Berichte des Meteorologischen Instituts
der Albert-Ludwigs-Universität Freiburg

Nr. 20

Andreas Matzarakis, Helmut Mayer

and Frank-M. Chmielewski (Eds.)

Proceedings of the
7th Conference on Biometeorology

Albert-Ludwigs-University of Freiburg, Germany
12-14 April 2010

Freiburg, April 2010

ISSN 1435-618X

Copyright reserved, particularly rights of reproduction, distribution and translation

Self-publishing company of the Meteorological Institute, Albert-Ludwigs-University of Freiburg, Germany

Print: Printing office of the Albert-Ludwigs-University of Freiburg

Editor: Prof. Dr. Helmut Mayer

Meteorological Institute, Albert-Ludwigs-University of Freiburg

Werthmannstr. 10, D-79085 Freiburg, Germany

Tel.: +49/761/203-3590; Fax: +49/761/203-3586

e-mail: meteo@meteo.uni-freiburg.de

Documentation: Ber. Meteor. Inst. Univ. Freiburg Nr. 20, 2010, 584 pp.

Editorial

Biometeorology represents a discipline with long tradition and interdisciplinary background. Therefore, it is very popular. The interactions between the atmosphere and the living environment are not only related to atmospheric exchange but also visible and sensitive from daily life to global warming issues. We have to keep in mind that climate change effects, finally, will at most influence and affect the living environment. Biometeorology can also be seen as part of climate impact in the global warming discussion.

The 7th Conference on Biometeorology (BioMet-7) is hosted from 12-14 April 2010 at the Meteorological Institute, Albert-Ludwigs-University of Freiburg, Germany, in collaboration with the Expert Committee on Biometeorology of the German Meteorological Society, the Humboldt-University of Berlin, Germany, the Society for the Promotion of Medicine-Meteorological Research in Germany, the International Society of Biometeorology, the German Weather Service and the Central Institute of Meteorology and Geodynamics in Vienna, Austria. It will provide an excellent opportunity to present and discuss new developments, approaches and methodologies from the whole spectrum of biometeorology.

The oral and poster presentations at the auditorium of the Albert-Ludwigs-University of Freiburg were subdivided into the fields: agricultural meteorology, animal meteorology, climate change, human-biometeorology, phenology, tourism climatology and urban bioclimate. The organisers of the Conference would like to express their thanks to the approximately 100 participants from over 30 countries. They are indebted to the authors of oral and poster presentations, the session chairs as well as the scientific and local organising committee.

In its present form, the proceedings volume contains extended abstracts of more than 80% of the presentations. The authors have the sole responsibility for the contents of their extended abstracts.

Andreas Matzarakis, Helmut Mayer and Frank-M. Chmielewski (Eds.)

Contents

Climate Change

Forest Meteorology

Human Biometeorology

Phenology

Tourism Climatology

Urban Bioclimate

Miscellaneous

Die Auswirkungen des Klimawandels auf die Landwirtschaft – die Aktivitäten des Deutschen Wetterdienstes im Rahmen des Projektes ZWEK

F.-J. Löpmeier, C. Frühauf

Deutscher Wetterdienst, Zentrum für Agrarmeteorologische Forschung Braunschweig

Zusammenfassung

Im Rahmen des Projektes ZWEK werden die Klimaszenarien der Regionalmodelle CLM, REMO, WETTREG und STAR mit der agrarmeteorologischen Beratungsroutine AMBER verrechnet. Durch die Verwendung der zurzeit in Deutschland häufig genutzten Regionalmodelle entsteht ein Ensemble von möglichen Ergebnissen für das Szenario A1b. Hierdurch erhält man einen Bereich, in dem die einzelnen agrarmeteorologischen Parameter in der Zukunft liegen können.

The effect of climate change on agriculture – activity of the german national weather service within the framework of the project ZWEK

Abstract

Climate scenario data of the regional models CLM, REMO, WETTREG and STAR were used as input for the agrometeorological model AMBER within the framework of the project ZWEK. An ensemble of possible results is generated by application of the in Germany most used regional models for the scenario A1b. The result is an array in which the agrometeological parameter can vary in future.

1. Das Projekt ZWEK des DWD

Kern des Vorhabens ist die Verrechnung der Klimaszenarien der Regionalmodelle CLM, REMO, WETTREG und STAR mit der agrarmeteorologischen Beratungsroutine AMBER. Die Ergebnisse der Regionalmodelle werden für zurückliegende Zeiträume (1971-2000) mit den Beobachtungen bzw. Messungen verglichen. Hierdurch kann bereits festgestellt werden, wie groß die auch in der Zukunft zu erwartenden Abweichungen vom späteren Wert sein können. Die Ergebnisse für die Zukunft werden als 30-jährige Mittelwerte für die Zeiträume 2021-2050 und 2071-2100 angegeben.

Bei der Anwendung der Daten der Regionalmodelle als Eingangsgrößen treten zum Teil fachlichen Probleme auf. Bereits die zeitliche Auflösung der Daten führt zu Schwierigkeiten, da zahlreiche agrarmeteorologische Modelle eine höhere zeitliche Auflösung (Stundenwerte) erfordern. Hier müssen erst mit geeigneten Verfahren Stundenwerte aus den vorhandenen Tageswerten erzeugt werden.

2. Vernalisation

Der Begriff Vernalisation bezeichnet die natürliche Induktion des Schossens und Blühens bei Pflanzen durch eine längere Kälteperiode im Winter. Zahlreiche ein- und zweijährige Pflanzenarten in Regionen mit ausgeprägten Unterschieden zwischen Winter- und Sommerbedingungen schossen und blühen erst, nachdem sie eine andauernde Peri-

ode mit niedrigen Temperaturen durchlebt haben. Treten im Winter Temperaturen über 12°C auf, wird dieser Effekt wieder aufgehoben. Die Pflanzen benötigen also nachfolgend wieder einen Kältereiz, um im Frühjahr in die generative Phase übergehen zu können. Für alle Wintergetreide ist die Vernalisation wichtig. Sind die Winter zu mild (fehlender Kältereiz) hat dies einen deutlichen Ertragsrückgang zu Folge. Ein Beispiel hierfür ist der Winter 2006/2007.

Untersucht wurde die Wahrscheinlichkeit für die Aufhebung des Vernalisationseffektes, d.h. wie oft treten im Winter Temperaturen über 12°C auf (siehe Tab. 1). Zur Übersichtlichkeit wird der Parameter für die vier Teilgebiete Norden, Osten, Westen und Süden Deutschlands angegeben.

Tab. 1: Anzahl der Fälle pro Winter mit Temperaturen oberhalb von 12°C

Table 1: Number of days with temperatures above 12°C in winter

Zeitraum		Norden	Osten	Westen	Süden
1971-2000	Messung	0,14	0,21	0,38	0,17
	REMO	0,24	0,41	0,41	0,41
	STAR	0,14	0,41	0,52	0,48
	CLM	0,10	0,07	0,17	0,07
	WETTREG	0,76	1,17	0,83	0,31
2021-2050	REMO	0,86	1,34	1,24	1,17
	STAR	1,17	1,86	2,17	1,90
	CLM	0,28	0,45	0,38	0,55
	WETTREG	0,66	0,52	0,90	0,24

Die meisten Regionalmodelle zeigen eine Zunahme der Häufigkeit der Aufhebung des Vernalisationseffektes für den Zeitraum 2021-2050 im Vergleich zu 1971-2000. Im Gegensatz dazu berechnet das Modell WETTREG für drei Bereiche Deutschlands eine Abnahme.

3. Bodenfrost

Kann Wasser in verdichtete Zonen des Bodens eindringen, führt Bodenfrost zu einer Lockerung des Bodens. Neben der Aufhebung der Bodenverdichtung wird durch die bessere Durchlüftung die Lachgasproduktion der Böden reduziert.

Mit den in der Zukunft prognostizierten milderen Wintern und der damit wahrscheinlich abnehmenden Bodenfrosteindringtiefe wird dieser Vorgang weniger häufig auftreten. Eine Lockerung der Böden mit mechanischen Mittel wird notwendig werden.

Abbildung 1 zeigt die Ergebnisse der Regionalmodelle für die Anzahl der Tage mit Bodenfrost von mindestens 25 cm Tiefe. Auffällig sind hier die starken Unterschiede zwischen den Modellen bereits in der Vergangenheit. Ursache hierfür sind die Unterschiede in der Schneebedeckung (siehe Abb. 2), denn eine Schneedecke wirkt isolierend. Hier wird deutlich, dass der Übergang von Regen in Schnee und der Aufbau einer Schneedecke von den Modellen hinreichend gut simuliert werden muss, um Aussagen in der Zukunft über die Frosteindringtiefe treffen zu können.

Schon aktuell ist es schwierig flächendeckend die Schneehöhe zu erfassen, obwohl Messungen der Schneehöhe vorliegen und Messmethoden über die Art des Niederschlages die Modellierung der Schneedecke erleichtern. Da für die Zukunft diese Informationen fehlen, sind Aussagen zum Bodenfrost nur schwer zu bewerten.

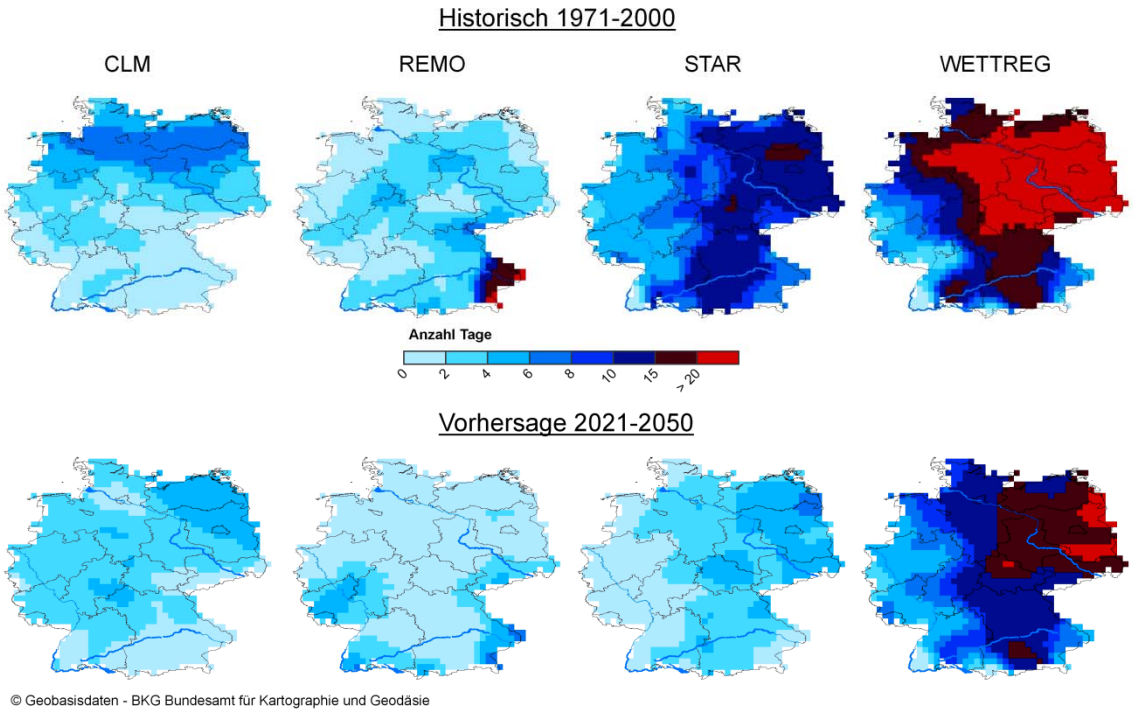

Abb. 1: Mittlere Anzahl von Tagen im Jahr mit Bodenfrost > 25 cm

Fig. 1: Mean number of days in the year with soil frost > 25 cm

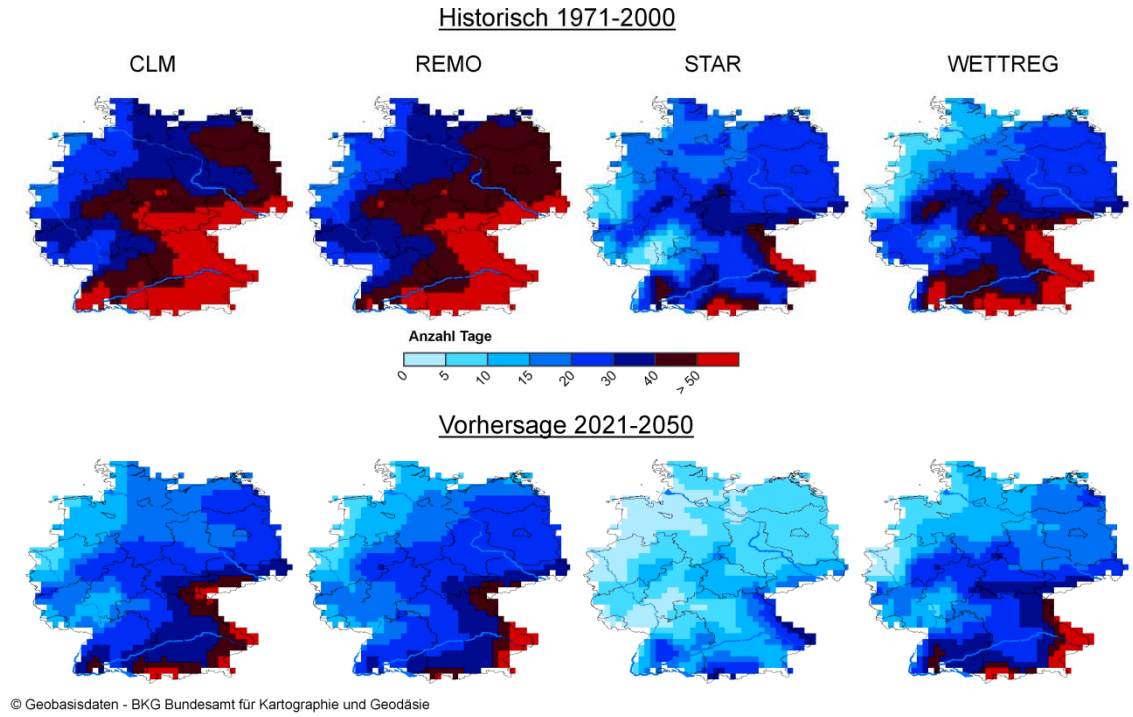

Abb. 2: Mittlere Anzahl von Tagen im Jahr mit einer Schneedecke > 3cm

Fig. 2: Mean number of days in the year with snow cover > 3 cm

4. Kornfüllungsphase

Viele Prozesse in der Pflanze sind an die Temperatur gekoppelt. Steigt die Temperatur, werden die Entwicklungsvorgänge beschleunigt. Ein beschleunigtes Durchlaufen der Wachstumszeit führt bei vielen Getreidearten zu einer Ertragsreduktion, da die Kornfüllungsphase verkürzt wird. Gleichzeitig arbeiten die Enzyme bei höheren Temperaturen nicht mehr so gut. In der Kornfüllungsphase werden dann statt großer Körner mit hoher Qualität, nur kleinere, minderwertige Körner ausgebildet.

Mit den steigenden Temperaturen setzt in Zukunft die Kornfüllungsphase früher ein. In Tabelle 2 sind die Kalendertage angegeben, an denen das Stadium BBCH 71 erreicht wird. Deutlich ist eine Verfrühung um durchschnittlich 10 Tagen für den Zeitraum 2021-2050 zu erkennen.

Tab. 2: Beginn der Kornfüllungsphase (Stadium BBCH 71: erste Körnerbildung), Angabe als Kalendertag (X - für den Zeitraum liegen keine Szenario-Daten vor)

Table 2: Start of grain filling (stage BBCH 71: first formation of grain), day of year (X – no scenario data)

Zeitraum	REMO	CLM	STAR	WETTREG
1961-1990	176	193	185	186
2021-2050	167	186	170	177
2071-2100	148	168	X	164

Tabelle 3 gibt einen Überblick, an wie vielen Tagen in der Kornfüllungsphase mit Maximumtemperaturen oberhalb von 25°C gerechnet werden muss. Es wurden zwei Zeiträume untersucht. In der Variante I wurde von heutigen Verhältnissen ausgegangen (165.-181. Kalendertag), während in der Variante II eine 10-tägige Verfrühung der Kornfüllungsphase berücksichtigt wurde (155.-171. Kalendertag). Es zeigt sich, dass die Unterschiede zwischen den beiden Varianten in der Regel kleiner sind als zwischen den einzelnen Regionalmodellen. Aus diesem Grund wurde keine weitere Anpassung für den Zeitraum 2071-2100 vorgenommen.

Tab. 3: Anzahl der Fälle mit einer Maximumtemperatur von >25°C innerhalb der Kornfüllungsphase für Deutschland, Variante I: Kornfüllungsphase entsprechend den heutigen Bedingungen (165-181), Variante II: Verfrühung der Kornfüllungsphase um 10 Tage durch höhere Temperaturen (155-171), mit Angabe der Änderung (Δ) zwischen den ausgewählten Zeiträumen

Table 3: Number of days with maximum temperature >25°C in the grain filling period for Germany, version I: normal grain filling period (165-181); version II: 10 days earlier grain filling period (155-171), under specification of change (Δ) between the selected time periods

Zeitraum	REMO				CLM				STAR				WETTREG			
	I	**Δ**	**II**	**Δ**	**I**	**Δ**	**II**	**Δ**	**I**	**Δ**	**II**	**Δ**	**I**	**Δ**	**II**	**Δ**
1961-1990	2,1		1,9		3,1		2,8		3,6		2,5		2,5		2,1	
		+0,2		+0,6		-0,1		+0,4		+1,4		+1,3		+2,0		+2,2
2021-2050	2,3		2,5		3,0		3,2		5,0		3,8		4,5		4,3	
		+2,8		+1,8		+3,4		+3,3						+2,0		+1,7
2071-2100	5,1		4,3		6,4		5,5		X		X		6,5		6,0	

5. Maisabreife

Mit der Zunahme von Biogasanlagen hat auch der Anbau von Mais als Silageprodukt stark zugenommen und die Flächen werden auch in Zukunft ausgeweitet werden. Mit dem früherem Vegetationsbeginn und der Temperaturzunahme ist davon auszugehen, dass auch in den nördlichen Gebieten Deutschlands später abreifende und damit mehr Biomasse produzierende Sorten angebaut werden können.

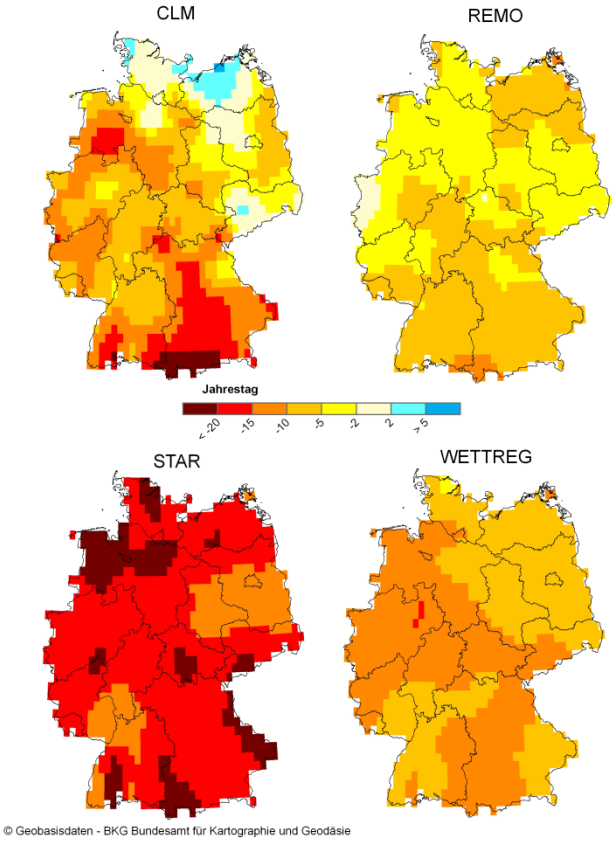

Abb. 3: Änderung des Termins Trockenmasse Mais (Gesamtpflanze) > 30% in Tagen; Zeitraum 2021-2050 im Vergleich zu 1971-2000; leichter Boden; frühe Sorte; negative Werte = Verfrühung

Fig. 3: Change of date in days dry matter maize (whole plant) > 30%; 2021-2050 in comparison to 1971-2000; sandy soil; early variety; negative values=earliness

Das Kriterium für die Ernte ist das Erreichen der Trockenmasse von ca. 28-32% je nach Verwendungszweck. Die Abbildung 3 zeigt für den Zeitraum 2021-2050 fast flächendeckend eine Verfrühung des Termins, an dem die Trockenmasse von 30% überschritten wird.

Adressen der Autoren:

Franz-Josef Löpmeier (franz-josef.loepmeier@dwd.de)
Dr. Cathleen Frühauf (cathleen.fruehauf@dwd.de)
Deutscher Wetterdienst, Zentrum für agrarmeteorologische Forschung Braunschweig
Bundesallee 50, D-38116 Braunschweig, Germany

Die Agrarmeteorologische Beratung des Deutschen Wetterdienstes unter spezieller Berücksichtigung von Sonderberatungen

Ramona Weßnigk, Jens Fildebrandt

Deutscher Wetterdienst, Zentrum für Agrarmeteorologische Forschung Braunschweig

Zusammenfassung

Kaum ein anderer Wirtschaftszweig ist so von Wetter und Klima abhängig wie die Landwirtschaft. Die Abteilung Agrarmeteorologie des Deutschen Wetterdienstes (DWD) bietet mit ihren fundierten Kenntnissen für diese Anforderungen praktische Umsetzungen. Diese beinhalten regionale Beratungsleistungen, wie die Routineprodukte „Wetterfax für die Landwirtschaft“, den Telefon- bzw. Fax-Service „Agrarwetter“ und das Internetangebot „agrowetter“. Darüber hinaus finden auf einem breiten Spektrum Sonderberatungen statt, die schwerpunktmäßig vorgestellt werden sollen.

Under special consideration of the agrometeorological advice of the German Weather Service

Abstract

Any other economic sector depends more on weather and climate than agriculture. The agrometeorological department of the German Weather Service provides specific agrometeorological consulting based on competent knowledge. This includes the regional information service, like “weather for farmers”, forecasts via phone and fax and the online service “agroweather forecast”. Furthermore individual advice offered for a wide range. These are presented exemplarily.

1. Standardberatungsprodukte

Die Abteilung Agrarmeteorologie des DWDs umfasst neben der fachlichen Leitung und dem Fachreferat für die Erstellung und Vertrieb agrarmeteorologischer Beratungsprodukte mit Sitz in Offenbach (am Main) vier Außenstellen: Braunschweig, Geisenheim, Leipzig und Weihenstephan. In Braunschweig ist gleichzeitig das Zentrum für Agrarmeteorologische Forschung (ZAMF) angesiedelt.

Ein Tätigkeitsfeld der Außenstellen, die regionale Ansprechpartner für die Landwirtschaft sind, ist die routinemäßige Erstellung von Beratungsprodukten. Diese sind speziell auf den Kundenkreis „Landwirtschaft“ zugeschnitten. Dazu gehört das „Wetterfax für die Landwirtschaft“. Es umfasst für die nächsten fünf bis sieben Tage eine auf den jeweiligen Vegetationsstand abgestimmte agrarmeteorologische Vorhersage zu den wichtigsten Kulturpflanzen und landwirtschaftlichen Arbeiten in dem jeweiligen Beratungsgebiet. Ein weiteres Kernprodukt stellt die Agrarwettervorhersage mit einer Wochenvorhersage und landwirtschaftlichen Hinweisen dar, die per Telefon, Fax oder aus dem Internet abrufbar sind. Weiterhin zeigen die Außenstellen in verschiedenen regionalen Landwirtschaftzeitungen mit Agrarwettervorhersagen Präsenz.

Das vom DWD angebotene Internetprodukt „agrowetter“ setzt sich aus einem Online-Beratungssystem für die Landwirtschaft und einer interaktiven Beregnungsberatung zusammen. Die „agrowetter Prognose“ enthält neben allgemeinen Wettervorhersagen in Text- und Zahlenform und der agrarmeteorologische Entwicklung des aktuellen Tages sowie der sechs Folgetage auch wichtige landwirtschaftliche Hinweise, unter

anderem zu optimalen Aussaatterminen, Grünlandschnitt, Getreideernte oder Maisernte. Diese Vorhersage wird für ca. 500 deutsche Wetterstationen berechnet.
Das Produkt „agrowetter Beregnung“ ist dagegen ein interaktives „Online-System“, welches für über dreißig Obst- und Gemüsekulturen die momentane und für die nächsten vier Tage zu erwartende Bodenfeuchte berechnet und gezielte Beregnungsempfehlungen gibt. Dabei werden die individuellen Gegebenheiten des Nutzers in Form von Kultur- und Bodeneigenschaften, sowie sein vor Ort gefallener Niederschlag und seine Beregnungsmengen berücksichtigt.

2. Beispiele für Sonderberatungen in Norddeutschland

In den letzten Jahren haben die Beratungsleistungen, die über Routinearbeiten hinausgehen, immer weiter zugenommen.
So ergeben sich auf unterschiedlichsten thematischen Bereichen Zusammenarbeiten, die von Bundesforschungsinstituten über den Fachverband für Feldberegnung bis hin zu Bundes- bzw. Landesministerien reichen.

2.1 Prognose Blüte Wiesenfuchsschwanz

Mit dem Niedersächsischen Ministerium für Ernährung, Landwirtschaft, Verbraucherschutz und Landesentwicklung findet eine Kooperation im Rahmen der NAU/BAU-Programme mit der Maßnahme „Förderung extensiver Grünlandnutzung durch Verringerung der Betriebsmittelanwendung“ statt. Daran teilnehmende Landwirte erhalten eine finanzielle Entschädigung. Es ist festgelegt, dass das Mähen der Grünlandflächen erst nach einem jährlich vom Ministerium vorgegebenen Termin erfolgen darf. Dieser Termin orientierte sich vor der Zusammenarbeit starr am 25. Mai. Dies führte in den vergangenen Jahren mit früher Vegetationsentwicklung dazu, dass das Erntegut schlechte Qualität aufwies. Nach der Kooperation richtet sich der Schnittzeitpunkt danach, wann der phänologische Stand des 25. Mai erreicht ist. Dies korreliert stark mit der Blüte des Wiesenfuchsschwanzes. Mit Hilfe des Phänologischen Meldenetzes vom Deutschen Wetterdienst kann der Blühzeitpunkt prognostiziert werden. Auf diesen für ganz Niedersachsen durchschnittlichen Blühtermin werden 13 Tage addiert. Für die Landwirte bringt diese Praxis deutliche Vorteile, da die Qualität des Schnittguts so meist eine gesicherte Verwendbarkeit gewährleistet.

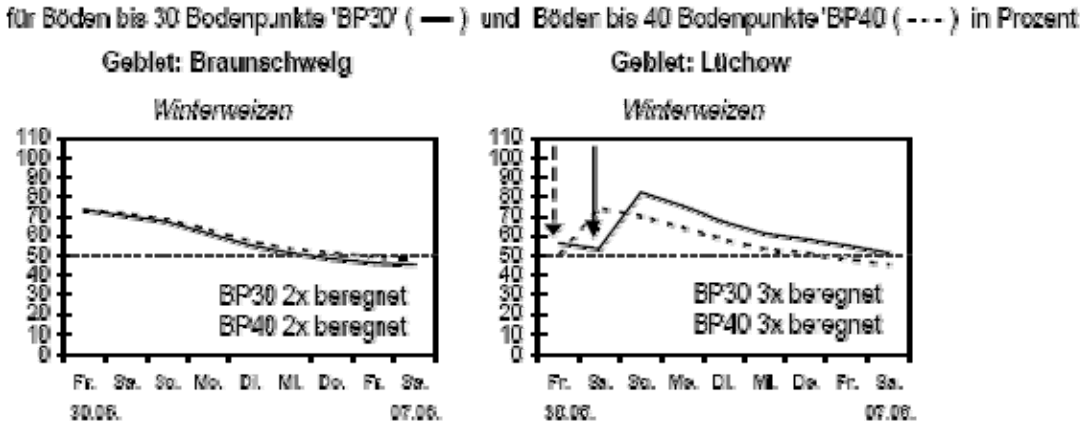

Abb. 1: Beispiele von Bodenfeuchteverlaufskurven
Fig. 1: Examples for soil moisture developing

2.2 Beregnungsberatung

Eine weitere Zusammenarbeit, die im Ergebnis über tausend niedersächsische Landwirte erreicht, ist die Beregnungsberatung mit dem Fachverband Feldberegnung e.V. und der Landwirtschaftskammer Niedersachsen. Die Beregnungsberatung beinhaltet einen während der Vegetationszeit wöchentlich erscheinenden Hinweis, der über Niederschlag und Verdunstung von über 70 niedersächsischen Stationen und die daraus resultierende Klimatische Wasserbilanz informiert. Darüber hinaus enthält der Bericht die Wetteraussichten für die kommenden sieben Tage, eine Wasserbedarfsrechnung für verschiedene Feldfrüchte, sowie exemplarische Bodenfeuchteverlaufskurven.

2.3 Grünlandertragsprognose

Die Landwirtschaftskammern Schleswig-Holstein und Niedersachsen beproben, je nach Vegetationsentwicklung und Standort im Zeitraum von Mitte April bis Anfang Juni wöchentlich spezielle Ackergras- und Gründlandflächen hinsichtlich grünlandspezifischer Parameter. Diese Daten werden vom Deutschen Wetterdienst mit Hilfe eines von der Universität Kiel entwickelten Ertragsmodells verrechnet. Zusätzlich fließen in das Modell die meteorologischen Vorhersagen wie Temperatur und Strahlung ein. Als Ergebnis werden die für den optimalen Schnittzeitpunkt von Grünland relevanten Parameter Ertrag, Rohfasergehalt, Nettoenergiekonzentration Laktation (NEL) sowie Rohproteingehalt für die nächsten sechs Tage prognostiziert. Die Ertragsprognosen werden auf den Seiten der Landwirtschaftskammern und in den niedersächsischen und schleswig-holsteinischen Landwirtschaftszeitungen veröffentlicht.

2.4 Agrarmeteorologische Auswertungen für Bundes- und Landesministerien

In der Vergangenheit ist es immer wieder witterungsbedingt zu Extremereignissen in der Landwirtschaft gekommen. In den letzten Jahren häufen sich die Ereignisse. Auf Grundlage der seit Februar 2009 überarbeiteten Rahmenrichtlinie der Europäischen Kommission können Landwirte, die durch solche Naturkatastrophen oder widrige Witterungsverhältnisse geschädigt wurden, zur Bewältigung staatliche Zuwendungen beantragen. Durch entsprechende Daten und Unterlagen muss das Vorliegen einer Naturkatastrophe gemäß der Rahmenrichtlinie bei nationalem Ausmaß vom Bundesministerium für Ernährung, Landwirtschaft und Verbraucherschutz (BMELV) und bei regionalem Ausmaß von der jeweiligen Landesregierung nachgewiesen werden. Die Bewertung der agrarmeteorologischen Situation wird durch den DWD durchgeführt. Bereits vor der Rahmenrichtlinie traten das BMELV und die Ministerien der Länder an den DWD heran. Im Zuge dessen wird beispielsweise dem BMELV eine monatlich erstellte Witterungsanalyse vom ZAMF Braunschweig bereit gestellt.

2.5 Beratungen von Bundesforschungsanstalten bei Forschungsvorhaben

Die Bundesforschungsanstalten Julius Kühn-Institut (JKI) und Johann Heinrich von Thünen-Institut (vTI) bekommen bei Forschungsarbeiten, die einen agrarmeteorologischen Bezug haben, Unterstützung vom Deutschen Wetterdienst.
Das JKI benötigte beispielsweise im Rahmen eines Forschungsprojektes zum Thema Guttation (Austreten von Xylemsaft an den Blatträndern von Pflanzen) meteorologische Parameter. Damit Guttation auftritt, müssen unter anderem bestimmte Witterungsbedingungen vorherrschen, die sich aus den Parametern relative Feuchte, Benetzungszeiten und Niederschlag zusammensetzen. Zur Koordinierung der deutschlandweiten Guttati-

onsbeobachtung wurden diese meteorologischen Größen, für die kommenden fünf Tage bereitgestellt.
Eine weitere Zusammenarbeit fand im Zuge des Projekts FACE (Free Air Carbon Dioxid Enrichment) statt. Dabei wird die Wirkung von erhöhter CO_2-Konzentration auf Pflanzen untersucht. Um gleichzeitig ein mögliches Klimaszenario zu simulieren, welches eine Zunahme der Sommertrockenheit voraussagt, wird ein Teil der Pflanzen vor signifikanten Niederschlagsereignissen mit Zelten abgedeckt. Als Entscheidungshilfe stellte der DWD spezielle Niederschlagsprognosen zur Verfügung.

2.6 Enthalpie

Ein vom DWD kostenfreies im Zeitraum etwa von Mai bis September über das Internet abrufbares Beratungsprodukt ist die Enthalpie. Die Enthalpie gibt den Gesamtwärmeinhalt der Luft an und dient als Kennzahl für die Wärmebelastung bei Geflügel. In einer Vereinbarung zwischen dem niedersächsische Landwirtschaftsministerium und der Geflügelwirtschaft über Mindestanforderungen in der Hühnermast sind Grenzwerte für die Enthalpie angegeben. Bei Überschreiten einer Enthalpie von 72 kJ/kg in den Stallungen tritt nach kurzer Zeit der Hitzetod ein. Da sich die Modellprognosen immer auf die Außenluft beziehen, wird hier mit einem Grenzwert von 67 kJ/kg gearbeitet. Somit können bei einem prognostizierten Überschreiten des Grenzwertes entsprechende Maßnahmen, wie die Ventilation in Ställen eingeleitet werden.

2.7 Temperaturprognose Nordzucker

Eine weitere Zusammenarbeit, die in den Wintermonaten erfolgt, ist eine spezielle Temperaturprognose für den Zuckerproduzenten Nordzucker.
Die Zuckerrüben müssen nach der Ernte häufig am Feldrand zwischengelagert werden, da die Verarbeitung von den Annahme- und Verarbeitungsmöglichkeiten der Zuckerfabriken abhängt. Mit zunehmend längeren Rübenkampagnen, die bis Ende Dezember, teils bis Januar andauern, nehmen gleichzeitig witterungsbedingte Risiken wie Frost, Schnee und Nässe zu. Die Lagerbedingungen der Zuckerrüben am Feldrand müssen der Witterung angepasst werden. Beispielsweise muss das Erntegut vor Nachtfrost und Tagestemperaturen von unter -4 °C mit Stroh und Vlies geschützt werden. Treten dagegen mehrere Tage mit Temperaturen von über 10 °C auf, so müssen die Rüben aufgedeckt werden um Atmungsverluste zu verringern. Wettervorhersagen werden täglich für die kommenden acht Tage erstellt, wobei der Schwerpunkt auf der Temperatur liegt. Zusätzlich wird ein Trend für bis zu 14 Tagen angegeben. Hiermit können kurz- und mittelfristig Maßnahmen eingeleitet bzw. geplant werden und die Qualität der Zuckerrüben trotz langer Lagerzeiten gesichert werden.

3 Schlussbetrachtung

Aus dieser kurzen Betrachtung der über die Routinearbeiten hinausgehenden Sondertätigkeiten wird das vielfältige Arbeitsspektrum der Agrarmeteorologie des Deutschen Wetterdienstes ersichtlich. Dieses wird sich auch in den kommenden Jahren weiter ausbauen, sei es im Bereich der Politikberatung, des Klimawandels oder bei weiteren Forschungsvorhaben.

Adressen der Autoren
Ramona Weßnigk (ramona.wessnigk@dwd.de), Jens Fildebrandt (jens.fildebrandt@dwd.de)
Deutscher Wetterdienst, Zentrum für Agrarmeteorologische Forschung
Bundesallee 50, 38116 D-Braunschweig

Klimatologische und phänologische Dürre-Indikatoren in der Agrarmeteorologie des DWD

Klaus-Peter Wittich[1], Ralf Becker[2]

[1] Deutscher Wetterdienst (DWD), Zentrum für Agrarmeteorologische Forschung, Braunschweig
[2] Deutscher Wetterdienst (DWD), Richard-Aßmann Observatorium, Lindenberg

Zusammenfassung

Im Rahmen der gegenwärtigen Klimadebatte wird überwiegend die Meinung vertreten, dass in Deutschland die Anzahl sommerlicher Dürren zunehmen wird. Aus diesem Grunde ist es sinnvoll, sich im Rahmen eines Umweltmonitorings mit Dürre-Indizes zu befassen.

In dem Artikel werden die gegenwärtigen agrarmeteorologischen Arbeitsgebiete des DWD's angesprochen. Im Einzelnen geht es um

- die Anwendung des Standardized Precipitation Index (SPI), dessen kürzere Zeitskalen (≤ 6 Monate) die wasserhaushaltsrelevanten Belange der Landwirtschaft abdecken (im Unterschied zu den längeren Zeitskalen, die hydrologische Fragestellungen beantworten),
- die Entwicklung eines satellitengestützten Dürreproduktes auf der Basis des *NDVI* und der Brightness-Temperatur, deren normierte Relativwerte zwischen 0 und 1 Pflanzenstress- bzw. Nichtstresssituationen anzeigen, und um
- die Einführung der farbphänologischen Beobachtung der Grasvergilbung, um auf Referenzflächen den Wassergehalt natürlicher Vegetation abzuschätzen.

Climatological and phenological drought indicators within the DWD's agrometeorology

Abstract

Most climate models project an increase in the number of droughts in Germany in the next decades. Therefore, drought monitoring is becoming more and more important. This article presents the DWD's agrometeorological activities in this context:

- application of the standardised precipitation index (SPI) whose short time scales (≤ 6 months) addresses agricultural drought issues,
- development of a satellite-based stress index using the *NDVI* and the brightness temperature of land surface to calculate a standardised relative number between 0 and 1 as indicator for stressed and non-stressed vegetation, and
- phenological observations of the yellowing level for assessing the leaf-water content of grassland.

1. Einführung

Bekanntlich sind landwirtschaftliche Kulturen hinsichtlich ihrer langfristigen Anbauwürdigkeit sowie ihrer saisonalen Ertragsfähigkeit von einer optimalen Wasserversorgung des Wurzelraumes abhängig. Eine der klassischen Hauptarbeitsgebiete der Agrarmeteorologie behandelt deshalb folgerichtig das Thema des Bodenwasserhaushalts. Speziell erwähnt sei die seit Jahrzehnten etablierte Beregnungsberatung, die zu den traditionellen Aufgabenfeldern des agrarmeteorologischen Beratungsdienstes zählt. Neben dieser Beratungsaufgabe befasst sich die Agrarmeteorologie allerdings auch mit anderen Aspekten des Wasserhaushalts. Hierzu gehört z.B. das Dürremonitoring. Dieses ist von steigendem Interesse, da einige Klimamodelle eine Zunahme der Dürreperioden in den nächsten Jahrzehnten andeuten.

Drei in jüngerer Zeit aufgenommene Tätigkeitsfelder behandeln innerhalb dieser Thematik z.B. einen farbphänologischen Indikator, der Auskunft über den Wassergehalt von Grasflächen gibt. Hierzu wird die prozentuale Vergilbung einer im natürlichen Wachstum befindlichen Grasbrache auf einer Freifläche beobachtet (Kap. 2). Während mit dieser Aufgabe phänologische Beobachter betraut werden können, bietet sich für das Monitoring größerer Flächen ein satellitengestützter Index an. Dieser basiert auf dem Normalized Difference Vegetation Index (*NDVI*) und der Helligkeitstemperatur (Kap. 3). Ferner sind statistische Aussagen von Interesse, die mittels eines Wahrscheinlichkeitsindexes (dem sog. Standardized Precipitation Index, *SPI*) die Einordnung der Niederschlagssituation in den klimatologischen Maßstab ermöglichen (Kap. 4).

2. Grasvergilbung

Seit einigen Jahrzehnten bereits werden in den größeren Waldbrandländern (Kanada, Australien, USA) Beobachtungsprogramme durchgeführt, um den Grad der Grasvergilbung in Feuerausbreitungs- bzw. -gefahrenmodelle einzubeziehen. Unter günstigen meteorologischen Bedingungen zeichnet sich abgestorbenes, vergilbtes Gras – im Unterschied zu grünem Pflanzenmaterial – durch raschere Wasserverluste aus, was mit einem schnellen Anstieg der Zündbereitschaft einhergeht. Insofern stellen z.B. unter sommerlichen Dürren vergilbte Grasflächen einen potentiellen Ausgangsort für Bodenfeuer dar.

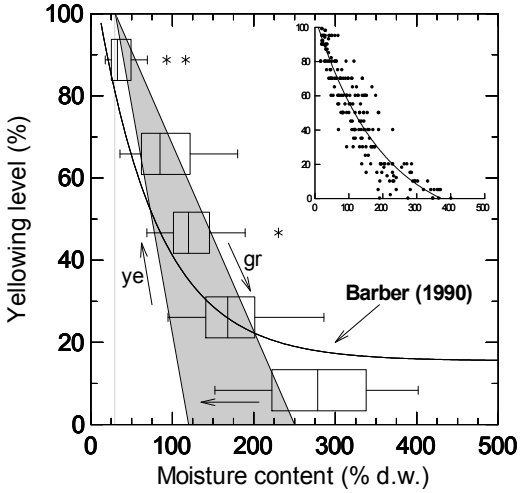

Abb. 1: Beziehung zwischen Blattwassergehalt und Vergilbungsniveau von Grasbrachen. Die Originaldaten sind in der Innengrafik dargestellt. Die Punktdarstellung wurde zur besseren Vergleichbarkeit mit Beobachtungen aus Australien (Barber) und den USA (graues Dreieck) in Boxplots überführt (aus Wittich, 2010)

Fig. 1: Relationship between leaf moisture and yellowing level of grassland. The original data are plotted in the inset whereas box plots of five subpopulations contained in the data pool are used for better comparison with Australian data (Barber's curve) and US data (shaded triangle) (adopted from Wittich, 2010)

Dem Vorgehen der genannten Waldbrandländer folgend begann der DWD im Jahr 2005 mit Voruntersuchungen, um aus dem Grad der Vergilbung den Wassergehalt abzuschätzen. Abb. 1 zeigt, dass der prozentuale Vergilbungsgrad mit dem Wassergehalt korre-

liert ist. Eine Einschränkung erfährt die Grasbeobachtung allerdings dadurch, dass sie nur auf jenen speziell ausgewählten Freiflächen durchgeführt werden darf, die einerseits mehrjähriges Graswachstum aufweisen, andererseits sich jeglicher Pflege und landwirtschaftlicher Nutzung entziehen. Nur unter diesen Bedingungen ist eine Vergleichbarkeit der Beobachtungsdaten gewährleistet, welche erfordert, dass die Flächen einem ungehinderten Niederschlags- und Strahlungseintrag unterliegen und die Vegetation während des gesamten Jahres eine ungestörte Wachstums- und Seneszenzphase durchlaufen kann. Abb. 2 zeigt einen typischen Verfärbungszyklus, der mit vergilbtem abgestorbenen (erfrorenem) Material am Ausgang des Winters beginnt, in das Ergrünen des Frühjahrs übergeht und schließlich – durch eine sommerliche Dürreperiode verstärkt – erneut in eine Vergilbungsphase eintritt.

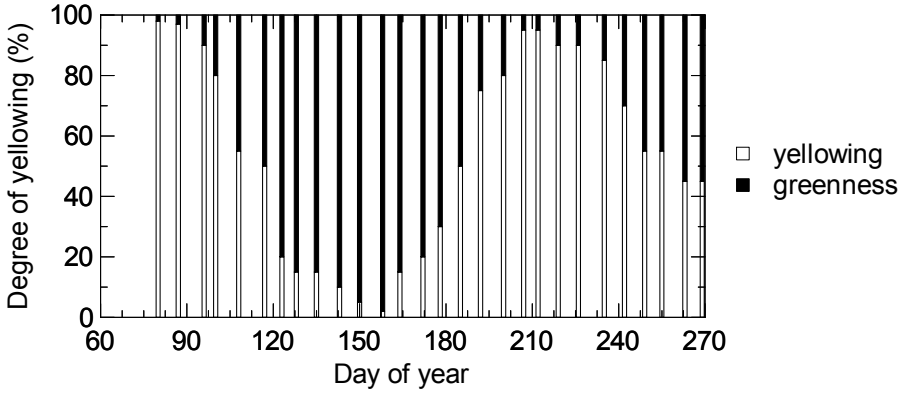

Abb. 2: Vergilbungsanteile einer Grasbrache während des Vegetationszeitraums 2006; Beobachtungsort: Vechelade (nach Wittich und Langhoff, 2007)

Fig. 2: Degree of yellowing during the growing season 2006; site: Vechelade (according to Wittich und Langhoff, 2007)

3. Satellitengestützter Dürre-Index

Da es sich bei den für die farbphänologische Beobachtung geeigneten Flächen um relativ kleine ökologische Nischen handelt, ist es sinnvoll, für ein größerskaliges Monitoring auf Satellitendaten zurückzugreifen. Als Dürre-Index wird der von Kogan (1995, 2001) vorgeschlagene sog. Stress-Index (*SI*) benutzt (siehe Becker et al., 2007), der sich aus den mit *w* linear gewichteten Komponenten des Vegetation Condition Index (*VCI*) und des Temperature Condition Index (*TCI*) gemäß

$$SI_i = w * VCI_i + (1 - w) * TCI_i$$

zusammensetzt ($0 \le (SI, w, VCI, TCI) \le 1$). Der *VCI* berechnet sich aus einem normierten *NDVI* nach der Beziehung

$$VCI_i = \frac{NDVI_i - NDVI_{\min,i}}{NDVI_{\max,i} - NDVI_{\min,i}}, \quad NDVI = \frac{\rho_2 - \rho_1}{\rho_1 + \rho_2},$$

wobei $\rho_{1,2}$ die Strahlungsreflexionen des Kanals 1 (sichtbarer Spektralbereich) und des Kanals 2 (nahes Infrarot) des NOAA-AVHRR sind. Der *TCI* gehorcht der Beziehung

$$TCI_i = \frac{T_{\max,i} - T_i}{T_{\max,i} - T_{\min,i}}$$

mit T als Brightness-Temperatur des AVHRR-Kanals 4 (10.3 – 11.3 µm). Die für jede Woche i gültigen *min-max*-Ränder ergeben sich aus den historischen Extremwerten zurückreichender Zeitreihen (1998 – 2004) eines Pixels und stellen Ökosystemgrenzen (*NDVI*) bzw. Temperaturgrenzen (T) dar. Stressbedingungen bzw. normale oder günstige Wachstumsbedingungen liegen bei $SI < 0.4$, $0.4 \leq SI \leq 0.8$ bzw. $SI > 0.8$ vor. Abb. 3 zeigt für die Referenzpixel Lindenberg (östliches Brandenburg) und Feldberg (Schwarzwald) und deren Umgebung (9 km^2) den historischen Schwankungsbereich des *NDVI* und der Helligkeitstemperatur während der Vegetationsperiode, wobei die Ränder mittels eines Polynoms 2. Grades geglättet wurden.

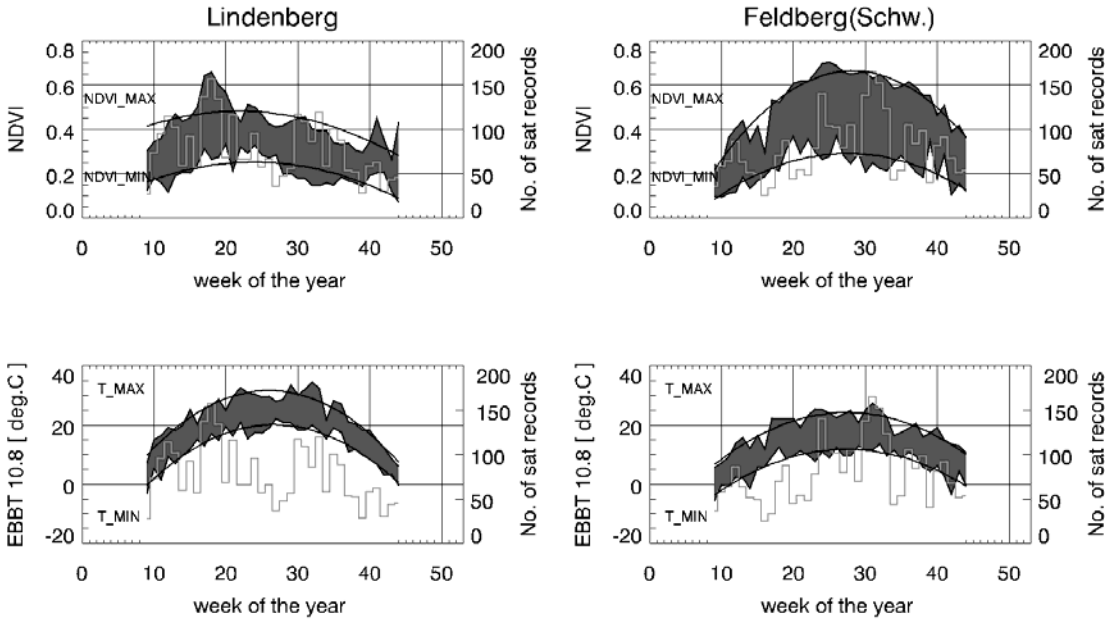

Abb. 3: Mehrjährige Randwerte des *NDVI* (oben) und der Helligkeitstemperatur (unten) als Basiseingaben für den *VCI* und den *TCI* für die Regionen Lindenberg und Feldberg (Schwarzwald).

Fig. 3: Multi-annual boundary values of NDVI (top) and brightness temperature (bottom) used for VCI and TCI calculation; sites: Lindenberg and Feldberg (Black Forest).

4. Standardized Precipitation Index

Der Standardized Precipitation Index (*SPI*; siehe McKee et al., 1993, 1995) gehört seit etwa einem Jahrzehnt zu den gebräuchlichsten klimatologischen Niederschlagsindizes, die eine Bewertung von Dürren und Niederschlagsüberschüssen auf statistischem Wege ermöglichen. Berechnungsgrundlage ist eine mindestens 30-jährige Zeitreihe, bestehend aus monatlichen Niederschlagssummen. Unter der Annahme, dass der Niederschlag gammaverteilt ist, wird die monatsweise gebildete Wahrscheinlichkeitsdichte (für $n \geq$ 30 Januare, $n \geq 30$ Februare, …) in eine kumulative Gammaverteilung umgerechnet und

diese in eine kumulative Standard-Normalverteilung transformiert, deren Abszisse den *SPI*-Wert für den gewählten Monat angibt. Um die Wirkung längerer Zeiträume darzustellen (Quartalsniederschlag, Halbjahresniederschlag, etc.), werden gleitende Niederschlagsmittel über 3, 6, etc. Monate gebildet. Die Berücksichtigung unterschiedlich langer Zeitskalen liefert Hinweise auf landwirtschaftliche Dürren (z.B. Zeitskalen ≤ 6 Monate) oder hydrologische Dürren (z.B. Zeitskalen ≥ 6 Monate). Als Dürre wird die Andauer einer negativen *SPI*-Periode bezeichnet, in welcher der *SPI* den Wert –1 erreichen bzw. unterschreiten muss (s. Tab. 1). Abb. 4 zeigt den Verlauf des Halbjahresniederschlages mit den zugehörigen *SPI*-Werten für die Station Braunschweig. Als Referenzzeitraum für die Kalibrierung der statistischen Parameter wurden die Jahre 1961 – 1990 gewählt. Innerhalb des vergangenen 15-jährigen Zeitraums treten deutlich die zu feuchten Jahre 2002 und 2007 sowie das zu trockene Frühjahr 1996 und der zu trockene Sommer 2003 hervor.

Tab. 1: Wahrscheinlichkeit unterschiedlicher *SPI*-Bereiche und Kategorien der Feuchtigkeitsverhältnisse (*Probabilities of SPI intervals and drought category*)

Probability (%)	***SPI***	**Category**
2.3	≥ 2.0	Extremely wet
4.4	1.5 bis 2.0	Severely wet
9.2	1.0 bis 1.5	Moderately wet
34.1	0.0 bis 1.0	Near normal (mildly wet)
34.1	-1.0 bis 0.0	Near normal (mild drought)
9.2	-1.5 bis -1.0	Moderate drought
4.4	-2.0 bis -1.5	Severe drought
2.3	≤ - 2.0	Extreme drought

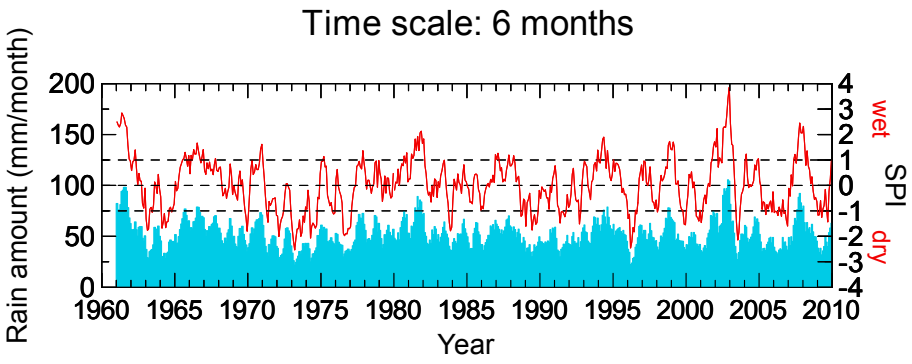

Abb. 4: Niederschlagszeitreihe (Balken) und *SPI*-Zeitreihe (Kurve) für Braunschweig (1961–2009) für die 6-monatige Zeitskala

Fig. 4: 6-monthly averaged rain totals (bars) and related SPI values (curve); site: Braunschweig (1961–2009)

5. Schlussbemerkung

Der Artikel beschreibt die gegenwärtigen Arbeitsfelder eines agrarmeteorologischen Dürremonitorings. Aufgrund dessen steigender Bedeutung werden die Tätigkeitsfelder weiter ausgebaut und in eine operationelle Anwendung überführt.

References

Becker, R., Wittich, K.-P., Koslowsky, D., 2007: A satellite-derived drought product to improve the agrometeorological consulting. Proceedings of the Joint EUMETSAT/AMS Meteorological Satellite Conference, Amsterdam, Sep. 24-28, 2007.

Kogan, F., 1995: Application of vegetation index and brightness temperature for drought detection. Adv. Space Res. 15, 91-100.

Kogan, F., 2001: Operational space technology for vegetation assessment. Bull. Amer. Meteorol. Soc. 82, 1949-1964.

McKee, T.B., Doesken, N.J., Kleist, J., 1993: The relationship of drought frequency and duration to time scales. Preprints, 8th Conference on Applied Climatology, 17-22 January, Anaheim, CA, Amer. Met. Soc., 179-184.

McKee, T.B., Doesken, N.J., Kleist, J., 1995: Drought Monitoring with multiple time scales. Preprints, 9th Conference on Applied Climatology, 15-20 January, Dallas, TX, Amer. Met. Soc., 233-236.

Wittich, K.-P., Langhoff, H., 2007: Farbphänologie: Beobachtung der Grasvergilbung. Phänologie-Journal Nr. 28, Deutscher Wetterdienst, Offenbach, 4-5.

Wittich, K.-P., 2010: Phenological observations of grass curing in Germany. Eingereicht in: Int. J. Biometeorol. (9. Nov. 2009, in der Begutachtung).

Authors' address:

Dr. Klaus-Peter Wittich (klaus-peter.wittich@dwd.de)
Zentrum für Agrarmeteorologische Forschung, Deutscher Wetterdienst (DWD)
Bundesallee 50, D-38116 Braunschweig, Germany

Ralf Becker (ralf.becker@dwd.de)
Richard-Aßmann-Observatorium, Deutscher Wetterdienst (DWD)
Am Observatorium 12, D-15848 Tauche/Lindenberg, Germany

Sensitivität des agrarmeteorologischen Modells AMBETI/BEKLIMA für Änderungen der meteorologischen Randbedingungen

Harald Braden

Deutscher Wetterdienst (DWD), Zentrum für Agrarmeteorologische Forschung, Braunschweig

Zusammenfassung

Mit dem Modell AMBETI/BEKLIMA wurden Rechnungen einerseits mit gemessenen und andererseits mit modifizierten meteorologischen Randbedingungen durchführt. Vergleiche der jeweils berechneten Modellergebnisse zeigen die Sensitivität des Modells für meteorologische Randbedingungen an. Zielgrößen sind dabei Bodentemperaturen, bodennahe Minimumtemperatur, Blattbenetzungsdauer, Bestandstemperatur sowie die Verdunstungskomponenten. Die modifizierten Randbedingungen sind Lufttemperatur und -feuchte, Globalstrahlung und langwellige Gegenstrahlung.
Die Ergebnisse erlauben Aussagen über den Einfluss sowohl von Unsicherheiten der vorhergesagten Klimadaten als auch von deren Trends auf agrarmeteorologische Zielgrößen.

Sensitivity of the agrometeorological model AMBETI/BEKLIMA for modified meteorological boundary conditions

Abstract

The sensitivity of the model AMBETI/BEKLIMA was tested by comparing its results of runs with original and modified meteorological data. The target variables are soil temperatures, minimum air temperatures near to the ground, leaf wetness duration and evaporation components. The modified boundary conditions are air temperature, global radiation and incident long-wave radiation. The results inform about the impact of uncertainness of the forecasted climatic data and of trends of the agrometeorological results.

1 Einleitung

Das Modell AMBETI/BEKLIMA ist ein (eindimensionales) SVAT-Modell, das vom DWD seit Jahren unter anderem im Rahmen der agrarmeteorologischen Beratung eingesetzt wird (Braden, 1995). Neuerdings wird es darüber hinaus auch als "Klimawirkmodell" mit Ergebnissen regionaler Klimamodelle betrieben. Dadurch werden Auswirkungen unterschiedlicher Klimaszenarien auf agrarmeteorologische Zielgrößen untersucht.
Die Sensitivität des Modells AMBETI/BEKLIMA bezüglich seiner meteorologischen Eingangsgrößen ist deshalb von Interesse.

2 Material und Methoden

Das eindimensionale SVAT-Modell AMBETI/BEKLIMA rechnet dabei mit einer Bestandsschicht und 13 Bodenschichten. Dadurch wird sowohl eine hohe räumliche und zeitliche Auflösung an der Oberfläche ermöglicht als auch eine untere Randbedingung in einer Tiefe unterhalb von 12 m erreicht, die dem Modell eine sehr gute Langzeitstabilität verleiht. Weil auch Gefriervorgänge und die Schneedecke berechnet werden, eignet sich das Modell gut für mehrjährige Modellierungen. Der externe Zeitschritt des Modells wird durch die meteorologischen Randbedingungen vorgegeben und sollte nicht größer als eine Stunde sein. Die erforderlichen meteorologischen Randbedingungen sind Lufttemperatur und –feuchte, Globalstrahlung, langwellige Gegenstrahlung, Wind-

geschwindigkeit und Niederschlag. Lufttemperatur und Luftfeuchte sind dabei in der Regel Werte aus der Höhe von 2 m, die Windgeschwindigkeit aus 10 m.

Die Rechnungen wurden mit Messwerten von Braunschweig aus dem Jahr 2008 durchgeführt, welches einen mittleren Jahresniederschlag aufweist. Gerechnet wurde für die Bodenart "schwach schluffiger Sand" (su2), jedoch ist die Modellsensitivität von diesen Eigenschaften weitgehend unabhängig.
Zur Ermittlung der Modellsensitivität wurden einerseits Modellrechnungen mit den ursprünglichen meteorologischen Randbedingungen durchgeführt ("Referenz"). Für unterschiedliche Szenarien wurden die Stundenwerte des gesamten Jahres einzelner meteorologischen Größen jeweils um einen festen Wert erhöht, bzw. mit einem Faktor multipliziert und die Ergebnisse mit der Referenz verglichen. Bei Winterweizen ("WW") wurde vom 27. Juli an und bei Zuckerrüben ("ZR") bis 4. Mai mit unbewachsenem Boden gerechnet.

3 Ergebnisse

Im Folgenden werden die Ergebnisse einzelner Modifikationen der meteorologischen Randbedingungen erläutert. Übersichten der Auswirkungen aller Modifikationen auf die Verdunstungskomponenten von Winterweizen ("WW") und Zuckerrüben ("ZR") sowie die Bodenevaporation eines unbewachsenen Bodens ("oB") finden sich in Tabelle 1, wo jeweils prozentuale Abweichungen der Verdunstungssummen gegenüber der Referenz für die Zeit März bis Oktober angegeben sind.

Tab. 1: Änderung der Verdunstungssummen von März bis Oktober (447 mm Niederschlag); ETP = Evapotranspiration, T = Transpiration, E_{Bo} = Bodenevaporation

Tab. 1: Impact on evaporation components (March to October, 447 mm of precipitation); ETP = evapotranspiration, T = transpiration, E_{Bo} = soil evaporation

	ETP_{oB}	ETP_{WW}	T_{WW}	$E_{Bo\ WW}$	ETP_{ZR}	T_{ZR}	$E_{Bo\ ZR}$	
tl:=tl+1	+0.4	+1.0	+2.4	–0.3	+0.3	+0.6	+0.4	%
tl:=tl+1, cf	+8.3	+6.8	+3.3	+9.5	+3.8	–1.0	+10.3	%
lg:=lg*1.05	+9.5	+4.6	+1.1	+8.9	+2.5	–0.6	+7.4	%
lg:=lg*1.05, tl:=tl+1	+10.2	+5.8	+3.4	+9.1	+2.9	–0.1	+8.1	%
lg:=lg*1.05, tl:=tl+1, cf	+18.1	+11.4	+4.2	+18.9	+6.2	–1.8	+18.5	%
rg:=rg*0.9	–6.0	–3.1	–2.2	–5.0	–1.7	±0	–5.7	%
rg:=rg*1.1	+6.1	+3.0	+2.2	+4.4	+1.7	+0.3	+4.9	%
Referenz	221.9	325.5	153.5	130.4	395.5	222.9	113.4	mm

Für die Referenz berechnete mittlere Temperaturen sowie die jeweiligen Temperaturänderungen für die einzelnen Szenarien sind in Tabelle 2 zusammengestellt. Tabelle 3 enthält die Benetzungsdauern der Referenz sowie deren Änderungen bei den einzelnen Szenarien. In beiden Tabellen werden für Winterweizen der Zeitraum März bis Juni und für Zuckerrüben der Zeitraum Mai bis Oktober benutzt. Für unbewachsenen Boden und für Gras erstreckt sich der Mittelungszeitraum in Tabelle 2 über das ganze Jahr.

3.1 Erhöhung der Lufttemperatur um 1 K ("tl:=tl+1")

Eine Erhöhung der Lufttemperatur um 1 K führte zu einem Anstieg der Temperaturen des unbewachsenen Bodens um 0.6 bis 0.8 K in 5 cm Tiefe. Auch in 1 m Tiefe stieg die Temperatur um 0.6 K an, wobei 90% des Anstiegs innerhalb von 60 Tagen erreicht wurden (siehe Tab. 2).

Tab. 2: Änderungen der Temperaturmittelwerte und Referenztemperaturen (WW: März bis Juni, ZR: Mai bis Oktober)

Tab. 2: Impact on average temperatures and reference temperatures (WW: March to June, ZR: May to October)

	$tb05_{oB}$	$tb1m_{oB}$	tm_{oB}	tm_{Gras}	tbe_{WW}	tbe_{ZR}	
tl:=tl+1	+0.69	+0.57	+0.83	+0.75	+0.90	+0.91	K
tl:=tl+1, cf	+0.53	+0.44	+0.73	+0.52	+0.84	+0.86	K
lg:=lg*1.05	+0.60	+0.49	+0.46	+0.70	+0.21	+0.23	K
lg:=lg*1.05, tl:=tl+1	+1.30	+1.06	+1.31	+1.45	+1.11	+1.14	K
lg:=lg*1.05, tl:=tl+1, cf	+1.15	+0.93	+1.25	+1.25	+1.06	+1.09	K
rg:=rg*0.9	–0.30	–0.25	–0.03	–0.02	–0.11	–0.14	K
rg:=rg*1.1	+0.29	+0.25	+0.03	+0.02	+0.10	+0.13	K
Referenz	11.4	11.3	6.4	4.6	11.3	15.7	°C

Die Evapotranspirations-Summe von März bis Oktober nimmt mit maximal 1% nur geringfügig zu (siehe Tab. 1). Ursache ist die mit der Temperaturerhöhung bei unveränderter relativer Feuchte einhergehende Erhöhung der absoluten Feuchte und damit eine nur geringfügige Erhöhung des Sättigungsdefizits. Dadurch wird auch eine leichte Erhöhung der Benetzungsdauern bei beiden Feldfrüchten bewirkt (siehe Tab. 3).

3.2 Erhöhung der Lufttemperatur um 1 K bei unveränderter absoluter Feuchte ("tl:=tl+1, cf")

Hält man hingegen die absolute Feuchte bei der Temperaturerhöhung konstant, so ergibt sich eine wesentlich stärkere Erhöhung des Sättigungsdefizits. Dadurch erhöhen sich die meisten Verdunstungskomponenten deutlich. Lediglich die Transpiration der Zuckerrüben sinkt geringfügig, verursacht durch einen verstärkten Wasserstress.

Aufgrund der verstärkten Bodenevaporation ist der Temperaturanstieg im unbewachsenen Boden mit 0.5 K in 5 cm Tiefe etwas geringer als bei der unveränderten relativen Feuchte ("tl:=tl+1").

Die Benetzungsdauern verringern sich aufgrund des großen Sättigungsdefizits und gegenüber der Referenz unveränderter Feuchte bei Winterweizen und – wegen des längeren Zeitraumes – besonders bei Zuckerrüben drastisch.

Tab. 3: Änderung der Benetzungsdauern und Referenz
Tab. 3: Impact on leaf wetness duration and reference

	Wi.-Weizen März-Juni	Zu.-Rüben Mai-Oktober	
tl:=tl+1	+28	+82	Stundendifferenz
tl:=tl+1, cf	–120	–236	Stundendifferenz
lg:=lg*1.05	–93	–195	Stundendifferenz
lg:=lg*1.05, tl:=tl+1	–73	–135	Stundendifferenz
lg:=lg*1.05, tl:=tl+1, cf	–198	–389	Stundendifferenz
rg:=rg*0.9	+21	+22	Stundendifferenz
rg:=rg*1.1	–11	–10	Stundendifferenz
Referenz	856	1348	Stunden

3.3 Erhöhung der langwelligen Gegenstrahlung um 5 % ("rl:=rl*1.05")

Ähnliche Auswirkungen auf die Verdunstungskomponenten und die Benetzungsdauern hat die Erhöhung der langwelligen Gegenstrahlung um 5 %. Der Temperaturanstieg im unbewachsenen Boden ist ähnlich wie bei der Erhöhung der Lufttemperatur um 1 K. Die Auswirkung auf die Lufttemperaturen in den Beständen von Winterweizen und Zuckerrüben sind schwächer als die durch Lufttemperaturerhöhungen bewirkten Änderungen, weil die langwellige Gegenstrahlung am Tage meist nur einen kleinen Einfluss auf den Energiehaushalt hat.

3.4 Erhöhung der langwelligen Gegenstrahlung um 5 % und der Lufttemperatur um 1 K ("tl:=tl+1, rl:=rl*1.05")

Die Erhöhung der langwelligen Gegenstrahlung um 5 % bei gleichzeitiger Erhöhung der Lufttemperatur um 1 K hat von allen getesteten Szenarien den stärksten Einfluss, sowohl auf die Bodentemperaturen als auch auf die Lufttemperaturen in den Beständen (siehe Tab. 2 und Abb. 1).

Die meisten Verdunstungskomponenten reagieren nur unwesentlich auf die zusätzliche Erhöhung der Lufttemperatur; Ausnahme ist die Transpiration beim Winterweizen, die dadurch um mehr als zwei Prozentpunkte steigt (siehe Tab. 1). Offenbar wird hier die, durch das vergrößerte Sättigungsdefizit und die größere Blattfeuchte erhöhte, potentielle Transpiration nur leicht durch Wasserstress begrenzt, weil die Wasserversorgung im Frühsommer relativ gut war. Bei Zuckerrüben wirkte sich der Wasserstress hingegen während seiner späteren Vegetationsperiode stärker aus.

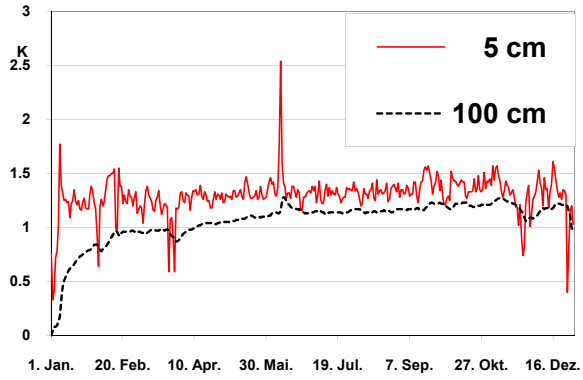

Abb. 1: Änderung der Bodentemperaturen (unbewachsen) bei um 5% erhöhter Gegenstrahlung und um 1 K erhöhter Lufttemperatur

*Fig. 1: Effect of elevated incident long wave radiation and air temperature on temperatures in bare soil ("tl:=tl+1, rl:=rl*1.05")*

3.5 Erhöhung der langwelligen Gegenstrahlung um 5 % und der Lufttemperatur um 1 K bei unveränderter absoluter Feuchte ("tl:=tl+1, cf, rl:=rl*1.05")

Wird demgegenüber die absolute Feuchte unverändert gehalten, so ergeben sich die größten Anstiege fast aller Verdunstungskomponenten. Eine Ausnahme stellt wieder die Transpiration der Zuckerrüben dar, die infolge des verstärkten Wasserstress sogar sinkt. Wie zu erwarten, sinken die Benetzungsdauern in diesem Fall am stärksten. Die Temperaturänderungen fallen gegenüber dem vorangehenden Szenarium ("tl:=tl+1, rl:=rl*1.05") geringfügig schwächer aus, weil mehr Energie für die Verdunstung aufgewandt wird.

3.6 Änderung der Globalstrahlung um ±10% ("Rg:=Rg ± 10%")

Die Erhöhung der Globalstrahlung um 10% hat nur mäßigen Einfluss auf die Verdunstungskomponenten, der zudem meistens geringer ist als durch die Erhöhung der langwelligen Gegenstrahlung um nur 5%. Auch der Einfluss auf die Benetzungsdauern ist gering. Die Bodentemperaturen reagieren im Mittel schwach (siehe Tab. 2). Ihre Tagesmaxima weisen jedoch einen deutlichen Jahresgang auf (Abb. 2). Wie zu erwarten, hat die Verringerung der Globalstrahlung um 10% in den meisten Fällen die entgegen gesetzte Wirkung zur Folge.

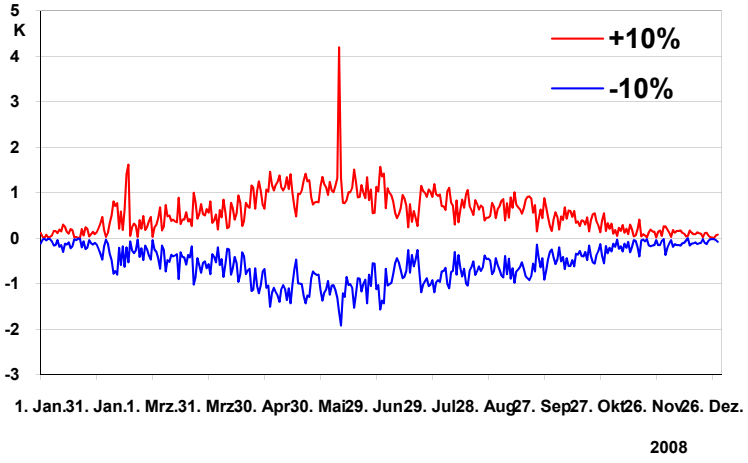

Abb. 2: Auswirkungen der Globalstrahlungsänderungen um ±10% auf die Bodentemperaturen in 5 cm Tiefe (Tagesmaxima)

Fig. 2 Impact of global radiation variations (±10%) on daily maxima of soil temperatures at 5 cm

4 Schlussfolgerungen

Die Ergebnisse der Untersuchung lassen erkennen, welche Auswirkungen unterschiedliche Klimaszenarien auf agrarmeteorologische Modellergebnisse haben können. Auch der Einfluss von Unsicherheiten der Klimamodellierung geht daraus hervor.

Es wurden jedoch weder der sich ändernde CO_2-Gehalt auf die Stomatawiderstände, noch andere pflanzliche Reaktionen, wie veränderte Reifeprozesse oder angepasste Wasserstressreaktionen, berücksichtigt, die mit Sicherheit durch züchterische Maßnahmen angestrebt werden. Zudem ist möglicherweise mit jahreszeitlich verschobenen Niederschlägen zu rechnen. Aus diesen Gründen ist insbesondere bei den Aussagen über die Verdunstungskomponenten keineswegs damit zu rechnen, dass sie einer zukünftigen Realität entsprechen. Die Aussagen über die Reaktionen als Klimawirkmodell sind davon jedoch unbenommen.

Literatur

Braden, H., 1995: The model AMBETI. – A detailed description of a soil-plant-atmosphere model, Berichte des Deutschen Wetterdienstes, Nr. 195, 117 p., Offenbach am Main.

Anschrift des Autors:
Dr. Harald Braden, Deutscher Wetterdienst, Zentrum für Agrarmeteorologische Forschung, Bundesallee 50, 38116 Braunschweig

Der Beitrag von Landschaftsstrukturen (z.B. Windschutzhecken) zur Ertragssituation im Ackerbau in Ostösterreich

Gerersdorfer Thomas[1], Josef Eitzinger[1], Enno Bahrs[2], Christiane Brandenburg[3]

[1] Institut für Meteorologie, Universität für Bodenkultur Wien, Österreich
[2] Institut für Landwirtschaftliche Betriebslehre, Universität Hohenheim, Deutschland
[3] Institut für Landschaftsentwicklung, Erholungs- und Naturschutzplanung, Universität für Bodenkultur Wien, Österreich

Zusammenfassung

Der Ackerbau im Osten Österreichs wird aufgrund der Folgen des Klimawandels und der begrenzten natürlichen Wasserversorgung der Agrarflächen zunehmend schwieriger und ohne entsprechende Anpassungsmaßnahmen möglicherweise partiell unmöglich werden. Landschaftsstrukturen, wie zum Beispiel Windschutzhecken, verändern das Mikroklima und verbessern die Wassernutzungseffizienz der angebauten Kulturen. Mithilfe eines Pflanzenwachstumsmodells (DSSAT) werden Erträge in der landwirtschaftlichen Produktion simuliert. Eine ökonomische Modellierung untersucht Grenzen und Chancen einer Landschaftsstrukturierung hinsichtlich eines betriebswirtschaftlichen Nutzens. Neben der rein ökonomischen Abschätzung werden darüber hinaus noch die zu erwartenden positiven externen Effekte der Landschaftsstrukturierung in Betracht gezogen.

1. Einleitung

In wenig strukturierten Agrarlandschaften ist die Untergliederung großer landwirtschaftlich genutzter Flächen mit Hecken ein möglicher Zugang, klimatische Extreme des freien Feldes abzuschwächen. Sie haben so auch eine bedeutende ökologische Funktion neben der bekannten Schutzfunktion gegen Wind und Erosion. Zudem leisten sie einen wichtigen Beitrag zum Bodenschutz und zur langfristigen Ertragssicherung und -verbesserung (EITZINGER und KÖSSLER, 2002). Die Optimierung lokalklimatischer und mikroklimatischer Verhältnisse durch Gestaltung der Landschaftsstrukturen ist ein wesentlicher Aspekt im ökologischen Landbau, da diese Elemente ebenso eine ökologische Nische für Nützlinge darstellen können. Das veränderte Mikro- und Lokalklima durch Landschaftselemente wirkt weiters auf den Pflanzenbestand und kann die Standortbedingungen (wie z.B. den Wasserhaushalt über die Verdunstung und die Taubildung) für den Pflanzenbau und die Ökologie entscheidend verändern, was aus vielen Untersuchungen bekannt ist, wie z.B. in Agro-Forestry Systemen (z.B. BENZARTI, 1999).

Eine Kammerung der Landschaft mit Landschaftsstrukturen, die gleichzeitig eine ökologisch sowie ökonomisch Nutzung ermöglicht, kann eine „vernetzte“ multifunktionale Landnutzung begründen. Die Implementierung von Landschaftsstrukturen kann eine Anpassungsmaßnahme an den Klimawandel darstellen und gleichzeitig zum Anbau eines Rohstoffes genutzt werden und somit unmittelbare und mittelbare wirtschaftliche Vorteile ermöglichen.

Zur Steigerung der Akzeptanz von Landschaftsstrukturierungen seitens der Landbewirtschafter kann ein nachweisbarer direkter wirtschaftlicher Nutzen durch eine Implementierung von Landschaftsstrukturen vorteilhaft sein.

2. Landwirtschaft und Klimawandel

Regionalisierte Klimaszenarien (Abb. 1 und 2) für den Osten Österreichs weisen auf eine deutliche Temperaturerhöhung bei ungefähr gleich bleibenden Niederschlagssummen hin. Für die 2020er Jahre ist eine Zunahme der durchschnittlichen Jahrestemperatur um ca. 1,9°C und für die 2040er Jahre um ca. 2,5°C im Vergleich zu den in der Klimanormalperiode 1961-1990 herrschenden Temperaturverhältnissen zu erwarten. Bei den Niederschlägen geht man von einer geänderten jahreszeitlichen Verteilung und höheren Intensitäten aus. Aufgrund der veränderten Temperaturbedingungen und der etwa gleich bleibenden Niederschlagssummen ist mit einer Zunahme der potentiellen Verdunstung von rund 18 % bis 25 % zu rechnen (EITZINGER et al., 2005).

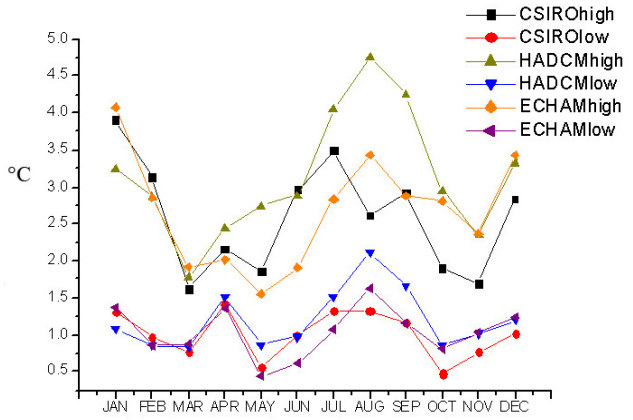

Abb. 1: Änderung der mittleren monatlichen Temperaturmaxima für die Periode 2040-2060 im Vergleich zur Referenzperiode 1971-2005 (RISCHBECK, 2007)

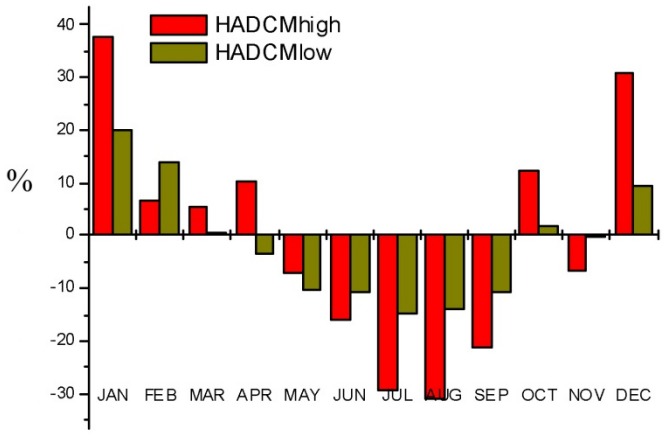

Abb. 2: Relative Veränderung der monatlichen Niederschlagsmengen für die Periode 2040-2060 im Vergleich zur Referenzperiode 1971-2005 (RISCHBECK, 2007)

Bei den skizzierten klimatischen Veränderungen muss in der Landwirtschaft mit erschwerten Wirtschaftsbedingungen und Ertragsverlusten gerechnet werden (STEININGER et al., 2003). Bereits in jüngster Vergangenheit wurden in Ostösterreich Schäden in der Landwirtschaft bedingt durch Trockenheit verzeichnet. In der Landwirtschaft ist mit einer längeren Vegetationsperiode und einer rascheren Pflanzenentwicklung zu rechnen. Der Bodenwasserspeicher wird im Winter häufiger aufgefüllt werden, die Schneeschmelze fällt aber geringer aus. Frostschäden an Winterungen können trotz höherer Wintertemperaturen zunehmen, wenn die schützende Schneedecke wegfällt. Der Entwicklungsbeginn der Winterungen kann früher einsetzen, und daher in eine feuchtere Phase fallen. Später, zur Zeit der Getreideblüte können Winterungen, aber vor allem Sommerungen, vermehrt von Trockenheit und Hitze betroffen sein. Die Ertragsvariabilität nimmt daher zu.

3. Klima- und Windschutzwirkung einer Hecke

Der Einflussbereich einer Hecke ist vom jeweils betrachteten meteorologischen Parameter abhängig und unterschiedlich groß (Abb. 3). Die Wirkung der Hecke ist grundsätzlich abhängig von ihrem Aufbau, ihrer Dichte (Durchlässigkeit), der Höhe und vor allem auch von ihrer Ausrichtung in Bezug auf die Himmelsrichtung und Hauptwindrichtung. Hecken verändern das Mikroklima des umliegenden Pflanzenbestandes, beispielsweise verringert ein verändertes Windfeld die Verdunstung und fördert Taubildung. Es ergibt sich somit - neben verringerter Winderosion - ein positiver Einfluss auf den Wasserhaushalt der Anbauflächen, weshalb gezielte Heckenpflanzungen der Optimierung mikroklimatischer Verhältnisse dienen können.

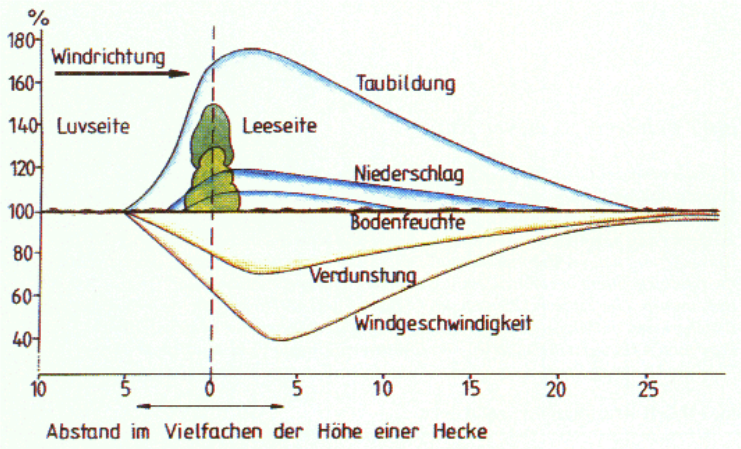

Abb. 3: Klimaschutzwirkung einer Landschaftsstruktur mit mehrjährigen verholzenden Pflanzen (FRIELINGHAUS et al.,1997, http://www.zalf.de/bfd/fr-merkb.htm)

Die in der Literatur zahlreich gefundenen Angaben zum Einflussbereich in Bezug auf Wind, Verdunstung, Niederschlag und Tau können durch eigene Messungen großteils bestätigt werden (GERERSDORFER et. al., 2009). So wird z.B. ermittelt, dass die Wind bremsende Wirkung der untersuchten Hecke mit 8 m Höhe bei vertikaler Anströmung bis ca. 100 m in das Feld hineinreicht, was dem 12-fachen der Heckenhöhe entspricht. Die direkte Messung der Referenzverdunstung zeigt eine steigende Ver-

dunstung mit zunehmender Distanz von der Hecke ebenfalls bis zum etwa 12-fachen der Heckenhöhe. Der Niederschlag wird eigenen Messungen nach nur im Nahbereich der Hecke beeinflusst. Im Luv der Hecke fällt geringfügig mehr Regen als im Lee. Ein besonders deutlicher Effekt auf den Wassereintrag kann durch Schneeablagerungen im März 2005 festgestellt werden, wo im Nahbereich der Hecke bis zu 30 % des Jahresniederschlages (ca. 160 mm) eingebracht wird. Die Schneeablagerungen reichen im Luv viel weiter in das Feld als im Lee - mit einer deutlichen Abhängigkeit von der Dichte der Hecke. Die Folge sind messbare positive Ertragseffekte in diesem Bereich.

4. Einfluss von Landschaftsstrukturen auf den Ertrag

Im unmittelbaren Nahbereich der Hecke weisen alle Erhebungen einen Minderertrag, vor allem durch die Wasserkonkurrenz der Gehölze der Windschutzanlage mit den Feldfrüchten auf. Dieser Bereich reicht bis zu einer Entfernung der 0,5- bis 1,5-fachen Höhe der jeweiligen Gehölzstruktur. Im Rahmen des interdisziplinären Monitoringprojektes „MUBIL“ (www.mubil.boku.ac.at) wurde u.a. der Ertragseinfluss einer 8 m hohen Hecke auf verschiedene biologisch bewirtschaftete Feldkulturen erhoben. Der Einflussbereich der Hecke reicht bis ca. 35 m (4-fache Heckenhöhe) bei Winterweizen und bis zu ca. 80 m (10-fache Heckenhöhe) bei Luzerne und Sonnenblumen, wobei in einem Jahr bei Winterroggen kein Einfluss der Hecke auf den Ertrag festgestellt wird (SURBÖCK et al., 2009).

Tabelle 1: Mehrerträge (in Prozent) im Einflussbereich von Windschutzanlagen. Zusammenfassung von Ergebnissen aus MUBIL und einer Literaturrecherche.

Kulturarten	Feldfrucht	Mehrertrag in Prozent
Wintergetreide	Winterweizen, Winterroggen	0 - 14
Sommergetreide	Sommergerste, Sommerhafer	5 – 17
Hackfrüchte	Zuckerrüben, Körnermais, Kartoffeln, Sonnenblumen	9 - 30
Futterleguminosen	Luzerne, Serradella	5 - 47

5. Ökonomische Modellierung

Ausgangspunkt für die im Rahmen des Projektes durchgeführte ökonomische Analyse ist die Annahme einer ortsüblichen Fruchtfolge bei konventioneller Bewirtschaftung im Osten Österreichs, deren Naturalerträge sowie Preisprognosen. Es erfolgt somit eine Trendabschätzung der ökonomischen Grenzen und Chancen einer Landschaftsstrukturierung in Hinblick auf unmittelbare ökonomische Auswirkungen sowie auch Folgewirkungen.

Für eine 5 m hohe und 6 m breite Landschaftsstruktur kann sich bei einer durchschnittlichen Windschutzwirkung der 10fachen Höhe der Struktur bereits bei einer angenommen 10%igen Ertragssteigerung (ausschließlich bezogen auf die Feldfruchternte) ein ökonomischer Vorteil für den Betrieb ergeben (Tabelle 2). Beträgt die durchschnittliche Windschutzwirkung sogar das 20fache der Höhe der Landschaftsstruktur, so kann bereits eine etwas mehr als 5%ige Steigerung des Feldfruchtertrages ausreichen, damit die Landschaftsstrukturierung für den landwirtschaftlichen Betrieb positiv in die Bilanzie-

rung eingeht. Ohne derartige Ertragssteigerungen ist der betriebswirtschaftliche Effekt der Landschaftsstrukturen negativ, da sie auf den von ihnen genutzten Flächen nicht den zuvor bestrittenen Feldfruchtanbau zulassen (Opportunitätskosten der von den Landschaftselementen genutzten Flächen).

Tabelle 2: Gegenüberstellung von Mehr- und Mindererträgen auf Ackerflächen durch Windschutzpflanzungen mittels Kurzumtriebspflanzungen und Hecken für eine exemplarische Fläche von 1 ha (100*100 m)

Schlag-länge in m	Schlag-breite in m	Schlag-größe in ha	Schutz streifen-breite in m	Netto-etrags-fläche in ha	Wind-schutz-wirkung in m Breite	Mehr-ertrags-fläche in ha	Mehrertrag auf Haupt-parzelle in € für den Durchs. der Fruchtfolge	Minderer-trag auf Schutzwall-fläche in € für den Durchs. der Fruchtfolge	Delta Mehr-ertrag zu Minder-ertrag in €
Kurzumtrieb und Hecken mit 6 m breitem und bis zu 5 m hohen Windschutzwirkung bzw. Landschafts-struktur ohne Mehrertragswirkung									
100	100	1	6	0,94				58,1	-58,1
10 % Mehrertragswirkung für alle Ackerfrüchte der Fruchtfolge auf der Hauptparzelle bei 10-facher Wir-kungsbreite									
100	100	1	6	0,94	50	0,5	48,4	58,1	-9,7
15 % Mehrertragswirkung für alle Ackerfrüchte der Fruchtfolge auf der Hauptparzelle bei 10-facher Wir-kungsbreite									
100	100	1	6	0,94	50	0,5	72,7	58,1	14,6
5 % Mehrertragswirkung f. alle Ackerfrüchte der Fruchtfolge auf der Hauptparzelle bei fast 20-facher Wirkungsbreite									
100	100	1	6	0,94	94	0,94	45,5	58,1	-12,6

6. Schlussfolgerungen

Es wird deutlich, dass nicht zwangsläufig sehr hohe Ertragsteigerungen auf der Hauptparzelle erforderlich sind, um eine einzelbetriebliche Vorzüglichkeit von Landschaftselementen als Windschutz zu induzieren, sofern die Landschaftsstrukturen selbst einer angemessenen bioenergetischen oder stofflichen Nutzung zugeführt werden können. Werden darüber hinaus auch noch die zu erwartenden positiven externen Effekte von Landschaftsstrukturen ins Kalkül gezogen, wie z. B. Erosionsvermeidung oder ein höheres Ausmaß an Biodiversität, können je nach Standort schnell gesamtwirtschaftliche Vorzüglichkeiten von Landschaftsstrukturierungen entstehen. Je nach Wertniveau der positiven externen Effekte sowie der Wirkungsbreite des Windschutzeffektes können bereits weniger als 5 % Mehrertragswirkung auf der Hauptparzelle zu einer gesamtwirtschaftlichen Vorzüglichkeit führen.

Die Gliederung einer agrarisch genutzten Landschaft mit Hecken stellt unter den hier getroffenen Annahmen eine klimatisch, ökologisch und ökonomisch sinnvolle Anpassungsmaßnahme an die sich ändernden klimatischen Verhältnisse in Ostösterreich dar, um eine Zunahme der Evapotranspiration zu reduzieren und damit die Höhe des Ertrages und die Bodenfruchtbarkeit langfristig zu erhalten. Auch heute schon ist im Hinblick auf eine Erhöhung der Ertragsstabilität und der Erhaltung der Bodenfruchtbarkeit

für die nächsten Generationen eine Strukturierung der ackerbaulich genutzten Landschaft als sinnvoll zu erachten.

Danksagung

Dieses Projekt wurde aus Mitteln des Lebensministeriums, der Bundesministerien für Gesundheit, für Wissenschaft und Forschung, der Österreichischen Hagelversicherung und der Verbund Austrian Hydro Power gefördert.

Literatur

Benzarti, J., 1999: Temperature and water-use efficiency by lucerne (Medicago sativa) sheltered by a tree windbreak in Tunisia. Agroforestry Systems, 43, 14.

Eitzinger, J., Kössler, C., 2002: Microclimatological characteristics of a miscanthus (Miscanthus cv. Giganteus) stand during stable conditions at night in the nonvegetative winter period. Theor. Appl. Climatol., 72(3-4), 12.

Eitzinger, J., Kubu, G., Formayer, H., Haas, P., Gerersdorfer, T., Kromp-Kolb, H., 2005: Auswirkungen einer Klimaänderung auf den Wasserhaushalt des Neusiedlersees. Forschungsbericht.

Gerersdorfer, T., Eitzinger, J., Laube, W., 2009: Monitoring des Witterungs- und Klimaverlaufs und mikroklimatischer Einflussgrößen in der Umstellung auf den biologischen Landbau. BOKU Wien.

Rischbeck, P., 2007: Der Einfluss von Klimaänderung, Bodenbearbeitung und Saattermin auf den Wasserhaushalt und das Ertragspotential von Getreide im Marchfeld. University of Natural Resources and Applied Life Sciences, Vienna, Vienna.

Steininger, K., Steinreiber, C., Binder, C., Schaffer, E., Tusini, E., Wiesinger, E., 2003: Adaptionsstrategien der von extremen Wetterereignissen betroffenen Wirtschaftssektoren: Ökonomische Bewertung und die Rolle der Politik.

Surböck, A., Heinzinger, M., Friedel, J. K., Freyer, B., 2009: Monitoring der Auswirkungen einer Umstellung auf den biologischen Landbau (MUBIL II), Teilprojekt 1: Pflanzenbau und Bodenfruchtbarkeit.

Adressen der Autoren

Dipl.-Ing. Thomas Gerersdorfer (thomas.gerersdorfer@boku.ac.at)
Institut für Meteorologie, Universität für Bodenkultur Wien, Peter-Jordan-Straße 82, 1190 Wien, Österreich

Ao.Univ.Prof. Dr. Josef Eitzinger (josef.eitzinger@boku.ac.at)
Institut für Meteorologie, Universität für Bodenkultur Wien, Peter-Jordan-Straße 82, 1190 Wien, Österreich

Prof. Dr. Enno Bahrs (bahrs@uni-hohenheim.de)
Institut für Landwirtschaftliche Betriebslehre, Universität Hohenheim, Schloß-Osthof-Südflügel, 70593 Stuttgart, Deutschland

Ao.Univ.Prof. Dr. Christiane Brandenburg (christiane.brandenburg@boku.ac.at)
Institut für Landschaftsentwicklung, Erholungs- und Naturschutzplanung, Universität für Bodenkultur Wien, Peter-Jordan-Straße 65, 1190 Wien, Österreich

Crop weather interaction studies in a natural sweetener plant (*Stevia rebaudiana* (Bert.) Bertoni) in Indian Western Himalaya

Rakesh Kumar[1], K. Ramesh[1]*, Sandeep Tehria[1], Bikram Singh[1] and Rajendra Prasad[2]

[1]Institute of Himalayan Bioresource Technology (CSIR) Palampur (HP), India
[2]CSK Himachal Pradesh Agricultural University, Palampur (HP), India
*Present address: Senior Scientist, Indian Institute of Soil Science (ICAR), Bhopal (MP), India.

Abstract

Agriculture and climate are closely linked in terms of crop growth, development and production, which are affected by both long-term meteorological factors (the climate) and short-term meteorological events (the weather). The major limiting factors for higher crop productivity are sunlight and temperature. Crop-weather interaction studies in medicinal plants are very meager and need particular attention to ensure higher molecule recovery depending on the stage of crop growth. The leaf of *Stevia rebaudiana* (Bert.) Bertoni contains specific glycosides, which produce a sweet taste, but have no calorific value. Stevia has thus become the hottest new cash crop opportunity for those in the agribusiness sector. In view of the growing importance of this crop world wide, crop-weather interaction studies were carried out from 2007 to 2008 at the experimental farm of Institute of Himalayan Bioresource Technology, Palampur (HP), India. The established agroclimatic indices for temperature studied elsewhere in the domain *viz*., temperature difference (TD), relative temperature disparity (RTD), growing degree days (GDD), heliothermal units (HTU) and photothermal units (PTU) were computed for stevia. The variation in development of different phenophases and harvesting of stevia after transplanting was manifested by varied accumulation of heat units. Day length showed highest correlation with accumulation of biomass and marker compounds. Obviously, late transplanted crop had shown shorter phenological stages and accumulated lower heat units than the early transplanted crop. Ambient temperature affects the crop growth and yield through photosynthesis, respiration, growth, dry matter production and its distribution with change in cumulative temperature difference, reproductive phenology duration changed accordingly. The dry leaf yield, stevioside and rebaudioside A contents correlated well with cumulative TD, RTD, GDD, HTU, PTU and bright sunshine hours. This implies that temperature has a major role in the biosynthesis and accumulation of these compounds in the plants.

1. Introduction

The genus stevia {*Stevia rebaudiana* (Bert.) Bertoni} (Asteraceae) consisting approximately 200 species of herbaceous, shrub and sub-shrub plants (Gentry, 1996), is one of the most distinctive genera within the tribe Eupatorieae Its leaves contain non- carcinogenic and non-calorific sweeteners (steviol glycosides), whose consumption could exert beneficial effect on human health. The sweeteners, steviosides extracted from the plants are 300 times sweeter than sugar and are used as natural alternative to artificial sweeteners (Soejarto et al., 1983; Midmore and Rank, 2002). The world wide demand of high potency natural sweeteners is expected to increase in years to come due to increase in number of diabetic people. Leaf is the principal sweet bearing part of the plant. Leaf extract of this plant has been used traditionally in the treatment of diabetes. Stevia has become the hottest new cash crop opportunity for those in the agribusiness sector, and rebaudioside A has become a valuable commodity in the ingredients, food and beverages industries.

Temperature plays a vital role in almost all biological processes of crop plants. It is one of the most important climatic factors affecting the growth, development and yield of the crops. Air temperature based agromet indices *viz*., GDD, PTU, and HTU can be successfully used for describing phenological behaviour and growth parameters (Singh et al. 2007; Kumar et al., 2008). Heat unit concept is based on idea that plants have a definite thermal requirement, therefore, they complete certain phenological stages as and when the thermal requirement is met. This provides an opportunity to build up quantitative relationships between heat unit system, biomass production, stevioside content and crop growth rates of stevia. Some work on crop management practices including the time of transplanting has also been carried out. However, variation in stevioside content with change in weather conditions and its interaction with temperature needs to be investigated for rationalizing time of harvest to achieve highest biomass or stevioside content. Keeping in view the above facts, the present study was undertaken to assess crop-weather interaction studies in stevia crop.

2. Materials and Methods

The study was conducted during 2007 and 2008 at the experimental farm of Institute of Himalayan Bioresource Technology (CSIR), Palampur (1325 m amsl, 32º06´05”N, 76º34´10”E), India. The soil of experimental area is acidic in reaction, low in available nitrogen (181 kg ha^{-1}), and medium in available phosphorus (12 kg ha^{-1}), potassium (202 kg ha^{-1}) and organic matter (0.5%). Palampur represents the sub temperate mid-hill region of western Himalaya and endowed with mild summers (18.0-31.3 °C) and severe winters (3.3-13.2 °C). The average rainfall is about 2500 mm of which about 77 % is received during June to September. Data on weather parameters *viz*., maximum and minimum temperatures, relative humidity, evaporation, bright sunshine hours, and rain fall for the crop season recorded at meteorological observatory of the C. S. K. Himachal Pradesh Agricultural University, Palampur are depicted in Fig. 1. Perusal of meteorological data reveals that the weekly maximum and minimum temperature ranged from 25.5-31.0 °C and 15.1-20.7 °C, respectively. BSS and day length ranged from 2.9 to 11.0 hrs and 11.9 to 13.9 hrs respectively.

The experiment was laid as per Split Plot design with five dates of transplanting in the main plots and two genotypes (Accession- I and Accession -II) in sub-plots. During 2007, stevia crop was transplanted from April 15 until August 15, at 1 month interval, whereas, during 2008 the crop was transplanted from May 29 till August 1, 2008, at 15 days interval. For calculation of GDD, base temperature for stevia crop was taken as 12^{o} C. Three replications were maintained. Sweet glycoside from dried leaves of stevia was extracted using acetonitrile and water 80:20 and the content of stevioside was calculated through HPLC using standards of stevioside.

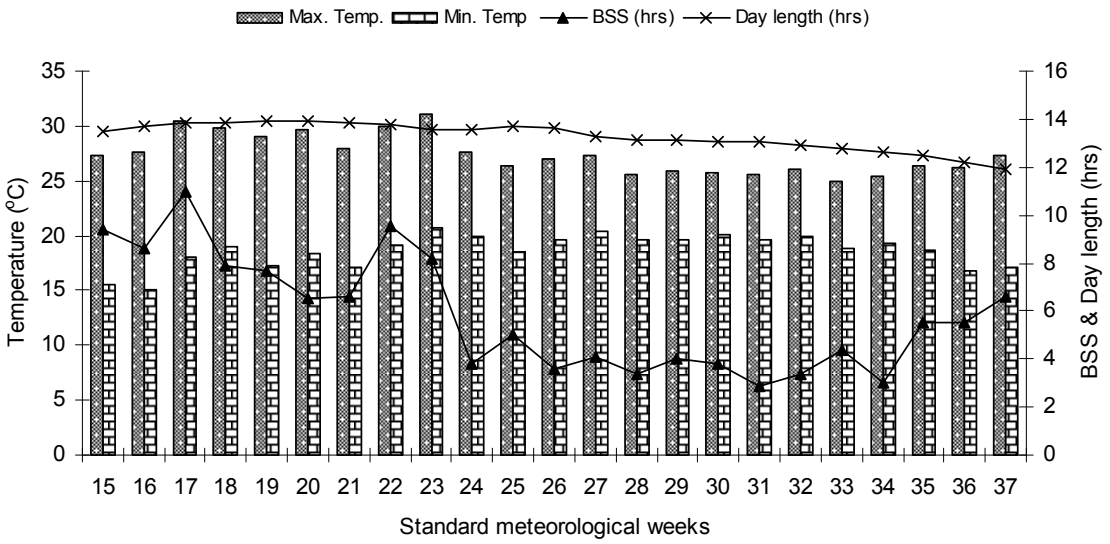

Fig. 1: Mean weekly weather data of Palampur during the crop season

3. Results and discussion

The heat unit requirement provides a scientific basis for determining the effect of temperature or photoperiod or phenological behaviour of the crop. Temperature indices *viz.,* RTD, GDD, HTU, PTU, and heat use efficiency (HUE) were computed for stevia under different growing environments from transplanting to harvesting and presented in Table 1.

Table 1: Agroclimatic indices from transplanting to harvesting of stevia

Treatment	TD	RTD (%)	GDD (ºC days)	HTU (ºC day hr)	PTU (ºC day hr)	Day length (hr)	BSS (hr)
Dates of Transplanting							
				2007			
D1	1270.5	5322.4	1748.6	11025.6	23361.0	1968.1	909.5
D2	968.3	4058.5	1422.4	8171.1	18808.7	1583.5	670.7
D3	640.0	2765.4	997.7	4631.2	12961.3	1169.2	417.1
D4	433.8	1886.6	671.2	3098.7	8545.8	782.6	289.8
D5	225.4	994.4	328.5	1478.3	4205.5	390.5	137.3
				2008			
D1	725.2	3241.6	1070.0	4328.4	14077.2	1365.0	404.5
D2	625.5	2850.3	928.4	3411.7	12071.7	1207.1	337.1
D3	476.2	2176.1	724.3	2632.4	9333.7	939.4	260.1
D4	363.0	1673.9	544.0	1980.8	6958.8	715.7	198.4
D5	277.0	1290.5	377.1	1507.9	4772.7	506.1	153.2

Date of transplanting played a major role in the accumulation of GDD and PTU from transplanting to harvesting of crop. The early sown crop accumulated higher values of RTD and GDD for the crop to mature, irrespective of the year of experimentation. The

shifting of transplanting dates corresponded to fluctuations in temperature causing either lengthening or shortening of the growth periods. With the subsequent transplanting, the values of RTD and GDD for crop maturity were found to diminish. The association between the leaf dry yield and HUE during different growing environments was significant ($R^2 = 0.8813$, Fig. 2).

Every crop needs a specific amount of growing degree days to enter its reproductive phase from vegetative phase. Early transplanting resulted in absorbing sufficient growing degree days due to prevalence of higher temperature and longer sunshine hours during post transplanting period. Therefore, early transplanted crop recorded higher growing degree days as compared to late. Similar results were also reported by Kanth et al. (2000) and Roy et al. (2005) for Brassica. Late transplanting compelled the plants to complete their life cycle with a short period of time resulting in decreased HTU. These results are in conformity to those of Masoni et al. (1990).

Attempt was made to correlate dry leaf yield, stevioside and rebaudioside content of stevia with different agroclimatic indices (Table 2). Correlation analysis between dry leaf yield and daily mean weather variable at harvesting stage revealed a significant positive correlation. Significant correlations were found between dry leaf yield and RTD, GDD, HTU, PTU, day length, and BSS during both years. This indicated that temperature, day length, sunshine hours play an important role and influence leaf yield and marker compound accumulation in stevia. More sunshine hours during reproductive phase might have helped in translocation of photosynthates to sink. Based on the above correlation coefficient, it is clear that the selected weather variables have correlations with dry leaf yield, marker compound accumulation.

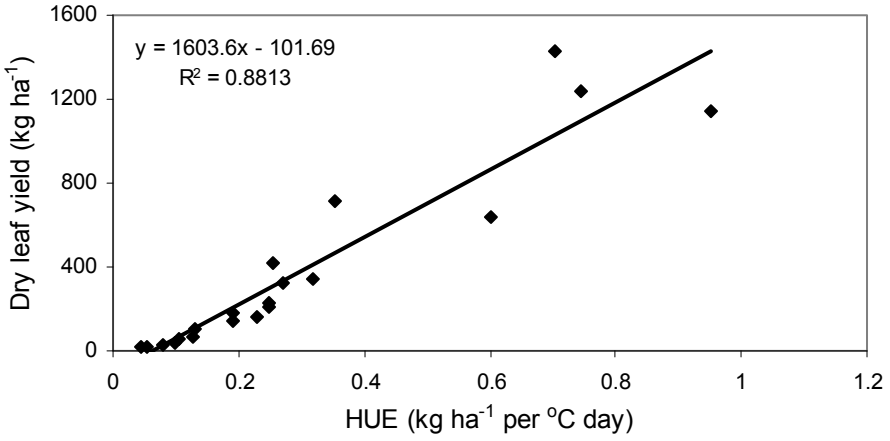

Fig. 2: Relationship between HUE (kg ha^{-1} per ^oC day) and dry leaf yield (kg ha^{-1}) of stevia

4. Conclusions

The weather variables *viz.*, temperature, bright sunshine hours, and day length at different growth phases had a definite bearing on growth and quality of stevia crop. Temperature influenced accumulation of biomass at vegetative stage of the crop. It may be inferred that growing degree days, photothermal index, and heat use efficiency indices may be used to understand the crop performance in assessing suitability of the variety to a particular locality depending on the thermal environment.

Table 2: Correlation coefficients between agro-meteorological indices and biometric observations of stevia

Parameters	RTD (%)	GDD (ºC days)	HTU (ºC day hr)	PTU (ºC day hr)	Day length (hr)	BSS (hr)
			2007			
Dry leaf yield (q/ha)	0.765	0.773	0.747	0.772	0.753	0.777
St (%)	0.958	0.970	0.948	0.969	0.951	0.968
Rb (%)	0.810	0.795	0.817	0.796	0.819	0.792
Total (St+Rb) (%)	0.945	0.947	0.940	0.947	0.942	0.945
			2008			
Dry leaf yield (q/ha)	0.834	0.830	0.875	0.835	0.858	0.822
St (%)	0.642	0.629	0.712	0.638	0.998	0.998
Rb (%)	0.624	0.624	0.708	0.633	0.670	0.610
Total (St+Rb) (%)	0.655	0.647	0.733	0.656	0.698	0.635

t value at 8 (10-2) df is 0.632 at 5% and 0.765 at 1%

Acknowledgement

The authors thank the Director, IHBT, Palampur (HP), India for providing necessary facilities for the studies. The authors are also thankful to Dr. R.D. Singh, Scientist, IHBT, Palampur for his constructive suggestions in the preparation of manuscript. The funding of Department of Science and Technology, Govt. of India is gratefully acknowledged.

References

Gentry, A.H., 1996: A field guide of the families and genera of woody plants of northwest south America (Colombia, Ecuador, Peru) with supplementary notes on herbaceous taxa. The University of Chicago Press, Chicago.

Kanth, R.H., Shah, M.H., Bali, A.S., 2000: Effect of different sowing dates on heat unit requirement for different phenophases of brown sarson (*Brassica campestris*) varieties and dynamics of aphid (*Lipaphis erysimi*) population. Ind. J. Agron. 45, 170-173.

Kumar, A., Pandey, V., Kumar, M., Shekh, A.M., 2008: Correlation study in soybean (*Glycine max*. [L] Mirrll) with response to prevailing weather parameter, agro-meteorological indices to seed and stover yield at Anand. American Eurasian J. Agron. 1, 31-33.

Masoni, A., Ercoli, L., Massantini, F. 1990: Relationship between number of days, growing degree days and photothermal units and growth in wheat (*Triticum aestivum* L.) according to seeding time. Agricoltura-Mediterrancea. 120, 41-51.

Midmore, D.J., Rank, A.H., 2002: A new rural industry stevia to replace imported chemical sweeteners. RIRDC Pub NO. W02/22, p.55.

Roy, S., Meena, R.L., Sharma, K.C., Kumar, V., Chattopadhyay, C., Khan, S.A., Chakarvarthy, N.V.K., 2005: Thermal requirement of oilseed Brassica cultivars at different phenological stages under varying environmental conditions. Indian J. Agric. Sci. 75, 717-721.

Singh. I.A., Rao, U.V.M., Singh, D., Singh, R., 2007: Study on agrometerological indices for soybean crop under different growing environments. J. Agrometerol. 9, 81-85.Soejarto, D.D., Compadre, C.M., Medon, P.J., Kamath, S.K., Kinghorn, A.D., 1983: Potential sweetening agents of plant origin. II. Field search for sweet-tasting *Stevia* species. Econ. Bot. 37: 71-79.

Authors' address:

Dr. Rakesh Kumar (rakeshkumar@ihbt.res.in), Natural Plant Products Division, Institute of Himalayan Bioresource Technology (CSIR), Post box no. 6, Palampur 176 061 (HP) India

Dr. K. Ramesh (ramechek@yahoo.co.in; kramesh@iiss.ernet.in), Senior Scientist, Indian Institute of Soil Science (ICAR), Nabi bagh, Berasia Road, Bhopal 462038, India.

Mr. Sandeep Tehria (sandeeptehria@gmail.com), Natural Plant Products Division,
Institute of Himalayan Bioresource Technology (CSIR), Post box no. 6, Palampur 176 061 (HP) India

Dr. Bikram Singh (bikramsingh@ihbt.res.in), Natural Plant Products Division,
Institute of Himalayan Bioresource Technology (CSIR), Post box no. 6, Palampur 176 061 (HP) India

Dr. Rajendra Prasad (rprasad57@gmail.com), Department of Agronomy, CSK Himachal Pradesh Agricultural University, Palampur 176 062 (HP) India.

Growing degree days at the Russian Far East

[1]E.A. Grigorieva, [2] A. Matzarakis

[1]Institute for Complex Analysis of Regional Problems, Far Eastern Branch, Russian Academy of Sciences, Birobidzhan, Russia
[2] Meteorological Institute, Albert-Ludwigs-University of Freiburg, Germany

Abstract

Concept of degree-days called growing degree-days (GDD) as a measure of the intensity of the growing season was used for assessment of thermal resources for the locations in the southern part of the Russian Far East. Daily maximum and minimum temperatures were used for calculating GDD at 17 locations of the Far East. Base temperatures of 0, 5, 10 and 15 ^{o}C as commonly used lower threshold temperatures, and upper threshold of 30 ^{o}C were utilized for assumption of growing degree days. GDD increases from north to south, from mountainous locations to the plain, and moving off the coast. Thermal conditions in the southern part of the study area cover the demands of all the plants cultivated here; low thermal resources are observed in the north, in the elevated areas and in the coastal regions. Temporal variability of GDDs shows mainly positive temporal changes over the 1966-2005 period; positive trend is observed for GDD0, indicating that study area has experienced a stretching of the warm period. GDD15 indicating thermal resources of summer season vary little or reveal zero trend.

1. Introduction

Air temperature is one of the main environmental factors for distribution, growing, biological development and yield production of the plant species (Cross & Zuber 1972, Russelle et al. 1984; Gordon & Bootsma 1993) and may be the main limiting factor for plant growth especially at temperate zones and high latitudes (Førland et al. 2004). Cumulative effect of daily temperatures over the long period reacts on the plants and their development (Wang 1960, Schwartz et al. 2006), may be estimated by index which illustrate heat accumulation necessary for development processes and named as growing degree days (GDDs).

Important changes have occurred in global climate during the 20th century. Marked increase in surface air temperature since 1970 (IPCC 2007) correlates with other climate and environmental characteristics first of all with increasing climatic variability and has a clearly visible ecological response: in natural and managed ecosystems from the species to the community level, in agriculture first of all in crop production, and in people living as well (Bootsma 1994, Karing et al. 1999, Schwartz et al. 2006). Changed climatic conditions and consequently agroclimatic resources forces mankind to find decision for possibilities of agriculture adaptation to all possible environmental changes (Karing et al. 1999).

The objective of the present study is to evaluate GDDs as one of the main climatic growing index for the locations at the southern part of the Russian Far East with the extreme annual temperature amplitude using daily maximum and minimum temperatures. The growing degree-days are analyzed and their linear trends are estimated for period from 1966 to 2005.

2. Methods and study area

Concept of degree-days named growing degree-days (GDD) as a measure of the intensity of the growing season is one of the widely used to determine development of living things and plant species first of all. GDD is based on the idea that the development of a plant or other organisms first of all poikilotherms will occur only when the temperature exceeds a specific base temperature for a certain number of days. It ignores additional environmental factors and different respond of plants to the same temperature during various stages of their life cycle but it has been widely used due to practical utility in agriculture, phenological and other studies (Wang 1960). Now GDD is used as a method to predict the growth stages of major crops like soya bean, maize, wheat (particularly temperate crops); it is also useful in taking precautionary measures against insect pest and diseases attack on crops (Gilmore & Rogers 1958, Wang 1960, Russelle et al. 1984, Gordon & Bootsma 1993, Bootsma 1994, Yang et al. 1995, McMaster & Wilhelm 1997, Roltsch et al. 1999, Cesaraccio et al. 2001, Førland et al. 2004, Matzarakis et al. 2007, Fealy & Fealy 2008). It may be calculated on the basis of long-term average daily mean temperature or it may be computed on data of a given year and in this case it will take into account weather variability.

There are several methods of GDD calculation including model estimation with their advantages and shortcomings (Roltsch et al. 1999). Method with using hourly temperature data (Cesaraccio et al. 2001) is the most accurate but needs data only from an automatic weather network. Assumption of GDD with mean temperature calculated as average from minimum and maximum daily temperatures is the most common in agricultural and phenological researches (Gilmore & Rogers 1958, Bootsma 1994, McMaster & Wilhelm 1997, Matzarakis et al. 2007, Fealy & Fealy 2008):

$$GDD = \sum_{i=1}^{m} (T_i - T_{base}),$$

where GDD – growing degree days, ^{o} C; $T_i = (T_{max} + T_{min})/2$ – mean temperature, ^{o} C; T_{base} – base or threshold temperature, ^{o} C; $i = 1, 2, \ldots m$ – days with temperature higher threshold temperature T_{base} in warm period; T_{max} – the daily maximum air temperature, ^{o}C; T_{min} – the daily minimum air temperature, ^{o}C (Gordon & Bootsma 1993, Bootsma 1994, McMaster & Wilhelm 1997). Thus all temperatures under the diurnal temperature curve and over threshold value are summed during period with this base temperature.

Typically in general assessments of climate and temperature impact on plant vegetation 0, 5, 10 and 15 ^{o}C are taken as base or threshold temperatures (Gordon & Bootsma 1993, Karing et al. 1999, Gordeev et al. 2006, Fealy & Fealy 2008, Grigorieva 2008) due to the close relationship of these temperatures with the onset and end of the main crops development. In the work by Gordeev et al. (2006), as in many other papers by Russian or by former USSR's researchers, thresholds 0, 5, 10 and 15 ^{o}C have stable meanings as, respectively: warm period; heat supply of the vegetation period for the main cold-resistant wild and cultivated plants; heat supply for the period of active plant growth; heat supply for the heat-loving plants (Gordeev et al. 2006).

High temperatures may decline or even stop development rate and main physiological functions of plants up to temperature or thermal stress and survival of plants or plant organs and poikilotherms (Wang 1960, Bootsma 1994, Roltsch et al. 1999). Cross and Zuber (1972) suggested to use optimum of 30 ^{o}C; excess temperature above 30 ^{o}C must

be subtracted to account for high temperature stress. In modern analysis this value is used as upper temperature threshold T_{UT} (Russelle et al. 1984, McMaster & Wilhelm 1997, Matzarakis et al. 2007). In the present paper the heat accumulation necessary for development process is described using GDD for four different lower thresholds 0, 5, 10 and 15 °C and with account of temperature upper limit 30°C.

The study area is the south of the Far Eastern Russia region, which has middle latitude monsoon climate characterized by an extreme continental annual temperature regime. Annual temperature here varies between -5.4 °C at Ekimchan to 5.7 °C at Pogranichnyi. The annual temperature range is from 28.2 °C at the coastal part of the study area to 52.7 °C at the continent.

The data used for 17 hydrometeorological stations (HMS) are daily maximum and minimum air temperature. The observational base is quite limited by very rare network of weather stations with data available that results in a paucity of observations in general. Data used consistes of year-long records from each site during 1966-2005.

3. Results

Using degree days as the heat unit, the thermal resources are calculated for each location with threshold temperatures described previously providing a useful indicator for assessing crop development at the Russian Far East (Fig. 1).

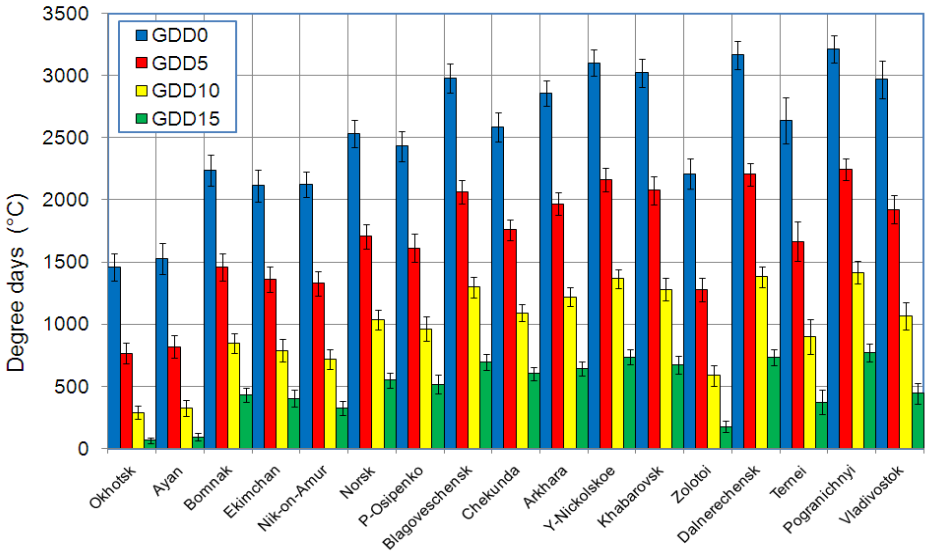

Fig. 1: GDDs at the Russian Far East for period 1966-2005

Analyzing the calculated data, we establish that the highest mean value GDD0, used to characterize warm period (Gordeev et al. 2006), is recorded at the continental southern part of the study area in Pogranichnyi (3212 °C), that is twice higher than the corresponding value of 1459 °C observed in Okhotsk – coastal location at the north with minimum thermal supply. High values are calculated mainly for the continental stations at the south Dalnerechensk, Yekaterino-Nickolskoe, Blagoveschensk and Khabarovsk.

Coastal areas have considerably lower thermal provision varying from 1530°C in Ayan, northern coast of the Okhotsk Sea, to 2208 °C in Zolotoi, and to 2968 °C in Vladivostok, southern coast of the Japan Sea. Lower thermal reserve is observed in mountains at Bomnak and Ekimchan (2236 and 2114 °C respectively).

Spatial distribution of the GDD5, used to describe heat supply of the vegetation period, is the same as for the previously described index. GDD5 varies from 767 ° C in Okhotsk at the northern coastal part of the study area to 2246 °C in Pogranichnyi at the southern continental part, data scattering is three times. GDD5 is lower in the mountains and on the sea shores of the study area; continental regions have higher values than those coastal.

The highest value of the GDD10 in Pogranichnyi (1416 °C) is five times as much the result for Okhotsk (290 °C). Large difference in GDD10 is between continental and coastal parts at the same latitude, this value is more expressed for the southern locations – up to 2.3 between Yekaterino-Nickolskoe and Zolotoi. Far to the north continental stations are situated in the mountains, and the contrast between continent and coast is not so large.

Thermal supply for the heat-loving plants (Gordeev et al. 2006) is described by GDD15. Eleven-time difference in GDD15 values between north and south – from 67 ° C in Okhotsk to 771 °C in Pogranichnyi – shows the intense and the largest contrast in the climatic characteristics between two extreme geographical points at summer period. Spatial distribution of previous GDDs and GDD15 is very similar but with a significant reduction in the absolute values.

Assessment of temporal changes of GDDs was done for the period 1966-2005. The significance of the trends was tested using Fisher F-test. Calculated F values are more than empirical F-value 4.08 for all GDDs' at the northern coastal stations (Okhotsk and Ayan), two continental HMS (Poliny-Osipenko and Blagoveschensk) and for all southern – coastal (Zolotoi, Ternei and Vladivostok) and continental ones (Dalnerechensk and Pogranichnyi). The results are large showing statistically significant positive trend at these locations. At the same time null-hypothesis was confirmed for all GDDs' at the coastal location Nickolaevsk-on-Amur and continental HMS (Bomnak, Ekimchan, Norsk, Chekunda, Arkhara, Yekaterino-Nickolskoe and Khabarovsk).

4. Discussion

The mean value of growing degree days varies considerably following the main geographical pattern of temperature distribution: the magnitude of the GDDs increases from north to south, moving off the coast, and from mountainous locations to the plain. The largest contrast is revealed for extremely different latitudinal locations Pogranichnyi (44°24') and Okhotsk (59°11' N). This spatial difference in thermal supply increases from the warm period to summer, – from two to eleven times. Significant spatial gradient is established for areas located at the same latitude that is explained by the influence of large water reservoirs (seas of the Pacific Ocean). Contrast for all degree days (0, 5, 10 and 15 °C) between Yekaterino-Nickolskoe at the continent (47°44' N, 130°58' E) and Zolotoi at the sea shore (47°19' N, 138°59' E) – is 1.4, 1.7, 2.3 and 4.2 times respectively. This difference is revealed in less degree further to the north, where mountainous influence is expressed at the continent. Thus, for example, GDDs gradient from

Bomnak (54°43' N, 128°56' E, 357 m asl) to Nickolaevsk-on-Amur (53°09' N, 140°41' E, 46 m asl) is 1.05, 1.1, 1.2 and 1.3 times. Ekimchan (53°04' N, 132°56' E, 540 m asl) shows even lower value for thermal resources of the warm period in comparison with the coastal stations due to its higher elevation.

Interannual variability of GDDs shows positive statistically significant temporal changes over the 1966-2005 period, confirming global warming trend. The most significant positive trend is observed for GDD0, indicating that study area has experienced a stretching of the warm period. But for some locations zero trend is marked as evidence that global climate change has regional features, expressed in some specific characters at the study area. It is known that global warming is emphasized mostly for winter time, and even cooling may be observed at some locations especially in summer (e.g. Grigorieva & Tunegolovets 2005) that is corroborated by our research. The largest increase in temperature has taken place in the southern part of the Sea of Japan near Ternei showing local spot with strong positive trend.

5. Conclusions

The study area at the south of the Far Eastern Russia region is characterized by an extreme continental annual temperature regime that is revealed in low winter temperatures and nevertheless high thermal supply of warm period. This study sets out to apply a conception of the growing degree days to this region to get valuable information for agricultural management. It is marked that the mean value of growing degree days varies considerably from one location to other following the main geographical characteristics of temperature distribution: the magnitude of the GDDs increases from north to south, moving off the coast, and from mountainous locations to the plain. Temporal variability of GDDs shows positive temporal changes over the period from 1966 to 2005, confirming the global warming trend. The most significant positive trend is observed for the sum of temperatures during warm season GDD0, indicating that study area has experienced a stretching of the warm period. GDD15 indicating thermal resources of summer season vary little or reveal zero trend.

Acknowledgment

The work was supported by Russian Fund for Basic Research: projects No 08-01-98505-r_vostok_a, 09-04-00146-a; FEB RAS: projects No. 09-I-П16-08, 09-III-A-09-498.

References

Bootsma, A., 1994: Long term (100 yr) climatic trends for agriculture at selected locations in Canada. Clim. Chang. 26, 65-88.

Cesaraccio, C., D. Spano, P. Duce, R.L. Snyder, 2001: An improved model for determining degree-day values from daily temperature data. Int. J. Biometeorol. 45, 161-169.

Cross, H.Z., M.S. Zuber, 1972: Prediction of flowering dates in maize based on different methods of estimating thermal units. Agron. J. 64, 351-355.

Fealy, R., R.M. Fealy, 2008: The spatial variation in degree days derived from locational attributes for the 1961 to 1990 period. Irish. J. Agric. Food. Res. 47, 1-11.

Førland, E.J., T.E. Skaugen, R.E. Benestad, I. Hanssen-Bauer, O.E. Tveito, 2004: Variations in thermal growing, heating, and freezing indices in the Nordic Arctic, 1900-2050. Arct. Antarct. Alp. Res. 36, 347-356.

Gilmore, E.C.Jr., J.S. Rogers, 1958: Heat units as a method of measuring maturity in corn. Agron. J. 50, 611-615.

Gordeev, A.V., A.D. Kleschenko, B.A. Chernyakov, O.D. Sirotenko, 2006: Bioclimatical potential of Russia: theory and practice (in Russian). Moscow, 512.

Gordon, R., A. Bootsma, 1993: Analyses of growing degree-days for agriculture in Atlantic Canada. Clim. Res. 3, 169-176.

Grigorieva, E., 2008: Spatial-Temporal Dynamics of Climate Thermal Resources for the Southern Part of the Russian Far East. 18th International Congress of Biometeorology, 22-26 September 2008. Tokyo: International Society of Biometeorology, 121.

Grigorieva, E., V. Tunegolovets, 2005: Change of climate on the south of the Russian Far East in the second half of the 20th century. Ann. Meteorol. 41, 209-212.

IPCC, 2007: Climate Change 2007: Impacts, Adaptation and Vulnerability. Contribution of Working Group II to the Fourth Assessment Report of the Intergovernmental Panel on Climate Change, M.L. Parry, O.F. Canziani, J.P. Palutikof, P.J. van der Linden and C.E. Hanson, Eds., Cambridge University Press, Cambridge, UK, 976.

Karing, P., A. Kallis, H. Tooming, 1999: Adaptation principles of agriculture to climate change. Clim. Res. 12, 175-183.

Matzarakis, A., D. Ivanova, C. Balafoutis, T. Makrogiannis, 2007: Climatology of growing degree days in Greece. Clim. Res. 34, 233-240.

McMaster, G.S., W.W. Wilhelm, 1997: Growing degree-days: one equation, two interpretations. Agric. For. Meteorol. 87, 291-300.

Roltsch WJ, Zalom FG, Strawn AJ, Strand JF, Pitcairn MJ (1999) Evaluation of several degree-day estimation methods in California climates. Int I Biometeorol 42:169-176.

Russelle, M.P., W.W. Wilhelm, R.A. Olson, J.F. Power, 1984: Growth analysis based on degree days. Crop. Sci. 24, 28-32.

Schwartz, M.D., R. Ahas, A. Aasa, 2006: Onset of spring starting earlier across the Northern Hemisphere. Glob. Change. Biol. 12, 343-351.

Wang, J.Y., 1960: A critique of the heat-unit approach to plant response studies. Ecology. 41, 785-790.

Yang, S., J. Logan, D.L. Coffey, 1995: Mathematical formulae for calculating the base temperature for growing degree days. Agric. For. Meteorol. 74, 61-74.

Authors' address:

Dr. Elena A. Grigorieva (eagrigor@yandex.ru)
Institute for Complex Analysis of Regional Problems
Far Eastern Branch, Russian Academy of Sciences
Sholom-Aleikhem, 4, Birobidzhan, Russia

Prof. Dr. Andreas Matzarakis (andeas.matzarakis@meteo.uni-freiburg.de)
Meteorological Institute, Albert-Ludwigs-University of Freiburg
Werthmannstr. 10, D-79085 Freiburg, Germany

Climate Change and Possible Late Frost Damages to Apple Trees in Germany

Frank-M. Chmielewski, Klaus Blümel and Yvonne Henniges

Humboldt-University of Berlin
Faculty of Agriculture and Horticulture, Professorship of Agricultural Climatology, Germany

Abstract

This paper will focus on possible impacts of climate change on late frost damages in 11 fruit growing regions in Germany in the next decades up to 2100 (WETTREG, Scenario A1B). For this reason phenological models were developed, which allow estimating the shift in the beginning of apple blossom due to climate change. On the basis of these results the frequency of late frost events up to 10 days after the beginning of apple blossom were evaluated. It was assumed that minimum temperatures between -2.0 and -4.0 °C could harm the opened flower buds between 10 and 90 %. In order to estimate the final damage to the apple yield further assumptions were made. The investigation showed, that in all fruit growing regions the beginning of apple tree blossom will be significantly advanced by about 15 days up to 2100. The mean probability for late frost (T_n<0 °C) after the beginning of blossom will significantly increase by 8 % (range: 6-14%). Lower damages of 10-50 % on the flowers are more likely than higher damages (50-100 %). The total frost-damage on the flowers increases in all growing-regions up to 2100, but only in a few regions this increase is statistically significant and leads to clear yield reductions.

1. Introduction

Climate change will probably increase the growth of trees due to increased atmospheric CO_2-content, rising temperatures and the extension of growing season, but it can also causes disturbances in the annual growth cycle of trees. Frost damages on trees and buds are usually not observed in winter, when dormancy and cold hardiness of trees is well developed, but in autumn if this stage is not reached yet or in spring if it is already broken. For this reason some authors used the time between the last frost in spring and the first frost in autumn to define the length of growing season.

An earlier blossom of fruit trees could also increase the danger of damages by late spring frosts. Injured flowers may appear to be normal, but if the pistils are killed no fruit will be produced. Frost risk depends on the fruit species/variety, as well as on the strength and the duration of frost. From dormancy of floral buds to fruit set the vulnerability to damage by a late frost increases progressively. For example, the closed floral bud of apples (pink stage) can stand minimum temperatures up to -4 °C for a short time without any damage, but already opened buds (king blossom bloom) can only stand short time temperatures up to -2 °C. After fruit set, minimum temperatures must not drop below -1 °C.

2. Data and Methods

2.1 Observation data

Phenological observations for the beginning of apple blossom (BBCH-stage 61) were derived from the German Weather Service (DWD) for the period 1961-2005. The beginning of flowering is registered when the first regular flowers have opened completely

in several places of the tree. For this developmental stage 5630 stations with observations between 1 and 45 years were available for Germany. 2411 stations had observations of more than 20 years and even 1214 stations had observations of more than 30 years. The spatial distribution of the stations was sufficient to cover the whole territory of Germany in terms of space and altitude.

In order to calculate phenological models for the beginning of apple blossom air temperature data were necessary, because the plant development in early spring is mainly driven by temperature. For this reason, also daily temperatures in the period 1961-2005 were derived from the DWD (523 stations with daily mean temperatures).

2.2 Climate change scenario

To estimate the impact of climate change on the late frost hazard of apple trees a regional climate change scenario was used. The scenario was based on a statistical weather-pattern downscaling method WETTREG for individual climate stations in Germany. The input for the downscaling procedure was derived from the SRES-A1B run of the coupled atmosphere and ocean model ECHAM5/OM of Max-Planck-Institute for Meteorology and Deutsches Klimarechenzentrum in Hamburg, Germany. For our study we used scenario-data for the decades 2011–2100. The control run of the model (20C) covers the years 1961–2000. For each scenario-decade and the control run ten 20-year simulations were available. So for each scenario-decade 200 years (10x20-year simulations=200 years in total) exist which represent the variability of climate in this period.

2.3 Methods

2.3.1 Development of phenological models

Phenological models are important tools to estimate the impact of global warming on plant development. In phenology the use of heat and chilling units is a common approach to describe the state of dormancy and the plant development.

In order to optimize phenological models on the basis of observation data, both the air temperature data and the phenological data (beginning of apple blossom) were gridded on a 10 x 10 km grid (horizontal resolution 0.088°) using the universal kriging method of second order. As a result, for 3703 grid points (Germany) data of daily air temperature and phenology in the period 1961-2005 were available. For modeling purposes only grid points up to 1000 m altitude were considered (altogether 3672 grid points), since in higher altitudes fruit growing is very rare.

To set up phenological models for the beginning of apple blossom in Germany the data base was spitted in two halves (fitting data: even years, verification data: odd years from 1961 to 2005). The model parameters were optimized for the fitting period at each grid point. Afterwards, mean model parameters were calculated on the basis of all 3672 points. The accuracy of the model was checked by the root mean square error (RMSE) or mean absolute error (MAE) between observed and estimated dates for the verification years. In order to optimize additionally models for individual fruit growing regions, the procedure was repeated, now for the grid points which define the growing regions (6-23 cells per growing area). In this case, only the chilling- (C^*) and forcing requirement (F^*)

as well as further individual model parameters were fitted to the regions. For the chilling- (T_{Bc}) and forcing base temperature (T_{Bf}) the previously optimized thresholds for Germany were used. To verify the phenological models for the fruit growing regions, the modeled data were compared with experimental data from the growing regions. The MAE was ranging between 1-6 days, depending on the region and apple variety.

Altogether 5 different phenological models for the beginning of apple blossom (t_2) were fitted, which are known from the literature. The simplest model was the so called '*thermal time model'*, which assumes that the chilling requirement is fulfilled to the beginning of the year (t_1 = 1 January). Thus only two model parameters have to be optimized (T_{Bf}, F^*).

$$S_f(t) = \sum_{i=t_1}^{t} R_f(T_i), \ \textit{where} \ S_f(t_2) := F^* \tag{1}$$

$$\begin{aligned} R_f(T_i) &= 0, && \textit{if} \ \ T_i \le T_{Bf} \\ R_f(T_i) &= \frac{28.4}{1+\exp\left(-0.185(T_i - T_{Bf} - 18.4)\right)}, && \textit{if} \ \ T_i > T_{Bf} \end{aligned} \tag{2}$$

Furthermore a '*sequential model*' was used which considers the state of chilling $S_c(t)$ and the state of forcing $S_f(t)$. Over and above this, the model assumes that an exponential relationship between the final chilling- (C^*) and forcing requirement (F^*) exist. Here even 5 parameters have to be fitted (t_1,T_{Bc}, T_{Bf}, a, b).

$$S_c(t) = \sum_{i=t_0}^{t} R_c(T_i), \ \textit{where} \ S_c(t_1) =: C^* \tag{3}$$

$$S_f(t) = \sum_{i=t_1}^{t} R_f(T_i), \ \textit{where} \ S_f(t_2) := F^* \ \textit{and} \ F^* = a \cdot \exp\left(b\, S_c(t_1)\right) \tag{4}$$

The state of chilling was calculated according to the following equations:

$$\begin{aligned} R_c(T_i) &= 0, && \textit{if} \ \ T_i \le 0.0 \ \textit{or} \ T_i \ge 10.0 \\ R_c(T_i) &= \frac{T_i}{T_{Bc}} && \textit{if} \ \ 0.0 < T_i \le T_{Bc} \\ R_c(T_i) &= \frac{T_i - 10.0}{T_{Bc} - 10.0} && \textit{if} \ \ T_{Bc} < T_i < 10.0. \end{aligned} \tag{5}$$

In order to calculate the forcing rate, equation (2) was used.

The next two models were *‚parallel models*'. These models assume that the process of chilling and forcing can run parallel. For the first model it was assumed that:

$$S_c(t) = \sum_{i=t_0}^{t} R_c(T_i), \ (i \ \textit{runs until} \ t_2), \textit{where} \ S_c(t_1) =: C^* \tag{6}$$

$$S_f(t) = \sum_{i=t_1}^{t} R_f(T_i), \ \textit{where} \ S_f(t_2) := F^* \ \textit{and} \ F^* = a \cdot \exp\left(b\, S_c(t_2)\right). \tag{7}$$

Here also 5 parameters (t_1, T_{Bc}, T_{Bf}, a, b) have to be optimized. The chilling- and forcing rates were calculated according to equations (5) and (2). t_2 is the smallest t that fulfills $S_f(t) \geq a \exp(b\, S_c(t))$ (see also equation (8), but with t_1 instead of t_0 in the sum on the left hand side).

The second parallel model also uses the equations (6) and (7), but for this model $F^*(S_c(t))$ and $S_f(t)$ were calculated for each day from t_0 (1 October) to t_2. In this case t_2 is the smallest t for that:

$$\left[S_f(t) = \sum_{i=t_0}^{t} R_f(T_i) \right] \geq \left[F^*(S_c(t)) = a \exp(b\, S_c(t)) \right]. \tag{8}$$

The rate of chilling was calculated as chilling days

$$\begin{aligned} R_c(T_i) &= 0, && \text{if } T_i \geq T_{Bc} \\ R_c(T_i) &= 1 && \text{if } T_i < T_{Bc} \end{aligned} \tag{9}$$

and the daily forcing rate according:

$$\begin{aligned} R_f(T_i) &= 0, && \text{if } T_i \leq T_{Bf} \text{ and } S_c < C^*, \text{ i.e. } t < t_1 \\ R_f(T_i) &= \left(K_m + \frac{1-K_m}{C^*} S_c \right) f(T_i), && \text{if } T_i > T_{Bf} \text{ and } S_c < C^*, \text{ i.e. } t < t_1 \\ R_f(T_i) &= f(T_i), && \text{if } T_i > T_{Bf} \text{ and } S_c \geq C^*, \text{ i.e. } t \geq t_1 \end{aligned} \tag{10}$$

$$f(T_i) = T_i - T_{Bf}\,.$$

In this model an additional parameter K_m exists. In total 6 parameters has to be optimized (T_{Bc}, C^*, T_{Bf}, a, b, K_m).

Finally a simple statistical regression model was also used. Here T_B was fixed to 3.8 °C.

$$t_2 = a + b \cdot T_M, \text{ wherby } \quad T_M = \frac{1}{t_2 - t_1 + 1} \sum_{i=t_1}^{t_2} \max(T_i - T_B, 0°C) \tag{11}$$

2.3.2 Evaluation of late frost risks, flower and yield damages

In order to estimate possible changes in the frequency of late frost up to 10 days after the beginning of apple tree blossom, the phenological models were used to calculate changes in the blossoming date up to 2100. Since the individual models showed slightly different shifts in the timing of blossom, the average trend of all 5 models was used. Then the probability for late frost after the beginning of blossom was estimated. It was necessary to classify the frost events according to their strength, because it influences the extent of flower damage. The total frost damage on the flowers (F_d) was estimated from (12). It was assumed that minimum temperatures of T_n= -2 °C would damage 10 % of the flowers and temperatures of T_n= -4 °C even 90 % of the flowers. Thus the flower damage (d_{FL}) can be calculated as follows:

$$d_{FL} = a \cdot \left[\exp\left(-b \cdot T_n\right) - 1 \right] \cdot 100\%, \quad a = 0.0142857,\ b = 1.03972$$
$$d_{FL} = 100\% \ \textit{for}\ T_n < -4.1°C \tag{12}$$

The yield damage (d_F) is different to the flower damage, because light flower damages would not have any effect on the apple yield. For this reason we assumed that 25 % of killed flowers could lead to yield losses by 10 % and 75 % of damaged flowers to yield losses of 70 %. For this reason we used 2 equations to estimate the yield losses due to late frost events:

$$d_F = \frac{0.10}{0.25} d_{FL},\ \textit{if}\ d_{FL} \le 0.25$$
$$d_F = 0.1 + \frac{0.90}{0.75} \cdot \left(d_{FL} - 0,25\right),\ \textit{if}\ d_{FL} > 0.25. \tag{13}$$

3. Results

The results indicate that the average beginning of apple blossom will be further advanced by 15 days to the end of this century (1971-2100). The shift slightly differs between the growing regions from -11 to -19 days. As a result the probability of late frost events (PR_{LF}) increases in all regions significantly between 6 and 14 % (Tab 1).

Tab.1: Calculated changes in the beginning of apple blossom (BF_{Ma}), in the probability for late frost up to 10 days after the beginning of blossom (P_F), in the probability of light (P_F^1: -2.0 < T_n < 0.0 °C), medium (P_F^2: -3.5°C < T_n ≤ -2.0°C) and strong (P_F^3: T_n ≤ -3.5°C) late frost events, which damage up to 10 % (P_F^1), between 10 - 50 % (P_F^2) and between 50 - 100% (P_F^3) of the flowers, changes in the total flower damage (d_{FL}) and changes on apple yield (d_F), 2071-2100 vs. 1961-1990, WETTREG, Scenario A1B, x: mean, s: standard deviation, bold numbers indicate a significant change (p≤0.05)

Fruit Growing Region	**BF_{Ma}** days	**P_F** **%**	**P_F^1** **%**	**P_F^2** **%**	**P_F^3** **%**	**d_{FL}** **%**	**d_F** **%**
Niederelbe	**-14.9**	**6.1**	**4.8**	**1.4**	-0.1	0.3	0.0
West-Mecklenburg	**-13.8**	**5.7**	**4.0**	**2.0**	-0.3	0.1	-0.1
Havelland/Brandenburg	**-11.0**	**6.7**	**4.8**	1.3	0.6	0.9	0.6
Süßer See/Thüringen	**-14.9**	**10.4**	**6.8**	1.9	1.7	2.2	1.9
Elbtal/Sachsen	**-13.0**	**6.1**	**4.5**	0.7	0.9	1.2	1.0
Franken	**-14.9**	**12.2**	**8.2**	**2.4**	1.6	**2.3**	1.8
Rheinland/Rheinhessen	**-15.8**	**5.6**	**4.8**	1.0	-0.2	0.2	0.0
Bergstraße	**-17.7**	**6.9**	**5.9**	0.9	0.1	0.4	0.3
Neckarregion	**-15.4**	**7.0**	**4.8**	**1.5**	0.6	1.0	0.7
Baden	**-18.8**	**7.3**	**4.5**	1.8	1.0	1.6	1.3
Bodenseegebiet	**-15.8**	**14.0**	**7.4**	**3.4**	**3.2**	**4.0**	**3.5**
x	**-15.1**	**8.0**	**5.5**	**1.7**	0.8	1.3	1.0
s	2.12	2.87	1.38	0.77	1.04	1.19	1.09

From Tab. 1 we can see that the probability for light frost events (P_F^1), which do not harm the flowers more than 10 %, increases at the very most, on average by 6 %. The probability for medium frost events, which harm 10 - 50 % of the flowers (P_F^2) is already lower and the probability for strong events, which damages more than 50 % of the opened flowers (P_F^3) is nominal. Thus, the total late frost damage at the flowers (d_{FL}) increases only slightly. Significant changes are only possible for two regions (Franken, Bodensee). As a result the final apple yield losses due to late frost (d_F) are probably also week. They range between -0.1 and 3.5 % of the apple yield (Bodensee) (negative values mean profit, positive loss).

4. Discussion and Conclusions

In the last decades (1961-2005) the blossoming time of apple trees has advanced on average by 15 days due to increasing temperatures in winter and in early spring. Up to the end of this century this date could shift once more by the same amount, so that the mean apple blossom in Germany would already start between 1 and 25 April. For this reason it is interesting to know how the frost hazard will change in the future.

Scheifinger et al. 2003 investigated trends in the last occurrence date of frost events and phenological trends in Central Europe (1951-1997). They found that trends of frost events appear more negative than those of the phenological phases. Therefore, they concluded that the risk of late frost damage for plants should have been lower during the last decade as compared to the previous decades. Stainer (2009) also showed that late frost damages in South Tirol have reduced in the last years. However, investigations by Sušnik and Žust (2001) for Slovenia point to an increase of spring frost frequency in 1990s and in 2001. In the Emilia-Romagna region (Italy) an increase in frost risk damage has been already observed in the last decades (e.g. Zinoni et al. 2002). After the extremely mild winter 2006/07, in many East-European countries late frost damages were observed with yield losses of more than 50 % such as in Hungary, Poland, Czech Republic, Slovakia, Lithuania and Latvia (Ellinger and Görgens 2007).

Our results show also a significant increase in the probability of late frost events after the beginning of apple blossom for all investigated regions. The study emphasise that a detailed approach is necessary to estimate the final consequences of a higher frost risk during fruit blossom. Doing this, we found that mainly the light frost events will significantly increase, so that according to this scenario the damages on the apple yield are probably moderate.

Acknowledgments

The authors are thankful to the Federal Ministry of Education and Research (BMBF) for funding the research project KliO (FZK: 01LS05024) within the scope of the research initiative klima*zwei*.

References

Scheifinger H., Menzel A., Koch E., Peter Ch., 2003: Trends of spring time frost events and phenological dates in Central Europe. Theor. Appl. Climatol. 74, 41–51.

Stainer R., 2009: Das Klima im Wandel – Südtirol im Klimastress. 4. umweltmedizinischen Fachtagung: „Klimaveränderungen und Gesundheit. Auswirkungen in Südtirol“, 28. November, Bozen (I).

Sušnik A., Žust A., 2001: Phenological model for forecasting blossoming dates of plum tree as a tool for frost risk assessment related to climate change, Conference abstract on Wageningen Phenology Conference, Holland, 5-7 December, 6 pp.

Zinoni F., Antolini G., Campisi T., Marletto V., Rossi F., 2002: Characterization of Emilia Romagna in relation with late frost risk. Chemistry and Physics of the Earth, 27, 1091-1101.

Ellinger, W., Görgens, M., 2007: EU-Kernobstschätzung 2007, Mitt. OVR, 62, 9, 320-327.

Authors' address:

Humboldt-University of Berlin
Faculty of Agriculture and Horticulture
Division of Agronomy and Crop Production
Professorship of Agricultural Climatology
Albrecht-Thaer-Weg 5, D-14195 Berlin
E-Mail: chmielew@agrar.hu-berlin

Using digital elevation models in agroclimatology: determination of potential frost-risk territories

Ákos Németh

Climate Analysis Division, Hungarian Meteorological Service, Budapest, Hungary

Abstract

Nowadays more and more hypothesis come out that the frost-risk decreases in Hungary and the importance of late spring frosts become negligible on account of the global climate change. But the result of climate data processing opposes this idea. According to the measurements of the Hungarian Meteorological Service, in the last decades (mainly in April) the frost frequency and intensity increased significantly. The day of the last frost is pushed later and later time. This tendency is very dangerous at the beginning of the growing season. These results flashed, that very important to determine the potential frost-risk lands.

Determination of potential frost-risk territories practically means the determination of cold air lakes. The method based on the 90m-resolution SRTM (Shuttle Radar Topography Mission) digital elevation model and the primary and secondary terrain parameters. We used the SAGA (System for Automated Geo-scientific Analysis) and DIGEM (Digitales Gelände-Modell) software to produce input parameters, ArcView 3.2 and AV Spatial Analyst software to create raster-category maps and spatial analysis and the SURFER 8 software to visualization. We demonstrate this method on the Southern-Balaton Winery (Hungary) as a sample area. The verification was done with satellite remote sensing techniques (with using land surface temperature data was calculated from NOAA-AVHRR images).

1. Introduction

Frosts (measured at two meters as well as frost above the ground) are harmful phenomena for plants. The sensitivity of plants to temperatures below zero is different in different periods of their growth. In Hungary's climate one can expect frost damages to occur in three seasons. In spring and fall air with temperature not much below the freezing-point causes losses to farmers, as in winter, the extreme cold weather can be damaging. In the Southern, warmest part of Hungary the frost free period is between 195 – 200 days. This period is 180 – 195 days in most parts of Hungary, but in the higher mountain areas it decreases below 180 days. Frost above the ground can even occur in the beginning of June (this is very rare), and in the end of August this phenomenon occurs again. So, if frost pocket places are not considered, ground frost does not occur only during summer in Hungary (Botos and Varga-Haszonits, 1974).

Climate change will probably cause temperature rising in Hungary as well. Numerous studies have been prepared on this topic to compensate its harmful effects. Decision makers are planning to make a governmental action plan. There is less emphasis on studying frost occurring in spring and autumn. According to the measurements of the Hungarian Meteorological Service (HMS) the frequency and durability of the (late) spring frost has risen in the last decades (Németh and Kalmár, 2006). This is an important phenomenon that gives us reason to devote more attention to the determination of frost risk territories.

Irradiation causes cold air to overlay the surface during the night. This cold air covers the surface homogeneously and in calm situation it does not move. But on the slopes,

like water, it starts to move because of its weight. Warmer air coming from higher layers replaces the cold air moving downward on the slopes. This circulation causes special surface wind on the slopes. Cold air flowing downward on the slopes collects in depressions. Moreover, masses of cold air follow the valleys and ditches even when they move. Flowing cold air collects in deep depressions or behind mounds perpendicular to the direction of movement, where it creates "cold air lakes". In this region the thickness of the cold masses rises, inside the masses the wind may be calm that may cause further cooling down. Severe frost can occur in this situation (Bridier et al., 2004).

2. The sample area

Our research locality was the Western or South-Western part of Hungary, areas to the South of the Lake Balaton (Figure 1.). The territory is about 300 km2 large with a picturesque morphology. There is a loess-mantled, relatively low and NW-SE directed hilly ridges dissected by erosion-derasion valleys. On the slope loess is formed good quality chernozem brown forest soil.

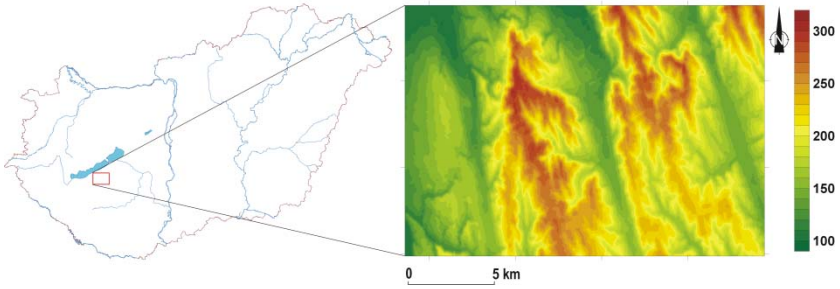

Fig. 1: Location and elevation of the sample area

This area has moderately warm and moderately wet climate with submediterranean climatic influence. The annual mean temperature is 10.2 °C. The frost free period is 205 days; usually it lasts between 5 April and 28 October. The annual mean precipitation is about 650 mm, and the annual sunshine duration is around 2000 hours.

The chosen land is an important agricultural area being part of the Southern-Balaton Winery. On this area beside grapes there are fruits (e.g. peach, apricot, cherry, sour cherry and apple) and cereals. On higher relief (especially on ridges of hills) we can find natural (Quercetum petreae-cerris pannonicum) or planted mixed forests.

3. Used data

To determine the potential frost risk territories, the most important task was to define weight factors of different effecting parameters. It happened in a subjective way, according to research of Bridier and her colleagues (Bridier et al., 2004). We marked the weight factors on a five-class scale. The most important factors got the weight factor 5, while the most unimportant ones got 1.

One of the bases of research was the digital terrain model (DTM), including parameters originating from it. We used the SRTM (Shuttle Radar Topography Mission) database developed in cooperation between NASA, the US National Imagery and Mapping Agency (NIMA), the German Space Agency (DLR), and the Italian Space Agency

(ASI); and the DTM generated from this database. The obtained results in three (angle) seconds resolution are freely available on the Internet. We had to consider, when we used this data that it was made by radar technology. Water surfaces give uncertain signs because of the waves, so we get false data on these surfaces (lakes, rivers and seas). A part of this data was filtered and these pixels were given ZERO values. Many of the pixels of mountain areas got ZERO values, mainly those that are so deep in the valleys that the radar echo did not return to the detector according to the radar shadow. Consequently, the higher the landscape, the more data is missing because of this phenomenon. Another fault in the database is that the height of buildings and trees appears in the data. This is caused by the fact that radio waves of few centimeters are not able to penetrate the thick leaves or even leaves of medium thickness, and they are reflected back from the roofs and buildings. The pixel size in the DTM is 90 m that is enough to determine the frost risk territories. Since the frost risk is not the direct function of the altitude (in SW-Hungary), we have to determine different parameters from the DTM.

One of these parameters is the slope category. In this classification we considered that cold air flows downward very fast on steep slopes, so these areas are not called frost risk lands. The movement of cold air slows down on moderate slopes, therefore cold air lakes can form behind smaller landmarks.

Beside the slope, another important secondary topographic attribute (Wilson and Gallant, 2000) is the convergence of the surface. The convergence index was calculated by the SAGA (System for Automated Geo-scientific Analyses) program developed by the Georg-August University, Göttingen (Germany). The interpretation of the convergence index is very simple. Negative values indicate areas where the surface is concave, so these are the places of collection. The positive index is typical for the convex surface - from these areas cold air masses flow downward.

Among the parameters of the DTM modeling, determining topographic solar radiation is the most difficult. There are several methods to determine radiation that reaches the surface. These actually only differ slightly (Kang et al., 2002). In general, because of the applied physical connections, there are few radiation models that can be used generally in regional scale (Németh, 2004). In our work, we used one of the SAGA models (Olaya, 2004). Using the model we determined the annual values of potential radiation energy in the sample area. The values of the radiation energy were classified in the abovementioned way. Those parts of the sample area where the incoming radiation energy is the smallest got the highest weight factor (5). On the contrary, lands that get lots of energy (in general the Southern slopes) were marked by a weight factor 1 (Németh, 2008).

Land use is slightly different from the previous parameters. Land use data were obtained from the Corine Land Cover database. The land use database that we used was made by visual fotointerpretation of Landsat TM shots. These space shots were made in the period of 1990-1992. The database was created according to the European methodology. In our study we simplified the original Corine Land Cover nomenclature. We extracted only three categories. Grapes and fruits plantations are in the first category that was given a weight factor 5. This is because most of the grapes and fruits are very sensitive to frost, particularly at the beginning of their growing period. The second category is composed of agricultural production lands. These lands were given a weight factor 3.

All the other lands are unimportant in our examination, so they were given a weight factor one (Németh, 2008).

4. Determination of potential frost-risk territories

The first step in determining frost risk territories was the classification of parameters and selection of weight factors according to the method of frost risk determination. According to the weight factors, we made each parameter's raster category map. After this we put these maps on each other and simply added the values of each cell. The process is presented in Figure 2. The next step after the addition was to reclassify the results, as a result we obtained the territory's frost risk map.

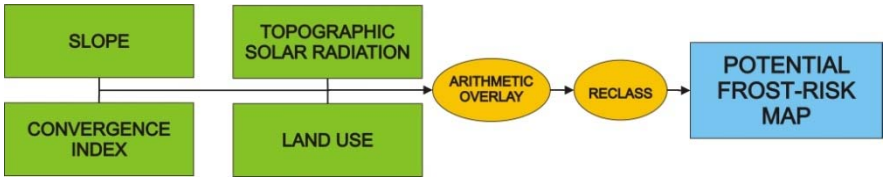

Fig. 2: Flowchart showing sequence for determining potential frost-risk map

We can see that the most of the risk occurs in the NW parts of the examined territories - in the valleys and where there are gentle slopes. We can see it more clearly if we put the potential frost risks map on the DTM. Those areas, which get 4 or 5 value after the reclassifying (blue colored on Figure 3.), are regarded potential frost-risky. Here the temperature above the surface may decreases below zero under certain synoptic conditions. These areas are usually located in the valleys. In some of them, especially the wider ones the local morphological depressions indicate the potential frost-risky areas.

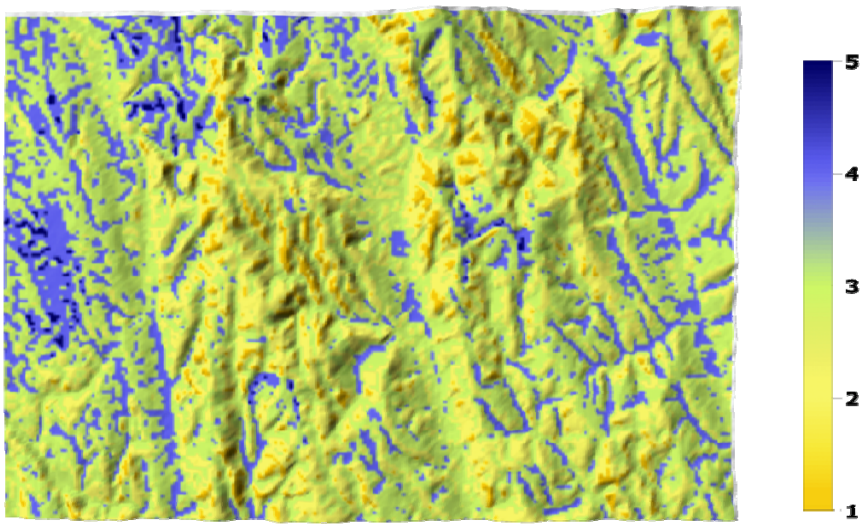

Fig: 3: Potential frost-risk map (Legend: 1 – not risk, 2 – slighty, 3 – moderate, 4 – frost-risk, 5 – highly frost-risk).

Our results shows that about 20 percentage of the study area are potential frost-risky. When we examine the vineyards only, the situation was much worse. More then half of it lies on potential frost-risky fields. The vineyards (and orchards), which lay such areas need protect from frost damage. There are much more different methods for protection.

Such methods are for example smoke or fog making, air heating, air mixing, etc. Using these methods increase the production cost.

4. Verification

For the preliminary verification of this method we used the remotely sensed land surface temperature (LST). For the LST calculation we applied a method that use a combination of the channels 4 (10.3 - 11.3 μm) and 5 (11.5 - 12.5 μm) of the AVHRR sensor. This technique is called Split-Window. The most common form of Split-Window algorithm is (Beik and Saradjian, 2003):

$$LST = T4 + A\,(T4 - T5) - B \quad , \tag{1}$$

where T4 and T5 are brightness temperatures in AVHRR channels 4 and 5, A and B are coefficients in relation to atmospheric effects, viewing angle and ground emissivity.

The mean horizontal resolution of the LST map is only 1.5 - 2 km (the original pixel size is 1 km). However it has worst spatial resolution than the potential frost-risk maps the LST is suitable for the qualitative verification. On the Figure 3., we can see four LST maps. We could distinguish the warmer and colder areas on these maps. The coldest regions on LST maps are coincide with areas that we classify as potential frost-risk predominantly. We have set ourselves the task to make the exact verification of the potential frost-risk map.

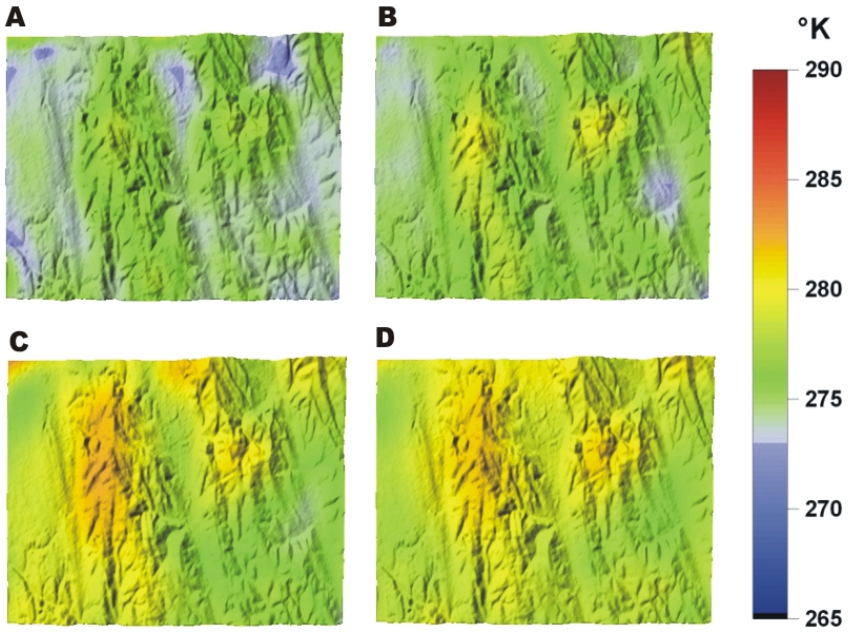

Fig. 3: Land surface temperature map of the sample area (A – 3 April 2005 1:49am UTC; B – 4 April 2005 1:34am UTC; C – 5 April 2005 1:26am UTC; D – 6 April 2005 1:15am UTC)

5. Conclusions

In our research we determined the potential frost risk areas. At present we are verifying this method, so this paper only contains preliminary results. During the verification we will conduct field measurements to determine exactly the frost-risk areas. Apart from this, we will make the temperature map of the area by analysing meteorological network data with applying the suitable interpolation. These together provide enough possibility to verify the results. The method is under development presently. The implementation of albedo values determined by satellite data would refine the current model.

Acknowledgement

This study was supported by the National Office for Research and Technology (NKTH) TECH-08-A4/2-2008-140 Programme.

References

Beik, F., Saradjian, M. R., 2003: Emissivity determination for Land Surface Temperature estimation of Iran using AVHRR Thermal Infrared Data. Proceedings of Map Asia Conference, 13-15 October 2003, Kuala Lumpur, Malaysia

Botos, L., Varga-Haszonits, Z. (eds.), 1974: Agroclimatology and cultivation. Ministry of Agriculture and Food, Budapest, Hungary (in Hungarian)

Bridier, S., Quénol, H., Beltrando, G., 2004: Cartographie du potentiel de refroidissement en situation radiative. Application au terroir des Fonds de Sillery dans le vignoble de Champagne. Revue internationale de géomatique 14, 1-14. (in French)

Kang, S., Kim, S., Lee, D., 2002: Spatial and temporal patterns of solar radiation based on topography and air temperature. Canadian Journal of Forest Resources 32, 487-497.

Németh, Á., 2008: DEM based method for determination of potential frost risk territories. Climatological and Agrometeorological Papers 9, 53-79. (in Hungarian with English abstract)

Németh, Á., 2004: Modelling of topographic solar radiation using digital elevation models. Proceedings of HUNDEM Conference, University of Miskolc, Hungary (in Hungarian)

Németh, Á., Kalmár, E., 2006: Winter and spring cold extremes in Hungary. Proceeding of VAHAVA (Weather and Climate, Effects and Arrangements) Final Conference, 9 March 2006, Budapest, Hungary (in Hungarian)

Olaya, V., 2004: System for Automated Geo-scientific Analysis v. 1.1; A gentle introduction to SAGA GIS, Georg-August University of Göttingen.

Wilson, J. P., Gallant, J. C., 2000: Secondary Topographic Attributes. In: Wilson, J. P., Gallant, J. C. (eds.): Terrain Analysis: Principles and Applications, 87-131.; John Wiley and Sons Inc.

Author's address:

Ákos Németh (nemeth.a@met.hu)
Climate Analysis Division, Hungarian Meteorological Service
Kitaibel P. u. 1., H-1024 Budapest, Hungary

Erweiterung und Optimierung der Geisenheimer Peronospora-Prognose und Umsetzung in die Rebschutz-Praxis im Rheingau

Cathleen Frühauf[1], Beate Berkelmann-Löhnertz[2], Bernd J. Loskill[2], Anja Schaldach[1], Harald Braden[1], Klaus-Uwe Gollmer[3], Markus Forster[3] und Klaus-Peter Wittich[1]

[1] Deutscher Wetterdienst, Zentrum für Agrarmeteorologische Forschung Braunschweig;
[2] Forschungsanstalt Geisenheim, Fachgebiet Phytomedizin;
[3] Fachhochschule Trier, Umweltcampus Birkenfeld.

Zusammenfassung

Genetische Studien und epidemiologische Untersuchungen auf drei Monitoring-Flächen im Rheingau haben die Bedeutung bodenbürtiger Peronospora-Infektionen aufgezeigt (Loskill et al. 2005, 2007). Aus diesem Grunde wurde das vorhandene Prognosemodell zur Vorhersage von Sekundärinfektionen in den Jahren 2002 bis 2005 optimiert. Einerseits ist es jetzt möglich, den Zeitpunkt der Primärinfektion präziser vorhersagen zu können. Andererseits können nachfolgende bodenbürtige Infektionen im weiteren Verlauf der Vegetationsperiode sicher prognostiziert und damit der Anteil falsch-negativer Prognose-Ergebnisse reduziert werden. Hierbei wurde neben den Parametern Oosporen-Reifung und Splash das Bestandesklima in der Laubwand berücksichtigt. Mit dem neuen Primärinfektionsmodell wurde ein redundantes System zur Bewertung des bodenbürtigen Infektionsrisikos geschaffen.

Plasmopara forecast based on the expanded and improved Geisenheim disease model and application in practise

Abstract

Genetic studies and epidemic analyses on three monitoring sites in the Rheingau region (Hesse, Germany) stressed the significance of soil borne *Plasmopara* infections (Loskill et al. 2005, 2007). With respect to this finding, the actually applied forecast model – focusing on the secondary disease cycle – was optimised in years 2002 to 2005. On the one hand, the precise prediction of the date of primary infection was improved; on the other hand, further soil borne infections in the later course of the growing period could be detected, thus resulting in a reduction of the amount of false negative forecast notes. The following parameters were taken into account: oospore maturation, splash, and the micro climate of the canopy. A redundant system was established by addition of the newly created primary infection model which enables to estimate the specific risk for soil borne infections.

1. Einleitung

Mit dem P.R.O.-Modell (HILL, 1989 a, b) für die Vorhersage des Falschen Rebenmehltaus, hervorgerufen durch *Plasmopara viticola*, wurde Ende der 80er Jahre ein Meilenstein gesetzt. Das Modell basiert auf der Vorhersage von Sekundärinfektionen des Pilzes. Hierfür werden unter anderem Reife- und Vermehrungsfaktoren verwendet. Der Termin der Primärinfektion wurde durch das Überschreiten einer kritischen Niederschlagsrate während der Entwicklungsphase der „Wintersporen“ (Oosporen) abgeschätzt. Nach mehreren Jahren der Anwendung zeigte sich Mitte der 90er Jahre, dass die Ergebnisse der P.R.O.-Prognose und die reale Krankheitsentwicklung auf so genannten Monitoring-Flächen (unbehandelte Kontrollflächen) nicht mehr kongruent waren. Im Weinberg kam es zur Überlagerung einzelner Infektionszyklen, während die Kurve der „prognostizierten Ölflecken“ deutlich darunter lag.

Um die Ursachen für die fehlende Übereinstimmung zwischen den Befallswerten der Prognose und der Krankheitsbonitur zu finden, wurden genetische Studien durchgeführt. Auf drei Monitoring-Flächen wurde jeweils eine Ölfleckenhälfte im Weinberg belassen, um den Epidemieverlauf möglichst wenig zu beeinflussen, die andere wurde mittels Mikrosatelliten-Technik genetisch analysiert. Mit Hilfe dieses Verfahrens war es möglich, „bodenbürtige“ Infektionen (Primärzyklus) von „blattbürtigen“ Infektionen (Sekundärzyklus) zu differenzieren. Es konnte gezeigt werden, dass sich starke „Pero-Jahre“ bzw. „schwierige Pero-Standorte“ durch einen hohen Anteil bodenbürtiger Infektionen im weiteren Verlauf der Vegetationsperiode von Jahren mit eher moderatem Peronospora-Befall bzw. weniger gefährdeten Standorten unterscheiden (Loskill et al., 2005).

2. Die Geisenheimer Peronospora-Prognose

Das neue Primärinfektionsmodell besteht aus Modulen zur Berechnung der Keimdauer, der Spritzhöhe und eines Primärinfektionsindexes (Berkelmann-Löhnertz et al., 2006; Loskill et al., 2007). Für die Nutzung in der Beratung wurde das Modell in die Agrar-Meteorologische BERatungssoftware (AMBER) implementiert (Abb. 1). Darin finden außerdem der Sekundärzyklus des Pilzes (EXPERO) sowie die Phänologie der Rebe Berücksichtigung (Adaption des Blattflächenentwicklungsmodells von Schultz, 1992).

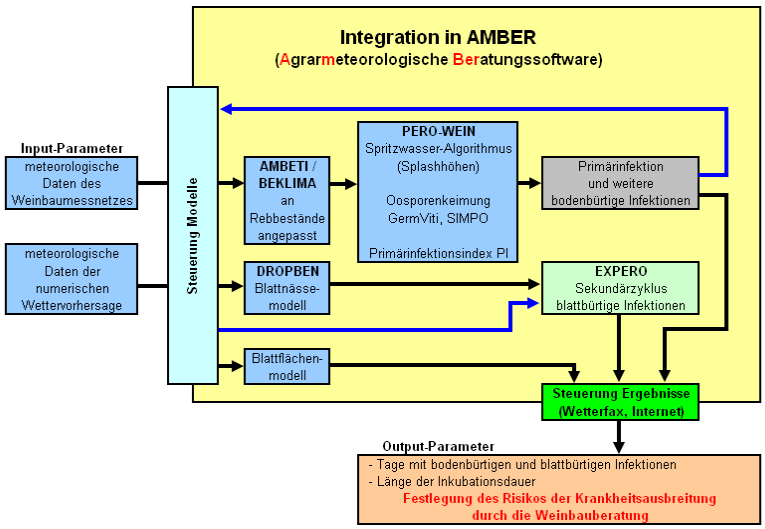

Abb.1: Einbettung der neuen Modelle in die AMBER-Umgebung
Fig. 1: Implementation of the new models into the AMBER software package

Leider befand sich das Modell im schwierigen „Peronospora“-Jahr 2005 noch in der Entwicklungsphase. Die rückwirkende Modellierung des Jahres 2005 gab den beobachteten Epidemieverlauf sehr gut wieder. Die erste bodenbürtige Infektion wurde am Standort Geisenheim für den 07.05.2005 berechnet (Abb. 2). Die folgenden Abbildungen zeigen den Verlauf des Primärinfektionsindexes (PI) und der Bodenfeuchte im Oberboden (oberste 5 cm). Für jedes Niederschlagsereignis ist die maximale Splashhöhe als Punkt dargestellt. Werden die Bedingungen für eine bodenbürtige Infektion erfüllt (keimbereite Oosporen, PI $\geq$ 0.7 und Splashhöhe $\geq$ 70 cm), so sind diese Punkte größer und in roter Farbe hervorgehoben.

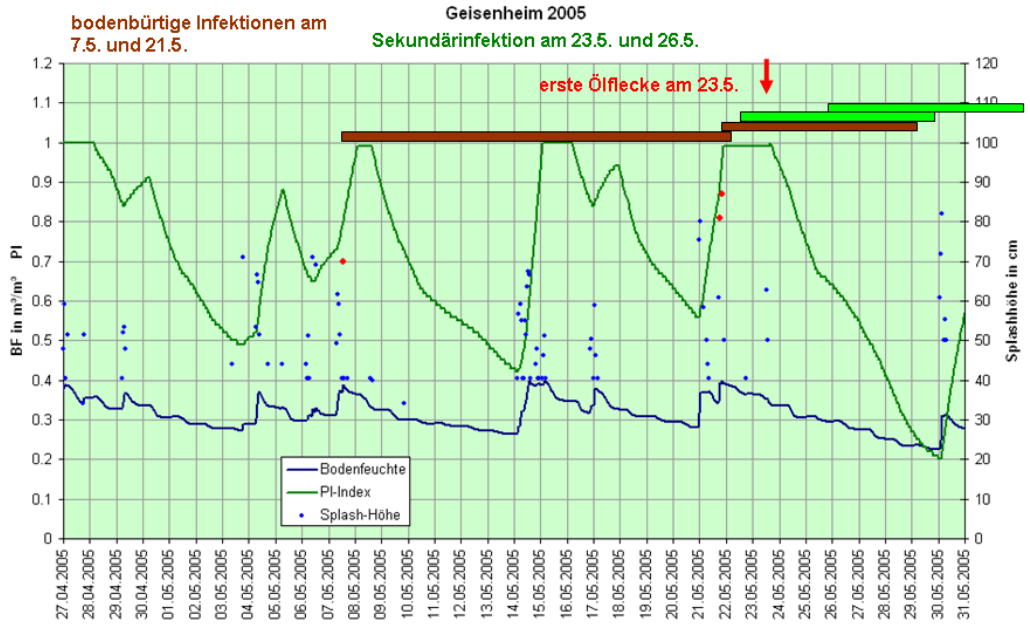

Abb. 2: Modellierung des Epidemieverlaufs von *Plasmopara viticola* und Boniturergebnisse für das Jahr 2005 – Standort Geisenheim

Fig. 2: Epidemiology of Plasmopara viticola *based on model results and disease development data based on oilspot assessment in the vineyard in year 2005 – experimental site Geisenheim, Germany*

Aufgrund der Anfang Mai herrschenden sehr kühlen Temperaturen ergab sich eine ungewöhnlich lange Inkubationszeit von 15 Tagen (dargestellt als brauner bzw. dunklerer Balken). Das Ende der Inkubationszeit fiel auf ein Wochenende, so dass erste Ölflecke erst am folgenden Montag (23.05.2005) bonitiert wurden. Bereits vor Sichtbarwerden der ersten Ölflecke kam es zur nächsten bodenbürtigen Infektion. In der Folge überlagerten sich die Inkubationszeiten dieser zweiten bodenbürtigen Infektion (kürzerer brauner bzw. dunklerer Balken) und der ersten Sekundärinfektion (grüner bzw. hellerer Balken), die direkt nach Ablaufen der Inkubationszeit der Primärinfektion startete. Die feucht-warmen, sommerlichen Temperaturen der dritten Mai-Dekade hatten kurze Inkubationszeiten (zwischen sechs und acht Tagen) und erneute Sekundärinfektionen zur Folge.

Der Standort Erbach zeichnete sich durch einen deutlich höheren Anteil bodenbürtiger Infektionen aus. Die Modelle berechneten hier am 03.05., 06.05., 07.05., 14.05., 21.05. und 23.05.2005 erfolgreiche bodenbürtige Infektionen (Abb. 3). Die ersten Ölflecke wurden ebenfalls am 23.05.2005 bonitiert. Zu diesem Zeitpunkt waren die Inkubationszeiten der ersten drei bodenbürtigen Infektionen bereits abgelaufen und drei weitere bodenbürtige Infektionen sowie zwei Sekundärinfektionen gesetzt. Erbach gehört somit zu den „schwierigen Pero-Standorten“, was sich mit den genetischen Studien von Loskill et al. (2005) deckt.

Insgesamt handelte es ich im Jahr 2005 um ein sehr ungewöhnliches „Peronospora“-Jahr, da eine sehr starke erste bodenbürtige Infektion auftrat, die zudem auf Grund der extrem langen Inkubationszeit unerkannt blieb. Diese Situation wurde von der weinbaulichen Praxis völlig unterschätzt. Nur einige wenige Betriebe, die kurz vor dem entscheidenden Wochenende (21./22.05.2005) Peronospora-Fungizide ausgebracht hatten,

blieben verschont. Wer nicht rechtzeitig gespritzt hatte, konnte den regional katastrophalen Epidemieverlauf nicht mehr stoppen. Interessanterweise hatten im Jahr 2005 viele der ökologisch wirtschaftenden Betriebe aufgrund des notwendigen frühen Applikationsbeginns mit kupferhaltigen Pflanzenschutzmitteln weitgehend „saubere Weinberge“.

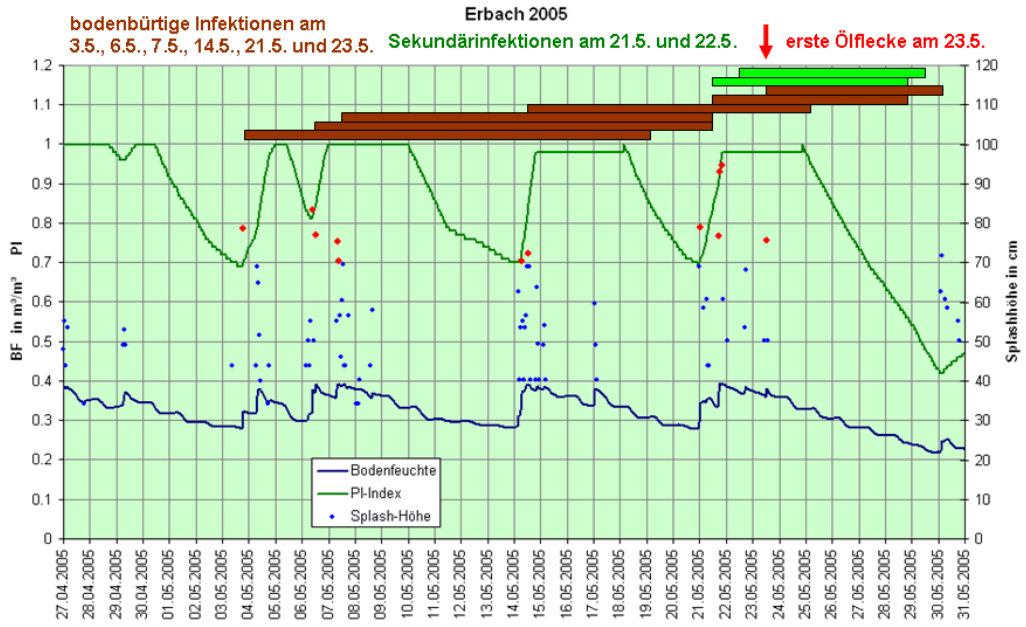

Abb. 3: Modellierung des Epidemieverlaufs von *Plasmopara viticola* und Boniturergebnisse für das Jahr 2005 – Standort Erbach

Fig. 3: Epidemiology of Plasmopara viticola *based on model results and disease development data based on oilspot assessment in the vineyard in year 2005 – experimental site Erbach, Germany*

Die nachfolgenden ersten Validierungsjahre 2006 und 2007 waren schwache „Peronospora“-Jahre. In 2006 traten erste bodenbürtige Infektionen am 19. und 20.05.2006 auf (keine Abbildung). Die Inkubationszeiten dieser beiden schwachen Primärinfektionen umfassten jeweils 13 Tage. Allerdings führten diese nur zu einem schwachen Epidemiestart, so dass die vereinzelt aufgetretenen Ölflecke nicht gefunden wurden. Die darauf folgende Sekundärinfektion startete am 04.06.2006. Erste Ölflecke wurden auf den Monitoring-Flächen am 19.06.2006, einige Tage nach Ablauf der Inkubationszeit der Sekundärinfektion, bonitiert.

Im Jahr 2007 kam es wie in 2005 bereits Anfang Mai zur Primärinfektion (09.05.2007). Die Inkubationszeit (brauner Balken) war nach elf Tagen abgelaufen (Abb. 4). Es handelte sich aber im Gegensatz zur Situation im Jahr 2005 um eine sehr schwache Primärinfektion, da die nur vereinzelt aufgetretenen Ölflecke nicht wahrgenommen wurden. Aufgrund der für den Pilz ungünstigen Witterungsbedingungen traten über einen Zeitraum von einem Monat keine weiteren Infektionen auf. Erst am 18. und 19.06.2007 kam es zu ersten Sekundärinfektionen. Mit Ablaufen der Inkubationszeiten dieser Sekundärinfektionen (grüne Balken) wurden am 26.06.2007 erste Ölflecken auf der Monitoring-Fläche festgestellt.

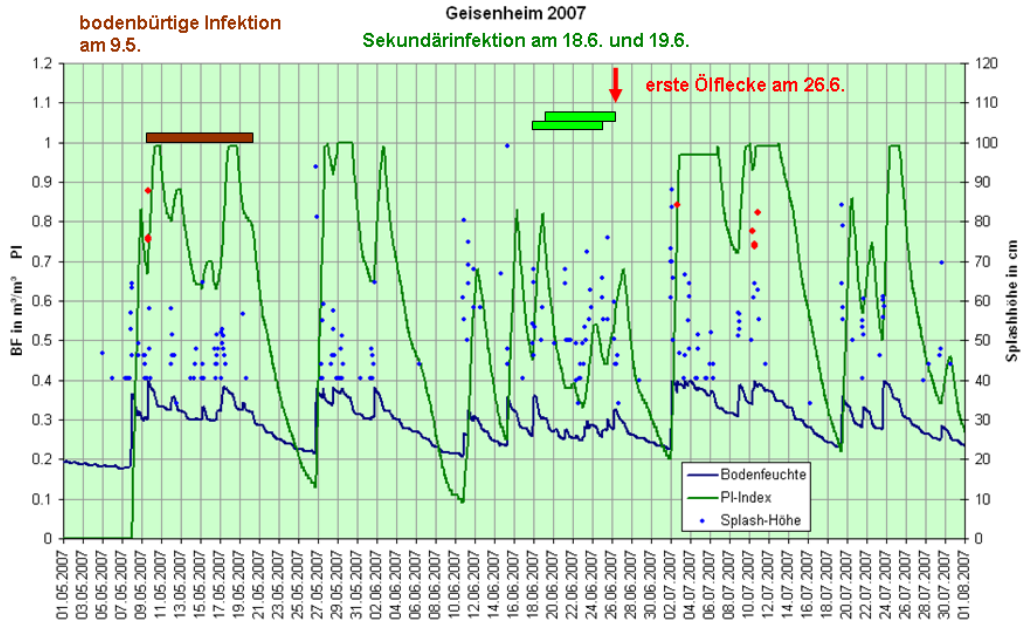

Abb. 4: Modellierung des Epidemieverlaufs von *Plasmopara viticola* und Boniturergebnisse für das Jahr 2007 – Standort Geisenheim

Fig. 4: Epidemiology of Plasmopara viticola *based on model results and disease development data based on oilspot assessment in the vineyard in year 2007 – experimental site Geisenheim, Germany*

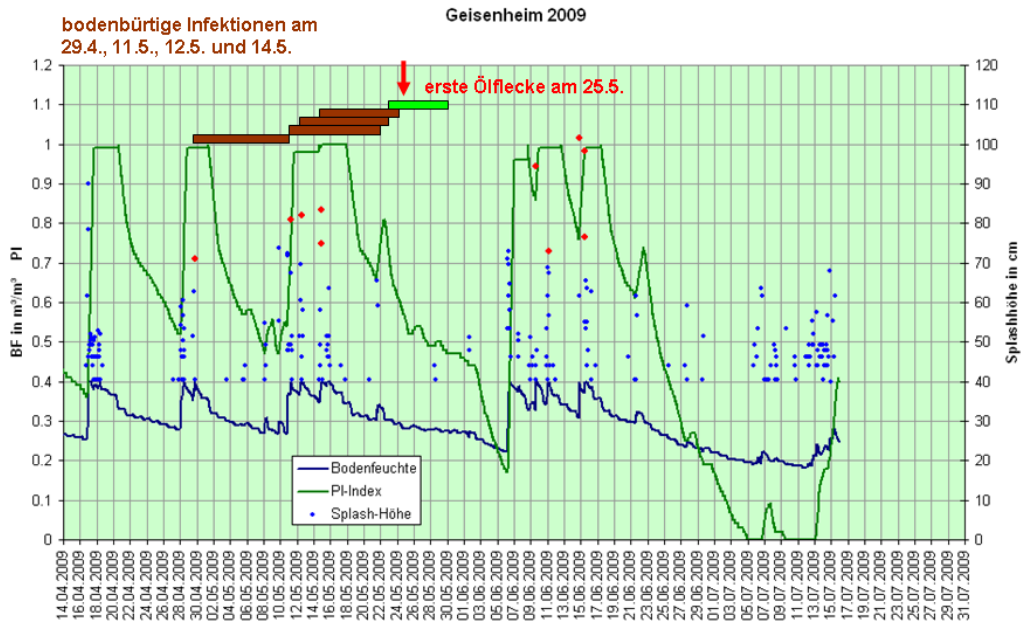

Abb. 5: Modellierung des Epidemieverlaufs von *Plasmopara viticola* und Boniturergebnisse für das Jahr 2009 – Standort Geisenheim

Fig. 5: Epidemiology of Plasmopara viticola *based on model results and disease development data based on oilspot assessment in the vineyard in year 2009 – experimental site Geisenheim, Germany*

Im Jahr 2008 ließ der extrem schwache Peronospora-Befall im Rheingau keine Validierung zu. Dies konnte erst im äußerst problematischen Peronospora-Jahr 2009 erfolgen (siehe Abb. 5). Es zeigte sich, dass der Zeitpunkt der Primärinfektion präzise prognostiziert und der nachfolgende Epidemieverlauf mit Hilfe des Modells sehr gut abgebildet werden konnte.

Die Prognoseergebnisse ergänzen im Rheingau die breite Datenbasis, die für die Weinbauberatung genutzt wird. Somit fließt der Modell-Output in aufgearbeiteter Form in das Beratungsinstrument „Wetterfax für den Weinbau“ ein.

Im durchaus schwierigen Peronospora-Jahr 2009 konnte eindrucksvoll gezeigt werden, dass Winzer, die ihre Peronospora-Bekämpfung gemäß den Empfehlungen des „Rheingauer Weinbaufaxes“ durchgeführt haben, keine Probleme mit dieser Krankheit hatten. Wichtig ist nach wie vor die exakte Terminierung der Peronospora-Fungizid-Applikationen sowie die Beachtung und entsprechende Berücksichtigung der Grenzen, die jedes Fungizid hinsichtlich Wirkungsdauer und/oder Kurativpotential aufweist.

Literatur

Berkelmann-Löhnertz B., Loskill B.J., Frühauf C., Gollmer K.-U., Forster M., Kuczera A., Braden H., Wittich K.-P., (2006): Downy mildew forecast regarding primary and further soil borne infections based on a splash algorithm and a microclimate model. Proceedings of the 5th International Workshop on Grapevine Downy and Powdery Mildew, 130.

Hill G., (1989a): Effect of temperature on sporulation efficiency of oilspots caused by *Plasmopara viticola* (Berk. et Curt., ex de Bary) Berl. & de Toni in vineyards. Vitic Enol. Sc., 44, 86-90.

Hill G., (1989b): Das Peronospora-Risikoprognosemodell Oppenheim (P.R.O.) im Praxistest. Der Deutsche Weinbau, 44, 514-517.

Loskill B.J., D. Gobbin, B. Berkelmann-Löhnertz, (2005): Bodenbürtige Peronospora-Infektionen. Der Deutsche Weinbau 7, 26-29.

Loskill B.J., A. Kuczera, K.-P. Wittich, H. Braden, C. Frühauf, K.-U. Gollmer, M. Forster, B. Berkelmann-Löhnertz, (2007): Neue Wege bei der Peronospora-Prognose – Mehr Licht in das Dunkel der Primärinfektion. Deutsches Weinbau-Jahrbuch 58, 76-81.

Schultz H.R., (1992): An empirical model for the simulation of leaf appearance and leaf area development of primary shoots of several grapevine (*Vitis vinifera* L.) canopy systems. Scientia Horticulturae 52, 197-205.

Adressen der Autoren:

Dr. Cathleen Frühauf (cathleen.fruehauf@dwd.de); Dr. Harald Braden (harald.braden@dwd.de)
Dr. Klaus-Peter Wittich (klaus-peter.wittich@dwd.de); Anja Schaldach
Deutscher Wetterdienst, Zentrum für agrarmeteorologische Forschung Braunschweig
Bundesallee 50, D-38116 Braunschweig, Germany

Prof. Dr. Beate Berkelmann-Löhnertz (berkelmann@fa-gm.de); Dr. Bernd J. Loskill
Forschungsanstalt Geisenheim, Fachgebiet Phytomedizin
Von-Lade-Str. 1, D-65366 Geisenheim, Germany

Klaus-Uwe Gollmer (k.gollmer@umwelt-campus.de); Markus Forster
Fachhochschule Trier, Umweltcampus Birkenfeld
Postfach 13 80, D-55761 Birkenfeld, Germany

Erfassung der Vegetationsentwicklung landwirtschaftlicher Bestände mit agrarmeteorologischen Strahlungssensoren

Klaus-Peter Wittich[1], Martin Kraft[2]

[1] Deutscher Wetterdienst (DWD), Zentrum für Agrarmeteorologische Forschung, Braunschweig, Germany
[2] Johann Heinrich von Thünen Institut (vTI), Institut für Technologie und Biosystemtechnik, Braunschweig, Germany

Zusammenfassung

Einem Artikel von Huemmrich et al. (1999) folgend wurden auf den Versuchsfeldern der agrarmeteorologischen Forschungseinrichtung des DWD in Braunschweig ein Albedometer und zwei PAR-Sensoren in einer geeigneten Kombination eingesetzt, um aus den Messdaten verschiedene breitbandige Vegetationsindizes (*NDVI*, *SAVI*, *DVI*) zu generieren. Zielkulturen waren Hafer und Raps. Die Messungen zeigen, dass die Indizes die Vegetationsentwicklung gut erfassen, d.h. sie weisen einen Anstieg bis zum Bestandsschluss und eine Abnahme während der Seneszenzphase auf. Die ausgewählten Indizes reagieren allerdings unterschiedlich sensitiv auf sowohl Boden- als auch Blütesignale. Die Indexverläufe werden dem unabhängig gemessenen *LAI* und dem fotographisch ermittelten Pflanzenbedeckungsgrad gegenübergestellt.

Measurements of the development of agricultural crops with agrometeorological radiation sensors

Abstract

Following the suggestion made by Huemmrich et al. (1999), an albedometer and two PAR sensors were installed on the experimental oat and rape plots of the Agrometeorological Research Centre of the Deutscher Wetterdienst at Braunschweig. Suitable combinations of spectral bands were used to calculate broadband vegetation indices (*NDVI*, *SAVI*, *DVI*). The indices reflect the canopy development well, showing an increase during plant growth and a decrease during senescence. They differ, however, in their sensitivity to soil brightness and flowering. The index curves are compared with the separately measured leaf area index and the percent vegetation cover obtained by means of digital cover photography.

1. Einführung

Zur sensorseitigen Verfolgung der Pflanzenentwicklung bieten sich in der Regel engbandige Spektroradiometer an, aus deren Strahlungsreflexionswerten sich Vegetationsindizes berechnen lassen (z. B. Nagai et al., 2010). Als eine kostengünstigere Alternative schlugen Huemmrich et al. (1999) die Verwendung routinemäßig eingesetzter agrarmeteorologischer Strahlungssensoren vor. Hierbei handelt es sich um ein Albedometer und zwei PAR-Sensoren (PAR = photosynthetisch aktive Strahlung), wobei einer der beiden Sensoren abwärts, der andere aufwärts gerichtet ist, um die PAR-Reflexion bestimmen zu können.

Im Folgenden sollen einige Vegetationsindizes mit typischen agrarmeteorologischen Parametern verglichen werden. Hierzu gehören der Blattflächenindex und der Pflanzenbedeckungsgrad, die wichtige Steuergrößen in SVAT (Surface-Vegetation Atmosphere Transfer) Modellen sind.

2. Vegetationsindizes

Unter der Vielzahl der bisher entwickelten Vegetationsindizes ist der von Rouse et al. (1974, zitiert in Jiang et al., 2006) vorgeschlagene Normalized Difference Vegetation Index, *NDVI*, der bekannteste und populärste. Der *NDVI* setzt sich aus der roten (Subskript *r*) and der nah-infraroten (Subskript *NIR*) Strahlungsreflexion zusammen gemäß

$$NDVI = \frac{\rho_{NIR} - \rho_r}{\rho_{NIR} + \rho_r} \quad , \quad \rho_\lambda = R_{\lambda,\uparrow} / R_{\lambda,\downarrow} \quad .$$

Hierbei ist die Reflexion ρ_λ durch die aufwärts ($R_{\lambda,\uparrow}$) und abwärts ($R_{\lambda,\downarrow}$) gerichtete Strahlungsflussdichte im Spektralbereich λ definiert.

Der *NDVI* zeigt eine unerwünscht hohe Sensitivität in Bezug auf die Helligkeit des Bodenhintergrundes. Um diese zu reduzieren, entwickelten Huete (1988, zitiert in Jiang et al., 2006) als *NDVI*-Variante den Soil-Adjusted Vegetation Index, *SAVI*. Er ist definiert durch

$$SAVI = \frac{\rho_{NIR} - \rho_r}{\rho_{NIR} + \rho_r + L}(1 + L) \ ,$$

wobei der Korrekturfaktor L, obwohl abhängig von der Bestandsdichte, in der Mehrzahl der bekannten Untersuchungen auf $L = 0.5$ gesetzt wird.

Einer der einfachsten Indizes ist der Difference Vegetation Index (*DVI*) nach Tucker (1979, zitiert in Jiang et al., 2006)

$$DVI = \rho_{NIR} - \rho_r \ ,$$

der relativ unsensibel auf Änderungen der Bodenhelligkeit reagiert.

3. Messort und Messverfahren

Die Messungen wurden auf dem Versuchsgelände der agrarmeteorologischen Forschungseinrichtung des DWD in Braunschweig (10° 26.55’ E, 52° 17.35’ N) über einem Haferbestand, über Sommerraps und über Winterraps durchgeführt. Die Bestände bedeckten eine Fläche von 34 × 20.5 m^2. Zum Einsatz kamen ein Albedometer (CM 7B; Kipp und Zonen, Delft, Niederlande), welches die Solarstrahlung im Spektralbereich 305 – 2800 nm erfasst, sowie zwei PAR-Sensoren (LI-190 SA, LiCOR, Lincoln, Nebraska, USA) mit einem Spektralbereich von 400 – 700 nm. Die breitbandige PAR-Reflexion, ρ_{PAR}, ersetzt in den oben genannten Vegetationsindizes die Reflexion im roten Spektralbereich ρ_r, während an die Stelle von ρ_{NIR} die Reflexion im sog. optischen Infrarot ρ_{OIR} tritt. Diese ergibt sich aus dem Quotienten der für beide Halbräume getrennt berechneten Differenz der Globalstrahlung und der PAR (Huemmrich et al., 1999).

Begleitend wurde wöchentlich der grüne Blattflächenindex (LAI_g) mithilfe eines LI-3000A Sensors (LiCOR) ermittelt. Zudem konnte mittels eines photographischen Verfahrens der Pflanzenbedeckungsgrad des Bodens erfasst werden, wozu eine Epson Photo PC 3000 Z und eine Nikon Coolpix 8800 VR Kamera zum Einsatz kamen. Die photographischen Aufnahmen erfolgten unter Ausschluss direkter Sonnenstrahlung, um störende Schattenbildung zu vermeiden. Mithilfe eines automatischen Klassifikationsverfahrens ließen sich unterschiedliche Bedeckungsanteile ermitteln (grüne Pflanzen, vergilbte Pflanzen, Blüten, unbewachsener Boden). Nahezu zeitgleich wurden Messungen mit einem engbandigen Spektroradiometer (FAL II Sensor, Institut für Technologie und Biosystemtechnik, Braunschweig) durchgeführt. Dessen Bänder liegen u.a. im grünen (545–554 nm), roten (666–676 nm) und nah-infraroten (774–785 nm) Spektralbereich.

4. Ergebnisse

Exemplarisch zeigt Abb. 1 die Reaktion der drei breitbandigen Vegetationsindizes auf die Entwicklung eines Sommerrapsbestandes während der Vegetationsperiode. Die Termine einiger markanter phänologischer Phasen sind durch den BBCH-Code kenntlich gemacht. Das Ergrünen und die Abreife werden von allen drei Indizes deutlich widergespiegelt. Der um den Tag 120 einsetzende Einbruch des *NDVI* ist auf eine durch Niederschläge hervorgerufene Bodenverdunklung zurückzuführen, während für den Einbruch um den Tag 180 die Rapsblüte verantwortlich ist. Der *SAVI* und der *DVI* reagieren weniger empfindlich auf derartige Einflüsse.

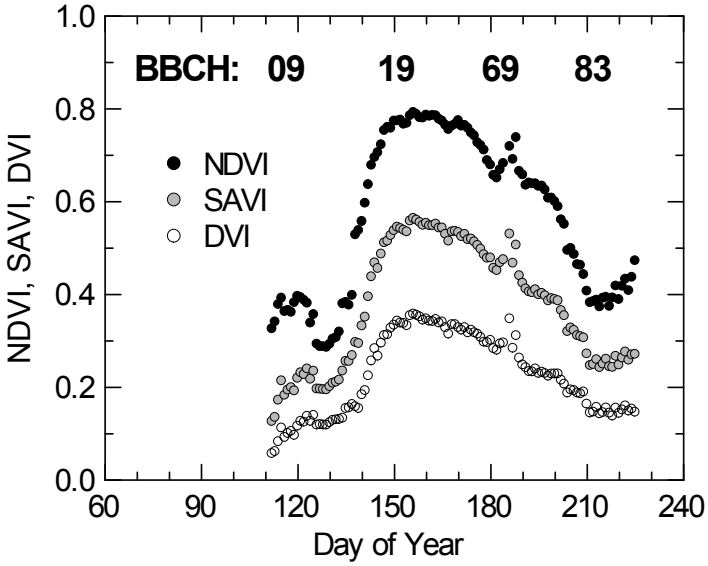

Abb. 1: Vegetationsindizes während der Wachstumsperiode eines Sommerrapsbestandes. Die Zahlen am Oberrand geben phänologische Stadien gemäß der BBCH-Skala an: 09 = Auflaufen, 19 = neun und mehr Blätter entfaltet, 69 = Ende der Blüte, 83 = 30 % der Schoten ausgereift

Fig. 1: Vegetation indices during the growth period of a summer rape crop. The numbers at the top stand for phenological stages described by the BBCH code: 09 = emergence, 19 = nine or more leaves unfolded, 69 = end of flowering, 83 = 30 % of pods ripe

Ein weiteres Beispiel bezieht sich auf die Beschreibung des grünen *LAI* durch den *NDVI*. Nachgewiesen sind exponentielle Abhängigkeiten, wobei der *NDVI* entsprechend der oben gegebenen Definitionsgleichung aus den Reflexionen des NIR- und des roten Spektralbereiches gebildet wird (s. z.B. Asrar et al, 1984). Die Frage ist deshalb, ob derartige Beziehungen sich durch die hier gemessenen breitbandigen *NDVI*s bestätigen lassen. Abb. 2 zeigt deshalb neben der Abhängigkeit des breitbandigen *NDVI*s vom grünen *LAI* auch jene des engbandigen roten und grünen *NDVI*s (letzterer basiert auf ρ_g anstelle von ρ_r). Als Referenzkurve ist die im engbandigen roten Spektralbereich über

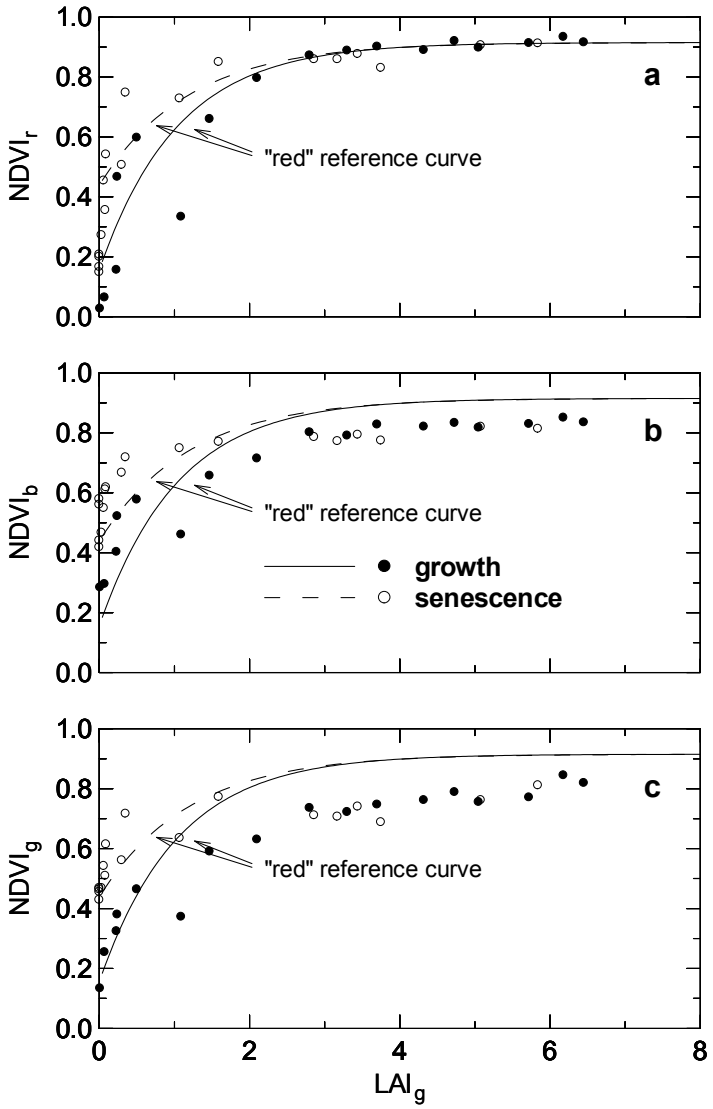

Abb. 2: Roter **(a)**, breitbandiger **(b)** and grüner **(c)** *NDVI* im Vergleich zum grünen *LAI* während der Wachstums- und Seneszenzphase eines Haferbestandes. Die eingezeichneten Verläufe der Referenzkurven basieren auf Messungen über Weizen gemäß Asrar et al. (1984) (aus Wittich and Kraft, 2008)

*Fig. 2: Red **(a)**, broadband **(b)** and green **(c)** NDVI compared to green leaf area index for growth and senescence periods of oat. The dashed and solid curves, inserted as a reference, are given by Asrar et al. (1984) for wheat (adopted from Wittich and Kraft, 2008)*

einem Weizenbestand aufgenommene exponentielle Funktion von Asrar et al. (1984) eingezeichnet. Diese wird durch die über Hafer im engbandigen roten Bereich durchgeführten Messungen bestätigt (Abb. 2a). Die im grünen Spektralbereich aufgenommenen Messdaten weichen in Richtung geringerer *NDVI*s ab (Abb. 2c), während die breitbandigen *NDVI*-Daten (Abb. 2b) zwischen den roten und grünen *NDVI*s liegen. Dieses Ergebnis entspricht aufgrund der breitbandigen spektralen Glättung der Erwartung.

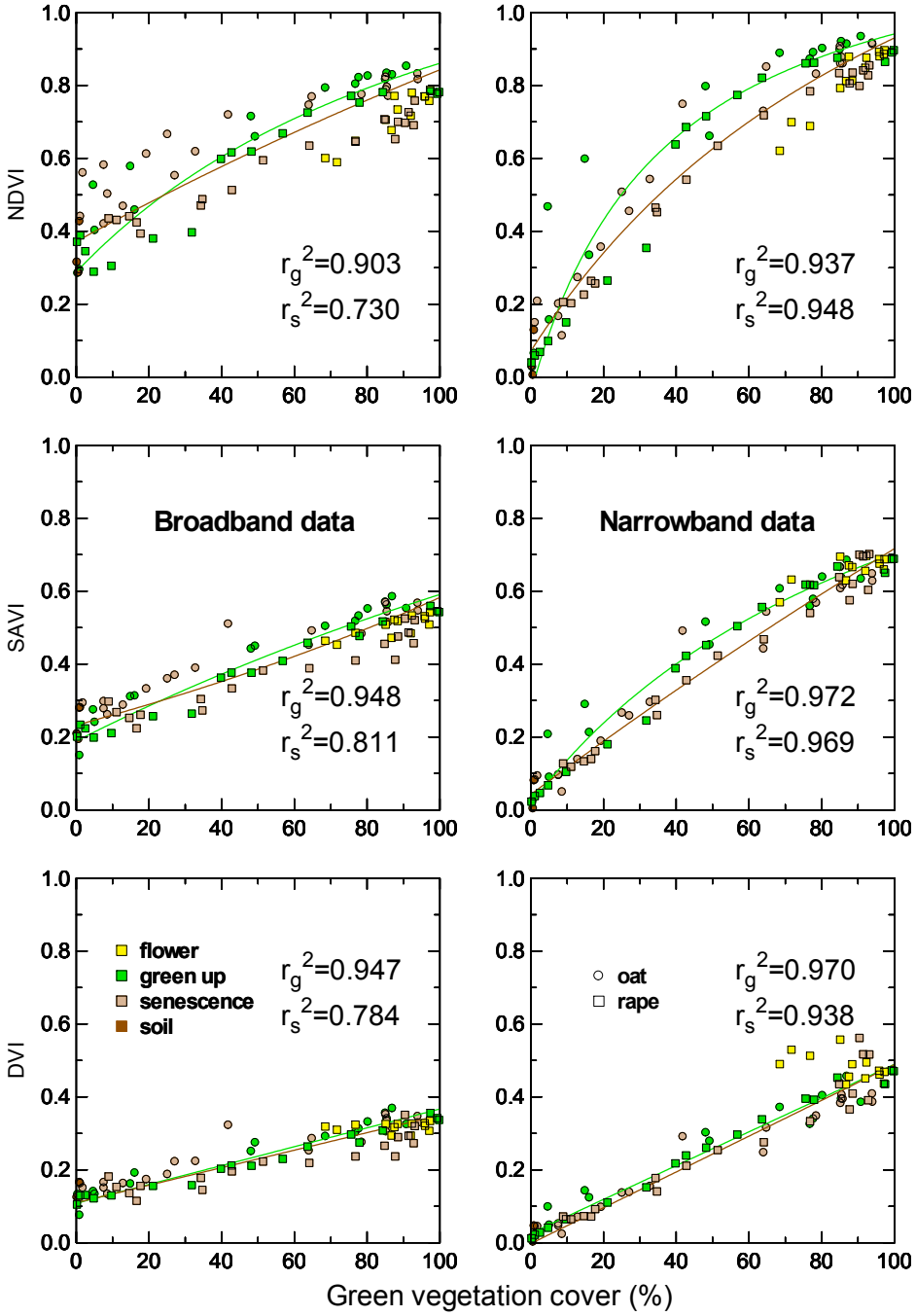

Abb. 3: Breit- und engbandige Vegetationsindizes in Abhängigkeit vom grünen Pflanzenbedeckungsgrad für Ergrünen und Abreife von Hafer und Raps

Fig. 3: Broad- and narrowband vegetation indices in dependence on green vegetation cover for green-up and senescence periods of oat and rape

Als weiteres Beispiel werden *NDVI*, *SAVI* und *DVI* gegenüber dem grünen Pflanzenbedeckungsgrad aufgetragen. Abb. 3 zeigt, dass aufgrund der spektralen Glättung die breitbandigen Indizes kleinere Jahresamplituden aufweisen und deshalb sich über engere Ordinatenbereiche erstrecken als die schmalbandigen Indizes. Darüber hinaus zeigt sich eine nichtlineare Abhängigkeit für den *NDVI*, während *SAVI* und *DVI* nahezu linear sind. Ferner weisen *SAVI* und *DVI* eine geringere Streuung auf als der *NDVI*.

5. Schlussfolgerungen

Die hier vorgestellten Messergebnisse zeigen, dass die Kombination üblicher agrarmeteorologischer Strahlungssensorik nützliche Information zur Bestandsentwicklung liefern kann. In der Literatur dokumentierte, auf *eng*bandigen Messungen beruhende Regressionsbeziehungen zwischen Bestandsparametern (z.B. LAI_g) und Vegetationsindizes dürfen allerdings nicht für *breit*bandige Eingabewerte verwendet werden, sondern müssen eine Koeffizientenanpassung erfahren. Darüber hinaus zeigt sich, dass der *NDVI* eine weniger geeignete Größe zur Beschreibung des Pflanzenbedeckungsgrades ist als der *SAVI* oder *DVI*.

References

Asrar, G., Fuchs, M., Kanemasu, E.T., Hatfield, J.L., 1984: Estimating absorbed photosynthetic radiation and leaf area index from spectral reflectance in wheat. Agron. J. 76, 300-306.

Huemmrich, K.F., Black, T.A., Jarvis, P.G., McCaughey, J.H., Hall, F.G., 1999: High temporal resolution NDVI phenology from micrometeorological radiation sensors. J. Geophys. Res. D 104, 27,935-27,944.

Jiang, Z. et al., 2006: Analysis of NDVI and scaled difference vegetation index retrievals of vegetation fraction. Remote Sens. Environm. 101, 366-378.

Nagai, S., Nasahara, K.N., Muraoka, H., Akiyama, T., Tsuchida, S., 2010: Field experiments to test the use of the normalized-difference vegetation index for phenology detection. Agric. Forest Meteorol. 150, 152-160.

Wittich, K.-P., Kraft, M., 2008: The normalised difference vegetation index obtained from agrometeorological standard radiation sensors: a comparison with ground-based multiband spectroradiometer measurements during the phenological development of an oat canopy. Int. J. Biometeorol. 52, 167-177.

Authors' address:

Dr. Klaus-Peter Wittich (klaus-peter.wittich@dwd.de)
Zentrum für Agrarmeteorologische Forschung, Deutscher Wetterdienst (DWD)
Bundesallee 50, D-38116 Braunschweig, Germany

Martin Kraft (martin.kraft@vti.bund.de)
Institut für Technologie und Biosystemtechnik, Johann Heinrich von Thünen Institut (vTI)
Bundesallee 50, D-38116 Braunschweig, Germany

The effect of climate on the phenology of wheat in Iran

Step 1: Homogenisation and calibration of observed temperature and ERA40 reanalysis in Iran

Elham Rahmani, Andreas Hense, Jan Keller, Petra Friederichs

Meteorological Institute, University of Bonn, Germany

Abstract

The impact of climate variability on wheat production in Iran is the main aim of this research. Over the last decade or so, climate change has gradually been recognized as an additional factor which, with other conventional pressures, will have a significant influence on the form, scale, and spatial and temporal impact on agricultural productivity. The basic research purposes are (1) Investigation of climate change in different areas of Iran in terms of qualitative and quantitative characteristics and determination of climate change trend on climatic parameters (2) Comparison of the result of different climate models in Iran, (3) Investigation for the effect of climate variability on wheat yield as a strategic crop and (4) determination of the effect of future climate change on wheat yield using results from (1) to (3). Given this general aims analysis of existing data in Iran was the first step. Climatic stations with long term data (42 years) in different locations of Iran were selected and temperature data considered in these stations. To achieve an accurate computation of mean daily data missing and wrong data had to be corrected and filled in as well. This has been done by means of a regression method using the available 3hourly data. In a second step the temperature data of the ECMWF Re-Analysis (ERA40) were compared with the Iran station temperature data. This comparison has been done for monthly and daily anomalies for the coldest and warmest month (February and August) as well as for the whole year by linear regression combined with bootstrapping. Then resulting spatial structures from the ERA40 data set can be combined with climate model output to perform a statistical downscaling.

1. Introduction

Several climate factors directly connect climate change and agricultural productivity: Average temperature increase, change in rainfall amount and patterns, rising atmospheric concentrations of CO2, pollution levels such as tropospheric ozone, change in climatic variability and extreme events. Most agricultural impact studies have considered the effects of one or two aspects of climate change on a particular farming activity. For instance the first factor, average temperature increase, an increase in average temperature can

1) Lengthen the growing season in regions with a relatively cool spring and fall
2) Adversely affect crops in regions where summer heat already limits production
3) Increase soil evaporation rates
4) Increase the chances of severe droughts (IPCC, 2007)

The frequency and magnitude of extreme weather events are assumed to increase with global warming. However, it is not clear how these events might affect agricultural crops and whether yield losses resulting from severe droughts or heat stress will increase in the future. (Semenov, 2009).

For other subtropical regions of the world it has been suggested that the projected climate change will have an apparently negative effect on wheat yield e.g. in Australia. This effect will only partly be compensated by increasing CO2 availability. These re-

sults have been obtained by combining results from global climate modelling (CSIRO's global atmosphere models CCAM-Mark2 and CCAM-Mark3) with the CropSyst model in Southeastern Australia. (Anwar et al., 2007)

2. Objectives

The specific objectives of the research presented below are

- Selecting the stations with long term data with a high temporal resolution of three hours in whole Iran,
- Quality control of the observed station temperatures in stations with a removal of the subdaily gaps using a regression method,
- Comparing the observed temperature data at the stations and the temperature data of ERA40 reanalyses by linear regression of monthly temperature anomalies of the coldest (February) and warmest month (August) as well as for the whole year. To estimate the sampling uncertainty bootstrapping will be applied.

3. Methodology

3.1. Quality control and missing data

From a data set of about 300 synoptic stations with three-hourly data we selected sixteen stations with long term data (42 years). These stations covered the whole Iran. Quality of the data was assessed visually by plotting all available data and registering obviously erroneous data or change points. Erroneous data were removed from the data set while no data in homogeneities could be identified. Overall the data quality was exceptional good. To fill up the gaps we developed a multivariate regression method for each station and each month based on the three-hourly values. The training data set was that part of the observed record which was complete. For each specific time of the day a multivariate regression was estimated using the remaining 7, 6 or 5 subdaily observations as predictors for the missing datum/data in case those 1 to 3 gaps of the three-hourly data were present. If more than three observations per day were missing, the complete day was considered as missing. This rather strict constraint could be relaxed in future e.g. if only daily averages are to be analysed. Figs (1, 2, and 3) show some time series in Tabriz in North West of Iran.

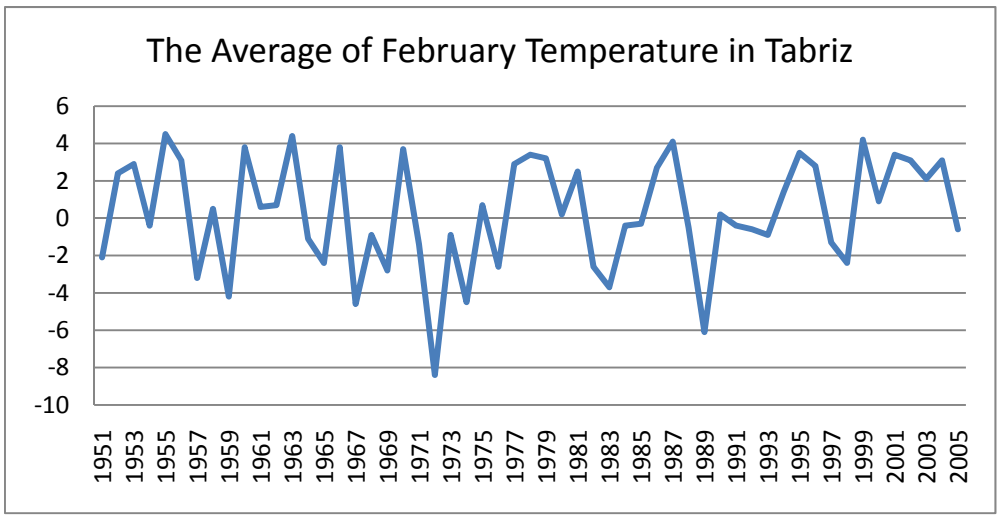

Fig. 1: The average of February temperature in 54 years time series in Tabriz

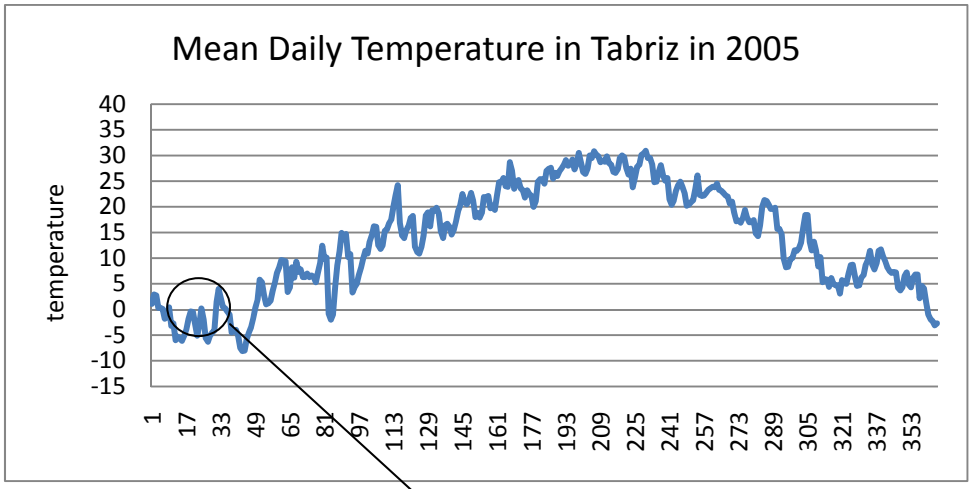

Fig. 2: The average of daily temperature in Tabriz in 2005

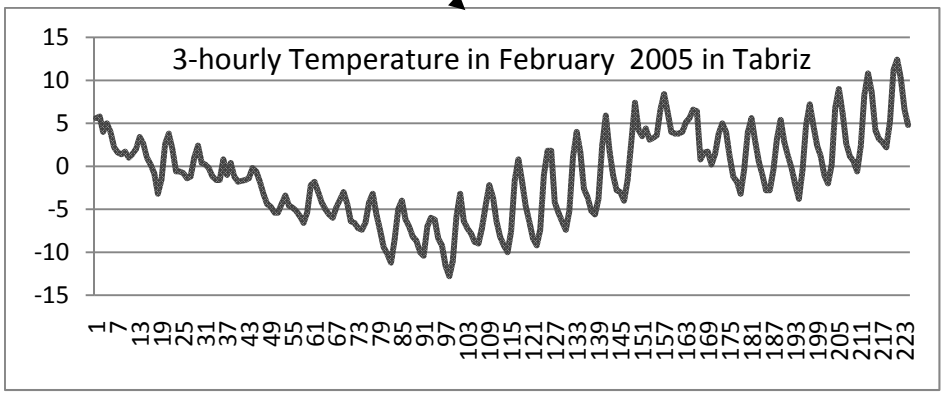

Fig. 3: The 3-hourly temperature in February 2005 in Tabriz

Relations between observed temperature data and ERA40 data

The aim of this part is to derive and present large scale representative patterns of near surface temperature as proxies for the local near surface temperature variability. We turned to ERA-40 reanalyses at 806 grid points covering Iran and parts of the neighbouring countries. Due to the complex orographic structure within Iran and the possible influence of two rather large water bodies (the Persian Gulf to the south and the Caspian Sea to the north) we performed a univariate linear regression between each ERA-40 grid point temperature as predictor and each single station as predictand.

$$T_{obs}=a+bT_{era}+E_i$$

Then the estimated regression coefficient b and the respective squared correlation coefficient are functions of the grid point coordinates and can be presented as maps. They are estimated from the data by minimizing the residual errors E_i. To avoid a contamination from the annual cycle monthly anomalies from the 42 year monthly means for the whole year were considered first. Additionally month specific regressions for February as the coldest month and August as the warmest month were estimated to document the seasonality in the regression.

3.2.1. Re-sampling the data based on bootstrap method

In case of the regression analysis for February or August the regression is based in 42 monthly mean values from ERA-40 and the respective station. To estimate the sampling uncertainty of the regression results we used bootstrapping.

The bootstrap method of resampling was invented in the 1970's by Bradley Efron. That is a computing intensive procedure that simulates a statistical population using the original sample set of data (Chernick, 2007). The simulated population is used to make judgments regarding the statistical analyses performed on the original sample set of data.

Instead of relying of the theoretical sampling distributions for certain sample sizes, the bootstrap procedure creates an empirical distribution for a sample statistic through a repeated sampling with replacement from the original sample (Chernick, 2007). For each newly simulated sample the statistics – in our case the regression results– are computed. The sampling uncertainty of the regression results is assessed by analysing the regression coefficients and squared correlation from the bootstrap sample which has in our case a sample size of 1000. The test of the Nullhypothesis $b=0$ at a significance level p can be performed by calculating the empirical $p/2$ and $1-p/2$ quantile of the bootstrapped regression coefficient. If the interval between these two quantiles contains the value $b=0$, the Nullhypothesis has to be accepted.

4. Results

Correlation and regression coefficient between bootstrapped anomalies of monthly temperature from observed data and ERA40 for selected stations in north, south, west and east of Iran as examples are shown in (Fig. 4) and (5). Grid points where the Nullhypothesis has to be accepted are marked with a grey dot. The colour shaded areas indicate the squared correlation as a measure for the strength of the linear relation between the station and ERA-40 data and the contour lines the estimated regression coefficients. Ideally one would expect $b \sim 1$ in the vicinity of the station. However, due to the fact that ERA-40 does represent larger scales in space and time than the local stations the regression coefficient must deviate from the ideal case.

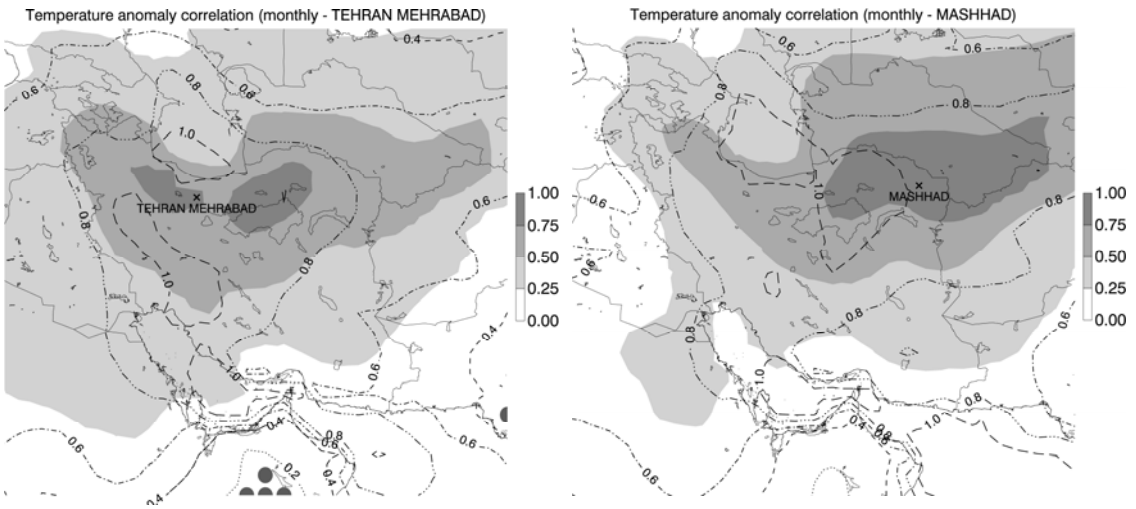

Fig. 4: Correlation and regression coefficient between bootstrapped anomalies of monthly temperature (whole year) for observed and ERA40 data at Tehran Mehrabad (left) and Mashhad (right)

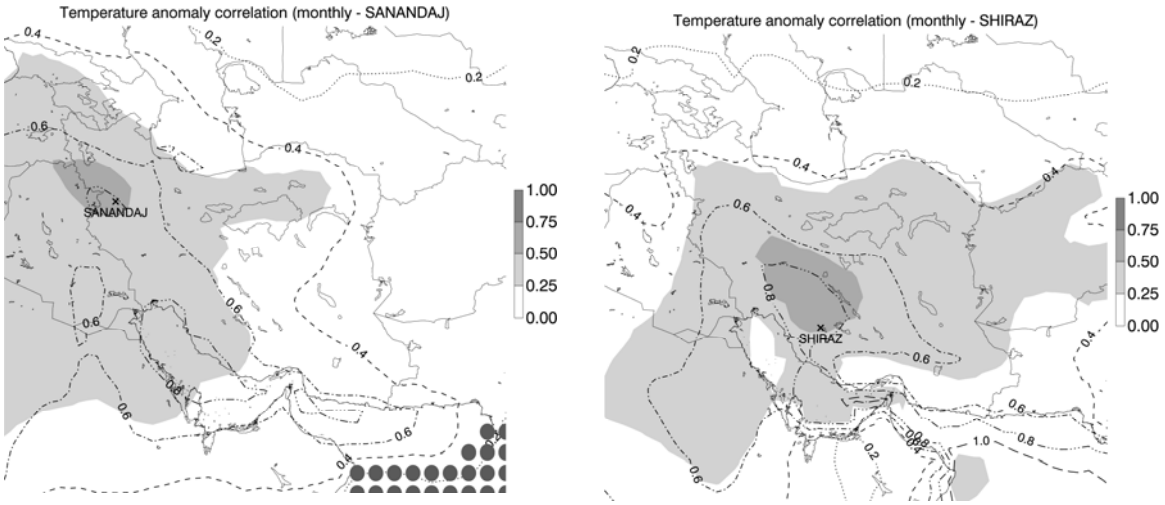

Fig. 5: same as Fig. (4) but for station Sanandaj (left) and Shiraz (right)

The results indicate a rather complex behaviour of temperature variability in Iran. The two northern station and more elevated Tehran Mehrabad and Mashhad (Fig. 4) give a very pronounced structure elongated in East-West direction with a clear influence of the Caspian Sea and of the mountain ranges Alborz Mountains. The latter can be seen by a comparison (not shown) with a station northwest from Tehran situated at the Caspian Sea shore. The other two stations to the west and to the south (Sanandaj and Shiraz, Fig. 5) leave a less clear fingerprint in the ERA-40 data although the squared correlation coefficients are still large and significantly nonzero.

The seasonality of the patterns can be viewed in Fig. (6) for the station Tehran Mehrabad. Both patterns resemble the "banana" shaped annual pattern (Fig. (4)) but the summer pattern is much smaller in its spatial extend. This can be expected because during summer local variability dominates much more the observed temperature record which is not represented in the ERA-40 data set. Overall the results indicated that simple spatial patterns like area averages or empirical orthogonal functions are not suitable for downscaling because they would not take into account the apparent dependency on the topographical settings of Iran.

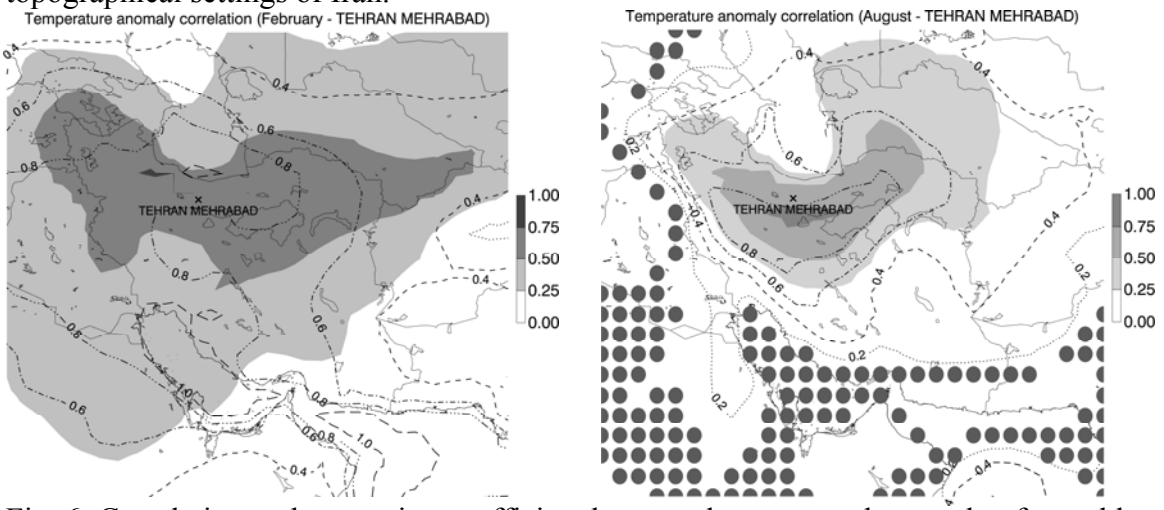

Fig. 6: Correlation and regression coefficient between bootstrapped anomaly of monthly temperature in February (left) and August (right) for observed and ERA40 data in Tehran Mehrabad

4. Conclusions

This study presented first results on a regional climate downscaling exercise which will be used for studying the effects of climate variability and climate change on wheat phenology and yield in Iran. Local temperature variability which is the important driver for phenology is well to very well represented in the ERA-40 data set. Coherent large scale structures can be used as predictors or fingerprints to related large scale information e.g. from a global climate model to local climate in a statistical sense.

Acknowledgment

The authors are indebted the German Academic Exchange Service, DAAD (Deutscher Akademischer Austausch Dienst) for funding the research project.

References

Anwar, M., O'Leary, G., McNeil, D., Hossain, H., Nelson, R., 2007: Climate change impact on rainfed wheat in south-eastern Australia. Field Crops Research. 104, 139-147.

Chernick, M., Bootstrap Methods: A Guide for Practitioners and Researchers. Second Edition, 400 pages, December 2007, Copyright © 2008 by John Wiley & Sons, Inc.

IPCC Working Group II, Fourth, 2007: Climate Change Science Program Synthesis and Assessment Product 4.3: The effects of global change on agriculture, biodiversity, land, and water resources, U.S. National Assessment, Agriculture Sector, U.S. Department of Agriculture Climate Change Resources.

Semenov, M., 2009: Impacts of climate change on wheat in England and Wales. J. R. Soc. Interface. 6, 343-350.

Author's address:

Elham Rahmani (erahmani@uni-bonn.de)
Andreas Hense (ahense@uni-bonn.de)
Jan Keller (jkeller@uni-bonn.de)
Petra Friederichs (pfried@uni-bonn.de)
Meteorological Institute, University of Bonn
Auf dem Hügel 20, 53121 Bonn, Germany

Guttation: Bedeutung, Beobachtung, Vorhersage

H. Braden

Deutscher Wetterdienst (DWD), Zentrum für Agrarmeteorologische Forschung, Braunschweig

Zusammenfassung

Das Auftreten von Guttation wurde an unterschiedlichen Pflanzenarten jeweils in den Morgenstunden beobachtet. Um eine eindeutige Unterscheidung zwischen Guttation und Taubildung zu ermöglichen, wurden unterschiedliche physikalische Eigenschaften getestet. Mit Hilfe des agrarmeteorologischen Modells AMBETI/BEKLIMA wurde versucht, das Auftreten von Guttation vorherzusagen. Weil das Modell jedoch keinen aktiven, durch osmotisch erzeugten Wurzeldruck verursachten, Wassertransport berücksichtigt, lässt sich das Auftreten von Guttation nur eingeschränkt berechnen. Die Häufigkeit des Auftretens von Guttation wird abgeschätzt.

Guttation, importance, observation, forecasting

Abstract

The occurrence of guttation on several plant species has been observed during the morning hours from May until September 2009. In order to properly distinguish between guttation and dew, different measuring methods have been tested. The model AMBETI/BEKLIMA was applied in order to forecast guttation. But this was of restricted success because the model does not consider osmotic water transport.

1 Einleitung

Guttation macht sich vor allem durch das Austreten von Xylemsaft an Blatträndern bemerkbar. Erfahrungsgemäß tritt Guttation vor allem bei guter Wasserversorgung der Pflanzen und bei geringer Verdunstungsbeanspruchung auf. An einigen Pflanzenarten, wie Frauenmantel, wird der Effekt besonders häufig beobachtet. Neuerdings steht dieser Effekt im Verdacht, für Bienensterben verantwortlich zu sein. Systemisch wirkende Pflanzenschutzmittel, die z.B. in Beizen von Saatgut enthalten sind, können auf diesem Weg zur Vergiftung von Bienen führen, die von den Tropfen trinken (Girolami et al., 2009; Wallner, 2009). Ziel dieser Untersuchungen war es daher, die Kenntnisse über das Phänomen zu erweitern, Aussagen über die Häufigkeit von Guttation zu machen und ihr Auftreten vorherzusagen.

2 Material und Methoden

Auf den Versuchsflächen des Zentrums für Agrarmeteorologische Forschung in Braunschweig wurden unterschiedliche Pflanzenarten in der Zeit von Mai bis September 2009 an insgesamt 60 Tagen jeweils in den Morgenstunden beobachtet, um festzustellen, ob Guttation aufgetreten war. Die Beobachtungen wurden an unterschiedlichen Pflanzenbeständen durchgeführt: an einem Winterweizen Bestand, an einer bewässerten Grasfläche, an Erdbeerpflanzen sowie an Frauenmantel.

Unterschiedliche physikalische Eigenschaften wurden versuchsweise herangezogen, um eine rasche, eindeutige Unterscheidung zwischen Guttation und Taubildung zu ermöglichen. Das wäre um so mehr wünschenswert, als beide Effekte oftmals gleichzeitig auftreten.

Der elektrische Widerstand wurde mit einem Vielfach-Messgerät direkt an (vermeintlichen) Guttationstropfen gemessen. Es konnte jedoch kein hinreichend kleiner Widerstand festgestellt werden, der eine Unterscheidung von Tau ermöglicht hätte.
Mit Hilfe von Universal-Indikatorpapier (pH 1-11) wurde versucht, Tau und Guttationstropfen aufgrund unterschiedlicher pH-Werte zu unterscheiden, jedoch lagen die pH-Werte nicht unterscheidbar im neutralen Bereich. Auch der Brechungsindex war in beiden Fällen mit Hilfe eines Refraktometers (ATP Messtechnik+Waagen, 0-32% Brix) von dem reinen Wassers nicht eindeutig zu trennen.
Eine Feldmethode zur Unterscheidung von Guttation und Tau konnte damit nicht gefunden werden. Die eindeutige Abgrenzung bleibt damit weiterhin aufwendigen Laboranalysen vorbehalten, bei denen im allgemeinen mit chromatographischen Methoden aus dem Boden stammende Stoffe wie Pflanzenschutzmittel nachgewiesen werden.
Für diese Untersuchungen musste daher ersatzweise weiterhin das optische Erscheinungsbild charakteristischer großer, vor allem an den Rändern auftretender Tropfen zur Unterscheidung genutzt werden. Zudem wurden die beobachteten Pflanzen (außer Winterweizen) in der Regel nachts abgedeckt, wenn kein Niederschlag zu erwarten war, damit kein Tau auftreten sollte.

Abb. 1: Guttation an Frauenmantel

Fig. 1: Guttation on Lady's Mantle

Mit Hilfe des agrarmeteorologischen Modells AMBETI/BEKLIMA (Braden, 1995) wurde versucht, das Auftreten von Guttation vorherzusagen. Das Modell AMBETI/BEKLIMA ist ein eindimensionales Modell des Energie- und Wasserhaushalts im System Boden-Pflanze-Atmosphäre. Der Wärme- und Wasserhaushalt des Bodens wird für mehrere Schichten berechnet. Der pflanzliche Wassertransport wird – angetrieben durch die Wasserpotentialdifferenz zwischen Pflanzenblättern und Boden – durch ein Leitungssystem von Wurzeln und Spross beschrieben. Das Blattwasserpotential ist zudem eine Regelungsgröße für die Transpiration.

3 Ergebnisse

Weil das Modell jedoch keinen aktiven, durch osmotische Potentiale verursachten Wassertransport berücksichtigt, lässt sich das Auftreten von Guttation auf diese Weise nicht direkt modellieren. Daher wurde nach Kriterien gesucht, bei denen das Auftreten von Guttation zu erwarten ist.

Am ehesten erfolgversprechend erschien dafür eine geringe Wasserpotentialdifferenz zwischen Blättern und Zentralwurzel, weil diese am leicht durch ein osmotisches Potential überwunden werden kann. Ebenfalls als aussichtsreich wurden geringe Flüsse von Transpiration und Bestandsverdunstung angesehen. Darüber hinaus wurde auch getestet, ob eine gute Wasserversorgung des Wurzelraums oder eine hohe Luftfeuchtigkeit im Bestand als Kriterium heran gezogen werden können.
Diese Modellergebnisse wurden mit den Beobachtungen während niederschlagsfreier Stunden an Gras verglichen, weil diese Beobachtungen zuverlässiger waren und in größerer Zahl vorlagen, als die anderer Pflanzenarten. An 23 der 60 Beobachtungstage wurden an Gras als Guttation interpretierte Tropfen beobachtet.
Bei Tests der einzelnen Kriterien mit unterschiedlichen Grenzwerten stellten sich folgende als die günstigsten heraus:

- "q": Transpirationsfluss < 1 g m²/h
- "p": Wasserpotentialdifferenz zwischen Blättern und Zentralwurzel < 0.001 Pa
- "w": Wassergehalt im Wurzelraum > 60% nutzbarer Feldkapazität
- "m": Luftfeuchte im unteren Bestandsraum > 96% .

Darüber hinaus wurden auch Kombinationen zweier Kriterien getestet, z.B. "p^q", wobei sowohl "p" als auch "q" zutreffen. In allen Fällen wurde geprüft, ob das jeweilige Kriterium in den Morgenstunden bis zum Beobachtungstermin aufgetreten war. Die Auswertung der Modellergebnisse nach diesen Kriterien wurden mit den Beobachtungen verglichen und ist in Tabelle 1 dargestellt. Dabei bedeutet "M^B" die Anzahl der Fälle, bei denen die jeweilige Modellauswertung in Übereinstimmung mit der Beobachtung Guttation ergibt. Unter "M^¬B" steht hingegen die Anzahl der Fälle, bei denen die Modellauswertung im Gegensatz zur Beobachtung "Guttation" anzeigt. Die beiden letzten Spalten geben die jeweiligen Anteile einerseits korrekter und andererseits nicht zutreffender interpretierter Modellergebnisse wieder.

Tab. 1: Auswertung von Modellergebnissen im Vergleich mit Guttationsbeobachtungen (siehe Text)

Tab.1: Interpretation of model results compared with observations of guttation (see text)

Kriterium	**M^B**	**M^¬B**	**¬M^B**	**¬M^¬B**	**korrekt**	**Irrtum**
"q"	22	22	1	15	**62%**	38%
"m^q"	19	20	4	17	60%	40%
"m"	20	21	3	16	60%	40%
"p"	21	20	2	17	**63%**	37%
"w"	18	25	5	12	50%	50%
"p^q"	21	19	2	18	**65%**	35%
"m^p"	19	17	4	20	65%	35%
"m^w"	16	15	7	22	**63%**	37%

Die Irrtumswahrscheinlichkeiten sind in allen Fällen beträchtlich, jedoch liefert die Modellinterpretation bei beobachteter Guttation nur wenige negative Aussagen (**¬M^B**). Das trifft insbesondere auf das Kriterium "q" (=Transpiration nur minimal) zu. Ähnliche Ergebnisse mit leicht erhöhtem Anteil korrekter Aussagen liefert das Kriterium "p" sowie die Kombination "p^q". Gegenüber den Beobachtungen liefert die Auswertung der Modellergebnisse übereinstimmend nach allen Kriterien annähernd die doppelte Häufigkeit von Guttation. Ursache dafür könnten, neben der zu erwartenden Unzulänglichkeit der Modellierung, auch zu späte Beobachtungszeiten sein. Möglicherweise waren Guttationstropfen bei der Beobachtung bereits wieder verschwunden.

Um die Häufigkeit von Guttationserscheinungen und die damit verbundene Gefährdung von Bienen abschätzen zu können, wurden mit dem Modell AMBETI/BEKLIMA Rechnungen für Braunschweig und Mannheim durchgeführt. Dabei wurde für Winterweizen vom 90. bis zum 190. Jahrestag und für Gras vom 90. bis zum 260. Jahrestag nach dem Kriterium "p^q" ausgewertet. Tabelle 2 enthält die sich jeweils ergebende Anzahl von Tagen sowie die davon für Bienen gefährlichen Tage, an denen morgens kein Niederschlag fiel und die Temperaturen nicht unter 12°C lagen.

Tab. 2: Anzahl der Tage mit Guttation nach Modellkriterium "p^q"
Tab. 2: Number of days with guttation according to criterion "p^q"

	BS 2009	BS 2009	MH 2002	MH 2003	MH 2004
	WiWei	Gras	Gras	Gras	Gras
"p^q"	61	131	115	91	108
bienengefährlich	34	77	76	65	69

Auch wenn die beobachtete Guttationshäufigkeit nach Tab. 1 durch die Modellierung erheblich überschätzt werden sollte, ist noch an vielen Tagen mit Guttation zu rechnen, die nach Ausbringen von Pflanzenschutzmitteln bienengefährlich sein kann.

4 Schlussfolgerungen

Die Untersuchungen haben gezeigt, dass das Auftreten von Guttation mit Hilfe des Modells AMBETI/BEKLIMA mit einigen Einschränkungen vorhergesagt werden kann. Bei der Beurteilung der Vorhersagequalität sollte auch der beschränkte Umfang der Beobachtungsdaten und der möglicherweise ungünstige Beobachtungszeitpunkt berücksichtigt werden. Auch wenn man von einer erheblichen Überschätzung der Guttationshäufigkeit ausgeht, ist an zahlreichen Tagen einer Vegetationsperiode mit Guttation zu rechnen, die nach Girolami et al. (2009) für Bienen eine tödliche Gefahr darstellen kann, wenn entsprechende systemische Pflanzenschutzmittel ausgebracht wurden.

Literatur:

Braden, H, 1995: The model AMBETI. – A detailed description of a soil–plant–atmosphere model, Berichte des Deutschen Wetterdienstes, Nr. 195, 117 p., Offenbach am Main.

Girolami, V., L. Mazzon, A. Squartini, N. Mori, M. Mararo, A. di Bernardo, M. Greatti, C. Giorio, and A. Tapparo, 2009: Translocation of Neonicotinoid Insecticides From Coated Seeds to Seedling Guttation Drops: A Novel Way of Intoxication for Bees. J. Econ. Entomol. 102(5): 1808-1815.

Wallner, K., 2009: Guttation: Tropfen, die es in sich haben. Deutsches Bienen-Journal (4) 18-19.

Anschrift des Autors:
Dr. Harald Braden, Deutscher Wetterdienst, Zentrum für Agrarmeteorologische Forschung, Bundesallee 50, 38116 Braunschweig

Climate Change and Fruit Growing in Germany (KliO)

Frank-M. Chmielewski[1], Klaus Blümel[1], Yvonne Henniges[1], Antje Müller[1], Roland W.S. Weber[2]

[1]Humboldt-University of Berlin,
Faculty of Agriculture and Horticulture, Professorship of Agricultural Climatology, Germany
[2]Fruit Growing and Consulting Service Jork, Germany

Abstract

The changing climate conditions could have increasingly strong implications for fruit growing at the end of this century. Fruit trees will need more irrigation in summer, trees and shrubs will blossom earlier and in particular their fruit will start to ripen earlier. The period for fruit development will therefore be shortened. Among other consequences, this could result in lower apple yields. The earlier apple blossom also increases the risk of late frost inflicting slight damage on the apple yield. Towards the end of the century, the markedly increasing temperatures in autumn and in winter could result in insufficient cold stimulation for the trees. Moreover, the higher temperatures will provide better development conditions for the codling moth, so more than one generation of this pest will be able to develop within the course of the year.

1. Introduction

The general objective of the BMBF research project KliO was to investigate the impact of climate change on fruit growing in Germany and to identify regional differences in potential vulnerability, in order to develop sustainable and practice-oriented adaptation strategies. To this end, climatic changes were analysed in eleven fruit growing regions in Germany on the basis of climate scenarios up to 2100. From this, the climate-related damages to apple production were estimated and evaluated in economic terms.

2. Data and Methods

Climatic data from the German Weather Service (period 1961-2005, reference period 1961-1990) and climate scenarios from the Max-Planck-Institute for Meteorology and Deutsches Klimarechenzentrum in Hamburg/Germany (ECHAM5/OM with the statistical downscaling method WETTREG, emission scenarios B1, A1B until 2100) were used to analyse recent and possible future climate changes in the German fruit growing regions. On the basis of different mechanistic models (phenological models, water-budged and yield models, pest models, etc.) the impact of climate change on apple growing in Germany was investigated. Altogether four different damages (due to a lack of chilling, late frost, the codling moth, and direct yield losses due to climate change) and methods to avoid these damages (adaptation strategies such as chemical applications to break dormancy, irrigation for frost protection, pest control, and summer-irrigation) were considered. In order to estimate the *total damage* D_{tot} the four *individual damages* d_i were sorted according to their temporal appearance within the year, in order to consider the extent of primarily damages (see later Fig. 2 and 3).

$$D_{tot} = 1 - \prod_{i=1}^{N} (1 - d_i) \quad \left[\neq \sum_i d_i \right] \tag{1}$$

However, the total *costs of adaptation measures*

(C_{tot}) can be calculated as the simple sum of the individual adaptation costs c_i.

Thus, the annual *cost of climate change* in the apple-growing sector (C_{CC} in Euros per ha and year) is the sum of the costs for damages and adaptation measures. The costs for damages can be estimated if D_{tot} is multiplied by the maximal revenue for apples per hectare without any damages (R_a in Euros per ha). All changes of damages and adaptation measures were calculated for two different periods (P_1: reference period, 1961-1990; P_2: future period e.g. 2071-2100).

$$C_{CC} = \left(\overline{D_{tot}}^{P_2} - \overline{D_{tot}}^{P_1}\right) R_a + \left(\overline{C_{tot}}^{P_2} - \overline{C_{tot}}^{P_1}\right) \quad (2)$$

Additionally, two adaptation strategies we considered in KliO. In the first strategy (w/o-strategy = with/without adaptation) only summer-irrigation and extensive pest control was done for the both periods (P_1, P_2). In the second strategy (w-strategy = with additional adaptation) only for future periods chemical products to break the dormancy, frost protection, and intensive pest control were introduced, beyond summer-irrigation. Over and above this, the cost and damages were estimated without any adaptation measures for current and future periods (o-strategy, not considered in this paper). Equation (2) can be used to estimate the sectoral costs of climate change for any periods and any adaptation strategies.

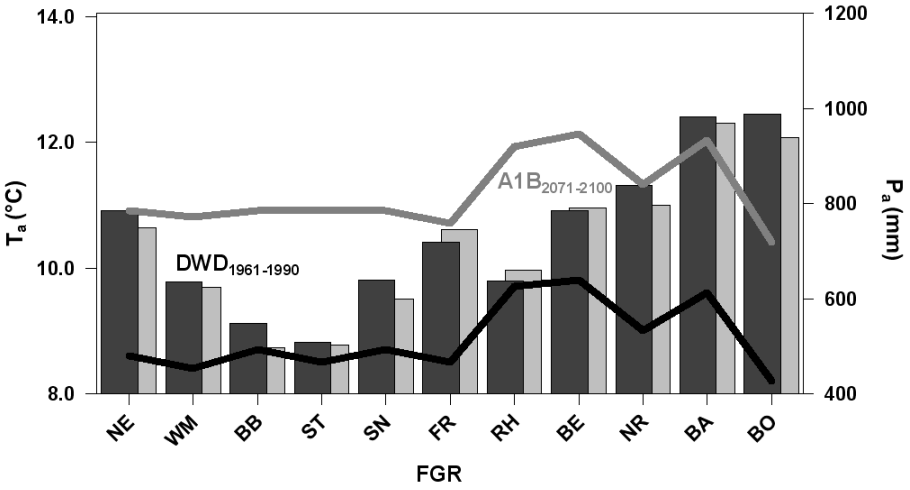

Fig. 1:
Possible changes in mean annual air temperature (T_a, lines) and annual precipitation (P_a, bars) in the fruit growing regions of Germany (FGR) (black: 1961-1990, gray: 2071-2100, WETTREG scenario A1B)
ΔT_a = + 2.3 °C***
ΔP_a = -17.3 mm^{ns}

3. Results

3.1 Possible Climate Change in the Fruit Growing Regions

The investigation has shown that the mean annual temperature in the German fruit growing regions could rise up to 2.3 °C (scenario A1B, mean of all eleven fruit growing regions, 2071-2100 vs. 1961-1990). The greatest temperature rises will be in winter (+3.8 °C), followed by summer (+2.3 °C) and autumn (+2.1 °C). Only in spring the temperature will rise by just 1.0 °C. Changes in the annual level of precipitation are insignificant, although there will be an identifiable shift of summer precipitation (-52 mm) to the winter months (+60 mm). In both scenarios, the strongest reduction of summer precipitation could occur in the area 'Neckarregion' (NR: scenario B1: -74 mm, scenario A1B -77 mm).

In all fruit growing regions the thermal growing season will be extended by at least one month (scenario B1). In most regions the extension of growing season is much stronger, for example in the region 'Niederelbe (NE)' between 69 (B1) and 95 days (A1B) and in the region 'West-Mecklenburg' by 57 (B1) and 82 days (A1B).

3.2 Climate Related Damages in Apple Growing

In the course of the project, changes of the following damages on apples were investigated:

- Possible damages due to insufficient chilling of trees (dormancy damage d_D),
- Damages by late frost events up to ten days after the beginning of apple blossom (late frost damage d_F),
- Damages due to an increased number of codling moth generations per year (codling moth damage d_C),
- Changes in apple yield due to climatic changes and changes in the length of ripening period (direct yield losses d_Y).

i) Dormancy damages

Generally, insufficient chilling has been recognized as an economic problem in fruit production. Symptoms of insufficient chilling are manifold. It can occur that the blossoming time of fruit trees is delayed and extended, the trees start to flower irregular, and in extreme cases a total lack of bud break can occur. For current climatic conditions the chilling requirement of apple trees is usually fulfilled to the end of the previous year or in the beginning of the harvest year. However, rising temperature in autumn and winter could influence the timing of dormancy release.

In KliO the probability for an insufficient chilling (P_C, 0…1) was calculated by different methods (phenological chilling/forcing models, chilling hour method). The yield-damage (d_D) was calculated as the product of P_C and 25 %. This means we assumed a 25% yield damage if the probability for an insufficient chilling is 1. In all investigated regions P_C was less than 0.20 up to the end of this century, so that these minor damages in individual years could be avoided by chemical applications (hydrogen cyanamide, e.g. Dormex). The adaptation costs c_D were balanced with 232 Euros per ha. An alternative solution would be to grow apple varieties with a lower chilling requirement, which is widely ranging between 1800 and less than 500 chilling hours.

ii) Late frost damages

In order to estimate changes in the frequency of late frost up to 10 days after the beginning of apple tree blossom, phenological models were used to calculate changes in the blossoming date up to 2100. Then the probability for late frost after the beginning of blossom was estimated. It was necessary to classify the frost events according to their strength, because it influences the extent of flower damage. The yield damage (d_F) is different from the flower damage, because light flower damages would not have any effect to the apple yield. For this reason we assumed that 25 % of killed flowers could lead to yield losses by 10 % and 75 % of damaged flowers to yield losses of 70 % (linear interpolation in between). The best method to avoid yield losses is frost sprinkling. For this, the cost could range between 212 Euros per ha (sites far away from ground water) and 172 Euros per ha (sites close to ground water). We assumed that a correct use of sprinklers in frost nights would prevent any damages.

iii) Codling moth damages

Already today, pest control is an important issue in fruit growing. The revenue for afflicted apples is only one third compared to dessert apples. Annual pest control is also necessary to avoid stronger infestation in the following year. These days, we have only one or in extremely warm years even 1.5 generations of codling moth per year, so that extensive pest control is sufficient. Rising temperatures and a longer growing season can lead to two or even more generations per year. In this case more efficient methods for pest control have to be applied (intensive pest control) which would increase the adaptation cost. The total management costs depend strongly on the number of codling moth generations per year. In KliO we calculated both the cost for pesticides (control) agents and the work efforts, depending on the number of generations per year. We also assumed that in both control strategies some damages remain which depend on the number of generations per year. Detailed information is given in Chmielewski et al. (2009a).

iv) Direct yield losses

Apple yields depend on a number of factors, so that it is very difficult to consider all of them in a simulation model. Site conditions (climate, soil), the variety, the tree density, the tree training (height, shape) as well as the age of the trees belong to these factors (Büchele, 2008). Additionally, fruit trees show alternating in yields. Despite these complex processes, we tried to implement a seven year old apple tree (constant age) into the water budged and yield formation model SIMWASER. Since the model was able to calculate the average apple yields for common varieties such as 'Elstar' or 'Jonagold' we used the model to estimate possible yield changes due to climate change. The direct CO_2-fertilisation effect, which could be important for fruit trees (Janssens et al., 2000; Ainsworth and Long, 2005), was not considered yet.

v) Summer-irrigation

Drop irrigation is a common practice in orchards. The model SIMWASER allows to simulate the soil moisture in individual soil layers for different crops, using daily weather data. Additionally, for each crop a set of plant parameters is necessary in order to calculate the plant development (phenology) and biomass increment. For all fruit growing regions the soil types of each simulated layer have to be known.

In KliO we considered a soil depth up to z=1.5 m. Irrigation was done if the mean relative available field capacity (W_{rel}) for the soil layers up to 0.6 m depth was below 0.5. In this case, on the next day irrigation was started. The amount of irrigation (IRR) was calculated in such a way that after the irrigation W_{rel}=0.8 in all upper layers up to 0.6 m depth. The required amount IRR can be calculated as follows:

$$IRR = \sum_{i=1}^{N} \left[0.8 - W_{rel}\right] \cdot \left(FC_i - WP_i\right) \cdot \Delta z_i \quad , \tag{3}$$

were FC_i is the field capacity and WP_i is the wilting point of the soil layer 'i'. The daily irrigation was limited to 24 mm per day. If the total amount of irrigation was higher than 24 mm the applications were spread on several days.

3.3 Possible Costs of Climate Change for Apple Growing in Germany

The changing climate conditions could have increasingly strong implications for fruit growing by the end of this century (Fig. 2, left). Fruit trees will need more irrigation in summer, the trees will blossom earlier and, in particular their fruit will start to ripen earlier. The period for fruit development would therefore be shortened. Among other consequences, this will result in some lower apple yields. The earlier apple blossom also increases the risk of late frost inflicting slight damage on the apple yield. Towards the end of the century, the markedly increasing temperatures in autumn and in winter could result in insufficient cold stimulation for the trees. Moreover, the higher temperatures will provide better development conditions for the codling moth, so more than one generation of this pest will be able to develop within the course of the year.

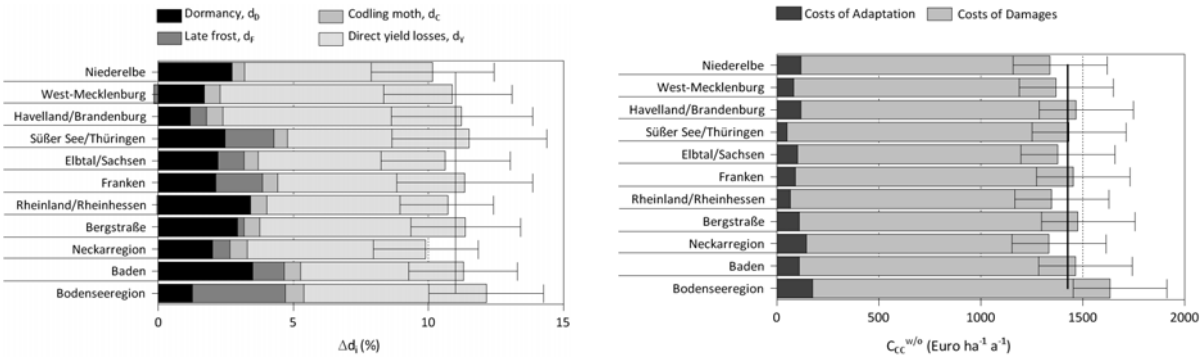

Fig. 2: Left: Changes of individual damages (Δd_i) due to climate change 2071-2100 vs. 1961-1990 and right: Costs of climate change ($C_{CC}^{w/o}$) for apple growing in Germany, 2071-2100 vs. 1961-1990, WETTREG Scenario A1B, without additional adaptation; only summer-irrigation and extensive codling moth control is done (w/o-strategy)

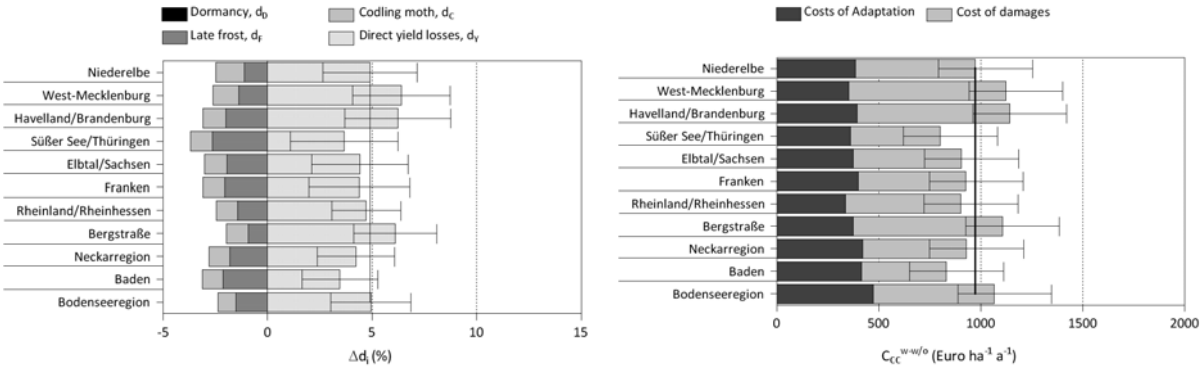

Fig. 3: Left: Changes of individual damages (Δd_i) due to climate change 2071-2100 vs. 1961-1990 and right: Costs of climate change ($C_{CC}^{w-w/o}$) for apple growing in Germany, 2071-2100 vs. 1961-1990, WETTREG Scenario A1B, with additional adaptation measures such as extended summer-irrigation, chemical solutions to break dormancy, frost protection, and intensive codling moth control between 2071-2100 (w-w/o-strategy)

Consequently, at the end of this century (2071-2100), climate change could inflict damages of more than € 40 million per year on German apple production (1400 Euros ha^{-1}a^{-1}, s=88 Euros ha^{-1}a^{-1}) if adaptation measures fail to go beyond the current standard measures such as irrigation and pest control (Fig. 2, right, see also Chmielewski et al. 2009b). Here, additional adaptation measures such as frost protection, extended pest control, and cultivar change could limit apple damages of over 10 percent to less than 5 percent in some fruit growing

regions (Fig. 3, left). By these measures, the mean cost of climate change can be limited to € 29 million per year (973 Euros ha^{-1} a^{-1}, s=118 Euros ha^{-1} a^{-1}, Fig. 3, right).

4. Discussion and Conclusions

This research project was the first comprehensive attempt to estimate the cost of climate change for an economic sector such as fruit growing. For this reason an economic approach was developed which allows to estimate the cost of climate change on the basis of costs for damages and adaptation measures.

The estimations in this project base on different simulation models and several assumptions. The models were testes on the base of sensitivity studies and the results were verified as far as possible. The cost of all adaptation measures were estimated by the Fruit Growing and Consulting Service in Jork. To evaluate the results of this project it is necessary to consider all the assumptions on which they base.

It was not possible to consider all climate related damages in this study. For instance we did not investigate any hail damages which are also very important for fruit growers. Beside the codling moth further pests and plant diseases can harm the orchards, if the climate is changing. In this case additional cost for plant protection would be necessary.

Acknowledgments

The authors are thankful to the Federal Ministry of Education and Research (BMBF) for funding the research project KliO (FZK: 01LS05024) within the scope of the research initiative klima*zwei*.

References

Ainsworth, E. A.; Long, S. P., 2005: What have we learned from 15 years of free-air CO_2 enrichment (FACE)? A meta-analytic review of the responses of photosynthesis, canopy properties and plant production to rising CO2, in: New Phytologist, Vol. 165, No. 2, S. 351–372.

Büchele, M., 2008: Höhere Baumerziehung im Kernobstbau: Rank und schlank für gehobene Qualitätsansprüche, in: Besseres Obst, 53. Jg., Nr. 9, S. 14–16.

Chmielewski, F.-M.; Blümel, K.; Henniges, Y.; Müller, A., 2009a: Klimawandel und Obstbau in Deutschland. Endbericht des BMBF-Verbundprojekts KliO., Eigenverlag, Humboldt-Universität zu Berlin, 237 S.

Chmielewski, F.-M.; Blümel, K.; Henniges, Y.; Müller, A.; Weber, R.W.S., 2009b: Klimawandel: Chancen, Risiken und Kosten für den deutschen Obstbau. In: Mahammadzadeh, M.; Biebeler, H.; Bardt, H. (Hrsg.): Klimaschutz und Anpassung an die Klimafolgen - Strategien, Maßnahmen und Anwendungsbeispiele, Institut der deutschen Wirtschaft Köln, Medien GmbH, 279-286.

Janssens, I. A.; Mousseau, M.; Ceulemans, R., 2000: Crop ecosystem responses to climate change, tree crops, in: Reddy, K. Raja / Hodges, Harry F. (Hrsg.): Climate change and global crop productivity, New York, S. 245–270.

Authors' address:

Humboldt-University of Berlin, Faculty of Agriculture and Horticulture, Division of Agronomy and Crop Production, Professorship of Agricultural Climatology, Albrecht-Thaer-Weg 5, D-14195 Berlin , E-Mail: chmielew@agrar.hu-berlin

Forecasting epidemic outbreaks of wheat leaf blotch based on meteorological parameters

J. Junk[1], M. El Jarroudi[2], F. Pogoda[1], T. Dubos[1],
K. Görgen[1], M. Beyer[1], L. Hoffmann[1]

[1]Centre de Recherche Public – Gabriel Lippmann, Belvaux, Luxembourg
[2]Université de Liège, Campus d'Arlon, Belgium

Abstract

Agricultural crops like wheat are under permanent pressure from plant diseases. In wheat, leaf blotch caused by the fungus *Septoria tritici* is the economically most important disease in the humid regions of Europe. Crucial steps of the pathogen's life cycle depend on the availability of liquid water and moderate temperatures. Between 2003 and 2009, four fields with winter wheat were equipped with automatic meteorological stations and with dielectric leaf wetness sensors from DECAGON DEVICES. Additionally, the level of disease was observed once a week during the growing season. Provided that the pathogen is present in a specific plot, the point of time when leaves are infected can be predicted based on standard meteorological measurements and leaf wetness data. The actual time of infection is particularly important, because fungicides are most effective when being applied during infection. If leaf wetness data are not recorded, they can be estimated from standard meteorological measurements using a non-linear statistical approach.

1. Introduction

Yield and quality of agricultural crops are reduced by different plant diseases. In wheat, leaf blotch caused by the fungus *Septoria tritici* is the y most damaging disease in the humid regions of Europe. Crucial steps of the pathogen's life cycle depend on the availability of liquid water and moderate temperatures. If the pathogen is present in a specific field, the point of time when leaves are infected can be predicted based on meteorological data. Since fungicides are most effective when being applied during infection, the point of time is particularly important.

2. Data acquisition and methods

Between 2003 and 2009, four fields of winter wheat were selected and equipped with automatic meteorological stations. The four fields at, Burmerange, Christnach, Everlange, and Reuler, are homogeneously distributed over Luxembourg. During the growing season, the level of disease was observed in the fields once per week. Meteorological observations of air temperature, precipitation and relative humidity were used as secondary forcing.

According to results from other authors, e.g. Chungu et al. (2001), detailed information about the leaf wetness during the growing season can help to improve the prediction of *Septoria tritici* progress on wheat plants. Therefore, the four test plots with winter wheat were also equipped with dielectric leaf wetness sensors (LWS) from DECAGON DEVICES Inc. The LWS were set up at 10 cm, 30 cm, 60 cm and 120 cm above the ground. To evaluate whether sensor orientation had any influence on the measurements,

two sensors mounted 120 cm above the ground were conversely oriented, one facing north and one facing south (Fig. 1).

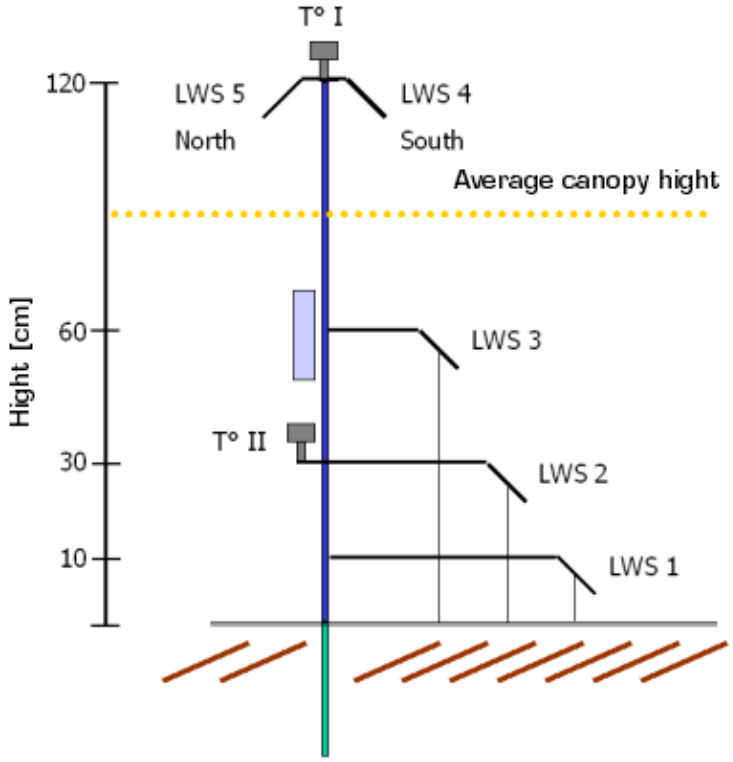

Fig. 1: Schematic of air temperature and leaf wetness sensors

Artificial neural networks (ANN) were applied successfully in various geoscience studies (e.g. Junk et al., 2007), including the estimation of leaf wetness duration (e.g. Francl and Panigrahi, 1997). ANNs can be used to derive a complex non-linear relationship among (observed) input and output data without knowing the exact physical interrelationships involved (Lopez et al., 1998).

Hourly measurements of leaf wetness, air temperature, relative humidity, and precipitation; as well as the calculated saturated vapour pressure, absolute humidity, and dew point temperature served as input data. The data set was randomly split into three sub sets: a training data set (70% of the data), a testing data set (15%), and a validation data set (15%). The training data set determines the adjusted weights between the neurons. During the training period, the network is tested against the test data to determine the accuracy of the derived statistical relationship. The training procedure is stopped, as soon as the mean average error remains unchanged. Finally, the ability of the derived ANN to reproduce the validation data is verified.

3. Results

Each epidemic outbreak is preceded by a unique set of meteorological conditions. With enough case studies, those meteorological conditions preceding epidemic outbreaks can

be identified. This can be done by subjecting the meteorological data to a cluster analysis. As a result, several groups of similar meteorological events are obtained.

After eliminating the scenarios, which were too dry to allow fungal spore germination and after eliminating humid scenarios that were not found in all case studies with epidemic outbreaks, a meteorological scenario at a temporal distance of about 20 days before the onset of an epidemic outbreak was identified. When plants reach the developmental stage that is critical for seed production (formation of upper three leaves), lower leaves are already infected, and the critical conditions derived above occur, then a fungicide should be applied to suppress the epidemic outbreak that is expected approximately 20 days later in order to limit yield loss.

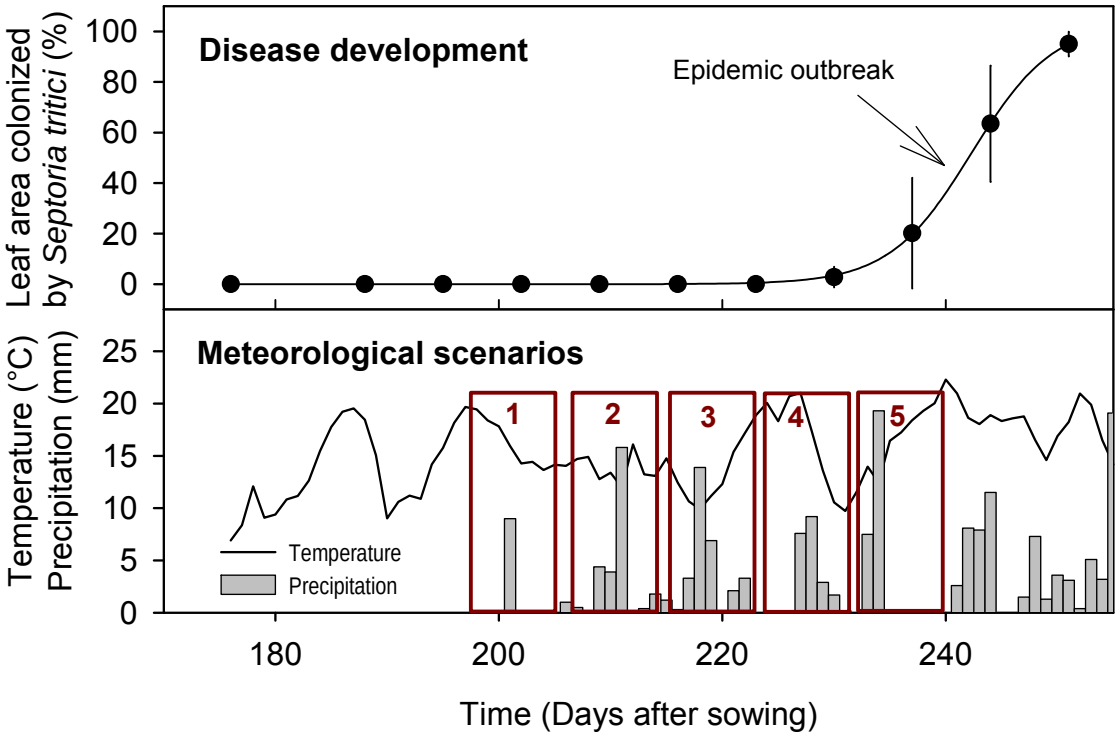

Fig. 2: Time evolution of wheat leaf blotch disease development, temperature and, precipitation in a wheat field near Burmerange, Luxembourg, in 2007

Some of these scenarios are too dry to allow *Septoria tritici* spore germination. In Fig. 2, one of the five meteorological scenarios, marked in red, must have given rise to the infection, which resulted in the epidemic outbreak. Scenarios 1, 2, 4, and 5 did not occur in all case studies with epidemic outbreaks, making scenario 3 the most likely cause of the infection.

The temporal distance between scenario 3 and the epidemic outbreak suggests a latent period of about 20 days, which is in agreement with previous results utilizing other methods. Average conditions during the infection scenario were: temperature = 13.6 ± 2.3°C, leaf wetness = 92.4 ± 4.2%, and at least one precipitation event (Henze et al., 2007).

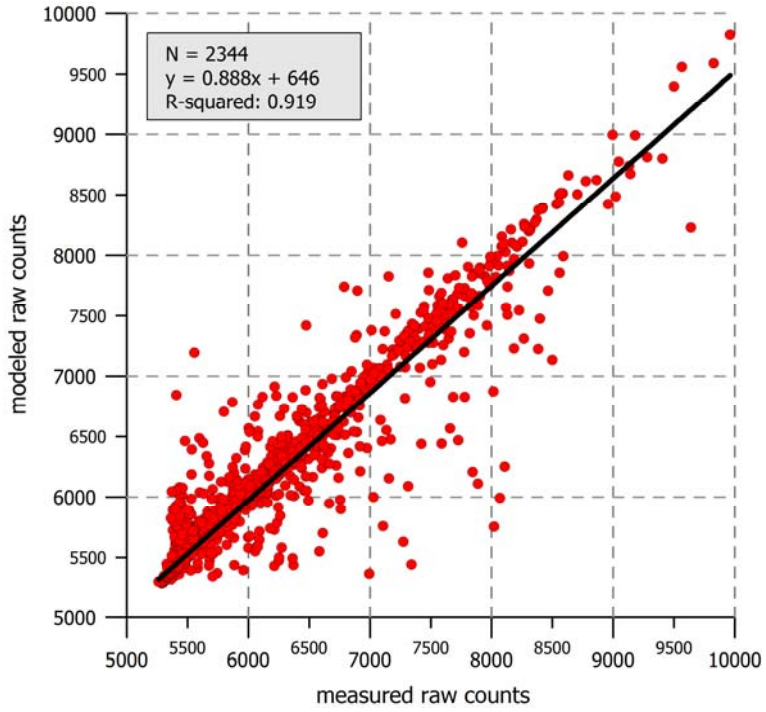

Fig. 3: Scatter plot of modeled and measured hourly cumulative raw counts of LWS 3 at Burmerange; data from 13.4.2007 to 19.7.2007

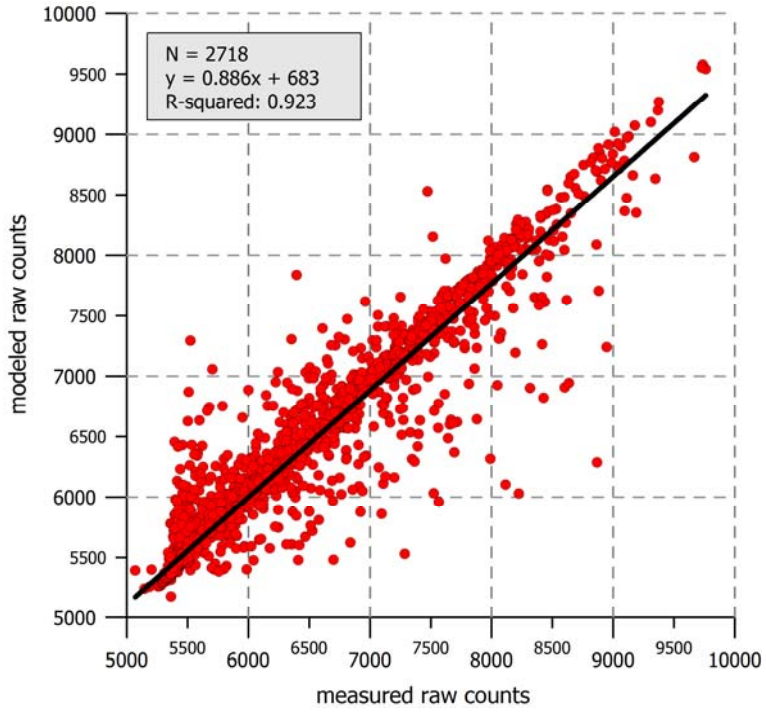

Fig. 4: Scatter plot of modelled and measured hourly cumulative raw counts of LWS 3 at Christnach; data from 2.4.2007 to 24.7.2007

If leaf wetness data were not recorded, they can be estimated from standard meteorological measurements. Due to the fact that a multiple linear stepwise forward regression shows no satisfactory results (R^2 <0.6) we used artificial neural networks to model the non-linear correlation among the leaf wetness (measured in raw counts) and the meteorological conditions.

Different ANN models for each test site were calculated. Validation results are shown for the test sites at Burmerange and Christnach (Fig. 3 and Fig. 4). The most relevant predictors for these sites are air temperature, relative humidity, dew point temperature, and time of day. Using the ANN model it is possible to reconstruct longer leaf wetness time series' for the past years using only the meteorological data as input variables (Junk et al., 2008).

Acknowledgements

The financial support of the 'Administration des Services Techniques de l´Agriculture', as well as the technical support by the 'Chambre d'Agriculture Luxembourg' are gratefully acknowledged.

References

Chungu, C., J. Gilbert, F. Townley-Smith, 2001: *Septoria tritici* blotch development as affected by temperature, duration of leaf wetness, inoculum concentration and host. Plant disease 85, 430-435.

Francl, L.J., S. Panigrahi, 1997: Artificial neural network models of wheat leaf wetness. Agric. For. Meteorol. 88, 57-65.

Henze, M., M. Beyer, H. Klink, J.-A. Verreet, 2007: Characterizing meteorological scenarios favourable for *Septoria tritici* infections in wheat and estimation of latent periods. Plant Disease 91, 1445-1449.

Junk, J., U. Feister, A. Helbig, 2007: Reconstruction of daily solar UV irradiation from 1893 to 2002 in Potsdam, Germany. Int. J. Biometeorol. 51, 505-512.

Junk, J., K. Görgen, M. El Jarroudi, P. Delfosse, L. Pfister, L. Hoffmann, 2008: Operational application and improvement of the disease risk forecast model PROCULTURE to optimize fungicides spray for the Septoria leaf blotch disease in winter wheat in Luxembourg. Advances in Sciences and Research 2, 57-60.

Lopez, G., M.A. Rubio, M. Martinez, M. Battles, 1998: Estimation of hourly global photo synthetically active radiation using artificial neural network models. Agric. For. Meteorol. 107, 279-291.

Authors' address:

Dipl. Geogr. Jürgen Junk (junk@lippmann.lu)
Centre de Recherche Public – Gabriel Lippmann
41, rue du Brill
L-4422 Belvaux, Luxembourg

The importance of meteorological variables in the bias of Potential evapotranspiration estimates in Crete, southern Greece

Fotios Xystrakis[1], Andreas Matzarakis[2]

[1] Institute of Silviculture, Albert Ludwigs University of Freiburg, Germany
[2] Meteorological Institute, Albert Ludwigs University of Freiburg, Germany

Abstract

Aim of the present study is to identify the importance of various meteorological variables in the absolute values of positive and negative bias of the estimates of the reference potential evapotranspiration (PET_{ref}) rates from two empirical equations in Crete, southern Greece. Daily values of PET_{ref} calculated by means of the standardised FAO Penman-Monteith equation in the meteorological station of Iraklio were used as a basis for the comparison between different methods. Wind velocity was detected as an important factor, yet it is the combination of various meteorological parameters that actually controls the magnitude of bias.

1. Introduction

Estimates of reference potential evapotranspiration (PET_{ref}) are important for a number of applications in biometeorology and especially in agricultural and forest meteorology. Since there are many difficulties for the direct measurement of PET_{ref}, it is usually estimated using the standardised, physically based equation of FAO Penman-Monteith (PET_{FAO}) (Allen *et al.*, 1998) which is widely accepted to provide the best estimates of PET_{ref} over various climatic types (Droogers and Allen, 2002; Gavilán *et al.*, 2006). This equation, nevertheless, is demanding in terms of input data (among others requires input of net radiation, wind speed, air humidity) which are not measured in the majority of the weather stations. To overcome this deficiency, a number of empirical equations, less demanding in terms of input data, has been proposed for the estimation of PET_{ref}.
Yet, due to the fact that the empirical equations are developed for specific regions and climatic types it is possible that their estimates will be deemed by source of bias deriving from site-specific conditions (Allen *et al.*, 1998; Grismer *et al.*, 2002). To exemplify, it has been observed that although the Hargreave's equation (PET_{Har}), results in adequate estimates for many regions (Temesgen *et al.*, 1999; DehghaniSanij *et al.*, 2004), it has a tendency to over-estimate PET_{ref} rates in high advection phenomena of semi-arid environments (Martínez-Cob, 1996; Berengena and Gávilan, 2005). It is important therefore, besides the general evaluation of the empirical equation prior to their use, to detect and identify the specific parameters that lead in partial failure of the empirical equations even when they overall perform well.
Within this concept, in the semi arid region of Crete, the performance of thirteen empirical equations was evaluated with respect to the PET_{ref} estimates obtained by the PET_{FAO} in seven meteorological stations. The evaluation has shown that two empirical equations (Hamon's and Turc's) perform considerably well (Xystrakis and Matzarakis, submitted). For the aforementioned equations, statistical analyses were used in order to identify the meteorological parameters that have a large impact in their over- or under-estimations with respect to the PET_{FAO} using data from the weather station situated in Iraklio.

2. Data and methods

Daily values (17155 days) of meteorological data, required for the calculation of PET_{FAO}, were obtained from one climate station (Irakleio – Lon: 25°10'0"; Lat: 35°19'0"; Alt: 39 m a.s.l.) on the island of Crete, southern Greece. The data included observations of mean air temperature, T_{mean} (°C); minimum air temperature, T_{min} (°C); Maximum air temperature, T_{max} (°C); Dew point temperature, T_{dew} (°C); relative humidity, RH (%); wind velocity, U_2 (m/s) and cloud cover, CL (octas).

The global (total) solar radiation data which are required for estimation of PET_{ref} by means of Turc's equation and not measured by the meteorological station of Irakleio, were estimated using the RayMan® model (Matzarakis and Rutz, 2007; Matzarakis *et al.*, 2007), taking into consideration the cloud cover, the latitude and the elevation of the meteorological station. To estimate the extraterrestrial radiation (R_a) and net radiation (R_n), required for the application of the PET_{FAO} equation, the method described by Allen *et al.* (1998) was followed. An albedo value of 0.23 was used (Allen *et al.*, 1998) in the calculation of R_n for the reference crop. The performance of the empirical equation was tested using the daily bias error (BE) measure, defined as:

$BE = E_i - O_i$

with E_i: Estimates from empirical equations and O_i: respective values from PET_{FAO} equation for day i

The empirical equations that, based on out unpublished data, show a generally good performance in Crete were these of Turc's (PET_{Tur}) described in Jacobs and Satti (2001) and Lu *et al*. (2005) and Hammon's (PET_{Ham}) described in Oudin *et al*. (2005). For these equations therefore, the meteorological factors that contribute to over- or under-estimation of PET_{ref} will be assessed.

To detect structure in the relationships between variables, factor analysis was performed (StatSoft, 2007) with the daily meteorological observations as the input variables. The principal component method was used as extraction method, the number of factors (axes) extracted was four and varimax rotation was applied for the estimation of sample scores. Stepwise multiple linear regressions were then performed using the absolute values of positive and negative values of BE and the scores of the axes of the factor analysis as the dependent and independent variables respectively. The load (importance) of each of the factors in the BE was estimated by their standardised beta coefficients in the regression models. Interception was forced to zero. The use of the negative and values of BE allowed us to account for the direction of bias (under- or over-estimation respectively). Both factor and regression analyses were performed in Statistica (StatSoft, 2007).

3. Results

The results of the factor analysis are summarised in table 1.

From the above table, and based on the correlation coefficients between the daily meteorological observations and the factors (axes), it can be concluded that the relative position of the days along the axes, indicates their meteorological conditions as described hereafter: Days that are characterised by high air temperatures are positively correlated with the first factor. Days with high RH are negatively correlated with the second factor. Days with high wind speed are negatively correlated with third factor and finally, days with high incoming radiation are positively correlated with the fourth factor. To exemplify, a day that is situated on the positive part of the first axis, on the nega-

tive part of the second axis, on the positive part of the third axis and on the negative part of the fourth axis of the factor analysis, is considered to be a warm, wet, with low wind velocity and low incoming radiation (cloudy) day.

Tab. 1: Factor analysis outputs. Correlation coefficients which are higher than 0.7 are bolded and underlined

Variables	Factor 1	Factor 2	Factor 3	Factor 4
T_{mean}	**0.891091**	0.256722	0.039950	0.357928
RH	-0.157786	**-0.951404**	0.169836	-0.190822
U2	-0.040839	0.145534	**-0.980987**	-0.108822
CL	-0.322499	-0.121923	-0.110805	**-0.909969**
T_{max}	**0.859845**	0.296496	0.110251	0.338196
T_{min}	**0.914387**	0.171401	-0.106921	0.252498
T_{dew}	**0.876975**	-0.324674	0.130110	0.311544
R_s	0.483314	0.177272	0.069425	**0.818468**

The results of the regression analysis between the absolute values of bias error of the empirical equations are presented in table 2

Tab. 2: Beta coefficients and their standard errors of the regression analyses. All but the underline factors are statistically significant at 0.01 level

Hammon's equation					
over-estimation (absolute values of positive BE)			**Under-estimation (absolute values of negative BE)**		
	beta	**Std. Err.**		**beta**	**Std. Err.**
Factor 1	0.529495	0.007387	**Factor 3**	-0.576253	0.005806
Factor 2	-0.007092	0.007474	**Factor 2**	0.493862	0.005820
Factor 3	0.467052	0.007648	**Factor 1**	-0.230526	0.005773
Factor 4	-0.243960	0.007635	**Factor 4**	0.167189	0.005837
Turc's equation					
over-estimation (absolute values of positive BE)			**Under-estimation (absolute values of negative BE)**		
	beta	**Std. Err.**		**beta**	**Std. Err.**
Factor 3	0.628697	0.006736	**Factor 3**	-0.647237	0.004399
Factor 4	0.452673	0.006794	**Factor 2**	0.486130	0.004380
Factor 1	0.126237	0.006650	**Factor 4**	-0.441899	0.004409
Factor 2	-0.041261	0.006576	**Factor 1**	0.095315	0.004389

The above table, combined with the results presented in table 1, shows that the over-estimation of Hammon's equation mostly depends on air temperatures as the absolute values of positive bias increase when values of factor one increase. The absolute values of positive bias also increase with an increase of the factor three, which is related with a decrease in wind velocity. Finally, the absolute values of positive bias decrease as sample scores along factor four increase with the latest signifying an increase in incoming radiation values. The relative humidity has not effect over the overestimation from Hammon's equations.

Table 2 also shows that under-estimation of PET_{ref} from the same empirical equation mostly depends on the factor related with wind speed. The absolute value of under-

estimation increases with decrease in the values of factor three (increase in U_2). The absolute values of under-estimation also increase with increasing values of factor two (decrease in RH). Additionally, increase in over-estimation is observed for decrease in factor's one values (decrease in air temperatures). Finally, the absolute values of under-estimation slightly increase with a respective increase in the values of factor four (increase in radiation intensity).
Summarising for Hammon's equation, large over-estimations are expected during warm, with low wind velocity and incoming radiation days, while large under-estimations are expected to occur during days with high wind velocity which are dry, cold and sunny.
Concerning the over-estimation of Turc's equation, the factor three, which is related to wind velocity, is identified to has the greater importance. As values of factor three increase (U_2 decreases), the absolute error of over-estimation increases. Similarly, when values of factor four increase (increased incoming radiation), the overestimation increases. When values of factor one increase (increase in air temperatures), the over-estimation decreases and finally, when values of factor two increase (decrease in relative humidity).
The factor with the greatest importance concerning the under-estimation of Turc's equation is identified as to be the factor three (related to wind speed). High values of factor three (low wind velocity) result in low under-estimations. Additionally, high values of factor two (low values of relative humidity) result in large under-estimations. Respectively, low values of factor four (low incoming radiation) result in large under-estimations. Finally, high values of factor one (high air temperatures) result in a slight increase in under-estimation of PET_{ref}.
Summarising for Turc's equation, high over-estimation bias is expected for days with low wind speed which are sunny, warm and dry. High underestimations are expected during days with high wind speed which are dry, cloudy and cold.

4. Discussion

The under-or over-estimation of these two empirical equations for the prevailing meteorological conditions in Irakleio, largely depends on wind velocity, as the factor three, which is related to this meteorological variable, has been identified as having the greatest relative importance in three of the four regression models. That can be explained from the fact that both of the empirical equations, unlike the PET_{FAO} do not account for wind velocity for the estimation of PET_{ref}.
Additionally, it is interesting to observe that the equations show a consistent pattern in terms of the effect that the meteorological variables have in over- or under-estimation of PET_{ref}. The regression coefficients of the independent variables (factors) have the opposite sign, for high over- and under-estimations (with the exception of air temperatures for Turc's equation). Fore example, high relative humidity is related with high over-estimations and with low underestimations. Nevertheless, it is obvious that the over- or underestimation form the empirical PET_{ref} equations does not depend in a single parameter but to their combination. Further research is required in order to be able to detect the important parameters that lead to deviation of estimates from PET_{ref} values and make use of this knowledge for an optimum calibration of the empirical equations at local conditions, taking into consideration the prevailing meteorological conditions.

Acknowledgements
We thank also the Hellenic National Weather Service for providing us the climate data of Crete.

References

Allen, R., Pereira, L., Raes, D. Smith, M. (1998) Crop evapotranspiration - Guidelines for computing crop water requirements., p. 300, FAO, Rome.

Droogers, P. Allen, R.G. 2002: Estimating reference evapotranspiration under inaccurate data conditions. Irrig. Drain. Syst. 16, 33-45.

Gavilán, P., Lorite, I.J., Tornero, S. Berengena, J. 2006: Regional calibration of Hargreaves equation for estimating reference ET in a semiarid environment. Agr. Water Manage. 81, 257-281.

Grismer, M.E., Orang, M., Snyder, R. Matyac, R. 2002: Pan evaporation to reference evapotranspiration conversion methods. J. Irrig. Drain. E.-ASCE 128, 180-184.

Temesgen, B., Allen, R.G. Jensen, D.T. 1999: Adjusting temperature parameters to reflect well-watered conditions. J. Irrig. Drain. E.-ASCE 125, 26-33.

DehghaniSanij, H., Yamamoto, T. Rasiah, V. 2004: Assessment of evapotranspiration estimation models for use in semi-arid environments. Agr. Water Manage. 64, 91-106.

Martínez-Cob, A. 1996: Multivariate geostatistical analysis of evapotranspiration and precipitation in mountainous terrain. J. Hydrol. 174, 19-35.

Berengena, J. Gávilan, P. 2005: Reference evapotranspiration estimation in a highly advective semiarid environment. J. Irrig. Drain. E.-ASCE 131, 147-163.

Matzarakis, A. Rutz, F. (2007) RayMan - Modelling of mean radiant temperature in urban structures - Calculation of thermal indices, Freiburg i. Br.

Matzarakis, A., Rutz, F. Mayer, H. 2007: Modelling radiation fluxes in simple and complex environments - application of the RayMan model. Int. J. Biometeorol. 51, 323-334.

Jacobs, J.M. Satti, S.R. (2001) Evaluation of reference evapotranspiration methodologies and AFSIRS crop water use simulation model: Final report, St. Johns River Water Management District.

Lu, J.B., Sun, G., McNulty, S.G. Amatya, D.M. 2005: A comparison of six potential evapotranspiration methods for regional use in the southeastern United States. J. Am. Water Resour. As. 41, 621-633.

Oudin, L., Hervieu, F., Michel, C., Perrin, C., Andreassian, V., Anctil, F. Loumagne, C. 2005: Which potential evapotranspiration input for a lumped rainfall-runoff model?: Part 2-Towards a simple and efficient potential evapotranspiration model for rainfall-runoff modelling. J. Hydrol. 303, 290-306.

StatSoft, I. (2007) STATISTICA-data analysis software system.

Xystrakis, F., Matzarakis, A.: Evaluation of thirteen empirical potential evapotranspiration equations (PETref) in the island of Crete, southern Greece. Agricultural Water Management (submitted).

Authors' addresses:
Dr. Fotios Xystrakis (xystrakis.fotis @waldbau.uni-freiburg.de)
Institute of Silviculture, Albert-Ludwigs-University of Freiburg
Tennenbacherstr. 4, D-79106 Freiburg i. Br., Germany

Prof. Dr. Andreas Matzarakis (andreas.matzarakis@meteo.uni-freiburg.de)
Meteorological Institute, Albert-Ludwigs-University of Freiburg
Werthmannstr. 10, D-79085 Freiburg i. Br., Germany

Development of a Climate Stress Index for Dairy Cows Housed Outside

John Gaughan, Jarrod Lees

School of Animal Studies, University of Queensland, Australia

Abstract

Climate change models are suggesting an increase in the severity of extreme weather events. Dairy cows are highly susceptible to heat stress due to their high level of metabolic heat production, which is required to meet the high levels of milk output. Current predictive models, such as the temperature humidity index (THI) and the heat load index (HLI) may not adequately describe the effect of hot climatic conditions on dairy cows kept outside.

The aims of this study were to (i) determine the effect of climatic factors on milk production (MP), (ii) assess the usefulness of THI and HLI in predicting cow responses to heat load (HL), and (iii) from these develop a heat load model that will predict the impact of climatic stress (specifically heat stress) on dairy cows kept outside. Results from the first summer of the study will be presented in this paper.

1. Introduction

Climate change models are suggesting an increase in the severity of extreme weather events. Dairy cows are more susceptible to heat stress than are beef cattle due to their high level of metabolic heat production, which is required to meet the high levels of milk output. Some of the negative effects of climate can be ameliorated by housing cows. However in countries which rely on pasture based nutrition or outdoor housing, cows are being exposed to an increasing number of heat load events. Therefore there is a need to have in place reliable methods of assessing the impact of these heat events on production and welfare of dairy cows. Milk production is influenced by a number of factors such as, days in milk, genetic capacity to produce milk, degree of acclimatisation, nutrition, health status and climatic conditions. The relationship between these factors is somewhat complex, and dynamic. It is not clear how cumulative stressors (e.g. prolonged exposure to high heat load) will affect milk production.

There are a number of climatic indices currently employed to measure heat load on cattle. A review of the thermal indices used in the livestock sector has recently been published (Hahn et al. 2009). The THI[1] provides a guide to the severity of the stress and a reasonable measure of heat load in cattle. The THI which has served as the defacto index for livestock for sometime considers that all animals will respond the same to a given climatic condition. THI is further limited in that it does not account for solar load or the effects of air movement. The heat load index (HLI[2]) developed by Gaughan et al.

[1] $THI = (0.8 \times T_A) + [(rh/100) \times (T_A - 14.4)] + 46.4$

[2] The HLI consists of 2 parts based on a BG threshold of 25 ^oC: $HLI_{BG>25} = 8.62 + (0.38 \times rh) + (1.55 \times BG) - (0.5 \times WS) + [e^{(2.4 - WS)}]$, and $HLI_{BG<25} = 10.66 + (0.28 \times rh) + (1.3 \times BG) - WS$. Where e = the base of the natural logarithm (approximate value of e = 2.71828).

(2008) for beef cattle is used extensively in the Australian feedlot sector, and has potential as an indicator of heat load in dairy cows (Schütz et al. 2009). Within the HLI beef cattle can be categorised based on thresholds so that genetics, level of production and health status can be accounted for.

2. Materials and Methods

Animals and facilities: The study was conducted at The University of Queensland dairy during summer (December 2008 to March 2009), with the approval of the University Animal Ethics Committee. The dairy consists of a 10 per side Herringbone equipped with rapid exit gates. Cows (n=150) were confined to a feedlot area (1.4 ha approx.) with occasional access to pasture. Cows had access to shade (1.6 m^2/cow) provided by an open sided shed with a steel roof, and a feed pad (1.3 m^2/cow) also with a metal roof. Sprinklers in the holding yard provided cooling prior to milking. Cows were milked twice daily at 0600 h and 1400 h. Milking cups were fitted with Westfalia In-Line milk meters. Individual MP was recorded (DairyPlan, GEA Farm Technologies). Because the cows varied in terms of days in milk (DIM) and level their of milk production (MP) they were grouped (for statistical analysis) into the following categories. DIM categorised as; 1 = <56 d, 2 = 57 to 100 d, 3 = 101 to 224 d, 4 = >224 d, and MP categorised as; 1 = <12 kg/d, 2 = >12 to 20 kg/d, 3 = >20 to 30 kg/d, 4 = >30 kg/d.

Nutrition: Cow were fed (45 kg/cow/day as-fed) a mixed ration of 70% sorghum silage, 15% brewers grain, 10% corn cobs, 5% lactating cow pellets (Ridley AgriProducts, Australia). Half of their feed allocation was provided at 0800 h and the remainder at 1400 h. Pasture consisted of rye grass, forage sorghum, alfalfa, and native grasses. Water was provided via two 720 L troughs at the feedlot and a 330 L trough at the holding yard. DMI could only be assessed on the herd level.

Climatic conditions: Climatic conditions were recorded at 10 minute intervals using an automated weather station (Easidata MK 3, Environdata Australia P/L, Warwick, QLD, Australia) located within 30 m of the cows. Climate variables consisted of ambient temperature (T_A; °C), relative humidity (rh; %), wind speed (WS; m/s), solar radiation (W/m^2), and black globe temperature (°C). The THI and HLI were calculated from the weather data. The mean THI (THI_M) and mean HLI (HLI_M) between 1100 and 1600 h was calculated each day. THI_M and HLI_M were then categorised as. thermoneutral = THI_M <72; moderate = THI_M is 72 to 78; hot = THI_{MEAN} is 78.1 to 86; and extreme = THI_M >86; HLI_M was categorised as; Thermoneutral = HLI_M <64.0; Moderate = HLI_M is 64.1 – 70.0; Hot = HLI_M is 70.1 – 76.0; and Extreme = HLI_M >76.

Animal observation: The cows were observed 3 times/day (0800, 1200, and 1400 h). Cow location (at feed, at water, under shade, in sun); posture (standing or lying); and panting score (PS) (Mader et al. 2006) (0 = regular breathing, 4 = open mouth, tongue out, excessive drooling) were recorded. Mean panting score (MPS) was then calculated on a herd to assess the severity of the heat stress (Gaughan et al. 2008).

Statistical analysis: Data were converted from animal numbers to proportion of the herd. Percentage of cows recorded for each PS was transformed to a normalised distribution using squared root arcsine transformation before being statistically analysed. The data were analysed using PROC GLM and PROC MIXED (SAS Inst. Inc., Cary, NC).

MP was analysed using repeated measures ANOVA. The model included the effects of the HLI_M and the THI_M categories, DIM category, MP category, month, time of day and day as fixed effects. The specific term for the repeated statement was cow within day. The transformed PS, and MPS were analysed using a repeated measures model which included day, time of day, month, HLI_M category, THI_M category DIM category, and MP category as fixed effects and cow as a random effect. The specified term for the repeated statement was day. The between month differences in the climatic variables were analysed using PROC GLM. Chi Square analysis was used to determine the differences between months for the number of cows lying or standing.

3. Results

Climatic conditions: The means over the study period for T_A, rh, THI and HLI were 27.6 ± 0.4 ^oC, 65.6 ± 1.9 %, 77.5 ± 1.4, and 87.4 ± 0.1 respectively. Conditions were sufficient to induce heat stress in some cows on most days.

HLI and THI: Both the HLI and THI were good predictors ($P<0.0001$; $r^2=0.56$) of changes in MP over a month, but were less reliable predicting day effects ($P<0.01$; $r^2=0.15$).

Mean Panting Score: The MPS increased ($P<0.0001$) as the severity of the heat load increased over summer. During December the MPS was 0.89. This increased to 1.34 in January, and 1.46 in February, and then fell to 1.22 in March. In contrast the average value in June/July (winter) was 0.17. When MPS >1.2 there will be a significant portion of the herd with PS≥2. The HLI and THI at the time of observation (0800, 1200 and 1400 h) had an effect on MPS ($P<0.0001$). This suggests that these indices have value in assessing stress levels at a given point in time. However the THI was not good at predicting MP when conditions were MOD or HOT whereas the HLI predicted MP decline during TNC, MOD, HOT and EXT.

Milk Production: The MP from low production cows <20 kg/d was not affected ($P>0.05$) by the climatic conditions to which they were exposed over the summer. Higher production cows (categories 3 and 4) had significant reductions ($P<0.001$) in milk yield during periods of extreme heat load (Table 1). There was an affect ($P<0.001$) of DIM within MP category in regards to declines in MP as heat load increased. There was considerable between cow variation for MP (within and between MP category), and between days for individual cows. The latter appeared to be independent of climatic factors ($r^2=0.35$ for MP of individual cows on 2 consecutive days).

Table 1: Milk production (kg/cow/d) of cows classified as high or low production cows under thermonuetral (TNC) and extreme (EXE) HLI_M categories

Milk Production Category[2]	TNC[1]	EXE[1]	SE	P-value
1	$9.97^{a,c}$	$9.86^{a,c}$	0.16	P>0.05
2	$16.88^{a,d}$	$16.63^{a,d}$	0.14	P>0.05
3	$24.04^{a,e}$	$23.35^{b,e}$	0.12	P<0.0001
4	$36.14^{a,f}$	$34.38^{b,f}$	0.22	P<0.0001

[1] Thermoneutral (TNC), HLI_M <64.0; (4) extreme (EXE), HLI_M >76. [2] MP categories; 1 = < 12 kg milk/day, 2 = > 12 & < 20 kg milk/day, 3 = > 20 & < 30 kg milk/day, 4 = > 30 kg milk/day.
[ab]Means within a row with the same superscript are not significantly different (P > 0.05); [cdef]Means within a column with the same superscript are not significantly different (P>0.05)

4. Discussion

Both of the indices provided an adequate assessment of the thermal load on the cows udder TNC and EXT. However the THI did not accurately predict the change in MP when cows were exposed to moderate and hot conditions. The low r-values for the prediction of milk production suggest that neither index is ideal for dairy cows housed outside. Therefore there is a need for a new index to be developed. It is also evident that there is a need to assess cows individually e.g. on the basis of days in milk, level of milk production). A whole herd approach is not sufficient. The HLI (beef cattle) accounts for animal variation (level of production, days in feedlot, health status, breed, coat color), and a similar approach is necessary for dairy cows. The HLI also uses wind speed and solar load (black globe temperature). These two factors are known to have major effects on the animals ability to dissipate heat. Berman (2005) noted that increased air velocity increased intermediate heat stress threshold temperatures; whereas humidity decreased threshold temperatures. This may explain some of the differences in the predictive abilities of HLI and THI on MP.

However there are inconsistencies in the published studies. Verwoerd et al. (2006) concluded that an increase in body temperature (T_B) could not be explained using THI. Legates et al. (1991) concluded that T_A had the biggest influence on respiration rate and T_B, followed by solar radiation and, to a lesser extent, air movement and vapour pressure. Eigenberg et al. (2005) found that T_A and solar radiation had the largest contribution toward respiration rate, with 51.4% and 32.2% respectively, followed by dew point temperature (8.9%), WS (5.7%) and body weight (2%). Berman et al. (1985) reported a decline in MP and reproductive performance of Holstein cows that when T_A reach 25 to 26°C. In the current study, T_A was, on average, greater that 26°C. This would indicate that even at TNC category (in the current study), cows may have been under some degree of heat load.

The lack of a response of MP to increased heat load in the current study was unexpected. West et al. (2003) established that on a given day DMI and MP were affected by both THI and mean T_A over the 2 days prior. It is possible that by analysing the present study from this perspective; that is removing the physiological time lag; a greater corre-

lation between MP and the climatic variables may be seen. Calculation of accumulated heat load (AHL) (Gaughan et al. 2008) and THI hours (Hahn & Mader 1997) may improve our understanding of the cumulative effects of continuous heat load on dairy cows. The accumulative effects of heat load will need to be accounted for in the development of a new model.

5. Conclusions

- Both THI and HLI can predict about 56% of the monthly decline in MP over summer.
- The THI can predict the impact of extreme conditions on MP, but does not accurately predict MP under moderate and hot conditions. Possibly because it does not account for solar load and wind speed.
- The HLI predicts the steady decline MP response of cows exposed to increasing heat load.
- The HLI was a good predictor of the stress response (panting score). Possibly because it does account for solar load and wind speed.
- Neither model accounts for differences between cows in terms of DIM and MP – these will be incorporated into the new model..

Work is currently underway (year 2 of the study) to develop a heat load model for dairy cows housed in an outdoor environment. It is clear from the first part of the study that the accumulative effects of heat load should be taken into account in the new model..

References

Berman, A., 2005: Estimates of heat stress relief needs for Holstein dairy cows. J. Anim Sci.. 83, 1377-1384.

Berman, A., Folman, Y., Kaim, M., Mamen, M., Herz, Z., Wolfenson, D., Arieli, A., Y. Graber, 1985: Upper critical temperatures and forced ventilation effects for high-yielding dairy cows in a subtropical climate. J. Dairy Sci. 68, 1488-1495.

Eigenberg, R.A., Brown-Brandl, T.M., Nienaber, J.A., G.L. Hahn, 2005: Dynamic response indicators of heat stress in shaded and non-shaded feedlot cattle, Part 2: Predictive relationships. Biosyst. Eng. 91, 111-118.

Gaughan, J.B., T.L. Mader, S.M. Holt, A. Lisle, 2008: A new heat load index for feedlot cattle. J. Anim. Sci. 86, 226-234

Hahn, G.L., Gaughan, J.B., Mader, T.L., R. Eigenberg, 2009: Thermal indicies and their application for livestock environments, in J DeShazer (ed.), *Livestock Energetics and Thermal Environmental Management*, ASABE, St Joseph Michigan USA, 113 - 130.

Hahn, G.L, T.L. Mader, 1997: Heat waves in relation to thermoregulation, feeding behavior and mortality of feedlot cattle, in R.W. Bottcher & SJ Hoff (eds), Bloomington, Mn, pp. 563-571.

Legates, J.E., Farthing, B.R., Casady, R.B., M.S. Barrada, 1991: Body temperature and respiratory rate of lactating dairy cattle under field and chamber conditions. J. Dairy Sci. 74,2491-2500.

Mader, T.L., Davis, M.S., T.M., Brown-Brandl, 2006: Environmental factors influencing heat stress in feedlot cattle. J. Anim. Sci. 84, 712-719.

Schütz, K.E., Rogers, A.R., Cox, N.R., C.B. Tucker, 2009: Dairy cows prefer shade that offers greater protection against solar radiation in summer: Shade use, behaviour, and body temperature. Appl. Anim. Behav, Sci. 116, 28-34.

Verwoerd, W., Wellby, M., G. Barrell, 2006: Absence of a causal relationship between environmental and body temperature in dairy cows (Bos taurus) under moderate climatic conditions. J. Therm. Biol. 31, 533-540.

West, J.W., Mullinix, B.G., J.K. Bernard, 2003: Effects of hot, humid weather on milk temperature, dry matter intake, and milk yield of lactating dairy cows. J. Dairy Sci. 86, 232-242.

Authors Address

Dr John Gaughan (j.gaughan@uq.edu.au)
School of Animal Studies, The University of Queensland
Gatton, Queensland, Australia 4343

Mr Jarrod Lees (jarrod.lees@uqconnect.edu.au)
School of Animal Studies, The University of Queensland
Gatton, Queensland, Australia 4343

Seasonal pattern of mortality and relationships between mortality and temperature humidity index in heavy slaughter pigs during transport and lairage

Andrea Vitali,[1] Franco Guizzardi,[2] Emilio Lana,[2] Massimo Amadori,[3] Umberto Bernabucci,[1] Alessandro Nardone,[1] Nicola Lacetera[1]

[1] Dipartimento di Produzioni Animali, Università degli Studi della Tuscia, Viterbo, Italy
[2] Distretto veterinario di Viadana, Mantova, Italy
[3] Laboratorio di Immunologia Cellulare, Istituto Zooprofilattico Sperimentale Lombardia ed Emilia Romagna, Brescia, Italy

Abstract

The two studies reported herein are based on Italian data collected during a five-years period (2003-2007) and were aimed at assessing seasonal variations of mortality and temperature humidity index (THI)–mortality relationships in heavy pigs during transportation to the slaughterhouse and lairage at the abattoir. Summer was the season with the highest frequency of deaths both during transport and lairage. Furthermore, within summer months, the risk ratio (RR) for mortality in July was significantly higher than in June and August. The THI-mortality relationship study pointed out a significant association between THI and mortality, with a higher risk of death under conditions of high THI. These results may be of help for the pig industry to ensure welfare and survival of pigs during transport and lairage at the abattoirs by adopting adaptation measures for reducing the adverse consequences of heat stress.

1. Introduction

Previous studies testified that the stress levels experienced from animals during transport to the slaughterhouse and lairage at the abattoir may be influenced by several factors including season and temperature (Warriss, 1998). Studies aimed at investigating the effects of season on pig losses during transport and lairage provided conflicting results. Some reported that the mortality rates of slaughter pigs during transportation and lairage at the abattoir were higher during summer months (Vecerek et al., 2006; Werner et al., 2007; Haley et al., 2008a; Haley et al., 2008b). Averos et al. (2008) indicated that the risk of mortality increases significantly when the external temperature during the journey increases, although no significant effects were found for the season. Conversely, others reported that in-transit pig losses were not associated with season or high temperatures (Ritter et al., 2006; Ritter et al., 2008).

Only little is known on the relationships between temperature humidity index (THI) and in-transit or lairage pig losses. The THI incorporates the effects of temperature and humidity and is commonly used to quantify the degree of heat stress in farm animals. Recently, Fitzgerald et al. (2009) reported that the increase of THI to the maximum value was associated with an increase of pig losses during transport and lairage at a commercial abattoir.

It has to be noticed that all these studies were refereed to pigs slaughtered at 115-140 Kg live weight, whereas no information are available for heavy pigs slaughtered at 160 Kg live weight, which is the slaughter weight to obtain meat suitable for producing the typical cured meats as crude Parma's ham.

The studies reported herein were aimed at investigating the seasonal variation of mortality and THI–mortality relationship in slaughter heavy pigs during transportation and lairage at the abattoir.

2. Materials and method

The two studies reported herein are based on Italian data collected during a five-years period (2003-2007). For each journey, the following information were available: date of the journey, farm code and municipality, destination (slaughterhouse), number of pigs transported, number of deaths recorded during transportation and during lairage at the abattoir.

2.1. Seasonal pattern study

Complete descriptive statistic of this study is reported in Table 1. Briefly, the study was carried out on mortality data referred to 24,098 journeys and 3,676,153 heavy pigs transported from 1,618 farms to three different slaughterhouses.

Table 1: Descriptive statistics of the studies

Study period (years)	2003-2007
Geographic area	North Italy
Seasonal pattern study	
Number of journeys	24,099
Number of in-transit pigs	3,676,153
Number of farms	1,618
Number of in-transit losses	1,161
Number of lairage losses	675
THI-mortality relationships study	
Number of journeys	14,316
Number of in-transit pigs	2,156,322
Number of farms	1,209
Number of in-transit losses	664
Number of lairage losses	399
N. of weather stations consulted	82
Weather station – farm/slaughterhouse distance (km)	14.07 ± 9.12

2.2. THI-mortality relationships study

Complete descriptive statistic of this study is also reported in Table 1. Briefly, the study was carried out on mortality data referred to 14,316 journeys and 2,156,322 heavy pigs transported from 1,209 farms to three different slaughterhouses.

Temperature and relative humidity data from 82 weather stations were utilized to characterize climate conditions of transports. The THI value attributed to each transport was the average of the mean daily THI recorded at the weather stations nearest to the farm (departure) and at the slaughterhouse (arrival). The THI value attributed to deaths recorded during lairage was the mean daily value calculated at the weather station nearest to the slaughterhouse.

THI was calculated with the following formula (Kelly and Bond, 1971):

$$THI = (1.8 \cdot AT + 32) - (0.55 - 0.55 \cdot RH) \cdot [(1.8 \cdot AT + 32) - 58]$$

where AT is the ambient temperature in °C, and RH the relative humidity as a fraction of the unit.

2.3. Statistical analysis

Seasonal variation of mortality and THI–mortality relationships were evaluated by univariate Poisson regression models.

For the seasonal pattern study, the dependent variables were the observed counts of pigs died during transport and lairage at the abattoirs for each season. Seasons was considered as the categorical independent variable, whereas THI was considered as the numeric independent variable. Pigs transported or kept in lairage were considered as the exposure variables.

For the THI-mortality relationship study, variables were smoothed by 5 THI units moving average prior to entry into the regression models. Pearson and G statistic test were performed to evaluate the goodness-of-fit. Regression coefficients were transformed into risk ratios (RR) by taking the exponent of the coefficients. A RR of > 1 means that the determinant increases the incidence rate of in-transit and/or lairage pigs losses compared with the reference. A risk ratio is statistically significant when the 95% confidence interval (CI) does not include 1. Statistical analyses were performed with NCSS software for windows (NCSS 2007 software, NCSS, Kaysville, Utah, USA).

3. Results

Values of the overall mortality rate during transport or lairage were 0.032 and 0.02%, respectively.

A significant association between season and deaths was found for pigs died both during transport and lairage (Table 2). Summer was the season with the highest risk of death both during transport and lairage, whereas winter and spring were the seasons with the lowest risk of death both for transport and lairage. The RR for summer were 1.107 (CI: 1.008 - 1.217; $P < 0.05$) and 1.143 (CI: 1.011 - 1.292; $P < 0.05$) for in-transit and lairage pigs losses, respectively. The analysis of the RR within the summer months revealed that the month of July had the highest risk of death: 1.220 (CI: 1.064 - 1.398; $p < 0.01$) and 1.272 (CI: 1.067 - 1.516; $p < 0.01$) for in-transit and lairage pigs mortality rates respectively.

Results of the THI–mortality relationship are reported in Fig 1. The regression analysis indicated that the risk ratio of death was THI dependent. The RR for one unit increment of THI were 1.016 (CI: 1.008 - 1.023; $p< 0.001$) and 1.029 (CI: 1.019 – 1.039; $p<0.001$) for the transport and lairage respectively. The slope and intercept provided by the model [$Y_{trasport} = e^{(-9,11361+ 0,01600*THI)}$ (R^2=0.529); $Y_{lairage} = e^{(-10,48755+ 0,02902*THI)}$ (R^2=0.476)], shows the relationship between the mortality rate with climatic condition expressed by average THI.

Table 2: 95% confidence interval (CI) estimates of risk ratios (RR) for season in heavy pigs died during transport to the slaughterhouse and in lairage

	RR	95% CI	P value
Trasport			
Winter	0.716	0.566 - 0.905	0.005375
Spring	0.565	0.435 - 0.734	0.000019
Summer	1.107	1.008 - 1.217	0.033166
Fall	1.023	0.906 - 1.154	0.708065
Lairage			
Winter	0.645	0.465 - 0.894	0.008624
Spring	0.575	0.409 - 0.808	0.001437
Summer	1.143	1.011 - 1.292	0.031910
Fall	0.973	0.828 - 1.144	0.745810

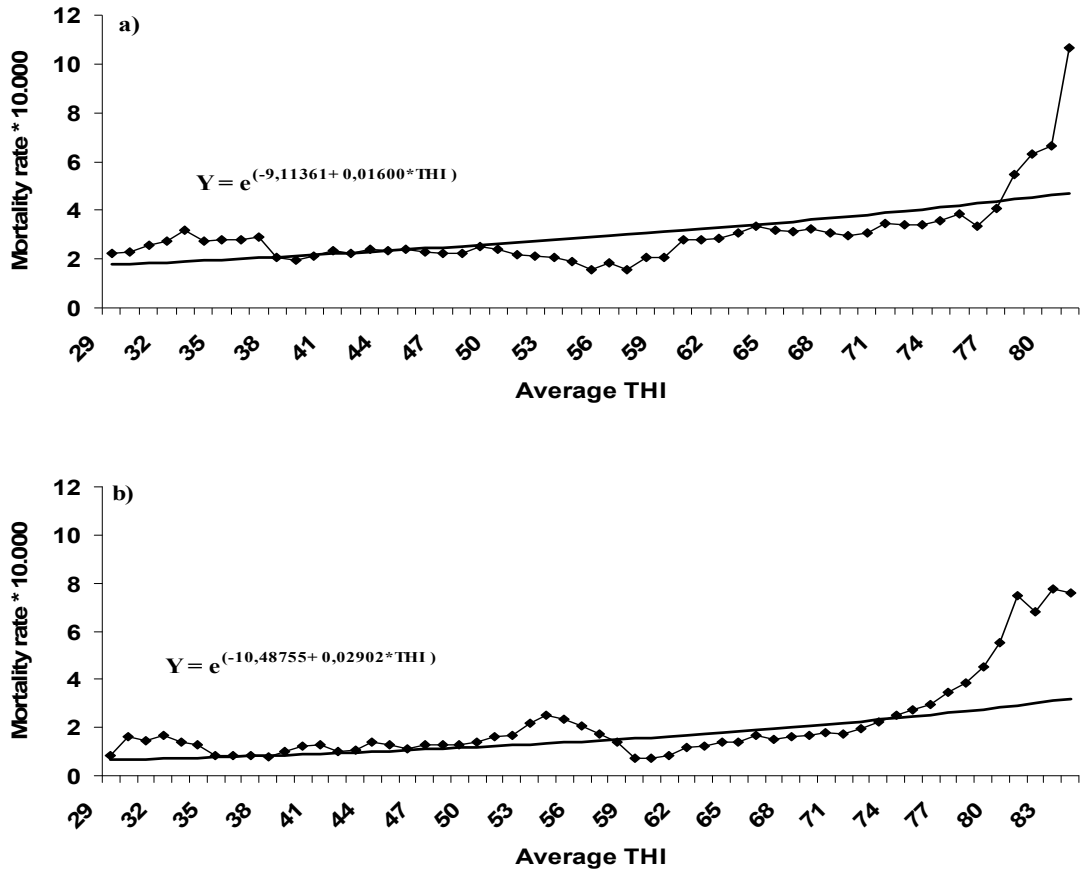

Fig. 1: Mortality rate moving average (—♦—), and linear regression of mortality rate (—) for incremental unit increases of the temperature-humidity index (THI) for pigs during transport to the slaughterhouse (a) and in lairage at the abattoir (b)

4. Discussion

First of all we wish to notice that the overall mortality rate recorded in our stydy was lower than that reported in previous European studies (Vecerek et al., 2006; Werner et al., 2007).

Results of the seasonal pattern study showed a significant association between season and deaths in heavy pigs during transport and laraige, and indicated that a higher number of deaths should be expected during summer. Furthermore, among summer months, the risk of death was significantly higher in July. These results are in line with some of those reported in previous studies.

In a German study, Werner et al. (2007) reported a significant increase of mortality rate in pigs during transport to the slaughterhouse and lairage at the abattoirs in the months of June, July and August. Analogously, in a Czech Republic study, Vecerek et al. (2006) reported an increase in mortality rates during the summer months of June, July and August in association with the average ambient temperature of 15.8 °C, 16.9 °C and 16.6 °C, respectively. Finally, in a Canadian study, Haley et al. (2008a) reported that August had the highest monthly in-transit losses and that August losses accounted for 20% of the total annual losses. The same research group (Haley et al., 2008b) reported a 3-fold increase of the in-transit loss ratio as the 90th percentile of internal trailer temperature increased from a range of 8.6°C to 23.3°C to a range of 23.4°C to 26.1°C, with an additional 2-fold increase as the range increased from 26.2°C to 28.9°C to a range of 29.0°C to 30.5°C.

The THI-mortality relationship analysis indicated a significant association between THI and mortality rates in heavy pigs during transport to slaughterhouse and in lairage at the abattoir. The RR for one unit increment of THI were 1.016 and 1.029 for the transport and lairage, respectively. During transport, the range of THI from 29 to 81 was associated with a 2.66 increase in mortality rates. Whereas, in the lairage at commercial abattoirs, the range of THI from 29 to 84 was associated with a 4.93 increase in mortality rates. These results are in line with those reported recently from Fitzgerald et al. (2009).

5. Conclusions

THI may represent a useful tool to predict the risk of heat related mortality in heavy pigs transported to the slaughterhouse and during lairage at the abattoir. These results may be of help for the pig industry to ensure welfare and survival of pigs during transport and lairage at the abattoirs by adopting adaptation measures for reducing the adverse consequences of heat stress.

Acknowledgement

This study was financially co-supported by Italian Ministry of Health (IZSLER 03/07, PRC 2007003) and Università degli Studi della Tuscia. The authors gratefully acknowledge Dr. Simona Bignami, Dr. Costantino Morini and Dr. Stefano Ambrosini (ASL Mantova, distretto di Viadana) for provision of the mortality data; Lombardia, Veneto and Emilia Romagna Environmental Protection Agency and the Research Unit for Agricultural Climatology and Meteorology (CRA-CMA) for providing meteorological data.

References

Averos, X., G. Knowles, S.N. Brown, P.D. Warriss, L.F. Gonsalvez, 2008: Factors affecting the mortality of pigs being transported to slaughter. Vet. Rec. 163, 386-390.

Fitzgerald, R.F., K.J. Stalder, J.O. Matthews, C.M. Schultz Kaster, A.K. Johnson, 2009: Factors associated with fatigued, injured, and dead pig frequency during transport and lairage at a commercial abattoir. J. Anim. Sci. 87, 1156-1166.

Haley, C., C.E. Dewey, T. Widowski, Z. Poljak, R. Friendship, 2008a: Factors associated with in-transit losses of market hogs in Ontario in 2001. Can. J. Vet. Res. 72, 377-384.

Haley, C., C.E. Dewey, T. Widowski, Z. Poljak, R. Friendship, 2008b: Association between in-transit loss, internal trailer temperature, and distance traveled by Ontario market hogs. Can. J. Vet. Res. 72, 385-389.

Kelly, C.F., T.E. Bond, 1971: Bioclimatic factors and their measurements. Page 7 in A guide to environmental research in animals. Natl. Acad. Sci., Washington, DC.

Ritter, M.J., M. Ellis, J. Brinkmann, J.M. DeDecker, K.K. Keffaber, M.E. Kocher, B.A. Peterson, J.M. Schlipf, B.F. Wolter, 2006: Effect of floor space during transport of market-weight pigs on the incidence of transport losses at the packing plant and the relationships between transport conditions and losses. J. Anim. Sci. 84, 2856-2864.

Ritter, M.J., M. Ellis, R. Bowman, J. Brinkmann, S.E. Curtis, J.M. DeDecker, O. Mendoza, C.M. Murphy, D.G. Orellana, B.A. Peterson, A. Rojo, J.M. Schlipf, B.F. Wolter, 2008: Effects of season and distance moved during loading on transport losses of market-weight pigs in two commercially available types of trailer. J. Anim. Sci. 86, 3137-3145.

Vecerek, V., M. Malena, M. Malena JR., E. Voslarova, P. Choupek. 2006: The impact of the transport distance and season on losses of fattened pigs during transport to the slaughterhouse in the Czech Republic in the period from 1997 to 2004. Veterinarni Medicina 51, 21-28.

Warriss, P.D., 1998: The welfare of slaughter pigs during transport. Anim. Welfare. 7, 365-381.

Werner, C., K. Reiners, M. Wicke, 2007: Short as well as long transportation duration can affect the welfare of slaughter pigs. Anim. Welfare 16(3), 385-389.

Authors' address:

Dr. Andrea Vitali (mail@andreavitali.it); Prof. Dr. Umberto Bernabucci (bernab@unitus.it); Prof. Dr. Alessandro Nardone (nardone@unitus.it); Prof. Dr. Nicola Lacetera (nicgio@unitus.it)
Dipartimento di Produzioni Animali, Università della Tuscia
Via S. Camillo de Lellis, 01100 Viterbo, Italy

Dr. Franco Guizzardi (franco.guizzardi@aslmn.it); Dr. Emilio Lana (mike80vet@hotmail.it)
Distretto veterinario di Viadana
Largo De Gasperi 7, 46019 Viadana (Mantova), Italy

Dr. Massimo Amadori (massimo.amadori@izsler.it)
Laboratorio di Immunologia Cellulare, IZSLER
Via Bianchi 7/9, 25124 Brescia, Italy

Biometeorological investigations in dairy cowsheds

Merike Fiedler[1], Gundula Hoffmann[1], Kristina von Bobrutzki[1], Andreas Matzarakis[2]

[1] Leibniz-Institute for Agricultural Engineering Potsdam-Bornim e.V. (ATB), Department of Engineering for livestock Management, Potsdam, Germany
[2] Meteorological Institute, Albert-Ludwigs-University of Freiburg, Germany

Abstract

The aim of this study was to investigate heat stress of dairy cows with regard to the current situation and the definition of evaluation parameters that evaluate heat stress of dairy cows. For this reason climate measurements (e.g. air temperature, air humidity, globe thermometer temperature, wind speed) in- and outside of dairy stables in northeastern Germany has been carried out. A common method for heat stress evaluation in animals is to determine the temperature humidity index (THI). This however does not consider the wind speed nor the radiation fluxes. Findings from the RayMan model have been applied in order to interpret the conditions of the stable in respect of the animal's thermal comfort.

1. Introduction

Modern dairy cows generally spend the entire day in the stable. The welfare of animals depends critically on the indoor environment. Dairy cows are most comfortable e.g. at air temperatures between 0° and 15° C. Therefore an optimal indoor environment must be created with a sufficient air ventilation to satisfy both, the air temperature and air humidity in the optimum zone. Additionally a good ventilation leads to a good air pollution control in the building and hence contribute to the welfare of animals. The DIN 18910-1 (2004) provides minimum air flow rates for dairy cows in the summer of 413 $m^3\ h^{-1}$. Nevertheless, there may be situations (e.g. large heat waves in summer) in which - despite exceeding the minimum ventilation rate - the great thermal output of high performance animals can not be compensated. This can lead to heat stress of the animals.

An annual economic loss of $900 million have been estimated for US dairy industry due to heat stress (Collier et al., 2006). But even in moderate climate the influence of heat stress in dairy cows is discussed. The increasing importance of heat stress is often associated with the global warming (e.g. more expected heat waves). Another reason is caused by the rising milk yield of the cows, which goes along with a metabolic energy performance. Lactating dairy cows produce a large quantity of metabolic heat and accumulate also additional heat through radiant energy. This two effects combined with insufficient cooling capability because of environmental conditions, result in heat load for the cow and finally a decreased productivity of the cow (West, 2003). This leads to an observed decrease of food intake which in turn results in reduced milk yield and quality.

2. Experimental set-up and methods

2.1 Investigated cowsheds

During summer 2008 the Leibniz-Institute for Agricultural Engineering Potsdam-Bornim (ATB) carried out a field measurement campaign to investigate the environ-

mental conditions inside and outside two naturally ventilated cowsheds in northeastern Germany. Aim of the study was to evaluate several parameters that should describe possible heat stress of dairy cows.
These two cowsheds (cowshed 1 and cowshed 2) are located parallel with a distance of 8 m to each other and are nearly identical in construction. The main difference between both investigated cowsheds consists of the roofs design: the roof of cowshed 1 is equipped without thermal insulation while the roof of cowshed 2 is thermal insulated. The two cowsheds can be described in more detail as follows:
Room size: length: 76.68 m (cowshed 1 and 2); width: 31.49 m (cowshed 1) and 28.50 m (cowshed 2); the roof top ranges from the side: 2.7 m (cowshed 1) and 2.5 m (cowshed 2) to 5.40 m (for both cowsheds) at the gable top, enclosing a volume of 10685 m^3 (cowshed 1) and 8648 m^3 (cowshed 2)
The keeping system is a lying box loose housing for both cowsheds. The liquid manure system (slurry channel) in cowshed 1 contains a slatted floor, while cowshed 2 is equipped with winch drawn dung channel cleaner.
Number of cows: 215 cows in each cowshed
Ventilation: At both cowsheds the natural ventilation is driven by adjustable openings in the side walls, by open doors in the gable walls and by permanently open ridge slots. Additionally cowshed 1 is equipped with a ceiling fan (diameter 4.30 m) near the gable door above the feeding alley for test purposes.

2.2 Measurements

Within the two cowsheds the following indoor environmental parameters were measured:

- Air temperature and air humidity
- Globe thermometer temperature
- Surface temperature of the structure by an infrared camera
- Air velocity measured by an ultrasonic anemometer in order to determine the air movement in the animal zone
- Air volume flow by using CO_2-balance model and a tracer gas technique by using radioactive gas Krypton 85 (Kr-85)

The external meteorological conditions were recorded by a measurement tower which was located at a distance of ~10H of the two cowsheds (H= height of the cowshed). The tower was equipped with two Ultrasonic anemometers (GILL wind master pro) at heights of 7.5 m and 10 m, respectively. Local wind of all three velocity components were sampled at a frequency of 10Hz and their turbulent quantities, e.g. turbulence intensity, were derived. Additionally, air temperature and relative air humidity sensors (Rotronic) were mounted at three heights (3, 6 and 9 m). The globe thermometer outside temperature was measured between the two cowsheds.

2.3 Evaluation methods

The main influencing factors on heat stress are air temperature, air humidity, the wind velocity and the direct solar radiation. In literature (e.g. CIGR, 2002; Mader et al., 2006) many models exist which combine the temperature and the humidity to the so called *Temperature Humidity Index* (*THI*), which can be defined as follows:

$$THI = 0.8 * T_a + \left[\left(RH / 100 \right) * \left(T_a - 143 \right) \right] + 46.4 \qquad (1)$$

where T_a is the ambient temperature in [°C] and RH is the relative humidity in percent [%]. Based on the daily maximum Temperature Humidity Index (THI_{max}) Brown-Brandl et al. (2005), citing Thom (1959), defined four categories to rate the level of possible heat stress: a) $THI_{max} < 74$ normal, b) $74 \leq THI_{max} < 78$ alert, c) $78 \leq THI_{max} < 84$ danger, d) $THI_{max} \geq 84$ emergency. Similar values are defined by CIGR (2006), citing Johnson et al. (1965), by a slightly different definition of the *THI*. In order to include the influence of the solar radiation effect some authors (e.g. Buffington et al., 1981; Panagakis and Deligeorgis, 2006) substitute the black globe temperature (T_{bga}) for the ambient temperature (T_a) in the *THI* equation:

$$BGTHI = 0.8*T_{bga} + [(RH/100)*(T_{bga} - 14.3)] + 46.4 \quad (2)$$

Mader et al. (2006) adjusted the THI for wind speed and solar radiation and proposed the following Equation:

$$THIV = [4.51 + THI - (1.992 * V) + (0.0068 * RAD)] \quad (3)$$

where V is the wind speed in [m s^{-1}] and RAD the solar radiation in [W m^{-2}].

Another approach to assess the climate impact on animals is to adapt the knowledge of thermal comfort for humans which has a long experience and provides special guidelines as e.g. DIN EN ISO 7730 (2003) which give guidance for the evaluation of the thermal comfort for humans. Pache et al. (2007) attempted to use this guideline to compare a light construction cowshed and a solid construction cowshed. Even though the concept for humans can not directly transferred to animal husbandry some of the parameters may be suitable for an evaluation regarding heat stress. Several studies, e.g. Pache et al. (2007) used a special measuring station for human thermal comfort to determine the *mean radiant temperature* (Eq. 4) inside the cowshed:

$$t_r = [(t_g + 273)^4 + 2.5*10^8*{v_a}^{0.6}*(t_g - t_a)]^{1/4} - 273 \quad (4)$$

where: t_r: mean radiant temperature in °C
t_g: globe thermometer temperature in °C
t_a: ambient dry temperature in °C
v_a: air velocity in m/s

The *mean radiant temperature* includes the effect of solar radiation and wind speed, but neglects the humidity. However, the definition of thermal comfort for animals is much more difficult than for humans and needs further investigations. The animal response on varying climatic impact factors cannot be neglected and have to be determined.

3. Selected results

3.1 THI and BGTHI

The obtained data were used to calculate the THI, BGTHI and THIV (Eqs. 1 through 3) and compare them with threshold values from literature. In fact, only at one day of a 28-day measurement period, the THI exceeded the threshold value 74 associated with the category "danger" (Fig. 1). Figure 1 illustrates the calculated THI (Eq. 1), the BGTHI

(Eq. 2) and the THIV (Eq. 3) for a selected three day period in cowshed 1. Three different wind speeds from velocity measurements were applied for calculating THIV; the lowest measured wind speed by V= 0.2 m s^{-1}, an average wind speed by V= 0.9 m s^{-1} and the highest measured wind speed by V= 2.0 m s^{-1}. The calculated THI, BGTHI and THIV with V= 2 m/s obtained similar results (Fig. 1). For lower wind speeds, higher THIV were observed. This fact may result in a different classification of heat stress. The differences between calculated THI from cowshed 1 and cowshed 2 are nominal due to the small differences of measured air temperature and air humidity. In most cases THI of cowshed 2 (with roof insulation) revealed higher values during evening and night hours due to higher observed air temperatures. These differences of THI between cowshed 1 and cowshed 2 became smaller during day time. On this basis no significant positive effect due to the roof insulation could be found.

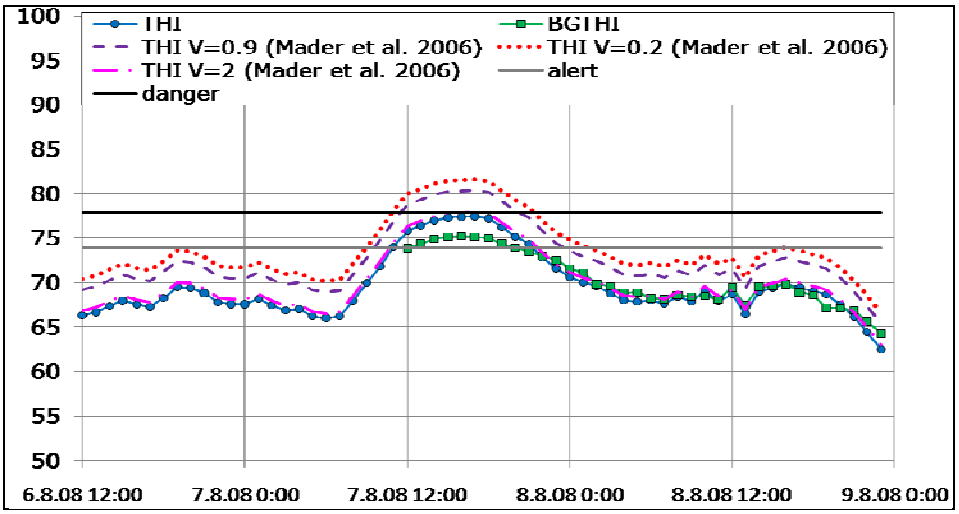

Fig. 1: Estimated THI, BGTHI and THIV in cowshed 1 for a selected period

3.2 Mean radiant temperature

Additionally to the received data, the mean radiant temperature was calculated (Eq. 4). It combined the black globe thermometer temperature, the ambient temperature and the wind speed. Figure 2 shows the run for the mean radiant temperature (with a considered wind speed of V= 0.8 m s^{-1}) for a selected period in both cowsheds and outside the cowsheds. The estimated radiation temperature ranged between 12.2 and 25.6°C in stable 1 and between 5.2 and 36.0 °C in stable 2 (with roof insulation) over the entire measurement period. For want of an adequate data set for connecting the animal response to the radiation temperature, it was not possible to define a critical threshold. Pache et al. (2007) found an increased respiration frequency and body temperature if the radiation temperature exceeded 36 °C. All data obtained within this study are beyond this value.

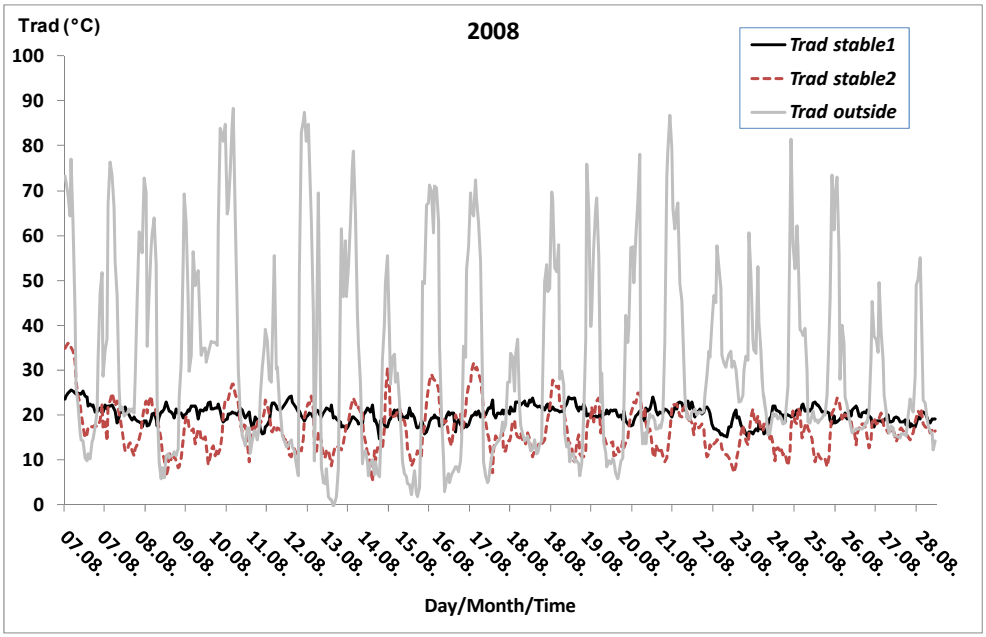

Fig. 2: Estimated in- and external mean radiant temperature of two cowsheds

4. Discussion and conclusions

The results of this study showed that the investigated roof insulation possessed only minor effects on the indoor environment. For performed temperature measurements in comparable cowsheds with and without roof insulation only differences smaller than 1 K could observed. Nevertheless, calculation of the radiation temperature mostly obtained higher values in cowshed 1 with differences up to 10 K. Thus, it should be aimed at implementing more parameters beside only air temperature and air humidity. Moreover, occurring environmental effects (e.g. air velocity) and the animal-related parameters (e.g. age, breed, milk yield and color) are crucial and have to be considered. As an outcome, further investigations over longer time periods are necessary, for defining most influencing parameters. The welfare of cows depends on many various factors including health, feeding, occupancy density of the stable and the treatment of the stable staff. Further, each animal shows different reactions toward heat as a stressful event. Therefore, more investigative methods should be developed for detecting individual stress of animals. Assessing the impact of the stable indoor environment on animal welfare, the whole husbandry system and the behavior of animals have to be considered. It is planned at first to use thermal climate indices from human biometeorology i.e. Physiological Equivalent Temperature (PET) and other radiation parameters calculated by the RayMan model, since it has a thermo physiological importance, particularly during the summer period (Matzarakis and Mayer, 1998; Mayer and Matzarakis, 1998).

References

Brown-Brandl, T.M., T.A. Eigenberg, J.A. Nienaber, G.L. Hahn, 2005: Dynamic response indicators of heat stress in shaded and non-shaded feedlot cattle, part 1: analyses of indicators. Bios. Eng., 90, 4, 451-462.

Buffington, D. E., A. Collazo-Arocho, G.H. Canton, D. Pitt, 1981: Black globe-humidity index (BGHI) as comfort equation for dairy cows. Trans. ASAE, 24, 3, 711-714.

CIGR Report, 2002: Climatization of Animal Houses. Editors: Pedersen, S., K. Sällvik, Working Group Report on: Heat and Moisture Production at Animal and House Level. Published by DIAS, Denmark.

CIGR Report, 2006: Animal Housing in Hot Climates: A multidisciplinary view. Editors: Nääs, I.A., D.J. Moura, Working Group Report. Published by DIAS, Denmark.

Collier, R.J., G.E. Dahl, M.J. VanBaale, 2006: Major advances associated with environmental effects on dairy cattle. J. Dairy Sci., 89, 1244-1253.

DIN 18910-1, 2004: Thermal insulation for closed livestock buildings-Thermal insulation and ventilation forced, part 1: Principles for planning and design for closed ventilated livestock buildings. Published by Beuth-Verlag, Berlin.

DIN EN ISO 7730, 2003: Ergonomics of the thermal environment-Analytical determination and interpretation of thermal comfort using calculation of the PMV and PPD indices and local thermal comfort. Published by Beuth-Verlag, Berlin.

Mader, T.L., M.S. Davis, T. Brown-Brandl, 2006: Environmental factors influencing heat stress in feedlot cattle. J. Anim. Sci., 84, 712-719.

Matzarakis, A., H. Mayer, 1998: Investigations of urban climate's thermal component in Freiburg, Germany. Prepr. 2nd Urban Environment Symposium, November 2-6, 1998, Albuquerque, New Mexico, American Meteorological Society, 140-143.

Mayer, H., A. Matzarakis, 1998: Human-biometeorological assessment of urban microclimates' thermal component. Proc. 2nd Japanese-German Meeting "Klimaanalyse für die Stadtplanung", Research Center for Urban Safety and Security, Kobe University, Special Report No. 1, 155-168.

Pache, S., S. Rössner, O. Hörig, U. Bergfeld, 2007: Requirements of the dairy cows for outdoor climate stables suited for summer – examinations to the thermo regularization, stable climate control and construction method. In: Proceedings of the 8th International conference on Construction, Engineering and Environment in Livestock Farming, 264-269.

Panagakis, P., S. Deligeorgis, 2008: Preliminary evaluation of the short term thermal comfort of dairy ewes reared under Greek summer conditions. In: Proc. International Conference on Agricultural Engineering AgEng 2008, paper-no. OP-705, Hersonissos, Crete, Greece, 23.-25.06.2008.

West, J.W., 2003: Effects of heat-stress on production in dairy cattle. J. Dairy Sci., 86, 2131-2144.

Authors' addresses

Dr. Merike Fiedler (mfiedler@atb-potsdam.de),
Dr. Gundula Hoffmann and Kristina von Bobrutzki
Leibniz-Institute for Agricultural Engineering Potsdam-Bornim e.V. (ATB)
Department of Engineering for livestock Management
Max-Eyth-Allee 100, 14469 Potsdam, Germany

Prof. Dr. Andreas Matzarakis (andreas.matzarakis@meteo.uni-freiburg.de)
Meteorological Institute, Albert-Ludwigs-University of Freiburg
Werthmannstr. 10, 79085 Freiburg, Germany

Evaluation of solar global radiation 1984-2008 over Czechia station network

Jiri Nekovar[1] , Rudolf Bagar[2]

[1]Czech Hydrometeorological Institute, Na Šabatce 17, CZ-14306 Prague 4 – Komořany
[2]CZ-62500 Brno, Oderská 8

Abstract

Eleven meteo stations form solar global radiation measuring network in the frame of Czech Hydrometeorological Institute. Regular series in the period 1984 - 2008 (25 year duration) have been measured. Evaluation of data series is given by regression linear correlation coefficients and polynomial regression significance according to the elevation is described - during calendar year and summer half-year periods.

1. Introduction

Solar global radiation is climatology characteristic conditioned climate behavior in the Earth planet, including Czechia, of course. It has important influence to climate change, including actual status of it. Let us express thanks to CHMI colleagues from Solar & Ozone Department (especially to Dr. Michal Janouch); they collect, organize, classify and kindly provide solar global radiation data series to permit us to compare these data for 25 years period.

Solar global radiation is defined (Sobíšek et al, 1993) like short-waved radiation flow to the earth surface; it is given like vertical direct sunshine radiation (the insolation) and diffused sunshine radiation incident to the horizontal surface from space angle 2π. It is important characteristic of sunshine energy into the atmosphere and to the Earth surface. Its intensity expands with Sun angle over the horizon and with atmospheric turbidity decrease; it depends also in the cloud amount. Wavelength is moved in interval between 0, 2 to 10 μ m.

2. Methodology

The aim of the presentation is to give sure overview over solar global radiation for last 25 years in Czechia and mainly to try to find sure tendency of data series development. This climate characteristic is measured in Czechia using the network of 11 stations from 1984 - by the care of mentioned Solar and Ozone Dpt being situated in Hradec Králové Observatory. Tendencies are evaluated usually with the regard to increasing evaluation of station position – from Prague-Karlov 232 m above sea level to the mountain station Churánov in 1122 m a. s. l.

We try to evaluate solar radiation tendency, based on correlation coefficient comparison - like significant relation indicator – to evaluate the significance of correlation between:

a) Accretion of solar radiation total during the period 1984 – 2008,
b) Lowland – Highland station position differences,
c) Polynomial curve & linear regression equation using,
d) Annual & summer half-year period differences, month step difference, too,
e) Solar radiation, sunshine duration and air temperature –1984-2008 tendency.

3.1 Results – global solar radiation tendency

Evaluated period has been from 1984 to 2008. Every station has its own 25-years' course. Nevertheless, general tendencies would be explained in this contribution. General results are repeated also in the Conclusion chapter.

Sunshine global radiation of all eleven studied stations has increasing tendency; more rapid in the lowland and less rapid in the mountain areas. The graphs of annual & summer half-year season of the lowest and highest studied stations (Prague-Karlov and Churánov) are given in fig. 1 to fig.4.

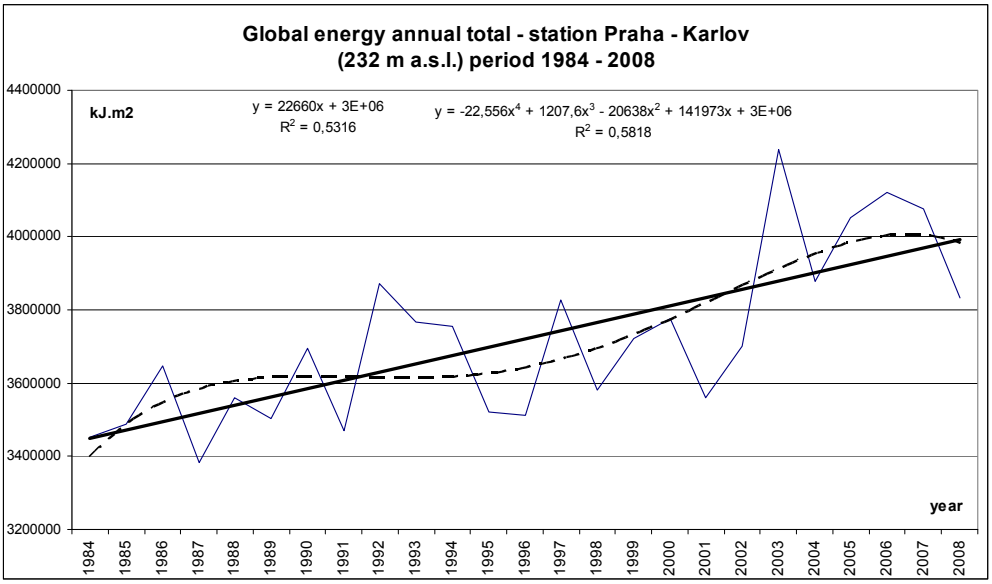

Fig. 1: Annual total of solar radiation value – station Prague – Karlov, period 1984 – 2008

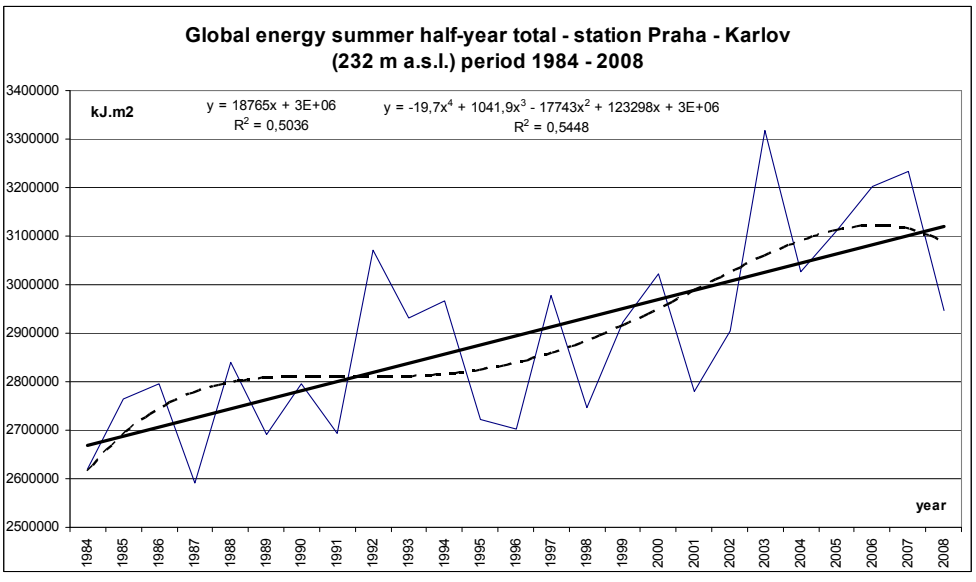

Fig. 2: Summer half-year (April to September) total of solar radiation, station Prague-Karlov, period 1984-2008

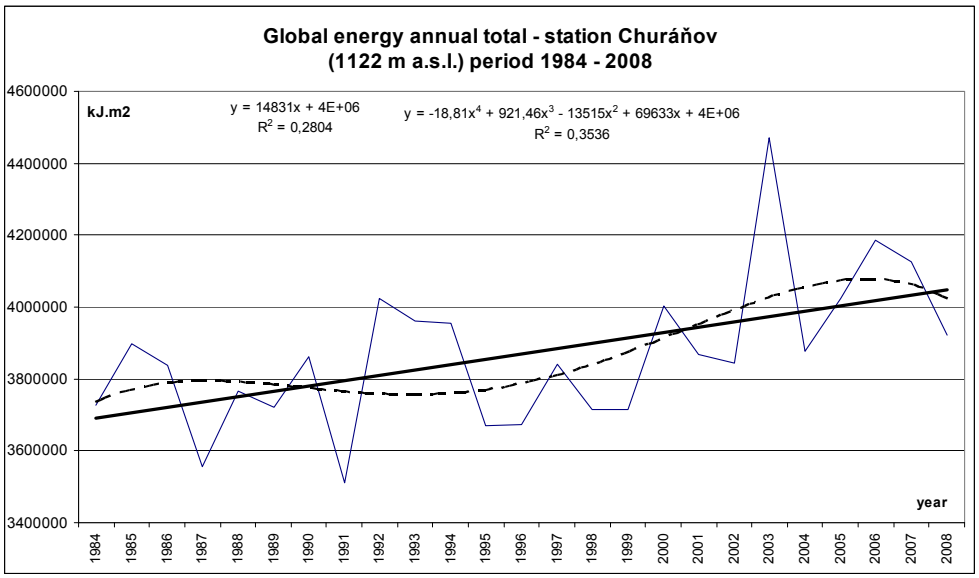

Fig. 3: Annual total of solar radiation value – station Churánov, period 1984 – 2008

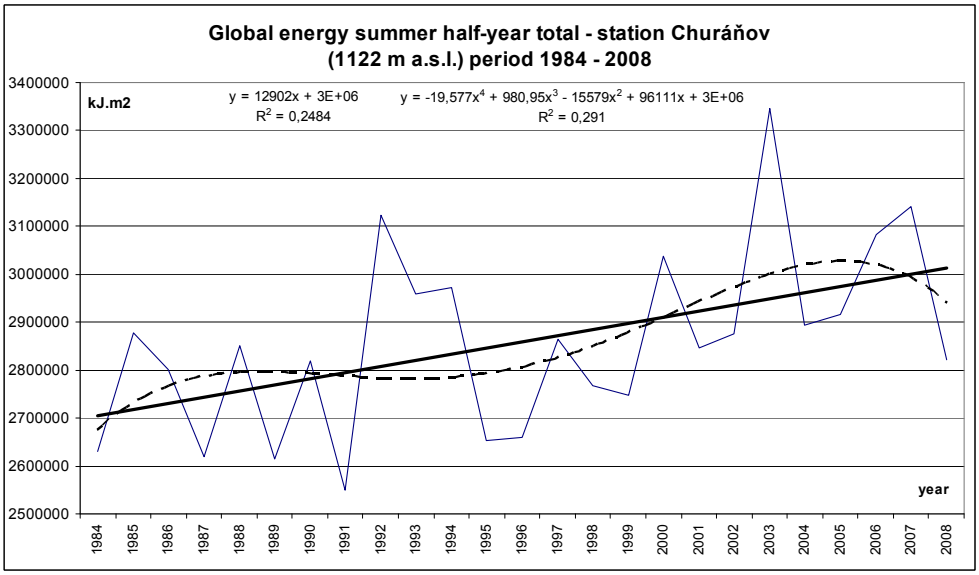

Fig. 4: Summer half-year (April to September) total of solar radiation, station Churánov, period 1984-2008

3.2 Results – sunshine global radiation correlation coefficients evaluation

Correlation coefficient of polynomial regression is – in the case of all eleven station tendency higher in comparison with linear regression results.

Correlation coefficient of annual solar global radiation data series is higher than the same one concerning in summer half-year period. Results are given in Tab. 1.

Table 1: Linear and polynomial regression dependence correlation coefficient of solar radiation series 1985 – 2008 according to CHMI climatic station network be given by ascending elevation

CHMI station	period	Corr. dependence linear	Corr. dependence polynomial
Praha	annual	0,5316 **	0,5819 **
232 m a.s.l.	IV. – IX.	0,5036 **	0,5448 **
Ostrava -Poruba	annual	0,5951 **	0,6451 **
242 m a.s.l.	IV. – IX.	0,5776 **	0,6165 **
Hradec Králové	annual	0,3036	0,3901 *
285 m a.s.l.	IV. – IX.	0,3208	0,3838 *
Tušimice	annual	0,5056 **	0,5188 **
322 m a.s.l.	IV. – IX.	0,4555 *	0,4832 *
Kuchařovice	annual	0,4769 *	0,5037 **
334 m a.s.l.	IV. – IX.	0,3898 *	0,4109 *
Ústí nad Labem	annual	0,5478 **	0,6679 **
377 m a.s.l.	IV. – IX.	0,4821 *	0,6208 **
Luká	annual	0,5960 **	0,6261 **
513 m a.s.l.	IV. – IX.	0,6037 **	0,6127 **
Kocelovice	annual	0,3833 *	0,4112 *
519 m a.s.l.	IV. – IX.	0,3519 *	0,3810 *
Košetice	annual	0,3640 *	0,5015 **
534 m a.s.l.	IV. – IX.	0,3120	0,3994 *
Svratouch	annual	0,4200 *	0,4418 *
735 m a.s.l.	IV. – IX.	0,3898 *	0,4089 *
Churáňov	annual	0,2804	0,3536 *
1122 m a.s.l.	IV. – IX.	0,2484	0,2910

3.3 Results – correlation comparison according to the station elevation

Correlation coefficient seems to be generally the higher one in lowland station and the lesser one in highlands.

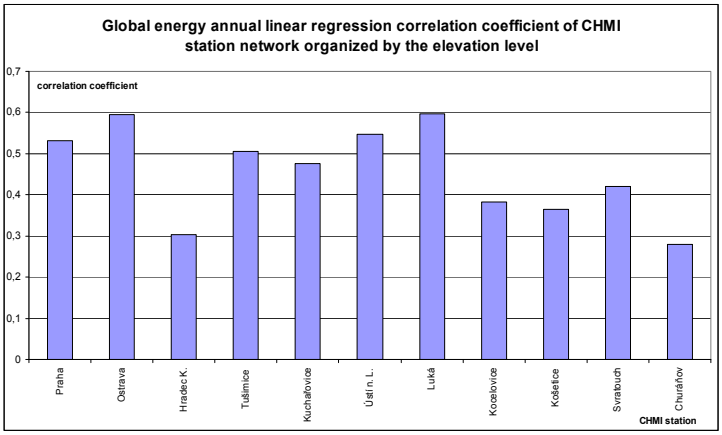

Fig. 5: Correlation coefficient of annual linear regression of solar radiation according to the station elevation increase

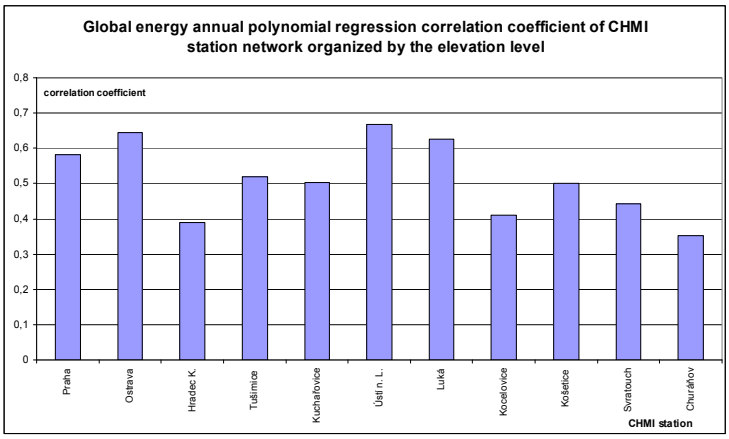

Fig. 6: Correlation coefficient of annual polynomial regression of solar radiation according to the station elevation increase

3.4. Results - Correlation between solar radiation, sunshine duration and air temperature

The highest correlation is between solar radiation and sunshine duration, absolutely lesser one between solar radiation and air temperature and the smallest one between sunshine duration and air temperature data series.

The highest correlation between solar radiation and air temperature is in June & July, between sunshine duration and air temperature in July (from June to August), between solar radiation and sunshine duration has the correlation significant relation in all months, but the highest one is in September (from May to October).

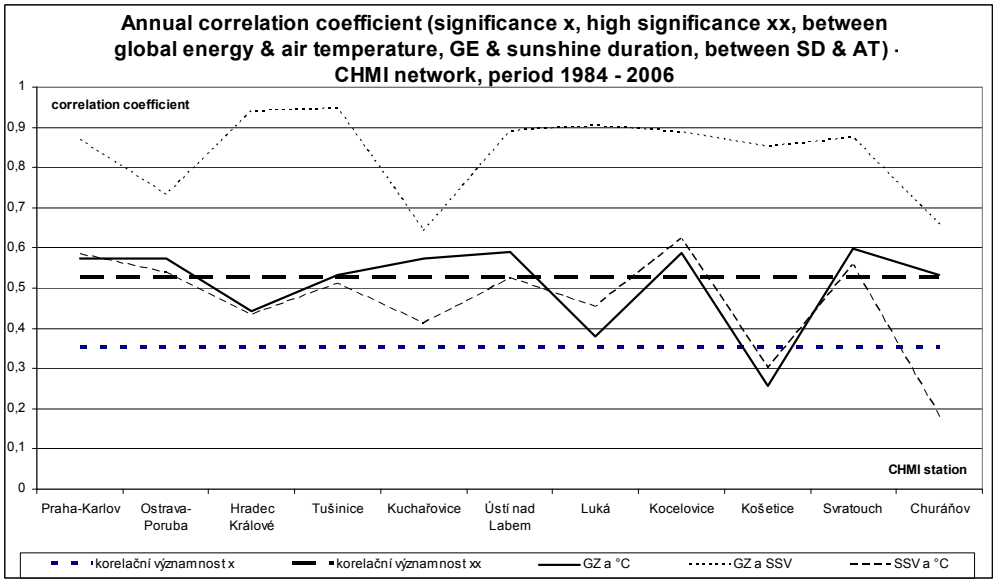

Fig. 7: Annual mean of the correlation coefficient value between solar radiation, sunshine duration and air temperature in the comparison with significant & very significant level

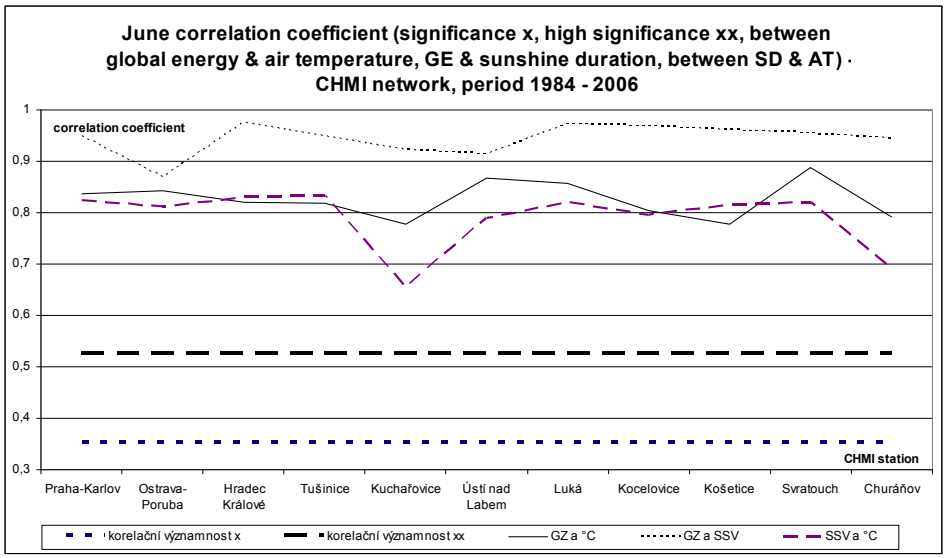

Fig. 8: Annual mean of the correlation coefficient value between solar radiation, sunshine duration and air temperature in the comparison with level significance

4. Conclusions

a) Global solar radiation of all eleven studied stations has increasing tendency; more rapid in the lowland and less rapid in the mountain areas.
b) Correlation coefficient of polynomial regression is – in the case of all eleven station tendency higher in comparison with linear regression results.
c) Correlation coefficient of annual solar global radiation data series is higher than the same one concerning in summer half-year period.
d) Correlation coefficient seems to be generally the higher one in lowland station and the lesser one in highlands.
e) Correlation is the highest one between solar radiation and sunshine duration (maximal in September), lesser one between solar radiation and air temperature (max. in June) and the smallest one between sunshine duration and air temperature (July).

Acknowledgement

Authors are indebted to:

- the Ministry of Education – for financial support of OC09029 (ES0603) project
- Dr. Michal Janouch, Ph.D., main researcher of P05OC033 project (Long-term changes and UV radiation climatology over Czechia; COST726) - for help and data acquisition
- As. Prof. Martin Klimánek, Ph.D., Mendel Agricultural and Forestry University Brno - for operative scientific-technical cooperation

References

Sobíšek et al., 1993: Meteorologický slovník výkladový a terminologický. /Meteorological dictionary/ Academia Praha & MŽP ČR, 594 pp. ISBN 80-85368-45-5

Janouch M., 2008: Long-term changes and UV radiation climatology over Czechia. P05OC033 (COST726) project - Final Report, Hradec Králové

Author's address:

Eng. Jiri Nekovar, Ph.D., (jiri.nekovar@chmi.cz) Czech Hydrometeorological Institute, Na Šabatce 17, CZ-14306 Prague 4 – Komořany, Czechia

As. Prof. Eng. Rudolf Bagar, Ph.D., Oderská 8, CZ-62500 Brno – Starý Lískovec, Czechia

Stadtplanung und Klimawandel
Eine Kooperation mit der Stadtentwicklungsverwaltung von Berlin

Angelika Grätz[1], Ursel Behrens [2], Jörn Welsch[3]

[1]Deutscher Wetterdienst, Zentrum für Medizin-Meteorologische Forschung Freiburg
[2]Deutscher Wetterdienst, Regionale Klima und Umweltberatung Potsdam
[3]Senatsverwaltung für Stadtentwicklung, Abteilung Geoinformation, Informationssystem Stadt und Umwelt, Berlin

Abstract

Wärmeinseleffekt und fortdauernde Klimaerwärmung legen nahe, dass in großen Städten die thermischen Bedingungen insbesondere im Sommerhalbjahr zunehmend belastender und folglich bei Stadtplanungsfragen an Bedeutung gewinnen werden. In diesem Zusammenhang ist die Kooperationsvereinbarung zwischen der Stadtentwicklungsverwaltung von Berlin und dem Deutschen Wetterdienst zu sehen, die sich das Ziel gesetzt hat, die räumliche Struktur und die Häufigkeit künftiger gesundheitlich relevanter Wärmebelastung zu bestimmen und für Berlin kleinräumig auszuprägen. Realisieren lässt sich das mit der Erweiterung des Stadtbioklimamodells UBIKLIM durch ein Modul, das die lokalen und die regionalen bioklimatischen Bedingungen miteinander verknüpft. Zum künftigen Bioklima in der Stadt kommt man dann, indem das erweiterte Stadtbioklimamodell mit den Resultaten regionaler Klimamodelle - im vorliegenden Fall REMO und WETTREG - angetrieben wird. Die Ergebnisse zeigen, dass innerstädtische Parkanlagen, die reichlich Schatten bieten, im Laufe dieses Jahrhunderts als Ausgleichsflächen für die zunehmend stärker belasteten versiegelten und bebauten Areale weiter an Bedeutung gewinnen werden.

1. Einführung

Mit dem Ziel, die räumliche Struktur und die Häufigkeit künftiger gesundheitlich relevanter Wärmebelastung im Stadtgebiet von Berlin und dem Umland zu bestimmen, haben die Senatsverwaltung für Stadtentwicklung, Abteilung ‚Geoinformation' Referat Informationssystem Stadt und Umwelt und der Deutschen Wetterdienst (DWD),

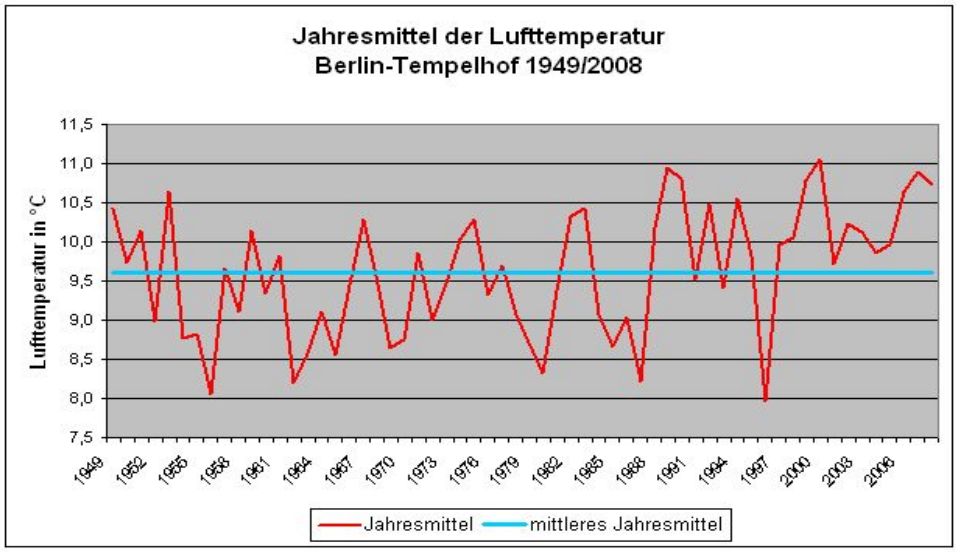

Abb. 1: Jahresmittel der Lufttemperatur an der Station Berlin-Tempelhof (1949-2008)

Abteilung ‚Klima- und Umweltberatung' eine Kooperation vereinbart. Damit sollen die Effekte des Klimawandels und die des urbanen Wärmeinseleffekts – auch unter Berücksichtigung städteplanerischer Veränderungen - zusammengefasst und gemeinsam betrachtet werden. Auswertungen klimatologischer Zeitreihen von Berliner Stadt- und Umlandstationen spiegeln thermische Veränderungen der letzten Jahrzehnte bis heute wider (Abb. 1) und liefern auch deutliche Hinweise für die positive Temperaturanomalie der Stadt gegenüber dem Umland. Über ein Downscaling regionaler Klimaprojektionen unter Verwendung und Fortentwicklung des Stadtbioklimamodells UBIKLIM lassen sich beide Effekte gemeinsam auswerten. Die Anwendung von Bioklimamodellen im Rahmen von Planungsfragen birgt dabei den großen Vorteil, dass die Ergebnisse immer eine Bewertung in Bezug auf das Wohlbefinden des Menschen beinhalten.

2. Das Kombinierte Stadtbioklimamodell

Das in den neunziger Jahren entwickelte Stadtbioklimamodell UBIKLIM (**U**rbanes **BI**o**KLI**ma**M**odell) basiert auf der Idee der Klimatope. Klimatope sind Gebiete mit ähnlicher mikroklimatischer Ausprägung. In der Ebene sind sie durch die dominante Flächennutzungsart geprägt, während in kupiertem Gelände außerdem der Einfluss von Höhe, Orographie und Exposition zu berücksichtigen ist.

Als Eingangsgrößen benötigt UBIKLIM neben einem hoch aufgelösten Höhenmodell geeignete Flächennutzungsinformationen. Dazu wird das Untersuchungsgebiet in eine endliche Anzahl von Arealen mit gleicher oder ähnlicher Nutzung unterteilt. Bebautes Gebiet wird weiter unterteilt und durch Versiegelungsgrad, überbauten Flächenanteil, Gebäudehöhe, Zahl der Gebäude pro Fläche und Durchgrünung eindeutig charakterisiert. Anhand dieser Eingangsdaten berechnet UBIKLIM in mehreren Schritten – vorrangig durch Anwendung des 1-dimensionalen Stadtklimamodells MUKLIMO_1 – für einen windschwachen, wolkenlosen Sommertag die meteorologischen Größen in 1 m Höhe über Grund für das gesamte Untersuchungsgebiet und analysiert sie anschließend pixelweise mit dem Klima-Michel-Modell (Piehl und Grätz, 1996; Friedrich et al., 2001). Damit werden die lokalen Unterschiede im Bioklima erfasst. Um eine Beziehung zum regionalen Klima herzustellen, werden die UBIKLIM-Ergebnisse mit von der Flächennutzung unabhängiger regionaler Bioklimainformation – im Folgenden als Hintergrundbelastung bezeichnet – verknüpft. Die Zusammenführung der unterschiedlichen Scales erfolgt anhand einer statistischen Modellgleichung.

Beschrieben wird die Hintergrundinformation mit der Zahl der Tage mit Wärmebelastung als 30-jähriger Jahresmittelwert. Ein Tag mit Wärmebelastung wird definiert als ein Tag, an dem tagsüber die Gefühlte Temperatur mindestens an drei Stundenterminen 32°C und damit starke Wärmebelastung erreicht oder überschritten hat - eine Definition, die angenähert die Tage erfasst, die als warnwürdig erachtet werden.

Um den Zusammenhang zwischen den thermischen Bedingungen an einem sommerlichen Strahlungstag einerseits und den mittleren klimatischen Bedingungen andererseits zu ermitteln, wurden für den Zeitraum 1971 - 2000 den Wetterdaten der synoptischen Stationen in Deutschland verschiedene Nutzungen/ Stadtstrukturen aufgeprägt. Alle Daten wurden anschließend mit dem Klima-Michel-Modell analysiert und auf Wärmebelastungstage hin untersucht. Da sich die UBIKLIM-Ergebnisse auf Strahlungstage beziehen, müssen zur Kopplung mit dem regionalen Bioklima auch die Wärmebelas-

tungstage berücksichtigt werden, die keine Strahlungstage sind. Damit besteht die resultierende Gleichung sowohl aus einer Regressionsbeziehung als auch aus einer Gewichtungsfunktion.

Die Kopplung der lokalen mit der regionalen Bioklimainformation wird durch folgenden Ansatz realisiert:

$WB = (r_1 * WB_{frei} + r_2 * dGT + r_3 WB_{frei} * dGT + geo) * strant + WB_{frei} * (1 - strant)$

mit WB: Tage mit Wärmebelastung an einem beliebigen Ort der Stadt

WB_{frei}: Hintergrundbelastung

dGT: Gefühlte Temperatur an einem beliebigen Ort der Stadt minus Gefühlte Temperatur über Freifläche außerhalb der Stadt (gemäß UBIKLIM)

geo: f(geograph. Breite und Länge sowie Höhe) = konstant für Berlin

strant: prozentualer Anteil von Strahlungstagen an den aufgetretenen Wärmbelastungstagen

r_i : Regressionskoeffizienten

3. Bioklima Berlin und Umland - heute und morgen

Bei der Anwendung des Kombinierten Bioklimamodells auf Berlin und Umland wurde aufgrund der geringen vertikalen Erstreckung die Höhe als konstant angenommen.

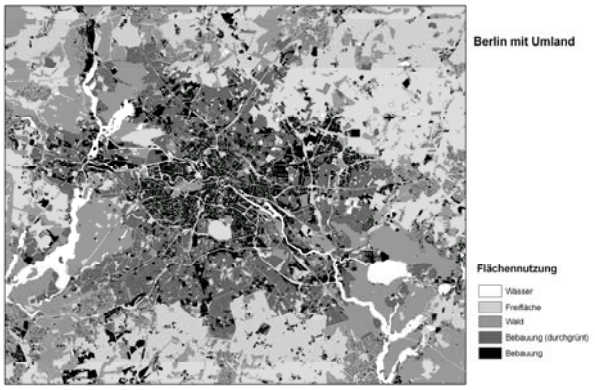

Karte 1: Flächennutzung (vereinfacht) Berlin und Umland

Die Informationen zu Flächennutzung und Stadtstruktur stellte die Senatsverwaltung für Stadtentwicklung im 25m x 25 m – Raster so zur Verfügung, dass sie entsprechend den Erfordernissen von UBIKLIM aufbereitet werden konnten. Es wurden ca 65 Strukturtypen unterschieden. (Karte 1 vereinfachte Flächennutzung Berlin und Umland). Auch potenzielle Planungsflächen mit einem Zeithorizont bis 2020 wurden bereitgestellt (Ausschnitt: Karte 3a).

Die Aktuelle Bioklimakarte für Berlin und Umland wurde anhand der Bestandsdaten für die Flächennutzung und einer Hintergrundbelastung berechnet, die aus den Beobach-

tungsdaten der synoptischen Station Berlin-Schönefeld abgeleitet wurde. Diese zeigt, dass die Berliner Innenstadt etwa doppelt so häufig belastet ist wie die unbebaute Umgebung. Allerdings brechen die Parkanlagen das innerstädtische Belastungsgefüge auf, und man findet hier oftmals noch recht angenehme thermische Bedingungen, wenn in der umliegenden Bebauung die Bedingungen bereits warnwürdige sind.

Für den Klimawandel in einer Stadt sind lokale Änderungen, die insbesondere durch Umnutzungen hervorgerufen werden, sowie an das globale Klima gekoppelte Änderungen verantwortlich. Mit dem Kombinierten Stadtbioklimamodell können beide Einflussfaktoren berücksichtigt werden, wobei die Hintergrundbelastung durch das globale beziehungsweise das daraus abgeleitete regionale Klima definiert wird.

Unter Beschränkung auf das A1B-Szenario (IPCC, 2001) wurden bei dieser Kooperation die Resultate der Regionalmodelle REMO (Jacob,2005) und WETTREG (Kreienkamp und Enke, 2006) herangezogen.

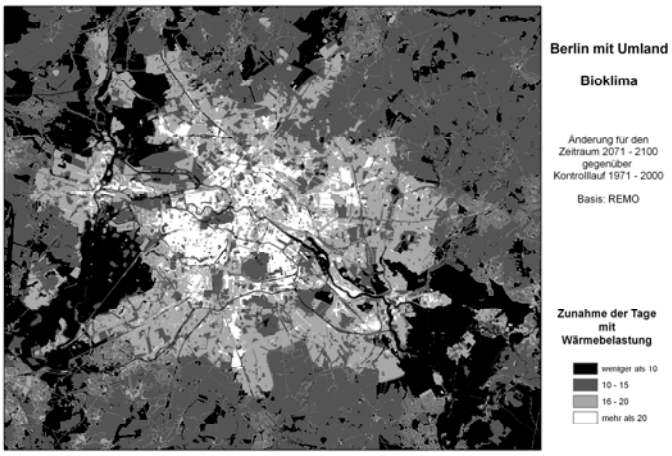

Karte 2: Zunahme der Tage mit Wärmebelastung (Jahresmittel) des Projektionszeitraums 2071 – 2100 gegenüber dem Kontrolllauf 1971 – 2000 mit REMO-Antrieb

Es wurden die Zeiträume 1971 – 2000, 2021 – 2050 und 2071 – 2100 untersucht. Für diese wurden zunächst anhand der jährlich ermittelten Tage mit Wärmebelastung aus den Mess- und Modelldaten Konfidenzintervalle für das 90%-Signifikanzniveau berechnet. Es zeigt sich zum einen, dass die Hintergrundbelastung, die sich aus den Modellen ergibt, die an der Station beobachtete Hintergrundbelastung gut widerspiegelt, zum anderen, dass es zu einer leichten, aber signifikanten Erhöhung der Anzahl an Wärmebelastungstagen bis zur Mitte dieses Jahrhunderts kommt. Für 2071 – 2100 ist die Zunahme der Tage mit Wärmebelastung dann deutlich stärker.

Wie bereits die Betrachtungen der Konfidenzintervalle vermuten lässt, zeigt sich, dass die thermische Belastung künftig im gesamten Untersuchungsgebiet zunimmt. Dabei intensiviert sich die Wärmebelastung in den heute schon am häufigsten betroffenen Arealen der Innenstadt am stärksten. Hier werden bis zum Ende des 21. Jahrhunderts

die Hälfte der Tage in den Sommermonaten wärmebelastet sein, im Umland und auch in den innerstädtischen mit Schatten spendenden Bäumen begrünten Parkanlagen nicht ganz ein Drittel (Karte2).

Die zusätzliche Berücksichtigung der potenziellen städtebaulichen Veränderung unterstreicht die Bedeutung der Parkanlagen für das Bioklima erneut. Bis Mitte des Jahrhunderts wird es hier nur geringfügig zu einem Mehr an Belastungstagen kommen und dort, wo Freiflächen mit Bäumen durchgrünt werden (Gebiet 1 in Karte 3), stellt sich die Situation sogar entspannter als heute dar. Wo dagegen versiegelt und dicht bebaut wird (Gebiet 2), nimmt die thermische Belastung gegenüber heute zu und zwar stärker als nur durch den Klimawandel bedingt.

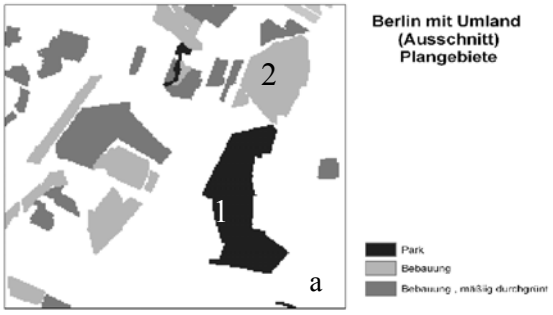

Karte 3a: Projektgebiete mit gesamtstädtischem Veränderungspotenzial (Ausschnitt)

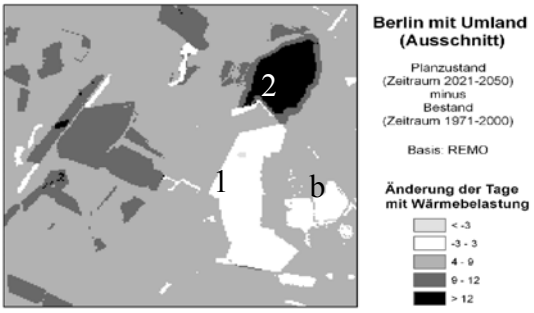

Karte 3b: Änderung der Anzahl der Tage mit Wärmebelastung (Jahresmittel) durch Umnutzung der Projektgebiete sowie den globalen Klimawandel für den Projektionszeitraum 2021 – 2050 gegenüber dem Kontrollzeitraum 1971 – 2000 mit REMO-Antrieb (Ausschnitt)

4. Schlussbemerkungen

Die vorgestellten Untersuchungen bauen bezüglich des Einsatzes der Regionalmodelle auf den Erfahrungen des beim Deutschen Wetterdienst angesiedelten Projektes ZWEK (Zusammenstellung von Wirkmodell-Eingangsdatensätzen für die Klimafolgenabschätzung) auf (Deutschländer et al., 2009). Dort wird darauf hingewiesen, dass erst die Zusammenschau mehrerer Modellsimulationen eine Aussage über die Zuverlässigkeit der gefundenen Ergebnisse näherungsweise erlaubt. Die Interpretation der Ergebnisse sollte grundsätzlich und gleichwertig die gesamte Ergebnispalette beinhalten (Ensemble-

Betrachtung). Es wird deshalb die Simulation mit weiteren Ensemble-Mitgliedern (zunächst STAR) angestrebt.Von Seiten der Senatsverwaltung für Stadtentwicklung Berlin ist vorgesehen, die Ergebnisse (unter Berücksichtigung der fachlich gebotenen Einschränkungen) als wesentliche Hilfe in den laufenden Prozess der Erarbeitung eines Stadtentwicklungsplanes Klima einfließen zu lassen (Stand 12.01.2010).

Literatur

Deutschländer, T., M. Koßmann, T. Steigerwald, J. Namyslo, 2009: Verwendung von Klimaprojektionsdaten für die Stadtklimasimulation. Klimastatusbericht 2008. Deutscher Wetterdienst, Offenbach, 13 – 17.

Friedrich, M., A. Grätz, G. Jendrtzky, 2001: Further development of the urban bioclimate model UBIKLIM, taking lokal wind systems into account. Meteorol. Z. 10, 267 – 272.

IPPC, 2001: Climate Change 2001: the scientific basis. In: Houghton, J.T., L.G. Meira Filho, J. Bruce, H. Lee, B.A. Callender, E. Haites, N. Harris, K. Maskell, eds. Contribution of the Working Group I to the Third Assessment Report of the Intergovernmental Panel on Climate Change. Cambridge- New York: Cambridge University Press.

Jacob, D, 2005: REMO climate of the 20th century run, UBA projekt, 0.088 degree resolution, run no. 006210, 1h data. World Data Centre for Climate. CERA-DB "REMO_UBA_C20_1_R006210_1H" http://cera-www.dkrz.de/WDCC/ui/Compact.jsp?acronym=REMO_UBA_C20_1_R006210_1H (Stand Februar 2009).

Kreienkamp, F., W. Enke, 2006: WETTREG 20C control run 1961-2000 und WETTREG A1B scenario run 2001-2100, UBA Project. (CERA-Datenbank: http://cera-www.dkrz.de/WDCC/ui/BrowseRxperiments.jsp?proj=WETTREG-UBA (Stand04/2009))

Piehl, H.-D., A. Grätz, 1996: Klimakarten für das Land Berlin. Teil1: Bioklima. Deutscher Wetterdienst, Potsdam.

Adresse der Autoren

Angelika Grätz (angelika.graetz@dwd.de)
Deutscher Wetterdienst, Zentrum für Medizin-Meteorologische Forschung
Stefan-Meierstr. 4, D-79104 Freiburg

Ursel Behrens (ursel.behrens@dwd.de)
Deutscher Wetterdienst, Regionale Klima und Umweltberatung Potsdam
Michendorfer Chaussee 23, D-14473 Potsdam

Jörn Welsch (joern.welsch@senstadt.berlin.de)
Senatsverwaltung für Stadtentwicklung Berlin, Abteilung Geoinformation, Informationssystem Stadt und Umwelt
Fehrbelliner Platz 1, D-10707 Berlin

Entwicklung der Wärmebelastung in Deutschland im 21. Jahrhundert

Birger Tinz[1], Thomas Deutschländer[2], Barbara Früh[2]

[1]Maritime Klimaüberwachung, Deutscher Wetterdienst Hamburg, Deutschland

[2]Zentrales Gutachtenbüro, Deutscher Wetterdienst Offenbach a.M., Deutschland

Zusammenfassung

Die Änderung der Anzahl der Tage mit mindestens mäßiger Wärmebelastung in Deutschland im 21. Jahrhundert wurde mit dem human-biometeorologischen Klima-Michel-Modell untersucht. Im Referenzzeitraum 1971-2000 gab es nach Daten von 102 Wetterstationen zum Termin 12 UTC im Norden etwa 25 und im Süden um 50 solcher Tage mit einer Gefühlten Temperatur $T_G \geq 26$ °C. Im Kontrolllauf des regionalen Klimamodells REMO zeigt sich bei den interessierenden hohen Werten der Gefühlten Temperatur ein positiver Bias. Mit einem stationsspezifischen Korrekturverfahren, das auf Anpassung der Quantilwerte der Gefühlten Temperatur beruht, ergibt sich bis zum Ende des 21. Jahrhunderts eine Verdopplung der Anzahl der Tage mit mindestens mäßiger Wärmebelastung gegenüber den heutigen Verhältnissen.

1. Einleitung

Die negativen gesundheitlichen Auswirkungen thermischen Stresses zeigen sich bei epidemiologischen Untersuchungen z.B. von Mortalitätsdaten. Mit zunehmendem Kältestress bzw. stärkerer Wärmebelastung nimmt die Mortalität überproportional zu, ohne einen bestimmten Schwellenwert aufzuweisen (Laschewski und Jendritzky, 2002; Koppe und Jendritzky, 2005). Deshalb spielen bei der Beurteilung der thermischen Verhältnisse weniger Mittelwerte eine Rolle, sondern eher Extremereignisse, die auch durch Auswertung von Überschreitungen bestimmter Schwellenwerte beschrieben werden können.

Kartendarstellungen thermischer Indizes bzw. der Ergebnisse von Bioklimamodellen gibt es in verschiedenen räumlichen Auflösungen; sie reichen von der globalen Skala (z.B. Matzarakis und Amelung, 2008; Jendritzky und Tinz 2009) bis hin zu einzelnen Straßenschluchten (Mayer et al., 2008).

Neu in dieser Untersuchung sind die Quantifizierung des Modell-Bias, die Untersuchung seiner Ursachen sowie die Vorstellung eines Verfahrens, das es ermöglicht den Fehler vollständig zu beseitigen.

2. Daten und Methoden

Mit dem Klima-Michel-Modell (KMM) des Deutschen Wetterdienstes werden die atmosphärischen Bedingungen der Wärmeabgabe des Menschen bewertet (Jendritzky et al., 1990). Es berücksichtigt, dass für das thermische Empfinden neben der Temperatur ebenfalls die Strahlungsflüsse, die Luftfeuchtigkeit und die Windgeschwindigkeit eine Rolle spielen. Ergebnis ist die thermo-physiologisch relevante Größe „Gefühlte Tempe-

ratur“ $T_{G,}$ der sich bestimmte Klassen von Kältereiz, Komfort und Wärmebelastung zuordnen lassen (weitere Details in Jendritzky et al., 2007).

Als Datengrundlage für das KMM dienen die Beobachtungen von 102 Stationen des Deutschen Wetterdienstes. Für den Referenzzeitraum 1971-2000 wurde die Gefühlte Temperatur berechnet und daraus die mittlere Anzahl der Tage mit mindestens mäßiger Wärmebelastung (Gefühlte Temperatur $T_G \geq 26$ °C) zum Termin 12 UTC abgeleitet. Diese Schwelle wurde gewählt, da einerseits deutschlandweit genügend Fälle für eine statistische Auswertung zur Verfügung stehen und andererseits bereits thermo-physiologische Wirkungen beim Menschen auftreten.

Die Anzahl der Wärmebelastungstage wurde ebenfalls mit den Daten des regionalen Klimamodells REMO (Max-Planck-Institut für Meteorologie in Hamburg; Jacob, 2005; Jacob et al., 2008) ermittelt. Das Deutschland, Schweiz, Österreich und angrenzende Bereiche umfassende Modellgebiet wurde mit einer räumlichen / zeitlichen Auflösung von etwa 10 km bzw. 1 Stunde zur Verfügung gestellt. Angetrieben wird REMO mit den globalen Klimasimulationen des ECHAM5-T63L31/MPI-OM des Max-Planck-Instituts für Meteorologie (Roeckner et al., 2006). Bisher beschränkt sich die Analyse auf den Lauf 1 des IPCC-Emissionsszenarios A1B (2001-2100) sowie den Kontrolllauf C20 (1951-2000).

3. Entwicklung der Anzahl von Wärmebelastungstagen in Deutschland

3.1 Validierung

Der Vergleich von Beobachtungs- und Klimamodelldaten trifft auf methodische Probleme, da Punkt- bzw. Gitterflächenwerte betrachtet werden. Während sich die Wetterstationen auf der realen Orographie befinden, repräsentieren die Gitterpunkte im Klimamodell ein Flächenmittel. Die Modellorographie kann dabei in Gebirgen deutlich von der realen Orographie abweichen, so dass im Extremfall der gleiche Gitterpunkt benachbarten Berg- und Talstationen zugeordnet werden muss. Hinzu kommt eine jedem Klimamodell innewohnende Modellunsicherheit, deren Ursache u.a. in der nicht vollständig erforschten Modellphysik und der Notwendigkeit der Parametrisierung subskaliger Prozesse liegt. Solche Fehler führen zum Modell-Bias, der die Abweichung des Modellwertes von den Beobachtungen darstellt. Je nach Modell hat er ein unterschiedliches Vorzeichen und ist räumlich unterschiedlich stark ausgeprägt.

Nach Beobachtungen treten in Deutschland im Zeitabschnitt 1971-2000 an den Küsten 10, im norddeutschen Flachland etwa 25 und in Teilen Süddeutschlands um 50 Tage mit mindestens mäßiger Wärmebelastung ($T_G \geq 26$ °C) auf. Dem REMO-Kontrolllauf zu folge kommt es zu einer Überschätzung um 10 Tage in Norddeutschland, während es in den Tälern Süddeutschland sogar 20 bis 30 Tage sind.

3.2 Analyse des BIAS am Beispiel von Hamburg

An der DWD-Referenzstation Hamburg wurde im Zeitraum 1971-2000 im Mittel um 12 UTC an 21,5 Tagen mindestens mäßige Wärmebelastung ($T_G \geq 26$ °C) registriert. Laut REMO sind es im Experiment C20 32,3 Tage. Es liegt also eine Überschätzung um etwa 11 Tage (50 %) vor. Dieser Unterschied spiegelt sich auch in der Häufigkeitsverteilung der Gefühlten Temperatur wider (Abb. 1a). Zwar stimmt die Form der Vertei-

lung des Experiments REMO-C20 mit derer der Beobachtungen (OBS) grundsätzlich gut überein, jedoch weisen die REMO-Häufigkeiten oberhalb einer Gefühlten Temperatur von ca. 14°C prinzipiell höhere Werte auf als die Beobachtungen. Speziell im warmen Bereich oberhalb von T_G = 26 °C liegt die Überschätzung der Gefühlten Temperatur bei etwa 1 bis 2 K (Abb. 1b). Dies führt zum Modell-Bias von REMO hinsichtlich der Anzahl der Wärmebelastungstage. Die in das Klima-Michel-Modell eingehenden meteorologischen Größen Lufttemperatur T_L, Taupunkt T_D, Windgeschwindigkeit v und mittlere Strahlungstemperatur T_{mrt} tragen dabei mit unterschiedlichem Gewicht zum Modell-Bias bei. Die Lufttemperatur wird von REMO für T_G -Werte ≥ 26 °C gut simuliert, nur bei den Häufigkeiten von T_L < 27 °C ist z.T. eine nennenswerte Überschätzung festzustellen (Abb. 1c). Der Taupunkt hingegen ist im Bereich T_D ≥ 14 °C deutlich zu hoch (etwa 2 bis 4 K; Abb. 1d), was zu einer höheren Anzahl an Tagen mit mäßiger Wärmebelastung führt. Die Windgeschwindigkeit und die mittlere Strahlungstemperatur leisten einen nur geringen Beitrag zum Bias (nicht gezeigt).

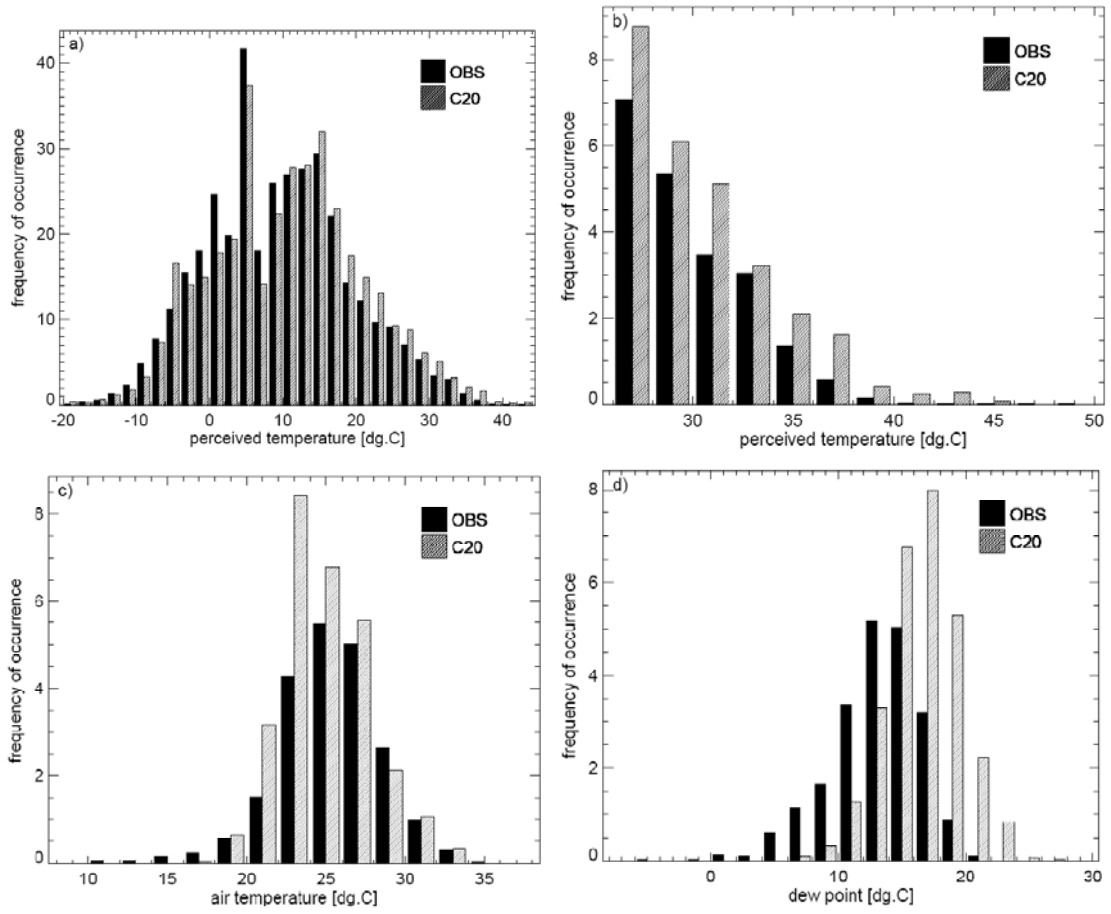

Abb. 1: Häufigkeitsverteilung der täglichen 12 UTC-Werte in Hamburg aus Beobachtungen (OBS) und REMO C20 für 1971-2000. Links oben a): alle Werte der Gefühlten Temperatur T_G in °C; rechts oben b): nur T_G ≥ 26 °C; links unten c): Lufttemperatur in °C (für T_G ≥ 26 °C); rechts unten d): Taupunkt in °C (für T_G ≥ 26 °C)

3.3 Implizite BIAS-Korrektur

Aufgrund des nichtlinearen Zusammenhangs zwischen der Häufigkeitsverteilung der Gefühlten Temperatur und dem Schwellenwert für mäßige Wärmebelastung (T_G = 26 °C, Abb. 1a) wird zur Bestimmung der Anzahl der Tage mit mindestens mäßiger Wärmebelastung auf der Basis der REMO-Modelldaten zunächst der Wert p der kumulativen Häufigkeitsverteilung für das 26 °C-Quantil an Hand der Beobachtungsdaten für 1971-2000 bestimmt. Für diesen Wert p wird dann das zugehörige Quantil aus dem REMO-Kontrollabschnitt ermittelt. Die Auszählung und Differenzenbildung der Tage mit mindestens mäßiger Wärmebelastung erfolgt dann unter Verwendung des auf diese Weise ermittelten korrigierten Schwellenwertes. Diese implizite Bias-Korrektur entspricht anschaulich einer Verschiebung der Häufigkeitsverteilung der Gefühlten Temperatur auf der Abszisse. Das Verfahren ist anwendbar, wenn sich die Form der Verteilungsfunktion der Beobachtungswerte und der Klimamodellexperimente nicht signifikant voneinander unterscheiden. Darüber hinaus muss der p-Wert des Quantils zur mäßigen Wärmebelastung auf Grund der statistischen Robustheit bei allen Datenkollektiven möglichst << 100 % sein.

3.4 Änderung der Wärmebelastung in Deutschland im 21. Jahrhundert

Mit dem stationsweise korrigierten Schwellenwert der Gefühlten Temperatur für mäßige Wärmebelastung wurde für die Experimente C20 und A1B die Anzahl der Tage mit mindestens mäßiger Wärmebelastung berechnet. Die auf diese Weise ermittelten Häufigkeiten laut dem Kontrolllauf von REMO stimmen für 1971-2000 im Rahmen der statistischen Unsicherheit mit den Beobachtungswerten überein.

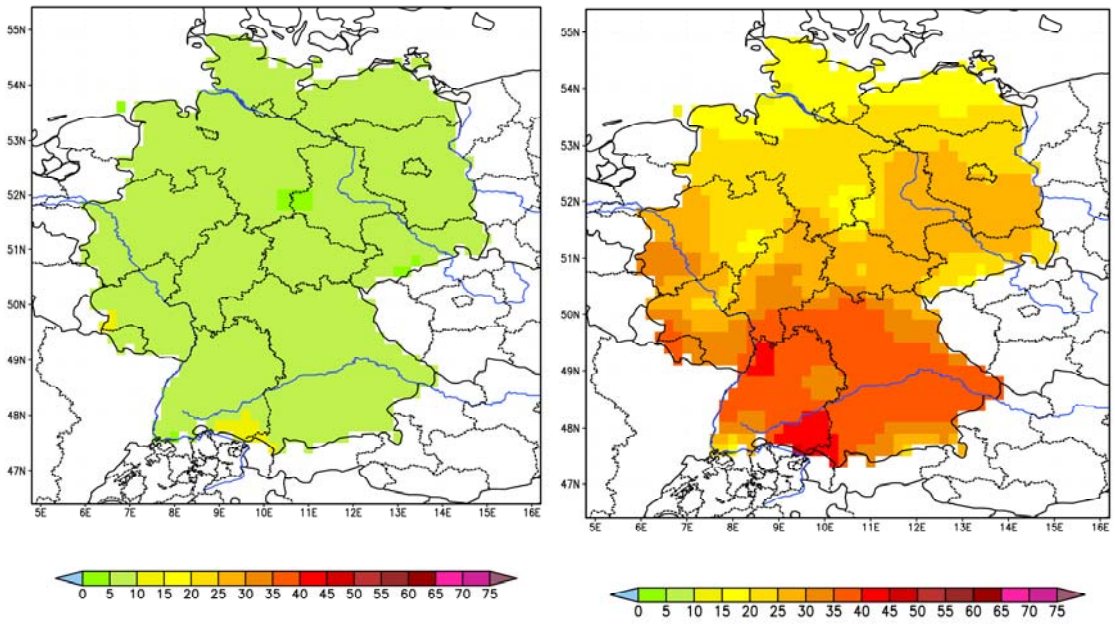

Abb. 2: Differenz der mit der impliziten Bias-Korrektur ermittelten Anzahl der Tage mit mindestens mäßiger Wärmebelastung in Deutschland gemäß REMO A1B – C20 (links 2021-2050 – 1971-2000, rechts 2071-2100 – 1971-2000)

Im Experiment A1B ergibt sich bis 2021-50 deutschlandweit eine Erhöhung um 5-10 Tage, wobei sich für Süddeutschland teilweise auch mehr als 10 Tage ergeben (Abb. 2). Dieser Anstieg setzt sich bis zum Ende des Jahrhunderts fort. Im Zeitraum 2071-2100 muss mit 15 zusätzlichen Tagen mit mindestens mäßiger Wärmebelastung an den Küsten und Teilen des Berglandes sowie mit 40 weiteren Tagen in den tiefen Lagen Süddeutschlands gerechnet werden. Dies entspricht einer Verdopplung der bisher beobachteten Häufigkeit. Der schon heute starke, von Nord nach Süd verlaufende, Gradient würde sich gemäß dieser Modellprojektion noch weiter verschärfen.

4. Diskussion

Im Laufe des Jahrhunderts ist gemäß dem Szenario A1B mit einer deutlichen Zunahme der Anzahl der Tage mit mindestens mäßiger Wärmebelastung in Deutschland zu rechnen. Sie kann verbunden sein mit häufigeren hitzebedingten Erkrankungen und steigender Mortalität beim Menschen. Besonders stark betroffen sein dürften vor allem ältere Menschen und Patienten mit Vorerkrankungen, wie es der Hitzesommer 2003 in Teilen Europas mit 55 000 zusätzlichen hitzebedingten Sterbefällen deutlich zeigte (Kosatzky, 2005). Die Verhältnisse in diesem Extremsommer würden nach den hier vorgestellten Berechnungen in Deutschland in etwa den Mittelwerten am Ende des 21. Jahrhunderts entsprechen.

Studien zeigen, dass Vorsorge- und Anpassungsmaßnahmen im Gesundheitswesen in Bezug auf sommerliche Hitzewellen wirksam sind und sich auch ökonomisch lohnen (Ebi et al., 2004). Prävention erfordert verschiedene Maßnahmen, angefangen von öffentlichen Hitzewarnsystemen bis hin zu Änderungen in der Stadtplanung und im Bauwesen (Matthies und Menne, 2009). Der Deutsche Wetterdienst beteiligt sich daran und betreibt seit einigen Jahren ein Hitzewarnsystem. Bei erwarteter starker Wärmebelastung ($T_G \geq 32$ °C) werden Behörden, das Gesundheitswesen sowie die Öffentlichkeit informiert (www.wettergefahren.de/warnungen/hitzewarnungen.html).

Die Auswirkungen zunehmender Wärmebelastung treffen aber nicht nur das Gesundheitswesen, sondern direkt und indirekt die gesamte Wirtschaft u.a. in Form von Produktionseinschränkungen und werden mit hohen Kosten verbunden sein (Beniston et al., 2007; Hübler et al., 2008).

Danksagung

Wir danken dem Max-Planck-Institut für Meteorologie für die Bereitstellung der Daten von REMO sowie dem Deutschen Klimarechenzentrum (beide Hamburg), wo ein Großteil der Berechnungen stattfand.

Literatur

Beniston, M., D.B. Stephenson, O.B. Christensen, C.A.T. Ferro, C. Frei, SC. Goyette, K. Halsnaes, T. Holt, K. Jylhü, B. Koffi, J. Palutikoff, R. Schöll, T. Semmler, K. Woth, 2007: Future extreme events in European climate; an exploration of Regional Climate Model projections. Climatic Change 81, 71-95.

Ebi, K., T.J. Teisberg, L.S. Kalkstein, L. Robinson, R.F. Weiher, 2004: Heat watch/warning systems save lives. Bull. of the American Meteorol. Soc. 85, 1067 - 1073.

Hübler, M., G. Klepper, S. Peterson, 2008: Costs of Climate Change - The Effects of Rising Temperatures on Health and Productivity in Germany. Ecological Economics 68, Elsevier, 381-393.

IPCC (Intergovernmental Panel on Climate Change, Solomon, S., et al., eds.), 2007: Climate Change 2007. The Physical Scientific Basis. Contribution of Working Group I to the Fourth Assessment Report (FAR) of the IPCC. University Press, Cambridge

Jacob, D., 2005: REMO Climate of the 20th century run No. 006210, 1950-2000 und AlB scenario run No. 006211, 2001-2100. UBA Project, 0.088 degree resolution, 1h Data.

Jacob, D., H. Göttel, S. Kotlarski, P. Lorenz, K. Sieck, 2008: Klimaauswirkungen und Anpassung in Deutschland – Phase 1: Erstellung regionaler Klimaszenarien für Deutschland. Climate Change Nr. 11, Umweltbundesamt, Dessau, Germany.

Jendritzky, G., 1990: Bioklimatische Bewertungsgrundlage der Räume am Beispiel von mesoskaligen Bioklimakarten. In: Jendritzky, G., G. Menz,, W. Schmidt-Kessen, H. Schirmer: Methodik der räumlichen Bewertung der thermischen Komponente im Bioklima des Menschen (Fortgeschriebenes Klima-Michel-Modell). Akad. f. Raumforschung und Landesplanung, Beiträge 114, 7-69.

Jendritzky, G., D. Fiala, G. Havenith, C. Koppe, G. Laschewski, H. Staiger, B. Tinz, 2007: Thermische Umweltbedingungen. Promet 33, 83-94.

Jendritzky, G., B. Tinz, 2009: The Thermal Environment of the Human Being on the Global Scale. Global Health Action, 2009; 3: 1-12: http://DOI: 10.3402/gha.v2i0.2005

Koppe C, G. Jendritzky, 2005 Inclusion of short-term adaptation to thermal stresses in a heat load warning procedure. Meteorol. Z. 14, 271-278.

Kosatsky, T., 2005: The 2003 European heat waves. Euro Surveill 10, 148-149.

Laschewski G, G. Jendritzky, 2002: Effects of the thermal environment on human health: an investigation of 30 years daily mortality data from SW Germany. Clim. Res. 21, 91-103.

Matthies, F., B. Menne, 2009: Prevention and management of health hazards related to heatwaves. International Journal for Circumpolar Health 68, 8-22.

Matzarakis, A., B. Amelung, 2008: Physiologically Equivalent Temperature as indicator for impacts of climate change on thermal comfort of humans. In: Thomson M.C., R. Garcia-Herrera, M. Beniston, eds. Seasonal Forecasts, Climate Change and Human Health. Advances in Global Change Research 30. Springer Sciences and Business Media

Mayer, H., J. Holst, P. Dostal, F. Imbery, D. Schindler, 2008: Human thermal comfort in summer within an urban street canyon in Central Europe. Meteorol. Z. 17: 241-250

Roeckner, E., R. Brokopf, M. Esch, M. Giorgetta, S. Hagemann, L. Kornblueh, E. Manzini, U. Schlese, U. Schulzweida, 2006: Sensitivity of Simulated Climate to Horizontal and Vertical Resolution in the ECHAM5 Atmosphere Model. J. Climate 19, 3771-3791.

Adressen der Autoren:

Dr. Birger Tinz (birger.tinz@dwd.de), Abteilung Klimaüberwachung, Deutscher Wetterdienst
Bernhard-Nocht Str. 76, 20359 Hamburg, Deutschland

Dr. Thomas Deutschländer (thomas.deutschlaender@dwd.de) und Dr. Barbara Früh (barbara.früh@dwd.de), Abteilung Klima- und Umweltberatung, Deutscher Wetterdienst
Frankfurter Straße 135, 63067 Offenbach a.M., Deutschland

Klimawandel bedingt neue luftgetragene Gesundheitsrisiken

Hans-Guido Mücke

Umweltbundesamt, Dienstsitz Berlin-Dahlem, Germany

Abstract

Climate change could have various direct and indirect implications for human health. On one hand there is reason for concern that, as a direct impact, more injuries and cardiovascular disorders will occur if extreme weather events – such as storms, floods and heat – become more frequent. Furthermore and as an indirect effect, climate change could result in an increase in infectious (e.g. vector-borne) and non-infectious diseases (e.g. allergies and asthma). A changed climate leads to a changed occurrence of biological species in the air. Extended vegetation periods result in an extended pollen season, new allergic species can be established. Insects, which transmit diseases or have allergenic potential, can extend their range or become domestic. For example, mild temperatures favour the presence and distribution of thermophile organisms of plants and insects (species such as ragweed and the oak processionary moth). Contact with pollen or stinging hairs of such species may not only lead to allergic skin, eye and pulmonary irritations, but may also cause serious asthma attacks. The presentation wants to give an insight and overview on the current situation and ideas on adaptation measures for public health protection in Germany.

1. Hintergrund

Jüngste Erkenntnisse der Klimafolgenforschung weisen darauf hin, dass sich mit einem weiteren Klimawandel auch thermophile (Wärme liebende) pflanzliche und tierische Organismen mit einem erhöhten Allergiepotential in Deutschland verstärkt ausbreiten können (Menzel und Behrendt 2008, Schmidt 2008). Sowohl das Vorkommen, die Verbreitung als auch die Dauer und Häufigkeit des Auftretens der Organismen und ihrer Allergene ist mit klimatischen Änderungen verbunden (WHO 2003). Obwohl die Klimaerwärmung in Deutschland bisher zunächst nicht dramatisch erscheint (Anstieg von 0,9 °C der bodennahen Lufttemperatur in den letzten 100 Jahren), begünstigt sie die Veränderung im Auftreten und in der Ausbreitung pflanzlicher und tierischer Schadorganismen, die mildes Klima bevorzugen. Dies kann zu einer Zunahme von nicht übertragbaren Krankheiten (beispielsweise von Allergien und Asthma) und damit zu einer erhöhten gesundheitlichen Belastung in der Bevölkerung führen (Sperk und Mücke 2009).

2. Auftreten und Ausbreitung Wärme liebender Schadorganismen

Die Einwanderung gebietsfremder Pflanzen- (Neophyten) und Tierarten (Neozoen) ist kein neues Phänomen. Der Mensch hat seit jeher Organismen bewusst eingeführt oder ungewollt verschleppt. Neu ist indes, dass durch den stetig wachsenden globalen Waren- und Reiseverkehr viele Arten oft ungewollt und zufällig verbreitet werden. Dabei werden geographische und klimatologische Barrieren überwunden. Typisch für viele eingeschleppte Arten ist, dass sie sich in ihrer ursprünglichen Heimat eher unauffällig zeigen und dort im Gleichgewicht zu konkurrierenden Arten stehen. Demgegenüber können sie sich in ihrer neuen Heimat stark ausbreiten. Dort können solche eingewanderten (invasiven) Arten oft ökologische, ökonomische oder gesundheitliche Probleme verursachen. Die Probleme und potentiellen Gefahren sind vielfältig, sie können die

heimischen Ökosysteme verändern, die Artenvielfalt verdrängen, wirtschaftliche Schäden z.B. in der Landwirtschaft bewirken, aber auch Krankheiten und Parasiten einschleppen sowie die Gesundheit des Menschen z.B. durch Allergien und Gifte gefährden. Ein bekanntes Beispiel für eine invasive, Wärme liebende Pflanze, die sich in unseren Breiten etabliert hat, ist das Beifuß-blättrige Traubenkraut, die so genannte Beifuß Ambrosie. Ihre Samen wurden aus Nordamerika eingeführt, als Verunreinigungen z.B. von Vogelfutter oder Saatsamen. Unterstützt durch das milde Klima in Mitteleuropa breitet sie sich zunehmend auch in Deutschland aus. Ihre hochallergen wirksamen Pollen intensivieren und verlängern die saisonale Beschwerdezeit von Pollenallergikern (beispielsweise Heuschnupfen) in vielen Fällen (WHO 2003, Menzel und Behrendt 2008, LGA 2009) (Abbildung 1).

Abb. 1: Ambrosiapflanze (Foto: wikipedia public domain)

Abb. 2: Eichenprozessionsspinner (Foto: wikipedia public domain)

Temperaturveränderungen begünstigen darüber hinaus aber auch die Verbreitung heimischer thermophiler Pflanzen- und Tierarten in neue Regionen innerhalb Deutschlands. So breiten sich zum Beispiel einheimische Nachfalter in den letzten Jahren in Deutschland in neue Regionen aus (Lehmann 2008, Lobinger 2008, Wulf 2008). Auch neue

Arten können sich etablieren. Auf die durch die Luft transportierten Allergene dieser Tiere kann der Mensch mit zum Teil erheblichen gesundheitlichen Beeinträchtigungen reagieren. So zeigt sich, dass beispielsweise eine Gesundheitsgefahr von den Brennhaaren (Setae) der Raupen des Eichenprozessionsspinners ausgeht, die neben juckenden Hautreaktionen (zum Beispiel Raupendermatitis) auch Reaktionen der Atemwege (zum Beispiel Atembeschwerden und Asthma) auslösen können (Spiegel et al. 2004, Maronna et al. 2008). Es wird angenommen, dass diese Brennhaare hochallergen sind (Abbildung 2).

3. Gesundheitsrelevanz und Anpassungsmanagement

Im Dezember 2008 verabschiedete die Bundesregierung die Nationale Anpassungsstrategie an den Klimawandel (DAS). Diese schafft einen Rahmen zur Anpassung an die Folgen des Klimawandels in Deutschland. Sie stellt vorrangig den Beitrag des Bundes dar und bietet auf diese Weise eine Orientierung für andere Akteure. Die Strategie legt den Grundstein für einen mittelfristigen Prozess, in dem schrittweise mit den Bundesländern und anderen gesellschaftlichen Gruppen die Risiken des Klimawandels bewertet, der mögliche Handlungsbedarf benannt, die entsprechenden Ziele definiert sowie mögliche Anpassungsmaßnahmen entwickelt und umgesetzt werden sollen. In ihr wird u.a. die vermehrte Aufklärung der Bevölkerung über die gesundheitlichen Gefahren des Klimawandels als notwendig identifiziert. Darüber hinaus kommt es bei der Erarbeitung von möglichen Anpassungsstrategien für Deutschland darauf an, dass Maßnahmen zur medizinischen Vorsorge und Versorgung der Bevölkerung erarbeitet werden (BMU 2008).

Das Wissen über den Wirkungszusammenhang zwischen Klimawandel und thermophilen Schadorganismen sowie über deren gesundheitliche Auswirkungen ist bislang noch eingeschränkt. Es besteht die Notwendigkeit mittels neuer Forschungsprojekte mehr über das klimabedingte Vorkommen dieser und anderer Schadorganismen sowie über Art und Ausprägung ihrer gesundheitlichen Auswirkungen auf den Menschen zu erfahren. Um das bereits vorhandene Wissen zusammenzustellen haben das Bundesministerium für Umwelt, Naturschutz und Reaktorsicherheit (BMU) und das Umweltbundesamt (UBA) im November 2009 gemeinsam ein erstes Expertentreffen zum Thema „Klimawandel und Gesundheit – welche Probleme verursachen Wärme liebende Schadorganismen?“ durchgeführt. Ziel der Veranstaltung mit internationaler Beteiligung war es, die vorhandenen Kenntnisse zusammen zu tragen sowie Perspektiven für die zukünftige Forschungsplanung und für den vorbeugenden Gesundheitsschutz der Bevölkerung zu entwickeln. Hierzu behandelte das Fachgespräch zum einen das Auftreten, die Aus- und Verbreitung Wärme liebender heimischer oder neu eingewanderter Pflanzen und Insekten, die sich begünstigt durch die Erwärmung des Klimas in Deutschland ausbreiten. Zudem wurden erste Erkenntnisse über die Wirkungen pflanzlicher und tierischer Organismen auf die Gesundheit des Menschen, zum Beispiel in Form von Kontaktekzemen oder Atemwegsallergien, vorgestellt. Darüber hinaus konzentrierte sich der Austausch auf die bisherigen Erfahrungen des Anpassungsmanagements durch Umwelt- und Gesundheitsbehörden, zum Beispiel hinsichtlich der Entwicklung von Strategien zur Bekämpfung von Schadorganismen sowie der Identifikation und Analyse von Allergieerkrankungsfällen, ausgelöst durch Wärme liebende Schadorganismen.

An dem interdisziplinären Fachgespräch mit internationaler Beteiligung - aus Österreich, der Schweiz und von der Weltgesundheitsorganisation - nahmen 50 Teilnehmer

aus Forschung und Wissenschaft, öffentlicher Verwaltung und angewandter Praxis teil. Aspekte, Erfahrungen und Perspektiven unterschiedlicher Ebenen (national, regional und lokal) wurden erörtert. Das Fachgespräch hat gezeigt, dass Wärme liebende Pflanzen (wie Ambrosia) und Tiere (wie Prozessionsspinnerarten) bereits veränderte Muster und Intensitäten in ihrem Auftreten und ihrer Verbreitung, vor allem im unmittelbaren Nachgang zum Hitzesommer 2003, in Deutschland aufweisen. Erste Studien des öffentlichen Gesundheitsdienstes zeigen anhand ausgewählter Beispiele aus Bayern und Nordrhein-Westfalen für die Jahre 2004/2005, dass es in Gebieten mit stark ausgeprägtem Befall des Eichenprozessionsspinners auch zu einem Anstieg und zu einer Häufung von Haut- und Atemwegserkrankungen in den Befallsgebieten kam. Trotz einer bislang moderaten Erhöhung der Jahresdurchschnittstemperatur ist dies ein Indiz dafür, dass sich Wärme liebende Pflanzen- und Tierarten in Deutschland zukünftig zunehmend etablieren und ausbreiten können. Auch wird die allergologische Bedeutung dieser Arten wachsen. Umso notwendiger sind beispielsweise auch im Rahmen der DAS neue Forschungsinitiativen, die sowohl die Kausalität zwischen Klimawandel und nicht übertragbaren Erkrankungen resp. Krankheiten auf den Menschen, als auch die speziellen gesundheitlichen Wirkmechanismen und potenziellen Gesundheitsschäden, insbesondere bei empfindlichen Personengruppen, untersuchen. Es ist damit zu rechnen, dass neue Arten zu einem Anstieg der Exposition der Bevölkerung gegenüber biologischen Luftschadstoffen, sogenannte biogene Aerosole, beitragen werden und dass dadurch auch das Potential für neue Umweltallergien steigen wird. Der Abschlussbericht zu diesem internationalen Fachgespräch wird im Frühjahr 2010 erscheinen (UBA/BMU 2010).

Im Rahmen des DAS-Anpassungsmanagements sollte die Einwanderung bzw. Einschleppung thermophiler Schadorganismen (Pflanzen und Tiere) zukünftig bundesweit beobachtet und überwacht werden, damit vor allem aus gesundheitsvorbeugender Sicht sowohl die Bevölkerung, der öffentliche Gesundheitsdienst als auch die in der Region behandelnden Ärzte frühest möglich über Befallsgebiete und gesundheitliche Gefahren gewarnt sowie über anpassende Verhaltensweisen aufgeklärt wird. Darüber hinaus sollte als Gesundheitsvorsorgemaßnahme eine flächenhafte Verbreitung gesundheitlich kritisch invasiver Arten rechtzeitig verhindert werden.

Literatur

Bundesministerium für Umwelt, Naturschutz und Reaktorsicherheit/BMU, 2008: Deutsche Anpassungsstrategie an den Klimawandel. http://www.bmu.de/klimaschutz/downloads/doc/42783.php

Landesgesundheitsamt Baden-Württemberg im Regierungspräsidium Stuttgart/LGA (Hrsg.), 2009: Einfluss klimatischer Faktoren und ihrer bisherigen sowie erwarteten Änderung bezüglich der Zunahme von Sensibilisierungen am Beispiel von Ambrosia-Pollen. Forschungsprogramm Herausforderung Klimawandel; Abschlussbericht des Verbundprojektes Ambrosia-Pollen, 234 S., Stuttgart.

Lehmann, M., 2008: Lästlinge im urbanen Grün und ihre Wertung aus der Sicht des Pflanzenschutzes. Jahrbuch der Baumpflege 2008, 177-186. Dujesiefken D und P Kockerbeck (Hg.). Haymarket Media.

Lobinger, G., 2008: Untersuchungen zur Überwachung und Bekämpfung des Eichenprozessionsspinners (Thaumetopoea processionea Lep., Thaumetopoeidae) in Bayerns Wäldern. Mitteilungen des Julius Kühn-Instituts, 417, 154.

Maronna, A., Stache, H., Sticherling, M., 2008: Lepidopterism - oak processionary caterpillar dermatitis: Appearance after indirect out-of-season contact. Journal der Deutschen Dermatologischen Gesellschaft, 9 (6), 747-750.

Menzel, A., Behrendt, H., 2008: Zunahme des Pollenflugs und die Gefahr von Allergien. Warnsignal Klima. Gesundheitsrisiken. Gefahren für Pflanzen, Tiere und Menschen, 132-135. Lozán J, Graßl H, Jendritzky G, Karbe L, Reise K und WA Maier (Hg.).Wissenschaftliche Auswertungen. Hamburg.

Schmidt, O., 2008: Südländische Insekten überwinden die Alpen. Warnsignal Klima. Gesundheitsrisiken. Gefahren für Pflanzen, Tiere und Menschen, 73-76. Lozán et al. (Hg.).Wissenschaftliche Auswertungen. Hamburg.

Sperk, C., Mücke, H.-G., 2009: Klimawandel und Gesundheit: Informations- und Überwachungssysteme in Deutschland. Ergebnisse der internetbasierten Studie zu Anpassungsmaßnahmen an gesundheitliche Auswirkungen des Klimawandels in Deutschland. UBA-Publikation ‚Umwelt & Gesundheit', Heft 3/2009, Umweltbundesamt (Hrsg), Dessau-Roßlau.

Spiegel, W., Maier, H., Meier, M., 2004: A non-infectious airborne disease. The Lancet, 363, 1438.

Umweltbundesamt/Bundesministerium für Umwelt, Naturschutz und Reaktorsicherheit, 2010: Klimawandel und Gesundheit: Welche Probleme verursachen Wärme liebende Schadorganismen? Abschlussbericht eines internationalen Fachgespräches am 09. und 10.11.2009 im Umweltbundesamt, Dienstsitz Berlin (im Druck).

World Health Organization/WHO, 2003: Phenology and Human Health: Allergic Disorders. Rom. http://www.euro.who.int/document/e79129.pdf

Wulf, A., 2008: Über die Zunahme thermophiler Schadorganismen in den Wäldern - Umbaupläne müssen dies berücksichtigen. In: Lozán et al. (Hg.).Warnsignal Klima. Gesundheitsrisiken. Gefahren für Pflanzen, Tiere und Menschen, 282-285. Wissenschaftliche Auswertungen. Hamburg.

Autorenadresse

Dr. Hans-Guido Mücke (hans-guido.muecke@uba.de)
Umweltbundesamt, Fachgebiet „Umweltmedizin und gesundheitliche Bewertung",
Corrensplatz 1, 14195 Berlin, Germany

Regional and local dimension of climate change: identification of the impact of climate variability and extreme events using the example of heat and drought in Baden-Württemberg

Paul A. Neumann and Andreas Matzarakis

Meteorological Institute, Albert-Ludwigs-University of Freiburg, Germany

Abstract

Within the start-up project "Regional and local dimension of climate change: identification of the impact of climate variability and extreme events using the example of heat and drought in Baden-Württemberg" an analysis of the impact of climate change will be conducted. The research is based on simulations of several regional climate models using A1B and B1 scenarios. The investigation area is Baden-Württemberg with focus on heat and drought. Especially the frequency and duration of climate events, short time events like heat waves or droughts, will be analysed. The impact of such climate events can influence sectors (water and energy) and different branches of industry (tourism, health and agriculture). Present research is focused on the identification of heat waves and droughts and on possible affects on viticulture during the 21st century. First results of the project are presented.

1. Introduction

Climate change and its positive and negative effects are a frequently discussed topic in science and in the general public. A worldwide increase of air temperature and a decrease of precipitation in some areas are assumed. According to the research group "Climate alteration and consequences for the water economy" a rising of air temperature as well as more precipitation in winter and less in summer for the period of 2021 to 2050 in Baden-Württemberg are expected (KLIWA, 2006). Their results are mainly based on the "Meteo-Research" MR-Model with a statistical-dynamical downscaling, using the SRES B2. Even more than climate trends, the impact of climate events, like heat waves or droughts, on economic and socio-economic systems can be enormous. The regional and local importance of such events is still not sufficiently investigated for many areas. According to Mehl and Tebaldi (2004) more intense, more frequent, and longer lasting heat waves in the second half of the 21st century in Europe and North America are expected, based on simulations of the "Parallel Climate Model" PCM. With such a development, the importance of heat waves for Baden-Württemberg could increase in the future.

In November 2009 the start-up project "Regional and local dimension of climate change: identification of the impact of climate variability and extreme events using the example of heat and drought in Baden-Württemberg" was initiated at the Meteorological Institute of the Albert-Ludwigs-University of Freiburg. The project's main goal is to research climate impacts based on existent results of regional climate simulations as well as to identify the limits of regional climate models. The results are based on simulations of the "Regional Modell" REMO of the Max-Planck-Institute for Meteorology and the COSMO model in climate mode COSMO-CLM or CLM of the Consortium for Small-scale Modeling. The emission scenarios SRES A1B and B1 were used for the simulation runs.

Hot days, summer days and tropical nights were examined as a first parameter to identify areas with increased heat stress. The impact of high air temperatures on human health can be of importance for health resorts and hospital facilities, which are numerous in Baden-Württemberg. Kovats and Ebi (2006) even proclaimed a requirement for a heat wave warning system because of higher mortality rates connected with heat waves. A first step in the field of agriculture was to investigate the development of viticulture during the 21st century. Viticulture is of great importance for the agriculture of Baden-Württemberg and climate change can influence the quantity and quality of wine (Petgen, 2007). For the investigation a possible expansion of suitable areas for viticulture was determined with the help of the Heliothermal Index (HI). To research the expected decrease of precipitation during summers, as a simple parameter dry days, days with precipitation less than 1 mm, were filtered out of scenario runs.

2. Data

Developed by the Max-Planck-Institute for Meteorology, the three-dimensional hydrostatic regional climate model REMO (Jakob et al., 2007; Jakob and Podzun, 1997) is an atmospheric circulation model, calculating the relevant physical processes dynamically. The simulation runs used are covering mainly the area of Germany in a resolution of 10km x 10km. The simulations were run from 1961 to 2100. Two runs from 2000 to 2100, one based on the SRES A1B and one based on the SRES B1 as well as a simulation for 1961 to 1990 were used. The parameters air temperature 2 meters above ground and total precipitation are both available in a resolution of one hour.
In the same way simulation runs of the model COSMO-CLM were used. The COSMO-CLM (Steppeler et al., 2003; Will et al., 2006) was developed by the "Consortium for Small-scale Modeling" COSMO. It is a non hydrostatic regional model also calculating the relevant physical processes dynamically. The simulation runs used, are in a 0.165° spatial resolution covering mainly the area of Europe. The simulations were run from 1961 to 2100. Two runs from 2000 to 2100, one based on the SRES A1B and one based on the SRES B1 as well as a simulation for 1961 to 1990 were used. The parameters air temperature 2 meters above ground and total precipitation are both available in a resolution of three hours.
The usage of other climate model runs as well as data of climate stations is planned, but not covered in this first report about the ongoing start-up project.

3. Impact of high air temperature

The expected rise of air temperature during the 21st century may affect human health as well as branches of industry in the form of heat stress or rising cooling costs. Many health resorts and hospital facilities are resident in Baden-Württemberg. For them a financial or image damage caused by changing environmental conditions may be possible. Using common parameters, a first estimation of the simulation runs can be made. The parameters used were: the number of hot days with a maximum air temperature ≥ 30 °C, the number of summer days with a maximum air temperature ≥ 25 °C and the number of tropical nights with a minimum air temperature ≥ 20 °C. More parameters like frost days with a minimum air temperature < 0 °C were examined, too. In figure 1 the increase of the mean annual amount of hot days during the 21st century in Baden-Württemberg is displayed. The periods shown are: 1961 to 1990, 2021 to 2050 and 2071 to 2100. The future periods are based on A1B.

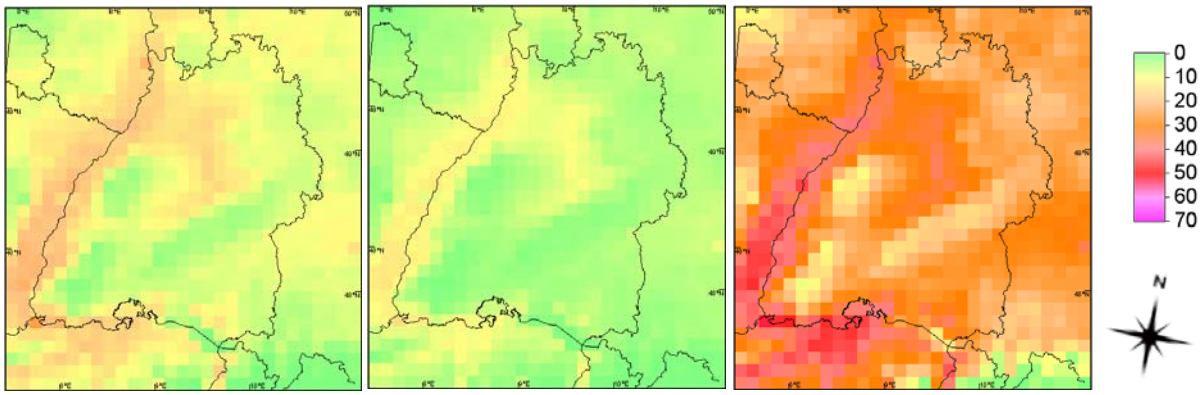

Fig. 1: Mean annual amount of hot days based on REMO with A1B. Periods are from left to right: 1961-1990, 2021-2050 and 2071-2100

An increase of hot days in the future is apparent. In the Upper-Rhine-Areas an increase of hot days from 10 - 20 in 1961 to 1990 to 20 - 30 in 2021 to 2050 is shown. For the period 2071 to 2100 it is simulated that hot days will be common in the whole federal state of Baden-Württemberg even mountainous areas. This kind of development will likely lead to an amplification of heat stress in the future. Simulation runs of the COSMO-EU have shown quite similar results.
Besides extreme temperatures the lack of possibilities to recover can be important as well. Such a problem can occur on days with a tropical night. Nowadays tropical nights are not an important matter for the general public in Germany, because of their rare occurrence. That fact may change in the future, especially in the Upper-Rhine-Areas as one of the warmest regions in Germany.

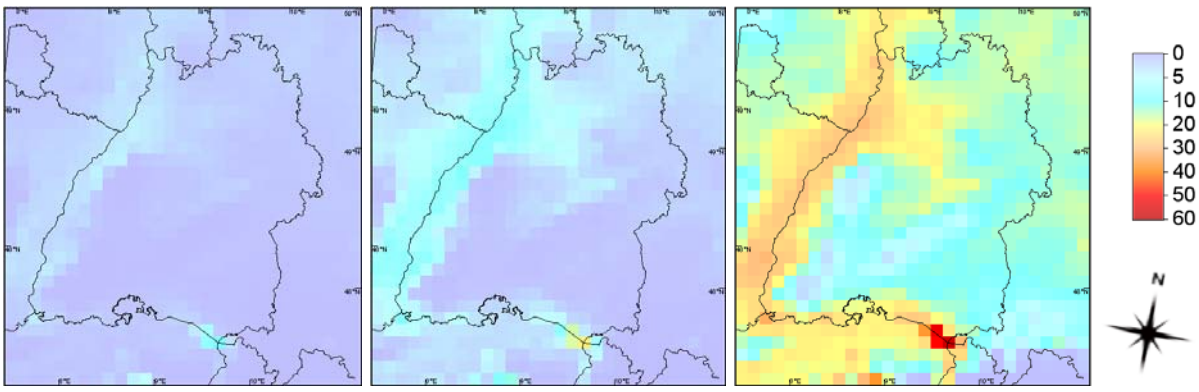

Fig. 2: Mean annual amount of tropical nights based on REMO with A1B. Periods are from left to right: 1961-1990, 2021-2050 and 2071-2100

In figure 2 the rising of the mean annual amount of tropical nights during the 21st century in Baden-Württemberg is displayed. The periods shown are: 1961 to 1990, 2021 to 2050 and 2071 to 2100. The future periods are based on the SRES A1B. A development from very few tropical nights in the Upper-Rhine-Area in 1961 to 1990 to up to 10 events in 2021 to 2050 as well as some in northern Baden-Württemberg is visible. In the period of 2071 to 2100 tropical nights will become a common incidence in the whole federal state of Baden-Württemberg with the exception of the mountainous areas. Simulation runs of the COSMO-EU have shown quite similar results. The development of summer days and frost days will be researched, too.

3. Viticulture

Viticulture is a considerable part of the agriculture in Baden-Württemberg. Changes in air temperature and precipitation are able to change the quantity and quality of a vintage (Mariani, 2009). Some of the negative effects of climate change for viticulture can be an intensified rottenness problem as well as an increase of vermin (Petgen, 2007). A positive aspect is a possible expansion of suitable areas for viticulture (Maracchi et al., 2005; Petgen, 2007). To investigate such a possible expansion the Heliothermal Index or Huglin Index (HI) was used. The HI is an often used index to identify suitable areas for grape-vine, so it was applied by studies of Tonietto and Carbonneau (2004) as well as Petgen (2007). For the HI, daily mean air temperatures T_M and daily maximum air temperature T_X as well as a length of day coefficient d are used for the growing period from April 4th to September 30th each year.

$$HI = \sum_{09.30.}^{04.01.} \frac{\left[(T_M - 10)(T_X - 10)\right]}{2} * d$$

The result can then be ranked in a class system to determine the best suited grape variety for the region. Some examples are given in table 1.

Table 1: Classes of the "Heliothermal Index" and suitable grape varieties (Tonietto and Carbonneau, 2004)

HI	≤1500	>1500 ≤1800	>1800 ≤2100	>2100 ≤2400	>2400 ≤3000	>3000
Class, Example grape varieties	Very cool, no vine or Gewürztraminer	Cool, Riesling	Temperate, Cabernet-Sauvignon	Temperate warm, Grenache	Warm, Nabeul	Very warm, Petrolina

An overview over the different HI values in Baden-Württemberg during the periods of 1961 to 1990, 2021 to 2050 and 2071 to 2100 is shown in figure 3. The future periods are based on the SRES A1B. An expansion of suitable areas for viticulture is visible. The HI is still an index based only on temperature and day length, many areas shown as suitable for viticulture may be unfitting because of different reasons, like thick forest or shadowing effects. Nevertheless, it may be necessary to think about seeding different grape varieties in the future.

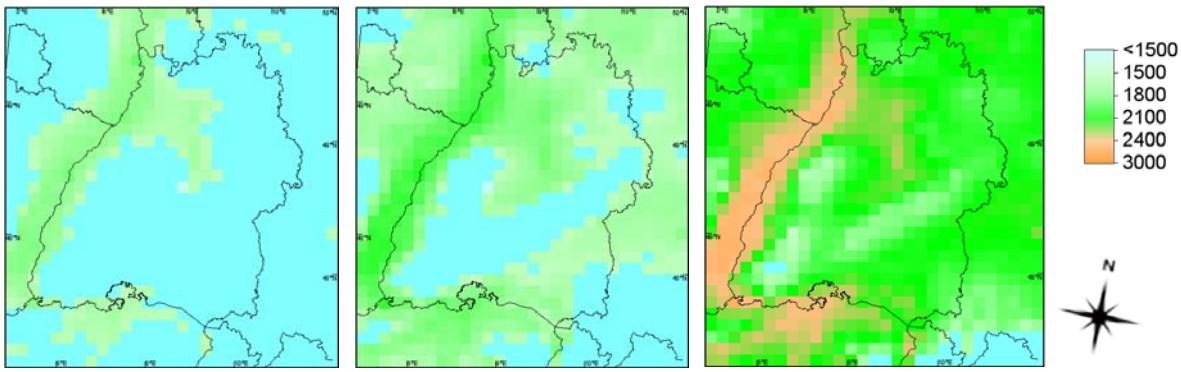

Fig. 3: Mean HI based on REMO with A1B. Periods are from left to right: 1961-1990, 2021-2050 and 2071-2100

4. Aridity and drought

A reduction of summer precipitation together with the presumed rising in air temperature can locally cause problems like droughts. To quantify future aridity, the mean annual amount of dry days, days with less than 1mm precipitation, were filtered out the simulation runs. This step is apparently only a start for research on the subject aridity and drought. Especially for agriculture, droughts in summer are more important than in winter, because of the growing season. For that reason the mean amount of dry days per summer half year from Mai to October is shown in figure 4. The periods are: 1961 to 1990, 2021 to 2050 and 2071 to 2100. The future periods are based on A1B.

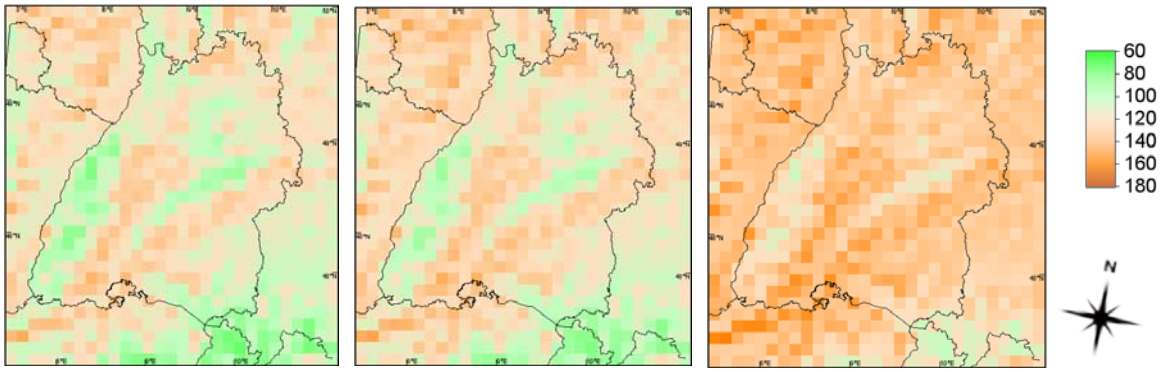

Fig. 4: Mean amount of dry days per summer half-year from Mai to October based on REMO with A1B. Periods from left to right: 1961-1990, 2021-2050 and 2071-2100

From the period 1961 to1990 to the period 2021 to 2050 the increase in dry day seems to be minor in comparison to the future periods where an increase of dry days is clearly visible.

4. Conclusion and Outlook

As a first approach the development of simple parameters during the 21st century was determined. Further steps are: adapting a definition for heat waves and droughts suitable for the region of Baden-Württemberg, finding appropriate indexes to describe changes during the century and evaluate their usefulness for the region. It may be necessary to develop or adjust one or more indexes. For agriculture also Growing Degree Day (GDD) and for health the Physiological Equivalent Temperature (PET) (Matzarakis and Amelung, 2008) will be analysed. With the suitable parameters and indexes, climate trends as well as intensity, duration and frequency of climate events, based on regional climate simulations, are intended to be investigated.

References

Jacob, D., L. Bäring, O. B. Christensen, J. H. Christensen, M. De Castro, M. Deque, F. Giorgi, S. Hagemann, M. Hirschi, R. Jones, E. Kjellström, G. Lenderink, B. Rockel, E. Sanchez, C. Shär, S. Seneviratne, S. Somot, A. Van Ulden, B. Van Den Hurk, 2007:An inter-comparison of regional climate models for Europe: model performance in present-day climate. Climatic Change 81, 31-52.

Jacob, D., R. Podzun, 1997: Sensitivity studies with the regional climate model REMO. Meteorol. Atmos. Phys. 63, 119-129.

KLIWA, 2006: Regionale Klimaszenarien für Süddeutschland Abschätzung der Auswirkungen auf den Wasserhaushalt. KLIWA-Berichte Heft 9.

Kovats, R.S., K.L. Ebi, 2006: Heatwaves and public health in Europe. European Journal of Public Health 16, 592-599.

Maracchi, G., O. Sirotenko, M. Bindi, 2005: Impacts of present and future climate variability on agriculture and forestry in the temperate regions: Europe. Climatic Change 70, 117-135.

Mariani, L., S. Parisi, O. Failla, G. Cola, G. Zoia, L. Bonardi, 2009: A long time series of harvest dates for Grapevine. Italian Journal of Agrometeorology 1, 7-16.

Matzarakis, A., B. Amelung, 2008: Physiologically Equivalent Temperature as indicator for impacts of climate change on thermal comfort of humans. In: M. C. Thomson, R. Garcia-Herrera, M. Beniston (eds.), Seasonal Forecasts, Climatic Change and Human Health. Advances in Global Change Research 30, Springer-Sciences and Business Media, 161-172.

Meehl, G.A., C. Tebaldi, 2004: More intense, more frequent, and longer lasting heat waves in the 21th century. Science 305, 994-997.

Petgen, M., 2007: Reaktion der Reben auf den Klimawandel. Schweiz. Z. Obst-Weinbau 9/07.

Steppeler, J., G. Doms, U. Schättler, H.W. Bitzer, A. Gassmann, U. Damrath and G. Gregoric, 2003: Meso-gamma scale forecasts using the non-hydrostatic model LM. Meteorology and Atmospheric Physics, 82, 75-96.

Tonietto, J., A. Carbonneau, 2004: A multicriteria climatic classification system for grape-growing regions worldwide. Agricultural and Forest Meteorology 124, 81-97.

Will, A., Keuler K., Block A., 2006: The Climate Local Model - Evaluation Results and Recent Developments. TerraFLOPS Newsletter 8, 2-3.

Authors' address:

Dipl.-Met. Paul A. Neumann (paul.neumann@meteo.uni-freiburg.de)
Meteorological Institute, Albert-Ludwigs-University of Freiburg
Werthmannstr. 10, D-79085 Freiburg, Germany

Prof. Dr. Andreas Matzarakis (andreas.matzarakis @meteo.uni-freiburg.de)
Meteorological Institute, Albert-Ludwigs-University of Freiburg
Werthmannstr. 10, D-79085 Freiburg, Germany

Variability of light quality and quantity in a mixed forest stand

Christian Hertel, Michael Leuchner

Fachgebiet für Ökoklimatologie, Technische Universität München

Abstract

Light quality and quantity affects different characteristics in growth and competition within forest stands. These parameters deliver crucial energetic information about the light environment to the plants. Especially the spectral waveband between 400 and 700 nm (PAR) is mainly responsible for photosynthesis and thus for plant growth. Spectral ratios e.g. red/far red (R/FR) and blue/red (B/R) give important information about the light quality within stands. The R/FR is important for the detection of competition, structure and architecture, and internode expansion. Blue light strongly influences development and growth of plants; e.g. an increase of B/R may lead to higher photosynthetic rates per unit leaf area. In addition to spectral properties, a higher fraction of diffuse radiation on overcast days can be used more effectively by plant organs.

In this study, the spectral composition and variability of solar radiation were analyzed for different sky conditions (CS: clear, OVC: overcast) and solar angles in six different vertical layers of a mixed European beech and Norway spruce stand in Bavaria.

Solar elevation and sky conditions have great impact on the absorption of the entire PAR band. While the frequency of sunflecks decreases strongly from the sun to the shade crown, it does not show high variability among the species, sky conditions, or phenological stages when compared at the same canopy level.

The B/R ratio shows significantly higher values for spruce in comparison to beech at CS conditions. For both investigated species a strong increase of B/R in the sun crown and a strong decrease in the shade crown can be observed. Low solar angles result in higher B/R values. Differences in R/FR between beech and spruce are the result of the architecture of the respective species. R/FR increases under OVC conditions, while it decreases under CS conditions and increasing canopy cover.

1. Introduction

Light quality and quantity affect different characteristics in growth and competition within forest stands. These parameters deliver crucial energetic information about the light environment to the plants (e.g. Lieffers et al. 1999). The spectral irradiance is strongly influenced by the architecture of the canopy. Plant canopies operate as light filter concerning the spectral and spatial distribution of light at the ground level (e.g. Grant 1997). Important ecological processes are controlled through changes in the light environment e.g. regeneration, establishment, and physiological processes of productivity

The photosynthetically active radiation (PAR: waveband between 400 nm and 700 nm) triggers or inhibits processes such as seed germination, stem growth, leaf expansion and orientation, flowering, and dormancy. The ratio of red (R: 655-665 nm) and far-red (FR: 725-735 nm) is determined as the status of the phytochrome photoequilibrium (e.g. Smith 1994) and is important for the detection of competition, structure and architecture, and internode expansion (e.g. Grant 1997). R light is strongly absorbed by photosynthetically active pigments, on the other hand FR is mostly transmitted or reflected. In contrary, blue light is primary sensed by cryptochromes as photoreceptors and influences growth, development of higher plants, and promotes stomatal opening more than

other spectral wavelengths (e.g. Matsuda et al. 2007). The blue range of the spectrum is characterized by low reflectance and high absorption in contrast to FR and near infrared. The aim of this work is to describe how light quality and quantity represented by the spectral ratios R/FR and B/R vary in deciduous and coniferous stands.

2. Experimental Design

All measurements were carried out in the mature Norway spruce (*Picea abies* [L.] Karst) and European beech (*Fagus sylvatica* L.) stand „Kranzberger Forst“ (48°25’08’’ N, 11°39’41’’ E, 485m a.s.l.) approximately 35 km northeast of Munich, Germany. The experimental site is part of the Sonderforschungsbereich 607 founded by the Deutsche Forschungsgemeinschaft (DFG). The 130 sensor multichannel measurement system covering the range of 360-1020 nm is described in detail by Leuchner et al. (2005). The spectral measurements were performed for five different stand heights (3, 14, 17, 20, 23 m above ground; Fig. 1) and above the canopy with a spectral resolution of 0.8nm. Data from all sensors were included in the analysis and separated by their affiliation to the respective tree species. Due to this experimental setup, it is possible to describe the spatiotemporal distribution of solar radiation for both species.

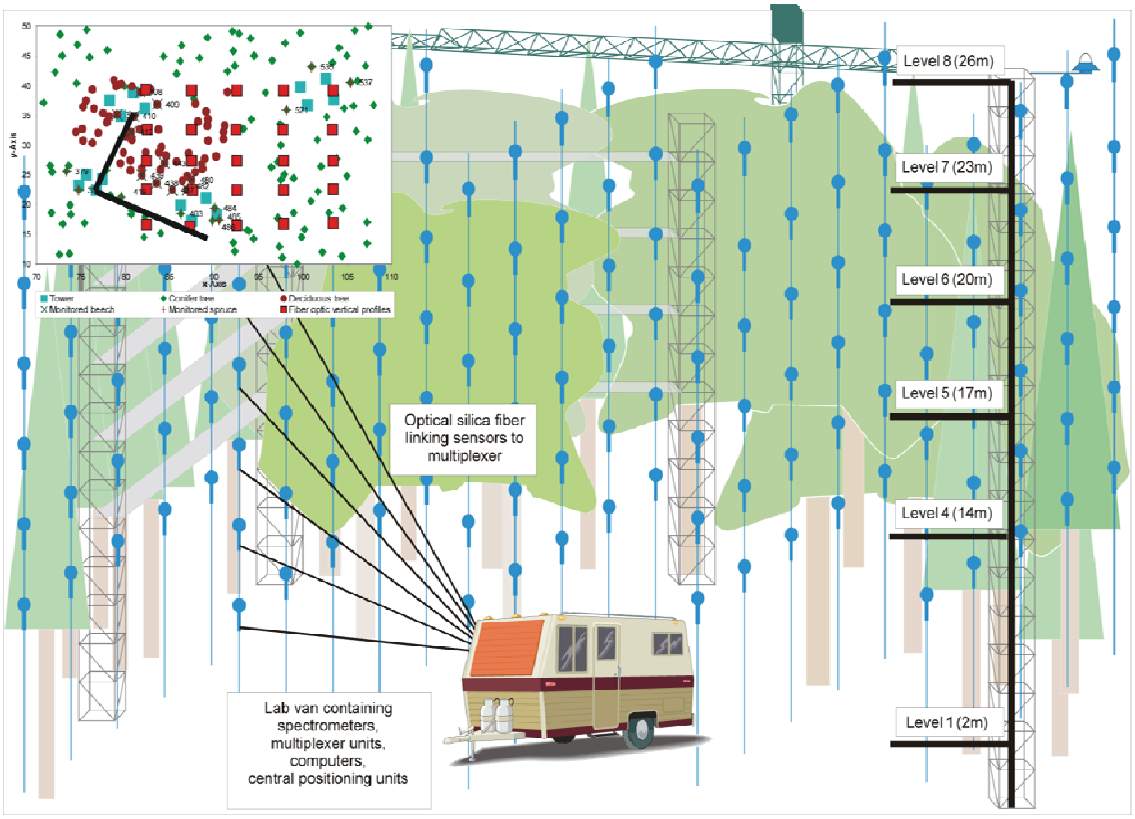

Fig. 1: Overview of the experimental site „Kranzberger Forst“ with the 130 sensor multichannel measurement system, covering the spectral range of 360-1020 nm

3. Results

When penetrating a canopy, light quantity as well as the spectral composition is changed significantly. Most of the absorption and spectral changes take place in the upper part of the sun crown. These processes are strongly dependent on solar elevation and sky conditions that determine the incoming radiation and the incident angle of direct irradiance.

This work shows that under clear sky conditions more PAR can penetrate the canopy at higher solar elevation. This effect is more pronounced for spruce than for beech due to the conical shape that allows photons from higher angles to enter the gaps in between trees in contrast to the more homogeneous surface of the beech canopy. The solar elevation is not a relevant factor at uniformly overcast conditions.

Differences in the vertical distribution of umbra and penumbra can be detected when comparing both species or different sky conditions, while the frequency of sunflecks is not strongly dependent on either factor. Not surprisingly, the highest frequency of sunflecks can be observed in the upper parts of the canopies. Only very few sunflecks can be measured in the shade crown and on the forest floor of this mature stand during foliation of beech.

Fig. 2 shows that sky conditions above the canopy have no great impact on the R/FR. Within the forest stand this situation changes in dependence of the species. The higher R/FR especially during OVC conditions is due to the fact that more diffuse unattenuated radiation can penetrate omni directional from the upper hemisphere into the forest stand and foliage gaps (e.g. Leuchner, 2007). The results show that deciduous canopies are denser than the clumped coniferous stands even under diffuse conditions where the impact of scattered light from all directions is quasi homogenous. R/FR determines the state of the phytochrome photoequilibrium and is to be seen as indicator for competition (Ammer 2003). The higher values in the upper layers of spruce during OVC and CS conditions are the effect of the special cone-shaped habit. The stepwise decrease of R/FR down to the layer of the shade crown (14m) underlines this result. In comparison, beech shows a strong decrease within the layers of the sun and shade crown, respectively, in the height of 23 and 20m linked to the dense, broadleaved architecture. The canopy density clearly affects the shading of the lower levels. Higher R/FR values at the forest basement are linked to scattered unattenuated radiation from the side, especially under low solar angles and OVC conditions. Low solar elevation angles are important for R/FR and the linked processes.

The analysis for B/R again shows the impact of biomass onto the ratio. All values under beech are lower than under spruce due to higher absorption of the broadleaved specie. For days with higher direct radiation an increase of the B/R ratio in the upper layers was evident for both species. Studies (e.g. Combes et al. 2000) have shown that more blue light is absorbed by biomass than red light. In our case the opposite behavior can be observed in the upper layers.

The B/R exhibits a strong dependence on the solar elevation angle. The variability of the values in the middle layers for spruce and the upper layers for beech show up to twofold increased values. The highest B/R ratios occur at low solar elevation independent of sky conditions.

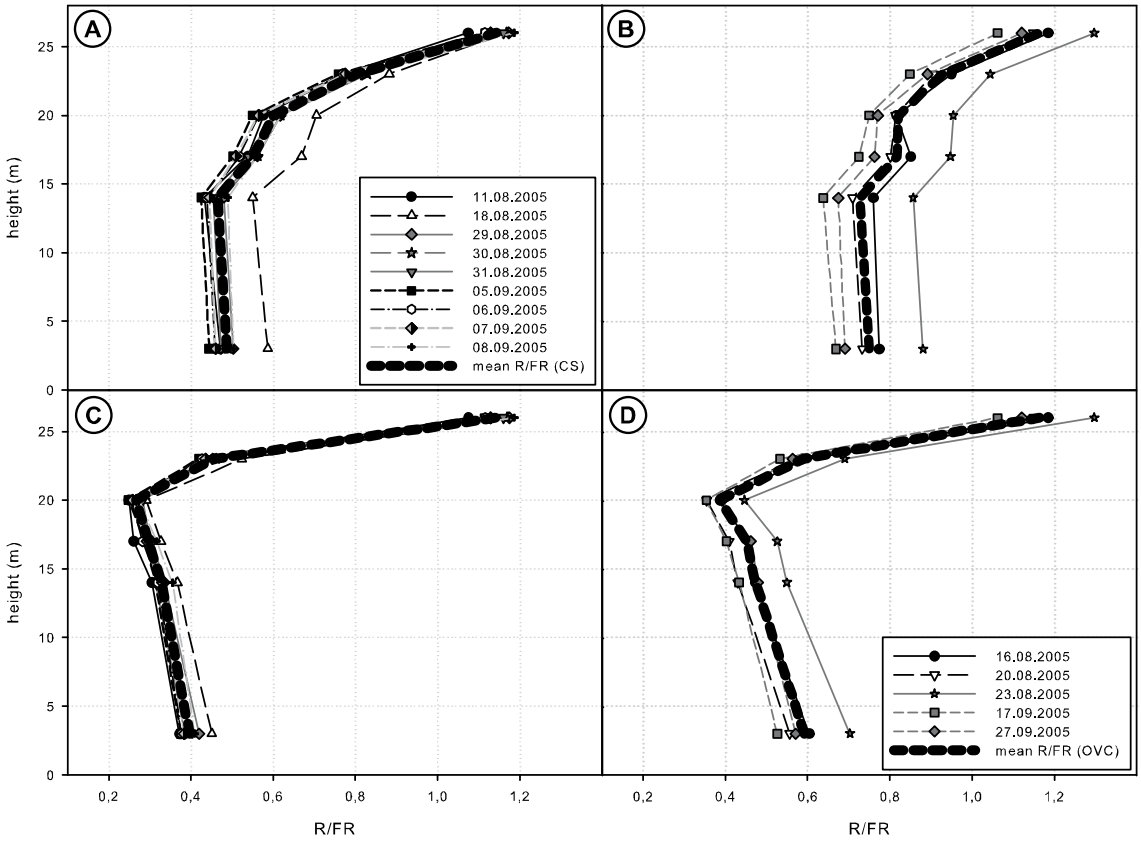

Fig. 2: Vertical profile of R/FR during CS and OVC conditions in the investigated layers. A) Spruce-CS, B) Spruce-OVC, C) Beech-CS, D) Beech-OVC

4. Conclusions

The main findings of our work are the spectral interactions of radiation with biomass under different sky conditions, solar angles and for different tree species. In particular the PAR waveband as well as the R/FR and B/R are investigated. The vertical distribution of sunflecks, penumbra, and umbra is compared under the above factors. Differences in R/FR in beech and spruce are the result of the special canopy structures. Only slight variations between the single vertical profiles in the investigated period show that R/FR behaves almost homogeneously for both sky conditions and species. For both investigated species sun leaves/needles seem to have a major effect onto the B/R ratio. It is evident that an increase of B/R is shown in the area of the sun crown. Also low solar elevation angles have a major effect by increasing the ratio.

Acknowledgement

This project is part of the Sonderforschungsbereich 607 (SFB 607) founded by the Deutsche Forschungsgemeinschaft (DFG). (further informations: http://www.sfb607.de)

References

Combes, D., Sinoquet, H., Varlet-Grancher, C., 2000: Preliminary measurements and simulation of the spatial distribution of the Morphogenetically Active Radiation (MAR) within isolated tree canopy. Ann. For. Sci. 57, 497-511.

Grant, R.H., 1997: Partitioning of biologically active radiation in plant canopies. Intl. J. Biometeorol. 40, 26-40.

Leuchner, M., Menzel A., Werner H., 2007: Quantifying the relationship between light quality and light availability at different phonological stages within a mature mixed forest. Agric. For. Meteorol. 142, 35-44.

Lieffers, V.J., Messier, C., Stadt, K.J., Gendron, F., Comeau, P.G., 1999: Predicting and managing light in the understory of boreal forests. Can. J. For. Res. 29, 796-811.

Matsuda, R., Ohashi-Kaneko, K., Fukiwara, K., Goto, E., Kurata, K., 2007: Analysis of the relationship between blue-light photon flux density and the photosynthetic properties of spinach (*Spinacia oleracea* L.) leaves with regard to the acclimation of photosynthesis to growth irradiance. Soil Sci. Plant Nutr. 53, 459-465.

Smith H., 1994: Sensing the light environment: the functions of the phytochrome family, In: R.E., Kronenberg G.H.M. (Eds.), Photomorphogenesis in plans, 2nd edn., Kluwer Academic Publishers, Dodrecht, 1994, 377-416.

Authors' address

Christian Hertel (hertel@wzw.tum.de)
Fachgebiet für Ökoklimatologie, Technische Universität München
Hans-Carl-von-Carlowitz-Platz 2, D-85354 Freising-Weihenstephan, Germany

Dr. Michael Leuchner (leuchner@wzw.tum.de)
Fachgebiet für Ökoklimatologie, Technische Universität München
Hans-Carl-von-Carlowitz-Platz 2, D-85354 Freising-Weihenstephan, Germany

Stem water storage of Norway spruce and its possible influence on tree growth under drought stress - application of ct-scannings -

Thomas Rötzer, Hans Pretzsch

Chair of Forest Yield Science, TU München, Germany

Abstract

From the forest site 'Fürstenfeldbruck 612' - a IUFRO experimental plot - 15 spruce trees of 3 different structured plots were harvested and up to 7 stem discs of every tree were scanned by computer tomography. Based on these data, heart and sapwood distributions on individual tree level are estimated as well as the stem water storage of each tree. Because stem water storage is closely linked with the diameter of a tree, we could scale the water storage from individual tree level to stand level. Using the physiologically based growth model BALANCE, assumptions were checked whether water storage in stems can mitigate drought stress.

1. Introduction

There is more and more evidence for a clear climate change within the next decades, the IPPC report (2007) showed the drastic consequences that global warming will have. Most likely precipitation and temperature will change substantially in the coming years. Additionally to the means the distribution within a year will probably differ from the current climate situation. And finally the frequency of climatic extremes, such as droughts, will increase in the coming decades (Meehl et al. 2000, Jonas et al. 2005). Therefore we studied the reaction of forest growth on extreme events, i.e. droughts, by simulating growth using the water balance and climate-sensitive model BALANCE. Hereby we considered stem water storage results that were gained from ct-scannigs.

2. Methods

2.1 Site description

The study site 'Fürstenfeldbruck 612' is located in Southern Germany, about 30 km west of Munich. In this area the annual mean temperature is 7.5 °C, the annual mean precipitation sums up to 825 mm. The trees grow on a loess soil. The three analysed plots are spruce stands with different stand densities (Table 1). At plot 14 the initial number of trees was 400, at plot 4 it was 1,000 trees and at plot 16 there were 2,500 trees. In 2006 - at a stand age of 37 - the number of trees of plot 14 had decreased to 200 with a basal area of 24.9 m², while the number of trees of plot 4 resp. plot 16 was reduced to 400 with 30.1 m² basal area resp. 800 with 35.8 m² basal area.

Table 1: Characterisation of the study site 'Fürstenfeldbruck 612'

plot no.		14	4	16
number of trees	initial	400	1000	2500
	2006	200	400	800
basal area [m²]		24.9	30.1	35.8

For this study 5 trees of each plot were harvested. From each of the harvested spruces up to 7 discs from every stem were analysed by computer tomography.

2.2 Ct-Scanning

Additionally to the heart and sapwood distribution, densities as well as moisture distribution in spruce stems were determined by ct-scanning. This X-ray based method commonly used in human medicine has been adopted for wood analysis (e.g. zu Castell et al. 2005). The suitability of ct-scanning for the detection of structures and water content in woody tissues was proven in several studies (e.g. Fromm et al. 2001, Vötter 2005, Nikolova et al. 2009).

For our studies a ‘‘Siemens Somatom AR.HP’’ medical scanner was used. The predefined acceleration voltage was 130 kV with a dose of 200 mAs for 2 s. The scanner features a density resolution of 14 bits and a reconstruction matrix of 512 x 512 pixel in the region of interest. Like traditional X-ray radiographs, ct-scanning - according to the Lambert Beer’s law - is based on the attenuation of X-rays by an object. Higher densities and differences in atomic weight lead to a modification of the attenuation coefficient. The obtained tomogram is a picture of known size and coordinates of each pixel. Combining the multiple tomograms along the axial vector of the object yields a fully 3D-representation. The constancy of density measurement was assured by regular maintenance based on tests of known densities. All stem discs were scanned twice: immediately after cutting, while the disc was still fresh and after drying. Water content and distribution within discs were assessed as the difference between density levels of dry and fresh scans, which were measured in ‘Hounsfield units’.

2.3 Tree growth model BALANCE

The physiological growth model BALANCE calculates the 3-dimensional development of individual trees or forest stands and estimates the consequences of environmental influences. As an individual tree based model BALANCE simulates growth responses on the single tree level, which enables an estimation of the influence of competition, stand structure, species mixture, and management impacts because tree development is described as a response to individual environmental conditions and environmental conditions change with individual tree development. Biomass of an individual tree is calculated from the dimensional variables tree position, tree- and crown base height, diameter, and crown radii. The increase in biomass is the result of the interaction of several physiological processes which depend on the physical and chemical microenvironment that is itself influenced by the stand structure.

Individual carbon-, water- and nutrient balances of the trees species beech, oak, spruce and pine are the fundamental processes for the simulation of growth. Each tree is structured in crown and root layers, which are in turn divided in up to eight crown- and root sectors. For each layer resp. each sector micro climate and water balance are calculated by using temperature, radiation, precipitation, humidity and wind. While these calculations are computed daily, the physiological processes assimilation, respiration, nutrient uptake, growth, senescence and allocation are calculated in monthly or decadal time steps (= 10-day periods) from the aggregated driving variables. This way, CO2-concentration, soil condition, competition between individuals, and stress factors, as for

example air pollution and nutrition deficiency, can be considered additionally to the weather conditions when modelling the growth of trees. Based on the individual carbon balance, dimensional changes and mortality of each tree are computed annually.

BALANCE includes different approaches for the estimation of the stand climate for each individual tree. The Penman-Monteith equation is the base of the water balance calculations. Via the stomatal closure water balance is connected with photosynthesis, which is calculated in BALANCE by using the approach of Haxeltine and Prentice (1996). Carbon and nitrogen allocation into roots, branches, foliage and stem is computed according to functional balance and pipe model principles. A more detailed description of the model can be obtained in Grote and Pretzsch (2002), Rötzer et al. (2005), Rötzer et al. (2009) and Rötzer et al. (2010).

3. Calculation of the stem water storage of single trees and entire stands

Based on the density analysis by ct-scanning and the measured diameter and height values of each single tree, stem water storage of the individual trees can be calculated by subtracting the dry mass of a tree from the fresh mass. Figure 1 shows the water storage in the stems of the 15 analysed spruces.

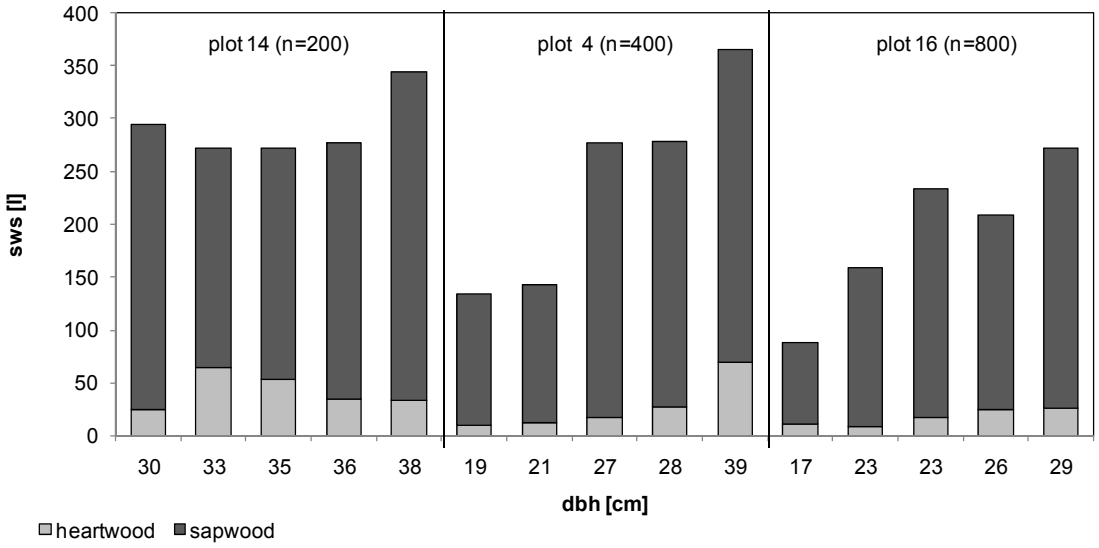

Fig. 1: Water storage in the sapwood and heartwood of the single spruces according to their diameters at breast height within the three plots in 'Fürstenfeldbruck 612' (Southern Germany)

Figure 1 shows a close relationship between stem water storage *sws* and diameter at breast height *dbh*. Based on the values of the 15 spruces, linear regression analysis results in a coefficient of determination of 83 % for the regression sws = a + b*dbh. Thus, stem water storage of the single trees can be calculated by using the diameter at breast height. After the estimation of the *sws* for all trees of the three plots, stem water storage of the entire spruce stands can be calculated (Fig. 2).

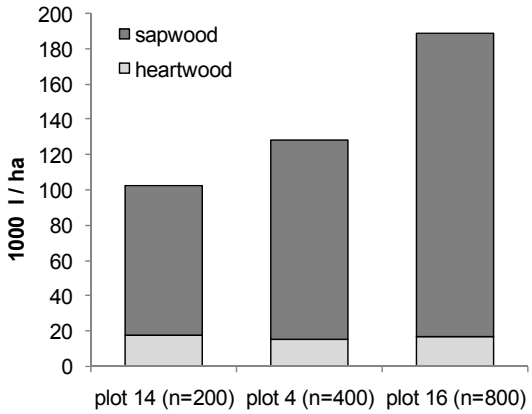

Fig. 2: Stem water storage of the three spruce plots in 'Fürstenfeldbruck 612' (Southern Germany)

While the low density plot 14 with only 200 trees can store 100,032 l water per ha, the stem water storage of plot 4 with 400 trees is 128,441 l /ha and the 800 trees of plot 16 store 189,454 l/ha.

4. Simulation of tree growth under water stress regarding stem water storage

If trees can use just a part of the stem water storage in periods with a poor water supply, then this is beneficial for the trees. To analyse this aspect simulation studies were done using the physiologically sensitive tree growth model BALANCE. For the simulations we assumed that a maximum of 10% of the stem water storage can be used for transpiration in dry periods.

As a test plot a spruce stand of the experimental site 'Kranzberger Forst' located 515 m asl and stocking on eutric cambisols was used. The mean diameter at breast height of the entire stand is 18.2 cm, the mean height is 17.4 m. Growth simulations were done for the years 1999 and 2003. 1999 was a normal year with an average temperature of 8.1 °C and an annual precipitation sum of 849 mm. These values are close to the long term means for the area. The dry year 2003 showed an average temperature of 8.8 °C with a precipitation sum of only 558 mm.

As response variables we analysed gross primary productivity *gpp* and net primary productivity *npp* as well as biomass increment *b-inc*. Additionally, we looked for the changes in the water balance by comparing the actual evapotranspiration sums (Tab. 2).

Table 2: gpp, npp, b-inc and transpiration of a spruce stand at the site 'Kranzberger Forst' (Southern Germany) for the years 1999 and 2003 with and without using stem water storage *sws*

	1999		2003	
	without sws	using sws	without sws	using sws
gpp [t dm /ha /a]	29.7	30.0	24.3	24.9
npp [t dm /ha /a]	16.8	17.1	10.5	11.0
biomass increment [t dm /ha /a]	18.1	18.5	8.1	8.6
transpiration [l/m²]	356	364	337	348

The differences for the simulation run with and without using *sws* are small for the year 1999, e.g. *gpp* increases from 29.7 to 30.0 t dm/ha. In 2003 the absolute values are smaller, e.g. *gpp* in 1999 was 29.7 t dm/ha, in 2003 it was 24.3 t dm /ha. However, there are bigger differences between the runs with and without using *sws. Gpp* for example rises from 24.3 t dm/ha to 24.9 t dm/ha.

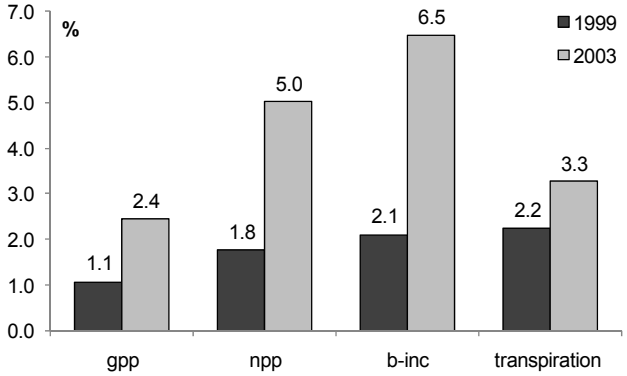

Fig. 3: Changes of gpp, npp, b-inc and transpiration of a spruce stand at the site 'Kranzberger Forst' (Southern Germany) for the years 1999 and 2003 with and without using stem water storage

Looking at the changes (100% = simulation without using s*ws*) we can see from figure 3 that particularly in 2003 *npp* and the biomass increment rise by 5.0 % resp. 6.5 % while transpiration increases only by 3.3 %.

5. Conclusions

Ct-scanning is a proper tool to uncover tree structures of single trees as for example stem moisture. Using the results and transferring the knowledge to models will be a further step in improving forest growth modelling. As shown in an example, trees can overcome stress periods much better and optimize productivity if they can use a part of the stem water storage in dry periods for transpiration. Up to now this issue is rarely considered when simulating the growth and water balance of forest stands.

Acknowledgement

The authors thank the German Weather Service and the Bayerische Landesanstalt für Wald und Forstwirtschaft for supplying meteorological data. The study was done in the frame of the Sonderforschungebereich SFB 607.

References

zu Castell, W., Schrödl, S., Seifert, T. 2005: Volume Interpolation of CT Images from Tree Trunks. Plant Biol. 7: 737–744.

Fromm, J.H., Sautter, I., Matthies, D., Kremer., J, Schumacher, P., Ganter, C. 2001: Xylem water content and wood density in spruce and oak trees by high-resolution computer tomography. Plant Physiol 127:416–425.

Grote, R., Pretzsch, H. 2002: A model for individual tree development based on physiological processes. Plant Biol. 4: 167-180.

Haxeltine, A., Prentice, I.C. 1996: A general model for the light use efficiency of primary production by terrestrial ecosystems. Functional Ecology 10: 551-561.

IPCC 2007: IPCC WGI Fourth Assessment Report to Climate Change: The Physical Science Basis; Summary for Policymakers. IPCC Secretariat, Geneva, Switzerland, 18p.

Jonas, M., Staeger, T., Schönwiese, C.D. 2005: Berechnung der Wahrscheinlichkeiten für das Eintreten von Extremereignissen durch Klimaänderungen – Schwerpunkt Deutschland -. UBA-Bericht 201 41 254, Dessau, 252p.

Meehl, G.A., David, T.K., Easterling, R., Changnon, S., Pielke, Jr. R., Changnon, D., Evans, J., Groisman, P., Knutson, T.R., Kunkel, K.E., Mearns, L.O., Parmesan, C., Pulwarty, R,, Root, I., Richard, T., Sylves, T., Whetton, P., Zwiers, F. 2000: An Introduction to Trends in Extreme Weather and Climate Events: Observations, Socioeconomic Impacts, Terrestrial Ecological Impacts, and Model Projections. Bulletin of the American Meteorological Society 81 (3): 413–416.

Nikolova, P, Blaschke, H, Matyssek, R, Pretzsch, H, Seifert, T (2009) Combined application of computer tomography and light microscopy for analysis of conductive xylem area in coarse roots of European beech and Norway spruce. Eur J Forest Res 128:145–153.

Rötzer, T., Grote, R., Pretzsch, H. 2005: Effects of environmental changes on the vitality of forest stands. European Journal of Forest Research 124: 349-362.

Rötzer, T., Seifert, T., Pretzsch, H. 2009: Modeling above and below ground carbon dynamics in a mixed beech and spruce stand influenced by climate. Eur J Forest Res 128: 171-182.

Rötzer, T., Leuchner, M., Nunn, A.J., 2010: Simulating stand climate, phenology, and photosynthesis of a forest stand with a process based growth model. Int. J Biometeorol. doi: 10.1007/s00484-009-0298-0.

Vötter, D. 2005: Splintholzerkennung mittels Computertomographie und Färbeverfahren an Fichte und Buche. Ein Methodenvergleich. Diploma thesis at the Chair of Forest Yield Science, Technische Universität München, Freising, p 151.

Authors' address:

Dr. Thomas Rötzer (thomas.roetzer@lrz.tu-muenchen.de)
Chair of Forest Yield Science, TU München
Hans Carl von Carlowitz Platz 2, D-85354 Freising, Germany

Prof. Dr. Hans Pretzsch (hans.pretzsch@lrz.tu-muenchen.de)
Chair of Forest Yield Science, TU München
Hans Carl von Carlowitz Platz 2, D-85354 Freising, Germany

Effects of climate change and adaptation strategies for Northwest European forest stands

Thomas Rötzer, Yan Liao, Hans Pretzsch

Chair of Forest Yield Science, TU München, Germany

Abstract

The project 'Transnational Forestry Management Strategies in Response to Regional Climate Change Impacts (ForeStClim)' will show regionalized climate change impacts on forest site characteristics, forest protection functions, forest yield, biodiversity, water resources and carbon sequestration across North-West Europe. Growth simulations based on the response of physiological processes are carried out with BALANCE, a model that includes the simulation of micro-climate and represents total water- and carbon flows in a forest ecosystem. This way, an understanding of the quantitative importance of various processes can be gained and ecosystem responses to environmental changes beyond the currently observed conditions can be analyzed. Results about growth responses - e. g. forest structure or environmental changes - can be used to adapt growth functions in the management oriented model SILVA. The step by step modelling of the growth of individual trees informs about the development of classical parameters as timber volume or basal area but also about financial yield, stability and diversity. Therefore, the model is an ideal tool for modern forest management which has to ensure multi-criterial sustainability. An example shows first results of physiologically based simulations**.**

1. The ForeStClim-project

At present there is great interest in forest science concerning studies about the responses of forests on climate changes. Most of this studies show a rise of photosynthesis and net primary production under higher CO2 concentrations and elevated temperatures (e.g. Zheng et al. 2002, Hamilton et al. 2002). The influence of other environmental parameters as for example nutrition, level of stress, stand structure, or management impact on growth in combination with climate change scenarios is, however, analyzed insufficiently up to the present. The project 'Transnational Forestry Management Strategies in Response to Regional Climate Change Impacts' (www.forestclim.eu) is part of the INTERREG IVB program in North-West Europe. Its goal is to develop proactive and adaptive regional forestry management and forest protection strategies in the face of expected climate change scenarios. In this study we focus on uncovering growth patterns influenced by changing climate conditions using different forest growth models. At first, we have to adjust and validate the growth models SILVA and BALANCE for selected NW-European regions. Afterwards we can run scenario simulations of forest growth and carbon sequestration depending on climate change scenarios and analyze the simulation results of different adaptation strategies for a sustainable forest management in different NW-European regions.

2. Methods

The uncovering of growth patterns and their utilization for forest economic and environment political decisions can be realised by using growth models. However, most of the growth models are either management oriented models or eco-physiologically based. Therefore they have to be connected. Growth patterns based on physiological analyses can be revealed for the present climate and for climate scenarios by using the

physiological model BALANCE. The detected reaction patterns can be transformed in functional algorithms and integrated in the management oriented model SILVA. This way changed growth relationships caused by environmental changes can be simulated by the model SILVA. By using this model also the testing of possible adaption strategies is possible.

2.1 The physiological growth model BALANCE

The single tree based growth model BALANCE calculates tree growth based on the response of physiological processes. It includes the simulation of micro-climate and represents total water- and carbon flows in a forest stand. With this model an understanding of the quantitative importance of various processes can be gained and research requirements can be high-lighted. Principally, ecosystem responses to environmental changes beyond the currently observed conditions (e.g. climate change) can be analysed. Results about growth responses - e. g. forest structure or environmental changes - can be used to adapt functions in management oriented models if the empirical basis for certain boundary conditions is poor. BALANCE calculates the 3-dimensional development of individual trees or forest stands and estimates the consequences of environmental influences. The simulation of growth responses on the single tree level enables an estimation of the influence of competition, stand structure, species mixture, and management impacts because tree development is described as a response to individual environmental conditions and environmental conditions change with each individual tree development. Dimensional tree growth is calculated once a year based on the biomass increase of the woody tissue that has been accumulated during the last year by each single tree. The increase in biomass is the result of the interaction of several physiological processes which depend on the physical and chemical microenvironment that is itself influenced by the stand structure. BALANCE includes different approaches for the estimation of the stand climate for each individual tree. The Penman-Monteith equation is the base of the water balance calculations. Via the stomatal closure water balance is connected with photosynthesis, which is calculated by using the approach of Haxeltine and Prentice (1996). Carbon and nitrogen allocation into roots, branches, foliage and stem is computed according to functional balance and pipe model principles. To depict the relationships between the environmental influences and growth the annual cycle of foliage development must be known. With the beginning of bud burst foliage, biomass, leaf area, light availability and radiation absorption change. Thus, the date of foliage emergence in a tree determines its assimilation and respiration rate but also affects the environmental conditions of the trees in its vicinity. Because tree development is described as a response to individual environmental conditions and environmental conditions change with the individual tree development, environmental influences can be assessed in any kind of species mixture or stand structure. A more detailed description of the model can be obtained in Grote and Pretzsch (2002) or Rötzer et al (2010).

2.2 The management oriented growth model SILVA

SILVA is a distance-dependent individual tree model (Pretzsch et al. 2002). It was primarily developed to support operational forest management planning (Moshammer 2006). The statistically based growth simulator SILVA reflects the spatial and dynamic character of pure and mixed, even- and uneven-aged stands with Norway spruce, silver

fir, European beech, Pedunculate oak, Scots pine, Douglas fir, European larch, ash and elder. The model simulates the effects of tending, thinning and regeneration on the stand dynamics. The step by step modelling of the growth of all individual trees informs about the development of classical parameters as timber volume or basal area but also about financial yield, stability and biodiversity. With models of this type a weighting between yield-related, socio-economic and ecological effects becomes possible. This broad range of information makes the model an ideal tool for modern forest management which has to ensure multi-criterial sustainability. 3-dimensional visualisation (realistic views, real-time walk- or fly-throughs) contribute towards illustrating natural developments and human operations in forests. In combination with SILVA the effect of forest management on the appearance of landscapes can be visualised as well as changes on landscape level. The smallest simulation time step with SILVA is a period of five years. This time interval corresponds with the time intervals provided by yield tables and with the standard time interval between two measurements on trial plots. Based on the individual-tree approach a module allows to create rules for a virtual thinning which likewise take place every five years. A recently implemented biomass module uses SILVA's individual-tree output to assess stem biomass, bark biomass, branch biomass, leaf or needle biomass, and the coarse root biomass for each tree separately. Detailed information about SILVA can be derived from Pretzsch (2002) or from Pretzsch et al. (2002).

3. First results

A first study area to adjust and validate the models BALANCE and SILVA and to run first simulations is located in Rhineland Palatinate, in Western Germany.

3.1 Site description

The 'Pfälzerwald' is located in the south of Rhineland Palatinate. It is in a low-mountain region ranging from 49° 02' N to 49° 37' N, and from 7° 30' E to 8° 09' E, extending southwards to Northern France. The 'Pfälzerwald' is one of the largest forests in NW Europe covering 1.798 km². Originally, the dominant tree species of the 'Pfälzerwald' are oak and beech. Due to economic reasons more and more pine and spruce trees have been planted in the last 150 years (Umweltbundesamt 2009). Soils are generally nutrient poor sands derived from red bed sandstones and limestones (Behrens et al.2006). The test plots BE1, BE3 and BE4 are located in the Merzalben and Johanniskreuz areas. The characteristics of these plots are shown in table 1.

Table1: Characteristics of test plots

site W-Germany	tree species		age		n
	principle	secondary	principle	secondary	
RLP-BE1	oak	beech	64	35	799
RLP-BE3	oak	beech	198	95	360
RLP-BE4	pine	beech	127	50	119

As soil information for the test plots field capacities and wilting point values in four layer from 0 - 6 cm (fc: 39.5 vol%, wp: 15.5 vol%), from 6 - 25 cm (fc: 33.5 vol%, wp: 11.5 vol%), from 25 - 55 cm (fc: 24.5 vol%, wp: 7.0 vol%) and from 55-80 cm (fc: 23.5

vol%, wp: 7.0 vol%) were assumed.

Climate information used as the driving forces of growth is based on the WETTREG simulations (Enke et al. 2006), emission scenario A1B for the Merzalben region. The first 30 years from 2001 - 2030 present the current climate, the years from 2071 - 2100 describe future climate conditions. Figure 1 shows the conditions of the two periods for temperature and precipitation.

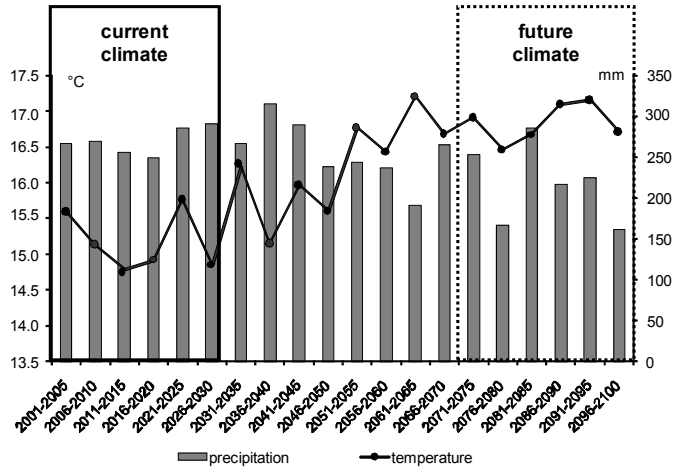

Fig: 1: Five years averages of temperature and precipitation for the test plots in the 'Pfälzerwald' simulated by WETTREG, scenario A1B

Table 2 shows the mean values of temperature and precipitation averaged for the year and the growing period under current and future climate conditions for the region Merzalben. While the mean annual temperature rises by 2.4 °C from current to future climate conditions, precipitation decreases by 20 mm on annual basis and by 51 mm within the growing season.

Table 2: Mean values of the current and future climate for the test plots in the 'Pfälzerwald'

period	temperature [°C]		precipitation [mm]		growing season [d]
	year	growing season	year	growing season	
2001-2030	8.3	15.2	621	270	157
2071-2100	10.7	16.8	601	219	189

3.2 Results

Figure 2 shows the biomass increment after 30 years under current and future climate conditions for the three test plots. In the period between year 2001 and 2030, the total living biomass increment of plot BE1 is 94 t C ha^{-1}, which is estimated to decrease to 32.6 t C ha^{-1} under future climate conditions in the period from 2071 to 2100. The living biomass change in BE3 and BE4 tell the same story. The total living biomass increments are 106.9 t C ha^{-1} resp. 51.4 t C ha^{-1}, in the first period under the present climate, but the increments drop to 72.8 t C ha^{-1} resp. 19.3 t C ha^{-1} in the next period under a future climate.

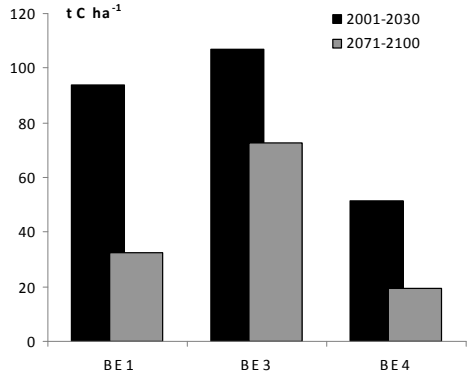

Fig: 2: Living biomass increment after 30 years at the three test plots under current and future climate conditions

Figure 3 depicts the dead biomass as sums of 30 years for the three test plots under current and future climate conditions. In contrast to the living biomass increment, the dead biomass shows smaller differences under present and future climate conditions. This is especially supported by the plot BE1 (the younger oak stand), where dead biomass only increases from 70.1 t C ha^{-1} to 71.4 t C ha^{-1}. Both test plots BE3 (old oak stand) and BE4 (old pine stand) have a slight decrease between the two tested periods in terms of the dead biomass.

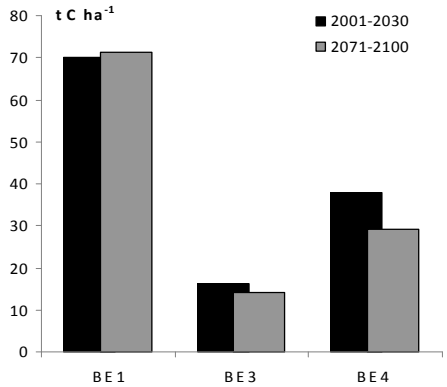

Fig: 3: Sum of the dead biomass within 30 years at the three test plots under current and future climate conditions

4. Conclusions

The first results show that BALANCE is able to realistically simulate forest growth in Western Germany. Further validation and sensitivity tests have to be done to confirm the results. The next step will be to reveal growth patterns for present and future climate scenarios, to transform them in functional algorithms and integrate them in the management oriented model SILVA. This way, possible adaption strategies of forest stands in Rhineland Palatinate under changed environmental conditions can be simulated and analysed.

Acknowledgement

The authors are indebted to the INTERREG IVB NWE Programme for funding the project FORESTCLIM. We thank our colleagues of the Research Institute for Forest Ecology and Forestry in Rhineland Palatinate for supplying data and giving us helpful advices.

References

Behrens T., Scholien T.P., Lagacherie A.B.M., Voltz, M., 2006: A Comparison of Data-Mining Techniques in Predictive Soil Mapping. In: Developments in Soil Science. Elsevier, 617pp.

Enke, W., Spekat, A., Kreienkamp, F., 2007: Neuentwicklung von regional hoch aufgelösten Wetterlagen für Deutschland und Bereitstellung regionaler Klimaszenarien mit dem Regionalisierungsmodell WETTREG 2005 für die SRES – Szenarien B1, A1B und A2. Projektbericht im Rahmen des F+E-Vorhabens 204 41 138 "Klimaauswirkungen und Anpassung in Deutschland – Phase 1: Erstellung regionaler Klimaszenarien für Deutschland", 94 S.

Grote, R., Pretzsch, H., 2002: A model for individual tree development based on physiological processes. Plant Biol. 4, 167-180.

Hamilton, J.G., DeLucia, E.H., George, K., Naidu, S.L., Finzi, A.C., Schlesinger, W.H., 2002: Forest carbon balance under elevated CO2. Oecologia 131, 250-260.

Haxeltine, A., Prentice, I.C. 1996: A general model for the light use efficiency of primary production by terrestrial ecosystems. Functional Ecology 10, 551-561.

Moshammer, R., 2006: Vom Inventurpunkt zum Forstbetrieb. AFZ- Der Wald 61, 1164-1165.

Pretzsch. H., 2002: Application and Evaluation of the growth simulator SILVA 2.2 for forest stands, forest estates and large regions. Forstwiss. Cbl. 212, 28-51.

Pretzsch, H., Biber, P., Dursky, J., 2002: The single tree-based stand simulator SILVA: construction, application and evaluation. For. Ecol. Manage. 162, 3-21.

Rötzer, T., Leuchner, M., Nunn, A.J., 2010: Simulating stand climate, phenology, and photosynthesis of a forest stand with a process based growth model. Int. J Biometeorol. doi: 10.1007/s00484-009-0298-0.

Umweltbundesamt 2009: Forest ecosystems: Palatinate Forest Biosphere Reserve. URL http://www.umweltbundesamt.de/specimen/upb39.htm

Zheng, D., Freeman, M., Bergh, J., Røsberg, I., Nilsen, P., 2002: Production of Picea abies in South-east Norway in Response to Climate Change: A Case Study Using Process-based Model Simulation with Field Validation. Scand. J. For. Res. 17: 35-46.

Authors' address:

Dr. Thomas Rötzer (thomas.roetzer@lrz.tu-muenchen.de)
Chair of Forest Yield Science, TU München
Hans Carl von Carlowitz Platz 2, D-85354 Freising, Germany

Yan Liao
Chair of Forest Yield Science, TU München
Hans Carl von Carlowitz Platz 2, D-85354 Freising, Germany

Prof. Dr. Hans Pretzsch (hans.pretzsch@lrz.tu-muenchen.de)
Chair of Forest Yield Science, TU München
Hans Carl von Carlowitz Platz 2, D-85354 Freising, Germany

Einfluss des Klimas auf die Kohlenstoffspeicherung von Moorwäldern

Steffi Röhling, Thomas Rötzer, Hans Pretzsch

Lehrstuhl für Waldwachstumskunde, Technische Universität München

Zusammenfassung

Im Rahmen des vom Johann Heinrich von Thünen-Instituts (vTI) geförderten Verbundvorhabens „Organische Böden“ wird im Teilprojekt „Wachstum und Kohlenstoffdynamik von Moorwäldern“ untersucht, wie viel Kohlenstoff in Moorwaldbeständen gespeichert ist und wie sich die Kohlenstoffspeicherung aufgrund von Absterbe- und Aufbauprozessen, sich ändernder Umweltbedingungen oder Behandlungsmaßnahmen verändert. In einem ersten Schritt erfolgte die Aufnahme von ertragskundlichen Kenndaten der Baumarten Erle (*Alnus glutinosa* (L.) GAERTN.), Fichte (*Picea abies* (L.) KARST) und Kiefer (*Pinus sylvestris* L.) auf vier Moorstandorten in Deutschland. Daraus konnten der jährliche Radialzuwachs sowie die jährliche Kohlenstoffspeicherung eines jeden Baumes abgeleitet werden. Im nächsten Schritt kann so der Zusammenhang der annuellen Kohlenstoffdynamik mit den einzelnen klimatischen Größen analysiert und der Einfluss von Temperatur sowie Niederschlag auf das Zuwachsverhalten von Moorwaldbeständen abgeschätzt werden.

Influence of climate on the carbon storage of forest stands in peatlands

Abstract

In the context of the joint research project “Organic Soils” funded by the Johann Heinrich von Thünen-Institut the subproject “Growth and carbon dynamics of forest stands in peatlands” examines how much carbon is accumulated in peatland forests. The change of the carbon storage due to growth and mortality processes, environmental changes or management measures will be analysed. In a first step the growth parameters of the alder, spruce and pine were collected at four peatland sites in Germany. Based on these data the annual radial increment and the annual carbon storage of each tree can be calculated. Thus the relationships of the annual carbon dynamic with the individual climate conditions were analysed and the influence of temperature and precipitation on the growth increment of peatland forests were estimated.

1. Einleitung

Obwohl Moore nur ca. 5 % der Landesfläche von Deutschland bedecken, gehören sie mit 2 bis 5 % der nationalen Treibhausgasemissionen zur größten Treibhausgasquelle in den Bereichen Landwirtschaft, Landnutzung, Landnutzungsänderung und Forstwirtschaft (vTI 2009). Moore wurden als größte Treibhausgashauptquelle außerhalb des Energiesektors identifiziert, wodurch erhöhte Anforderungen für die Berichterstattung gemäß dem Kyotoprotokoll gelten. Da derzeit keine belastbaren Zahlen für Emissionen aus genutzten Mooren als auch Referenzemissionen aus natürlichen Mooren in Deutschland existieren, ist eine regelkonforme Berichterstattung entsprechend der Anforderungen des Intergovernmental Panel on Climate Change (IPCC) nicht möglich. Deshalb müssen Grundlagen für die Klimaberichterstattung geschaffen sowie Managementszenarien und Entscheidungshilfen für die deutsche Verhandlungsposition im Klimaschutzprozess entwickelt werden. Um den internationalen Vereinbarungen zum Klimaschutz gerecht zu werden, wurden 11 Testgebiete (Abb. 1 und Tab. 1) mit unterschiedlichen organischen Bodentypen in Deutschland ausgewählt, auf denen die fehlen-

den Aktivitätsdaten zur Moorverteilung, Mooreigenschaften, Landnutzung, Hydrologie sowie Emissionsfaktoren ermittelt werden sollen. Eine wesentliche Steuergröße für den Spurengasaustausch ist die Vegetation. Um Unsicherheiten in den Emissionsfaktoren ausschließen zu können, ist eine räumliche und zeitliche Modellierung erforderlich. Ein wichtiger Beitrag dazu ist, das Wachstum und die Kohlenstoffdynamik der Moorwaldbestände in den ausgewiesenen Testgebieten modellhaft abzubilden.

2. Material und Methoden

2.1 Testgebiete

Die 11 Testgebiete sind über ganz Deutschland verteilt (Abb. 1), wobei die organischen Bodentypen Anmoor, Niedermoor sowie Hochmoor abgedeckt werden. Die dargestellten Ergebnisse beziehen sich auf die untersuchten Testgebiete Freisinger Moos, Graben-Neudorf, Mooseurach und Spreewald die auf Niedermoor- und Hochmoorstandorten liegen (Tab. 1, Abb. 1). Die Jahresmitteltemperaturen der 4 Testgebiete schwanken innerhalb des Unter-suchungszeitraums von 1990 bis 2008 zwischen 8,5 und 11,3 °C, die Jahresniederschläge von 548 bis 1161 mm.

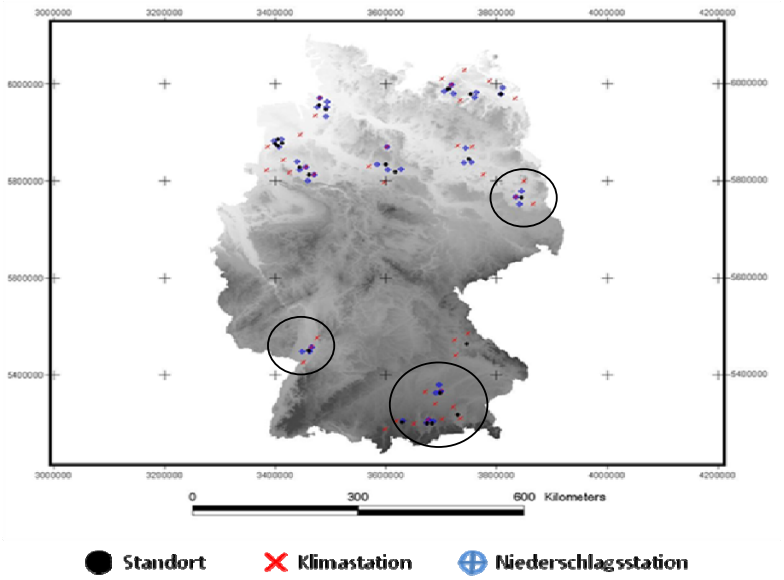

Abb. 1: Testgebiete mit zugeordneten Klima- und Niederschlagstationen

Fig. 1: Test plots with attributive climate and precipitation stations

2.2 Aufnahmemethodik

Nach Anlage von jeweils 2 gleichgroßen Parzellen mit 0,04 bis 0,16 ha in den 4 Testgebieten wurden von allen Bäumen innerhalb der Parzellen und den unmittelbar angrenzenden Umfassungsbäumen die ertragskundlichen Parameter Baumart, x,y-Koordinaten, Durch-messer, Höhe, Kronenansatz sowie Kronenradien aufgenommen. Zusätzlich erfolgte die Entnahme von Bohrkernen an jedem Baum innerhalb einer Parzelle. In den Tabellen 2 und 3 sind die wichtigsten Ergebnisse der Ertragskenndaten in den einzelnen Testgebieten dargestellt.

Tab. 1: Lage der Testgebiete, organische Bodentypen, Jahresmitteltemperaturen [JMT] und Jahresniederschläge [JNS] 1990 - 2008

Table 1: Test plots, soil types, annual mean temperature [JMT] and precipitation sums [JNS] 1990 - 2008

TG	Standort	Bodentyp	Koordinaten		Höhe	JMT	JNS
			Länge [°]	Breite [°]	[m ü. NN]	[°C]	[mm]
1	Ahlen-Falkenbergermoor	Hochmoor	8,786	53,698	3	10,0	821
2	Dümmer	An-/Niedermoor	8,310	52,520	40	9,9	786
3	Peenetal	Niedermoor	13,282	53,866	8	9,0	596
4	Paulinenaue	An-/Niedermoor	12,717	52,683	31	9,6	565
5	**Freisinger Moos**	**Niedermoor**	**11,685**	**48,372**	**500**	**8,5**	**822**
6	**Mooseurach**	**Hochmoor**	**11,262**	**47,538**	**576**	**9,0**	**1161**
7	Westermoor/Leegmoor	Hochmoor	7,595	53,028	7	10,0	815
8	Dummerstorf	An-/Niedermoor	12,244	53,995	43	9,2	576
9	Großes Moor bei Gifhorn	Hochmoor	10,610	52,559	59	9,7	670
10	**Spreewald**	**Niedermoor**	**14,017**	**51,917**	**50**	**9,7**	**548**
11	**Graben-Neudorf**	**Niedermoor**	**8,460**	**49,177**	**106**	**11,3**	**701**

Tab. 2: Ertragskenndaten der Erle in den Testgebieten 5, 10 und 11 (Abkürzungen: N = Stammzahl, H_G = Höhe des Grundflächenmittelstammes, H_O = Oberhöhe, D_G = Durchmesser des Grundflächenmittelstammes, D_O = Durchmesser des Oberhöhenstammes, G = Grundfläche, VD = Derbholzvolumen)

Table 2: Yield characteristics of alder in the test plots 5, 10 and 11 (Abbreviations: N = stand density, H_G = height of the median basal area tree, H_O = dominant height, D_G = diameter of the median basal area tree, D_O = diameter of the dominant height tree, G = basal area, VD = compact wood volume)

TG	BA	Parzelle	Alter	Größe [ha]	N [Bäume/ha]	H_G [m]	H_O [m]	D_G [cm]	D_O [cm]	G [m²/ha]	VD [m³/ha]
5	Erle	I	44	0,0411	973	19,7	22,8	21,7	32,0	35,9	330
5	Erle	II	44	0,0395	1089	19,6	23,4	20,3	30,1	35,4	319
10	Erle	I	55	0,0513	721	24,0	25,7	21,9	30,4	33,2	371
10	Erle	II	55	0,0550	709	21,5	24,2	23,0	28,6	29,4	287
11	Erle	I	68	0,0601	707	28,5	33,0	32,0	45,0	56,8	851
11	Erle	II	68	0,0627	702	28,0	33,7	31,8	46,4	55,7	817

Tab. 3: Ertragskenndaten von Fichte und Kiefer im Testgebiet 6 (Abkürzungen: VS = Schaftholzvolumen)

Table 3: Yield characteristics from spruce and pine in the test plot 6 (Abbreviation: VS = stem wood volume)

TG	BA	Parzelle	Alter	Größe [ha]	N [Bäume/ha]	H_G [m]	H_O [m]	D_G [cm]	D_O [cm]	G [m²/ha]	VS [m³/ha]
5	Fichte	I	44	0,0806	608	20,3	22,0	25,4	33,5	30,8	305
5	Fichte	II	44	0,0820	512	19,9	21,5	26,1	32,6	27,5	267
5	Kiefer	I	44	0,1543	279	15,6	16,3	20,4	23,9	9,15	66
5	Kiefer	II	44	0,1633	322	14,7	16,5	21,3	25,4	11,52	80

2.3 Auswerteverfahren

Nachdem aus den Radialzuwachswerten jedes Einzelbaumes die Durchmesser *D* für den Untersuchungszeitraum von 1990 bis 2008 rekonstruiert worden sind, konnte aus diesen

Werten die Stammbiomasse jedes Baumes abgeschätzt werden. Die Stammbiomasse *B* wurde nach ZIANIS et al. (2005) aus der allometrischen Biomassegleichung $B = a*D^b$ berechnet, wobei a und b baumartenspezifische Faktoren sind. Der jährliche Stammbiomassezuwachs eines Baumes ergibt sich aus der Differenz der Biomassen zweier aufeinander folgender Jahre. Für die Umrechnung der Trockenmasse in Kohlenstoffgehalte wurde ein Wert von 0,5 angenommen.
Für vergleichende Analysen zum Einfluss von Temperatur und Niederschlag auf das Zuwachsverhalten der Moorwaldbestände in den Testgebieten wurden Daten des Deutschen Wetterdienstes verwendet. Die Klimareihen von mehreren umliegenden Klima- und Niederschlagstationen wurden dabei abstands- und höhengewichtet für das jeweilige Testgebiet umgerechnet, so dass für jedes Testgebiet plausible Tageswerte der Temperatur und des Niederschlags zur Verfügung standen.

3. Ergebnisse

Abbildung 2 zeigt den jährlichen oberirdischen Kohlenstoffzuwachs im Vergleich zu Temperatur und Niederschlag in der Vegetationszeit im Untersuchungszeitraum von 1990 bis 2008 am Beispiel der Baumart Erle im Testgebiet Freisinger Moos.

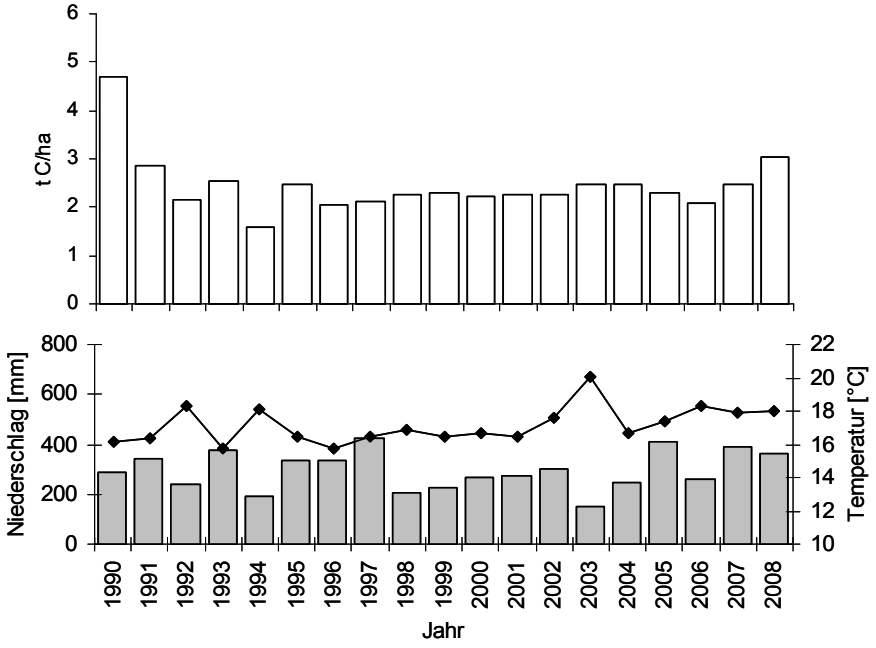

Abb. 2: Jährlicher Kohlenstoffzuwachs der Erle im Vergleich zu Temperatur und Niederschlag in der Vegetationszeit von 1990 bis 2008 im Testgebiet Freisinger Moos

Fig. 2: Annual carbon increment of alder compared to temperature and precipitation in the growing seasons from 1990 to 2008 in the test plot Freisinger Moos

Im Zeitraum von 1990 bis 2008 schwankten die jährlichen Kohlenstoffzuwächse zwischen 1,58 (1994) und 4,69 t C/ha (1990). Dem gegenüber liegen die Niederschlagsummen während der Vegetationsperioden von Mai bis September zwischen 274 (2003)

und 659 mm (2007), die Temperaturen zeigen Werte von 14,4 (1991) bis 17,6 °C (2003).
Die mittleren jährlichen Kohlenstoffzuwächse getrennt nach Baumarten und Testgebieten sind der Abbildung 3 zu entnehmen. Der stärkste Kohlenstoffzuwachs mit 3,35 t C/ha ist bei der Fichte in Mooseurach (TG 6) mit Niederschlägen von 652 mm und Temperaturen von 15,8 °C zu erkennen. Bei gleichen Witterungsbedingungen weist die Kiefer hingegen nur 0,75 t C/ha Zuwachs auf.
Mit Werten von 1,72 und 1,76 t C/ha zeigen die Erlen in den Testgebieten Spreewald (TG 10) und Graben-Neudorf (TG 11) bei Temperaturen von 16,8 bzw. 18,2 °C und Niederschlägen von 278 bzw. 323 mm in der Vegetationszeit ähnliche Zuwachsverhaltensweisen. Im Freisinger Moos (TG 5) hingegen liegt der mittlere Kohlenstoffzuwachs bei Temperaturen von 15,5 °C und Niederschlägen von 452 mm bei 2,45 t C/ha.

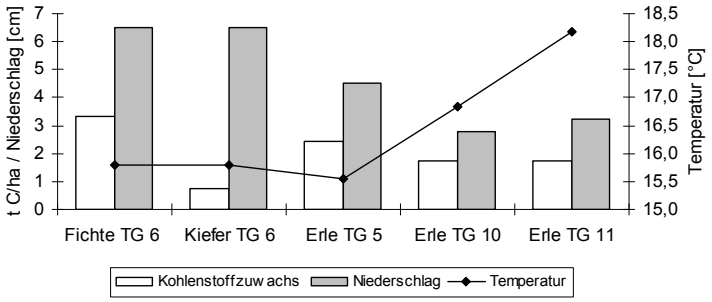

Abb. 3: Mittlerer jährlicher Kohlenstoffzuwachs, Temperatur und Niederschlag in der Vegetationszeit in den Testgebieten 5, 6, 10 und 11
Fig. 3: Mean annual carbon increment, temperature and precipitation in the growing season in the test plots 5, 6, 10 and 11

Die Auswirkungen des Trockenjahres 2003 auf den Kohlenstoffzuwachs von Moorwaldbeständen zeigt Abbildung 4.

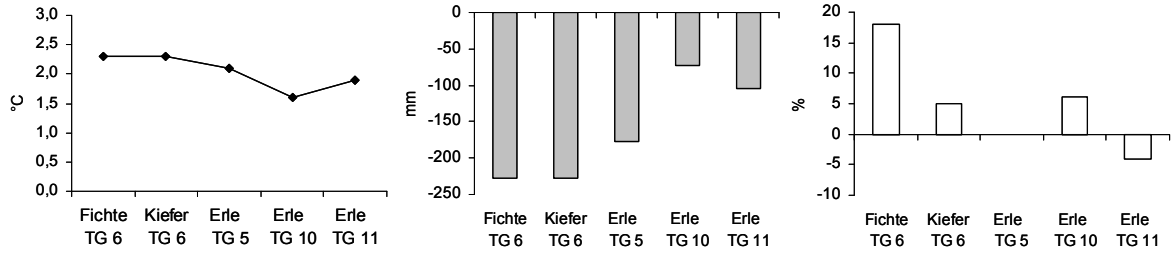

Abb. 4: Temperatur- und Niederschlagsänderung sowie relativer Kohlenstoffzuwachs 2003 gegenüber dem Untersuchungszeitraum 1990 - 2008
Fig. 4: Temperature and precipitation changes as well as relative carbon increment of 2003 compared to the period 1990 - 2008

Aus Abbildung 4 ist zu erkennen, dass Fichte in Mooseurach (TG 6) im Jahr 2003 gegenüber dem langjährigen Mittel bei um 2,3 °C höheren Temperaturen und um 228 mm geringeren Niederschlägen einen um 18 % höheren Kohlenstoffzuwachs zeigt, während die Zuwachs-steigerung der Kiefer unter gleichen klimatischen Bedingungen nur bei 5 % liegt.

Unterschiedliche Reaktionen im Zuwachsverhalten weisen die Erlen auf. Die stärkste Änderung des Kohlenstoffzuwachses mit + 6 % im Jahr 2003 gegenüber dem langjährigen Mittel zeigt sich im Spreewald (TG 10). Hier liegen im Jahr 2003 die Temperatur um 1,6 °C höher und der Niederschlag um 72 mm niedriger als im Mittel der Jahre 1990 - 2008. Im Testgebiet Graben-Neudorf (TG 11) weist die Erle einen Zuwachsrückgang von 4 % im Jahr 2003 auf. Hier beträgt die Temperatur- bzw. Niederschlagsänderung 2003 gegenüber dem langjährigen Mittel 1,9 °C bzw. - 105 mm. Keine Änderung des Zuwachses der Erle im Jahr 2003 ist im Freisinger Moos (TG 5) erkennbar. Dort zeigt die Temperatur einen Anstieg von 2,1 °C, der Niederschlag eine Abnahme von 178 mm im Vergleich des Trockenjahres 2003 mit dem langjährigen Mittel.

4. Schlussfolgerungen

Anhand der dargestellten Ergebnisse lässt sich erkennen, dass Temperatur und Niederschlag einen unterschiedlich starken Einfluss auf die Kohlenstoffbilanzen der einzelnen Baumarten in den Moorwaldbeständen haben. Das Trockenjahr 2003 erweist sich bei Fichten- und Kiefernbeständen auf Moorböden als Zuwachs steigernd (Abb. 4). Demgegenüber zeigen Fichten und Kiefern auf Mineralstandorten in Süddeutschland für das Jahr 2003 deutliche Zuwachseinbußen (z.B. KLEMMT et al. (2009)).

Erlen weisen auf Moorböden bei höheren Temperaturen geringere Kohlenstoffzuwächse auf. Sowohl bei einer Gegenüberstellung der Testgebiete (Abb. 3) als auch im Vergleich des Trockenjahres mit dem Mittel aller Jahre (Abb. 4) ist dieser Trend zu erkennen.

In den nächsten Schritten muss untersucht werden, in wie weit die jährlichen Klimadaten, die Bestandesstruktur und weitere Standortverhältnisse diese Ergebnisse widerspiegeln.

Danksagung

Das dargelegte Projekt wird im Rahmen des Verbundvorhabens „Organische Böden“ bearbeitet. Die Förderung erfolgt durch das Johann Heinrich von Thünen-Institut.

Literaturverzeichnis

Johann Heinrich von Thünen-Institut (2009): Forschungs- und Entwicklungsvertrag zum Verbundvorhaben „Organische Böden“. 52 S.

Muukkonen, P., Mäkipää, R. (2006): Biomass Equations for European Trees: Addendum. Silva Fennica 40 (4), S. 763-773

Klemmt, H.-J., Heindl, M., Werner, R., Hussendörfer, E., Pretzsch, H. (2009): Auswirkungen von Trockenjahren auf das Wachstum von Mischwaldbeständen. AFZ – Der Wald 23, S. 1247 – 1249

Röhling, S., Rötzer, T., Pretzsch, H. (2010): Verbundvorhaben: Klimaberichterstattung „organische Böden“ – Ermittlung und Bereitstellung von Methoden, Aktivitätsdaten und Emissionsfaktoren für die Klimaberichterstattung LULUCF/AFOLU. Jahresbericht 2009, 17 S.

Zianis, D., Muukkonen, P., Mäkipää, R., Mencuccini, M. (2005): Biomass and Stem Volume Equations for Tree Species in Europe. Silva Fennica 4: 63 S.

Anschrift der Autoren

Steffi Röhling (Steffi.Roehling@lrz.tu-muenchen.de)
Lehrstuhl für Waldwachstumskunde, Technische Universität München
Hans-Carl-von-Carlowitz-Platz 2, D-85354 Freising, Deutschland

Dr. Thomas Rötzer (Thomas.Roetzer@lrz.tu-muenchen.de)
Lehrstuhl für Waldwachstumskunde, Technische Universität München
Hans-Carl-von-Carlowitz-Platz 2, D-85354 Freising, Deutschland

Prof. Dr. Dr. Hans Pretzsch (Hans.Pretzsch@lrz.tum.de)
Lehrstuhl für Waldwachstumskunde, Technische Universität München
Hans-Carl-von-Carlowitz-Platz 2, D-85354 Freising, Deutschland

Klimatische Anbaueignung von Sorghumhirsen in Deutschland unter gegebenen und veränderten Klimabedingungen

Maendy Fritz[1], Uwe Hera[2], Thomas Rötzer[3]

[1] Technologie- und Förderzentrum, Straubing, Germany
[2]geoKLIM consulting, Karlsfeld, Germany
[3] TU München, Lehrstuhl für Waldwachstumskunde, Freising, Germany

Abstract

Für den Anbau landwirtschaftlicher Kulturen spielen neben den Bodenbedingungen die klimatischen Verhältnisse eines Standortes eine zentrale Rolle. Dies ist besonders für den Anbau von Pflanzen mit hohen klimatischen Ansprüchen wie den stark wärmebedürftigen Sorghumhirsen von Bedeutung. Um Landwirten in Deutschland die Möglichkeit zu geben, sich frühzeitig auf die zu erwartende Klimaänderung einzustellen, und die Anbaueignung von Hirse für die jetzige und zukünftige Situation in ihrer Region zu beurteilen, wurden Anbaueignungskarten für Sorghumhirsen erstellt. Als Daten standen Klimadaten des Deutschen Wetterdienstes für den Zeitraum 1961 bis 1990 sowie Klimaprojektionen (WETTREG-Simulationen, SRES-Szenarien A1B und B1) für den Zielzeitraum 2011 bis 2040 zur Verfügung. In einem ersten Schritt wurden die klimatischen Ansprüche für jeden Entwicklungsabschnitt der Sorghumhirse definiert. Im Anschluss daran konnten über multiple Regressionsanalysen Regionalisierungen der Anbaueignung durchgeführt werden. Die daraus entstandenen Karten bilden mit dem Referenzzeitraum 1961 bis 1990 die Gegenwart ab, die zwei Standardszenarien A1B und B1 des Zeitraums 2011 bis 2040 zeigen die Verhältnisse unter veränderten Klimabedingungen. Es zeigt sich, dass sich die Klimabedingungen für den Anbau der wärmeliebenden Kultur Sorghumhirse in vielen Regionen Deutschlands verbessern werden. Gleichzeitig verändern bzw. verschlechtern sich ggf. die Bedingungen für heimische Kulturen, so dass die Bedeutung des Sorghumhirseanbaus zunehmen könnte.

1. Einführung

Wachstum und Ertrag von Kulturpflanzen hängen neben den Parametern Bodenart, Düngung, Krankheitsbefall und Kulturmaßnahmen im Wesentlichen von den klimatischen Verhältnissen der Anbauregion ab. Das Klima ist jedoch im Wandel begriffen, wobei die Veränderungen einzelner Klimaelemente regional sehr unterschiedlich ausfallen werden (IPCC 2007). Wie sich diese Änderungen auf das Pflanzenwachstum auswirken werden, ist bislang noch weitest gehend ungeklärt (Jacob et al. 2006). Die in Deutschland noch recht neue Kultur Sorghumhirse erscheint aufgrund ihrer Trockenheitstoleranz und ihrer hohen Wassernutzungseffizienz als vielversprechender Nachwachsender Rohstoff, dessen Bedeutung besonders im Hinblick auf die Klimaänderung weiter zunehmen könnte.

Ziel der vom Bayerischen Staatsministerium für Ernährung, Landwirtschaft und Forsten geförderten pflanzenbaulichen Forschung und Beratung bezüglich Sorghumhirsen ist auch die Klärung der Fragestellung, ob die klimatischen Gegebenheiten Deutschlands einen Anbau in flächenmäßig bedeutendem Umfang mit potenziell ausreichenden Erträgen und Qualitäten zulassen.

2. Methodik

In einem ersten Projektabschnitt wurde zunächst eine klimatische Anbaueignungskarte für Sorghumhirse unter gegebenen klimatischen Bedingungen (1961 – 1990) erstellt. Zur Verfügung standen Klimadaten von 407 Stationen des Deutschen Wetterdienstes für Temperatur (Mittelwert, Minimum, Maximum), Sonnenscheindauer, relative Feuchte, Windgeschwindigkeit und Niederschlag, zudem das Digitale Geländemodell DGM1000 des Bundesamtes für Kartographie und Geodäsie, die Bodenübersichtskarte BÜK500 sowie die Daten des CorineLandCover-Projekts (CLC1990). Auf Grundlage dieser Daten sowie weiterer daraus abgeleiteter Geoparameter wie Höhe über NN, geographische Länge und Breite, Landnutzungs- und Bebauungsindizes, Luv-/Lee-Effekte oder Kaltlufteinzugsgebiete (Rötzer und Würländer 1994, Dirscherl 1995, Mues 2000), konnten durch multiple Regressionsanalysen sämtliche klimatisch relevanten Parameter für den Hirseanbau (Auflaufen, Spätfrostgefährdung etc., vgl. Tabelle 1) an allen Klimastation berechnet werden.

Tabelle 1: Parameterliste für die Anbaueignung der Sorghumhirse in Deutschland

Parameter	Einheit	Beschreibung
Auflaufen	d	5 Tage hintereinander T > 12° C, danach kein wesentliches Absinken mehr
Spätfrostgefährdung	%	Häufigkeit von Frösten ab 1. Mai (Tmin < 0°C)
Temperatursumme Vegetationsperiode	%	Summe der Temperaturen > 8°C von Mai bis September
Temperatursumme Hauptwachstumszeit	°C*d	Summe der Temperaturen > 16°C von Juli bis September
Niederschlag Vegetationszeit	mm	Niederschlagssumme von Mai bis September
Trockenheitsindex	-	Verhältnis tatsächliche zu potentieller Verdunstung für 4 Bodenarten (Wasserhaushaltsmodell HYMO), Mittel Juli bis September
Tatsächliche Verdunstung	mm	tatsächliche Verdunstungssumme für 4 Bodenarten (Wasserhaushaltsmodell HYMO), Mai bis September
Frühfrostgefährdung	%	Häufigkeit von Frösten vor 15. Oktober (Tmin < 0°C)
Sonnenscheindauer Hauptwachstumszeit	h	Summe der Sonnenscheinstunden von Juli-September
Sonnenscheindauer Vegetationsperiode	h	Summe der Sonnenscheinstunden von Mai - September
Dauer der Vegetationsperiode	d	Beginn: siehe Auflaufen, Ende : 5 Tage hintereinander < 8°C

Auf Basis der ermittelten Regressionsgleichungen und einer Interpolation der Residuen wurde eine Regionalisierung der klimatisch relevanten Parameter durchgeführt (siehe dazu Rötzer et al. 1997), die sich daraus ergebenden 11 Karten der einzelnen Parameter wurden anschließend standardisiert. Grundlagen der klimatisch relevanten Paarmeter und Schwellenwerte waren unter anderem Parzellenversuche an bis zu zehn Standorten in Bayern, an denen auch klimatische und agronomische Schwellenwerte für den Sorghumhirseanbau ermittelt wurden. Durch eine Addition der standardisierten Werte aller klimatisch relevanten Parameter an jedem Rasterpunkt des Untersuchungsgebietes ergab sich abschließend eine Karte der Anbaueignung von Sorghumhirsen unter gegenwärtigen Klimabedingungen.

In einem zweiten Projektabschnitt wurden die Daten der Klimastationen des DWD durch die entsprechenden Projektionsdaten der WETTREG-Simulationen (Enke et al. 2006) ersetzt. Unter Verwendung der zuvor beschriebenen Methodik wurden für jede Klimastation alle klimatischen Parameter (Auflaufen, Spätfrost etc.) für die SRES-Szenarien A1B und B1 sowie für den Kontrolllauf C20 über den Zeitraum 2011 – 2040 neu berechnet. Die Regionalisierung erfolgte in gleicher Weise wie bei den Karten unter gegebenen Klimabedingungen. Anschließend wurde die Differenz (= Änderung) zwischen den Karten des Kontrolllaufes und den Karten der SRES-Szenarien ermittelt. Diese Differenzkarten der einzelnen für Sorghumhirsen klimatisch relevante Parameter wurden dann zu den jeweiligen Karten der Klimazeitreihe 1961 -1990 addiert und bildeten, nach Szenarien getrennt, wiederum die Grundlage für eine Standardisierung, aus der – wie im ersten Projektabschnitt – letztlich die Anbaueignungskarten für die beiden SRES-Szenarien A1B und B1 errechnet wurden.

3. Anbaueignung unter gegebenen Klimabedingungen

Abbildung 1 zeigt die klimatische Anbaueignungskarte für Sorghumhirsen in Deutschland unter gegebenen Klimabedingungen (1961 – 1990).

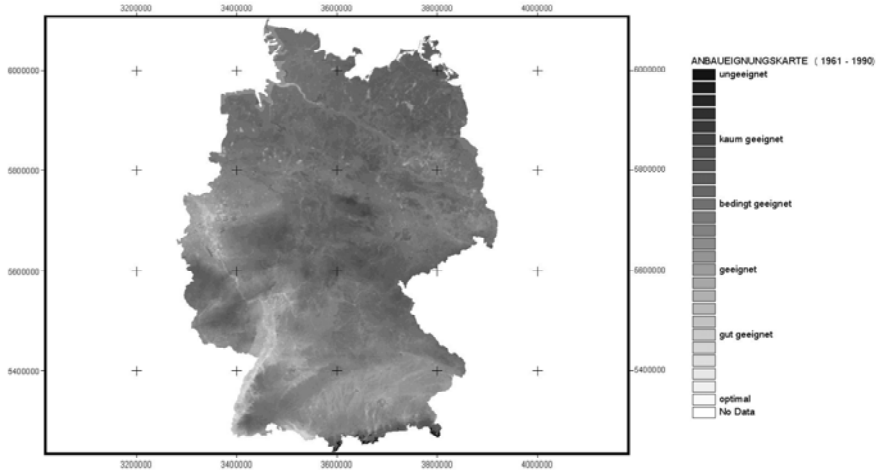

Abb. 1: Klimatische Anbaueignungskarte für Sorghumhirse in Deutschland (1961 – 1990)

Aus ihr wird ersichtlich, dass nur ein sehr geringer Teil (ca. 1,5 %, entsprechend 5.264 km²) gar nicht oder kaum für den Anbau von Hirse geeignet ist. Diese Flächen finden sich ausschließlich in den Hochlagen des deutschen Alpenanteils sowie im Bereich der

deutschen Mittelgebirgsschwelle im Harz und vereinzelt im Thüringer Wald. Ursächlich hierfür sind vor allem ein spätes Auflaufen, eine hohe Spätfrostgefährdung, geringe Temperatursummen während der Vegetations- bzw. Hauptwachstumszeit, eine hohe Frühfrostgefährdung sowie eine daraus resultierende kurze Vegetationszeit.

Als „bedingt geeignet“ für den Anbau von Hirse erweist sich der weitaus größte Teil Deutschlands (ca. 75,2 %, entsprechend 271.568 km²). In dieser Klasse unterscheiden sich Regionen mit geringeren Indexwerten (wie etwa die tieferen Lagen der Alpen bzw. der Mittelgebirge sowie ein großer Teil Mecklenburg-Vorpommerns und Niedersachsens) von jenen, die etwas günstigere Anbaubedingungen bieten (etwa Schleswig-Holstein, Teile von Nordrhein-Westfalen, Brandenburg, Sachsen und Sachsen-Anhalt, das westliche Niedersachsen und Nordbayern).

Etwa 23,4 % der Landesfläche Deutschlands weisen geeignete oder gut geeignete Bedingungen für den Hirseanbau auf. Es sind dies vor allem die Regionen südlich der Donau von der Schwäbischen Alb bis hin zum Bayerischen Wald einschließlich der Gegend um den Bodensee, die von relativ hohen Temperatursummen während der Hauptwachstumszeit, von hohen Niederschlägen und von hohen Werten der Sonnenscheindauer während der Vegetations- und Hauptwachstumszeit profitieren, des weiteren das Oberrheintal sowie die Gegend um den Niederrhein, die durch einem frühen Aufgang, eine geringe Spätfrostgefahr, hohe Temperatursummen während der Vegetations- und Hauptwachstumszeit, ausreichenden Niederschlägen und einer geringen Frühfrostgefährdung gekennzeichnet sind.

Die optimal geeigneten Gebiete für den Hirseanbau in Deutschland finden sich in Sonderlagen im Oberrheintal sowie am Nordrand des Bodensees mit Indexwerten bis zu 9,0. Diese Flächen fallen aber mit einem Gesamtanteil von nur 0,02 % der Gesamtfläche Deutschlands (entsprechend etwa 61 km²) kaum ins Gewicht.

4. Anbau unter möglichen künftigen Klimaverhältnissen

Vor allem die Gebiete südlich der Donau, im Südwesten und Westen Deutschlands zeigen positive Veränderungen der Anbaueignung (Abbildung 2).

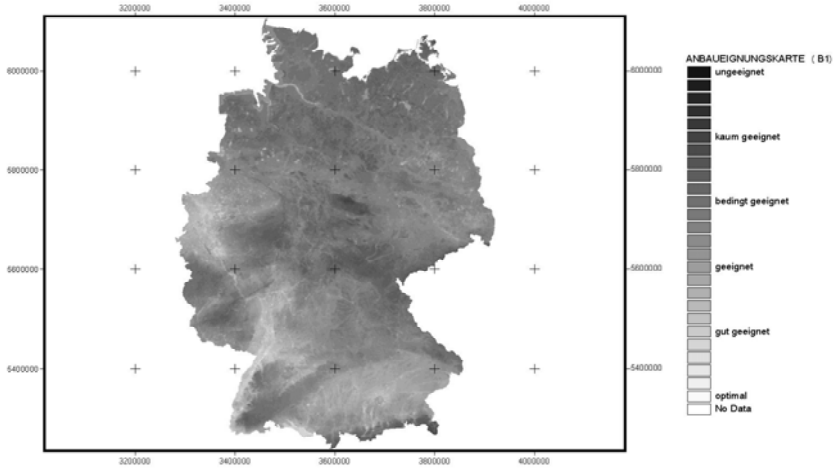

Abb. 2: Klimatische Anbaueignungskarte für Sorghumhirse in Deutschland (Szenario B1 2011 – 2040)

Die Änderung der Flächenausdehnung geeigneter, gut geeigneter und optimaler Anbaugebiete ist in Tabelle 2 dargestellt. Im Vergleich zur Anbaueignungskarte unter gegebenen Klimabedingungen mit 8,4 Mio. Hektar werden für den Zeitraum 2011 bis 2040 unter den klimatischen Bedingungen des Szenarios A1B circa 11,0 Mio. Hektar und unter den Bedingungen des Szenario B1 nahezu 14,5 Mio. Hektar als geeignete bzw. bessere Anbauflächen ausgewiesen. Vor allem die als geeignet und gut geeignete kategorisierten Flächen nehmen deutlich zu.

Tabelle 2: Flächen der klimatischen Anbaueignung für Sorghumhirse für die jetzigen (1961 bis 1990) und zukünftigen (2011 bis 2040) Klimabedingungen (Szenarien A1B und B1)

Flächenkategorie	Fläche [ha]		
	Gegenwart (1961 – 1990)	Szenario A1B (2011 – 2040)	Szenario B1 (2011 – 2040)
ungeeignet	44.600	0	0
kaum geeignet	481.835	306.736	145.619
bedingt geeignet	27.156.837	24.776.859	21.494.541
geeignet	7.749.811	10.094.601	12.961.804
gut geeignet	682.310	933.948	1.512.236
optimal	6.101	8.993	6.937
Σ geeignet, gut geeignet und optimal	8.438.222	11.037.542	14.480.977

5. Bewertung

Auf der Grundlage der klimatischen und agronomischen Schwellenwerte von Sorghumhirse sowie unter Berücksichtigung der klimatischen Gegebenheiten Deutschlands von 1961 bis 1990, konnten für die Gegenwart große Bereiche Deutschlands identifiziert werden, die für den Anbau von Sorghumhirse potenziell geeignet bis gut geeignet sind. Bei einer Gegenüberstellung dieser Karte mit den beiden Anbaueignungskarten der IPCC-Standardszenarios A1B und B1 für den Zeitraum 2011 bis 2040 zeigt sich eine deutliche Verbesserungen in den Anbaubedingungen, d.h. vor allem eine Ausweitung der geeigneten und gut geeigneten Regionen.

Im gleichen Maße, wie sich die Klimabedingungen für den Anbau der wärmeliebenden und trockenheitstoleranten Kultur Sorghumhirse verbessern, verändern und ggf. verschlechtern sich die Bedingungen für heimische Kulturen, sofern sie nicht mit züchterischen Methoden an die Klimaänderung angepasst werden können. Es ist davon auszugehen, dass unter den sich ändernden Klimabedingungen relativ kurzfristig die Attraktivität der Hirsen als Alternativ- und Ergänzungskultur, vor allem im Bereich der Nachwachsenden Rohstoffe, steigen wird.

Für die Beratung der landwirtschaftlichen Praxis ermöglicht das Aufzeigen kartographisch dargestellter Gunst- und Ungunstgebiete für den Hirseanbau eine einfache Erkenntnisvermittlung und längerfristige Betriebsplanungen.

Literatur

Dirscherl, A., 1995: Untersuchungen zur Parametrisierung des Topographieeinflusses das Klimaelement Frost. Unveröffentlichte Diplomarbeit, vorgelegt am Lehrstuhl für Photogrammetrie und Fernerkundung der Technischen Universität München, 55 Seiten.

Enke, W., Spekat, A., Kreienkamp, F., 2007: Neuentwicklung von regional hoch aufgelösten Wetterlagen für Deutschland und Bereitstellung regionaler Klimaszenarien mit dem Regionalisierungsmodell WETTREG 2005 auf der Basis von globalen Klimasimulationen mit ECHAM5/MPI – OM T63L31 2010 bis 2100 für die SRES – Szenarien B1, A1B und A2. Projektbericht im Rahmen des F + E-Vorhabens 204 41 138 "Klimaauswirkungen und Anpassung in Deutschland – Phase 1: Erstellung regionaler Klimaszenarien für Deutschland", 94 S.

Intergovernmental Panel on Climate Change (IPCC) 2007: Climate Change 2007 - The Physical Science Basis. Contribution of Working Group I to the Fourth Assessment Report of the IPCC. URL http://ipcc-wg1.ucar.edu/wg1.

Jacob, D., Lorenz, P., Göttel, H., Möller, M., Kotlarski, S., 2006: Klimaänderungen in Deutschland, Österreich und der Schweiz bis 2100: erste Analysen des regionalen Klimamodells REMO - Mittelwerte und Extrema. http:/www.umweltbundesamt.de/klimaschutz/veranstaltungen/04jacob2.pdf.

Mues, V., 2000: GIS-gestützte Regionalisierung von Klima- und Depositionsdaten in Niedersachsen. Diss. Uni Göttingen 223 S.

Rötzer, T., Häckel, H., Würländer, R., 1997: Der Agrar- und Umweltklimatologische Atlas von Bayern. Selbstverlag Deutscher Wetterdienst Weihenstephan.

Rötzer, T., Würländer, R., 1994: Neuartige phänologische Karten von Bayern und deren Anwendungsmöglichkeiten in der Landschaftsökologie und Landschaftsplanung. Berichte der Bayer. Akademie für Naturschutz und Landespflege, Kirchzarten 18: 131-145.

Authors' addresses:

Dr. Maendy Fritz (maendy.fritz@tfz.bayern.de)
Technologie- und Förderzentrum im Kompetenzzentrum für Nachwachsende Rohstoffe
Schulgasse 18, D-94315 Straubing, Germany

Dr. Thomas Rötzer (thomas.roetzer@lrz.tu-muenchen.de)
TU München
Lehrstuhl für Waldwachstumskunde
Am Hochanger 13, 85354 Freising

Dr. Uwe Hera (hera@geoklim.com)
geoKLIM consulting
Birkenstraße 33a, 85757 Karlsfeld, Germany

Comparison of Methods for Heat Determination

Katharina Gabriel[1,2]

[1]Leibniz-Institute of Freshwater Ecology and Inland Fisheries, Berlin, Germany
[2]Department of Geography, Humboldt-University of Berlin, Germany

Abstract
When analyzing meteorological data concerning heat, a limiting value has to be defined at first. Its exceedance is described as thermal stress. To determine this threshold, in the expert literature different methods are applied as, for example, fixed values, percentile values or values determined by the regression of temperature and mortality, the so called Hockey-Stick-Method; next to the parameter of 'air temperature' indices like 'Humidex' are also taken as a basis.
In the presented research these different methods were applied to data from stations in the Berlin-Brandenburg area. The 'air temperature' as well as the 'perceived temperature' was available for this research. Over a period of 17 years (1990-2006) the respective thresholds as well as the amount of days exceeding this value were determined. This survey offers an attempt to comparatively classify the results of studies using different methods.

1. Introduction

When analyzing meteorological data concerning heat, first a limiting value has to be defined that is specific to the study area. Its exceedance describes thermal stress. Up to now, there is no generally accepted definition or an internationally consented mathematical formula. In fact, different methods are applied in the expert literature to determine the threshold of heat stress.
The most simple approach uses a fixed but more or less randomly chosen value of air temperature and can be applied to either the daily average (T_{av}) or the daily maximum (T_{max}). For France the limiting value of 27°C is used for T_{max} [Fouillet et al. 2008], while a threshold of 35°C is applied on daily maximum temperature in Adelaide and Shanghai [Nitschke et al. 2007; Tan et al. 2007]. In Germany, days with maximum temperature exceeding 25°C or even 30°C are characterized as a 'summer day' or a 'heat day', respectively. Nights with a minimum temperature above 20°C are called 'tropical nights'.
Assuming that ‚heat' is a rare phenomenon, the limiting value of a city or region often is identified by determining a percentile of the observed temperatures. A value often used is the 95th percentile (P95) [e.g. Gosling et al. 2007; Ishigami et al. 2008], especially if data of the whole year form the basis of analysis. Using only the data from April to September, Saez et al. [1995] applied the 85th percentile. This means that the top 5 % (resp. 15 %) of the observed temperatures are regarded as ‚heat'. The method is implemented on the daily average [Ishigami et al. 2008], the daily maximum [Gosling et al. 2007] as well as on the combination of daily maximum and minimum temperature [Rey et al. 2007]. Medina-Ramón et al. [2006] state 'heat' on those days, on which nighttime temperature does not fall below the 99th percentile (P99).
The correlation of thermal stress and human well-being can be illustrated by opposing temperature and health-data – i.e. mortality data – graphically. Starting 1976 [Rogot & Padget 1976] studies have shown a U-, V- or J-shaped connection between the two variables. [e.g. Curriero et al. 2002 for North America, Garssen et al. 2005 or Kunst et al. 1993 for Europe]. Because of the resulting shape the method is called hockey-stick-

method: the long descending line reflects the annual development of mortality, which is highest during winter and decreases with rising temperatures towards summer; the short(er) ascending line reflects sensitivity of the population regarding further rising temperatures. Thus, the lowest point of the regression line can be seen as the thermal optimum and is taken as the threshold. In the scientific literature it is specified as a single value [e.g. Curriero et al. 2002; Díaz et al. 2002; Garssen et al. 2005; Gosling et al. 2007; Kunst et al. 1993] as well as a range of 3 K [Keatinge et al. 2000]. The method is implemented on daily maximum temperature [e.g. Díaz et al. 2002] but more often on the daily average value [e.g. Curriero et al. 2002; Garssen et al. 2005; Kunst et al. 1993]. Only sporadic it is implemented on thermal indices as the 'apparent temperature' (AT) [Davis et al. 2003].
Thermal Indices offer a more complex approach for determining a limiting value than the previous mentioned methods. In addition to air temperature further meteorological parameters like humidity or wind speed are considered. Some indices also take into account human characteristics: next to age and sex the way of clothing and the amount of exercise influence the individual sensitivity to thermal strain. In the scientific literature (available to the author) only the use of 'apparent temperature' [Davis et al. 2003], 'humidex' [Mastrangelo et al. 2007], and 'perceived temperature' [Laschewski & Jendritzky 2002] was found in connection with the determination of heat occurrence.
For thermal indices classes of strain are determined. Their limiting values are used as fixed thresholds. Applying HeRATE [Koppe 2005], at least for the 'perceived temperature' short-term acclimatization can be considered.
The aim of this study is to point out the differences between three of the methods mentioned in the expert literature by applying them to one single station and area.

2. Data and Methods

Data of the meteorological station of Berlin-Dahlem form the basis of the present study. For a period of 27 years (1980 – 2006) daily values of air temperature (max, min) are on hand. For 17 years (1990 – 2006) the perceived temperature was provided by the German Meteorological Service (DWD) in 3-hourly steps. To implement the hockey-stick-method daily mortality data (1990 – 2006) of the city of Berlin were obtained from the State Statistical Institute Berlin-Brandenburg.
To detect 'heat', first the 95^{th} percentile was defined for the daily maximum and minimum of the air temperature. To consider a possible trend in the data a limiting value was determined for each year individually by taking the ten precedent years as the basis. Days and nights with air temperature reaching or exceeding these values were considered to be heat stressed.
Second, the regression of temperature and mortality was performed, each for minimum and maximum temperature. The regression line was determined as well as the air temperature value of its lowest point. Days and nights with measurements exceeding these values inclusively were considered to be heat stressed.
As a third method the limiting values of the perceived temperature were applied on the data. To be able to compare the results within the study, a singular day-time- as well as a singular night-time-value was determined before. Averaging the data of 09:00, 12:00 and 15:00 the daily maximum was derived; the same was done with the data of 00:00 and 03:00 for daily minimum.
Limiting values were chosen according to the classes of strain after VDI [1998] and in analogy to the standard of the German heat watch/warning system [Becker 2005]. Days

and nights with values exceeding these limits inclusively were considered to be heat stressed.

3. Results

The thresholds determined by the 95th percentile vary within the investigated 17 years. Its values range from 27,0°C in 1990 to 28,7°C in 2004. Days and nights with temperatures reaching or exceeding these values occurred from April to October, with the main focus on the months of meteorological summer (see fig. 1). While in spring especially the daily maxima are affected, in the end of summer the nights hold thermal stress more enduring than the days. The inter-annual comparison shows that some years were more affected by heat stress than others: during the summers of 1994, 2006, and 2003 long lasting periods of heat occurred while in 1993 the limiting value was violated only scarcely.

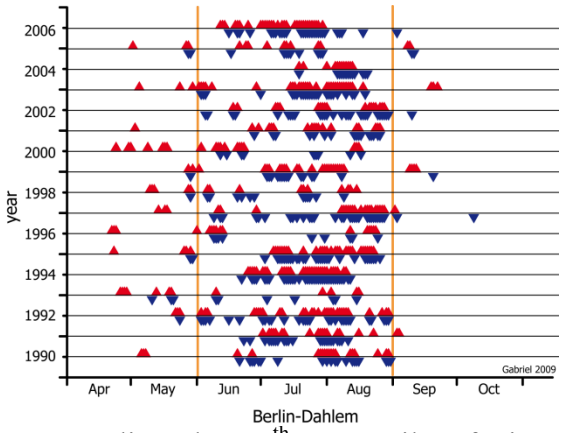

Fig. 1: Days per year exceeding the 95th percentile of air temperature at Berlin-Dahlem (max: ▲, min: ▼) [Gabriel 2009]

The thresholds determined by the regression of air temperature at Berlin-Dahlem and mortality data of Berlin are 23,0°C for maximum and 12,3°C for minimum temperatures. During the 17 years of investigation temperatures exceeding these values occurred from April to the end of October (see fig. 2). Periods of continuous thermal stress are much longer and more coherent than those defined with 95th percentile. Because of the high amount of days and nights exceeding the limits, a differentiation between years with more and years with less thermal stress is not that obvious.

Using an index like 'perceived temperature' to investigate thermal stress, it often brings along the application of predetermined classes of strain. Here, the upper limit was set with the thermal perception of the atmosphere being 'hot' at 32°C PT; the lower limit was set at 20°C PT, above which the thermal perception is no longer comfortable but slightly warm. As the 'perceived temperature' includes other meteorological parameters than just air temperature, the limits themselves cannot be compared directly with the aforementioned ones. However, by adjusting the number of days and nights exceeding these thresholds this method can be put into relation to the other techniques.

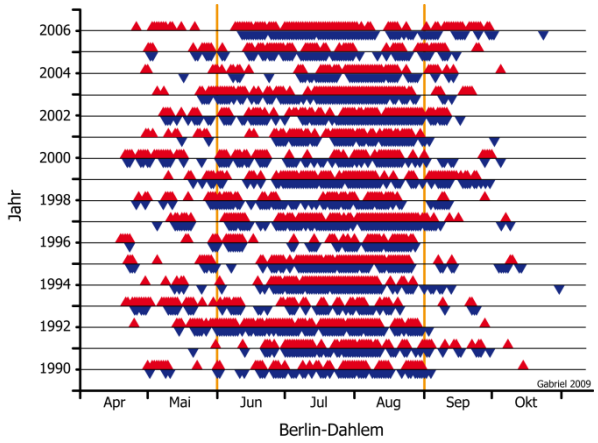

Fig. 2: Days per year exceeding the threshold gained by the regression of air temperature at Berlin-Dahlem and mortality data of Berlin (max: ▲, min: ▼) [Gabriel 2009]

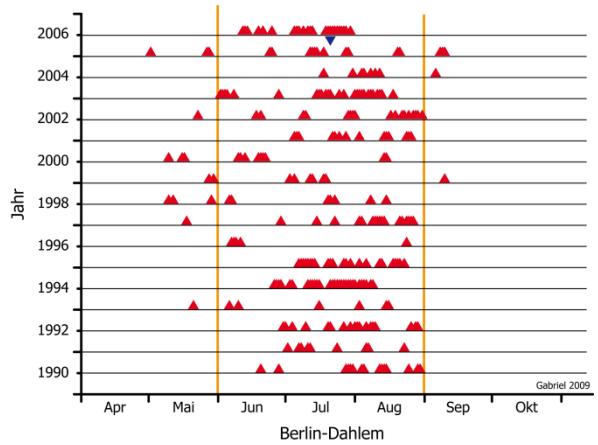

Fig. 3: Days per year exceeding the limiting value of 'perceived temperature' at Berlin-Dahlem (max: ▲, min: ▼) [Gabriel 2009]

For the data of 1990 to 2006, an exceedance of the limiting values can only be determined for five months from May to September. In addition, the violation is predominantly observed during daytime; just one single night in 2006 exceeded 20°C PT and thus fulfilled the requirements for thermal stress after this definition. Again, the interannual comparison clearly shows differences concerning the amount of heat stress in the individual years.

4. Conclusions

Regarding the classification of thermal stress the three methods show a varying sensitivity (see Tab. 1). The limiting values determined by regression of air temperature and mortality show the lowest magnitude. Roughly 18 % of all days and nights during the observed 17 years exceed these limits.

The thresholds defined by the 95th percentile are about 5 K higher than those of the regression method. This span conforms to findings of other European cities, like London and Lisbon [Gosling et al. 2007]. Accordingly, only 6 % of the days and nights are regarded as heat stressed.

Tab. 1: Limiting values at the meteorological station Berlin-Dahlem determined by percentile, regression and the index 'perceived temperature'

		regression	**percentile**	**index**
limiting values	day	23,0°C	27,0°C-28,7°C	32,0°C PT
	night	12,3°C	15,1°C-16,0°C	20,0°C PT
percentage of events exceeding the limit	day	~ 18 %	~ 6 %	~ 4 %
	night	~ 18 %	~ 6 %	< 1 %

Though the limits of the perceived temperature are not directly comparable with the previous mentioned methods they can be seen as the tightest thresholds: only 4 % of the days are declared as heat stressed, while during nights the limiting value is exceeded even more scarcely (0,02 %).
By applying the different methods mentioned in the expert literature to one single station and area differences in sensitivity can be observed. So, this survey offers an attempt to comparatively classify the results of other studies using these methods.

Acknowledgement

The author was funded by the Federal State of Berlin (NaFöG). Financial support from the German Research Foundation (DFG) enabled data acquisition.

References

Becker, P. 2005: Das Hitzewarnsystem des Deutschen Wetterdienstes. Notfallvorsorge 02/2005, 22-23.

Curriero, F. C., K.S. Heiner, J.M. Samet, S.L. Zeger, L. Strug, J.A. Patz, 2002: Temperature and Mortality in 11 Cities of the Eastern United States. Amer J Epidemiol 155, 80-87.

Davis, R.E., P.C. Knappenberger, W.M. Novicoff, P.J. Michaels, 2003: Decadal changes in summer mortality in U.S. cities. International Journal of Biometeorology 47, 166-175.

Díaz, J., A. Jordán, R. García, C. López, & J.C. Alberdi, E. Hernández, A. Otero, 2002: Heat waves in Madrid 1986 - 1997: effects on the health of the elderly. Int Arch Occup Environ Health 75, 163-170.

Fouillet, A., G. Rey, V. Wagner, K. Laaidi, P. Empereur-Bissonnet, A. Le Tertre, P. Frayssinet, P. Bessemoulin, F. Laurent, P. De Crouy-Chanel, E. Jougla, D. Hemon, 2008: Has the impact of heat waves on mortality changed in France since the European heat wave of summer 2003? A study of the 2006 heat wave. International Journal of Epidemiology 37, 309-317.

Gabriel, K., 2009: Gesundheitsrisiken durch Wärmebelastung in Ballungsräumen. Eine Analyse von Hitzewellen-Ereignissen hinsichtlich der Mortalität im Raum Berlin-Brandenburg. PhD-Thesis at Humboldt-University of Berlin, 149 p.

Garssen, J., C. Harmsen, J. de Beer, 2005: The effect of the summer 2003 heat wave on Mortality in the Netherlands. Eurosurveillance 10, 165-167.

Gosling, S.N., G.R. McGregor, A. Páldy, 2007: Climate change and heat-related mortality in six cities. Part 1: Model construction and validation. International Journal of Biometeorology 51, 525-540.

Keatinge, W.R., G.C. Donaldson, E. Cordioli, M. Martinelli, A. E. Kunst, & J.P. Mackenbach, S. Nayha, I. Vuori, 2000: Heat related mortality in warm and cold regions of Europe: obser-

vational study. British Medical Journal 321, 670-673.
Koppe, C., 2005: Gesundheitsrelevante Bewertung von thermischer Belastung unter Berücksichtigung der kurzfristigen Anpassung der Bevölkerung an die lokalen Witterungsverhältnisse. Fakultät für Forst- und Umweltwissenschaften (pp. 208), Freiburg i. Br.: Albert-Ludwigs-Universität.
Kunst, A. E., C.W.N. Looman, & J.P. Mackenbach, 1993: Outdoor Air Temperature and Mortality in the Netherlands: A Time-Series Analysis. Am. J. Epidemiol. 137, 331-341.
Laschewski, G., G. Jendritzky, 2002: Effects of the thermal environment on human health: an investigation of 30 years of daily mortality data from SW Germany. Climate Research 21, 91-103.
Mastrangelo, G., U. Fedeli, C. Visentin, G. Milan, E. Fadda, P. Spolaore, 2007: Pattern and determinants of hospitalization during heat waves: an ecological study. BMC Public Health 7, 8 p.
Medina-Ramón, M., A. Zanobetti, D.P. Cavanagh, J.Schwartz, 2006: Extreme Temperatures and Mortality: Assessing Effect Modification by Personal Characteristics and Specific Cause of Death in a Multi-City Case-Only Analysis. Environmental Health Perspectives 114, 1331-1336.
Nitschke, M., G.R. Tucker, P. Bi, 2007: Morbidity and mortality during heatwaves in metropolitain Adelaide. Medical Journal of Australia 187, 662-665.
Rey, G., E. Jougla, A. Fouillet, G. Pavillon, P. Bessemoulin, P. Frayssinet, J. Clavel, D. Hémon, 2007: The impact of major heat waves on all-cause and cause-specific mortality in France from 1971 to 2003. International Archives of Occupational and Environmental Health 80, 615-626.
Rogot, E., S.J. Padget, 1976: Associations of coronary and stroke mortality with temperature and snowfall in selected areas of the United States, 1962-1966. American Journal of Epidemiology 103, 565-575.
Saez, M., J. Sunyer, J. Castellsagué, C. Murillo, J.M. Antó, 1995: Relationship between Weather Temperature and Mortality: A Time Series Analysis Approach in Barcelona. Int. J. Epidemiol. 24, 576-582.
Tan, J. & Y. Zheng, G. Song, L.S. Kalkstein, A.J. Kalkstein, X. Tang, 2007: Heat wave impacts on mortality in Shanghai, 1998 and 2003. International Journal of Biometeorology 51, 193-200.
VDI (1998): Guideline VDI 3787, Part 2: Environmental Meteorology. Methods for the human biometeorological evaluation of climate and air quality for urban and regional planning at regional level. Part I: Climate. VDI-Handbuch Reinhaltung der Luft, Bd. 1b.

Author's address:

Katharina Gabriel (gabriel@igb-berlin.de)
Leibniz-Institute of Freshwater Ecology and Inland Fisheries
Müggelseedamm 310, D-12587 Berlin, Germany

The Universal Thermal Climate Index UTCI

Gerd Jendritzky[1], Peter Bröde[2], Dusan Fiala[3], George Havenith[4],
Philipp Weihs[5], Ekaterina Batchvarova[6], and Richard DeDear[7]

[1] Meteorological Institute, University of Freiburg, Germany
[2] Leibniz Research Centre of Working Environment and Human Factors (IfADo), Dortmund, Germany
[3] Institute of Building Technologies, IBBTE, University of Stuttgart, Germany
[4] Department of Ergonomics (Human Sciences), Loughborough University, U.K.
[5] University of Soil Culture, Vienna, Austria
[6] National Institute for Meteorology and Hydrology, Sofia, Bulgaria
[7]Faculty of Architecture, Design & Planning, The University of Sydney, Australia

Abstract

The existing assessment procedures of the thermal environment in the fields of public weather services, public health systems, urban planning, tourism & recreation and climate impact research show more or less significant shortcomings. Thus the idea came up to develop a Universal Thermal Climate Index UTCI based on the progress in science within the last 3 to 4 decades both in thermo-physiology and in heat exchange theory. Following extensive validation of accessible models of human thermoregulation, the advanced multi-node 'Fiala' model was adopted for this study. This model was coupled with a state-of-the-art clothing model considering the behavioural adaptation of clothing insulation by the general urban population to actual environmental temperature.
UTCI was developed conceptually as an Equivalent Temperature (ET). Thus, for any combination of air temperature, wind, radiation, and humidity, UTCI is defined as the air temperature in the reference condition which would elicit the same dynamic response of the physiological model. A 10 points stress assessment scale from "extreme heat stress" to "extreme cold stress" was defined. Polynomial regression equations facilitate fast predictions of ET values over relevant climate combinations. Comparisons to existing thermal stress/strain assessment procedures showed good conformity. However, in difference to these procedures, UTCI is based on contemporary science. The software of the operational UTCI procedure is available under www.utci.org.

1. Introduction

One of the fundamental issues in human biometeorology is the assessment and forecast of the thermal environment in a sound, effective and practical way. This is due to the need for human beings to adapt their heat budget to the thermal environment in order to optimise comfort, performance and health.
The heat exchange between the human body and its environment takes place by sensible and latent heat fluxes, radiation and (generally negligible) conduction. Consequently dealing with the thermo- physiologically significant assessment of the thermal environment requires the application of a complete heat budget model that takes all mechanisms of heat exchange into account (Buettner, 1938; Parsons, 2003). Input variables include air temperature, water vapour pressure, wind velocity, mean radiant temperature including the short- and long-wave radiation fluxes of the atmosphere, in addition to metabolic rate and clothing insulation. However, none of the more than 100 available

assessment procedures can be taken as sufficient considering thermo-physiology and heat exchange theory and the vast majority of them show unacceptable shortcomings.
A decade ago the International Society on Biometeorology ISB recognised this issue and –proposed by the former ISB president P. Höppe- established the Commission 6 ”On the development of a Universal Thermal Climate Index UTCI”(Working title) (Jendritzky et al., 2002). Since 2005 these efforts could be reinforced by the COST Action 730 (Cooperation in Science and Technical Development, supported by the EU RTD Framework Programme) that provided the basis that at least European scientists from 19 countries plus experts from Australia, Canada, Israel and New Zealand can join together on a regular basis in order to achieve significant progress in deriving such an index (www.utci.org). Aim was an international standard based on scientific progress in human response related thermo-physiological modelling of the last four decades including the acclimatisation issue. The term “universal” must be understood in terms of appropriate for all assessments of the outdoor thermal conditions in the major human biometeorological fields such as daily forecasts and warnings of extreme weather, to bioclimatic mapping, urban and regional planning, environmental epidemiology and climate impacts research. This covers the fields of public weather service, the public health system, precautionary planning, and climate impact research in the health sector.

The Universal Thermal Climate Index UTCI must meet the following requirements:

1) Thermo-physiological significance in the whole range of heat exchange conditions of existing thermal environments
2) Valid in all climates, seasons, and scales
3) Useful for key applications in human biometeorology.

2. Approach and result

As the assessment of thermal stress should be based on the physiological response of the human body (thermal strain) ISB Commission 6 decided already in the very beginning that this was to be simulated by one of the most advanced (multi-node) thermo-physiological models. After accessible models of human thermoregulation had been evaluated, the multi-node ‘Fiala’ thermoregulation model was selected (Fiala et al., 1999; 2001; 2003), extensively validated (Psikuta, 2009; Psikuta et al., 2007), and extended for purposes of the project (Fiala et al., 2007). In the next step a state-of-the-art adaptive clothing model was developed and integrated (Richards & Havenith, 2007). This model considers

1) the behavioural adaptation of clothing insulation observed for the general urban population in relation to the actual environmental temperature,
2) the distribution of the clothing over different body parts providing local insulation values for the different model segments, and
3) the reduction of thermal and evaporative clothing resistances caused by wind and the movement of the wearer, who was assumed walking 4 km/h on the level.

UTCI was then developed following the concept of an equivalent temperature. This involved the definition of a reference environment with 50% relative humidity (but vapour pressure not exceeding 20 hPa), with calm air and radiant temperature equalling air temperature, to which all other climatic conditions are compared. Equal physiological conditions are based on the equivalence of the dynamic physiological response predicted by the model for the actual and the reference en-

vironment. As this dynamic response is multidimensional (body core temperature, sweat rate, skin wettedness etc. at different exposure times), a strain index was calculated by principal component analysis as single dimensional representation of the model response (Bröde et al., 2009a; 2009b), cf. Figure 1. The UTCI equivalent temperature for a given combination of wind, radiation, humidity and air temperature is then defined as the air temperature of the reference environment, which produces the same strain index value.

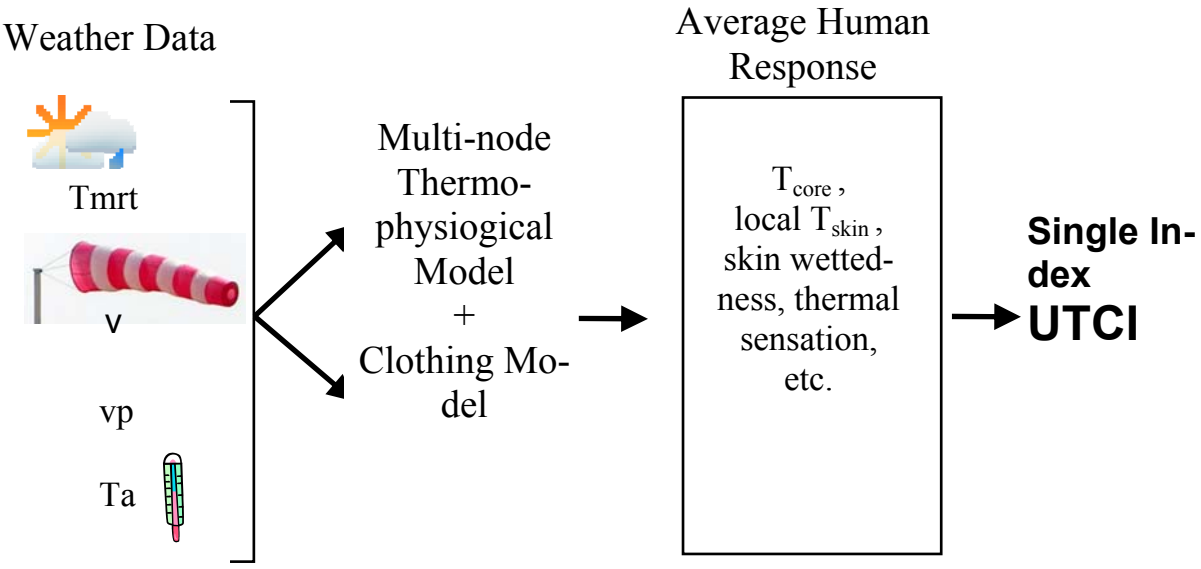

Fig. 1: Concept for calculating UTCI of an actual condition, which is defined as air temperature of the reference condition yielding the same dynamic physiological response

As calculating the UTCI equivalent temperatures by running the thermoregulation model repeatedly could be too time-consuming for climate simulations and numerical weather forecasts, several options to speed up this calculation were considered. These included look-up tables of pre-calculated index values for a grid of all relevant combinations of climate parameters and polynomial regression equations predicting the UTCI equivalent temperature values over the same grid (Bröde et al., 2008; 2009a).

3. Conclusion

The main objective of the joint activities of a group of over 40 scientists from 22 countries (Europe, IL, CA, AUS, NZ) was to develop and make easily available a physiologically assessment model of the thermal environment based on one of the "most advanced thermo-physiological models" in order to significantly enhance applications related to health and well-being in the fields of: public weather service, public health system, precautionary planning, and climate impact research. The development of UTCI required co-operation of experts from thermo-physiology, thermo-physiological modelling, occupational medicine, met data handling and in particular radiation modelling, application development etc. Thus, after many decades of frustrating attempts by „lone researchers" and single discipline teams in this issue, pooling considerable multidisciplinary expertise in a network of biometeorologists, physiologists and individuals from

the application community created the essential research synergies. It is thus evident that for such a multidisciplinary task a COST Action provided an adequate framework to derive a health related climate index as a standard.

The Universal Thermal Climate Index UTCI provides an assessment of the outdoor thermal environment in bio-meteorological applications based on the equivalence of the dynamic physiological response predicted by a model of human thermoregulation, which was coupled with a state-of-the-art clothing model. The operational procedure, which is available as software from the UTCI website (www.utci.org), showed plausible responses to the influence of humidity and heat radiation in the heat, as well as to wind speed in the cold and was in good agreement with the assessment of other standards concerned with the thermal environment. Local cooling of exposed skin, including frostbite risk (wind chill effects), should best be regarded as a transient, rather than a steady-state phenomenon. The consensus final procedure still remains to be determined.

Unlike to former indices UTCI is based on contemporary science (i.e. progress within the last 3-4 decades). Fiala's multi-node model of thermoregulation represents probably the best ever evaluated procedure. The use of UTCI standardizes applications and makes research results comparable.

The work was done under the umbrella of WMO- Commission on Climatology CCl and will finally be made available in a WMO "Guideline on the Thermal Environment" (in preparation) so that everybody dealing with human biometeorological assessments, in particular NMSs (National Meteorological Services), but also universities, public health agencies, epidemiologists, environmental agencies, city authorities, planners etc. can then easily apply the state-of-the-art procedure for their specific purposes. International initiatives such as the creation of WMO, WHO, CEN and ISO standards and guidelines are considered. Due to the difficulty to calculate precisely radiant fluxes based on different meteorological data levels (observations, numerical simulations), it is recommended to run the UTCI model for the fundamental application in Numerical Weather Predictions and climate assessments operationally in Regional Specialised Meteorological Centres or Regional Climate Centres, respectively.

Acknowledgement

The project has been done as teamwork of COST Action 730, funded by EU TRD Framework Programme over 4 years, and ISB Commission 6 on UTCI.

References

Bröde, P., Fiala, D., Blazejczyk, K., Epstein, Y., Holmér, I., Jendritzky, G., Kampmann, B., Richards, M., Rintamäki, H., Shitzer, A., Havenith, G., 2009a: Calculating UTCI Equivalent Temperature. In: Castellani, J.W., Endrusick, T.L. (eds.): Environmental Ergonomics XIII, University of Wollongong, Wollongong, pp 49-53.

Bröde, P., Fiala, D., Kampmann, B., Havenith, G., Jendritzky, G., 2009b: Der Klimaindex UTCI - Multivariate Analyse der Reaktion eines thermophysiologischen Simulationsmodells. In: Gesellschaft für Arbeitswissenschaft (ed.): Arbeit, Beschäftigungsfähigkeit und Produktivität im 21. Jahrhundert, GfA-Press, Dortmund, pp 705-708.

Bröde, P., Kampmann, B., Havenith, G., Jendritzky, G., 2008: Effiziente Berechnung des klimatischen Belastungs-Index UTCI. In: Gesellschaft für Arbeitswissenschaft (ed.): Produkt- und Produktions-Ergonomie - Aufgabe für Entwickler und Planer, GfA-Press, Dortmund, pp 271-274.

Buettner, K., 1938: Physikalische Bioklimatologie. Probleme und Methoden. Akad. Verl. Ges., Leipzig, 155pp.

Fiala, D., Lomas, K.J., Stohrer, M., 1999: A Computer Model of Human Thermoregulation for a Wide Range of Environmental Conditions: the Passive System. Journal of Applied Physiology, Vol. 87, No. 5, pp 1957-1972.

Fiala, D., Lomas, K.J., Stohrer, M., 2001: Computer Prediction of Human Thermoregulatory and Temperature Responses to a Wide Range of Environmental Conditions. International Journal of Biometeorology, Vol. 45, No. 3, pp 143-159.

Fiala, D., Lomas, K.J., Stohrer, M., 2003: First Principles Modeling of Thermal Sensation Responses in Steady-State and Transient Conditions. ASHRAE Transactions, Vol. 109, No. 1, pp 179-186.

Fiala, D., Lomas, K.J., Stohrer, M., 2007: Dynamic Simulation of Human Heat Transfer and Thermal Comfort. In: Mekjavic, I.B., Kounalakis, S.N., Taylor, N.A.S. (eds.): Environmental Ergonomics XII, Biomed, Ljubljana, pp 513-515.

Havenith G., 2001: An individual model of human thermoregulation for the simulation of heat stress response, *Journal of Applied Physiology*, **90**: 1943-1954.

ISO 11079, 2007: Ergonomics of the Thermal Environment - Determination and Interpretation of Cold Stress When Using Required Clothing Insulation (IREQ) and Local Cooling Effects. International Organisation for Standardisation, Geneva.

ISO 7243, 1989: Hot Environments; Estimation of the Heat Stress on Working Man, Based on the WBGT-Index (Wet Bulb Globe Temperature). International Organisation for Standardisation, Geneva.

ISO 7933, 2004: Ergonomics of the Thermal Environment - Analytical Determination and Interpretation of Heat Stress Using Calculation of the Predicted Heat Strain. International Organisation for Standardisation, Geneva.

Jendritzky, G., Maarouf, A., Fiala, D., Staiger, H., 2002: An Update on the Development of a Universal Thermal Climate Index. 15th Conf. Biomet. Aerobiol. and 16th ICB02, 27 Oct – 1 Nov 2002, Kansas City, AMS, 129-133.

Kampmann, B., Bröde, P., 2009: Physiological Responses to Temperature and Humidity Compared With Predictions of PHS and WBGT. In: Castellani, J.W., Endrusick, T.L. (eds.): Environmental Ergonomics XIII, University of Wollongong, Wollongong, pp 54-58.

Osczevski, R., Bluestein, M., 2005: The New Wind Chill Equivalent Temperature Chart. Bulletin of the American Meteorological Society, Vol. 86, No. 10, pp 1453-1458.

Parsons, K.C., 2003: Human thermal environments: the effects of hot, moderate, and cold environments on human health, comfort and performance. – Taylor & Francis, London, New York, 527pp.

Psikuta, A., 2009: Development of an 'artificial human' for clothing research. PhD Thesis, IESD, De Montfort University, Leicester, UK.

Psikuta, A., Fiala, D., Richards, M., 2007: Validation of the Fiala Model of Human Physiology and Comfort for COST 730. In: Mekjavic, I.B., Kounalakis, S.N., Taylor, N.A.S. (eds.): Environmental Ergonomics XII, Biomed, Ljubljana, p 516.

Richards, M., Havenith, G., 2007: Progress Towards the Final UTCI Model. In: Mekjavic, I.B., Kounalakis, S.N., Taylor, N.A.S. (eds.): Environmental Ergonomics XII, Biomed, Ljubljana, pp 521-524.

Tanabe, S.I., Kobayashi, K., Nakano, J., Ozeki, Y., Konishi, M., 2002: Evaluation of thermal comfort using combined multi-node thermoregulation (65MN) and radiation models and computational fluid dynamics (CFD). *Energy and Buildings*, **34**, 637-646.

Author's address:

Prof. Dr. Gerd Jendritzky (gerd.jendritzky@meteo.uni-freiburg.de)
Meteorological Institute, Albert-Ludwigs-University of Freiburg
Werthmannstr. 10, D-79085 Freiburg, Germany

Future thermal comfort in Germany

Insa Thiele-Eich[1], Susanne Brienen[2], Alice Kapala[1], Gerd Jendritzky[3], Clemens Simmer[1]

[1]Meteorological Institute, University of Bonn, Germany
[2]Deutscher Wetterdienst, Offenbach, Germany
[3]Meteorological Institute, Albert-Ludwigs-University of Freiburg, Germany

Abstract

To study future thermal comfort in Germany, the perceived temperature *PT* is utilized, a thermal index which refers to a reference environment in which the sensation of cold and heat would be the same as under actual conditions.

To calculate the thermal index *PT*, the German Weather Service DWD employs the Klima Michel Modell KMM, a complete heat budget model of the human body, which was developed by Jendritzky in 1979 as an operational tool for thermal assessment. The necessary input parameters for the KMM were obtained from different climate scenario runs conducted with the regional climate model of the German weather service, the COSMO-CLM.

The results for the period 2001-2050 show an overall increase in number of days with perceived temperatures in the range of thermal comfort (0-20°C), although no significant trend can be detected for Freiburg. Several spatiotemporal trends are discerned, i.e. a larger increase in coastal areas compared to southern parts of Germany. The rise in number of days with thermal comfort takes place at the expense of a decrease in number of days with a slight cold stress.

1. Introduction

In the context of the ongoing discussion about observed and projected global warming, variations in the thermal environment can be expected. These effects not only include a possible increase in heat waves, but can also procure changes in the daily thermal environment of humans. Because the thermal environment has a direct impact on the health and well-being of humans, an assessment of the range of changes in future thermal comfort in Germany is needed.

Although regional climate models do not offer enough spatial resolution to resolve the biometeorological processes on the scale of one individual person, regional climate models can still be used to detect possible trends in the thermal environment of a certain area and to discuss the effect on thermal comfort in the future.

2. The Klima Michel Modell and the COSMO-CLM

To determine the change of future thermal comfort, the thermal index *perceived temperature PT* is utilized. This index is defined as the air temperature of a reference environment (air temperature T_a equal to mean radiant temperature T_{mrt}, relative humidity=50 % , calm wind and a metabolic rate of 135 W/m^2) in which the perception of thermal comfort would be identical as under actual conditions (Staiger, 1990). To compute *PT*, the Klima Michel Modell of the German Weather Service DWD was used, which represents a complete heat budget model of the human body and calculates the thermal comfort perceived by a human 35 year-old male, 1.75 meters tall and weighing 75 kg. In addition, the model allows for behavioral adaptation such as removing or putting on clothing, which has an effect on the thermal resistance of the clothing layer (Jendritzky, 1979).

The data required to calculate *PT* for the future was taken from regional climate scenarios computed by the Model and Data Group of the Max Planck Institute for Meteorolo-

gy in Hamburg, Germany. These so-called consortial runs use the climate version CLM 2.4.11 of the DWD's COSMO-Modell to simulate the regional climate of the past (runs C20_1, C20_2; 1960-2000) as well as future years (runs A1B_1, B1_1; 2001-2050) with a grid cell spacing of approx. 18x18 km^2 (Böhm et al., 2006). The two runs for the future are initialized using the IPCC climate projections A1B and B1 (Christensen et al., 2007).
Table 1 shows the necessary input variables needed for the calculation of *PT*, as well as describing the variables obtained from the consortial runs of the COSMO-CLM, including their aggregation time. The wind speed in 1 m height is generated by applying a logarithmic wind profile to the wind speed vector composed of U_10M and V_10M. Then, three-hourly means were computed. In accordance with VDI 3789/Part 2, cloud cover at different levels is used to determine the mean radiant temperature T_{mrt}.

Table 1: COSMO-CLM output and variables needed for *PT*

Variable	**Aggregation**	**Description**	**Variable needed for *PT***
T_2M	every 3 h	2 m air temperature in K	ambient temperature T_a
TD_2M	every 3 h	2 m dew point temperature in K	water vapor pressure *e*
U_10M	every 1 h	u-component of 10m wind in m/s	wind speed in 1 m height
V_10M	every 1 h	v-component of 10m wind in m/s	wind speed in 1 m height
ALB	every 3 h	surface albedo in fraction of 0-1	albedo α
CLCL	every 3 h	low cloud cover in fraction of 0-1	mean radiant temperature T_{mrt}
CLCM	every 3 h	medium cloud cover in fraction of 0-1	mean radiant temperature T_{mrt}
CLCH	every 3 h	high cloud cover in fraction of 0-1	mean radiant temperature T_{mrt}
CLCT	every 3 h	total cloud cover in fraction of 0-1	mean radiant temperature T_{mrt}

3. Validation with synoptic data

Before being able to evaluate the effects of climate change on future thermal comfort with the COSMO-CLM, the model runs were validated using synoptical data from the DWD. For the period of 1960-2000, relevant output parameters of the consortial runs C20_1 and C20_2 were compared to data taken from 98 stations distributed over Germany.

Table 2: Thermal classes according to ASHRAE

Thermal class 1	$PT \leq$ -39 °C	very cold
Thermal class 2	-39 °C < $PT \leq$ -26 °C	cold
Thermal class 3	-26 °C < $PT \leq$ -13 °C	cool
Thermal class 4	-13 °C < $PT \leq$ 0 °C	slightly cool
Thermal class 5	0 °C < PT < 20 °C	comfortable
Thermal class 6	20 °C $\leq PT <$ 26 °C	slightly warm
Thermal class 7	26 °C $\leq PT <$ 32 °C	warm
Thermal class 8	32 °C $\leq PT <$ 38 °C	hot
Thermal class 9	$PT >$ 38 °C	very hot

Analyses showed that the COSMO-CLM is not able to reproduce the average diurnal cycles of T_a and T_{mrt} correctly, thus resulting in a shifted cycle of *PT*.

For this reason, the perceived temperatures calculated from the runs A1B_1 and B1_1 were grouped into thermal classes based on the thermal sensation scale developed by the American Society of Heating, Refrigerating and Air-Conditioning Engineers ASHRAE (ISO 7730). Table 2 shows a modified version of this scale with corresponding *PT* values.

4. Exemplary results of the future development of thermal comfort for Freiburg

To evaluate the future development of human thermal comfort, the number of days (NOD) in a certain thermal class was determined for each year. *PTs* calculated from COSMO-CLM output are available for different times of the day, the following discussion concentrates on those computed from the 12 UTC model output. Although analyses were performed all over Germany, results presented here are only exemplarily shown for Freiburg. As the model has a grid of 18x18 km^2, the variables for Freiburg were approximated by averaging the grid points surrounding Freiburg.

Figure 1 shows a time series of the NODs in thermal class 5 (thermal comfort) from both run A1B_1 and B1_1 for Freiburg, Germany.

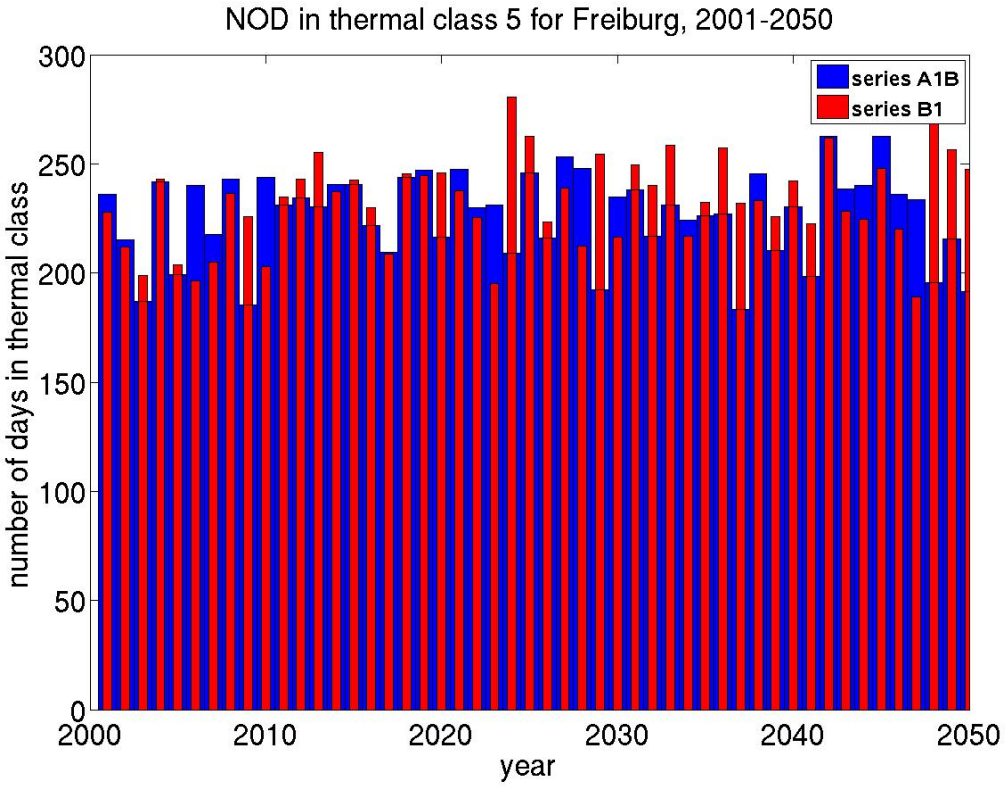

Fig. 1: Number of days NOD in thermal class 5 calculated from COSMO-CLM runs A1B_1 and B1_1 for Freiburg at 12 UTC, 2001-2050; blue bars represent NOD from A1B_1, red bars NOD from B1_1

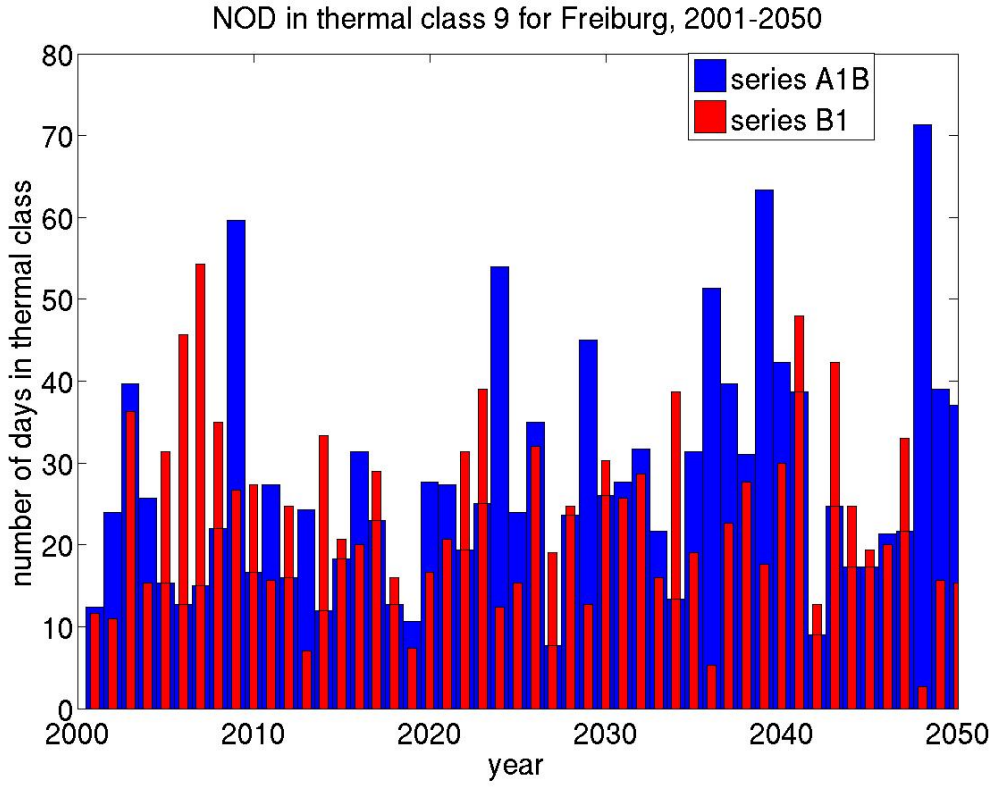

Fig. 2: Number of days NOD in thermal class 9 calculated from COSMO-CLM runs A1B_1 and B1_1 for Freiburg, 2001-2050; blue bars represent NOD from A1B_1, red bars NOD from B1_1

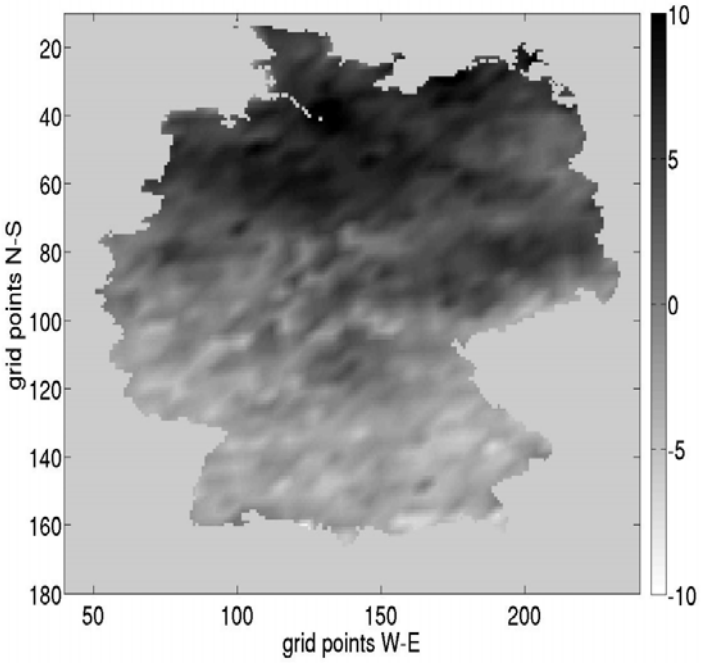

Fig. 3: Difference in the number of days in thermal class 5 compared to the period of 1970-2000 for the decadal means of 2031-2040 of scenario run A1B_1 over Germany

The mean number of days in thermal class 5 for run A1B_1 is 226.8, with a standard deviation of 20.0 (min 183, max 263), while run B1_1 has a slightly higher mean NOD of 232.8 with a standard deviation of 20.6 (min 189, max 281).
Even though the number of days in thermal class 5 increases slightly over Germany as a whole, a Mann-Kendall test did not confirm any significant trend for Freiburg.

Future human thermal comfort is not only affected by a change in NOD in thermal class 5, but also by the occurrence of days with *PTs* in thermal class 9, which corresponds to an extreme thermal sensation of "very hot". The mean number of days in thermal class 9 for run A1B_1 is 27.7, with a standard deviation of 14.3 (min 8, max 71), while run B1_1 has a mean NOD of 23.8 with a standard deviation of 11.3 (min 3, max 54).
While no trend is evident in thermal class 9 over Germany as a whole, the number of days in thermal class 9 increases significantly for Freiburg when evaluating data obtained from scenario run A1B_1. Run B1_1 shows no significant trends in this class.

To quantify the amount of future change, the number of days in a certain thermal class was averaged over ten years, resulting in five decadal means, which were then compared to the average number of days calculated from synoptical data for the period 1970-2000. Figure 3 shows the difference in the number of days in thermal class 5 for the decadal mean of 2031-2040 of scenario run A1B_1 over Germany.
A general increase in number of days with comfortable conditions can be seen for the coastal regions, which is compensated by a decrease in the same order of magnitude in thermal class 4 ("slightly cool"). Compared to the period of 1970-2000, on average southern Germany is expected to have fewer days with thermal comfort for the period of 2031-2040, although some of these effects can be due to the model used, which is not able to represent orographic structures such as the Alps entirely correctly.

5. Conclusion

To make a statement on the development of thermal comfort in the future, perceived temperatures *PT* were calculated by the Klima Michel Modell using output from regional climate model runs conducted with the COSMO-CLM. The two scenarios A1B_1 and B1_1 show similar results for Germany as a whole, with an overall increase in the number of days with thermal comfort (thermal class 5). However, a specific analysis for the area surrounding Freiburg did not detect any significant trend.
When focussing on thermal class 9, which represents *PTs* over 38 °C, the scenario A1B_1 displays a statistically significant increase in NOD for Freiburg, while B1_1 shows no trend.
Spatial trends can also be detected, i.e. a larger increase in coastal areas compared to southern parts of Germany. The rise in number of days with thermal comfort takes place at the expense of a decrease in number of days with a slight cold stress.

References

Böhm, U., M. Kücken, W. Ahrens, A. Block, D. Hauffe, K. Keuler, B. Rockel, and A. Will, 2006: CLM – The Climate Version of the LM: Brief Description and Long-Term Applications. Consortium of Small-Scale Modelling (COSMO) – Newsletter No. 6, 225-235.

Christensen, J.H., B. Hewitson, A. Busuioc, A. Chen, X. Gao, R. Held, R. Jones, R.K. Kolli, W. Kwon, R. Laprise, V. Magaña Rueda, L. Mearns, C.G. Menéndez, J. Räisänen, A. Rinke, A. Sarr, and P. Whetton, 2007: Climate Change 2007: The Physical Science Basis. Contribution of Working Group I to the Fourth Assessment Report of the Intergovernmental Panel on Climate Change. University Press, Cambridge. Chapter 11, 847-940.

ISO 7730, 2005: Ergonomics of the thermal environment – analytical determination and interpretation of thermal comfort using calculation of the PMV and PPD indices and local thermal comfort criteria.

Jendritzky G., W. Sönning, HJ. Swantes, 1979: Ein objektives Bewertungsverfahren zur Beschreibung des thermischen Milieus in der Stadt- und Landschaftsplanung. Akad. f. Raumforsch. u. Landesplanung Hannover. 28, 1–85.

Staiger H., K. Bucher, G. Jendritzky, 1990: Gefühlte Temperatur. Die physiologisch gerechte Bewertung von Wärmebelastung und Kältestress beim Aufenthalt im Freien in der Maßzahl Grad Celsius. Ann. Meteorol. 33, 100–107.

Authors' addresses:

Insa Thiele-Eich (imteich@uni-bonn.de), Dr. Alice Kapala (akapala@uni-bonn.de),
Prof. Dr. Clemens Simmer (csimmer@uni-bonn.de)
Meteorological Institute, University of Bonn
Auf dem Huegel 20, D-53121 Bonn, Germany

Dr. Susanne Brienen (susanne.brienen@dwd.de)
Deutscher Wetterdienst
Klima und Umwelt - Zentrales Gutachtenbüro
Frankfurter Straße 135, D-63067 Offenbach, Germany

Prof. Dr. Gerd Jendritzky (gerd.jendritzky@meteo.uni-freiburg.de)
Meteorological Institute, Albert-Ludwigs-University Freiburg
Werthmannstraße 10, D-79085 Freiburg, Germany

Spatial and temporal variability of the rate of change of the winter thermal comfort conditions in Bulgaria

Ilian Gospodinov and Anna Tzenkova-Bratoeva

National Institute of Meteorology and Hydrology, Bulgarian academy of sciences

Abstract

The winter season of 2009/10 in the Northern hemisphere showed wide regional variations of thermal conditions. For example, Western and Central Europe experienced a long extreme cold period while Southeast Europe enjoyed relatively mild first half of winter. However, the overall mild weather was interrupted with three short but violent cold snaps which resulted in rapid change of the thermal comfort conditions. People considered this unusual, unexpected and causing discomfort. Since November 2008 the National institute of meteorology and hydrology (NIMH), which is the national meteorological service of Bulgaria, has been producing daily analysis, at 11am local time, of the winter thermal comfort condition based on the Wind Chill Index (WCI). The result is visualized in the form of comprehensive maps available to the public through internet. The aim of this work is to study the variability of the rate of change of the thermal comfort conditions. Firstly we study its spatial distribution by comparing the archived country analyses of the WCI for winter 2008/09 and 2009/10. Secondly we attempt to estimate its temporal distribution by examining weather data from the central meteorological observatory of NIMH in the capital city of Sofia.

1. Introduction

The problem of estimating the perceived temperature has been widely studied and various indices of thermal comfort have been developed. The most recent effort of developing a Universal Thermal Comfort Index (UTCI) of the group under the EU COST action 730 has been finalized and resulted in the so called UTCI index. It is supposed to be approved by the World meteorological organization as a guiding one and recommended for implementation in the operational practices of the national meteorological services (for details see Bröde et al. 2009). Especially for the cold season, however, simple indices exist. The so called Wind Chill Index (WCI) is a very good measure of the perceived temperature in the cold season in Bulgaria. We use the WCI developed by the American National Oceanic and Atmospheric Administration (NOAA) and implemented in the operational practice of the American meteorological service in year 2000 (for details see the brochure of NOAA NWS). The perceived temperatures estimated by any of these indices are classified in a certain scale of categories of thermal comfort or discomfort. We use the following categories according to WCI: 1. Comfortable (>10ºC); 2. Slight discomfort (-1ºC<WCI<10ºC); 3. Cold (-10ºC<WCI<-1ºC); 4. Very cold (-18ºC<WCI<-10ºC); 5. Possible frostbite (-27ºC<WCI<-18ºC); 6. Frostbite within 10 to 30min (-35ºC<WCI<-27ºC); 7. Frostbite within 5 to 10min (-47ºC<WCI<-35ºC); 8. Frostbite within 5min (WCI<-47ºC). The first half of the winter season of 2009/10 in the Northern hemisphere has been marked by extreme cold periods in sensitive places like Western and Central Europe. In the same time Southeastern Europe enjoyed relatively mild first half of winter. However, the overall mild weather was interrupted with three short but violent cold snaps which resulted in rapid change of the thermal comfort conditions. People considered this unusual, unexpected and causing discomfort. In addition, the second half of January 2010 and the beginning of February were very cold.

This motivated our study of the rate of change of the thermal comfort conditions in winter season in Bulgaria.

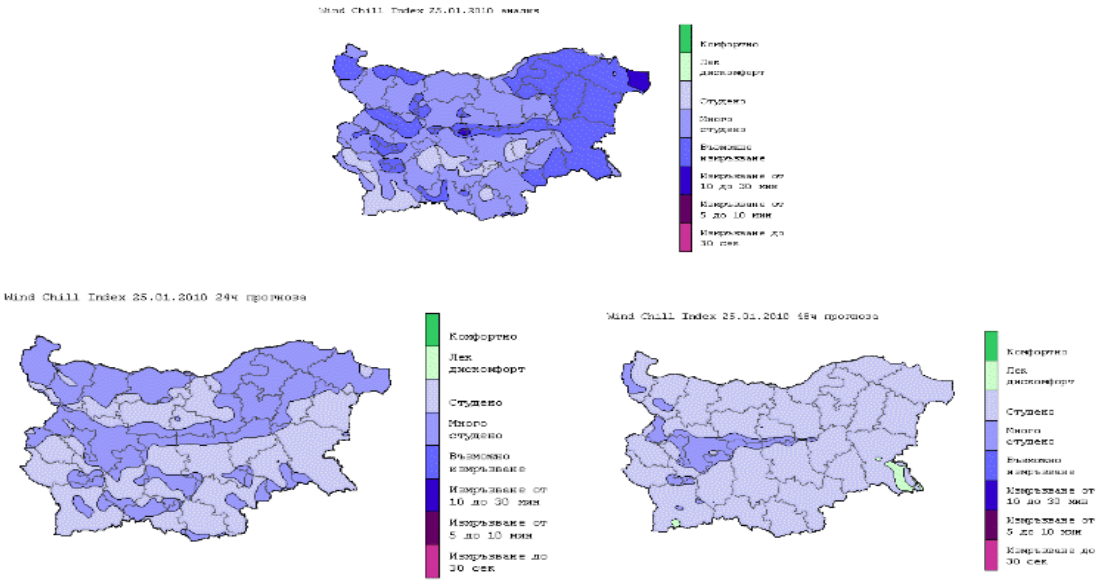

Fig. 1: Daily analysis at 11am local time (top), 24h-forecast (bottom left), and 48h-forecast (bottom right) of the WCI, 25.01.2010

2. Data source and definitions

Since November 2008 the NIMH has been producing daily analysis at 11am local time of the winter thermal comfort condition based on the WCI and forecast for the following two days at the same local time. We have chosen 11am as reference time because it is in the middle of day and can therefore serve as a good estimate of the average daily thermal comfort conditions. It also matches the time of observation at the synoptic stations from the meteorological network of NIMH. The result is visualized in the form of comprehensive maps available to the public through internet. Figure 1 shows an example of the daily analysis (top) and the two forecast maps (bottom left and right) for 25 January 2010. In parallel the NIMH is also testing experimentally the new UTCI in the aim to replace the WCI or to use both indices. The meteorological base used to calculate the WCI and UTCI has two components. The first one is a system of objective analysis of the latest measured data (at 11am local time) at the 40 synoptic stations from the meteorological network of NIMH. They are adjusted to a first guess taken from the regional numerical weather prediction (NWP) model of NIMH (for details see Gospodinov et al., 1999). The second one is the forecast of wind and temperature at 11am for the following two days produced by the NWP model. The system has already been operational for two winter season. We use the data from 20 November to the end of March for winter 2008/09 and from the beginning of November to 15 February for season 2009/10.

We define the rate of change of the thermal comfort conditions as the number of days within which the perceived temperature estimated by any index changes within certain range. As a better measure, we also look at the number of days within which the category of thermal comfort changes within certain range. Then, we seek the minimum number of days for a whole cold season from November to March within which either the

perceived temperature or the thermal comfort category changes within certain range. We use this number as a measure of the volatility of the thermal comfort conditions in a given winter season. In order to estimate the spatial variability in Bulgaria of the rate of change of WCI we use the gathered data from our WCI mapping system from the two cold seasons of 2008/09 and 2009/10. We dispose with archived daily fields of the perceived temperature according to WCI at 11am local time in a regular grid with horizontal resolution of about 9km. In order to estimate the temporal variability of the rate of change of the thermal comfort conditions we use data from the central meteorological observatory of NIMH in Sofia from 1991 to 2010. It is a synoptic station and we use archived data for the cold season for air temperature at 2m above ground and wind speed at 10m above ground available for every 3 hours.

3. Spatial variability of the rate of change of the thermal comfort conditions

We find the minimum number of days within which the perceived temperature at 11am according to WCI changes within certain range within a whole cold season from November to March. We ignore rates of change above 30 days. The most interesting range of change of the perceived temperature is for 25ºC decrease and 20ºC increase (not shown in this paper). In categories of thermal comfort, the most interesting rate of change is either decrease or increase of three categories. Figure 2 (left) shows the spatial distribution of the strongest negative rate of change in number of days of three categories of WCI in winter 2008/09 and Fig. 2 (right) shows the same for winter 2009/10. Figure 3 shows the same as Fig. 2 but for the strongest positive rate of change. Apart from the mountainous area of the country, we can see now that Northeastern Bulgaria is prone of higher volatility of the thermal comfort conditions in winter. Both the negative and positive rates of change are the strongest in large part of the northeast in both winter seasons. This is easy to explain. The northeastern part of the country is flat and the most exposed to the cold arctic air advection. Very often in winter it suffers the combination of low temperatures and strong northeastern winds. In contrast, the southwest of the country is protected by mountainous barriers and even though the temperatures can drop as much as in the northeast the winds are insignificant. The warm southern winds in winter manage to replace the cold air at the surface more rapidly in Eastern Bulgaria than in the western more mountainous part of the country. The comparison of the spatial distribution of the rate of change in Fig. 2 and 3, however, shows that the volatility of the thermal comfort conditions in winter 2009/10 is much higher that in winter 2008/09. This supports the general perception of the public that the first half of the current winter was “unusual”. The strongest negative rate of change occurred in the very northeastern corner of the country in the region of Dobrich, near the synoptic station of Shabla at the Black Sea coast (See Fig. 2 (right)). In the first days of January 2010 there, the thermal comfort category at 11am dropped from 1 (comfortable) to 4 (very cold) within 1 or 2 days only (See Fig. 4).

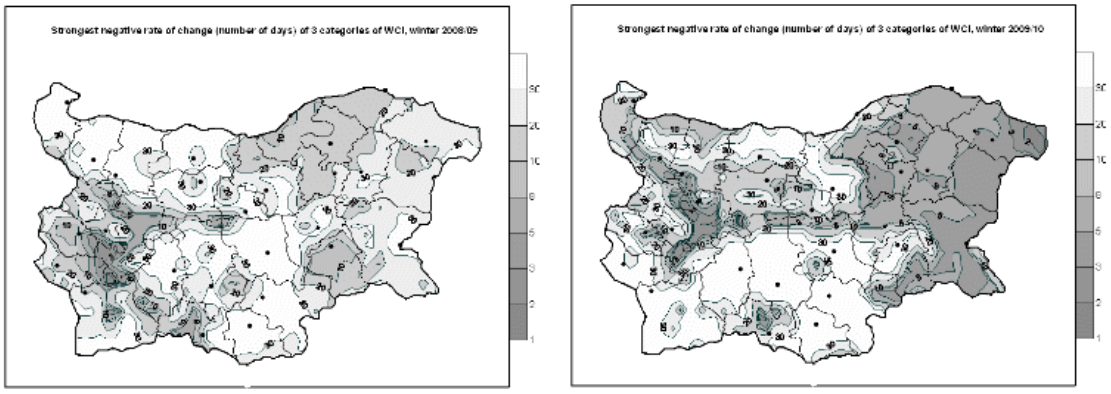

Fig. 2: Strongest negative rate of change (number of days) of 3 categories of WCI, winter 2008/09 (left) and winter 2009/10 (right)

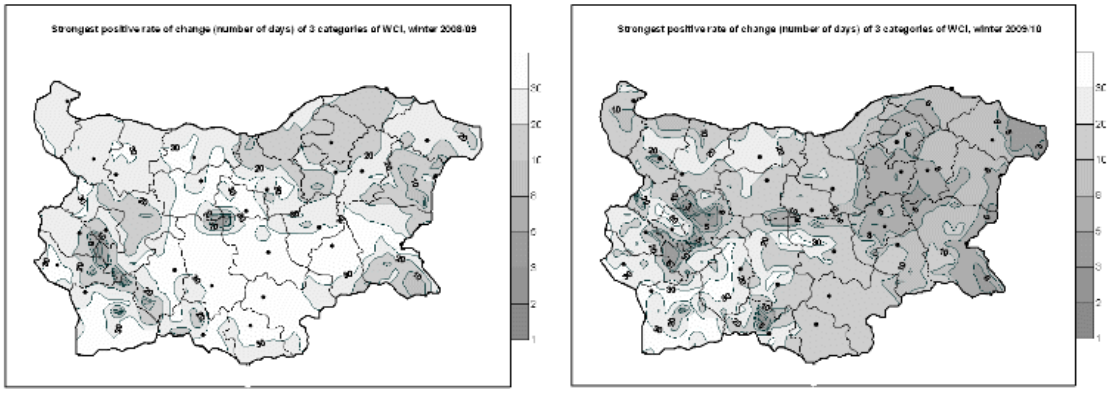

Fig. 3: Strongest positive rate of change (number of days) of 3 categories of WCI, winter 2008/09 (left) and winter 2009/10 (right)

The strongest positive rate of change occurred again in the region of Shabla but is with a day or two slower than the negative rate of change (See Fig.3 (right)). The strongest positive rate of change there occurred after 25 January 2010. On 24-25 January Northeastern Bulgaria experienced very harsh snow blizzard with temperatures as low as -15 ÷ -20ºC and northeastern winds as strong as 15 ÷ 20m/s. As can be seen on Fig.1 (top), on 25 January 2010 at 11am the WCI category of thermal comfort in the very northeast corner of Bulgaria was as low as 6 (Frostbite within 10 to 30min). The WCI never dropped as low in the winter of 2008/09. Figure 1 (bottom left and right) show the forecast of the WCI for the following two days. It can be seen that rapid improvement of the thermal comfort conditions was forecast. It indeed materialized and the WCI climbed up with 3 categories from 6 to 3 (cold) within the following 2 days (See Fig. 4).

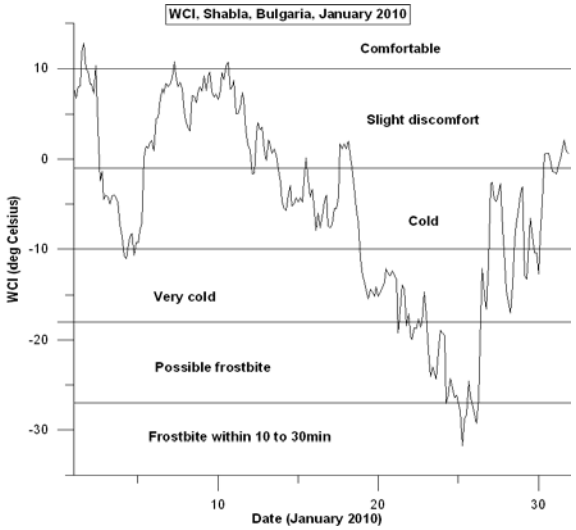

Fig. 4: Perceived temperature (WCI), Shabla, Bulgaria, January 2010

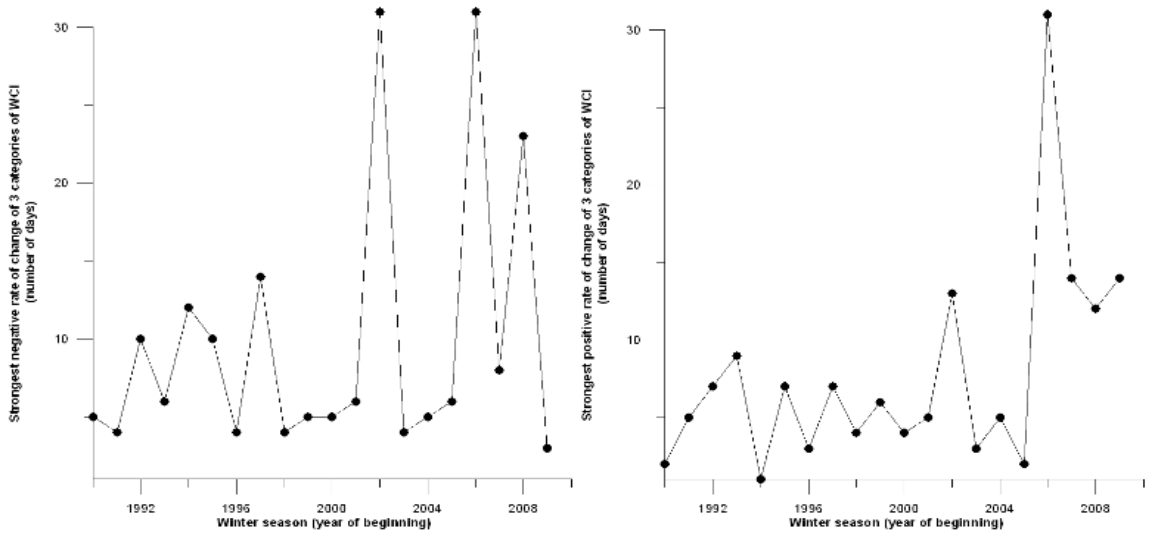

Fig. 5: Strongest rate of change of 3 categories of WCI for Sofia for winter seasons from 1990/91 to 2009/10. (left) - negative rate of change; (right) - positive rate of change

4. Temporal variability of the rate of change of the thermal comfort conditions

We analyze data from a single synoptic station, namely the station of Sofia, for all winter seasons from 1990/91 to 2009/10. We find the strongest rate of change of 3 categories for all winter seasons and look at their temporal distribution. Figure 5 shows the distribution by year (Fig.5 (left) – strongest negative rate of change and Fig.5 (right) – strongest positive rate of change). The most interesting result is that the strongest negative rate of change in Sofia is 3 days and actually occurred in the current winter (See Fig.5 (left)). Two of the previous 3 winters in Sofia are among the calmest since winter 1990/91 with the strongest negative rate of change above 20 days. This contrast should have probably been behind the perception of the public of unusual winter. The most

rapid drop of WCI occurred in Sofia in the first days of January when the thermal comfort category dropped from 1 (comfortable) to 4 (very cold). In the same time, however, the warm was slow to build up. Indeed, Fig.5 (right) shows that this winter is among the 4 least volatile years in terms of strongest positive rate of change. This should have been behind the perception of the public of cold winter in the second half of January and the first half of February.

5. Conclusions

The WCI mapping system implemented in the operational practice of the Bulgarian weather service proved to be a useful tool for alerting the public for the latest and the expected winter thermal comfort conditions. Additionally, the rate of change of the thermal comfort conditions can be seen as one of the factors staying behind the general perception of the public of the character of the winter season. Even if, in terms of mean seasonal temperature anomaly, a given winter season can be classified as relatively warm the general perception of the public may be for a cold winter season or unusual season. This perception depends also on the rate of change of the thermal comfort conditions.

References

Bröde P, Fiala D, Blazejczyk K, Epstein Y, Holmér I, Jendritzky G, Kampmann B, Richards M, Rintamäki H, Shitzer A, Havenith G, 2009: Calculating UTCI Equivalent Temperature. In: JW Castellani & TL Endrusick, eds. Proceedings of the 13th International Conference on Environmental Ergonomics, USARIEM, Natick, MA (5pp. on CD-rom)

Gospodinov, I., Spiridonov, V., Bogatchev, A. and Gaytandjieva, L., 1999: Aladin-Bulgaria – The operational limited-area numerical-weather-prediction model of the NIMH. In Black Sea GOOS Report n.1 – Workshop on operational marine services, 11-15 October 1999, Albena, Bulgaria.

NOAA, National Weather Service, USA: Wind Chill Temperature Index. http://www.weather.gov/os/windchill/index.shtml

Authors' address:

Ilian Gospodinov (ilian.gospodinov@meteo.bg)
Anna Tzenkova-Bratoeva (ani.tzenkova@meteo.bg)
National Institute of Meteorology and Hydrology
Tsarigradsko shose 66, Sofia 1784, Bulgaria

Differences in bioclimatic conditions in four European cities: Budapest Paris, Rome and Warsaw

Danuta Idzikowska

Faculty of Geography and Regional Studies, University of Warsaw, Poland

Abstract

The aim of the paper is to examine the main features of bioclimatic conditions of four European cities using a new Universal Thermal Climate Index. Daily values of meteorological variables for 12 UTC for the cities for 1990-2002 were used in the study. Using frequency of *UTCI* and one-way Anova the results showed that in all four cities "no thermal stress" dominated throughout the year. "Extreme" values of heat as well as "cold stress" were observed and there was only one day with "extreme cold stress" in Warsaw. The values of *UTCI* differed for all four cities in each studied year. The cities differed from each other in each month during the whole year with the exception of spring – March, April and summer – June, July.

1. Introduction

It is commonly known that climate and weather influence human beings in many ways. Therefore, it is of great importance to deliver information about the bioclimatic conditions of the cities which are densely populated, to indirectly help people improve their living conditions.

The importance of outdoor urban climate is neglected by planners and architects due to the lack of knowledge about the influence of urban structure and building design on climate and the lack of methods and measures to evaluate climatic impacts on human health and well-being (Taesler, 1991).

Table 1: *UTCI* categorized in terms of thermal stress

***UTCI* (°C) range**	**Stress category**
above +46	extreme heat stress
38.1 – 46.0	very strong heat stress
32.1 – 38.0	strong heat stress
26.1 – 32.0	moderate heat stress
9.1 – 26.0	no thermal stress
0.1 – 9.0	slight cold stress
-12.9 – 0.0	moderate cold stress
-26.9 : -13.0	strong cold stress
-39.9 : -27.0	very strong cold stress
≤-40	extreme cold stress

Unfortunately, there was not much research done in the area of bioclimatic conditions of Paris, Rome, Budapest and Warsaw. Usually the temperature related factors are studied. For example, J. Amigo and C. Ramirez, (1998) marked macrobioclimatic regions of Chile on the basis of temperature and precipitation regime. To assess thermal environment different biometeorological indices such as Humidex or Wind Chill Index as well as heat budget models such as Missenard effective temperature (Jauregui et al, 1997) or Predicted Mean Vote (Matzarakis, Mayer, 1997) are used. In the present study the Universal Thermal Climate Index was used. For each index value there is a corresponding

and unique thermo-physiological state of the human organism. *UTCI* equivalent temperature was categorized in terms of thermal stress (table 1).

The *UTCI* can be calculated using different input data so it can be adapted by different users. It may also be applied in many scientific fields such as weather forecast for general public, forecast of thermal extremes, epidemiology, bioclimate mapping, urban bioclimatology and planning, tourism and recreation, climate change impact research or climate therapy (Jendritzky et al, eds., 2009, Blazejczyk et al, 2010).

2. Materials and methods

Climate characteristic of the cities

Budapest is situated in the North of Hungary at the Danube river at latitude 47°30'N, 102 m above sea level and within temperate warm climate zone. The mean temperature is the highest in July (20.8°C) and the lowest in January (-1.6°C). The annual total of precipitation is 516 mm (CLINO, 1996).

Paris is situated in the Paris Basin at latitude 48°58'N, 33 m above sea level and within temperate warm maritime climate zone. The mean temperature varies from about 3.4°C in January to about 18.4°C in July. The precipitation is at almost the same level throughout the whole year with the annual total of 650 mm (CLINO, 1996).

Rome is situated in the middle of the highlands of central Italy at latitude 41°54'N, 37 m above sea level and the climate of it is subtropical. The mean temperature is the highest in August (about 23.6°C) and the lowest in January (about 8.2°C). The annual total of precipitation is 876 mm (CLINO, 1996).

Warsaw is situated in the centre of Poland at Vistula river at latitude 52°10'N, about 106 m above sea level in temperate warm transition climate zone. The mean temperature varies from -3.3°C in January to 18.0°C in July. The annual total of precipitation is 515 mm (CLINO, 1996).

The four cities have been chosen for the study due to their location in different parts of Europe and consequently in different climates.

Meteorological data

The meteorological data for Budapest, Paris and Rome used in the study came from the data base established for Assessment and Prevention of Acute Health Effects of Weather Conditions in Europe (PHEWE) project. The data for Warsaw came from the data base established for the 3 P04E 012 23 project entitled "The influence of the environment on humans' health and well being", carried out in the Institute of Geography and Spatial Organization of the Polish Academy of Sciences.

The data used in the study consists of the daily values of air temperature, dew point temperature, wind speed (m/s), total cloud cover (octas) and relative humidity for 12 UTC for Budapest, Paris, Rome and Warsaw for the period 1990-2002. The data for 1990 and 1991 was accessible only for Paris and it was impossible to compare it with the three other cities. The data for 2002 was accessible only for Warsaw and it was not included in the comparison. Similarly, there was no data for 1992 for Warsaw, for 2000 for Paris and for 2001 for Paris and Rome. The comparable period for the four cities was 1993-1999.

Methods

On the basis of the above data the Universal Thermal Climate Index (*UTCI*) for each single day was calculated using BioKlima v. 2.6 software and the *UTCI* calculator (Blazejczyk et al, 2010).

For the statistical analysis frequency of *UTCI* in certain categories as well as one-way Anova was used.

3. Results and discussion

In all four cities most often *UTCI* occurred in the category "no thermal stress" with the values from +9°C to +26°C (Fig. 1). More than 50% of such cases occurred in Rome whereas in Paris and Budapest it was 38% and in Warsaw 33%. In Paris and Warsaw *UTCI* very often indicated "moderate cold stress" (25%) and in Paris also "slight cold stress" was frequent (23%). The situation was similar in Budapest where "moderate cold stress" and "slight cold stress" reached 20% both. It could have been caused by the fact that Paris is situated in temperate warm maritime climate where the cooling effect of the Atlantic Ocean occurs. Budapest has got temperate warm climate but it is situated inside the continent and thus the continental air masses might have come to the region with a similar effect as in Paris. Additionally, Warsaw might have been under the influence of similar air masses to Paris. Similar results were obtained by Matzarakis et al (2009) for Entzheim (rural town in France) where cold temperatures, analysed through the frequency of thermal sensitivity and the grade of thermal stress (*PET*), dominated throughout the whole year. However, in Rome, which represents subtropical climate zone, it was "moderate heat stress" (*UTCI* from 26°C to 32°C - 18%) that occurred more frequently after "no thermal stress". "Slight cold stress" and "strong heat stress" occurred in Rome with similar frequency, 14 and 11% respectively.

.

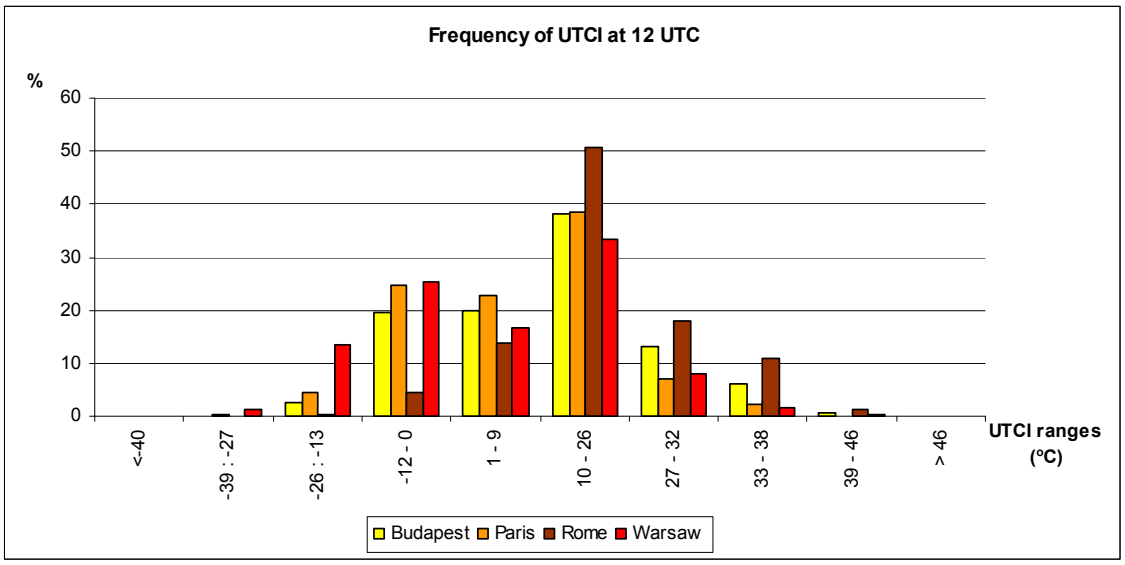

Fig. 1: The frequency of UTCI in Paris, Rome, Budapest and Warsaw in 1990-2002

Analysing the extreme cases in the four cities, it was only Rome and Budapest where "very strong heat stress" occured on 1% of days and in Rome there was one day with *UTCI* above +46°C which corresponds with "extreme heat stress". Considering cold

extremes, in Warsaw "strong cold stress" (*UTCI* from -13°C to -27°C) was noted on 490 days (13%), however in Paris and Budapest it was only 4% and 2% (Fig. 1). There were also 7 days in Paris and 2 in Budapest with "very strong cold stress" (*UTCI* from -27°C to -40°C), contrary to Warsaw were there were 44 such days. They did not appear in Rome. "Extreme cold stress" (*UTCI* ≤-40°C) occurred only on one day in Warsaw
The average value of *UTCI* was calculated for each year for all four cities. As shown in table 2 the values of *UTCI* differed for all four cities in each studied year (P<0.001). The closest to the mean value of *UTCI* for the four cities was always Budapest. The value of *UTCI* for Rome was above the mean and for Paris and Warsaw below it. It can be explained taking into account the fact that Rome is situated in lower latitudes (41°54'N) than Budapest (47°30'N), Paris (48°58'N) and Warsaw (52°10') and consequently in a warmer climate.

Table 2: *UTCI* (°C) values in the chosen cities in studied years
SE – standard error
A,B,C, D - significant differences among the groups at P<0.001;

Year	City				Mean	SE
	Budapest	Paris	Rome	Warsaw		
1990	·	9.44	·	·	·	·
1991	·	8.44	·	·	·	·
1992	12.77^{B}	8.18^{A}	18.74^{C}	nd	13.24	0.66
1993	11.77^{C}	6.85^{B}	18.31^{D}	4.15^{A}	10.28	0.70
1994	13.14^{C}	8.97^{B}	19.60^{D}	5.45^{A}	11.80	0.71
1995	11.26^{C}	8.94^{B}	17.79^{D}	4.91^{A}	10.73	0.74
1996	11.12^{C}	6.37^{B}	17.89^{D}	**3.65^{A}**	9.76	0.72
1997	12.23^{C}	9.65^{B}	19.66^{D}	4.48^{A}	11.50	0.68
1998	12.17^{C}	7.10^{B}	**20.21^{D}**	4.50^{A}	10.99	0.67
1999	11.94^{C}	8.30^{B}	18.80^{D}	5.91^{A}	11.17	0.72
2000	14.28^{B}	·	19.48^{C}	6.79^{A}	13.48	0.68
2001	12.71^{B}	·	·	4.36^{A}	8.53	0.78
2002	·	·	·	6.25	·	·

The average value of *UTCI* was also calculated for each month for the four cities. The cities differed from each other during the whole year (P< 0.001), except for March, April, June and July. Table 3 shows that in March Warsaw (-4.97°C), with lower values of *UTCI*, as well as Rome (12.11°C), with higher values of *UTCI*, differed from Paris (3.34°C) and Budapest (4.17°C), but the last two did not. However, in April it was Paris (6.61°C) and Warsaw (6.42°C) which had much lower values of *UTCI* than Rome (13.65°C) and Budapest (12.38°C). It might have been caused by different air masses coming over the cities which change very often during spring time.

Also in summer months, June and July, the bioclimatic conditions were similar in Paris and Warsaw with the lowest values of *UTCI* (June – 17.43°C, 18.41°C, respectively; July – 22.23°C, 22.10°C, respectively). The situation was different in Budapest with *UTCI* 24.42°C in June and 26.94°C in July and in Rome where *UTCI* values were the highest (27.33°C in June and 31.35°C in July).

The cities might also be divided into two groups in terms of thermal conditions felt by individuals. The first one with cold winters and comfort summers includes Paris and

Warsaw. The second one with cold or cool winters and hot summers includes Rome and Budapest. In winter the regional differentiation of bio-thermal conditions among the four cities is greater than in summer. Budapest, for example, is exposed to cold arctic or continental air masses (Blazejczyk, McGregor, 2007).

Table 3: *UTCI* (°C) values in the chosen cities in certain months
SE – standard error
A,B,C,D – significant differences among the groups at P<0.001;

Month	City				Mean	SE
	Budapest	Paris	Rome	Warsaw		
1	-3.12^{C}	-6.11^{B}	7.92^{D}	-11.75^{A}	-3.56	0.41
2	-0.12^{C}	-2.69^{B}	10.08^{D}	-9.75^{A}	-0.90	0.46
3	**4.17^{B}**	**3.24^{B}**	**12.11^{C}**	**-4.97^{A}**	3.39	0.46
4	**12.38^{B}**	**6.55^{A}**	**13.65^{B}**	**6.42^{A}**	9.65	0.51
5	21.21^{C}	15.07^{A}	22.59^{D}	16.61^{B}	18.81	0.40
6	**24.42^{B}**	**17.43^{A}**	**27.33^{C}**	**18.41^{A}**	21.76	0.39
7	**26.94^{B}**	**22.23^{A}**	**31.35^{C}**	**22.10^{A}**	25.50	0.37
8	28.55^{C}	23.52^{B}	32.99^{D}	22.35^{A}	26.68	0.36
9	19.59^{C}	15.64^{B}	26.33^{D}	12.94^{A}	18.43	0.37
10	14.28^{C}	8.56^{B}	20.60^{D}	5.45^{A}	12.00	0.42
11	2.75^{C}	0.33^{B}	13.17^{D}	-5.93^{A}	2.30	0.42
12	-3.75^{C}	-5.81^{B}	8.35^{D}	-12.35^{A}	-3.74	0.40

4. Conclusions

Firstly, on the base of the UTCI it was showed that in all four cities "no thermal stress" dominates throughout the year. Extreme values of heat appeared in Rome and Budapest. Cold stress was observed in Warsaw, Paris and Budapest.

Secondly, the values of *UTCI* differed for all four cities in each studied year. Budapest reached the middle values of UTCI. The values of UTCI in Rome were usually in higher ranges and in Paris and Warsaw in lower.

Thirdly, the cities differed from each other during the whole year. Rome appeared to be exceptional reaching the highest values of UTCI in studied months.

Finally, UTCI may help to differentiate cities in terms of thermal stress.

Acknowledgements The data for the study was accessible thanks to prof. dr hab. Krzysztof Blazejczyk from the Faculty of Geography and Regional Studies, University of Warsaw and dr Glen McGregor from the University of Auckland (New Zealand).

References

Amigo, J., C. Ramirez, 1998: A bioclimatic classification of Chile: woodland communities in the temperate zone. Plant Ecology 136, 9–26.

Błażejczyk, K., G. McGregor, 2007: Warunki biotermiczne a umieralnosc w wybranych aglomeracjach europejskich (Biothermal conditions and mortality in selected european agglomerations). Przeglad Geograficzny 79, 3 i 4, 401-423.

Błażejczyk, K., P. Broede, D. Fiala, G. Havenith, I. Holmér, G. Jendritzky, B. Kampmann, 2010: UTCI – nowy wskaznik oceny obciazen cieplnych czlowieka (UTCI – New index for assessment of heat stress in man). Przeglad Geograficzny 82, 1, 5–27.

Climatological normals (CLINO) for the period 1961-1990, 1996, WMO, 847, Geneva, Switzerland.
Jauregui, E., J. Cervantes, A. Tejeda, 1997: Bioclimatic conditions in Mexico city – an assessment. International Journal of Biometeorology 40, 166-177.
Jendritzky, G., G. Havenith, P. Weihs, E. Batchvarova (eds.), 2009: Towards a Universal Thermal Climate Index UTCI for assessing the thermal environment of the human being. Final Report, COST Action 730.
Matzarakis, A., M. De Rocco, G. Najjar, 2009: Thermal bioclimate in Strasbourg - the 2003 heat wave. Theoretical and Applied Climatology 98, 209–220.
Matzarakis, A., H. Mayer, 1997: Heat stress in Greece. International Journal of Biometeorology 41, 34-39.
Taesler, R., 1991: The bioclimate in temperate and northern cities. International Journal of Biometeorology 35, 161-168.

Author's address:

Danuta Idzikowska (danuta.idzikowska@student.uw.edu.pl)
Department of Climatology, Faculty of Geography and regional Studies, University of Warsaw
KrakowskiePrzedmieście 30, 00-927 Warsaw, Poland

Compact and wearable measurement system for Lagrangian Human Biometeorology

Makoto Nakayoshi[1], Manabu Kanda[1]

[1] Graduate School of Science and Engineering, Tokyo Institute of Technology

Abstract

Human Biometeorology is currently on the basis of the Euler concept; i.e., meteorological factors are evaluated by fixed-point observations. However, the Euler concept cannot evaluate the actual micro climates we are exposed and thermal load histories, which is increasingly gaining attentions. We introduced a Lagrangian concept to Human Biometeorology, named Lagrangian Human Biometeorology (LHM). The concept of LHM is to investigate and evaluate micro climates along human pathways carrying small bio-meteorological sensors. In this report, proposed was a new-sensor technology for meteorological factors that can enhance the portability. The new technology is to estimate wind velocity, short- and long-wave radiation flux from three compact globe thermometers with different radiative properties. A physiological measurement system was also developed: the bracelet-size observational system, where the sensors for pulse rate, perception of heat, and metabolic equivalent are implemented.

1. Introduction

Human Biometeorology is currently on the basis of the Euler concept; i.e., meteorological factors are evaluated by fixed-point observations (e.g., Mayer and Höppe: 1987). However, due to the locality of urban environments, meteorological data at fixed points cannot represent urban environments. In addition, the actual environments we are exposed and our physiological responses to them are also largely different by individuals depending on their pathways, health conditions, and physical-activity states. It is impossible to evaluate them in the Euler concept. We introduced a Lagrangian concept toward Human Biometeorology, named Lagrangian Human Biometeorology: hereafter LHM (Nakayoshi and Kanda, 2009). The concept of LHM is to investigate the continuous change of micro climates and the physiological responses along human pathways carrying compact bio-meteorological sensors. LHM can make the capture of the environments in urban canyons easy and contribute to the self-management of health of citizens.

In order to disseminate LHM, essential are developments of compact- and portable-meteorological sensors specific to LHM, because they are currently designed for Euler observations, and not applicable to LHM; they are large in size and less portable.

The meteorological sensors, which are introduced here, meet the demand of LHM. The main objective of this report is (1) to propose a new algorithm for the measurements of wind velocity, short-and long-wave radiation flux, and (2) to introduce a prototype of physiological measurement system, which detects pulse rate, perception of heat, and metabolic equivalent.

2. Meteorological sensors

Air Temperature (Ta), relative humidity (RH), wind velocity (U), and short- and long-wave radiation flux (SW and LW, respectively) are targeted for the meteorological sensors; all of the thermal-comfort indices can be computed from these five variables.

Among them, the commercially-available sensors of U, SW, and LW are not applicable for Lagrangian observations because of their less portability. They are large in size and their installation angle should be kept constant during observations. To break through the problems, we developed a new sensing technology for U, SW, and LW. The technology is that they are estimated from the heat budget equations (hereafter HBE) of three globe thermometers (hereafter GT) with different radiative properties (Figure 1). The spherical shape of GT can resolve the problem of the installation-angle dependency of sensors on the accuracy. In addition, replacing the ordinary GT with smaller one with 40-mm diameter can also enhance the portability.

A heat budget equation of a GT is shown in equation (1).

$$C\frac{dT_g}{dt} = (1-\alpha)SW_g + \varepsilon LW_g - \varepsilon\sigma T_g^4 - C_p\rho C_H U\left(T_g - T_a\right) \quad (1)$$

Here, SW_g and LW_g are the input of SW and LW to a GT, respectively. T_g is globe temperature. C, α, and ε are the physical quantities of a GT: heat capacity, albedo, and emissivity, respectively. Because the methods of the identification of albedo and emissivity of GT were not established, we proposed the methods. The detailed information of the methods is presented in the work of Nakayoshi and Kanda (2010).

2.1 Globe anemometer

Globe anemometer uses two GTs with the same radiative properties: white-paint GTs: albedo 0.6 and emissivity 0.8. A constant heat is input at the center of one GT. Subtracting two HBE results in equation (2). Due to the same radiative properties, the radiation terms are cancelled out. U is estimated from each globe temperature, T_{g1} and T_{g2}:

$$C\frac{T_{g1}-T_{g2}}{dt} = -\varepsilon\sigma\left(T_{g1}^4 - T_{g2}^4\right) - C_p\rho C_H U\left(T_{g1} - T_{g2}\right) + H_{input}. \quad (2)$$

Because of the heat input in the GT, globe temperature no longer represents its surface temperature. Therefore we directly monitored the surface temperatures of each GT.

Figure 2 (a) and (b) show the accuracy of the globe anemometer compared to a 3-D ultra sonic anemometer (CYG 81000, Campbell Scientific corp.). Figure 2 (a) indicates the result of the wind tunnel experiments and Figure 2 (b) is the result of the outdoor experiments. In the wind tunnel validation, U from globe anemometer is well correlated that of the ultra sonic anemometer with one-minute averaged data (correlation coefficient 0.98). Meanwhile under the atmospheric environments, the correlation coefficient decreased to 0.76 in spite of using ten-minute averaged data. The fluctuations of wind fields in the atmosphere caused the decrease of the accuracy. Since the heat capacity of GT buffers, globe temperatures cannot follow the fluctuations in real time. Using smaller GTs possibly contribute to the improvement of the accuracy.

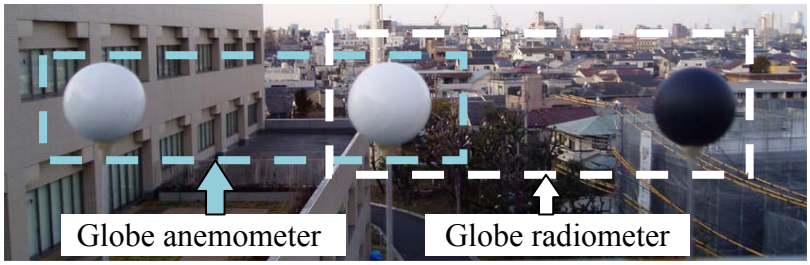

Fig. 1: Picture of Globe anemometer and radiometer

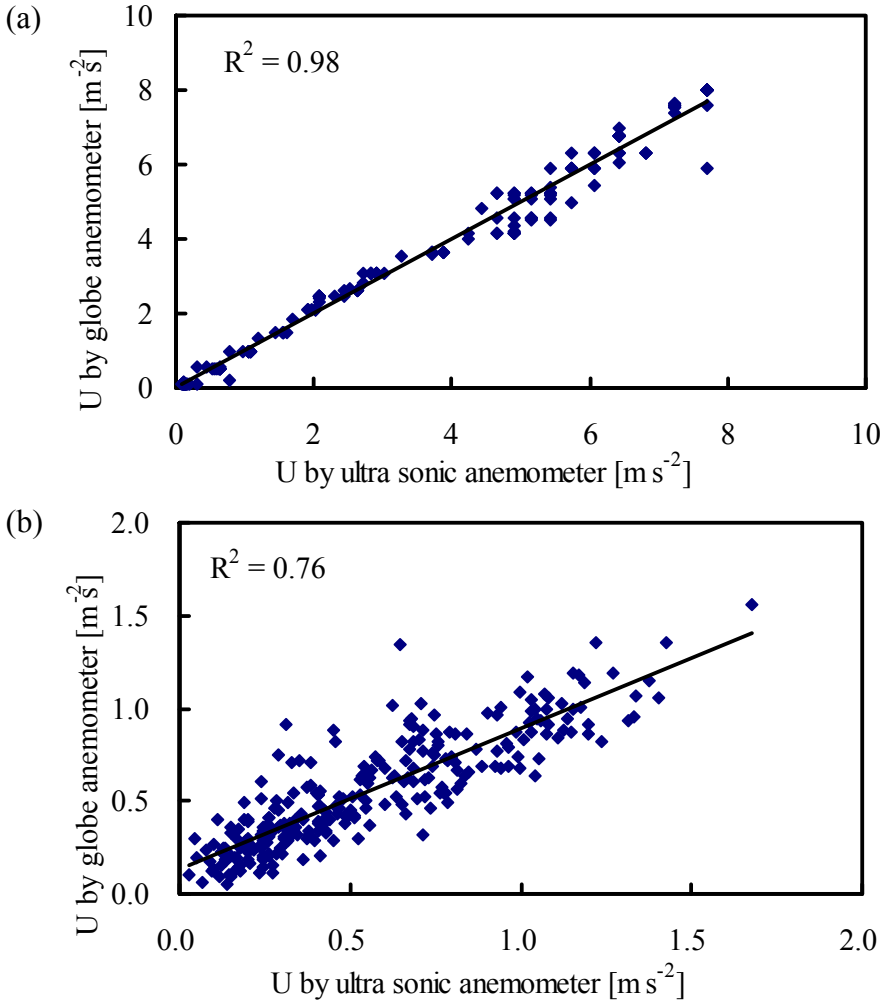

Fig. 2: Accuracy of globe anemometer compared with ultra sonic anemometer.
(a) Wind tunnel experiment at 1Hz monitoring and one-minute averaged data
(b) Outdoor experiment at 1Hz monitoring and ten-minute averaged data

2.1 Globe short- and long-wave radiometer

Globe radiometer uses two GTs with different radiative properties: white- and black-paint GTs: albedo 0.1 and emissivity 0.8 for the black GT. Substitute Ta, T_g for each GT, and U in their HBEs, then SW_g and LW_g are obtained by solving the simultaneous equations. Figure 3 shows the accuracy of the globe radiometer. The net radiometer (CNR1, Campbell Scientific corp.) was used for the validation of the accuracy. The relations between the readings of the net radiometer (SW_{up}, SW_{dn}, LW_{up}, and LW_{dn}) and those of the globe radiometer (SW_g and LW_g) are followed by the equations (3):

$$\begin{aligned} SW_g &= 0.25 \times S_{dir} + 0.5 \times \left(SW_{up} + SW_{dif}\right) \\ SW_{dn} &= SW_{dir} + SW_{dif} \\ LW_g &= 0.5 \times \left(LW_{up} + LW_{dn}\right), \end{aligned} \tag{3}$$

where SW_{dir} and SW_{dif} are the downward direct and diffuse solar radiation flux, respectively. The ratio of SW_{dir} to SW_{dn} was set to 0.8 assuming clear-sky days. Figure 3 shows that globe radiometer can well estimate both SW and LW.

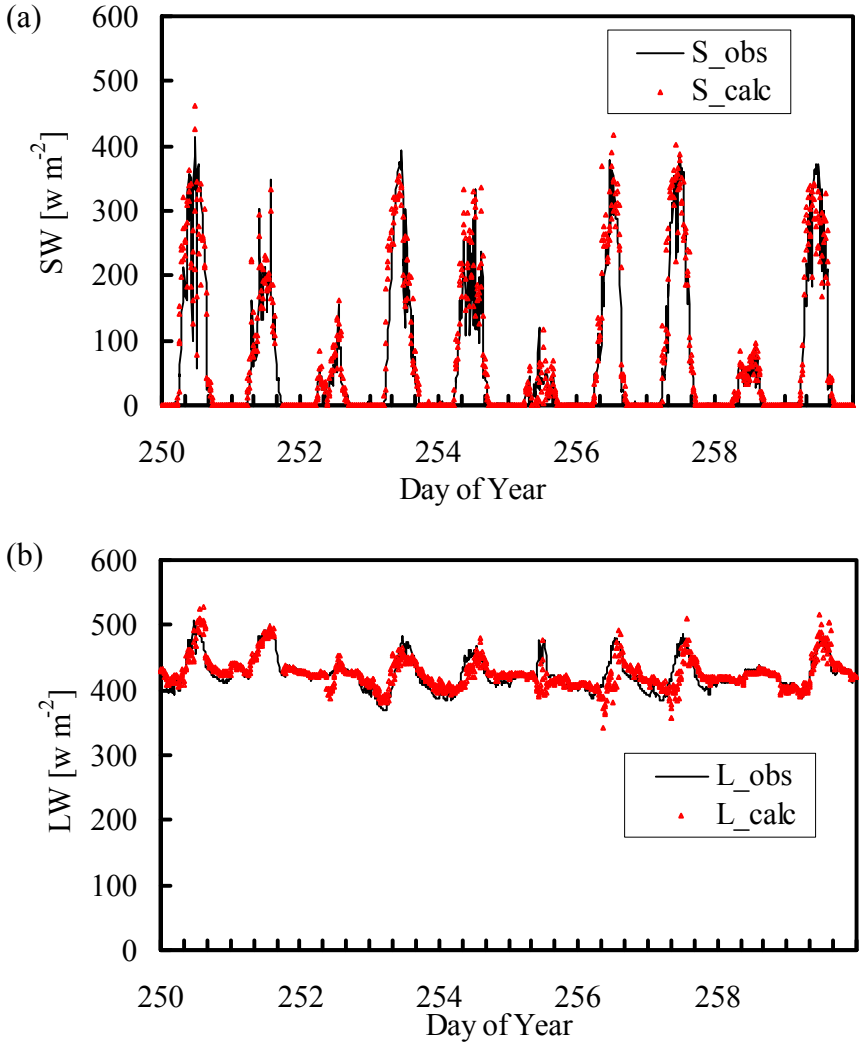

Fig. 3: Accuracy of globe radiometer: (a) Short wave radiation and (b) Long wave radiation. S_obs and L_obs mean SW and LW observed by the net radiometer, and S_calc and L_calc stand for those by the globe radiometer

3. Physiological Sensors

Pulse rate (PR), body surface temperature (BT), and perception of heat are targeted for physiological sensors. Those three components respond well to thermal environments and are fundamental in Thermal Physiology. In addition to these three variables, metabolic equivalent (MET) is also measured. MET is required for the calculation of thermal comfort indices and for the decoupling the effect of thermal loads and exercises to physiological responses. BT can be monitored by the commercially-available small temperature logger, ibottons (Maxim Integrated Products). They are often used by animal physiologists to measure the body temperature of various kinds of animals (e.g., Seebacher et al, 2003: Lovegrove and Genin, 2008). For PR, perception of heat, and MET, we made the prototype of the bracelet-type measurement system (Figure 4). The PR sensor continuously detects the digital pulse volumes at 16Hz and the PRs are estimated by a frequency analysis. Figure 5 shows that the sensor outputs are well corre-

lated with the actual PR measured by the palpation method. Perception of heat is an essential component for Human Bio-meteorological studies and is surveyed in the form of a questionnaire. Those questionnaire-base surveys are time consuming. Here, we introduced the simple sensor for it using adjustable resistors (Figure 4). Subjects adjust the resistor anytime anywhere, corresponding to their thermal comforts. Then the correspondent voltages are converted to digital data and recorded on the microcontroller. MET is estimated from signals of an acceleration sensor. The variance of the acceleration signals increases with MET. Thus as we expected, the standard deviation of them shows a good correlation with MET (Figure 6).

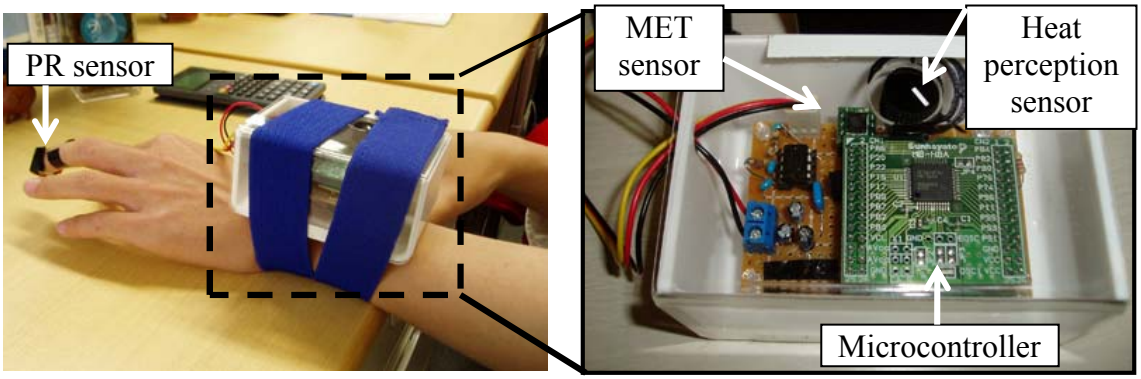

Fig. 4: Prototype of Langrangian physiological system

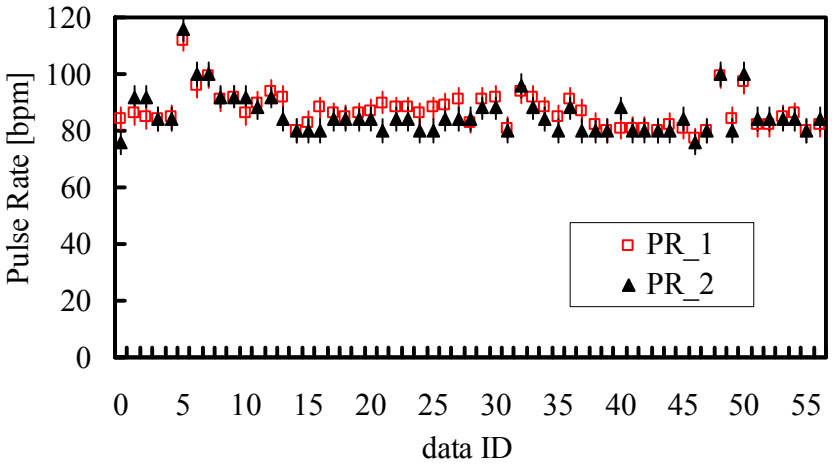

Fig. 5: Accuracy of the PR sensor. PR_1 and PR_2 indicate the PR-sensor outputs and PR measured by the palpation method, respectively

4. Conclusions

Proposed was a new algorithm for the measurements of U, SW, and LW. They were estimated from the HBE of three GTs with different radiative properties. In spite of its simple algorithm, these meteorological factors were estimated well.

Introduced was a prototype of physiological measurement system, which detects PR, perception of heat, MET.

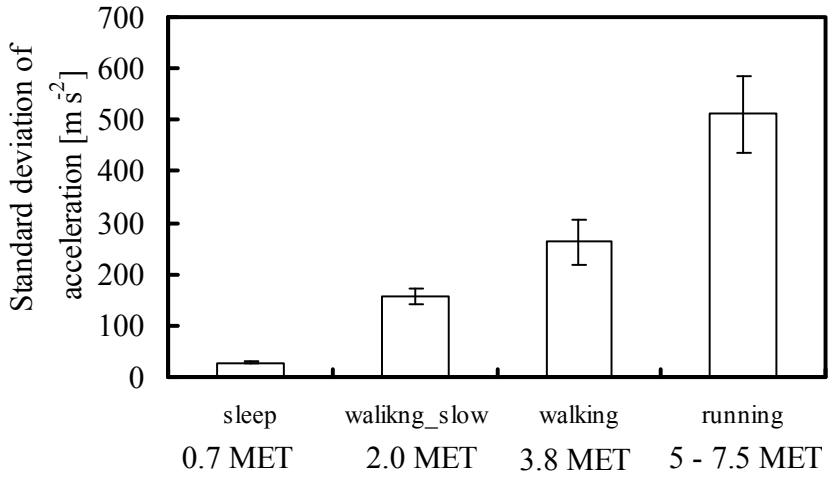

Fig. 6: The relations between standard deviation of acceleration signals and MET

References

Lovegrove, B.G., F. Génin, 2008: Torpor and hibernation in a basal placental mammal, the lesser hedgehog tenrec Echinops telfairi. J. Comp. Physiol. B 178, 691-698.

Mayer, H., P. Höppe, 1987: Thermal Comfort of Man in Difference Urban Environments. Theor. Appl. Climatol. 38, 43-49.

Nakayoshi, M., M. Kanda, 2009: Lagrangian Human Bio-meteorology. The 7th International Conference on Urban Climate. P4-31.

Nakayoshi, M., M. Kanda, 2010: Development of Lagrangian Human Biometeorological sensors: Annual Journal of Hydraulic Engineering, 54, 271-276. (Japanese with English abstract).

Seebacher F., H. Guderley, R. M. Elsey, P. L. Trosclair, 2003: Seasonal acclimatisation of muscle enzymes in a reptile (Alligator mississippiensis). J. Exp. Biol. 206, 1193–1200.

Authors' addresses:

Master Makoto Nakayoshi (nakayoshi.m.aa@m.titech.ac.jp)
Graduate School of Science and Engineering, Tokyo Institute of Technology
Ishikawadai 4th Bldg. Room 409, 2-12-1 Ookayama Meguro-ku, Tokyo, 152-8552, Japan

Associate Prof. Manabu Kanda (kanda.m.aa@m.titech.ac.jp)
Graduate School of Science and Engineering, Tokyo Institute of Technology
Ishikawadai 4th Bldg. Room 402, 2-12-1 Ookayama Meguro-ku, Tokyo, 152-8552, Japan

Estimating down- and up-welling thermal radiation for use in mean radiant temperature

Henning Staiger[1], Andreas Matzarakis[2]

[1] Former affiliation: German Meteorological Service, Germany
[2] Meteorological Institute, Albert-Ludwigs-University of Freiburg, Germany

Abstract

Thermal radiation significantly impacts the energy balance of human beings, and is usually assessed via mean radiant temperature T_{mrt}. The longwave down-welling radiation (*LDR*) and the up-welling from ground (*LUR*) are rarely measured, but are in the same order of magnitude as daily means of shortwave irradiation. This study evaluates simple, but theoretically based algorithms for *LDR* and *LUR* by comparison with measurements in regionally differing climates of Germany. *LDR* is modelled via the clear-sky algorithm (LDR_c) of Prata in a version converging against a realistic value for a completely dry atmosphere. Its advantage is an improved predicted variance. To account for cloud impact, a shortwave cloud modification factor (CMF_{sol}) derived from frequently measured solar global irradiation is applied for daylight hours and observed total cloudiness at night-time, respectively. It is accounted for the diurnal course in the effective temperature via relative humidity, whose impact is modulated dependent on cloud cover and altitude. *LUR* is modelled using the parameterisation of the Klima-Michel-Model. The selected algorithms show a universal applicability. A CMF_{sol} is more closely related to hemispherical cloud base emittance than any cloud correction scheme requiring synoptic cloud observations. The *LUR* model accounts for 90 − 97 % of variance in observations. The uncertainty in T_{mrt} due to estimated *LDR* and *LUR* is comparable to that of the shortwave radiation components.

1. Introduction

Atmospheric longwave down-welling radiation (*LDR*) and up-welling from the ground (*LUR*) are in the same magnitude as daily means of shortwave irradiation. Their impact on the energy balance of human beings is usually assessed by mean radiant temperature T_{mrt} (Matzarakis et al. 2007, ASHRAE 2001, Jendritzky et al. 1990). Furthermore, *LDR* and *LUR* are required in estimating the latent heat flux used in applied agricultural and forest meteorology.

Because of mostly unavailable observations of longwave radiation, *LDR* and *LUR* must be parameterised. Modelling of *LDR* in applied bioclimatology is usually restricted to simple, nevertheless theoretically based algorithms, because a complete radiation transfer calculation is time-consuming, and frequently lacks in required profiles.

LUR is the sum of longwave radiation emitted based on the surface temperature and the usually relative small part of *LDR* reflected by the surface. The surface temperature can strongly deviate from temperature T_0 (K) at screen-level (2 m above ground), and thus, it must be predicted from T_0 (K) and further observations.

This study assumes that the shortwave fluxes are observed and is concerned with the longwave components. It evaluates the performance of the algorithms by comparison with observations in regionally differing mid-latitude climates of Germany. The uncertainty in T_{mrt} using predicted *LDR* and *LUR* instead of observations will be assessed.

2. Methods

Mean radiant temperature (T_{mrt})

In operational human biometeorology the radiation fluxes required in calculation of T_{mrt} (K) are related to an upright standing or walking person, respectively (Matzarakis et al. 2007, Jendritzky et al. 1990). Most frequently the complex structured environment of a person is unknown. Thus, an un-shadowed plane is assumed with solid angles f_a of the surface and the sky set at 0.5: Then T_{mrt} (K) is given by:

$$T_{mrt} = \left\{ \sigma^{-1} \cdot \left[f_a \cdot LDR + f_a \cdot LUR + \alpha_{ir} \cdot \varepsilon_p^{-1} \cdot \left(f_a \cdot D_{sw} + f_a \cdot R_{sw} + f_p \cdot I_{sw} \right) \right] \right\}^{0.25} \qquad (1)$$

σ is the Stefan Boltzmann constant. D_{sw} denotes the isotropic diffuse and R_{sw} the surface reflected shortwave radiation flux. I_{sw} is the direct and by definition an-isotropic shortwave radiation flux. $\alpha_{ir} = 0.7$ is the effective shortwave and $\varepsilon_p = 0.97$ the effective longwave absorptance of the body surface (clothing and skin). The projected area factor f_p accounts for the directional dependence and is a function of the solar zenith angle and assumed body posture.

Longwave down-welling radiation (*LDR*)

LDR is a function of all-sky emissivity ε and T_0: $LDR = \varepsilon \cdot \sigma \cdot T_0^4$. In general, *LDR* modelling predicts first a value for a cloudless sky (LDR_c). This is than adjusted to account for clouds, which increase the atmospheric emittance beyond its clear-sky value, because cloud droplets also emit in the atmospheric window.

Clear-sky parameterisation

$LDR_c = \varepsilon_{ac} \cdot \sigma \cdot T^4_{atm}$ (W·m^{-2}) can be regarded in terms of a grey body emitting at uniform temperature. ε_{ac} is the effective atmospheric clear-sky emissivity, which is closely related to precipitable water u (kg·m^{-2}) in the atmospheric column. T_{atm} (K) is an effective temperature of the atmospheric boundary layer. Approximately 63 % of LDR_c is due to emission within the lowest 100 m of the atmosphere, less than 5 % originates from layers above an altitude of 2 km altitude (Schmetz et al. 1986). This enables LDR_c to be estimated from T_0 (K) and water vapour e_0 (hPa) at screen-level taking climatological profiles as a basis. Prata (1996) develops an analytical solution of the radiation transfer equation, which corresponds to a slab emissivity model with a continuum correction. It provides ε_{ac} as function of u (kg·m^{-2}):

$$\varepsilon_{ac} = 1 - \left(1 + u/u_P\right) \cdot \exp\left(-\sqrt{\left(a_1 + a_2 \cdot u/u_P\right)}\right) \qquad (2)$$

$u_P = 10$ (kg·m^{-2}) is a scaling constant. Using a temperature lapse rate and an inverse scale height for water vapour pressure derived from the US standard atmosphere, precipitable water can be predicted by $u \approx 465 \cdot e_0 / T_0$. This study deviates from Prata's (1996) original coefficients and sets a_1 at 0.068. Thus $\varepsilon_{ac} \rightarrow 0.23$ for $u \rightarrow 0$ (completely dry atmosphere), a more realistic value accounting for CO_2 and additional greenhouse gases (Skarveit et al. 1996, Konzelmann et al. 1994). The coefficient a_2 is selected so that the absolute difference of ε_{ac} between the formula with the original and the adjusted coefficients falls into to the broad minimum in the e_0/T_0 interval 0.004 - 0.080. This modified version deviates less then 3 % from the original in the range $e_0/T_0 > 0.024$. Prata (1996) provides an altitude correction $\delta\varepsilon_p$ to be subtracted from ε_{ac}.

$$\delta\varepsilon_p = 0.05 \cdot \left(1013.25 - p\right)/303.25 \qquad (3)$$

p (hPa) is the barometric pressure at site altitude.

All-sky parameterisations

The all-sky emissivity ε is derived correcting ε_{ac} for clouds. For observed total fractional cloud cover n (0−1), ε is calculated using Eq. (4) of Maykut and Church (1973):

$$\varepsilon = \varepsilon_{ac} \cdot \left(1 + 0.2234 \cdot n^{2.75}\right) \qquad (4) \qquad\qquad \varepsilon = \varepsilon_{ac} \cdot \left(1 - n\right) + n \qquad (5)$$

Due to unavailable synoptic cloud observations, Crawford and Duchon (1999) introduce a cloud fraction term n = 1-CMF_{sol}. The solar cloud modification factor CMF_{sol} is the ratio of measured solar global irradiation to that of the cloudless atmosphere. In this study, the ESRA clear-sky algorithm (Rigollier et al. 2000) is applied. The required Linke turbidity factors are taken from Remund et al. (2003). ε than is given as fractional reduction of the longwave radiation loss (Eq. 5).

Diurnal variations of emissivity

For cloudless skies, Long and Turner (2008) provide a relative humidity dependent factor for ε_{ac} in Eq. (4) and (5), which accounts for diurnal variations due to haze and dew formation. Under cloudy skies these diurnal variations will be reduced. Additionally, it has to be accounted for the site altitude:

$$fact_{rh} = 1 + \left(3.36 \cdot 10^{-12} \cdot rh^{5.1938} \cdot CMF_{sol} / 1.24\right) \Big/ \left(1 + 20 \cdot \delta\varepsilon_p\right) \qquad (6)$$

rh (%) is the relative humidity and $\delta\varepsilon_p$ is given by Eq. (3). In case of observed total fractional cloud cover, CMF_{sol} in Eq. (6) has to be replaced by (1-$n^{2.75}$).

Longwave up-welling radiation (*LUR*)

LUR is predicted according to Jendritzky et al. (1990): $LUR\,(\mathrm{W \cdot m^{-2}}) = 0.95 \cdot \sigma \cdot T_s^4 + 0.05 \cdot LDR$. T_s (K) is the surface temperature, which usually is unknown. It is parameterised dependent on the shortwave radiation balance, on assumptions concerning physical properties of the soil, the Bowen ratio, and on the flux of sensible heat between atmosphere and surface. The parameterisation is solved via a Newton approximation using the screen-level temperature as first guess.

3. Observational data

This study uses for southwest Germany the same measurements for the sites Bremgarten (212 m) and Feldberg (1489 m) from 1991–1996 as described by Iziomon et al. (2003). For northeast Germany, the observations at Warnemuende (4 m) from 2001-2003 are available. The site is located directly on the Baltic Sea. In screen level are observed: down-welling and up-welling longwave and shortwave radiation, direct shortwave irradiation via a SONIe sunshine duration sensor, as well as ambient temperature, relative humidity, and wind speed.

Synoptic observations of total cloudiness are available for Bremgarten (1991 –Feb. 1993), for Feldberg (1991-1995) and for Warnemuende (June 2001 –2003).

4. Results and discussion

Table 1 summarises the comparison of modelled and observed LDR_c and LDR. An hour is identified as “clear-sky”, if its $CMF_{sol} > 0.95$ at daylight hours, or $n = 0$ at night-time,

respectively. Comparison with LDR_c from Prata's original and other theoretically based algorithms shows within an individual site that the scattering in the correlation coefficients between the algorithms is quite low. However, the slope of the regression line (the modelled variance) is closer to unity for the scheme with adjusted coefficients.

Table 1: Predicted compared to observed longwave down-welling radiation for clear-sky (LDR_c obs) and all-sky (LDR obs) conditions. Bias is predicted minus observed radiation, RMSE is the root mean square error, SE the standard error

	clear-sky					all-sky				
site	LDRc obs	bias	RMSE	SE	corr. coeff.	LDR obs	bias	RMSE	SE	corr. coeff.
	W/m²	W/m²	W/m²	W/m²		W/m²	W/m²	W/m²	W/m²	
daylight hours										
Bremgarten	319.7	8.2	22.8	17.6	0.931	327.7	7.6	19.0	16.3	0.932
Feldberg	265.7	-0.6	27.0	25.1	0.837	291.0	-0.6	22.1	20.9	0.883
Warnemuende	318.0	0.8	30.5	26.3	0.848	338.4	-1.9	18.1	17.1	0.928
day and night										
Bremgarten	307.9	3.3	23.8	22.4	0.918	323.9	2.6	21.1	20.6	0.907
Feldberg	241.7	2.9	29.0	26.6	0.834	286.9	-12.9	37.0	33.0	0.745
Warnemuende	300.8	-4.4	23.9	23.4	0.921	329.4	-3.6	20.2	19.8	0.925

The *LDR* cloud correction scheme of Crawford and Duchon (1999) performs the best provided that it is based on CMF_{sol}. At night-time CMF_{sol} is undefined, and thus cloud correction requires a synoptic observation as input. Concerning bias, the Maykut and Church (1973) cloud correction scheme is at the lowland sites comparable with the CMF_{sol} scheme. However, related to the CMF_{sol} scheme, the root mean square error (RMSE) is increased by 33 %. Under all-sky conditions, the RMSE is noticeably reduced compared to clear-sky at daylight hours. This may result from the high number of all-sky hours. Nevertheless, it indicates that the main part of scattering in modelling is due to estimation of clear-sky emissivity.

LUR modelling applies the Bowen ratio for land use "settlements". Dependent on the site, the *LUR* model can determine 90 % (Feldberg) to 97 % (lowland sites) of the observed variance. At Feldberg, the five months with snow cover conflict somewhat with modelling assumptions. Most frequently the current surface albedo will not be available. The additional modelling error due to a set albedo of 20 % and due to scattering in modelled *LDR* is approximately 2 %.

Table 2: T_{mrt} based on modelled versus T_{mrt} based on observed *LDR* and *LUR*

sites	Tmrt obs	STD	bias	RMS error	SE
	K	K	K	K	K
Bremgarten	296.2	18.9	0.6	2.5	2.4
Feldberg	287.0	19.5	-0.5	4.7	4.5
Warnemuende	290.7	19.1	-0.5	2.2	2.1

The mean radiant temperature T_{mrt} (K) is calculated applying Eq. (1). Measured diffuse irradiation is unavailable for Bremgarten and Feldberg, thus it is modelled from observed global irradiation applying the algorithm of Skartveit et al. (1998). A predicted T_{mrt} is calculated based on

observed global irradiation and modelled *LDR* and *LUR*, assuming a shortwave surface albedo of 20 % and predicting diffuse irradiation via the algorithm of Skartveit et al. (1998). The bias (Tab. 2) is within ±0.6 (K), the RMSE is less than 3 (K) for the low-land sites, and 5 (K) for Feldberg. The coefficient of determination for modelled values is greater than 95 %.

Figure 1 exemplifies the result for the site Bremgarten. Dependent on the time, the residuals reveal a slight daily course with highest values during noon and lowest around midnight. This may be influenced by estimating the cloud impact at night-time based on observed cloud cover with a tendency toward too low predicted *LDR* especially at the mountain site, where the daily course is most pronounced.

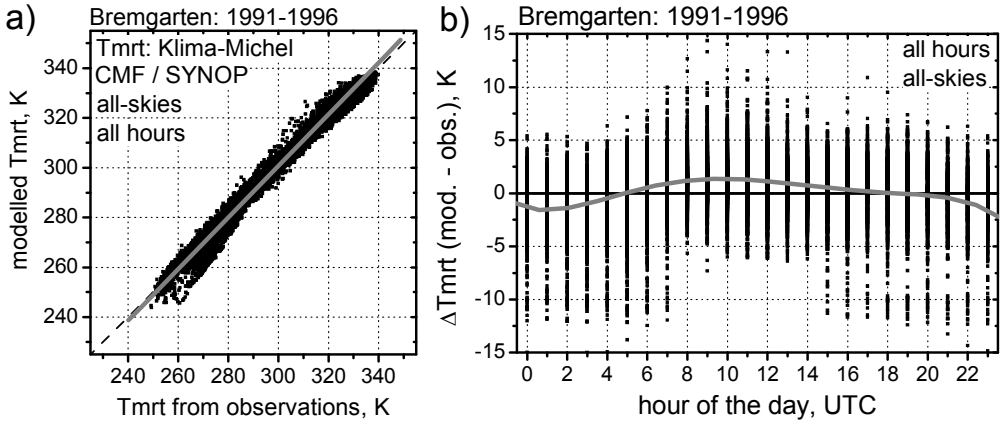

Fig. 1: Bremgarten: (a) Scatter-gram and (b) residuals for modelled versus observed T_{mrt}

5. Conclusions

Prata's (1996) scheme for LDR_c with adjusted coefficients has advantages, because modelled variances are closer to observations. The algorithm of Long and Turner (2008) improves the results, because it can be accounted for diurnal variations in effective temperature of the atmospheric boundary layer. The *LDR* cloud correction scheme of Crawford and Duchon (1999) using CMF_{sol} performs the best and should be preferred. If only observed total cloud cover is available, the Maykut and Church (1973) algorithm shows a comparable low bias, but an enlarged RMSE. Referring to publications, a universal applicability of the schemes can be anticipated.

The *LUR* algorithm performs well and with low uncertainty.

The uncertainty in T_{mrt} due to estimations of *LDR* and *LUR* can be expected to be in the magnitude of that of the shortwave radiation components in T_{mrt}.

Acknowledgement

This study has been performed in the framework of the COST-Action 730 on "Universal Thermal Climate Index (UTCI)". The southwest German sites used for this study were operated within the framework of a regional climate project (REKLIP) founded by the Ministry of Science and Research, Baden-Württemberg, Germany. The German Meteorological Service (DWD) has provided the observations at the northeast German site.

References

ASHRAE, 2001: ASHRAE Handbook: Fundamentals, 8. American Society of Heating and Air-Conditioning Engineers, Atlanta, GA.

Crawford, T. M., C. E. Duchon, 1999: An improved parameterization for estimating effective atmospheric emissivity for use in calculation daytime downwelling longwave radiation. J Appl Meteorol 38, 474-480.

Iziomon, M. G., H. Mayer, A. Matzarakis, 2003: Downward atmospheric longwave irradiance under clear and cloudy skies: Measurement and parametrization. J Atmos Sol-Terr Phys 65, 1107-1116.

Jendritzky, G., H. Schirmer, G. Menz, W. Schmidt-Kessen, 1990: Methode zur raumbezogenen Bewertung der thermischen Komponente im Bioklima des Menschen (Fortgeschriebenes Klima-Michel-Modell). Akad Raumforschung Landesplanung, Hannover, Beiträge 114.

Konzelmann, T., R. S. W. van der Wal, W. Feuell, R. Bintanja, E. A. C. Henneken, A. Abe-Ouchi, 1994: Parameterization of global and longwave incoming radiation for the Greenland ice sheet. Global Planet Change 9, 143-164.

Long, C. N., D. D. Turner, 2008: A method for continuous estimation of clear-sky down-welling longwave radiatiave flux developed using ARM surface measurements. J Geophys Res 113, D18206, doi: 101029/2008JD009936.

Matzarakis, A., F. Rutz, H. Mayer, 2007: Modelling radiation fluxes in simple and complex environments - application of the RayMan model. Int J Biometeorol 51, 323-334.

Maykut, G. A., P. Church, 1973: Radiation Climate of Barrow, Alaska 1962-66. J Appl Meteo-rol 12, 620-628.

Prata, A. J., 1996: A new long-wave formula for estimating downward clear-sky radiation at the surface. Q J Roy Meteor Soc 122, 1127-1151.

Remund, J., L. Wald, M. Lefevre, T. Ranchin, 2003: Worldwide Linke Turbidity Information. Proceedings of ISES Solar World Congress, 16-19 June 2003, Göteborg, Sweden, CD-ROM published by the International Solar Energy Society

Rigollier, C., O. Bauer, L. Wald, 2000: On the Clear Sky Model of the ESRA - European Solar Radiation Atlas - With Respect to the HELIOSAT Method. Sol Energy 68, 33-48.

Schmetz, P., J. Schmetz, E. Raschke, 1986: Estimation of daytime downward longwave radia-tion at the surface from satellite and grid point data. Theor Appl Climatol 37, 136-149.

Skartveit, A., J. A. Olseth, G. Czeplak, M. Rommel, 1996: On the estimation of atmospheric radiation from surface meteorological data. Solar Energy 56, 349-359.

Skartveit, A., J. A. Olseth, M. E. Tuft, 1998: An hourly diffuse fraction model with correction for variability and surface albedo. Sol Energy 63, 173-183.

Authors' address:

Dipl. Met. Henning Staiger (Henning.Staiger@gmx.de)
Alte Yacher Str. 43, D-79215 Elzach, Germany

Prof. Dr. Andreas Matzarakis (Andreas.Matzarakis@meteo.uni-freiburg.de)
Meteorological Institute, Albert-Ludwigs-University of Freiburg
Werthmannstr. 10, D-79085 Freiburg, Germany

Association of meteorological factors with emergency calls of ambulance in Vilnius, Lithuania

Judita Liukaityte[1,2], Justinas Savanevicius[2]

[1]Lithuanian Hydrometeorological Service under the Ministry of Environment
[2]Vilnius University

Abstract

The aim of research was to determine what kind of impact meteorological parameters make on human health in Vilnius, Lithuania. The meteorological indices like ambient air temperature, relative humidity, atmospheric pressure and others, PET index and weather classes were used. The response variable was the daily number of emergency patients admitted with two types of disease: cardiovascular and respiratory. Analysis was performed on data from years 2007-2008. Cardiovascular diseases are more frequent in wintertime. Generally, each illness has it own meteorological index (or indices) that correlate best. For example, there is a significant increase in arterial hypertension when ambient air temperature falls below 0°C, myocardial infarcts are much more frequent when atmospheric pressure is higher than 1010 hPa (reference altitude), strokes and heart deficiently increase when the precipitation exceeds 8 mm per day. Some respiratory diseases are more frequent in winter, other - in summer time, mostly because of strong linkage to temperature, atmospheric pressure and their diurnal alternations. Some illnesses like bronchial asthma or chronic obstructive pulmonary disease have no annual cycle – they are depended on separate gradation of meteorological indices.

1. Introduction

Various kinds of meteorological parameter complexes may bring significant influence on human health. Anecdotal evidence (dating back to Hippocrates) and some more modern research support their contention, but scientists cannot agree with one another on this issue. However, several studies have quantitatively revealed the impact of meteorological factors on the incidence of emergency hospital admissions. Analysis in Fukuoka, Japan, showed that the number of emergency patients admitted daily with cerebrovascular disease was significantly associated with temperature on the day of admission (Makie et al, 2001).

Also, many other experts affirm that temperature is affecting the state of health mostly. Especially dangerous phenomena are heat waves and cold spells, significantly increasing the incidence of various diseases and related mortality rate. Some studies of extremely high temperature show comparatively smaller increases in increases in hospital admissions than in mortality (Kovats, Hajat and Wilkinson 2004). In 12 US cities, there was an association between hot weather and a rise in admissions for heart diseases in the ≥65 age group (Schwartz, Samet and Patz, 2004). High temperatures were associated with an increase in admissions for acute myocardial infarction and congestive heart failure in Denver, CO (Koken et al, 2003). Studies in 12 European cities showed that high temperatures have an impact on hospital admissions for respiratory causes. This effect is more evident in the elderly population, which is consistent with their reduced capacity for coping with heat stress (Michelozzi et al, 2009).

Not only temperature, but also atmospheric pressure and humidity are very important meteorological elements determining not only physical but also psychological human

illnesses. There has been significant number of investigations carried out worldwide to determine impacts on human health made by moving atmospheric fronts of different types, various weather patterns and other geophysical factors.

The aim of this paper was to determine a relationship between cardiovascular and respiratory system diseases and meteorological factors in Vilnius in 2007-2008.

2. Data and methodology

Data used in this paper are collected from daily emergency call tables of the Vilnius ambulance station. Analysis was performed on data from years 2007-2008. The incidence of diseases of the circulatory system (ICD-10: I00-I99) and diseases of the respiratory system (ICD-10, J00-J99) was analyzed. Only those diseases were selected, which annual incidence exceeded 300 cases. Days that tended to give violent number of calls (like holidays, weekends and epidemic periods) were eliminated.

In this paper also are used the data from Trakų Vokė meteorological station, obtained from archives of the Lithuanian Hydrometerological Service. Some variations of parameters (average, minimal and maximal air temperature, atmospheric pressure, wind speed and relative humidity) from day to day were calculated. We used "Rayman" model to calculate PET (Physiological Equivalent Temperature) index (Matzarakis, Rutz and Mayer, 2009). We sought any impacts of PET daytime values in excess of 30 on exacerbations of particular diseases. We looked and for the main weather class of the day, which could have impact on human health. This paper utilizes a medical-meteorological weather classification developed in the German Weather Service (DWD) (Bucher and Haase, 1993).

Cardiovascular and respiratory diseases were analyzed separately because of ambiguity in their annual variations. Every illness was analyzed using several methods: reviewing of annual variations and correlation with meteorological information; analyzing homogeneity by Student's criteria.

3. Results

3.1 Cardiovascular diseases

Totally 11 cardiovascular diseases were determined having over 300 occurrences during the year. Having reviewed most reference sources (Spencer et al., 1998; McGregor, 2004), The Authors unambiguously affirm that cardiovascular diseases have distinct annual course as peak of diseases is observed during cold period of the year, and their low – during the warm one. Not exceptional is the distribution of emergency calls received by Vilnius ambulance station, analyzed in this study (Fig.1).

Such distribution of calls is typical for the most cardiovascular diseases, since both course and attacks of these deceases are also closely related as well as the most other diseases are correlated and one disease (e.g. arterial hypertension) can be a cause of the other.

It was determined that myocardic infarcts become very frequent when atmospheric pressure exceeds 1010 hPa ($t = 5{,}46$) – on such days a number of emergency calls increases up to 29% percents. Also, a number of emergency calls increases with tempera-

ture oscillating between 0 and -5°C (t = 2,70), and even more when falling below 5°C (t = 3,72). Stroke incidence decreases under prevailing cool weather (5-10°C).

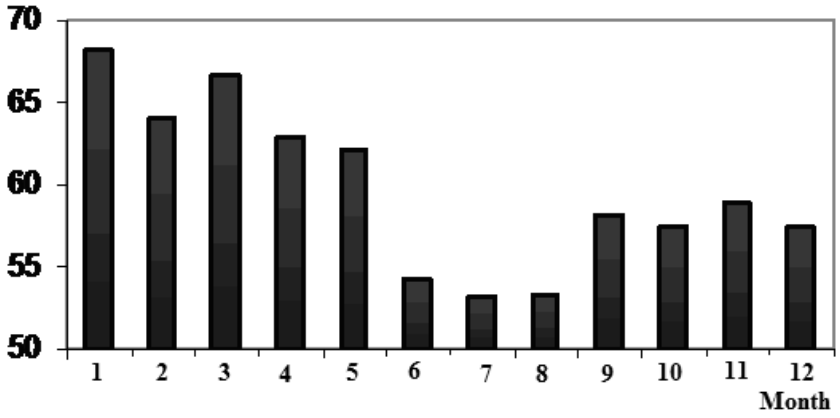

Fig. 1: Average number of daily emergency calls due to cardiovascular diseases by months in the city of Vilnius in 2007 – 2008

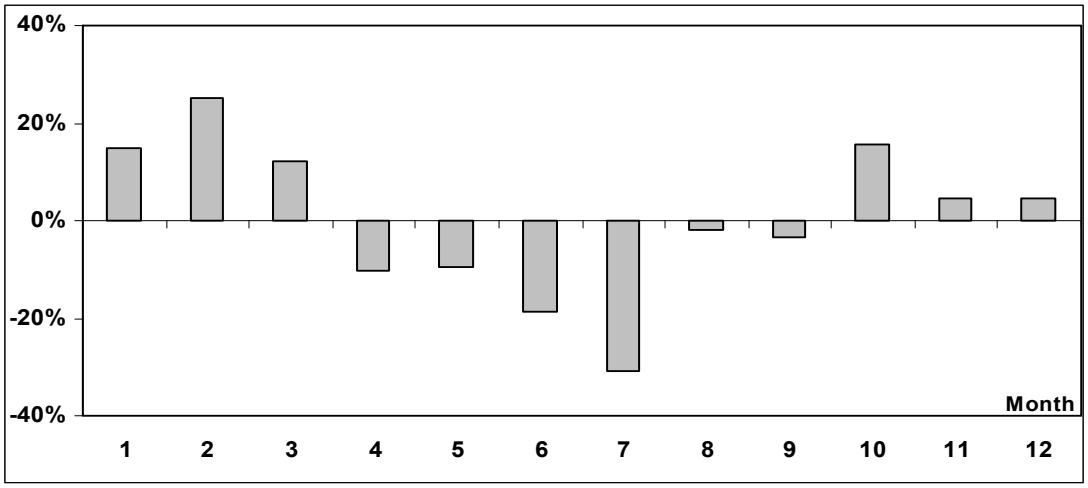

Fig. 2: Annual course of emergency calls related to myocardic infarcts in 2007 – 2008 (axis X represents averaged monthly call deviations from medium population figures)

Heart conduction disorder increases are correlated with mean air temperature and atmospheric pressure. Negative impacts are caused by daily temperatures from 10 to 15°C (t = 2,56), and when the atmospheric pressure is below 980 hPa, calls are increasing (r = 2,84), and when higher than 1010 hPa – decreasing (t = -2,22). Analyzing contribution of particular parameters to exacerbations of paroxysmal tachycardia, it become clear that negative impacts come from high pressure(>1010 hPa) (t = 2,43), and less numbers of cases happened under 0-5°C temperature conditions (t = -2,68). Heart atrium vibration and flutter often occur when atmospheric pressure falls below 980 hPa, noticeably increasing the number of calls (by 12% over general average). Negative impact on exacerbations of this disease has also wind speed from 4 to 6 m/s. Wind speed is mostly

significant for arterial hypertension. Exacerbations occur mostly under 4-6 m/s wind speed conditions and this correlation is statistically reliable, its Student criterion: t = 3,39. Meanwhile, cardiopathy cases are increasing under wind speed above average 6 m/s.

When looking for a weather class having the highest effect on diseases, we do not found significant association between diseases and anticyclonic circulation. But when the anticyclone begins to weaken and we have - 3 weather class - down slide motion at the edge of an anticyclone. Patients having paroxysmal tachycardia and complaining for higher blood pressure should be careful about weather conditions prevailing under this weather class, because a number of incidents is statistically significantly increasing. Under 4 weather type conditions (warm air advection in front of a cyclone), stroke incidence is statistically significantly increasing. In warm sector, brain stroke occurrences are increasing (t = 2,15). When we have easterly air flow (Class 9), number of cardiopathy cases is statistically significantly increasing (t = 2,81); this weather class is also dangerous for patients suffering from unstable angina pectoris. Heart atrium vibration and flutter are statistically significantly increasing (t = 3,55) under prevailing type 10 of weather (Indifferent weather situation (no dynamic processes)).

Examining correlation between PET index and cardiovascular diseases, it was established that under PET index in excess of 30°C threshold, a number of brain infarct cases is increasing (t = 2,55). There is also a correlation between cardiac insufficiency and PET, the index in excess of 30°C leads to increase of the number of cases (t = 2,23).

3.2 Respiratory diseases

Analyzed respiratory diseases' variety of causes and irritants is larger comparing to cardiovascular diseases. Variety of causes and irritants respiratory diseases is greater comparing to cardiovascular ones. 'J' group disease distribution over the year to present would be not purposeful, since different diseases have absolutely opposing patterns of their distribution. Essentially, respiratory diseases can be attributed to 2 groups: flaring up in summer and flaring up in winter. During warm period prevailing respiratory system diseases are acute tonsillitis (J03) and acute pharyngitis (J02), while during cold period - Acute nasopharyngitis and rhinitis (J00), acute laryngitis and tracheitis (J04) and other acute viral respiratory infections (J06).

„Wintry" cold diseases, as expected, have inverted linear dependence on mean, maximal and minimal temperature values. Their strongest correlation is with J04 group diseases. Similar dependence is observed, though slightly weaker, from dewpoint temperature and duration of sunshine. Exacerbation of almost all diseases is influenced also by relative humidity. Number of cases of acute viral respiratory infections increases with increasing humidity and decreasing temperature.

Relative air humidity and atmospheric pressure variations approaching threshold values, increases number of calls due to respiratory system diseases. Then, statistically significant increases the number of calls due to chronic obstructive lung disease, acute bronchitis and pneumonia. Temperature seems to be the most important factor determining exacerbations of cold diseases. Acute laryngitis and tracheitis unfavoured negative temperatures, while rhinitis and nasal pharyngitis more unfavourable are temperatures 0-10°C. 'Summerly' cold disease distribution regularities are opposite to 'wintry' ones.

Exacerbation of diseases is prompted by high temperature and precipitation as well as duration of sunshine. Number of cases increases with steadier increase of temperature. Inverse dependence is observed in relation to wind and air humidity as well as air pressure variations.

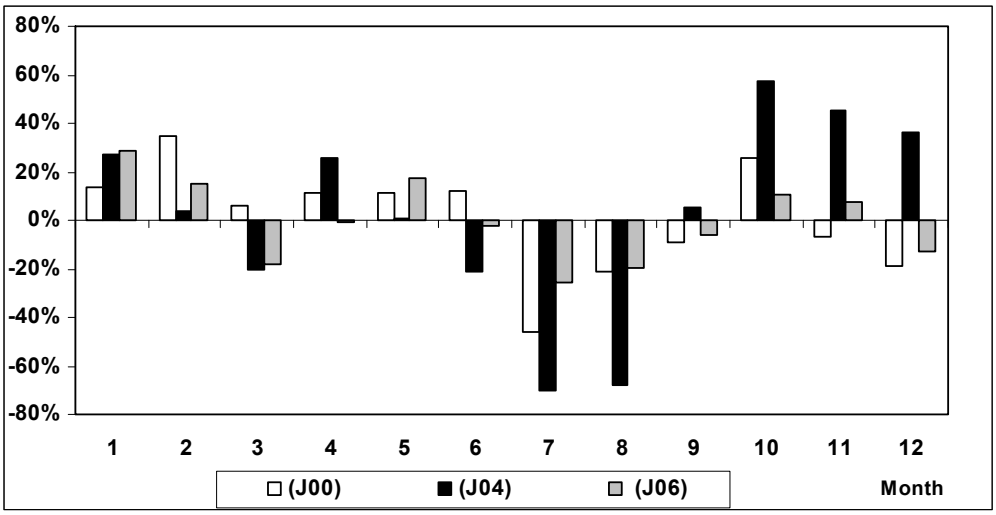

Fig. 3: Annual course of emergency calls related to „Wintry“ cold diseases in 2007 – 2008 (axis X represents averaged monthly call deviations from medium population figures)

Examining correlation between PET index and respiratory diseases, it was established that under PET index in excess of 30°C threshold ($t_{J02} = 2,86$, $t_{J03} = 2,89$). When looking for a weather class having the highest effect on diseases, we do not found significant association between respiratory diseases and weather classes. Only pneumonia statistically significantly decreasing (r = -2.88) under prevailing type 10 of weather (Indifferent weather situation (no dynamic processes)).

4. Conclusions

Nowadays medicine has passed into a new level in researches on diseases. Scientists are looking for the alternative ways in diagnosing and treatment of illnesses. People have noticed already that weather cannot only determine the mood. Various kinds of meteorological parameters complexes may bring significant influence on human's health. Our previously research already showed that the reaction of human constitution to the meteorological phenomenon changing and frequency was determined by making an inquisition. It turned out that to the most part of respondents' weather has high (50%) impact, especially when the weather is changing (83%). Because of this reason most of the people need biometeorological weather forecasts (Liukaityte, 2008).

Now we found that different meteorological parameters and has relationships with circulatory, cardiac, respiratory systems diseases. But our research based only on two years data of emergency visits to the patients. That to produce medical-meteorological

information and make special forecast for people with circulatory, cardiac, respiratory systems diseases, we need more research in this field.

Acknowledgement

The Author would like to thank the Lithuanian Hydrometeorological Service for enabling preparation of this presentation as well as rendering all necessary assistance and information. Also, the lecturers of the Department of Hydrology and Climatology of the Vilnius University for their guidance in the course of the work.

References

Bucher K., C. Haase, 1993: Meteorotropy and medical-meteorological forecasts. Experientia 49: 759-768.

Koken P.J.M., et al., 2003: Temperature, air pollution, and hospitalization for cardiovascular diseases among elderly people in Denver. Environ Health Perspect. 111(10): 1312–1317.

Kovats R.S, S. Hajat, P. Wilkinson, 2004: Contrasting patterns of mortality and hospital admissions during hot weather and heat waves in Greater London, UK. Occup. Environ. Med. 61(11): 893-898.

Liukaityte, J., 2008: Weather impacts on human health in Lithuania. Proc. 18th Int. Congress of Biometeorology 2008.

Makie T., et al., 2001: Association of meteorological and day-of-the-week factors with emergency hospital admissions in Fukuoka, Japan. Int J Biometeorol 46: 38–41.

Matzarakis, A., F. Rutz, H. Mayer, 2010: Modelling radiation fluxes in simple and complex environments: basics of the RayMan model. Int. J. Biometeorol 54(2): 131-139.

McGregor G.R., 2004: Winter North Atlantic Oscillation, temperature and ischaemic heart disease mortality in three English counties. Int. J. Biometeorol. 49, 197–204.

Michelozzi P., et al., 2009: High temperature and hospitalizations for cardiovascular and respiratory causes in 12 European cities. Am J Respir Crit Care Med. 179(5):383-389.

Spencer F.A., et al., 1998: Seasonal distribution of acute myocardial infarction in the second National Registry of Myocardial Infarction. J Am Coll Cardiol, 31, 226-1233.

Schwartz J., J. Samet J. Patz 2004: Hospital admissions for heart disease: the effects of temperature and humidity. Epidemiology 15:755–761.

Authors' address:

Judita Liukaityte, Justinas Savanevicius (judita.liukaityte@gf.vu.lt)
Department of Hydrology and Climatology,Vilnius University
M. K. Čiurlionio 21 / 27, LT – 01513 Vilnius, Lithuania

Mortality spatial variations in a small scale during heat waves in Lisbon - who is at risk?

Paulo Canário, Henrique Andrade

Centre of Geographical Studies, Institute of Geography and Spatial Planning, Univ. of Lisbon

Abstract

Impacts of heat waves in morbidity and mortality are largely known. Climate Change is expected to increase the climate health impacts in summer while during the winter these impacts will be probably favored.

The health impacts of extreme thermal events are mainly studied at a national or regional level, considering macro or mesoscale thermal features. But it can be assumed that local variations in mortality must exist, associated, in one hand, with local climatic differences, due to features such as land use and urbanization and, in other hand, with vulnerability factors, depending on demographic and socio-economic characteristics of populations. A model of hazard – vulnerability – risk was developed, to analyze the spatial variations of mortality in extreme thermal events, at the level of city district, in the Lisbon Metropolitan Area, Portugal. Small scale variation of meteorological features, in extreme thermal events, were simulated with a Regional Atmospheric Model (Brazilian Regional Atmospheric Modeling System - BRAMS) and the results were validated and calibrated using observation data from an urban network of termohigrometers placed in sites with different urban characteristics. These data along with thermal patterns data (obtained from the urban network of termohigrometers) and air quality information (ozone and PM) were then used to characterize heat stress events.

The relationship between temperature and daily mortality (especially during heat wave events) at a small scale, considering vulnerability factors, is an ongoing research. Spatial variations of mortality at this scale will be characterized, the most important vulnerability factors identified and risk areas will be delimitaded.

1. Introduction

A model of hazard – vulnerability – risk was developed, to analyze the spatial variations of mortality in extreme thermal events, at the city district level, in Lisbon Metropolitan Area (Portugal). The model fits into the global risk assessment framework for natural disasters (Zêzere, 2001) and is intended to be used primarily in urban areas. Risk is considered as the product of hazard, vulnerability and value (fig. 1).

Hazard is defined as the occurrence probability of extreme temperatures that, directly or indirectly, induce death. Several dimensions should be considered in hazard assessment: physical, chemical and biological. The physical dimension includes the thermal complex variables: air temperature, mean radiant temperature, wind and humidity (Matzarakis, 1998) and in what concerns the chemical dimension, those associated with air quality (ozone, PM_{10} and $PM_{2,5}$). The biological dimension refers to those elements whose influence in mortality is enhanced by physical and/or chemical elements of hazard: pollens, bacteria, virus and fungi.

In this investigation vulnerability is defined as the degree of loss (death rate) of the population at risk in a given area, as a result of the occurrence of a dangerous climate framework (extreme temperatures), for a certain period of time and it's a function of population sensitivity and exposure (Sanchez and Bertolozzi 2007, Confalonieri et al 2007). Whereas specific risk expresses the probability of deaths associated with certain extreme weather frameworks, total risk refers to the product between specific risk and

value. “Value” is defined as the values of human losses measurable as “years of life lost” – YLL (Campbell-Lendrum and Woodruff 2007; WHO 2008; Ezzati et al. 2002).

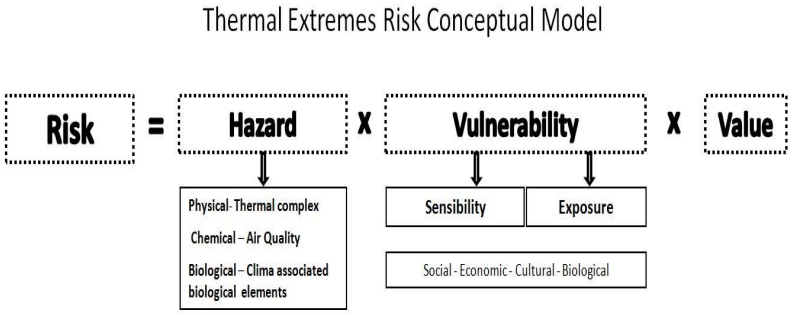

Fig. 1: Thermal Extremes Risk Conceptual Model

2. Hazard Assessment Methodology

Hazard assessment will require spatial modeling of the meteorological elements at the study area. Small scale variations of meteorological features, in extreme thermal events, are being simulated with a Regional Atmospheric Model (Brazilian developments on Regional Atmospheric Modeling System - BRAMS) on this ongoing research. Various types of input data will feed the model (fig.2). Sea surface temperature, topography (1 Km resolution), vegetation, a Normalized Difference Vegetation Index (NDVI) and soil humidity are needed to run the model.

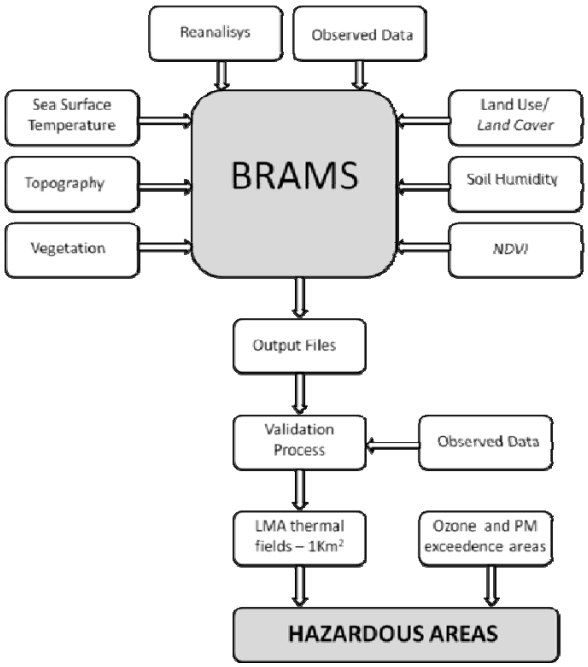

Fig. 2: Hazardous areas assessment

Reanalysis files (from NCEP-Reanalysis - Kalnay et al., 1996) to be used in the model will be downloaded containing u-wind, v-wind, geopotential, air temperature and relative humidity in several pressure levels. Land use/land cover information files will be provided to the model. In a downscaling study as this one, the BRAMS model allows assimilation of observed data in order to enhance the results accuracy. Thus, an urban

network of seventeen termo-higrometers placed in sites with different urban characteristics within the Lisbon Metropolitan Area (fig.3) was implemented and air temperature and humidity data from this sites are being inserted into the model.

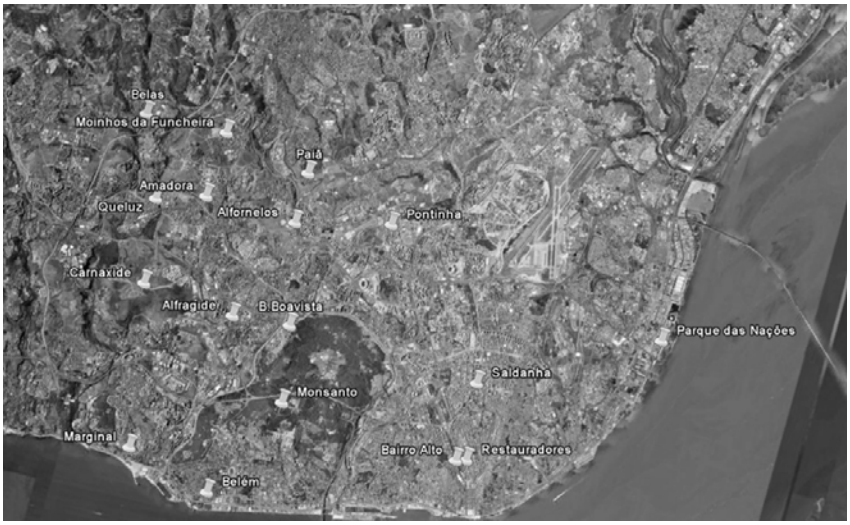

Fig. 3: Urban network of termo-higrometers in Lisbon Metropolitan Area

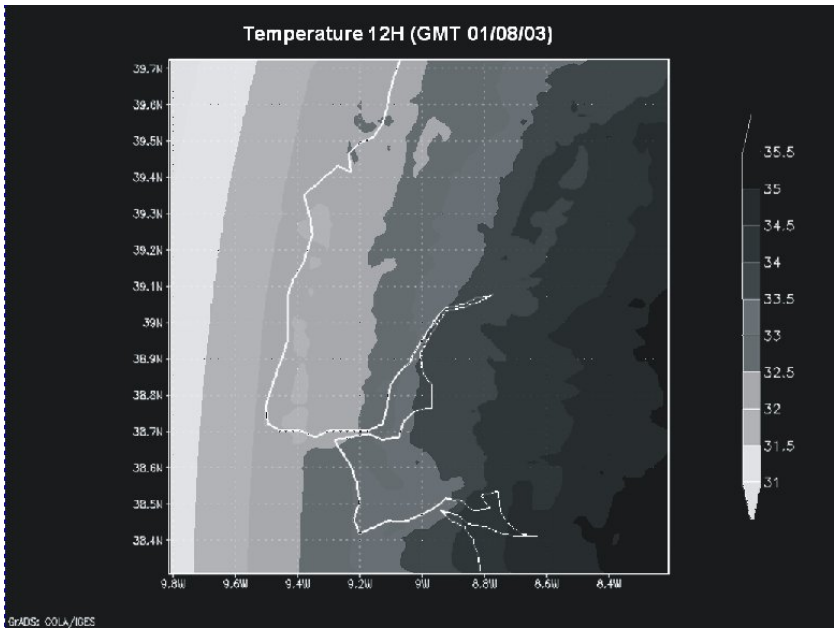

Fig. 4: Example of thermal fields in Lisbon Metropolitan Area during 2003 summer heat wave.

Data from radiosoundings (temperature, humidity and wind) will, as well, introduced into the model. A three nested grid methodology is being performed and the final model outputs will have one square kilometer resolution. The model outputs will be validated using data from the same registers network.

The results will show the thermal fields local variation during extreme thermal events in LMA with a square kilometer resolution. The BRAMS model is still being calibrated and parameterized in order to achieve the best accuracy possible. Figure 4 shows a first

output of a day, during the 2003 summer heat wave, in which more than five hundred people have died in consequence of extreme heat in the Lisbon Metropolitan Area.
Ozone and PM exceedence areas during extreme thermal events in Lisbon Metropolitan Area will be modeled as well (with the same resolution intend for thermal fields). Information generated by the two models will be integrated and the hazardous areas identified within the LMA.

References

Campbell-Lendrum, D., Woodruff, R., 2007: Climate change: quantifying the health impact at national and local levels. Editors, Prüss-Üstün A, Corvalán C. World Health Organization, Geneva. (WHO Environmental Burden of Disease Series No. 14).

Confalonieri, U., Menne,B., Akhtar,R., Ebi,K.L., Hauengue,M., Kovats,R.S., Revich,B.and Woodward,A.,2007: Human health. Climate Change 2007: Impacts, Adaptation and Vulnerability. Contribution of Working Group II to the Fourth Assessment Report of the Intergovernmental Panel on Climate Change, ML Parry, OF Canziani, JP Palutikof, PJ van der Linden and CE Hanson, Eds., Cambridge University Press, Cambridge, UK: 391-431.

Ezzati, M. Lopez, A.D., Rodgers, A., Hoorn, S.V., Murray, C.J.L. and the Comparative Risk Assessment Collaborating Group, 2002: Selected major risk factors and global and regional burden of disease. Lancet 360: 1347–60.

Kalnay, E., M. Kanamitsu, R. Kistler, W. Collins, D. Deaven, L. Gandin, M. Iredell, S. Saha, G. White, J. Woollen, Y. Zhu, M. Chelliah, W. Ebisuzaki, W. Higgins, J. Janowiak, K.C. Mo, C. Ropelewski, J. Wang, A. Leetmaa, R. Reynolds, R. Jenne, and D. Joseph, 1996: The NCEP/NCAR 40-Year Reanalysis Project., Bull. Amer. Meteor. Soc., 77, No. 3, 437-470

Matzarakis, A., Beckröge, W. and Mayer, H.,1998: Future perspectives in applied urban climatology. In Proc Second Japanese-German meeting, Report of Research Center for Urban Safety and Security, Kobe University, Special Report no 1: 109–122.

Sánchez, A., Bertolozzi, M., 2007: Pode o conceito de vulnerabilidade apoiar a construção do conhecimento em Saúde Coletiva? Ciência & Saúde Coletiva, 12(2):319-324.

World Health Organization, 2008: The Global Burden of Disease: 2004 Update. Department of Health Statistics and Informatics in the Information, Evidence and Research Cluster of WHO. Geneva, Switzerland.

Zêzere, J.L.,2001: Distribuição e Ritmo dos Movimentos de Vertentes na Região a Norte de Lisboa. Centro de Estudos Geográficos. Área de Geografia Física e Ambiente. Relatório nº 38.

Author's Adresses:
Paulo Canário (pmscanario@gmail.com)
Centre of Geographical Studies, Institute of Geography and Spatial Planning, Univ. of Lisbon
Edifício da Faculdade de Letras, Alameda da Universidade, 1600-214 Lisboa, Portugal

Prof. Dr.Henrique Andrade (henr.andr@gmail.com)
Centre of Geographical Studies, Institute of Geography and Spatial Planning, Univ. of Lisbon
Edifício da Faculdade de Letras, Alameda da Universidade, 1600-214 Lisboa, Portugal

Relation between climate and mortality in Vienna based on human-biometeorological data

Stefan Muthers[1], Andreas Matzarakis[1] and Elisabeth Koch[2]

[1] Meteorological Institute, University of Freiburg, Germany
[2] Central Institute for Meteorology and Geodynamics, Vienna, Austria

Abstract

The relation between heat stress and mortality has been analyzed for the period 1970-2007 in Vienna. PET (Physiologically Equivalent Temperature) was applied, to assess heat stress in a thermo-physiological manner. A significant increase of mortality was found for days with PET ≥ 29° C at 14 CET. For lower PET the mortality between April-October is significant below the baseline (-1.8 %). The highest values occur on days with extreme heat stress (PET ≥ 41° C) with +13 %. The mortality of women during heat stress is significant higher compared to men, and a slight increase was found for cardiovascular and respiratory diseases, compared to the overall mortality.

1. Introduction

The influence of the thermal environment on the human body is known since many years and is not reduced to single heat waves. An increase in mortality was found for cold stress too (Eurowinter, 1997). Additionally the influence is not limited to mortality, but mortality data is often used as an indicator for the general effect on human health, since mortality is recorded in many countries for a long time (Kovats und Shakoor 2008).

Thermal stress is a combination of many factors. Important meteorological components are the air temperature, water vapor, wind speed and different radiation fluxes. But also physiological components are involved; thermal sensation is influenced, by age, sex, activity level and others factors. Hence, simple meteorological indexes do not consider all the terms that are important for the human body.

In this study, the Physiologically Equivalent Temperature (PET) was used for an assessment of the thermal environment (Höppe und Mayer 1987). PET is based on the human energy balance model MEMI (Munich energy-balance model for individuals) (Höppe, 1984). It describes the thermal environment using all important meteorological components and combines them with physiological component. PET is defined as a distinct air temperature related to fixed standard indoor conditions where the heat balance of the human body shows the same core and skin temperature equal to the outdoor conditions assessed (Höppe, 1999). Compared to other thermal indices PET has the advantage of using a commonly known unit (°C), which makes the result easily understandable, also for people who may be unfamiliar with the human-biometeorological terminology.

Matzarakis and Mayer (1996) made an assignment of PET ranges to nine different grades of physiological stress for middle European countries, like Austria. The assignment reaches from extreme cold stress to extreme heat stress.

The relation between thermal stress and mortality varies from region to region (Keatinge et al. 2000). In this study, the relation between heat stress and mortality was analyzed using the 1.6 million population of Vienna.

2. Data and Methods

The analysis is based daily mortality data for the period 1970-2007. The data is classified by gender and cause of death according ICD-10.

The ZAMG climate station (Central Institute for Meteorology and Geodynamics) "Hohe Warte" in Vienna was selected to be representative for the population of Vienna. Climate data for 7, 14 and 19 CET was selected; the period is limited to the month April till October, since heat stress is absent in the other months.

Based on the climate data, the thermo-physiological conditions were assessed by the human-biometeological parameter PET. The calculation of PET and the required mean radiant temperature (T_{mrt}) is estimated by the RayMan model (Matzarakis et al., 2007).

Heat waves in early summer are known to have a higher impact on the human body compared to heat waves of the same magnitude in later summer (Hajat et al., 2002), since the body adapts physiologically to the thermal conditions (e. g. the sweat productions becomes more effective) and the people change their behavior (e. g.. the clothing selected). Due to this, an approach developed by Koppe and Jendritzky (2005) was applied to consider the short-term adaption effects. The approach uses the grades of physiological stress (Matzarakis and Mayer, 1996) and modifies the upper and lower limit of thermal comfort (PET 18° C and 23° C) to reflect the short-term adaption. The thermal conditions of the prior 30 days are described by an one-fold Gaussian smoother (Schönwiese, 2006). If this values is above the thermal comfort range, the upper limit is modified, by adding 1/3 of the Gaussian smooth value to the static threshold; for values below 18° C, one third is subtracted. The modification of the upper threshold (23° C) was done using the PET of 14 CET, for the lower threshold (18° C) the morning value was used. The limits of the other stress grades are moved accordingly.

To identify the additional mortality due to thermal stress, a baseline mortality was calculated. In this analysis a complex smoothing approach developed by Koppe and Jendritzky (2005) was used to calculate the baseline mortality. Basically this approach is based on a Gaussian smooth of one year, which is modified to reflect the real annual amplitude of the mortality values. This expected mortality was used to calculate the percentage daily deviations, which are called relative mortality below.

The analysis of the relation between thermal stress and mortality in Vienna is structured into different parts. First the general relation was examined by scatterplots of daily mortality and daily PET a 2 p. m in combination with a lowess smooth with a bandwidth of 0.75 (Cleveland and Devlin, 1988). In a second step the temporal reaction to thermal stress was studied. All days of the reference period were classified according grades of thermo-physiological stress (Matzarakis and Mayer; 1996). For each class, the mean mortality on the day and the following 30 days was calculated. To assess the impact of duration of heat stress situations, the mean mortality for subsequent days with PET $\geq$ 35° C and PET $\geq$ 41° C was calculated. The main analysis is based on four different grades of thermal stress, since the prior results allowed reducing of table 1. The heat

stress grades above 29° C were retained, but all grades below 29° C were combined to one grade.

For each class, the mean mortality was calculated and checks for significant differences in the mean value were done using T-tests. First the overall mortality, for men, women and all causes of death was used, afterwards differences between men and women as well as for death due to cardiovascular or respiratory diseases (C+R) were analyzed. This was done for the period 1970-2007 and per decade.

Sensitivity changes - changes in the relation between thermal stress and relative mortality - were analyzed by calculating the mean mortality for each thermal stress grade and each year and fitting a linear regression. Significant trend in this regression line were analyzed by T-tests.

The impact of the three heat stress classes was calculated, by combing the mean mortality per grade with the number of days for each grade and year for 1970-2007 and per decade. The product of both, the mean mortality and the number of days, is called cumulated heat related mortality and it describes the cumulated daily deviations of the mortality from the expected value for one year.

5. Results

Mortality rises sharply with PET values between 28° and 30°C. At lower values the mean relative mortality is slightly below the baseline and for higher values a sharp increase in the mean mortality was found. On the other side of the PET scale a slight increase was found. For cold stress this increase would be higher if the winter month and/or a lag of some days are considered.

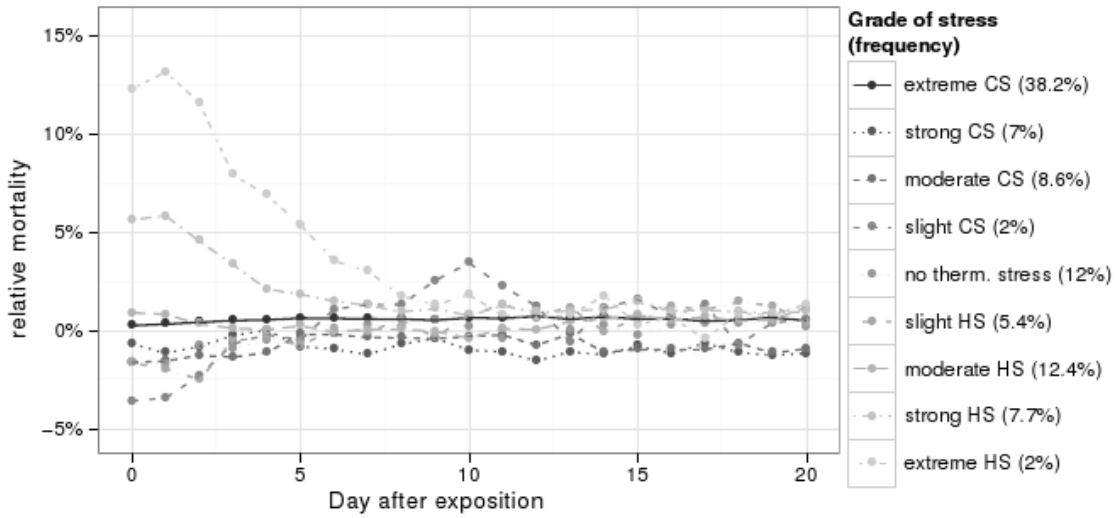

Fig. 1: Temporal reaction to different grades of thermal stress (Vienna, 1970-2007)

Figure 1 shows, that a strong increase of mortality exists on and after days with strong (PET 35-41° C) or extreme (PET ≥ 41° C) heat stress. In both cases, the mortality increases on the second day, but the differences were not significant. For strong and extreme the mortality stays eight days significantly above the baseline. Also the mortality

due to moderate (PET 29-25° C) heat stress is slightly raised. For this figure, the whole year was considered, to analyze the impact of cold stress classes. This shows that all other classes, except strong cold stress, are characterized by mortality values below the baseline, with a minimum on and after days with slight cold stress.

Strong cold stress is not of importance during April to October. Hence, the grades of physiological stress (table 1) were simplified and only the four highest heat stress levels and a large class with PET < 29° C ("thermal acceptability") were considered.

The previous approach does not consider the thermal conditions following days zero. Analyzing heat periods, were the thresholds 35° C or 41° C was exceeded on consecutive days, it was found that, the mean relative mortality rises during the first days. For days with PET ≥ 35° C from 2.6 % (CI: 1.4, 3.8) to 15.6 % (CI: 10.1, 21.2) on the sixth days. Periods with PET ≥ 41° C are characterized by a mean mortality of 8.9 % (CI: 6.4, 11.5) on the first day, increasing to 27.4 % (CI: 13.6, 41.3) on the fourth day.

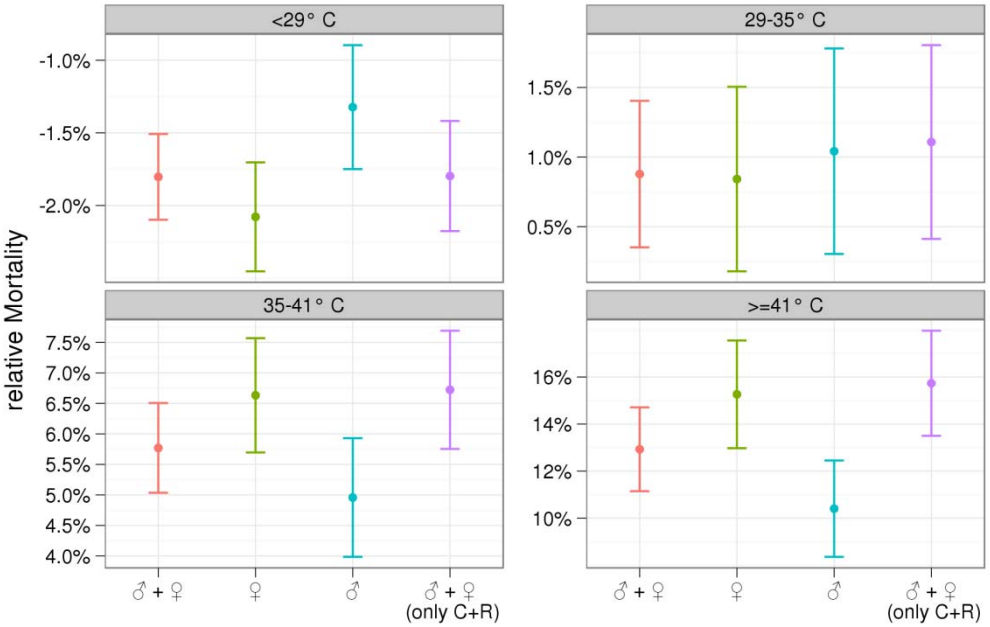

Fig. 2: Mean relative mortality and confidence interval for all causes and both sexes, women, men and cardiovascular and respiratory diseases (Vienna, 1970-2007)

Using the four levels of thermo-physiological stress (Fig. 2), it was found, that mortality is significant below the baseline on days with thermal acceptability (-1.8 %, CI: -2.1,-1.5). On days with heat stress, a significant increase was notices, with 0.9 % (CI: 0.4, 1.4) on days with moderate heat stress, 5.8 % (CI: 5.0, 6.5) on days with strong heat stress and 13.0 % (CI: 11.1, 14.7) on days with extreme heat stress. The differences between the classes were in any case significant. For women, the mortality was even higher with 15.3 % (CI: 13.0, 17.6) compared to men (10.4 %, CI: 8.4, 12.5) on days with extreme heat stress. The differences between men and women were significant, except on days with moderate heat stress. Additionally the mortality was higher for the causes

of death groups cardiovascular or respiratory diseases (C+R). But the differences were only in the highest grade significant (significance level 90%).

The mean mortality per grade was not constant during 1970-2007 (Fig. 3). The mean mortality per grade and year shows a significant decline of mean mortality on days with moderate (-0.08 % per year, CI: -0.05, -0.11) and strong (-0.10 % per year, CI: -0.06, -0.13) heat stress, whereas the number of days with heat stress increased during the last decades.
To assess the impact of the different heat stress levels for the heat related mortality during a typical year, the mean mortality has been combined with the number of days per stress grade. The product, the cumulated heat-related mortality, is highest on days with strong heat stress, but the differences to the extreme heat stress grade, where not significant. During the period of examination the relation changed, due to the significant decreases in mean mortality in the mid-grades. In 2001-2007 the days with extreme heat stress were responsible for the majority of heat related deaths.

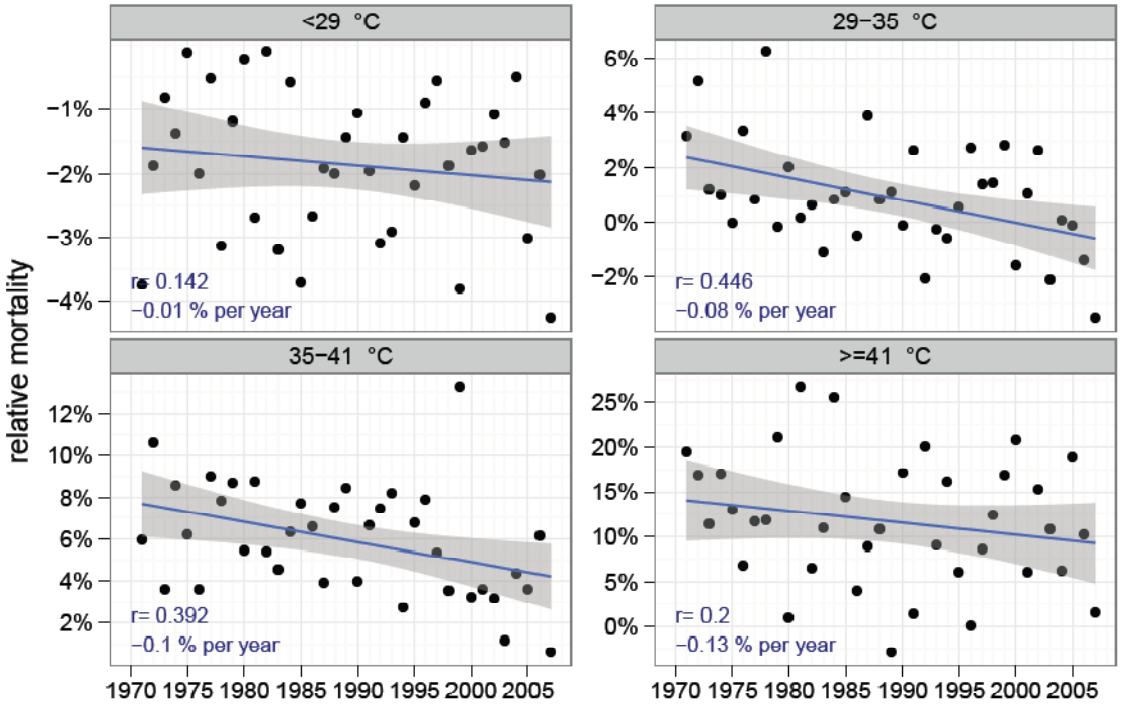

Fig. 3: Sensitivity changes in Vienna 1970-2007: Relative mortality per thermal stress grade and year and fitted linear regression with confidence interval

4. Conclusions

A strong relation between heat stress and mortality was found for Vienna. As in other regions (Koppe, 2005) an inverse relation exists, between the mean mortality and the frequency of heat stress situations.

The threshold between thermal acceptability in Vienna is situated around 29° C (PET). No changes of this threshold were found during the period of examination. Above this threshold, the increase of mortality is significantly higher for women compared to men. Additionally, patients with cardiovascular or respiratory diseases are at higher risk.

A significant decrease in mean mortality on moderate and strong heat stress grades was found between 1970 and 2000. This could indicate a successful adaptation process. On days with strong heat stress, a slight but not significant decrease was found. This could be the effect of a slight adaptation, combined with an increase in the absolute values of thermal stress.

Acknowledgement:
Thanks to the Austrian ministry for science and research for funding this study and to Gerhard Hohenwarter from ZAMG for providing the climate data.

References

Cleveland, W. S. and S. J. Devlin, 1988: Locally Weighted Regression: An Approach to Regression Analysis by Local Fitting. J Am Stat Assoc 83(403), 596–610.

Eurowinter: Keatinge, W. R., G. C. Donaldson, K. Bucher, G. Jendritzky, E. Cordiolo, M. Martinelli, L. Dardanoni, K. Katsouyanni, A. E. Kunst, J. P. Mackenbach, C. McDonald, S. Nayha, I. Vuori, 1997: Cold exposure and winter mortality from ischaemic heart disease, cerebrovascular disease, respiratory disease, and all causes in warm and cold regions of Europe. The Lancet 349(9062), 1341-1346.

Hajat, S., R. S. Kovats, R. W. Atkinson, A. Haines, 2002: Impact of hot temperatures on death in London: a time series approach. J Epidemiol Commun H 56, 367-372.

Höppe, P. 1984: Die Energiebilanz des Menschen. Diss. Fakultät für Physik der Ludwig-Maximilians-Universität München.

Höppe, P., H. Mayer, 1987: Planungsrelevante Bewertung der thermischen Komponente des Stadtklimas. Landschaft Stadt 19, S. 22–29.

Höppe, P. (1999), The physiological equivalent temperature - a universal index for the biometeorological assessment of the thermal environment. Int J Biometeorol 43, 71-75.

Keatinge, W. R., G. C. Donaldson, E. Cordiolo, M. Martinelli, A. E. Kunst, J. P. Mackenback, S. Nayha, I. Vuori 2000: Heat related mortality in warm and cold regions of Europe: observational study. Brit Med J 321(7262), 670-673.

Koppe, C., Jendritzky, G. 2005: Inclusion of short-term adaption to thermal stresses in a heat load warning procedure. Meteorol. Z. 14(2), 271-278.

Kovats, S., H. Shakoor 2008: Heat Stress and Public Health: A Critical Review. Annu Rev Publ Health 29, 41–55.

Matzarakis, A., Mayer, H. 1996: Another kind of environmental Stress: Thermal Stress' in WMO Newsletter 18

Matzarakis, A., Rutz, F., Mayer, H. 2007: Modelling radiation fluxes in simple and complex environments - application of the RayMan model. Int J Biometeorol 51(4), 323-334.

Schönwiese, C. D. 2006: Praktische Statistik für Meteorologen und Geowissenschaftler. Stuttgart: Gebrüder Borntraeger.

Authors' address:

Stefan Muthers (stefan.muthers@mars.uni-freiburg.de) and Prof. Dr. Andreas Matzarakis (andreas.matzarakis@meteo.uni-freiburg.de), Meteorological Institute, Albert-Ludwigs-University of Freiburg, Werthmannstr. 10, D-79085 Freiburg, Germany

Dr. Elisabeth Koch (elisabeth.koch@zamg.ac.at), Central Institute for Meteorology and Geodynamics, Hohe Warte 38, A-1190 Vienna, Austria

Environmental impacts on human health during a Saharan episode at Crete Island, Greece

P. T. Nastos[1,2*], K. N. Giaouzaki[3], N. A. Kampanis[2], P. I. Agouridakis[4] and A. Matzarakis[5]

[1]Laboratory of Climatology and Atmospheric Environment, Faculty of Geology and Geoenvironment, University of Athens, Greece
[2]Institute of Applied & Computational Mathematics, Foundation for Research & Technology-Hellas, Greece
[3]Department of Cardiology, School of Medicine, University of Crete, Greece
[4]Department of Emergency Medicine, School of Medicine, University of Crete, Greece
[5]Meteorological Institute, University of Freiburg, Germany

Abstract

The objective of this study is to examine the relationship of the environmental variability (weather and particulate air pollution conditions) with cardiovascular and respiratory syndromes, in Heraklion city at the northern part of Crete Island, during a Saharan dust episode on March, 22-23 2008. Daily counts of admissions for cardiovascular and respiratory syndromes were obtained from the two main hospitals in Heraklion. The corresponding daily meteorological parameters, such as maximum and minimum air temperature, relative humidity, wind speed, cloudiness and atmospheric pressure, from the meteorological station of Heraklion (Hellenic National Meteorological Service), were manipulated in multivariate analyses. Besides, the bioclimatic conditions expressed by the Physiologically Equivalent Temperature (PET), based on the energy balance models of the human body, are analyzed. Dust concentrations were derived from the SKIRON forecast model of the University of Athens.

The findings showed that the respiratory admissions were 3-fold than the mean daily admissions on the same day of the emergence of the Saharan dust episode (key day). The admissions concerning the cardiovascular syndromes did not appear any significant change. The analysis of the bioclimatic conditions on the key day revealed that thermal stress existed and this may be attributed mainly to the geomorphology of the island which is responsible for extreme weather conditions.

1. Introduction

Changes in the frequencies of extreme heat and cold and the profile of local or transboundary air pollution and aeroallergens would directly affect human health. These environmental changes are caused in specific cases by miscellaneous phenomena, such as Föhn winds - hot and dry winds - associated with extreme bioclimatic conditions and Saharan dust transport. Crete Island (Fig. 1), being in the Southeastern Mediterranean basin is affected by frequent Saharan dust episodes, resulting in very high particulate matter (PM) concentrations, which are associated with either short or long term effects on human health.

Long-term particulate matter exposure is connected with accelerated heart and lung disease because it contributes to pulmonary and systemic oxidative stress, inflammation, sybclinical chronic inflammatory lung injury, atherosclerosis and increased risk of ischemic heart disease and death (Pope et al., 2004; Souza et al., 1998). But besides the problem of exposure to PM over a long period (months or years), exposures from minutes to hours or days can also affect heart and lung function.

Short term exposures result in: increased rates of myocardial infraction associated with hospital admissions or death (Pope et al., 2006; Peters et al., 2001; Sullivan et al., 2005), heart rate disturbances such as paroxysmal atrial fibrillation or other arrhythmias (Lipsett et al., 2006; Rich et al., 2006; Grigoropoulos et al., 2009) and reduced lung function with episodes of acute asthma and bronchitis (Ho et al., 2007; Nastos, 2008; Monteil et al., 2009). Many studies have shown that short-term increase in mean daily levels of PM may also precipitate acute cardiac decompensation leading to hospitalization, especially in patients with ischemic heart disease (Wellenius et al., 2005).

Fig. 1: Crete Island, Greece. Heraklion city is indicated by a rectangular frame

The present study evaluates the role of short-term increases of dust concentrations in daily counts of admissions for cardiovascular and respiratory syndromes at the wider area of Heraklion, Crete Island, Greece, during a Saharan dust episode on March, 22-23 2008.

2. Data and Analysis

Daily counts of admissions for cardiovascular (acute coronary syndrome, arrhythmia, decompensation of heart failure) and respiratory (pulmonary infection, acute exacerbation of chronic obstructive pulmonary disease, acute asthma crisis and syncoptic-presyncoptic) syndromes were obtained from the two main hospitals in Heraklion, during March-April 2008. The corresponding daily meteorological parameters, such as maximum and minimum air temperature, air humidity, wind speed, cloudiness and atmospheric pressure, were acquired from the meteorological station of Heraklion (Hellenic National Meteorological Service. Besides, the bioclimatic conditions expressed by the Physiologically Equivalent Temperature (PET), based on the energy balance models of the human body, are analyzed (Matzarakis et al., 1999). Dust concentrations were derived from the SKIRON forecast model of the University of Athens, while daily composite anomalies (reference period: 1968-1996) of the air temperature and vector wind from the middle to the lower atmospheric levels (500hPa – mean sea level) on March, 23 2008, calculated from the reanalysis datasets of the National Centers for Environmental Prediction/National Center for Atmospheric Research (NCEP/NCAR) (Kalnay et al., 1996).

3. Results and Discussion

The examined Saharan dust episode affected Crete Island firstly at noon on March, 22 2009 and became more appreciable the next day, as it is depicted in Fig. 2, where the aerosol optical thickness, the dust concentration (μg m^{-3}) at 10 m and the dry deposition (mg m^{-2}) over the wider area of Heraklion are presented from the SKIRON forecast model of the University of Athens.

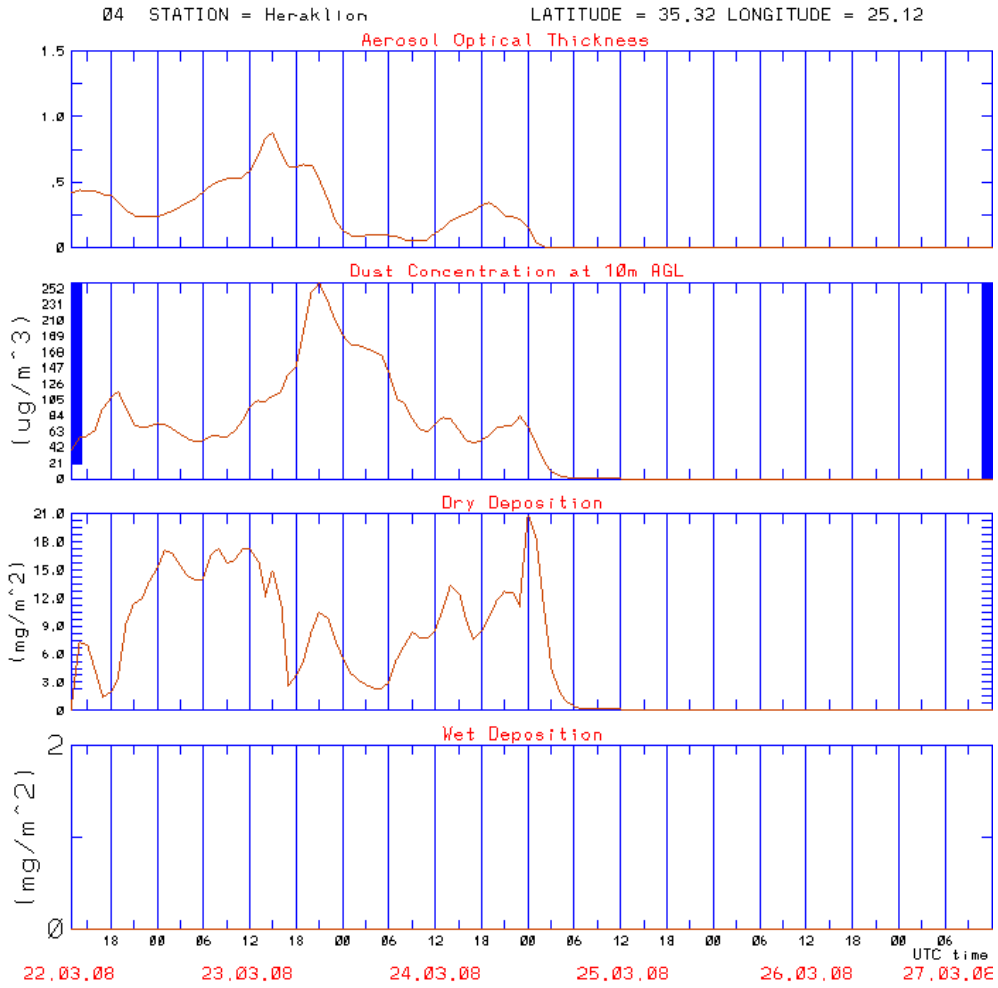

Fig. 2: Output (dustgram) from SKIRON forecast model of the University of Athens, concerning aerosol optical thickness, dust concentration at 10m, dry and wet deposition over Heraklion, Crete on March, 22-27 2008

High values of dust concentrations (252 μgm^{-3}) appeared over the city causing an asphyxiating environment. Moreover, the south-eastern wind blow was the main factor for extreme bioclimatic conditions, which could be attributed to the Föhn phenomenon, a normal situation under these synoptic conditions.

The daily composite anomaly (reference period: 1968-1996) of the air temperature from the middle to the lower atmospheric levels (500hPa – mean sea level) on March, 23 2008 (Fig. 3) revealed that positive anomalies (~ +5 ^{o}C at the 500hPa isobaric level, ~ +12 ^{o}C at the 850 hPa isobaric level, ~ +7^{o}C at surface) appear. Additionally, high positive daily composite anomalies of south-eastern winds (~ +25 m/s at the 500 hPa isobar-

ic level, ~ +17 m/s at the 850 hPa isobaric level, ~ +10m/s at surface) show the strong transport of Saharan dust over Crete area.

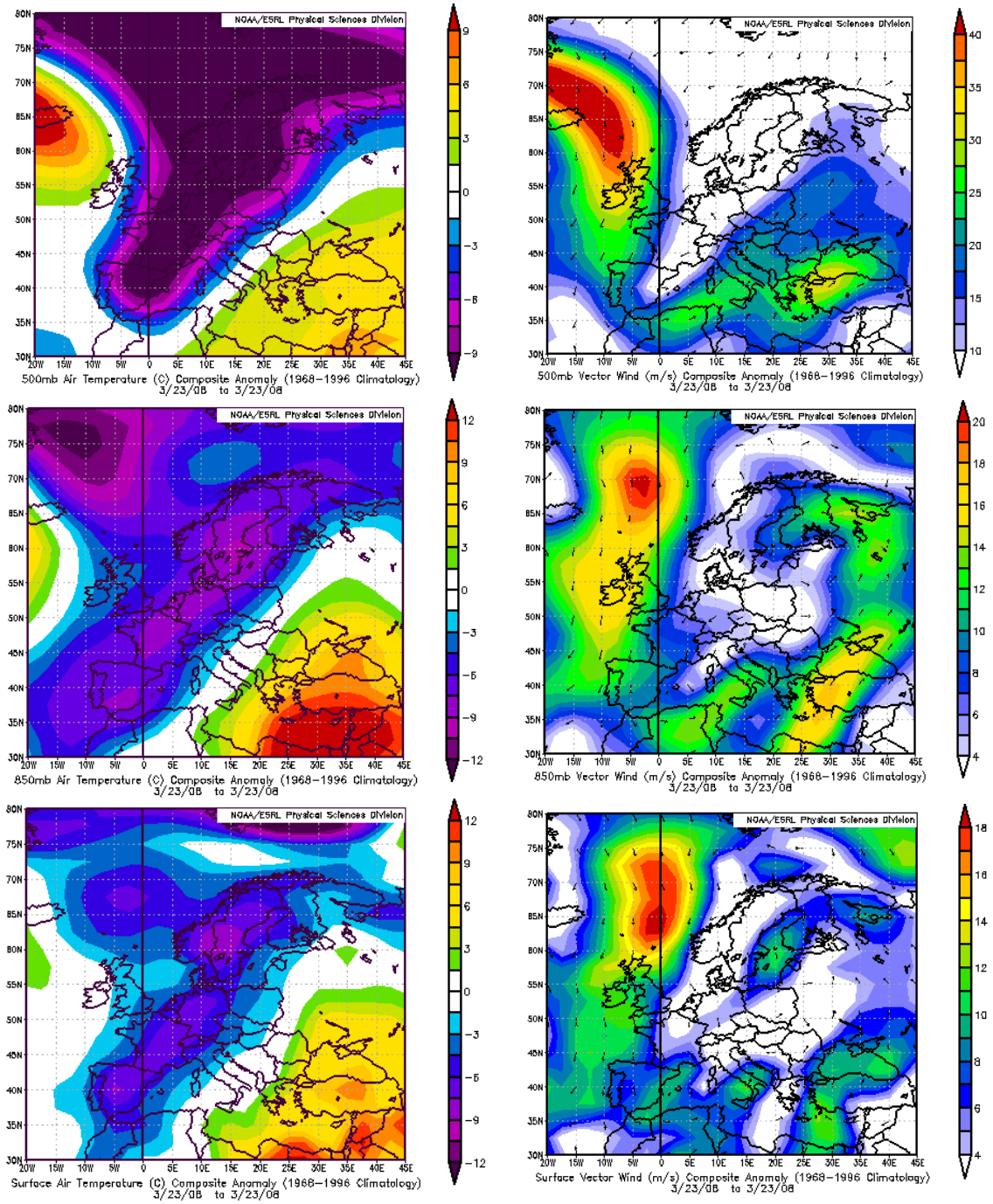

Fig. 3: Daily composite anomalies (reference period: 1968-1996) of air temperature (left graphs) and vector wind (right graphs) for 500 hPa level (upper graphs), 850hPa level (middle graphs) and surface (lower graphs) on March, 23 2008, calculated from the NCEP/NCAR reanalysis data

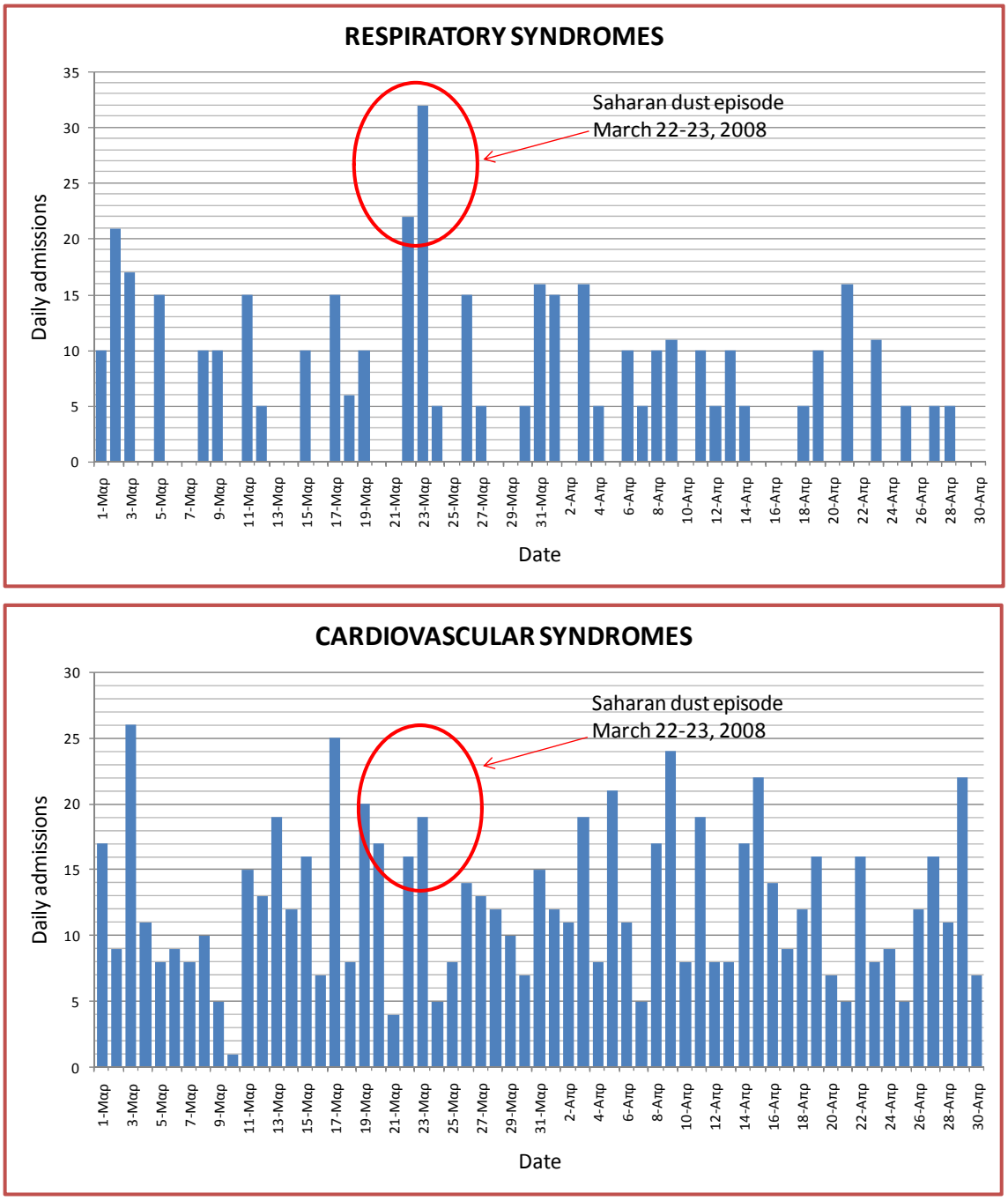

Fig. 4: Daily admissions concerning respiratory (upper graph) and cardiovascular (lower graph) syndromes at Heraklion, Crete Island, in March-April 2008

As far as the bioclimatic conditions are concerned, the physiologically equivalent temperature (PET), estimated from RAYMAN model (Matzarakis et al., 2007), reached 29.3 ^{o}C at 13:00 UTC on March, 23 2008, giving evidence of moderate heat stress at the beginning of Spring season, when Saharan dust episodes are more frequent (Kosmopoulos et al., 2008).

The daily counts of admissions for cardiovascular and respiratory syndromes, which were obtained from the two main hospitals in Heraklion city, are depicted in Fig. 4. It is clear the impact of the Saharan dust episode in the increased incidence of respiratory

syndromes, giving evidence that high dust concentrations, which are associated with high PMs concentrations (Mitsakou et al., 2008), trigger respiratory syndromes outbreak. The daily counts were approximately 5-fold than the mean daily counts (6.6 admissions) on the same day of the emergence of the Saharan dust episode. On the other hand, it seemed not to be any significant increase in the cardiovascular syndromes attributed to the Saharan episode. Cardiovascular syndromes appeared high variability within the examined period.

Acknowledgement

The authors would like to acknowledge the NOAA/ESRL Physical Sciences Division, Boulder Colorado, for the provided daily composite images and the Atmospheric Modeling and Weather Forecasting Group (AM&WFG), School of Physics, National and Kapodistrian University of Athens for the output of SKIRON model on March, 23 2008.

5. Conclusions

The Saharan dust episode on March, 22-23 2009 affected Crete Island, Greece, establishing moderate heat stress bioclimatic conditions and increased dust concentrations over Heraklion city (case study). These outdoor factors linked to respiratory syndromes outbreak, while cardiovascular syndromes were not associated with high dust concentrations resulted from Saharan episode.

References

Grigoropoulos, K.N., P.T. Nastos, G. Feredinos, 2009: Spatial distribution of PM1 and PM10 during Saharan dust episodes in Athens, Greece. Advances in Science and Research 3, 59–62.

Ho, W-C., W. Hartley, L. Myers, M-H. Lin, Y-S. Lin, C-H. Lien, R-S. Lin, 2007: Air pollution, weather and associated risk factors related to asthma prevalence and attack rate. Environmental research 104, 402-409.

Kalnay, E. and Coauthors, 1996: The NCEP/NCAR Reanalysis 40-year Project. Bulletin of American Meteorological Society 77, 437-471.

Kosmopoulos, P.G., D.G. Kaskaoutis, P.T. Nastos, H.D. Kambezidis. 2008: Seasonal variation of columnar aerosol optical properties over Athens, Greece, based on MODIS data, Remote Sensing of Environment 112, 2354–2366.

Lipsett, M., F. Tsai, L. Roger, M. Woo, B. Ostro, 2006: Coarse particles and heart rate variability among older adults with coronary artery disease in the Coachella Valley, California. Environmental Health Perspectives 114, 1215-1220.

Matzarakis, A., H. Mayer, M.G. Iziomon, 1999: Applications of a universal thermal index: physiological equivalent temperature. International Journal of Biometeorology 43, 76-84.

Matzarakis, A., F. Rutz, H. Mayer, 2007: Modelling Radiation fluxes in simple and complex environments – Application of the RayMan model. Int. J. Biometeorol. 51, 323-334.

Mitsakou, C., G. Kallos, N. Papantoniou, C. Spyrou, S. Solomos, M. Astitha, C. Housiadas. 2008: Atmospheric Chemistry and Physics Saharan dust levels in Greece and received inhalation doses. Atmospheric Chemistry and Physics 8, 7181–7192.

Monteil, M.A., R. Antoine, 2009: African dust and asthma in the Caribbean: medical and statistical perspectives. International J Biometeorology 53, 379-381.

Nastos, P.T., 2008: Weather, Ambient Air Pollution and Bronchial Asthma in Athens, Greece. Advances in Global Change Research (AGLO), M. C. Thomson et al. (eds.), Seasonal Forecasts, Climatic Change and Human Health. © Springer Science + Business Media B.V. 2008

ISBN 978-1-4020-6876-8 e-ISBN 978-1-4020-6877-5, DOI 10.1007/978-1-4020-6877-5, Library of Congress Control Number: 2007942723, 173-188.

Peters, A., D.W. Dockery, J.E. Muller, M.A. Mittleman, 2001: Increased particulate air pollution and the triggering of myocardial infarction. Circulation 103, 2810-2815.

Pope, C.A. III, J.B. Muhlestein, H.T. May, D.G. Renlund, J.L. Anderson, B.D. Horne, 2006: Ischemic Heart Disease Events Triggered by Short-Term Exposure to Fine Particle Air Pollution. Circulation 114, 2443-2448.

Pope, C.A. III, R.T. Burnett, G.D. Thurston, M.G. Thun, E.E. Calle, D. Krewski, J.J. Godleski, 2004: Cardiovascular mortality and long-term exposure to particulate air pollution: epidemiological evidence of general pathophysiological pathways of disease. Circulation 109, 71-77.

Rich, D., M. Mittleman, M. Link, J. Schwartz, H. Luttmann-Gibson, P. Catalano, F. Speizer, D. Gold, D. Dockery, 2006: Increased risk of paroxysmal atrial fibrillation episodes associated with acute increases in ambient air pollution. Environmental Health Perspectives 114, 120-123.

Souza, M.B., P.H.N. Saldiva, C.A. III Pope, V.L. Capelozzi, 1998: Respiratory changes due to long-term exposure to urban levels of air pollution: a histopothologic study in humans. Chest 113, 1312-1318.

Sullivan, J., L. Sheppard, A. Schreuder, N. Ishikawa, D. Siscovick, G. Kaufman, 2005: Relation between short-term fine particulate matter exposure and onset of myocardial infarction. Epidemiology 16, 41-48.

Wellenius, G., T. Bateson, M. Mittleman, J. Schwartz, 2005: Particulate Air Pollution and the rate of hospitalization for Congestive Heart Faillure among medicare Beneficiaries in Pittsburgh, Pennsylvania. American Journal of Epidemiology 161(11), 1030-1036.

Corresponding Author's address:
Assoc. Prof. Dr. Panagiotis Nastos (nastos@geol.uoa.gr)
Laboratory of Climatology and Atmospheric Environment, Faculty of Geology and Geoenvironment, University of Athens, Panepistimiopolis GR 157 84, Athens, Greece

Untersuchungen zum Einfluss des Klimawandels in Deutschland auf den Start der Pollensaison, die Saisonlänge und die Pollenkonzentration der wichtigsten allergenen Pollen anhand der Pollendaten der Referenzstationen des Polleninformationsdienstes PID

Uwe Kaminski[1], Tom Glod[2]

[1]Deutscher Wetterdienst Freiburg, Zentrum für Medizin-Meteorologische Forschung
[2]Universität Trier, FB Geographie

Zusammenfassung

Mehr als fünfzehn Millionen Deutsche leiden jedes Jahr an Heuschnupfen. Klinische Studien haben gezeigt, dass es zwischen Pollenexposition und dem Auftreten von allergischem Schnupfen eine eindeutige Dosis-Wirkungs-Beziehung gibt. Die Anzahl von Atemwegserkrankungen aufgrund von Pollen in der Luft hat in den letzten Jahrzehnten weltweit zugenommen. Welchen Einfluss haben hierbei veränderte klimatische Bedingungen? Anhand der Pollendaten der PID Referenzstationen (Polleninformationsdienst) wird für die wichtigsten allergenen Pollen (Hasel, Erle, Birke, Gräser und Beifuss) und für die Regionen Nordwest-, Nordost- und Süddeutschland untersucht, ob sich im Rahmen des Klimawandels der Start der Pollensaison, die Saisonlänge und die Gesamt- sowie die Peak-Pollenkonzentration im Laufe der letzen Jahre (1988-2009 für Nordwest- und Süddeutschland und 1994-2009 für Nordostdeutschland) verändert haben. Mögliche Trends werden mit dem Mann-Kendall Test auf ihre Signifikanz überprüft. Die Ergebnisse zeigen, dass hinsichtlich des Starts des Pollenflugs und der Pollenmenge in Süddeutschland und Nordostdeutschland die stärksten Veränderungen eingetreten sind.

Abstract

More than fifteen million people in Germany each year suffer from hay fever and rhinitis. Clinical studies showed that there is a clear dose-response-relationship between pollen exposition and the occurrence of allergic rhinitis. The number of respiratory diseases due to pollen in the air increased in the last decades world-wide. What influence do changed climatic conditions have? On the basis of the pollen data of the PID reference-stations (Pollen Information Service) we examined for the main allergic pollen (hazel, alder, birch, grasses and mugwort) and for the regions Northwest, Northeast and South Germany whether in the context of changing climate the start of the pollen season, the season length and the total amount as well as the peak pollen concentration changed in the course of the last years (1988-2009 for Northwest and South Germany and 1994-2009 for Northeast Germany). Possible trends are analysed by means of the Mann-Kendall test for their significance. Regarding the start of the pollen season and the total pollen amount, the results demonstrate that the changes are strongest in South- and Northeast Germany.

1. Einleitung

Betrachtet man in Deutschland den Zeitraum 1901-2000, dann hat in allen Jahreszeiten eine ziemlich gleichmäßige Erwärmung in der Größenordnung von 1 °C stattgefunden. Der global gemittelte jährliche Vergleichswert beträgt + 0,7 °C. Diese, wie alle Klimatrends, sind zeitlich nicht stabil und so zeigt sich in den letzten beiden Jahrzehnten 1981-2000 ein deutliches Erwärmungsmaximum mit +2,3°C im Winter, gefolgt von +1,3°C im Frühling; die Herbsttemperatur zeigt keinen Trend (Schönwiese et al. 2005). Wärmere, kürzere Winter sowie höhere Frühlingstemperaturen und ein früherer Frühlingsanfang stellen Pflanzen und natürlich auch die Allergiker schon heute vor

große Herausforderungen. Räumlich gesehen fällt die Erwärmung im Süden am stärksten aus, im Nordwesten Deutschlands ist sie geringer. In den Gebirgen ist die Nullgradgrenze in den letzten 50 Jahren um 210 m höher gewandert. Phänologische Beobachtungen zeigen ebenfalls, dass sich der Blühbeginn von z.B. Hasel und Erle um etwa 10 Tage nach vorne verschoben haben. Spiegeln sich diese Klimaänderungen aber auch in den Pollenauswertungen wider?

2. Auswertung der Daten

Als Datengrundlage wurden die täglichen Pollenmesswerte des Polleninformationsdienstes an den Referenzstationen Delmenhorst, Hannover, Bad Lippspringe, Mönchengladbach (Nordwestdeutschland), Greifswald, Berlin, Dresden (Nordostdeutschland) und Fulda, Freiburg, München (Süddeutschland) herangezogen (Abb. 1). Untersucht wurden die allergenen Pollen Hasel, Erle, Birke, Gräser und Beifuss hinsichtlich einer Verschiebung des Startzeitpunktes des Pollenfluges, der Saisonlänge und der Gesamt-Pollen- sowie der Peak-Pollenkonzentration. Roggenpollen wurde bewusst ausgeklammert, da Roggen eine Kulturpflanze ist, deren Anbau und Verbreitung zeitlich variiert und damit Trendaussagen schwierig macht.

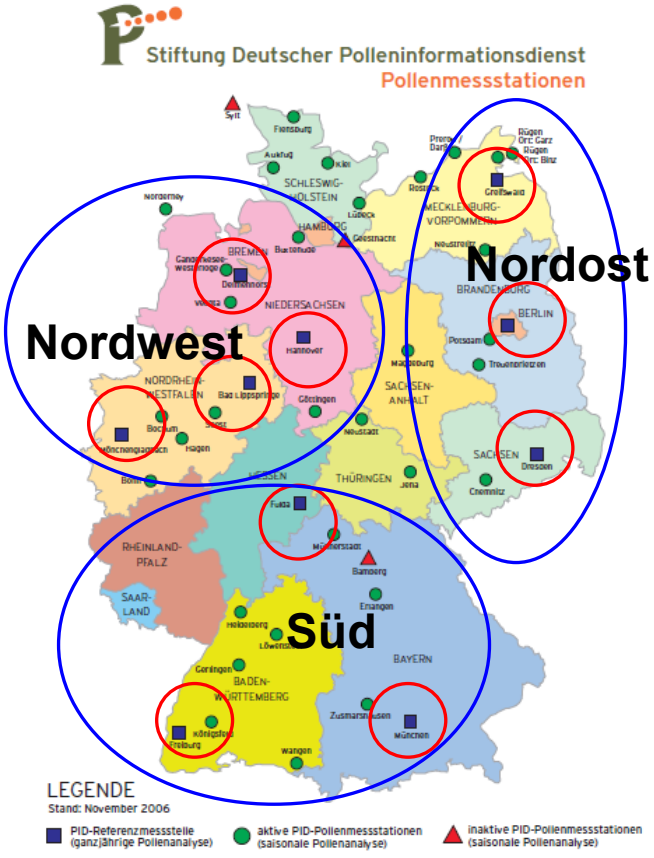

Abb. 1: Pollen Referenzstationen des PID (rote Kreise) und die Gebiete Nordwest, Nordost und Süd, für welche die Auswertungen zusammengefasst wurden

Häufig setzt der Pollenflug einer bestimmten Art nicht sofort mit starker Intensität ein, sondern der Pollenflug wird vor Beginn und nach Ende der Hautpollenflugsaison von zeitlich unregelmäßig auftretenden Pollen geringer Anzahl geprägt, deren Auftreten von

verschiedensten eher zufälligen Faktoren oder durch Ferntransport bestimmt wird. Da eine statistische Auswertung durch diese unscharfe Eingrenzung der Hauptpollensaison erschwert wird, wendet man die verschiedensten Verfahren zur Bestimmung der Hauptpollensaison an. Jato et al. (2006) geben eine Überblick über diese Verfahren. In der vorliegenden Untersuchung wurde zur Bestimmung der Hauptpollensaison der Ansatz von Andersen (1991) gewählt: Er definiert diesen Zeitraum als die Periode, ab der die Summe der täglichen mittleren Pollenkonzentration 2,5% der gesamten Pollenmenge erreicht bis zu dem Zeitpunkt, an dem die Summe 97,5% beträgt, d.h. die Hauptpollensaison umfasst 95% der gesamten Pollenmenge.

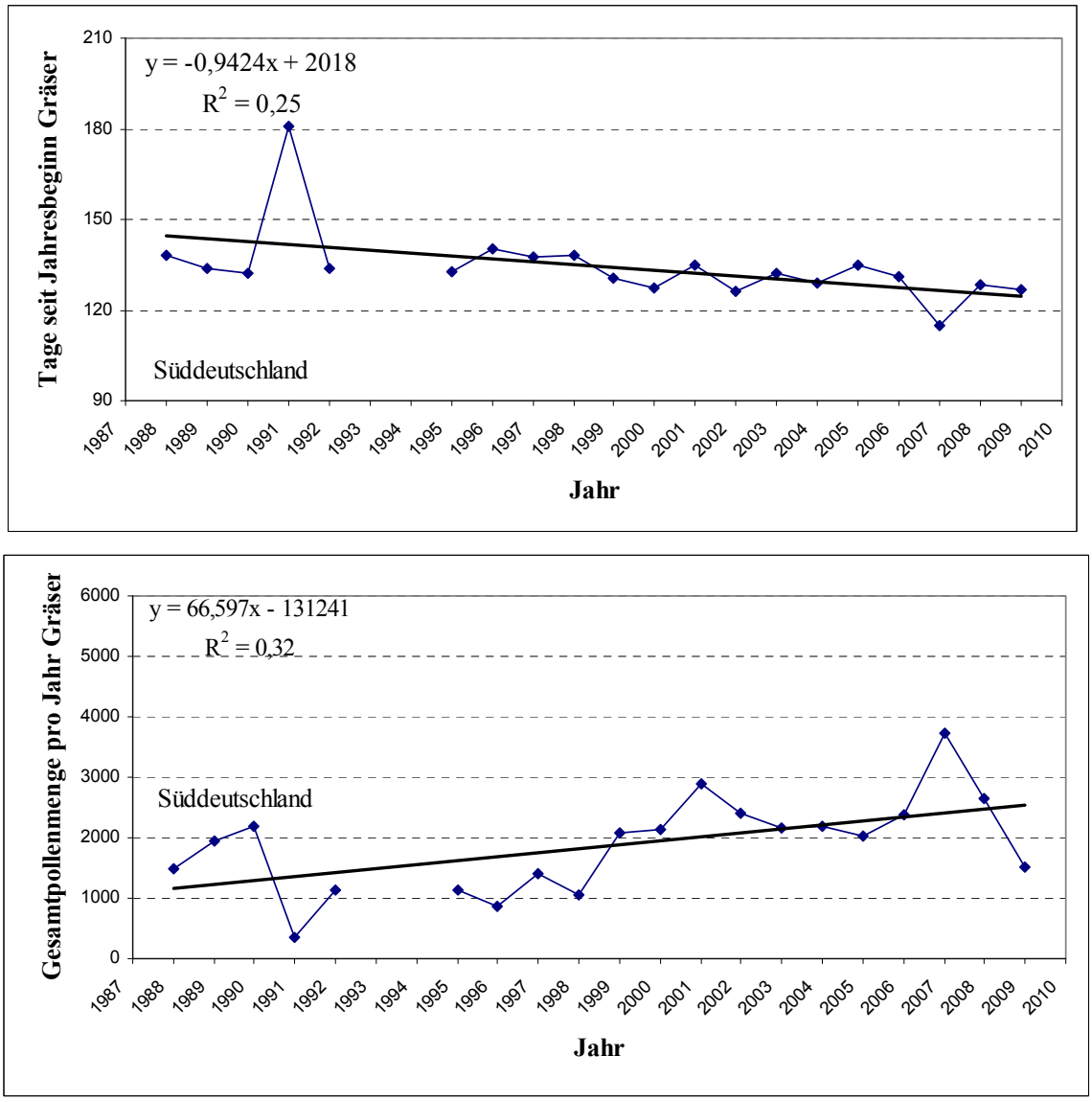

Abb. 2: Zeitlicher Verlauf (1988-2009) des Starts der Haupt Pollensaison für Gräser mit Regressionsgerade (oben) und Gesamt-Pollenmenge mit Regressionsgerade (unten) während der Haupt Pollensaison und den Bereich Süddeutschland

Auf diese Weise wurden für alle Stationen, alle Jahre und die genannten Pollenarten der Start- und der Endtermin der Hauptpollensaison bestimmt. In der sich daraus ergebenden Pollensaison wurde die gesamte Pollenmenge aufsummiert und die Peak-Konzentration ermittelt. Diese Ergebnisse wurden dann zu Gebietsmitteln für die Be-

reiche Nordwest, Nordost und Süd zusammengefasst. Ein Beispiel für Gräserpollen und den Südbereich zeigt die Abb. 2. In Süddeutschland setzt der Pollenflug von Gräsern gegenüber 1988 um 20 Tage früher ein (Tag 125 statt Tag 145), gleichzeitig hat sich die jährliche Pollenmenge mehr als verdoppelt (von 1150 auf 2550 Pollen).

Ob die derart ermittelten möglichen Trends auch statistisch signifikant sind, wurde mit dem Mann-Kendall Test ermittelt (Mann, 1945; Kendall, 1970). Dieser Test prüft, auf welchem Signifikanzniveau oder mit welcher Irrtumswahrscheinlichkeit ein monotoner An- oder Abstieg in den Daten vorhanden ist, vorausgesetzt den Daten ist kein saisonaler oder anderer Zyklus überlagert, wovon aber bei den kurzen Pollenepisoden ausgegangen werden kann.

Der Starttermin für den Pollenflug ist in den meisten Fällen an das Erreichen einer bestimmten Temperatursumme über einen bestimmten Zeitraum gekoppelt. So setzt z.B. in Freiburg der Birkenpollenflug ein, wenn die Temperatursumme der Tagesmaxima, ausgehend vom Starttermin 1. Februar, einen Wert von etwa 576°C erreicht hat (Eistage werden hierbei auf 0°C gesetzt). Die Gesamtpollenkonzentration einer Art, die im Laufe eines Jahres ausgezählt wurde, ist in erster Näherung von der Witterung während der Pollenflugsaison abhängig.

3. Ergebnisse und erkennbare Trends

Die Pollensaison der Gräser setzt in Süddeutschland im Mittel (lineare Regression) 20 Tage früher ein, dauert 24 Tage länger (1988 waren es 76 Tage, im Jahr 2009 im Mittel 100 Tage) und die Gesamt- wie auch die Peak-Pollenkonzentration hat sich etwa verdoppelt. Der Birkenpollenflug setzt verglichen mit 1988 heute zwar 10 Tage später ein, aber die Gesamt-Pollenmenge ist um mehr als Faktor 4 angestiegen. Ebenso bei Haselpollen und Erlenpollen (etwa Faktor 5). Der Start des Beifuss Pollenflugs setzt 20 Tage später ein, Saisonlänge und Pollenmengen zeigen aber keinen signifikanten Trend.

In Nordostdeutschland, wo nur der Zeitraum 1994-2009 vorhanden ist, sind keine signifikanten Veränderungen hinsichtlich des Beginns des Pollenflugs sichtbar, aber auch hier haben die Gesamt-Pollenmengen von Hasel (Faktor 16), Erle (Faktor 8), Birke (Faktor 6) und Gräsern (ähnlich wie in Süddeutschland etwa Faktor 2) zugenommen. Die Saisonlänge des Beifuss Pollenflugs hat sich um 13 Tage verlängert (von 34 auf 47 Tage).

In Nordwestdeutschland zeigt nur die Erle einen signifikanten um 30 Tag früher einsetzenden Pollenflug und die Saisonlänge hat sich von 26 auf 49 Tage fast verdoppelt. Bei der Hasel stieg die Gesamt-Pollenmenge um etwa Faktor 3 an. Beim Beifuss Pollenflug ist zwar die Saisonlänge im Mittel von 28 auf 42 Tage angestiegen, die Gesamt- und Peak-Pollenmengen sind aber nur noch halb so hoch wie zu Beginn der Messreihe.

Die kompletten Ergebnisse des Mann-Kendall Tests zeigt die Tabelle 1. Die Symbole in der Tabelle 1 haben folgende Bedeutung:

+	signifikanter Trend	$\alpha = 0{,}1$	Signifikanzniveau 90%
*	sehr signifikanter Trend	$\alpha = 0{,}05$	Signifikanzniveau 95%
**	hoch signifikanter Trend	$\alpha = 0{,}01$	Signifikanzniveau 99%
***	höchst signifikanter Trend	$\alpha = 0{,}001$	Signifikanzniveau 99,9%

Tabelle 1: Signifikante Trends für **S**üddeutschland (oben), **N**ord**o**stdeutschland (Mitte) und **N**ord**w**estdeutschland (unten). Rote und grau hinterlegte Symbole zeigen eine Zunahme der Werte an

	S				
	Hasel	Erle	Birke	Gräser	Beifuss
Start Pollensaison			*	**	*
Pollenmenge	+	+	***	*	
Saisonlänge				*	
Peakkonzentration	+		*	*	

	NO				
	Hasel	Erle	Birke	Gräser	Beifuss
Start Pollensaison					
Pollenmenge	***	**	*	*	
Saisonlänge					+
Peakkonzentration	*	*	+	**	

	NW				
	Hasel	Erle	Birke	Gräser	Beifuss
Start Pollensaison		*			
Pollenmenge	*			+	*
Saisonlänge		*			*
Peakkonzentration	*				**

4. Schlussfolgerungen

Die Untersuchungen zeigen, dass in den Pollendaten deutliche Trends vorhanden sind. Im Nordwesten setzt der Flug von Erlenpollen um 30 Tage früher ein, im Süden der Pollenflug von Gräsern um 20 Tage. Besonders signifikant ist eine deutliche Erhöhung der Gesamt-Pollenmenge und zum Teil der Peak-Konzentrationen. Die meistens Trends treten in Süddeutschland auf und gehen damit mit der stärksten regionalen Erwärmung einher.

Ein bei einigen Arten früherer Beginn der Pollensaison, eine teilweise längere Pollenflugzeit und höhere Pollenmengen haben die Belastung der Allergiker in den letzten Jahren verstärkt. Klimaprojektionen sagen einen weiteren CO_2-Anstieg und davon ausgehend eine weitere Temperaturzunahme vorher, welche die Bildung von Biomasse und die Pollenproduktion begünstigt. Somit wird wahrscheinlich auch in der Zukunft das Allergiepotential weiter ansteigen.

Literatur

Andersen, T.B., 1991: A model to predict the beginning of the pollen season, Grana 30, 269-275.

Jato, V., Rodríguez-Rajo, F.J., Alcázar, P., De Nuntiis, P., Galán, C., Mandrioli, P., 2006: May the definition of pollen season influence aerobiological results? Aerobiologia 22, 13-25.

Kendall, M.G., 1970: Rank Correlation Methods. Griffin, London.

Mann, H.B., 1945: Nonparametric test against trend. Econometrica, 13, 245-259.

Schönwiese, C.-D., Staeger, T., Trömel, S., 2005: Klimawandel und Extremereignisse in Deutschland. Klimastatusbericht des DWD 7 , 7 - 17.

Authors' address:

Uwe Kaminski (uwe.kaminski@dwd.de)
Zentrum für Medizin-Meteorologische Forschung
Stefan-Meier-Str. 4-6, D-79104 Freiburg, Germany

Climate Change and Adaptation Strategies for Pollens in Korea

Young-Jean Choi[1], Ki-Jun Park[1], Kyu Rang Kim[1], Hye-Rim Lee[1], Chae Yeon Yi[1] and Jae-Won Oh[2]

[1]Applied Meteorology Research Laboratory, National Institute of Meteorological Research, Korea Meteorological Administration, Seoul, Korea

[2]Departments of Pediatrics, Hanyang University College of Medicine, Guri, Korea

Abstract

Airborne pollen is known as one of the major causal agents to respiratory allergic reactions. Daily number of pollen grains was monitored using Burkard volumetric spore traps at eight locations including Seoul and Jeju island in the Republic of Korea during 1997-2009. Pollen grains were observed throughout the year especially from February to November. They showed similar distribution patterns of species among locations except in Jeju, where Japanese cedar vegetation is uniquely found. Peak seasons for pollen grains from trees, grasses, and weeds were March to May, May to September, and August to October, respectively. Tree pollens were mainly composed of pine, oak, alder, and birch. Weed pollens were mainly from Japanese hop, sagebrush, and ragweed. Statistical analyses including simple correlation and multiple regression were conducted between the day-to-day fluctuations of pollens and various meteorological variables so that we can estimate the increase of pollens as the consequences of the climate change. Diameter of pollen grains, which has a typical range of 20~60㎛, has close relationship with allergenicity. Pollens from trees and weeds have higher allergenicity than those from grasses in general. The allergenicity of the pollen grains is observed to depend on the concentration of atmospheric carbon dioxide. The elevated level of pollen allergenicity together with the increased number of airborne pollens can be more harmful to the allergic patients in the future.

1. Introduction

With many people spending their time outdoors, a growing number of people contract allergic diseases caused by pollens. The advanced countries in Europe and North America have long realized its importance and have warned the people, who are sensitive to allergies, of the seriousness of allergic diseases (Buck et al, 1985, Vazquez et al., 2003, Smith and Emberlin, 2006, Stach et al, 2007). In 1819, John Bostock disclosed that pollens can cause diseases to the human body. Since the late 1960s, the United States and European nations have continued epidemiological studies of pollens. In the 1970s, scientists in Japan, the Philippines, and Taiwan released the outcome of studies on pollens. In the 1980s, research was conducted on the relationship between pollens and allergic diseases (Oh et al., 1998). Korea, however, remains at the early stage in terms of its research on pollen forecasts.

2. Methods

There are eight pollen observation sites, which are operated by the Korean Academy of Pediatric Allergy and Respiratory Disease and KMA throughout Korea. Pollen grains are sampled by Burkard Seven Day Recording Volumetric Spore Traps. Then the pollen grains are counted using a microscope and the counted data are stored in a pollen database. The pollen data used in this study are provided by the Korean Academy of Pediatric Allergy and Respiratory Disease. Fig. 1 shows the pollen collector.

The daily pollen data at each observation site were grouped by month and pollen classes (tree, grass, and weed). They are analyzed by correlation and multiple regression analyses using weather conditions as independant variables.

Fig. 1: The pollen trap installed at the KMA's Shindaebang-dong field in Seoul, Korea

3. Results

Airborne pollen is known as one of the major causal agents to respiratory allergic reactions. Daily number of pollen grains was monitored using Burkard volumetric spore traps at eight locations including Seoul and Jeju during 1997-2009. Pollen grains were observed throughout the year especially from February to November. They showed similar distribution patterns of species among locations except in Jeju, where Japanese cedar vegetation is uniquely found. Peak seasons for pollen grains from trees, grasses, and weeds were March to May, May to September, and August to October, respectively. Tree pollens were mainly composed of pine, oak, alder, and birch. Weed pollens were mainly from Japanese hop, sagebrush, and ragweed. Diameter of pollen grains, which has a typical range of 20~60□, has close relationship with allergenicity. Allergenicity of tree and weed pollens is higher than that of grass pollens in general.

The pollen calendar in Fig. 2 shows the pollen species and their monthly distribution. Generally, pollens are observed all the year round, except for the winter months (November to February). The distribution differs for each species of pollen. The pollens of trees and shrubs are observed from March to May; those of grass from May to September; and those of weeds from August to October. In the case of trees and shrubs, pine trees account for about 70% of all tree pollens. However, pine pollens are weak allergens. The remaining 30% of tree pollens, including alder trees, white birches, and oaks, are moderate to strong allergens despite the smaller numbers. Also despite their small numbers, grass and weeds are also highly likely to cause allergies. Especially, the pollens of *Artemisia vulgaris* and *Humulus japonicus* are highly likely to cause allergies. The allergenicity of each pollen species of interest in Korea was investigated in a separate research by interviewing selected patients everyday during the pollen seasons. The allergenicity calendar was developed based on the number of observed pollens considering their allergenic properties (Fig. 3).

Daily fluctuations in the number of pollens have to do with a variety of meteorological factors, such as temperature, rainfalls, and the duration of sunshine. Correlation analyses were performed between the daily number of pollens and various meteorological factors grouped by month and pollen classes – tree, grass, and weed. Air temperature and sunshine hours were major driving variables in daily observed pollens: higher temperature and sunshine hours induced more pollens. Cumulative degree-day represented physiological age of the plants so that the flowering season could be explained by it with many pollen analyses. Rainfall supressed daily

number of pollens because of its wash-out effect. Wind speed promoted the number of pollens through enhancing the release and dispersal of pollens. In some cases it suppressed the number of pollens by diluting the pollen concentration if there was not much release at the source. Based on these relationships between the weather conditions and the number of pollens, we developed forecasting equations for allergenicity of each pollen class and for each observatory. They were able to forecast daily allergenicity of pollens with ca. 60% of accuracy.

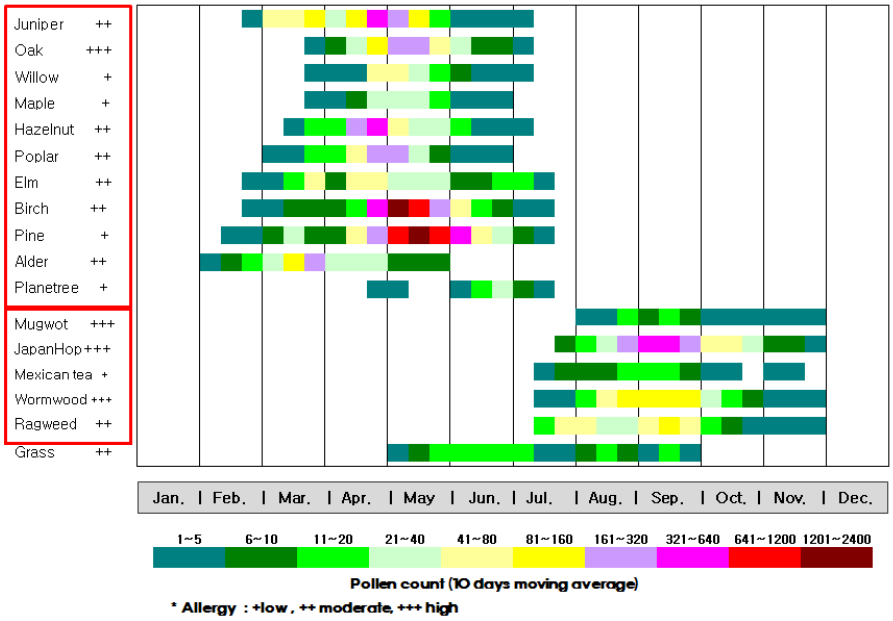

Fig. 2: A pollen calendar of Seoul. The calendar was created based on the pollen count data measured over the past eleven years (1997-2008)

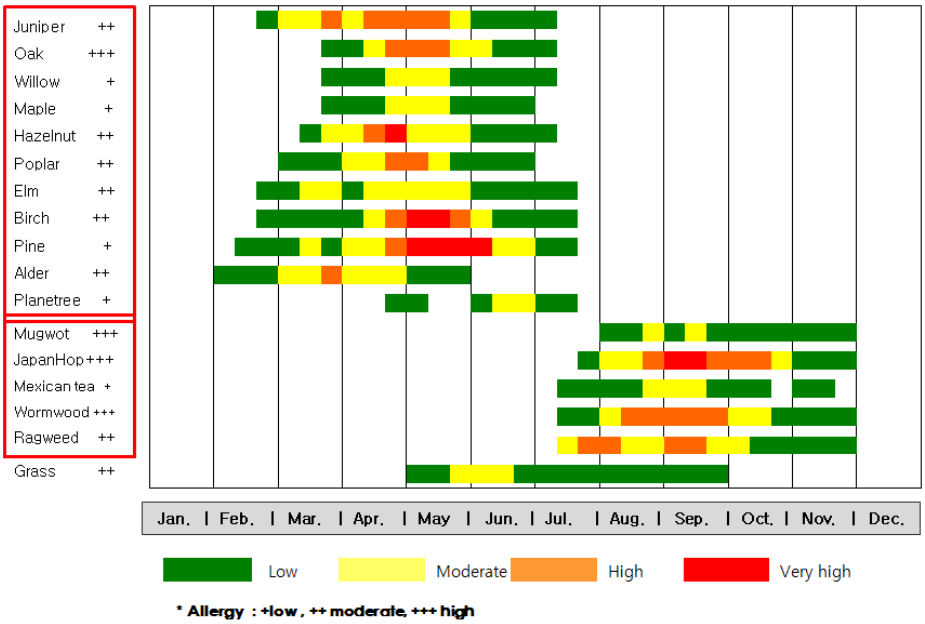

Fig. 3: Pollen allergenicity calendar based on daily observation of pollen counts in Seoul during 1997-2008

4. Conclusions

Korea Meteorological Administration has a plan to develop an accurate pollen index forecast model by improving the existing forecast equations. It is going to build a nationwide pollen observation network in close cooperation with related agencies for the purpose of securing quality data of pollens. In a short time, it will supply the people with comprehensive pollen forecasts over the Internet.

We can also apply these forecasting equations to climate change scenarios so that we can estimate the amount and allergenicity of pollens in the future. In addition to the increase of temperature, the climate change scenario includes increasing CO2 concentration. Singer et al. (2005) reported that rising atmospheric CO2 concentration is related to increasing Amb a 1 content, which is the major allergen of ragweed. The elevated level of allergenicity of pollens along with their increased numbers can be more harmful to the allergic patients in the future.

The projected increase in warning levels in the future based on the increased number and allergenicity of the pollens would be helpful for the decision makers to prepare against pollinosis in the changing climate.

Acknowledgement

This study was financially supported by Advanced Research on Industrial Meteorology of National Institute of Meteorological Research (NIMR) / Korea Meteorological Administration (KMA).

References

Buck P, E. Levetin, 1985: Airborne pollen and mold spores in a subalpine environment, Ann Allergy, 55, 794-801.

Oh, J.-W., H.-B. Lee, H.-R. Lee, B.-Y. Pyun, Y.-M. Ahn, K.-E. Kim, S.-Y. Lee and S.-I. Lee,1998: Aerobiological study of pollen and mold in Seoul, Korea. Allergology International, 47:263-270.

Singer, B. D., L.H. Ziska, D.A. Frenz, D.E. Gebhard, J.G. Straka, 2005: Increasing Amb a 1 content in common ragweed (*Ambrosia artemisiifolia*) pollen as a function of rising atmospheric CO2 concentration. Functional Plant Biology 32, 667-670.

Smith, M. and J. Emberlin, 2006: A 30-day-ahead forecast model for grass. Int J Biometeorol., 50:233-242.

Stach A, Smith M, Skjoth C. A, Brandt J, 2007: Examing ambrosia pollen episodes at Poznan (poland) using back-trajectory analysis, Int J Biometeorol 51, 275-286.

Vázquez, L. M., C. Galán, E. Domínguez-Vilches, 2003: Influence of meteorological parameters on olea pollen concentrations in Cordoba (South-Western Spain). Int J Biometeorol., 48:83-90.

Authors' address:

Dr. Young-Jean Choi (yjchoi@kma.go.kr), Ki-Jun Park, Dr. Kyu Rang Kim (krk9@kma.go.kr), Hye-Rim Lee, Chae Yeon Yi
Applied Meteorological Research Laboratory,
National Institute of Meteorological Research,
45 Gisangcheong-gil, Dongjak-gu, Seoul, Republic of Korea

Dr. Jae-Won Oh, MD, PhD (jaewonoh@hanyang.ac.kr)
Department of Pediatrics, Hanyang University College of Medicine
Hanyang University Guri Hospital, Guri, Republic of Korea

Ambrosia Pollen-Konzentrationen in Baden-Württemberg

Uwe Kaminski[1], Beate Alberternst[2], Thomas Gabrio[3], Michael Böhme[3], Stefan Nawrath[2], Heidrun Behrendt[4]

[1]Deutscher Wetterdienst Freiburg, Zentrum für Medizin-Meteorologische Forschung
[2]Arbeitsgruppe Biodiversität Friedberg
[3]Landesgesundheitsamt Baden-Württemberg im Regierungspräsidium Stuttgart
[4]ZAUM - Zentrum für Allergie und Umwelt, TU München

Zusammenfassung

Die Beifuss-Ambrosie auch Beifussblättriges Traubenkraut genannt, besitzt ein starkes allergenes Potential. In welchem Ausmaß stellen die Pollenemissionen vorhandener Ambrosia-Bestände in Baden-Württemberg bereits eine Belastung für die Anrainer-Bevölkerung dar? Zur Beantwortung dieser Frage wurde der Ambrosia-Pollenflug in einem Gebiet mit großen Ambrosia-Beständen (Waghäusel) mit einem Kontrollgebiet mit geringen Ambrosia-Beständen (Ravensburg, Bad Waldsee-Reute) verglichen. Die gemessenen Pollenkonzentrationen, der derzeit in Baden-Württemberg vorhandenen Ambrosia-Populationen sind noch nicht so hoch wie in Ungarn oder Frankreich, wo sich die Ambrosie massiv ausgebreitet hat und Pollenkonzentrationen von mehreren Tausend erreicht werden können. Die Untersuchungen zeigen jedoch, dass in der unmittelbaren Nähe größerer Ambrosia-Vorkommen höhere Pollenkonzentrationen erreicht werden können. Luftmassenherkunftsanalysen ergaben, dass die höchsten Ambrosia Pollen-Konzentrationen bei Ferntransport aus Südfrankreich beobachtet werden.

Abstract

Ambrosia or Ragweed exhibits the strongest pollen allergen world-wide. To which extent do pollen emissions of existing Ambrosia plants in Baden-Württemberg already represent a load for the population nearby? To answer this question, the number of Ambrosia pollen was compared in an area with large Ambrosia in place (Waghäusel) with a control area without Ambrosia or with only small Ambrosia populations (Ravensburg, Bad Waldsee-Reute). At present the measured pollen concentrations of existing Ambrosia populations in Baden-Württemberg are not yet as high as in Hungary or France, where Ambrosia plants substantially spread and pollen concentrations are in the order of several thousands. However, there are higher pollen concentrations in the direct proximity of larger Ambrosia populations in Germany than in a greater distance of the source. Air mass origin analyses showed that the highest Ambrosia pollen concentrations occurred with long-range transport from Southern France.

1. Einleitung

Die Beifuß-Ambrosie (*Ambrosia artemisiifolia* L. 1753), auch Beifußblättrige Ambrosie, Beifußblättriges Traubenkraut oder Common Ragweed genannt, ist eine einjährige Pflanzenart, die in Nordamerika beheimatet ist und von dort unbeabsichtigt nach Europa eingeschleppt wurde. Die Pollen dieser Pflanzenart besitzen ein hohes allergenes Potenzial und sind in Nordamerika Hauptverursacher von Atemwegsallergien im Spätsommer. Auch in verschiedenen europäischen Ländern wie z.B. Ungarn (Kadocsa und Juhász, 2002; Makra et al., 2005), Slowenien, Kroatien (Cvitanovic et al., 2007), Frankreich (Déchamp und Méon, 2002; Laaidi et al., 2003) und Norditalien (Asero, 2007), wo sich die Ambrosie in den letzten Jahren bis Jahrzehnten stark ausgebreitet hat, verursacht sie zunehmend allergische Erkrankungen und stellt damit eine gesundheitliche Belastung für die Bevölkerung dar. Die Beifuß-Ambrosie wurde auch nach Deutschland eingeschleppt und tritt hier in verschiedenen Regionen wie z.B. in der Niederlausitz, in

Südhessen und in Baden-Württemberg (z.B. in der Oberrheinebene) zunehmend auf. Aufgrund seiner geografischen und meteorologischen Lage zählt Baden-Württemberg zu den Regionen in Deutschland, in denen sich *Ambrosia artemisiifolia* möglicherweise bevorzugt ausbreiten könnte, wie beispielsweise im klimatisch begünstigten Oberrheingraben. Untersuchungen aus den USA und Australien deuten darauf hin, dass der Klimawandel den Ausbreitungsprozess der Art fördert (Wayne et al., 2002; Ziska et al., 2003).
Allergische Haut- und Atemwegserkrankungen gehören in den hochentwickelten Industrienationen zu den häufigsten Erkrankungen. Eine Ausbreitung der Beifuß-Ambrosie in Deutschland und damit auch eine Zunahme der Pollenbelastung der Luft könnte zu einer Erhöhung der Sensibilisierungsrate und zu einer Zunahme allergischer Erkrankungen führen, da Studien gezeigt haben, dass Sensibilisierungen mit der Menge der inhalierten Pollen korrelieren (Jäger, 2000).

2. Projektbeschreibung, Projektziele und Vorgehensweise

In einer interdisziplinär angelegten Studie wurde zwischen 2006 und 2008 vom Landesgesundheitsamt Stuttgart (LGA), vom Zentrum für Allergie und Umwelt München (ZAUM), vom Deutschen Wetterdienst (DWD) und von der Projektgruppe Biodiversität und Landschaftsökologie, Friedberg (PBL) in zwei Regionen Baden-Württembergs untersucht, wie weit die Beifuß-Ambrosie in den Untersuchungsgebieten verbreitet ist, welche Pollenmengen in der Luft nachweisbar sind und ob bereits Sensibilisierungen gegen diese Pollen bei Kindern der 4. Klasse vorliegen (Alberternst et al., 2009).
Wesentliche Ziele des hier beschriebenen Projektes waren:
a) die Abschätzung des von *Ambrosia artemisiifolia* ausgehenden Risikos für die menschliche Gesundheit durch:

- die Erfassung der vorhandenen Pflanzenbestände in zwei unterschiedlich stark mit der Art besiedelten Regionen Baden-Württembergs.
  Verglichen wurde eine Region mit relativ häufigen und zum Teil großen Vorkommen der Beifuß-Ambrosie (Waghäusel, Kreis Karlsruhe, Oberrheinebene) und eine mit nur wenigen und kleinen Ambrosia-Vorkommen (Bad Waldsee-Reute, Kreis Ravensburg, Oberschwaben). In beiden Regionen wurden jährlich flächendeckende Bestandserhebungen auf einer Fläche von jeweils ca. 20 km^2 durchgeführt. Weiterhin erfolgten selektive Bestandserhebungen in der Umgebung der beiden Gebiete sowie eine Untersuchung der Bestandsdynamik und der Einschleppungswege.
- Parallele Messung der Pollenkonzentrationen in den beiden Untersuchungsregionen mit Abschätzung der lokalen Einträge und des Ferntransports z.B. von Frankreich nach Baden-Württemberg und
- Bestimmung der Sensibilisierungsrate gegenüber den Allergenen der Ambrosie an Kindern der vierten Klasse.
  Vom Landesgesundheitsamt Stuttgart (LGA) und dem Zentrum für Allergie und Umwelt der Technischen Universität München (ZAUM) wurde im Rahmen eines Serum-Allergiescreenings eine Testung auf die Ambrosia-Allergene vorgenommen und auch eine solche auf die bekannten kreuzreaktiven Allergene wie z.B. Beifuß und Wermut durchgeführt. Durch die zusätzliche Testung auf Pan-Allergene und spezifische Minor-Allergene wurde versucht abzuklären, welche Bedeutung einer Sensibilisierung auf Ambrosia-Allergene im Rahmen von

Polysensibilisierungen zukommt. Die Ermittlung der klinischen Relevanz erfolgte in dieser „Pilotstudie“ vor allem anhand entsprechender Fragebogenangaben.

b) das Schaffen einer Datengrundlage für eine zukünftige Abschätzung, ob es im Verlauf der Zeit zu einer relevanten Zunahme der Ausbreitung der Beifuß-Ambrosie gekommen ist oder ob es aufgrund der eingeleiteten Präventionsmaßnahmen möglich war, diese Ausbreitung zu verhindern.

3. Ergebnisse

Ambrosia artemisiifolia ist gegenwärtig regional unterschiedlich weit verbreitet. In Waghäusel und Umgebung (Oberrheinebene) tritt die Pflanze deutlich häufiger auf als in Bad Waldsee-Reute und Umgebung (Oberschwaben) (s. Abb. 1). In und um Waghäusel wurden auch große Ambrosia-Bestände mit mehreren tausend Pflanzen nachgewiesen. In Waghäusel traten die meisten Bestände im Randbereich der Siedlungen auf, während in Bad Waldsee-Reute die meisten Vorkommen in Gärten im Siedlungsbereich wuchsen (Alberternst et al., 2009). Vogelfutter stellt derzeit einen sehr bedeutenden Einschleppungsweg dar. Viele der nachgewiesenen Ambrosia-Bestände wurden in beiden Regionen mit verunreinigtem Vogelfutter eingebracht. Auch Neueinschleppungen in Waghäusel erfolgten mehrfach über Aussaat von Vogelfutter und durch außerhalb von Gärten abgelagerten organischen Abfall (Gartenabfall, Vogelkäfigstreu).

Abb. 1: Lage der beiden Untersuchungsgebiete Waghäusel und Bad Waldsee-Reute in Baden-Württemberg

Trotz der stärkeren Verbreitung von Ambrosia-Pflanzen in Waghäusel im Vergleich zu Bad Waldsee-Reute, wurden in beiden Regionen ähnlich niedrige Pollen-Konzentrationen ermittelt (Kaminski et al., 2010). Die derzeit vorhandenen Ambrosia-Pflanzen führten noch nicht zu hohen Pollenmesswerten. Pollenmessungen in unmittelbarer Nähe zu einem Ambrosia-Bestand zeigten jedoch, dass hier im Vergleich mit den weiteren Messstellen relativ viele Pollen in der Luft vorhanden waren. Auch wurde zu keinem Zeitpunkt ein kontinuierlicher, über mehrere Tage anhaltender Ambrosia-Pollenflug, der auf lokale Emissionsquellen zurückgeführt werden könnte, detektiert. Es liegt deshalb nahe, dass die gegenwärtig detektierten Pollen quantitativ vor allem auf den Ferntransport aus Südfrankreich zurückzuführen sind.

Auch im Hinblick auf die Häufigkeit einer Sensibilisierung von Kindern und Erwachsenen sowohl gegen native Ambrosia-Pollen-Extrakte als auch gegen das Major-Allergen Amb a 1, konnte kein Unterschied zwischen den beiden Untersuchungsregionen festgestellt werden. Die relativ hohen Prävalenzen von ca. 17% gegenüber Ambrosiapollen-Extrakten sind wahrscheinlich (noch) nicht ursächlich mit einer relevanten Exposition zu erklären, sondern sind eher in Verbindung mit bekannten Kreuzreaktivitäten zwischen Korbblütlern allgemein, insbesondere aber mit Beifuß, zu sehen (Fernandez et al, 1993; Weber, 2005). Die Tatsache, dass alle auf Ambrosia getesteten Probanden auch im allgemeinen Inhalationsscreen (sx1) positiv reagierten, weist insbesondere auf Ko-Sensibilisierungen mit Beifußpollen, aber auch mit anderen Baum- und Graspollen über kreuzreaktive (Pan-)Allergene in einem insgesamt polysensibilisierten Kollektiv hin.
Allerdings zeigen die Vergleichsuntersuchungen mit erwachsenen Probanden sowie die Auswertung der Fragebögen, dass der Verbreitung der Ambrosia eine klinische Relevanz zukommt. Kinder zeigten in der hier vorliegenden Studie häufiger eine Sensibilisierung gegenüber Amb a 1 als Erwachsene. Dies könnte als Hinweis interpretiert werden, dass bei der gegenwärtig noch relativ geringen Verbreitung der Ambrosia in Baden-Württemberg sich erste Effekte bezüglich einer spezifischen Sensibilisierung gegenüber Ambrosia zuerst bei Kindern manifestieren.
Derzeit zeigt sich in Baden-Württemberg eine ähnliche Situation wie in Norditalien Mitte der 1990er Jahre mit geringen messbaren Pollenmengen, Polysensibilisierungen und bereits relativ hohen Sensibilisierungsraten. Dort wurden keine Gegenmaßnahmen ergriffen, die Ambrosie hat sich seither rasant in Norditalien ausgebreitet und ist dort mittlerweile von hoher allergologischer Relevanz (Asero, 2007). Diese Erfahrungen, aber auch weitere aus anderen Ländern zeigen, dass die Verbreitung der Ambrosia im Sinne der Vorsorge in Deutschland unterbunden werden sollte.

4. Schlussfolgerungen

Gegenwärtig kommt in Baden-Württemberg bezüglich der Belastung der Umgebungsluft mit *Ambrosia artemisiifolia*-Pollen dem Ferntransport eine große Bedeutung zu. Emissionen aus lokalen Beständen tragen nur zu einem geringen Anteil zur Belastung der Umgebungsluft bei, obwohl die Pollenkonzentrationen in unmittelbarer Nähe eines Ambrosia-Bestandes relativ hoch sein können. Auch Zink (2009) kommt in einer Modellsimulation des Ambrosiapollenfluges mit COSMO-ART zu dem Ergebnis, dass der Ferntransport eine wichtige Quelle für Ambrosiapollen in Deutschland darstellt.
Die Witterung während der Wachstumsperiode der Ambrosia und das Wetter während der Blütezeit haben einen erheblichen Einfluss auf die Pollenkonzentration (Barnes et al., 2001). Ambrosiabestände in Baden-Württemberg sind zu klein, um flächendeckend derart hohe Pollenanzahlen zu erzeugen wie in Ungarn oder Südfrankreich. In Brandenburg haben wir aber bereits so große Bestände und auch entsprechende Pollenkonzentrationen. Das derzeitige Pollenmessnetz ist zu grobmaschig, um Pollen lokaler Bestände zu erfassen. Es lässt sich abschließend nicht klären, ob eine lokal erhöhte Pollenkonzentration bei langfristiger Einwirkung bereits zu einer Sensibilisierung der unweit der Pflanzenbestände wohnenden Bevölkerung oder ggf. zu klinischen Symptomen führen kann.
Derzeit zeigt sich in Baden-Württemberg eine ähnliche Situation wie in Norditalien Mitte der 1990er. Da dort keine Gegenmaßnahmen ergriffen wurden, konnte sich die Ambrosie in Norditalien rasant ausbreiten und ist dort von hoher allergologischer Relevanz. Um neu auftretende gesundheitliche Risiken durch die Ausbreitung invasiver Ar-

ten und die durch sie ausgelösten Krankheiten frühzeitig erkennen zu können, ist ein fortlaufendes Monitoring der Pflanzenverbreitung, des Pollenfluges und der gesundheitlichen Auswirkungen erforderlich, welches frühzeitig Tendenzen aufzeigt. Ein solches Monitoring sollte aufgebaut werden. Der Deutsche Wetterdienst hat daher die Pflanze Ambrosia auch in das Meldeprogramm der phänologischen Sofortmelder aufgenommen.

Danksagung

Die Autoren danken dem Umweltministerium Baden-Württemberg und der Landesanstalt für Umwelt, Messungen und Naturschutz Baden-Württemberg (LUBW), die die Mittel für das Forschungsprogramm zur Verfügung gestellt und das Forschungsprogramm jederzeit mit fachlichem Rat begleitet haben.

Literatur

Alberternst, B., Behrendt, H., Gabrio, T., Kaminski, U., 2009: Abschlussbericht – Forschungsprogramm, Herausforderung Klimawandel - Verbundprojekt Ambrosia-Pollen: Einfluss klimatischer Faktoren und ihrer bisherigen sowie erwarteten Änderung bezüglich der Zunahme von Sensibilisierungen am Beispiel von Ambrosia-Pollen, Hrsg. LGA Baden-Württemberg im Regierungspräsidium Stuttgart, Stuttgart.

Asero, R., 2007: The changing pattern of ragweed allergy in the area of Milan, Italy. Allergy 62, 1097-1099.

Barnes, C., Pacheco, F., Landuyt, J., Hu, F., Portnoy, J., 2001: The effect of temperature, relative humidity, and rainfall on airborne ragweed pollen concentrations. Aerobiologia 17, 61-68.

Cvitanovic, S., Znaor, L., Kanceljak-Macan, B., Macan, J., Gudelj, K., Grbic, D., 2007: Allergic rhinitis and asthma in southern Croatia: impact of sensitization to Ambrosia elatior. Croat. Med. J. 48(1), 68-75.

Déchamp, C., Méon, H., 2002: Ambroísíes, Polluants Bíologíques. Arpam-Edition, Lyon, 287 Seiten, ISBN 2.902913.37.11

Fernandez, C., Martin-Esteban, M., Fiandor, A., 1993: Analysis of cross-reactivity between sunflower pollen and other pollens of the Compositae family. J. Allergy Clin. Immunol. 92, 660-667.

Jäger, S., 2000: Ragweed (Ambrosia) sensitisation rates correlate with the amount of inhaled airborne pollen. A 14-year study in Vienna, Austria. Aerobiologia 16, 149-153.

Kadocsa, E., Juhász, M., 2002: Study of airborne pollen composition and allergen spectrum of hay fever patients in south Hungary (1990-1999). Aerobiologia 18, 203-209.

Kaminski, U., Alberternst, B., Gabrio, T., Böhme, M., Nawrath, S., Behrendt, H., 2010: Ambrosia Pollen-Konzentrationen in Baden-Württemberg. Umweltmed Forsch Prax 15 (1). In press.

Laaidi, M., Laaidi, K., Besancenot, J.-P., Thibaudon, M., 2003: Ragweed in France: an invasive plant and its allergenic pollen. Ann Allergy Asthma Immunol 91**,** 195–201.

Makra, L., Juhasz, M, Beczi, R. Borsos, E., 2005: The history and impacts of airborne Ambrosia (Asteraceae) pollen in Hungary. Grana 44, 57-64.

Wayne, P., Foster S., Connolly, J., Bazzaz, F., Epstein, P., 2002: Production of allergenic pollen by ragweed (*Ambrosia artemisiifolia* L.) is increased in CO_2-enriched atmospheres. Annals of Allergy, Asthma & Immunology 88, 279-282.

Weber, R. W., 2005: Cross-reactivity of pollen allergens: recommendations for immunotherapy vaccines. Curr Opin Allergy Clin Immunol 5(6),6-569.

Zink, K., 2009: Modellierung der Ausbreitung von Ambrosiapollen mit COSMO-ART. Diplomarbeit im Fach Meteorologie. Institut für Meteorologie und Klimaforschung Universität Karlsruhe (TH)/ Forschungszentrum Karlsruhe. 83 Seiten.

Ziska, L. H., Gebhard, D. E., Frenz, D. A., Faulkner, S., Singer B., Straka, J. G., 2003: Cities as harbingers of climate change: Common ragweed, urbanization, and public health. J. Allery Clin. Immunol. 111(2), 290-295.

Authors' address:

Uwe Kaminski (uwe.kaminski@dwd.de)
Zentrum für Medizin-Meteorologische Forschung
Stefan-Meier-Str. 4-6, D-79104 Freiburg, Germany

Beate Alberternst und Stefan Nawrath
Arbeitsgruppe Biodiversität Friedberg
Hinter´m Alten Ort 9, D-61169 Friedberg, Germany

Thomas Gabrio
Landesgesundheitsamt Baden-Württemberg im Regierungspräsidium Stuttgart
Nordbahnhofstr. 135, D-70191 Stuttgart, Germany

Michael Böhme
Landesgesundheitsamt Baden-Württemberg im Regierungspräsidium Stuttgart
Nordbahnhofstr. 135, D-70191 Stuttgart, Germany

Heidrun Behrendt
ZAUM - Zentrum für Allergie und Umwelt, TU München
Biedersteiner Str. 29, D-80802 München, Germany

Ambrosia in Berlin: pollen emission, spread and control

Sandra Kannabei[1], Thomas Dümmel[1]

[1] Meteorological Institute, Free University of Berlin, Germany

Abstract

Climate warming leaves its mark on metropolises like Berlin. Thus the thermophilic ambrosia could spread and establish in the last years. As a consequence of this the pollen concentration reached or even exceeded the critical threshold (~10 pollen / m³ air) for allergic persons (Taramarcaz et. al. 2006). Since the start of the "Action program against Ambrosia in Berlin" over 600 locations of *Ambrosia artemisiifolia* and 104 locations of *Ambrosia coronopifolia* have been determined as sources of emission in the year 2009, which are spread all over the city area, massing with ~25 locations of over 100 plants in the south-eastern part of Berlin. Here the seed of the species *Ambrosia coronopifolia* is often spread by displacement of soil during construction works. The remaining part of the 48 main findings and most of the smaller findings up to a quantity of 100 plants consist of the annual *Ambrosia artemisiifoli*a.

1. Introduction

Many scientific studies proved that the ongoing climate warming has an effect on especially the biosphere. Thus it is not remarkable that neophytes like Ambrosia spread out in Germany and threaten to establish.

Since 2006 the spread of the highly allergenic Ambrosia in Berlin has been studied in detail. This has been motivated by analyses of intra urban dust that have shown increased concentrations of Ambrosia pollen.

To identify the sources of emission and to research the introduction and spread of the plant as well as to develop strategies to combat further spreading in Berlin, the "Action program against Ambrosia in Berlin" was initiated in early summer of 2009 under leadership of the Meteorological Institute (Free University Berlin), supported by the senate offices of urban development, health, environment and consumer protection. In 2009 the project initiators in corporation with employment institutions have begun to compile a register, to gather all relevant meta-data of the findings and to destroy as much as possible of the Ambrosia population.

2. Ambrosia pollen concentration in Berlin

Since an increased occurrence of Ambrosia has been noticed in 2006, staff members of the pollen information service of the Free University are analysing pollen trap obtained aerosol samples for the existence of Ambrosia pollen. Data for the years between 1998 and 2005 were derived from reanalysis of older samples. As the pollen trap was deactivated in the first two weeks of September until 2005, data for the years between 1998 and 2005 is just available for this time span, although the season of pollen flight lasts until October. Additionally, due to their bad condition, samples of the year 2000 could not be reanalysed. The results of the analysis, the annual trend of pollen concentrations of Ambrosia/m³ air in Berlin-Steglitz for the years 1998 to 2009, are shown in figure 1.

Note that year 2000 has been left out due to the aforementioned circumstances.

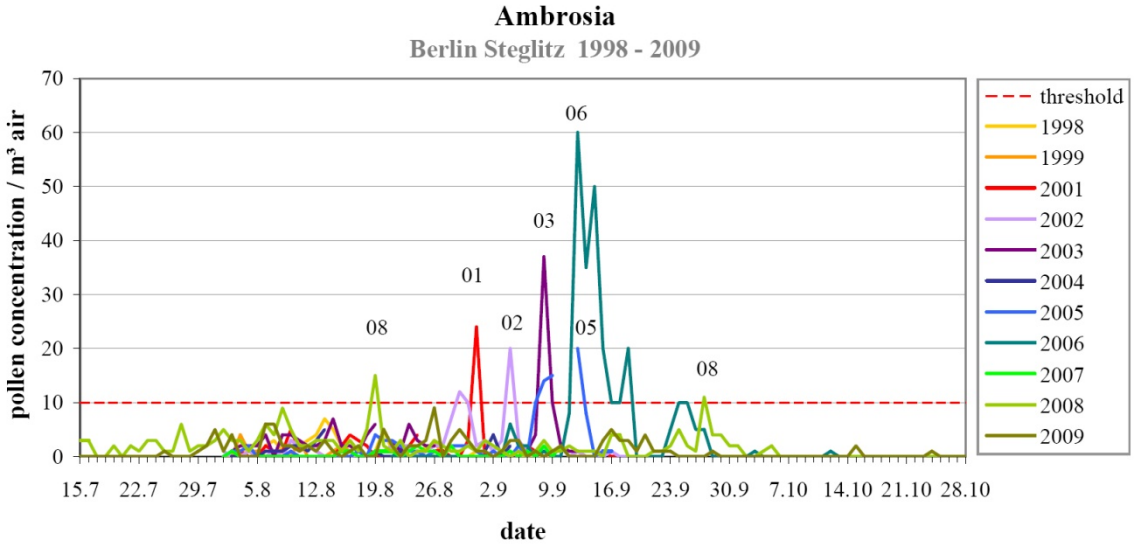

Fig. 1: Pollen concentration of Ambrosia in Berlin-Steglitz 1998-2009 (without 2000)

It can be identified that pollen flight of Ambrosia starts in the midst of July until early August. Concentrations range under 10 pollen/m³ air. The main phase of blossom starts in late August while the critical threshold for allergic persons has been exceeded in the years 2001, 2002, 2003, 2005, 2006 and 2008 (Taramarcaz et. al. 2006). It is not possible to prove an increased concentration in the remaining years preceding 2005 due to missing data. The maximum of measured pollen has been reached on 12.09.2006 with 60 pollen/m³ air. According to the analysis since 1998 it is assumed that especially in hot summers an increased concentration of Ambrosia pollen has to be expected.

3. Ambrosia locations in Berlin

Mapping the locations of Ambrosia in the city area of Berlin by the members of the "Action program" has helped to identify the sources of emission. In the first year of the project about 30% of the city area was systematically searched to get a first impression of the spread and the distribution of Ambrosia. Figure 2 shows a map of all Ambrosia found in 2009.

Data analyses have shown that not only the annual *Ambrosia artemisiifolia* but also the perennial *Ambrosia coronopifolia* are widespread in Berlin. Especially in the south-east of Berlin an increased occurrence of the perennial ambrosia was determined in 25 findings of over 100 plants, which were predominantly spread by displacement of soil during construction works. With a total of ~55.000 plants they constitute almost half of all Ambrosia specimen found. The main portion (60%) is made up of small findings of up to 10 plants, which have almost all been destroyed. Spread of *Ambrosia artemisiifolia* is often caused by birdseed.

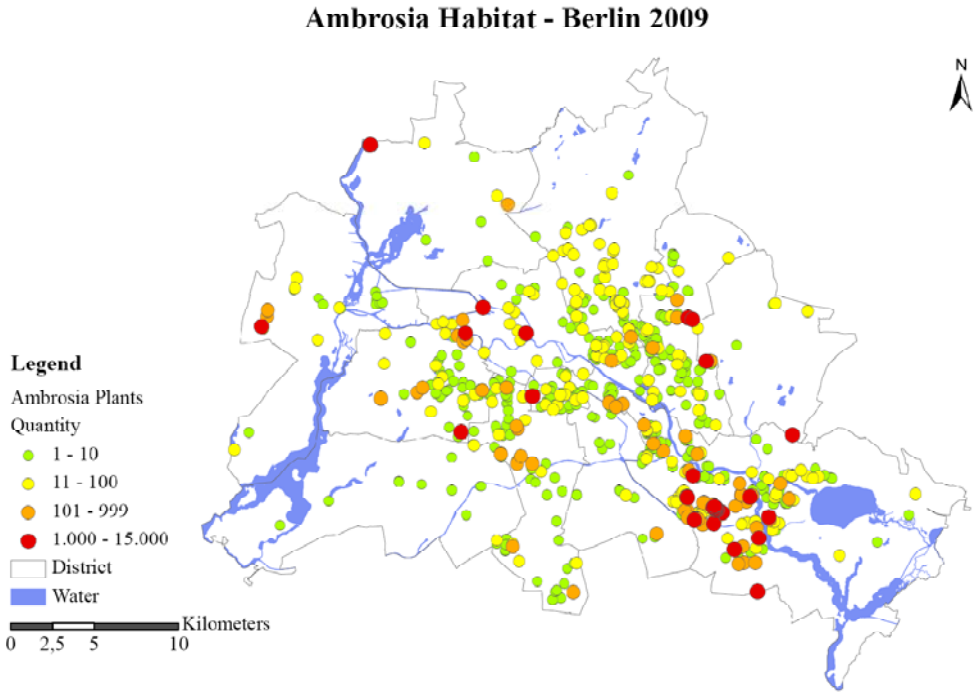

Fig. 2: Ambrosia Habitat in Berlin 2009, geodatabase source: senate department for urban development of Berlin

4. Conclusions

With the help of all members of the "Action program against Ambrosia in Berlin" this research has succeeded in producing first results regarding the identification of the distribution and causes of spread of Ambrosia in Berlin.

If birdseed is purged of Ambrosia seed, e.g. by governmental regulation, the citizens are sensitised to the issue of Ambrosia and small findings are regularly destroyed, a further spread in Berlin could be stopped. The main findings are more problematic, as a great number of pollen are produced and can be emitted to the air during blossom. These plants are spread throughout the city by displacement of pollen-contaminated soil during construction works. It remains highly important for the future to find appropriate solutions for these kinds of locations in order to destroy the large-area populations on the one hand and to prevent the further spreading of the plants through contaminated soil on the other hand.

References

Taramarcaz, P., Lambelet, C., Clot, B., Keimer, C., Hause, C., 2005: Ragweed (Ambrosia) progression and its health risks: will Switzerland resist this invasion? Swiss Med WKLY 135: 538-548.

Author's address:

Dipl.-Geogr. Sandra Kannabei (sandra.kannabei@met.fu-berlin.de)
Institute of Meteorology, Free-University of Berlin
Carl-Heinrich-Becker-Weg 6-10, D-12165 Berlin, Germany

The effect of temperature and thermal atmospheric conditions on mortality in Bangladesh

Katrin Burkart,Wilfried Endlicher

Humboldt-Universität zu Berlin, Department of Geography, Climatological Section

Abstract

Mortality underlies seasonal fluctuations and seems to be associated with temperature and other meteorological parameters. Most studies on the atmosphere-health relationship have been conducted in industrialized countries of the mid-latitudes. Due to the strong variations between different regions and locations, as well as the confounding effect by non-atmospheric parameters, results obtained from those studies cannot be directly applied in the context of a tropical developing country. In this paper we present some selected results obtained from our combined analysis of mortality and meteorological data.

1. Introduction

Climate and air pollution have major impacts on human health and wellbeing. Non-linear relationships have been observed with increased mortality at high or low temperatures (Kunst et al., 1993; Braga et al., 2001a, b, c; Braga et al., 2002). Both hyperthermia and hypothermia are generally linked to cardio-respiratory morbidity and mortality (Braga et al., 2001a; Kunst et al., 1993; Schär and Jendritzky, 2004), bur also infectious diseases such as acute respiratory infection or diarrhoea are temperature-dependent (Burkart and Endlicher, 2009, 2010). In many regions of the world a seasonal variation of morbidity can be observed. In countries of the mid-latitudes death rates in winter are generally higher than those in summer, although heat waves can cause excess mortality (Braga et al., 2002; McMichael, 2001; Rau, 2007). For tropical regions usually a mortality peak during the hot or rainy season has been observed which is mainly attributed to infectious disease in general and diarrhoeal disease in particular (McMicheal et al., 2008). The heat-mortality and -morbidity relationship varies across time periods, regions and populations. Time-series studies have shown that different cities and population groups exhibit different responses to heat. For instance, the relationship between heat and mortality differed for Delhi, São Paulo and London (Hajat et al., 2005), and the impact of heat waves on mortality differed by city for a study of London, Milan and Budapest (Hajat et al., 2006). Klinenberg (2002) noted that the urban poor and people with fewer social connections were most at risk of death during the Chicago heat wave of 1995. Furthermore, the risk for heat-related mortality was higher among the African-American population (Kaiser et al., 2007). Smoyer et al. (2000) showed that the strongest relationship between heat and mortality in Southern Ontario occurred in cities with relatively high levels of urbanisation and high costs of living.

This work aims at providing a general overview of the relationship about season, heat and mortality in Bangladesh. Mortality data collected by the Bangladesh Bureau of Statistics was analysed and linked to meteorological data from the Bangladesh Meteorological Department.

2. Data and Methods

Nationwide meteorological data were collected from the Bangladesh Meteorological Department (BMD); these data included air temperature, barometric pressure, radiation, rainfall, wind-speed and -direction and cloud coverage. Data were collected every third hour from 2002 to 2007. Mortality data were provided by the Bangladesh Bureau of Statistics (BBS) for the period of 2002 to 2007. The data were collected within the Vital Sample Registration System (VSRS), which exists in its current version since 2002.
Thermophysiological parameters were calculated from 3-hourly meteorological data. Indices calculated were the Heat Index and Windchill Index (HI/WCI), whenever threshold criteria were met. Additionally, the physiological equivalent temperature (PET) and the standardized equivalent temperature (SET) were calculated using the Software RayMan (Version 1.2) (Höppe, 1999; Matzarakis et al., 2007). The Universal Thermal Climate Index was calculated using the Software BioKlima (Version 2.6). For assessing seasonal fluctuations of mortality, daily mortality counts were smoothed by locally-weighted scatterplot smoothing (LOESS). The relationship between daily mortality and (equivalent) temperature were assessed using generalized additive models (GAMs).

3. Exemplary results

From an epidemiological perspective three seasons can be distinguished. The cold season, from November to March, the hot and humid season, from March to May, and the rainy (monsoon) season with heavy rainfalls from May to October. About 90 % of precipitation falls from May to October, while the rest of the year is rather dry. Looking at the distribution of temperature and the selected thermophysiological parameters it can be observed that lowest values of all parameters are reached in December and January. In the case of maximum avarage values, the peak of temperature, HI/WCI, PET, or UTCI occurs temporarily displaced. While average mean temperatures are almost equally high from April to September, HI peaks in August, while PET and UTCI reach maximum values from June to August. Especially, in the warm season, thermophysiological indices are surpassing temperature values (Figure 1).

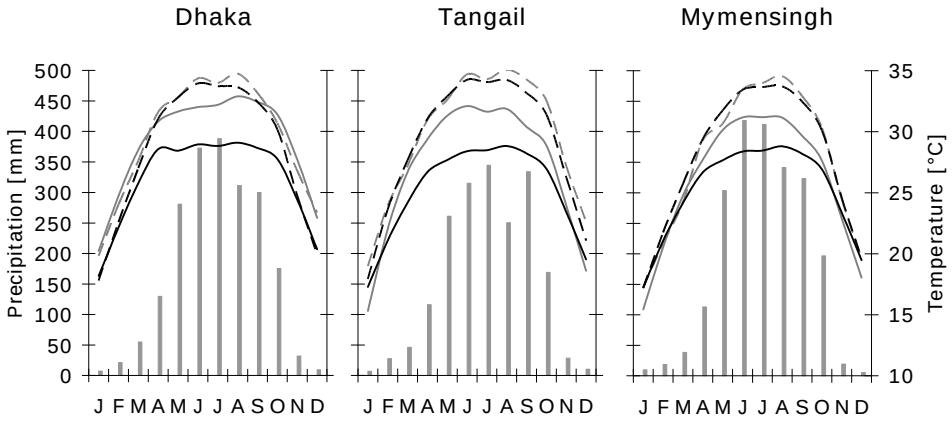

Fig. 1: Annual variations of monthly mean temperature (black solid line), mean HI/WCI (grey dashed line), mean PET (grey solid line) and mean UTCI (black dashed line) in Dhaka, Tangail and Mymensingh

All-cause mortality exhibits a marked seasonality with a bimodal distribution. The primary maximum occurs during the cold and dry season (October to February), and the secondary maximum occurs from May to July, at the end of the summer season and the beginning of the monsoon season (Figure 2a). Cardiovascular mortality peaks during the cold season.

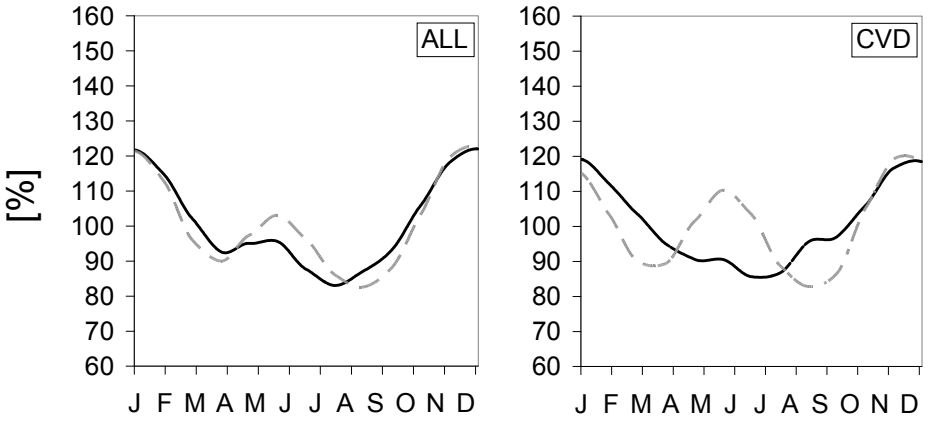

Fig. 2: Annual seasonal mortality variations of all-cause mortality (ALL), respiratory mortality (RE), cardiovascular mortality (CVD), and diarrhoeal mortality (DIA) in rural (black solid line) and urban (grey dashed line) areas displayed as percentage deviation from average mortality

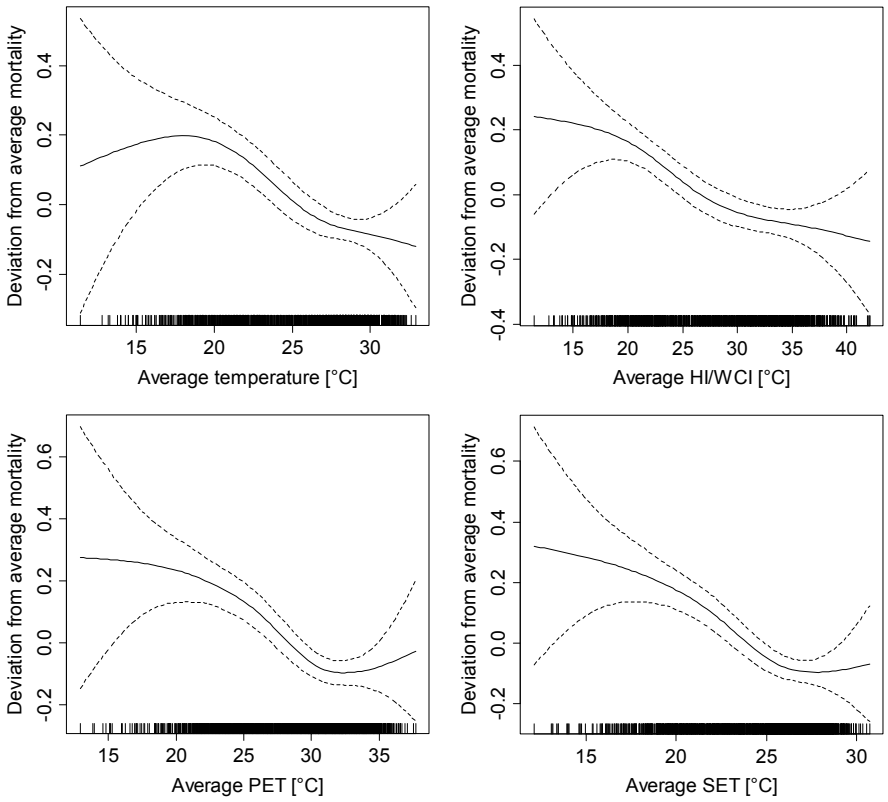

Fig 3: Relationship between cardiovascular mortality and temperature, as well as between selected thermophysiological indices (solid black lines represent estimated spline curves, dashed lines show the 95% confidence intervals)

However, in urban areas cardiovascular mortality shows a very pronounced secondary peak during summer. This clearly demonstrates the increased vulnerability of urban populations toward heat, which could be partly caused by the urban heat island. However, it is also likely that urban populations are more vulnerable towards heat as they face a higher burden of cardiovascular disease.Only minor differences of all-cause and cardiovascular seasonality could be observed between males and females and between regions with high and low SES (data not shown).
Regression analysis showed that mortality rises between approximately 10 and 18 °C. After surpassing a breakpoint temperature of approximately 18 °C there is an inverse, almost linear trend between temperature and mortality. Looking at the association between mortality and Heat Index or Windchill Index respectively, an inverse trend can be observed over the whole data range. In the case of the physiological and standardized equivalent temperature, mortality decreases with increasing temperature until a value of 31 ° (PET) or 26 ° (SET). Above these breakpoints an increase of mortality can be observed. Distinguishing between rural and urban areas those observed threshold temperatures are approximately 1 to 2 degrees lower in urban areas compared to rural areas. Furthermore, the increase in mortality after passing the breakpoint equivalent temperature a sharper rise of mortality could be observed for urban areas (data not shown).

4. Conclusion

For the analysed data a clear association between season, temperature and all-cause as well as cardiovascular mortality could be observed. We showed that the influence of season and thermal conditions depends on certain preconditions existing on-site. While tropical regions have been, and still are, associated with a marked excess of mortality in summer, only a weakly pronounced secondary summer peak could be observed for Bangladesh, possibly due to reduced diarrhoeal fatalities. We hypothesize that Bangladesh is undergoing an epidemiological transition from summer toward winter excess mortality as a consequence of changes in socioeconomic conditions and health care. The study further demonstrated the importance of considering seasonal impacts on mortality and revealed several target groups and diseases for which the consideration of seasonality could especially help to improve disease prevention. For instance, general protection measures against cold or heat among infants or those under hospital care can help to avoid or overcome critical states of health. We recommend further research in this area and highlight that, especially in times of climate change, knowledge on the interaction between seasons, atmosphere, and health is necessary.

Acknowledgement

This work was supported by the German Research Foundation (DFG) within the frame of the Priority Programme 1233 “Megacities-Megachallenges – Informal Dynamics of Global Change”. We owe special thanks to Anwar Hossain, Project Director of the Vital Sample Registration System, established by the Bangladesh Bureau of Statistics. Furthermore, we sincerely thank Prof. Mohammad Kabir from the Jahangirnagar University, Department of Statistics for his cordial support of our research.

References

Braga, A.L., A. Zanobetti, J. Schwartz, 2001: The Lag Structure Between Particulate Air Pollution and Respiratory and Cardiovascular Deaths in 10 US Cities. Journal of Occupational and Environmental Medicine 43 (11), 927-933.

Braga, A.L., A. Zanobetti , J. Schwartz, 2001: The Time Course of Weather Related Deaths. Epidemiology 12 (6), 662-667.

Braga, A.L., P.H. Saldiva, L.A. Pereira, J.J. Menezes, G.M. Conceição, C.A. Lin, A. Zanobetti, J. Schwartz, D.W. Dockery, 2001: Health Effects of Air Pollution Exposure on Children and Adolescents in São Paulo, Brazil. Pediatric Pulmonology 31 (2), 106-113.

Braga, A.L., A. Zanobetti, J. Schwartz, 2002: The Effect of Weather on Respiratory and Cardiovascular Deaths in 12 U.S. Cities. Environmental Health Perspectives 110 (9), 859-863.

Burkart, K., W. Endlicher, 2009: Assessing the Atmospheric Impact on Public Health in the Megacity of Dhaka, Bangladesh. Die Erde 140(1):93-109.

Burkart K, W. Endlicher 2010 (in print): Bioclimate and Thermal Stress in the Megacity of Dhaka. In: Krämer A, Kraas F, Khan M, editors. Health in Megacities and Urban Areas Springer. .

Hajat, S., B.G. Armstrong, N. Gouveia, N., P. Wilkinson, 2005: Mortality Displacement of Heat Related Deaths: A Comparison of Delhi, São Paulo, and London. Epidemiology 16 (5): 613-620.

Hajat, S., B. Armstrong, M. Baccini, A. Biggeri, L. Bisanti, A. Russo, A. Paldy, B. Menne, T. Kosatsky, 2006: Impact of High Temperatures on Mortality: Is There an Added Heat Wave Effect? Epidemiology 17 (6), 632-638.

Höppe P., 1999: The physiological equivalent temperature - a universal index for the biometeorological assessment of the thermal environment. International Journal of Biometeorology 43, 71-5.

Kaiser, R., A. Le Tertre, J. Schwartz, C.A. Gotway, W.R. Daley, C.H. Rubin, 2007: The Effect of the 1995 Heat Wave in Chicago on All-Cause and Cause-Specific Mortality. American Journal of Public Health 97 (1), 158-162.

Klinenberg, E. 2002: Heat Wave: A Social Autopsy of Disaster in Chicago. Chicago.

Kunst, A.E., C.W.N. Looman, J.P. Mackenbach 1993: Outdoor Air Temperature and Mortality in the Netherlands: A Time-Series Analysis. American Journal of Epidemiology 137 (3), 331-341.

Matzarakis, A., F. Rutz and H. Mayer, 2007: Modelling radiation fluxes in simple and complex environments—application of the RayMan model. – International Journal of Biometeorology 51, 323–334.

McMichael, A.J., 2001: Global Environmental Change as "Risk Factor": Can Epidemiology Cope? – American Journal of Public Health 91 (8): 1172-1174.

McMichael, A.J., P. Wilkinson, R.S. Kovats, S. Pattenden, S. Hajat, B. Armstrong, N. Vajanapoom, E.M. Niciu, H. Mahomed, Ch. Kingkeow, M. Kosnik, M.S. O'Neill, I. Romieu, M. Ramirez-Aguilar, M.L. Barreto, N. Gouveia, B. Nikiforov, 2008: International Study of Temperature, Heat and Urban Mortality: The 'ISOTHURM' Project. International Journal of Epidemiology 37(5): 1121-1131.

Rau, R. 2007: Seasonality in Human Mortality: A Demographic Approach. Berlin et al.

Ren, C., G.M. Williams, S. Tong, 2006: Does Particulate Matter Modify the Association between Temperature and Cardiorespiratory Diseases? Environmental Health Perspectives 114 (11): 1690- 1696.

Schär, C., G. Jendritzky 2004: Climate Change: Hot News from Summer 2003. Nature 432 (7017):559-560.

Smoyer, K.E., D.G.C. Rainham, J.N. Hewko, 2000: Heat-Stress-Related Mortality in Five Cities in Southern Ontario: 1980-1996. International Journal of Biometeorology 44 (4): 190-197.

Authors' addresses:

Katrin Burkart, M.Sc.
Humboldt-Universität zu Berlin
Department of Geography
Unter den Linden 6
10099 Berlin
katrin.burkart@geo.hu-berlin.de

Wilfried Endlicher, Prof. Dr.
Humboldt-Universität zu Berlin
Department of Geography
Unter den Linden 6
10099 Berlin
wilfried.endlicher@geo.hu-berlin.de

Changes in heat related mortality in Vienna based on regional climate models

Stefan Muthers[1], Andreas Matzarakis[1] and Elisabeth Koch[2]

[1] Meteorological Institute, University of Freiburg, Germany
[2] Central Institute for Meteorology and Geodynamics, Vienna, Austria

Abstract

The development of mortality due to heat stress in Vienna was assesses by using two regional climate models in the emissions scenarios A1B and B1. Heat stress was described using the human-biometeorological index PET. Two approaches were applied, to estimate the increases with and without long-term adaptation. Until 2011-2040 no significant changes compared to 1971-2000 were found. In the following decades heat-related mortality could increase up to 129 % until the end of the century, if no adaptation takes place. The strongest increase occurred due to extreme heat stress (PET $\geq 41°$ C). With long-term adaptation the increase is less pronounced, but still notably. This encourages the need for additional adaptation measurements.

1. Introduction

The huge number of heat-related death in summer 2003 (Robine et al. 2007) in combination with the probability of an increase of heat waves in frequency and duration due to climate change (Schär et al., 2004) creates the need to assess the future development of heat-related mortality.

2. Data and Methods

The study uses the prior found relation between heat stress and mortality (Muthers et al. 2010), and applies this relation to regional climate model data.

To analyze the relation, daily mortality data for the period 1970-2007 and climate data from the ZAMG climate station (Central Institute for Meteorology and Geodynamics) "Hohe Warte" in Vienna was used. The human-biometeorological index PET (Physiologically Equivalent Temperature) at 14 CET was applied, to assess the thermo-physiological impact of heat stress on the human body (Höppe und Mayer 1987, Höppe, 1984). Based on the station data PET was calculated by the RayMan model (Matzarakis et al., 2007). To estimate the baseline mortality and to include short-term adaptation processes, two approaches by Koppe and Jendritzky (2005) were applied. Percentage deviations from the baseline were used as relative mortality.

The impact of climate change on the heat related mortality was assessed using the two regional climate model REMO (Jacob and Podzun, 1997) and CLM (Böhm et al. 2006; Rockel et al. 2008) in the emissions scenarios A1B and B1. For REMO the climate data for 13-14 CET was selected. For CLM, where only three hour periods were available, the 12-15 CET period was selected. For each day, the PET was estimated using RayMan (Matzarakis et al., 2007). The study is limited to the month April to October, since it focuses on the impact of heat stress.

In a first step, the projected change in the number of days per year for four different grades of thermo-physiological stress was considered. Compared to Matzarakis and

Mayer (1996) the number of grades is limited to four grades, since it was found that PET < 29° C are characterized by a mean mortality significantly below the baseline, while the other three heat stress grades show significantly higher mortality values (Muthers et al., 2010). The comparison was made relative to the period 1971-2000 and for the three future periods 2011-2040, 2041-2070 and 2071-2100.

The assessment of the development of heat related mortality is a difficult and complex topic, since it depends on the levels of adaptations (Kalkstein and Greene, 1997). Two different approaches were applied, to assess the possible range of future sensitivity, i. e. the relation between thermal stress and mortality. The first approach is a rather pessimistic approach, which applied the mean relation of the period of examination (1970-2007) to the three future periods. In this approach no adaptation is assumed. For the three periods, the mean mortality for each heat stress grade is combined with the number of days per year. The product of both is called cumulated heat-related mortality and describes the cumulated deviations of the mortality from the baseline for a year.

The first approach is probably too pessimistic, since significant decreases in the heat related mortality in some grade were found in the period of examination. Hence, the mean value of 1970-2007 is already too high at the beginning of the 21th century. To assess the future level of adaptation, significant trends of the period of examination were extrapolated using the statistically most conservative trend line (Fig. 1 – "significant trend"). If no significant trends were found between 1970 and 2007, the sensitivity at the end of the period of examination was used (Fig. 1 – "no significant trend"). Since this approach assumes continuous long-term adaptation, it could be too optimistic.

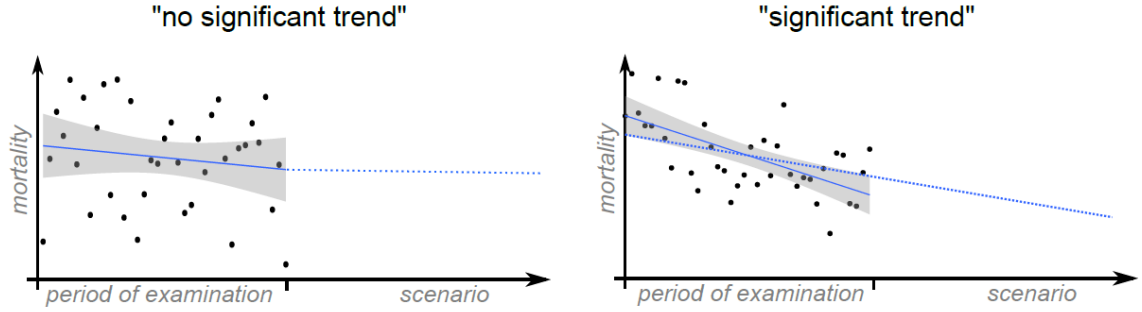

Fig. 1: Diagram of the two approaches to assess the future development of sensitivity to thermal stress. Size of period of examination and scenario is not to scale

For both approaches, the mean mortality per grade (with or without adaptation) was combined with the number of days per year for each grade and the relative changes in cumulated heat related mortality were compared to the period of investigation.

3. Results

The first approach assumes the relation between thermal stress and mortality to be constant until 2100. In this case, significant higher relative mortality exists on days with moderate heat stress (PET 29-35° C, relative mortality: 0.9 %, CI: 0.4, 1.4), on days with strong heat stress (PET 35-41° C, rel. mortality: 5.8 %, CI: 5.0, 6.5) and extreme heat stress (PET ≥ 41° C, rel. mortality 13.0 %, CI: 11.1, 14.7). These values including CI were combined with the projected relative change in the number of days per grade.

In the first period (2011-2041), no significant change in the number of days per grade compared to 1971-2007 occurs (except moderate heat stress in REMO-A1B). Until 2041-2070 heat stress increases significantly in A1B in most of the grades and in B1 in the extreme heat stress grade (~ 50 %). In the last period (2071-2100) significant increase were found for all heat stress classes, with the highest relative values on days with extreme heat stress. In Vienna, the number of days could increase between 57 % (REMO-B1) and 129 % (CLM-A1B), compared to 7 days between 1971 and 2000. Days with strong heat stress could increase by 29 % to 43 % (Fig. 2).

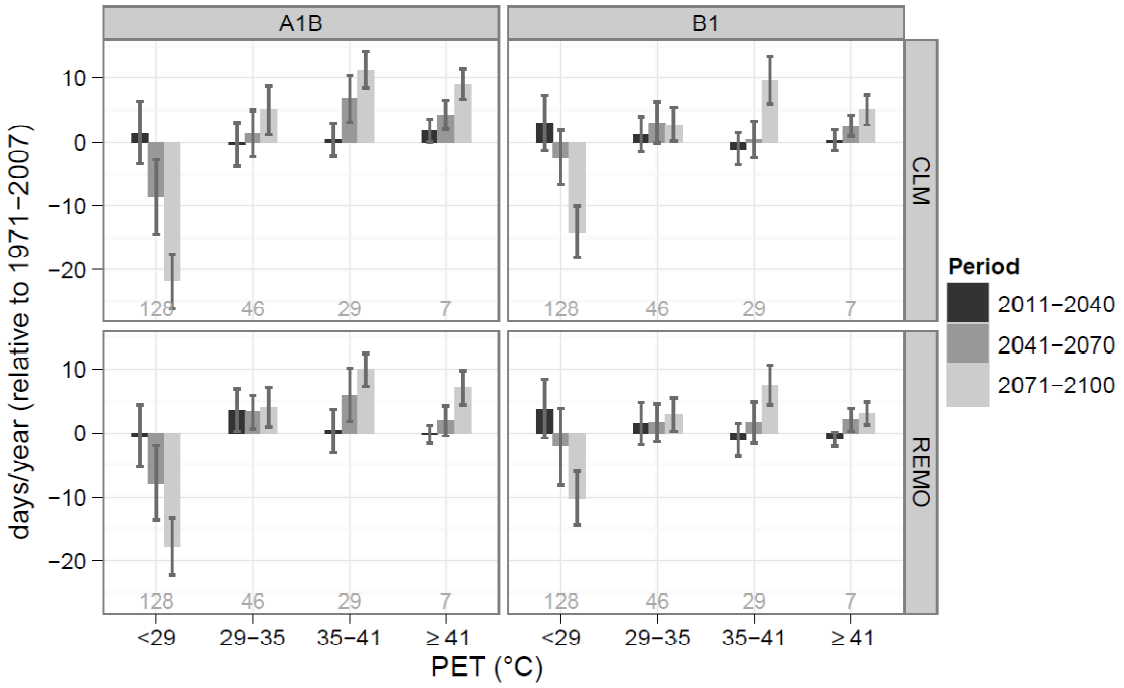

Fig. 2: Number of days per grade of thermo-physiological stress in two regional climate models and two SRES-scenarios

In the first approach (no adaptation, Fig. 3), no significant increases in heat related mortality were found for the first period (2011-2040). For 2041-2070 increases were detected in most cases. Until 2071-2100 heat related mortality could increase by 41 % to 121 % on days with extreme heat stress and 26 % to 39 % on days with strong heat stress. The changes on days with moderate heat stress are marginal.

The increases were higher for the female population as well as for cardiovascular or respiratory diseases, since these groups show a higher sensitivity to thermal stress.

A different development was found, when long-term adaptation is included (Fig. 4). Due to significant trends in the grades of moderate and strong heat stress (Muthers et al., 2010), mortality on these days decreases continuously. For moderate heat stress, the mean mortality already fell below the baseline at the end of the period of examination.

Hence, this grade is omitted in the following. On days with strong heat stress, a trend of -0.06 % per year is used. This results in proceeding reduction of cumulated heat-related mortality on these days, although the number of days per year increases. At the end of the 21th century, mortality on days with extreme heat stress is only slightly raised, by

6 % in REMO-B1 and 7 % in CLM-A1B and it is considerable lower compared to the period of examination.

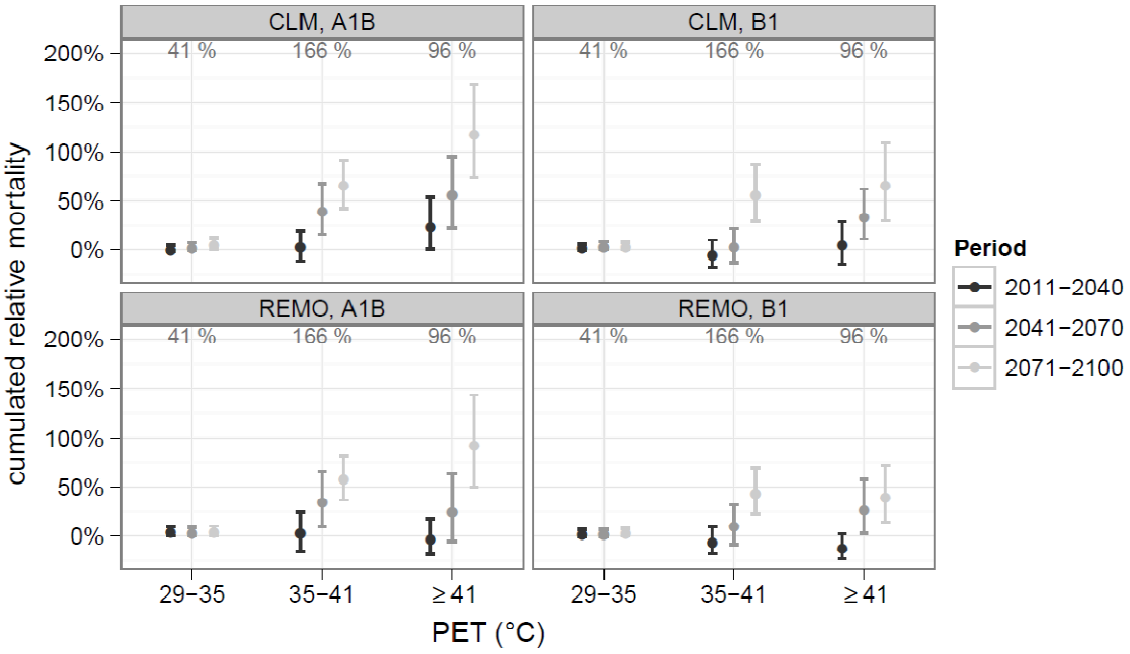

Fig. 3: Changing cumulated heat related mortality without adaptation. The value of the period of examination is shown in grey in the upper margin of each panel

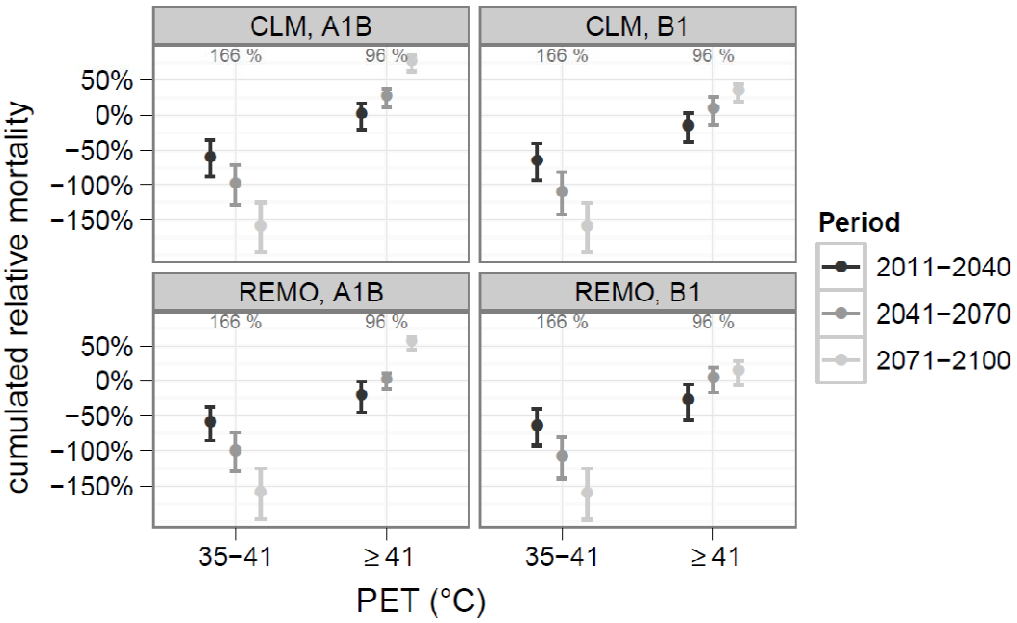

Fig. 4: Changing cumulated heat related mortality including long-term adaptation. The value of the period of examination is shown in grey in the upper margin of each panel. Days with moderate heat-stress were omitted

For mortality due to extreme heat stress, no significant trend was found. Hence, the sensitivity at the end of the period of examination (10.5 %) is used. This results in an increase of cumulated heat-related mortality on days with extreme stress. From 2041-2070 on the increase could be significant (CLM-A1B). Until 2071-2100 increases between 15 % (REMO-B1) and 77 % (CLM-A1B) relative to the 96 % of the period of examination were found.

For women, the increase on days with extreme heat stress was higher, with values between 25 % (REMO-B1) and 106 % (CLM-A1B) for 2071-2100. For cardiovascular or respiratory an increase between 14 % and 85 % was found.

4. Conclusions

Two different approaches were applied, so assess the range of development of heat related mortality in the future. The upper limit is formed by an approach without any long-term adaptation; the lower limit assumes continuous adaptation. In both approaches the heat related mortality could increase significantly till the end of the 21th century.

No significant changes compared to the period of investigation were found for 2011-2040. Hence, time for planning and implementation of additional adaptation measures is available. Measures could g. e. consider the topic of heat stress in urban planning by reducing the radiation component of the thermal environment (Mayer et al. 2008; Lin et al. 2010). On a larger scale heat health warning systems could form a promising step, to reduce the health impact of extreme heat waves (WHO 2004).

Acknowledgement:
Thanks to the Austrian ministry for science and research for funding this study and to Gerhard Hohenwarter from ZAMG for providing the climate data.

References

Böhm, U., M. Kücken, W. Ahrens, A. Block, D. Hauffe, K. Keuler, B. Rockel, A. Will 2006: CLM - The Climate Version of LM: Brief Description and Long-Term Application. COSMO-Newsletter 6, 225–235.

Jacob, D. R. Podzun 1997: Sensitivity Studies with the Regional Climate Model REMO. Meteorol Atmos Phys 63, 119–129.

Höppe, P. 1984: Die Energiebilanz des Menschen. Diss. Fakultät für Physik der Ludwig-Maximilians-Universität München.

Höppe, P., H. Mayer 1987: Planungsrelevante Bewertung der thermischen Komponente des Stadtklimas. Landschaft Stadt 19, 22-29.

Kalkstein, L. S., J. S. Greene 1997: An Evaluation of Climate/Mortality Relationships in Large U.S. Cities and the Possible Impacts of a Climate Change. Environ Health Persp 105(1), 84-93.

Koppe, C., Jendritzky, G. 2005: 'Inclusion of short-term adaptation to thermal stresses in a heat load warning procedure, Meteorol. Z. 14(2), 271-278.

Lin, T.-P., A. Matzarakis R.-L. Hwang 2010: Shading effect on long-term outdoor thermal comfort. Build Environ 45(1), S. 213–221.

Matzarakis, A., Mayer, H. 1996: Another kind of environmental Stress: Thermal Stress. In WMO Newsletter 18.

Matzarakis, A.; Rutz, F., Mayer, H. 2007: Modelling radiation fluxes in simple and complex

environments - application of the RayMan model, Int J Biometeorol 51(4), 323-334.
Mayer, H., J. Holst, P. Dostal, F. Imbery, D. Schindler 2008: Human thermal comfort in summer within an urban street canyon in Central Europe. Meteorol Z 17(3), S. 241–250.
Muthers, S., Matzarakis, A., Koch, E. 2010: Relation between climate and mortality in Vienna based on human-biometeorological data. In: Ber. Meteorol. Inst Univ. Freiburg No. 20, 229-234.
Robine, J. M., S. L. Cheung, S. Le Roy, H. Van Oyen, F. R. Herrmann 2007: Report on excess mortality in Europe during summer 2003. European Commission.
Rockel, B., A. Will, A. Hense 2008: The Regional Climate model COSMO-CLM (CCLM). Meteorol Z 17(4), 347–348.
Schär, C., P. Luigi Vidale, D. Lüthi, C. Frei, C. Häberli, M. A. Liniger, C. Appenzeller 2004: The role of increasing temperature variability in European summer heatwaves. Nature 427(6972), 332–336.
WHO 2004: Heat-Waves: risks and responses. Health and Global Environmental Change, Series No. 2. World Health Organisation.

Authors' address:

Stefan Muthers (stefan.muthers@mars.uni-freiburg.de) and Prof. Dr. Andreas Matzarakis (andreas.matzarakis@meteo.uni-freiburg.de), Meteorological Institute, Albert-Ludwigs-University of Freiburg, Werthmannstr. 10, D-79085 Freiburg, Germany

Dr. Elisabeth Koch (elisabeth.koch@zamg.ac.at), Central Institute for Meteorology and Geodynamics, Hohe Warte 38, A-1190 Vienna, Austria

Melatonin secretion in various climate zones

Joanna Maroszek[1,2], Takeshi Morita[3], Krzysztof Błazejczyk[1,4]

[1] University of Warsaw, Faculty of Geography and Regional Studies (Poland)
[2]University of Warsaw, Interfaculty Individual Doctoral Studies in Mathematics and Natural Sciences supported by Operational Program Human Capital EU.
[3] Fukuoka Woman University (Japan)
[4] Institute of Geography and Spatial Organization, Polish Academy of Sciences (Poland)

Abstract

Melatonin is a major hormone of pineal gland. It is responsible for diurnal and seasonal biological cycles. Local geographical factors (depended on latitude), like a midday Sun altitude and day length in connection with climate conditions (cloudiness, solar radiation etc.) directly affect regional differences in melatonin rhythm. The smallest values of melatonin secretion was noted during the day time and in Winter. At Spring and Summer the biggest values were observed for Polish participants, in Autumn and Winter for the Japanese. From Spring to Autumn in Poland maximum melatonin secretion was over 50 pg/ml, at Winter only 20 pg/ml. Time Peak was noted between 2 and 3 a.m. at Polish subjects, at Japanese between 3 and 5 a.m. and at Vietnamese between 4 and 6 a.m.

1. Introduction

Melatonin is a major hormone produced by pineal gland. It is responsible for diurnal and seasonal biological cycles. The previous researches confirm that melatonin secretion in humans strongly depends on lighting factors (artifical or/and natural), e.g. light intensity, colour corresponded temperature (CCT), time of dim/bright light exposure (Morita at al., 1997, 2002; Morita, Tokura, 1998; Blazejczyk at al, 2005; Ueno-Tawatari at al, 2007). Peak of melatonin concentration is recorded at night.

The previous researches (Blazejczyk K. et all 2005) suggested that there are significant regional differences in melatonin secretion. Local geographical factors (depended on latitude), like a midday Sun altitude and day length together with climate conditions (cloudiness, solar radiation etc.) directly affect regional differences in melatonin rhythm.

The purpose of the paper is to examine melatonin secretion characteristics (depended on natural lighting conditions) in 3 geographical regions, which represent various climate zones: Poland (Warsaw, 52°N, moderately warm transient climate), Japan (Fukuoka, 33°N, subtropical marine monsoon climate) and Vietnam (Hanoi, 21°N, tropical monsoon climate).

2. Materials and methods

The research were taken at three base regions: Poland (Warszawa, 52ºN), Japan (Fukuoka, 33ºN) and in Vietnam (Hanoi, 21ºN) four times a year: in Spring and Autumn equinox as well as in Winter and Summer solstice. The experimental period was from Monday to Friday. In every experiment diurnal cycle of melatonin secretion was examined at volunteers (Poland – 15, Japan – 18, Vietnam – 15), young male and female (21-33 years). Participants were required to sleep from 23:00 until 7:00 in total darkness

and to take they ordinary activity during the day. Cigarettes, coffee and alcohol was banned.

During whole experiment, several environmental parameters were registered automatically every 1 minute (outdoor): intensity of global 0.4-3.0 µm and visible 0.4-0.76 µm solar radiation as well as air temperature and humidity (HOBO Micro Station). Additionally spectral characteristics of solar light (irradiation, CCT, peak wave length) were measured several times a day (by LightSpex, GretagMacbeth).

Furthermore for each subject individual characteristics of: activity level, light intensity (with the use of ActiWatch, Mini Mitter Comp., Inc) and totals of energy of visible radiation in 7 spectral ranges the subject was expose (HandyLight) were controlled.

Saliva samples were collected at 3h intervals, beginning at 10:00h on Thursday with subsequent sampling times at 13:00, 16:00, 19:00, 22:00, 01:00, 04:00 and 07:00h on Friday. Saliva specimens were collected using a saliva collection tubes (Buhlmann Laboratories AG Swiss). Saliva samples were frozen at -24ºC until the analysis. Melatonin concentration (MC) was measured by commercials ELISA kit tests (Buhlmann Laboratories AG Swiss).

3. Results

The studied areas were significant differentiated by lighting conditions. The highest Sun altitudes were observed in Hanoi and the lowest ones in Warsaw (Fig. 1). Difference in maximum Sun altitude among this locations was more than 20°. Day length at Spring and Autumn equinox was similar (about 12 hours) at each location. The greatest seasonal differences in day length were observed for Warsaw. The longest day (22 of June) lasted 16 h 47 min while the shortest only 7 h 42 min (22 of December). Those differences have significant impact at solar radiation totals and in consequence at melatonin rhythm.

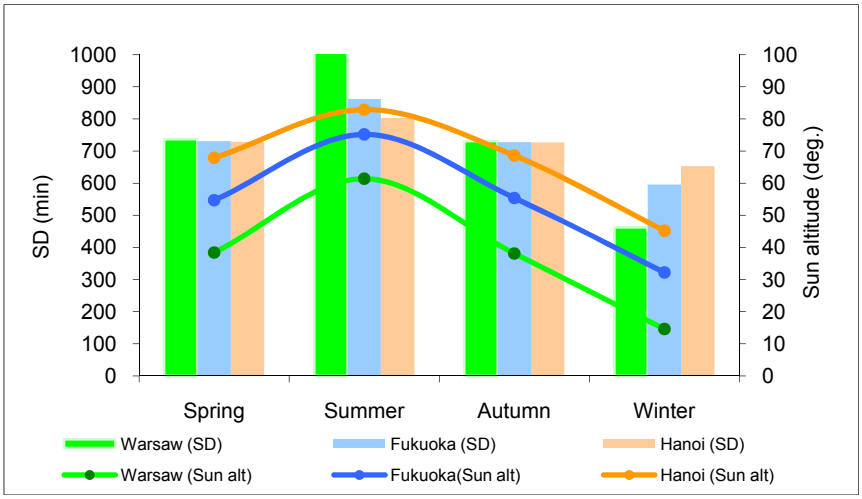

Fig. 1: Seasonal values of environmental factors at studied locations: Day length (SD, min) and Sun altitude (deg.)

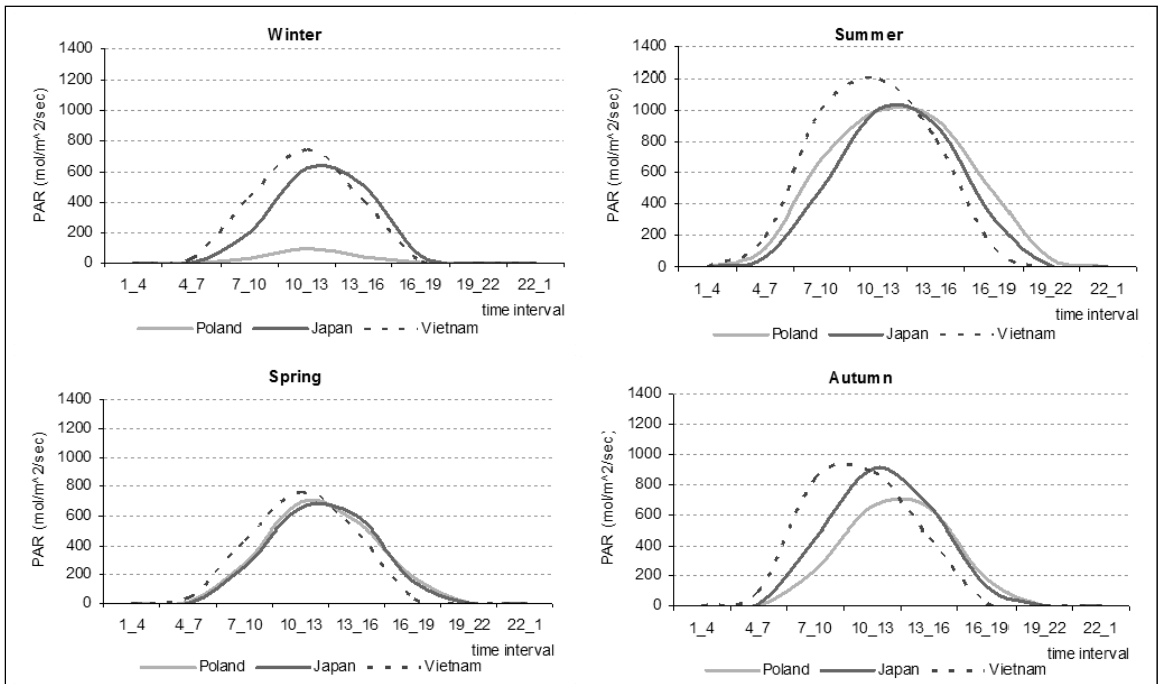

Fig. 2: Seasonal mean values of photosynthetically active radiation (PAR) at studied locations

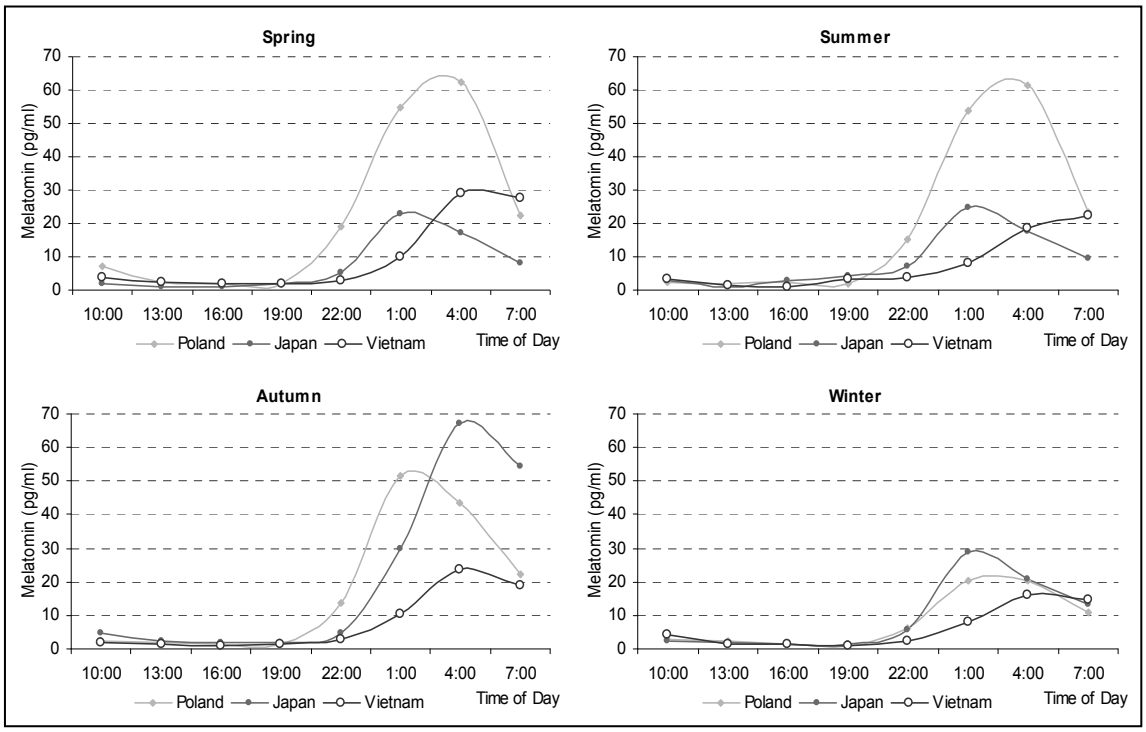

Fig 3: Mean diurnal melatonin secretion (pg/ml) in seasons at studied locations

Figure 2 presents seasonal mean values of photosynthetically active radiation (PAR) (400 - 710 nm) in 3 hours intervals during experiment time. The highest values in each season were observed for Vietnam (Hanoi), the smallest for Poland (Warsaw). Maxi-

mum of PAR intensity usually occurred between 10 a.m. and 1 p.m. In Hanoi PAR maximum was observed earlier than in other locations. The biggest differences of PAR distribution among the locations occurred in Autumn.

Figure 3 shows mean diurnal melatonin secretion, in studied exposition time. The smallest values were observed during the day time and in Winter. At Spring and Summer the biggest values were observed for Polish participants, in Autumn and Winter for the Japanese. From Spring to Autumn in Poland maximum melatonin secretion was over 50 pg/ml, at Winter only 20 pg/ml. Seasonal differences between participants were even bigger. The level of melatonin secretion observed for Vietnamese participants was similar in each season.

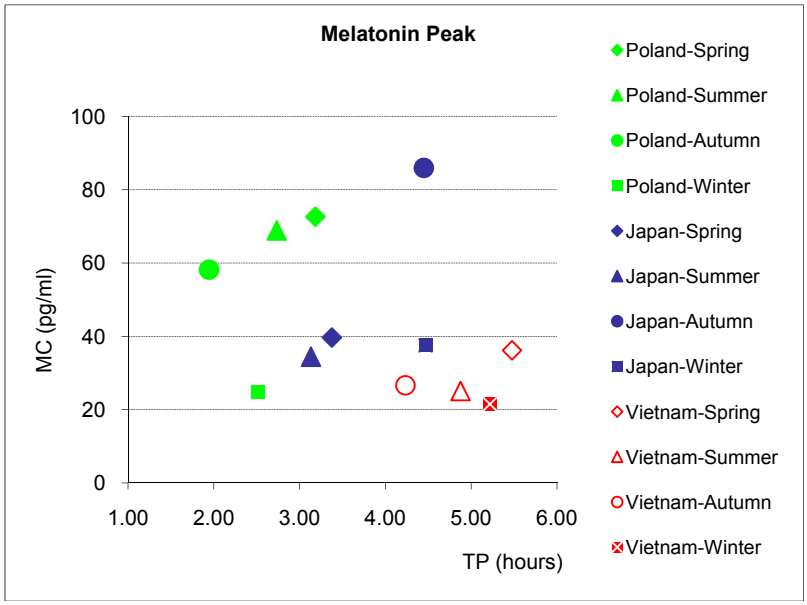

Fig. 4: The highest melatonin secretion (MC) and the Time Peak (TP) of its occurrence in different seasons at studied locations

Relationships between melatonin secretion and the time peak of its occurrence are presented at figure 4. Values of MC were determined based on interpolation of measured melatonin concentration. Melatonin peak in each location has occurred few hours or just before sun rise. The earliest occurrence of melatonin peak was noted for Poland, the latest for Vietnam. At Polish subjects time peak was noted between 2 and 3 am, at Japanese between 3 and 5 am and for Vietnamese between 4 and 6 am. Melatonin concentration levels at Polish participants in all season except Winter was higher than in participants from other locations.

4. Conclusions

Environmental factors have significant impact at solar radiation totals and in consequence at melatonin rhythm. The most stable lighting conditions (as consequence of geographical location) was observed in Vietnam. Melatonin secretion in Hanoi (Vietnam) was similar in all seasons, which confirm mainly impact of solar radiation at melatonin diurnal and seasonal cycles.

The lowest values of melatonin in saliva samples were observed during the day time, where highest intensity of solar radiation was observed. That may suggest that Winter should be the season with the biggest melatonin secretion in humans. Experimental data do not confirm that.. Winter proved the season with the smallest melatonin secretion. This may suggest that melatonin peak can be depend on other factors, eg. radiation totals absorbed during the day time or on length of daily exposure at outdoor conditions. Further studies should be conduced.

The Time Peak of melatonin secretion depends on moment of sun rise and day length, which confirms regional and seasonal differences.

Acknowledgments

This research was partly supported by Japan Society for the Promotion of Science grant No 16207021.

References

Blazejczyk K., Morita T., Kanikowska D., Tokura H., Wiktorowicz K., Ueno T., Bakowska M., 2005, Regional differences in diurnal and seasonal cycles of lighting conditions and melatonin secretion. DWD, Annalen der Meteorologie, 41, 1, 17th International Congress of Biometeorology ICB 2005, 301-304.

Morita T., Koikawa R., Ono K., Terada Y., Hyun K., Tokura H., 2002, Influence of the amount of light recived during the day and night on the circadian rhythm of melatonin secretion in woman living diurnally. Biological Rhythm Research, 33, 3, 271-277.

Morita T., Rutkowska D., Ohyama M., Tokura H., 1997, Absence of an effect of light of different wavelengths on the nocturnal fall of core temperature and rise of melatonin secretion in color-deficient subjects. Biological Rhythm Research, 28, Supplement, 104-110.

Morita T., Tokura H., 1998, The influence of different wavelengths of light on human biological rhythms. Applied Human Science, 17(3), 91-96.

Ueno-Towatari T., Norimatsu K., Blazejczyk K., Tokura H., Morita T., 2007, Seasonal variations of melatonin secretion In young females under natural and artificial Light conditions In Fukuoka, Japan. Journal of Physiological Anthropology, 26(2), 209-215.

Author's adresses:

Mgr Joanna Maroszek (joanna.maroszek@gmail.com)
University of Warsaw, Interfaculty Individual Doctoral Studies
in Mathematics and Natural Sciences, Zwirki i Wigury 93, Warsaw, Poland

Prof. dr hab. Krzysztof Blazejczyk (kblazejczyk@uw.edu.pl)
University of Warsaw, Faculty of Geography and Regional Studies, Krakowskie Przedmiescie 28/30, Warsaw, Poland

Prof. dr hab. Takeshi Morita (morita@fwu.ac.jp)
Fukuoka Woman University, Faculty of Human Environment Science, Higashi-ku, Fukuoka 813-8529, Japan

Clothing as an indicator of human thermal comfort

Katarzyna Lindner

Faculty of Geography and Regional Studies, University of Warsaw, Poland

Abstract

The aim of the paper was to discuss the clothing habits of young Polish during the summer time, in relation to dynamically changing weather conditions. The values of air temperature as well as biometeorological indexes (*PET* and *Iclp*) were compared to both: subjective thermal sensations of subjects and clothing worn in the given moment. This allowed to determine 5 types of clothing, used in different biometeorological conditions, by people that described their thermal sensation as comfortable or sub comfortable. Moreover it was examined if insulation of clothing worn by respondents was consistent with the values by *Iclp* (Insulation Predicted index).

1. Introduction

In order to maintain thermal comfort, people adjust to changing conditions of atmospheric environment by using clothes of appropriate thermal insulation. The relation between clothing and current thermal conditions has been already described by Donaldson et al. (1998), Mäkinen et al. (2006) or Goodwin et al. (2000), but these studies focused mainly on cold seasons. Strong contribution field has been made by Donaldson et al. (2001) who gathered the data of clothing applied outdoors from 6538 individuals from 8 regions of Europe. The present study provides additional information by investigating clothing types applied by young people (20 – 25 years) in the summer in Poland.

2. Materials and methods

The data analyzed in this research had been collected within three field observation series. They took place in July in the surroundings of Cracow (south Poland), at Dobczycki Reservoir region, in the years 2003, 2006 and 2009. Meteorological conditions during observations were representative for the climate in this region in the summer.

During the study air temperature and biometeorological indexes (*PET* – Physiological equivalent temperature and *Iclp* – Insulation Predicted), that characterize current state of biothermal environment, were compared with responses given by subjects in weather perception questionnaire, that has been carried out simultaneously with meteorological measurements. Respondents - geography students in the age of 20-25 years, who were specially instructed first, described their subjective perception of particular weather elements and characterized the type of currently used clothing. In the second part, the study focused only on cases, in which current sensible conditions were described as tolerable (neutral and slightly cool/slightly warm). Subsequently it was determined what kind of clothing used by subjects to ensure them thermal comfort in different biometeorological conditions. Thermal insulation of the clothing used by subjects was determined on the basis of total insulation values suggested by Krawczyk (1993), modified in order to adjust to the specificity of young people clothing style.

3. Subjective thermal perception with respect to biometeorological conditions

Field researches were carried our in various types of weather. In the analyzed period mean air temperature was 20.4°C, minimal temperature was 11.5°C and maximal 33.6°C. Some measurements were performed for 24 hours periond, so also after sunset, what could to extent influence perception of sensible conditions. The weather in the time of research was not very windy (v = 1.3 m/s), but due to the presence of a big water reservoir (Dobczycki Reservoir) it was rather humid (RH = 69.2%). Mean value of the *PET* index in analyzed period was 20.8°C, what corresponds to thermal comfort, but the values varied from 5.1°C („cold") to 46.6°C („very hot") (Matzarakis et al. 1999).
Subjects were evaluating their thermal perception using seven point scale, in which value -3 meant "cold", 0 - "thermal comfort" and +3 represented "hot". In analyzed period nearly 40% of respondents assessed their thermal perception as comfortable, and about 70% described it as acceptable (comfort and sub comfort). At the same time subjective perception of comfort was present in all ranges of thermal perception scale for *PET* index (Fig. 1). Besides individual preferences of each person, this was a consequence of efficient adaptation of clothing to the current biometeorological conditions. The most precisely subjects have assessed extreme states – "hot" (+3) and "cold" (-3). They were present only in marginal ranges of the thermal perception scale for *PET* (over 29°C – „warm" and „hot"; below 13°C – „ cool" and „cold").

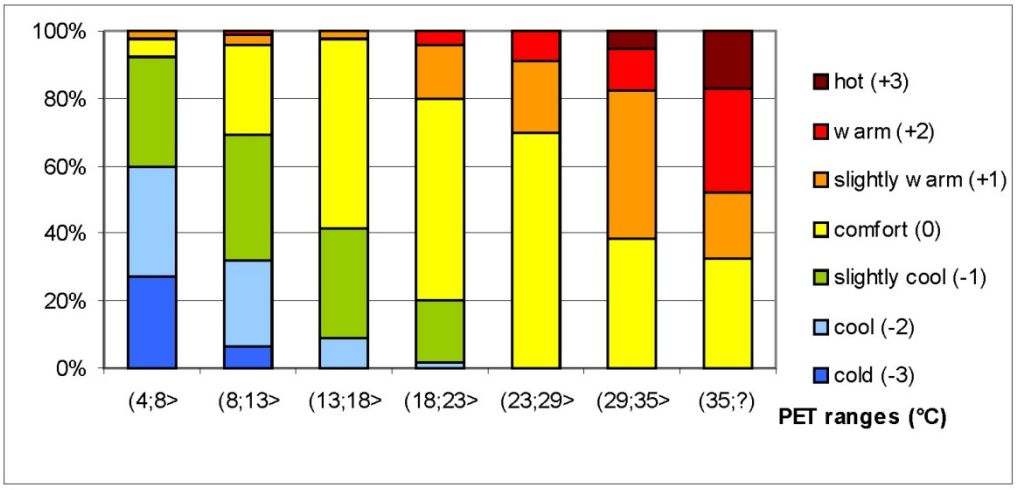

Fig. 1: Subjective thermal perception in particular ranges of thermal scale for *PET* index

4. Clothing used in specific thermal conditions

Clothing thermal insulation (*Icl*) that was calculated for clothes used by respondents, who described their perception as comfortable or sub comfortable, is a function of ambient air temperature (Fig. 2). A third order polynomial was used to fit the data:

$$y = 0.0006 \cdot Icl^3 - 0.0341 \cdot Icl^2 + 0.5795 \cdot Icl - 1.5592.$$

The coefficient of determination is 0.75, with a standard error of estimation is 0.29 clo.

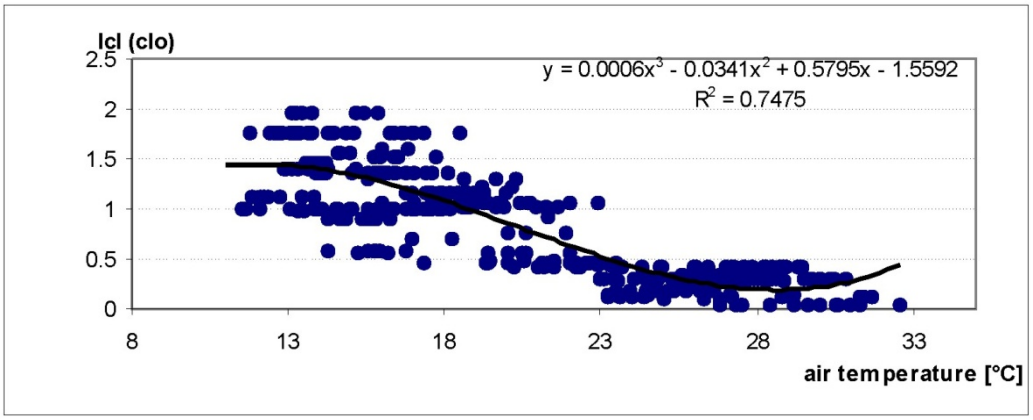

Fig. 2: Relation between clothing insulation (Icl) and air temperature

Figure 3 shows air temperature and *PET* values plotted against mean insulation of clothing, worn by individuals assessing the sensible conditions as acceptable. At air temperature of 10-14°C the mean thermal insulation of clothing equals 1.54 clo and with the increase of temperature it is observed a steep decrease of clothing insulation. It slows down at around 22°C, when people use clothing of 0.35 clo. Further reducing of worn clothing is limited by factors related to modesty and acceptance of scant clothing by the person itself as well as by the society (Parsons 2002).

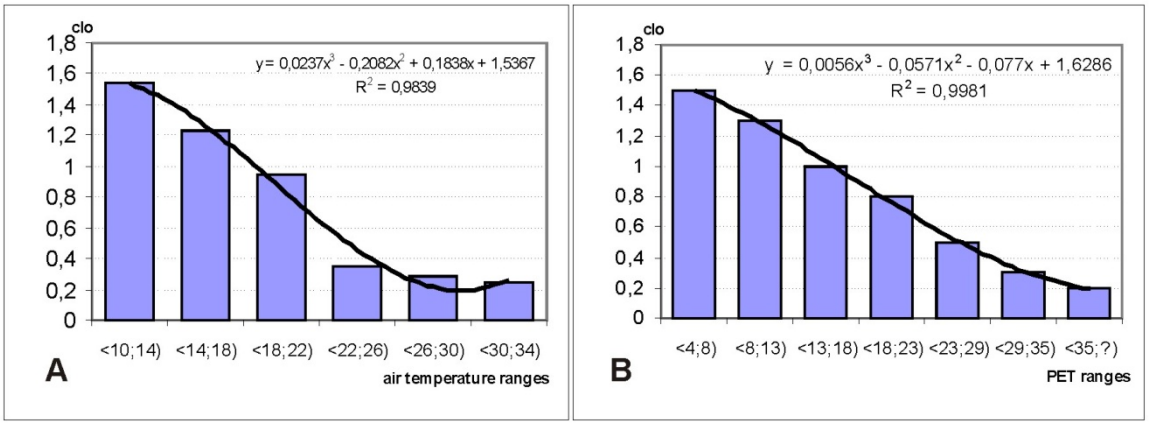

Fig. 3: Mean values of thermal insulation of worn clothing with reference to air temperature (a) and *PET* index values (b)

The similar trend is observed for *PET* index. At *PET* values of 4-8°C, when it is sensibly cold, clothing of 1.5 clo is worn, whereas in the upper scale (over 35°C), when it is sensibly hot and very hot, it is of 0.2 clo and its further reduction is limited. The mean value of clothing thermal insulation in the cases in which *PET* had neutral values equaled to 1 clo.

The clothing worn by respondents may be divided into several types (Tab. 1). Type A corresponds to light summer clothing (up to 0.4 clo) comprised of short skirt or shorts, sandals or flip-flops and depending on subtype: bikini, short top, vest (A1) or T-shirt (A2). As far as males are concerned subtype A1 includes also situation with no top

clothing, which is characteristic of certain places (like recreation zones) and activities that don't require formal clothing. Type B comprises of similar clothing as in subtype A2 but in this case trousers or long skirt and sometimes normal shoes are worn.

Table 1: Types of clothing worn by respondents in terms of thermal insulation values

type	description	Icl (clo)
A1	shorts/short skirt, bikini/top/vest, sandals or flip-flops	<0;0,2)
A2	shorts/short skirt, bikini/top/T-shirt, sandals or flip-flops	<0,2;0,4)
B	trousers/long skirt, T-shirt, sandals or flip-flops	<0,4;0,6)
C	Like type B + long sleeve blouse/shirt, shoes	<0,6;1)
D1	trousers/long skirt, 3 layers of top clothing (T-shirt, blouse/shirt and long sleeve blouse/light sweater - 0,8 clo), shoes	<1;1,3)
D2	Like D1, but warmer top clothing (with sweater or polar) - 1-1,2 clo	<1,3;1,45)
E	trousers/long skirt, 4 layers of top clothing (over 1,2 clo), the forth layer constitutes windjammer or one-layer jacket	<1,45;2)

The most seldom used clothing type is type C (Fig.4). It comprises of trousers or long skirt,
T-shirt, second layer of clothes like blouse or shirt and shoes or sandals. It is probable that type C would be more often used in other types of environment, for example in the city. Type D consists of two subtypes. Subtype D1 resembles type C but includes third layer of top clothing. As a result in this subtype the top clothing is quite warm (insulation reaching 0.8 clo), whereas bottom clothing consists of trousers, socks and shoes. Subtype D2 is characterized by higher than D1 thermal insulation of third top clothing layer (polar or sweater) that may reach 1-1.2 clo. Finally, individuals that were in the conditions with *PET* values corresponding to "cold" (4-8°C) or "cool" (8-13°C) in order to assure their thermal comfort used the type E clothing (Fig. 5) which includes, in addition to clothing from type D, fourth layer (windjammer, one-layer jacket) that increases thermal insulation value of top clothing to over 1.2 clo.

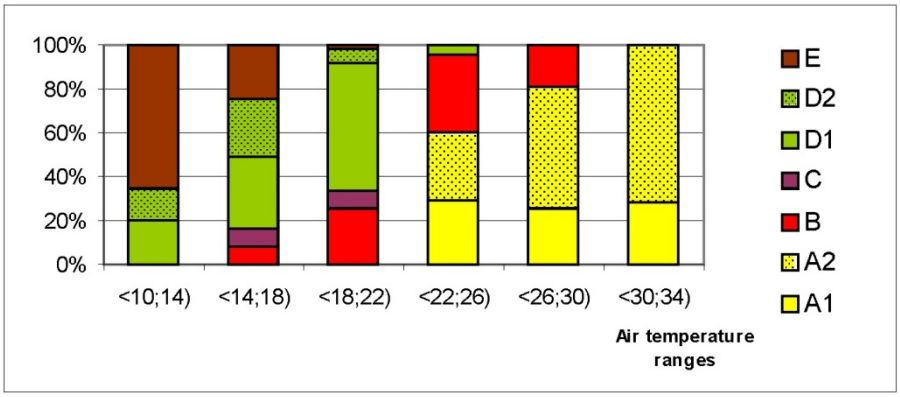

Fig. 4: Frequency of wearing different clothing types plotted against air temperature. A1- E - types of clothing used by subjects. For explanations see table 1

Figures 4 and 5 show frequency of wearing particular types of clothing with respect to air temperature ranges and *PET* index values, determined using thermal sensation scale.

In higher air temperatures and *PET* value above 23°C most commonly used clothing type was type A. Conversely in air temperatures around 14-22°C and *PET* values 13-18°C ("slightly cold") much more often type D clothing was used. In addition in the conditions described by *PET* index as comfortable respondents achieved comfort and sub comfort using type B clothing.

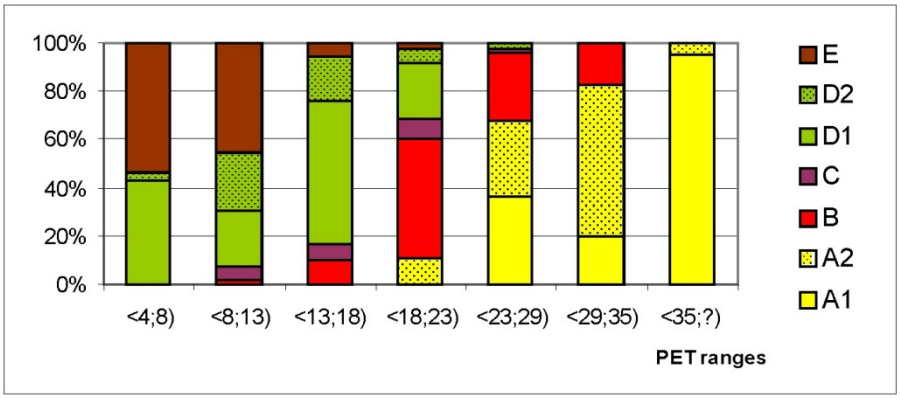

Fig. 5: Frequency of wearing different clothing types plotted against PET thermal sesation scale. A1- E types of clothing used by subjects. For explanations see table 1

5. Insulation of used clothing vs. predicted insulation (*Iclp*)

Insulation of clothing used by respondents, was compared to Predicted insulation index (*Iclp*), that specify clothing insulation necessary to maintain thermal balance of the human organism (Blazejczyk 2004). Taking under considerations only the clothing used by people assessing their subjective thermal perception as comfortable and sub comfortable, it was expected, that the clothing insulation values would be similar to values calculated with *Iclp* index. In fact, significant differences between these two measures occurs (Fig. 6).

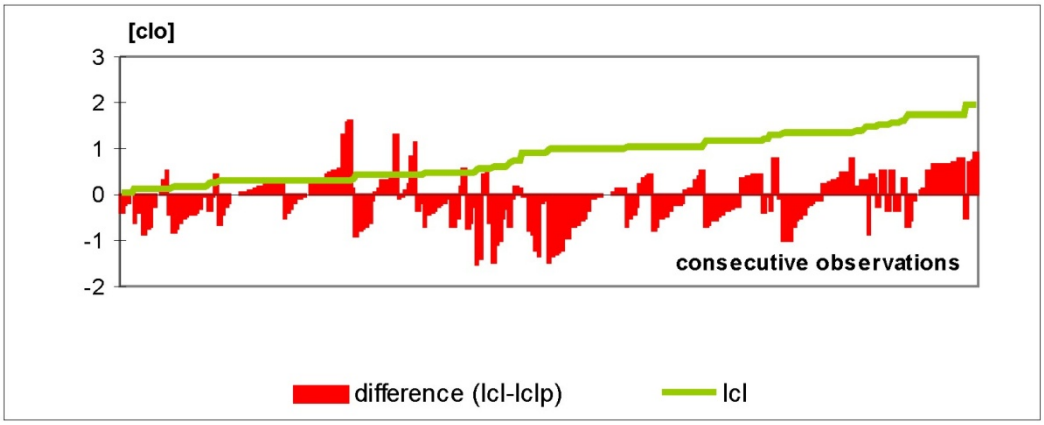

Fig. 6: Differences between thermal insulation of used clothing (*Icl*) and predicted insulation (*Iclp*) index values.

In addition it has been observed that many individuals wore too light, with respect to thermal conditions, clothing (so called "underdressing"), however this trend was not very clear. This observation is in agreement with data from Jendritzky et al. (2009), who analysed clothing habits of Europeans. On the other hand, in case of subjectively per-

ceived coolness (and therefore in case of using clothing of a high thermal insulation), respondents tend to wear warmer clothes than predicted by *Iclp* index. This inclination to "overdressing" was observed especially during night measurements, when subjects were influenced by the lack of solar radiation and probably felt a little uncomfort in connection with changing their biorhythm and lack of sleep.

6. Conclusions

The results presented in the paper proves the rationality of analyzed population behavior and shows that the people are able, to a certain extent, to assure thermal comfort by using appropriate clothing. The relations observed between clothing insulation and air temperature as well as *PET* index allow to conclude that as far as the clothing habits of the given population are identified, it is possible to assess actual sensible conditions from analysis of used clothing and subjective sensations of subjects. It is however important to take into account, that this kind of analysis will bear a significant error, as each person has individual preferences. Moreover intensive physical activity requires different clothing as the metabolic production is higher. Assessing sensible conditions from the point of view people are dressed can be also difficult in cases, when adjusting worn clothing to short term changes of thermal conditions is not possible or is ignored by the subjects, because of the impermanent character of weather changes.

References

Blazejczyk, K., (2004): Bioklimatyczne uwarunkowania rekreacji i turystyki w Polsce (Bioclimatic principles of recreation and tourism in Poland), Prace Geograficzne 192, pp. 291.

Donaldson, G.C., Tchernjavskii, V., Ermakov, S.P., Bucher, K., Keatinge, W.R., (1998): Winter mortality and cold stress in Yekaterinburg, Russia: interview survey. BMJ 316, 514-518.

Donaldson, G.C., Rintamäki, H., Näyhä, S. (2001): Outdoor clothing: its relationship to geography, climate, behavior and cold-related mortality in Europe. Int. J.Biometeorol. 45, 45–51.

Goodwin, J., Taylor, R.S., Pearce, V.R., Read, K.L., (2000): Seasonal cold, excursional behavior, clothing protection and physical activity and old subjects. Intl. J. Circumpolar Health, vol. 59, 195-203.

Jendritzky G., Havenith G., Weihs P., Batchvarova E. (eds.), 2009, Towards a Universal Thermal Climate Index UTCI for assessing the thermal environment of the human being. Final Report COST Action 730.

Krawczyk, B., (1993): Typologia i ocena bioklimatu Polski na podstawie bilansu cieplnego ciała człowieka (The typology and evaluation of the bioclimate of Poland on the basis of the human body heat balance). Prace Geograficzne 160, pp. 102.

Mäkinen, T.M., Raatikka, V-P., Rytkönen, M., Jokelainen, J., Rintamäki, H., Ruuhela, R., Näyhä, S., Hassi, J., (2006): Factors affecting outdoor exposure in winter: population-based study. Int. J. Biometeorol. 51, 27–36.

Matzarakis, A., Mayer, H., (1996): Another kind of environmental stress: thermal stress, WHO News 18, 7-10.

Parsons, K., (2002): The effects of gender, acclimation state, the opportunity adjust clothing and physical disability on requirements for thermal comfort. Energy and Buildings 34, 593-599.

Authors' address:

MA Katarzyna Lindner (katarzyna_lindner@yahoo.com)

Faculty of Geography and Regional Studies, University of Warsaw, Krakowskie Przedmiescie 30, 00-927 Warsaw, Poland.

Klimawandel und Hautkrebserkrankungen – Zusammenhang und Wirkungen

Jobst Augustin

Umweltbundesamt, Berlin
Universitätsklinikum Hamburg-Eppendorf, Hamburg

Zusammenfassung

Hautkrebs (Karzinom, Melanom) ist die häufigste Form von Krebs in Deutschland (140.00 Neuerkrankungen in 2008). Die Inzidenz ist stark ansteigend. UV-Strahlung wird als vollständiges Karzinogen bei Hautkrebserkrankungen angesehen und ist damit auch der Hauptrisikofaktor. Ozon gilt als ist der wichtigste natürliche Schutz gegenüber der UV-Strahlung. Werden die natürlichen Einflussfaktoren von Hautkrebserkrankungen beschrieben, wird häufig nur das Ozon (-loch) als UV-strahlungsbeeinflussender Faktor thematisiert, nicht aber der Klimawandel. Anhand eines Kausalitätsmodells und zweier Beispiele sollen die Zusammenhänge näher beschrieben werden.

Climate change and skin cancer - relation and effects

Abstract

Skin cancer (Melanoma, squamos cell carcinoma, basal cell carcinoma) is the most frequent cancer in Germany (140.000 cases in 2008). The incidence is increasing rapidly. Because of UV-radiation is verified as a complete carcinogen, UV-radiation is the main risk factor for skin cancer diseases. Ozone is the most important natural protection against UV-radiation. Mostly ozone and the hole in the ozone layer are regarded as important factors with an impact on skin cancer. Climate change is in many studies not included. By the help of a causal model and two examples, the relation between climate change and skin cancer diseases should describe.

1. Einleitung

Mit 140.000 Neuerkrankungen (2008) zählt Hautkrebs (Karzinom, Melanom) zu den häufigsten Krebserkrankungen in Deutschland. Auffallend ist die besonders starke Zunahme der Hautkrebsinzidenz während der letzten 30 Jahre, denn die Erkrankungshäufigkeit hat sich in diesem Zeitraum etwa verzehnfacht. Hauptrisikofaktor für die Entstehung von Hautkrebs ist die UV-Strahlung, deren karzinogene Wirkung nachgewiesen ist. Das stratosphärische Ozon gilt als wichtigster natürlicher Schutzfaktor vor den kurzwelligen und aus biologischer Sicht besonders schädlichen UV-Strahlungsanteilen (UV-B). Insbesondere der Eintrag ozonzerstörender Substanzen – vor allem Fluorchlorkohlenwasserstoffe (FCKWs) – hat dazu geführt, dass sich die UV-Strahlung erhöht hat. Dies kann neben einem sich verändernden Schönheitsideal als wesentlicher Faktor für die Zunahme der Hautkrebserkrankungen angesehen werden.

Bislang ungeklärt ist die Entwicklung der Hautkrebshäufigkeit unter dem Einfluss des Klimawandels. Ein Grund hierfür mag in den teilweise sehr komplexen und vielfältigen Zusammenhängen zwischen klimatischen Veränderungen, der UV-Strahlung, dem menschlichen (Expositions-) Verhalten und der Hautkrebsinzidenz liegen. In der Abb. 1 ist ein Kausalitätsmodell ersichtlich, dass die Zusammenhänge zwischen dem Klima und Hautkrebserkrankungen vereinfacht beschreibt. Dabei zeigt sich, dass die strato-

sphärische Ozonkonzentration von einer Vielzahl von Faktoren (chemisch und dynamisch) beeinflusst wird, die ihrerseits dem Einfluss klimatischer Veränderungen unterliegen. Neben dem Einfluss der Aerosole und der Bewölkung wirkt sich das stratosphärische Ozon auf die UV-Strahlungsintensität aus, die wiederum unter Berücksichtigung des Präventions- und Expositionsverhaltens für eine Karzinogenese verantwortlich ist. Ein in diesem Kontext wichtiger Link besteht zwischen dem „Klima“ und dem „Expositionsverhalten“, denn thermische bzw. meteorologische Veränderungen können das menschliche Expositionsverhalten gegenüber der UV-Strahlung beeinflussen.

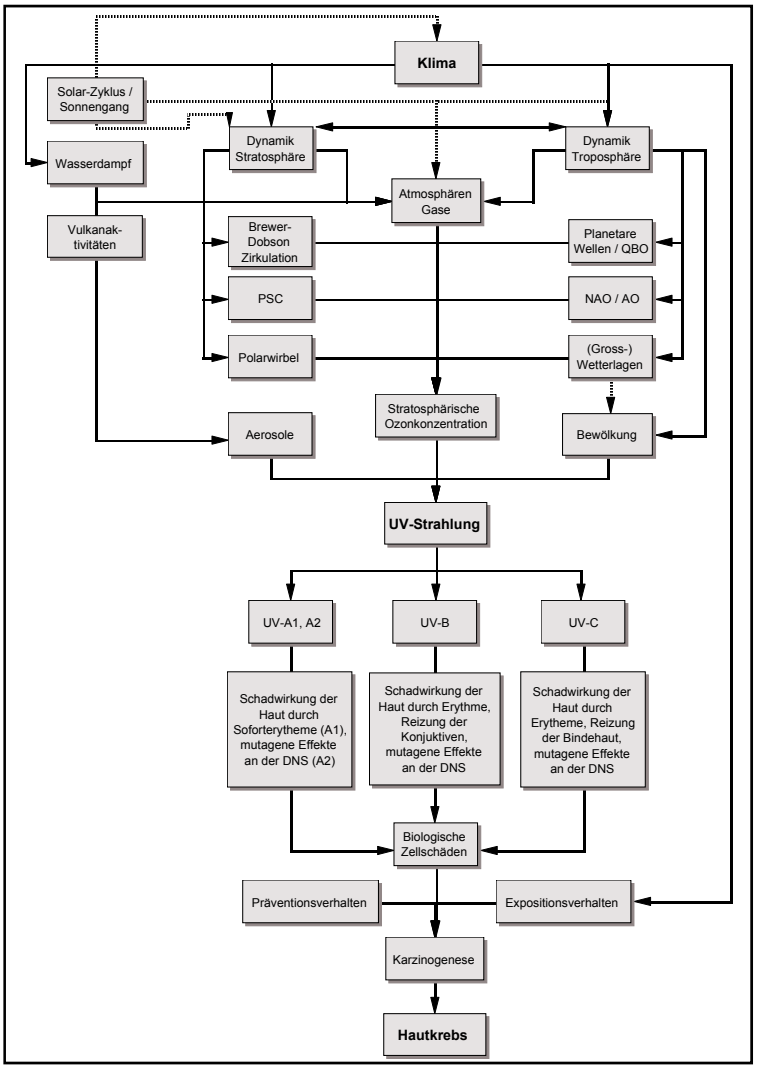

Abb. 1: Kausalitätsmodell Klima und Hautkrebserkrankungen

2. Veränderung strahlungsbeeinflussender Faktoren – das Beispiel Ozon

Klimatische Veränderungen können sich sowohl auf die Ozondynamik (Ozonverteilung) als auch auf die Ozonchemie auswirken. Die Dynamik der Atmosphäre kann die chemischen Prozesse temporär überlagern, da sie das Ozon in der Atmosphäre verteilt und beispielsweise ozonarme Luftmassen aus den polaren oder äquatorialen Breiten nach Mitteleuropa befördert (Streamer). Eine für die Ozonchemie bedeutende und durch die globale Erwärmung beeinflusste Größe ist die Temperatur der Stratosphäre. Baldwin

und Dameris (2006) konnten eine langfristige Abnahme der Stratosphärentemperatur von 0,5 K pro Dekade beobachten. Die Abkühlung der Stratosphäre hat verschieden Ursachen. Zum einen spielt die Hebung der Tropopause eine Rolle, die auf der klimatisch bedingten Erwärmung der Troposphäre basiert. Im Gegenzug zur Troposphärenerwärmung tritt dabei eine Stratosphärenabkühlung ein. Zum anderen tritt eine Abkühlung der Stratosphäre durch den verstärkten Ozonabbau während der letzten Jahrzehnte ein, da weniger UV-Strahlung durch Ozon absorbiert wird. Ein weiterer Aspekt liegt im Eintrag von Treibhausgasen, denn Treibhausgase beeinflussen die Strahlungsbilanz der Troposphäre und Stratosphäre. In der Troposphäre absorbieren sie die langwellige Strahlung der Erde, die zur Erwärmung führt (Treibhauseffekt). In der Stratosphäre ist dies etwas anders, denn der verstärkte Eintrag von CO_2 kann netto zu einer Abkühlung führen, da mehr langwellige Strahlung emittiert als absorbiert wird. Die Abkühlung der Stratosphäre ist für die Ozonzerstörung von hoher Bedeutung, da diese unter anderem die Stabilität des Polarwirbels und damit die Bildungswahrscheinlichkeit Polarer Stratosphären Wolken (PSC) erhöht. Polare Stratosphärenwolken sind in hohem Maße mitverantwortlich für den Abbau des stratosphärischen Ozons in den polaren Breiten („Ozonloch“). Ihr Entstehen und Vorkommen ist an sehr kalte Temperaturen gebunden, die über längere Zeit oftmals nur im Inneren des Polarwirbels erreicht werden. Der Polarwirbel führt zu einer Isolation der kalten Luftmassen. Im polaren Winter (keine Photolyse zur Ozonbildung) finden starke ozonzerstörende Prozesse statt, da kein Austausch mit ozonreichen und/oder wärmeren Luftmassen außerhalb des Wirbels eintritt. Erst die zunehmende Instabilität – bedingt durch die Temperaturerhöhung im Frühjahr – lässt den Wirbel zunächst mäandrieren und schließlich ganz zusammenbrechen. In diesem Zusammenhang wichtige Ereignisse sind Low-Ozone Events (LOEs) und Ozone-Miniholes (OM). Sie werden definiert über Schwellenwerte der Ozonkonzentration (z.B. OM < 220 DU), die allerdings nicht einheitlich geregelt sind. LOEs und OMs sind im Winter und Frühjahr auftretende starke, temporäre Ozonverluste über eine im Vergleich zum „Ozonloch“ jedoch verhältnismäßig kleine Fläche. Die Advektion warmer, subtropischer Luftmassen in der Tropopause im Zusammenhang mit dem Brechen von Wellen ist der entscheidende Prozess, der zur Ausbildung von LOEs und OM führt. Die Advektion polarer, ozonarmer Luftmassen ist ebenfalls von Bedeutung (z.B. mäandrieren des Polarwirbels) und kann zu den regional niedrigen Ozonwerten beitragen (Brönnimann und Hood, 2003). Die Häufigkeit der OM-Ereignisse hat in den letzten 20 Jahren über dem europäisch-atlantischen Sektor zugenommen (Stenke und Grewe, 2003). Hauptursache hierfür ist eine lokale Veränderung der atmosphärischen Dynamik (beispielsweise aufgrund der NAO) oder ein veränderter stratosphärischer Transport mit daraus resultierenden geringen Ozonwerten (vgl. Brönnimann und Hood, 2004; Reid et al., 2000). Mit dem Auftreten solcher Extremereignisse gehen teilweise stark erhöhte UV-Intensitäten einher, die insbesondere im Frühjahr eine kritische Wirkung auf die zu diesem Zeitpunkt kaum sensibilisierte Haut haben können. In der Abb. 2 ist für den 05.02.1990 das Auftreten eines LOEs in Mitteleuropa erkennbar. Die Abbildung zeigt die Abweichung der erythemwirksamen UV-Tagesdosis vom 05.02.1990 bezogen auf das langjährige (1984-2003) Monatsmittel im Februar in J/m². Durch die Abnahme des stratosphärischen Ozons innerhalb von zwei Tagen auf 277 DU (langjähriges Monatsmittel 355 DU) stieg die erythemwirksame UV-Tagesdosis auf 510 J/m² und liegt damit kurzzeitig 46 % über dem langjährigen Monatsmittel von 277 J/m² (Beispiel Potsdam). Dabei zeigt sich, dass die ozonarmen Luftmassen vermutlich aus den äquatorialen Bereichen stammen, und es sich um einen Streamer handelt. Dies wird dadurch

gestützt, dass zeitgleich eine zyklonale Südwestlage (SWZ) herrschte, die ozonarme Luftmassen aus den niederen Breiten nach Europa transportiert hat – der Grund für die erhöhte Strahlungsintensität war somit dynamischer Herkunft.

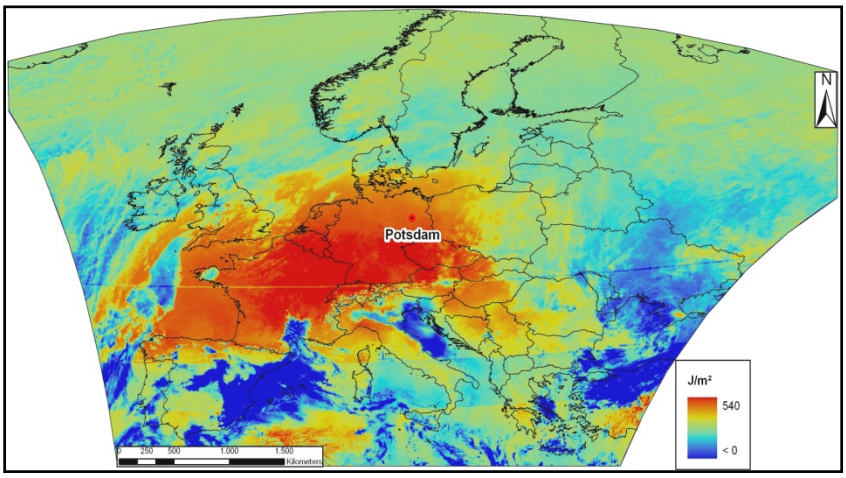

Abb. 2: Abweichung des 05.02.1990 vom langjährigen (1984-2003) Monatsmittel (Februar) der mittleren erythemwirksamen Tagesdosis in J/m²

3. Veränderung expositionsbeeinflussender Faktoren – das Beispiel Physiologisch Äquivalente Temperatur (PET)

Aus der Veränderung der UV-Strahlung alleine lassen sich keine Rückschlüsse auf eine sich verändernde Hautkrebshäufigkeit ableiten, denn erst die (übermäßige) Exposition gegenüber der UV-Strahlung kann zu Hautschäden und Mutationen führen. Damit kommt der Exposition bzw. der Expositionsmotivation des Menschen eine besondere Bedeutung zu. Insbesondere die „thermisch motivierte“ Exposition ist vor dem Hintergrund des Klimawandels ein zunehmend bedeutender Aspekt, der bislang jedoch kaum untersucht worden ist. Bentham (2001) geht von einer Veränderung des Freizeit- und Kleidungsverhaltens aufgrund einer Temperaturzunahme aus und prognostiziert dadurch erhöhte UV-Exposition in der Bevölkerung. Obwohl die Urlaubsexposition nicht zu vernachlässigen ist, ist die „heimische“ Exposition von hoher Bedeutung. Wie eine Untersuchung von Knuschke et al. (2007) gezeigt hat, können in Abhängigkeit von den meteorologischen Bedingungen ähnlich hohe Strahlungsdosen in Deutschland erreicht werden, wie im Mittelmeerraum. Als Grund für diese hohen Expositionen kann in erster Linie die gefühlte Temperatur angenommen werden. Im Sommer wird die Sonne im Mittelmeerraum aufgrund der hohen Wärmebelastung – vor allem in den Mittagsstunden – gemieden und Schatten aufgesucht. Aufgrund des eher geringeren Temperaturniveaus in Deutschland (vor allem an der Küste) wird die Sonnenwärme und damit die UV-Exposition auch über die Mittagsstunden gesucht. Bezogen auf die Tagesdosis kann damit die UV-Exposition selbst in thermisch etwas ungünstigeren Regionen relativ hoch sein.

Es zeigt sich, dass meteorologische Gegebenheiten (Temperatur, Bedeckungsgrad, Feuchtigkeit, Sonnenscheindauer, Niederschlag) einen wesentlichen Faktor in der UV-Exposition spielen und auch gut mit dieser korrelieren. Vor diesem Hintergrund stellt sich die Frage nach der Veränderung dieser Faktoren. Als Beispiel dient hier die Phy-

siologisch Äquivalente Temperatur (PET). Bei der PET handelt es sich um einen so genannten „thermischen Indize“, das heißt ein Verfahren zur Beschreibung und Bewertung der thermischen Umgebung des Menschen. Die PET ist für eine beliebige Stelle im Freien definiert als diejenige Lufttemperatur, bei der in einem typischen Innenraum die Wärmebilanz eines Menschen bei gleichen Werten der Haut- und Kerntemperatur ausgeglichen ist wie unter den Bedingungen im Freien (vgl. VDI, 1998). Jeder PET kann das thermische Empfinden (z.B. kalt, behaglich, heiß) und eine thermische Belastungsstufe (z.B. nach Matzarakis und Mayer, 1996) zugeordnet werden. Dadurch lässt sich ableiteten, ob ein thermischer Komfort bzw. Diskomfort besteht und eine Strahlungsexposition (unter anderem in Abhängigkeit der „gefühlten Temperatur“) wahrscheinlich ist. In der Abb. 3 ist die mittlere PET für den Monat Juli (1961-2008) abgebildet. Es zeigt sich eine tendenzielle Zunahme der PET von Norden in Richtung Süden. Die eher geringen Werte an der Küste lassen sich unter anderem auf die im Mittel geringeren Lufttemperaturen, aber auch auf den Einfluss des Windes zurückführen, der den thermischen Komfort herabsetzt.

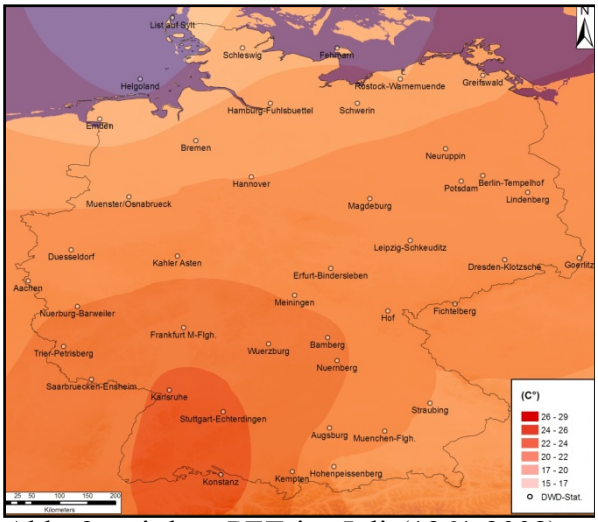

Abb. 3: mittlere PET im Juli (1961-2008) in C°

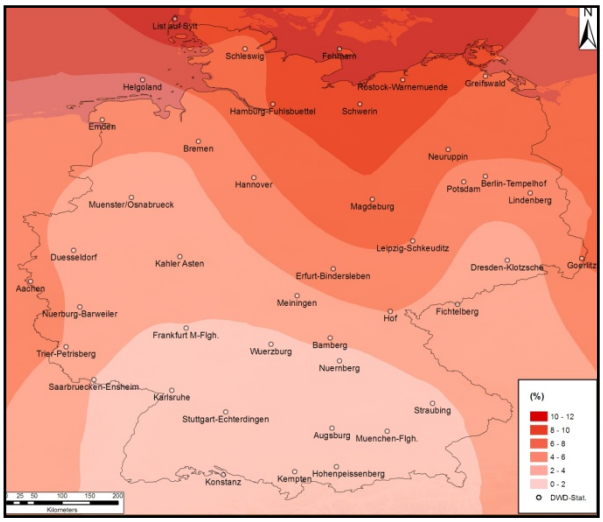

Abb. 4: Veränderung der PET im Juli (1961-2008) in %

In Abb. 4 ist die Veränderung (%) der PET für den Monat Juli zwischen 1961-2008 erkennbar. Es zeigt sich insbesondere in den Küstenregionen eine Zunahme der PET, hingegen bleibt diese im Süden Deutschlands nahezu unverändert. Die Ursache für diese Veränderungen bedarf weiterer Untersuchungen, jedoch zeigt das Beispiel, dass sich die thermischen Bedingungen – vor allem im Norden Deutschland – unter langjähriger Betrachtung begünstigt haben. An dieser Stelle ist aber zu erwähnen, dass die Temperatur nur ein expositionsbeeinflussender Faktor darstellt und zudem eine langfristig sehr starke Temperaturerhöhung auch zum verstärkten Diskomfort und einer Verschlechterung der Expositionsbedingungen führen könnte.

4. Zusammenfassung

Das Beispiel Ozon hat verdeutlicht, dass Zusammenhänge zwischen dem Klima und dem stratosphärischen Ozon bestehen, diese aber komplex und noch unsicher sind. Allerdings wurde in den letzten 10 Jahren aufgrund der chemischen, dynamischen und strahlungsphysikalischen Rückkopplungen deutlich, dass der Ozonhaushalt weitaus en-

ger mit dem Treibhauseffekt in Verbindung steht als bislang angenommen (vgl. Shindell und Grewe, 2002). So kann nach Winkler (2003) beispielsweise 30 % des stratosphärischen Ozonverlustes auf den langfristigen Anstieg der Tropopause zurückgeführt und zudem eine (globale) Zunahme von Streamern modelliert werden – beides Faktoren, die dem Einfluss klimatischer Prozesse unterliegen und die UV-Strahlungsintensität verändern. Das sich verändernde (Exposition-) Verhalten der Menschen unter dem Klimawandel ist ein weiterer zentraler Aspekt in dieser Thematik. Die Untersuchung von Knuschke et al. (2007) verdeutlicht, welche hohe Bedeutung meteorologische Bedingungen für die Exposition haben können. Die komplexen Zusammenhänge und Unsicherheiten verdeutlichen den großen Forschungsbedarf. Das am Universitätsklinikum Hamburg-Eppendorf angesiedelte Kompetenznetzwerk *CLIMAderm* plant in einem interdisziplinären Forschungsprojekt erstmalig die zukünftige Hautkrebshäufigkeit unter dem Einfluss des Klimawandels zu prognostizieren.

Literatur:

Baldwin, M., Dameris, M. 2006: Climate-Ozone connections. World Meteorological Organisation (WMO) (2006) Scientific Assessment Report of Ozone Depletion: 2006. Geneva, Switzerland.

Bentham, G. 2001: UV-radiation. Health Effects of Climate Change in the U.K. Expert Group of Climate Change and Health in the U.K., :218-227. London.

Brönnimann, S., Hood, L.L. 2003: Frequency of low-ozone events over northwestern Europe in 1952-1963 and 1990-2000. Geophys. Res. Lett., 30, 2118. doi: 10.1029/2003GL0018431.

Brönnimann, S., Hood, L.L. 2004: Low ozone events over north-western Europe in the 1950s and 1990s. Zerefos, C. 2004: Ozone. Proceedings of the XX Quadrennial Ozone Symposium (1-8 June 2004), 1:302-303. Kos, Greece, Athens.

Reid, S.J., Tuck, A.F., Kiladis, G. 2000: On the changing abundance of ozone minima at northern midlatitudes. J. Geophys. Res., 105(10):169-180.

Stenke, A., Grewe, V. 2003: Impact of ozone mini-holes on the heterogeneous destruction of stratospheric ozone. Chemosphere, 50:177-190.

Knuschke, P., Unverricht, I., Ott, G., Janssen, M. 2007: Personenbezogene Messung der UV-Exposition von Arbeitnehmern im Freien. Abschlussbericht zum Projekt „Personenbezogene Messung der UV-Exposition von Arbeitnehmern im Freien“ – Projekt F 1777. Bundesanstalt für Arbeitsschutz und Arbeitsmedizin (Hrsg.), Dortmund.

Verein Deutscher Ingenieure (VDI) 1998: Umweltmeteorologie – Methoden zur humanbiometeorologischen Bewertung von Klima und Lufthygiene für die Stadt- und Regionalplanung, Teil I: Klima. VDI 3787, Blatt 2.

Matzarakis, A., Mayer, H. 1996: Regionalisierung der Physiologisch Äquivalenten Temperatur für Griechenland. Annalen der Meteorologie, 33, 3. Fachtagung BIOMET am 4. und 5. Dezember 1996 in München. Deutscher Wetterdienst (DWD), Offenbach.

Shindell, D.T., Grewe, V. 2002: Separating the influence of halogen and climate changes on ozone recovery in the upper stratosphere. J. Geophys. Res., 107(12), 4144. doi: 10.1029/2001JD000420.

Winkler, P. 2003: Dokumentation der UV-Belastung in Bayern. Fachgespräch „Gesundheitsgefahren durch UV-Strahlung“ im Auftrag des Bayerischen Staatsministeriums für Umwelt, Gesundheit und Verbraucherschutz.

Anschrift des Autors:

Dr. Jobst Augustin (jobst.augustin@uba.de)
Umweltbundesamt, FG II 1.5, Umweltmedizin und gesundheitliche Bewertung ,
Corrensplatz 1, D-14195 Berlin

Acute coronary syndromes and biometeorological conditions at Crete Island, Greece

P. T. Nastos[1,2*], K. N. Giaouzaki[3], N. A. Kampanis[2], P. I. Agouridakis[4] and A. Matzarakis[5]

[1]Laboratory of Climatology and Atmospheric Environment, Faculty of Geology and Geoenvironment, University of Athens, Greece
[2]Institute of Applied & Computational Mathematics, Foundation for Research & Technology-Hellas, Greece
[3]Department of Cardiology, School of Medicine, University of Crete, Greece
[4]Department of Emergency Medicine, School of Medicine, University of Crete, Greece
[5]Meteorological Institute, University of Freiburg, Germany

Abstract

The relationship between the biometeorological conditions with the non fatal Acute Coronary Syndromes (ACS), is examined in the Ierapetra area, with mild climate, in the Southeastern Crete Island, Greece, during the period 2004-2007. Daily ACS counts were acquired from the General Hospital of Ierapetra and corresponding meteorological parameters, such as maximum and minimum air temperature, relative humidity, wind speed and cloudiness, from the meteorological station of Ierapetra (Hellenic National Meteorological Service). Besides, the daily values of the thermal index Physiologically Equivalent Temperature (PET) were evaluated, in order to interpret the grade of the physiological stress.

The find out the possible association between ACS and the meteorological variables we applied on one hand the Pearson's χ^2 test, the most widely used method of independence control of groups in lines and columns in a table of frequencies. The use of contingency tables instead of Pearson correlation is considered more accurate, because the medical data present large divergence from a Gaussian (regular) distribution. On the other hand, the application of the Generalized Linear Models (GLM) with Poisson distribution resulted in quantitative relationships between the examined parameters.

The ACS syndromes present a multiple variation within the year, with the primary maximum in August and the secondary in May, while relative high ACS frequencies exist in early winter time. The impacts of the weather variability on ACS are not statistically significant (C.L. 95%) and indicate that mild climates without temperature extremes within the year do not appear a clear evidence of influence on ACS.

1. Introduction

There is strong evidence, supported by a consensus of world's leading scientists that the earth's climate is changing, causing a harmful impact on human health. It is already recognized that extreme weather events place an extra burden on public health systems. Hippocrates (430 BC) was the first to establish in his treatises that bioclimatic conditions play an important role in the pathogenesis of disease. The last 30 years several studies indicated that climatic indices such as daily temperature (average, minimum, maximum), humidity, wind speed and barometric pressure increase mortality and morbidity rates of ischemic heart disease, especially in the older people (Glantz, 1993; Colwell, 1998; Fish et al., 1985; Rooney et al., 1998). Even more, in January 1985 a smog episode, that took place in parts of West Germany caused many deaths, the majority of them were due to cardiovascular or cardiopulmonary diseases (Wichmann et al., 1989). In a more recent work (Grigoropoulos et al., 2009), it is showed that the ultra

fine particulate matter with diameter less than 1 μm (PM_1) is in close relation with sinus arrhythmias registered in the emergency units of the hospitals in Athens.
The exploitation of the effects of the bioclimatic conditions variability and human health is of principal interest and one of the current trends of the related sciences. This acquires more importance, as the climate change influence enforce extreme weather phenomena and increases their frequency of occurrence, driving all the more to a permanent degradation of the bioclimatic conditions.
The objective of this study is a preliminary approach to identify if there is a significant relationship between intra annual weather variability and acute coronary syndromes in the Ierapetra area, in South Eastern part of Crete Island, Greece.

2. Data and Analysis

In this study, the daily counts of admissions for non fatal Acute Coronary Syndromes (ACS) - either Acute Myocardial Infraction (AMI) or Unstable Angina (UA) - were obtained from the cardiology emergency department of the General Hospital of Ierapetra, during the period 2004-2007. Acute myocardial infraction (STEMI: ST segment elevation myocardial infarction or NSTEMI: non-ST segment elevation myocardial infarction) is the clinical syndrome that results from an injury to myocardial tissue due to prolonged ischemia. The corresponding meteorological parameters, such as maximum and minimum air temperature, relative humidity, wind speed and cloudiness, were provided from the meteorological station of Ierapetra (Hellenic National Meteorological Service).The geographical position of Ierapetra, Crete Island, appears in Fig. 1.

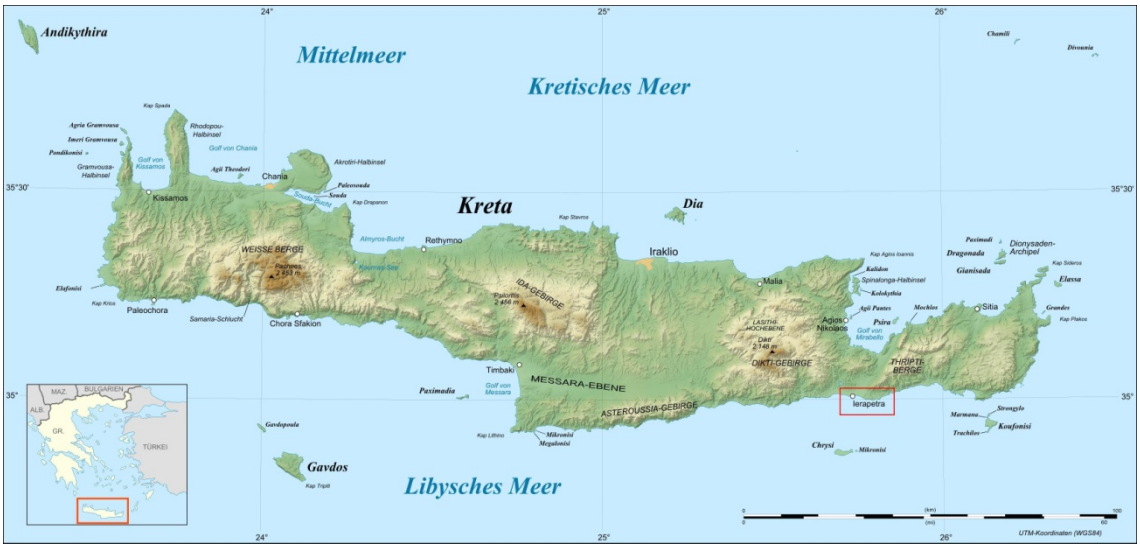

Fig. 1: Crete Island, Greece. Ierapetra city is indicated by a rectangular frame

The relationship between ACS/STEMI and the aforementioned meteorological parameters was calculated by the application of: a) Pearson χ^2 test, the most widely used method of independence control of groups in lines and columns in a table of frequencies and b) Generalized Linear Models with Poisson distribution (McGullagh and Nelder, 1997), a method of analysis, which has been performed satisfactorily in previous studies (Nastos and Matzarakis, 2006; Nastos et al., 2008). The values of each meteorological parameter and ACS/STEMI, were grouped in four quartiles, so that the first quartile contain the lowest 25% and the fourth quartile the highest 25% of the values. In the

process, the number of days for the quartiles of ACS/STEMI was calculated for each quartile of the parameters and then a contingency table was constructed for every parameter. Besides, the bioclimatic conditions expressed by the Physiologically Equivalent Temperature (PET), based on the energy balance models of the human body, are analyzed (Matzarakis et al., 1999).

3. Results and Discussion

Ierapetra is Europe's southernmost town, characterized by very mild climate and mean air temperature rarely drops below 12°C in the winter. The temperate climate of Ierapetra is of typical Mediterranean type, defined by cold and rain period (October-March) and warm and dry period (April–September). The mean maximum air temperature is 31.8 °C in July and August and the mean minimum air temperature is 8.7 °C, in February. The mean annual rainfall is 494 mm and is rare during the summer months. The mean annual number of sunshine hours is 3066 while the prevailing wind direction is of the North sector and the mean wind speed ranges from 7.1 kts in May to 12.4 kts in July.

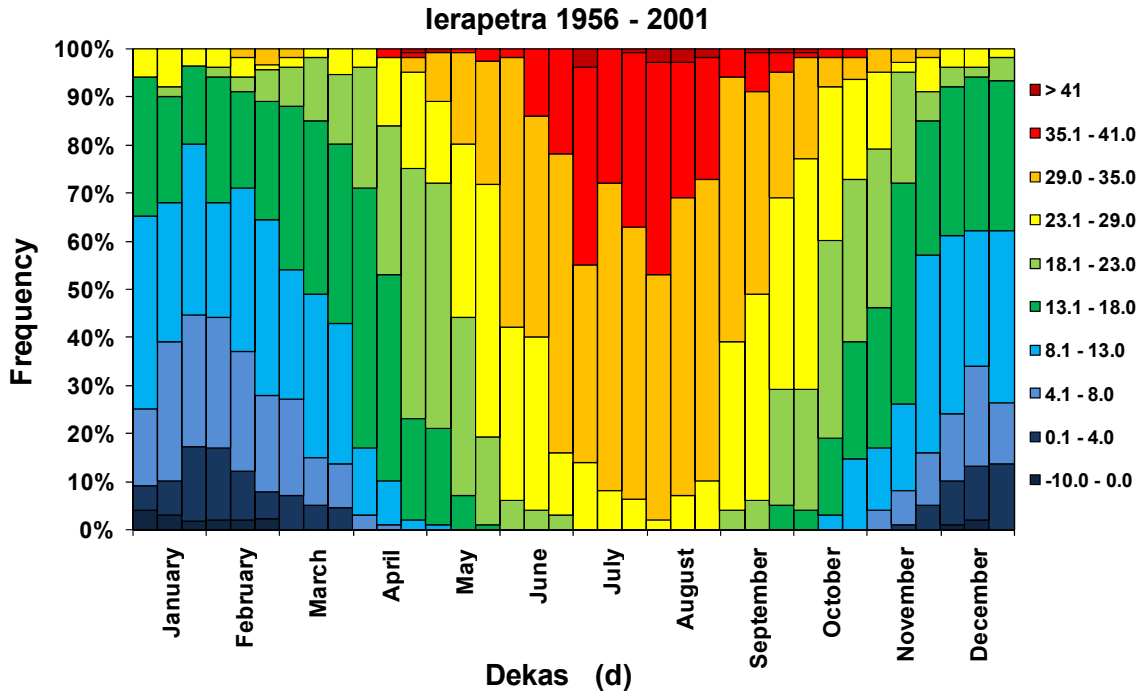

Fig. 2: Bioclimatic diagram with respect to PET classes per ten days interval, for Ierapetra, Crete Island, Greece, during the period 1956-2001

The mild climatic conditions at Ierapetra are depicted in the more descriptive bioclimatic diagram concerning PET classes per ten days interval, during the period 1956-2001 (Fig. 2). The PET values, estimated from RayMan model (Matzarakis et al., 2007), give evidence of strong heat stress for approximately 20% -30% of the days within the period from July to August. The temperate climatic regime of Ierapetra, as described before, brings difficulties in the evaluation of the impact of heat in human health, which

particularly appear in regions with mild climate, without temperature extremes (Gnecchi Ruscone et al., 1985; Ku et al., 1998).

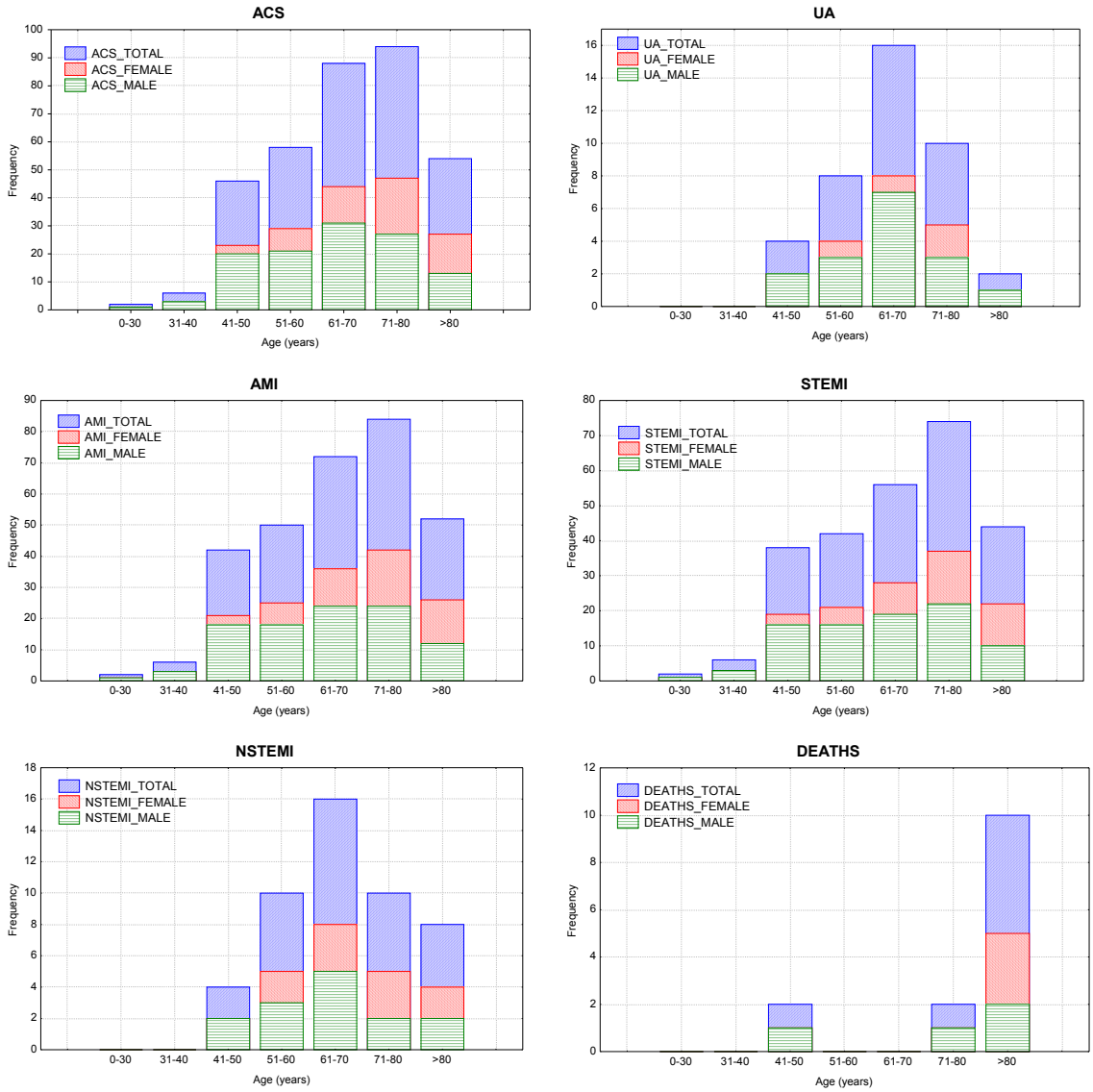

Fig. 3: Stacked graphs with respect to male, female and total counts for ACS, UA, AMI, STEMI, NSTEMI and Deaths, for different classes of age, in Ierapetra area, Crete Island, for the period 2004-2007

As far as the cardiovascular diseases depend on sex and age, Fig. 3 depicts the frequency of each examined cardiovascular syndrome per sex and age classes. It is crystal clear that males appear higher frequency than females for all the syndromes. Regarding only deaths, females predominate within the age class greater than 80 yrs. Moreover, females with age greater than 70 yrs seem to be a little more vulnerable than males in NSTEMI syndromes. These findings are in agreement with the results of an analysis concerning the projected prevalence of the cardiovascular syndromes in the Americans with age greater than 20 years old (American Heart Association, 2003).

The frequencies of the ACS or STEMI admissions within the quartiles of the examined meteorological parameters (contingency tables) were tested by the application of the Pearson χ^2 test (not shown). The results revealed that the null hypothesis is fulfilled;

namely the meteorological parameters examined are not associated with the emergence of the cardiovascular syndromes. Notwithstanding the results are not statistically significant (C.L. 95%), ACS and particularly STEMI syndromes seem to be influenced by high maximum and minimum air temperature (the highest 25% quartile).

Table 1: Results of the application of Generalized Linear Models (GLM) with Poisson distribution, (dependent variable is the ACS/STEMI admissions, while independent covariates are the aforementioned meteorological parameters)

ACS			**STEMI**		
variable	**b coefficient ± standard error**	**significance level p**	**variable**	**b coefficient ± standard error**	**significance level p**
T_{max} (^{o}C)	0.0180±0.0129	0.163061	T_{max} (^{o}C)	0.0217±0.0147	0.140714
T_{min} (^{o}C)	0.0192±0.0142	0.179036	T_{min} (^{o}C)	0.0209±0.0162	0.196644
RH (%)	-0.0041±0.0093	0.657128	RH (%)	-0.0078±0.0107	0.467654
WS (m/s)	-0.0019±0.0301	0.950132	WS (m/s)	-0.0155±0.0348	0.656980

Because the medical data do not follow normal but Poisson distribution, the application of Generalized Linear Models with Poisson distribution is considered the most appropriate method of checking the impact of weather on cardiovascular syndromes. The results of this analysis are presented in Table 1, where an insignificant correlation between ACS/STEMI and meteorological variables exist (C.L. 95%). The insignificance of the results could be attributed to several factors. The predominant factor is the temperate climate without extremes, while the employment of the population in the greenhouses seems to be beneficial. Another reason of local interest that might be mentioned is the regulated climatic conditions inside the many greenhouses in the region, which protect the health of the people working in there against the cold weather conditions, which is responsible for the acute coronary syndromes exacerbation.

4. Conclusions

In this study, the impact of weather variability on non fatal Acute Coronary Syndromes (ACS), obtained from the cardiology emergency department of the General Hospital of Ierapetra, Crete Island, Greece, during the period 2004-2007, was examined. The results from the performed analysis showed that there was not any statistically significant relationship (C.L. 95%) between ACS and weather parameters. This could be attributed to the temperate climate of Ierapetra, supporting the assumption that mild climates without temperature extremes have minor impacts on ACS incidence. Further research is needed in order to confirm our findings and understand better the involved pathophysiological mechanisms.

References

American Heart Association, 2003: Heart and stroke statistical update. Dallas.

Colwell, R.R., Epstein, P.R., Cubler, D., Maynard, N., McMichael, A.J., Patz, J.A., et al., 1998: Climate change and human health. Science 13, 279(5353), 968-969.

Fish, P.D., Bennett, G.C., Millard, P.H., 1985: Heat wave morbidity and mortality in old age. Age Aging 14(4), 243-5.

Glantz, S.A., 1993: Heart disease and the environment. Journal of the American College of Cardiology 21, 1473-1474.

Grigoropoulos, K.N., P.T. Nastos, G. Feredinos, 2009: Spatial distribution of PM1 and PM10 during Saharan dust episodes in Athens, Greece. Advances in Science and Research 3, 59–62.

Gnecchi Ruscone, T., Crosignani, P., Micheletti, T., Sala, L., Santomauro, D., 1985: Meteorological influences on myocardial infarction in the metropolitan area of Milan. International Journal of Cardiology 9. 75– 80.

Ku, C.S., Yang, C.Y., Lee, W.J., Chiang, H.T., Liu, C.P., Lin, S.L., 1998: Absence of a seasonal variation in myocardial infarction onset in a region without temperatures extremes. Cardiology 89, 277– 82.

Matzarakis, A., Mayer, H., Iziomon, M.G., 1999: Applications of a universal thermal index: physiological equivalent temperature. International Journal of Biometeorology 43, 76-84.

Matzarakis, A., Rutz, F., Mayer, H., 2007: Modelling Radiation fluxes in simple and complex environments – Application of the RayMan model. International Journal of Biometeorology 51, 323-334.

Nastos, P.T., Matzarakis, A., 2006: Weather impacts on respiratory infections in Athens, Greece. International Journal of Biometeorology 50, 358-69.

Nastos, P.T., Paliatsos, A.G., Papadopoulos, M., Bakoula, C., Priftis, K.N., 2008: The effect of weather variability on pediatric asthma admissions in Athens, Greece. Journal of Asthma 45, 59–65.

McGullagh, P., Nelder, J.A., 1997: Generalized Linear Models. 2nd ed. Chapman & Hall.

Rooney, C., McMichael, A.J., Kovats, R.S., Coleman, M.P., 1998: Excess mortality in England and Wales and in Greater London, during the 1995 heat wave. Epidemiology of Community Health 52(8), 482-486.

Wichmann, H.E., Mueller, W., Allhoff, P., Beckmann, M., Bocter, N., Csicsaky, J.M., Jung, M., Molik, B., Schoeneberg, G., 1989: Health effects during a smog episode in West Germany in 1985. Environmental Health Prospective 79, 89-99.

Corresponding Author's address:

Assoc. Prof. Dr. Panagiotis Nastos (nastos@geol.uoa.gr)

Laboratory of Climatology and Atmospheric Environment, Faculty of Geology and Geoenvironment, University of Athens, Panepistimiopolis GR 157 84, Athens, Greece

The WBGT-Index – a heat index, used in international sporting events

Petra Gebauer

Institute for Meteorology, Free University Berlin, Germany

Abstract

Heat stress affects all people. Particularly affected in their well-being are the elderly and sick. A limitation of their performance notice especially athletes, which do not reach under extreme physical strain on one hand their objective during an athletic contest, on the other hand, however, they could take physical damage, mainly due to miscalculations by excessive heat stress. In order to put the athletes a decision criterion in their hand, is increasingly at international sporting events the WBGT index used as a measure to prevail the heat stress. In Berlin, every year since 2007, meteorological measurements accompany the real,-BERLIN MARATHON, in 2009, there were direct measurements performed in sports complexes during the 12th IAAF World Championships in athletics.

1. Introduction

The physicians, who take care about a sporting event, become increasingly considered in the international framework to provide information about the meteorological conditions under which the athletes achieve their performance.
Especially by the Medical Board of the real, - BERLIN MARATHON, normally in the end of September, already existed for years the desire to make studies at the course on the prevailing conditions as temperature, humidity and wind and collect for several years, a usable data set of meteorological data as well as medical information. Finally, the aim is to optimize the preparation of the athletes but also the preparation of the medical teams with the help of warning systems on the basis of weather forecasts.
This monitoring program was made possible with support of the NaT-Working project led by the Institute for Meteorology, Free University Berlin, sponsored by the Robert Bosch Foundation, in cooperation with several secondary schools in Berlin. Through the use of portable measuring instruments and various groups of pupils was a 10-minute recording of the parameters of temperature, humidity and wind directly on the running course at all possible. Long- and short-term weather forecasts made by meteorologists of the Association Berliner Wetterkarte e.V. support the project.
In 2009 was the first time that measuring instruments are used to detect directly the WBGT index as the heat index, and display it. Under the supervision of students of the Institute of Meteorology of the Free University of Berlin, the measurement program took place during the Athletics World Championships in Berlin in August 2009.

2. Definition of the WBGT index

The performance of an athlete depends on

"internal factors" such as
- age
- condition
- health

"external factors" such as
- clothing
- weather conditions
- air temperature
- air humidity
- wind velocity

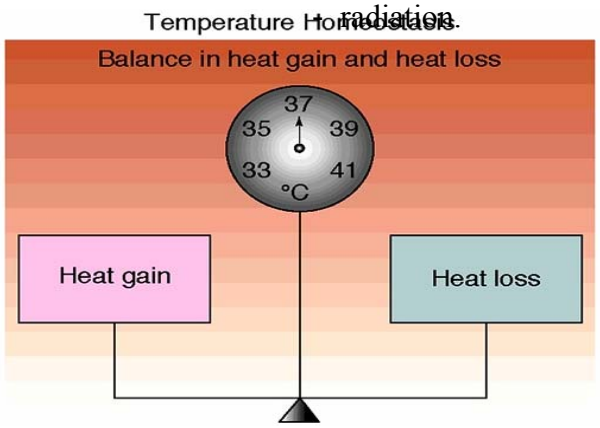

Fig. 1: Thermoregulation

These external, uncontrollable weather conditions affect the thermal regulation of the human body. The goal of the body is to keep the temperature inside it constant regardless of the changing environmental conditions within a narrow range. The more the environment is full of stress factors, the more the thermoregulation system must be active.
A heat loss may be compensated by clothing. A heat gain on the other hand, leads to inevitable heat stress. The resulting heat stress can be identified by a heat index.
In the international area is increasingly used at sporting events, the Wet Bulb Globe Temperature (WBGT index). It was developed in 1956 by the United States Marine Corps at Parris Iceland, South Carolina, to set limits of carrying capacity at high temperatures and to reduce heat damage for recruits. It is used by safety representatives, athletes and military.
It is a composite temperature to estimate the effect of temperature, humidity, wind speed and solar radiation on people (heat stress), measured in 1,5 m above ground.

Wet Bulb Globe Temperature:

WBGT = 0.7 Tw + 0.2 Tg + 0.1Td

- Tw = natural wet bulb → is a measure of the humidity and thus the possibility of heat dissipation by evaporative sweating, supported by wind
- Tg = "black globe temperature" → Globe thermometer: also black globe thermometer, to measure the solar radiation, with a black ball, similar to the absorptive capacity of the skin. This radiation temperature is a measure of the thermal radiation that a person feels.
- Td = dry bulb temperature → reflects the possibility of heat by convection and conduction
- units of the temperatures are in °Celsius or °Fahrenheit

If there is no possibility to measure the black globe temperature following approximation may be used:

WBGT = 0.567 Td + 0.393 e + 3.94 (apply in full sunshine and light winds)

- Td = dry bulb temperature (°C)
- e = vapour pressure (hPa) e = (RF/100) 6.105 exp (17.27 Td / (237.7 + Td))
- RF = relative humidity (%)

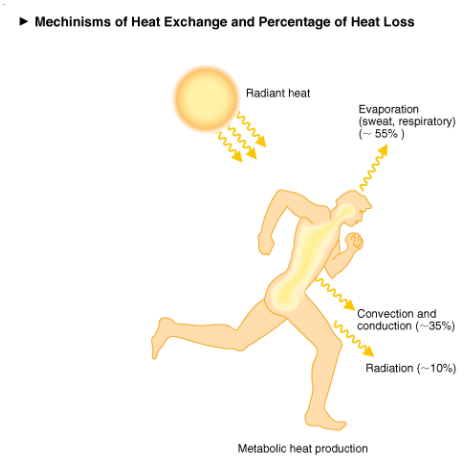

Fig. 2: Potential loss of heat through the human body

The following limits on the WBGT index are based on the guidelines of the American College of Sports Medicine.

Table 1: Warning classes according to the WBGT index

warning flag	risk	for	WBGT (°C)	WBGT (°F)
black	extrem	hyperthermia	> 28,0°C	> 82,0°F
red	high		23,1°C – 28,0°C	73,1°F – 82,0°F
yellow	moderat		18,1°C – 23,0°C	65,1°F – 73,0°F
green	low		10,1°C – 18,0°C	50,1°F – 65,0°F
white	increasing	hypothermia	≤ 10,0°C	≤ 50,0°F

3. Measurements of the WBGT index

In the first two years the individual parameters such as temperature and humidity were recorded with mobile multi-function devices, for the registration of the wind speed was a hand anemometer used.

Fig. 3: Measuring teams at the real,- BERLIN MARATHON course

Since 2009 a comprehensive measuring system was purchased with a special black globe thermometer, according to DIN EN 27243 with a diameter of 150 mm, measuring height should be 1.1 m above ground.

Fig. 4: Measuring system to record the WBGT index, due to guidelines of the organizing team of the 12th IAAF World Championships in Athletics in Berlin 2009 and TV specifications not the best place to measure

For mobile application there were several hand sets purchased. Here the diameter of the black globe is 40 mm.

(1) black globe temperature sensor
(2) relative humidity and dry temperature sensor, remove protection to arrange it for natural ventilation by the wind

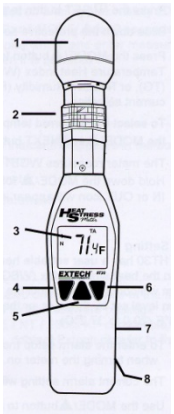

Fig. 5: Mobile hand set to record the WBGT index

Every ten minutes the data was detected and stored into a data base. Published over the web everyone could observe the actual situation.

4. Results of the monitoring program

In the years 2007 and 2008 only temperature, humidity and wind velocity were recorded by the mobile measuring teams. In both years WBGT index, calculated with the approximation formula, is in category 1 (< 21.0°C).

In the last year, it was the warmest marathon day after 2006 in the history of the BERLIN MARATHON, the WBGT index reached the second warning class at several stations along the course.

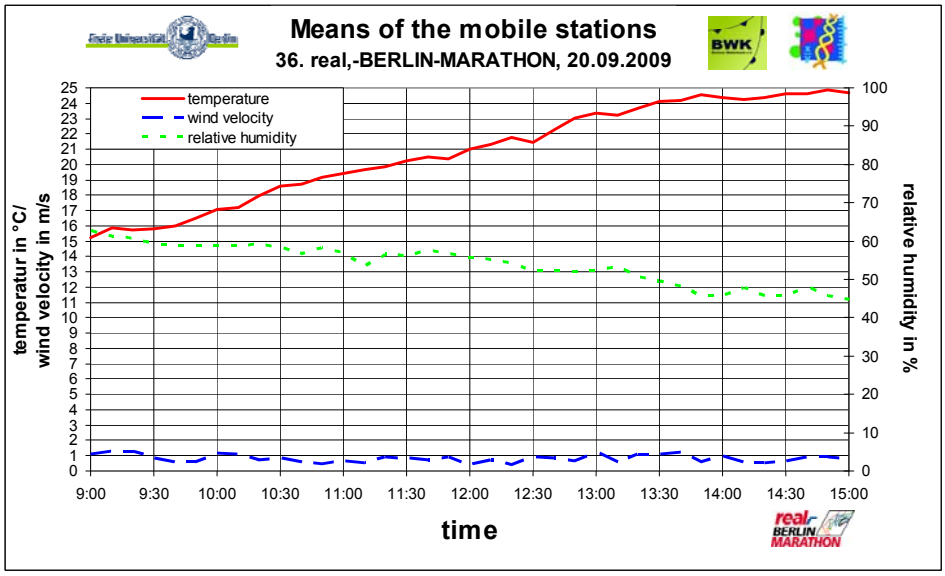

Fig. 6: Means of the mobile stations in Berlin on 20 September 2009

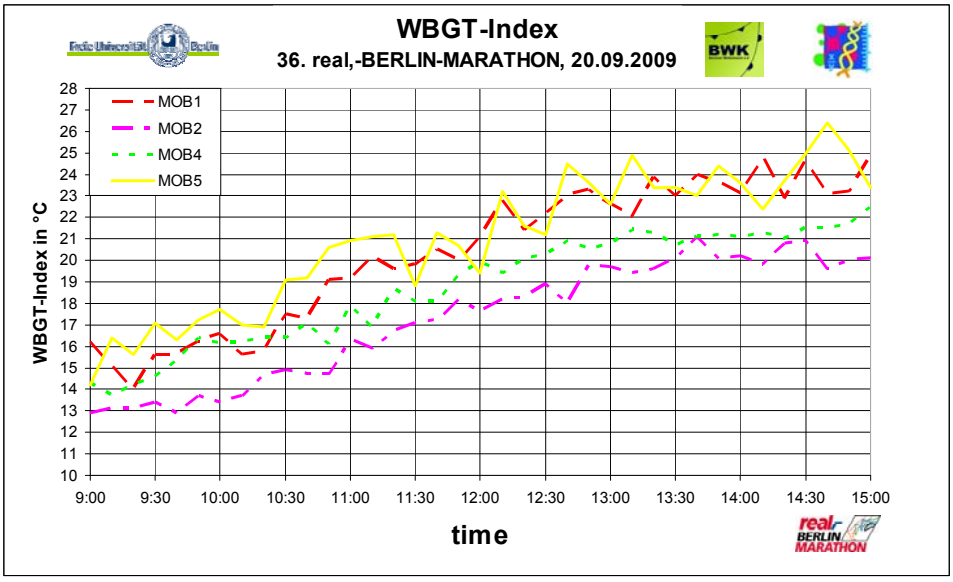

Fig. 7: Differences between the WBGT index measurements along the real,- BERLIN MARATHON course on 20 September 2009

The WBGT index was progressive with time of day and depending on the situation in the town within the yellow to red region of the warning area for the risk of overheating.

The quantity of heat injuries was higher than in the years before. Even the fastest racers had no chance to win in world record time.

5. Conclusions

The measuring program during sporting events is a first step to lead to the development of a heat warning system. The meteorological data base as well as the medical reports are currently not comprehensive enough to make a final conclusion. But the collaboration between meteorologists and physicians was started. The intention to create a warning system, especially for the athletes may be expanded to lead to a heat stress warning system for the whole city of Berlin. Routine measurements of the black globe temperature are embedded in the monitoring network of the Institute of Meteorology at the main observation station Dahlem.

References

American College of Sports Medicine, 1984: Prevention of thermal injuries during distance running - Position Stand. Med.J.Aust. Dec. 876.

American Society of Heating Refrigerating and Air Conditioning Engineers (ASHRAE), 2001: Thermal comfort. In ASHRAE Handbook: Fundamentals (p. 8.1-8.29). Atlanta, GA: ASHRAE.

Armstrong, L. E., Casa D. J., Millard-Stafford, M. Moran D.l S., Pyne S. W., Roberts W. O., 2007: Exertional Heat Illness during Training and Competition. MEDICINE & SCIENCE IN SPORTS & EXERCISE, Official Journal of the American College of Sports Medicine, 556-572, http://www.acsm-msse.org

Budd, G. M., 2008: Wet-bulb globe temperature (WBGT)—its history and its limitations. Journal of Science and Medicine in Sport, Volume 11, Issue 1, Pages 20-32.

Department of the army, 1980: Prevention, Treatment and Control of Heat Injury, Washington, DC: Department of the Army, Technical Bulletin No. TB MED 507, pp. 1-21

DIN EN 27243, 1993: Warmes Umgebungsklima: Ermittlung der Wärmebelastung des arbeitenden Menschen mit dem WBGT-Index (wet bulb globe temperature). Berlin, Beuth-Verlag.

Roberts WO., 1998: Medical management and administration manual for long distance road racing. In: Brown CH, Gudjonsson B, eds. IAAF Medical Manual for Athletics and Road Racing Competitions: a Practical Guide. Monaco: International Association of Athletics Federations, 39-75.

Authors' address:

Dipl.-Met. Petra Gebauer (petra.gebauer@met.fu-berlin.de)
Institute for Meteorology, Free University Berlin
Carl-Heinrich-Becker-Weg 6-10, D-12165 Berlin, Germany

Modeling of *UTCI* index in various types of landscape

Anna Kunert

Institute of Geography and Spatial Organization, Polish Academy of Sciences, Poland

Abstract

In the paper the influences of the relief's features and the land use on locally observed values of new *UTCI* index in different meteorological conditions are discussed. The consideriation were derived from general assumption, that the basic meterological elements (solar radiation, wind speed, air temperature and humidity) vary in different types of landscape.

It was calculated expected (in particular weather scenarios) values of this meteorological elements and the mean radiant temperature. Then *UTCI* was simulated for every type of landscape, taking in consideration different meteorological scenarios. Finally, *UTCI* deviations from it's value observed at reference landscape were calculated for every type of relief, land use and ground moisture. The calculations were made for in each of defined weather conditions.

The results show, that *UTCI* deviation in different types of local landscape, depending on weather conditions, is ranged from -11.5^{o}C to +35.5^{o}C. The negative deviations occur always in water banks, wetlands, meadows, and on northern, eastern and western slopes as well as on tops and upper parts of hills. Positive deviations occur in ground transportation belts and built-up areas, on south slopes as well as in wide and narrow valleys. The deviations of *UTCI* index in forests, in the intra-forest-settlement and also in narrow valleys can attain either negative or positive values, depending on meteorological conditions.

1. Introduction

The *UTCI* index represents air temperature of the reference condition with the same physiological response as the actual condition. Values of *UTCI* vary at different meteorological conditions (Jendritzky et al. eds, 2009; Blazejczyk et al., 2010). There are well known, in general, differences between meteorological elements (air temperature, humidity, wind speed, solar radiation) observed at standard landscape conditions and elements noted in specific kinds of landscapes (forests, urbanized areas, valleys, slopes etc).

The aim of the paper is to present the results of simulations of modification of *UTCI* index in various types of landscape in different weather conditions.

2. Method

Based on coefficients of changes (Blazejczyk 2002) of solar radiation, wind speed, air temperature and humidity in different types of local landscapes (Table 1), predicted values of basic meteorological elements and the mean radiant temperature for various weather scenarios were calculated.

Next, simulations of *UTCI* for every type of the landscape were made, taking into account different meteorological scenarios: the solar radiation intensity of 200, 500 and 800 W/m^2, air temperature of 10, 20, 30 and 35^{o}C, relative humidity of air (20, 50 and 80%) and wind speed (2, 4, 8 m/s). The code of simulated weather consists of four

numbers, e.g. 200-20-50-4, where first number refers to solar radiation, second to air temperature, third to relative humidity of air and forth – to wind speed. All together, for each of the landscape, 108 different values of *UTCI* index were calculated.

Table 1: Coefficients at changes in solar radiation (*zr*), air temperature (*zt*), wind speed (*zv*) and air humidity (*zf*) in selected types of landscape (due to Blazejczyk 2002, modified by author)

Selected types of landscape		**Deviations**			
		zr	*zt*	*zv*	*zf*
Relief features	plains	1	1	1	1
	tops and upper parts of hills	1	1	1.4	1
	correction because of absolute altitude	0.0065 / 100 m	1	-	-
	Valley's bottoms (H – is valley depth, W – is valley wide):				
	> 20 m H and < 200 m W	0.95	0.85	0.7	1.1
	< 20 m H and < 200 m W	1.05	0.9	0.8	1
	> 20 m H and > 200 m W	1.05	0.95	0.9	1.05
	< 20 m H and > 200 m W	1	1	1	1
	Slopes:				
	south, elevation 20 - 50 m	1.2	1.2	1	1.1
	south, elevation > 50 m	1.2	1.2	1	1.1
	north, elevation 20 - 50 m	0.8	0.85	1	0.95
	north, elevation > 50 m	0.8	0.85	1	0.95
	east (west), elevation 20 - 50 m	1	0.95	1	1
	east (west), elevation > 50 m	1	0.95	1	1
	correction because of elevation above valley's bottom (h)	-	t -0.6 * h / 100	0.0075*50 +0.6833	-
Land use	fields and westlands	1	1	1	1
	meadows	1	0.95	1	1
	forests	0.3	0.9	0.2	1.1
	ground transportation belts	1	1.05	0.95	0.9
	rural settlement	1	1.1	0.8	1
	intra-forest-settlement	0.6	0.95	0.6	1
	downtown	0.8	1.25	0.6	0.9
	industrial areas	0.8	1.3	0.6	0.9
	water banks	1	0.85	1.1	1.2
Ground moisture	dry	1	1	1	1
	humid	1	0.95	1	1.1
	wet	1	0.9	1	1.2

In the next step deviations of *UTCI* value in every type of the landscape from the value of *UTCI* index in the reference landscape condition (dry plains with low vegetation) in each of defined weather conditions were calculated.

3. Results

The relief features have the greatest influence on modification on thermal conditions. Differences of *UTCI* index between the warmest and the coldest areas, in similar weather conditions, rise above 30^{o}C. Definitely, the most warmest sites are southern slopes, however the coldest are narrow deep valleys and northern slopes (Fig. 1).

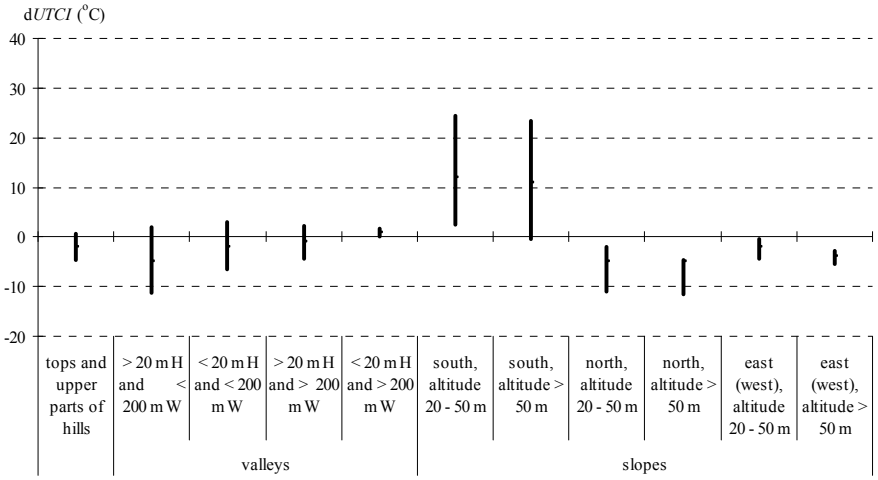

Fig. 1: Deviations of *UTCI* in different relief types, H – is valley depth, W – is valley wide

On northern, eastern and western slopes as well as on upper parts of hills and on its tops *UTCI* index attains the lower values then in the reference landscape. Value of d*UTCI* increases with altitude. Lower parts of weak insolated slopes are much warmer in low air temperatures, irrespective of wind speed and air humidity (Fig. 2).

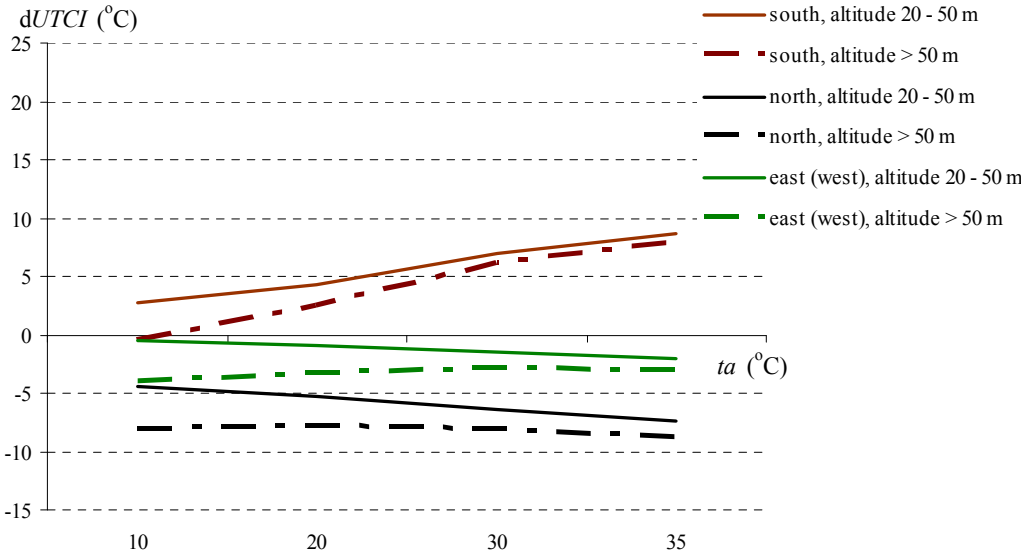

Fig. 2: Deviations of *UTCI* in different types of slopes, at various air temperature (*ta*); weather conditions 800-xx-20-2 (xx is various air temperature)

The higher parts of slopes are the warmest during days with strong solar radiation and strong wind. The coldest days are noted at hot and wet weather. Thermal conditions very close to reference landscape are noted in lowest parts of eastern and western slopes at temperature of 10°C.

On southern slopes the *UTCI* deviations can attain value up to 23°C, and d*UTCI* values increase with altitude. The highest *UTCI* deviations on southern slopes occur in hot days with high humidity of air. Wind speed impacts d*UTCI* only in higher parts of northern slopes at low air temperature. Higher parts of northern slopes are always cold-

er, the biggest deviations in relation to lower parts occur at low air temperature (10 and 20°C). Irrespective of solar radiation, negative deviations of *UTCI* index can appears in these relief types.
In narrow and wide valleys deviations of *UTCI* are ranged from -11.2°C to 3°C, nevertheless the lowest values are observed in narrow, well shadowed deep valleys with reduced air movement.
Due to rise in air temperature an increase of *UTCI* deviations is observed. The biggest negative deviations can be noted at hot and sultry days with strong wind. Positive deviations in narrow valleys are observed in cool days (10°C) with moderate and strong wind. Thermal conditions similar to reference landscape condition, (d*UTCI* about 1°C) was observed in wide and shallowed valleys.
Deviations of *UTCI* index in different types of land use, depending on weather conditions are ranged from -11.5°C to +35.5°C. *UTCI* differences between the warmest and the coldest areas can reach 45°C. The biggest negative deviations are noted on water bodies and in forests, however the biggest positive deviations are observed at urbanized areas: downtown and industrial zones (Fig. 4).

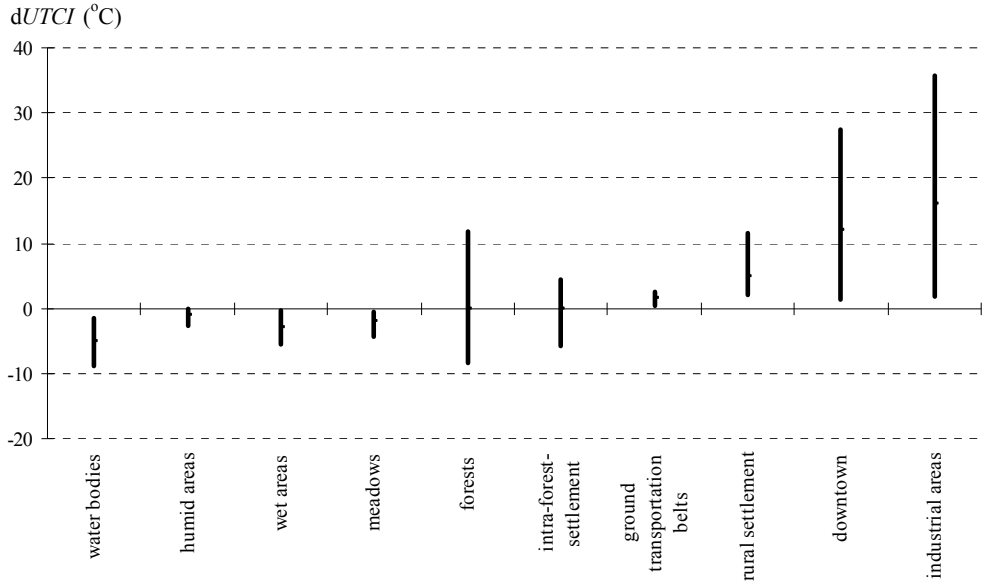

Fig. 4: Deviations of *UTCI* in different types of land use

Deviations of *UTCI* in forests can have negative or positive values, from -8.3°C to 11.7°C, depending on meteorological conditions. Thermal conditions in forests are modified by wind, air temperature and also the solar radiation. Positive deviations are observed during cold days with low solar radiation. Increase of wind speed is noted in cold days; the value of *UTCI* deviations can rise even of 10°C. Negative deviations are noted at soft winds, irrespective of air temperature, except of weather conditions 200-10-20-2. The biggest negative *UTCI* deviations occur in hot days with low wind speed and high solar radiation.

At open areas, with free air flow and also at areas with increased humidity negative deviations of *UTCI* index always occur. At these areas, *UTCI* values are determined espe-

cially by air temperature and wind speed. The highest deviations are noted in hot windy days with high humidity of air (Fig. 5).

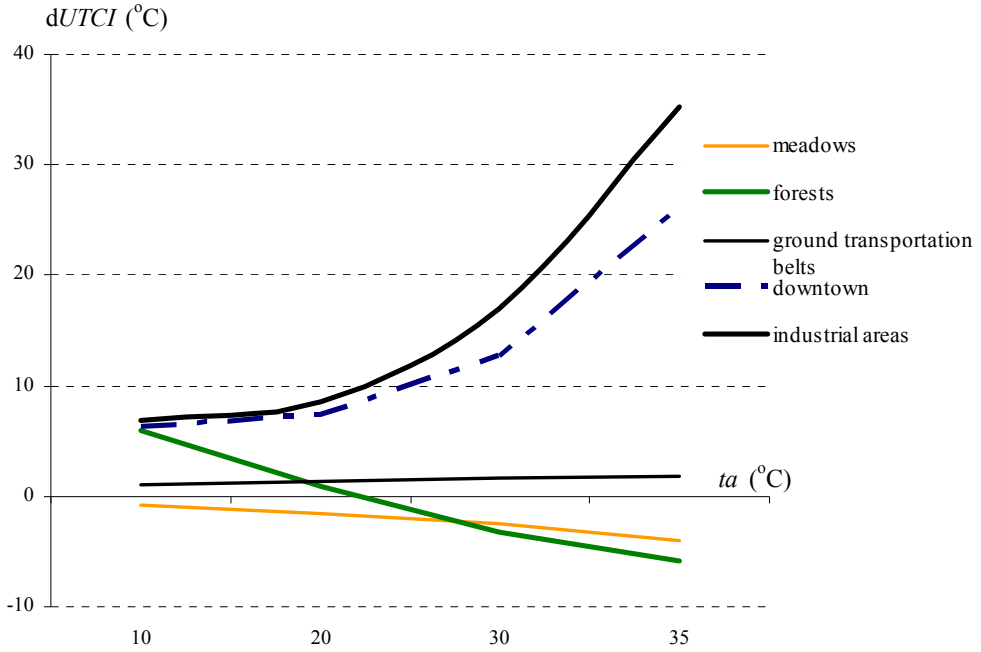

Fig. 5: Deviations of *UTCI* in selected types of land use, at various air temperature (*ta*); weather conditions: 800-xx-80-8, (xx is various air temperature)

Positive deviations of *UTCI* index occur at ground transportation belts and at built-up areas; the highest values of deviations are noted at industrial areas. In built-up areas value of *UTCI* deviations is modified by solar radiation (deviations at weak solar radiation are higher of about 2°C then at intensive radiation), and also by wind speed, especially in low air temperature.

4. Conclusion

The model of *UTCI* distribution presented in the paper was used to create maps for Warsaw Lowland. Some examples of *UTCI* maps will be presented at the poster.
Spatial distribution of *UTCI* well represent differentiation of landscape of the Warsaw Lowland. The spatial picture of *UTCI* is similar to that obtained by Blazejczyk and Kunert (2002) for the same area with the use different bioclimatic index (*STI* – subjective temperature index, Blazejczyk, 2005).

References

Blazejczyk K., 2002: Influence of air circulation and local factors on climate and bioclimate of Warsaw agglomeration. Dok. Geogr. 26, IGiPZ PAN, Warsaw 2002.

Blazejczyk K., Kunert A., 2002: Topoclimatic and biotopoclimatic maps of Warsaw Lowland. Dok. Geogr. 26, IGiPZ PAN, Warsaw 2002.

Blazejczyk K., 2005: New indices to assess thermal risks outdoors. [in:] I. Holmér, K. Kuklane, Ch. Gao (eds.), Environmental Ergonomics XI, Proc. Of the 11th International Conference, 22-26 May, 2005 Ystat, Sweden, p: 222-225.

Blazejczyk K., Broede P., Fiala D., Havenith G., Holmér I., Jendritzky G., Kampmann B., 2010: UTCI – nowy wskaźnik oceny obciążeń cieplnych człowieka (UTCI – New index for assessment of heat stress in man), Przeglad Geograficzny, 82, 1, p: 5–27.

Jendritzky G., Havenith G., Weihs P., Batchvarova E. (eds.), 2009: Towards a Universal Thermal Climate Index UTCI for assessing the thermal environment of the human being. Final Report COST Action.

Author address:

MSc. Anna Kunert (a.kunert@twarda.pan.pl)
Department of Geoecology and Climatology,
Institute of Geograpfy and Spatial Organization, Polish Academy of Sciences
Twarda 51/55, 00-818 Warsaw, Poland

Limits of phenological modelling in tree species

Peter Braun[1] and Markus Müller[1,2]

[1]Dept. of Pomology, Geisenheim Research Centre, Germany

[2]Meteorological Institute, University of Bonn, Germany

Abstract

In Mid-Europe perennial species have a dedicated phase during late autumn and winter, where no growth can be observed, the so-called endodormancy. To go through and finish this phase cool temperatures are required. Following this, a period of warmer temperatures is required to see new visible growth. Modelling the then visible phenological stages such as bud break and flowering is difficult and currently only achieved by relatively simplified modelling techniques. Such models are basically black box models and are not mechanistic. Nevertheless, such models, once fitted to a given environment, can be very good for prediction for the next few years. In this time frame the uncertainty of the models can be quantified well. However, when applying them to mid and long-term forecasts such as required in impact modelling of climate change research, the uncertainty is not quantifiable any more and predictions consequently are of little value. This paper demonstrates the basic problems in phenological modelling of early season growth stages and presents possible solutions.

1. Introduction

Phenological stages such as leaf unfolding or full bloom are in their timing highly dependent on the climatic conditions leading up to the respective event and, with climate conditions changing, this will cause large effects on the species in question. Therefore, phenology in general is now widely accepted as being a very easy to observe indicator of climate variations and thus climate change. However, interest in phenological observations, particularly in plants, traditionally come from agriculture or horticulture with the main purpose of describing the suitability of a region for certain crops or varieties in a more or less constant and known environment. The changing role of phenological observations in the light of the climate change debate has increased the demand for accuracy of phenological models and thus the demand for understanding the underlying physiological mechanisms leading to a given event in the growth of a plant. In tree species, this is particularly true for predicting the timing of early season growth stages such as bud break and flowering. We will shortly describe the history of such phenological models and from there define the requirements for models suitable for using them in the climate change debate.

2. Development of phenological models

Phenological observations were historically first used as a simple indicator of whether a certain crop or variety would fit into a certain environment. This was largely done by comparing similarly reacting species and then judging the suitability of a region for growing this species/ variety. The first widely known approach to model early spring phases such as flowering of fruit tree species was the so-called ‘Utah Model’ (Richardson et al., 1974). These authors acknowledged that trees originating from more tempe-

rate or cooler zones have a period from late autumn into winter, where no visible growth occurs and cool temperatures are required to fulfil the so-called chilling requirement, which again is genetically fixed and varies largely between species. Once the chilling requirement is fulfilled, warmer temperatures will result in beginning development and growth leading to bud break and flowering. The latter period is often called forcing. Such a concept became widely accepted after the work by Richardson et al. (1974), who defined temperatures over a particular threshold become as becoming effective and a given accumulated quantity is needed to arrive at a particular growth stage. The follow-up of these periods is illustrated schematically in Fig. 1 where the forcing period in late winter/ early spring follows after the chilling period in late autumn and early winter. Anderson et al. (1984) introduced a weighting for both chilling and forcing in a way that more effective temperatures are weighted more and less effective or even detrimental ones less or negative, respectively. Chuine (2000) summarized numerous variations of these approaches and presented a more generalized model.

However, all of these approaches have two main problems in common. Firstly, they all assume temperature to be the only and absolutely dominant climatic variable driving development. This is mainly caused by an inherent cross-correlation between air temperature and many other climate variables such as global radiation, cloud cover, rainfall and soil temperature and any analysis of variance will always result in air temperature being the dominant if not only variable having a significant effect. That suits modellers since air temperature is a relatively easy to obtain information. However, the interdependency and relationship between these variables differs largely between locations. The other problem is that they are based on a statistical fit of historical data of temperature and corresponding observations of bud break or flowering. These visible phenological stages are a result of two consecutive periods, chilling and forcing and it is even unknown, how much overlap there can be between those periods.

In summary, the effective temperature range, the length of the respective periods, the possible overlap between chilling and forcing and the cross-correlation with other possible climate variables and their unknown influence all make it impossible to deduct the mechanism driving plant development into early spring. Since the existing models are always purely statistical they can only be valid in a situation, where the future is largely similar to the past because the model only has the information from the past as a basis. This can be expected to be the case in the near future and therefore such models are in a given situation relatively good to predict what will happen for the next few years. In the longer term and thus with climate change, the climatic conditions change considerably. As the basis for the model development disappears an unknown uncertainty of the predictions is the result. This is illustrated in Fig. 1, where the situation A is the present time and the model is with acceptable uncertainty able to predict the date of bud break or flowering. If climatic conditions during autumn, winter and early spring change, then it might be that the required chilling is fulfilled in a shorter period. Also, a warmer winter/ spring causes as well a shorter period needed for forcing resulting in a much earlier begin of bud break or flowering (Situation B, Fig. 1). Or it might that the chilling requires much more time for it to be fulfilled since future climates may lift the actual temperatures too often above the optimum. This effect could be so large, that it actually causes a delay in bud break or flowering (Situation C, Fig. 1). At least it will partially offset the effect seen due to higher temperatures on the forcing period, which then shortens.

Since statistical approaches are not likely to give better results than currently available, the only way leading to a more precise way of predicting the likely results

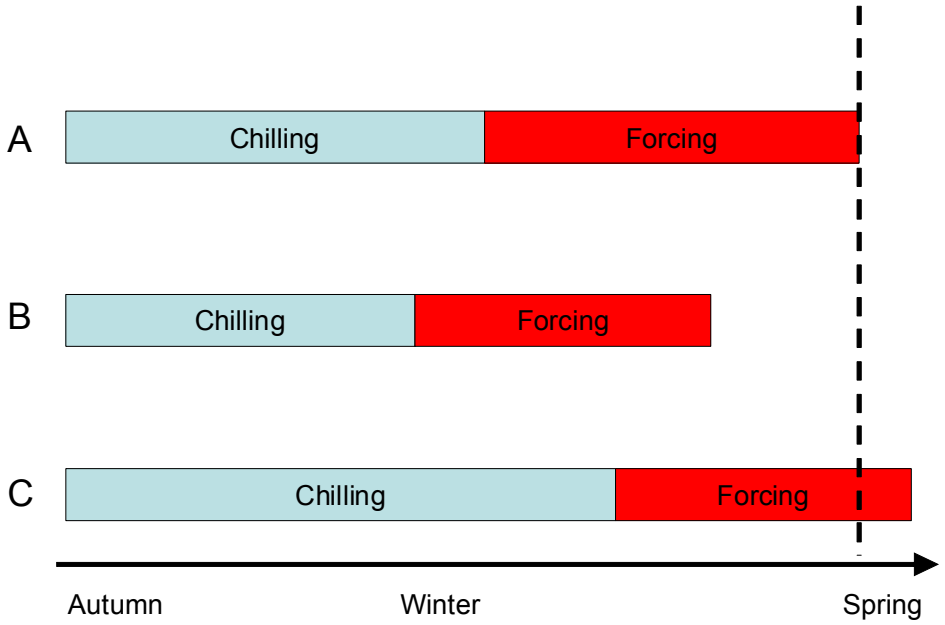

Fig. 1: Schematic representation of the follow-up of chilling and forcing periods in trees. A represents the current situation, B represents a situation with shorter periods required for chilling and forcing and C a situation with a longer period for chilling and a shorter one for forcing

of climate change on phenology will be through a more mechanistic model representing at least the major influencing factors correctly. A major stumbling block is here the determination of the time of the fulfilment of the chilling requirement and the start of the effectiveness of warmer temperatures for forcing. If this would be known, determining the remaining variables for just the chilling period or the forcing period statistically should be easier and could be done with currently existing information. It is known, that the water content and the water uptake capacity of buds is greatly reduced, when they are in endodormancy and, leaving endodormancy, the water uptake capacity increases drastically again. So this might be a physiological measure to determine the end of endodormancy experimentally. This could then be correlated with a molecular approach, where one or several of the gene products related to the beginning activity are identified. The molecular approach would then have the advantage that it can easily be done in a number of locations and species while the physiological measurements might be restricted to a few species allowing such measurements. However, as long as there is no clear separation of chilling and forcing and a more universally valid and thus mechanistic model is possible, phenological models will be of limited use and the results should be viewed with caution.

References

Anderson, J. L., E. A. Richardson, C. D. Kesner, 1986. Validation of chill unit and flower bud phenology models for “Montgomery” sour cherry. Acta Hort. 184, 71–78.

Chuine, I., 2000. A Unified Model for Budburst of Trees. J. theor. Biol. 207, 337–347.

Richardson, E. A., Seeley, S. D. and Walker, D. R. 1974. A model for estimating the completion of rest for “Redhaven” and “Elberta” Peach Trees. Hort Sci. 9, 331–332.

Authors’ address:

Prof. Dr. Peter Braun (braun@fa-gm.de)
Geisenheim Research Centre, Dept. of Pomology,
Von Lade Str. 1, D-65366 Geisenheim, Germany

Markus Müller (muellerm@uni-bonn.de)
Meteorological Institute, University of Bonn
Auf dem Hügel 20, D-53121 Bonn, Germany

Defining the vegetation period by temperature sums

Wolfgang Janssen

Deutscher Wetterdienst

Abstract

The vegetation period can be defined by plants and is described by their phenological stages. Using 58 stations where temperature and phenological observations are available, most plausible and accurate approaches were determined, to calculate phenological observation dates with the help of the temperature values. The beginning of vegetation period is defined by the phenological phase "gooseberry, leaf unfolding," and the end of growing by the phase "European beech, leaf fall". As most appropriate approach a temperature sum above a reference temperature from a fixed start day was found. When the temperature sum exceeds 164 °C starting at 18.2. with reference temperature of 0 °C the growth of vegetation begins. The end of vegetation growth is reached, when temperature sum falls below -1383 °C starting at 2.8. with a reference temperature of 30 °C.

The founded approach reproduces the growing season in most years well and shows the observed extension of the growing season up to 15 days in the last 40 years.

1. Einleitung

Es gibt zahlreiche Definitionen zum Vegetationsanfang und wenige zum Vegetationsende, die alle unterschiedliche Ergebnisse liefern. Im Zusammenhang mit Klimaszenarienrechnungen muss eine verbindliche Definition gefunden werden, die hilft, die zukünftige Veränderung der Vegetationszeit zu erfassen. Da in allen Klimamodellen am verläßlichsten die Temperaturen vorhergesagt werden, wird der neue Ansatz über dieses Element hergeleitet.

Die Vegetationszeit der Pflanzen ist unterschiedlich, da jede Pflanze ein anderes Wärmebedürfnis und Wachstumsverhalten hat, was die Findung einer allgemeingültigen Definition erschwert. Nach der Definition der phänologischen Jahreszeiten beginnt die Vegetation im Erstfrühling mit Auftreten der Pflanzenphase „Stachelbeere, Blattentfaltung“ und endet zum Winteranfang mit der Pflanzenphase „Stieleiche, Blattfall“. Die Untersuchung wurde mit Hilfe der phänologischen Sofortmelder durchgeführt, die für ganz Deutschland ab 1992 zur Verfügung stehen. Leider wird in diesem Beobachtungsprogramm nicht der Blattfall der Stieleiche beobachtet, so dass ersatzweise der Blattfall der Rotbuche für die Auswertung verwendet wurde, die im Mittel etwas früher auftritt.

Da phänologische Beobachtungen auf engstem Raum durch Wärmeinseleffekte oder individuelle Interpretation der Beobachter stark variieren können, wurden die endgültigen Beziehungen über interpolierte Eintrittstermine ermittelt. Hierunter ist zu verstehen, dass in einem Gebiet die lineare Abhängigkeit der Eintrittstermine von der Stationshöhe und geographischen Lage über das kleinste Fehlerquadrat optimal angepaßt wird. Mit der so ermittelten Abhängigkeit und den gegebenen Stationskoordinaten läßt sich der wahrscheinlichste (interpolierte) Eintrittstermin berechnen. Diese gewählte Vorgehensweise reduziert die Streuung der gesuchten Beziehungen und reduziert den Einfluß von Falschmeldungen.

Nachfolgender Ansatz erwies sich am zweckmäßigsten und erzielte mit geringem Aufwand bereits hohe Übereinstimmung, die nur unwesentlich durch Berücksichtigung weiterer anderer Variablen erhöht werden konnte.

(Gl. 1) $$T_S = \sum_{Starttag} (T_M - T_B)$$

Liegt die Tagesmitteltemperatur T_M über einer Bezugstemperatur T_B, so wird die Differenz ab einem Starttag bis zum Eintrittstermin als Temperatursumme T_S aufaddiert. Mit Hilfe einer multiplen Regression wurde die optimale Beziehung ermittelt und in einem darauffolgenden Schritt angewendet und mit den tatsächlich beobachteten Werten verglichen. Aus dem Vergleich der so berechneten zu den beobachteten Werten wurde die Streuung berechnet, die als Maß für die Güte der Anpassung verwendet wurde.

2. Vegetationsanfang

Für den Vegetationsanfang wurde die Blattentfaltung der Stachelbeere für die Auswertung herangezogen. Im Mittel tritt diese Phase am 27.3. (86. Tag) jeden Jahres in Deutschland auf, kann jedoch von Jahr zu Jahr oder Region um bis zu 60 Tage schwanken. Erste Versuche mit Gl. 1 zeigten sehr schnell, dass sowohl die Wahl des Starttages als auch die Bezugstemperatur die Güte der Anpassung stark beeinflusst. Um die optimale Anpassung zu erlangen, wurden für alle verfügbaren 58 Stationen und 18 Jahre jeweils die Streuung für 61 unterschiedliche Starttage und 31 unterschiedlichen Bezugstemperaturen berechnet. In der nachfolgenden Grafik ist diese Streuungsmatrix der Berechnungen dargestellt.

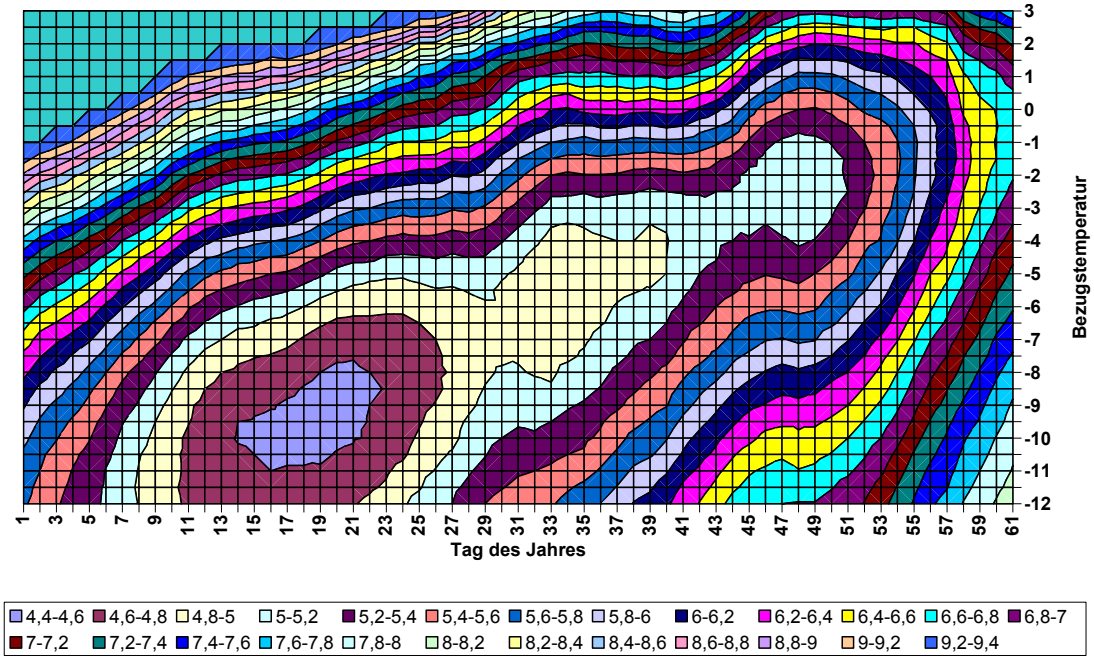

Abb. 1: Streuungsmatrix in Tagen für unterschiedliche Starttage (x-Achse) und Bezugstemperaturen (y-Achse) aus Gl. 1 für den Vegetationsanfang

Mit 4,5 Tagen ergibt sich die geringste Streuung bei dem 19.1. als Starttag und -9,5 °C als Bezugstemperatur. Überraschend sind weniger die vom 1.1. abweichenden optimalen Starttage, sondern eher die negativen Bezugstemperaturen, die eigentlich keinen

Pflanzenwachstum erlauben. Damit dieser Widerspruch zum Pflanzenwachstum verschwindet, wurde trotz schlechter Ergebnisse im Ansatz eine Bezugstemperatur von 0°C und 18.2. als Starttag verwendet. Wird mit diesen Werten eine Temperatursumme von 164 °C überschritten, so beginnt die Vegetation. Im langjährigen Mittel treten zur Zeit des Starttages die letzten Temperaturminima des Winters auf.

Auch für andere Pflanzenphasen lassen sich solche Streuungsmatrizen aufstellen und interessanterweise ergeben sich unterschiedliche Streumuster. So ähnelt die Matrix vom Ergrünen des Dauergrünlandes sehr der Abb. 1, spätere Blühphasen sind dagegen stärker auf einen engen Temperatur- und Starttagebereich begrenzt. Dieses kann damit erklärt werden, dass die früh im Jahr beobachteten Pflanzenphasen eine höhere Schwankung als die später im Jahr beobachteten Phasen aufweisen, wodurch sich automatisch eine größere Spanne der möglichen Starttage ergibt.

Dieser Ansatz wurde sowohl an Zeitreihen und in Einzelljahren in der Fläche mit den Beobachtungen verglichen und zeigte gute Übereinstimmung. Beispielhaft wird die Zeitreihe von Braunschweig in der nachfolgenden Abb.2 gezeigt.

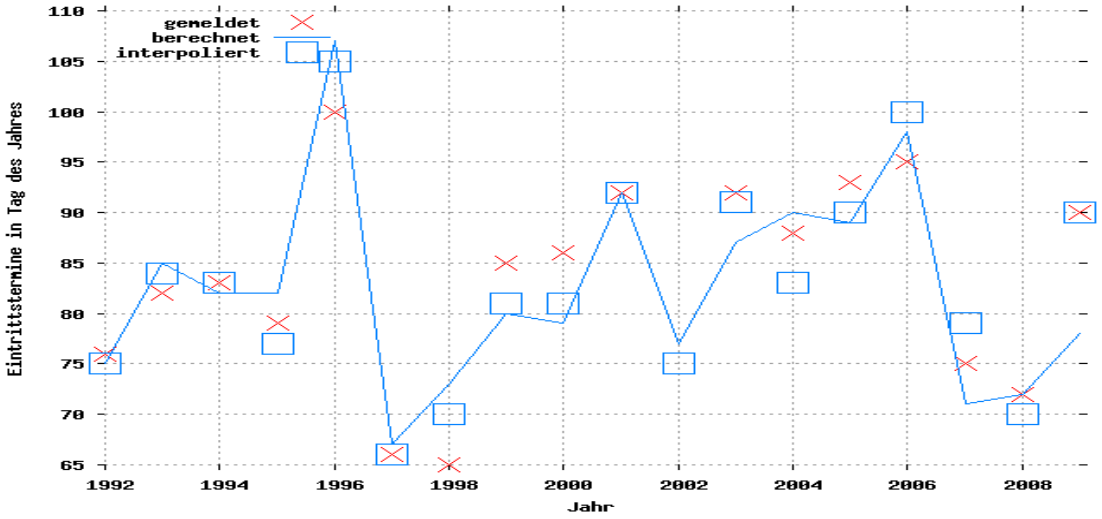

Abb. 2: Verlauf des beobachteten (x), berechneten (---) Vegetationsanfanges in Braunschweig in den Jahren 1992 - 2009

Selbst die extreme Schwankung des Vegetationsanfanges zwischen 1996 und 1997 wird von dem Ansatz gut reproduziert.

3. Vegetationsende

Zur Definition des Vegetationsendes bietet sich der Blattfall an, da die Pflanze danach keine Photosynthese und somit Wachstum betreiben kann. Der untersuchte Blattfall der Rotbuche wird im Mittel am 27.10. (300. Tag) eines Jahres in Deutschland beobachtet. Wie bei dem Vegetationsanfang wurde wieder mit Gl. 1 gearbeitet, allerdings ist beim Ende der Vegetation nicht der Anstieg, sondern Abfall der Temperatur ausschlaggebend, so dass von einer hohen Bezugstemperatur und einer negativen Temperatursumme auszugehen ist. Zur Findung des optimalen Starttages und Bezugstemperatur wurden die Streuungen für 81 Starttage mit jeweils 31 unterschiedlichen Bezugstemperaturen berechnet. Die Ergebnisse sind in der Abb. 3 dargestellt.

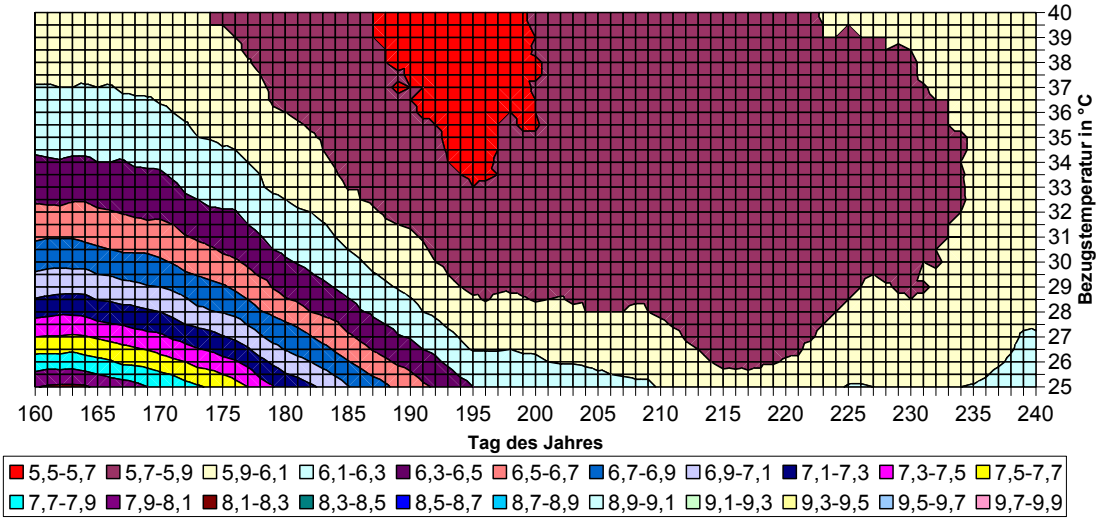

Abb. 3: Streuungsmatrix in Tagen für unterschiedliche Starttage (x-Achse) und Bezugstemperaturen (y-Achse) aus Gl. 1 für das Vegetationsende

Die geringsten Streuungen werden mit dem 196 Tag des Jahres als Starttag und einer Bezugstemperatur von 38 °C erzielt. Unwesentlich schlechtere Ergebnisse bekommt man mit dem 214 Tag (2.8.) des Jahres als Starttag, der für die Definition des Vegetationsendes verwendet wurde. Dieser Starttag hat den Vorteil, dass die Abhängigkeit von der Bezugstemperatur nahezu verschwindet. Mit einer Bezugstemperatur von 30 °C muss die Temperatursumme von -1383 °C für das Ende der Vegetation unterschritten werden. Obwohl der Starttag fast drei Monate vor dem eigentlichen Zieltermin liegt, sind die Streuungen überraschend gering. Zur Zeit des Starttages werden im Mittel über das Jahr die höchsten Temperaturen beobachtet. Andere Phasen wie der Blattfall von Apfelbäumen, die noch später auftreten haben ebenfalls einen Starttag zu dieser Zeit.

Dieser Ansatz wurde wieder anhand der Zeitreihe von Braunschweig überprüft. Das Ergebnis ist in Abb. 4 dargestellt.

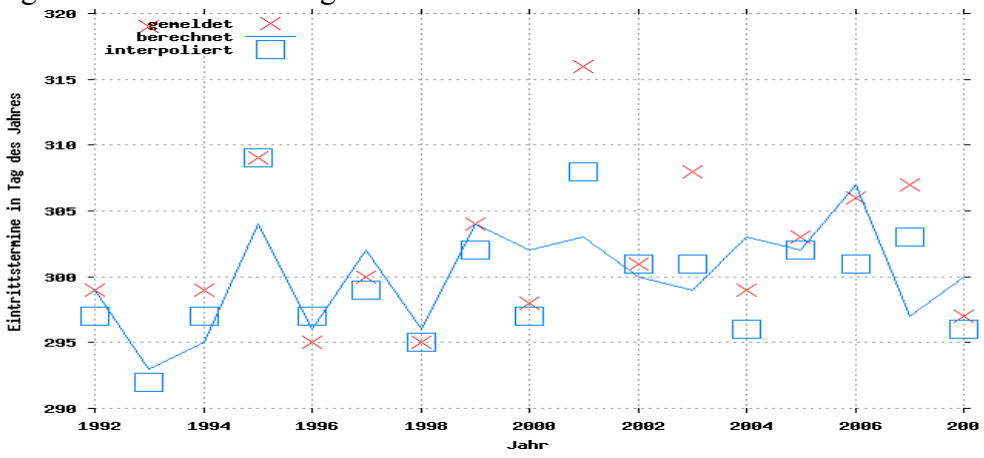

Abb. 4: Verlauf des beobachteten (x), berechneten (---) Vegetationsendes in Braunschweig in den Jahren 1992 - 2009

Insgesamt wird der Verlauf nicht so genau wie bei dem Anfang reproduziert und Einzelljahre wie 2001 zeigen starke Abweichungen. Entgegen langläufiger Meinung wurde ist in den trockenen Jahren 2003 und 2006 kein früheres Vegetationsende beo-

bachtet worden. Obwohl die Streuung mit dem gefundenen Ansatz relativ gering ist, könnte diese mit Berücksichtigung weiterer Faktoren noch weiter reduziert werden.

4. Vegetationszeit

Mit den hergeleiteten Beziehungen für den Vegetationsanfang und das –ende soll abschließend einmal beispielhaft an der Stationen Braunschweig die Änderungen der Vegetationszeit über den langen Zeitraum 1961 – 2008 untersucht werden. Da die Werte von Jahr zu Jahr stark schwanken und somit schlecht ein Trend zu erkennen ist, wurde zusätzlich der gemittelte (Zeitraum -5 - +5 Jahre) Verlauf in der nachfolgenden Abb.5 dargestellt.

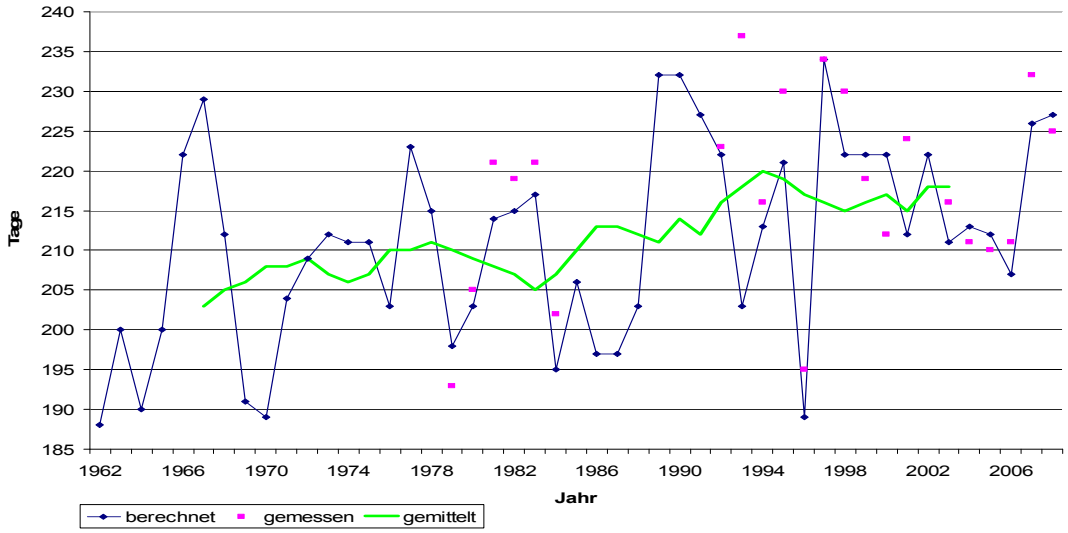

Abb. 5: Verlauf der beobachteten (•) und berechneten (---) Vegetationszeit in Braunschweig für die Jahre 1961 – 2008. Kurve (---) ist gleitendes Mittel

Die klimatologische Entwicklung hat sich verlängernd auf die Vegetation ausgewirkt. Im Mittel über 40 Jahre kam eine Verlängerung von ca. 15 Tagen zustande, was sich gut mit den phänologischen Beobachtungen (Differenz zwischen den Eintrittsterminen der beiden Zeigerphasen und als rote Punkte in Abb. 5 markiert) deckt. Für diese Verlängerung ist maßgeblich eine stärkere Verfrühung des Vegetationsanfanges verantwortlich, da besonders in der ersten Jahreshälfte stärkere Temperaturerhöhungen stattgefunden haben.

Interessant ist ebenfalls, ob sich über diesen Ansatz regionale Unterschiede in Deutschland ergeben haben. Hierzu wurde für alle verfügbaren Stationen eines Jahres der Vegetationsanfang und das –ende über die neuen Definitionen berechnet und deren Differenz auf ein Raster von 1 x 1 km für jedes Jahr interpoliert. Aus diesen Jahresrastern wurde dann die durchschnittlichen Vegetationszeit für die Zeiträume 1961 – 1990 und 1991 – 2009 sowie deren Differenz bestimmt und in nachfolgenden Abb. 6a -c dargestellt.

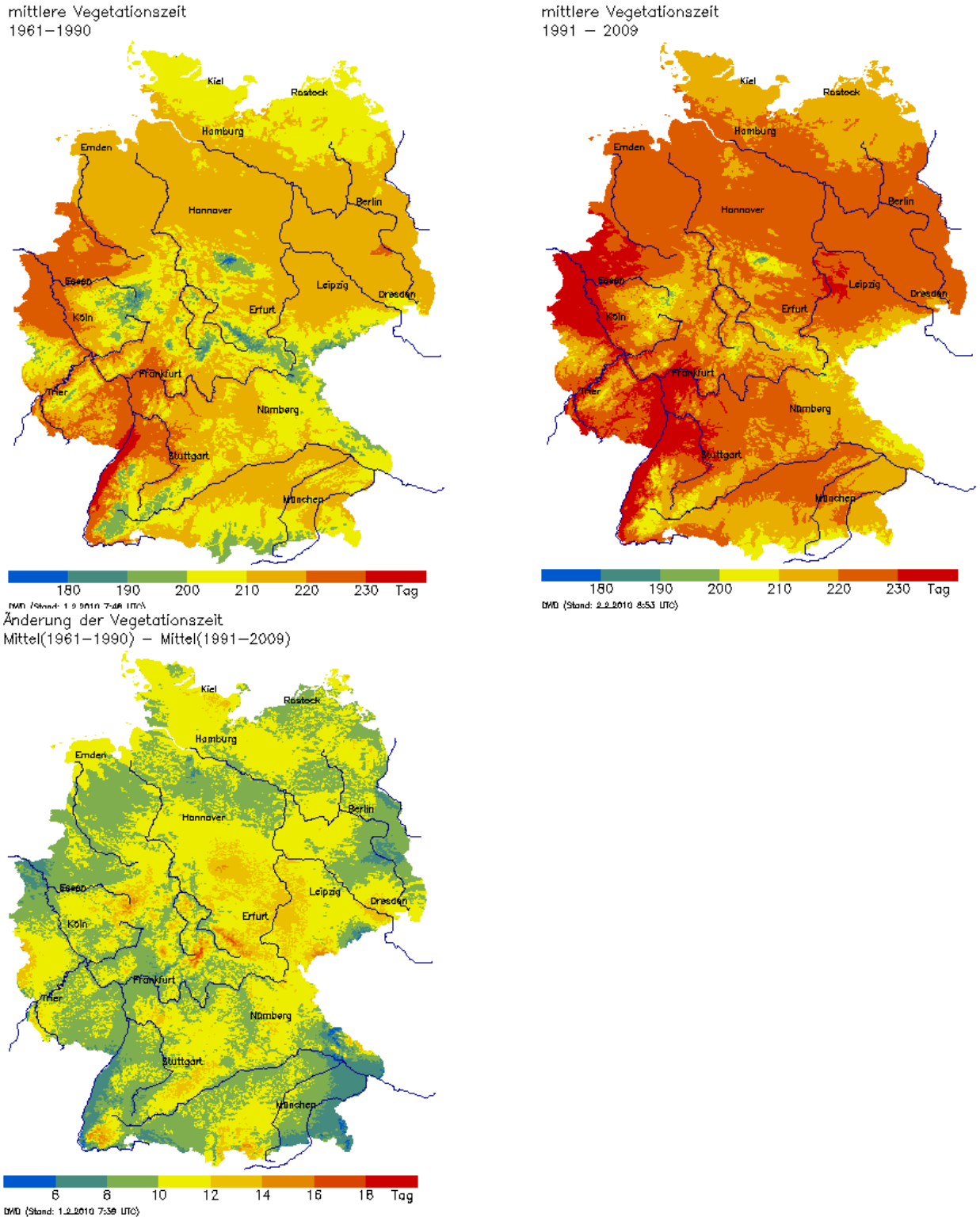

Abb.6a-c: mittlere Vegetationszeiten für die Zeiträume 1961 – 1990, 1991–2009 sowie deren Differenz

In ganz Deutschland hat sich die Vegetationszeit zwischen 6 – 18 Tage in den untersuchten Zeiträume verlängert. Hierbei treten Unterschiede in der räumlichen Verteilung auf. Die größten Zuwächse sind in den Bergen, also Gebieten mit kürzerer Vegetations-

zeit, und die geringsten Zuwächse in den Gebieten mit ohnehin langer Vegetationsperiode festzustellen.

5. Ausblick

Um eine größere Datenbasis bzgl. Stationsanzahl und Jahren zu bekommen, sollte die Auswertung noch einmal mit den phänologischen Jahresmeldern durchgeführt werden. Mit diesen umfangreicheren Daten kann dann die regionale und zeitliche Varianz des Starttages untersucht werden, die evtl. auch eine Abhängigkeit zur Temperatur aufweist. Mit dem Wissen solcher Zusammenhänge könnten gezielt kalte und besonders warme Jahre analysiert werden, um bessere Erkenntnisse für zukünftige Entwicklungen abschätzen zu können, denn extrem warme Jahre in der Vergangenheit sollten schon die Strukturen

Future climatic conditions and their impact on viticulture in the Upper Moselle region

Steffi Urhausen[1], Susanne Brienen[2], Alice Kapala[1], Clemens Simmer[1]

[1]Meteorological Institute, University of Bonn, Germany
[2]Deutscher Wetterdienst, Offenbach, Germany

Abstract

Climate, especially temperature, light and precipitation, plays a decisive role in growing and maturating processes as well as for the health of the vine. Several studies have investigated the relationships between climate and phenology. The study presented here is primarily focused on the region of the Upper Moselle, especially on the viticulture in Luxembourg. First, we analysed climatic and phenological data of the last 40 years in order to detect trends and to find possible relationships between climate and phenology. Second, phenological models based on multiple regression methods, are set up in order to calculate, out of meteorological data, the phenological events. We focused on bud burst and flowering events and further on must density and acidity at harvest time for seven different vine varieties. As these models use mainly meteorological data, they can also be computed based on climate model output. In this project the consortial runs of the regional climate model CCLM are used, in order to estimate the phenological events until 2050.

1. Introduction

Viticulture depends strongly on meteorological conditions, thus monitoring the changing climate and investigating its impact on viticulture is of high interest. In over 9 different European regions, annual mean temperature has risen significantly (Jones et al, 2005a), although the amount is varying from region to region and from period to period. These climatic changes affect agriculture in general and viticulture in particular, because amongst other effects, the vegetative period is extended. Clear changes in vine phenology are observed in Europe (e.g. Bois, 2007; Jones and Davis, 2000; Jones et al, 2005b; Menzel, 2005).

Different types of phenological models have been developed. Some models are based on correlations (Lüers, 2003) others on regression methods (Jones and Davis, 2000; Santos et al, 2009). We present a model for the Upper Moselle region which is characterised by a high variety of wine sorts. The predictors for the phenological stages are restricted to meteorological data, with long time series, which can easily be measured and which are also provided by climate models.

2. Climatic conditions and its variability

Annual maximum, minimal and mean temperature show increasing trends. The maximum temperature shows low values around the 1970s, while the lowest annual temperature was measured in 1954. After a period of slightly decreasing maximum temperature, a significant increasing trend (+0.07°C/year) is observed from 1980 onwards. The minimum and mean temperatures show a monotonically increasing trend of 0.02°C/year.

A closer look at the seasons shows a positive trend for all temperature time series. They are only significant for spring and summertime. Maximum temperature in spring is lower between 1951 and 1979, but increases from 1978 to 2006 significantly. Minimum and mean temperature rise during the entire spring time series.

The annual precipitation at the Upper Moselle region is about 770 mm per year. The year to year variability is high and no significant trend is detectable for annual or seasonal precipitation.

3. Phenological data

Bud burst event occurs on average on the 118th day of the year, which means end of April (Fig. 1). Until 1985 the bud burst date was very late, mainly in May. After 1988 bud burst events were always observed before the mean date. With 90% significance, it occurs each year 0.20+/-0.15 days earlier. All vine varieties behave similarly for the bud burst event (Table 3). The standard deviation is about 7 days and the range between the earliest and the latest event one month.

The time series of must density and acidity of Riesling is shown in Fig. 1. The years between 1973 and 1987 alternate from sweeter to more acid wine styles, but after 1988 must density is increasing and acidity decreasing continuously. Both trends are significant at the 99% level. This behaviour of wine quality is similar for the other vine varieties, although they are differing in the averaged must density and acidity (Table 4 and Table 5). Elbling is characterised by a low must density and a high acidity. Traminer has the highest must density and the lowest acidity.

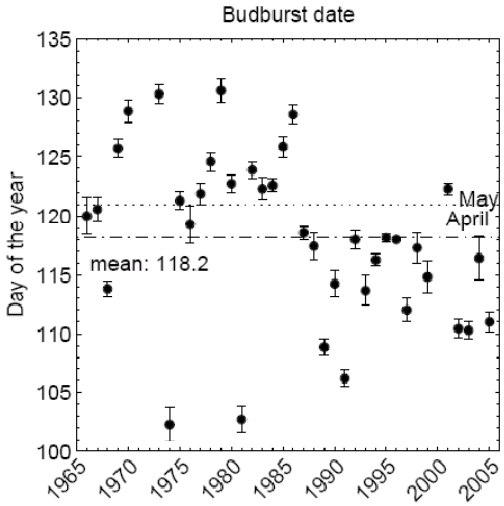

Fig. 1: Mean bud burst date (points). The bars around the point indicate the standard deviation due to the different vine varieties

Table 3: Statistical characteristics of bud burst event in the Upper Moselle region for the mean and the different vine varieties

	mean value	stand. dev.	range	minimum	maximum	1st quartile	3rd quartile
All	118.1	7.1	28.3	102.3	130.6	113.8	112.6
Auxerrois	118.4	6.9	27.0	103.0	130.0	114.0	123.0
Elbling	117.1	7.3	30.0	100.0	130.0	112.8	122.0
Pinot Blanc	118.2	7.2	28.0	103.0	131.0	114.0	123.0
Pinot Gris	118.1	7.2	29.0	102.0	131.0	113.5	123.0
Riesling	119.0	7.0	28.0	104.0	132.0	115.0	123.0
Rivaner	118.2	7.1	28.0	102.0	130.0	114.0	123.0
Traminer	117.6	7.2	30.0	101.0	131.0	113.0	123.0

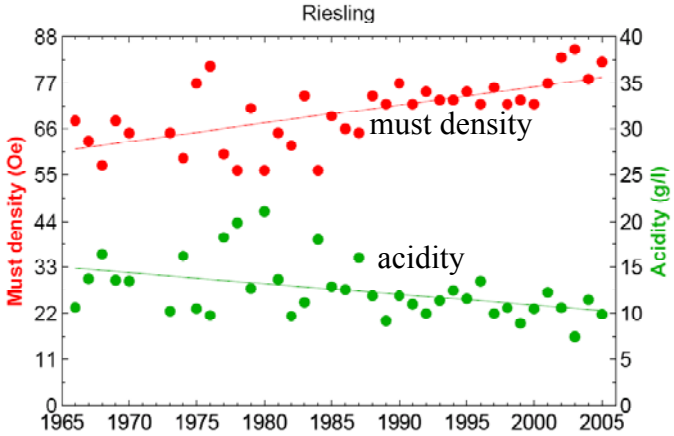

Fig. 1: Must density and acidity for the Riesling species

Table 4: Statistical characteristics of must density for the mean and the different vine varieties

	mean value	stand. dev.	range	minimum	maximum	1st quartile	3rd quartile
All	69.4	6.9	30.0	55.3	85.3	64.9	72.6
Auxerrois	70.6	7.6	31.7	53.3	85.0	66.0	75.0
Elbling	59.8	5.9	26.4	48.6	75.0	56.0	63.0
Pinot Blanc	70.0	7.1	32.0	54.0	86.0	66.0	75.0
Pinot Gris	74.6	7.8	35.0	58.0	93.0	69.0	80.7
Riesling	70.5	8.3	33.0	56.0	89.0	65.0	75.0
Rivaner	62.6	6.3	29.0	50.0	79.0	57.0	66.0
Traminer	78.6	8.5	38.0	61.0	99.0	73.0	83.1

Table 5: Statistical characteristics of acidity for the mean and the different vine varieties

	mean value	stand. dev.	range	minimum	maximum	1st quartile	3rd quartile
All	10.0	2.2	9.1	5.8	14.8	8.4	11.6
Auxerrois	8.5	2.1	8.7	4.9	13.5	7.1	9.6
Elbling	12.2	2.7	11.1	6.7	17.8	10.3	14.1
Pinot Blanc	10.7	2.1	9.2	6.2	15.4	9.0	12.2
Pinot Gris	9.7	2.0	8.3	5.5	13.8	8.3	11.2
Riesling	12.5	3.2	13.6	7.5	21.1	10.5	13.6
Rivaner	8.5	1.4	5.9	5.7	11.6	7.4	9.2
Traminer	8.0	2.3	9.7	3.9	13.6	6.2	9.4

4. Modelling strategy and modelling results

The phenological models are based on a stepwise linear multiple regression method which contains forward and backward steps. Every potential predictor is tested for an increase of the explained variance. The first predictor is chosen based on the highest correlation. The second one is added also in order to get the highest explained variance. This procedure is the forward step in the stepwise regression method. If more than three predictors have been determined, one has to check if all predictors are still significant. Otherwise this predictor is taken out of the regression equation. After these backward steps, the forward steps follow again. This technique is continued until no further significant predictor can be found.

The predictors tested in this study are meteorological parameters like temperature, temperature indices, precipitation and sunshine duration for different time periods. Previous

phenological events are also taken into account as long as they can be calculated from meteorological data.
In contrast to must density and acidity, the bud burst and flowering events are similar for the vine species, the phenological model can be set up using the mean over the different varieties. The final model for bud burst events contains degree days of March, maximum temperature in April and the amount of frost days from January to March. The model has a correlation of 0.91 with the observation and explains about 83% of the variance.

5. Estimation of the future phenological events

The future meteorological conditions are computed using the consortial runs of the regional climate model CCLM of the German Weather Service. The spatial resolution is of about 18 km. The computed time period is divided into two parts: the 20th century (C20) from 1960 until 2000 and the future period from 2001 until 2100 divided into the two scenarios A1B and B1. The population development is the same for the two scenarios, but they differ in technology and energy resources. Where the A1B scenario has a balance across all sources (fossil and non-fossil), the B1 scenario introduces clean and resource efficient technologies.

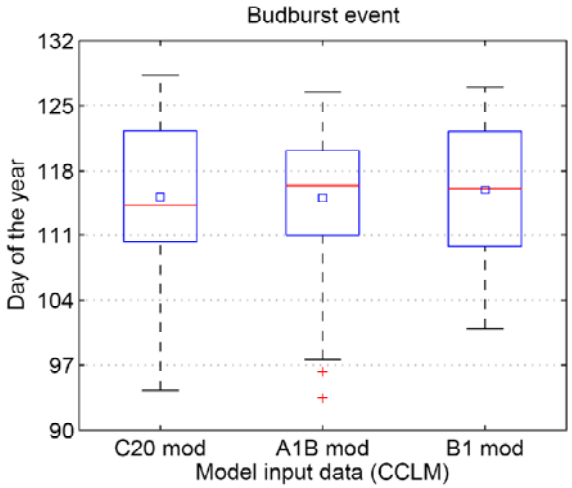

Fig. 2: Distribution of bud burst events calculated with the regional climate model for the past century (C20) and the future scenarios A1B and B1. The middle line is the median, the square the mean value

The bud burst event is calculated using the climate model data from the 20th century and the two future scenarios from 2001 until 2050. Their distribution is visualised in Fig. 2. The variance of budburst events is high in C20 and lowest in the B1 scenario. A trend toward later or earlier events is not detectable out of the distributions. Looking at the time series of the A1B and B1 scenarios (Fig. 3), we do not see a clear behaviour to earlier or later bust bursts until 2030. Between 2030 and 2050, however, the two scenarios show a trend toward earlier bud burst dates.

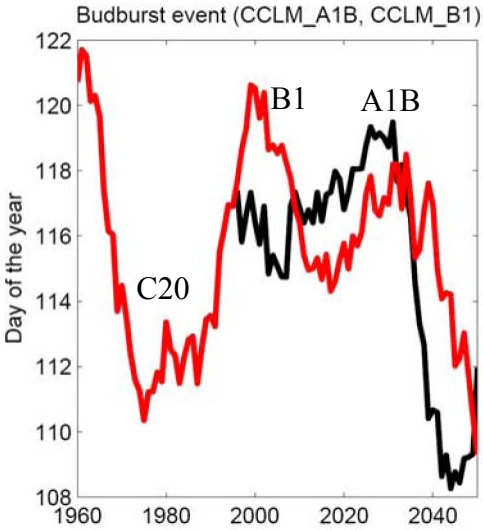

Fig. 3: Time series of bud burst events (moving average of 10 years) from 1960 until 2050 using the C20, A1B and B1 scenarios

6. Conclusions

Significant trends in annual as well as in spring and summer temperatures have been found. Mean and minimum temperature show lower increasing rates as maximum temperature. Analysing precipitation data reveals no significant trend on annual or seasonal scales. Phenological events, like bud burst or flowering events show a clear trend toward earlier dates, with a trend of 2 days/decade.

The phenological models developed in this study are based on meteorological data and are in good agreement with the observation. They work not only well for bud burst and flowering events but also for wine quality. Using the CCLM data we cannot find a clear trend direction for bud burst events (as well as for flowering events), but afterwards a rapid decrease in bud burst date may be possible.

Acknowledgements:

This work has been funded by "Fonds National de la Recherche (Luxembourg)" under grant TR-PHD BFR06-090. We thank the "Institut Viti-Vinicole (Luxembourg)", "Deutscher Wetterdienst (Germany)" and „Administration des Services Techniques de l'Agriculture (Luxembourg)" for the phenological and meteorological data.

References:

Bois, B., 2007 : Ce que nous apprennent le climat récent et les observations phénologiques sur les effets du changement climatique en Gironde viticole. Acte de la 8ème Journée Technique du CIVB, Bordeaux-Lac.

Jones, G. V., Davis, R. E., 2000: Climate Influences on Grapevine Phenology, Grape Composition, and Wine Production and Quality for Bordeaux, France. American Journal of Enology and Viticulture 51(3):249–261.

Jones, G. V., Duchêne, E., Tomasi, D., Yuste, J., Braslavaska, H., Schultz, H., Martinez, C., Boso, S., Langellier, F., Perruchot, C., Guimberteau, G., 2005a: Changes in European Winegrape Phenology and Relationships with Climate. GESCO.

Jones, G. V., White, M. A., Cooper, O. R., Storchmann, K., 2005b: Climate change and global wine quality. Climatic Change 73:319–343.

Lüers, J., 2003: Agrarklimatologische und phänologische Auswertungen für das Mittlere Moseltal. Auswirkungen des Klimawandels auf die Weinrebe im Moselraum. PhD thesis, Universität Trier.

Menzel, A., 2005: A 500 year pheno-climatological view on the 2003 heatwave in Europe assessed by grape harvest dates. Meteorologische Zeitschrift 14(1):75–77.

Santos, J. A., Malheiro, A. C., Pinto, J. G., 2009: Modelling of grapevine productivity in the Port Wine region for present and future climate conditions. submitted to Agricultural and Forest Meteorology.

Authors' address:

Dr. Alice Kapala (akapala@uni-bonn.de),
Prof. Dr. Clemens Simmer (csimmer@uni-bonn.de)
Meteorological Institute, Rheinische Friedrich-Wilhelms-Universität, Bonn, Germany
Auf dem Huegel 20, D-53121 Bonn, Germany

Dr. Susanne Brienen (susanne.brienen@dwd.de)
Deutscher Wetterdienst
Klima und Umwelt - Zentrales Gutachtenbüro
Frankfurter Straße 135, D-63067 Offenbach, Germany

Bestimmung amphibischer Aktivität mittels Phänologie

Kerstin Höbart[1], Christina Czachs[1], Christiane Brandenburg[1], Manfred Pintar[2], Erich Mursch-Radlgruber[3]

[1]Institut für Landschaftsentwicklung, Erholungs- und Naturschutzplanung,

[2]Institut für Zoologie, [3]Institut für Meteorologie

Universität für Bodenkultur Wien, Österreich

Zusammenfassung

Sowohl Tiere als auch Pflanzen werden in ihrer Entwicklung und ihrem Lebensrhythmus von äußeren Einflüssen gesteuert. Vor allem Wetter bzw. Klima spielen hier eine große Rolle. Im Rahmen einer Diplomarbeit an der Universität für Bodenkultur in Wien wurde der Frage nachgegangen, inwieweit pflanzenphänologische Ereignisse und amphibische Aktivität korrelieren. Die daraus resultierenden Erkenntnisse sollen helfen, die Lebensphasen der Amphibien besser voraussagen zu können um Schutzmaßnahmen für sie zeitlich besser abstimmen zu können. Die Untersuchungen haben gezeigt, dass es vor allem im Frühjahr Übereinstimmungen zwischen den Aktivitätsmustern der Amphibien und den pflanzenphänologischen Ereignissen gibt. Ob diese Erkenntnisse tatsächlich für den Amphibienschutz nutzbar sind, wird sich erst nach mehrjähriger Untersuchung der Fragestellung zeigen.

Determination of amphibious activity using plant phenology

Abstract

Both animals and plants are controlled in their development and their rhythm of life by influences coming from the outside. Especially weather and climate have a major influence. As part of a diploma thesis at the University of Natural Resources and Applied Life Sciences Vienna, plant phenological events and amphibian activities have been compared. The results should help to predict the life stages of amphibians. These findings could be used to set amphibian protection measures on time. The investigations have shown that there are connections between the life stages of amphibians and plant phenological events, especially in spring. If these conclusions are effectively useable for the protection of amphibians remains to be seen after long lasting research.

1. Einleitung

Amphibien zählen zu den am stärksten vom Aussterben bedrohten Arten. Nach HÖDL et al. (1997) ist dies vor allem auf die Zerstörung bzw. Veränderung ihrer Lebensräume zurückzuführen. Die Tatsache, dass diese Tiere im Laufe eines Jahres mehrere unterschiedliche Lebensräume besiedeln und sie hierfür teilweise weite Wanderungen unternehmen müssen, die in der heutigen Landschaft nicht mehr gefahrlos durchgeführt werden können, tut ihr übriges hinzu. In Wien sind Amphibienpopulationen hauptsächlich in den Randgebieten anzutreffen, jedoch sind auch diese stark gefährdet (TIEDEMANN, 1990).

Amphibien suchen im Lauf des Jahres mehrere Lebensräume (Sommer- und Winterquartier, Laichplatz) auf, legen dabei meist große Distanzen zurück und setzen sich bei Querung von Straßenabschnitten großen Gefahren aus. Zu ihrem Schutz ist es daher erforderlich, den Zeitpunkt ihrer Wanderung möglichst genau zu bestimmen. Die wichtigste und zugleich schwierigste Frage bei der Vorhersage von Lebens- und Aktivitätsphasen von Amphibien ist, wann deren Laichwanderung beginnt. Zahlreiche Untersuchungen zeigen, dass viele Amphibienarten im Frühjahr ab einer Temperatur von ca. 5°C und Niederschlag ihre Wanderung zum Laichgewässer beginnen (vgl. BLAB, 1986). Mit Hilfe der Meteorologie kann somit der Beginn der Laichwanderungen der Amphibien mehr oder weniger genau vorhergesagt werden. Da jedoch die meteorologischen Verhältnisse der jeweiligen Laichgebiete bekannte sein müssen und meteorologische Messstationen oft nicht in der unmittelbaren Nähe des Untersuchungsgebietes liegen, ist die Prognose der Laichwanderung mittels meteorologischer Parameter mit einem hohen Aufwand verbunden. Phänologische Ereignisse können hingegen nahezu überall und nach entsprechender Einschulung von nahezu jeder Person beobachtet werden.

Die Phänologie ist folglich eine Möglichkeit interessierten Menschen leicht sichtbare Anhaltspunkte zu geben, wann welche Aktivitätsphase der Amphibien im Jahreszyklus beginnt. Somit können diverse Hilfsaktionen (Aufstellen von Amphibienschutzzäunen, Errichten von Straßensperren, Reduktion der Höchstgeschwindigkeit, Aufruf zum Verzicht auf Autofahrten auf bestimmten Straßen usw.) zeitlich fixiert werden, damit u.a. bei der Frühjahrswanderung möglichst wenige Tiere zu Schaden kommen.

2. Daten und Methoden

Das im Folgenden vorgestellte Forschungsprojekt bediente sich Methoden aus drei Fachbereichen. Es wurden ein Amphibienmonitoring, phänologische Erhebungen und meteorologische Aufnahmen durchgeführt.

Der Untersuchungszeitraum erstreckte sich vom 08.03.2009 bis zum 16.07.2009. Während dieser Zeit wurde die Phänologie der Pflanzen an zwei Standorten beobachtet. Untersuchungsgebiet war die Jägerwaldsiedlung im 14. Wiener Gemeindebezirk sowie der Türkenschanzpark und das Gelände der Universität für Bodenkultur im 18. Wiener Gemeindebezirk. Der Standort Türkenschanze wurde als Referenzort ausgewählt, da die Eigenschaften der jeweiligen Standorte einen entscheidenden Einfluss auf den Eintrittszeitpunkt phänologischer Ereignisse haben. Die Erhebung der Amphibien erfolgte in der am Rande des Wienerwaldes liegenden Jägerwaldsiedlung an einem künstlich für den Amphibienschutz angelegten Gewässer.

Phänologische Erhebungen

Die phänologischen Aufnahmen wurden basierend auf der „Anleitung zur phänologischen Beobachtung in Österreich“ (ZAMG, 2000) durchgeführt. Für die Untersuchung wurden ausschließlich Wildpflanzen ausgewählt, da auf Grund der Lage der Untersuchungsgebiete innerhalb des Stadtgebietes von Wien keine landwirtschaftlichen Kulturpflanzen sowie Obst und Weinreben angebaut werden. Um die Eintrittszeitpunkte besser untereinander vergleichen zu können, wurden - wenn möglich - jeweils an beiden Standorten zwei Pflanzen der gleichen Art ausgewählt. Da sich das Untersuchungsgebiet in

der Stadt befindet musste natürlich auch der Einfluss von städtebaulichen Elementen auf die Phänologie der Pflanzen beachtet werden (KARSTEN, 1986)

Auf Grund der Hauptaktivitätszeit (CABELA et al., 2001) und damit auch Hauptgefährdungszeit der Amphibien in den Frühjahrsmonaten wurden die phänologischen Jahreszeiten Vor-, Erst – und Vollfrühling sowie Früh- und Hochsommer beobachtet (ZAMG, 2000).

Amphibienmonitoring

Während des Aufnahmezeitraumes wurden täglich die am Teich und auf den umliegenden Wegen und Straßen angetroffenen Tiere auf Artniveau bestimmt und gezählt. Es konnten neun Amphibienarten am Teich beobachtet werden. Zusätzlich wurde das Geschlecht aufgenommen und zwischen verpaarten und unverpaarten Tieren unterschieden.

Meteorologische Aufnahmen

Abgesehen von den beiden genannten Methoden wurden meteorologische Messungen vorgenommen. Die ausgewählten Parameter Lufttemperatur, relative Luftfeuchte, Bodentemperatur und Bodenfeuchtigkeit dienten dabei lediglich zur Unterstützung der Auswertung. Daher soll hier nicht näher darauf eingegangen werden.

Die so erhobenen Daten wurden zusammengeführt und mittels deskriptiver Analyse ausgewertet. Zentrale Fragestellung war der Zusammenhang zwischen den phänologischen Eintrittszeitpunkten der beobachteten Pflanzen (Austrieb, Blattentfaltung, Erste Blüte und Maitrieb) und der phänologischen Lebensphasen der Amphibien (z.B. Erstes Auftreten, Hauptwanderung, Erste Paarungsrufe).

3. Ergebnisse

Eine erste Auswertung der Daten hat vielversprechende Ergebnisse geliefert. Die erhobenen Individuenzahlen von Erdkröte, Grasfrosch und Springfrosch und deren Änderungen im Zeitverlauf konnten mit den phänologischen Eintrittszeitpunkten in Verbindung gebracht werden. Für alle anderen Arten (Bergmolch, Teichmolch, Alpenkammolch, Laubfrosch, Feuersalamander und Gelbbauchunke) können jedoch nur vage Angaben gemacht werden. Eine Verknüpfung mit der Phänologie der Pflanzen wurde zwar versucht, es ist jedoch fraglich, inwieweit diese tatsächlich zutrifft.

Anhand eines Beispiels soll der Zusammenhang zwischen den Eintrittsdaten der pflanzenphänologischen Phasen und den erhobenen Amphibienzahlen von Springfrosch, Grasfrosch und Erdkröte dargestellt werden. Abbildung 1 zeigt die Verschneidung der phänologischen Eintrittsdaten der Hasel (*Corylus avellana)* am Standort Türkenschanze und Jägerwaldsiedlung mit den gezählten Individuenzahlen von Springfrosch (*R. dalmatina*),Grasfrosch (*R.temporaria*) und Erdkröte (*B. bufo*).

Aus der grafischen Darstellung ist deutlich ablesbar, dass die erste Blüte von *Corylus avellana* zeitgleich mit dem Beginn der Laichwanderung von *R. dalmatina* eintritt. Diese pflanzenphänologische Phase eignet sich demnach gut um rechtzeitig entsprechende Amphibienschutzmaßnahmen zu treffen. Die Blattentfaltung setzt hingegen erst gegen Ende der Hauptaktivität von *R. dalmatina*, *R.temporaria* und *B. bufo* ein. Das Ende der

Hauptaktivität von *R. dalmatina* fällt auf den 30. März, von *R. temporaria* auf den 19. bzw. 27. April und jene von *B. bufo* auf den 07.April. Wobei mit dem Überbegriff „Hauptaktivität“ jene Tage gemeint sind, an welchen die Individuenzahl das Mittel der insgesamt gezählten Tiere einer Art übersteigt. Die Blattentfaltung der Haselpflanzen trat zwischen 06. und 09. April ein.

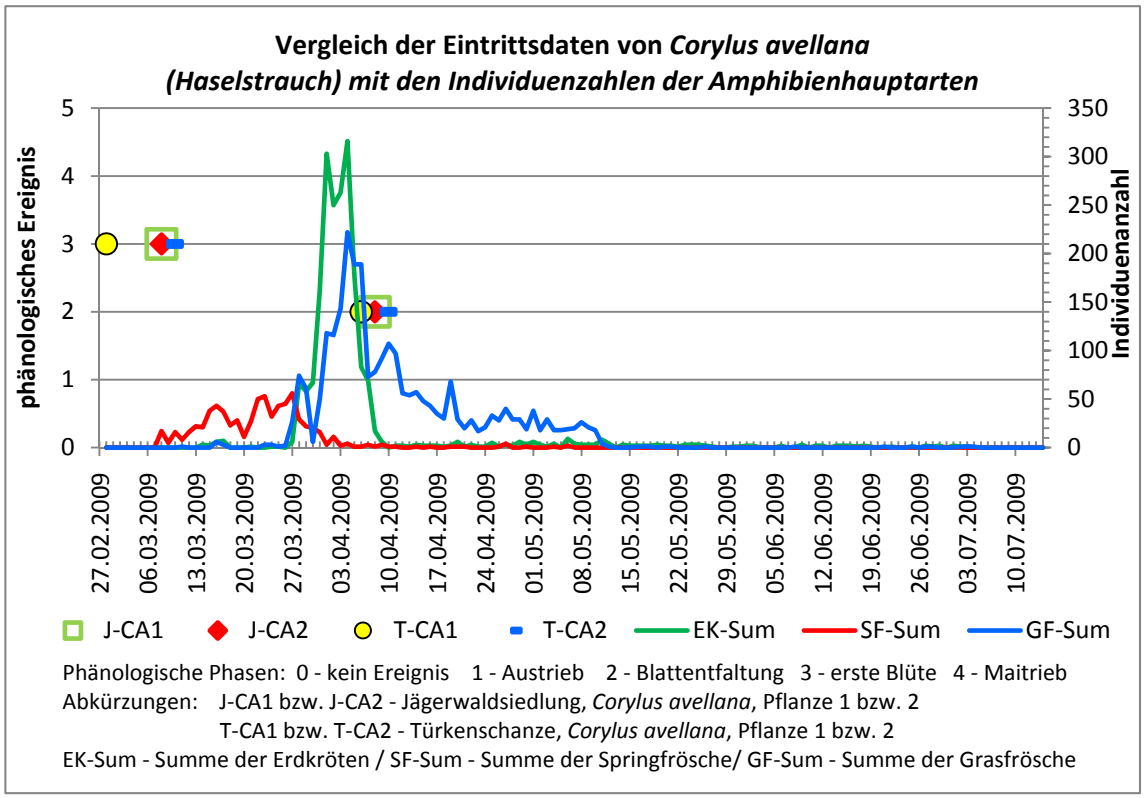

Abb. 1: Eintrittsdaten phänologischer Ereignisse von *Corylus avellana* im Vergleich mit den gezählten Individuen der drei Hauptarten Erdkröte (*B. bufo*) Springfrosch (*R. dalmatina*) und Grasfrosch (*R. temporaria*) am Laichgewässer

Tabelle 1 zeigt eine vollständige Übersicht der korrelierenden Ereignisse der pflanzenphänologischen Phasen mit den amphibischen Eintrittszeitpunkten. Hier sind sämtliche Pflanzen und Amphibienarten aufgelistet, die im Zuge des Forschungsprojektes beobachtet bzw. erhoben wurden.

Tabelle 1: Vergleich der phänologischen Eintrittsdaten von Pflanzen und Amphibien

Vergleich der phänologischen Eintrittsdaten von Pflanzen und Amphibien			
Datum	**Ereignisse Amphibien**	**Ereignisse Pflanzen JWS**	**Ereignisse Pflanzen TSP**
08.03.	SF erstes ♂ / BM erstes ♂	*Corylus avellana* erste Blüte	---
10.03.	SF erste Rufe / TM erstes ♂	---	*Leucojum vernum* & *Galanthus nivalis* erste Blüte
14.03.	EK erstes ♂ / SF erster Laich	*Leucojum vernum* & *Galanthus nivalis* erste Blüte	---
16.03.	GF erstes ♂/ BM erstes ♀	---	*Acer pseudoplatanus* Austrieb

01.04.	EK erste Rufe; meiste Paare; meiste Straßenfunde/ SF letztes Paar / GF meiste Straßenfunde	*Salix caprea* erste Blüte	---
03.04.	EK erster Laich; erste abwandernde ♀ / BM meiste Straßenfunde	*Anemone nemorosa* erste Blüte	---
04.04.	EK meiste ♂ & ♀ / GF meiste Tiere; meiste Paare; erstes abwanderndes ♀	*Larix decidua* Blattentfaltung	---
05.04.	GF meiste ♀	---	*Forsythia suspensa* erste Blüte / *Taraxacum officinale* erste Blüte
06.04.	GF meiste ♂; letztes Paar/ GBU erstes ♂	*Forsythia suspensa* erste Blüte	*Forsythia suspensa* erste Blüte / *Corylus avellana* Blattentfaltung / *Aesculus hippocastanum* Blattentfaltung
07.04.	TM erstes ♀ / BF erste Larve	*Taraxacum officinale* erste Blüte	*Fagus sylvatica* Blattentfaltung
09.04.	EK letztes Paar	*Betula pendula* erste Blüte	---
10.04.	BM meiste ♀	---	*Betula pendula* erste Blüte
15.04.	AKM erste Sichtung	*Picea abies* Maitrieb / *Tilia cordata* Blattentfaltung	*Aesculus hippocastanum* erste Blüte
16.04.	SF letztes ♀		*Acer pseudoplatanus* erste Blüte
20.04.	TM meiste Tiere	*Aesculus hippocastanum* erste Blüte	---
21.04.	TM meiste ♂	*Fagus sylvatica* Blattentfaltung	---
16.05.	FS erste Larve	---	*Sambucus nigra* erste Blüte
11.06.	AKM letzte Sichtung	---	*Tilia cordata* erste Blüte

SF – Springfrosch (*Rana dalmatina)* BM – Bergmolch (*Triturus alpestris*)
GF – Grasfrosch (*Rana temporaria*) TM – Teichmolch (*Triturus vulgaris*)
EK – Erdkröte (*Bufo bufo*) AKM – Alpenkammmolch (*Triturus carnifex*)
BF – Braunfrosch (*Rana sp.*) FS – Feuersalamander (*Salamandra salamandra*)

4. Schlussfolgerung

Die vorliegende Untersuchung zeigt eine mögliche Eignung pflanzenphänologischer Phasen als Indikator amphibischer Aktivität. Jedoch können aus einem Jahr Aufnahmetätigkeit lediglich Vermutungen und Tendenzen abgeleitet werden und es kann nicht ausgeschlossen werden, ob es sich dabei um zufällige Korrelationen handelt, oder diese auch in kommenden Jahren Bestand haben. Daher sind weitere Beobachtungen an demselben Standort und anderen Standorten notwendig um gesicherte Aussagen treffen zu können.

Danksagung

Ein besonderer Dank gilt Ao.Univ.Prof. Dipl.-Ing. Dr.nat.techn. Christiane Brandenburg, Ass.Prof. Dr.phil. Mag.rer.nat Manfred Pintar und Ao.Univ.Prof. Dr.phil. Erich Mursch-Radlgruber von der Universität für Bodenkultur Wien, welche mit sehr viel Engagement, guten Ideen die Diplomarbeiten betreut haben. Ebenfalls bedanken möchten wir uns bei Dr. ElisabethKoch (Zentralanstalt für Meteorologie und Geodynamik Wien) für Antworten auf phänologische Fragen.

Literaturverzeichnis

Blab, J., 1986: Biologie, Ökologie und Schutz von Amphibien (3. Auflage), Schriftenreihe für Landschaftspflege und Naturschutz, Heft 18, KILDA Verlag, Greven

Cabela A., Grillitsch, H.; Tiedemann, F., 2001: Atlas zur Verbreitung und Ökologie der Amphibien und Reptilien in Österreich: Auswertung der Herpetofaunistischen Datenbank der Herpetologischen Sammlung des Naturhistorischen Museums in Wien, Umweltbundesamt Wien

Hödl, W., Jehle, R., Gollmann, G., 1997: Populationsbiologie von Amphibien – Eine Langzeitstudie auf der Wiener Donauinsel, A3 Werbeservice Linz

Karsten, M., 1986: Eine Analyse der phänologischen Methode in der Stadtklimatologie am Beispiel der Kartierung Mannheims, Geografisches Institut der Universität Heidelberg, Heidelberg

Tiedemann, F. (Hrsg.), 1990: Lurche und Kriechtiere Wiens, J & V Edition Wien Verlagsges.m.b.H

ZAMG - Zentralanstalt für Meteorologie und Geodynamik Wien, 2009: http://zacost.zamg.ac.at/phaeno_portal/

Anschrift der Autoren

Bakk.techn. Kerstin Höbart
Universität für Bodenkultur Wien
Gregor Mendel Straße 33, A-1180 Wien, Österreich

Bakk.techn. Christina Czachs
Universität für Bodenkultur Wien
Gregor Mendel Straße 33, A-1180 Wien, Österreich

The Pan European Phenological Database PEP725

E. Koch, S. Adler, W. Lipa, M. Ungersböck, S. Zach-Hermann

Zentralanstalt für Meteorologie und Geodynamik, Hohe Warte 38, 1190 Vienna

Abstract

From 2004 to 2005 the COST-action 725 was running with the main objective to establish a European reference data set of phenological observations that can be used for climatological purposes, especially climate monitoring, and detection of changes. So far the common database/reference data set of COST725 comprises about 8 million data in total from 15 European countries plus the data from the International Phenological Gardens IPG. 7300 observation sites cover the timeframe from 1951 to 2000. ZAMG is hosting the database. In January 2010 PEP725 began its work as follow up project with funding from EUMETNET the network of European meteorological services and of ZAMG the Austrian national meteorological service. PEP725 not only will take over the part of maintaining, updating the database, but also to bring in phenological data from the time before 1951, developing better quality checking procedures and ensuring an open access to the database. An attractive webpage will make phenology and climate impacts on vegetation more visible in the public enabling a monitoring of vegetation development.

1. Introduction

Phenology though active in the 19th century, was for long time an abandoned field: But during the past decade phenology has rapidly become an important tool for climate change impact studies. In the 4th assessment report of IPCC (Rosenzweig et al., 2007) the results of phenological research play a major role in assessing the observed changes in natural and managed systems. The impacts of climate change on plants can be easily observed which is also one of the reasons why phenology has gained a huge public interest and phenological topics are often found in the media. But phenological data are also important to have ground truth observations for NDVI-data (Schwartz and Hanes, 2009). Both data sets together with meteorological measurements are for instance used for crop-yield modelling. Vegetation influences the albedo, the evapo/transpiration and thus the energy budget of the earth – atmosphere system. The knowledge about and the input of the status of vegetation leads also to a better performance of NWP models. The interaction between atmosphere and biosphere is a crucial area of study for increasing knowledge of critical exchanges in the planetary carbon balance. The earlier onset of spring and the emergence of invasive species in wide parts of Europe as e.g. ragweed has prolonged the pollen season, with all its negative effects on allergic persons (Vliet et al., 2002).

2. PEP 725 a project funded by EUMETNET and ZAMG

In 2004 a five year COST-action 725 started with its main objective to establish a European reference data set of phenological observations that can be used for climatological purposes, especially climate monitoring, and detection of changes. Secondary objectives were the harmonisation of techniques for the observations by developing recommendations for monitoring and collection procedures, quality control of observations and last

but not least increasing the knowledge concerning relations between climate and phenology. The COST-action 725 succeeded to collect phenological data from all over Europe, to apply a common code-system (BBCH code) to the data and to combine them in one database www.zamg.ac.at/cost725 (Koch et al., 2009). So far the common database of COST725 comprises 7687248 data in total from 15 countries plus International PG from 7285 observation sites spanning the timeframe from 1951 to 2000. ZAMG is hosting the database www.zamg.ac.at/cost725.

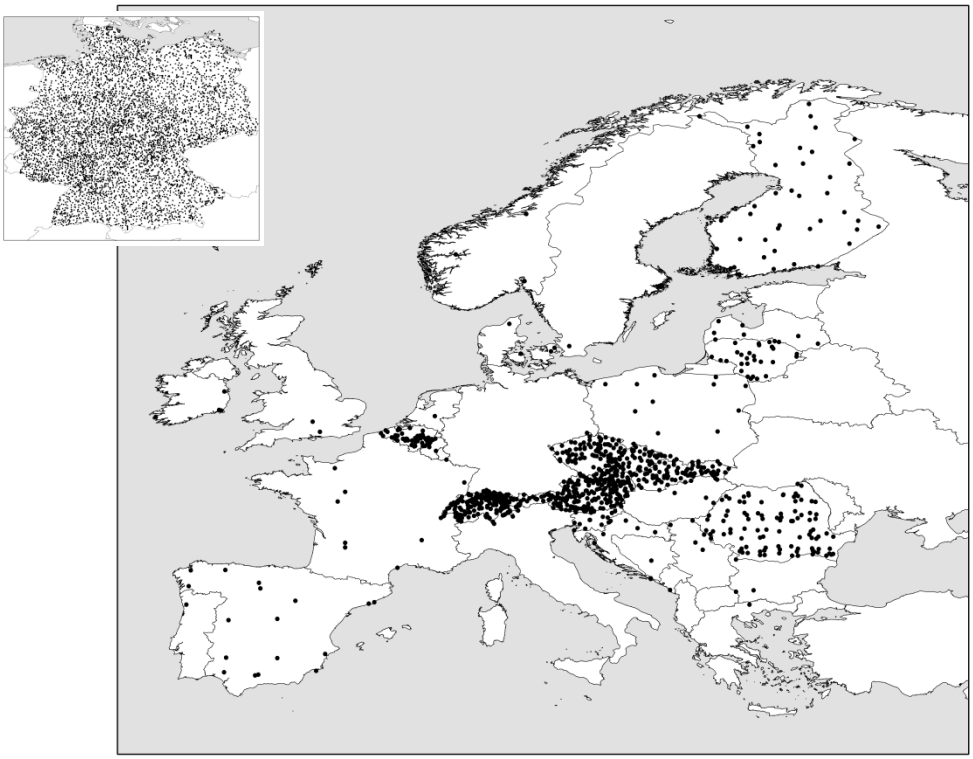

Fig. 1: map of observation-sites stored in the COST725 database

PEP 725 funded by EUMETNET and ZAMG will not only maintain and update the database, but will also bring in phenological data from the time before 1951 and develop better quality checking procedures and ensure an open access to the database. The existing webpage will get more attractive and user friendly thus making phenology and climate impacts on vegetation better and more visible in the public and enabling a monitoring of vegetation development

3. Exemplary results of climate change impacts on plant development

Many studies (for instance Chmielewski 2004, Menzel et al., 2006, Maurer et al., 2009) proved a strong dependence of phenological phases on temperature in Europe as can be seen in figure 2 where the grape harvest dates were collected from historical sources mainly from archive of the monastery Klosterneuburg.

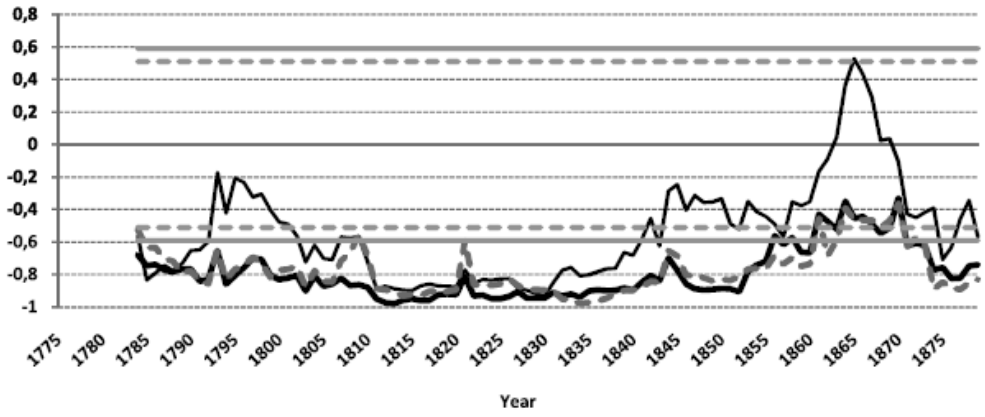

Fig. 2: Running correlation between different mean temperatures from Vienna and grape harvest dates from Klosterneuburg for the period 1785–1879 using a moving 10 year window; black thick line is running correlation with May to July mean temperature, black thin line is running correlation with mean June temperature, grey thick dashed line is running correlation with April to July mean temperature, and horizontal grey solid and horizontal grey dashed lines are 95% and 90% significance level (source Maurer et al., 2009)

The recent trend to an earlier plant development is of course also obvious by the data stored in the pan European database www.zamg.ac.at/cost725 as can be seen from figure 3.

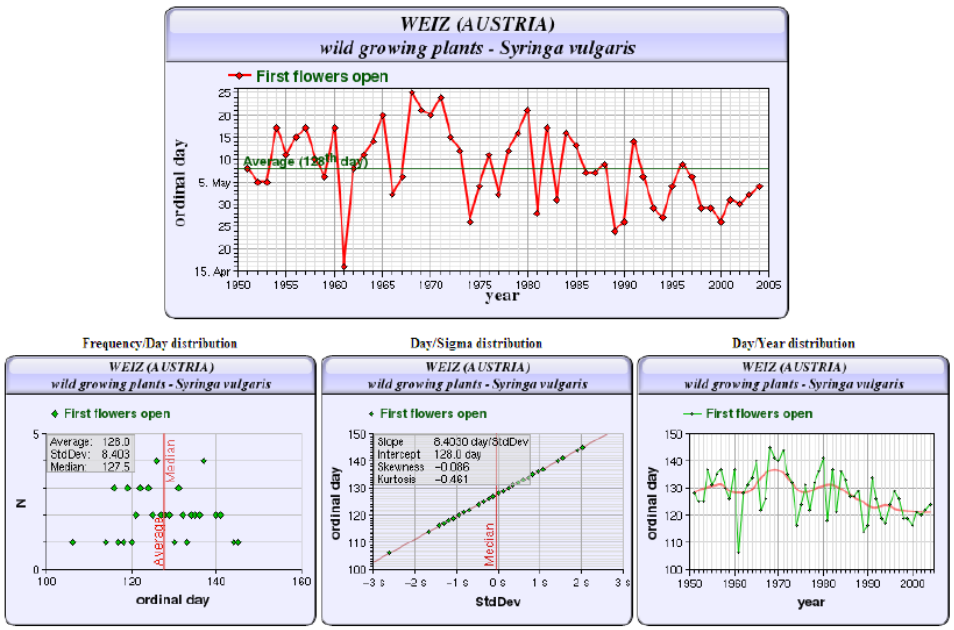

Fig. 3: time series and statistics from *Syringa vugaris*, first flowers open (BBCH 61), a screen shot from the webpage www.zamg.ac.at/cost725

Menzel et al. (2006) could show that European phenological response to climate change matches the warming pattern.

4. Conclusions

Phenological observations are an easy tool to monitor climate change impacts. There are worldwide efforts to install and / or maintain phenological networks and building up phenological databases. The USA National Phenology Network USA – NPN was launched in 2007. Europe is in the fortunate situation to have a long tradition in phenology starting in 1751 when Carl von Linné outlined in his work Philosophia Botanica methods for compiling annual plant calendars of leaf opening, flowering, fruiting and leaf fall together with climatological observations "so as to show how areas differ". Over the last decade the barriers towards phenological collaboration between European countries have been broken down. COST725 has made a substantial contribution to that collaboration and PEP725 will continue on this way.

Acknowledgement

The authors are indebted to EUMETNET the Network of European Meteorological Services and to Zentralanstalt für Meteorologie und Geodynamik (ZAMG) and the Austrian Ministerium für Wissenschaft und Forschung (bm:w_f[a]) funding the research project PEP725.

References

Chmielewski, F.-M.; A.Müller, E. Bruns, E., 2004: Climate changes and trends in phenology of fruit trees and field crops in Germany, 1961-2000, Agricultural and Forest Meteorology 121(1-2), 69-78.

Koch, E., A. Donelly, W. Lipa, A. Menzel, J. Nekovar, 2009: Final Scientific Report of COST725, COST Office, ISBN 978-92-898-0048-8, doi: 10.2831/10279.

E. Koch, E. Dittmann, W. Lipa, A. Menzel, J. Nekovar, T. H. Sparks, and A. J. H. van Vliet, 2009: COST725 – establishing a European phenological data platform for climatological applications: major results. Adv. Sci. Res., 1, 1–4, 2009 www.adv-sci-res.net/1/1/2009/.

Maurer, Ch., E. Koch, Ch. Hammerl, T. Hammerl, and E. Pokorny, 2009: Klosterneuburg Wine and Climate Change in Lower Austria (BACCHUS) temperature reconstruction for the period 16th to 18th centuries from Viennese and Klosterneuburg grape harvest dates, J. Geophys. Res., Vol. 114, D22106, doi:10.1029/2009JD011730.

Menzel, A, T. H. Sparks, N. Estrella, E. Koch, A. Aasa, R. Ahas, K. Alm-Kübler, P. Bissolli, O. Braslavská, A. Briede, F. M. Chmielewski, Z. Crepinsek, Y. Curnel, Å. Dahl, C. Defila, A. Donnelly, Y. Filella, K. Jatczak, F. Måge, A. Mestre, Ø. Nordli, J. Peñuelas, P. Pirinen, V. Remisová, H. Scheifinger, M. Striz, A. Susnik, F.-E. Wielgolaski, A. v. Vliet, S. Zach, A. Zust (2006): European phenological response to climate change matches the warming pattern, Global Change Biology 12.

Rosenzweig, C., G. Casassa, D.J. Karoly, A. Imeson, C. Liu, A. Menzel, S. Rawlins, T.L. Root, B. Seguin, P. Tryjanowski, 2007: Assessment of observed changes and responses in natural and managed systems. Climate Change 2007: Impacts, Adaptation and Vulnerability.Contribution of Working Group II to the Fourth Assessment Report of the Intergovernmental Panel on Climate Change, M.L. Parry, O.F. Canziani, J.P. Palutikof, P.J. van der Linden and C.E. Hanson, Eds., Cambridge University Press, Cambridge, UK, 79-131.

Schwartz, M. D., J. M. Hanes, 2009: Intercomparing multiple measures of the onset of spring in eastern North America. Int. J. Climatol. DOI: 10.1002/joc.2008.

Vliet A. J. H. van, A. Overeem, R. S. De Groot, A. F. G. Jacobs, F. T. M. Spieksma, 2002: The influence of temperature and climate change on the timing of pollen release in the Netherlands. Int. J. Climatol. Vol 22 Issue 14, 1757-1767.

Authors' address:

Dr. Elisabeth Koch (elisabeth.koch@zamg.ac.at)
Mag. Silke Adler (silke.adler@zamg.ac.at)
Dr. Wolfgang Lipa (wolfgang.lipa@zamg.ac.at)
Mag. Markus Ungersböck (markus.ungersboeck@zamg.ac.at)
Zentralanstalt für Meteorologie und Geodynamik
Hohe Warte 38, A-1190 Wien, Austria

Influence of climate change on summer tourism potential in the Pannonian basin

Ksenija Zaninović[1], Lidija Srnec[1], Mirta Patarčić[1], Melita Perčec Tadić[1], János Mika[2], Ákos Németh [2]

[1] Meteorological and Hydrological Service of Croatia, Zagreb
[2] Hungarian Meteorological Service, Budapest

1. Introduction

The Pannonian lowland is located in central Europe spreading among nine countries, with a great part situated in Hungary and Croatia. Besides the main agricultural activity in the region, it is also an important tourist resource. The most popular tourist destination is the "Hungarian sea" – Lake Balaton, but there are also several spas as well as a lot of cultural and historic heritage. The spa tourism has been developed but there is a lot of potential to make it even more pronounced.

Besides other factors such as geographic location, landscape, flora and fauna, climate is one of the principal resources in tourism. It can be limiting as well as the attracting factor, determining the suitability of locations for a wide range of tourist activities (Perry, 1972). On the other hand it has an important influence on tourism industry in the planning of tourism capacities and on operating costs. Thus, changes in climate could have considerable implications on tourism and its competitive relationships between destinations and therefore the profitability of tourism enterprises (Landau et al, 2009, Simpson et al, 2008).

There are many climate-related criteria people use to make decisions about tourism (de Freitas and Matzarakis, 2005). Among other important factors in determining the pleasantness of climate conditions, thermal component of the climate is especially important for summer tourism. In order to analyse possible changes of summer thermal conditions in the part of Pannonian basin, the two sets of integrations for present and future climate scenario have been performed using the regional climate model RegCM3 (Pal et al 2007). The initial and boundary conditions for regional model were provided from the global circulation model EH5OM. The climate change has been studied by an analysis of the differences between future and present bioclimate focusing on physiologically equivalent temperature (PET).

2. Data and method

Climate simulations based on the regional climate model RegCM3 were used for the tourism related climatic analyses. RegCM3 is a 3-dimensional, sigma-coordinate, primitive equation model (Giorgi et al, 1993a,b). In our study regional model was forced by coupled atmosphere-ocean general circulation model EH5OM (Roeckner et al, 2003) from Max Planck Institute in Germany. Emission scenario A2 for the time period 2041–2070 was considered and compared to the 30 years of "present" climate 1961–1990. The model resolution was 35 km, with the central point at 46°N and 7.5°E. The vertical number of levels was 23, extending from the surface to 100 hPa. For the convection parameterisation, the Grell scheme (Grell, 1993) was chosen with the Fritch-Chappell closure scheme (Fritsch and Chappell, 1980). The studied area was the part of the Pan-

nonian basin between Balaton Lake and river Sava (between 45°N and 47°N, 17°E and 19°E with altitudes mainly between 100 to 300 m). Regional model output was interpolated to the regular 0.168° grid with 182 points in the analyzed area (Fig. 1). Results are shown for summer season defined as period from June to August at 12 UTC, i.e 1 p.m. local time.

Fig. 1: The area of analysis in the Pannonian basin

The input meteorological data for the biometeorological calculation were: air temperature, wind speed, cloudiness and water vapour pressure. These data were extracted in regular grid points for the studied area and according to them further calculation has been done. Temperature at 2 m, wind components and specific humidity are the components of the direct model output in monthly surface files. The wind is calculated as sqrt(u^2+v^2), and water vapour pressure as it follows:

$$e = s * p_0 /(0.623 + 0.377 * s) \quad (1)$$

where e[hPa] is water vapour pressure, s is specific humidity and p_0[hPa] is air pressure reduced to 0 °C (hPa).

Total cloudiness is calculated by means of cloud fractional cover (cld) as a part of radiation model output. Clouds that form in individual layers are assumed to be randomly overlapped in the vertical. So the total cloudiness for the whole column at each grid point is calculated as:

$$total\_cloud(i,j) = 1-(1-cld(i,j,1))*(1-cld(i,j,2))*...*(1-cld(i,j,23)) \quad (2)$$

Total cloudiness is originally expressed in tenths and for further calculation it has to be expressed in octas.

The physiologically equivalent temperature (PET), as the physiologically significant assessment of the thermal environment based on human energy balance (Gulyás and Matzarakis, 2009, Höppe, 1999 and Matzarakis et al., 1999) was calculated for the present and future climate for 182 grid points. In order to evaluate the influence of climate change on tourism potential, the differences between thermal acceptability and heat stress between two periods are calculated. The thermal acceptability is defined as 18 °C < PET < 23 °C, strong heat stress as PET > 35 °C and extreme heat stress PET > 41 °C (Matzarakis and Mayer, 1996).

3. Results

According to the present climate (1961–1990) provided by climate model the mean summer temperature at 1 p.m. in the analyzed area is 21.7 °C, varying between 20 °C in the northwestern to 23.5 °C in the southeastern part of the area. The water vapour pressure pattern shows minimum in the south and maximum in the north. The northern part has somewhat stronger wind and more cloudiness than the southern part. As the result of such spatial distribution of the meteorological parameters important for thermal sensation, the physiological equivalent temperature pattern is consistent with temperature distribution with maximum in the southeast and minimum in the northwest. However, due to the influence of cloudiness and wind the difference between minimal PET in the north and maximal PET in the south is about 1–2 °C greater than the difference between temperatures (not presented). In the whole area PET is higher than the air temperature, more pronounced in the south than in the north.
The rate of thermal acceptability or heat stress is substantial for planning the level of activities rather than mean values. In the analyzed area the number of thermal acceptable summer afternoons (18 °C < PET < 23 °C) varies between 19 and 25 (the mean value being 22), indicating that about quarter of days is convenient for different activities even during the warmest part of the day. On the other hand, strong heat stress (PET > 35 °C) is not very frequent with maximum of 16 days in the southeast and minimum of 3 days in the northwest in the area of Lake Balaton. The extreme heat stress (PET >41 °C) appears rather rare, only once in 2 years in the northwest and 5 times per year in the southeast. Generally, the northern part is thermally more convenient than the southern, and southeastern part has the most unfavourable thermal environment.

The climate change could modify the tourism potential of the area. The differences between thermal environment in future and present climate indicate distinct changes in the region. The main objection is that the warmest southeast part, the wetland Drava-Danube estuary, will suffer the greatest warming. The mean values of PET at 12 UTC are expected to change between present and future climate for from 3.2 in the northwest to 4.1 °C in the southeast. This can be also seen from the change of thermal acceptable days (Figure 2) and especially from the increase of heat stress (Figure 3). The number of thermal acceptable afternoons will increase in the northern part of the region, suggesting even more favourable conditions in the region of Lake Balaton in the future. On the other hand the frequency of thermal acceptable afternoons will reduce in the south, mostly in the southwest (for around 7 days). Heat stress is expected to be more frequent in the whole region, with increase varying between 6 to even 13 days for strong heat stress, and 2 to 8.5 days for extreme heat stress, mostly again in the southeast.

Analyzing the influence of individual meteorological parameters on thermal environment changes, the similarity between temperature and thermal environment pattern is evident (Figure 4). Simultaneous decrease in cloudiness and wind speed in the whole area additionally contributes to the warming, with the most intensive decrease of cloudiness in the south.

The comparison with the PET at 2 p.m. calculated using the data from the meteorological stations Osijek (45°32'N, 18°44'E) (Zaninovic et al, 2008) and Siofok (46°53'N, 18°03'E) indicates the considerable underestimation of the model calculations, even bearing in mind the difference between terms of observed (2 p.m.) and calculated data (12 UTC i.e. 1. p.m.). The differences between real and modelled data are greater in

Osijek (southeast) than in Siofok (northwest). This comparison suggests that the thermal environment in the future would be even warmer than provided by climate model.

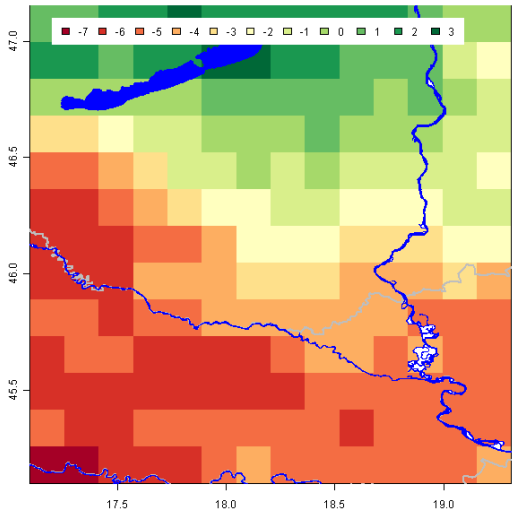

Fig. 2: Changes in thermal neutrality (18 °C < PET < 23 °C) at 12 UTC during summer, 2041/2070 – 1961/1990.

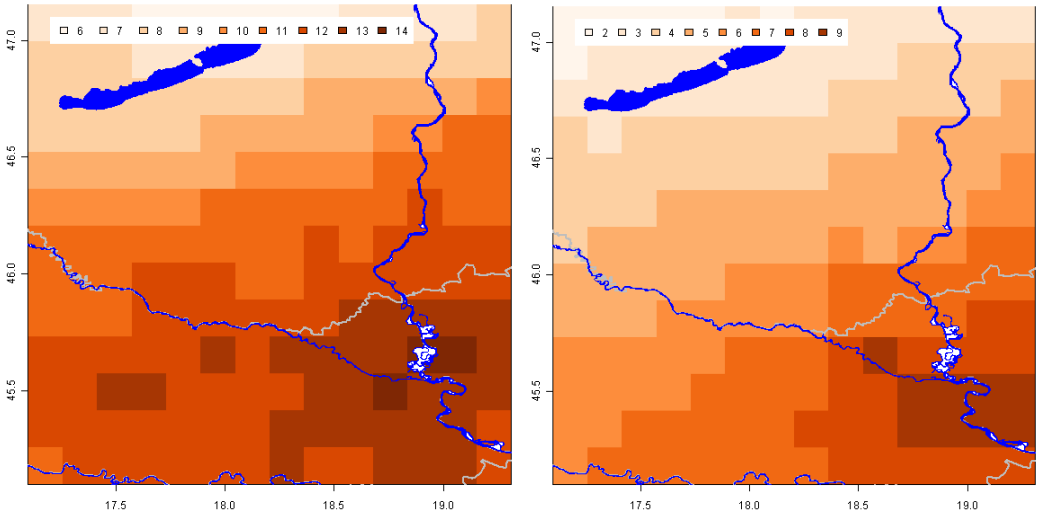

Fig. 3: Differences between number of days with discomfort: strong heat stress (PET > 35 °C, left), extreme heat stress, PET > 41 °C, right) at 12 UTC during summer, 2041/2070 – 1961/1990.

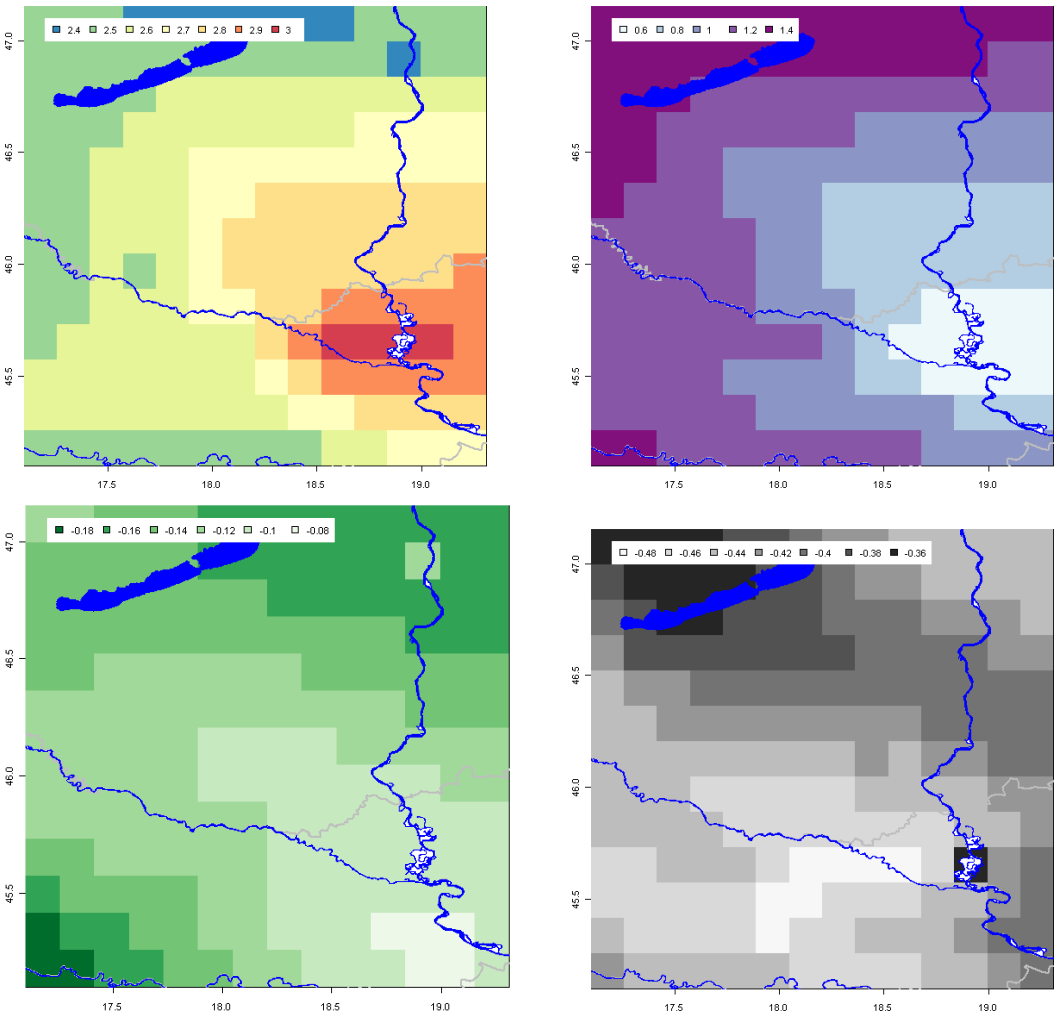

Fig. 4: Differences between mean temperatures (°C) (upper left), water vapour pressure (hPa) (upper right), wind speeds (m/s) (down left) and cloudiness (octas) (down right) at 12 UTC during summer, 2041/2070 – 1961/1990.

4. Conclusions

The analysis based on PET indicates possible changes in tourism potential of the area due to the warming. The change is not the same all over the region. The wetland part of eastern Slavonia (National park Kopački rit in Drava-Danube delta) in the southeast of the area will be mostly affected by warming. The tourist area around Lake Balaton will suffer less warming, but although it seems according to the model results that the tourism potential in the area around the Lake Balaton would be even improved, the differences between real and model data don't permit such conclusion.

It would be of interest to examine the influence on tourism potential for other seasons and for the nearer future (2011-2040). Besides, the investigation of other meteorological parameters important for tourism such as precipitation, wind, cloudiness, cold stress for winter would give more complete picture.

References:

de Freitas, C. R., Matzarakis, A., 2005: Recent Development in Tourism Climatology. Bulletin of the German Meteorological Society 1/2005:2-4.

Fritsch, J. M. and C. F. Chappel, 1980: Numerical predictions of convectively driven mesoscale pressure systems. Part I: Convective parameterization. J. Atmos. Sci. 37, 1722-1733.

Giorgi, F., M. R. Marinucci and G. T. Bates, 1993a: Development of a second-generation regional climate model (RegCM2), Part I: Boundary-layer and radiative transfer processes. Mon. Wea. Rev. 121, 2794-2813.

Giorgi, F., M. R. Marinucci, G. T. Bates and G. De Canio, 1993b: Development of a second-generation regional climate model (RegCM2), Part II: Convective processes and assimilation of lateral boundary conditions. Mon. Wea. Rev. 121, 2814-2832.

Grell, G. A., 1993: Prognostic evaluation of assumptions used by cumulus parameterizations. Mon. Wea. Rev. 121, 764-787.

Gulyás, Á., Matzarakis, A., 2009: Seasonal and spatial distribution of physiologically equivalent temperature (PET) index in Hungary. Időjárás 113, 221-231.

Höppe, P., 1999: The physiological equivalent temperature – a universal index for the biometeorological assessment of the thermal environment. Int. J. Biometeorol. 43, 71–75.

Landau, S., Legro, S., Vlasic, S., 2009: A Climate for Change, UNDP in Croatia, pp 284.

Matzarakis A, Mayer H, 1996: Another kind of environmental stress: Thermal stress. WHO Newsletter 18, 7-10.

Matzarakis, A., Mayer, H., Iziomon, M.G., 1999: Applications of a universal thermal index: physiological equivalent temperature. Int. J. Biometeorol. 43,76-84.

Pal, J. S., and Coauthors, 2007: Regional climate modeling for the developing world: The ICTP RegCM3 and RegCNET. Bull. Amer. Meteor. Soc. 88, 1395-1409.

Perry, A. H., 1972: Weather, climate and tourism. Weather 27, 199-203.

Roeckner E., and Coauthors, 2003: The atmospheric general circulation model ECHAM5. Part I: Model description. Max-Planck Institute for Meteorology Rep. 349, Hamburg, 127 pp.

Simpson, M. C, Gössling, S., Scott, D., Hall, C. M., Gladin, E., 2008: Climate Change Adaptation and Mitigation in the Tourism Sector: Frameworks, Tools and Practices. UNEP, University of Oxford, UNWTO, WMO: Paris, France, pp. 136.

Zaninović, K., Gajić-Čapka, M, Perčec Tadić, M. et al., 2008: Klimatski atlas Hrvatske / Climate atlas of Croatia 1961-1990, 1971-2000, Meteorological and Hydrological service of Croatia, Zagreb, pp. 200.

Acknowledgement

The article is prepared in the framework of bilateral Croatian-hungarian project sponsored by the Ministry of science, education and sports of the Republic of Croatia and National Office fore Research and Technology of the Republic of Hungary.

Authors' address:

Ksenija Zaninovic (ksenija.zaninovic@cirus.dhz.hr)
Meteorological and Hydrological service of Croatia
Gric 3, HR-10000 Zagreb, Croatia

Evaluation of climatic characteristics for tourism and recreation in a specific area, Tortum, in Eastern Anatolia region of Turkey

Hasan Yılmaz[1], Sevgi Yılmaz[2], Süleyman Toy[3], Nalan Demircioglu Yıldız[4]

[1] Atatürk Univ. Fac. of. Agric. Dept. of Landscape Architecture, 24240, Erzurum Turkey
[2] Atatürk Univ. Fac. of. Agric. Dept. of Landscape Architecture, 24240, Erzurum Turkey
[3] Landscape Architect and Engineer in Met Office., Erzurum Turkey
[4] Atatürk Univ. Fac. of. Agric. Dept. of Landscape Architecture, 24240, Erzurum Turkey

Abstract

Eastern Anatolia Region of Turkey is a relatively less developed area with its untouched nature. The region has considerably high alternative tourism potentials due to its distinct geological structures, vegetation and water reserves. Tourism and recreational activities have been taking place in the region more in recent years by providing new development opportunities for local people. District of Tortum, which is governed by Erzurum city, has very high alternative tourism and recreation potentials with its very famous waterfall, a naturally formed lake and unique geological features. In the study, climatic characteristics of the area were evaluated for tourism and recreation activities using one of the new tourism climatic indices, Climate-Tourism-Information-Schemes (CTIS) and it was found that the climatic characteristics of the area are very suitable for these activities in especially summer period when tourist density is more than other seasons.

1. Introduction

Increasing devastation in natural and cultural environment notwithstanding the recent improvements in science and technology has created an ill fate for man. An uncontrollable, unmanageable and unhealthy living environment has been brought about by the processes of development, industrialization and urbanisation, causing population movements and cluttering (Yilmaz et al., 2003; Yilmaz and Bulut, 1997). Consequently, recreation demands for natural areas have become larger than ever before.

North eastern part of Turkey is of a distinctive feature for alternative tourism and recreation activities because of its untouched nature and unique geography. In this region, the city of Erzurum occupies the largest surface area and is the most important city of the region. Its northern part can provide very diverse alternative tourism opportunities. Tortum district is located in the northern part of Erzurum and has very rich potentials for very different tourism and recreation types with its famous waterfall and natural lake. This are attracts vistors from both its close proximity and far regions.

Climate can affect all kind of human activities carried out on earth surface. Tourism and recreation activities are among the activity types which are affected by climatic elements the most. Today very different types of tourism climate index have been developed for the assessment of a location's climatic potentials for tourism and recreation (e.g. Mieczkowski 1985). In recent years, a tourism climate index developed by Matzarakis (2007; CTIS; Climate and Toursim Information Schemes) has been in use. This index is a very useful and easy – to – use device for the assessment of the climatic characteristics based on daily meteorological data. The aim of this study is to evaluate suit-

ability of climatic characteristics of Tortum district for tourism and recreation activities using CTIS index.

2. Material and method

The district of Tortum is located in the north-eastern part of Turkey at an elevation of 1572 m and 40.17 N and 41.33 E (Fig.1). It has a very famous waterfall in Turkey and a natural lake which can attract very serious number of tourists every year (Fig. 2). Around the lake and waterfall, recreational activities such as picnicking, fishing and nature hiking can be performed by local people. As alternative recreational activities, mountain climbing, camping, chasing, parasailing, cave visiting, bird watching and botanical education can also be done. The area is very suitable for the recreational activities based on water. The area which can provide visual opportunities based on water is also suitable for camping activity. In addition to visual properties these areas can provide various opportunities based on water such as fishing, sailing, waterskiing and swimming for camping people in the area. Because people who prefer camping as a recreational activity tend to be interested in all the values of the area they visit, historical and archaeological sites near the camping areas pull the attractions of such people.

In the study, CTIS (Climate and Tourism Information Schemes) method of Matzarakis (2007) was used to evaluate the climate of the district. However, not all of the results obtained from the calculations required for the index are given in the study except for those related to PET values (for details see Matzarakis 2007). Calculations were performed using a meteorological dataset over a 35 – year period from 1975 to 2009.

Fig.1: Location of Tortum in Erzurum and Turkey

3. Results

Distribution of PET (Physiological Equivalent Temperature) index values for Tortum is given in Fig. 3. According to the figure "cold" and "very cold" ranges are dominant in a period from November to the end of March. The beginning of the period when "comfortable" range is prevalent is April. However, this period ranges mainly from May to the end of September. In summer, excessive heat stress caused by "hot" and "very hot" ranges has very little percentage values. Calculated maximum, minimum and mean PET values are 47.2, -17.8 and 13.6ºC, respectively.

Fig. 2: Tortum Lake visual landscape

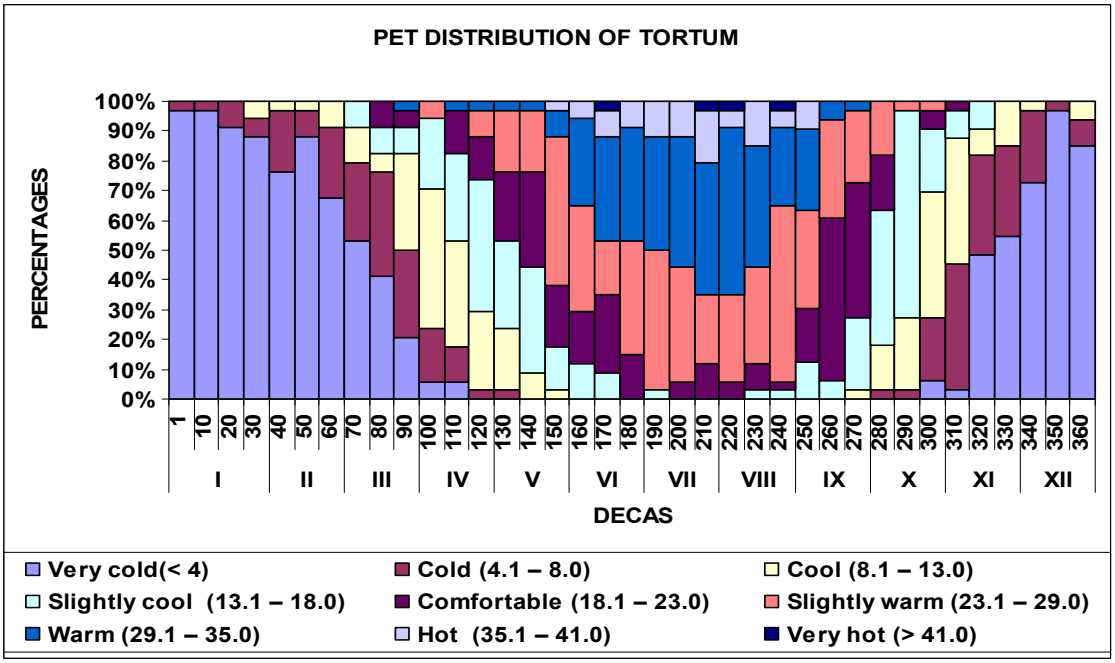

Fig. 3: Distribution of PET values for Tortum

4. Conclusions

It is widely known that tourism and recreation activities are important elements to support the development of an area. Weather and climate are important factors for the recreation and tourism activities carried out in an area. Assessment of these factors for a specific area can provide benefits for this area because people organise their activities considering mostly climate and weather information. Therefore, such studies as the present one can introduce the areas having potentials of being tourist destinations by showing the favourable features of these areas.

As the consequence of the present study it can be stated that the district shows very favourable climatic and bioclimatic features especially in summer months when recreational and tourism activities are expected to take place. This favourable situation can be combined with the rich reserves of the area.

Although the study area is an important attraction centre for native and foreign people with its natural, historical and cultural wealth, it has not yet been introduced well. The area should be introduced using various ways. Variety of the tourism and recreational activities in the area such as rural tourism activities should be increased. Quality and quantity of the studies emphasizing on all of the characteristics of the area should also be increased.

References

Matzarakis A., 2007: Assessment method for climate and tourism based on daily data. In: A. Matzarakis, C. R. de Freitas, D. Scott (Eds.), Developments in Tourism Climatology, 52-58.

Mieczkowski Z., 1985: The tourism climatic index: a method of evaluating world climates for tourism. Can Geogr, 29(3):220–233.

Yilmaz, H., Yilmaz, S., Kelkit, A., & Bulut, Y. (1997). Problems caused by land-misuse in cities and Proposals for their solutions. Settlement and Environmental Problems Çanakkale City, 9-13 September, DEU Engineering Faculty, Proceedings Book İzmir, Turkey.

Yilmaz, H., Yilmaz, S., & Yildiz, N.D.,2003:Determination of recreational demand and trend of city people in Kars. Atatürk Univ. Journal of Agricultural Faculty. 34 (4),353-360.

Authors' address:

Prof. Dr. Hasan Yılmaz (hyilmaz@atauni.edu.tr)
Ataturk Univ., Fac. of Agric., Dept. of Landscape Architecture, 25240, Erzurum/ Turkey

Associate Prof. Dr. Sevgi Yılmaz (syilmaz_68@hotmail.com; sevgiy@atauni.edu.tr)
Ataturk Univ., Fac. of Agric., Dept. of Landscape Architecture, 25240, Erzurum/ Turkey

PhD candidate Süleyman TOY (s_toy2@hotmail.com) Landscape Architect & Engineer at Meteorology Office, Erzurum/Turkey

Assist. Prof. Nalan Demircioglu Yildiz (nalandemirci25@hotmail.com)
Ataturk Univ., Fac. of Agric., Dept. of Landscape Architecture, 25240, Erzurum/ Turkey

Anticipating the Impacts of Climate Change on Tourism in Lisbon Metropolitan Area – Assessing Tourist Perceptions

Raquel Machete, Carlos Ferreira, Eduardo Brito-Henriques, Henrique Andrade, José Couto

Centre of Geographical Studies, Institute of Geography and Spatial Planning, Univ. of Lisbon

Abstract

According to the *Intergovernmental Panel on Climate Change* latest findings, average air temperature in southern Europe can raise from 2ºC to 6ºC until 2100. Longer, warmer summers and smoother winters can be expected, along with changes in the precipitation regime and quantities. In tourism, as well as in other climate sensitive economic sectors – such as agriculture - considerable impacts are likely to happen. Changes in what concerns tourism flows and seasonality can be anticipated, as well as in the activities in which tourists engage. Impacts of climate change in tourism can be either positive or negative, although most literature on the subject has emphasized costs more than benefits. The purpose of this paper is to reflect upon these matters that are currently in an early stage of debate. Taking into account the results of interviews to tourists carried out in the Lisbon Metropolitan Area, as a part of the international project "Urban Tourism and Climate Change", we try to assess to what extent climate changes will impact on tourism trends and tourist perceptions, behaviour and preferences, and also how these can influence the attractiveness of urban destinations.

1. Introduction

For many regions of the world tourism has become a noteworthy, if not the most important, source of income (De Freitas, 2003), acting as a trigger for a number of businesses. Despite often being pointed out as one of the largest and fastest growing industries in the world (Amelung et al, 2007, De Freitas 2003, Lise and Tol, 2002; Wall, 2007), tourism is extremely vulnerable to several aspects, such as economy, politics, the occurrence of crisis and threats or demographic changes. Tourism trends are, therefore, subject to a great deal of variability.

Climate is among the features that we must take into account when considering international tourism flows. Being a resource in itself and lending many destinations their attractiveness, climate also influences environmental assets that are vital to tourism and recreation and the operating costs related to the tourism activity (De Freitas, Matzarakis, Scott 2006). Hence, bearing in mind both the weight of the tourism industry for global economy and the importance of climate for tourism, it is imperative that we try to assess the impacts that may arise from climate change.

According to the recent findings of the *Intergovernmental Panel on Climate Change* (Wilbanks *et al*, 2007), there is evidence that climate has changed when compared to the pre-industrial era and is expected to continue changing. It is anticipated that, until 2100, average temperatures can increase 2º to 6º C in southern Europe. Likewise, longer, warmer summers and smoother winters can be expected. Considering the *Scenarios, Impacts and Adaptation Measures* (SIAM) project's forecast for Portugal (Miranda *et*

al, 2006), a 3º C (in coastal areas) to 7º C (in inner areas) increase in average temperature until 2100 can be estimated. Heath waves are likely to be longer and occur more often. With a greater deal of uncertainty, inland annual precipitation can undergo a severe reduction of 20 to 40 per cent, whereas heavy rainfall events are like to become more recurrent. Such changes will also have indirect environmental impacts, such as biodiversity loss and ecosystems dilapidation, as well as effects in public health (Casimiro *et al*, 2006). Another expected outcome of climate change is an average sea level raise which can, among other consequences, cause the erosion of the coastal line (Andrade et al, 2006).

Therefore, even though the effects of climate change remain, to a considerable extent, highly uncertain, especially at the regional scale (Alcoforado and Andrade, 2008), there is a widespread agreement on the need to take action to minimize negative impacts and take advantage of the opportunities that may take place. Climate change will bring about structural transformations for the tourism industry calling for adaptation measures. Strategies can encompass a wide range of initiatives, according to the vulnerabilities of a given region. Infrastructure adjustment, diversification of the tourism commodities available, changes in schedules or activity agenda are some of the measures that can be included in adaptation plans.

On the other hand, the transformations in land use, the emission of greenhouse gas (GHG), and the use of energy and water resources entailed by tourism are also aggravating climate change. Mitigation measures to reduce tourism's environmental impact are, thus, just as crucial as adaptation strategies.

2. Objectives, study case and methodology

Most literature on the impacts of climate change for tourism has emphasized its consequences for seaside and mountain tourism. On the one hand, these tourism destinations are climate dependent and, at the same time, they are regions that display greater vulnerability to climate change impacts. However, the effects of climate change for other tourism destinations, namely urban tourism, have not been thoroughly assessed, even tough it is highly unlikely these will be similar.

The most widespread views on this matter estimate major changes in tourism trends. Under the expected future climate scenario, tourism flows would tend to reorient towards higher latitudes, thus leading to the decline of many traditional international tourism destination (Hamilton *et al*, 2003). Usually thought of only as a seaside and beach destination, the Mediterranean has been pointed out as one of the potentially top losing regions.

With the current study on *Tourism and Climate Change*, framed under the Urban-Net project, we intend to question to what extent these scenarios are adequate and can be applied to tourism in urban areas. In order to do so, we try to assess tourists' environmental awareness and their perceptions on the attractiveness of Lisbon under future climate scenarios. The research, still in progress, is being developed in the Lisbon Metropolitan Area, the second most important tourism region in Portugal, after the Algarve (having registered 21,8% of the country's overnights in 2007). From the 1990s onwards the tourist demand has grown fast, boosted by a number of events to promote Lisbon's international image (Brito Henriques, 2003)

3. Results

The following results draw from 218 interviews to tourists (randomly sampled), conducted in the Lisbon Metropolitan Area in the autumn of 2009. In what concerns the sample's age structure, more than half of the interviewed are under 35 years old (55%), whereas 29% is between 35 and 55 years old; only 15% is over 55 years old. There is a majority of tourists recording a high education level (78% hold, at least, a bachelor degree). The data highlight the importance of the Spanish market in the city's tourism international demand (1/5), followed by other noteworthy origin markets: Germany (11%); France (11%); United Kingdom (9%). It is also worth pointing that 43% of foreign tourists represent other nationalities (26 different countries), which demonstrates a heterogeneous tourist demand in the region.

The majority of the interviewed is alert to climate change. When assessing the concern about climate change risks, over half the respondents (59 %) expressed preoccupation on the matter, whereas 19% demonstrated to be moderately concerned; for 22% of the enquired, however, risks arising from climate change do not constitute a mater of worry.

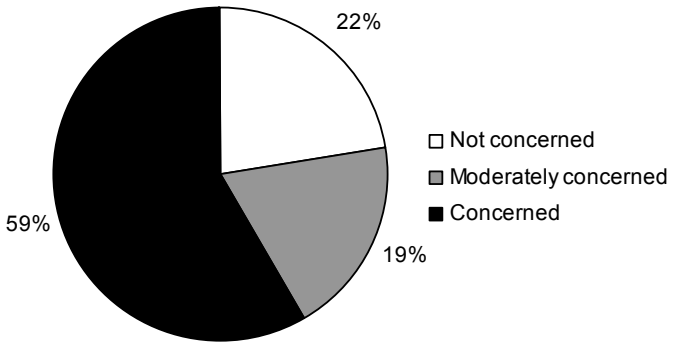

Fig. 1: Concern with climate change risks

When crossing the replies with the interviewees' nationalities (using the Chi-Square test) we can observe that there is a significant statistical relation ($p < 0.01$) between these variables. Tourists from United Kingdom and Germany appear to be more worried than tourists arriving from France, Spain and domestic tourists.
Establishing a comparison between the concern and the respondents' age, we can see that young and middle aged people reveal to be more apprehensive about climate change risks than people that are over 55 years old. This may be explained by the evolution of environmental education and raise of awareness to the subject, recent trends in societies. Furthermore, it can also express elder's lower levels of concern for the future.

During the interview, tourists were confronted with two hypothetical climate change scenarios for the region in 2050, based on the projections presented in Miranda *et al* (2006): a moderate and an extreme future scenario. According to the first scenario, a 2ºC raise in average temperatures can be expected, as well as a 150 mm decrease in average annual precipitation and a more frequent occurrence of heat waves. In an extreme future scenario, a 5ºC increase in average temperatures is estimated; heat waves are

likely to take place more often and for longer time periods, while annual precipitation is expected to severely decrease (300 mm). A 7 point Lickert scale was used in order to assess the tourists' perception on the region's attractiveness, facing these two scenarios.

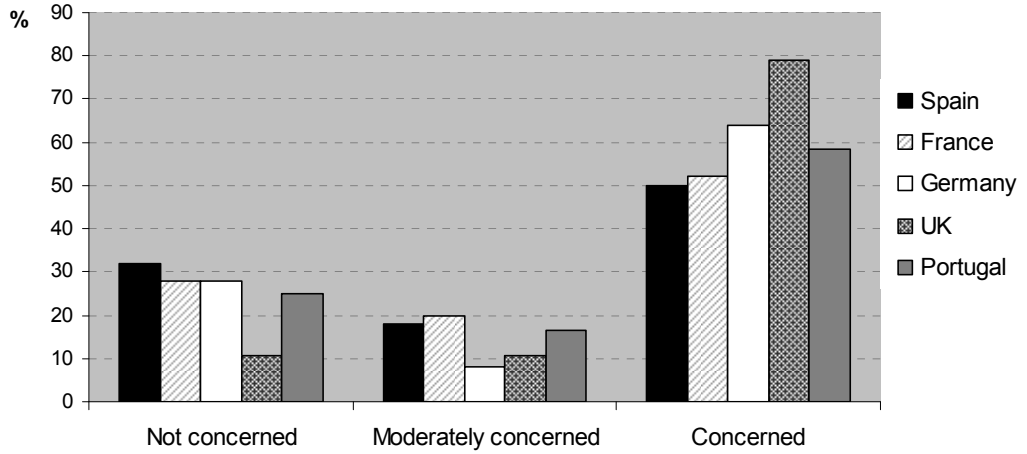

Fig.2: Concern with climate change risks in relation to the interviewees' nationality

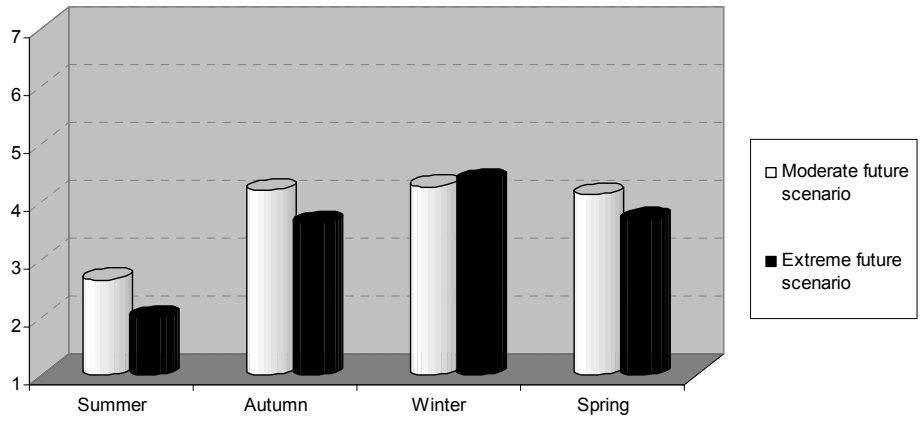

Fig. 3: Tourists opinion on the regions' attractiveness facing two distinct future climate scenarios for 2050 (average values in a 7 point Lickert scale, 1 expressing disagreement and 7 expressing total agreement)

In general, according to the tourists' opinion, summer's attractiveness will suffer harshly, especially before an extreme future scenario. The data reveals that intermediate season's pleasantness will undergo a slight decrease in the second scenario, remaining, nevertheless, positive. In face of the expected climate assessment, the winter is seen as the most agreeable season for visiting, particularly under an extreme future scenario.

On the other hand, recreation and tourism activities also demand certain specific climate conditions. Considering possible impacts on tourist practices, the interviewed were asked whether climate changes would influence the activities in which they engage. Over half the respondents answered that, facing climate change, they would prefer indoor activities in the summer, in order to escape excessive heat whereas, in the winter, the climate would largely encourage engaging in outdoor activities.

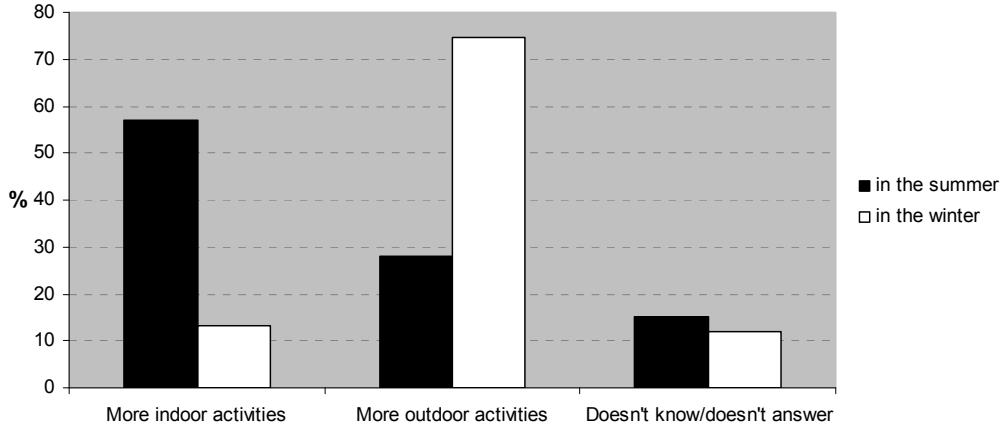

Fig. 4: Opinion on the effects of climate change on tourist preference for indoor or outdoor activities

4. Conclusions

The results of the research, although preliminary, suggest that tourists are aware of climate change, although the extent of concern with the risks that it may entail widely varies, namely according to the respondents age and nationality.

Considering tourist perceptions on the attractiveness of the region before two future climate scenarios we can see that the winter is perceived as the most pleasant season for visiting. Moreover, looking at recent tourism trends, city and short breaks or golf tourism are increasingly favouring shoulder months and winter. Therefore, milder autumns and winters can be quite positive for the attractiveness of a given region and lead us to anticipate possible seasonal shifts in the tourist demand patterns.

The variety of practices and activities in which tourists can engage in urban destinations, on the other hand, allow for adjustments and do not necessarily entail a decline of a given region.

Acknowledgement
This study was developed in the framework of the research project "Climate Change and Urban Tourism" (URBAN/AUR/0003/2008), financed by FCT and framed under the Urban-net program, in cooperation with the University of Ankara and the University of Gothenburg.

References

Alcoforado, M.J., Andrade, H. 2008, «Global Warming and the Urban Heat Island», Urban Ecology, An International Perspective on the Interaction Between Humans and Nature, ed J. M. Marzluff, E. Sulenberger, W. Endlicher, M. Alberti, G. Bradley, C. Ryan, U. Simon and C. ZumBrunnen, Springer US, pp. 249-262.

Amelung, B., Blazejczyk, K., Matzarakis, A. 2007: Climate Change and Tourism: Assessment and Coping Strategies, . Maastricht, Warsaw, Freiburg.

Andrade, C., Pires, H. O., Silva, P., Taborda, R., Freitas, M. C., 2006, «Zonas Costeiras», Alterações climáticas em Portugal. Cenários, Impactes e Medidas de Adaptação, Projecto SIAM II, ed. F. D. Santos, P. Miranda, Gradiva, Lisboa, pp. 169-208.

Brito-Henriques, E., 2003, «Distracção, fruição e evasão: as funções cultural e recreativa na AML.» ed. J. A. Tenedório, Atlas da Área Metropolitana de Lisboa. Junta da Área Metropolitana de Lisboa, Lisboa: 189-208.

Casimiro, E. Calheiros, J., Santos, F. D., Kovats, S., 2006, National Assessment of Human Health Effects of Climate Change in Portugal: Approach and Key Findings. Environmental health perspectives, 114 (12): 1950-1956.

Freitas, C.R. 2003, «Tourism Climatology: Evaluating Environmental Information for Decision Making and Business Planning in the Recreation and Tourism Sector», International Journal of Biometeorology, vo.48, pp. 45-54.

Hall, C. M., Higham, J. 2005, Tourism, Recreation and Climate Change, ed. C.M. Hall, J. Higham, Channel View Publications, Clevedon,

Hamilton, J. M, Maddison, D. J., Tol, R. S .J., 2003 Climate Change and international Tourism: A simulation Study, Research Unit Sustainability and Global Change, University of Hamburg.

Instituto Nacional de Estatística, I.P., 2008, Anuário Estatístico da Região Lisboa 2007, Lisboa.

Instituto Nacional de Estatística, I.P., 2009, Estatísticas do Turismo 2008, Lisboa.

Lise, W, Tol, R.S.J. 2002, «Impact of Climate on Tourism Demand», Climatic Change, vo.55, pp. 429-449.

Miranda, P.; Valente, A.; Tomé, A. R.; Trigo, R.; Coelho, F.;Aguiar, A.; Azevedo , F., 2006, «O clima em Portugal nos Séculos XX e XXI», Alterações climáticas em Portugal. Cenários, Impactes e Medidas de Adaptação, Projecto SIAM II, ed. F. D. Santos, P. Miranda, Gradiva, Lisboa, pp 45-113.

Perry, A, «The Mediterranean: How Can the World's Most Popular and Successful Tourist Destination Adapt to a Changing Climate?» Tourism, Recreation and Climate Change, ed. C.M. Hall, J. Higham, Channel View Publications, Clevedon, pp. 86-96.

Scott, D. et al, 2007, «Climate Change and Tourism: Responding to Global Challenges», Second International Conference on Climate Change and Tourism, Davos.

Wilbanks, T.J., P.Romero Lankao, M.Bao, F. Berkhoust, S. Cairncross, J.-P- Ceron, M. Kapshe, R. Muir-Wood and R. Zapata-Marti, 2007: «Industry, settlement and society», Climate Change 2007: Impacts, Adaptation and Vulnerability. Contribution of Working Group II to the Fourth Assessment report of the Intergovernmental Panel on Climate Change, M.L. Parry, O.F. Canziani, J.P. Palutikof, P.J.van der Linden and C.E Hanson, ed., Cambridge University Press, Cambridge, UK, pp. 357-390.

Authors' address:

Centro de Estudos Geográficos da Universidade de Lisboa, Edifício da Faculdade de Letras, Alameda da Universidade, 1600-214 Lisboa, Portugal, Tel: + 351 217940218
raquelmachete@gmail.com carlosferreira@campus.ul.pt eduardo@campus.ul.pt henr.andr@gmail.com coutojos@gmail.com

Summer sea breeze influence on human comfort in Funchal (Madeira Island) - Application to urban climate and tourism planning

A. Lopes[1], S. Lopes[1], A. Matzarakis[2], M.J Alcoforado[1]

[1] Centre for Geographical Studies, University of Lisbon, Portugal
[2] Meteorological Institute, Albert-Ludwigs-University of Freiburg, Germany

Abstract

The influence of sea breeze on human comfort in Funchal (Madeira Island) is presented in this study. Two groups of days (with sea breezes and hot days) from June to September 2006 were analysed. The Physiologically Equivalent Temperature (PET) was used to evaluate thermal comfort. It was concluded that most of the sites in the city are slightly comfortable during breeze days. When hot days occurs only shore line and the higher green places can be comfortable. It is advisable that during hot periods more vulnerable tourists visit higher altitude places, gardens and acclimatized buildings in order to prevent thermal stress situations. Urban planners should not promote dense construction near the shoreline that prevents the renovation of the air inside the city.

1. Introduction

Thermal comfort is the psychological state of mind that expresses satisfaction of people with the thermal surroundings and is usually referred to in terms of whether someone is feeling too hot or too cold (Mayer 2008). Human thermal complex is therefore balanced by thermal surroundings and metabolic processes.

Madeira (32°38' N and 16°55' W) is a mountainous Atlantic island (Pico do Areeiro: 1816 m and Pico Ruivo: 1862 m), 660 km away from the North Africa coast and 980 km from Lisbon. A great part of its population (245 000 inhabitants in 2001 census) is concentrated in the city of Funchal (41%), located in the southern slope (fig.1).

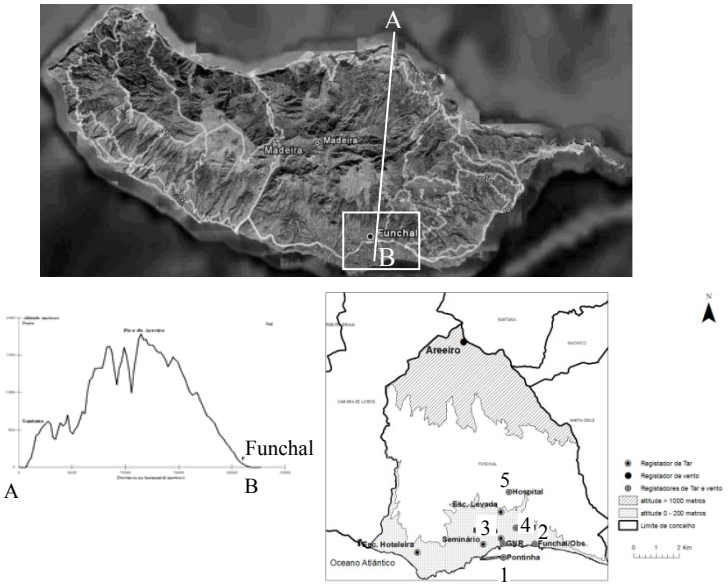

Fig. 1: Madeira Island and Funchal region. Meteorological observation sites: 1-Pontinha; 2-Funchal/Obs.; 3-Police station; 4-Firemen station; 5-Hospital. Sources: Image©2010 SRES DRIGOT; ©2010 Tele Atlas; Data SIO, NOAA, U.S. Navy NGA, GEBCO; ©2010Google and Lopes (2007)

The location in the Atlantic, the mountains, the *laurissilva* forest, and the compact city of Funchal originates a great variety of local climates.
The local economy is centred in the tourism activity of the two islands (Madeira and Porto Santo). According to the Statistics Bureau of Madeira the archipelago receives more than one million tourists per year (that corresponds to a revenue of 297 Million Euro). Recently the region was distinguished as an excellent travel destination by the CED (World Centre of Excellence for Destinations). Despite its importance, little attention is given to one of the attractiveness potential factors of the islands: its climate. For example, the most important climate information in the official site of Madeira Tourism is seasonal air and sea temperatures and only a "climate chart" (with monthly averages temperatures, total sunshine hours and precipitation) was found. This information is insufficient because present market rules impose accurate reporting to the consumers. In a previous study, Alcoforado et al. (1999) concluded that the climate information that was given to the tourists was fuzzy, incomplete or inaccurate, although climate is referred to by operators as an attraction factor for tourism. Climate information is often directed to specific high latitudes groups from North America or Europe, associating paradise tropical landscapes and climate/weather. Based on a methodology of weather types (with thresholds based on the sunshine hours, rainfall, maximum air temperature, vapour pressure and wind speed, measured at noon), the authors concluded that weather types where favourable for tourism and outdoor leisure activities even in wintertime where 50% of the days of December and January were considered "favourable for tourism and outdoor leisure activities" (Andrade et al, 2007).

2. Sea breeze in Funchal

Sea breezes are an in important wind system to ameliorate urban environment and thermal comfort conditions. In Lisbon it was found that even if the breezes do not travel very far inland, they play an important role in cooling the urban air near the river bank, where air temperature may be up to 4◦C lower than in the city centre (Alcoforado et al., 2009). In Funchal several types of sea breezes, defined by their characteristics (predominant wind direction and speed, duration, existing of veering dynamics or intermittence) were identified by Lopes (2007). During the period studied (May to September 2006), sea breezes occurred in 84% of the days, showing the persistence and the importance of this local wind system in the southern part of Madeira. The principal characteristics of the breezes are shown in table 1. They usually start in the morning (after 9:30 am) and end at night (after 10:00 pm), with an average total duration of about 11 hours and a mean velocity of 3 m/s.

Table 1: Characteristics of the sea breeze in Funchal (Pontinha), from May to September 2006. Source: Lopes, 2007

Type	Dominant direction	Beginning	End	Duration in hours (Avg.)	Mean wind speed (m/s)
		Median			
Regular	SW	9:20	22:40	10:35	4.0
	SW interrupted	9:25	22:40	10:35	3.2
	S and SE	10:00	21:25	12:20	1.9
Irregular	Other with veering	9:30	22:20	11:10	3.0
General Characteristics		≈9:30	≈22:20	≈11:00	2.9

On the top of the mountain (Pico do Arieiro) the wind blows prevailingly from the NE with a mean speed of about 6.7 m/s. The central mountain of Madeira acts as a barrier to the synoptic wind and on the southern slope the wind is highly modified by the relief. Therefore, due to its persistence, sea breeze is an important factor to ameliorate the human comfort in Funchal.

3. Methods and data

In the present research two groups of days from June to September 2006 were analysed: the first group corresponds to days where sea breeze occurred (total of 10 days from June to August); in the second group the temperatures were much higher than the averages for the period (3 to 6 September) and sea breezes hardly ever occur. For both groups wind speed and direction, air temperature, relative humidity and global radiation at 12:00 h and 18:00 local time were observed. Rayman software was used to calculate among other parameters the Physiologic Equivalent Temperature (PET) (Matzarakis et al., 2007). PET is defined as the air temperature at which, in a typical indoor setting (without wind and solar radiation), the heat budget of the human body is balanced with the same core and skin temperature as under the complex outdoor conditions to be assessed (Höppe, 1999). The observation network (table 2) is operated by the LREC (Regional Engineering Laboratory) and the Portuguese Institute of Meteorology (IM).

Table 2: Urban characteristics of the observations sites (see locations in fig.1)

Site	Altitude (m)	Urban/topographic characteristics
Pontinha	5	Sea shore (marina)
Police station (GNR)	10	Urban near the shore line
Firemen brigade station (BVM)	50.	Urban (bottom of valley)
Funchal/Observatory (IM).	58	Suburban medium density.
Hospital	380	High city; suburban surrounded by vegetation.

The characteristics of the groups were chosen to give theoretical differences between places and to analyse the importance of the wind breeze in human comfort.

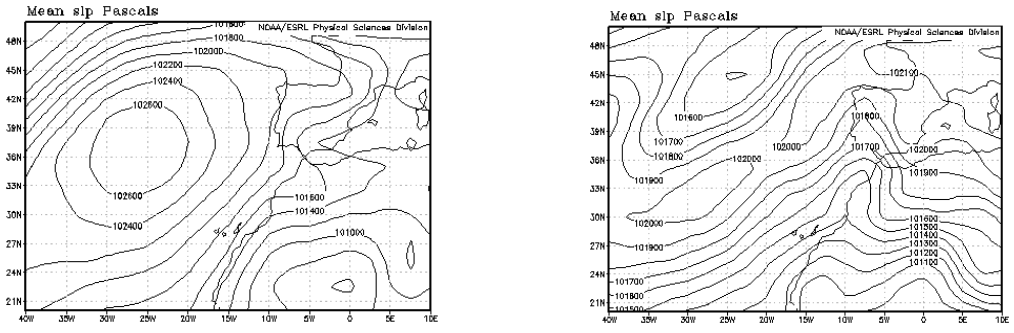

a b

Fig. 2: NCEP/NCAR reanalysis of the 1st of August (a), representing breeze days and 3rd of September 2006 (b), showing the "African" eastern flux

During the period from the 3rd to 6th September 2006 the eastern flux from North Africa was regular and the wind blew with an average speed of 2.5 to 3 m/s (respectively at 12:00h and 18:00 h). This wind was replaced at the end of the afternoon by a land breeze, maintaining high air temperatures during the night (mean temperatures between 26ºC at 12:00h and 27ºC at 18:00h). Relative humidity was very high, with values about 90% near the shore and above 50% at the other observation points. Although the concept of heat wave can be discussed, according to WMO (WCDMP.No.47, WMO.TD No. 1071*)*, a heat wave occurs when a period of six consecutive days have temperatures 5ºC superior to average in the reference normal. The average temperature in September in Funchal is 23ºC. Within the hot period presented in this study all the observation sites (except near the shore) registered temperatures around 30ºC. When the sea breeze occurs, the eastern flank of the Azores anticyclone rules this part of the Atlantic. The northeast wind is dominant, but in the Funchal region it can be replaced by a breeze from the south and south west directions.

4. Results and discussion

As can bee seen in fig. 3 the hot days that occurred with the eastern flux from Africa are clearly uncomfortable especially at noon inside the city of Funchal. The better situation is near the shore line (Pontinha) were the wind speed is blowing more intensively (2.5 to 3 m/s) than the inner city (1.3 to 1.7 m/s). In the afternoon of the period from 2 to 6 September (hot days) a reduction of the uncomfortable situations (from hot to warm) can be explained by the reduction of global radiation (870 w/m^2 at noon to 240 w/m^2 at 18:00 pm) and a consequent decrease of 17ºC of the Mean Radiant Temperature $T_{mrt.}$

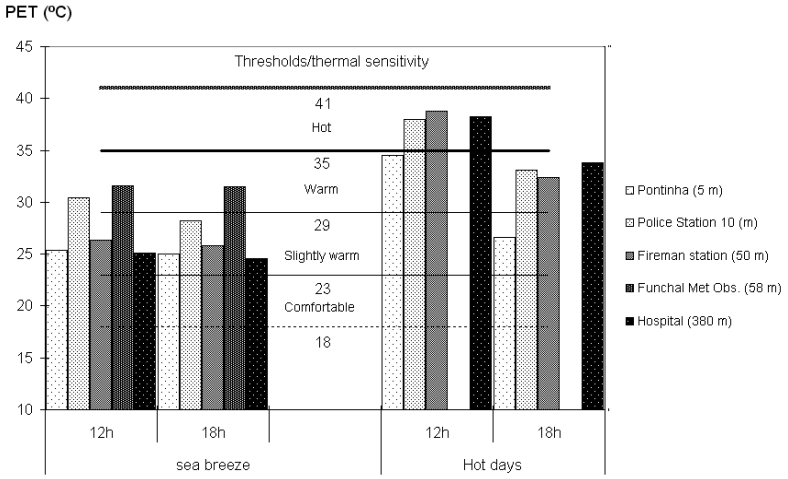

Fig. 3: Estimated PET for the two groups of days. Thermal sensitivity "Slightly warm" class corresponds to a grade of physiological stress of "Slight heat stress"; "Warm" to "Moderate heat stress"; and "Hot" to "Strong heat stress" (according to Matzarakis, 2006)

In both cases near the shore line (Pontinha) is always comfortable, more than the other places. During the breeze days, individuals can have better levels of thermal comfort only in the suburban elevated places of Funchal (such as near the Hospital, located at 380m, and surrounded by green spaces). Even near the ocean, but surrounded by dense construction (Police Station site), the environment may be warmer and stressful.

The hourly data presented in fig. 4 (PET, wind speed and south sea breeze direction and air temperatures) during the hot period reveal the role of the urban structure in the impoverishment of human comfort condition and the importance of sea breeze in the amelioration near the coast line. The better comfort conditions of higher places in the Funchal suburban green areas (near the Hospital observation site) are obvious; there PET values are in average 7ºC lower than inside the urban compact structure (Firemen and Police Station). Due to the proximity of the ocean the shore line is another comfortable location during hot periods, especially when south breeze attains inland. However this system does not produce effects inside the urban dense areas. This can be seen in the differences between the Firemen and Police Station observation sites and Pontinha (the last 4 to 5ºC lower in average) with a maximum difference of 16 to 19ºC during the day.

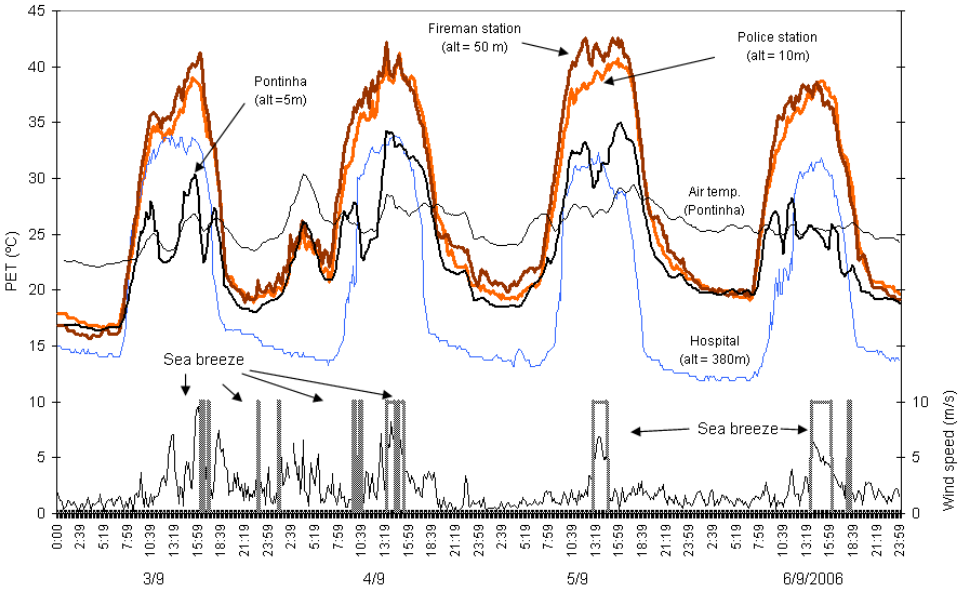

Fig. 4: PET within the warm period from 3 to 6 September 2006. Vertical bars (in the bottom of the graphic) correspond to southern sea breeze

5. Conclusions

Most of the tourists that choose the Madeira Island as a travel destination are people aged between 40 and 70 years old from north European countries (50% from UK and Germany). Therefore, tourism planning should attend to the thermal comfort issues and perception of such travellers. During the analyzed periods no absolute comfort situation was observed, although most of the sites in the city are slightly comfortable during breeze days. During heat waves like the one that occurred in September 2006, it is desirable that tourism agents can programme solutions to ameliorate the thermal comfort, especially northern Europe seniors who are not well acclimatized to hotter environments. As a response to escape too high temperatures, it is advisable to plan short trips to higher altitude superior to 400 m (outside the city of Funchal) or in controlled environments (visit to gardens and acclimatized buildings) during hot periods. Local authorities can also advise more exposed people to heat to remain near the shore line during the hours of higher air temperatures. As sea breezes are an important system to con-

trol heat stress urban planners should not promote dense construction near the shoreline that can act as a barrier to the renewable of the air inside the city.

Acknowledgement

This research is part of the European SECOA project, "Solutions for Environmental Contrasts in Coastal Areas" (FP7. ENV.2009.2.1.5.1).

References

Alcoforado, M. J., Dias, A., Gomes, V., 1999: Bioclimatologia e Turismo, exemplo de Aplicação ao Funchal. Islenha. 25: 29-37.

Alcoforado, M.J., H. Andrade, A. Lopes, J. Vasconcelos, 2009: Application of Climatic Guidelines to Urban Planning. The Example of Lisbon (Portugal), Landscape and Urban Planning, 90:56.65. http://dx.doi.org/10.1016/j.landurbplan.2008.10.006.

Andrade, H., Alcoforado, M.J, Oliveira, S., 2007: Methodologies to Assess the Effects of Climate on Tourism: Weather Type and Individual Perception, in A. Matzarakis, C. R. de Freitas, D. Scott (ed) Development in tourism climatology, Commission on Climate and Recreation, International Society of Biometeorology, Freiburg, p.74-79.

Höppe, P., 1999: The physiological equivalent temperature. A universal index for the biometeorological assessment of the thermal environment. International Journal of Biometeorology, 43(2): 71-75.

Kalnay et al., 1996: The NCEP/NCAR 40.year reanalysis project, Bull. Amer. Meteor. Soc., 77, 437-470.

Lopes, S., 2007: Summer wind regimes in Funchal related with thermal patterns, Master Thesis in Geography, Climate and Society, FLUL, Lisbon, (in Portuguese with an extended abstract in English).

Matzarakis, A., 2006: Weather and climate related information for tourism. Tourism and Hospitality Planning & Development 3, 99-115.

Matzarakis, A., F. Rutz, H. Mayer, 2007: Modelling Radiation fluxes in simple and complex environments – Application of the RayMan model. Int. J. Biometeorol. 51, 323-334.

Mayer, H, 2008: KLIMES – a joint research project on human thermal comfort in cities Berichte des Meteorologischen Instituts der Albert-Ludwigs Universität Freiburg, Vol. 17, 101-117.

Authors' address:

António Lopes (antonio.lopes@campus.ul.pt)
Instituto de Geografia e Ordenamento do Território,
Al. da Universidade (ed. FLUL), 1600-214 Lisboa, Portugal.

Sérgio Lopes (lopes.sergiodasilva@gmail.com) - PhD Student
Instituto de Geografia e Ordenamento do Território,
Al. da Universidade (ed. FLUL), 1600-214 Lisboa, Portugal.

Andreas Matzarakis (andreas.matzarakis@meteo.uni.freiburg.de)
Meteorological Institute, Albert.Ludwigs.University of Freiburg
Werthmannstr. 10, D.79085 Freiburg, Germany

Maria João Alcoforado (mjalcoforado@campus.ul.pt)
Instituto de Geografia e Ordenamento do Território,
Al. da Universidade (ed. FLUL), 1600-214 Lisboa, Portugal.

The impact of snow poor winter seasons in ski touristic demand

Robert Steiger

Institute of Geography, University of Innsbruck, Austria

Abstract

The vulnerability of ski areas in South Tyrol to snow poor winter seasons has reduced since the 1980s. While warm winters in the 1980s caused losses of ski lift transports of up to 33 %, the impact in the 2000s was comparably low with losses of 2 % due to heavy investments in snowmaking technology. In 2006/07 the vulnerability of ski areas in Tyrol and South Tyrol was different. Especially low altitude and small to medium size ski areas in Tyrol had losses of 30-44 % despite installed snowmaking systems. This higher vulnerability is due to the lower mean altitude of ski areas in Tyrol.

1. Introduction

Winter tourism is highly sensitive to climate change due to its dependency on snow. A projected rising number of snow-deficient winter seasons will have impacts on the economy of many alpine destinations but also on the alpine economy as a whole, where about 10-12 % of the jobs are generated by tourism (Abegg et al., 2007). Supply side studies (e.g. Steiger 2010, this issue) using numerical computer models to simulate potential ski season length showed that by the middle of the 21st century the reduction of potential skiing days could question the profitability of ski businesses in regions being economically dependent on winter tourism (for an overview on these studies refer to Scott et al., 2008). Modeling ski season length offers the possibility to assess the time pattern in which the current operation can be maintained (e.g. by snowmaking), but it cannot give information on how demand is likely to develop.

One possibility to assess the potential shifts in demand is to use the analogue-year approach. By choosing extraordinary warm and snow poor winter seasons of the past and analyzing the effect on touristic demand (e.g. overnight stays, frequencies in ski areas, turnover of ski areas etc.), it is possible to identify years serving as a climatic analogue for future average seasons. Studies investigating the impact of extraordinary warm winter seasons on the ski tourism sector were conducted in Canada (Scott, 2006) and the US (Dawson et al., 2009). The impact on demand in winter seasons representative of an average winter in the 2050s was found to be relatively small with reductions in skier visits of 7 % in Ontario/Canada, 10 % in Quebec/Canada and 11 % in the US Northeast region. It was concluded that supply side studies tend to overestimate the potential impacts if common adaptation strategies like snowmaking are not regarded. So far snowmaking was only incorporated in models by Scott (e.g. Scott et al., 2003), Hennessy (Hennessy et al., 2003) and Steiger (Steiger and Mayer, 2008; Steiger, 2009; Steiger, 2010, this issue). In this paper the impact of snow poor winter seasons on ski touristic demand is assessed by analyzing climate and tourism statistics in the provinces of Tyrol/Austria and South Tyrol/Italy allowing to draw conclusions of the potential vulnerability of the winter tourism sector to climate change.

Tourism is an important economic factor contributing about 15.4 % to the GDP in Tyrol (Tirol Werbung, 2010) and 8.2 % in South Tyrol (ASTAT, 2009a). In Tyrol winter is

the main touristic season with 25.6 million overnight stays (59 % of annual overnight stays). Per capita spending is significantly higher in winter (€ 137) compared to the summer season (€ 96) (Tirol Werbung, 2010). Thus the tourists' expenses can be estimated to € 3.5 billion per year not including day trippers. In South Tyrol 11.0 million overnight stays are generated in the winter season, about 39 % of total stays (ASTAT, 2009b). The mean touristic spending is very similar to Tyrol with € 140 in winter and € 105 in summer (ASTAT, 2009b) summing up to € 1.5 billion in the winter season excluding day trippers.

2. Methodology

Climate data was analyzed to identify winter seasons with an extraordinary small number of days suitable for skiing (snow depth threshold of 30 cm). The data was provided by the hydrographic services of the provinces of Tyrol and South Tyrol and by the Central Institute for Meteorology and Geodynamics "ZAMG". The impact of climatic anomalies on ski tourism was assessed using statistics of ski lift transports and overnight stays provided by the bureau of statistics of each province. As no sufficiently long data series of ski lift transports was available for Tyrol, past vulnerability of the ski tourism sector to warm winter seasons was only investigated for South Tyrol.

Some ski areas were excluded due to data gaps. In total 60 ski areas in Tyrol representing about 85 % of the transport capacity and 29 ski areas in South Tyrol with 91 % of total transport capacity were included. The ski areas range from 545-3,433 m with 7,200 ha of ski slopes in Tyrol and 930-3,391 m with approximately 4,000 ha ski slope area in South Tyrol.

In order to detect potential differences in the ski areas' vulnerability to warm winter seasons, a detailed analysis of tourism and ski area statistics of the 2006/07 winter season was conducted. The preceding three seasons were averaged to get a benchmark to compare the 2006/07 season with, as the study areas are among the few marketplaces in the world with still significant growth in ski lift transports (Vanat, 2009): 6.2 % per annum between 2001/02 and 2005/06 (WKO, 2003, 2004, 2005, 2006, 2007) in Tyrol and 4.1 % in South Tyrol (Autonome Provinz Bozen-Südtirol, 2009).

The ski areas were categorized by their mean altitude and size: The ski areas' mean altitude is below 1,500 m in the low altitude category, between 1,500 m and 1,999 m in the mid altitude category and at 2,000 m and above for high altitude ski areas. Additionally, four categories concerning lift capacity as an indicator for ski area size were defined: Small with a capacity of less than 5,000 persons per hour (p/h), medium (5,000 – 9,999 p/h), large (10,000 – 19,999 p/h) and extra large (20,000 p/h and above).

3. The development of ski areas vulnerability in South Tyrol since the 1980s

In South Tyrol five winter seasons characterized by extraordinary bad snow conditions were identified in the 1980/81 to 2007/08 period (Tab. 1). While the 1980/81 season was very cold and dry, all other seasons were too warm, 2001/02 also exceptionally dry. The degree of the lack of snow was similar throughout the province, even the highest elevated climate station available for this paper had losses in ski season length of between 41-85 %.

Table 1: Losses in ski season length at three climate stations and mean climatic anomalies at eight stations compared to a 20-years average (1981/82-2000/01)

	Toblach (1,250m)	Wehr (1,365m)	Weissbrunn (1,900m)	Temp (°C) (Nov-Apr)	Precipitation (%) (Nov-Apr)
	Losses in ski season length (%)			Mean of eight stations	
1980/81	-50	-23	-85	-1.9	-54
1988/89	-77	-83	-41	+2.6	-12
1989/90	-95	-98	-77	+1.3	+15
2001/02	-98	-100	-62	+0.8	-75
2006/07	-62	-94	-71	+2.9	+13

In the 1980s the ski tourism sector was heavily influenced by these snow poor winter seasons with losses in ski lift transports of 21 % (1980/81), 33 % (1988/89) and 29 % (1989/90) with some ski areas actually being out of operation the entire season. The impact on the accommodation sector in ski resorts was less but still significant with 9 %, 15 % and 17 % less recorded overnight stays. The two snow poor seasons in the 2000s (2001/02 and 2006/07) had almost no impact on ski lift transports (-2 %) on the province level. Losses of single ski areas were up to 70 % in 2001/02 and 23 % in 2006/07. In the accommodation sector even slight gains of overnight stays were recorded (+4 % and +2 %) continuing the positive trend of the preceding years.

Since the 1980s the ski businesses have heavily invested in snowmaking. The number of snowmaking guns increased from 511 in 1994 to 1,976 in 2007 covering about 75 % of the total ski slope area (Autonome Provinz Bozen-Südtirol, 2009). As snow is an essential natural resource for ski tourism it must be assumed that these investments are the main reason for the reduced vulnerability of ski areas towards snow poor winter seasons.

4. The impact of the 2006/07 season on ski tourism in Tyrol and South Tyrol

In many parts of the Alps the 2006/07 season was the warmest winter on record, very likely even the warmest in the last 500 years (Luterbacher et al., 2007). Although in both study areas 75 % of the ski slopes were covered by snowmaking in 2007 (Fachverband der Seilbahnen Österreichs 2007; Autonome Provinz Bozen-Südtirol, 2009), the impacts were considerably different (Tab. 2 and Tab. 3).

While ski areas in South Tyrol only experienced comparably small losses in ski lift transports (see Chap. 3), especially low elevated and small to medium sized ski areas in Tyrol were hit hard.

A reason for these huge losses at low altitude ski areas despite the high snowmaking coverage can be found regarding the number of days suitable for snowmaking (Fig. 1). In December prior to the Christmas holidays only seven days with minimum temperatures suitable for snowmaking ($\leq$ -5°C) were recorded at climate station Aschau (1,005 m) and six at Ehrenbachhöhe (1,790 m). The following warm phase until the

third week of January made it impossible to produce the much needed snow leading to closures of some ski areas in the middle of the season.

Table 2: Change in ski lift transports 2006/07 by ski area size compared to the 2003/04-2005/06 mean (in %)

	Small size	Medium size	Large size	Extra large size
Tyrol	-44 (n=9)	-30 (n=21)	-13 (n=18)	-6 (n=12)
South Tyrol	-8 (n=11)	-6 (n=8)	-9 (n=6)	+1 (n=4)

Table 3: Change in ski lift transports 2006/07 by ski area's mean altitude compared to the 2003/04-2005/06 mean (in %)

	Low altitude	Mid altitude	High altitude
Tyrol	-33 (n=18)	-9 (n=22)	-2 (n=20)
South Tyrol	-8 (n=1)	-1 (n=15)	-9 (n=13)

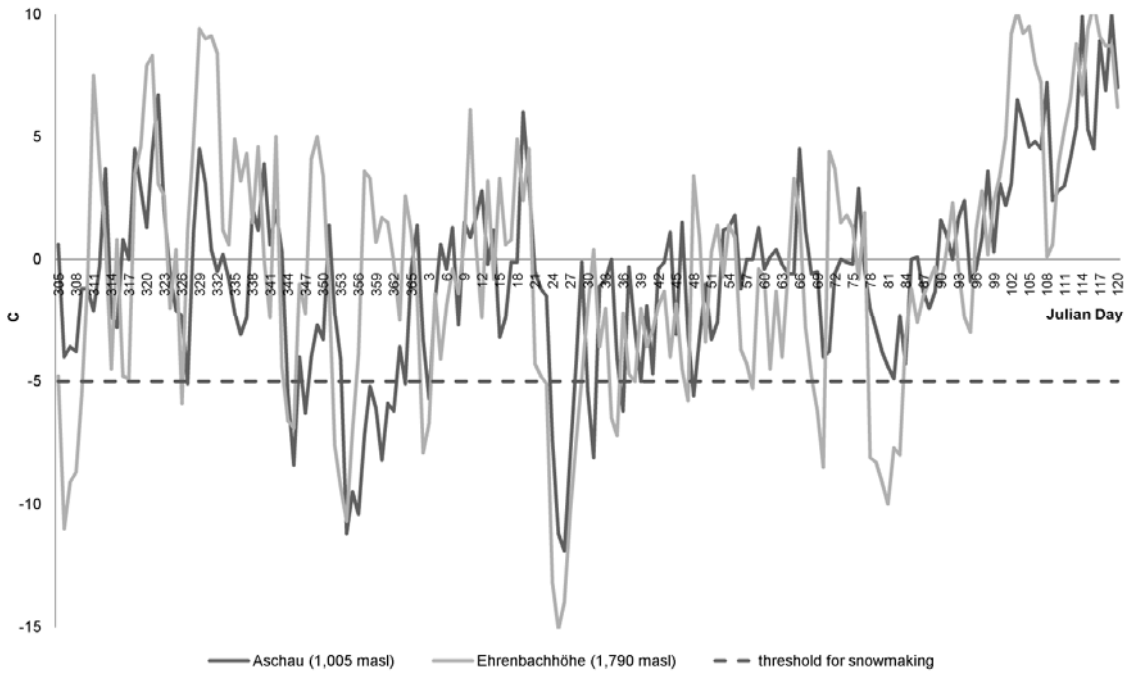

Fig. 1: Daily minimum temperatures at two climate stations in the 2006/07 season

Several reasons are plausible for the different demand reaction in the study areas: The mean altitude of ski areas in South Tyrol is 300 m higher than in Tyrol. As coherence between the impact on demand and ski area altitude can be seen in Tyrol, this seems to be one explaining factor. Another reason could be the media coverage and the perception of the tourists: In interviews conducted in Tyrol in 2007 and 2008 ski area managers mentioned that the perception of snow conditions was very much influenced by the press releases showing green ski hills, although skiing conditions were quite good in the upper regions of many ski areas. Especially Kitzbühel gained a lot of media attention

when the world famous "Streif" downhill ski race had to be cancelled due to a lack of snow, which had happened several times in the history of the traditional race.

5. Conclusions and Discussion

The combined analysis of data of the climate and tourism statistics revealed two major findings:

1) Ski areas' vulnerability to snow poor winter seasons significantly decreased in South Tyrol since the 1980s due to investments in snowmaking technology, and

2) In the 2006/07 winter season, the vulnerability of ski areas in Tyrol was considerably higher than in South Tyrol. As only low altitude ski areas were severely affected and as only one ski area in South Tyrol was within this category, this different vulnerability can be mainly addressed to the ski areas mean altitude being about 300 m higher in South Tyrol.

Climatically, the record season 2006/07 is representative of an average winter in the 2060s to the 2080s depending on the emission scenario used (A1B and B1 respectively). Several conclusions for climate change vulnerability can be drawn from the findings of the presented analysis: Even though snowmaking is an indispensable technology to reduce the risk of closures, it is no guarantee to reach the desired season lengths every year. Snowmaking hours were rare in the analyzed season not only in the valley floors but also at altitudes where many ski areas have their highest ski lift (see Fig. 1). Therefore, further investments in snowmaking or ski infrastructure in general should only be done after a cost-benefit analysis of the planned investments. In such an analysis not only average seasons should be regarded, but also extreme seasons which are very likely to become more frequent with the ongoing climate change. According to statements of ski area managers in personal interviews in the research area, this is currently done seldom. Furthermore, it must be considered that one extraordinary season is likely to have different impacts than a series of warm winters or deteriorating skiing conditions in the medium-term. If tourists are confronted with bad snow conditions repeatedly, they are very likely to change their behaviour concerning the time and the destination of their vacation. A series of several marginal winter seasons could have significant impacts on the financial status of ski areas. Especially small to medium sized ski businesses could be threatened, as financial reserves are generally less than in bigger companies (Scott et al., 2008). The reinvestment-ratio of 50 % of the ski companies in Tyrol in the last years must thus be regarded critically.

Acknowledgement

The author would like to thank the FWF for funding the research project.

References

Abegg, B., S. Agrawala, F. Crick, A. de Montfalcon, 2007: Climate change impacts and adaptation in winter tourism. In: Agrawala, S. (ed.), Climate Change in the European Alps. Adapting Winter Tourism and Natural Hazards Management, OECD, Paris.

ASTAT, 2009a: Das Tourismus-Satellitenkonto für Südtirol – 2005. Autonome Provinz Bozen-Südtirol, Bozen.

ASTAT, 2009b: Tourismus in Südtirol - Tourismusjahr 2007/08. Autonome Provinz Bozen-Südtirol, Bozen.

Autonome Provinz Bozen-Südtirol, 2009: Seilbahnen in Südtirol 2008. Amt für Seilbahnen, Bozen.

Dawson, J., D. Scott, G. McBoyle, 2009: Climate change analogue analysis of ski tourism in the northeastern USA. Climate Research 39(1), 1–9.

Fachverband der Seilbahnen Österreichs, 2007: personal speech Ingo Karl (president oft he Austrian Cable Car Association).

Hennessy, K., Whetton, P., Smith, I., Bathols, J., Hutchinson, M., Sharples, J., 2003: The impact of climate change on snow conditions in mainland Australia, http://www.cmar.csiro.au/e-print/open/hennessy_2003a.pdf (accessed on 03.02.2010).

Luterbacher, J., M. A. Liniger, A. Menzel, N. Estrella, P. M. Della-Marta, C. Pfister, T. Rutishauser, E. Xoplaki, 2007: Exceptional European warmth of autumn 2006 and winter 2007: Historical context, the underlying dynamics, and its phenological impacts. Geophysical Research Letters 34, L12704.

Scott, D., 2006: Global Environmental Change and Mountain Tourism. In: Gössling, S., M.C. Hall (eds.), Tourism and Global Environmental Change. Routledge, London.

Scott, D., J. Dawson, B. Jones, 2008: Climate change vulnerability of the US Northeast winter recreation– tourism sector. Mitig Adapt Strat Glob Change 13, 577–596.

Scott, D., G. McBoyle, B. Mills, 2003: Climate change and the skiing industry in southern Ontario (Canada): exploring the importance of snowmaking as a technical adaptation. Climate Research 23, 171–181.

Steiger, R., 2009: SkiSim - A tool to assess the impact of climate change on ski season length and snowmaking In: Schweizer, J., A. van Herwijnen (eds.), Proceedings of the International Snow Science Workshop, 27. September to 2 October 2009, Davos, Switzerland.

Steiger, R., and M. Mayer, 2008: Snowmaking and Climate Change. Future Options for Snow Production in Tyrolean Ski Resorts. Mountain Research and Development 28(3/4), 292–298.

Tirol Werbung, 2010: Tirol in Zahlen. http://www.presse.tirol.at/xxl/de/tirol-zahlen/. (accessed on 03.02.2010)

Vanat, L., 2009: 2009 International report on mountain tourism, http://www.vanat.ch/RM-world-report-2009.pdf.

WKO, 2003-2007: Berichtsblätter Wintersaison 2001/02 bis 2005/06. WKO, Die Seilbahnen, Wien.

Authors' address:

Robert Steiger (robert.steiger@uibk.ac.at)
Institute of Geography, University of Innsbruck
Innrain 52, A-6020 Innsbruck, Austria

Prediction of acclimatization thermal loading for climatic extremes

C.R. de Freitas[1] and E.A. Grigorieva[2]

[1]School of Environment, University of Auckland, New Zealand
[2] Institute for Complex Analysis of Regional Problems,
Far Eastern Branch, Russian Academy of Sciences, Birobidzhan, Russia

Abstract

Tourists are often exposed to thermal conditions that are quite different to those at home. There is an important period following arrival during which an unacclimatized individual experiences additional thermal loading that can affect their comfort or even threaten their physiological wellbeing. The first signs of thermal strain show up in the respiratory organs. The research reported here is a case study for thermally contrasting climates of Khabarovsk, the administrative center of the Russian Far East, and the holiday destination of Haikou, Hainan Island, China. Khabarovsk has a classic mid-latitude continental climate of thermal extremes and Haikou an equable tropical climate popular with Russian vacationers during the Northern Hemisphere winter. The Acclimatization Thermal Strain Index (ATSI) is used to quantify the consequences of acclimatization thermal loading experienced in travelling between these places, where ATSI is the ratio of a difference between respiratory heat losses at the traveler's home location to respiratory heat losses at the trip destination. Mean daily climatic data for 2008-2009 are used to identify acclimatization thermal loading that would be experienced by individuals outdoors during the period December to February. Results for destination Haikou travelling from Khabarovsk show that in January ATSI ranges from +23 to +43%. The potential for equally severe thermal strain scenarios exists on the return home. ATSI at destination Khabarovsk travelling from Haikou in January varies between -30 and -74%. In the light of these findings, it is possible that travelers may suffer serious consequences unless appropriate measures are taken to avoid severe discomfort or harm.

1. Introduction

The human body will experience heat or cold strain when metabolic heat produced is not equal to heat lost to the surrounding environment. Quite apart from this, there is a period of acclimatisation during which the body adjusts to changed conditions. During this period of acclimatisation the body experiences an additional thermal loading. For example, when tourists are exposed to climates that are quite different to that to which they are accustomed, there is an important period following arrival during which an individual experiences additional thermal loading, which can affect their comfort or even threaten their physiological wellbeing. The first signs of the physiological strain associated with this additional thermal loading show up in the respiratory organs. There are several reasons for this. Respiration is the body-environment heat exchange process in which the body is in closest contact with the ambient air. The respiratory tract is not protected and humans can do nothing to prevent the ambient air entering into the body's core area, the lungs, through the respiratory tract.

For individuals moving from warm to cold conditions, the initial effects are greater respiratory heat losses due to large difference in temperature and humidity between the body and ambient air, leading to increased cooling and drying of the respiratory organs. Cooling and drying move deeper into central airways and lungs (Cole, 1954; McFadden, 1983) and may cause cold injury (Simonova, 1980). The first response of the respi-

ratory system is aimed at reducing pulmonary ventilation, referred to as bronchoconstriction, which occurs within about 10 to 15 minutes (Giesbrecht, 1995). At the same time the body responds to the cold by elevating heat production from increased metabolism (Scholander et al., 1958; Divert et al., 2006), which affects respiration and leads to an increase in minute volume ventilation. This process is known as "polar dyspnea" (Shishkin et al., 1998) or hyperventilation (Bandopadhyay, Selvamurthy, 1993). The first stage of acclimatization is the body's attempt to adapt by reducing pulmonary ventilation and respiratory heat loss (Simonova 1980; Burgess and Whitelaw, 1988; Giesbrecht, 1995; Grishin and Ustuzaninova, 2007). This change in breathing pattern manifests itself as a reduction in ventilation rate (Simonova, 1980; Diesel et al., 1990; Kozyreva and Simonova, 1994) and length of expiration – time taken for inspired air to be removed from the lungs (Simonova, 1980; Giesbrecht, 1995). There are other changes that take place. Constant exposure to cold environments results in pulmonary morphological changes such as increased numbers of goblet cells and mucous glands, hypertrophy of airway muscular fascicles and increased muscle layers of terminal arteries and arterioles, increase of surfactant production (Giesbrecht, 1995). When acclimatization is complete, respiratory heat losses are reduced by 25-40 % (Simonova, 1980).

For individuals moving from cold to hot conditions, heat gain by the body might exceed heat loss. Respiratory heat loss is reduced because of a decreased lungs-to-air thermal gradient. To counter this, there is a need for a rise in evaporative and sensible respiratory heat loss (Rasch et al., 1991; Mariak et al., 1999; Cabanac and White, 1995; White, 2006). For people acclimatised to heat, the temperature of exhaled air is higher than for those who are unacclimatized. To achieve the equivalent respiratory heat loss, unacclimatized individuals must maintain higher pulmonary ventilation (Beaudin et al., 2009; Simonova, 1980). This latter contributes additional thermal strain, as large as 30 % (Simonova, 1980).

The research reported here is a case study for thermally contrasting climates of Khabarovsk, the administrative center of the Russian Far East, and the holiday destination of Haikou, Hainan Island, China. Khabarovsk has a classic mid-latitude continental climate of thermal extremes and Haikou an equable tropical climate popular with Russian vacationers during the Russian winter.

2. Materials and Methods

The respiratory heat exchange between the lungs and the outside air (Q_r) takes place by forced convection and involves both a dry heat flux and evaporative (latent) heat flux (Hanson, 1974; de Freitas, 1985; Varene, 1986; de Freitas and Ryken, 1989; Rusanov, 1989; Rasch et al., 1991). De Freitas and Grigorieva (2009) show that this can be quantified as:

$$Q_r = P_l + LE, \tag{1}$$

$$P_l = 2 \times 10^{-5}\, w\, b\, (T_l - T), \tag{2}$$

$$LE = 2.9 \times 10^{-2}\, w\, (l_l - l), \tag{3}$$

where Q_r (W) is heat loss via respiratory organs, P_l (W) is heat loss from the respiratory track caused by heating of inhaled air, LE (W) evaporative heat loss caused on moisture loss from a surface of respiratory organs, w (l min^{-1}) is the volume of inhaled air set at

8 l min^{-1}, T (^{o}C) is temperature of inhaled (surrounding) air, T_l is temperature of exhaled air set at 35^{o}C; l (hPa) is vapor pressure of inhaled air, l_l is vapor pressure of exhaled air set at 56.3 hPa, and b (hPa) is atmospheric pressure taken to be 1000 hPa. The coefficients (2 x 10^{-5}) and (2.9 x 10^{-2}) for terms P_l and LE, respectively, take into account metabolic rate. Wind accompanied by cold ambient air temperatures can affect respiratory heat loss by increasing lung ventilation and heat loss from respiratory organs (Assman 1963; Rusanov 1989; Rusanov 2004). According to Rusanov (2004) this can be taken into account by adjusting air temperature, given as

$$T_A = T - 2V, \tag{4}$$

where T_A (^{o}C) is adjusted air temperature, T (^{o}C) is the temperature of the air outdoors and V (m s^{-1}) is wind speed. The adjustment is applied only when T < 0^{o}C.

During the period of acclimatisation, the body experiences an additional thermal loading the first signs of which show up in heat exchange through the respiratory organs Q_r (Rusanov, 1989). De Freitas and Grigorieva (2009) showed that the physiological significance of different climatic conditions at the trip destination may be expressed as an "acclimatization thermal loading" (ATL) and used the ATL in an index form to quantify the thermophysiological impact of the change due to a lack of acclimatization. The Acclimatization Thermal Strain Index (ATSI) describes the additional thermal loading on respiratory organs until full acclimatization is achieved. ATSI is defined as the ratio of the difference between heat losses that would occur at the traveler's home location to losses of heat at the holiday or trip destination upon first arriving there, expressed as a percentage:

$$\text{ATSI} = 100\ (Q_{rh} - Q_r')\ /\ Q_{rh}\ , \tag{5}$$

where Q_{rh} (W) is heat loss from respiratory organs at the home location and Q_r' (W) is heat loss at the trip destination. An ATSI value of zero marks the transition of ATL for individuals unacclimatized to either heat or cold (Rusanov, 1989). The most favorable conditions at the trip destination are considered to exist when ATSI values are zero-to-slightly-positive-or-negative. ATSI values less than zero indicate ATL due to lack of acclimatization to cold conditions, with increasing severity as the values become progressively more negative. For example, this would be the case if thermal conditions at the home location were warmer than the trip destination (that is, $Q_{rh}<Q_r'$). Rising positive values of ATSI above zero indicate the onset of ATL due to lack of acclimatization to hot conditions, with the possibility of causing heat strain should ATSI values climb well above the 15-20 level. The ATSI applies to ATL over the short-term only, as in due course (a matter of weeks or months) the acclimatization process will be complete.

The acclimatization thermal loading for thermally contrasting climates of Khabarovsk and the holiday destination of Haikou, Hainan Island, China is examined using the above approach. Khabarovsk has a classic mid-latitude continental climate of thermal extremes and Haikou an equable tropical climate popular with Russian vacationers during the Russian winter. The hydrometeorological station (HMS) Khabarovsk (WMO-index 31735, 48^{o}31 N, 135^{o}10 E) is situated at an altitude 88 m above sea level. The HMS at Haikou (WMO-index 59758, 20°02 N, 110°21 E) is at an altitude of 15 m above sea level. Mean daily climatic data for 2008-2009 are used to identify acclimatization thermal loading that would be experienced by individuals outdoors during the period December to February. Q_r was calculated for a person standing relaxed for a me-

tabolic rate of 90 W m^{-2} (for 1.5 m^2 human body area) across the full range of mean daily conditions for the same period for both locations, namely Khabarovsk and Haikou.

3 Results and discussion

The range of air temperature and relative humidity conditions encountered over the study period are shown in Table 1. The results in Table 2 show Q_r and ATSI for changed conditions and lack of acclimatization in moving between Khabarovsk and Haikou.

Table 1: Monthly mean values of air temperature T_a (^oC) and relative humidity rh (%) with standard deviation (± σ) for Khabarovsk and Haikou for the period 01.12.2008 to 28.02.2009

HMS	December		January		February	
	T_a	rh	T_a	rh	T_a	rh
Khabarovsk	-15.8 ±7.11	69 ±14.1	-19.1 ±5.24	75 ±8.9	-17.0 ±4.64	71 ±15.8
Haikou	19.2 ±2.35	76 ±13.8	16.2 ±3.04	76 ±16.2	22.7 ±3.73	81 ±14.2

Table 2: Monthly mean (with standard deviation, ± σ) and maximum and minimum values of respiratory heat loss Q_r (W) and ATSI (%) for Khabarovsk and Haikou for the period 01.12.2008 to 28.02.2009

Month	December			January			February		
	Mean ± σ	Min	Max	Mean ± σ	Min	Max	Mean ± σ	Min	Max
Location	**Respiratory heat loss Q_r (W)**								
Khabarovsk	21.9 ±1.5	18.9	24.1	22.3 ±0.6	20.8	23.5	22.1 ±0.7	20.9	23.6
Haikou	14.2 ±1.0	12.1	15.8	14.8 ±1.2	12.5	16.6	12.6 ±0.8	11.3	13.6
Travel	**ATSI (%)**								
Khabarovsk-Haikou	35 ±7.1	20	49	33 ±5.8	23	43	43 ±4.5	37	50
Haikou-Khabarovsk	-55 ±17.2	-24	-96	-51 ±13.0	-30	-74	-76 ±10.8	-59	-98

The results for destination Haikou show that the highest ATSI (of about 50 %) occur in December and February. The potential exists for a significantly more ATL on the return home to Khabarovsk, where ATSI ranges from -96% in December to -98% in February. These peaks occur on December 12 and February 19, respectively; during which times air temperature in Khabarovsk was -20^{o}C and +25^{o}C in Haikou, with wind speeds as high as 10 m s^{-1} in Khabarovsk.

Maximum positive ATSI of 50% occurs in February and maximum negative ATSI -98% in the same month. However, it is not clear from the research literature whether or not sensitivities (per ATSI) are the same for unit-values in the negative range as they are within positive range. Nevertheless, the results show that the thermal loadings due to lack of acclimatization are significant and serious enough to affect human wellbeing.

4. Conclusion

Travelers can experience climatic conditions that are quite different to those to which they have acclimatized at home. The impact of the change on physiological well-being centers on the respiratory organs. Results for destination Haikou travelling from Khabarovsk show that in January ATSI values are high. The potential for equally severe thermal strain scenarios exists on the return home. The most severe ATL occurs during December and February when low air temperatures in Khabarovsk are accompanied by high winds. Knowledge of the risks involved could be useful in planning outdoor activity. Further work is required to refine the index and its meaning across the positive and negative ranges and the relevance of using more detailed meteorological data over shorter time periods.

Acknowledgement

The work was supported by Russian Fund for Basic Research: project No 08-01-98505-r_vostok_a, FEB RAS: project No. 09-III-A-09-497, 09-III-A-09-498.

References

Assman, D., 1963: Die Wetterfühligkeit des Menschen. Fischer, Jena (in German).

Bandopadhyay, P., W. Selvamurthy, 1993: Respiratory changes due to extreme cold in the Arctic environment. Int. J. Biometeorol. 37, 32-35.

Beaudin, A.E., M.E. Clegg, M.L. Walsh, M.D. White, 2009: Adaptation of exercise ventilation during an actively-induced hyperthermia following passive heat acclimation. Am. J. Physiol. Regul. Integr. Comp. Physiol. 297, R605-R614.

Burgess, K.R., W.A. Whitelaw, 1988: Effects of nasal cold receptors on pattern of breathing. J. Appl. Physiol. 64, 371-376.

Cabanac, M., M.D. White, 1995: Core temperature thresholds for hyperpnea during passive hyperthermia in humans. Eur. J. Appl. Physiol. 71, 71-76.

Cole P., 1954: Recordings of respiratory air temperature. J. Laryngol. Otol. 68, 295-307.

De Freitas, C.R., 1985: Assessment of human bioclimate based on thermal response. Int. J. Biometeorol. 29, 97-119.

De Freitas, C.R., E.A. Grigorieva, 2009: The Acclimatization Thermal Strain Index (ATSI): a preliminary study of the methodology applied to climatic conditions of the Russian Far East. Int. J. Biometeorol. 53, 307-315.

De Freitas, C.R., M. Ryken, 1989: Climate and physiological heat strain during exercise. Int. J. Biometeorol. 33, 157-164.

Diesel, D. A., A. Tucker, D. Robertshaw, 1990: Cold-induced changes in breathing pattern us a strategy to reduce respiratory heat loss. J. Appl. Physiol. 69(6), 1946-1952.

Divert, V.E., G.M. Divert, S.G. Krivoschekov, 2006: Temperature homeostasis and work efficiency in the cold. Alaska Medicine. 49(2 Suppl), 222-227.

Giesbrecht, G.G., 1995: The respiratory system in a cold environment. Aviat. Space. Environ. Med. 66, 890-902.

Grishin, O.V., N.V. Ustuzaninova, 2007: The influence of cold on energy expenditure at rest and during exercise in person in the North. Alaska Med. 49(2 Suppl), 231-236.
Hanson, RG., 1974: Respiratory heat loss at increased core temperature. J. Appl. Physiol. 37, 103-107.
Kozyreva, T.V., T.G. Simonova, 1994: Peripheral thermal input and respiratory regulation in men. Proc. Sixth Int. Conf. on Environmental Ergonomics, 38-39.
Mariak, Z., M.D. White, J. Lewko, T. Lyson, P. Piekarski, 1999: Direct cooling of the human brain by heat loss from the upper respiratory tract. J. Appl. Physiol. 87, 1609-1613.
McFadden, E.R.Jr., 1983: Respiratory heat and water exchange: physiological and clinical implications. J. Appl. Physiol. 54, 331-336.
Rasch, W., P. Samson, J. Cote, M. Cabanac, 1991: Heat loss from the human head during exercise. J. Appl. Physiol. 71, 590-595.
Rusanov, V.I., 1989: Appraisal of meteorological conditions defining human respiration (in Russian). Bull. Russian Acad. Med. Sci. 1, 57-60.
Rusanov, V.I., 2004: Bioclimate of the Western Siberia Plain. Tomsk, Institute of Atmospheric Optics SB RAS (in Russian).
Scholander, P.F., H.T. Hammel, K.L. Andersen, Y. Løyning, 1958: Metabolic acclimation to cold in man. J. Appl. Physiol. 12, 1-8.
Shishkin, G.S., V.K. Preobrazhenskaya, G.P. Krasulina, N.P.Bistrova, N.D. Umahtceva, V.V. Gultyaeva, 1998: Defense reaction of upper airway system on long action of ecological factors (in Russian). Vestnik RAMS. 9, 45-48.
Simonova, T.G., 1980: Adaptive changes in human respiratory system in cold conditions. PhD thesis (in Russian).
Varene, P., 1986: Computation of respiratory heat exchanges. J. Appl. Physiol. 61, 1586-1589.
White, M.D., 2006: Components and mechanisms of thermal hyperpnea. J. Appl. Physiol. 101, 655-663.

Authors' addresses:

Prof. Dr. C. R. de Freitas (c.defreitas@auckland.ac.nz)
School of Environment, University of Auckland,
PB 92019 Auckland, New Zealand

Dr. Elena A. Grigorieva (eagrigor@yandex.ru)
Institute for Complex Analysis of Regional Problems
Far Eastern Branch, Russian Academy of Sciences,
Sholom-Aleikhem, 4, Birobidzhan, Russia

Determination of the winter human thermal comfort distributions in a ski-centre

Sevgi Yılmaz[1], Süleyman Toy[2], Hasan Yılmaz[3]

[1] Ataturk Univ., Fac. of Agric., Dept. of Landscape Architecture, 25240, Erzurum/ Turkey
[2] Landscape Architect & Engineer at Meteorology Office, Erzurum/Turkey
[3] Ataturk Univ., Fac. of Agric., Dept. of Landscape Architecture, 25240, Erzurum/ Turkey

Abstract

Erzurum is located in the eastern part of Turkey at an elevation of 1850 m. In the city, a harsh continental climate is prevalent, which means winters are long and extremely cold. In 2011, UNIVERSIADE winter university games will be held in the city. The city has a very important ski centre and in winter months a considerably large number of tourists visit the city. The aim of this study is to determine the distribution of human thermal comfort conditions in winter months using a very popular bioclimatological comfort index PET (Physiological Equivalent Temperature) and bioclimate RayMan.

1. Introduction

North eastern part of Turkey is of a distinctive feature for alternative tourism and recreation activities because of its untouched nature and unique geography. In this region the city of Erzurum occupies the largest surface area and is the most important city of the region. The city of Erzurum has a very famous winter sports centre and can attract very large number of tourists. The city is the second highest city in Turkey. The city of Erzurum is the largest and the most crowded city in its region. However, negative effects of climate and air pollution mainly caused by its harsh climate can adversely affect quality of urban life. Presence of Atatürk University, which is one of the largest universities in the country, can increase social and environmental life quality.

The city of Erzurum has a high winter tourism capacity. In 2011, UNIVERSIADE winter university games will be held in the city. For that reason, the city will host a considerable number of students from all over the world. This will be an opportunity for the city.

In the assessment of climate characteristics for tourism and recreation, perhaps the most preferred bioclimatic comfort index is Physiological Equivalent Temperature (PET; Höppe, 1999; Matzarakis et al., 1999). PET index is the most widely used thermal comfort index. It can be used for a very wide range of studies including the evaluation of climate and bioclimate of an area for tourism and recreation (Matzarakis 2007).

The aim of this study is to evaluate the climatic characteristics of Erzurum city for winter sports considering PET index calculated over a 35 – year period.

2. Material and method

The city of Erzurum is located in north-eastern part of Turkey at an elevation of 1850 m and 39.57 N, 41.10 E (Fig. 1). A very famous winter sports centre in Turkey is located very near the city centre and it can attract very serious number of tourists (Fig. 2).

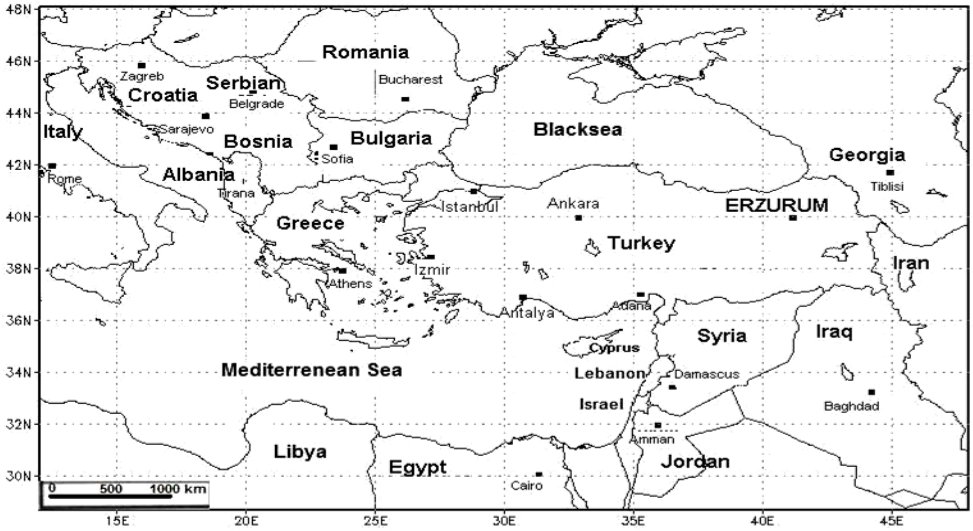

Fig. 1: Location of Erzurum in Turkey

In the study, PET (Physiological Equivalent Temperature) index (Höppe, 1999; Matzarakis et al., 1999) was used to evaluate the comfort conditions of the city for winter tourism. Calculations were performed using a meteorological dataset over a 35 – year period from 1975 to 2009 using Rayman thermal comfort calculation model (Matzarakis et al. 2000; 2007 and Matzarakis and Rutz 2005).

Fig. 2: A view from Palandöken winter sports centre in Erzurum (original)

3. Results and discussion

Distribution of PET (Physiological Equivalent Temperature) index values for Erzurum is given in Fig. 3. PET values were calculated according to the values obtained from the meteorological station located at city's airport.

According to the figure, a very long period of excessive heat stress is prevalent in the city. “Cold” and “very cold” ranges are prevalent in period beginning from September and lasting until the end of April. “Comfortable” range is limited only to summer months and no heat stress is experienced in the summer period. Maximum, minimum and mean PET values were found to be 43.0, -30.1 and 6.4 ºC in Erzurum, respectively.

From the results of the study, it seems that the city can be suitable for the activities in summer; however, it should be considered that the calculation of thermal comfort values was performed considering the constant values in Rayman model (e.g. Clo and activity values), which may be not suitable for the calculation of thermal conditions in a winter sports centre.

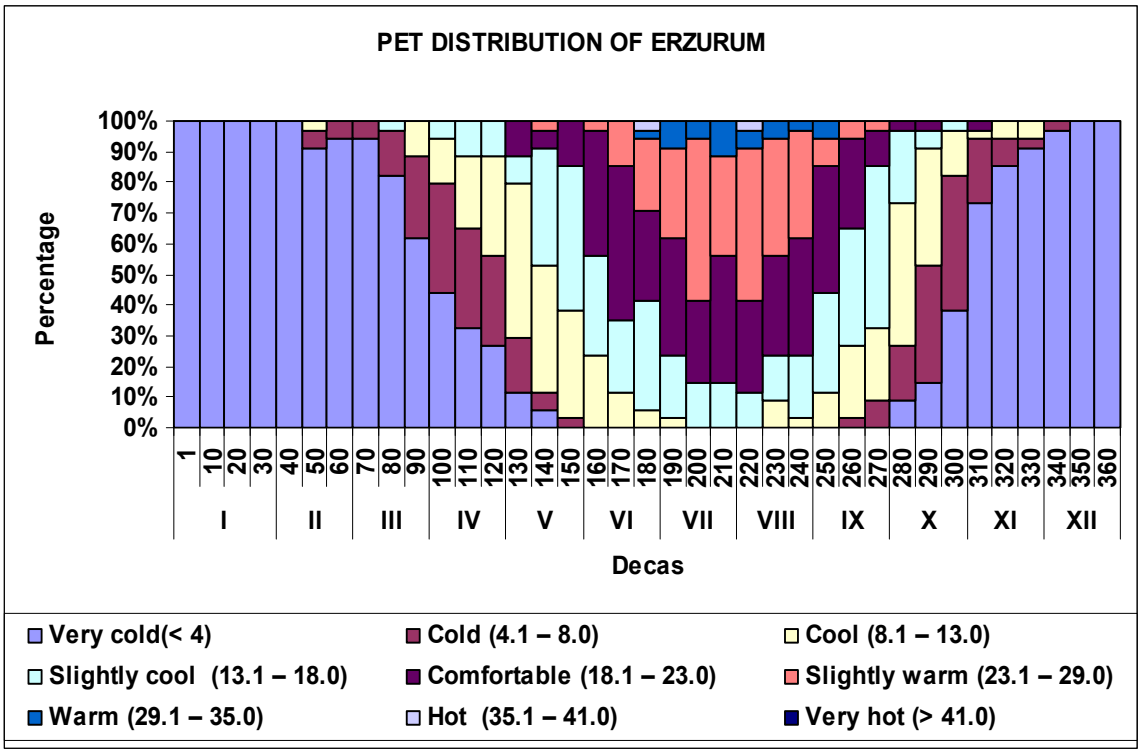

Fig. 3: Distribution of PET values for Erzurum

4. Conclusion

As the consequence of the study it may be sated that even though in winter extreme cold stress is prevalent in the city, this may not be valid for a skier while he/she performs his/her activities due to the isolating effects of sport kid and working activities.

In addition, since the values used in the present study were from the meteorological station in the city centre, a more detailed and accurate data set can be obtained from an automatic weather station which has just been established in the centre. Therefore, data and constant values used for the calculations should be reconsidered in the future studies.

Quality and quantity of such studies which can contribute to the potentials of the area should be increased. Since the study area has very high winter sports potentials with its physical and climatic characteristics, several new organisations in addition to UNIVERSIADE can be implemented in the area by introducing it in every environment.

References

Matzarakis A., 2007: Assessment method for climate and tourism based on daily data. In: A. Matzarakis, C. R. de Freitas, D. Scott (Eds.), Developments in Tourism Climatology, 52-58.

Höppe P., 1999: The physiological equivalent temperature - a universal index for the biometeorological assessment of the thermal environment. Int. J. Biometeorol. 43:71-75.

Matzarakis A., Mayer H., Iziomon M. G., 1999: Applications of a universal thermal index: physiological equivalent temperature Int J Biometeorol 43:76–84.

Matzarakis, A., Rutz, F., Mayer, H., 2007: Modelling Radiation fluxes in simple and complex environments – Application of the RayMan model. International Journal of Biometeorology 51, 323-334.

Matzarakis, A., Rutz, F., 2005: Application of RayMan for tourism and climate investigations. Annalen der Meteorologie 41, (2), 631-636.

Matzarakis, A.; Rutz, F., Mayer, H., 2000: Estimation and calculation of the mean radiant temperature within urban structures. In: Biometeorology and Urban Climatology at the Turn of the Millenium (ed. by R.J. de Dear, J.D. Kalma, T.R. Oke and A. Auliciems): Selected Papers from the Conference ICB-ICUC'99, Sydney, WCASP-50, WMO/TD No. 1026, 273-278.

Authors' address:

Associate Prof. Dr. Sevgi Yılmaz (syilmaz_68@hotmail.com; sevgiy@atauni.edu.tr)
Ataturk Univ., Fac. of Agric., Dept. of Landscape Architecture, 25240, Erzurum/ Turkey

MsC. Süleyman TOY (s_toy2@hotmail.com) Landscape Architect & Engineer at Meteorology Office, Erzurum/Turkey

Prof. Dr. Hasan YILMAZ (hyilmaz@atauni.edu.tr)
Ataturk Univ., Fac. of Agric., Dept. of Landscape Architecture, 25240, Erzurum/ Turkey

Gauging the sensitivity of tourism climate to change by way of an integrated thermal bioclimatic assessment scheme

C. R. de Freitas[1] and Andreas Matzarakis[2]

[1] School of Environment, University of Auckland, New Zealand
[2] Meteorological Institute, University of Freiburg, Germany

Abstract

Climate is a key factor in attracting visitors to certain regions, thus any change in climate, whatever the cause, will affect the value of this toursim resource. The problem is we are unable to adequately predict future climate. Sensitivity assessment circumnavigates this problem and informs planning decisions without knowing precisely the magnitude of climate change that might occur. The impact of change will depend on the net effect of the changed variables as well as the climate of the region in question. For example, an average 1°C air temperature rise may be of little consequence where high temperatures, high solar heat loads, high relative humidity and low wind speeds are commonplace. Conversely, marginal tourism climates may be highly sensitive and respond dramatically to even the smallest change in climatic conditions in an already short tourist season. Two well-tested schemes for integrating thermal bioclimatic variables are used to assess sensitivity to change in Australia and New Zealand. The approach produces integrated output indices in the form of the ASHRAE thermal sensation scale (TSN) and Physiologically Equivalent Temperature (PET). Data for a 30-year period is used to produce monthly charts. The results describe the net effects of various climate scenarios and show that the changes in thermal conditions will be greater than implied by using air temperature alone, especially during summer. The changes for the winter result in net increases one to two TSN stress levels or about 5°C PET. The findings show that quantification of the thermal impact of changed climate cannot be adequately assessed using temperature alone. The results are useful for identifying areas of high sensitivity to climate change as well as the extent to which potential impact on thermal climate appeal for tourism is likely to be negative or positive.

1. Introduction

Many tourist destinations rely heavily on thermal environmental assets that create a generally agreeable climate to attract visitors. Climate change, whether natural or anthropogenic, could modify these assets and result in significant impacts, posing both risks and opportunities. There are two ways assessing the effect of these changes on tourism climate, these are the so called top down or bottom up approach. The top down method is by far the most common. In this approach, a future climate state is identified using global climate models and impacts evaluated. But this method is hampered by the unreliability of climate models. The fact is that there are no dependable predictions of future climate, especially at the regional scale; consequently the topic of future climate and possible impacts is plagued with uncertainty (de Freitas and Fowler, 1989). Another problem is that there is often an implicit assumption that a specific changed climate condition is predicted. This is reinforced by the fact that global climate models are limited to calculating a single equilibrium response condition. Clearly, the consequences of models being 'wrong' could have serious planning implications. To make matters worse, there are large discrepancies between predictions from different global climate models, especially when model output is transformed into impacts at the regional scale, the very scale at which planners and policy-makers typically operate.

An additional problem is that top down climate change impact assessment often relies on a greatly simplified picture of climate, mainly because it usually deals with change in terms of single climate variables that allow for only elementary statistical connections to be made with impacts.. This approach is of limited use since the significance of change will depend on the net effect of the changed variables. Clearly, thermal climate in terms of human comfort is a function of the combined effect of several atmospheric variables, including air temperature, humidity, solar radiation and wind, as well a the body's metabolic rate and clothing.

The alternative bottom up approach, circumnavigates many of these problems. First sensitivity of a tourism activity to climate is assessed, and then the question asked: What is the net effect of change on the tourism activity or tourism-related socioeconomic exposure unit? By identifying its sensitivity to climate and evaluating this in terms of the adaptive capacity of the exposure unit, vulnerability of tourism to change may be determined and assessed. With this information, planning decisions would be possible without knowing precisely what future climate will be like.

In the current study bottom up approach is used to assess the sensitivity to change of the thermal environmental assets that create a generally agreeable climate to attract visitors. Two regions that are heavily used for outdoor tourism activities are considered together for comparative purposes. The Southern Hemisphere is used as this part of the global often neglected in regional climate assessments. To overcome the deficiency caused by using a single climate variable, typically air temperature, a body-atmosphere energy balance approach is employed. This approach deals with thermal climate in terms human comfort as a function of the combined effect several atmospheric variables as well as the individual's activity level, posture and clothing. Thus he information provided is an expression of the integrated effect of all thermal aspects of climate. From here the significance of change can be related to overall sensitivity of the climate condition to those aspects of climate that do change. For example, an average 1^{o}C air temperature rise may be of little consequence where high temperatures, high solar heat loads, high relative humidity and low wind speeds are commonplace. On the other hand, marginal tourism climates may be highly sensitive and respond dramatically to even the smallest change in thermal conditions in an already short tourist season. Also, more subtle changes in climate can be assessed, such as those due to changes in cloud cover, which affects the solar heat load on the human body and thus the body net thermal state.

2. Method

Two refined and well-tested schemes for integrating thermal bioclimatic variables are used to assess sensitivity of the climate of Australia and New Zealand generally to climate change. The tourism focus in both cases is outdoor recreation. In addition, two of regions that are well heavily used tourist locations, namely the Auckland region of the North Island of New Zealand and the Sunshine and Gold coasts of southeast Queensland Australia, are the subject of more in depth analysis. Detailed assessment of data from the climate stations at Auckland and Brisbane Australia are used as indicative of the climate of these important tourist regions.

Two refined and well-tested schemes for integrating thermal bioclimatic variables are used to assess sensitivity to climate change in a variety of regions of the world well known tourist locations globally. The integrated output index is in the form of the ASHRAE Tempera-

ture Sensation Scale (TSN) and Physiologically Equivalent Temperature (Höppe, 1999, Matzarakis et al., 1999). TSN quantifies comfort/discomfort based on human-assessed response to thermal stress. TSN is one of the most widely used thermal indices (McGregor et al., 2002). Physiological Equivalent Temperature (PET) integrates all thermal variables relevant to the body-atmosphere energy balance and expresses the result in terms of an "effective air temperature" (Höppe, 1999, Matzarakis et al., 1999).

The method adopted uses response surfaces to quantify sensitivity of regional climates to change. A response surfaces is a two-dimensional representation of the sensitivity of a specific response variable (TSN for example) to change in the two controlling features of climate (for example, temperature change and change in sunshine/cloudiness as it affect the solar heat load on the body). The relationship between the response variable and climate is determined from a pre-tested set or relationships, usually in the form of an empirical model, called a transfer function.

3. Results

The output from the groups of determinants can be plotted using values relative to a baseline representing no climate change (Fig. 1 and 2). The latter representation is a step removed from absolute input and output but does have the advantage of providing a direct measure of sensitivity. For example, a 20 % response to a 10 % change in a controlling climate variable is clearly an example of impact amplification. Response surface isolines are a summary of a matrix of response points associated with various combinations of changes to the two groups of driving climate variables (Figs. 1 and 2). The required data are derived from repeated runs of the transfer function with the prescribed changes to the input. The slope and closeness of the isolines are an indicator of sensitivity and discontinuities an indicator of change in response. Plotting climate change scenarios on the response surface enables it to be used for impact analysis. For example, a scenario of a 10 % increase in temperature and a 20 % increase in the cloud, for example, can be plotted on the response surface to assess the anticipated impact on the response variable, say change in the TSN (Figs. 1 and 2).

4. Conclusions

The results can be used to describe the net effects of various IPCC scenarios and show that the changes in thermal conditions will be greater than implied by using air temperature alone, especially during summer. The changes for the winter result in net increases one to two TSN stress levels or about 5°C PET. Overall the results show that the quantification of the thermal impact of changed climate cannot be adequately assessed using temperature alone. The generalised mapped results are useful for identifying areas of high sensitivity to climate change as well as the extent to which potential impact on thermal climate appeal for tourism is likely to be negative or positive.

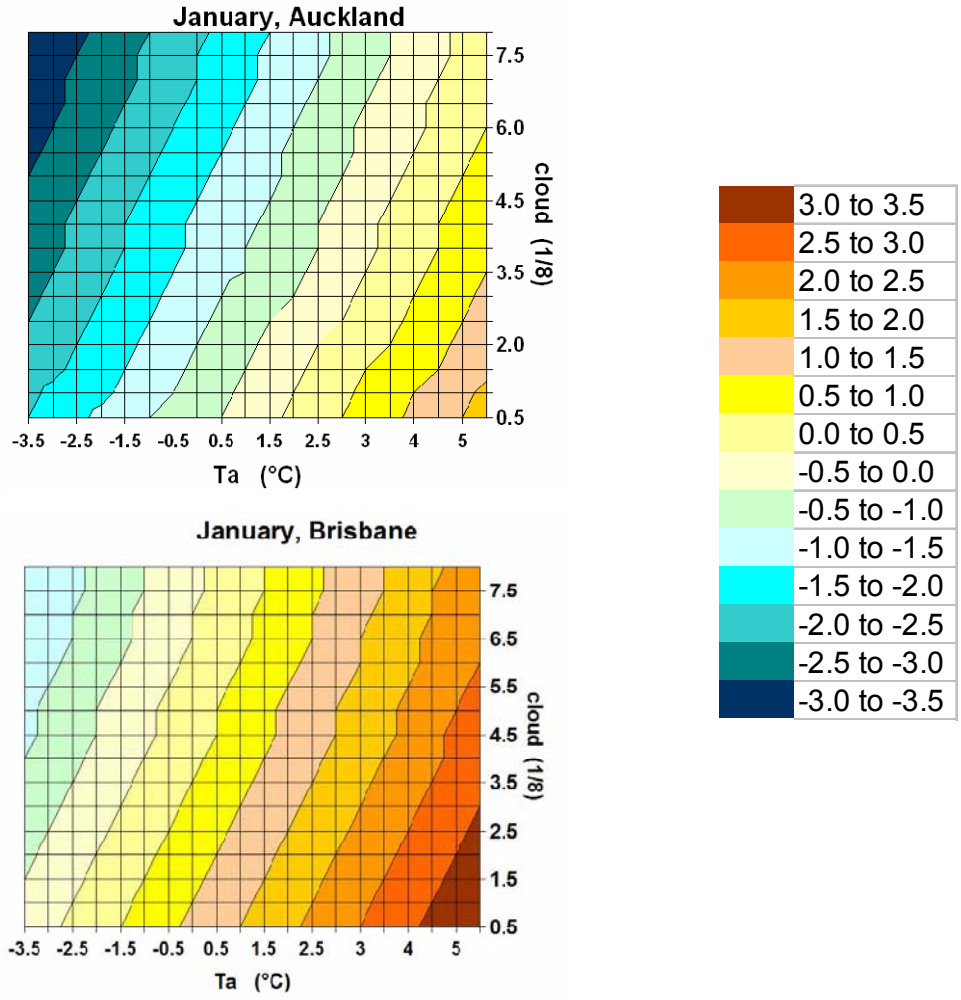

Fig. 1: Sensitivity of TSN to changes in air temperature (deg C) and cloud cover. Mean cloud for Auckland is 3.9 and 3.1for Brisbane. TSN is calculated from an integrated human body-atmosphere energy budget holding relative humidity, wind and solar radiation constant at mean January values. Calculations consider conditions at solar noon. Activity and clothing level are 80 W m^{-2} and 0.5 clo, respectively

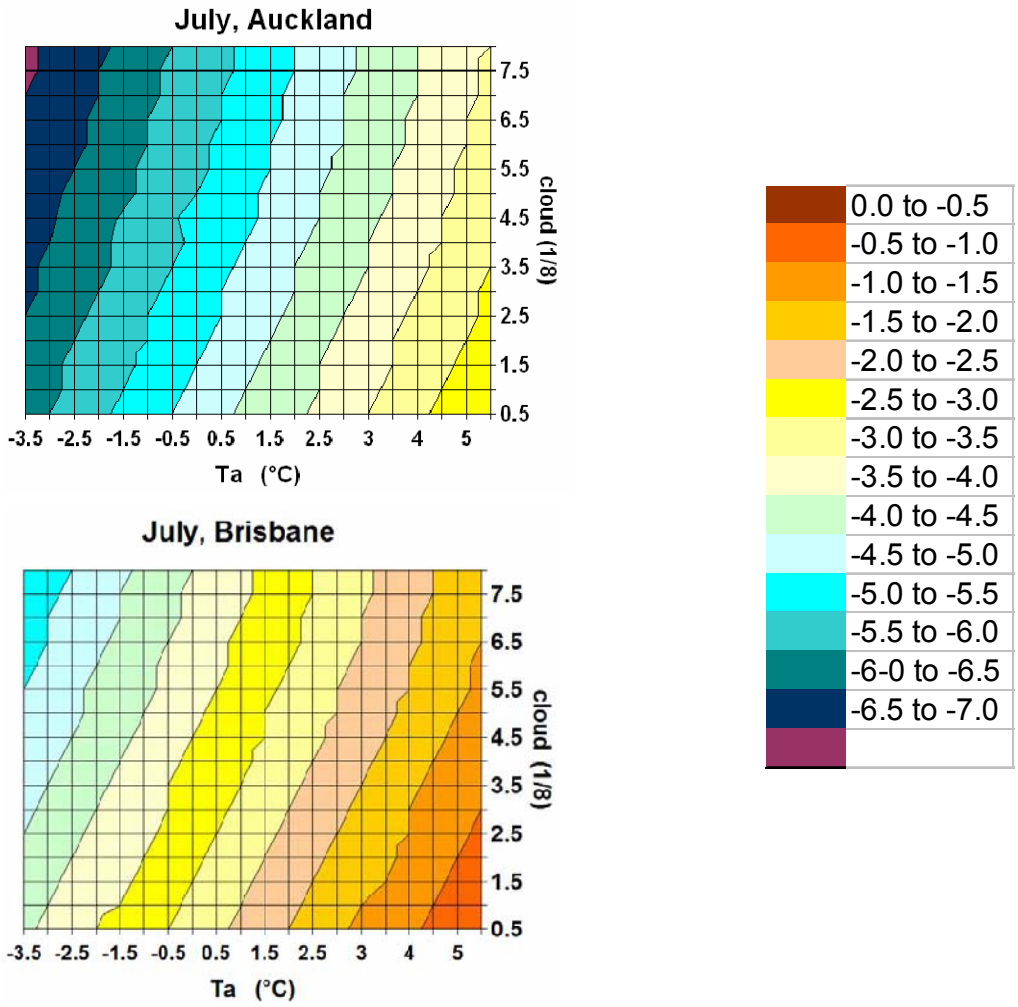

Fig. 2: Sensitivity of TSN to changes in air temperature (deg C) and cloud cover. Mean cloud for Auckland is 4.5 and 3.2 for Brisbane. TSN is calculated from an integrated human body-atmosphere energy budget holding relative humidity, wind and solar radiation constant at mean July values. Calculations consider conditions at solar noon. Activity and clothing level are 80 W m^{-2} and 0.5 clo, respectively

Given that, for many regions, climate is the main impetus for attracting visitors, it forms an important part of the natural resource base for tourism. Any change in climate will affect not only the resource but also demand for the resource. The capacity of society to respond will depend on tourism's sensitivity to changing climate. This will vary from region to region. An advantage of the response surface method is that it less likely to obscure inherent sensitivities to change that can occur in top down approach. Another is its flexibility. A wide range of new or changed scenarios can be easily handled by plotting them on the response surface. This avoids the need to rerun the transfer function, thus facilitating use by non-climate specialists such as planners and policy makers wanting to reassess impacts. In the top down approach the impression is given that a future climate state will occur at a particular time. This may not be particularly useful since a variety of planning time frames may be required. In contrast, the response surface me-

thod has an additional advantage of allowing, through interpolation, both longer and shorter term impacts to be assessed by way of response envelopes.

References

de Freitas, C.R., Fowler, A.M., 1989: Identifying sensitivity to climatic change at the regional scale: the New Zealand example. Proceedings of 15th Conference New Zealand Geographical Society, R. Welch (ed.), New Zealand Geographical Society Conference Series, No. 15, Dunedin, 254-261.

de Freitas, C.R., 2003: Tourism climatology: evaluating environmental information for decision making and business planning in the recreation and tourism sector. International Journal of Biometeorology, 47 (4), 190-208.

Höppe, P., 1999: The physiological equivalent temperature – a universal index for the biometeorological assessment of the thermal environment. - International Journal of Biometeorology 43: 71-75.

Matzarakis, A., Mayer, H., and Iziomon, M.G., 1999: Applications of a universal thermal index: physiological equivalent temperature. Int. J. Biometeorol. 43: 76-84.

McGregor, G.R., Markou, M. T., Bartzokas, A., Katsoulis, B.D., 2002: An evaluation of the nature and timing of summer human thermal discomfort in Athens, Greece. Clim. Res. 20: 83-94.

New, M., Hulme, M., Jones, P., 1999: Representing twentieth century space-time climate variability. Part 1: development of a 1961-1990 mean monthly terrestrial climatology. J. Clim. 12: 829-856.

New, M., Hulme, M. and Jones, P.D., 2000: Representing twentieth century space-time climate variability. Part 2: development of 1901-96 monthly grids of terrestrial surface climate. J. Clim. 13: 2217-2238.

VDI, 1998: Methods for the human-biometerological assessment of climate and air hygiene for urban and regional planning. Part I: Climate, VDI guideline 3787. Part 2. Beuth, Berlin.

Authors' addresses:

Prof. Dr. C. R. de Freitas (c.defreitas@auckland.ac.nz)
School of Environment, University of Auckland,
PB 92019 Auckland, New Zealand

Prof. Dr. Andreas Matzarakis (andreas.matzarakis@meteo.uni-freiburg.de)
Meteorological Institute, Albert-Ludwigs-University of Freiburg
Werthmannstr. 10, D-79085 Freiburg, Germany

Assessment of climate for tourism purposes in Germany

Christina Endler, Andreas Matzarakis

Meteorological Institute, Albert-Ludwigs-University of Freiburg, Germany

Abstract

The topic of climate and tourism is increasingly of high relevance due to the ongoing discussion about climate change. The close relationship between climate and tourism is confirmed by many studies. In the context of climate change adaptation to a changing climate becomes significant. The general objective of the BMBF joint research project CAST was both an analysis of climate, especially for tourism purposes and development of possible and potential adaptation strategies, in two climatic sensitive regions in Germany: the North Sea and the Black Forest.

1. Introduction

Due to the high relevance of climate and weather in industrial sectors such as tourism an adequate, easy understandable and complete assessment is required. Current climate conditions and weather thereby control, limit, and favour demand and supply in tourism and can affect decisively the motivation for travelling (UNWTO, 2008). Small changes in climate conditions can already result in huge losses in revenues. Higham and Hall (2005) identify climate change as the new challenge and determinant in tourism. It can be seen both as chance or risk and as chance and risk, especially in mountainous and coastal regions. Independent of the dimension of climate change a tourism industry without adaptation is faced with risks in many places. In order to estimate climatic, changes for tourism and recreation an integral assessment is required that is defined in the next section.

2. Method and Data

2.1. An integral assessment of climate

The assessment of climate for tourism and recreation is based on the climate facets introduced by de Freitas (2003): aesthetical, physical, and thermal. In this context, the thermal facet is regarded as the most important (Matzarakis et al., 2009).

Humans are exposed to and affected by the thermal environment. Büttner already stated 1938 that if one wants to assess the influence of climate on the human organism in the widest sense, it is necessary to evaluate the effects not only of a *single* parameter but of *all thermal components*. This leads to the necessity of modeling the human heat balance.

The Physiologically Equivalent Temperature (PET) is one thermal index based on the human energy balance and considering all relevant thermal components, especially short- and long wave radiation fluxes (Höppe, 1999).

From this it follows, that not only air temperature and precipitation ought to be included in the quantification of climate, which are the most common parameters in meteorology and climatology, but also parameters such as wind, snow, cloud cover, and a kind of perceived temperature, e.g. PET (Fig. 1). Furthermore, frequencies ("*number of days with*") of parameters considered in an analysis are more appropriate than mean values.

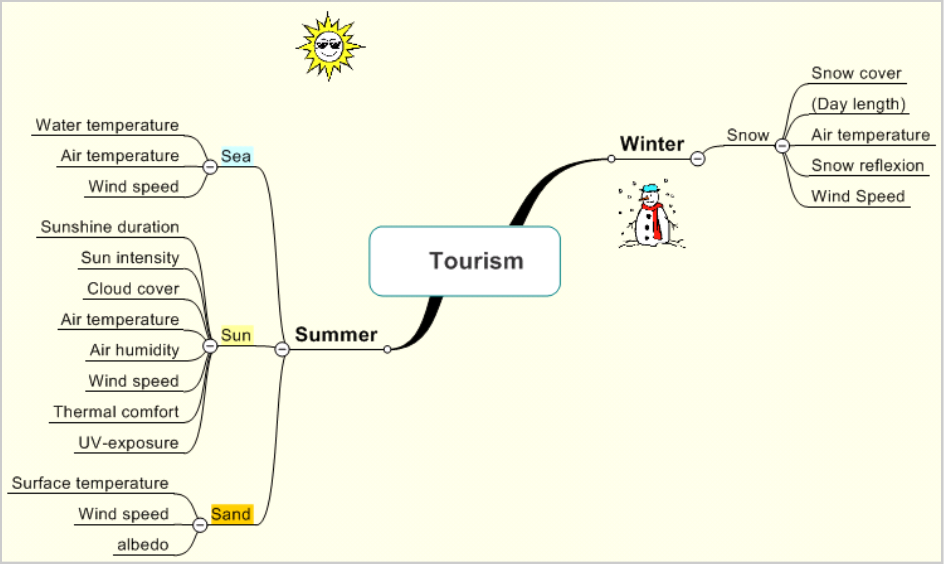

Fig. 1: Overview of the "*Quadruple S*" defined in tourism and corresponding parameters (Matzarakis, 2006)

2.2. Regional climate simulations

In order to reveal and assess the magnitude of vulnerabilities due to climate change climate simulations of two regional climate models (RCM) are used: REMO and CLM. The analysis considers the following parameters:

- Thermal acceptance:	18 °C < PET < 29 °C
- Cold stress:	PET < 0 °C
- Heat stress:	PET > 35 °C
- Humid-warm ("sultry")	conditions: vapour pressure > 18 hPa
- Sunny day:	cloud cover < 4 eights
- Fog:	relative humidity > 93 %
- Dry day:	precipitation ≤ 1 mm
- Wet day:	precipitation > 5 mm
- Stormy day:	wind velocity > 8 ms^{-1}
- Ski potential:	snow cover > 30 cm

Regional climate simulations used in this study have a spatial resolution of 0.088° (~10 km) for REMO (Jacob et al. 2001) and 0.167° (~18 km) for CLM (Steppeler et al. 2003). Both RCMs are driven by EHCAM5-MPI-OM (Roeckner et al., 2003, Marsland et al., 2003).
Future climate conditions are analysed for 2021-2050 compared to the reference 1971-2000. Two SRES scenarios, A1B and B1, are considered.

3. Results

3.1. North Sea

Till 2050, an increase in air temperature of about 1 °C is expected in the North Sea region. In this context, winter and autumn will stronger warm compared to summer and

spring resulting in strong decrease in cold stress. Additionally, major changes are referred to humid-warm conditions up to 5-15 days (Fig. 2, Table 1).

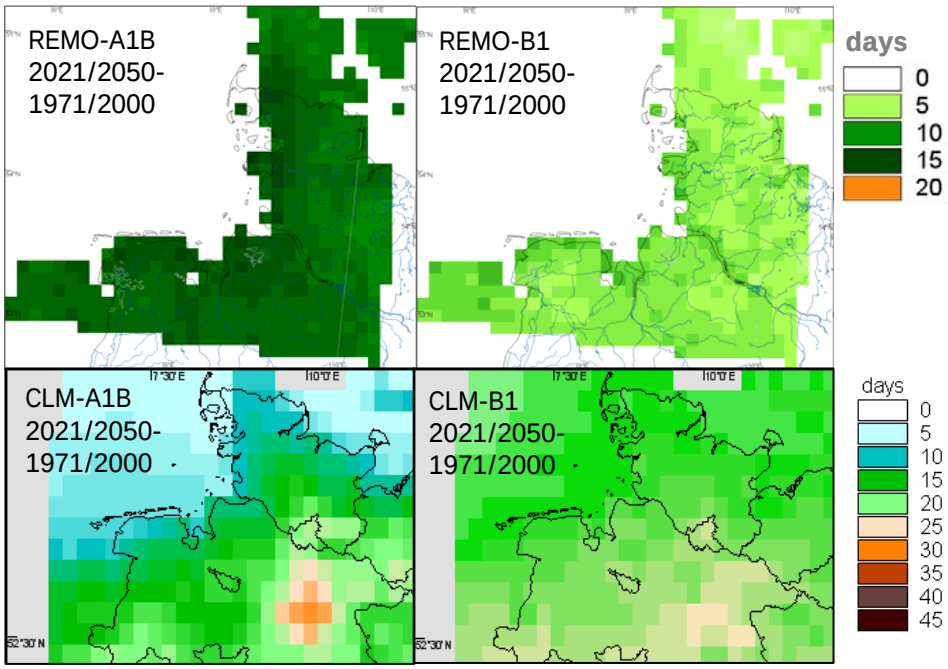

Fig: 2: Changes in humid-warm conditions for the North Sea region for 2021/2050 vs. 1971/2000 for both REMO (*upper panel*) and CLM (*lower panel*)

Thermal comfort will slightly increase. Due to the vicinity of the offshore, thermal and heat stress will not play any role in future.

Table 1: A qualitative summary of parameters analysed for the North Sea region based on the two regional climate models CLM and REMO. The notation "--/++" defines a moderate decrease/increase, "-/+" a slight decrease/increase, "0" no changes in the model, and "n. s." not specified due to huge variations between the scenarios A1B and B1

Parameter	**CLM**	**REMO**
Thermal acceptance	+	+
Cold stress	--	--
Heat stress	0	0
Humid-warm („sultry") conditions	+	++
Sunny day	-	n. s.
Dry day	--	n. s.
Wet day	+	+
Fog	n. s.	n. s.
Stormy day	+	n. s.

Annual changes in precipitation might be not expected but redistribution throughout the year. In this context, winter precipitation will increase while summer precipitation will decrease. This pattern is also reflected by changes in dry or wet days, respectively.

Changes in sunny and stormy days as well as fog are not significant (Table 1).

3.2. Black Forest

The strong winter warming will have also an impact on changes in cold stress as well as on snow depth and ski potential decreasing about 15-20 days. These both parameters and humid-warm conditions show largest changes.

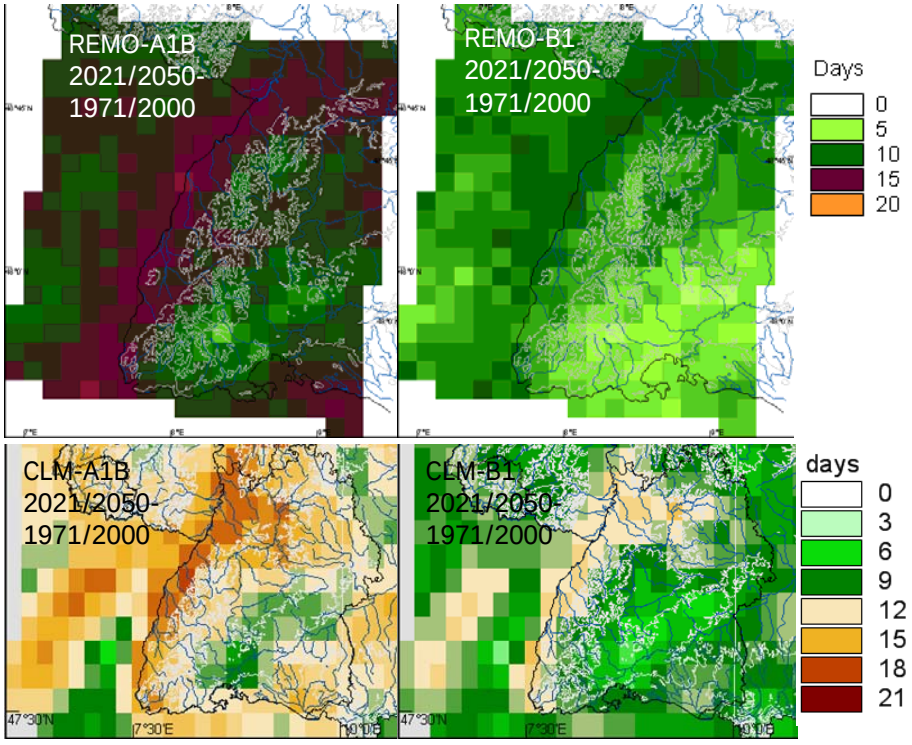

Fig: 3: Changes in humid-warm conditions for the Black Forest region for 2021/2050 vs. 1971/2000 for both REMO (*upper panel*) and CLM (*lower panel*)

Both cold stress and snow days (ski potential) will decrease about 15-20 days, whereby lower regions are more affected. In contrast, humid-warm conditions will only increase during summer by about 5-15 days (Fig. 3). In this context, higher regions are hardly affected.

Changes in precipitation are slightly more pronounced compared to the average of Germany due to processes induced by orography in the Black Forest affecting the hydrological cycle.

Changes in wind and cloud cover are hardly visible due to the challenge of modelling, among other (Table 2).

Table 1: A qualitative summary of parameters analysed for the Black Forest region based on the two regional climate models CLM and REMO. The notation "--/++" defines a moderate decrease/increase, "-/+" a slight decrease/increase, "0" no changes in the model, and "n. s." not specified due to huge variations between the scenarios A1B and B1

Parameter	CLM	REMO
Thermal acceptance	+	-
Cold stress	--	--
Heat stress	+	n. s.
Humid-warm („sultry") conditions	++	++
Sunny day	-	n. s.
Dry day	-	n. s.
Wet day	+	+
Fog	n. s.	n. s.
Stormy day	0	0
Ski potential	--	--

4. Conclusion

Model results for the North Sea and the Black Forest show that climatic changes are not so pronounced until 2050 compared to the end of the 21st century. In general, changes in B1 are somewhat lower compared to A1B.

Both models show generally same tendencies but differing in their magnitudes. One exception is the thermal acceptance in the Black Forest. While it increases in CLM, it will decrease in REMO.

Moreover, REMO indicates a wider range of the possible development of climate between A1B and B1. Although the evolution of emissions and GHG concentration is rather homogenous until 2040 and both RCMs are driven by the same general circulation model, differences can be due to RCM formulation and parameterization.

Main changes are referred to the thermal component, in particular cold stress and humid-warm conditions, and to snow. Altogether they tend to affect both summer and winter tourism. Hence, adaptation strategies, especially in the Black Forest are essential.

Acknowledgement

Thanks to the Federal Ministry of Education and Research (BMBF) for funding the sub research project "*Weather and Climate Analysis*", which is part of the joint research project CAST (promotional reference: 01LS05019) within the scope of the research initiative klima*zwei*.

References

Büttner, K., 1938: Physikalische Bioklimatologie. Akademische Verlagsgesellschaft Leipzig.

de Freitas, C.R., 2003: Tourism climatology: evaluating environmental information for decision making and business planning in the recreation and tourism sector". Int. J. Biometeorol. 48, 45–54.

Hall, C.M., J. Higham, 2005: Tourism, Recreation and Climate Change. Channel View Publications, Clevedon, UK.

Höppe, P., 1999: The physiological equivalent temperature - a universal index for the biometeorological assessment of the thermal environment. Int. J. Biometeorol. 43, 71–75.

Jacob D, B.J.J.M. an der Hurk, U. Andræ, G. Elgered, L.-P. Graham, C. Fortelius, S.D. Jackson, U. Kartens, Chr. Koepken, R. Lindau, R. Podzun, B. Roeckel, F. Rubel, B.H. Sass, R.N.B. Smith, X. Yang, 2001: A comprehensive model inter-comparison study investigating the water budget during the BALTEX PIDCAP period. Meteorol. Atmos. Phys. 77, 19–43.

Marsland G.A., H. Haak, J.H. Jungclaus, M. Latif, F. Röske, 2003: The Max Planck Institute global/sea-ice model with orthogonal curvilinear coordinates. Ocean Model 5, 91–127.

Matzarakis, A., 2006: Weather- and Climate-Related Information for Tourism. Tourism and Hospitality Planning and Development 3, 99–115.

Matzarakis, A., H. Mayer, M. Iziomon, 1999: Applications of a universal thermal index: physiological equivalent temperature“. Int. J. Biometeorol. 43, 76–84.

Roeckner, E., G. Bäuml, L. Bonaventura, R. Brokopf, M. Esch, M. Giorgetta, S. Hagemann, I. Kirchner, L. Kornblueh, E. Manzini, A. Rhodin, U. Schlese, U. Schultzweida, A. Tompkins, 2003: The atmospheric general circulation model ECHAM5. Part I: Model description. Max Planck Institute for Meteorology, Report No. 349. Hamburg

Steppeler J, G. Doms, U. Schaettler, H.W. Bitzer, A. Gassmann, U. Damrath, G. Gregoric, 2003: Meso-gamma scale forecasts using the nonhydrostatic model LM. Meteorol. Atmos. Phys. 82, 75–96.

UNWTO, 2008: Climate Change and Tourism - Responding to Global Challenges. UNWTO, World Tourism Organization und the United Nations Environment Programme, Madrid, Spain.

Authors' address:

Dipl.-Met. Christina Endler (christina.endler@meteo.uni-freiburg.de)
Prof. Dr. Andreas Matzarakis (andreas.matzarakis@meteo.uni-freiburg.de)
Meteorological Institute, Albert-Ludwigs-University of Freiburg
Werthmannstr. 10, D-79085 Freiburg, Germany

Application of Physiologically equivalent temperature for assessment of extreme climate regions at the Russian Far East

[1]E.A. Grigorieva, [2] A. Matzarakis

[1]Institute for Complex Analysis of Regional Problems, Far Eastern Branch, Russian Academy of Sciences, Birobidzhan, Russia
[2] Meteorological Institute, Albert-Ludwigs-University of Freiburg, Germany

Abstract

Assessment of climatic conditions at the southern part of the Russian Far East has been carried out by the use of the physiologically equivalent temperature (PET) based on the body-atmosphere energy balance; results are presented as bioclimatic maps for spatial assessment of climate. The spatial patterns for all southern part of the Russian Far East are constructed to get general (on the climatic data) and more or less adequate bioclimate information for areas with low density of hydrometeorological stations. They allow identifying areas with extreme and uncomfortable thermal conditions for every season and every month. The results of the present study can be helpful in applied climatology especially in tourism and recreation researches, in regional planning and environmental medicine as well.

1. Introduction

Many different models and indices were developed during the second half of the 20th century for estimating the complex influence of atmospheric thermal environment on human being. Assessment of thermal bioclimate may be done by using climate indices, e.g. Heat stress index, Discomfort index (Thom, 1959), Wind-chill index (Steadman, 1971) or similar ones that are based on atmospheric parameters such as air temperature, humidity, wind speed etc. But they did not include the effect of radiation fluxes, did not account thermo-physiological regulatory processes and had a lot of various limitations (Mayer and Höppe, 1987; Höppe, 1999).

To estimate relations between atmospheric environment and human health in a more relevant way the methods of heat balance of humans are used (Burton and Edholm 1955; Fanger, 1972; Höppe, 1999). Physiologically equivalent temperature (PET) is developed on the base of body-atmosphere energy balance and may be calculated by the RayMan model which has been developed for applied climate studies. The main feature and advantage of RayMan to other similar models is the calculation of short- and long-wave radiation fluxes and the possibility to evaluate thermal environment throughout the whole year and use of commonly known unit (^{o}C). RayMan has a boarder use for a variety of application: for assessing climate in human biometeorology, in applied climatology, and for recreational issues and environmental medicine (Matzarakis et al., 2007b).

The objective of the present paper is to give an application of PET for the assessment of the thermal environment for the extreme thermal climate of the Russian Far East located at the temperate monsoon climatic zone characterized by an extreme continental regime of annual temperatures. Spatial visualization on monthly and seasonal PET bioclimate maps is constructed on the base of climatic values, for the whole study area, where terri-

tories with extreme and uncomfortable thermal bioclimatic conditions and heat stress affection are identified.

2. Methods and study area

The RayMan model is based on the energy-balance equation of the human body and is evolved founded on (VDI, 1994; VDI, 1998). The model is developed for urban climate studies and has a broader use in applied climatology and tourism investigations as well. Finally several thermal indices such as Predicted Mean Vote (PMV), Physiologically Equivalent Temperature (PET) and Standard Effective Temperature (SET*) may be calculated for the assessment of human bioclimate in a physiologically relevant manner as shown in several applications (Matzarakis et al., 1999; Blazejczyk, Matzarakis, 2007; etc). All indices have the known grades of thermal perception for human beings and physiological stress (Höppe, 1999).

PET is defined as a certain air temperature related to fixed standard indoor conditions at which the heat balance of the human body is maintained with core and skin temperature equal to those under the conditions being assessed (VDI, 1998; Höppe, 1999). Compared to other thermal indices it has the advantage of commonly known unit (^{o}C) which makes results to be easily understandable to people unfamiliar with the human-biometeorological terminology. Other advantage of PET is that values may be calculated for each day and time of the year in different climates with easy and complex environment (Matzarakis et al., 1999; Matzarakis et al., 2007b). They can be attributed for different grades of thermal perception and physiological stress with a valid assumption for standard person with the definite internal heat production (80 W) and thermal resistance of the clothing (0.9 clo) (Matzarakis and Mayer, 1996).

All meteorological parameters influence the human energy balance including air temperature, vapor pressure, wind speed, as well as short- and long-wave radiation parameterized by the mean radiation temperature (MRT) of the surroundings. Data on short- and long-wave radiation are generally not available in climate records. In the case of the absence of radiation data, MRT may be estimated by cloud cover, time of the year and type of surface cover (Matzarakis et al., 2007b).

In the current study, spatial distribution of PET is used to assess thermo-physiologically the thermal conditions of meteorological environment in the Far-Eastern Federal Okrug of the Russian Federation. The study area is situated at the northern latitude from 40^{o} to 60^{o} and at the eastern longitude from 125^{o} to 145^{o} in Khabarovsky Krai, Primorsky Krai (Primorye), Amursk Region, Jewish Autonomous Region and is named as the southern part of the Russian Far East. The topography of the area is varied, comprising extensive mountainous regions stretching mainly from south-west to north-east. It has temperate monsoon climate characterized by an extreme continental regime of annual temperatures. The annual air temperature range is near 45-50 ^{o}C, which characterizes the continentality of Middle Siberia; the annual mean temperatures are between -7.3 ^{o}C and 5.0 ^{o}C. Annual precipitation varies between 400 and 1000 mm, and nearly 80 % of it falls in the period of summer monsoon from June till September.

Several authors (e.g. Gorbatcevich, 1894; Matukhin, 1971) have highlighted the extreme bioclimates found in these areas: conditions in the southern Far East in long cold winter are similar to that in Siberia; and in summer, like that of the warm, humid tropics. Human discomfort in monsoon climatic conditions of the Far East is a

combination of the low temperatures and wind in winter and of high air temperatures with high relative humidity creating an unpleasant, sultriness feeling, in summer (Grigorieva, 2007).

Standard climate data such as air temperature, relative air humidity, wind speed and cloud cover are used to quantify the thermal bioclimatic conditions. These data are available through the International Water Management Institute World Water and Climate Atlas (New et al., 2002): the climatology was interpolated from a data set of station means for the climate normal period centered on 1961 to 1990 and was constructed of a 0.1° latitude (longitude) data set of mean monthly surface climate.

3. Results

The spatial visualization of thermal conditions for human-biometeorological significant analysis may be obtained from spatial distribution of PET; for this purpose monthly and seasonal PET bioclimate maps are constructed including a combination of climate parameters. Thus, instead of daily resolution we may offer only mean monthly and season conditions as basic information of average state of thermal bioclimatic conditions.

The map for the winter period (December, January and February) shows that PET values vary from -15 to -40 ^{o}C increasing from south-east to north-west of thermo-physiological extreme cold stress level (Fig. 1). Low values in the north-western part of the study area (up to -45 ^{o}C in high mountains) reflect the great continentality of this region. The coastal locations along the coasts of the Japanese sea show the maritime influence of the Pacific Ocean with sufficiently high values near -15 ^{o}C at the extreme south. Comparatively high air temperatures in the lowlands at the Amur River basin give low PET values due to the impact of the strong winds.

During spring (March, April and May) PET values range from -5 to +15 ^{o}C in the range of thermo-physiological extreme cold stress level at the north and in mountainous regions (e.g. in Dzugdzur Mountain Range along the coasts of the Okhotsk sea PET reaches -5 to -10 ^{o}C) to slight cold stress at the south continental regions. Plane areas are expressed in comparatively high PET values close to favorable bioclimate conditions.

In summer months (June, July and August), PET conditions may reach values from 5 to 25 ^{o}C (Fig. 2). Particularly in summer, the dependence of PET value on the location results in a marked variation between PET values calculated for different places. Plane sites with slight heat stress show much higher thermal stress than mountainous ones. Favorable conditions with thermal comfort (PET values without thermal stress) are obtained only in higher elevated areas but only at the central part of the study area; northern mountains are situated in the zones with thermal moderate cold stress even in the summer period.

In autumn (September, October and November), PET ranges from -30 to 0 ^{o}C. The spatial distribution is similar to that in summer. The highest values characterize the southern locations and sites along the coasts of the Japanese Sea. The coldest parts are at the elevated locations at the north-west and in the mountains. As a whole autumn is much colder than spring that may be explained by the cold (air temperatures are very close to winter values) and windy November.

In all seasons, the lowest PET values are observed in elevated areas, e.g. in Sikhote-Alin and Dzugdzur; the highest at the continental lowlands near the Middle Amur and at extreme south at the coastal region of the Japanese Sea.

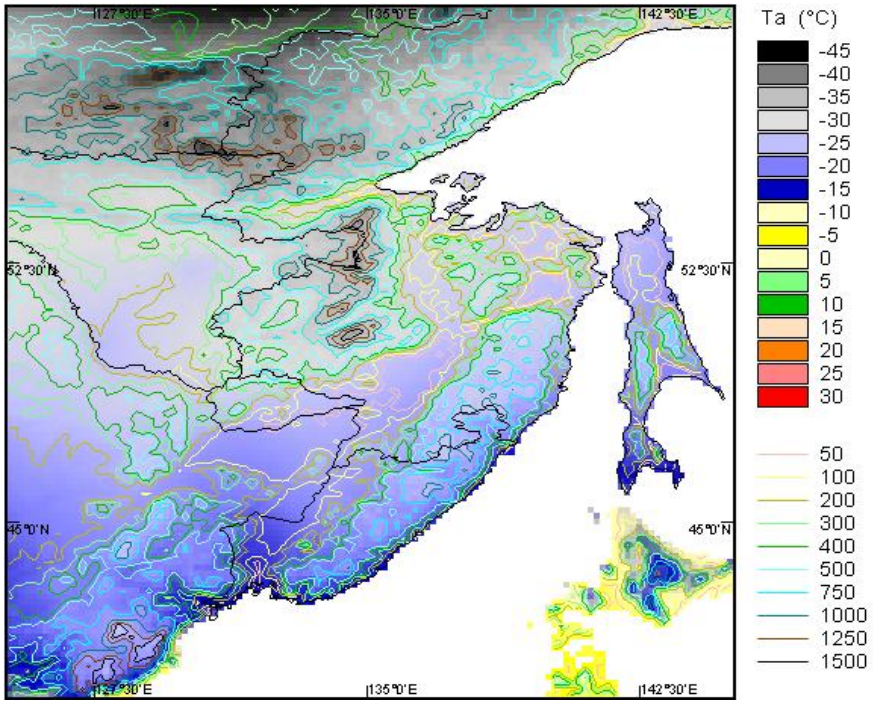

Fig. 1: Physiologically equivalent temperature for winter (December, January, February in the Far East Russia for the period 1961-1990

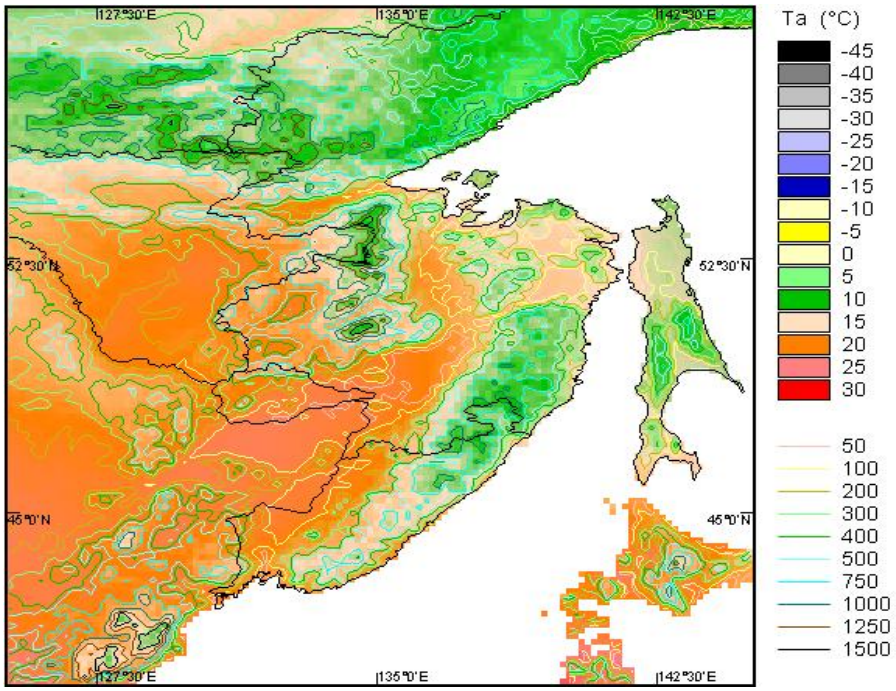

Fig. 2: Physiologically equivalent temperature for summer (June, July, August) in Far East Russia for the period 1961-1990

4. Discussion

Human-biometeorological assessment of climatic conditions at the southern part of the Russian Far East has been carried out by using the physiologically equivalent temperature based on the body-atmosphere energy balance; results are presented as bioclimatic maps for spatial assessment of climate.

As it was shown earlier (Matzarakis et al., 1999) one of the main advantages of PET is that it may be used for any time of the year in different climates and in temperate as well. We use it successfully for bioclimatic evaluation of temperate monsoon climatic zone with extreme thermal regime of the Russian Far East. The spatial patterns are constructed to get general (on the climatic data) and more or less adequate bioclimate information about areas with low density of hydrometeorological stations. They allow to identify regions with extreme and uncomfortable thermal conditions for every season and every month. We assume that this approach gives a method for the solution of a concrete task using meteorological information for example in assessment of heat (or cold) waves that may influence additional mortality in humans at the study area.

We may compare spatial distribution of PET with other regions of the world i.e. with Europe (Matzarakis et al., 2007a) or with Japan (Matzarakis, 2008). The PET conditions in winter in studied locations in Russia are considerably lower in comparison even to Northern Europe. Only PET values for the extreme southern part of the target area are similar for the northern Europe and Japan. During summer, the PET conditions in the southern and central parts of the study area are more similar to the conditions of central and northern Europe and Japan. We assume that this approach gives a method to get general and more or less adequate bioclimate information for areas with low density of climate stations. Bioclimatic maps are of interest because they can be applied in climate and health and also in climate impact research for analyzing thermal stress situations, in tourism and recreation for selection of holiday destination.

5. Conclusion

Physiologically equivalent temperature is well suited for the human-biometeorological evaluation of the thermal environment of different climates including extreme climate regimes of the Russian Far East. Spatial visualization on seasonal PET bioclimate maps gives a general evaluation of thermo-physiologically relevant information. Nevertheless we may assume more or less detail spatial assessment when territories with extreme and uncomfortable thermal conditions and heat stress affection may be identified. The results of the present study can be helpful in applied climatology especially in tourism and recreation researches, in regional planning and environmental medicine as well.

Acknowledgement

The work was supported by RHSF: project No. 09-02-88202a/T, and FEB RAS: projects No.09-III-A-09-497 and 09-III-A-09-498.

References

Blazejczyk, K., A. Matzarakis, 2007: Assessment of bioclimatic differentiation of Poland based on the human heat balance. Geographia Polonica. 80, 63-82.

Burton, A.C., O.G. Edholm, 1955: Man in cold environment: physiological and pathological effects of exposure to low temperatures. Edward Arnold, London, 273.
Fanger, P.O., 1972: Thermal comfort. McGraw-Hill, New York, 244.
Gorbatcevich, E.F., 1894: A climate of Khabarovsk. Hygienic studies (in Russian). Priamurye Military District Press, Khabarovsk, 78.
Grigorieva, E.A., 2007: Acclimatization demands of recreationists moving within the southern region of the Russian Far East. In: Developments in Tourism Climatology (A. Matzarakis, C.R. de Freitas and D. Scott, Eds.) University of Freiburg, Freiburg, 214-220.
Höppe, P.R., 1999: The physiological equivalent temperature – a universal index for the biometeorological assessment of the thermal environment. Int. J. Biometeorol. 43, 71-75.
Matukhin, V.A., 1971. Bioclimatology of human in the monsoon conditions (in Russian). Nauka, Leningrad, 136.
Matzarakis, A., H. Mayer, 1996: Another kind of environmental stress: Thermal stress. NEWSLETTERS No. 18, WHO Collaborating Centre for Air Quality Management and Air Pollution Control. 7-10.
Matzarakis, A., 2008: Relevance of thermal bioclimate for tourism in Japan. In: Global Environmental Research 12, 129-136.
Matzarakis, A., H. Mayer, M.G. Iziomon, 1999: Application of a universal thermal index: physiological equivalent temperature. Int. J. Biometeorol. 43, 76-84.
Matzarakis, A., T. Georgiadis, F. Rossi, 2007a: Thermal bioclimate analysis for Europe and Italy. Il Nuovo Cimento. 30 C, 623-632.
Matzarakis, A., F. Rutz, H. Mayer, 2007b: Modelling radiation fluxes in simple and complex environments – Application of the RayMan model. Int. J. Biometeorol. 51, 323–334.
Mayer, H., P.R. Höppe, 1987: Thermal comfort of man in different urban environments. Theor. Appl. Climatol. 38, 43-49.
New, M., D. Lister, M. Hulme, I. Makin, 2002: A high-resolution data set of surface climate over global land areas. Clim. Res. 21, 1-25.
Steadman, R.G., 1971: Indices of windchill of clothed person. J. Appl. Meteorol. 10, 674-683.
Thom, E.C., 1959: The Discomfort Index. Weatherwise. 12, 57-60.
VDI, 1994: Environmental Meteorology, Interactions between Atmosphere and Surface; Calculation of the short- and long wave radiation. VDI- guideline 3789. Part 2. Beuth, Berlin, 48.
VDI, 1998: Methods for the human-biometeorological evaluation of climate and air quality for urban and regional planning. Part I: Climate. VDI-guideline 3787. Part 2. Beuth, Berlin, 29.

Authors' address:

Dr. Elena A. Grigorieva (eagrigor@yandex.ru)
Institute for Complex Analysis of Regional Problems
Far Eastern Branch, Russian Academy of Sciences
Sholom-Aleikhem, 4, Birobidzhan, Russia

Prof. Dr. Andreas Matzarakis (andeas.matzarakis@meteo.uni-freiburg.de)
Meteorological Institute, Albert-Ludwigs-University of Freiburg
Werthmannstr. 10, D-79085 Freiburg, Germany

Climate-Tourism-Information-Scheme (CTIS)

Andreas Matzarakis, Timm Schneevoigt, Olaf Matuschek, Christina Endler

Meteorological Institute, Albert-Ludwigs-University of Freiburg, Germany

Abstract

For the assessment of weather and climate in tourism regions the Climate-Tourism-Information-Scheme (CTIS) has been developed. CTIS represents frequencies, probabilities and thresholds of tourism climatic and bioclimatic factors. In addition, CTIS is a software that can operate this relevant data from text-based files and generate highly customizable diagrams. It can easily be used and implemented for diverse applications i.e. decision making or information about tourism industry.

1. Introduction

Weather and climate are important factors for tourism and recreation which are both promoting and limiting factors (Matzarakis 2006). For an integral assessment and implementation of the different facets of climate in tourism (Fig. 1) for both experts and tourism industry a clear and user friendly visualization is needed for information transfer. The results have, however, to be based on scientific knowledge.

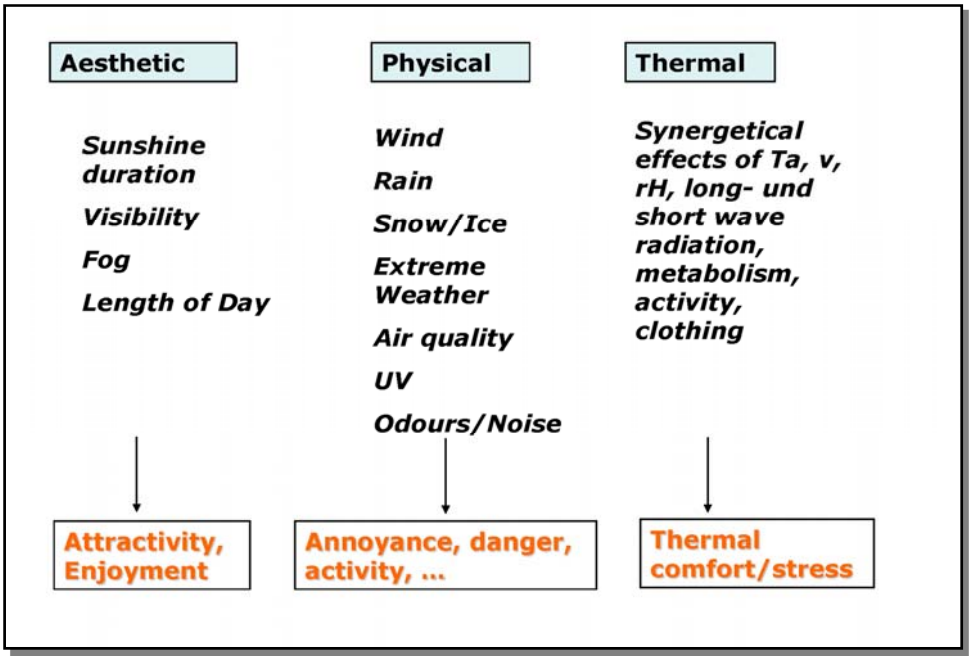

Fig. 1: Facets of climate in tourism (based on de Freitas, 2003)

Based on these demanded requirements the Climate-Tourism-Information-Scheme (CTIS) (Matzarakis 2007, Lin and Matzarakis 2008, Matzarakis et al. 2009) has been developed to create a simply representation and visualization of all these factors.

2. Climate-Tourism-Information-Scheme

CTIS (Matzarakis 2007, Lin and Matzarakis 2008) represents frequencies and probabilities of different bioclimatic and tourism climatic factors from all facets. It combines thermal components like physiological-equivalent-temperature ranges and thresholds, aesthetic components like cloudiness and fog, and physical components like wind speed, precipitation, and vapor pressure. The frequencies of these factors are presented in 10-day intervals visually grouped by months. An example is shown in Fig. 2 for Feldberg for the period 1971-2000. The definitions and thresholds of the different factors are shown in Table 1 (Matzarakis 2009).

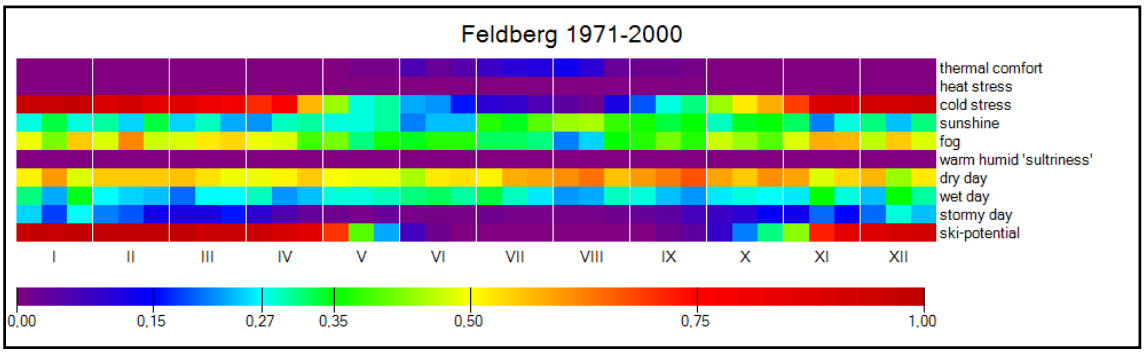

Fig. 2: CTIS for the Feldberg (Period: 1971-2000) in a temporal resolution of 10-days based on data from the German Weather Service (DWD)

Table 1: Factors, ranges, and sources for thresholds included in CTIS (after Matzarakis, 2007)

Factor	**Range**	**Literature**
thermal comfort	18 °C < PET < 29 °C	Matzarakis, 2007
heat stress	PET > 35 °C	Matzarakis und Mayer, 1996
cold stress	PET < 0 °C	Matzarakis, 2007
sunshine	sky cover < 5/8	Gómez Martín, 2004
fog	Relative humidity > 93 %	Matzarakis, 2007
warm humid („sultriness“)	vapor pressure > 18 hPa	Scharlau, 1935
dry day	precipitation ≤ 1 mm	Matzarakis, 2007
wet day	precipitation > 5 mm	Matzarakis, 2007
stormy day	wind speed > 8 m/s	Besancenot, 1990; Gómez Martín, 2004
ski-potential	snow cover> 30 cm	OECD, 2007

*PET = Physiologically Equivalent Temperature

3. CTIS software

CTIS has been developed in a user friendly way. It reads text based data files that contain frequencies of all climatic factors the user wants to present in his diagram. These factors have to be scaled on a uniform scale like 0 to 1 or 0 to 100. The CTIS program consists of two parts: the main window including data import and basic preparation (Fig. 3) and second, the report window for fine tuning the resulting image in size and font with real-time preview (Fig. 4).

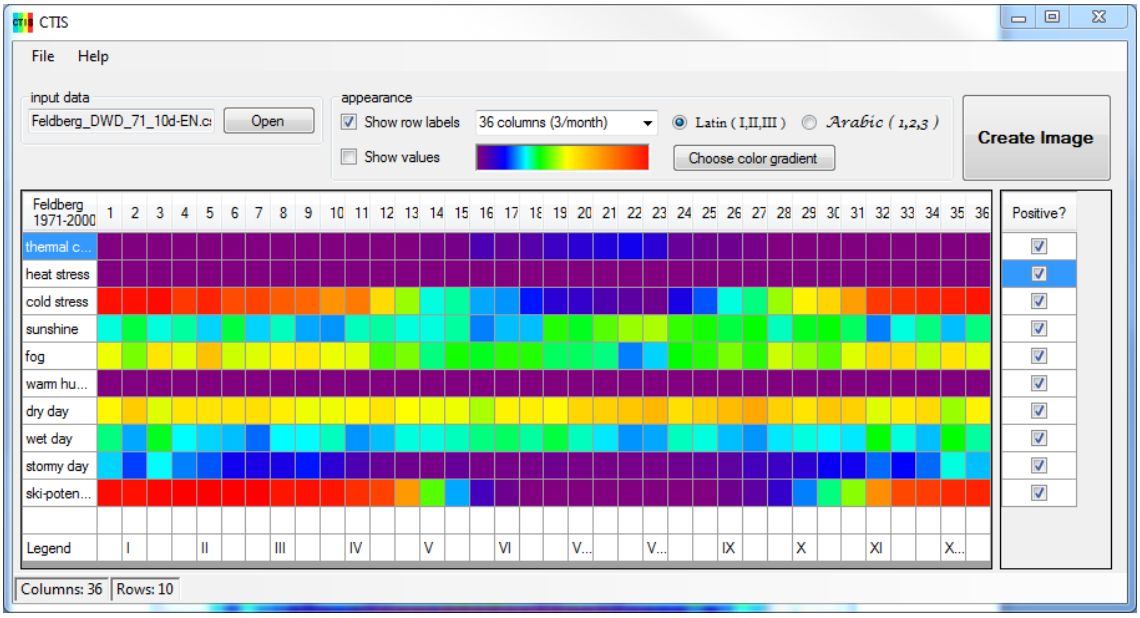

Fig. 3: CTIS main window for import of data, visual options and preparation of the factors (positive or negative)

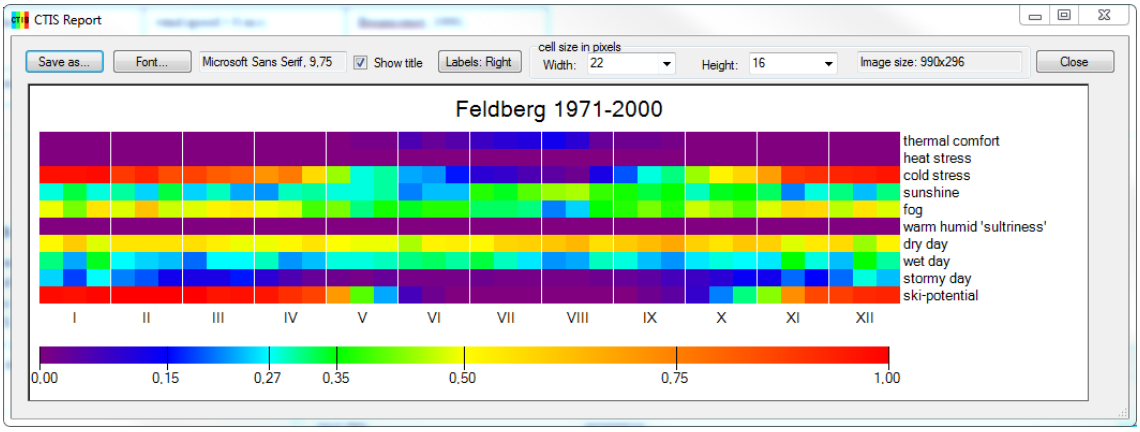

Fig. 4: CTIS report window for further visual options, font type and image size

As seen in Fig. 3 factors may be rated as positive or negative resulting in an inversion of the assessment scale for those rows. This rating is intended to use with classification coloring, not with colors interpolated according to frequencies.

After importing data the user is able to customize labeling options and time resolution options for visual grouping of intervals like 10-day periods grouped to months. Possible options are:

Time intervals:

- 1 value per month (12 columns)
- 3 values per month (36 columns)
- 1 value per hour (24 columns)
- 1 value per week (52 columns)

Legend numbering:

- Latin (I, II, III, …)
- Arabic (1, 2, 3, …)

Font type:

- Font type and size can be chosen from the standard windows font type dialog

Other visual options:

- Show or hide data values in diagram cells
- Show or hide factor (row) descriptions
- Place factor descriptions left or right of the diagram
- Show or hide diagram title

The dialogs for these choices are shown in Fig. 5 and Fig. 6.

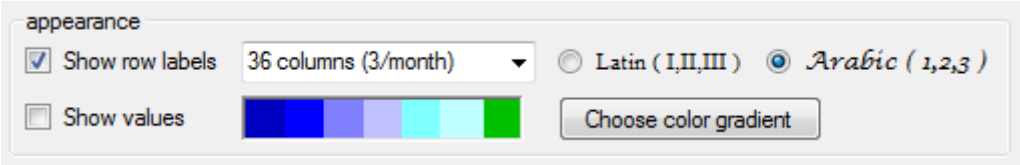

Fig. 5: Set of options in the CTIS main window

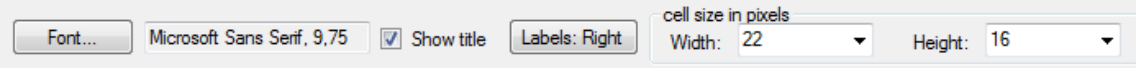

Fig. 6: Set of options in the CTIS report window

Moreover, the user can freely modify the color gradient used to classify frequencies or probabilities. Color values can be interpolated or classified as shown in Fig. 7.

Fig. 7: Color gradient comparison of an interpolated gradient (left) and classified gradient (right), both based on the same thresholds

For this purpose there is an additional dialog for creating value-color mappings and specifying assessment classes and descriptions. As shown in Fig. 8 values can be assigned to colors and a description. If *Interpolate Colors* is deactivated those descriptions appear in the diagram legend as class names. Advanced options are colors for error values and optical restriction of decimal places. The complete color gradient configuration can be saved and reused with other datasets without going through the setup process again.

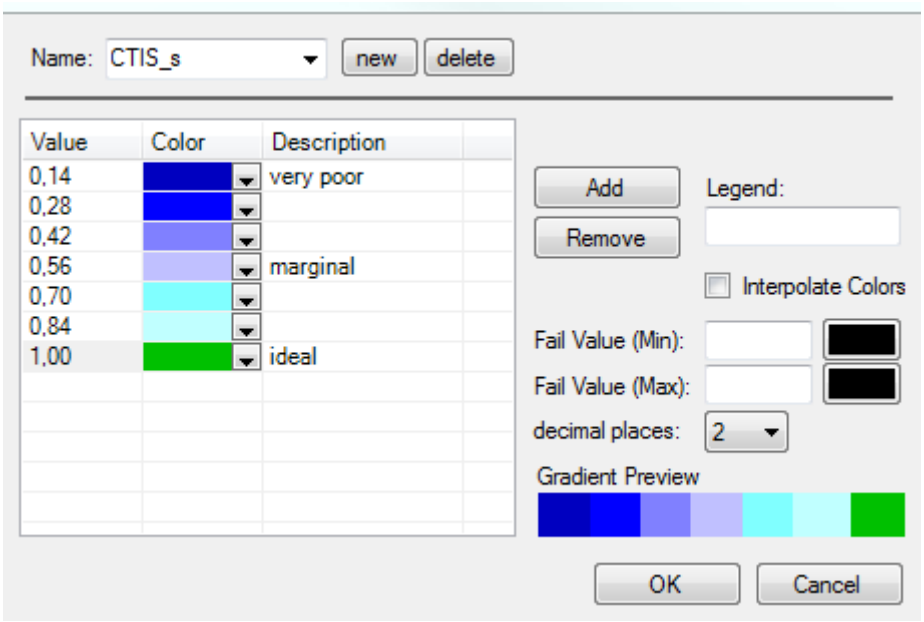

Fig. 8: Color gradient dialog

Finally, Fig. 9 shows a CTIS of the same data used for Fig. 2 but with the classification gradient of Fig. 8 and positive or negative ranked factors (Zaninovic and Matzarakis, 2009).

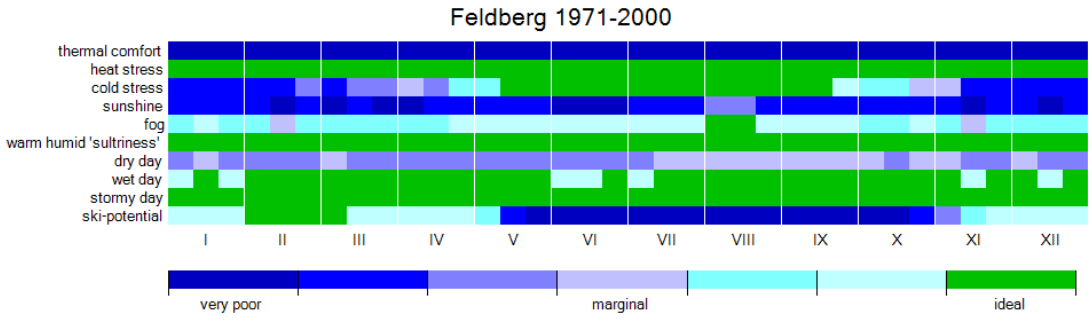

Fig. 9: CTIS with classes for the Feldberg (period: 1971-2000) in a temporal resolution of 10-days based on data from the German Weather Service (DWD)

The result image can be saved as .gif, .jpg or .png image file. sing Office 2007 the user can directly import the saved image to a new Word or PowerPoint document.

In order to improve the workflow when regularly creating multiple diagrams from different data sets or with different visual setups the complete program state can be saved in a settings file. The ability to load these previously saved setting files allows for a quick switch between different tasks working with numerous CTIS diagrams.

4. Conclusions

Required climate and climate relevant information has to be presented and visualized in an easily understandable way for non experts. Because of the plenty of kinds of tourism and the diverse requirements on climate information an integral assessment of weather and climate in one single factor or value is very difficult and too complex to understand. One single value let too many information and factors unconsidered. This lack can be filled by CTIS including the most relevant factors based on the climate facets in tourism and recreation.

Specific kinds of tourism possibilities based on CTIS can be assessed, quantified and periods with occurrence of specific extremes e.g. heat waves or periods of strong wind can detected.

The CTIS-Software is available under http://www.urbanclimate.net/climtour.

References

de Freitas C. R., 2003: Tourism Climatology: evaluating environmental information for decision making and business planning in the recreation and tourism sector. Int. J. Biometeorol. 48, 45–54.

Matzarakis, A., 2006: Weather and climate related information for tourism. Tourism and Hospitality Planning & Development 3, 99-115.

Matzarakis, A., 2007: Assessment method for climate and tourism based on daily data. In: A. Matzarakis, C. R. de Freitas, D. Scott (Eds.), Developments in Tourism Climatology, 52-58

Matzarakis, A., Möller, A., Kreilkamp, E., Carstensen, I., Bartels, C., Burandt, S., Endler, C., 2009: Anpassungsstrategien zum Klimawandel touristischer Pilotdestinationen in Küsten- und Mittelgebirgsregionen. In: Mahammad Mahammadzadeh, Hendrik Biebeler, Hubertus Bardt (Hrsg.): Klimaschutz und Anpassung an die Klimafolgen. Köln: Institut der Deutschen Wirtschaft Köln Medien GmbH, 253-262.

Lin, T.-P., Matzarakis, A., 2008: Tourism climate and thermal comfort in Sun Moon Lake, Taiwan. Int. J. Biometeorol. 52, 281-290.

Zaninovic, K., Matzarakis, A., 2009: The Biometeorological Leaflet as a means conveying climatological information to tourists and the tourism industry. Int. J. Biometeorol. 53, 369-374.

Authors' addresses:

Prof. Dr. Andreas Matzarakis (andreas.matzarakis@meteo.uni-freiburg.de)
Timm Schneevoigt (timm.schneevoigt@saturn.uni-freiburg.de)
Olaf Matuschek (olaf.matuchek@uni-freiburg.de)
Christina Endler (christina.endler@meteo.uni-freiburg.de)
Meteorological Institute, Albert-Ludwigs-University of Freiburg
Werthmannstr. 10, D-79085 Freiburg, Germany

The tourism climate of Engadin, Switzerland

Christine Ketterer and Andreas Matzarakis

Meteorological Institute, Albert-Ludwigs-University of Freiburg, Germany

Abstract

Tourism is vitally important for the economy in Engadin, Switzerland. Climate and weather are presumed to be a natural capital of the region and therefore an economic capital. The context of climate change poses the question on the change of the tourism climate in Engadin. Using measured data of MeteoSwiss and the climate models REMO and CLM the thermal, physical and aesthetical facets are analyzed during the time period 1961–2100 and visualized by the Climate-Tourism-Information Scheme (CTIS). The consequences of climate warming are going to be more distinct from mid-century to 2100 than in the future years. The number of days with thermal comfort is going to increase, while the number of days with cold days is going to decrease. This trend is more distinctive using the A1B scenario than using B1 scenario. Increasing thermal comfort and decreasing duration and frequency of precipitation is going to be of particular importance for the summer tourism. For the winter tourism Engadin is going to feature snow reliable conditions, even if the probability of snow high over 30 cm is going to decrease - especially the snow conditions in early and late winter worsen- in Engiadina Bassa more than in the higher Engadin`Ota around St. Moritz.

1. Introduction

The economic branch of tourism is vitally important for Engadin, because tourism creates 68 % and 59 % of the regional added value in Engadina`Ota and Egadina Bassa (Kronthaler und Cartwright 2008). Jobs and income, preservation of the agriculture were preserved through tourism and rural exodus can be stopped (Schweizer Tourismus Verband 1999). Landscape, flora and fauna, climate and the existing infrastructure provide a basis for tourism, but the weather can be seen as the Achilles-heel.

Tourists react to weather forecast as well as on the weather on site or the commercial: St. Moritz promotes with *sun* as a protected trademark for the climate favour of Engadin since 1930. Climate and weather are presumed to be a natural capital of the region and therefore as economic capital. If the weather is not as good as expected, the tourists avoid outdoor activities or even cancel their stay. The weather on sight can be separated in different aspects, the integrated thermal aspects, considered using the thermal index *Physiologically Equivalent Temperature*, the physical aspect, like sun, wind or rain and aesthetical aspects, as sunshine duration or cloudiness (de Freitas 2003).

In the context of climate change pose a question on the change of the tourism climate and its potential in Engadin.

2. Method

Therefore the tourism climate of Engadin is analyzed using existing data of the netwok of MeteoSwiss and data of the climate models REMO (A1B, B1 scenario) and CLM (A1B scenario) over the period 1961-2100. The regional climate model REMO has been performed by Max Planck Institute for Meteorology and encompasses the region of Germany, Austria and Switzerland ((Jacob 2001; Jacob et al. 2001). Based on the local model of the Deutschen Wetterdienst CLM has a resolution of 18 km (Steppeler et al. 2003; Böhm et al. 2006).

To control the quality of the climate models, its data were compared with the measuring data of Buffalora, Scoul, Sta. Maria and Sils Maria.
Following parameters matter for the tourists: thermal comfort, snow, precipitation, sunshine duration and wind. The thermo-physiological perception has been calculated with the aid of the thermal Index *Physiologically Equivalent Temperature*, based on the human energy balance. Furthermore the conditions for winter sport, like snow high and skiing potentials and their future change should be studied.
At the end the results are presented as frequencies and exceeding of thresholds in a climate-tourism-information scheme (CTIS) (Matzarakis 2007).

Tab. 1: Parameter and their Thresholds used for CTIS

Parameter	**Thresholds**	**literature**
cold stress	PET < 0 °C	Mayer und Matzarakis (1999)
Thermal acceptability	18 °C < PET < 29 °C	Matzarakis (2007)
Heat stress	PET > 35 °C	Matzarakis und Mayer (1996)
Sunshine	Cloud Cover < 4/8	Gómez Martín (2004)
Wind	v > 8 m/s	Gómez Martín (2004)
Light Rain	RR > 1 mm	Matzarakis (2007)
Long rain	RR > 5 mm	Matzarakis (2007)
Ski potential	Snow > 30 cm	Uhlmann et al (2009), OECD (2007)

3. Exemplary results

The climate model CLM describes the climatic conditions not so appropriate than REMO. CLM underestimates precipitation about 50% and more. REMO pictures air temperature, precipitation, wind velocity and air moisture in the highly reliefed region with acceptable variations. The measured air temperature average 2.5 °C in Sils Maria over a period of 1998 - 2008 and the calculated air temperature 2.6 °C, the measured precipitation 1047 mm und the estimated 952 mm. In Sta. Maria the averaged air temperature is 5.4 °C and the estimated 5.1 °C from1961 – 90, the measured precipitation 791 mm and the estimated is 773 mm. The seasonal characteristic of precipitation can be seen in the model data, but the precipitation in winter is overestimated and so also the snow depth is twice high as measured.
The averaged annual PET is -7.1 °C on the 3300m high Mountain Corvatsch, in Sils Maria 0.7 °C, in Samedan 2.4 °C, on Buffalora 3.7 °C and in Scoul 7.8 °C. The rang of PET ranges from -62 °C on the top of Corvatsch to 31 °C in Scoul and Sils Maria during 1981 – 2000.

Over a period 1981 – 2000 the winter sport in Engadin profits by low rainfall and plenty of sunshine. PET values under -10 °C are no rareness at noonday in Engadin. In Sils Maria has to be anticipated PET values under -10 °C to 65 %, in Scoul to 20 % and on the mountain Corvatsch to 90 %.

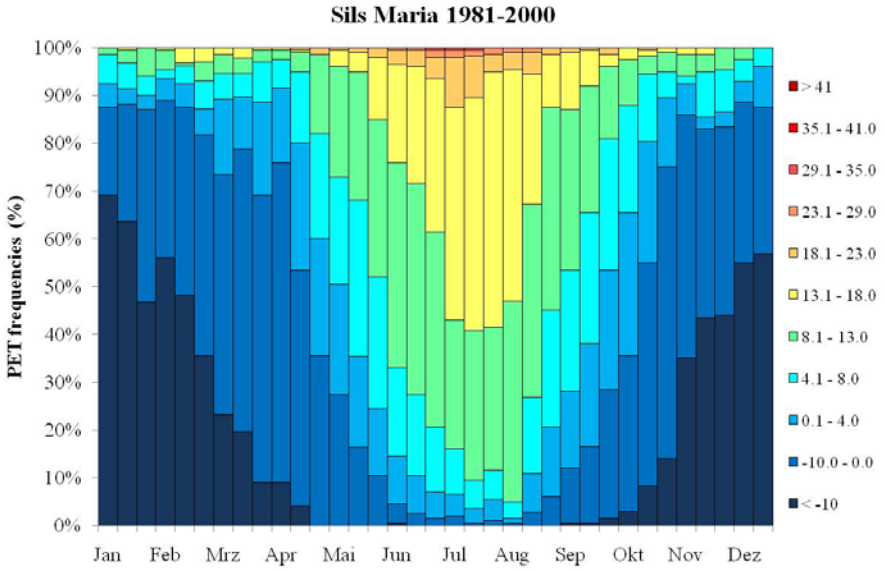

Fig. 2: Frequencies of the appearance of different PET classes in Sils Maria during the time period 1981 - 2000

Ski potential persists from November to April in Engadin` Ota and in Engadina Bassa from December to April. February features the best snow conditions, less precipitation and also warmer air temperatures. On the top of the mountains has to be bargained with an occurrence of 50 % with wind velocity stronger than 8 m/s.
Thermal acceptability appear on 64% of the days in Engadina Bassa from June to August, in Engadin`Ota in contrast only on maximal four days a month. The highest probability of cloudiness, rain duration and frequency occurs over summer. Indeed colder but dry conditions may be expected during September and October. The so called *Malojawind* can lead especially during summer to high wind velocity, which can be drop down the valley. On the mountains the wind velocity is over summer smaller than in winter.

The number of days with cold stress is expected to decrease mainly in early and late winter due to climate warming till 2025. Ski potential regresses in early winter most intensely under use of A1B scenario but in late winter using B1scenario. Nevertheless can be expected a probability over 98 % with a snow depth over 30 cm in Sils Maria and to 80 % in Scoul. Increasing rainfall duration and frequency during winter can lead to a higher danger of avalanches.
Using A1B Scenario the probability of days with thermal acceptability is increasing during summer. Using B1 Scenario minor increasing of the warming is expected. The precipitation is decreasing from May to September, with the exception of July. Heat stress is irrelevant in Engadin. In autumn climatic conditions, rainfall duration and precipitation change for ore pleasant conditions.
Classic winter tourism cannot be bargained for any more in Engadina Bassa, because the snow deph over 30 cm will only be exceed in a likelihood of 33 % in December and 58 % in February using B1 scenario till end of the century. Using A1B the maximal likelihood is 25 %. Because of the warming the participation of cold stress decreases and snow fall changes into rainfall and at the same time the rain duration will increase.

A high ski potential over 85 % using B1 and 65 % using A1B scenario consists furthermore In Engadin`Ota from January to.

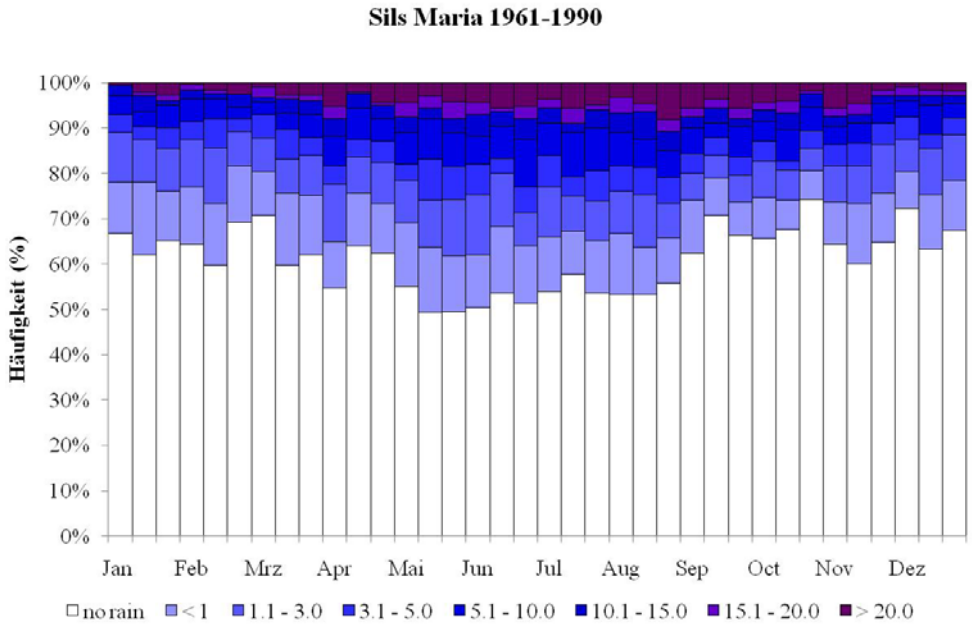

Fig. 3: Frequencies of the appearance of rain duration classes and the monthly rain sum (mm) in Sils Maria during the time period 1961 - 1990

The tourist during summer can expect optimal conditions in Engadin. The likelihood of thermal acceptability is about 60 % in the valley and rainfall amount is declining. In Engadina Bassa heat stress can occur to only 4 %, so that Engadin profits from the climate warming in contrast to low-lying or southern regions (Zaninovic and Matzarakis 2009, Matzarakis and Endler 2008). Especially Engadin`Ota exhibits a higher ski potential than other low-lying ski destinations in future years (Bürki et al. 2007). But problems like warm periods over winter and a higher avalanches risk can cause a bad image.

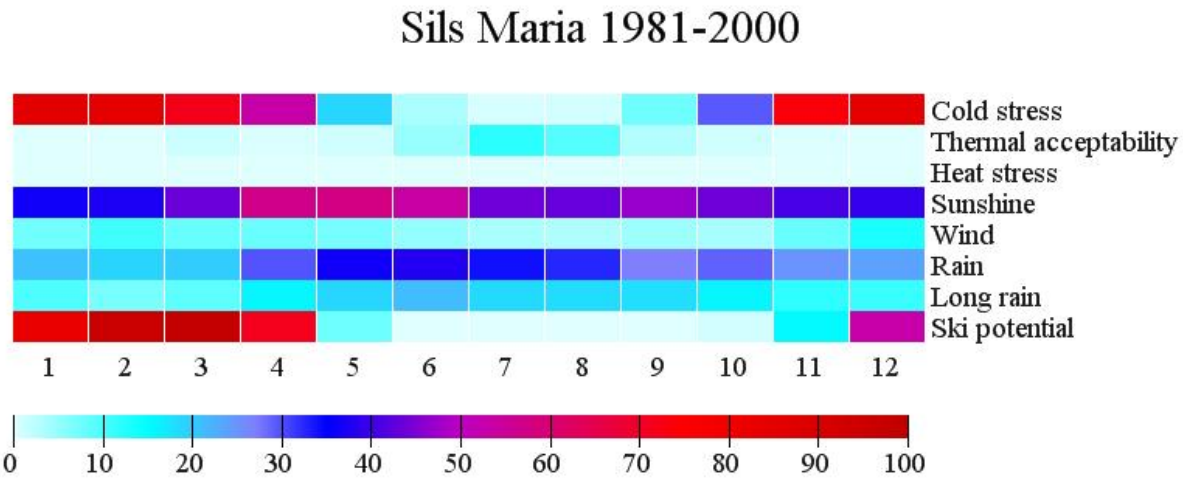

Fig. 4: Climate-Tourism-Information-Scheme for Sils Maria, based on measuring data of MeteoSwiss for the time period 1981-2000

5. Conclusions

Tourism adds 5% to the world wide CO_2 emission. Ascending level of motorisation, short breaks and secondary residences have a share to the Emissions in the Alps. Tourism as a part of the causes of climate change and also sufferer should not only react, but also see the change as Chance.

In the Alps and in Engadin are lots of good practice examples, like the project "Clean Energy St. Moritz", which was started 2003 on the occasion of the Ski WM. It contains the provision of energy sources like water, sun, biogas and geothermal energy from 1770 to 3057 m height. Photovoltaic-installations profit from 322 days with sunshine and temporary increase in efficiency through albedo-effects caused by snow cover at about 50 %. The first hotel of St. Moritz and one school covers 80 % and 70 % of their energy needs with the aid of heat pump installation, which extracts energy of the 4 °C warm water of Lake St. Moritz.
In Scoul snowmaking installations were built to the value of CHF 2.5 Mio. Climate and weather are important factors for visitors and tourism.

References

Böhm, U., Kücken, M., Ahrens, W., Block, M., Hauffe, D., Keuler, K., Rockel, B., Will, A., 2006: CLM - the climate version of LM: Brief Description and long term application. COSMO Newsletter 6, 225–235.

Bürki, R., Abegg, B., Elsasser, H., 2007: Climate Change and Tourism in the alpine regions of Switzerland. In: Amelung, B., K. Blazejczyk und A. Matzarakis (Hrsg.) (2007): Climate Change and Tourism. Assessment and Coping Strategies. S.165-172.

de Freitas, C. R., 2003: Tourism climatology: evaluating environmental information for decision making and business planning in the recreation and tourism sector. Int. J. Biometeorology 48, 45 -54.

Gómez, M., 2004: An evaluation of the tourist potential of the climate in Catalonia (Spain): a regional study. Geogr Ann 86A, 249–264.

Jacob, D., 2001: A note on the simulation of the annual and inter-annual variability of the water budget over the Baltic Sea drainage basin. Meteorol. Atmos. Phys. 77, S. 61–73.

Jacob, D., B.J.J.M. van der Hurk, U. Andræ, G. Elgered, C. Fortelius, L-P Graham, S.D. Jackson, U. Kartens, Chr. Koepken, R. Lindau, R. Podzun, B. Roeckel, F. Rubel, B.H. Sass, R.N.B. Smith und X. Yang, 2001: A comprehensive model inter-comparison study investigating the water budget during the BALTEX PIDCAP period. Meteorol. Atmos. Phys. 77, S. 19–43.

Kronthaler, F., Cartwright, J., 2008: Wertschöpfung des Tourismus in den Regionen Graubündens – Stand und Entwicklung, 45 -54.

Matzarakis, A., 2007:: Entwicklung einer Bewertungsmethodik zur Integration von Wetter und Klimabedingungen im Tourismus. Ber. Meteorol. Institut Univ. Freiburg. 16, 73-79.

Matzarakis, A., Endler, C., 2008: Climate Change and tourism in Germany – North Sea and Black Forest. Proceedings 18th International Congress on Biometeorology, Tokio 22-26 September 2008, 1-4.

Mayer, H., Matzarakis, A., 1999: Die Richtlinie VDI 3787 Blatt 2. Methoden zur humanbiometeorologischen Bewertung von Klima und Lufthygiene für die Stadt- und Regionalplanung. Teil I: Klima. In: Komission Reinhaltung der Luft im VDI und DIN (1999): Umweltsimulation. Methodik, Anwendung, Nutzen. Tagung Düsseldorf. September 1999. 31: 53-62.

Schweizer Tourismus Verband (1999): Tourismus in der Schweiz.

Steppeler, J., G. Doms, U. Schaettler, H.W. Bitzer, A. Gassmann, U. Damrath, G. Gregoric, 2003: Meso-gamma scale forecast using the nonhydrostatic model LM. Meteorol. Atmos. Phys. 82, 75–96.

Uhlmann, B., Goyette A., Beniston, M., 2009: Sensitivity analysis of snow patterns in Swiss ski resorts to shift in temperture, precipitation and humidity under conditions of climate change. Int. J. Climatology 29, 1048-1055.

www.clean-energy.ch

Zaninovic, K., Matzarakis A., 2009: The bioclimatological leaflet as a means conveying climatological information to tourists and the tourism industry. Int. J. Biometeorology 53, 369-374.

Authors' address:

Christine Ketterer (christine.ketterer@gmx.de)
Meteorological Institute, Albert-Ludwigs-University of Freiburg
Werthmannstr. 10, D-79085 Freiburg, Germany

Prof. Dr. Andreas Matzarakis (andreas.matzarakis@meteo.uni-freiburg.de)
Meteorological Institute, Albert-Ludwigs-University of Freiburg
Werthmannstr. 10, D-79085 Freiburg, Germany

Artificial snow making in the Southern Black Forest

Philipp Schmidt[1], Robert Steiger[2], Andreas Matzarakis[1]

[1]Meteorological Institute, Albert-Ludwigs-University of Freiburg, Germany
[2]Institute of Geography, University of Innsbruck, Austria

Abstract

Ski resorts react to warm winter seasons by investing in snowmaking. But snowmaking in warm winter seasons is at risk, because sufficiently low temperatures become less frequent in the future. In the study area of the Black Forest, Germany the region of Feldberg is the biggest ski area in Baden-Württemberg with 14 lifts and 16 ski slopes. The impact of climate change is extraordinary important, because for the whole area the winter tourism is the main source of revenue. The study area is in an altitudinal range from 850m – 1450 m. At the moment in 1/3 of the Feldberg area it is possible to work with artificial snowmaking. In the near future, till 2020, an artificial snowmaking of the whole Feldberg area is planned. On the basis of this, more detailed investigations of season length and the needed volume of produced snow are necessary. A ski season simulation model ("SkiSim 2.0") developed at the Department of Geography University Innsbruck, Austria was applied in order to assess the snow potential of natural and technical snow for today and for the climate scenarios A1B and B1 based on the regional climate models (REMO and CLM). In addition the model has been fitted with climate data from stations of the German Weather Service. The model operates and produces the monthly changes from 1961-2100 of the two emission scenarios (A1B and B1). These changes are downscaled to each weather station with a weather generator ("LARS-WG") producing daily data as input for SkiSim which calculates snow depth (natural and technically produced snow) and the required amount of artificial snow for 100 m altitudinal bands.

1. Introduction

Ski tourism has been identified as highly vulnerable to climate change (Abegg 1996, Breiling et al. 1997, Scott et al. 2003, 2006). Less snow, a shorter ski season, an increase of the snow line up to 1500m are the negative impacts of climate change on ski tourism (Beniston 2003, Breiling et al., 1997).

The most common method to define snow-reliability is the 100-days-rule stating that ski resorts can be considered as snow-reliable "if in 7 out of 10 winters, a sufficient snow covering of at least 30-50 cm is available for ski sport on at least 100 days between December 1 and April 15" (Abegg 1996). This methodology was adopted by the recent OECD study (Abegg et al. 2007) with the result that – with a 2 °C warming – only 60 % of today's existing ski areas in the European Alps will remain snow-reliable. Technical development outdated this methodology, as today snowmaking is widely spread all over the Alps and the adjacent low mountain regions – in the Feldberg area, for example, 1/3 of the skiing area is covered by snowmaking facilities. In the near future, till 2020, an artificial snowmaking of the whole Feldberg area is planned.

2. Methods

The chosen study area is the region of the Feldberg, Germany. The Feldberg is the highest point (1492 m) in the low mountain range Black Forest in Baden-Württemberg which is in the southwest of Germany (Willmanns, 2001).

For the present analyses the following stations are selected: Feldberg, Freiburg, Hinterzarten and Titisee (Fig.1.). These stations are representative for the ski destinations in the region of Feldberg.

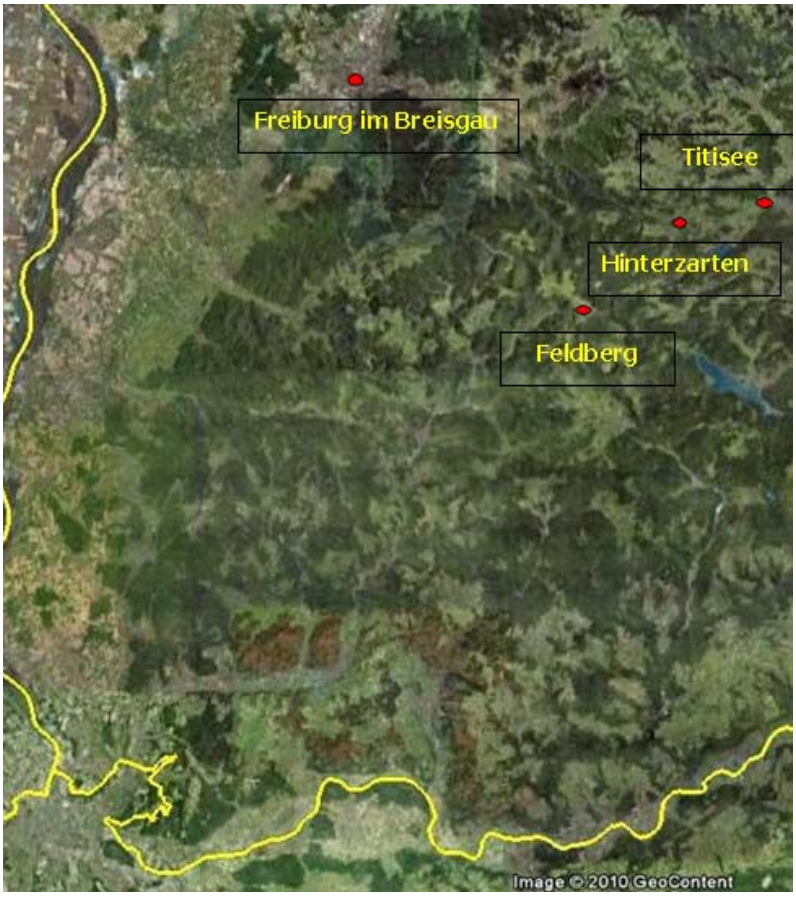

Fig. 1: Study area

For the computation of the snow potential the A1B and the B1 scenarios are used. The calculation is carried out by use of the regional climate model REMO from the Max-Planck-Institute of Meteorology in Hamburg with a spatial resolution of 10 km and data is available from 1950 until 2100. The period 1961 until 1990 is used as the reference period for future climate change (Jacob et al., 2007, Röckner et al., 2003, Will et al., 2006).

To assess the snow potential of natural and technical snow for today and for the climate scenarios A1B and B1 a ski season simulation model ("SkiSim 2.0") developed at the Department of Geography University Innsbruck, Austria was applied.

The model operates with monthly changes from 1961 until 2100 of the two emission scenarios A1B and B1. These changes are downscaled to each weather station with a weather generator ("LARS-WG") producing daily data as input for "SkiSim" which calculates snow depth (natural and technically produced snow) and the required amount of artificial snow for 100 m altitudinal bands (Steiger 2009).

For the computation of the snow potential the A1B and the B1 scenarios are used. The calculation is carried out by use of the regional climate model REMO from the Max-Planck-Institute of Meteorology in Hamburg with a spatial resolution of 10 km. Monthly changes of temperature and precipitation of two future time frames – 2030s

(2021-2050) and 2080s (2071-2100) – compared to the 1961-1990 baseline period are downscaled to each weather station with the "LARS-WG" weather generator (Semenov, 1997). The resulting daily weather data is used as input for SkiSim 2.0 calculating snow depth (natural and technically produced snow) and the required amount of artificial snow for 100 m altitudinal bands (Steiger, 2009).

3. Results

The results are shown for the station on Feldberg (modelled height: 1076 m). The Feldberg represents the area with 14 lifts and 16 slopes and is the highest point and is taken as case study being the largest and most important ski area of the study area.

Table 1: Potential ski days for the whole winter season in time period from the 1st November to the 30th April for thirty year periods for each altitudinal range (e.g. Alt_min means the "Talstation" 945m)

	SD_SM_BASE	SD_SM_A1B_2030	SD_SM_A1B_2080	SD_SM_B1_2030	SD_SM_B1_2080
Alt_min	50	27	5	33	12
Alt_mid	130	117	42	123	81
Alt_max	140	130	64	134	108
Weighted	113	92	26	100	56

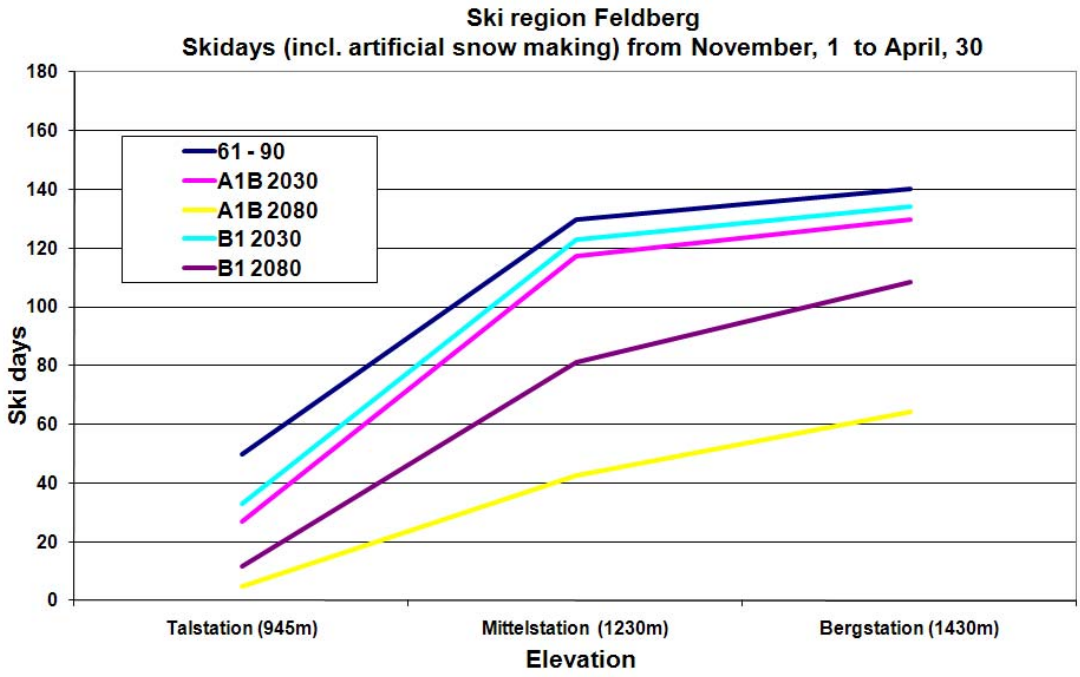

Fig. 2: Possible ski days for the whole winter season in time period from the 1st November to the 30th April each year for each altitudinal range (e.g. Alt_min means the "Talstation" 945 m)

Table 1 and Figure 2 show equally like Table 2 and Figure 3 the potential ski days for the whole winter season in the time period from the 1st November to the 30th April for a thirty year period for each altitudinal range. On the basis of the number of the possible ski days a conclusion is possible if ski operation is cost-covering or not. These results are shown that in the whole winter season the possible ski days decreases rapid until the year 2100 in each climate scenario. In the particular one the possible ski days in the lower ranges decreases even much more important than the possible ski days in the higher ranges. The numbers of the possible ski days are shown, that despite artificial snowmaking a cost covering manage which is reach with a number of ski days from more than 100 is not in guarantee in every altitudinal range.

Table 2: Possible ski days for the whole winter season in time period from the 1st November to the 30th April each year for each altitudinal range

ALT	SD_SM_BASE	SD_SM_A1B_2030	SD_SM_A1B_2080	SD_SM_B1_2030	SD_SM_B1_2080
900	50	27	5	33	12
1000	78	46	8	53	20
1100	102	69	13	80	36
1200	118	99	25	107	57
1300	130	117	42	123	81
1400	140	130	64	134	108

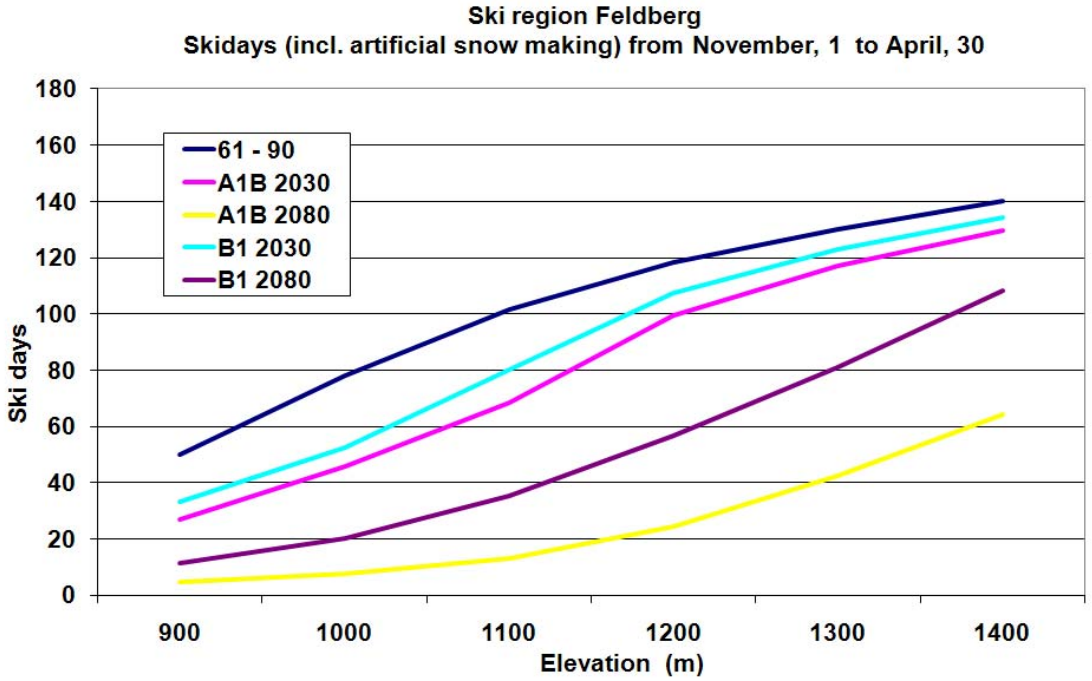

Fig. 3: Possible ski days for the whole winter season in time period from the 1st November to the 30th April each year for each altitudinal range

4. Discussion and conclusions

In general it is to be determined that a considerable change in season lengths only appears in the time period from 2050 to 2100. On a closer analysis it is evident, that the season lengths for each climate scenarios (A1B and B1) differ significantly. The decline of the season length is especially distinctive in climate scenario A1B. In the A1B scenario even the peak of the highest ski area of the study region falls below the 100 operation days. In the B1 scenario only the peak remains snow reliable while the rest of the ski area is projected to fall below the 100-days threshold. Even in high elevated ski resorts of the Feldberg area it is not secured, that the ski resorts has more than 100 operating days. Therefore artificial snowmaking is not the cure-all strategy. On the basis of this the whole Feldberg region and the adjacent ski resorts should think about an alternative strategy to the dominant ski tourism in the winter month.

Acknowledgement

Thanks to the Federal Ministry of Education and Research (BMBF) for funding the sub research project "*Weather and Climate Analysis*", which is part of the joint research project CAST (promotional reference: 01LS05019) within the scope of the research initiative klima*zwei*.

REFERENCES

Abegg, B., 1996: Klimaänderung und Tourismus: Klimafolgenforschung am Beispiel des Wintertourismus in den Schweizer Alpen. Zürich.

Abegg, B. et al., 2007: Climate Change impacts and adaptation in winter tourism. In: Agrawala, S. (ed.), Climate change in the European Alps. Paris, OECD, 25-60.

Beniston, M., 2003: Climate change in mountain regions: a review of possible impacts. Climate Change 59, 5-31.

Breiling, M., P. Charamza, O. Skage, 1997: Klimasensibilität österreichischer Bezirke mit besonderer Berücksichtigung des Wintertourismus. Rapport 1, 1997. Departement of Landscape Planning Alnarp, Swedish University of Agricultural Sciences.

Jacob, D., L. Bärring, O.B. Christensen, J.H. Christensen, S. Hagemann, M. Hirschi, E. Kjellström, G. Lenderink, B. Rockel, C. Schär, S.I. Senevirante, S. Somot, A. van Ulden, B. van den Hurk, 2007: An inter-comparison of regional climate models for Europe: Design of the experiments and model performance. Climate Change, 81, 31-52.

Roeckner, E., G. Bäuml, L. Bonaventura, R. Brokopf, M. Esch, M. Giorgetta, S. Hagemann, I. Kirchner, L. Kornblueh, E. Manzini, A. Rhodin, U. Schlese, U. Schultzweida, A. Tompkins, 2003: The atmospheric general circulation model ECHAM5. Part I: Model description. Max Planck Institute for Meteorology, Report No. 349. Hamburg

Scott, D., G. McBoyle, B. Mills, 2003: Climate change and the skiing industry in southern Ontario (Canada). Clim. Res.23 (2): 171-181.

Scott, D., G. McBoyle, A. Minogue, B. Mills, 2006: Climate Change and the Sustainability of Ski-based Tourism in Eastern North America: A Reassessment. Journal of Leisure Research 14: 376- 98.

Semenov, M., E. Barrow, 1997: Use of a stochastic weather generator in the development of climate change scenarios. Climatic Change 35, 397–414.

Steiger, R., 2009: SkiSim - A tool to assess the impact of climate change on ski season length and snowmaking In: Schweizer, J., A. van Herwijnen, Proceedings of the International Snow Science Workshop, 27. September to 2 October 2009, Davos, Switzerland.

Will, A., Keuler K., Block A., 2006: The Climate Local Model - Evaluation Results and Recent Developments. TerraFLOPS Newsletter 8, 2-3.

Willmanns, O., 2001: Exkursionsführer Schwarzwald – eine Einführung in Landschaft und Vegetation. Verlag Eugen Ulmer GmbH & Co.

Authors' address:

Philipp Schmidt (Philipp.Schmidt@students.unibe.ch)
Meteorological Institute, Albert-Ludwigs-University of Freiburg
Werthmannstr. 10, D-79085 Freiburg, Germany

Robert Steiger (robert.steiger@uibk.ac.at)
Institute of Geography, University of Innsbruck
Innrain 52, A-6020 Innsbruck, Austria

Prof. Dr. Andreas Matzarakis (andreas.matzarakis@meteo.uni-freiburg.de)
Meteorological Institute, Albert-Ludwigs-University of Freiburg
Werthmannstr. 10, D-79085 Freiburg, Germany

Climate change impact assessment in winter tourism

Robert Steiger

Institute of Geography, University of Innsbruck, Austria

Abstract

A ski season simulation model ("SkiSim 2.0") was developed to simulate ski season length and snowmaking requirements. Maximum differences between modelled and measured ski season length at three sample ski areas of two days mark SkiSim 2.0 as an appropriate tool for assessments on the impact of climate change on winter tourism. The snow reliable skiing terrain is projected to be reduced by 3 %, 12 % and 29 % until the 2030s, 2050s and 2080s (A1B scenario). The required increase of snow production of 24-79 % suggests that economic limits of snowmaking might be reached earlier than climatic limits.

1. Introduction

Winter tourism in mountainous areas is highly vulnerable to climate change due to its dependency on snow. The continuing warming trend is likely to derogate the availability of the natural resource snow. Snowmaking – currently the most used technical adaptation strategy – can balance out the decreasing amount of natural snow (Steiger, 2007b). Nevertheless, as temperatures below a certain threshold are needed for snowmaking, ski areas are expected to be significantly affected within the next decades (Scott et al., 2008).

Ski areas are important for the regional economy of many alpine regions. In Austria guests in the ski areas generate an annual gross turnover of € 5.8 billion (Fachverband Seilbahnen Österreichs, 2009). Due to the economic importance of that tourism sector and the strong dependency on a climate driven natural resource, "the multinational research literature on climate change and skiing is perhaps the best developed in the tourism sector" (Scott, 2006, p. 55, see also for a literature overview). So far, snowmaking was only considered in a comparably small number of studies (Australia: Hennessy et al., 2003, Canada and US: Scott et al., 2003, 2008, Germany: Steiger, 2007a and Austria: Steiger and Mayer, 2008; Steiger, 2009).

The objective of this study was to adapt the ski season simulation model "SkiSim" applied in Canada and the US (Scott et al., 2003; Scott et al., 2008) to the Alps. Based on the modelled daily snow depths, the potential impacts on the ski tourism industry in the research area of Tyrol/Austria and South Tyrol/Italy can be assessed. The research area consists of 109 ski areas not including ski areas with only one ski lift or short lifts for beginners close to the villages. Climate data was provided by the Hydrographic Service of Tyrol and the Central Institute of Meteorology and Geodynamics ("ZAMG"). Data on ski season length was derived from the annual railway statistics of Austria. The ski areas range from 545-3,433 m (mean altitude 1,800 m) with a total ski slope area of 11,200 ha (ski routes and off-piste terrain not included). The world market share considering the annual 37 million skier days is 9.3 % (Autonome Provinz Bozen-Südtirol, 2009; Manova, 2009; Vanat, 2009). Comparing to the leading marketplaces - the US (58 million skier visits) and France (54 million) (Vanat, 2009) - the economic impor-

tance of ski tourism for the research area with only 1.2 million inhabitants becomes apparent.

2. Methodology

A ski season simulation model (further referred to as "SkiSim 2.0") was developed calculating daily snow depth and snowmaking requirements for each 100 m altitudinal band. As input data only temperature and precipitation data is needed. These low data requirements increase the number of available climate stations thus being able to consider regional climate characteristics (e.g. areas with frequent Foehn winds, cold air pockets, etc.). SkiSim 2.0 consists of a natural snow module and a ski operations module. Temperature and precipitation data are extrapolated with lapse rates of 0.65°C/100m and 3 %/100 m respectively.

2.1 Natural snow module

The natural snow module is a temperature index model with a variable degree-day factor. The module was developed based on a snow model of Kleindienst (Kleindienst, 2000). The degree-day factor increases in the course of the season due to more incoming radiation and the reducing albedo of an ageing snowpack. Fresh snow reduces the degree-day factor as it increases the albedo. The temperature threshold for the separation of snow and rain is calibrated for each climate station separately using daily snow depth data. If temperature is below the lower threshold, 100 % of precipitation occurs as snow, if it is above the upper threshold 100 % occurs as rain, in between the snow/rain ratio is interpolated linearly. In the calibration process the lower and upper temperature thresholds are chosen based on a comparison of modelled and measured snow cover days. Fresh snow density is calculated temperature-dependent following Meister (1986). Snow pack metamorphosis and overlying fresh snow causes snow compaction until the maximum snowpack density of 450 kg/m³ is reached.

Potential snowmelt is calculated as a product of the degree-day factor and the mean daily temperature. Effective snowmelt only occurs, if enough energy is available to increase the snowpack temperature to 0°C. The snowpack temperature equals the mean air temperature of the previous day, with 0°C as the upper limit. The required energy to reach isothermal conditions and to cause effective melt is calculated based on Brooks et al. (2003).

Modelled snow cover days were compared to snow depth data. The model bias at the 31 climate stations used in this study is +/-10 %, or -1.9% in the average. These differences are acceptable regarding the purpose of the model.

2.2 Ski operations module

The ski operations module was developed based on the "SkiSim" model of Scott et al. (2003, 2008). Ski area managers of the research area provided information to consider snowmaking decision rules and strategies being different from the original model. It was further adapted to fit the semi-distributed character of the natural snow module, by calculating snowmaking requirements for each 100 m altitudinal band separately.

The daily snow depth of the natural snow module is transferred to the ski operations module. The snowpack on ski slopes is different from a natural snowpack due to the daily grooming. Thus the snowpack density is recalculated with a minimum density of 350 kg/m³ (Fauve et al., 2002). The snow depth threshold for a potential operation day is set to 30 cm (Abegg et al., 2007; Scott et al., 2003 and interviews). Potential snowmaking hours are calculated based on a linear interpolation of daily minimum and maximum temperatures being a simplification of the diurnal temperature cycle. Snowmaking is only possible if temperature is below the threshold of -5°C (Scott et al., 2003 and interviews) within the snowmaking season (Nov 1 - Mar 31). Snowmaking is split into two operational types: base layer snowmaking and improvement snowmaking (Steiger and Mayer, 2008). Base layer snowmaking enables the ski area to open with a sufficient snow depth. In the average 30 cm of snow are produced with that operational type, regardless of natural snowfalls and snow depth. Improvement snowmaking is required to assure a continuous ski operation until the scheduled end of the season. In most ski areas in the research area the ski season is terminated at the end of the Easter weekend, except on glaciers and at a few high altitude ski areas. Improvement snowmaking is calibrated to maintain a sufficient snow depth of 30 cm until April 1 (based on statements of ski areas managers in the interviews). The snowmaking capacity of 10 cm per day represents the state-of-the-art snowmaking technology.

The ski operations module was validated comparing modelled with recorded ski season length of three sample ski areas at different altitudes and in different climatic subregions of the research area (Steiger, 2009). With differences between 0-2 days SkiSim 2.0 seems appropriate to simulate ski season lengths incorporating snowmaking technology.

2.3 Climate change impact assessment

Climate model data of a regional climate model “REMO” (10x10 km resolution) driven by two emission scenarios (B1 and A1B) was provided by the “DKRZ”. Temperature and precipitation changes compared to the 1971-2000 baseline period were downscaled to each climate station with the “LARS” weather generator (Semenov and Barrow, 1997). The resulting daily data was taken as input into SkiSim 2.0.

The 100-days rule (Abegg et al., 2007) was applied to calculate snow reliable ski slope terrain. If the modelled ski season length of an altitudinal band is below 100 days, it is defined as not snow reliable and it is assumed that ski operation will be abandoned on these ski slopes in the future. Thus the change of snow reliable ski area compared to the baseline can be calculated. As the focus of this paper is to assess the impact of climate change on tourism destinations rather than on single ski areas, the results were aggregated to the level of tourism boards which in most cases match tourism destinations.

3. Results

For clarity reasons only results for the A1B emission scenario and for three future time frames (2030s, 2050s, 2080s) are presented in this paper. In the B1 scenario the same developments occur approximately two decades later than in the A1B scenario. The climate change signals derived from REMO for these timeframes show a 9-15 % increase of precipitation and a warming of 1.1°C, 2.4°C and 4.2°C compared to the base-

line period. The projected losses of snow reliable skiing terrain on the level of tourism boards are illustrated in Fig. 1.

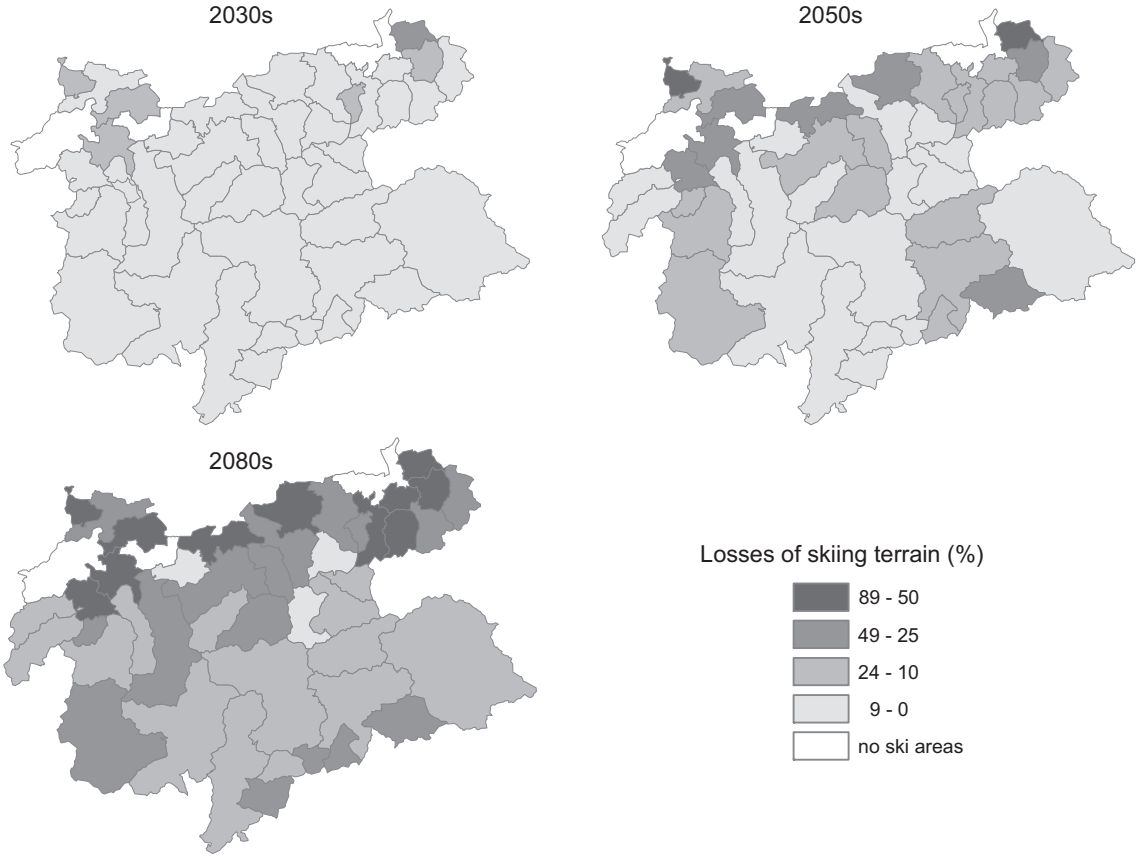

Fig. 1: Losses of skiing terrain in the 2030s, 2050s and 2080s

In the 2030s the losses of snow reliable skiing terrain are below 10 % in 38 out of 44 tourism board regions (86 %). Five regions have projected losses between 10-24 % and one region has 27 %. The mean altitude of the ski area in the last category is at 1,000 m. In the 2050s only 18 of the regions have losses of less than 10 %. Losses of up to 25 % are projected for 17 regions, seven have losses of up to 50 % and two lose more than 50 % (62 % maximum) of their skiing terrain. The mean altitude of ski areas with 25 % losses and more is shifted upwards to 1,401 m. In the 2080s three regions are still little affected, 14 lose up to 25 %, 16 lose up to 50 % and 11 lose more than the half of the skiing terrain, with extreme values of up to 89 %. The mean altitude of ski areas losing at least 25 % is at 1,581 m.

The tourism board regions being affected at first are in the north-western (Tannheim valley, Ehrwald and Imst region) and north-eastern part (Kössen, St. Johann i.T. and Wildschönau region) of the research area. Until the 2050s the entire northern part (north and east of the Inn valley) is heavily affected with famous destinations like “SkiWelt Wilder Kaiser” (largest ski area in Austria) and Kitzbühel. Especially small and thus financially weak ski businesses are likely to drop out of the market. Some of the larger ski areas in that region might be able to continue ski operation but at significantly higher costs (more snowmaking needed) and less income (shortened ski season). At the end of the century the losses in the northern part are likely to force virtually all ski areas

to drop out of the market or at least to reduce their business to the highest parts of the ski area. But it is questionable if these downsized ski areas can compete with the less affected ski areas in the southern part of the research area (e.g. Ischgl, Ziller valley, central Dolomites).

Summing up potentially lost skiable terrain for the entire research area, 3 % are lost in the 2030s, 12 % in the 2050s and 29 % in the 2080s. To limit the losses to these values, the production of artificial snow has to be increased: For the 2030s an increase in water demand of 24 % is projected, 54 % for the 2050s and 79 % for the 2080s. Assuming a temperature independent snowmaking technology (introduced at Pitztal glacier in 2009) preventing any losses of snow reliable skiing terrain, an increase in water demand of 31 %, 81 % and 164 % is projected for the 2030s, 2050s and 2080s. As none of the ski stations in the research area has the snowmaking capacity defined in the model (100 % of ski slopes covered combined with 10 cm production capacity) current water usages are likely to be lower than calculated by the model. Unfortunately, no data on water demand of snowmaking is available to compare to the model results. Thus it has to be assumed that the real increases of water demand are significantly higher than the projected changes.

4. Conclusion and Discussion

The model results of SkiSim 2.0 reveal that the potential impacts of climate change on the ski tourism sector can vary significantly depending on the altitudinal range of the ski area. The projected snow reliability of ski areas is higher compared to studies not considering snowmaking: Abegg et al. (2007) estimated that with a 2°C warming the number of snow reliable ski areas in the research area would be reduced by 39 %. The results produced by SkiSim 2.0 were significantly less severe with a total loss of ski slope area of 12 % in the 2050s A1B scenario (+2.4°C). On the other hand it can be clearly seen that current snowmaking technology can at most delay the withdrawal from the ski market in most of the northern regions. The projected increases in required snow production suggest that economic limits might be reached earlier than the climatic limits of snowmaking at some places. A temperature independent snowmaking technology cannot be a suitable adaptation strategy for all ski areas, as the required increase of snow production and water demand (about the factor of 2.5) until the end of the century is neither economically viable nor ecologically justifiable.

Acknowledgement

The author is grateful to the FWF for financing the project, Daniel Scott for his support and for insight in his ski season model, Andreas Matzarakis for data processing of the climate scenario data provided by the DKRZ and Hans Stötter for supervision.

References

Abegg, B., S. Agrawala, F. Crick, A. de Montfalcon, 2007: Climate change impacts and adaptation in winter tourism. In: Agrawala, S., Climate Change in the European Alps. Adapting Winter Tourism and Natural Hazards Management, OECD, Paris.

Autonome Provinz Bozen-Südtirol, 2009: Seilbahnen in Südtirol 2008. Amt für Seilbahnen, Bozen.

Brooks, K., P. Ffolliott, H. Gregersen, L. DeBano, 2003: Hydrology and the management of watersheds. Third Edition, Iowa State Press, Ames.

Fachverband Seilbahnen Österreichs, 2009: Die österreichische Seilbahnbranche und ihre ökonomische Bedeutung, Wien. http://www.seilbahnen.at/presse/aktuell/2009-10-01wertschoepfung (accessed on 03.02.2010).

Fauve, M., H. Rhyner, M. Schneebeli, 2002: Pistenpräparation und Pistenpflege. Das Handbuch für den Praktiker. Eidg. Institut für Schnee- und Lawinenforschung, Davos.

Hennessy, K., Whetton, P., Smith, I., Bathols, J., Hutchinson, M., Sharples, J., 2003: The impact of climate change on snow conditions in mainland Australia, http://www.cmar.csiro.au/e-print/open/hennessy_2003a.pdf (accessed on 03.02.2010).

Kleindienst, H., 2000: A Model for Distributed Snow Cover Simulation at Alpine Scale, unpublished dissertation, Bern.

Manova, 2009: Wirtschaftsbericht der Seilbahnen, Wien. http://www.seilbahnen.at/presse/wirtschaftsdaten/files/berichtsblaetter_tm_winter0708.pdf (accessed on 03.02.2010).

Meister, R., 1986: Density of new snow and its dependence on air temperature and wind. Zürcher Geographische Schriften 23, 73–79.

Scott, D., 2006: Global Environmental Change and Mountain Tourism. In: Gössling, S., M.C. Hall, Tourism and Global Environmental Change. Routledge, London.

Scott, D., G. McBoyle, B. Mills, 2003: Climate change and the skiing industry in southern Ontario (Canada): exploring the importance of snowmaking as a technical adaptation. Climate Research 23, 171–181.

Scott, D., J. Dawson, B. Jones, 2008: Climate change vulnerability of the US Northeast winter recreation– tourism sector. Mitig Adapt Strat Glob Change 13, 577–596.

Semenov, M., E. Barrow, 1997: Use of a stochastic weather generator in the development of climate change scenarios. Climatic Change 35, 397–414.

Steiger, R., 2007a: Der Klimawandel und seine Auswirkungen auf die Skigebiete im bayerischen Alpenraum. Salzwasser-Verlag, Bremen.

Steiger, R., 2007b: Snowmaking - A suitable Adaptation Strategy? Examples from Tyrol / Austria, In: Matzarakis, A., C.R. de Freitas, D. Scott (eds.), Developments in Tourism Climatology. Commission Climate, Tourism and Recreation, International Society of Biometeorology, Freiburg.

Steiger, R., 2009: SkiSim - A tool to assess the impact of climate change on ski season length and snowmaking In: Schweizer, J., A. van Herwijnen, Proceedings of the International Snow Science Workshop, 27. September to 2 October 2009, Davos, Switzerland.

Steiger, R., and M. Mayer, 2008: Snowmaking and Climate Change. Future Options for Snow Production in Tyrolean Ski Resorts. Mountain Research and Development 28(3/4), 292–298.

Vanat, L., 2009: 2009 International report on mountain tourism. http://www.vanat.ch/RM-world-report-2009.pdf (accessed on 03.02.2010).

Authors' address:

Robert Steiger (robert.steiger@uibk.ac.at)
Institute of Geography, University of Innsbruck
Innrain 52, A-6020 Innsbruck, Austria

The climate as an important factor in a multicriteria decision analysis for the developmnet planning of wellness tourism

Eleni Didascalou[1], Panagiotis Nastos[2], P. Tsartas[3]

[1] Department of Business Administration, University of Piraeus, Piraeus, Greece
[2] Laboratory of Climatology and Atmospheric Environment, University of Athens, Athens,Greece
[3] Department of Business Administration, University of the Aegean, Chios, Greece

Abstract

Health and wellness tourism is an important contemporary growth sector. Many people nowadays are concerned about their physical, social and psychological well-being and they are prepared to travel long distances to experience different forms of wellness tourism. For a wellness tourism consultant, as this market is rapidly changing, it is important to use new tools and techniques when he advises investors or tourism organisations, as for example about where to place a new wellness center, which is quite a complex problem. As more stakeholders are involved, Group decision making increases the project's approval. A Group Decision Support System improves group decision. The study illustrates the use of Web-HIPRE software in a case dealing with the ranking of the prefectures of Ahaia, Arkadia, Ilia, Korinthia, Messinia in the region of Peloponnese Greece, when a decision had to be made about the location of a new wellness centre. The criteria used for constructing the model concern climate, tourism development and attractions. The group preferences consist of three individual preferences, the preferences of a climatologist, a tourism development consultant and a wellness tourism consultant.

1. Introduction

A "spa" in the first place meant European destination resorts where guests went to "take the waters" to restore a healthy balanced life. Many people who were suffering from serious ailments preferred to head for local spa resorts (Kevan, 1993). Today the term "spa" is used to describe many different types of facilities in hospitality indusrty. Health and Wellness Tourism is a rapidly growing sector as many people are concerned about their physical, social and psychological well-being and they are prepared to travel long distances to experience different forms of wellness tourism.Spas are no longer just indulgences during annual vacations, they are important centres for overal well-benig and healthy mind and body maintenance (Monteson, 2004)

Wellness tourism is one of the most ancient forms of tourism if one considers the scrupulous attention paid to wellbeing by Greeks and Romans. This earliest form of health tourism is directly related to contemporary health and wellness and includes visits to mineral and hot springs (Didaskalou and Nastos, 2003). Today wellnes can be defined in various ways and it is not a static concept. It is subjective and relative, thus always in flux. The needs of wellness tourists will clearly vary enormously at different times and stages of their lives (Smith, 2006). Trends changes rapidly and any decision making in the area of product characteristics has to be driven by the use of effective tools and techniques.

The focus of this paper is on developing 'Wellness Tourism' across five prefecures (Ahaia, Arkadia, Ilia, Korinthia, Messinia) of Peloponesse region, concerning either destination spas or resort-based spas. Destination spas are entities unto themselves and

create environments that reinforce their specific missions. The destination spa offers a complete spa experience in an overnight setting (most require a two-or three-night minimmum stay). Their purpose is to set guests on a healthier path for life and serve healthy spa cuisine, provide education on lifestyle improvement, offer fitness activities that built self-esteem while motivating take-home habits and future bodywork and pampering therapies that complement wellness programmes (McNeil and Ragins, 2005). At a resort-based spa, on the other hand, the spa is one of the many recreational and social activities typically available at a full-service resort (Monteson, 1992).

The authors, due to lack of marketing studies, defined through literature review the dimensions that must be encompassed when a decision had to be made about the location of a new wellness center. The criteria that authors have teken into consideration when ratting destinations for the construction of a spa resort/hotel are: climate regime, existing tourism development and attractions (Didaskalou et al., 2009). Especially climate considerations pay a major role when choosing spesific holiday destinations (Amelung, 2007). The results of I-Test survey confirm that climate is a crusial factor in choosing Europeans' holiday destinations as this was rated 8.3 out of a possible 10. Safety and the quality of accommodation are also crucial for Europeans (8.4 viz. 8.2) (FiA, 2009). Two other factors that play an important role are: the accessibility and the subsidy one can receive for the construction of the operation but as these factors are in general the same for the region of Peloponesse, the authors did not take them into account in the model, but for other areas or districts where the differences are significant, these factors must be considered. Also an asset is the presence of a hot/mineral spring (Didaskalou et al., 2007),

2. Model Construction

Multicriteria decision analysis (MCDA) and computer based decision support systems provide ways to systematically structure and analyse complex decision problems (Mustajoki, 2004), like decisions regarding policy and long-range planning on wellness tourism. Important decisions in organizational settings are normally taken by a group of people whose collective decision making ability is considered to be more pragmatic than individual opinions. One widely recognized method to improve the effectiveness of group decisions is the use of Group Decision Support Systems (GDSS) (Limayem, 2006). Group decision support systems (GDSSs) combine communication, computer, and decision support technologies to support problem formulation and solution in group meetings (Poole, Homes and DeSanctis, 1988). In the study the group preferences consists of three individual preferences, the preferences of a climatologist, a tourism development consultant and a wellness tourism consultant.

When decision-making process involves several Decision Makers determining single attribute value functions and weighting the objectives is likely to be difficult. The value tree analysis can be applied in group decision-making to aggregate the values of the individual DMs. After the criteria has been established, from the authors through literature review, the GDSS tool which will be used for constructing the model is the software Web-HIPRE which is on-line available from Helsinki University of Technology at http://www.hipre.hut.fi/. Web-HIPRE is a Web implementation of the earlier HIPRE 3+ software and according to Mustajoki (2004) is the first web-based general purpose MCDA software that provides tools for problem structuring, preference elicitation and

sharing the results over the internet. In Web-HIPRE the problem is structured hierarchically to form a value tree. In this value tree each criterion is divided to its subcriteria, which are weighted by their importance to the decision maker (on the lowest level criteria the alternatives are weighted).The total weights of the alternatives are calculated from these local weights. The resulting model is called a value tree or a hierarchy of criteria and objectives depending on the tradition referred to. Table 1 gives the construction of the value tree of the individuals decision makers.

Table 1: The evaluation framework

Goal	Dimension	Criteria
Destination	Climate	Temperature (^oC)
		Relative humidity (%)
		Sunshine (hours)
		Wind speed (knots)
		Precipitation (days)
	Development	5* Hotels
		Index Defert
	Attractions	Nature (% of protected areas in km^2)
		Archaeological sites (number)
		Museums (number

Weighting Methods supported by Web-HIPRE

Direct Weighting: *The simplest way is to give them directly by point allocation*
SMART: *10 points are first given to the least important attribute.Then, more points are given to the other attributes depending on the relative importance of their ranges.*
SWING: *The method is similar with SMART but the procedure starts from the most important attribute keeping it as the reference.*
SMARTER: *In the SMARTER-technique you are asked to rank the attributes in the order of importance for the attribute changes from their worst level to the best level.*
AHP: *It is based on pairwise comparisons of the importance of both the attributes and the alternatives. The ratio scale of integers from 1 to 9 is used in the comparisons.*

3. Group Decision support with Web-HIPRE

Web-HIPRE supports group decision making with a possibility to create group hierarchies. Then, the individual values for the alternatives are combined with the weighted arithmetic mean method, i.e. the ovarall value is the weighted sum of individual values. In the group hierarchy each of the decision makers is presented as an element of the hierarchy. These elements can be weighted with any of weighting methods available in Web-HIPRE. The component values of decision maker elements are the overall values of each decision maker. These are obtained directly from the models of the decision makers (http://www.hipre.hut.fi).

The results of the GDSS model concerning the rating of the five prefecures are presented in Table 2.

Table 3: Composite Priorities

	Ahaia	Arkadia	Ilia	Korinthia	Messinia
Climatologist	0.147	0.193	*0.275*	0.157	0.248
Tourism Development Consultant	0.195	0.230	0.203	0.213	*0.247*
Wellness Tourism Consultant	0.155	0.157	*0.242*	0.230	0.216
Overall	0.166	0.193	**0.240**	0.200	0.237

The value tree of GDSS model is presented in Figure1. The total weights of the alternatives are given by bar graph in Figure 2

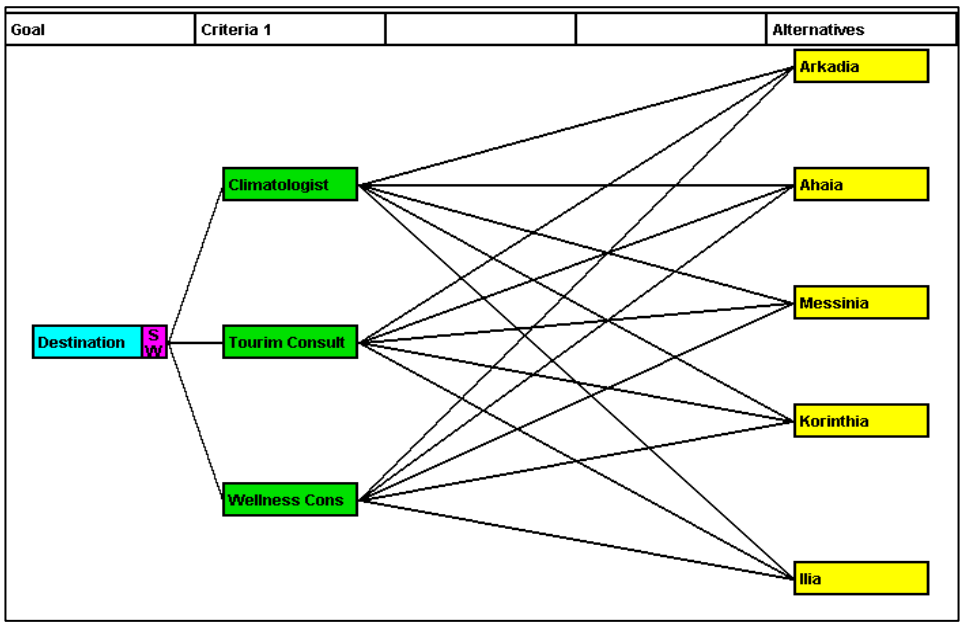

Fig. 1: The value tree of GDSS model

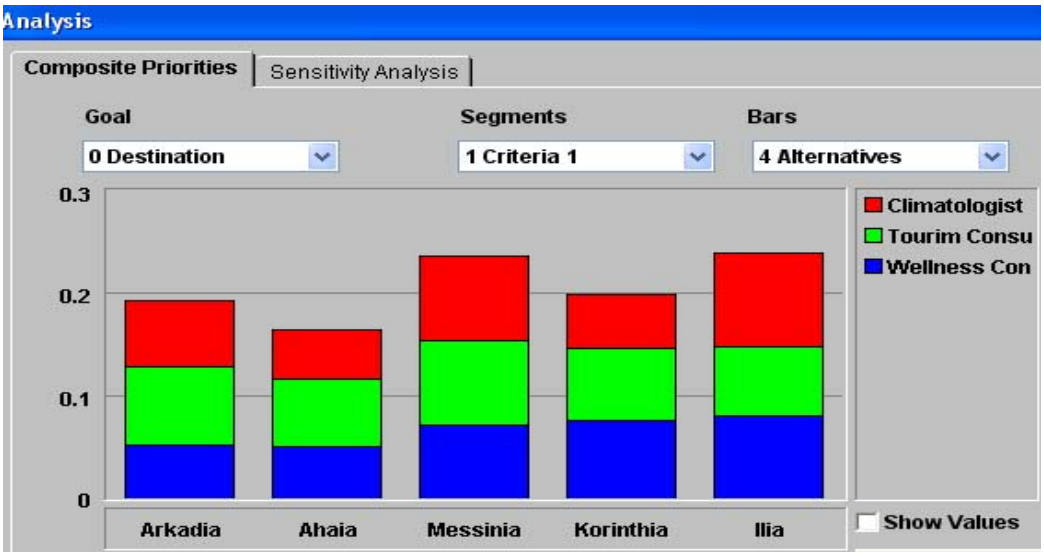

Fig. 2: Group preferences when raking the five destinations

An important dimension for the individuals decisions is climate. Figure 3 shows the preferences concering climate.

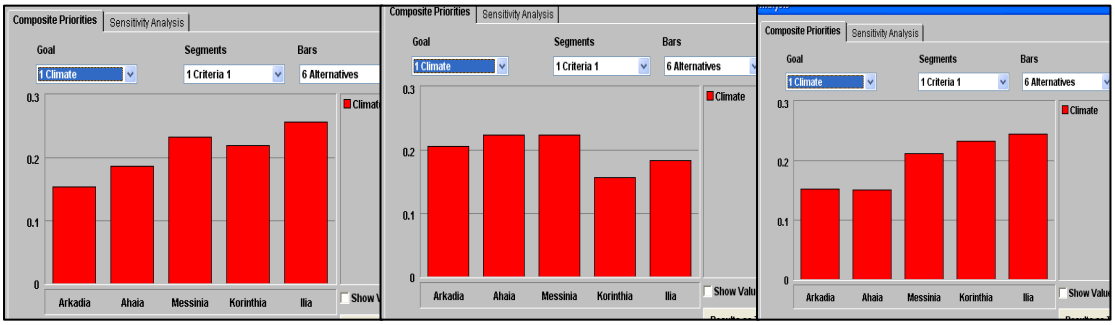

Fig. 3: Climate Priorities of a climatologist, a tourism decelopment consultant, a wellnes tourism consultant.

4. Conclusions

As stressed above, this study leans on making better decisions concerning wellness tourim, using new tools. As with any experimental study, we may not be able to genaralize our findings but our main goal was to acquaint planners about easy of use of new tools on tourism development decision making. The evaluation framework and the evaluation results given by Web-HIPRE can be used as a guide for public or private institutions to enhance decision quality as regards the developent of wellness tourism in the prefectures of Ahaia, Arkadia, Ilia, Korinthia, Messinia region of Peloponnese, Greece.

References

Amelug, B., Nicholls, S. And Viner, D. 2007: Implications of Global Climate Change for Tourism Flows and Seasonality. Journal of Travel Research 45, 285-296.

Didaskalou, E.A., Lagos D. and Nastos, P.Th. 2009: Wellness tourism: evaluating destination attributes for tourism planning in a competitive segment market, 4th International Conference Planning for the Future Learning from the Pasr: Contemporary Developments in Tourism, Travel & Hospitality, University of the Aegean, 3-5 April 2009, Rhodes, Greece.

Didaskalou, E.A, Nastos, P.Th & Matzarakis, A. 2007: Spa destination development using a decision support system-the role of climate and bioclimate. In A. Matzarakis, C.R. de Freitas and D. Scott (Eds.), Developments in Tourism Climatology, Freiburg: Commision on Climate, Tourism and Recreation, International Society of Biometeorology.

Didaskalou, E.A & Nastos, P. 2003: The role of climatic and bioclimatic conditions in the development of health tourism product. Anatolia, 14, 107-126.

FiA, 2009: The Eurocouncil of the Fédération Internationale de l'Automobile European Bureau, Press Release, Brussels, 8th October 2009, http://www.fiabrussels.com/download/news/press_releases/200910pressreleaseitest.pdf

Kevan, S.M. 1993: Quest for cures: a history of tourism for climate and health. International Journal of Biomometerology 37, 113-124.

Limayem, M., Banerjee, P. and Ma, L. 2006: Decision Support Systems 42, 945-957.

McNeil, K.R. and Ragins, E.J. 2005: Staying in the spa marketing game: trends, challenges, strategies and techniques. Journal of Vacation Marketing 11, 31-39.

Monteson, P. and Singer, J. 1992: Turn your spa into a winner. Cornell Hotel and Restaurant Administration Quarterly 33, 37-44

Monteson, P. and Singer, J. 2004: Marketing a resort-based spa. Journal of Vacation Marketing 10, 282-287.

Mustajoki, J., Hämäläinen, R. And Marttunen, M. (2004): Participatory multicriteria decision analysis with Web-HIPRE: a case of lake regulation policy. Environmental Modelling & Software 19, 537-547.

Poole, M.S., Homes, M. and DeSanctis G. 1988: Conflict management and group decision support systems, Proceedings of the 1988 ACM conference on Computer-supported cooperative work, Portland, Oregon, United States, 227-243.

Smith, M. and Kelly, C. 2006: Wellnes Tourism. Tourism Recreation Research 31, 1-4.

Authors' address:

Ph.D. Teachnig Staff Eleni Didaskalou (edidask@unipi.gr) University of Piraeus, Department of Business Administration, 80 Karaoli & Dimitriou St.,185 34 Piraeus, Greece

Associate Prof. Panagiotis Nastos (nastos@geol.uoa.gr), University of Athens, Faculty of Geology and Geoenvironment, Department of Geography and Climatology, Laboratory of Climatology and Atmospheric Environment, University of Athens Panepistimiopolis 157 84, Athens, Greece.

Prof. Paris Tsartas (ptsar@aegean.gr), University of the Aegean, Department of Business Administration, Michalio Bldg, Michalon 8, 82100 Chios, Greece

Modifikationen des lufthygienischen Wirkungskomplexes in der ruandischen Stadt Kigali

Sascha Henninger

Lehreinheit Physische Geographie, Technische Universität Kaiserslautern, Deutschland

Abstract

Rwanda is a landlocked republic in Equatorial Africa. The capital Kigali (1°57`S, 30°04`E) can be mentioned as a typical African city due to its rising population and the rising rate of motorization. Different pollutants produced e.g. by a high-usage rate of mopeds or open fireplaces burning woods for cooking and household chores could be detected. Climatological parameters as well as air pollutants were measured within the urban area. Additionally highly frequented spatial and temporal mobile measurements of particulate matters were taken during the dry spells of 2008 and 2009 regarding different conditions. These values indicated an UHI, which tended to rise from 1971 till 2009. Also a temporary phenomenon for the air pollution indicators is visible during clear and calm weather situations, e.g. the distinctive relief caused an accumulation within small valleys called "Marais" in the night time. Unfortunately, these are the favorite places of living and agriculture. So there is no infrequence in values of PM_{10} > 1.000 µg m^{-3}. The origin of the different airborne particles was verified by using a scanning electron microscope (SEM) and it could be mentioned that most particles were from the combustion of biomass fuels and traffic.

1. Einleitung

Kigali (1°57`S, 30°04`E), Hauptstadt des äquatornahen tropischen Berglandes Ruanda, weist, vergleichbar mit anderen Millionenstädten im subsaharischen Afrika, eine sehr schnell wachsende Bevölkerung auf. Im Laufe des Jahres 2010 wird Kigali wohl deutlich die 1-Million-Einwohner-Grenze überschritten haben. Mit steigender Bevölkerungszahl wächst auch das Problem der Luftverschmutzung. Der Grad der Motorisierung nimmt zu, vor allem mit Fahrzeugen, die keinerlei technischem Standard mehr genügen (Han und Naeher, 2006; Gwilliam, 2003). Neben dem Kfz-Verkehr stellt der private Hausbrand einen weiteren Emittenten dar. Über die Verbrennung von Holz, Dung und Kerosin in einfachen Öfen und auf offenen Feuerstellen gelangen zusätzlich luftbelastende Stoffe in die Stadtatmosphäre (Baumbach et al., 1995).

Das ausgeprägte Relief Ruandas spiegelt sich auch im Großraum von Kigali wieder. Die Einkaufs- und Geschäftsviertel, die Regierungs- und Diplomatenviertel, sowie deren Wohnbereiche befinden sich auf den Kuppenlagen der Hauptstadt. Hier herrscht während der Tagstunden die höchste Verkehrsdichte. Entlang der Berghänge und im Tal, den sog. „Marais", lebt die ärmere Bevölkerung. Diese ehemaligen Sumpf- und Feuchtgebiete stellen nicht nur den größten Wohn- und Lebensraum dar, dort findet sich auch ein Großteil der landwirtschaftlichen Subsistenzwirtschaft. Die Topographie dieses urbanen Raumes im Zusammenspiel mit den dort herrschenden meteorologischen Verhältnissen bedingen vor allem während autochthoner Wetterlagen, dass dort, wo die meisten Menschen leben, die höchsten Konzentrationen unterschiedlichster Luftschadstoffe erfasst werden (Henninger, 2009a).

2. ReCCiR-Projekt

Die Analyse der lufthygienischen Verhältnisse im Zusammenhang mit den meteorologischen Gegebenheiten im Stadtgebiet von Kigali ist ein Teil des ReCCiR-Projektes (**Re**cent **C**limate **C**hange **i**n **R**wanda), welches sich mit den Veränderungen der klimatischen Bedingungen in Ruanda im Hinblick auf den globalen Klimawandel beschäftigt (Henninger, 2009b). Schwerpunkt ist die Bewertung der Auswirkungen der lufthygienischen Situation und der damit einhergehenden gesundheitlichen Belastung der Bevölkerung (Van Wijnen et al., 1995).

3. Mess- und Analysemethodik

Die während der „kleinen Regenzeit“ im Februar 2008 erstmals durchgeführten Untersuchungen zur lufthygienischen Situation im Großraum Kigali wurden im gleichen Zeitraum des Jahres 2009 wiederholt. Dabei hat sich gezeigt, dass episodisch auftretende meteorologische Verhältnisse zusätzliche Auswirkungen auf die ohnehin angespannte lufthygienische Situation innerhalb der Stadthinderschicht haben. Lufttemperatur, relative Luftfeuchtigkeit, Niederschlag, Globalstrahlung, Windgeschwindigkeit und -richtung wurden mit dem WXT5000 (Fa. Driesen & Kern) an drei Standorten im Stadtgebiet erfasst. Da sich herausstellte, dass sich die WXT5000 aufgrund der Ansprechzeiten auch für den mobilen Einsatz eigneten, wurde ergänzend zu den stationären Messungen eine Messstrecke durch die Stadt entworfen. Die Messroute wurde in verschiedene Streckenabschnitte unterteilt, die unterschiedliche Flächennutzungen (Wohn-, Geschäfts-, Industrieviertel etc.) aufwiesen (Henninger, 2009b). Das gleichzeitige stationäre und mobile Erfassen von Meteorologie und Lufthygiene ermöglichte eine sowohl räumlich als auch zeitlich hohe Auflösung der Daten (Henninger, 2005). Feinstaub wurde ebenfalls an den drei kontinuierlich messenden Stationen und während der mobilen Messfahrten registriert. Der DustTrak 8534 DRX-Aerosolmonitor (Fa. Driesen & Kern) ermöglichte nicht nur eine schnelle Analyse der Partikelkonzentrationen, sondern auch eine Aufschlüsselung der unterschiedlichen Fraktionsgrößen (PM_{10}, $PM_{2,5}$, PM_1). Die insgesamt 45 mobilen Messungen wurden zu drei unterschiedlichen Tageszeiten durchgeführt (09.00 Uhr - 10.00 Uhr; 16.00 Uhr - 17.00 Uhr; 02.00 Uhr - 03.00 Uhr).

Ergänzend zur meteorologischen und lufthygienischen Analyse der urbanen Situation in Kigali wurden im Verlauf der Messkampagnen Luftproben mittels Filterwägung (Mettler Toledo XP2U; Fa. Mettler Toledo) genommen (Haryono et al., 2009). Die anschließende Analyse der Proben erfolgte in Deutschland. Mithilfe eines Rasterelektronenmikroskops sollten Rückschlüsse auf den originären Ursprung der luftgetragenen Teilchen geschlossen werden.

4. Feinstaub in der bodennahen urbanen Atmosphäre

Die Ergebnisse der Feinstaubanalyse treten nochmal deutlicher hervor, wenn zum Vergleich der Kurzzeitgrenzwert der WHO von 50 µg m^{-3} ergänzend in die Abbildungen 1 und 2 eingetragen wird (gestrichelte, schwarze Linien; WHO, 2006). Exemplarisch sollen die Ergebnisse der mobilen PM_{10}-Tagesmessungen dargestellt werden. Abbildung 1 zeigt die durchschnittlichen Streckenabschnittsmittelwerte der Messfahrten von 2008 und 2009, in Abhängigkeit der jeweiligen Tageszeit. Allerdings zeigt sich, dass es nahezu unerheblich ist, welche Tageszeit in dieser Betrachtung berücksichtigt wird. In die

Ergebnisdarstellung von Abb. 1 wurden alle Messfahrten aufgenommen, die während allochthoner Wetterlagen mit v > 1,5 m s^{-1} durchgeführt wurden (~ 2/3 aller Messungen).

Die Messungen in den Morgenstunden (Abb. 1, gepunktete & durchgezogene Linie) weisen etwas geringere Konzentrationen auf als die Messfahrten am Nachmittag (doppelte & gestrichelte Linie). In Abhängigkeit des Streckenabschnittes variieren die Konzentrationen zwischen 50 µg m^{-3} und 690 µg m^{-3}. Der Verlauf der Route ist anhand des erfassten Konzentrationsmusters sehr gut nachzuvollziehen. Die höchsten Werte werden im Bereich der Streckenabschnitte 10 bis 16 erreicht, dort, wo die Messstrecke auf die Hügellage der „Oberstadt“ führt, entlang des durch den Kfz-Verkehr hochfrequentierten Innenstadtbereiches. Vergleichbar mit den Morgenstunden weisen die Messungen der Nachmittagsstunden einen spiegelbildlichen Verlauf auf. Jedoch steigen die PM_{10}-Durchschnittswerte leicht auf 282 µg m^{-3} (vergl. Morgenstunden: 219 µg m^{-3}) an.

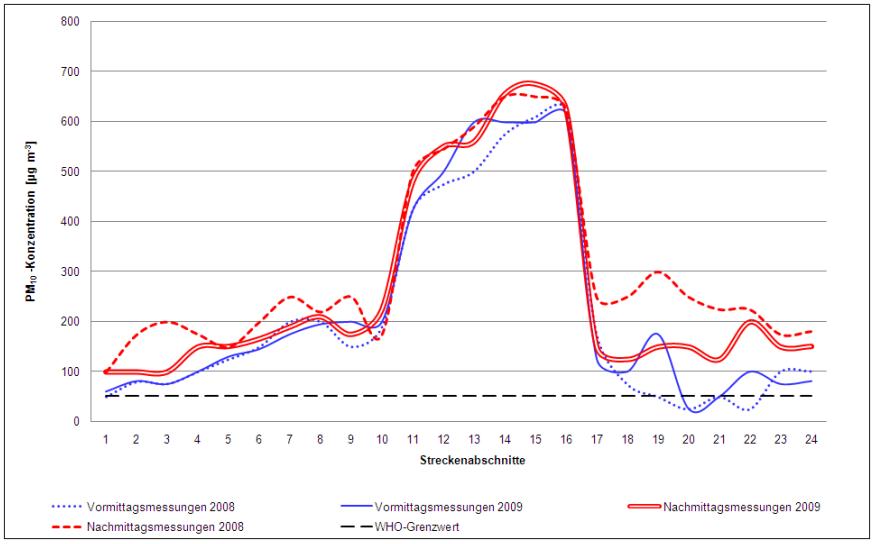

Abb. 1: Streckenabschnittsmittelwerte der PM_{10}-Konzentrationen aller Messfahrten durchgeführt am Vor- bzw. Nachmittag für die Messperioden 2008 und 2009 entlang der Messstrecke durch das Stadtgebiet von Kigali

Letztendlich wird in Abb. 1 die sehr gute Reproduzierbarkeit der Ergebnisse entlang der gesamten Messstrecke aufgezeigt, mit einem nahezu deckungsgleichen Konzentrationsverlauf, sowohl am Vor- als auch am Nachmittag.

Eine deutliche Verschlechterung der lufthygienischen Situation konnte während autochthoner Wetterlagen registriert werden. In Abb. 2 ist erneut der für die Messroute typische Konzentrationsverlauf sehr gut zu erkennen, jedoch offenbaren bereits die morgendlichen Messungen (untere Liniendarstellungen) aufgrund der eingeschränkten Austauschbedingungen (v < 1 m s^{-1}) PM_{10}-Konzentrationen zwischen 175 µg m^{-3} und 900 µg m^{-3}. Vergleichbar mit den allochthonen Nachmittagsmessungen (s. Abb. 1) zeigt sich auch für die eigenbürtigen Bedingungen, dass im Vergleich zum Morgen höhere Werte erreicht werden (Abb. 2, obere Liniendarstellungen). Allerdings äußert sich dieser Anstieg in Werten zwischen 1.400 µg m^{-3} und > 2.000 µg m^{-3}. Dies deutet darauf hin, dass der Luftaustausch der Stadtatmosphäre so stark eingeschränkt ist, dass es zu einer stetig fortlaufenden Akkumulation der Schadstoffe kommt. Erstaunlicherweise werden die

höchsten Konzentrationen dort gemessen, wo die Straße geteert und in einem recht guten Zustand ist. Ganz im Gegensatz zu Untersuchungen der Feinstaubkonzentration im Stadtgebiet von Ouagadougou (Burkina Faso) kann hier kein direkter Zusammenhang zwischen den aufgewirbelten Staubpartikeln der ungeteerten Pisten und den hohen Konzentrationen festgestellt werden (Linden, 2006; Linden et al., 2008). Vielmehr ergibt sich hier ein eindeutiger Hinweis auf die verheerende Situation der Kraftfahrzeuge. Die Daten der permanenten stationären Messungen bestätigten die mobilen Messergebnisse.

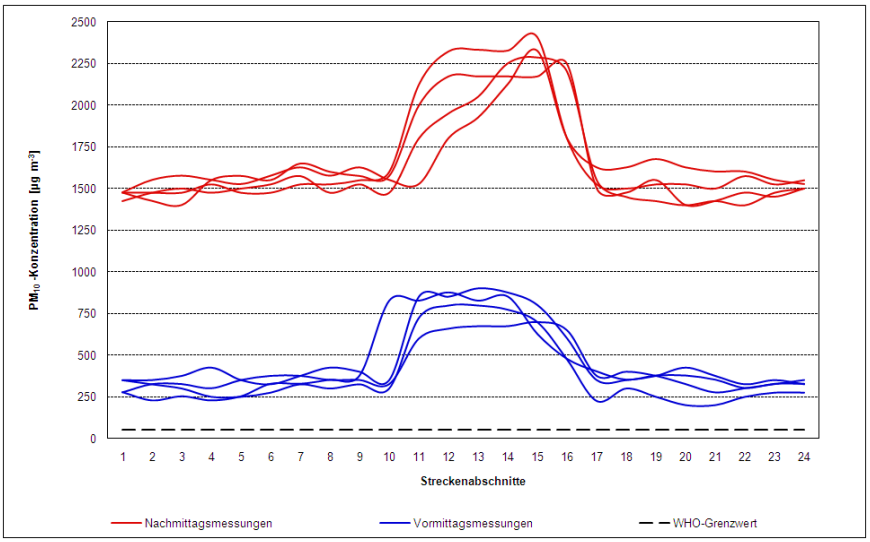

Abb. 2: Streckenabschnittsmittelwerte der PM_{10}-Konzentrationen entlang der Messstrecke durch das Stadtgebiet von Kigali für autochthone Wetterlagen während der Messperioden 2008 und 2009

5. Analyse der Staubproben

Da sowohl in den Vierteln der wohlhabenden als auch der armen Bevölkerung das PM_{10} die Grenzwerte der WHO um ein Vielfaches überschritten hat, kann dies als Indiz dafür angesehen werden, dass nicht nur der Kfz-Verkehr allein, sondern auch der private Hausbrand zu einer fatalen Verschmutzung der urbanen, bodennahen Atmosphäre beiträgt. Ebenso wurde die Vermutung aufgestellt, dass aufgrund der während der Messungen herrschenden „kleinen Trockenzeit“ der natürliche Anteil der anorganisch luftgetragenen Partikel einen entscheidenden Anteil am Gesamtstaub haben müsste. Die daraufhin durchgeführte Analyse der Staubproben mit dem Rasterelektronenmikroskop ermöglichte eine schnelle Zuordnung der Stäube, die aus der urbanen Luft der Hauptstadt herausgefiltert werden konnten. Die mit dem SEM-Verfahren abgetasteten Partikeloberflächen der Aerosole wiesen teilweise recht eindeutige Ergebnisse auf. So konnte die Flugasche aus der Verbrennung von Biomasse sehr gut von den durch Dieselmotoren produzierten Rußteilchen unterschieden werden. Auch organische Partikel sowie anorganischer Bodenstaub waren zu differenzieren. Wie aus Abbildung 3 hervorgeht, zeigt sich für das gesamte Untersuchungsgebiet, dass anthropogen produzierte Stäube rund zwei Drittel der Aerosole in der urbanen Luft ausmachen. Dies bestätigt die im Voraus angestellten Vermutungen, dass der zunehmende Bevölkerungsdruck und der steigende Motorisierungsgrad erheblichen Einfluss auf die lufthygienische Situation nehmen. Die dominanten Anteile der anthropogenen Aerosole sind Dieselruß (29 %; hohe Dichte veralteter Fahrzeuge mit Dieselmotoren), Flugasche (25 %; traditionelle

Art der Feuerung) und Kerosin (13 %; Ersatzbrennstoff aufgrund des sinkenden Holzverkommens). Pollen und andere organische Aerosole nehmen mit 12 % den geringsten Anteil ein. Stäube geogenen Ursprungs erreichen knapp 21 %.

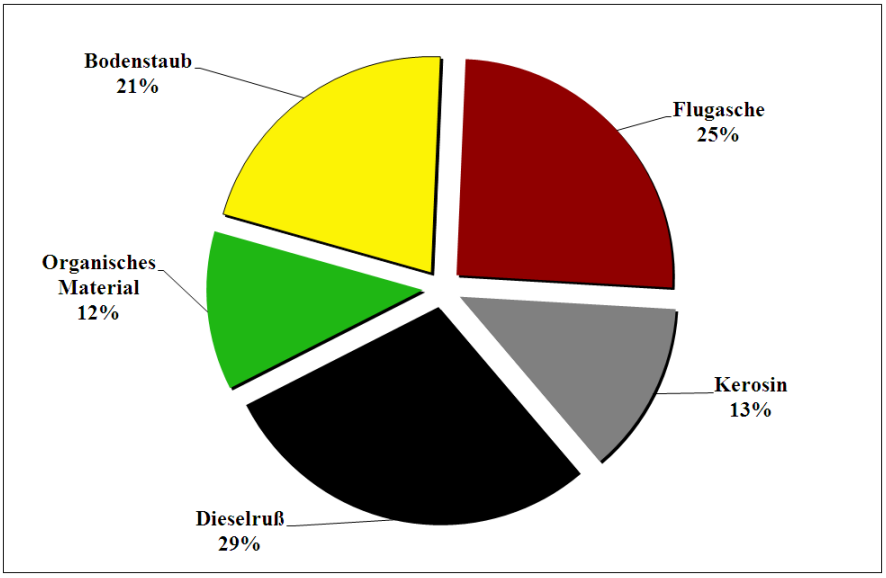

Abb. 3: Aufschlüsselung der natürlichen organischen und anorganischen Aerosole, sowie der Anteil der anthropogenen, luftgetragenen Partikel der urbanen Atmosphäre von Kigali

6. Zusammenfassung und Ausblick

Erste Untersuchungen zur lufthygienischen Situation in Ruandas Hauptstadt Kigali haben offenbart, dass die Luftverschmutzung kaum mehr nachvollziehbare Werte erreicht. Die Betrachtung des Feinstaubes zeigt, dass die durchschnittlichen Tageswerte mit rund 650 µg m^{-3} die Grenzwerte der WHO weit überschreiten. Damit stellt allein die Feinstaubbelastung der Stadthindernisschicht eine immanente gesundheitliche Gefährdung für die Bevölkerung in Kigali dar. Forciert wird die durch den Menschen verursachte Verschmutzung der urbanen Atmosphäre durch die alten Dieselfahrzeuge und die Verbrennung von Biomasse. Zunehmende Temperaturen und ein verringerter Luftaustausch aufgrund einer in den letzten Jahren signifikanten Zunahme autochthoner Wetterlagen verschärfen die Situation zusehends. Dies resultiert in einer fortschreitenden Akkumulation luftverunreinigender Stoffe. Die Analyse weiterer Luftinhaltsstoffe soll nun zeigen, inwieweit auch diese ein gesundheitsgefährdendes Potenzial aufweisen. Ergänzend dazu wird eine Analyse der lufthygienischen Situation im Inneren der Lehmhütten durchgeführt (Balakrishnan et al., 2002; Kousa et al, 2002). Die Messperiode wird auf mindestens ein Jahr ausgeweitet, um einen besseren Überblick über die Veränderungen der lufthygienischen Situation zu erhalten, u.a. durch den Wechsel zwischen Trocken- und Regenzeiten.

Literatur

Baumbach, G., U. Vogt, K.R.G. Hein, A.F. Oluwole, O.J. Ogunsola, H.B. Olaniyi, 1995: Air pollution in a large tropical city with a high traffic density – Results of measurements in Lagos, Nigeria. The Science of the total Environment 169, 25-31.

Balakrishnan, K., J. Parikh, S. Sankar, R. Padmavathi, K. Srividya, V. Venugopal, S. Prasad, V.L. Pandey, 2002: Daily average exposures to respirable particulate matter from combustion of biomass fuels in rural households of southern India. Environmental Health Perspectives 110/11, 1069-1075.

Gwilliam, K., 2003: Urban transport in developing countries. Transport Reviews, 23, 106-120.

Han, X., L.P. Naeher, 2006: A review of traffic-related air pollution exposure assessment studies in the developing world. Environmental International 32 (1), 106-120.

Haryono, S., A. Budihardjo, N. Hardyanti, 2009: Black carbon concentration in kitchens using fire-wood and kerosene fuels. Journal of Applied Sciences in Environmental Sanitation 4/1, 55-62.

Henninger, S., 2005: Analyse der atmosphärischen CO_2-Konzentrationen am Beispiel der Stadt Essen. Essener Ökologische Schriften, 23, Westarp Verlag Hohenwarsleben, 192 p.

Henninger, S., 2009a: Urban climate and air pollution in Kigali, Rwanda. ICUC 2009, 1038-1041.

Henninger, S., 2009b: Urbane Luftverschmutzung am Beispiel einer afrikanischen Großstadt. Umweltchemie und Ökotoxikologie 3, 58-60.

Kousa, A., L. Oglesbyd, K. Koistinea, N. Kunzlib, M. Jantunena, 2002: Exposure chain of urban $PM_{2.5}$ – Associations between ambient fixed site, residential outdoor, indoor, workplace and personal exposures in four European cities in the EXPOLIS-study. Atmospheric Environment 36, 3031-3039.

Linden, J., 2006: Urban Project – Urban climate and air pollution in Ouagadougou, Burkina Faso. IAUC Newsletter 20, 10-12.

Linden, J., S. Thorsson, I. Eliasson, 2008: Carbon monoxide in Ouagadougou, Burkina Faso – A comparison between urban background, roadside and intraffic-measurements. Water, Air and Soil pollution 188, 345-353.

Van Wijnen, J.H., A.P. Verhoeff, H.W. Jans, M. Bruggen, 1995: The exposure of cyclists, car driver and pedestrians to traffic-related air pollutants. International Archives of Occupational and Environmental Health 67, 187-193.

WHO (2006): Air quality guidelines for particulate matter, ozone, nitrogen dioxide and sulfurdioxide – Global update 2005 – Summary of risk assessment, Geneva, 22 p.

Adresse des Autors

Jun.-Prof. Dr. rer. nat. Sascha Henninger (henninger@rhrk.uni-kl.de)
Lehreinheit Physische Geographie, Technische Universität Kaiserslautern
Pfaffenbergstr. 95, D-67663 Kaiserslautern, Deutschland

Spatial and temporal variability of surface temperature of tree crowns in an urban environment

Fred Meier, Dieter Scherer, Jochen Richters

Chair of Climatology, Department of Ecology, Technische Universität Berlin, Germany

Abstract

This research analyses surface temperature of tree crowns using a high-resolution thermal-infrared (TIR) camera and meteorological measurements in the city of Berlin, Germany. For temporal analysis, the TIR camera recorded one image per minute over a period of five days from 5th to 10th August 2009 and for spatial analysis, we selected 108 trees with dense crowns. The daily mean crown temperature ranged from 23.5 °C to 24.7 °C. The maximum range was recorded around 14:00 CET (27.5 °C to 30.8 °C). Isolated columnar tree crowns e.g. *Populus nigra* showed the lowest daytime temperature in the investigated area. The results show that crown temperature depends on the tree location within the city and its canopy architecture.

1. Introduction

The importance of trees for the urban environment was already emphasised within urban climate research (Brahe 1974, Heisler 1986, Oke 1989). In particular, this includes the reduction of air temperature by evaporation, the reduction of surface temperature and building energy use by shadowing and the improving of air quality (e.g. Akbari et al. 2002). In addition, tree shadow has an effect on human thermal comfort because of modified incoming solar and thermal radiation part of the human energy balance (Matzarakis and Streiling 2004, Thorsson et al. 2004, Mayer et al. 2009).

However, there are only few studies regarding the spatial and temporal variability of tree crown temperature in cities (e.g. Kjelgren and Montague 1998, Leuzinger et al. 2010). The foliage temperature has important consequences for the tree itself, but also for the urban environment surrounding the tree. The surface temperature of tree a crown depends on each leafs energy balance. The leaf energy balance is affected on the one hand by type-specific properties of the leaf e.g. transpiration controlled by stomata conductance, leaf mass, leaf size, shape, emissivity and albedo (Monteith and Unsworth 2008). On the other hand, the leaves or tree crowns interact with the surrounding atmosphere. Consequently, temperature and humidity of the urban atmosphere, wind speed and incoming radiation are relevant to the energy balance of trees. Especially in the city, these atmospheric variables show a high spatial and temporal variability. The aim of this study is to answer the following questions:

1.) Are there differences between urban trees in the study area (Berlin, Germany) concerning the foliage temperature and if so, how big are these differences?
2.) What influence has the location within the city on the surface temperature of tree crowns?

2. Methods

In answering these questions, we analysed data from a meteorological station and TIR imagery. We could identify 108 tree crowns in the TIR image whereas genus or species of 34 trees are known. The TIR camera recorded one image per minute over a period of

five days from 5th to 10th August 2009. The fixed camera position ensured a valid comparison between the multi-temporal imagery. The measured radiance was converted into directional brightness temperature using firmware calibration parameters. For details on pre-processing, radiometric and geometric corrections of TIR imagery, please see Meier et al. (2010). Here, we assumed an emissivity of 1.0 since no data for the investigated trees were available and no atmospheric correction was applied. Though we did not derive thermodynamic surface temperatures, we use the term 'surface temperature' and not 'directional brightness temperature'. Inside the field of view (FOV), the meteorological station measured air temperature (Tair), relative humidity (RH), wind speed (WS), wind direction (WD) and global radiation in a height of 20 m above ground. Fig. 1 illustrates the experimental setup (left) and a photo showing approximately the FOV of the TIR camera.

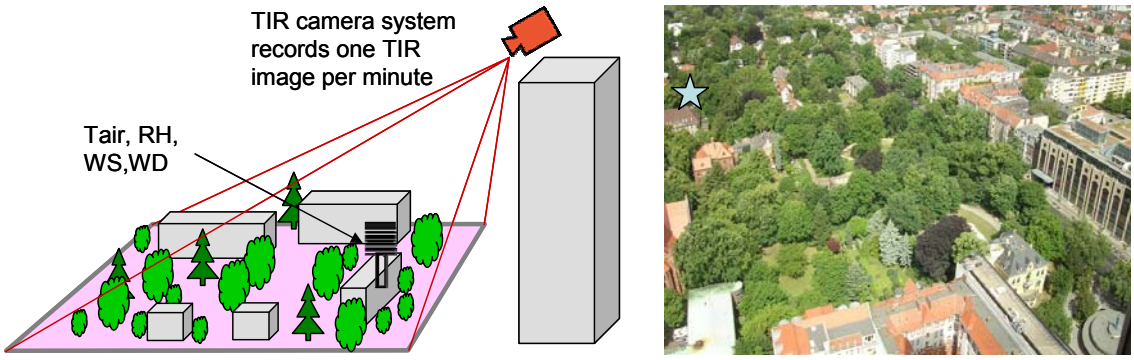

Fig. 1: Experimental setup (left) and field of view (FOV) of the thermal infrared (TIR) camera. The asterisk symbol marks the meteorological station

3. Results and Discussion

The average single crown temperature ranged from 23.5 °C to 24.7 °C. Fig. 2 shows the temporal variability of all tree pixels for the average diurnal cycle (30 min averages).

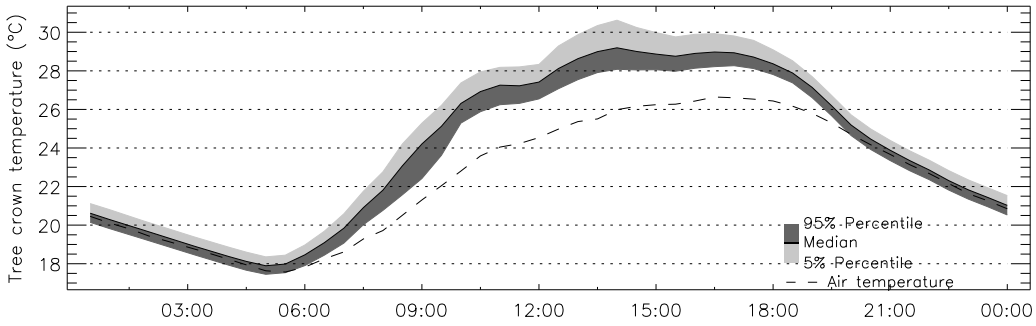

Fig. 2: Spatio-temporal variability of tree crown temperature during a diurnal cycle

During the night, maximum temperature difference was ca. 1.5 K. For instance temperature varied between 18.5 °C and 20.1 °C at 03:00 CET. The maximum range was recorded at 14:00 CET and ranged from 27.5 °C to 30.8 °C. During the day, the tree temperature was always greater than Tair. Please note, that the meteorological station is

situated in a very green and low building density area. The maximum leaf-to-air temperature difference amounts to 4.9 K at 13:30 CET. In the study of Leuzinger et al. (2010) leaf-to-air temperature difference reached up to 5 K at an ambient temperature of ca. 25 °C.

In terms of differences between tree species or tree genera, no general statement is possible, because the number investigated trees per species is limited. Table 1 presents all derived values of four species, two genera and all identified conifers. The data shows, that *Populus nigra* had the lowest mean and most notable the lowest daytime crown temperature. The highest values showed *Taxus baccata*. The difference between deciduous species (*Fagus sylvatica, Quercus robur*) or genera (*Acer, Tilia*) was less than 1 K. The trees with big crowns showed a slight higher spatial standard deviation (σ) than those with small crowns.

Table 1: Comparison between air temperature (Tair), relative humidity (RH) and tree crown temperature of four species, two genera and all identified conifers

	Tair (°C)	RH (%)	*Fagus sylvatica*	*Quercus robur*	*Acer*	*Tilia*	*Taxus baccata*	*Populus nigra*	Conifer
Number of trees			10	7	6	5	3	3	8
Pixels			8.267	7622	4596	3937	1277	846	2858
Mean	22.5	52.6	23.9	23.8	24.0	24.0	24.6	23.7	23.9
13:30-14:00	26.0	40.7	29.3	28.6	29.4	29.1	30.0	27.8	29.0
02:30-03:00	18.9	65.1	18.9	19.1	18.9	19.0	19.6	19.3	19.0
Mean spatial σ			0.19	0.23	0.20	0.23	0.08	0.12	0.20
13:30-14:00			0.74	0.63	0.82	0.70	0.43	0.31	0.49
02:30-03:00			0.23	0.26	0.18	0.17	0.08	0.09	0.23

The high values of *Taxus baccata* could be attributed to the influence of the tree location within the city, because all three crowns stand within an intensive sealed area (concrete pavement). Fig. 3 shows the spatio-temporal distribution of all selected tree crowns and the corresponding thermal pattern of all surfaces in the FOV of the TIR camera. All trees over sealed surfaces, most notable in the day pattern (Fig. 3B), show higher temperatures in comparison to park trees. Only very high crowns that overlap the street canyon or courtyard are not so hot. It is particularly noticeable that at night all tree crowns are slightly warmer than roofs (Fig. 3C).

4. Conclusions

The results show that tree crown temperature varies up to 3.8 K in the examined urban environment. The daily mean crown temperature ranged from 23.5 °C to 24.7 °C. Also at night, tree crown temperature varies up to 1.5 K.

Trees in street canyons or over sealed surface have higher crown temperature than those over grass and non-sealed surfaces, which is in accordance to further studies (Leuzinger et al., 2010; Kjelgren and Montague, 1998).

Isolated columnar tree crowns e.g. *Populus nigra* showed the lowest temperature in the investigated area. The study shows that crown temperature depends on the tree location within the city and its canopy architecture.

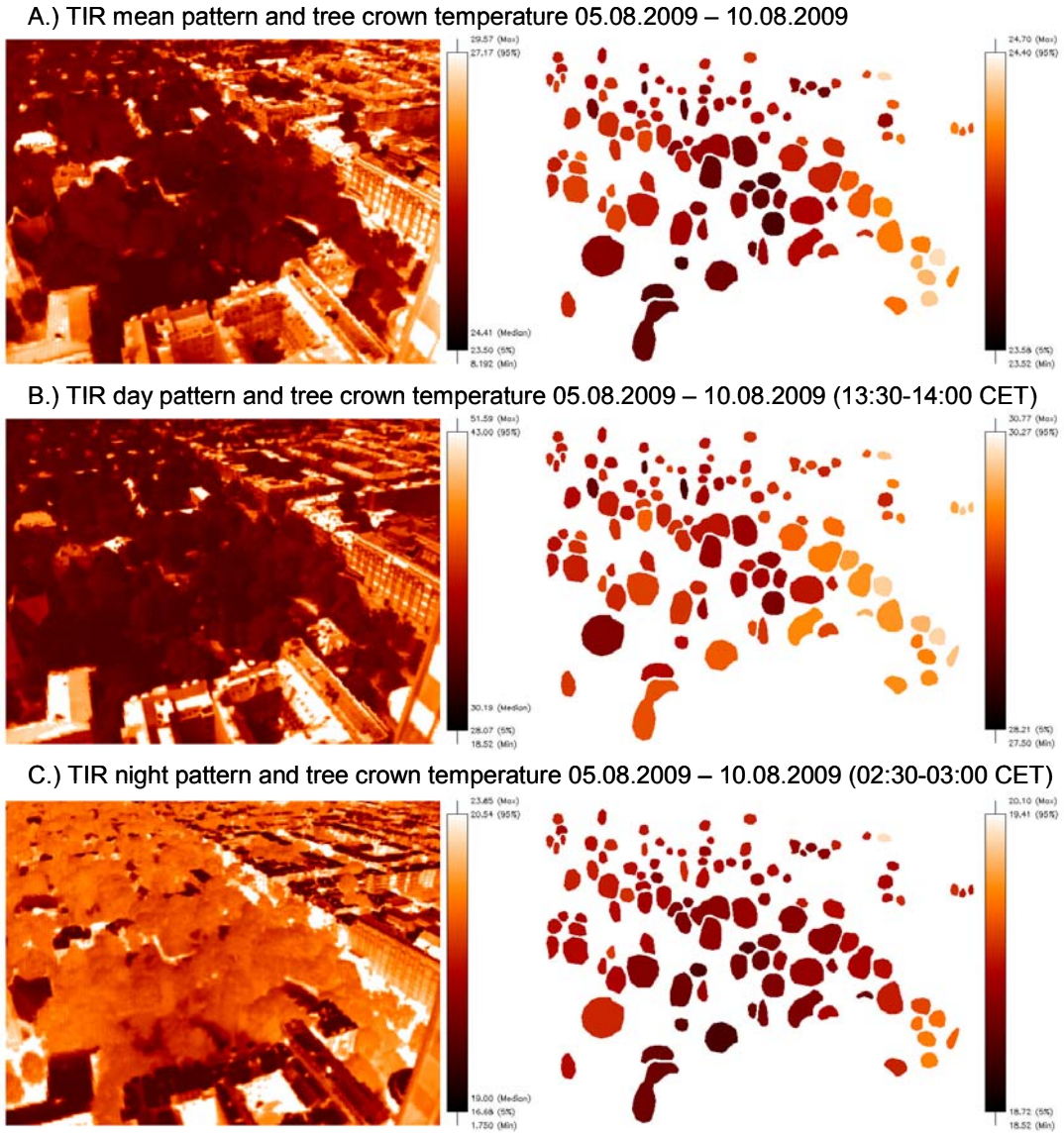

Fig. 3: Spatio-temporal mean pattern (A) of surface temperatures derived from 7.200 TIR images. Day pattern (B) and night pattern (C) of tree crown temperatures derived from 150 TIR images

Acknowledgement

The authors would like to thank Marco Otto (Chair of Climatology, TU Berlin) and Moritz von der Lippe (Chair of Ecosystem Science / Plant Ecology, TU Berlin) for help during the rapid field mapping of trees species in winter and data analysis.

References

Akbari, H., M. Pomerantz, H. Taha, 2001: Cool surfaces and shade trees to reduce energy use and improve air quality in urban areas. Solar Energy, 70, 295-310.

Brahe, P., 1976: Klimatische Auswirkungen von Gehölzen auf umbauten Stadtplätzen. Das Gartenamt, 23, 61-70.

Heisler, G.M. 1986: Effects of individual trees on the solar radiation climate of small buildings. Urban Ecology, 9, 337-359.

Kjelgren, R., T. Montague, 1998: Urban tree transpiration over turf and asphalt surfaces. Atmospheric Environment, 32, 35-41.

Leuzinger, S., R. Vogt, C. Körner, 2010: Tree surface temperature in an urban environment. Agricultural and Forest Meteorology, 150, 56-62.

Matzarakis, A., S. Streiling, 2004: Stadtklimatische Eigenschaften von Bäumen. Falluntersuchung in Freiburg im Breisgau. Gefahrstoffe-Reinhaltung der Luft, 64, 307-310.

Mayer, H., S. Kuppe, J. Holst, F. Imbery, A. Matzarakis, 2009: Human thermal comfort below the canopy of street trees on a typical Central European summer day. In: Mayer, H., A. Matzarakis (Eds.): 5th Japanese-German Meeting on Urban Climatology. Berichte des Meteorologischen Instituts der Albert-Ludwigs-Universität Freiburg, Nr. 18, 211-219.

Meier, F., D. Scherer, J. Richters 2010: Determination of persistence effects in spatio-temporal patterns of upward long-wave radiation flux density from an urban courtyard by means of Time-Sequential Thermography. Remote Sensing of Environment, 144, 21-34.

Monteith, J., M. Unsworth, 2008: Principles of Environmental Physics. Third Edition, Academic Press, 418 pp.

Oke, T.R., 1989: The micrometeorology of the urban forest. Philosophical Transactions of the Royal Society of London. Series B, Biological Sciences, 324, 335-349.

Thorsson, S., M. Lindqvist, S. Lindqvist, 2004: Thermal bioclimatic conditions and patterns of behaviour in an urban park in Göteborg, Sweden. International Journal of Biometeorology, 48, 149-156.

Authors' address:

Fred Meier (fred.meier@tu-berlin.de)
Prof. Dr. Dieter Scherer (dieter.scherer@tu-berlin.de)
Dr. Jochen Richters (jochen.richters@tu-berlin.de)

Chair of Climatology, Department of Ecology, Technische Universität Berlin
Rothenburgstr. 12, D-12165 Berlin, Germany

Use of a mobile platform for assessing urban heat stress in Rotterdam

Bert G. Heusinkveld[1], L.W.A. van Hove[1,2], C.M.J. Jacobs[2], G.J. Steeneveld[1], J.A. Elbers[2], E.J. Moors[2], A. A. M. Holtslag[1]

[1]Department of Meteorology and Air Quality, Wageningen University, The Netherlands
[2]Earth System Science and Climate Change Group, Wageningen UR, The Netherlands

Abstract

In this study, an assessment of the intensity of the urban heat island (UHI) in Rotterdam was carried out using an innovative mobile bio-meteorological measuring platform mounted on a cargo bicycle. The goal was to assess whether or not heat stress is currently or likely to become a critical issue. Physiological equivalent temperatures were calculated directly from the measurements. Preliminary results show how effective urban parks and greenery are in reducing the UHI. The maximum UHI was about 7 K warmer than the rural area, whereas greener urban configurations were under 3 K warmer. City parks show marked cooling effects during daytime. The preliminary results clearly demonstrate the presence of a considerable UHI in Rotterdam, which is expected to be found in other Dutch cities, and confirms the important role of green spaces in mitigating urban heat stress.

1. Introduction

The majority of the world's population now live in urban environments. The average temperature of built-up areas is higher than the surrounding rural area, which enhances heat stress, and is called the Urban Heat Island (UHI) effect (Oke, 2006). Because The Netherlands has a mild Cfb climate and is situated close to the sea, it was never considered an issue for urban planning even though the level of urbanization began to increase rapidly. Currently the built-up area is over 15% of the total land area and increasing. Recent heat waves of the year 2003 and 2006 caused an excess in mortality in The Netherlands of between 1400 and 2200 people. Climate projections predict that heat waves in The Netherlands will likely become more frequent in the next decades, which will compound the environmental stresses of urban life and lifestyles. However, information regarding UHI in Dutch cities is completely lacking, both from observational and model perspectives, which hampers the design of suitable adaptation and heat mitigation strategies. Even moderate heat waves should not be underestimated for a maritime climate. The reason is that the population has no time to acclimatize since adaptation of human thermoregulation usually takes about 1 week.

Spatial planning and urban growth projections using various scenarios all point to a large expansion of urbanized space (Nijs et al., 2002). The scenarios of the Dutch National Nature Outlook study (MNP, 2002) which are based on various IPCC-scenarios, also supports this. Comparing these scenarios to the current situation (2010), urban growth seems to follow the 'Global Market' scenario. This scenario suggests strong population growth, free trade, strong technological developments, limited role of government, strong decrease in agricultural land and a luxury consumption pattern. The most important land use changes in The Netherlands over the last 10 years are related to the increase of urban and nature reserve lands at the expense of agricultural land (Hazeu, 2006), and mixing of different land-use types in both urban and rural areas (Ritsema et al., 2006. The Land Use Scanner tool (LUS) was used to simulate how The Netherlands land use would look like in 2040. The LUS is a GIS-based logit model that si-

mulates future land use (Hilferink and Rietveld, 1999) and has been used for various policy-related research projects.

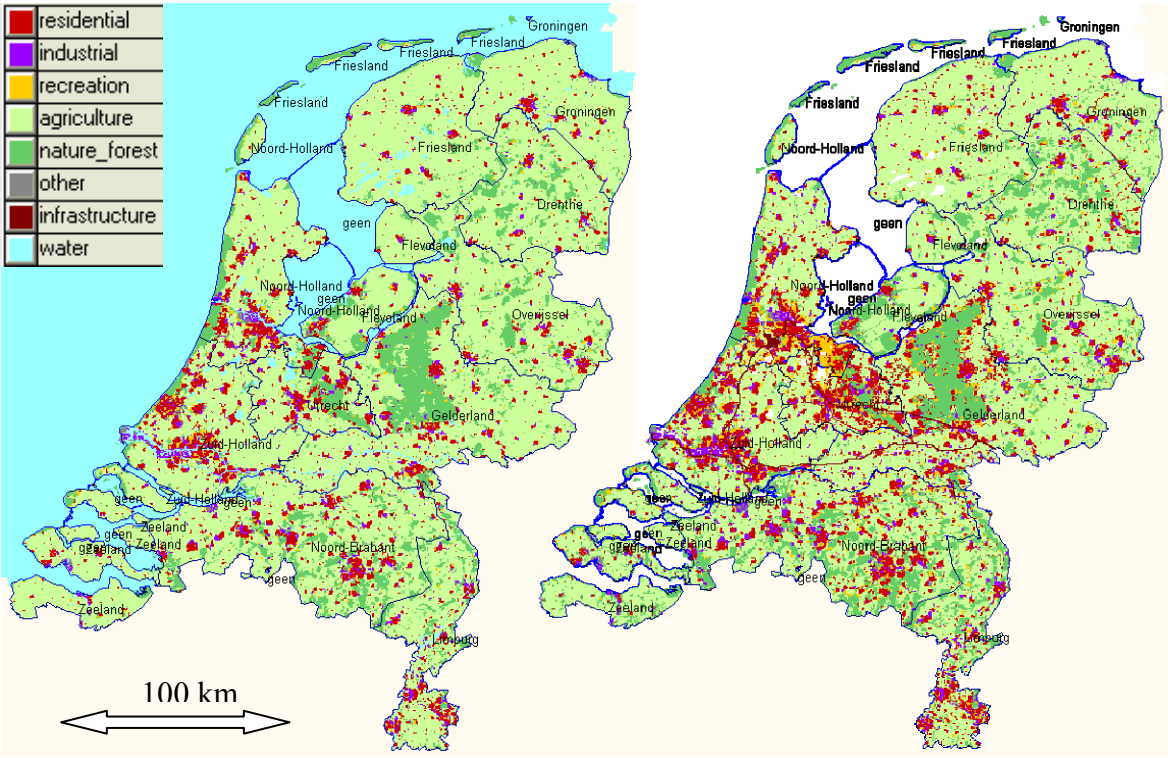

Fig. 1: Land use scenario, left side year 2000, right side year 2040

The 'Global Market' scenario simulation estimates 20 % urbanization in 2040 (Fig. 1). The definition of urban space also includes infrastructure and industry but there are some differences in the definition and the Dutch planning office includes, for example, urban greenery and urban infrastructure but not external infrastructure. The impact of infrastructure on surface heating is significant and therefore should not be excluded from such analyses.

This study examines the extent of the urban heat island effect (UHI) of the city of Rotterdam, which is part of the largest urban conglomeration of The Netherlands with more than 1.2 million inhabitants on 870 km^2.

2. Materials and methods

Traverse measurements were performed in Rotterdam using two cargo bicycles as a mobile platform, equipped with innovative instruments to quantify the micrometeorological conditions inside urban canyons. The cargo bicycles greatly facilitated data acquisition through the narrow streets and urban canyons of pedestrian areas. The bicycles were equipped with a shielded thermometer, a humidity sensor, a 2-dimensional sonic anemometer and 12 radiation sensors to measure solar radiation and thermal infrared radiation exchange from six directions (Fig. 2). Wind speed measurements were corrected for bicycling speed.

Fig. 2: Mobile biometeorological station mounted on a cargo bicycle

The data were recorded at 1 Hz and combined with concurrent readings from a GPS device. The instruments were powered by a solar panel mounted on the baggage carrier. Measurements were performed along two previously determined routes through a number of characteristic urban districts, including an industrial area, an older residential area, a city park and a harbour area. The routes were photographed at fixed intervals from 0.5 m above the ground with a fisheye lens pointing upwards. The observations were carried out during three 2 h time intervals on 6 August 2009. This was a warm day with maximum air temperatures of about 30°C. Data from the traverse measurements were compared with recordings from a nearby synoptic weather station outside the urban area. Fig. 2 shows a detailed view of the front of the bicycle.

A very important factor in the human energy balance is the mean radiant temperature (T_{MRT}), and this can be calculated directly from the 12 radiation sensors and correlates very well with perceived human comfort (Matzarakis et al., 2007) (Eq. 1).

$$T_{MRT} = \sqrt[4]{\frac{Q_a}{\varepsilon\sigma}} - 273.15 \qquad (1)$$

Where Q_a is the total shortwave and thermal radiation absorbed by the human body (W m^{-2}), ε is the thermal emissivity (-) and σ is the Stefan Boltzmann constant (W m^{-2} K^{-4}). Directional dependant weighing factors and shortwave radiation absorption coefficients need to be considered for calculating radiation load on a human.

The advantage of these extensive measurements are that the human micro-climate can be quantified using physiologically relevant indices that are much more accurate than indices derived from standard weather station data. Examples include the physiologically equivalent temperature (PET) (Höppe and Mayer 1987) or predicted mean vote (PMV) (Fanger, 1972). PET is defined as the physiological equivalent temperature at any given place, and thus complex outdoor microclimates can be compared with a climate chamber with temperature of air, floor, walls and ceiling at PET temperature (wind speed 0.1 m/s and relative humidity of 50%). The higher accuracy for human micro-climate indices derived from such a mobile station is mainly related to its ability to measure omnidirectional radiative fluxes. These flux measurements determine T_{MRT}, which is the most important meteorological parameter for calculating the human energy balance under summer conditions (Clark and Edholm, 1985).

3. Preliminary results and discussion

An initial analysis shows that the UHI is very large after sunset with an air temperature difference of more than 8 K between city center and rural environment (grassland). An interesting observation was an industrial zone with dark flat roofs. This area appears to have the hottest surface temperature of all urban areas in Landsat thermal infrared images. However the bicycle measurements did not find this area hotter than the city center, especially not during the evening hours. This might be related to the low thermal inertia of the flat roofs. The UHI is strongest after sunset and gradually declines during the night. Air temperature remains higher than the rural area due to the slow release of solar heat storage originating from daytime solar radiative forcing.

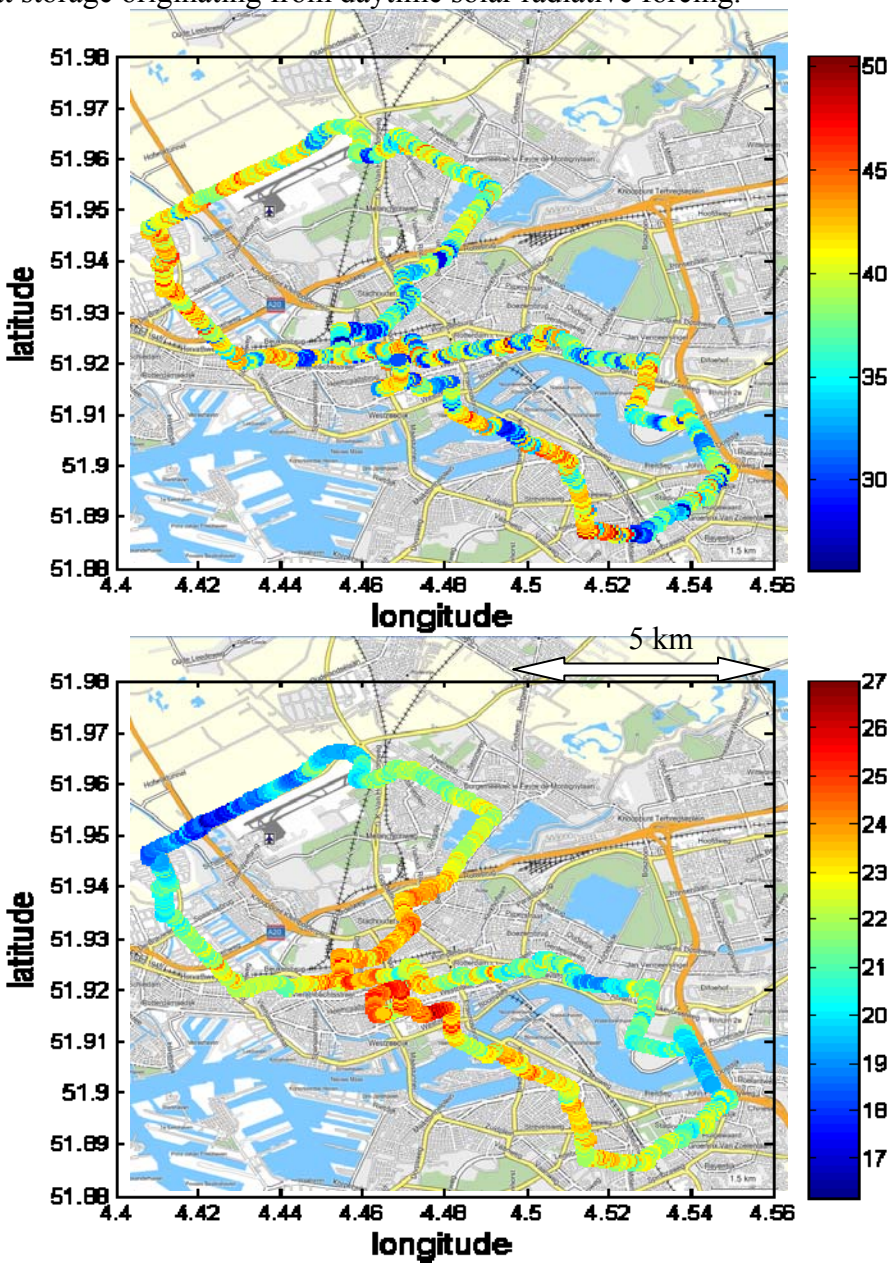

Fig. 3: Traverse measurements of Rotterdam, PET, Upper panel 14:00-16:00 h. lower panel 22:00 – 24:00 h (Central European Time)

PET (Fig. 3) could be easily calculated because of the direct measurements of all the radiation components. Rayman software was used to compute PET without the need to calculate complex city canyon radiation distribution because T_{MRT} was measured on the bicycle (Matzarakis et al., 2007). The measurements show some interesting features. A park in the southeast side was the coldest spot during daytime whereas a neighborhood just east of the city center was the coolest urban spot during the evening hours. Both routes were documented using fish-eye photography.
An isolated tree in an urban canyon does not seem to have much influence on PET during evening hours (Matzarakis et al., 2007). However the bicycle data shows that a neighborhood with scattered trees does have a marked impact on air temperature during evening hours. On the other hand, a nearby park shows the opposite, which may be related to the closed canopy cover. This is also evident in the calculated PET.

4. Concluding remarks

In a changing climate and with future urban space projection scenarios showing Dutch urban density increasing from 14% in 2000 to 20% by the year 2040, it is likely that the UHI impact will become much more serious. The UHI effect may also accelerate even faster because many isolated and growing urban clusters will start to influence each other, an issue worthy of further investigation.
The presented biometeorological measurements using a cargo bicycle proved to be a valuable tool for investigating urban biometeorological conditions. While traversing the city of Rotterdam PET ranged from 25 to over 50 °C during a hot afternoon (6 August 2009). The neighborhood with the lowest PET during daytime and evening hours appears to be an urban configuration with low buildings and extensive greenery.

Acknowledgements
This research was part of the project “Heat stress in the city of Rotterdam” (HSRR05) funded by the first phase of the Knowledge for Climate Program and the municipality of Rotterdam. We also like to thank the students Joel Schröter, Marina Sterk and Suzanne Visser for their support on the measurement days.

References

Clark R.P., Edholm, O.G., 1985: Man and his thermal environment. E. Arnold, London
Fanger, P.O., 1972: Thermal comfort. McGraw-Hill, New York
Hazeu, G.W., 2006: Land use mapping and monitoring in The Netherlands (LGN5). 2nd EARSeL Workshop on Land Use and Land Cover, 28-30 September 2006, Bonn, Germany. Conference proceedings.
Hilferink, M. & P. Rietveld (1999), *Land Use Scanner: An integrated GIS based model for long term projections of land use in urban and rural areas*, in: Journal of Geographical Systems, 1(2): 155-177.
Höppe, P., 1999: The physiological equivalent temperature -a universal index for the biometeorological assessment of the thermal environment. Int J Biometeorol (1999) 43:71–75 1987.
Matzarakis, A., Rutz, F., Mayer, H., 2007: Modelling Radiation fluxes in simple and complex environments – Application of the RayMan model. International Journal of Biometeorology 51, 323-334.
Nijs, T. de, Crommentuijn L., Farjon H., Leneman, H., Ligtvoet, W., De Niet, W., Schotten, K., 2002: *Vier scenario's van het Landgebruik in 2030, Achtergrondrapport bij de Nationale Natuurverkenning 2*, RIVM rapport 408764 003, RIVM, Bilthoven.
MNP (2002) Nationale Natuurverkenning 2, 2000–2030, Milieu- en Natuurplanbureau/Kluwer, Alphen aan de Rijn

Oke, T.R., 2006: Towards better scientific communication in urban climate. Theor. Appl. Climatol. 84, 179-190.

Ritsema, J., and E. Koomen. 2008: Characterising urban concentration and land-use diversity in simulations of future land use. Ann Reg Sci (2008) 42:123–140 DOI 10.1007/s00168-007-0141-7.

Author address:
Dr. Bert G. Heusinkveld (bert.heusinkveld@wur.nl)
Dept. of Meteorology and Air-Quality, Wageningen University
Droevendaalsesteeg 4, P.O. Box 47, NL-6700AA Wageningen, The Netherlands

Evaluation of the relationship between air pollution and climatic elements in urban areas in the sample of Erzurum city in the respect of landscape architecture

Sevgi Yilmaz[1], Yahya Bulut[1], Süleyman Toy[2], Işık Sezen[1]

[1] Department of Landscape Architecture,Erzurum/ Turkey
[2] Landscape Architect & Engineer at Meteorology Office, Erzurum/Turkey

Abstract

This study aims to determine the effects of air pollution on climatic elements and mention about its unfavourable effects on everyday lives of people suggesting some solution proposals in the respect of landscape architecture. Due to its direct and indirect effects on public health and everyday life, air pollution is an important phenomenon. In Erzurum city, where fossil fuels are densely used in extremely cold winter months, when especially Siberian high pressure centre is prevalent in the region, for heating and transportation purposes this phenomenon is of vital importance for people. Unfavourable effects of air pollution on people were determined in a previous study and in the present study effects of air pollution on climatic parameters especially on temperature were investigated, but no relationship was determined since the measurement points were too far from each other. Since the subject matter of landscape architecture discipline is centred on human comfort, this meteorological event interests also landscape architects to the aspect of reducing its unfavourable effects on people. This study is important because, according to the results, some solutions for the reduction of unfavourable effects of this phenomenon were presented in the respect of landscape architecture in order for local people to live in a more comfortable and healthy environment.

1. Introduction

Air pollution is one of the most important elements affecting human life today (WMO 1999). The city of Erzurum is the second highest settlement in Turkey and therefore its climate is one of the harshest. Long and extremely cold winters are prevalent in the city. Even though there are almost no heavy industries in the city, fossil fuel consumption for domestic heating can cause serious air pollution. In the city people found air pollution to be the most important environmental problem (e.g. Yilmaz and Sezen, 2004; Beyhun et al. 2008). Particulate pollution is a serious health problem throughout the world (e.g. El-Fedal and Massound, 2000; Beckett et al., 2000), exacerbating a wide range of respiratory and vascular illnesses in urban areas (e.g. Free-Smith et al., 1997), In Erzurum, particulate pollution is a very real problem with the potential to cause the most severe and damaging health effects of any pollutant currently in the locale. While it is universally accepted that trees improve the quality of urban life (e.g. Beckett et al., 1998) and while it has been known since ancient times that vegetation can purify the air, relatively little scientific research has been conducted in Turkey on the direct benefits street trees and woodlands provide by absorbing pollutant particles in our country. Landscape architects need to increase the public's awareness of trees in urban areas to enhance the concrete landscape for beauty and for healthy living.

Turkey's urban environment has an extremely high development density with Palandoken hillsides cut into terraces and retained with stone walls to provide geotechnical stability for densely-packed roads and buildings. Little ground-level space

is left for amenity planting on town lots, resulting in a cramped city matrix with inadequate green cover.

Landscape architecture occupation is a discipline whose one objective is to provide comfortable environments for people. Therefore everything in the environment is the subject of landscape architects.

In the present study, it was aimed to present the situation of Erzurum city for air pollution and its effects on climatic elements by giving some solution proposals considering this specific area from the perspective of landscape architecture occupation. The objective of this study is to assess the relative atmospheric concentrations of particulate matter in vegetated vs. unvegetated areas of Erzurum during the period from 1980 to 2009 to assess the value of street tree and other urban planting programs.

2. Material and method

The city of Erzurum is located in the north-eastern part of Turkey at an elevation of 1850 m and 39.57 N, 41.10 E (Fig.1). The city is one of the places where the harshest climate characteristics are seen in Turkey due to its elevation and remoteness to maritime effect. Long (nearly eight months from late September to early May) and extremely cold (ever recorded minimum temperature is -37.2ºC) winters are prevalent in the area. Means of some meteorological parameters are presented in Table 1.

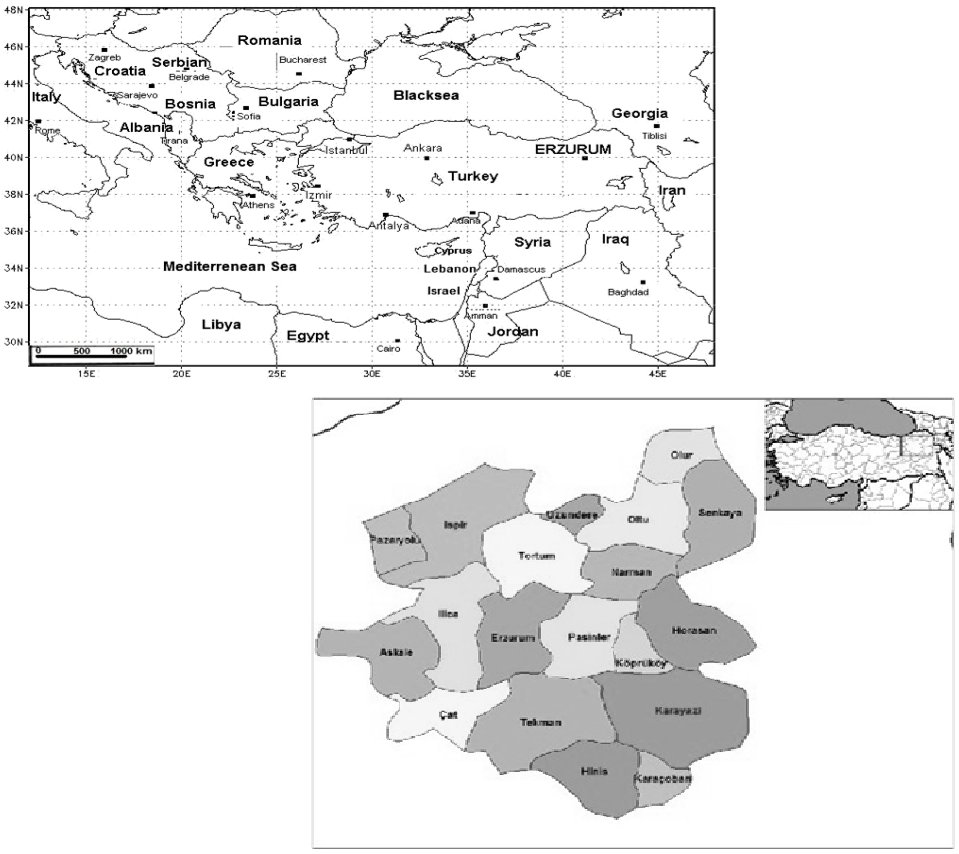

Fig. 1: Location of Erzurum in Turkey

The city is located outskirt of a mountain range in its south, Palandöken with a height above 3000 meters. Therefore its topography is very suitable for valley fogs in especially winter months when Siberian High Pressure Centre shows its effect on the region. If the ground is covered with snow and the sky is clear then the temperature can fall below – 30 ºC. At these times, people have to consume more fossil fuel for heating and if the quality of the coal is low then air pollution becomes a very serious problem even threat for people.

Table 1: Some of the meteorological parameters in Erzurum

Meteorological variables	**Means**
Annual mean temperature (ºC)	5.3
Annual mean maximum temperature (ºC)	12.0
Annual mean minimum temperature (ºC)	-1.5
Annual rainfall (kg/m²)	407.3
Relative humidity (%)	65.9
Annual mean wind speed (m/sec)	3.0
The number of snow covered day (day)	106.0

In the city, air quality measurements have been taken since 1986 and meteorological observations have been taken since 1929. Although these periods of time seem to be enough for the comparison of the data and to obtain clear results, locations of the observation are different. Therefore, in the comparison of the particle amounts in the air and air temperature in winter months in Erzurum no relationships have been found.

3. Results and discussion

With the comparison of air temperature and particle values from 1980 to 2009 in only winter months, no relationship was found between the parameters. However, as the consequence of the geographical and meteorological conditions of the city, air pollution can be seen as a very serious danger for the city especially in winter.

Even though the city is lack of heavy industrial facilities, heavy air pollution is caused only by fossil fuel consumption for domestic heating and vehicle traffic. If the city had industrial facilities the situation could be more serious.

In recent years, the use of natural gas has been increasing in the city. In a study (e.g. Eren and Turan 2007), it was determined that the use of natural gas could mitigate air pollution in winter months after 2005.

4. Conclusion

In order for landscape architects to mitigate the effects of air pollution in Erzurum, it is very important that new settlement areas should be selected with great care. Since the topography of the city is suitable for the formation of dense fogs, direction of prevalent wind should not be closed.

In order to make an air circulation at least in the city centre, some solid cares should be taken. For this aim, green area amount in the city should be increased beyond the stan-

dard of Turkey at least 10 m square per person. Dense and intricate building construction should be avoided.

Local administrations should encourage the use of natural gas in every building efficiently instead of low quality coal. Additionally, protection and preservation of street trees have lacked statutory means and a coordinated policy. This assessment method can usefully provide the data necessary to establish and test new planning practices in Erzurum's municipalities.

References

Beckett, KP., P.H. Freer-Smith, G. Taylor, 1998: Urban woodlands: their role in reducing the effects of particulate pollution. Environmental Pollution 99 (3), 347-360.

Beckett, K.P., P.H.Freer-Smith, G. Taylor, 2000: Particulate pollution capture by urban trees: effect of species and windspeed. Global Change Biology, Vol. 6(8): 995-1003.

Beyhun, N. E., S.Vançelik, H. Acemoğlu, Z. Koşan, A. Güraksin, 2008: Ambient air pollution in Erzurum City Center during 2003-2006. TAF Preventive Medicine Bulletin, 7(3), 237-242.

El-Fadel, M., M. Massound, 2000: Particulate matter in urban areas: health based economic assessment. The Science of The Total Environment, 257 (2-3), 133-146.

Eren, Z., T. Turan, 2007: The change of air pollution originated from fossil fuels in Erzurum City with use of natural gas. 7th National Environmental Engineering Congress. Life and Environment Technology , 24-27 October – İzmir Chamber of Environment Engineers.

Freer-Smith, PH., S. Holloway, A. Goodman, 1997: The uptake of particulates by an urban woodland: site description and particulate composition. Environmental Pollution 95 (1), 27-35.

WMO, 1999: Climate and human health. World climate News 14, 3-5.

Yilmaz, S. I.Sezen, 2004: Determination of public awareness fora ir pollution in Erzurum. Journal of Agriculture Faculty Akdeniz University 17(2), 199-206.

Authors' address:

Associate Prof. Dr. Sevgi Yilmaz (syilmaz_68@hotmail.com; sevgiy@atauni.edu.tr)
Ataturk Univ., Fac. of Agric., Dept. of Landscape Architecture,
25240, Erzurum/ Turkey

Associate Prof. Dr. Yahya Bulut (yahyabul@hotmail.com, ybulut@atauni.edu.tr)
Ataturk Univ., Fac. of Agric., Dept. of Landscape Architecture,
25240, Erzurum/ Turkey

PhD candidate Süleyman Toy (s_toy2@hotmail.com) Landscape Architect & Engineer at Meteorology Office, Erzurum/Turkey

PhD. Isik Sezen (sezen002@hotmail.com).
Ataturk Univ., Fac. of Agric., Dept. of Landscape Architecture,
25240, Erzurum/ Turkey

Calibration of thermal comfort in different climates for urban planning concerns

Antje Katzschner

Department of Environmental Meteorology, University Kassel, Germany

Abstract

For decision making architects and urban planners need qualitative and quantitative information concerning the urban microclimate and its thermal effects on the urban population. Comparative studies in Hong Kong, Freiburg and Kassel, based on urban climatic analysis, describe the effects of urban climate on spatial usage and furthermore calibrate thermal perception based on empirical data.
PET (physiological equivalent temperature) is used as an indicator for thermal comfort related to humans. This indicator is calibrated to evaluate heat stress in different climatic regions and give reference to urban planners.

1. Introduction

Comparative studies in Hong Kong, Freiburg and Kassel, based on urban climatic analysis, describe the effects of urban climate on spatial usage and furthermore calibrate thermal perception based on empirical data.

To assess global climate change influences on urban climate the analysis furthermore assesses heat stress and possibilities to minimize this effect by the means of urban and open space design. PET (physiological equivalent temperature) is used as an indicator for thermal comfort related to humans. This indicator is calibrated to evaluate heat stress in different climatic regions and give reference to urban planners.

Thermal perception was measured with the help of interviews while parallel meteorological measurements were carried out. These data is furthermore related to urban structures and is directly linked to the subjective perception. Using this approach it was possible to calibrate the PET index. Results show a close correlation between the urban heat island and the thermal perception whereas the inhomogeneity of the urban climate has positive influences on thermal perception.

A comparison of heat perception in tropical and moderate climates shows differences in the comfort zone of approximately 6 °C (PET). This means a standard calibration of PET is not possible but has to be matched the respective climate region. The analysis beyond that shows there is no linear relationship concerning PET and subjective perception.

According to recent studies concerning climate change an increase of temperature in middle Europe is predicted. This background situation is intensified by the urban heat island effect with the consequence that the quality of human life in urban quarters will be affected more frequent, over longer periods and stronger in the future. In this context human comfort is coming to the fore. As cities throughout middle Europe have been more concerned about accumulation of heat in the past there is supposed to be potential of heat stress. The aim of the project KLIMES (Strategies and concepts for urban planning to mitigate the impacts of climate extremes on well-being and health of people in

cities), was, taking into account existing urban structures, to develop planning strategies to ensure outdoor human thermal comfort during extreme heat waves in the summer. The research design covers various methods which are carried out by different work groups. The present paper presents, amongst other aspects, the particular project doing experimental investigations of the microclimatic conditions and parallel interviews with people on site concerning their thermal perception.

To understand thermal comfort the air temperature is not an adequate indicator. Instead different thermal indices are used. In this case the physiological equivalent temperature (PET) is used to calibrate urban climate classification in different climatic areas.

1.1 Research project KLIMES

The joint research project "Development of strategies to mitigate heat stress in urban quarters due to regional climate change in Central Europe", abbreviated by KLIMES, was carried out by four German research groups within the scope of the research initiative "*klima*zwei" funded by the German Federal Ministry of Education and Research (BMBF) from 2006 to 2009. One general aim was the quantification of the perception of human thermal comfort (discomfort) in different urban quarters (outdoors) during extreme summer heat in different urban quarters.

To achieve this aim, a coordinated design of different methods was applied in KLIMES: This included experimental investigations on the perception of heat by people in different urban quarters in Freiburg (SW Germany), which is the warmest city in Germany, through questionnaires about citizens' current perception of heat under consideration of their thermal history and their use of open spaces (see also Knez and Thorsson, 2006).

2. Experimental design of the subproject KLIMES KAS-1

The approach of KLIMES was to evaluate influences of certain urban structures or elements on human thermal comfort conditions to give advice to planners. This was realized through measurements with a temporary reference station and two mobile recording systems by the subproject from Freiburg University. The meteorological parameters measured are air temperature, wind and humidity, but also radiation coming from the horizontal and vertical directions. Furthermore another mobile system was used, measuring the same parameters but only where interviews were carried out (subproject University Kassel). Using this methodology every person and its subjective perception can be related to objective data of the mobile station. The mobile station measures three minute means of meteorological data being transferred into the thermal index PET.

There are several bio meteorological indices. In this study the index PET (Höppe 1999) was chosen due to different reasons. The first reason is that – compared to other indices – it was adapted to outdoor settings. The second reason is that it is internationally used which provides comparability. In addition to its wide distribution it is furthermore continuously developed by several work groups. Another reason to decide for PET was that the parameters needed to calculate are easy to be conducted.

PET, which is based on the heat balance of man from Höppe (2002), is an index used to describe the thermal situation of a person including the meteorological parameters Mean Radiant Temperature (Tmrt), Air Temperature (Ta), Wind Speed (v) and Vapor Pres-

sure (RH). It "is defined as the air temperature at which, in a typical indoor setting (without wind and solar radiation), the heat budget of the human body is balanced with the same core and skin temperature as under the complex outdoor conditions to be assessed." (Höppe 1999).

The reason for the use of the thermal index PET is mainly to be seen in the above mentioned effect of global warming. As we expect more heat stress days, PET is quite sensible towards long- and short wave radiation. So if heat storage is increased thermal stress will be increased at the same time.

Investigations were carried out in the city of Kassel, situated in the central part of Germany and Freiburg located in the south. The microclimatic conditions include mesoscale information of the urban heat island and ventilation. Important effects on thermal comfort are building structure, surface conditions and ventilation. On this level every interviewee could be allocated to a certain space and therefore certain microclimatic conditions.

2.1 Interviews

The method to carry out on-site interviews and parallel meteorological measurements at the exact point were the subjective perception was conducted, ensures a direct comparison of subjective and objective data.

The subjective perception was measured by an eight point scale with the categories very hot, hot, very warm, warm, neutral, cool, very cool and cold. As the main focus of the study was on heat stress four categories were used in the above neutral categories, measuring the differences in heat perception. For further evaluation of the conducted data measurements were carried out in colder weather as well. The interviews took place in Freiburg, Germany, as it is the city with the most sun hours. Comparing measurements were carried out in Kassel, Germany. Each interview is furthermore linked to the meteorological parameters at that exact point where the interview took place. The parameters, measured with a mobile meteorological station, were afterwards used to calculate the Physiological Equivalent Temperature (PET).

3. Comparison of thermal comfort in different climate zones

To study thermal comfort the indices have to be considered differently depending on the regional climate and the urban situation. Therefore it is not possible to use one index value world wide. A calibration of PET, using ordinal regression analysis, of the data from Hong Kong and Germany, shows the difference in perception concerning heat stress. Mobile measurements and interviews were conducted in two different climates during different seasons in Germany and Hong Kong. The data was used to calibrate the PET (table 1).

The comfort zones vary by 6 °C PET. But it becomes obvious that in the warmer categories differences decline (table 1). So the subjective perception of hot, meaning strong heat stress, in both climates starts around a value of 35 °C (PET).

As the interest lies in the heat stress situation the most important value is the benchmark between comfortable and warm, as this is were heat stress starts. Therefore 28 °C (PET)

in Germany and 30 °C (PET) in Hong Kong can be determined as a benchmark towards heat stress.

Looking to the cool classification, values were very difficult to compare, as in Hong Kong nearly no cool sensation from interviews could be found. The main focus during the investigation was on the comfortable and hot zones as health risks are expected after a certain point of heat stress.

Table 1: Calibration of PET (°C) in Germany (n = 776) and Hong Kong (n = 1958) based on empirical data

PET (°C) (Germany)	PET (°C) (Hong Kong)	subjective perception	level of stress
more than 42	more than 45	very hot	extreme heat stress
35 - 41	35 - 45	hot	strong heat stress
29 - 34	30 - 35	warm	moderate heat stress
18 - 28	12 - 30	comfortable	no thermal stress
13 - 17	9 - 12	slightly cool	weak cold stress
less than 13	less than 8	cool	cold stress

3.1 Aspects of planning

The perception of places concerning its thermal comfort is closely linked to psychological matters. Its outer appearance influences thermal comfort as well as, for example, the people's attachment to a place (Knez, 2005; Knez, Thorsson 2006). So thermal perception does not only rely on the microclimate but is also dependent on psychological issues. Further studies show that a high variation of microclimates tends to be evaluated positively (Katzschner 2006). One central issue of the project is to evaluate whether certain urban structures affect heat stress more than others, concerning the microclimate on the one hand and the subjective perception on the other hand. So a fountain affects the microclimate rarely but it does influence the subjective perception as being felt cooler. Thermal conditions are dependent on buildings, surface conditions and open space obstacles causing climates from very hot to cool in the summer period. Therefore, taking into account psychological issues, variation of microclimates and the microclimate itself, guidelines should be found, including issues taken off all disciplines. There is previous evidence (RUROS, 2004) that there are two dominant factors effecting thermal sensations. One is mean radiation temperature and the other is wind speed. Especially higher wind speed seems to be negatively perceived by people living in moderate climates but positively perceived in warmer climates. Considering the predicted increase of temperature, and first findings from KLIMES approve of that matter, wind is becoming more important in our regions and should be taken into account in further planning.

Future city developments, under the consideration of adaptation aspects, have to take into account how open spaces are used by people and how this usage is connected to heat conditions. People avoid warm places on urban spaces in summer conditions (figure 1). Shadows are used intensively. The calculations can serve as an analysis of the actual situation as well as it could give perspectives for change of the thermal situation

through materials or structures. Focus should be given to facades, shadow and sufficient ventilation.

Fig. 1: Picture of an open urban space in Kassel (Opernplatz) and the spatial distribution of conducted interviews on 07/31/2008 (Source: www.googlemaps.com)

Thermal situations moreover should be considered always in connection to the use of open spaces. The interviews on thermal sensations suggest a very inhomogeneous microclimate as best conditions for people. During hot summer days shadow as well as moderate microclimates is needed in walking distances. Open spaces are used for communication as well as recreation areas. The variation in thermal conditions can be seen in dependence of surface, vegetation and buildings so that a bioclimatic design of that open space can be conducted due to the specific needs of the urban population in the respective climate.

4. Conclusions

Thermal comfort represents an indispensable prerequisite for the quality of life within cities. It is essential for efficiency, well-being and health of citizens. Human thermal comfort within urban structures depends on the large-scale meteorological background conditions, which are modified within cities by their specific meteorological features in a way that the thermal level is enhanced. Based on current studies it is common sense that longer lasting, more intense and more frequent heat waves will occur in the future. This, through the global climate change, intensified background conditions lead to more thermal stress situations for citizens, which can be quantified by the application of thermal indexes.

As shown in the present paper the index PET cannot be applied in all climates the same but has to be calibrated regarding the specific local climate. But the calibration is a helpful instrument for planners and architects to evaluate human thermal comfort and heat stress under consideration of global climate change. Especially as urban planning is developed for longer periods with a lifespan having to deal with the outcome of climate change.

Acknowledgement

The author is indebted to the Federal Ministry of Education and Research (BMBF) for funding the sub research project KLIMES KAS-1 (FZK: 01LS05021), which were part of the joint research project KLIMES; within the scope of the research initiative klima*zwei*.

Furthermore I like to thank the other sub projects of KLIMES.

References

Höppe, P. 2002: Different aspects of assessing indoor and outdoor thermal comfort. Energy and Buildings Vol. 34 pp 661–665.

Höppe, P., 1999: The physiological equivalent temperature – a universal index for the biometeorological assessment of the thermal environment. International Journal of Biometeorology. Vol. 43: pp 71-75.

Katzschner, L. 2006: Microclimatic thermal comfort analysis in cities for urban planning and open space design, Comfort and Energy Use in Buildings, Network for Comfort and Energy use in Buildings (NCUB), www.nceub.or.uk, London.

Knez, I., S. Thorsson, 2006: Influences of culture and environmental attitude on thermal, emotional and perceptual evaluations of a public square. Int. J. Biometeorol. 50, 258-268.

Knez, I. 2005, Attachment and Identity as related to a place and its perceived climate. In: Journal of Environmental Psychology Vol. 25 pp 207-218.

RUROS 2004: Designing open spaces in the urban environment: a bioclimatic approach. Key Action 4, City of Tomorrow, Fifth Framework Programme EU, CRES Athen.

Authors address:

Antje Katzschner, MA (akatzschner@asl.uni-kassel.de)
Department of Environmental Meteorology, University Kassel
Henschelstr. 2, D-34127 Kassel, Germany

Summer human thermal comfort in urban open spaces in Hong Kong

Yuk Yee Yan, Ho Yan Cheng

Department of Geography, Hong Kong Baptist University, Hong Kong

Abstract

This study investigated human thermal comfort and perception outdoors in an urban park and a pedestrian district in Causeway Bay, Hong Kong. Microclimatic variable measurements and questionnaire interviews were conducted simultaneously at the two open spaces during the summer months (May to October). It was noted that majority of the respondents reported warm to hot thermal sensation in both study sites. Findings also revealed that respondents preferred having stronger wind, lower temperature and drier air in the two open spaces. Results of regression analyses discovered that temperature and wind speed were the most significant variables affecting human thermal comfort. Findings of this study provided better insight into the urban microclimate in Hong Kong.

1. Introduction

Quality of urban open spaces has recently received increased research attention. It has been acknowledged that these spaces influence people's well being, for instance health and quality of life in cities. People access these open spaces, such as urban parks, pedestrian districts, urban streets and plazas, to enjoy recreation and outdoor activities. It has been recognized that microclimate is a prominent factor affecting the way these spaces are used; and thermal comfort conditions influence people's behavior and usage of urban open spaces (Nikolopoulou et al., 2001; Nikolopoulou and Lykoudis, 2007).

The aims of the present study are (1) to examine the human response and perception on thermal comfort and (2) to investigate the relationship between microclimate and actual human thermal sensation in urban open spaces in Causeway Bay, Hong Kong.

2. Study area

Causeway Bay is in the northern part of Hong Kong Island. It is a commercial and residential district with dense, tall buildings and pedestrian crowds. Hong Kong has a subtropical climate with hot humid summers from May to September. Since high temperatures persist till mid-October, the summer month period in this study lasted from May through October.

Two open spaces were selected for the present study. They were the Victoria Park and the pedestrian district at Paterson Street (Fig. 1). Victoria Park, a large urban park with an area of over 19 hectares, is located close to the waterfront (Fig. 2a). Paterson Street is a full-time pedestrian district that provides a safe and comfortable walking environment (Fig. 2b). Two tall buildings are situated on both sides of Paterson Street, producing a H/W ratio of 5.6.

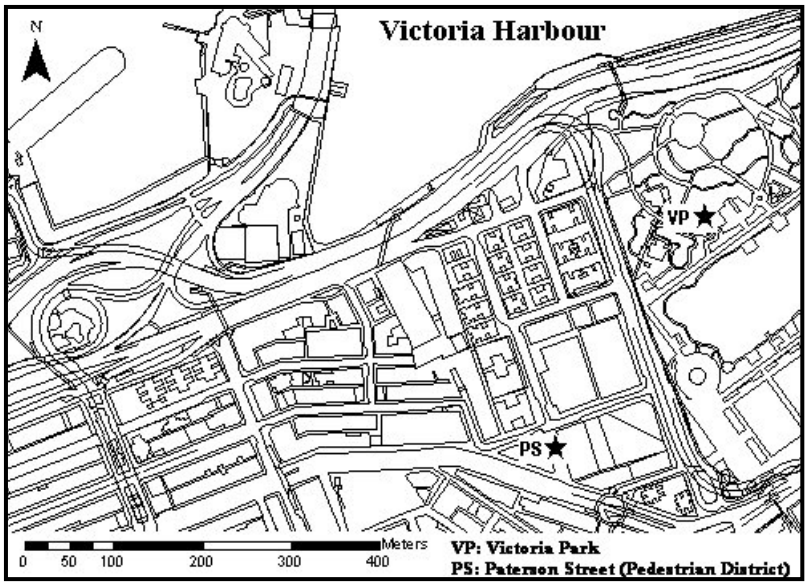

Fig. 1: Locations of the study areas

(a)

(b)

Fig. 2: Photographs showing (a) Victoria Park and (b) Paterson Street (pedestrian district) in Causeway Bay, Hong Kong

3. Methods

Field surveys were conducted from May 2007 to October 2007. The surveys took place at three different time periods: morning (7-9 a.m.), afternoon (1-3 p.m.) and evening (7-9 p.m.) on Tuesday, Friday and Saturday during the first week of each month. Both structured interviews and measurements of microclimatic variables were performed at the two selected urban open spaces simultaneously.

People's thermal sensation, perception and preferences were examined by structured questionnaires. People walking past or staying in the study areas were randomly selected for interviews that were conducted in Cantonese. The subjects were asked to report their actual thermal sensation according to a 7-point scale (varying from "much too cold" to "too hot"), thermal perception on a 5-point scale and thermal preference on a 3-point scale. Questions were also comprised of respondents' demographic characteristics. Portable weather stations (PortLog by Rain Wise Inc.) were used to measure the microclimatic variables, including temperature, wind speed, relative humidity and solar radiation. The weather stations were placed near pedestrian height and at the open point in each urban open space to avoid the influence of warm facades (Johansson and Emmanual, 2006), and to be in the sun during the field surveys. However, this was not possible for safety reason (pedestrian traffic) and the actual positions were quite far from ideal. Measurements were taken every 5 minutes.

It is assumed that respondents' perception of the thermal environment would affect their overall thermal comfort, which in turn would affect their preference. These relationships were evaluated by correlation coefficients. To investigate the relationship between the respondents' level of thermal sensation and the recorded microclimatic data, multiple stepwise regression analysis was applied.

4. Results and discussion

A total of 565, 544 and 511 people were interviewed for the morning, afternoon and evening sessions correspondingly in the two study areas, of which 52.6%, 71.1% and 65.6% respectively were males. These respondents were at the age between 14 and 80.

4.1 Thermal environment

The two study areas were characterized with high air temperatures and low wind speed (Table 1). At Victoria Park, with minimum impact of urban morphology, its temperatures were greatly affected by the amount of solar radiation received. The high H/W ratio at Paterson Street provided shaded areas both in the morning and afternoon. Nevertheless, high H/W ratios have negative impact in the evening and at night. Because shading reduces heat loss through long wave radiation, and thus high temperatures persist. This is the reason why Paterson Street was warmer than Victoria Park in the evening.

4.2 Thermal sensation

In the morning, 45.6% and 40.1% felt "too warm" and "too hot" in Victoria Park and Paterson Street respectively. About 60.0% of respondents at Victoria Park believed temperatures were high as compared to 50.2% respondents at Paterson Street. However, over 50% of the interviewees at Paterson Street disagreed that the solar radiation was strong. A large portion of respondents at both sites preferred having lower temperatures (over 70%), stronger winds (over 70%) and lower relative humidity (60%).

In the afternoon, over 58.5% of respondents at both study sites felt “too warm” and “too hot”. Majority thought that temperatures were too high (over 65%), winds were weak (over 64%), air was too humid (over 41%) and solar radiation was too strong (over 55%). A high percentage of respondents wanted lower temperatures (over 80%), higher wind speed (over 80%), lower relative humidity (over 50%) and less solar radiation (over 36%).

Table 1: Summary of measured microclimatic variables

		Victoria Park			Paterson Street		
		Morning	**Afternoon**	**Evening**	**Morning**	**Afternoon**	**Evening**
Temp (^oC)	Max	31.5	34.7	29.9	30.2	34.0	31.0
	Min	23.5	23.7	22.7	24.4	25.3	24.8
	Mean	27.2	30.6	27.4	27.7	30.4	29.0
	st dev	2.3	3.0	2.3	1.8	2.5	1.9
Wind speed (ms^{-1})	Max	2.1	2.8	2.4	4.7	2.7	2.1
	Min	0.1	0.4	0.0	0.7	0.4	0.3
	Mean	1.0	1.9	1.0	1.4	1.4	1.1
	st dev	0.6	0.7	0.6	0.9	0.7	0.5
Relative humidity (%)	Max	100.0	97.8	90.5	84.0	80.9	81.2
	Min	54.3	45.8	61.0	74.2	47.6	55.7
	Mean	77.0	64.8	75.5	50.8	61.7	67.6
	st dev	11.7	13.8	7.1	8.6	9.8	6.3
Solar radiation (Wm^{-2})	Max	136.6	545.2		16.8	162.9	
	Min	4.8	54.5		0.0	0.0	
	Mean	77.5	312.7		0.9	61.4	
	st dev	37.5	149.2		4.0	60.6	

In the evening, similar patterns of thermal sensation, perception and preference were recorded. About 61.4% of the responses at Paterson Street felt “too warm” and “too hot” as compared to 50.0% at Victoria Park. Majority of the respondents at both sites perceived the high temperatures (over 50%) and low winds (over 70%) were the major factors causing this thermal discomfort. A large portion of responses favored lower temperatures (over 71%) and stronger wind (over 80%).

General demands for lower temperatures, stronger winds and drier air are further supported by the correlation analyses between the thermal responses and measured microclimatic variables, as presented in Table 2.

Among the four measured microclimatic parameters, temperature was the most prominent factor determining the overall thermal comfort, as indicated by the highest correlation coefficients. Solar radiation, adding direct radiant heat flux on the body, was another important variable affecting thermal sensation in the afternoon. Wind speed had a negative impact since wind flow brings heat away from the human body by convection. For high temperatures, relative humidity is a significant factor causing the sultry sensation.

Table 2: Correlation coefficients between responses to thermal perception (x), thermal sensation (y) and thermal preference (z) (*p<0.05; **p<0.01)

		Victoria Park		Paterson Street	
		Rxy	**Ryz**	**Rxy**	**Ryz**
Morning	**Temperature**	0.568**	-0.501**	0.479**	-0.435**
	Wind speed	-0.186*	0.388**	-0.203**	0.356**
	Relative humidity	0.000	-0.122*	0.075	-0.128*
	Solar radiation	0.353**	-0.468**	0.125*	-0.260**
Afternoon	***Temperature***	0.587**	-0.351**	0.542**	-0.315**
	Wind speed	-0.115	0.297**	-0.142*	0.209**
	Relative humidity	-0.075	-0.015	0.066	-0.128*
	Solar radiation	0.533**	-0.440**	0.426**	-0.323**
Evening	**Temperature**	0.396**	-0.399**	0.427**	-0.396**
	Wind speed	-0.113	0.270**	-0.223**	0.273**
	Relative humidity	0.142*	-0.099	0.159*	-0.210*

The signs of R_{yz} were opposite to that of the respective R_{xy} because of the reverse inclination of perception and preference of thermal comfort. Respondents' preference reflects their desire for an ideal thermal condition. They all desired lower temperatures, less humid air and stronger wind speed.

4.3 Thermal comfort and microclimatic variable relationship

Regression analyses were employed to ascertain the relationship of thermal sensation and measured microclimatic variables, and the results are shown in Table 3. As expected, temperature and relative humidity were positively associated with thermal comfort. High temperature and humidity will cause sultry and oppressive sensation. The negative connection of wind speed and thermal comfort suggests that wind flows help relieve thermal discomfort by bringing heat away. It is proposed that urban wind speeds of 1.0-2.0 ms^{-1} are required to sustain thermal comfort in shade on sunny days, and a higher wind speed up to 5.0 ms^{-1} in areas exposed to the sun will be beneficial for alleviating thermal discomfort in summer days in Hong Kong (Cheng and Ng, 2006).

Table 3: Relationship between thermal comfort and microclimatic variables (p<0.05)

	Victoria Park			Paterson Street		
	Morning	**Afternoon**	**Evening**	**Morning**	**Afternoon**	**Evening**
Temperature	0.368	0.298	0.336	0.260	0.252	0.303
Wind speed	-------	-------	-0.190	-0.324	-0.247	-0.343
Relative humidity	0.013	0.020	0.028	-------	--------	0.041
Adj r^2	0.482	0.373	0.321	0.250	0.315	0.237

5. Conclusion

This paper presents the preliminary findings of a comprehensive study on thermal comfort in urban open spaces conducted in Hong Kong. It is discovered that a large portion of respondents reported warm to hot sensation, and they preferred having lower temperature, higher wind speed and less humid air. Results of this research provide useful information for planners to better understand urban microclimate and thus develop future standards in designing quality urban open spaces in Hong Kong.

Acknowledgement

This research project was funded by the Competitive Earmarked Research Grant (CERG) (HKBU2438/06H).

References

Cheng V., E. Ng, 2006: Thermal comfort in urban open spaces for Hong Kong. Archit. Sci. Rev. 49, 236-242.

Johansson E., R. Emmanual, 2006: The influence of urban design on outdoor thermal comfort in the hot humid city of Colombo, Sri Lanka. Int. J. of Biometeorol. 51, 119-133.

Nikolopoulou M., N. Baker, K. Steemers , 2001: Thermal comfort in outdoor urban spaces: the human parameter. Solar Energy. 70(3), 227-235.

Nikolopoulou M., S. Lykoudis, 2007: Use of outdoor spaces and microclimate in a Mediterranean urban area. Build. Environ. 42, 3691-3707.

Authors' address:

Dr. Yuk Yee Yan (yyan@hkbu.edu.hk)
Department of geography, Hong Kong Baptist University,
Kowloon Tong, Hong Kong

Mr. Ho Yan Cheng
Department of geography, Hong Kong Baptist University,
Kowloon Tong, Hong Kong

Development of Climate Analysis Software for Urban and Environmental Planning of Seoul

Chae Yeon Yi[1], Young-Jean Choi[1], Jeong-Hee Eum[*3], Geun Hoi Kim[1], Kyu Rang Kim[1], Dieter Scherer[2], Ute Fehrenbach[2]

[1] Applied Meteorology Research Laboratory, National Institute of Meteorological Research, Korea Meteorological Administration, Seoul, Korea

[2] Technische Universität Berlin, Berlin, Germany

Abstract

The general objective of this study is to develop tools on urban and environmental plannings in order to mitiagate urban heat stress in Seoul by preserving wind path in densely construted built-up areas. This study seeks to develop software for analyzing and evaluating climate conditions for urban and environmental planning of Seoul, which is called CAS (Climate Analysis Seoul), and to establish input data used for CAS. Three different levels of study domain were considered for CAS: Model Region, Study Region and Detail Region. Land cover information, Digital Elevation Model, and urban structural information were utilized as input data. The mesoscale wind and temperature fields were simulated by MetPhoMod. The results reflect the ventilation and air temperature conditions influenced by land cover and topography of Seoul and its surroundings. CAS software was tested with suitable input data to analyze further climate conditions like local air production/transport/stagnation, air quality and thermal situations. Using CAS software, effects of urban development on climate conditions can easily be analyzed and evaluated. However, intensive validation of CAS by using ground observation data at the study regions are remained as a further study.

1. Introduction

As interests of urban climate information in urban and environmental planning have been increased, attempts to consider urban climate information as a factor of spatial planning have been made in Korea (Eum et al., 2001; Kim et al., 2001). However, such consideration is not easy, because there are no available tools to analyze climate conditions for entire urban areas in Korea. In this study, we developed software for analysis and evaluation of climate conditions in urban areas – specifically in Seoul - to support environmental planning, which is called CAS (Climate Analysis Seoul). The processes to establish input data for CAS are also described.

2. Study area and data processing

Three different levels of domain were considered for CAS (Fig. 1). They are Model Region (MR), Study Region (SR) and Detail Region (DR). The Model Region (1000m horizontal resolution, 200x200km^2) was used as the numerical atmospheric modeling domain with the MetPhoMod model (Perego, 1999). The Study Region (25m horizontal resolution, 50x40km^2) is the basic study area, which covers Seoul and its surrounding areas. The Detail Region (5m horizontal resolution, 4x2.5km^2) focuses on a part of

* Current address: Korea Environment Institute, Seoul, Korea

Seoul in detail. The high resolution of DR allows detailed analysis of the interactions between land-cover and atmosphere. It meets the specific needs of urban planning.

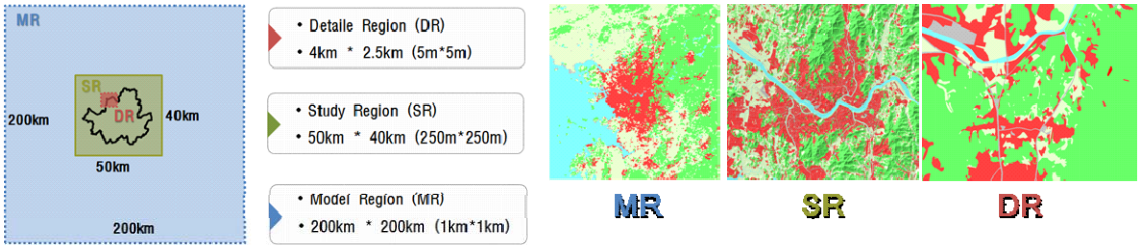

Fig.1: Three different levels of CAS and their resolution and domain area [MR/SR/DR]

As input data, land-cover information, digital elevation model and urban structural parameters including the network of main roads were established. An important part of input data processing procedures is the integration of GIS vector data into the climate analysis procedures (Fig. 2).

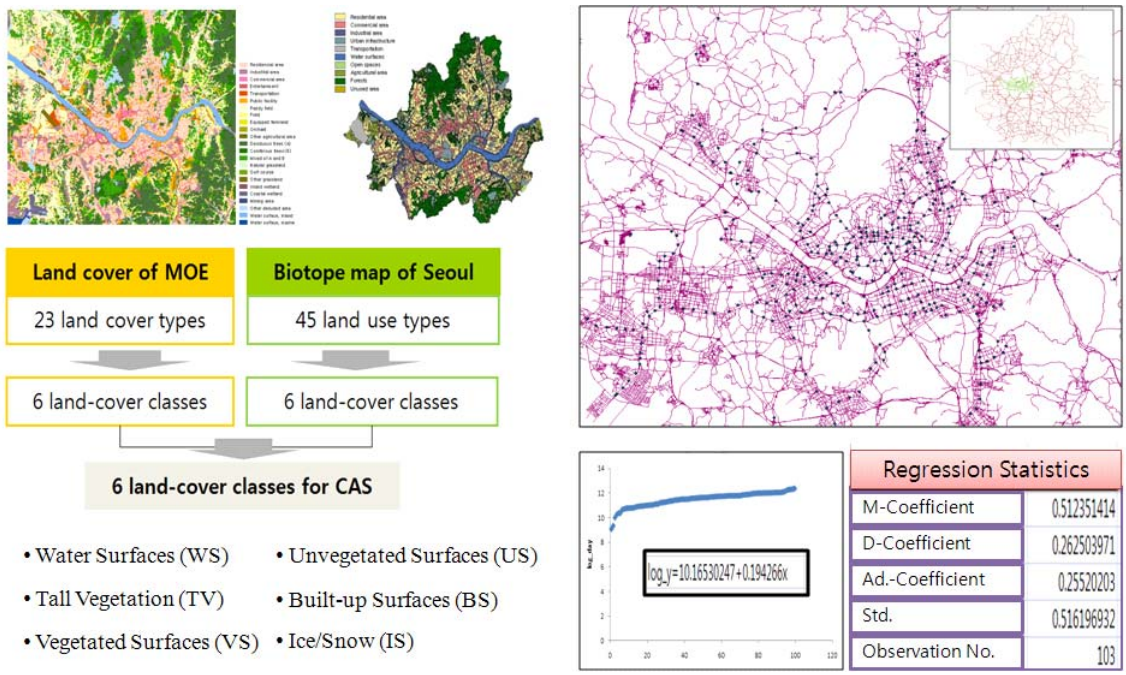

Fig. 2: Land-cover and main road dataset as input data of CAS

While land-cover (LC) data required for all domains were basically derived from suitable satellite data to ensure full data coverage, accurate GIS data on land cover and land use within the Seoul city area (Biotope map, vector data) were utilized so far as possible in CAS. The vector-raster conversion procedure allowed overlaying of the GIS data over satellite data at arbitrary horizontal resolution, increasing the level of detail both in the SR and DR. Subsequently a refinement of class definitions has become necessary for the LC data layers in the three domains. The scheme comprises water surfaces (WS),

ice/snow (IS), tall vegetation (TV), vegetated surfaces (VS), unvegetated surfaces (US) and built-up surfaces (BS) as so-called primary LC types (Fig. 3).

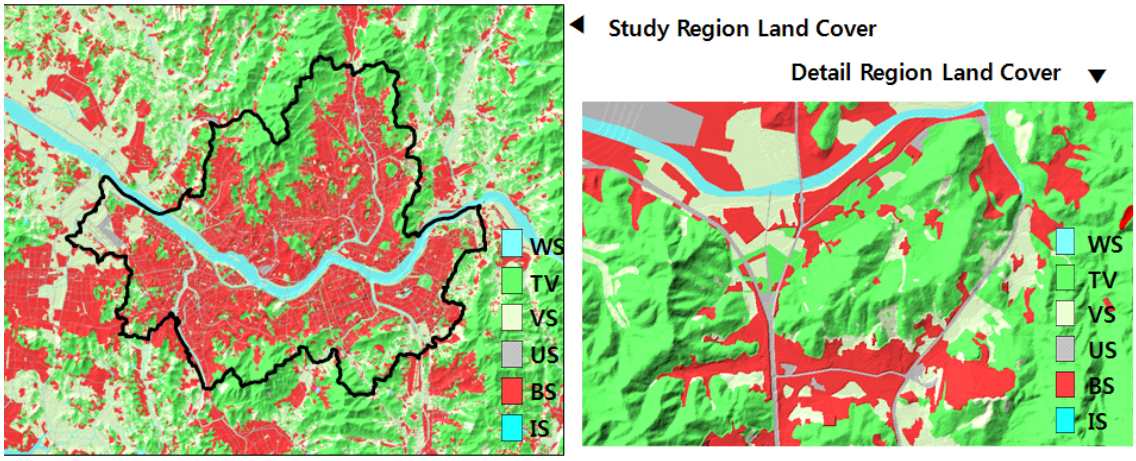

Fig. 3: Land cover of Study Region and Detail Region (raster dataset)

Spatially distributed data on fractional coverage (FC) of the primary LC types were computed for various horizontal resolutions. Structural parameters as well as areal types (AT) were derived from FC data. Thus, even small fractions of primary LC types influenced the computations instead of being disregarded by majority-based algorithms.

To calculate the urban structural parameters, the Seoul Biotope map with urban attributes like building heights was used, and attributes associated to each polygon were converted to raster dataset. In some cases a slight reduction of the spatial differentiation in structural parameters may be possible. However, this does not affect the quality of the climate analysis results, since data on structural parameters from separate data sources can be directly included to the process. For instance, if data from a digital surface model (DSM) is available at very high spatial resolution (e.g. from air-borne laser altimetry), building heights may no longer be derived statistically from FC data but directly at very high accuracy from the DSM. In case of CAS, DSM data was derived from band math of DTM and building height raster dataset (Fig. 4).

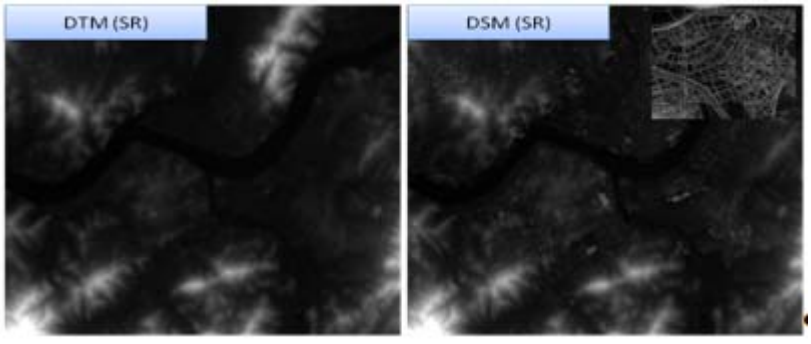

Fig. 4: DTM and DSM of Study Region (band math)

The MetPhoMod simulation had operated in a one-way nested mode using the SR as inner domain within MR (Fig. 5). The MetPhoMod simulation results of SR were spatially interpolated to the 250m horizontal resolution used by the other climate analysis

procedures in the SR. Nesting greatly improved the wind and air-temperature field simulations in CAS.

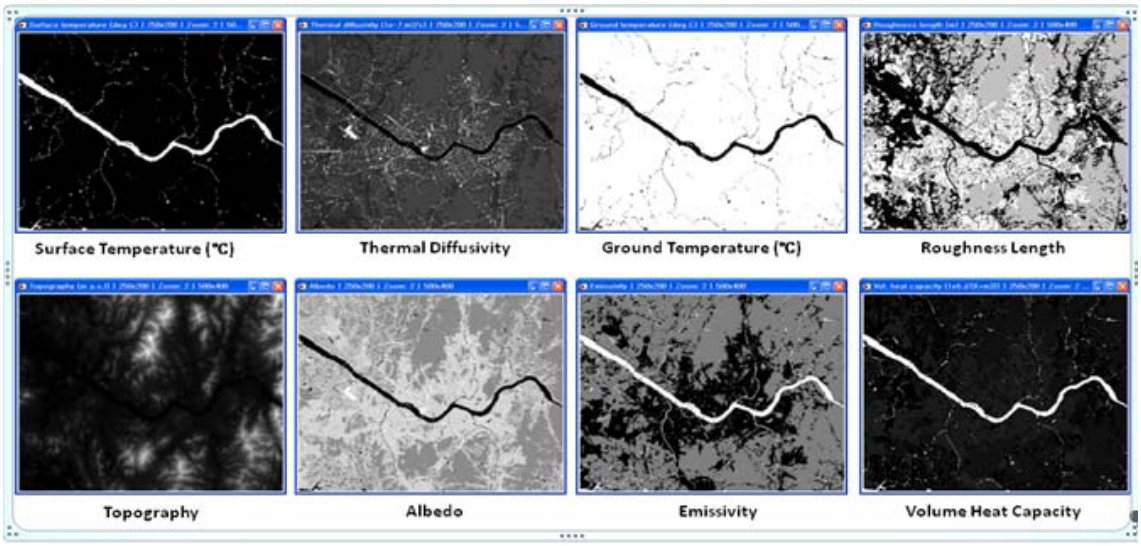

Fig. 5: MetPhoMod Simulation Input Dataset of Study Region

3. CAS Software

CAS has Graphical User Interface with five menus: project, workflow, view results, make maps and help. A larger part of the CAS was coded using the scientific programming environment IDL (Interactive Data Language). Some of the modules only exist as separate IDL routines not fully integrated in the CAS workflow. Before the processing using IDL routines, preprocessing of input files should be done without the use of IDL routines. Fig. 6 shows the structure and GUI of CAS software.

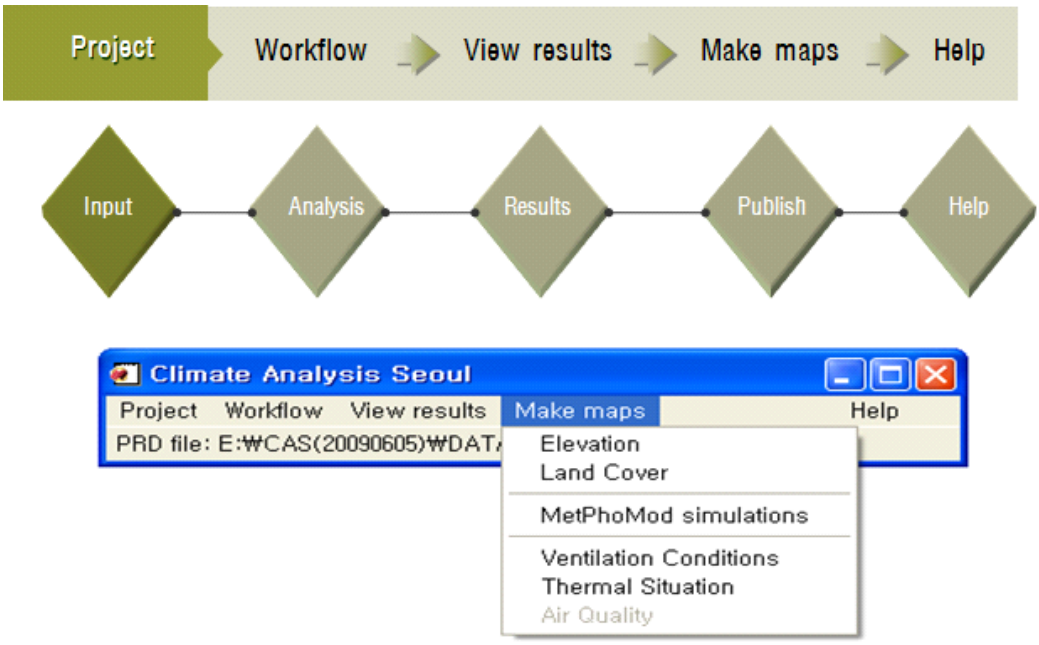

Fig. 6: Structure and GUI (graphic user interface) of CAS

4. Verification of the analysis results of CAS

We have been testing CAS with suitable input data to analyze ventilation conditions like local cold air production/transport/stagnation, mesoscale wind and thermal simulations, and environmental loads like air quality and thermal conditions. The mesoscale simulation of MetPhoMod was compared with that of other mesoscale (WRF) model. The results produced by CAS were also verified by measurement data (Fig. 7).

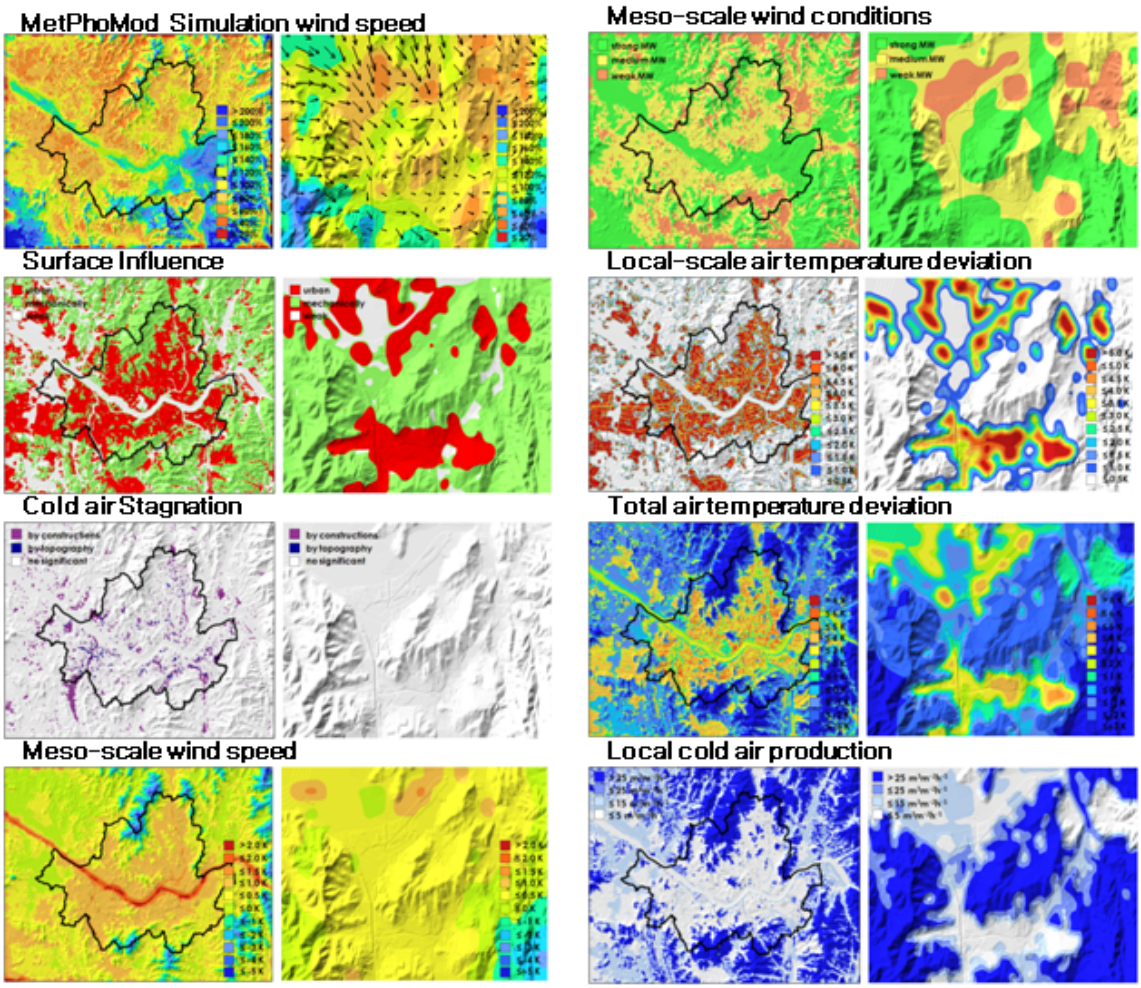

Fig. 7: Analysis results from the CAS software and MetPhoMod in SR and DR

5. Conclusions

CAS was able to analyze the spatial variation of thermal and wind conditions in Seoul. The results will be utilized in urban planning to help preserving wind path and reducing urban heat island. However, more intensive validation of CAS by using ground observation data at the study regions are remained as a further study.

Acknowledgement

This study was financially supported by Advanced Research on Industrial Meteorology of National Institute of Meteorological Research (NIMR) / Korea Meteorological Administration (KMA).

References

Eum, J.H., Woo, J.H. Yang, B.E, 2001. A study on the urban open space planning using the ventilation path: A case study of Yong-In city in Korea, *Journal of Korea Planners Association*, 36(1), 231-241.

Kim, W. S., Kim, H. Y., Eum, J. H., Jo, M. H., Oh, S. N., 2001. An experimental study for considering climates as a factor in urban design, *Seoul Studies*, 2(1), 1-21.

Perego S., 1999. Metphomod - a numerical mesoscale model for simulation of regional photosmog in complex terrain: model description and application during Pollumet 1993 (Switzerland), *Meteorol. Atmos. Phys.*, 70, 43- 69.

Authors' address:

Chae Yeon YI (prpr2222@korea.kr), Dr. Young-Jean Choi (yjchoi@kma.go.kr), Geun Hoi Kim, Dr. Kyu Rang Kim (krk9@kma.go.kr)
Applied Meteorology Research Laboratory
National Institute of Meteorological Research
45 Gisangcheong-gil, Dongjak-gu, Seoul , Republic of Korea

Jeong-Hee Eum(jeonghee.eum@googlemail.com)
Korea Environment Institute
290 Jinheungno, Eunpyeong-gu, Seoul, Republic of Korea

Prof. Dr. Dieter Scherer (dieter.scherer@tu-berlin.de), Ute Fehrenbach
Department of Ecology
Berlin Institute of Technology (TUB)
Rothenburgstr. 12 12165 Berlin Germany

The use of street trees for heat mitigation in hot and arid regions Case study: Beer Sheva, Israel

L. Shashua-Bar[1], S. Cohen[2], O. Potchter[1,3], Y. Yaakov[3], J. Tanny[2], P. Bar-Kutiel[1]

[1] Dept. of Geography & Environmental Development,Ben Gurion University in the Negev,Israel
[2] Inst. Soil, Water & Environmental Sciences, ARO, Volcani Center, Israel
[3] Dept. of Geography, Tel Aviv University, Israel

Abstract

This study analyzes the impact of shade trees on microclimate in urban streets of Beer-Sheva city, Israel, located in a hot-arid region. The study is part of a collaborative project between Israel and Germany on the contribution of vegetation to urban heat island mitigation. Two NW-SE oriented parallel streets were chosen: a pedestrian mall with vegetation and mature Jacaranda trees predominating, and a bare street with no trees. Both streets have the same width of 15 m and similar heights of surrounding buildings (1 to 2 stories). In situ measurements were made in 2009 during two periods: the beginning of summer (June) and the end of summer (September). Results show significant differences between the two time periods as indicated in the trees' impact on air and surface temperatures and in tree transpiration rate. These differences were larger for exposed surfaces than for those in tree shade indicating that the hotter the area's microclimate the stronger the trees' potential mitigating effect.

1. Introduction

Greenery in cities has long been recognized as a tool for urban heat island mitigation (Oke, 1989). Planting of trees along street canyons for sustainable passive cooling is becoming important in urban planning in terms of energy savings and improved human comfort (Simpson and McPherson, 1996: Steemers, 2003; Grimmond, 2007). Numerous empirical studies have investigated the impact of urban forest on the city climate (Arnfield, 2003; Milles, 2008), most of these studies deal with urban parks. Empirical studies investigated the effect of urban street trees on temperatures reduction at pedestrian level found that the reduction can reach 2˚-4˚C (i.e. Shashua-bar et al. 2010; Tsiros, 2010), at some sites in extreme climatic conditions the cooling effect may reach up to 5-8˚C (Miller et al, 2006).

Previous studies showed that the actual extent of this cooling may vary significantly, depending on the attributes of the plants, including the vegetation species, irrigation regime and the climatic region (Shashua-bar et al. 2010: Leuzinger, 2010). Trees respond to and interact with the environment in a variety of ways. Besides the shading effect, most important is the cooling influence of water vapor through transpiration. In considering tree water use we note that when aerodynamic components of the climate exert a high demand for evaporation, stomata can exert a large degree of control on water use (McNaughton & Jarvis, 1983). Thus, if soil water is not available the tree will become stressed, close stomata and reduce water loss, resulting in a reduction in evaporative cooling. Therefore, it is important to understand tree water relations for management of urban trees. Other more subtle interactions are the influence of shading (perhaps by buildings) on tree growth form and on tree water relations, as found in studies where trees were shaded by screens (Cohen et al., 2005). In the urban context, the

interaction between vegetation and environment has additional urban factors which were found to interact with the vegetation impact on the urban microclimate (Shashua-Bar et al., 2010). The potential tree cooling effect can be larger in hot, arid regions than in temperate regions due to the efficiency of evaporation cooling. The objective of this study is to analyze the factors that govern the cooling effect of trees planted along an urban street canyon in a hot arid climate, and study to what extent each parameter is influenced.

2. Sites and Methods

The study was conducted in the desert city of Beer Sheva, in southern Israel (characterized by BW climate according to Kapan classification). Two NW-SE oriented parallel streets were chosen for the study: a pedestrian mall with vegetation and mature Jacaranda trees predominating, and a bare street with no trees or other vegetation. Both streets have the same width, 15 m, and similar height of surrounding buildings (1 to 2 stories). Measurements were made in 2009 during two periods: the beginning of summer with clear sky conditions (7-11 June, 2009), following the wet season, and the end of summer, with variable clear-to-cloudy sky conditions (6-10 September, 2009) following the dry season.

Five fixed meteorological stations were installed and measured continuously during five days at each time period; besides, mobile climate measurements were made along the two streets. Two additional stations were located in KKL street, planted with a variety of plants with Jacaranda predominating: one station at the Northern section under the trees shade (KKL_N) and the second at the Southern section of the mall street in an unshaded position (KKL_S). Two stations were located on Stern Street which is a bare street without trees (Stern_N and Stern_S). A reference station was set up on a roof (10 m height) of a nearby three-story building in order to measure the climatic conditions of the above-canopy boundary layer. Fig. 1 shows the northern sections in the two streets.

Fig. 1: Observation points of Stern-N Street (left) and of KKL-N pedestrian mall (right), Beer-Sheva, Israel

3. Results

Table 1 shows some climatic data of the five measurement days in June and in September. Maximum air temperature reached up to 35˚C for Stern Street while at KKL street with trees, temperatures were lower reaching up to 32.2˚C. As shown in Table 1, apart from the temperature, minor differences were recorded in the water vapour pressure.

Wind velocity was reduced in KKL_N station as compared to the other locations, presumably due to the larger air flow resistance induced by the trees. In September, in all the street stations the temperatures were higher than those measured on the roof. The results in September show the same trends observed but with a lower values than in June, reaching up to 33.1˚C for Stern Street and 31.7˚C to 33.1˚C at KKL Street.

Table 1: Meteorological data for the fixed stations at the studied sites. Averages for the days of measurements of June 7-11 2009, Beer Sheva, Israel

Climatic variable	June 7-11 2009					September 6-10 2009				
	KKL_S	KKL_N	Stern_S	Stern_N	Roof	KKL_S	KKL_N	Stern_S	Stern_N	Roof
Max air temp. T_a (°C)	32.2	32.0	35.0	----*	32.9	33.1	31.7	33.1	32.9	31.4
Min air temp. T_a (°C)	20.6	20.7	20.8	19.4	20.5	20.1	20.5	20.4	20.6	20.0
Max water vapour pressure VP (hPa)	27.6	26.5	27.5	25.5	19.2	24.3	24.7	25.6	26.7	25.2
Min water vapour pressure VP (hPa)	20.0	19.6	20.8	----*	19.2	20.1	19.6	19.8	21.3	20.8
Max wind speed v ($m\ s^{-1}$)	0.7	0.3	0.8	----*	3.4	0.5	0.4	0.8	0.9	2.7

*- data unavailable due to technical problems.

The findings presented in the following sections focus on the trees impact on individual microclimatic parameters namely, air and surface temperatures and tree transpiration rate. These parameters indicated the most significant differences of the trees impact between the two time periods.

3.1. Air temperature differences

Figure 2 shows the air temperature differences between the two stations at KKL mall (KKL_N and KKL_S) and the station at Stern street (Stern_N), in June and in September. The cooling effect between the vegetated street and the bare one is most pronounced during afternoon hours while in the early morning a small heating effect occurs probably due to less long wave heat exchange than in the bare Stern street. Due to the fact that the south station was located at exposed place while the north one was under the trees canopy makes KKL_N cooler than KKL_S, a difference found larger in September. However, the maximum cooling effect was found to be larger in June (up to 3K) than in September (up to 1.4K), enhancing the significance of the trees cooling in hot environment. The various cooling effects are due to lower soil moisture following the dry season (September) than following the wet season (June) and to different meteorological conditions, especially cloudy conditions in September and clear sky in June.

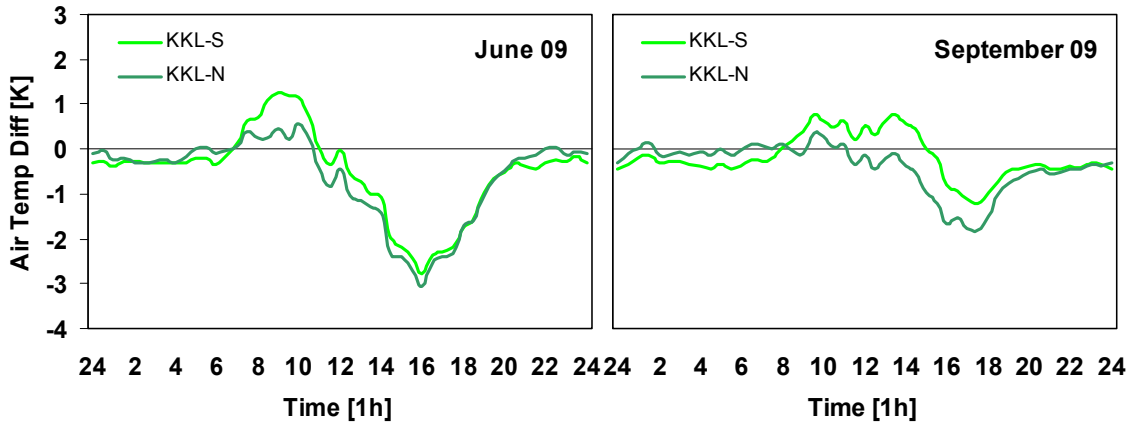

Fig. 2: Diurnal courses of difference in air temperature between KKL-N and Stern-N (dark green line) and KKL-S and Stern-N (light green line) Beer-Sheva, Israel

3.2. Transpiration

The transpiration rate was measured using the sap flow method which relates the transpiration rate to the speed of sap flow in the tree trunk (Granier, 1985). The results show (Fig. 3) high rates of transpiration from the trees. The daily transpiration rate was on the average 2.8 L/m^2 in June and 2.3 L/m^2 in September. The transpiration rate is related to the trees properties in the studied KKL street. Leaf area index (LAI) was estimated using a linear photosensor array probe (Decagon Sunlink) which measured a grid from South to North along KKL, giving an average of 4.4 in June and of 4.9 in September. Also the trees coverage (estimated by fish-eye) in June was about 10% less than in September, indicating a larger area of transpiration at the end of summer (September) than at the beginning (June) shortly after the deciduous period.

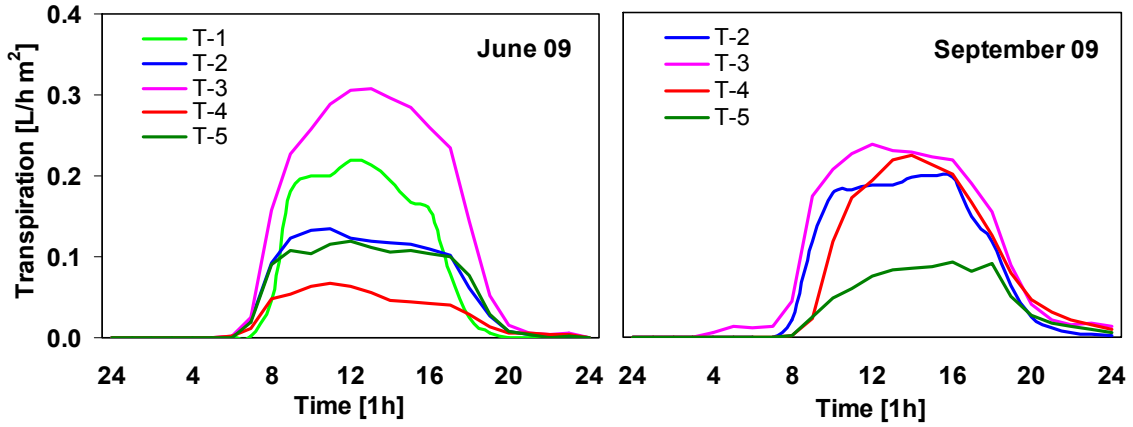

Fig. 3: Diurnal courses of transpiration rate in five trees in KKL-N mall Beer-Sheva, Israel. Each line is one tree

3.2. Surface temperature differences

The third variable that showed significant differences of the trees impact was the surface temperatures. Figure 4 shows results of measured surfaces in the KKL vegetated

street and in the Stern bare street in June. Surface temperatures reached a maximum of 50˚C to 60˚C for exposed ground and exposed car shields, respectively. In KKL street surface temperature reached a maximum of 30˚C to 32˚C under tree shade, including shaded ground, walls and the lower trees' canopy. All temperatures of surfaces shaded by the trees were close to air temperature, demonstrating the trees' ability to dissipate excess radiative heat as latent heat and thus provide a cooler and more comfortable shade microclimate. In September, similar trends were recorded. The differences between the two periods were larger for exposed surfaces than for those in tree shade, indicating that the hotter the area's microclimate the stronger the trees' potential mitigating effect. This mitigating effect was also expressed at hour of max surface temperature at trees' shade which occurred 2 hours after the maximum of the exposed surfaces.

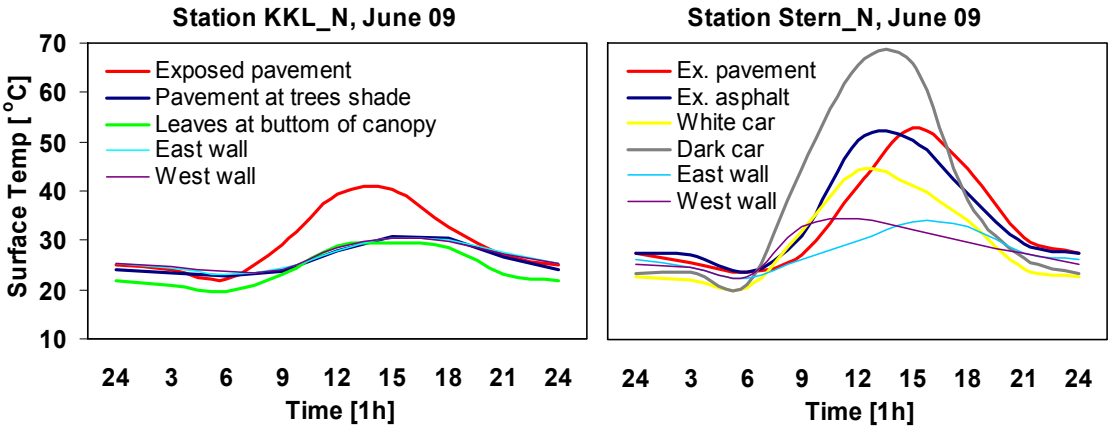

Fig. 4: Surface temperatures measured at KKL-N Boulevard (left) and at Stern-N Street (right), June 09, Beer-Sheva, Israel

4. Summary and Conclusions

Results focus on the trees' impact on air and surface temperatures and on tree transpiration rate. They indicate significant differences between the two time periods. In June, maximum air temperature reached up to 35˚C for the bare street while the vegetated street was up to 3˚C cooler. The daily transpiration reached an average of 2.8 L/m^2. In September the cooling effect was lower than in June due to lower soil moisture and different meteorological and synoptic conditions. Air temperature cooling was only up to 1.4˚C and an average transpiration rate of 2.3 L/m^2. In both periods, surface temperatures reached a maximum of 50˚C for exposed ground and 30˚C to 32˚C under tree shade, including shaded ground, walls and the lower trees' canopy. Differences between the two periods were larger for exposed surfaces than for those in tree shade, indicating that the hotter the area's microclimate the stronger the trees' potential mitigating effect.

Acknowledgement

The research was funded by GIF – German Israel Foundation, under contract number: 955-36.8/2007. We thank Avraham Grava, Uri Dicken, Tal Kanety and Michael Bahar for their help with the experiments.

References

Ali-Toudert, F., Mayer, H., 2007: Effects of asymmetry, galleries, overhanging facades and vegetation on thermal comfort in urban street canyons. Solar Energy 81, 742-754.

Arnfield, A.J., 2003: Two decades of urban climate research: A review of turbulence, exchanges of energy and water, and the urban heat island. International Journal of Climatology 23, 1-26.

Cohen, S., Raveh,E., Li,Y., Grava, A., E.E. Goldschmidt 2005: Physiological responses of leaves, tree growth and fruit yield of grapefruit trees under reflective shade screens. Scientia Horticulturae 107, 25-35.

Granier, A. 1985: Une nouvelle methode pour la measure du flux de seve brute dans le tronc des arbes. Ann. Sci. For. 42, 193-200.

Grimmond CSB. 2007. Urbanization and global environmental change: local effects of urban warming. Geographical Journal 173, 83-88.

Leuzinger, S., R.Vogt, C. Körner. 2010: Tree surface temperature in an urban environment. Agricultural and Forest Meteorology. 150, 56-62.

Mayer, H., Matzarakis, A., 2006: Impact of street trees on the thermal comfort on people in summer: A case study in Freiburg (Germany). Merhavim- Studies in the Geography of Israel and the Middle East, 5, 285-300.

Miller, J.A., D.A. Hartz, B.C. Hedquist, C. Atkinson-Palombo, 2006: The role of vegetation, density, and sky view factor on the microclimate of Tempe, Arizona, USA. Proceeding of the Fifth International Conference of Urban Climate, Lodz, Poland. 366-369.

Mills, G., 2008: Micro-and mesoscal climtology. Progress in Physical Geography, 32: 293-301

Oke, T.R., 1989: The micrometeorology of the urban forest. Philosophical Transactions - Royal Society of London, B324, 335-349.

Shashua-bar, L., O. Potchter, A. Bitan, D. Bolanski, Y. Yaakov, 2010: Micro-climate modeling of street tree species within the varied urban morphology in the Mediterranean city of Tel Aviv. International Journal of Climatology, 30, 44-57.

Simpson, J.R., E.G. McPherson, 1996: Potential of tree shade for reducing residential energy use in California. Journal of Arboriculture. 22, 10-18.

Steemers, K.., 2003: Energy and the city: density, buildings and transport. Energy and Buildings 35, 3-14.

Tsiros, I., 2010: Assessment and energy implications of street air temperature cooling by shade trees in Athens Greece under extremely hot weather conditions. Renewable Energy (In print)

Authors' address:

Dr. Limor Shashua-Bar (shashual@bgu.ac.il)
Prof. Dr. Pua Bar-Kutiel (kutiel@bgu.ac.il)
Deapartment of Geography and Environmental Development
Ben Gurion University in the Negev. P.O.B. 653 Beer Sheva, Israel

Dr. Shabtai Cohen (vwshep@volcani.agri.gov.il)
Dr. Josef Tanny (tanai@volcani.agri.gov.il)
Department of Soil, Water and Environmental Sciences
Agricultural Research Organization - the Volcani Center
P.O.B. 6, Bet-Dagan, 50250 Israel

Dr. Oded Potchter (potchter@post.tau.ac.il)
Yaron Yaakov (yaronws@post.tau.ac.il)
Department of Geography and Human Environment
Tel-Aviv University, P.O. Box 39040, Tel-Aviv 69978, Israel
And Department of Geography and Environmental Development
Ben Gurion University in the Negev. P.O.B. 653 Beer Sheva, Israel

Comparative study of trees impact on human thermal comfort in urban streets under hot-arid and temperate climates

O. Potchter[1,3], J. Holst[2], L. Shashua-Bar[3], S. Cohen[4], Y. Yaakov[1], J. Tanny[4]
P. Bar-Kutiel[3], H. Mayer[2]

[1] Dept. of Geography, Tel Aviv University, Israel
[2] Meteorological Institute, Albert-Ludwigs-University of Freiburg, Germany
[3] Dept. of Geography & Environmental Development,
Ben Gurion University in the Negev, Israel
[4] Inst. Soil, Water & Environmental Sciences, ARO, Volcani Center, Israel

Abstract

The paper compares the impact of trees on human thermal comfort in contrasting temperate and hot-arid urban environments. Studies were conducted on urban bare and vegetated streets in a residential area in Freiburg, Germany (temperate climate) and in the city area of Beer Sheva, Israel (hot-dry climate), during the summer of 2009. The simulation tool for thermal comfort analysis is based on the physiologically equivalent temperature, PET, a widely used thermo-physiological comfort index. PET simulations were compared with in situ measurements of human-biometeorological variables and interviews of pedestrians recorded on well-tested questionnaires, in order to evaluate pedestrian perception of ambient thermal environment. Pedestrian perception was used to evaluate the suitability of the human thermal index PET for local populations in the two climates. PET values for the vegetated streets were lower than for bare streets indicating the trees' potential to reduce heat stress to a level of 28°C (compared to 41°C at a bare site in the same street) at Freiburg and to 29°C (compared to 46°C at a bare street) at Beer-Sheva. Thus, a larger impact on heat stress was observed in the hot dry region than in the temperate one. Statistical analyses of the questionnaires in both cities showed the better adaptation of pedestrians in Beer Sheva to the thermal load.

1. Introduction

The use of urban trees for sustainable passive cooling in urban planning for mitigating the heat island intensity is becoming important for energy savings and improved human comfort (Steemers, 2003; Grimmond, 2007). Numerous studies have investigated the impact of street trees on temperatures reduction in urban street canyons at pedestrian height and found that the reduction can reach 2˚-4˚C (Dimudi and Nikapoulodo 2003: Shashua-Bar et al. 2010; Tsiros, 2010); at some sites in extreme climatic conditions the cooling effect may reach up to 5-8˚C (Miller et al, 2006).

Previous studies focused on the impact of street trees on human comfort and found that the impact on micro-climate at pedestrian level is more pronounced than the cooling effect itself due to the effect of the trees on Mean Radian Temperature (T_{mrt}), which is related to the tree shading effect (Mayer and Matazrkis, 2006: Ali-Toudert and Mayer 2007:). However, it seems that there is a dearth of studies that quantify the impact of street trees on the thermal comfort of people using thermal physiologically significant indices (Mayer and Matzarakis, 2006). Therefore the objective of this study is to extend our knowledge on the reduction of thermal stress on people below the trees canopy in hot summer conditions.

This study investigated the impact of street trees on human comfort in contrasting temperate and hot-arid urban environments in order to analyze the effect of street trees upon microclimate conditions and their impact on human thermal comfort and human reaction in the two different climatic regions. Studies were conducted on urban bare and vegetated streets in a residential area of ALUF at Freiburg, Germany (temperate climate) and in the city area of Beer Sheva, Israel (hot-dry climate), during the summer of 2009. The study is part of a collaborative project between Israel and Germany on the contribution of trees to urban heat island mitigation.

2. Methodology

The methodology of the study included three stages: in-situ measurements, human comfort calculation and questionnaires.

The first stage included empirical study in the old city of Beer Sheva, south region of Israel (hot-dry climate), and in a residential area of ALUF at Freiburg, Germany (temperate climate). In both cities human-biometeorological meteorological measurements (radiative fluxes, air temperature, air humidity, wind speed and direction) were conducted simultaneously at sites without trees and sites influenced by mature trees.

The second stage was the calculation of PET using the PC modelling program, RayMan (Matzarakis et al., 2007) for the Israeli data. The RayMan model, developed according to Guideline 3787 of the German Engineering Society (VDI, 1998) calculates the radiative fluxes in simple and complex environments on the basis of various parameters, such as air temperature, air humidity, degree of cloud cover, time of day and year, the albedo of the surrounding surfaces, elevation and location. According to the model, the calculation of thermal sensation requires input of the following constants: body surface area was standardized to 1.9 m^2, which represents a human with a height of 1.75m and a bodyweight of 75 kg (Hoppe, 1984); the metabolic rate (Met) was fixed at an average value of 80 W/m^2 for a standing person; the insulation factor of clothing (Icl) was standardized to 0.9 for light summer clothing (Jendritzky et al., 1990).

The third stage included questionnaires. During the experiments, pedestrians were interviewed at the observation points using questionnaires for estimating their perception of thermal comfort. The questionnaires used were the same for both cities according to ASHRAE.

At the third stage, the calculated PET values were compared with interviews of pedestrians recorded on the questionnaires, in order to evaluate pedestrian perception of ambient thermal environment and the suitability of the human thermal index PET for local populations in the two climates.

3. Sites and Measurements

At each of the studied sites, several fixed meteorological stations were installed and measured continuously, and mobile measurements were made to address the meteorological variables which need to be determined for estimating microclimate and human thermal comfort.

In Beer-Sheva city, two NW-SE oriented parallel streets were chosen for the study: a pedestrian mall street with vegetation and mature Jacaranda trees predominating, and a

bare street with no trees or other vegetation. Both streets have the same width, 15 m, and similar heights of surrounding buildings (1 to 2 stories). Five fixed meteorological stations were installed and measured continuously during five days (6-10 September, 2009) along with mobile climate measurements that were made along the two streets. Two stations were located in KKL Street, planted with a variety of plants with Jacaranda predominating, one station at the Northern section under the trees shade (KKL_N) and the second at the Southern section of the mall street at an exposed place (KKL_S). Additional two stations were located at Stern Street which is a bare street without trees (Stern_N and Stern_S). In Freiburg city data from measurements in the NNW-SSE oriented Albertstrasse are presented (29 July 2009). There, measurements were conducted on the northern sidewalk in a green section below a mature deciduous tree (fixed human-biometeorological station) and in a bare section (mobile station). Fig. 1 shows the observation stations in the two cities.

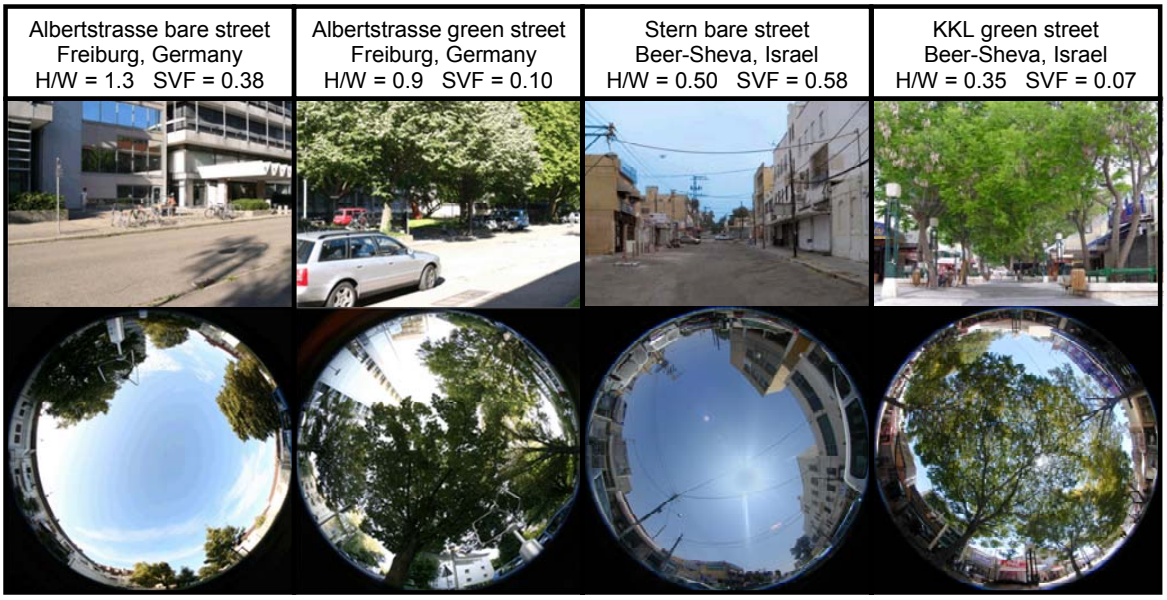

Fig. 1: Observation points of Albertstrasse street, bare section (1st left, "AS_bare") and green section with trees (2nd left, "AS_green"), at Freiburg Germany, and stations of bare street (3rd left, "Stern_N") and of green street (4rd left, "KKL_N"), at Beer-Sheva Israel. Bottom: fish-eye view of the four corresponding streets

3. Empirical results

The investigated climatic variables referring directly to the tree canopy thermal behaviour such as the transpiration rate and the recorded temperature values of air and of surfaces at the trees' shade indicated the potential role of the trees in reducing heat stress. Larger differences between the climatic variables at the exposed surfaces and at the trees shade, in the two climatic regions (Germany and Israel), indicate that the hotter the area's microclimate the stronger is the trees' mitigating effect (Table 1).

Table 1: Data of fixed meteorological stations at the studied sites at Beer Sheva, Israel (Averages of 6-10.9.2009), and at Freiburg, Germany (29 July 2009)

meteorological variable September 6-10 2009	Beer Sheva sites, Israel			Freiburg sites, Germany		
	KKL_N Green street	Stern_N Bare street	Station above roof level	Albertsr Green section	Albertstr Bare section	Station above roof level
Max air temperature Ta (°C)	31.7	33.1	31.4	29.6	29.5	30.0
Min air temperature Ta (°C)	20.5	20.4	20.0	17.5	18.0	16.6
Max water vapour pressure VP (hPa)	24.7	25.6	25.2	20.7	17.2	15.8
Min water vapour pressure VP (hPa)	19.6	19.8	20.8	16.7	10.2	9.7
Max wind speed v ($m\ s^{-1}$)	0.4	0.8	2.7	2.0	4.1	4.3
Max mean radiant temperature Tmrt (°C)	27	61	61	34	67	57
Max physiological equivalent temp PET (°C)	29	46	44	28	41	37

4. PET calculations

Figure 2 shows the PET calculations at the two stations in Beer Sheva (KKL_N, Stern_N) and at the two stations at Freiburg (AS_green, AS_bare). PET values for the vegetated streets were distinctly lower indicating the trees' potential for reducing heat stress to a level of 28°C at both Freiburg and Beer-Sheva. Figure 3 shows the PET calculations and their relation to the subjective thermal sensation at Beer Sheva and at Freiburg. It can be seen that although the cooling effect of street trees is around 1.5°C, reduction of PET is much more pronounced- 13°C in Freiburg and 20°C in Beer Sheva.

Statistical analysis of questionnaires regarding the comfort sensation in both cities showed that the comfort thermal sensation in Beer Sheva is only 2°C higher that in Frieburg, but the temperature at which people feel sever heat stress is almost 5°C higher in Beer sheva in comparison to Freiburg.

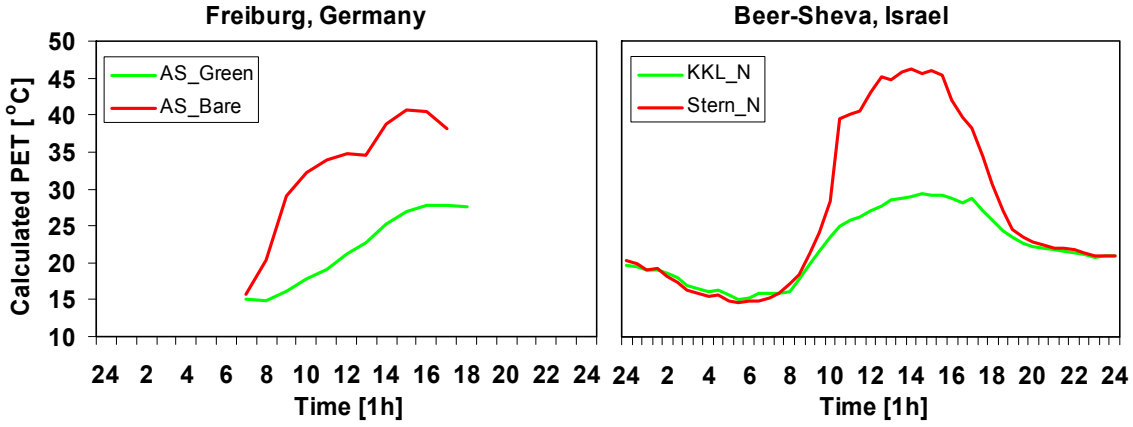

Fig. 2: PET calculations at Albertstrasse, Freiburg, Germany, 24 July 2009 (left) and at Stern-N and KKL-N streets, 8 September 2009, Beer-Sheva, Israel (right)

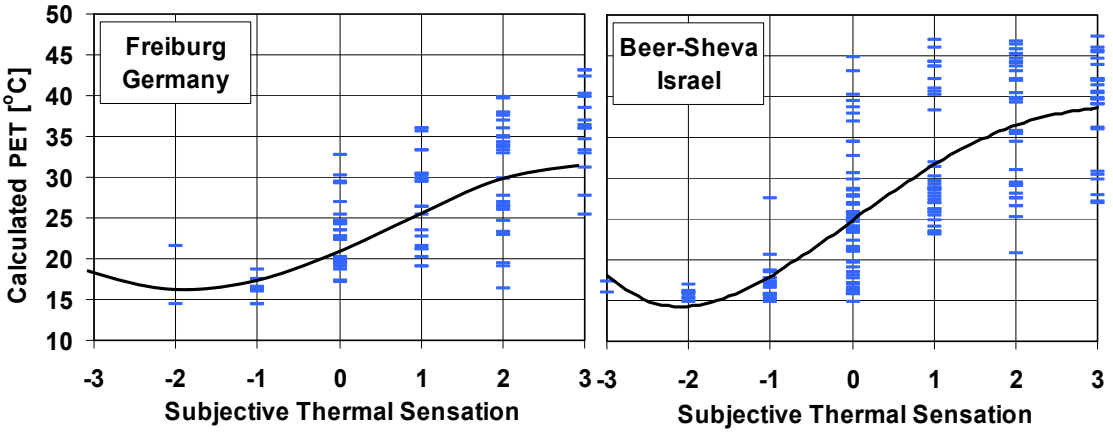

Fig. 3: Comparison of PET calculations with subjective thermal sensation at Albertstrasse, Freiburg, Germany (left) and at Stern-N and KKL-N streets, Beer-Sheva, Israel (right), during daily hours (6:00-18:00), summer 2009

5. Summary and Conclusions

Street trees have shown a better cooling effect and a better reduction in T_{mrt} in the most extreme climate, and as a result show a better improvement in human comfort. The cooling effect by trees was mainly caused by the reduction of T_{mrt} due to shading. Since PET is strongly influenced by T_{mrt}, this shading effect directly showed up in PET. The influence of street trees on air temperature is comparatively low.

Statistical analyses of climatic comfort questionnaires in both cities showed better adaptation of pedestrians in Beer Sheva to the thermal load.

Acknowledgement

The research was funded by GIF – German Israel Foundation, under contract number: 955-36.8/2007. The authors are indebted to the Federal Ministry of Education and Research (BMBF) for funding the sub research projects KLIMES ALUF-1 and KLIMES ALUF-2 (FZK: 01LS05020), which are part of the joint research project KLIMES; within the scope of the research initiative klima*zwei*. We thank Avraham Grava, Uri Dicken, Tal Kanety and Michael Bahar for their help with the experiments.

References

Ali-Toudert, F., Mayer, H., 2007: Effects of asymmetry, galleries, overhanging fac¸ades and vegetation on thermal comfort in urban street canyons. Solar Energy 81, 742-754.

Dimoudi, A., M. Nikolopoulou, 2003: Vegetation in the urban environment: microclimate analysis and benefits. Energy and Buildings 35, 69-76.

Grimmond CSB. 2007. Urbanization and global environmental change: local effects of urban warming. Geographical Journal 173, 83-88.

Jendritzky, G., G, Menz., H, Schirmer. W, Schmidt-Kessen. 1990: Methodik zur räumlichen Bewertung der thermischen Komponente im Bioklima des Menschen. *Beiträge der Akademie für Raumforschung und Landesplanung*. Bd. 114, Hannover,

Mayer, H., A. Matzarakis, 2006: Impact of street trees on the thermal comfort on people in summer: A case study in Freiburg (Germany). Merhavim- Studies in the Geography of Israel and the Middle East, 5, 285-300.

Matzarakis, A., F, Rutz, H, Mayer, 2007: Modelling radiation fluxes in simple and complex environments: basics of the RayMan model. Int. J. Biometeorol. 51, 323-334.

Miller, J.A., D.A. Hartz, B.C. Hedquist, C. Atkinson-Palombo, 2006: The role of vegetation, density, and sky view factor on the microclimate of Tempe, Arizona, USA. Proceeding of the Fifth International Conference of Urban Climate, Lodz, Poland. 366-369.

Shashua-Bar, L., O. Potchter, A. Bitan, D. Bolanski, Y. Yaakov, 2010: Micro-climate modeling of street tree species within the varied urban morphology in the Mediterranean city of Tel Aviv. Int. J. Climatol., 30, 44-57.

Steemers, K., 2003: Energy and the city: density, buildings and transport. Energy and Buildings 35, 3-14.

Tsiros, I., 2010: Assessment and energy implications of street air temperature cooling by shade trees in Athens Greece under extremely hot weather conditions. Renewable Energy (In print)

Authors' address:

Dr. Oded Potchter (potchter@post.tau.ac.il)
Department of Geography and Human Environment
Tel-Aviv University, P.O. Box 39040, Tel-Aviv 69978, Israel
And Department of Geography and Environmental Development
Ben Gurion University in the Negev. P.O.B. 653 Beer Sheva, Israel

Dr. Limor Shashua-Bar (shashual@bgu.ac.il)
Deapartment of Geography and Environmental Development
Ben Gurion University in the Negev. P.O.B. 653 Beer Sheva, Israel

Dr. Shabtai Cohen (vwshep@volcani.agri.gov.il)
Department of Soil, Water and Environmental Sciences
Agricultural Research Organization - the Volcani Center
P.O.B. 6, Bet-Dagan, 50250 Israel

Yaron Yaakov (yaronws@post.tau.ac.il)
Department of Geography and Human Environment
Tel-Aviv University, P.O. Box 39040, Tel-Aviv 69978, Israel

Dr. Josef Tanny (tanai@volcani.agri.gov.il)
Department of Soil, Water and Environmental Sciences
Agricultural Research Organization - the Volcani Center
P.O.B. 6, Bet-Dagan, 50250 Israel

Prof. Dr. Pua Bar-Kutiel (kutiel@bgu.ac.il)
Department of Geography and Environmental Development
Ben Gurion University in the Negev. P.O.B. 653 Beer Sheva, Israel

Prof. Dr. Helmut Mayer (helmut.mayer@meteo.uni-freiburg.de) and Dr. Jutta Holst (jutta.holst@meteo.uni-freiburg.de)
Meteorological Institute, Albert-Ludwigs-University of Freiburg
Werthmannstr. 10, D-79085 Freiburg, Germany

Comparison of the urban-rural comfort sensation in a city with warm continental climate

Ágnes Gulyás[1], Andreas Matzarakis[2], János Unger[1]

[1] University of Szeged, Department of Climatology and Landscape Ecology, Hungary
[2] Meteorological Institute, Albert-Ludwigs-University of Freiburg, Germany

Abstract

The aim of this study is to show the effect of the complex urban environment on the human bioclimatic conditions on local scale in a Central-European city with warm and relatively dry continental climate (Szeged, Southern Hungary). According to the practice in urban climate studies, the characteristics of two distinct locations were compared in bioclimatic aspects. The modifying effect of the city can be studied at the location situated in the built-up city center, while the effect of the city is negligible at a location on an arable land with open horizon. Hourly average values of each meteorological parameter (collected between 1999-2008) were used to calculate Physiologically Equivalent Temperature (PET) bioclimate index values. Based on these datasets the difference in physiological stress on urban and rural residents was described. Considering the average of the PET through the whole 10-year period between the urban and rural areas, it was 2.9 °C higher in the urban area. While the difference in the length of the *hot* and *very hot* period is 0,5% (compared to the full length of the studied term), this difference is 10% between the *cold* and *very cold* categories. According to our study the human bioclimatic modifying effect of the city is more pronounced in the physiologically more demanding cold periods.

1. Introduction

Characteristic climatic phenomena, occurring in cities (urban climate, urban heat island) generates special environments for their residents. The climatic effects of the cities can enhance the thermal stress of the residents (in summer, especially during heat waves), or attenuate it (in winter). The highest intensity of the urban heat island is formed several hours after sunset keeps the extent of the heat stress at high levels in addition to the strong heat stress during the daytime.

Table 1: Physiologically Equivalent Temperature (PET) for different grades of thermal sensation and physiological stress of human beings (internal heat production: 80 W, heat transfer resistance of the clothing: 0.9 clo) (Matzarakis and Mayer, 1996 modified)

PET (ºC)	**-4**	**4**	**8**	**13**	**18**	**23**	**29**	**35**	**41**
thermal sensation	extr. cold	very cold	Cold	cool	sligh. cool	comfortable	sligh. warm	warm	hot	extr. hot
Level of the physiology. stress	extreme		Strong	mod	slight	no stress	slight	mod.	strong	extr.
	cold stress						heat stress			

One of the most popular thermal index in the bioclimatic researches is the PET (Physiologically Equivalent Temperature). PET is defined as the air temperature at which the human energy budget for the assumed indoor conditions is balanced by the same skin

temperature and sweat rate as under the actual complex outdoor conditions to be assessed (e.g. Mayer and Höppe, 1987; Höppe, 1999). Ranges of the PET index are shown in Table 1. While the original scale does not contain, due to the homogeneity in winter we introduced a new category: below -4 °C PET it is named extreme cold thermal sensation.

The aim of this study is to compare the bioclimatic situation of a city and the surrounding rural area on the example of a Southern Hungarian city (Szeged) in a then-year period (1999-2008). Additionally, summer averages of 10 years were compared to the summer of 2003, when successive heat waves caused high heat load (Sch. Kriston and Schlanger, 2003). This comparison can provide data, how the bioclimatic stress is modified in extremely hot periods and how these changes are affected in urban and rural areas.

2. Study area and methods

Szeged is located in the southern part of Hungary (46ºN, 20ºE) at 79 m above sea level on a flat plain. The base of the street network is a circuit-avenue system, with several different land-use types from the densely built centre to the detached housing suburb region (Fig. 1 A, B). Szeged is in the climatic region *D.1* according to Trewartha's classification (continental climate with a long warm season). The annual mean temperature is 10.4 ºC and the amount of precipitation is 497 mm, the annual mean sunshine duration is 2100 hours.

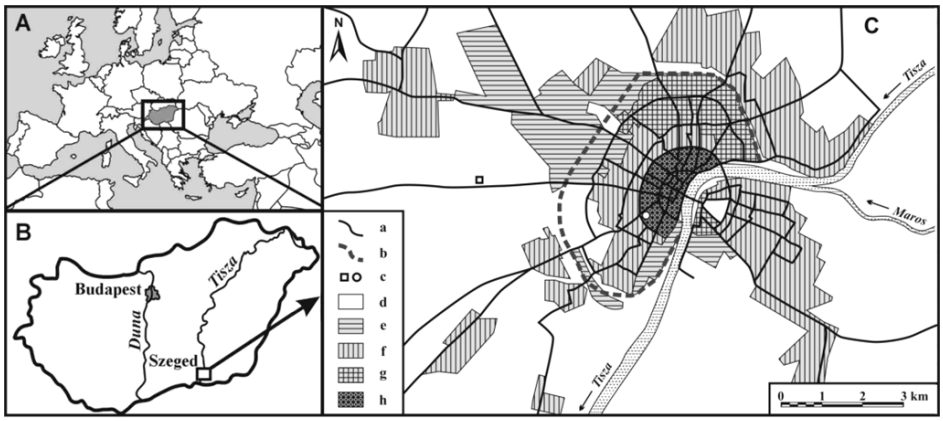

Fig. 1: Geographical location of Hungary in Europe (**A**), of Szeged in Hungary (**B**), characteristic land-use types and road network of Szeged (**C**) **a**: road **b**: circle dike **c**: measuring point in the city centre (○) and in the rural area (□) **d**: agricultural rural area **e**: industrial area **f**: 1-2 storey detached houses, **g**: 5-11 storey apartment buildings **h**: historical city core with 3-5 storey buildings

According to the widely used practice in urban climate studies, the characteristics of two distinct locations were compared from bioclimatic aspects. The modifying effect of the city can be studied at the location situated in the built-up city center (**h**), while the effect of the city is negligible at a location on an arable land with an open horizon (**h***) (Fig. 1C). Human biometeorological relevant data (air temperature (T_a), relative humidity (RH), wind velocity (v) and global radiation (G) were measured on these two different sites of the city with Vaisala meteorological stations. Wind speed data measured on the different height (station urban: 26 m, station rural: 10 m) were reduced to the 1.1 m

bioclimatologically standard height (Lee, 1979; Gál and Unger, 2009). Hourly average values of each meteorological parameter (collected between 1999 – 2008) were used to calculate PET values, using the RayMan model (Matzarakis et al., 2007). Based on these datasets the difference in physiological stress on urban and rural residents was described. PET categories were created according to the heat sensations levels (Table 1). Preliminary results show the results of the descriptive statistical analyses (e.g. absolute and relative frequency).

3. Results

Comparing the daily averages of PET index higher values can be observed in the city than in the surrounding rural area through the whole year (Fig 2).

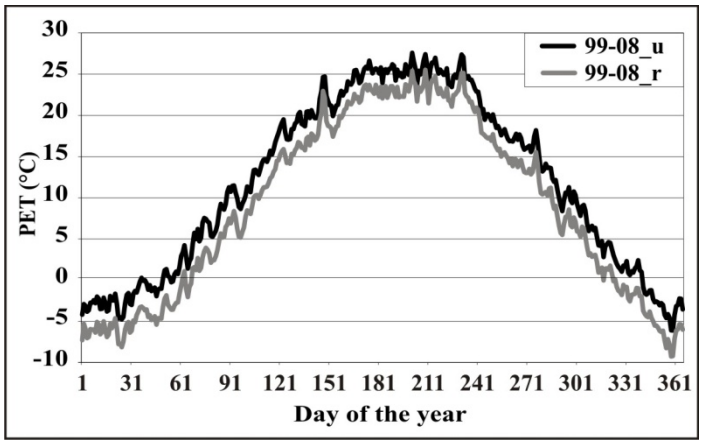

Fig. 2: Mean daily values of the PET index on the urban (u) and rural (r) area between 1999-2008 in Szeged

Considering the average of PET through the 10-year period, the difference is 2.9 ºC higher in the urban areas. While there is no considerable difference between highest PET values of the two examined areas (0.9 ºC), the difference between the minimum PET values is much higher (10.6 ºC) (Fig 3). Extremities have higher occurrence in the rural areas compared to the urban ones: frequency distribution of the strong or extreme heat stress (hot and very hot heat sensations categories) is 0.5 %, of the strong or extreme cold stress (between cold and extreme cold heat sensations) 9.5 % during the examined period. The occurrence of the periods without thermal stress is nearly two times higher in the city, than outside: 3.9 % compared to the full length of the studied term.

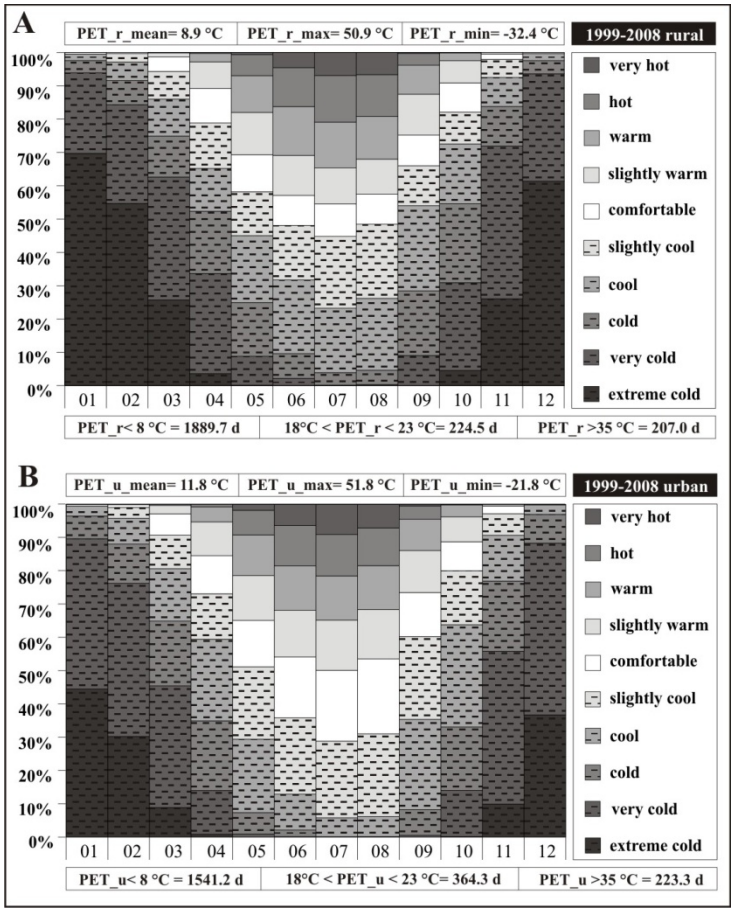

Fig. 3: Frequency of the PET (hourly averages) and the different grades of thermal sensation on the rural (**A**) and the urban (**B**) area between 1999-2008 in Szeged

It can be concluded from the averages that the city has equalizing effect on the thermal stress conditions. It reduces the extremities, furthermore this reduction is more pronounced on the cold extremities. Examining years what are significantly warmer than the average can predict the effect of global warming on bioclimatic situations, especially in case of the inhabitants of cities.

A very hot summer with several heat waves hit Europe and also Hungary in 2003. Very high daytime temperatures mostly in anticyclonic situation dominated between May and August with mainly low wind speed (Sch. Kriston and Schlanger, 2003). This period is compared to the averages of 10 years (Fig 4). During extreme hot periods, the frequency of the high heat stress periods is increased in both examined areas. Preliminary results show that in contrast to the average of the 10-year period, the increase is slightly higher in the rural areas compared to the city. Considerable increase of periods with comfort category was observed in the urban areas. This category remained unchanged outside the city, only the cold stress periods became shorter in the urban areas. The decrease of the cold stress periods was more pronounced in the city, the extent of the stress was also reduced to weak in the urban areas.

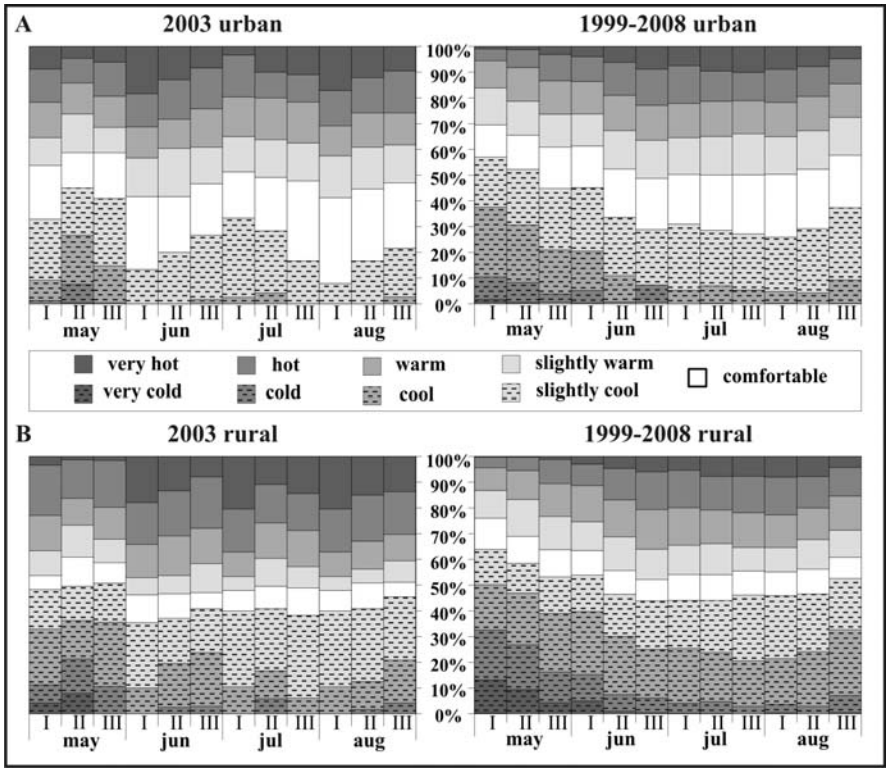

Fig. 4: Frequency of the PET (hourly averages) in then-day periods and the different grades of thermal sensation on the urban (**A**) and the rural (**B**) area between May and August in 2003 and 1999-2008 in Szeged

This phenomenon can be explained by the urban heat island (UHI) at night caused by reduced long wave radiation. These circumstances have physiologically disadvantageous effect in summer, because it can shorten the regeneration possibilities of urban inhabitants during the night.

4. Conclusions

The aim of this study was to compare the bioclimatic situation of a city with continental climate and the surrounding rural area.

(i) Using the PET index, we could detect significant difference between the two areas.

(ii) Examining data collected during long time periods, the reduction of the length of cold stress terms caused by urban effects is observed. In parallel the length of heat stress terms was slightly increased. This may increase the comfort of the residents of the city, especially in spring, autumn and winter, because cold stress is lower during the nights. Long term analysis shows that the city has a moderating and compensating effect on the human comfort conditions.

(iii) In heat waves however, this even heat load is not unequivocally positive phenomenon. Due to the lower direct radiation caused by smaller sky view factor values (obstacles of the city: buildings, trees), the occurrence of the extreme high heat stress is lower in the urban areas. During the night however the decrease of the heat load is significantly smaller (due to the UHI) in the city than in the surrounding rural areas. This effect reduces the regeneration chance of the human bodies before the heat stress of the

next day. Thus the occurrence of the comfort thermal sensation category is higher in the city apparently, but it does not mean better bioclimatic situation especially during the heat waves.

(iv) Our data predicts, that the extreme heat waves, occurring more frequently and higher intensity due to the global warming, will increase the heat stress more on the residents of the big cities, compared to their surrounding rural area.

Acknowledgements

This research was supported by the Hungarian Scientific Research Fund (OTKA K-67626).
Special thanks for Noémi Kántor for her help in preparing the figures.

References

Gál, T., J. Unger, 2009: Detection of ventilation paths using high-resolution roughness parameter mapping in a large urban area. Build. Environ. 44, 198-206.

Gulyás, Á., J. Unger, A. Matzarakis, 2006: Assessment of the microclimatic and human comfort conditions in a complex urban environment: modelling and measurements. Build. Environ. 41, 1713-1722.

Höppe, P., 1999: The physiological equivalent temperature – an universal index for the biometeorological assessment of the thermal environment. Int. J. Biometeorol. 43, 71-75.

Lee, D.O., 1979: The influence of atmospheric stability and the urban heat island on urban-rural wind speed differences. Atmos. Environ. 13, 1175-1180.

Matzarakis, A., F. Rutz, H. Mayer, 2007: Modeling radiation fluxes in simple and complex environments – Application of the RayMan model. Int. J. Biometeorol. 51, 323–334.

Mayer, H., P. Höppe, 1987: Thermal comfort of man in different urban environments. Theor. Appl. Climatol. 38, 43-49.

Sch. Kriston, I., Schlanger, V. 2003: 2003 nyarának időjárása. Légkör 48, 39-40. (in Hungarian)

Authors' address:

Ágnes Gulyás (agulyas@geo.u-szeged.hu)
János Unger (unger@ geo.u-szeged.hu)
Department of Climatology and Landscape Ecology, University of Szeged
Egyetem u. 2., H-6722 Szeged, Hungary

Andreas Matzarakis (andreas.matzarakis@meteo.uni-freiburg.de)
Meteorological Institute, Albert-Ludwigs-University of Freiburg
Werthmannstr. 10, D-79085 Freiburg, Germany

Influence of air circulation and geographical factors on daily rhythm of biothermal conditions

Monika Bakowska

Institute of Geography, Kazimierz Wielki University

Abstract

The paper shows the characteristic of daily variability of the biothermal conditions in Poland over the period 1991-2000. The bioclimatic conditions were evaluated by Universal Thermal Climate Index (UTCI). The analyses concern of daily course of UTCI in Koszalin, Warsaw and Wroclaw in different air masses: arctic, polar-maritime, polar-continental and tropical. Moreover the 3-hour data were approximated by the polynomial function and the maximal and minimal values of the UTCI in different air masses were estimated. The calculations show also the frequency of an occurrence of specific ranges of UTCI.

1. Introduction

Both the geographical factors and the air circulation modify biothermal conditions. A lot of bioclimatological indices are used in the studies regarded the impact of climatic condition on human thermal sensations (Blazejczyk, Matzarakis, 2007). Many of them are derived from the heat exchange between man and environment but they didn't simulates human heat transfer inside the body and heat exchanges between particular layers of the body. Universal Thermal Climate Index (UTCI) includes all these factors and it allows to qualify heat stress in wide range of thermal conditions in different climatic zones (Blazejczyk et al., 2010; Jendritzky et al.. eds. 2009). In the paper the UTCI it was applied for evaluation of heat stress in man in different region of Poland in particular air masses.

2. Data and methods

The purpose of the paper is to analyse the effect of geographical factors and air circulation on daily rhythm of biothermal conditions in Poland over the period 1991-2000. There were chosen three cities, represented various regions of Poland: Koszalin placed on north at the seashore, Warsaw represented central part of the country and Wroclaw situated at south-west. Selected cities allowed to show the spatial range of daily changeability of biothermal conditions in Poland.

Based on air temperature, dew point, wind speed and mean radiant temperature UTCI was computed and averaged for days with the particular air masses (*Codzienny biuletyn* 1991-2000). The air masses were divided into four groups: arctic air (PA), maritime polar air (PPm), continental polar air (PPk) and tropical air (PZ).

The analysis contained the character of daily variability of the UTCI in particular air masses during all months. In the next step, the minimal and maximal values of the UTCI were approximated data by polynomial function of 3-hours observation terms. The approximated time of an appearance of extreme UTCI values in different air masses were calculated as well. Moreover, the frequency of the occurrence of extreme heat stress and thermal neutrality in separated air masse were described. The analysis of the frequency of various heat stress classes was made for three months periods and it regarded winter (from December to February) and summer season (from June to August).

3. Results

Daily course of Universal Thermal Climate Index in particular air masses

The Universal Thermal Climate has the lowest values in Wroclaw on February, during advection of polar-continental air masses. In that situation the UTCI value achieved -28ºC at midnight hours; that refers to occurrence of very strong cold stress. The warmest conditions are during inflow of tropical air masses in Warsaw on July, when the index grows up to 34ºC at 3 p.m. This value causes strong heat stress.

Daily courses of UTCI in arctic air masses are similar in Warsaw and Wroclaw (Fig. 1). At these stations the strong cold stress occurs during winter season. Koszalin characterises by moderate cold stress at the same air mass. In the summer season the slight cold stress occurs at early-morning hours only in Warsaw and Wroclaw. The thermal strain does not exist from May to October at daily hours in all the stations.

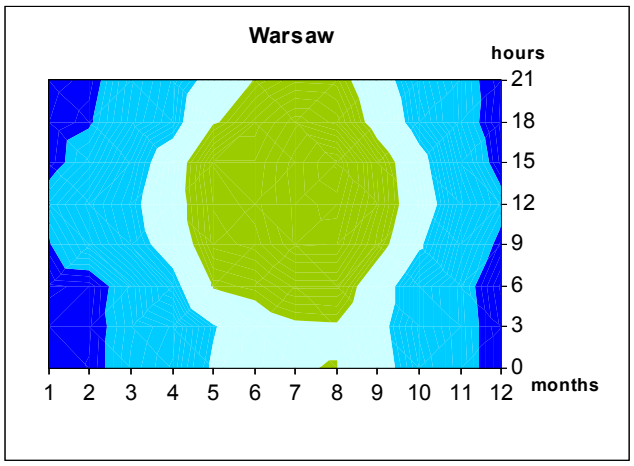

Fig. 1: Daily course of UTCI in particular months in Warsaw in arctic air mass strong cold stress moderate cold stress slight cold stress no thermal stress

Daily courses of UTCI index are similar in all the stations during advection of polar-maritime air masses. The moderate cold stress appears 24 hours a day in the winter season and no thermal stress occurs in summer.

UTCI values at polar-continental air mass are very differentiated. Because of Baltic sea influence the warmest station during winter season is Koszalin. The strong cold stress is noted only in the early-morning and evening hours in that station. However, such sensations occurs in Warsaw and Wroclaw during all day. The strong cold stress appears occasionally before sunrise in Wroclaw at polar-continental mass. There is no thermal stress on June and October almost 24 hours in all the cities. On July the moderate heat stress dominate from 6 a.m. to 3 p. m. UTCI exceeds 32ºC at noon hours and it points to strong heat stress which lasts till 3 p. m. in Wroclaw (Fig. 2).

The tropical air masses are warmest but they occur rarely during winter season (Bakowska, Wieclaw, 2009). They appear on January in Wroclaw and they causes slight and moderate cold stress. The UTCI during 24 hours period indicates no thermal stress on April, May and August. However, the index reach the range of moderate and strong heat stress on June and July.

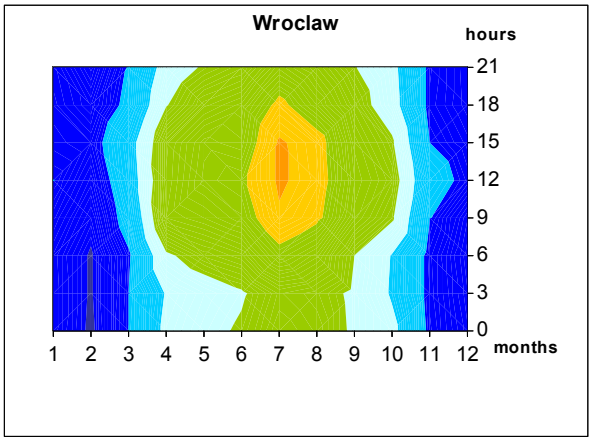

Fig. 2: Daily course of UTCI in particular months in Wroclaw in polar-continental air mass ■ very strong cold stress ■ strong cold stress ■ moderate cold stress ■ slight cold stress ■ no thermal stress ■ moderate heat stress ■ strong heat stress

The extreme values of UTCI in particular air masses

Because of thermal features the highest maximal values of UTCI are noted at tropical air mass. Maximum of the index oscillate between 34 and 39ºC, so they cause strong and very strong heat stress. Polar-continental air masses effect very high maximal UTCI values in the summer season. During advection of this kind of mass the moderate heat stress is noted. But in winter season the UTCI maximum is the lowest.

Polar-maritime air masses are cooler in the summer. For example, in Koszalin they are cooler than arctic air (Fig. 3). These masses cause no thermal stress during summer season and slight cold stress at winter months. At arctic air masses the maximum of UTCI decreases to -14ºC and that refers to strong cold stress.

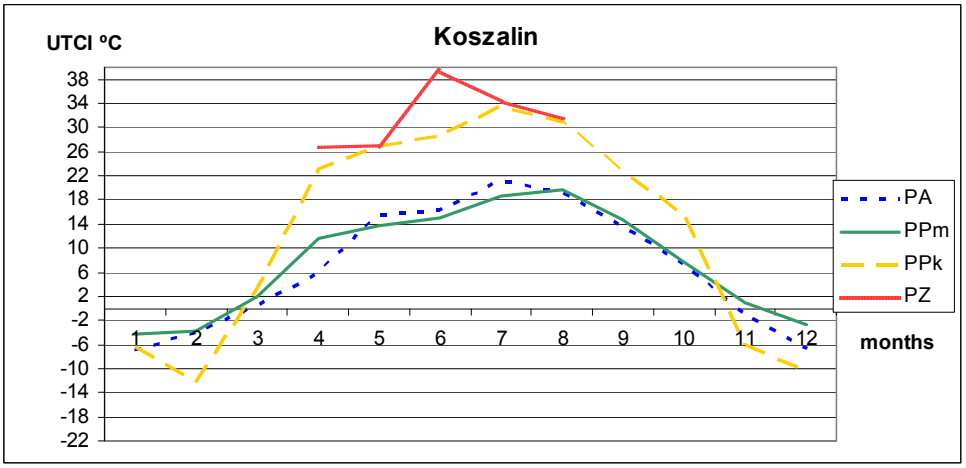

Fig. 3: The annual course of maximum values of UTCI in Koszalin in particular air masses

The course of minimal UTCI values is very similar to course of maximal ones. The observed UTCI minimum reaches about 18ºC in Koszalin at tropical air in the summer and

they decrease to -20ºC in polar-continental mass in winter season. In Warsaw and Wroclaw the minimal values oscillate between 15ºC in tropical air masses and -30ºC in polar-continental air (Fig. 4). This means that index indicates that biothermal conditions oscillate from "no thermal stress" to "very strong cold stress".

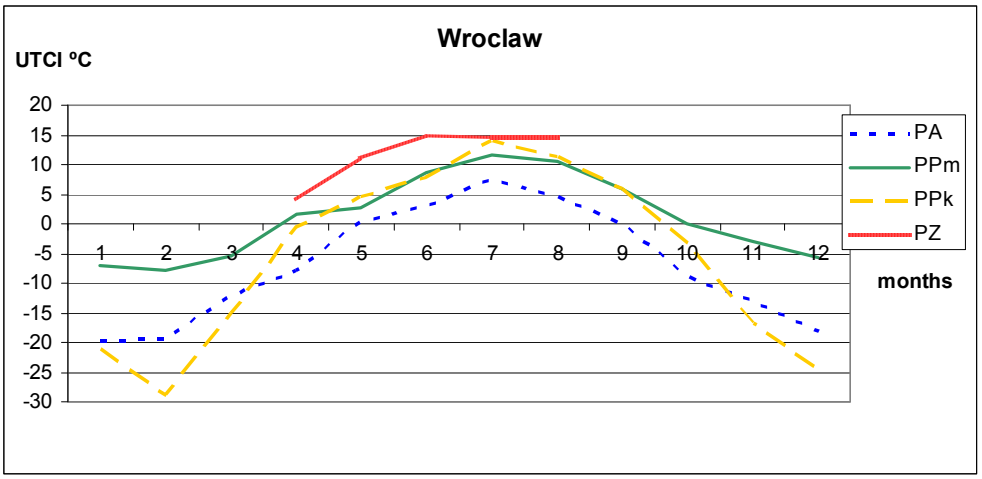

Fig. 4: The annual course of minimal values of UTCI in Wroclaw in particular air masses

There is seen tendency in the course of a time when maximal UTCI values occur. The winter months are characterised by earlier appearance of maximum in arctic and polar-maritime masses; the UTCI maximum is observed between 11:30 a. m. and the noon. In the summer the maximal UTCI values occur later – after noon hours (Fig. 5).

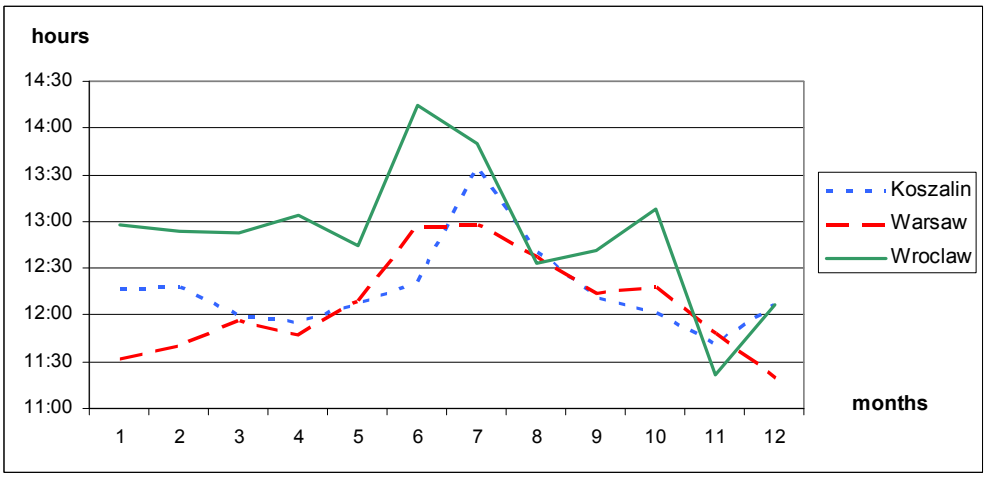

Fig. 5: The time of maximal UTCI values in arctic air in Koszalin, Warsaw and Wroclaw

In polar-continental air mass the maximal UTCI values occur between 11 a.m. and 12:30 p.m.. Wroclaw is an exception; in that station daily maximum of index is significantly delayed in comparison to other stations.

When considering annual course of the time when minimal values of the index occur the similar tendences in all air masses are seen. The UTCI minimum is noted later in winter season than in summer (Fig. 6). They appear at 2-3 a.m. from December to February and between 1 a.m. and 1:30 a.m. in the summer months.

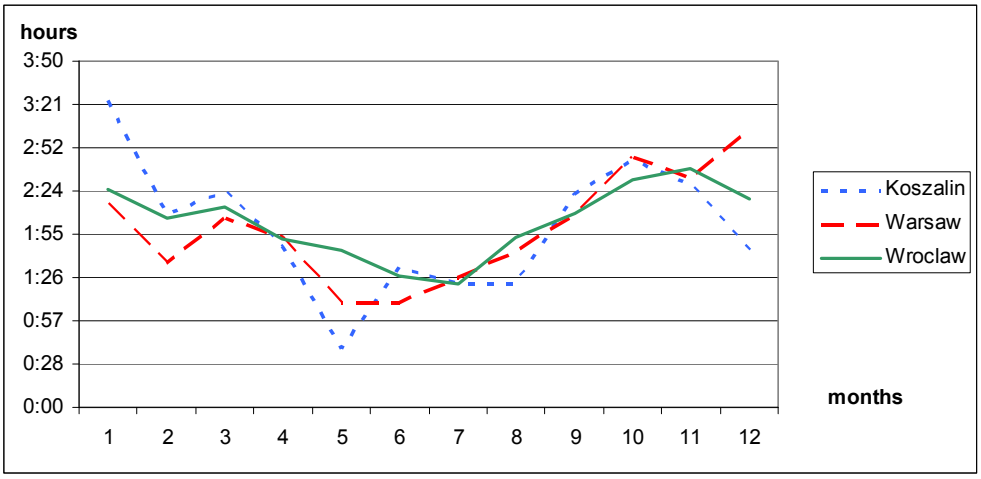

Fig. 6: The time of minimal UTCI values in polar-maritime air in Koszalin, Warsaw and Wroclaw

The frequency of neutral and extreme biothermal conditions

No thermal stress in the summer is noted each day but with different frequency in particular air masses. The neutral conditions appear in the polar-continental and tropical air masses during evening and night hours (Fig. 7). Only in Koszalin the rate of thermal neutrality does not exceed 20%.

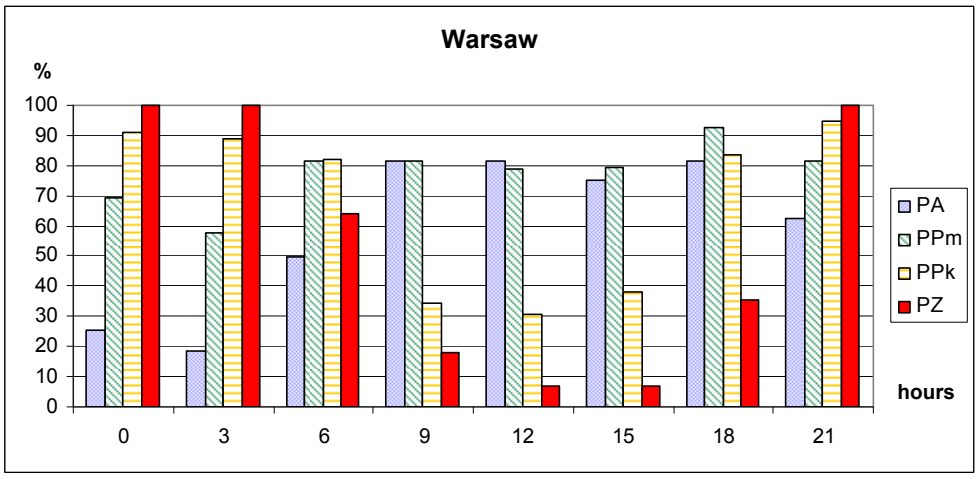

Fig. 7: Frequency of no thermal stress during summer in Warsaw in particular air masses

Generally, during day hours “no thermal stress” is noted in polar-maritime and arctic air masses. However, in day time hours tropical air is responsible for appearance of the very strong heat stress. The neutral conditions occur rarely in the winter season. They

are usually noted from 9 a.m. to 3 p.m. in Warsaw during advection of polar-maritime air.
In Warsaw and in Wroclaw strong cold stress is registered only in polar-continental and arctic air masses. In Wroclaw in continental mass it can reach 30% during night hours. However, during daily hours it decreases to 10-15%. In the arctic air its frequency is even smaller.

4. Conclusions

The analysis show that advections of polar-continental air masses in winter months bring most sever bioclimatic conditions in Poland. These masses are responsible for the occurrence of strong and occasionally very strong cold stress in Warsaw and in Wroclaw. The minimum UTCI values (even -30ºC) in polar-continental air mass appear between 2 and 2:30 a. m. On the other hand these masses are responsible for occurrence of strong heat stress in summer season. The maximum UTCI values are noted afternoon and they reach 34ºC. The flow of the arctic air causes the appearance of strong cold stress in winter season. Only in Koszalin the moderate cold stress is typical because of the influence of Baltic sea. The UTCI indicates thermoneutral conditions in summer in polar-maritime and arctic air. During summer season advection of tropical air causes strong heat stress in day-time hours and no thermal stress in the night.

References

Bakowska M., Wieclaw M., 2009, Dobowy przebieg wybranych wskaźników biometeorologicznych w różnych masach powietrza w Bydgoszczy, (Daily course of chosen biometeorological indices in different air masses in Bydgoszcz) Ekologia i Technika (Ekology and Technology), vol. XVII, nr 2, p. 53-59:

Blazejczyk K., Matzarakis A., 2007, Regional and local bioclimatic differentiation of Poland, Geographia Polonica, vol. 80 No. 1, Spring, p. 63-82.

Błażejczyk K., Broede P., Fiala D., Havenith G., Holmér I., Jendritzky G., Kampmann B., 2010, UTCI – nowy wskaźnik oceny obciążeń cieplnych człowieka (UTCI – New index for assessment of heat stress in man), Przeglad Geograficzny, 82, 1, p. 5–27.

Codzienny Biuletyn Meteorologiczny (Daily meteorological Bulletin), 1991-2000, IMGW, warszawa.

Jendritzky G., Havenith G., Weihs P., Batchvarova E. (eds.), 2009, Towards a Universal Thermal Climate Index UTCI for assessing the thermal environment of the human being. Final Report COST Action 730.

Author's adress:
mgr Monika Bakowska (monika.bakowska@gmail.com)
Institute of Geography, Kazimierz Wielki University
Minska 15, 85-428 Bydgoszcz, Poland

Urban thermal patterns, environmental conditions associated and synoptic factors in Lisbon

Henrique Andrade, Maria João Alcoforado; Paulo Canário

Centre of Geographical Studies, Institute of Geography and Spatial Planning, Univ. of Lisbon

Abstract

Urban Heat Island is the most studied feature of urban climate, but its actual importance to the urban quality of life should be analysed considering its association with other environmental features, such as air quality and the occurrence of thermal extremes. Furthermore, the urban thermal field is conditioned by wind and pressure regional patterns. The knowledge of the frequency of these patterns allows to extrapolate the frequency of urban thermal patterns, beyond the shorter period for which we possess urban air temperature measurements.

A network of seven thermo-hygrometers was installed in 2004 in Lisbon (Portugal) with the aim to deepen the knowledge about urban thermal fields. Thermal patterns were classified, using the k-means method, and seven main types where identified. In this paper, different features will be described: (i) hourly and seasonal thermal patterns variation; (ii) UHI association with regional wind and sea level patterns iii) association with environmental stress features (thermal extremes; particulate matter and ozone concentration).

The final objective of the present research is to understand the relationship among urban climate, environmental conditions and larger scale synoptic factors.

1. Introduction

The study of the Lisbon's Urban heat Island (UHI) began in the eighties (Alcoforado, 1992) based in observational methods and it is still carried out, combining observations and modelling (Alcoforado and Andrade, 2006; Andrade and Alcoforado; 2008; Lopes, 2003). The main aim of these studies was to produce useful information to urban planning, what has been achieved by working in collaboration with the Lisbon's municipality (Alcoforado et al., 2009). The knowledge of the urban thermal field is important, because of the impacts of temperature in thermal comfort (therefore in energy consumption) and health (Tan et al, 2010; Silva et al. 2010). But an average situation cannot be assumed; there are different configurations of the thermal field and it is necessary to know its frequency and conditioning factors, namely at the synoptic scale. Moreover, is important to know the association of the different thermal patterns with the conditions that can affect the human health and comfort, such as thermal extremes and air quality.

The classification and cartographic representation of Lisbon's thermal patterns was performed, based in observational data from a network of fix thermo-hygrometers and a statistical model of the relationship between temperatures and geographical factors; the analysis of the synoptic framework of each of the thermal patterns allows to extrapolate its frequency beyond the measurement period. Finally, the environmental conditions (considering thermal extremes and PMs and ozone concentration) was analysed, to identify the thermal patterns more frequently associated with uncomfortable or dangerous conditions.

2. Materials and methods

With the aim to deepen the knowledge about the thermal field in Lisbon, a network of seven thermo-hygrometers has been installed in 2004 (fig. 1), reaching a sample of near

1400 days with registration. The devices were installed in relatively open places, avoiding the influence of microclimatic factors. A cluster analysis, using the k-means method was performed, with the aim to classify the spatial thermal patterns, at three moments of the day: 6 am (near the time of the occurrence of the minimum temperature), 3 pm (near the maximum temperature) and 10 pm (beginning of the nigh that corresponds, frequently, to the period of higher intensity of the UHI). As the aim is the classification of spatial thermal patterns, it was necessary to normalise the values (to eliminate the differences associated with seasonal and daily temperature variations). Therefore calculated, for each time period, was calculated the difference between each measurement and the average of the seven values.

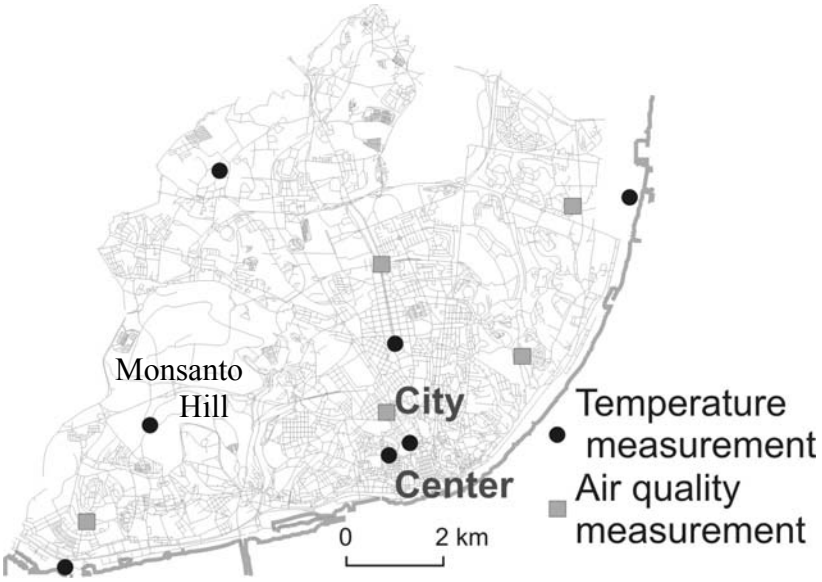

Fig: 1: Location of the measurement sites

These normalized values were used in the classification. The variation of the daily (between the three periods of the day considered) and seasonal frequency of the different clusters was analysed.

The next step was the cartographical representation of the normalized temperatures (for which there were only punctual data) in whole the city. The method of cartographical interpolation described in Alcoforado and Andrade (2006) was followed, based in the multiple regression between temperature and different geographical factors. The main factors were altitude (*alt*), distance to the Tagus river (*DistR*), latitude (*Lat*), an index of building density and volumetry (*Build*) and an index of green space (*Green*). Build was calculated as the product of the proportion of building area (within a square of 100 m side, centred in the measurement sites) versus the average height of the buildings; *Green* was simply the proportion of Green space in the same square as the previously described. A stepwise procedure was used to select, to each cluster, the best regression function, having the normalized temperatures as dependent variable and the referred geographical factors as in dependent variables. The spatial generalization was obtained through the use of a Geographical Information System, being the independent variables the different layers.

In the analyses of the synoptic conditions data from NCEP-Reanalysis (Kalnay et al., 1996) were used. A statistical analysis of the barometric fields over a window centred on Lisbon was performed, with classification and calculation of average patterns. A

second steep, ongoing, will be the determination of the probability of occurrence of the clusters for different barometric fields.
In the analysis of the atmospheric environmental conditions associated with each cluster, two features were considered: thermal extremes (cold and hot situations) and air quality. As *hot day*, the 5% hottest days at 3pm were selected and as warm nights, the 5% warmest at 6h. The cooler days and nights were selected as the 5% cooler situations at the same hours. The coincidence of such conditions with the different clusters was analysed and tested.
To the analysis of air quality, hourly data from ozone (O_3) and PN10 were used data from four measurement pollution stations (fig. 1), from the Portuguese Environmental Agency. The frequency of exceedence of 120 µg/m3 hourly concentrations to O_3 and 150 µg/m3 daily concentrations to PM_{10} (WHO, 2005) was analysed in each cluster.

3. Results

Seven clusters of cases were obtained using the k-means method. The maps of three of these clusters are presented in figures 2 to 4:
Cluster 1 is the more frequent (47% of cases), being more frequent by nightime (fig. 5), but in winter days too. In these situations, there is a UHI in the southern/Central part of the city (due to the urban density, but also to the topographic shelter from the wind), and the cooler areas are in the north of the city and in the Monsanto Hill (fig. 1). This cluster is mainly associated with North or Northwest wind (average barometric field shown in figure 5) and also, with a relatively high frequency, with Northeast wind. In these last situations, this cluster is very frequently associated with cool nights and days.
Cluster 2 has an average pattern similar to the former, but the spatial contrasts are stronger and the influence of urbanization more clear. This cluster has a global frequency of only 17%, but is more frequent in the summer nights (when it corresponds to 30 %). This cluster is particularly frequent when Portugal is located in the eastern border of the Atlantic anticyclone, being reached by a Norwest wind but with a low speed (average 1.7 m/s). It is too the cluster more often associated with hot nights and, with some frequency, with high concentrations of O_3.
Cluster 3 occurs only in 3% of the cases, but it is particularly frequent during the summer days (25% of the 3pm observations). The synoptic situations that corresponds to this pattern have frequently low pressure gradient and mainly eastern or north-eastern fluxes. In many situations, Lisbon is affected by sea or estuary breezes (Alcoforado et al., 2006), with a strong cooling effect in the southwester area of the city and high temperatures in the north. It is the cluster more frequently associated with hot days and also with high O_3 and PM_{10} concentrations.

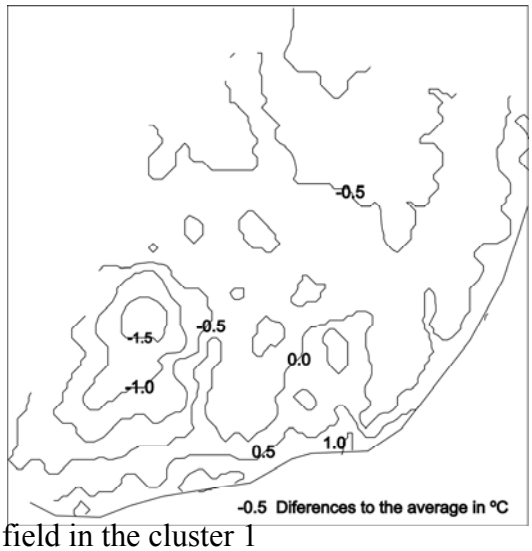

Fig: 2: Average thermal field in the cluster 1

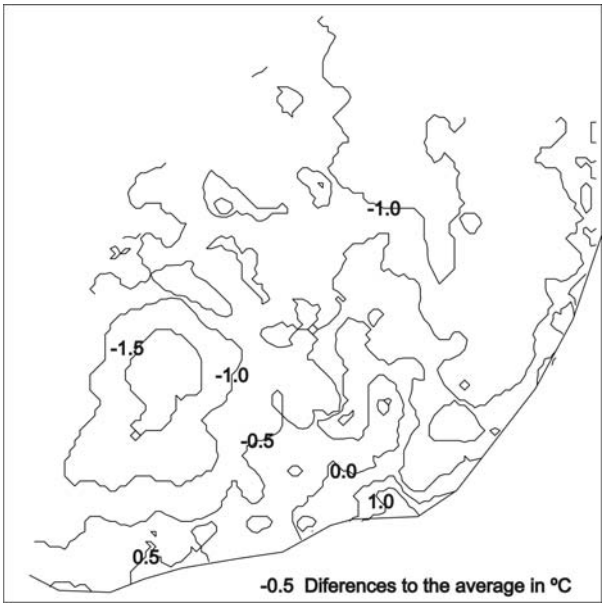

Fig: 3: Average thermal field in the cluster 2

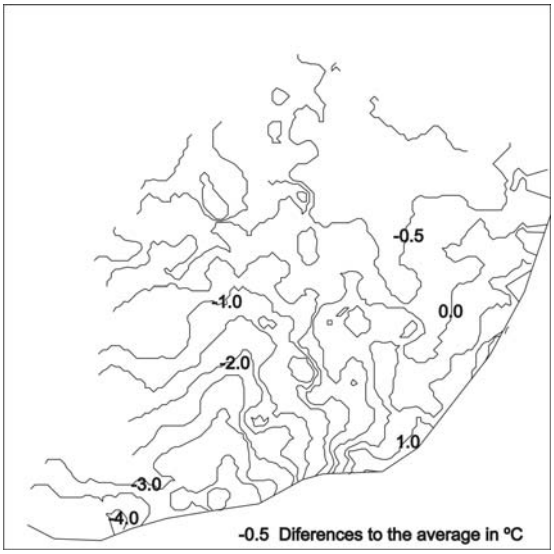

Fig: 4: Average thermal field in the cluster 3

5. Conclusion

The methodology applied allows the classification of different types of urban thermal patterns and the knowledge of its frequency, during the measurement period. The identification of the synoptic conditions associated with type allows the extrapolation of this knowledge beyond that period. It was possible to identify the thermal patterns associated with pernicious conditions and the spatial variation of these conditions in Lisbon.

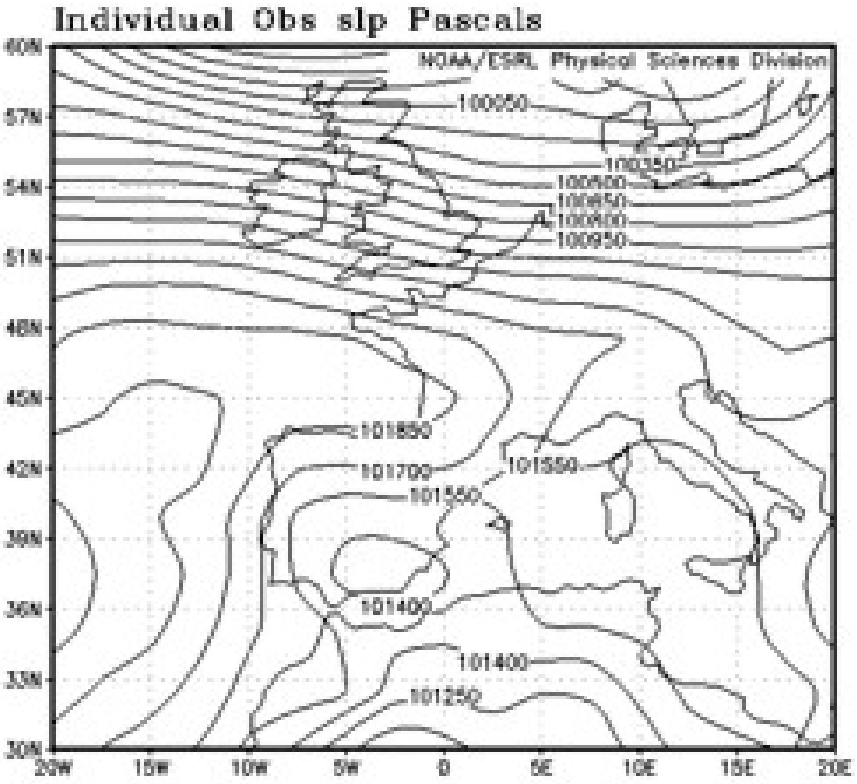

Fig: 5: Average barometric field associated with cluster 1 (NCEP-Reanalysis)

Acknowledgement

This study was developed in the framework of the project "URBKLIM: Climate and urban sustainability. Perception of comfort and climatic risks" (POCI/GEO/61148/2004), co-financed by FCT and FEDER (Operational Programme for Science and Innovation 2010). The authors would like to thank Dr Sofia Baltazar for providing the cartographical data basis for the modelling of the urban Thermal Patterns.

References

Alcoforado M. J. 1992: The climate of the Lisbon's region. Contrasts and thermal rhythms (PhD Thesis). Memórias do Centro de Estudos Geográficos. Lisboa: CEG 15 (in Portuguese with abstract in English).

Alcoforado, M. J., H Andrade, A. Lopes, J. Vasconcelos, 2009: Application of Climatic Guidelines to Urban Planning. The example of Lisbon (Portugal). Landscape and Urban Planning, Volume 90, Issues 1-2, 56-65.

Alcoforado, M. J., H. Andrade, 2006: Nocturnal urban heat island in Lisbon (Portugal): Main features and modelling attempts. Theor. Appl. Climatol. 84 (1–3), 151-159.

Alcoforado, M. J., H Andrade, A. Lopes, J. Vasconcelos, R. Vieira, 2006: Observational studies on summer winds in Lisbon (Portugal) and their influence on daytime regional and urban thermal patterns. Merhavim6, 88–112 (Special Issue: Climate Environ.).

Andrade, H., M. J. Alcoforado, 2008: Microclimatic variation of thermal comfort in a district of Lisbon (Telheiras) at night. Theor. Appl. Climatol. 225 (3–4), 225–237.

Silva, H. R., P. E. Phelan, J. S. Golden, 2010: Modeling effects of urban heat island mitigation strategies on heat-related morbidity: a case study for Phoenix, Arizona, USA. Int J Biometeorol (2010) 54, 13–22.

Tan, J., Y. Zheng, X. Tang, G. Changy, L. Liping, S. Guixiang, X, Zhen, D, Yuan, A. J. Kalkstein, F. Li, H. Chen 2010: The urban heat island and its impact on heat waves and human health in Shanghai. Int J Biometeorol (2010) 54,75–84

Kalnay et al. 1996: The NCEP/NCAR 40-year reanalysis project, Bull. Amer. Meteor. Soc., 77, 437-470.

Lopes A. 2003: Changes in Lisbon's urban climate as a consequence of urban growth. Wind, surface UHI and energy budget (in Portuguese, with abstract in English). PhD Thesis, University of Lisbon, Lisbon

WHO 2005: Air quality guidelines - global update 2005. World Health Organization, Copenhagen.

Authors' address:

Centro de Estudos Geográficos da Universidade de Lisboa, Edifício da Faculdade de Letras, Alameda da Universidade, 1600-214 Lisboa, Portugal, Tel: + 351 217940218 /

henr.andr@gmail.com mjalcoforado@campus.ul.pt pmscanario@gmail.com

CITY2020+ - assessing climate and demographic change impacts for the City of Aachen

Christoph Schneider[1], Marten F. Brunk[2], Wolfgang Dott[3], Heather Hofmeister[4], Carmella Pfaffenbach[1], Christine Roll[5], Klaus Selle[6], Kunibert Wachten[7], Mareike Buttstädt[1], Katja Eßer[5], Julia Hahmann[4], Lotta Hülsmeier[3], Gunnar Ketzler[1], Marion Klemme[6], Antje Kröpelin[2], Hendrik Merbitz[1], Sabrina Michael[3], Timo Sachsen[1], Agata Siuda[1]

RWTH Aachen University, Germany:
[1]Department of Geography, Faculty of Material Sciences and Geosciences
[2]Construction Business and Building Services, Faculty of Civil Engineering
[3]Institute of Hygiene and Environmental Medicine, Faculty of Medicine
[4]Institute for Sociology, Philosophical Faculty
[5]Department of History, Philosophical Faculty
[6]Faculty of Architecture
[7]Urban Design and Regional Planning, Faculty of Architecture

Abstract

The research initiative *CITY 2020+* assesses the risks and opportunities for residents in urban built environments under projected demographic and climate change for the year 2020 and beyond, using the City of Aachen as a case study. Organized into 3 clusters, *CITY 2020+* develops scenarios, options and tools for planning and developing sustainable future city structures. We investigate how urban environment, political structure and residential behavior can best be adapted, with attention to the interactions among structural, political, and sociological configurations and with their consequences on human health.

1. Introduction

Europe has an aging infrastructure and an aging population. Demographers project that in the EU-25-States by 2050, approximately 30% of the population will be over age 65. An aging workforce and population combined with higher energy prices, environmental concern, and technological changes are likely to transform living and working arrangements. Also by 2050, average temperatures are projected to rise by 1 to 2 K, and summers in Central Europe may exhibit prolonged dry periods (IPCC 2007). Combined, Europe can expect enhanced thermal stress and higher levels of particulate matter. Within *CITY 2020+* (see Fig. 1) there are among other sub-projects three climatological projects dealing with

(1) a micro-scale assessment of vegetation impacts to low-level cold-air drainage flow into the city centre,
(2) a detailed analysis of the change of probability density functions related to the occurrence of heat waves during summer,
(3) a meso-scale analysis of particulate matter concentrations depending on topography, local meteorological conditions and synoptic-scale weather patterns.

First results from measurement campaigns and surveys regarding environment and governance are presented.

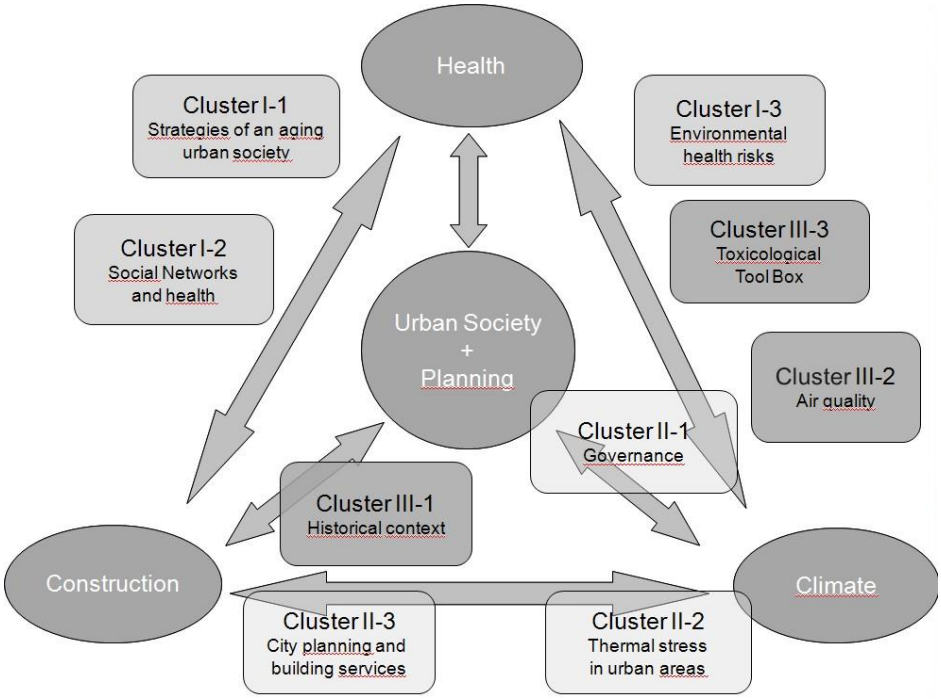

Fig. 1: Structure of the research project City2020+

2. Optimizing suburban vegetation structures for enhanced cold air drainage flow, maximum air quality and bioclimatic effects

The topography of Aachen in a basin causes air quality problems as the exchange of air in the city centre is limited. Cold air drainage flows are able to reduce this problem, as they bring fresh and cool air into the city centre. Due to increasing temperatures related to global warming these cold air drainage flows become even more important in the future, since cities are more suffering from thermal stress than rural areas (e.g. Matzarakis et al. 2009). In order to investigate the impact of vegetation on the cold air drainage flow four measurement units (small and medium-sized weather stations) were set up in two different valleys in the south fringe of Aachen. Most of them are placed in vegetation stands to allow measurements of the cold air flow within the vegetation stands (Fig. 2). Additionally, data is collected by cross valley profiles and balloon measurements (Fig 3). The cold air flow reaches up to 27 m above ground. Since the valley is about 200 m wide and wind speeds are typically around 1 ms^{-1} this inflow to the city is of major importance regarding air quality of the city centre of Aachen.

Fig. 2: Suburban valley with the same weather station in March (left) and July 2009

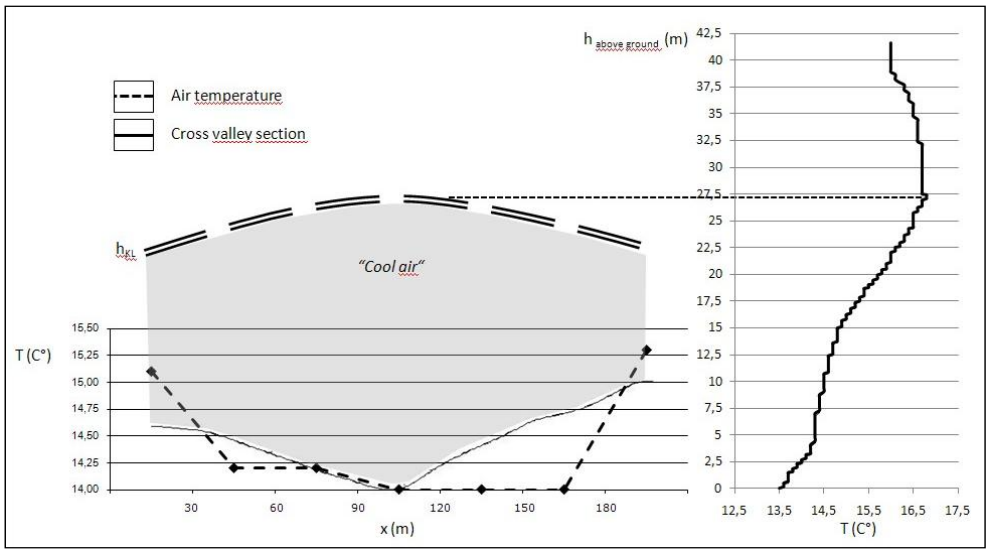

Fig. 3: Cross valley profile (left, 13.06.2009, 21:15 – 21:35pm) and balloon measurement (right, 13.06.2009, 21:26 – 22:04pm) showing cold air quantities at location "Kannegießertal"

3. Climate change and probability of summer heat waves in urban areas

Ongoing global warming, which is detected since the end of the 19th century by observational data is going to continue as suggested by the outputs of global and regional climate models (IPCC 2007). Besides increasing mean temperatures the climate change implicates an alteration in the probability of occurrence of extreme events (e.g. Beniston et al. 2007, Wigley 2009). Various studies show that climate change causes longer lasting and intensified periods of hot summer days resulting in an enhanced probability of heat stress situations (Meehl & Tebaldi 2004; Schär et al. 2004; Della-Marta et al. 2007) and associated public health risks (Kirch 2005, Gosling et al. 2009). In order to address this issue, weather station data from Aachen (German weather service, DWD) and the output from the regional climate model STAR2 (Orlowsky et al. 2008), based on IPCC SRES scenario. Fig. 4 illustrates daily summer and winter maximum temperatures for the City of Aachen showing a shift in the probability density functions (PDF) to warmer conditions. Heat wave situations in summer are likely to occur in future more often supporting findings from earlier studies mentioned above.

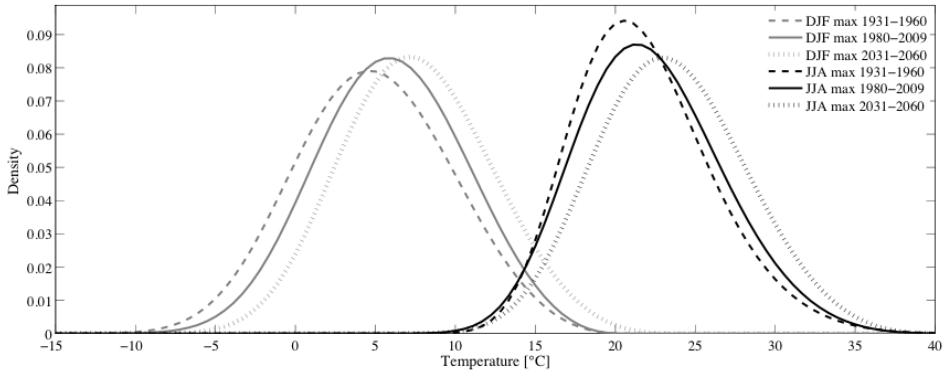

Fig. 4: Probability density functions for different 30-year periods for daily summer and winter maximum temperatures

4. Weather dependent concentrations of air pollutants in the City of Aachen

Particulate matter and gaseous pollutants are common important environmental cofactors for many different cardiovascular and respiratory diseases (Valavanidis et al. 2008). The spatio-temporal distribution of PM10 and PM2.5 levels in the City of Aachen are investigated by small scale measurements and geo-statistical analyzes. The influences of geographic factors and synoptic scale weather types are considered. Aachen is situated in a basin which negatively affects the exchange conditions (Havlik & Ketzler 2000). Measurements of particulate matter (PM10, PM2.5) in an inner city area of 2.5 x 2.5 km² are combined with meteorological investigations and analyzes of gaseous pollutants. For the investigation of both particulate and gaseous species, two locations are selected from the PM-measurement grid (figure 5) which covers 40 measurement points. The first site is located in an average urban environment with minor local emission-sources while the second location lies within a heavily polluted street canyon. In addition to the spatial comparison of the urban and the traffic site, the temporal variability of particulate and gaseous pollutants dependent on meteorological influences is examined. Two weather types with different impacts on air quality are analyzed. The impact of weather types and meteorology on PM10 concentrations in the area of Aachen has been investigated by Merbitz (2009), identifying the wind speed as primary factor governing PM concentrations in the inner urban area, especially during winter. Additionally, precipitation impacts PM10 levels considerably. Wind speed being related to atmospheric exchange conditions and precipitation are negatively correlated determinants for the daily PM10 levels in urban areas (e.g. Klinger & Sähn 2008; Holst et al. 2008), affecting local air quality especially at near-traffic locations. Beside the meteorological analyzes the investigation includes a chemical characterization of sampled gaseous pollutants. The air-sampling system consists of specific sorbent tubes (Tenax TA and Carbosieve™) for the detection of different volatile compounds. The identification of the composition is carried out via gas chromatography.

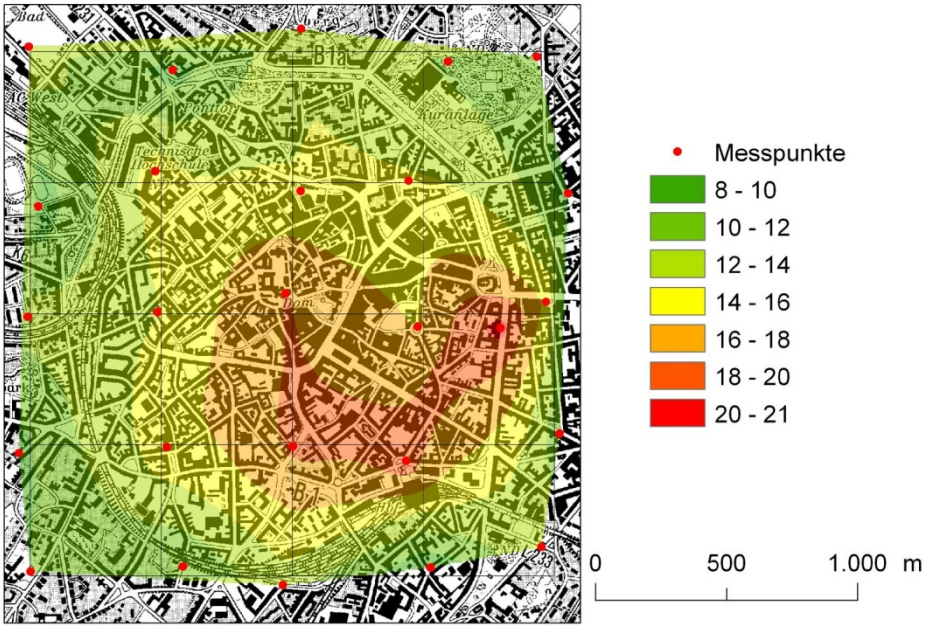

Fig. 4: Selected air quality measurement locations in Aachen and mean interpolated level of PM10 concentrations in µg/m³ in autumn 2009

5. Implication of demographic and climate change for governance best practice

City2020+ also addresses the local conditions under which changes are implemented. How do urban actors notice climate and demographic changes? How do they estimate problems and risks? Which courses of action do they know and under what circumstances are they willing to implement them? We try to answer these questions with a "governance perspective" (Mayntz 1997, Schimank 2007, Selle 2008) considering urban development policy in Aachen. Among other activities a workshop was carried out in December 2009 where local actors were asked to discuss climate and demographic change as subject of local governance processes. The two days workshop was attended by 45 participants, from the fields of research and practice. It become evident that there are already many different players who by now have started outreaching initiatives to cope with the effects and consequences of demographic and climate changes. However, these stakeholders need to join forces especially because local government cannot allocate sufficient financial resources for new measures and activities. Communication and cooperation between local protagonists are key issues in order to address climate mitigation and adaption as an integrated part of urban development strategies. Further research will address the deficiencies and hindrances of measures aiming at climate mitigation and climate adaptation.

6. Conclusions

The first results from measurement campaigns and surveys show the importance of cold air flow for air quality, likely increased occurrence of heat waves in the future, high spatial and temporal variability of PM concentrations and growing awareness amongst stakeholders towards climate and demographic changes in cities. At a later stage *City2020+* will propose new strategies based on cooperation from the fields of medicine, geography, sociology, history, civil engineering, and architecture for adapting the city for future needs.

Acknowledgement

The Project *CITY 2020+* is part of the interdisciplinary Project House HumTec (Human Sciences and Technology) at RWTH Aachen University funded by the Excellence Initiative of the German federal and state governments through the Deutsche Forschungsgemeinschaft (German Research Foundation, DFG).

References

Beniston, M., D. Stephenson, O. Christensen, C. Ferro, C. Frei, S. Goyette, K. Halsnaes, T. Holt, K. Jylhä, B. Koffi, J. Palutikof, R. Schöll, T. Semmler & K. Woth, 2007: Future extreme events in European climate: an exploration of regional climate model projections. Climatic Change, 81(0), 71-95.

Della-Marta, P. M., M. R. Haylock, J. Luterbacher & H. Wanner, 2007: Doubled length of western European summer heat waves since 1880. Journal of Geophysical Research, 112.

Gosling, S. N., J. A. Lowe, G. R. McGregor, M. Pelling & B. D. Malamud, 2009: Associations between elevated atmospheric temperature and human mortality: a critical review of the literature. Climatic Change, 92, 299-341.

Havlik, D. & G. Ketzler, 2000: Gesamtstädtisches Klimagutachten Aachen (Urban Climate Survey Aachen).
Holst, J., H. Mayer & T. Holst, 2008: Effect of meteorological exchange conditions on PM10 concentration. Meteorologische Zeitschrift, Vol. 17, No. 3, 273-282.
IPCC, 2007: Climate change 2007: The physical science basis. Contribution of working group I to the 4th assessment report of the intergovernmental panel on climate change. Cambridge, New York, Cambridge University Press.
Kirch, W., 2005: Extreme weather events and public health responses.
Klinger, M. & E. Sähn, 2008: Prediction of PM10 concentration on the basis of high resolution weather forecasting. Meteorologische Zeitschrift, Vol. 17, No. 3, 263-272.
Mayntz, R. 1997: Soziale Dynamik und politische Steuerung: theoretische und methodologische Überlegungen. Frankfurt a.M./New York [Campus]
Matzarakis, A., M. de Rocco & G. Najjar, 2009: Thermal bioclimate in Strasbourg – The 2003 heat wave. Theor Appl Climatol 98:209–220.
Meehl, G. & C. Tebaldi, 2004: More intense, more frequent, and longer lasting heat waves in the 21st century. Nature, 305, 994-997.
Merbitz, H., 2009: Feinstaubkonzentration in Abhängigkeit von Witterung und Großwetterlagen im Raum Aachen (Influence of weather types on Particulate Matter in the area of Aachen). Aachener Geographische Arbeiten 46.
Orlowsky, B., F.-W. Gerstengarbe & P. C. Werner, 2008: A resampling scheme for regional climate simulations and its performance compared to a dynamical RCM. Theoretical and Applied Meteorology, 92, 209-223.
Schär, C., P. L. Vidale, D. Lu□thi, C. Frei, C. Häberli, M. A. Liniger & C. Appenzeller, 2004: The role of increasing temperature variability in European summer heatwaves. Nature, 427, 332-336.
Schimank, U., 2007: Elementare Mechanismen. In: Arthur Benz u.a. (Hg.) Handbuch Governance. Theoretische Grundlagen und empirische Anwendungsfelder. Wiesbaden [VS] S. 29-45.
Selle, K., 2008: Stadtentwicklung aus der »Governance-Perspektive« Eine veränderte Sicht auf den Beitrag öffentlicher Akteure zur räumlichen Entwicklung - früher und heute. In: Altrock, Uwe u.a. (Hg.) Wer entwickelt Stadt? Kassel.
Wigley, T. M. L., 2009: The effect of changing climate on the frequency of absolute extreme events. Climatic Change, 97, 67-76.
Valavanidis A., Fiotakis K., Viachogianni T., 2008: Airborne Particulate Matter and Human Health: Toxicological Assessment and Importance of Size and Composition of Particles for Oxidative Damage and Crcinogenic Mechanisms. Journal of Environmental Science and Health Part C, 26:339-362

Authors' address:

Prof. Dr. Christoph Schneider (christoph.schneider@geo.rwth-aachen.de)
Department of Geography, RWTH Aachen University
Wüllnerstr. 5b, D-52056 Aachen, Germany

All authors may be addressed by their names, university units (see first page) and the post box of RWTH Aachen University: D-52056 Aachen, Germany

Effect of pavements albedo on long-term outdoor thermal comfort

Tzu-Ping Lin[1], Andreas Matzarakis[2], Ruey-Lung Hwang[3], Ying-Che Huang[1]

[1] Department of Leisure Planning, National Formosa University, Taiwan
[2] Meteorological Institute, Albert-Ludwigs-University of Freiburg, Germany
[3] Department of Architecture, National United University, Taiwan

Abstract

The outdoor thermal environment is impacted by the built environment, e.g. anthropogenic heat, evaporation and evapotranspiration of plants, shading by trees and man-made objects, and ground surface covering, such as natural grass and artificial pavement. Due to the albedo of pavements affect the quantity of global radiation reflected to the sky, the pavement with low albedo value is one of the main factor causes the high air temperature and thermal uncomfortable for human beings. Therefore, this research focus on 4 different pavements, i.e. grass, interlocking blocks, concrete and asphalt, located in university campus, measuring the albedo value and other thermal physical parameters. The net radiation is measured by CNR1 with up and down side short- and long-wave radiation. The field experiments are conducted in different season and the albedo value of each pavement are calculated. Meanwhile, the long-term thermal comfort is calculated in the RayMan model which has been calibrated with the local climate. The analytical result indicated that the low albedo pavement (i.e. asphalt) contribute longer period for hot hours (PET > 42 °C) than the high albedo ones (i.e. grass). The result could be applicable in the design of outdoor environment for the mitigation of urban heat island and improvement of human's thermal comfort.

1. Introduction

Outdoor thermal environment factors, such as air temperature, air humidity, wind speed, and solar radiation, affect evaluations of thermal comfort, e.g. thermal perception, preference and satisfaction. Studies conducted in temperate regions showed that many people visit outdoor urban spaces when the thermal conditions is high in both winter and summer (Nikolopoulou et al. 2001; Thorsson et al. 2004; Thorsson et al. 2007). However, research conducted in hot and humid regions indicated that few people visit squares or other public spaces when the thermal index is high (Lin 2009). The largest numbers of people visit squares when the thermal condition is close to their thermal comfort range. Therefore, outdoor thermal environments affect evaluations of thermal comfort and usage of outdoor spaces; the degree of impact varies with the thermal requirements of people in different climatic regions.

In general, outdoor thermal environment is impacted by the built environment, e.g. anthropogenic heat, evaporation and evapotranspiration of plants, shading by trees and man-made objects (Lin et al. 2010), and ground surface covering, such as natural grass and artificial pavement. Due to the albedo of pavements affect the quantity of solar radiation reflected to the sky, the pavement with low albedo value is one of the main factor cause the high air temperature and thermal uncomfortable for human beings.

Previous studies have generally performed field experiments on only a few days to investigate how pavement affect thermal environment. However, such experimental results merely elucidate the characteristic measured (or simulated) on a particular day and may not represent annual thermal conditions. On the other hand, tolerance of outdoor

thermal environments also varies for people in different climates, and they have different thermal perception given by the same thermal environment (Nikolopoulou and Lykoudis 2006; Lin and Matzarakis 2008). Therefore, one must discuss long-term thermal comfort based on the thermal requirements and characteristics of local residents.
The aim of the research is to realize the albedo value of some popular ground surface by field experiment. The long term thermal comfort is then calculated and the threshold of each thermal perception in Taiwan is then applied to understand the effect of pavement on long-term thermal comfort of for local people.

2. Method

2.1 Field measurement

This research focus on 4 different pavements, i.e. grass, bricks (red), concrete (gray) and asphalt (black), located in at the National Formosa University (NFU) campus in Taiwan. The physical microclimate parameters, i.e. air temperature, relative humidity, globe temperature, wind velocity/direction, direct/reflect short- and long-wave solar radiation. All the parameters are collected in a one-minute interval from 8:00 to 17:00 through the conducted day. The albedo value is calculated by the proportion of reflected short-wave solar radiation over long-wave radiation.

Fig. 1: The instrumentation of the filed experiments

2.2 Assessment of Outdoor Thermal Comfort

Several indices integrating thermal environmental factors and heat balance of the human body are applied for accessing thermal comfort. As PET is already included in the VDI

(German Association of Engineers) guideline 3787 (VDI 1998) for human biometeorological evaluation of climates in urban and regional planning, and has been employed in several studies of outdoor thermal comfort (Andrade and Alcoforado 2007; Oliveira and Andrade 2007; Thorsson et al. 2007). PET was adopted as the primary thermal index in this study. PET is estimated using the RayMan model, which has been used in urban built-up area with complex shading patterns and generated accurate predictions of thermal environments (Matzarakis et al. 1999; Gulyas et al. 2006; Lin et al. 2006; Matzarakis et al. 2007)

2.3 Thermal sensation classifications for locals

To account the subjective thermal perceptions under different PETs, one must define the PET ranges in which local people feel comfortable, i.e., the "thermal comfort range" for the PET. To estimate the thermal comfort range of Taiwan's residents, this study uses the data from an outdoor field study that conducted 1644 interviews in Taiwan (Hwang and Lin 2007; Lin and Matzarakis 2008). Table 1 is the thermal sensation classifications for Taiwan, combined with classifications for people living in Western/middle European climates (Matzarakis and Mayer 1996)

Table 1: Thermal sensation and PET classes for Taiwan and Western/Middle European classes. (Source: Lin and Matzarakis, 2008 Matzarakis and Mayer, 1996)

Thermal sensation	PET range for Taiwan **(°C PET)**	PET range for Western/middle European **(°C PET)**
very cold		
	14	**4**
Cold		
	18	**8**
Cool		
	22	**13**
Slightly cool		
	26	**18**
Neutral		
	30	**23**
Slightly warm		
	34	**29**
Warm		
	38	**35**
Hot		
	42	**41**
Very hot		

2.4 Long-term thermal comfort evaluations for different pavements

After validation of the RayMan model, long-term meteorological data from weather stations are imported into the model with each albedo settings for predicting long-term variations in thermal environmental conditions and thermal indices. The meteorological data applied in this study were from the nearest weather station, which is located in Chiayi. Hourly data for the 10-year period of 1998–2007 were selected. The parameters imported into the RayMan model were the air temperature, air humidity, wind speed and mean cloud cover. The albedo value for each pavement is obtained by the field experiment.

3. Results and discussion

3.1 Mean albedo value of each pavement

Fig. 2 is the mean albedo value of 3-5 field experiments for each pavement. The grass (albedo=0.177) have the highest value among the four pavement while the asphalt (albedo=0.087) have the smallest.

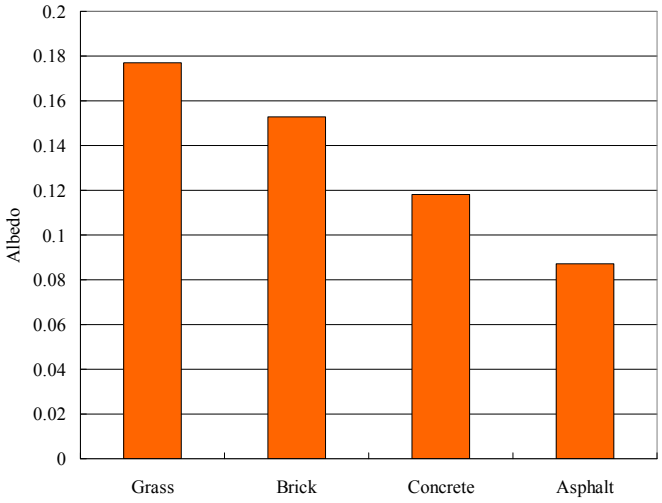

Fig. 2: Mean albedo value of each pavement

3.2 Frequencies and of long-term thermal comfort

Figures 3 show modelled PET frequency distribution graphs for each pavement in the noon (10:00–14:00) during 1998–2007 at 10-day intervals. Owing to that the frequency maps are almost the same while 24 hour data of each day is presented among the pavements; only the noon time data, i.e. 10:00–14:00 are displayed in this figure. As shown in fig 3, however, the results still almost the same for each pavement. Slightly differences occur in the frequencies of PET > 42 °C (very hot) among each pavement. Asphalt have the highest frequencies of PET > 42 °C while grass have the relative low frequencies.

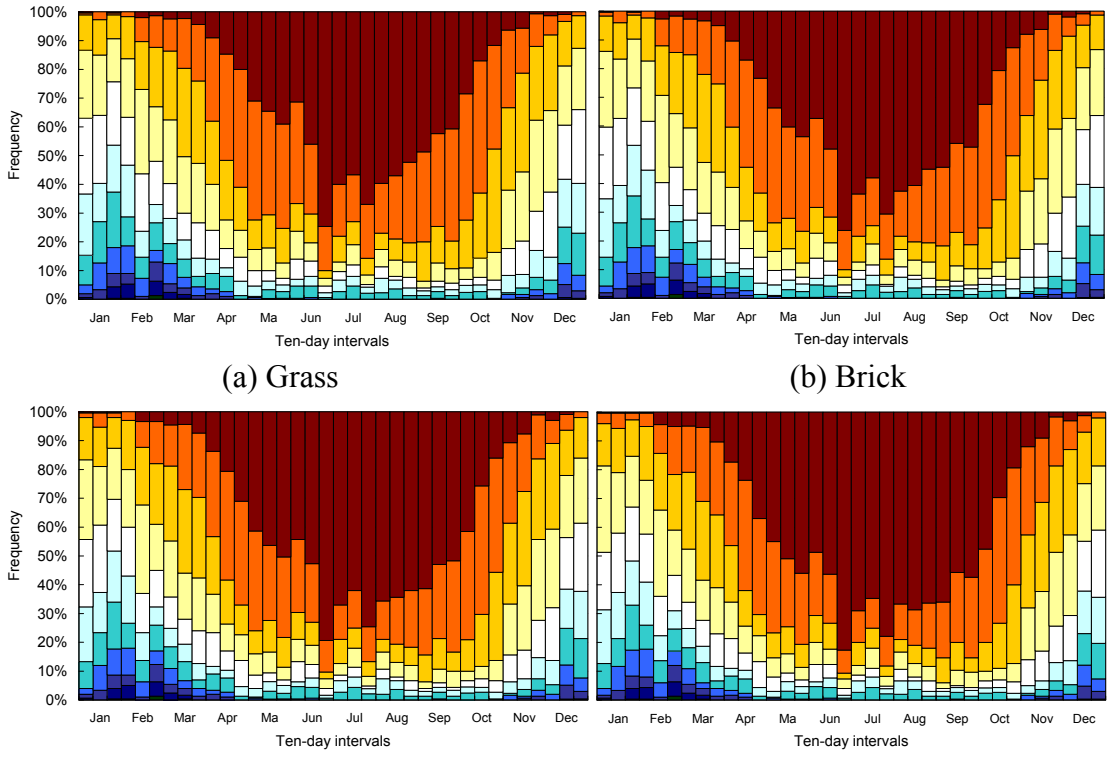

(a) Grass (b) Brick

(c) Concrete (d) Asphalt

Fig. 3: Estimation of annual PET frequencies at 10:00-14:00 during 1998-2007

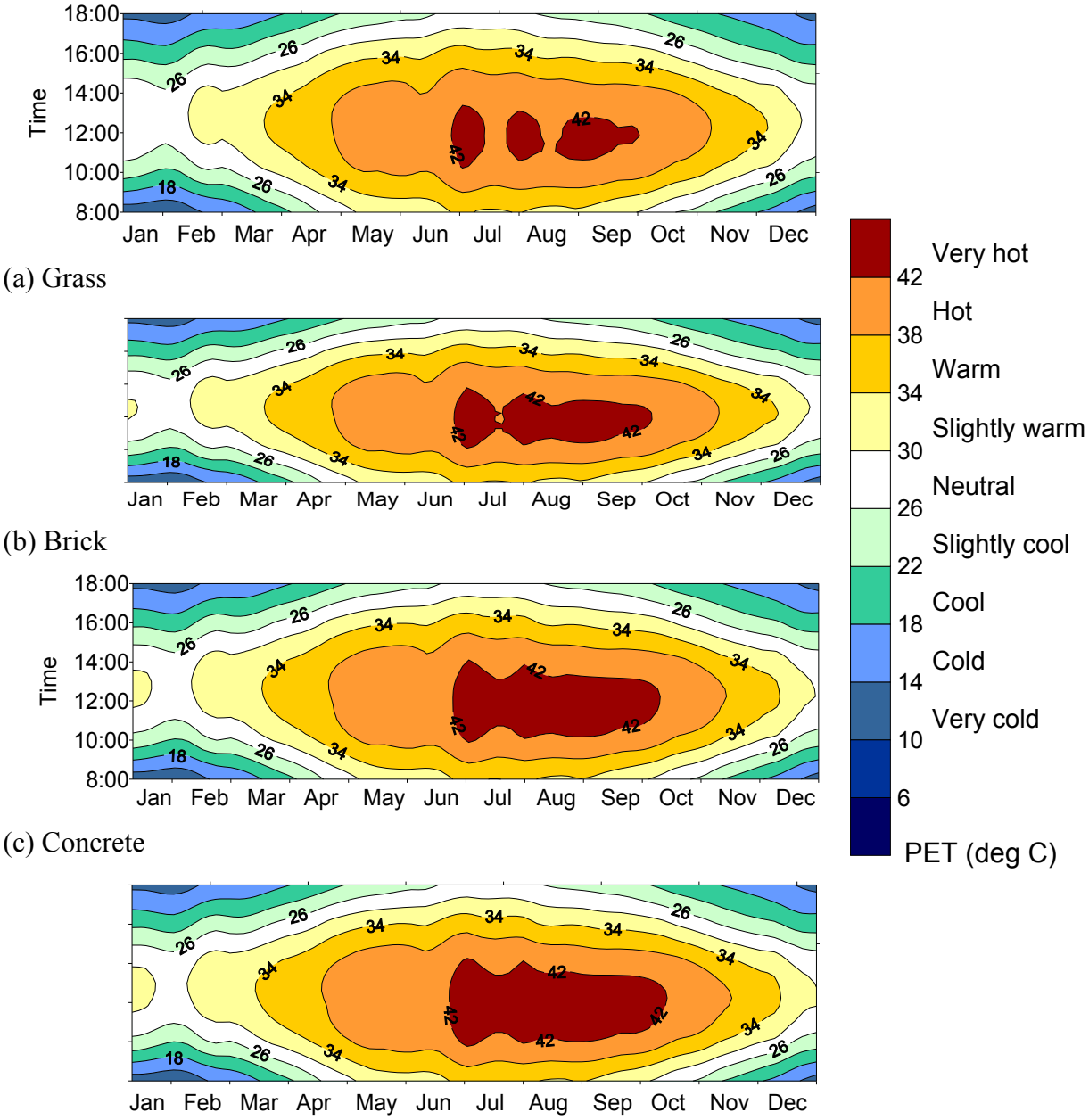

(a) Grass

(b) Brick

(c) Concrete

(d) Asphalt

Fig. 4: Estimation of annual PET contour maps at 8:00 - 18:00 during 1998-2007

3.3 Annual distribution long-term thermal comfort

From figure 4, it is more obvious to find the differences among each pavement. The area of PET>42 are largest for asphalt while the grass got the smallest PET>42 area. The comparative results indicate that the albedo value indeed affect the long-term thermal comfort, especially for the high temperature conditions.

4. Conclusions

This study conducted field experiment on four types of pavements to obtain the albedo value through the measurement. Although the estimated long-term frequencies of PET are similar for each pavements, the significant differences exist among the occurrence

of PET>42, i.e. very hot condition for Taiwanese people. The results indicate that high albedo pavement (or ground covering), i.e. grass, and will help to mitigate the hot condition. The results are also helpful for the outdoor environment design for the increased problem of urban heat island and global warming.

Acknowledgement

The authors would like to thank the National Science Council (NSC) of Taiwan and German Academic Exchange Service (DAAD) for financially supporting this research under the Project-Based Personnel Exchange Programme between the NSC and DAAD. Thanks to Shih-Pin Chou and Ruei-Lung Chiou for data collection.

References:

Andrade, H., M.-J. Alcoforado, 2007: Microclimatic variation of thermal comfort in a district of Lisbon (Telheiras) at night. Theor. Appl. Climatol. 92, 225-237

Gulyas, A., J. Unger, A. Matzarakis, 2006: Assessment of the microclimatic and human comfort conditions in a complex urban environment: Modelling and measurements. Build. Environ. 41, 1713-1722

Hwang, R.L., T.P. Lin, 2007: Thermal comfort requirements for occupants of semi-outdoor and outdoor environments in hot-humid regions. Architectural Science Review 50, 60-67

Lin, T.P., 2009: Thermal perception, adaptation and attendance in a public square in hot and humid regions. Build. Environ. 44, 2017-2026

Lin, T.P., A. Matzarakis, 2008: Tourism climate and thermal comfort in Sun Moon Lake, Taiwan. Int. J. Biometeorol. 52, 281-290

Lin, T.P., A. Matzarakis, J.J. Huang, 2006: Thermal comfort and passive design of bus shelters. Proc. 23rd Conference on Passive and Low Energy Architecture (PLEA2006),

Lin, T.P., A. Matzarakis, R.L. Hwang, 2010: Shading effect on long-term outdoor thermal comfort. Build. Environ. 45, 213-221

Matzarakis, A., H. Mayer 1996: Another kind of environmental stress: thermal stress. WHO Collaborating Centre for Air Quality Management and Air Pollution Control,

Matzarakis, A., F. Rutz, H. Mayer 1999: Estimation and calculation of the mean radiant temperature within urban structures., In: de Dear RJ, Kalma JD, Oke TR, Auliciems A (eds) Biometeorology and Urban Climatology at the Turn of the Millenium. Selected Papers from the ICB-ICUC'99 conference, Sydney, WCASP-50, WMO/TD No. 1026. World Meteorological Organization, Geneva, pp 273-278

Matzarakis, A., F. Rutz, H. Mayer, 2007: Modelling radiation fluxes in simple and complex environments - Application of the RayMan model. Int. J. Biometeorol. 51, 323-334

Nikolopoulou, M., N. Baker, K. Steemers, 2001: Thermal comfort in outdoor urban spaces: understanding the human parameter. Sol. Energy. 70, 227-235

Nikolopoulou, M., S. Lykoudis, 2006: Thermal comfort in outdoor urban spaces: Analysis across different European countries. Build. Environ. 41, 1455-1470

Oliveira, S., H. Andrade, 2007: An initial assessment of the bioclimatic comfort in an outdoor public space in Lisbon. Int. J. Biometeorol. 52, 69-84

Thorsson, S., T. Honjo, F. Lindberg, I. Eliasson, E.M. Lim, 2007: Thermal comfort and outdoor activity in Japanese urban public places. Environment and Behavior 39, 660-684

Thorsson, S., M. Lindqvist, S. Lindqvist, 2004: Thermal bioclimatic conditions and patterns of behaviour in an urban park in Goteborg, Sweden. Int. J. Biometeorol. 48, 149-156

VDI, 1998: Methods for the human biometeorological evaluation of climate and air quality for the urban and regional planning. Part I: Climate. VDI guideline 3787. Part 2. Beuth, Berlin

Authors' address:
Asso. Prof. Tzu-Ping Lin(tplin@nfu.edu.tw)
and Ying-Che Huang (kevin110014@yahoo.com.tw)
Department of Leisure Planning, National Formosa University
64 Wen-hua Rd, Huwei, Yunlin 632, Taiwan

Prof. Dr. Andreas Matzarakis (andreas.matzarakis@meteo.uni-freiburg.de)
Meteorological Institute, Albert-Ludwigs-University of Freiburg
Werthmannstr. 10, D-79085 Freiburg, Germany

Asso. Prof. Ruey-Lung Hwang (rueylung@nuu.edu.tw)
Department of Architecture, National United University
1 Lienda, Miaoli 360, Taiwan

Area usage and thermal sensation vs. thermal comfort conditions – Open air thermal comfort project in Szeged, Hungary

Noémi Kántor, Ágnes Gulyás

Department of Climatology and Landscape Ecology, University of Szeged, Hungary

Abstract

The aim of this study is to throw some light on the outdoor human thermal comfort investigations in Szeged. Methodology is described, which consists of micrometeorological measurements on the site, observation of visitors' area usage together with their characteristics, as well as questionnaire-based interviews on the subjective thermal sensation, human comfort and open air activity. As important part of the measurements, visitors' exact locations are marked on a map of the investigated resting place. Integrating these spatial data with the measured subjective and objective information within geoinformatical software (ArcView GIS in our case), make it possible to visualize the area usage according to many categorization, and to reveal relationships between the thermal environment, the usage of the area and the visitors' behavioural adaptation.

1. Introduction

Because of the current state of urbanization more and more people have to live or work in cities, which mean increasing number of citizens, affected by the strains of urban environments – thermal stress among others. This is the reason for many urban climate studies aim to analyze the thermal conditions in different urban structures. Large scale thermal comfort projects such as RUROS (e.g. Nikolopoulou and Lykoudis, 2006), Urban Climate Spaces (e.g. Knez and Thorsson, 2006) and KLIMES (e.g. Mayer et al., 2008) have multi- and interdisciplinary field of interest, and bring together human biometeorology (which is a complex scientific discipline itself), urban planning and psychology under a common roof.

There were no projects focusing on the thermal component of urban climate in a physiologically significant manner in Hungary until the 2000's. The first examination had performed in the city of Szeged (46° N, 20° E) (Gulyás et al., 2006). Similarly, the first investigation which used also human monitoring (questionnaire-based data collection) by the objective measurements and comfort-index calculations was also in this South-Hungarian city (Kántor et al., 2006). The aim of this study is to describe the diverse methodology applied in the proceeding long-term outdoor thermal comfort project in Szeged in the last 2 years and discuss the possible outcome of the results.

2. Study areas and measurement periods

Parks and squares may mitigate the harmful effects of cities by offering places for recreation and relaxation, functioning as "green islands" in the heavily build-up areas. Accordingly, two inner city squares were selected to study the area usage, the outdoor staying and thermal sensation of people in accordance with thermal comfort conditions. Due to the lack of mobile biometeorological station until summer 2009, sampling areas adjacent to the automatic meteorological station of the University of Szeged were selected. Szeged is a famous educational centre in Hungary attracting many students on the weekdays.

The first investigation site is a ca 5500 m^2 green area in the Ady Square and locates between the buildings of the University and the Information Centre. It is regularly visited by a high number of students throughout the academic year, which makes it suitable for thermal comfort studies using also human monitoring. The ca 6000 m^2 Honvéd Square lies also near to the automatic station and functions not only as resting place, but as playground too. It is visited by more age-groups than the other square where the younger subjects (in their twenties) dominate. Shading conditions are remarkably different between the two areas. In the first site visitors can chose from sunny, penumbra or shady exposures thanks to shading of buildings and/or various kinds of trees. Contrarily, the second square allows to take place mainly at the same penumbra conditions.

Three study periods were conducted till now: in late spring (April and May) 2008 and 2009, as well as in early autumn (September and October) 2009 (Table 1 shows details). Field surveys were carried out on every Tuesday, Wednesday and Thursday from 12 to 3 p.m. (CET, summer time), as early afternoon is the warmest period of day.

Table 1: Outdoor thermal comfort investigation periods in Szeged according to study area and methodology

STUDY AREA	**HUMAN MONITORING**		
	OBSERVATIONS		QUESTIONNAIRES
	Momentary attendance	Cumulative attendance	
Ady Square	spring 2008, 2009, autumn 2009 13 + 14 + 15 days	spring 2008, 2009, autumn 2009 14 + 14 + 14 days	autumn 2009 9 days
Honvéd Square	spring 2009, autumn 2009 15 + 15 days	spring 2009, autumn 2009 15 + 15 days	autumn 2009 5 days
	STATIONARY STATION		MOBILE STATION
	MEASUREMENT OF METEOROLOGICAL VARIABLES		

3. Observations and stationary measurements

Thermal comfort investigations which concentrate on urban public areas need specified and detailed information about the investigated area and about the visitors. Human monitoring with simultaneous measurement of meteorological variables (to calculate thermal comfort indices) can provide these data.

At the time of the first two investigation periods (spring 2008 and 2009) biometeorological station was no available for recording the thermal comfort variables in the height of 1.1 m a.g.l. reference height. Therefore questionnaires were dispensed and observations were carried out only in squares adjacent to the automatic stationary station (Table 1). Temperature and humidity sensors locating at 2 m a.g.l. while wind velocity and global radiation sensors locating at the top of the university building (Table 2). Wind speed data were reduced at the reference height of 1.1 m. The comfort indices PMV (Predicted Mean Vote) and PET (Physiologically Equivalent Temperature) are calculated with the RayMan model (Matzarakis et al., 2007), and refer to a person (default: 1.75 m, 75 kg, 35 years old standing male) who stays in the sun (because there was no radiation reduction). Comparing the observations data with these indices we are able to study the weather-related area usage and behavioral adaptation of visitors.

Table 3: Instrumentation of the stationary and mobile stations

PARAMETER	STATIONARY STATION	MOBILE STATION	
air temperature	HMP 35D, Vaisala, 2 m a.g.l.	THERMOCAP	as part of WXT 520, Vaisala, 1.2 m a.g.l.
relative humidity	HMP 35D, Vaisala, 2 m a.g.l.	HUMICAP	
wind speed	WAA 15A, Vaisala, 26 m a.g.l.	WINDCAP	
short-wave radiation	CM 11, Kipp & Zonen, 20 m a.g.l.	CM 3	as part of CNR 1, Kipp & Zonen, 1.1 m a.g.l.
long-wave radiation		CG 3	
data recording	MILOS 500, Vaisala	pendrive	
averaging period	10 min	1 min	

Observations consisted of counting people lingering on the squares in every 10 minutes (momentary attendance) on the one hand and measuring the visitors cumulatively in given time intervals on the other hand (Tables 1 and 3). In the Ady Square – beyond the total number of subjects – we noted also how many people stayed in the sun, penumbra and shade. In the case of the other site the momentary counting was made according to whether the subject was rather passive (stand, sit, lie) or active (play, walk around).

The cumulatively measurements occurred between 12 and 3 p.m. in six half hour and twelve 15-minute intervals in the Ady and Honvéd Square respectively. The locations of the visitors staying at least 5 minutes in a given time-period were marked with ID numbers on the map of the area. Each interval on each measurement day has its own map and a connected table containing some characteristics of the marked visitors (see detailed in Table 3). The cloud cover was also noticed (clear / cloudy / overcast), as determination of the subjects' exposure was possible only when it was shiny. It is important to note, that the above presented observation method can cope only with "resting place conditions" and mainly sedentary visitors, as marking the spatial position of too many active subjects can not accomplish. Therefore, we ignored the lots of children on the playground on the Honvéd square and measured only the visitors sitting on benches.

Interval-observations data (tables of personal characteristics and investigation maps) were digitized within geoinformatical software ArcView GIS. Then the 15-minute or half hour averages of the thermal comfort measures derived from the stationary station were attached to these subjective data according to the time of the measurement.

Table 3: Recorded parameters in the course of observations

	ADY SQUARE	HONVÉD SQUARE
Momentary attendance	*in every 10 minutes* according to exposure (sun / penumbra / shade)	*in every 10 minutes* according to activity (active / passive)
Cumulative attendance + Table of characteristics	*in half hour intervals* location (marked on a map with ID number) gender (male / female) age (child / young / middle aged / old) clothing (<0.5 clo / 0.5-1 clo / 1 clo<) activity (active / passive) exposure (sun / penumbra / shade)	*in 15-minute intervals* location (marked on a map with ID number) gender (male / female) age (child / young / middle aged / old) clothing (<0.5 clo / 0.5-1 clo / 1 clo<) (*only visitors sitting on benches*)

4. Questionnaires and measurements with mobile biometeorological station

Since autumn 2009 the examinations have been completed with structured interviews and on-site measurements with a biometeorological station. This unit is well suited to record thermal variables on different points of the study area next to the questioned individual and includes appropriate rotatable instrument to measure the short- and long-wave radiation flux densities from the 6 main directions. All meteorological variables necessary for PET and PMV are measured at the adequate height of 1.1-1.2 m (Table 2).

To calculate PMV exactly, we enter these data into the RayMan model together with the personal data (sex, age, height, weight), clothing, activity and position (posture) of the interviewee, recorded in the first part of the questionnaire. The noted clothes and activity are converted to clothing insulation value and heat generated by activity (active metabolism) according to Fanger (1972) as well as VDI 3787 (1998).

Beyond these personal parameters the subjects were asked to tell about their health conditions, general feelings, urban vs. open-air attitude, time spent in the place, housing area, reasons for their visit and opinions on the design of the area. To construct the list of queries many ideas from Lin (2009), Knez and Thorsson (2006) and Nikolopoulou and Lykoudis (2006) were adopted and modified more or less.

The main part of the questionnaire concerned to the thermal environment. The questioned individuals reported their thermal sensation – named Actual Sensation Vote or TSV Thermal Sensation Vote – based on a semantic differential scale. This scale (left side of Fig. 2), in contrast with the usually adopted ones, allows of marking thermal sensation more precisely. Consequently, subjective feelings could be compared to the index values (which are rarely round numbers) calculated from the measured parameters. After thermal sensation, the interviewees reported also their assessment of their overall comfort state (discomfortable / comfortable).

Another semantic differential scales were used for measuring the respondents' perceptions about the momentary air temperature, wind velocity, air humidity and solar radiation (Fig 2. right side). There were also four questions for the preference for better conditions, i.e. any changes (decrease / no change / increase) in the cases of the individual weather parameters.

The last two questions referred to behavioral adaptation to hot and cold conditions, as it is an important factor in outdoor thermal comfort. The interviewees were asked to choose maximum 3-3 adaptation measures they would take if they feel it is too hot or too cold (according to Lin, 2009).

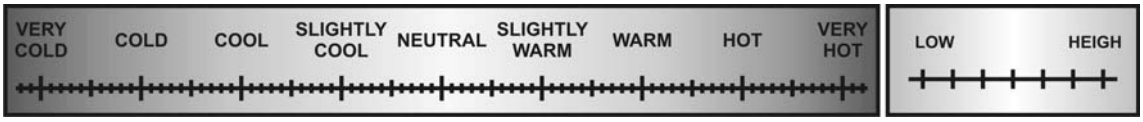

Fig. 2: Semantic differential scales used to measure the interviewees' thermal sensation (left side) and perception of individual weather parameters (right side)

Spatial locations of the subjects were marked with ID numbers on the map of the area (Ady Square or Honvéd Square) and digitized within ArcView in the same way as in the cases of interval-based observations.

5. Discussion: main possibilities of analysis

I. Momentary attendance in the function of the actual thermal conditions

Taking the dataset from the 10-minute observations and the 10-minute meteorological data measured by the stationary station, area usage of the investigated squares can be discussed in accordance with the weather and thermal comfort conditions. Besides total number of visitors, relative attendance of certain groups (made on the basis of position or activity) can also be represented in the function of the selected objective parameters.

II. Behavioural adaptation to and area usage patterns by different thermal situations – derived from observations in different intervals

In the cases of both squares, we are able to study the weather-related area usage of people grouped either gender or age-categories, as well as to study their behavioral adaptation by analyzing the changes of clothing-categories according to the measured or calculated thermal parameters. This can be pointed out with activity categories and visitors' exposure similarly, from the more detailed dataset collected in the first square.

In the case of Ady Square, the use of ArcView make it possible to show the presence in spatio-temporal manner and make area usage maps according to different categorization. The markers of visitors may be coloured by any measured or observed data, e.g. day and/or time-interval of the presence; weather parameters or thermal comfort during the interval of the observations; the numerous personal data collected on the field measurements. Determination of what are the preferred sectors (sub-areas) at different weather conditions might be a very important result. The commonly used forms representing the results of statistical analyses (diagrams, tabulations, statistical measures) become very informative together with these area usage maps (e.g. Fig. 3).

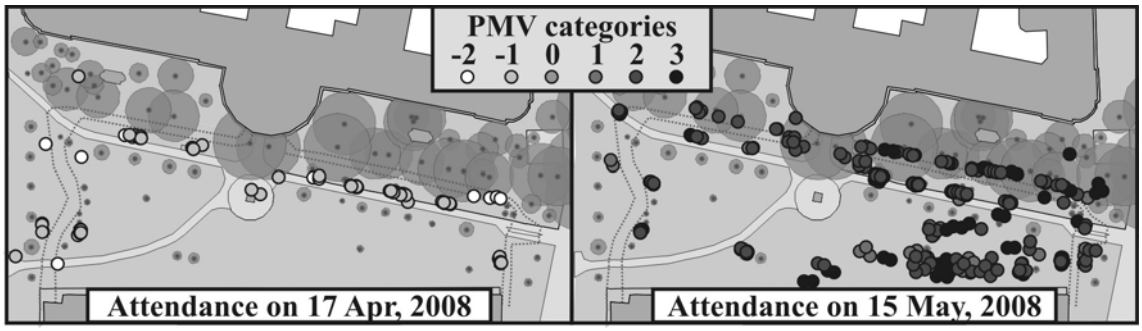

Fig. 3: Visitors' distribution on the Ady Square on two days – markers are coloured according to the thermal comfort conditions during the observation intervals

III. Results from evaluation the questionnaire survey

The simultaneously collected meteorological and personal data make it possible to compare the actual thermal sensation, the weather perceptions and preferences with the objective measures of thermal environment and to reveal objective and subjective factors affecting thermal sensation, human comfort and area usage. The use of the GIS software makes easy the data management and helps to demonstrate exactly the circumstances of the interviews.

6. Conclusion

This paper described the outdoor thermal comfort project proceeding in Szeged from methodological point of view. Investigations focus on urban parks and squares, as there is an increasing need for urban public environments offering places for relaxation, recreation and promoting the social activity. The project aims to reveal relationships between the thermal environment and the visitors' reactions manifests itself in their thermal sensation, weather perception and preference, behavioural adaptation as well as area usage patterns. The required data for the comprehensive analysis derived from field surveys: observations and structured conversations conducted together with measurements of the thermal environment.

The observation method consists of marking the visitors' exact spatial locations together with their personal characteristics can cope only with sedentary people, consequently it can be used only in resting places. However, momentary counting of people, interviews and on-site biometeorological measurements can be carried out in other city structures, too. The use of the GIS software to represent the spatial results i.e. the created area usage maps may easies the communication with urban planners and decision makers.

Acknowledgement

The research is supported by the grant of the Hungarian Scientific Research Fund (OTKA K-67626)

References

Fanger P O, 1972: Thermal Comfort. McGraw Hill Book Co., New York, 244 p.

Gulyás Á, Unger J, Matzarakis A, 2006: Assessment of the microclimatic and thermal comfort conditions in a complex urban environment: modelling and measurements. Build. Environ. 41, 1713-1722.

Kántor N, Gulyás Á, Égerházi L, Unger J, 2009: Objective and subjective aspects of an urban square's human comfort - case study in Szeged (Hungary). Ber. Meteor. Inst. Univ. Freiburg No. 18, 241-246.

Knez, I, Thorsson S, 2006: Influences of culture and environmental attitude on thermal, emotional and perceptual evaluations of a public square. Int. J. Biometeorol. 50, 258-268.

Lin T P, 2009: Thermal perception, adaptation and attendance in a public square in hot and humid regions, Build. Environ. 44, 2017–2026.

Matzarakis A, Rutz F, Mayer H, 2007: Modelling radiation fluxes in simple and complex environments – application of the RayMan model. Int. J. Biometeorol. 51, 323-334.

Mayer H, 2008: KLIMES – a joint research project on human thermal comfort in cities. Ber. Meteor. Inst. Univ. Freiburg No. 17, 101-117.

Nikolopoulou M, Lykoudis S, 2006: Thermal comfort in outdoor urban spaces: Analysis across different European countries. Build. Environ. 41, 1455-1470.

VDI 3787, 1998: Methods for the human-biometeorological assessment of climate and air hygiene for urban and regional planning. − Part I: Climate. VDI guidline 3787. Beuth, Berlin, 29 p.

Authors' address:

Noémi Kántor (kantor.noemi@geo.u-szeged.hu)
Ágnes Gulyás (agulyas@geo.u-szeged.hu)
Department of Climatology and Landscape Ecology, University of Szeged
Egyetem u. 2, 6722, Szeged, Hungary

Assessment of air quality indices in Seoul region by land use type

Hyunjung Lee[1], Jutta Holst[1], Helmut Mayer[1]

[1] Meteorological Institute, Albert-Ludwigs-University of Freiburg, Germany

Abstract

As a response to the need to improve well-being and health of human, various air quality indices were developed. Many air quality indices are related to the impact on human beings. The study was based on air pollution data from three different sites with different land use types (residential, commercial and industrial area) in Seoul/Korea for the period 2006-2008. The two air quality indices DAQx (Daily Air Quality Index), developed in Germany, and CAI (Comprehensive Air-Quality Index), developed in Korea, were used. Both indices refer two the impacts of short-term pollution for citizens. Results show that the maximum frequency of DAQx was recorded in the class 5 (poor air quality) at all sites (residential area: 41%, commercial area: 40%, industrial area: 43%). However, the frequency of DAQx class 6 (very poor air quality) at industrial area was the highest among three kinds of sites (residential area: 9%, commercial area: 10%, industrial area: 11%). It is known that the dominant impact factors which determine DAQx were arranged with PM_{10}, NO_2, O_3. In contrast, CAI had its the peak frequency of all sites for the same period in class 2 (satisfying air quality) of CAI standard.

1. Introduction

Increasing urbanization and industrialization have caused the urban environment to deteriorate. Urban structures locally affect the atmospheric background conditions and severely ambient air quality which is attributed to human health. Various indices for assessing air quality were developed to address the betterment of human health. However, indices which are not impact related to human beings or which use single air pollutants are insufficient in view of the persistent demands for the assessment of the air quality (Mayer and Kalberlah, 2009). Based on indices which include a mixture of air pollutants, which are typical for the ambient air, an integrated air quality evaluation on well-being and health of people is possible (Mayer et al., 2008).

This study aims to assess air quality by land use type. Based on DAQx (Daily Air Quality Index), which is developed in German, and CAI (Comprehensive Air-Quality Index), which is applied in Korea, evaluation of air quality within urban structures was carried out. Results of DAQx and CAI were compared in order to identify differences the two air quality assessment indices.

2. Materials and methods

2.1 Study area

Three sites of the study area are located in Seoul (37° 33' N, 126° 58' E), Korea (Fig. 1). Seoul, which is the capital city of Korea, occupies 6th place in the world rankings of population density (16700 people per km^2 in 2009). In order to assess the impact of air quality in urban spatial structures, three sites were selected by the land use type: residential, commercial and industrial area. Air pollution data were used in the period 2006 to 2008.

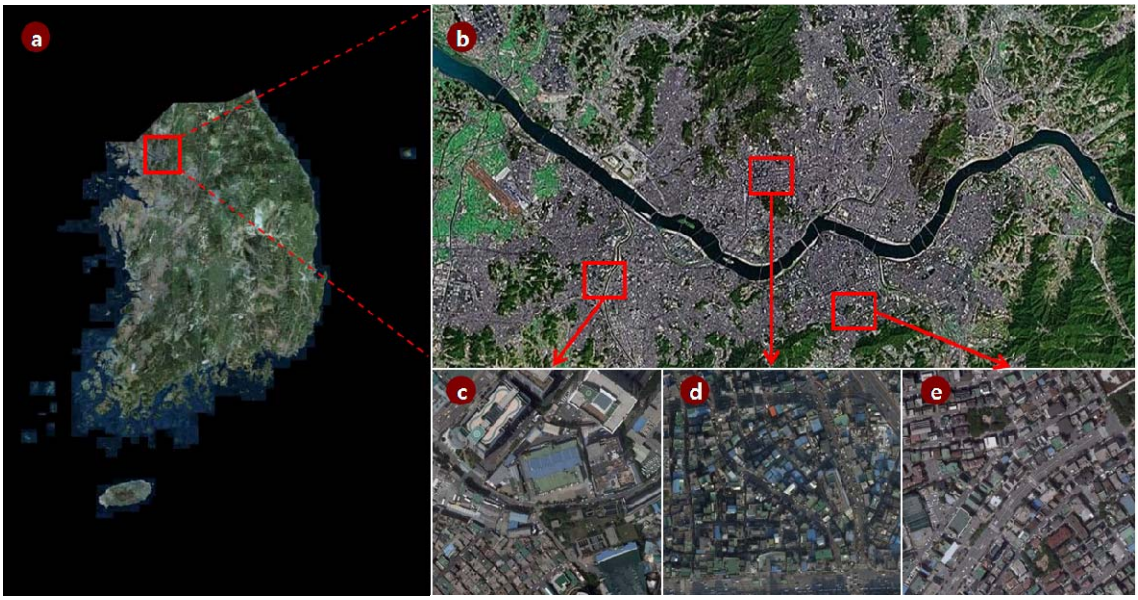

Fig. 1: Geographic location of (a) and (b) Seoul, (c) Guro (commercial area), (d) Hyoje (industrial area) and (e) Dogok (residential area)

2.2 Air quality index DAQx (Daily Air Quality Index)

The index DAQx was developed by the Research and Advisory Institute for Hazardous Substances, Freiburg, Germany, and the Meteorological Institute, University of Freiburg, Germany. It considers the most important air pollutants of ambient air related ability to negatively affect human health on a short-term basis. All these air pollutants' concentrations are assigned to different, pollutant specific ranges (Table 1), which correspond to six index classes.

Table 1: Assignment of ranges of air pollutant specific concentration (NO_2, O_3 and SO_2: daily peak 1-hr concentration, CO: daily highest 8-hr running mean concentration, PM_{10}: daily mean concentration) to DAQx values and classes inclusive of classification means (Mayer et al., 2004)

NO_2 *($\mu g/m^3$)*	*SO_2* *($\mu g/m^3$)*	*CO* *(mg/m^3)*	*O_3* *($\mu g/m^3$)*	*PM_{10}* *($\mu g/m^3$)*	*DAQx* *value*	*DAQ* *class*	*Classification*
0-24	0-24	0.0-0.9	0-32	0.0-9.9	≤1.4	1	very good
25-39	25-49	1.0-1.9	33-64	10.0-19.9	1.5-2.4	2	good
40-99	50-119	2.0-3.9	65-119	20.0-34.9	2.5-3.4	3	satisfying
100-199	120-349	4.0-9.9	120-179	35.0-49.9	3.5-4.4	4	sufficient
200-499	350-999	10.0-29.9	180-239	50.0-99.9	4.5-5.4	5	poor
≥500	≥1000	≥30.0	≥240	≥100	≥5.5	6	very poor

The index for each component ($DAQx_i$) is caluculated according to Eq. 1 (EPA, 1999).

$$DAQx_i = \left[\left(\frac{DAQx_{i,up} - DAQx_{i,low}}{C_{i,up} - C_{i,low}} \right) \cdot (C_i - C_{i,low}) \right] + DAQx_{i,low} \qquad \text{(Eq. 1)}$$

In Eq. 1, $C_{inst.}$ is the daily peak 1-hr concentration of the single air pollutant i: NO_2, SO_2 and O_3, daily highest 8-hr running mean concentration of CO, or daily mean concentration of PM_{10} respectively, C_{up} and C_{low} are the upper and lower thresholds of the specific air pollutant concentration range as well as $DAQx_{up}$ and $DAQx_{low}$ are the DAQx values corresponding to C_{up} and C_{low} (Mayer and Kalberlah, 2009).

The highest single index class among the air pollutants determines DAQx value (Fig. 2, Mayer et al., 2004).

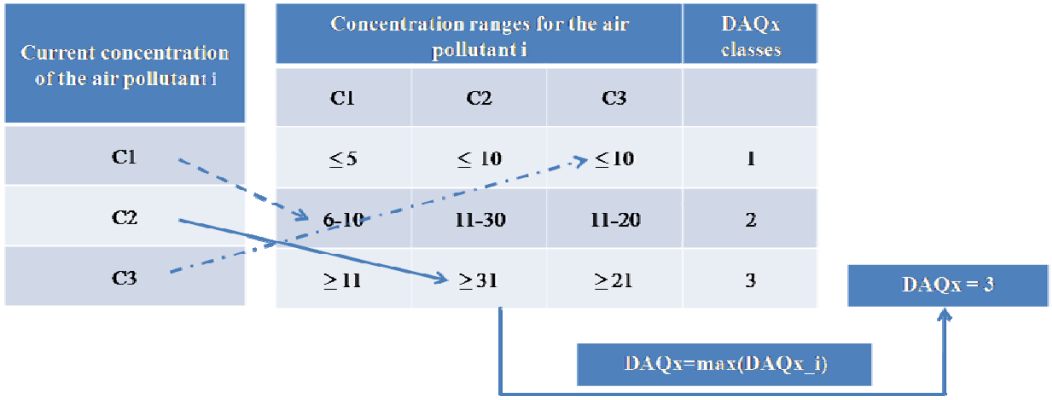

Fig. 2: Scheme for the determination of DAQx (Mayer et al., 2004)

Table 2: Assignment of ranges of air pollutant specific concentration (SO_2, NO_2, CO and O_3: daily peak 1-hr concentration, PM_{10}: daily mean concentration) to CAI values (Source: National Institute of Environmental Research, 2006)

Index / *Classification*		*A* *Good*		*B* *Satisfying*		*C* *Sensitive*		*D* *Poor*		*E* *Very poor*		*F* *Danger*	
Score	I_{LO}	0		51		101		151		251		351	
	I_{HI}	50		100		150		250		350		500	
Concentration		C_{low}	C_{up}	C_{low}	C_{up}	C_{low}	C_{up}	C_{low}	C_{up}	C_{low}	C_{up}	C_{low}	C_{up}
SO_2(ppm)	1hr	0	0.020	0.021	0.050	0.051	0.100	0.101	0.150	0.151	0.400	0.401	1
NO_2(ppm)	1hr	0	0.030	0.031	0.060	0.061	0.150	0.151	0.200	0.201	0.600	0.601	2
CO(ppm)	1hr	0	2.00	2.01	9.00	9.01	12.00	12.01	15.00	15.01	30.00	30.01	50
O_3(ppm)	1hr	0	0.040	0.041	0.080	0.081	0.120	0.121	0.300	0.301	0.500	0.501	0.600
PM10($\mu g/m^2$)	24hr	0	30	31	80	81	120	121	200	201	300	301	600

2.3 Air quality index CAI (Comprehensive Air-Quality Index)

CAI is also divided into six levels, reflecting the actual pollution influence on human body and includes the same the five major air pollutants. The calculation of CAI follows EQ. 1. The thresholds for each air pollution component are listed in Table 2. But instead of index borders ($DAQx_{i,up}$ and $DAQx_{i,low}$), air quality scores (I_{HI} and I_{LO}) are the basis

of CAI (National Institute of Environmental Research, 2009). As for DAQx, the highest value class among single air pollutants governs the resulting CAI class. If two single substances, which have high values under sensitive grade respectively, exist, the pollutant with the highest value is chosen as primary factor and 50 extra points is added to the score. In the case of more than three substances, 75 extra points is added to the value of the highest pollutant.

3. Results

3.1 Results of DAQx analysis

Fig. 3 shows the result of frequency analysis of DAQx by land use type during the three years from 2006 to 2008. The result reveals that the maximum frequency of DAQx was recorded in the class 5 (poor air quality) at all sites: residential area (Dogok) 41%, commercial area (Hyoje) 40% and industrial area (Guro) 43%.

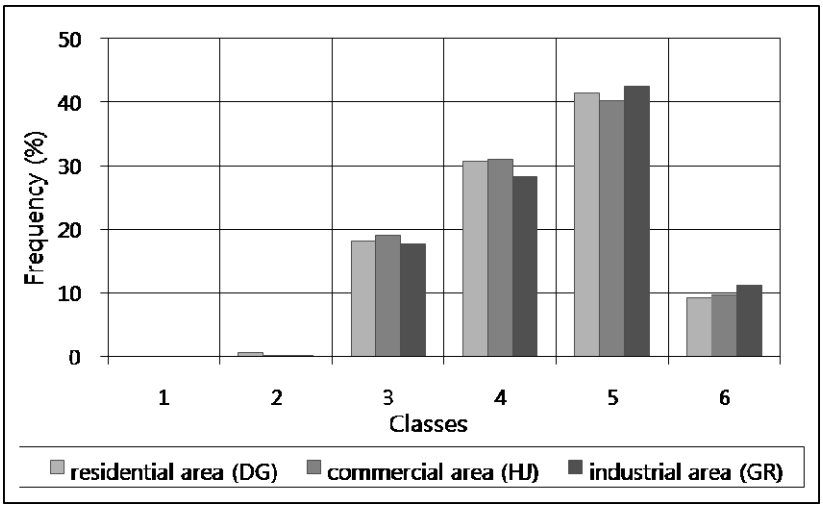

Fig. 3: Frequency of DAQx by land use type in the period 2006 to 2008

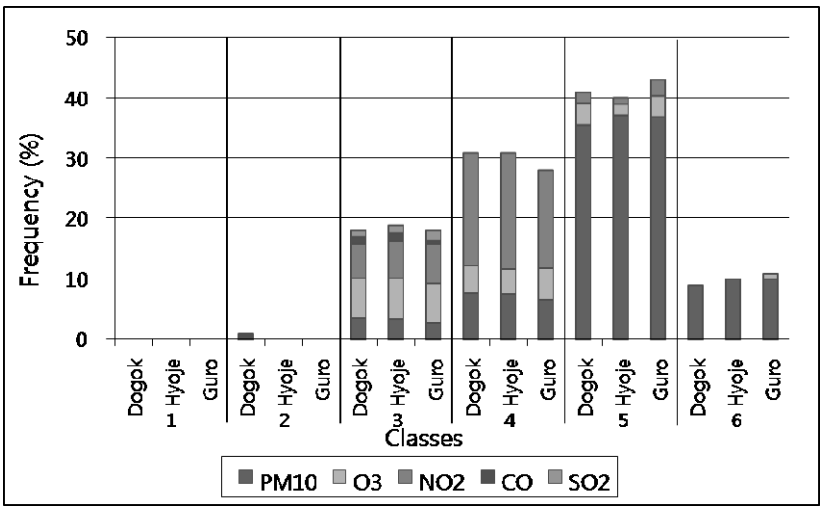

Fig. 4: Comparative air pollutant related frequency of DAQx by land use type in the period 2006 to 2008

Although the result found no significant differences by land use type, the frequency of DAQx class 6 (very poor air quality) at industrial area was recorded the highest value. The primary impact factor in class 5 and 6 which determined DAQx was PM_{10} (Fig. 4).

3.2 Results of CAI analysis

According to CAI, the dominating frequency occurred in the CAI class 2 (satisfying air quality). As for DAQx, no significant difference among three sites (residential area (Dogok) 54%, commercial area (Hyoje) 59% and industrial area (Guro) 57%) could be found (Fig. 5).

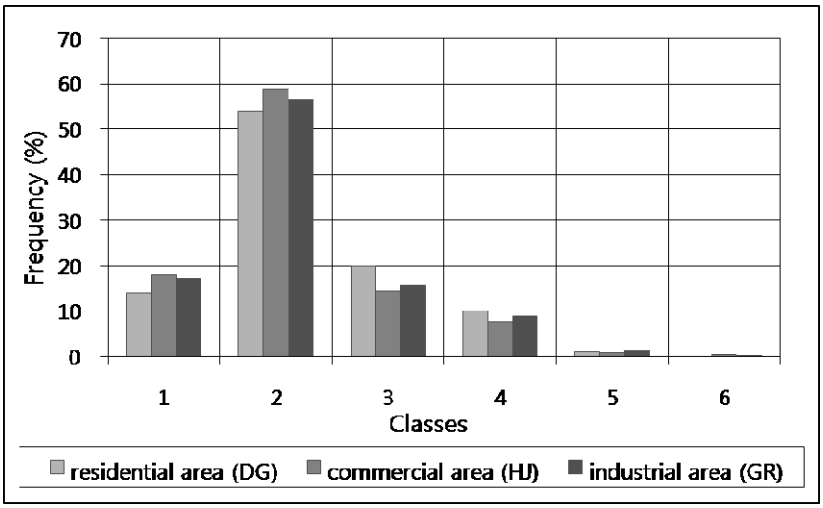

Fig. 5: Frequency of CAI by land use type in the period 2006 to 2008

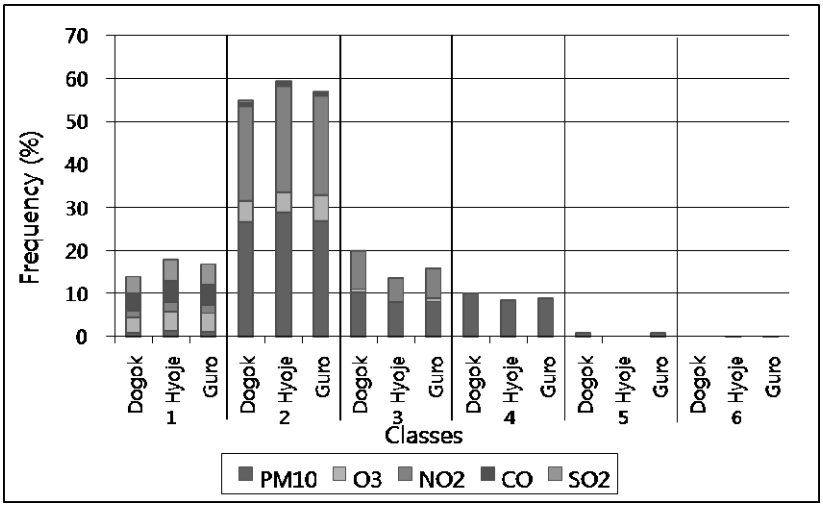

Fig. 6: Comparative air pollutant related frequency of CAI by land use type in the period 2006 to 2008

Best air quality was observed at the commercial area, where nearly 80% of the time, air quality assessment was “good” or “very good”. NO_2 as well as PM_{10} turned out to be the dominant pollutants in CAI classes 2 and 3, whereas the main substance was PM_{10} in the DAQx class 5 shown the highest frequency (Fig. 6).

4. Conclusions

The assessment of air quality by land use type was carried out based on two kinds of air quality indices: DAQx, which was developed in Germany, and CAI used in Korea. While two indices have similar calculation method, they have the different substance specific class ranges considered human health factors and national environmental standard.

In the case of using DAQx, the maximum frequency lies in the class 5 (poor air quality) at all sites. Air quality of the industrial area was the most severe in the DAQx classes 5 and 6. Compared to DAQx results, CAI showed the highest frequency in class 2 (satisfying air quality). The commercial area showed the best air quality based on CAI.

References

Mayer, H., Makra, L., Kalberlah, F., Ahrens, D. and Reuter, U., 2004: Air stress and air quality indices. Meteorological Zeitschrift. 13, 395-403.

Mayer, H. and Kalberlah, F., 2009: Two impact related air quality indices as tools to assess the daily and long-term air pollution. Int. J. Environment and Pollution 36, 19-29.

Mayer, H., Holst, J., Schindler, D., Ahrens, D., 2008: Evaluation of the air pollution in SW Germany evaluated by the long-term air quality index LAQx. Atmospheric Environment. 42, 5071-5078.

National Institute of Environmental Research, 2006: Development of comprehensive assessment method on air quality. Republic of Korea.

Authors’ address:

Hyunjung Lee (catharina96@gmail.com)
Dr. Jutta Holst (jutta.holst@meteo.uni-freiburg.de)
Prof. Dr. Helmut Mayer (helmut.mayer@meteo.uni-freiburg.de)
Meteorological Institute, Albert-Ludwigs-University of Freiburg
Werthmannstr. 10, D-79085 Freiburg, Germany

Impact of vegetation areas on the microclimate of Dresden, Germany

Cornelia Kurbjuhn[1], Valeri Goldberg[1], Christian Bernhofer[1]

[1] Institute of Hydrology und Meteorology, Chair of Meteorology, Technische Universität Dresden, Germany

Abstract

Aim of this research is to determine capabilities of vegetated areas and open areas in the inner city of Dresden to attenuate microclimatic extremes. The study is embedded in the project "city nature and open area structures under climate change" of the German Federal Agency for Nature Conservation. The diversity of impacts of different urban areas on the microclimate is presented by mobile measurements and model simulations. Simulations were carried out with the coupled vegetation-boundary layer model HIRVAC-2D and the 3D microclimate model ENVI-met. Model output agrees quite well with measurements of air temperature on sunny days in the year 2009. E. g., the maximum temperature difference between high and dense vegetation areas and the sealed and built city surrounding reaches up to 4 K at a hot and sunny summer day.

1. Introduction

Large cities are rougher, warmer and mostly drier than the surrounding landscape and show the so called urban heat island effect (Oke, 1987). Especially during the night the reduced cooling is significant in the urban area compared to the city surrounding. Heat island intensity of cities and, hence, urban warming mainly depends on the density of urban structures and sealing of urban areas. Therefore, determining heating and cooling effects in a city needs an analysis of the urban environment. Against the background of a probable increase of summer temperature in Central Europe, actual urban planning strategies should consider the importance of open areas and vegetation in the centre of cities for the urban microclimate. This study deals with the effect of interaction between open areas and vegetation structures on the urban micro climate of Dresden, Germany. Investigations are embedded in the project "city nature and open area structures under climate change" of the German Federal Agency for Nature Conservation which aims to demonstrate impacts of different urban structures based on climatic factors and to identify their capability for adaptation. Main topic of this research is the determination of the capabilities of given vegetated areas and open areas in the inner city of Dresden to attenuate microclimatic extremes. The diversity of impacts of vegetated and open areas on the urban microclimate is presented by mobile bicycle measurements and model simulations. Simulations were carried out with the coupled vegetation-boundary layer model HIRVAC-2D and the three-dimensional microclimate model ENVI-met.

2. Data and methods

The three-dimensional microclimate model ENVI-met (Bruse and Fleer, 1998) was designed to simulate the surface-plant-atmosphere interactions in urban environment and allows the derivation of bioclimatic factors like Predicted Mean Vote (PMV) for different urban structures. PMV describes the thermal perception of a human body which can result in cold (PMV values up to -3.5) or heat stress (PMV values up to +3.5). PMV values of -0.5 to + 0.5 describe a comfortable thermal perception (VDI, 1998). Simula-

tions with ENVI-met were carried out to define the cooling effects of urban areas and to estimate microclimate effects on humans. The typical resolution of ENVI-met ranges between 0.5 and 10 m in space and 10 s in time. ENVI-met is a prognostic model based on the fundamental laws of fluid dynamics and thermodynamics. The model includes the simulation of flow around buildings, exchange processes of heat and vapour at the ground surface and at walls, as well as the exchange at vegetation and bioclimatology. The main model input parameters are wind speed and wind direction, roughness length, temperature of the atmosphere, specific humidity, relative humidity, specific plant and soil types present, cloud cover, background CO_2 concentration, as well as soil temperature and relative soil water storage in three layers. ENVI-met is used for modelling the cooling effects of green spaces and for medium-scale simulation approaches. To illustrate the variability of urban structures model input data like building heights, vegetation structures in different heights (grass, hedges and trees) and several soil structures (loamy soil, loamy sand, brick road and asphalt road) have to be specified. Simulations with ENVI-met were carried out for different urban structures with a sealed surrounding as reference area.

The model HIRVAC (HIgh Resolution Vegetation Atmosphere Coupler) was firstly developed as a 1D boundary layer model with 120 layers between 0 and 2 km including a highly resolved canopy (60 layers between 0 and 30 m). Vegetation is considered by additional terms in the model equations for momentum, temperature and humidity which are parameterised by the output (leaf boundary layer and stomata resistance) of a mechanistic photosynthesis module for C3 plants (PSN6, Falge et al., 1996; Goldberg and Bernhofer, 2001). Precipitation, interception, and soil moisture distribution are calculated by multi-layer models for interception and groundwater (Baums et al., 2005). In context with the research project TurbEFA (funded by DFG – German Research Foundation) a 2D model version of HIRVAC was developed using the same vertical structure as in HIRVAC-1D. HIRVAC-2D was applied in the current study to quantify interactions between vegetation and surrounding urban, open and sealed areas. In a first case about 30 simulations with HIRVAC-2D were carried out to derive an easy manageable analytic function, which describes the link between maximum temperature difference ΔT in 1.5 m height (domain of the strongest thermal interaction between city dwellers and atmospheric vicinity) related to a dry reference area without vegetation and volume density of vegetation (gvd) and area size of high plants:

$\Delta T_{max,\,H} = 0{,}0284 gvd^{0{,}487} area^{0{,}383}$,with $\Delta T_{max,\,H}$ in Kelvin, gvd in m³/m² and area in m².

The output of this analytic function clearly shows the interaction of gvd (high vegetation), area size and the maximum cooling effect compared to the reference area on a cloudless summer day (Fig. 1). For example, a vegetation area of 6 ha size and a gvd of 5 m³/m² has a cooling effect of about 4 K.

Low vegetation areas (as, for example, grass) do not have a remarkable shading effect dependent on gvd. For that reason, an analytic function for the temperature difference of green areas with a small vegetation height (< 1m) in relation to the reference area was found which only depends on the area size:

$\Delta T_{max,\,N} = 1{,}65(1 - e^{-area/97736})$ with $\Delta T_{max,\,N}$ in Kelvin.

Finally, a weighted analytic function was derived which considers the partitions of areas with low (h< 1 m: f_N), middle (1 - 3 m: f_M) and high (h> 3 m: f_H) vegetation in the city district regarded:

$$\Delta T_{max} = \Delta T_{max,H} \cdot f_H + \Delta T_{max,N} \cdot f_N + 0.5(\Delta T_{max,H} + \Delta T_{max,N}) \cdot f_M \quad \text{(in Kelvin)}$$

The temperature difference of green areas with a middle vegetation height (1 - 3m) was calculated as the weighted (by area partition f_M) average between the results of the analytic functions for low and high vegetation.

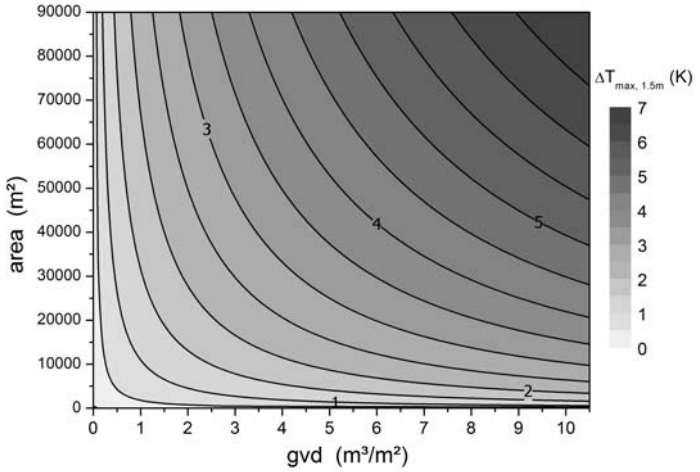

Fig. 1: Interaction of gvd (high vegetation), area size and maximum cooling effect, based on the analytic approximation of HIRVAC-2D results

To show the effect of different types of green spaces using ENVI-met, information about the vegetation is needed. For determining the proportion of green areas and vegetation volume in urban districts, urban biotope types are applied to define vegetation structures and their assessment by type, dimension and location. The vegetation structure of urban biotope types was analysed in areas with vegetation (in different heights) and without vegetation (built-up areas, other kinds of sealed soil surfaces and open ground).

3. Exemplary results

Interactions of different urban structures with the microclimate of Dresden were determined by calculating the temperature differences of various urban structure types to a reference area and by the distribution of PMV. Vegetated and open areas have a large potential for cooling down the urban area (Oke, 1987), which can be demonstrated with the ENVI-met model output. The interaction between typical urban vegetation structure types and the microclimate was simulated for a sunny summer day in the city of Dresden. Fig. 2 and Fig. 3 show the air temperature differences and thus the cooling and heating effects of several urban structures compared to the sealed vicinity for July 16th 2009 at 02:00 p.m. and 10:00 p.m. The given difference of the mean temperature of an urban structure and mean temperature of the sealed surrounding illustrates the importance of the vegetation inventory and the shading effects of trees for the microclimate during a sunny day. Because of these shading effects combined with a good ventilation, mixed green and urban structures are cooler (dark bars) than the sealed vicinity. Sealed

urban structures with less shadowed areas and ventilation, e.g. traffic areas, showed the highest temperature. Vegetation and the built environment cause shading effects and control the radiation budget to cool down the temperature. At night traffic areas and built-up areas are warmer than the sealed surrounding and show a heating effect, while vegetated areas still have the potential for cooling. Mixed open and vegetated urban structures have cooling effects during day and night and have thus a positive impact on the microclimate of Dresden.

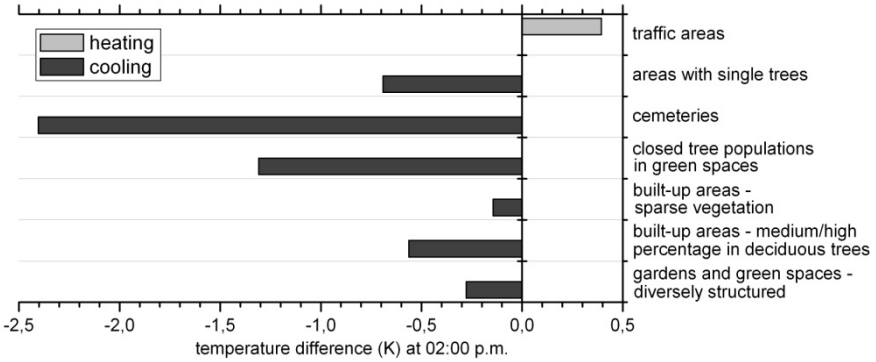

Fig. 2: Temperature difference in 1.2 m height on 16th of July 2009 at 02:00 p.m.

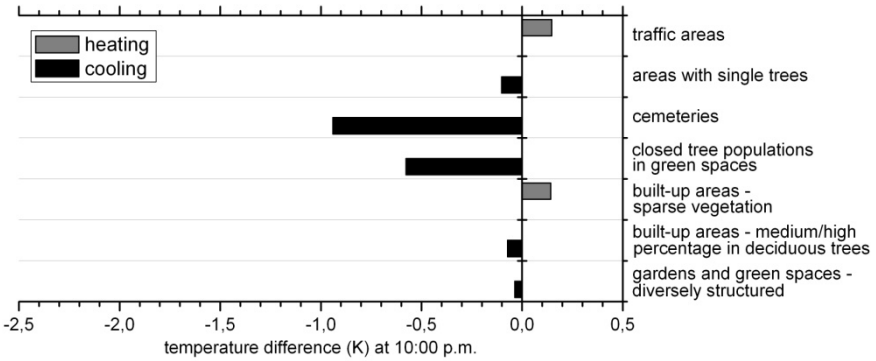

Fig. 3: Temperature difference in 1.2 m height on 16th of July 2009 at 10:00 p.m.

Fig. 4 shows the microclimate effect of different urban biotope types in the city of Dresden with different volume densities of vegetation and area size based on the analytic function shown above. The large green area of the city park Großer Garten shows the highest cooling effect compared to the vicinity. The built-up areas appear with almost no cooling effect.

Fig. 5 shows the PMV distribution in a part of the park Großer Garten (area: 200 ha), modelled with ENVI-met for July 16th 2009 at 02:00 p.m. in 1.2 m height. PMV inside this park showed distinctly lower values (dark grey) implying a pleasant thermal environment for humans compared to the sealed areas in the vicinity. Built-up areas and sealed surfaces are easy identifiably due to their higher PMV values (light grey).

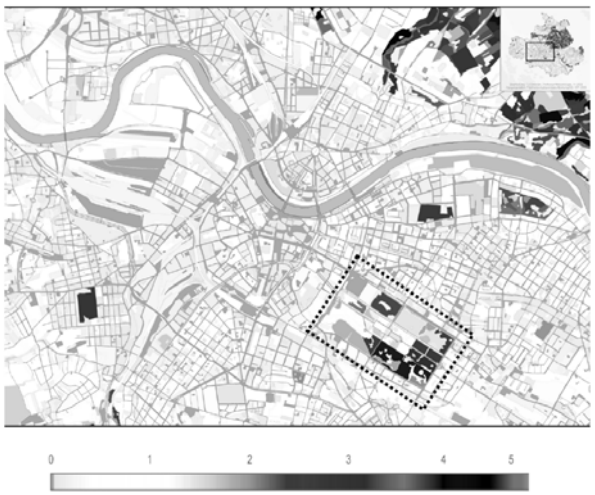

Fig: 4: Cooling effects (ΔT_{max} in K), based on the analytic functions derived from HIRVAC-2D simulations (dotted line shows the park Großer Garten)

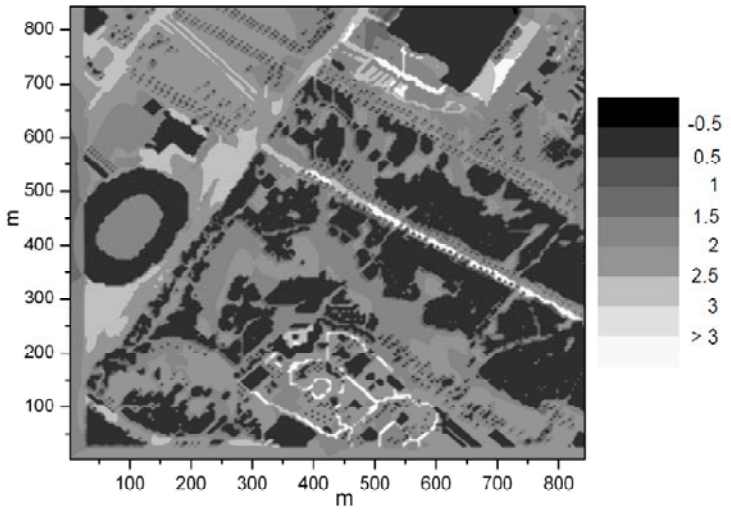

Fig: 5: Distribution of PMV in a part of the city park Großer Garten in 1.2 m height on July 16th 2009 at 02:00 p.m.

4. Summary and Conclusions

Interactions of different urban structures and microclimate were quantified by simulated temperature differences to a reference area and by the distribution of PMV. Model output of temperature and PMV clearly showed the effects of vegetated areas in Dresden to the thermal environment of humans. For example, the largest park of the city indicated a temperature drop of about 4 K on a hot and sunny summer day compared to the surrounding with less vegetation. PMV inside the park showed distinct lower values (means conditions in a range of thermal comfort of a human) compared to the sealed areas in the vicinity. Model output of ENVI-met and HIRVAC-2D was compared to measurements of air temperature and air humidity on sunny days in the year 2009. Results of the measurements confirm the model simulations adequately in the centre of the largest city park Großer Garten.

It should be mentioned that the distribution of ΔT_{max} based on HIRVAC-2D results does not show boundary effects between neighboured areas with sharp temperature gradients. The area of interaction between adjacent areas reaches up to few 100 meters and depends on meteorological conditions (wind, radiation) and roughness of the surrounding. Further studies will be directed to quantify these effects using a 3D-microclimate model (as ENVI-met or HIRVAC-3D which is currently developed at our institute) and a lot of computer power.

Acknowledgement

This study is embedded in the project "City nature and open area structures under climate change", funded by the German Federal Agency for Nature Conservation. We would like to thank Anna Westbeld (formerly Technische Universität Dresden) for assisting in data collection and preparation. Special thanks also go to Michael Bruse (University of Mainz) for permission to use the model ENVI-met.

References

Baums, A.-B., V. Goldberg, C. Bernhofer, 2005: Upgrading the Coupled Vegetation Boundary Layer Model HIRVAC by New Soil Water and Interception Modules. Met. Z. 14 (2), 211-218.

Bruse, M., H. Fleer, 1998: Simulating surface-plant-air interactions inside urban environments with a three dimensional numerical model. Environ. Modell. Softw. 13, 373-384.

Falge, E., W. Graber, R. Siegwolf, J. D. Tenhunen, 1996: A model of the gas exchange response of Picea abies to habitat conditions. Trees 10, 277-287.

Goldberg, V., C. Bernhofer, 2001: Quantifying the coupling degree between land surface and the atmospheric boundary layer with the coupled vegetation-atmosphere model HIRVAC. Annales Geophysicae 19, 581-587.

Oke, T. R., 1987: Boundary layer climates. Second edition. Routledge, London, 435 pp.

VDI, 1998: Human-biometeorologische Bewertung von Klima und Luft für die Stadt- und Regionalplanung. Verein Deutscher Ingenieure. VDI-Richtlinie 3787, Bl. 2, 29 pp.

Authors' address:

Prof. Dr. Christian Bernhofer (Christian.bernhofer@tu-dresden.de)
Dr. Valeri Goldberg (valeri.goldberg@tu-dresden.de)
Cornelia Kurbjuhn (cornelia.kurbjuhn@mailbox.tu-dresden.de)

Technische Universität Dresden
Institute of Hydrology and Meteorology
Chair of Meteorology
Pienner Straße 23
01737 Tharandt
Germany

Influence of mean radiant temperature on thermal comfort of humans in idealized urban environments

Jan Herrmann and Andreas Matzarakis

Meteorological Institute, Albert-Ludwigs-University of Freiburg, Germany

Abstract

Studies about thermal comfort of humans in urban areas require the meteorological parameters air temperature, air humidity, wind speed, short- and long wave fluxes. The radiation fluxes can be expressed for these studies by the mean radiant temperature, a parameter with high variability in urban area at least by the modification of the global radiation. Wind speed in urban areas is influenced by the urban obstacles and their orientation. These two factors mean radiant temperature and wind speed can be modified or changed by different height to width ratio or orientation.

1. Introduction

Aim of the study is to quantify the influence of the height to width ratio and effect of the orientation in a typical urban canyon in a western middle size European City. Usually the parameters which at most can influence thermal bioclimatic conditions in urban areas and which can also be modified by urban planning or architectural issues are the radiation fluxes (described in human-biometeorology in terms of the mean radiant temperature) and the wind speed (Lin et al., 2010). Analysing typical urban configurations with typical dimensions the influence on the two above mentioned parameters can be described. Here we analysed the effect of typical structures on the mean radiant temperature and the thermal index physiologically equivalent temperature (Höppe, 1999, Matzarakis et al,. 1999) based on over 10 year measurements of the urban climate station Freiburg (Matzarakis and Mayer, 2008) and the application of the RayMan model (Matzarakis et al., 2007).

2. Methods and data

Modern human biometeorological methods use the human energy balance of the human body (Höppe 1993) in order to extract thermal indices and describe the effects of the thermal environment on humans (Mayer, 1993, VDI, 1998). For this purpose, hourly measurements of air temperature, air humidity, wind speed and global radiation of an over ten year period (1.9.1999 to 31.12.2009) have been used in order to calculate the mean radiant temperature and the physiologically equivalent temperature. The simulations have been done by the use of the RayMan model, which is able to transfer the global radiation from an area with free horizon to urban structures. Main target is the estimation of mean radiant temperature due to atmospheric influences firstly by clouds and other meteorological compounds as vapour pressure or particles. In addition, the influences of topographical or urban morphologies in terms of obstacles modify mostly not only wind but also radiation properties in the micro scale (Lin et al., 2010).
The following configurations and setups have been used. The canyon has a length of 300 m and can be changes in his width and height. In addition the canyon can be rotated

in steps of 15 °. The height and width of the canyon starts from 5 to 40 m. As typical dimension of height and width of the urban canyon, 15 m has been chosen.

3. Exemplary results

First the data has been analysed in terms of the PET-Classes in order to quantify the background conditions at the urban climate station. Figure 1 shows the PET-Classes for the period 1.9.1999 to 31.12.2009. Figure 2 shows the mean monthly frequency distribution of PET-Classes for the same period as in Fig. 1.

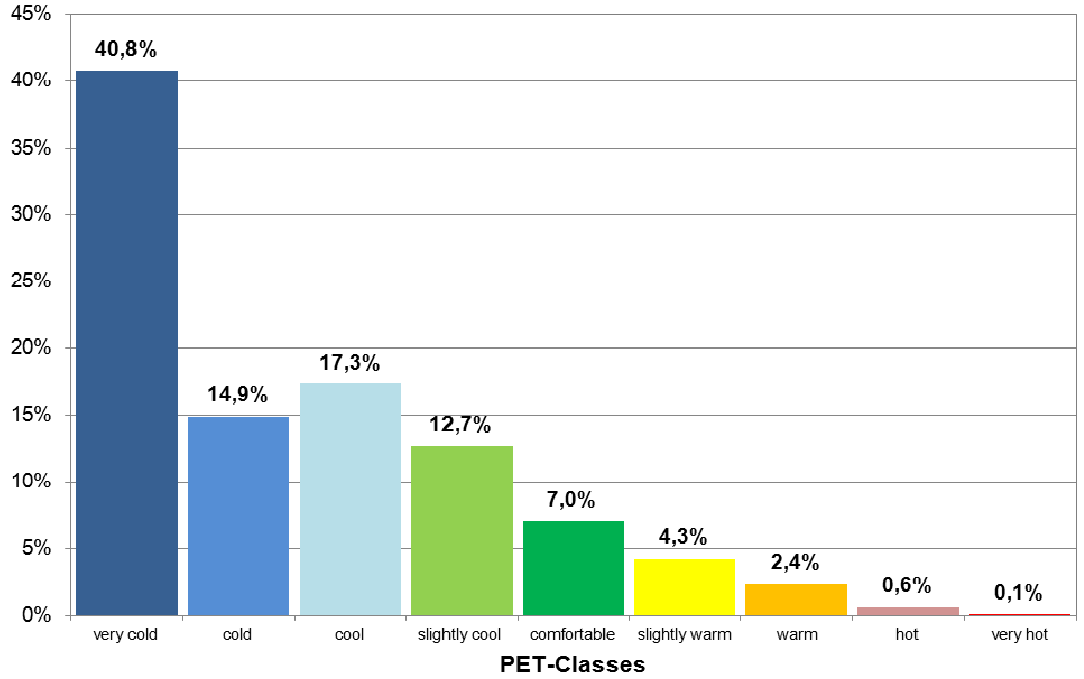

Fig. 1: PET-Classes at the urban climate station Freiburg for the period September, 1st 1999 to December 31st, 2009

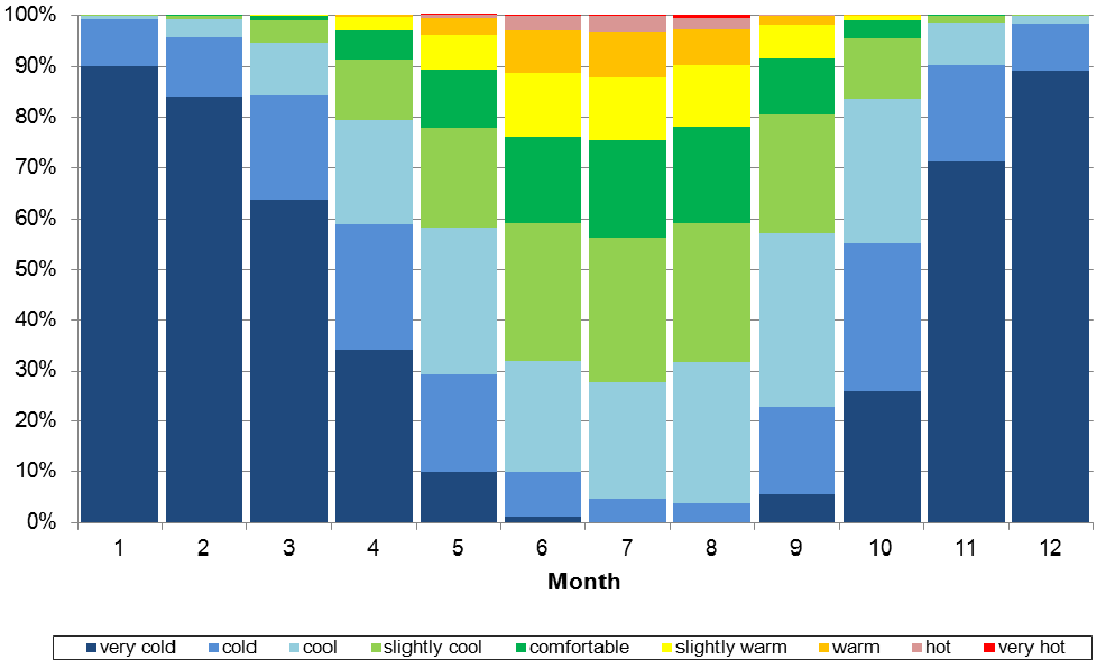

Fig. 2: Monthly Frequency distribution of PET at the urban climate station Freiburg for the period September, 1st 1999 to December 31st, 2009

Fig. 3 and 4 show respectively the diurnal course of the T_{mrt} of an idealized urban canyon in Freiburg in North-South (Fig. 3) and East-West (Fig. 4) orientation. The height of the canyon in both cases is 15 m height and the width is variable from 5 to 40 m. In addition, in the figure is the T_{mrt} at the urban climate station Freiburg included.

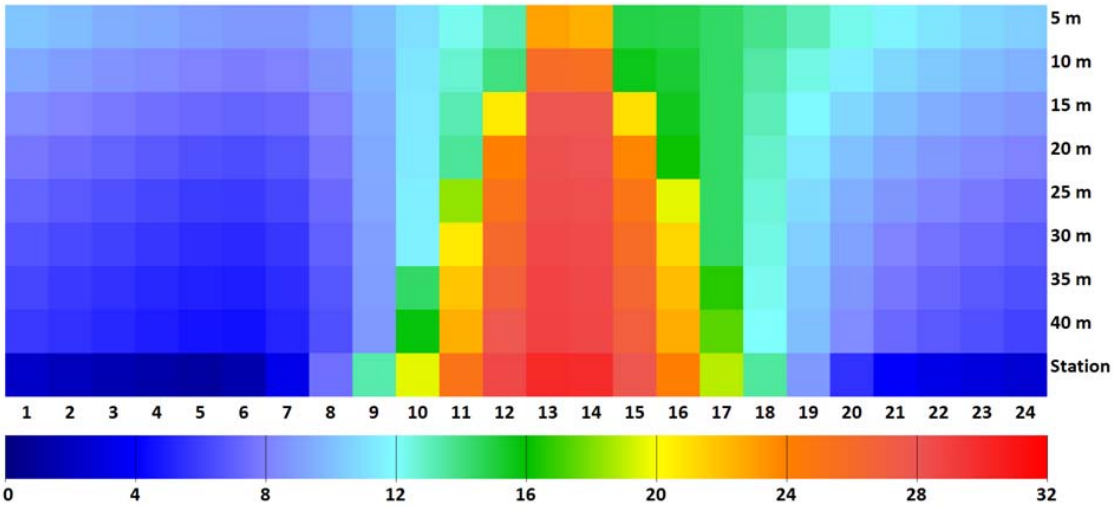

Fig. 3: Diurnal course of T_{mrt} (°C) for an urban canyon with Nord-South orientation, 15 m height and variable width (5 to 40 m) based on the data of the urban climate station and for the period September, 1st 1999 to December 31st, 2009

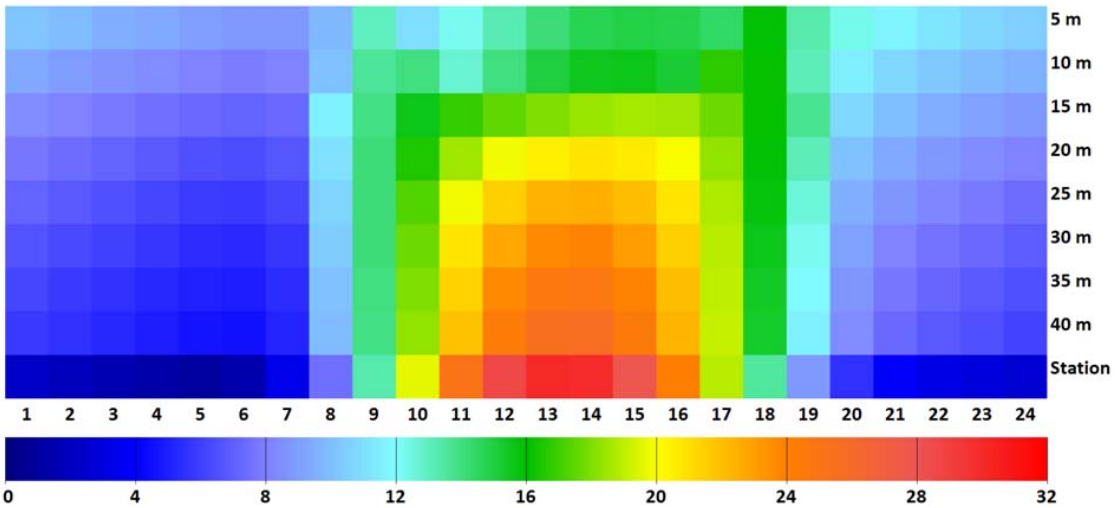

Fig. 4: Diurnal course of T_{mrt} (°C) for an urban canyon with East-West orientation, 15 m height and variable width (5 to 40 m) based on the data of the urban climate station and for the period September, 1st 1999 to December 31st, 2009

From both figures 3 and 4 is can be seen that during the night hours the conditions are similar because of the absences of the global radiation. During the day hours the picture

is very clear and at highest in the North-South orientation with width > 15 m reach the highest values. For the East-West orientation (Fig. 4) the increase is lower and do not reach the high T_{mrt} values up to 40 m.

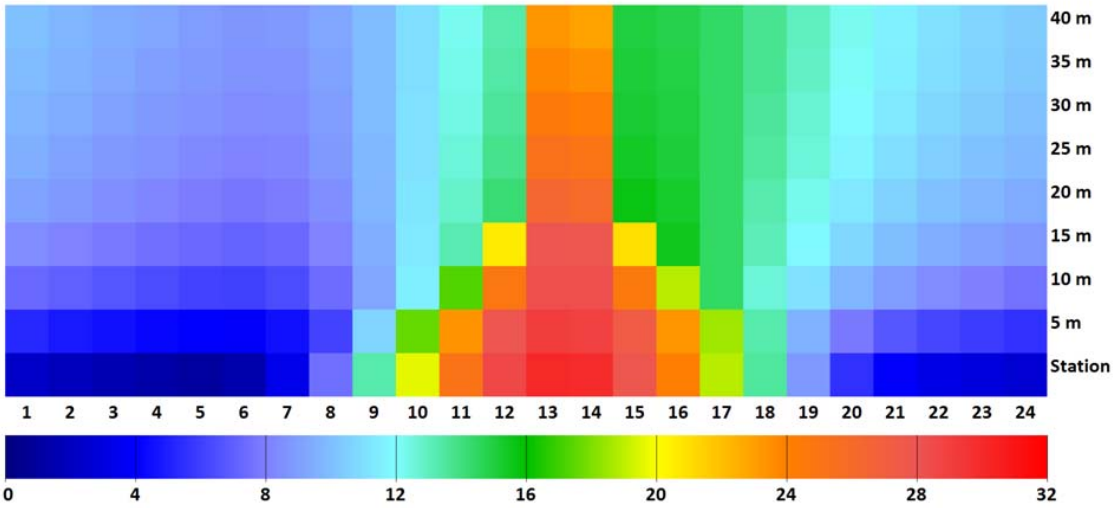

Fig. 5: Diurnal course of T_{mrt} (°C) for an urban canyon with North-South orientation, variable height (5 to 40 m) and 15 m width based on the data of the urban climate station and for the period September, 1st 1999 to December 31st, 2009

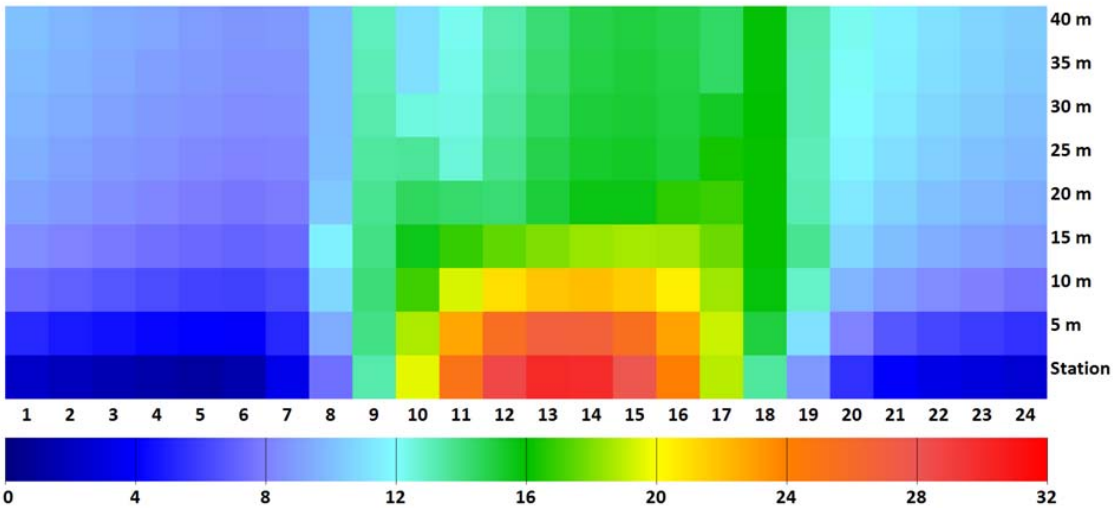

Fig. 6: Diurnal course of T_{mrt} (°C) for an urban canyon with East-West orientation, variable height (5 to 40 m) and 15 m width based on the data of the urban climate station and for the period September, 1st 1999 to December 31st, 2009

Fig. 5 and 6 show respectively the diurnal course of the T_{mrt} of an idealized urban canyon in Freiburg in North-South (Fig. 5) and East-West (Fig. 6) orientation. The width of the canyon in both cases is 15 m and the height is variable from 5 to 40 m. In addition in the figure is the T_{mrt} at the urban climate station Freiburg included. From Fig. 5 and 6 it can be seen that during the night the differences in both orientations and configurations

do not differ significantly. Concerning the different orientation the conditions depend of the different height of buildings used.

Fig. 7 shows the step wise (15 °) rotation of the urban canyon with a height and width of 15 m.

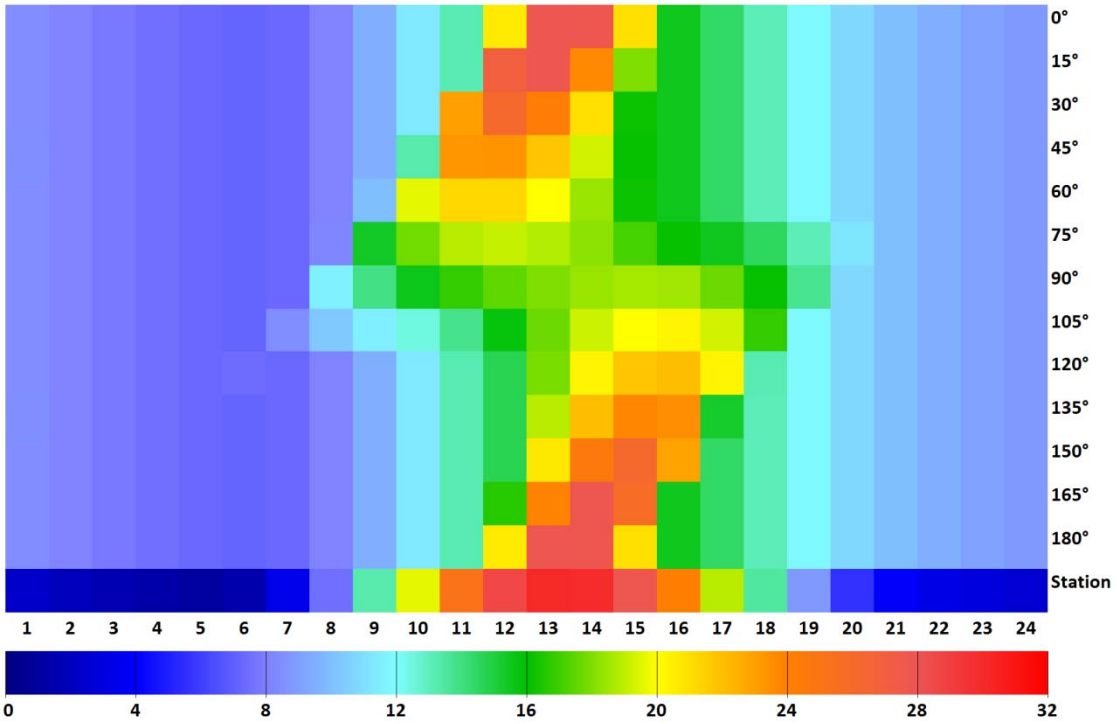

Fig. 7: Diurnal course of T_{mrt} (°C) for an urban canyon with steps of 15 ° rotation for a 15 m height and 15 m width based on the data of the urban climate station and for the period September, 1st 1999 to December 31st, 2009

The orientations 0 ° and 180 ° in Fig. 7 are identical and are marked as North-South orientation in the previous Figures. Equally, East-West is marked as 90 ° in Fig. 7. The results of these orientations can be also found in the other diurnal courses of T_{mrt} (Fig. 3, 4, 5, 6).

Fig. 7 shows that North-South and East-West orientations are the two extrema with highest values of T_{mrt} for North-South and lowest values for East-West during midday. The rotation in both directions starting at 0 ° reduces the values during midday and offset the maximum value of T_{mrt} towards the morning or the evening while the overall daytime values are decreasing. This leads to the described situation for 90 °. The conditions during the night are very similar due to the lack of global radiation, but the orientation of the canyon also affects the timing of the first increase of T_{mrt} in the morning.

4. Discussion and conclusion

The performed simulations show that the mean radiant temperature and also the thermal bioclimate conditions in urban areas can be affected strongly by the urban configura-

tion. Width, height and orientation of an urban canyon are all very important parameters for the evaluation of specific thermal bioclimatic conditions. It is evident that based on radiation fluxes estimations and simulations results can be derived which are important not only for basic research but also for urban planning issues in order to quantify the mean thermal bioclimatic conditions of a region or location.

In this study, existing long-term data of an urban climate station were used for a micro-scale urban bioclimatic simulation. As far as specific biometeorological measurements are not an option because of effort, time, costs or conditions, it is a good alternative to obtain required thermal bioclimatic data. Especially the comparison of different street configurations with the same input data, like realized in this study, is a realistic scenario. It could be an effective way for a global comparison of different urban areas in different climate regions.

References

Höppe, P., 1993: Heat balance modelling. Experientia 49, 741-746.

Höppe, P., 1999: The physiological equivalent temperature – a universal index for the biometeorological assessment of the thermal environment. Int. J. Biometeorol. 43, 71-75.

Lin, T.-P., Matzarakis, A., Hwand, R.-L., 2010: Shading effect on long-term outdoor thermal comfort. Building and Environment 45, 213-211.

Matzarakis A, Mayer H, 2008: Importance of urban meteorological stations - the example of Freiburg, Germany. Ber. Meteor. Inst. Univ. Freiburg 17, 119-128.

Matzarakis, A., F. Rutz, H. Mayer, 2007: Modelling Radiation fluxes in simple and complex environments – Application of the RayMan model. Int. J. Biometeorol. 51, 323-334.

Mayer, H., 1993: Urban bioclimatology, Experientia 49, 957-963.

Röckle, R.; Richter, C.-J., Höfl, H.-C.; Steinicke, W.; Streifeneder; M.; Matzarakis, A., 2003: Klimaanalyse Stadt Freiburg. Auftraggeber Stadtplanungsamt der Stadt Freiburg. November 2003.

VDI, 1998: Methods for the human-biometerological assessment of climate and air hygiene for urban and regional planning. Part I: Climate, VDI guideline 3787. Part 2. Beuth, Berlin.

Authors' address:

Jan Herrmann (jh.mail@t-online.de)
Prof. Dr. Andreas Matzarakis (andreas.matzarakis@meteo.uni-freiburg.de)
Meteorological Institute, Albert-Ludwigs-University of Freiburg
Werthmannstr. 10, D-79085 Freiburg, Germany

Designing with Urban Wind for Hong Kong

Edward Ng[1], Xipo An[1], Lutz Katzschner[2]

[1] School of Architecture, Chinese University of Hong Kong, Hong Kong SAR
[2] Department of Environmental Meteorology, University Kassel, Germany

Abstract

Hong Kong is one of the world's highest-density cities, with over sixty thousand persons per square kilometer in its urban areas. High-rise, bulky and closely packed buildings are the norm, This reduces urban air ventilation. Since 2003, the Hong Kong Government has commissioned studies on the issue; an air ventilation assessment (AVA) study was carried out. One of the key issues regarding the AVA assessment and the planning quest for better urban ventilation is a need for a better understanding of the wind environment. In a nutshell, what kind of wind are we designing for in our city? What are the characteristics of this wind? This paper elaborates piloted efforts to understand the Hong Kong's wind environment based on a detailed analysis of Hong Kong observatory's ten year wind data. It can be concluded that designing for the available wind can be a very complicated matter especially when the city is affected by various phenomena like topography, land and sea breezes, and so on.

1. Introduction

High density city design is a topical issue. There is a need to deal with the scarcity of land, to design for a viable public transport system, and to re-build the community of our inner cities. High density living is increasing an issue that planners have to confront with. Hong Kong is a high density city with a population of 8 millions living on a piece of land of 1,000 square kilometres. The urban density of Hong Kong is close to 60,000 persons per square kilometre. The site development density can be up to 3000 persons per hectare.

The unfortunate events of Severe Acute Respiratory Syndrome (SARS) in 2003 have brought the Government and inhabitants of Hong Kong to the realization that a "quality" built environment should be an aim for Hong Kong. Gradation of development height profiles, provision of breezeways, layout planning and disposition of building blocks to allow for more open spaces, greater building setbacks to facilitate air movement, reduction of development intensity, increase open space provisions especially in older districts and more greenery, are coined as measures in the Team Clean Report 2003 to improve the built environment. The report also highlights the need to establish an objective assessment method of urban air ventilation to guide future planning actions. [1] In 2006, the Government of Hong Kong promulgated the Air Ventilation Assessment (AVA) Method that has now been adopted in Hong Kong to guide developments.

Wind Velocity Ratio (VRw) is used as an indicator. $V\infty$ is the wind velocity at the top of the wind boundary layer not affected by the ground roughness, buildings and local site features (typically assumed to be a certain height above the roof tops of the city centre and is site dependent). Vp is the wind velocity at the pedestrian level (2m above ground) after taking into account the effects of buildings. $Vp/V\infty$ is the Wind Velocity Ratio (VRw) that indicates how much of the wind availability of a site can be experi-

enced and enjoyed by pedestrians on ground taking into account the buildings in between. As VRw is solely affected by the buildings of the location, it is a simple indicator one may use to assess the effects of proposals – higher the value of VRw, lesser the impact of buildings on wind availability. (Figure 1)

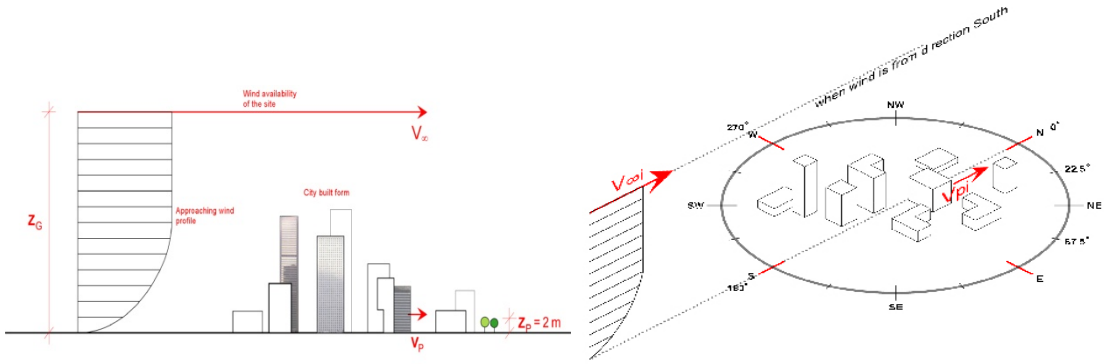

Fig. 1: The figures show how VRi and VRw are calculated

The wind performance understanding of the AVA method replies on the V∞, being the wind velocity at the top of the wind boundary layer not affected by the ground roughness. This is the synoptic wind of the city. In order for the city to capture this available, its directions and speeds are important to note; and since AVA is a weak wind assessment method, the directions of the available wind at low and medium speeds are of greater concern.

2. Observed wind

The Hong Kong Observatory observed data serves as the first step understanding the available wind of the city. There are more than 40 stations positioned in various places in Hong Kong (Figure 2). The data is extracted and presented as wind roses in Figure 3 and 4).

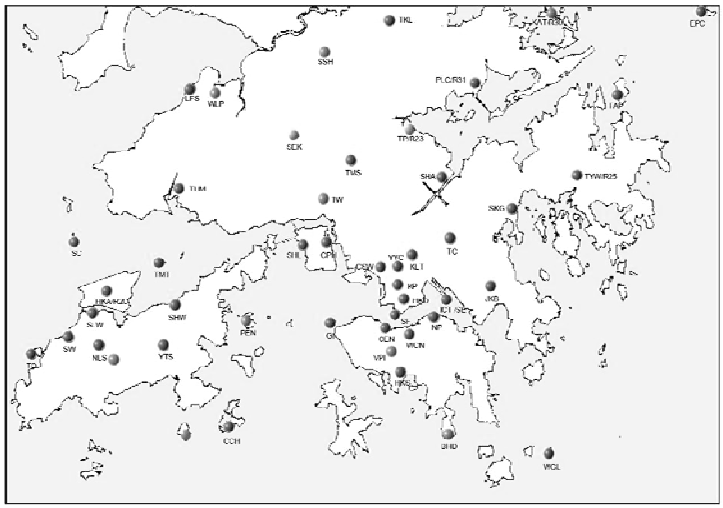

Fig. 2: Locations of Hong Kong Observatory wind stations

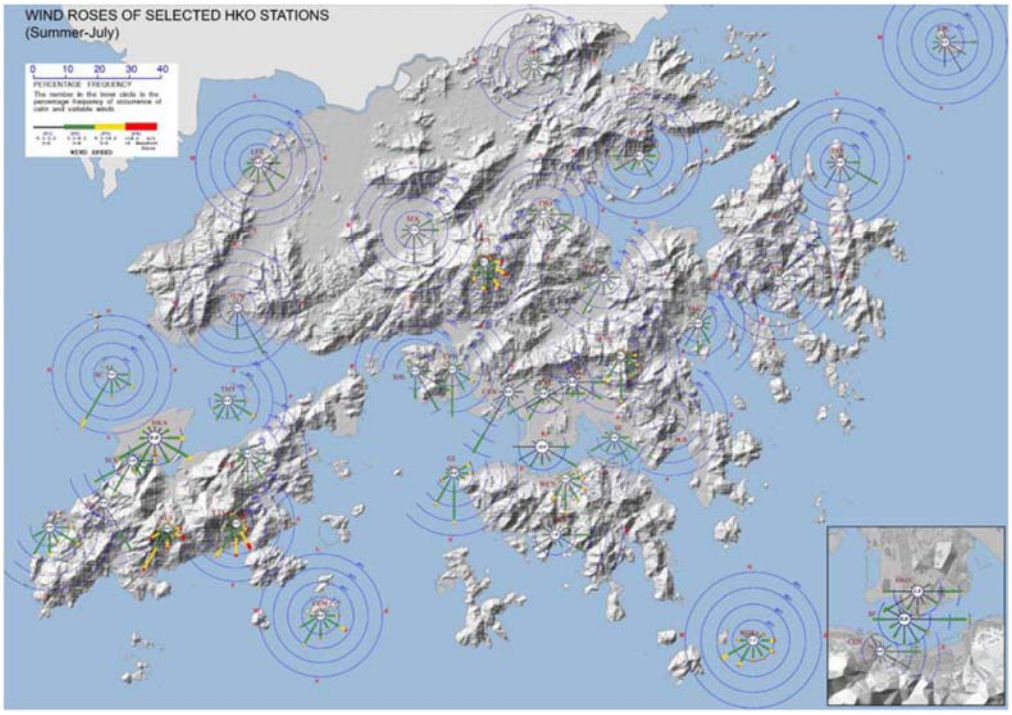

Fig. 3: Wind roses of Hong Kong Observatory wind stations (summer months of June to August). The topography of the land is show. The highest mountain is about 1000m above sea level

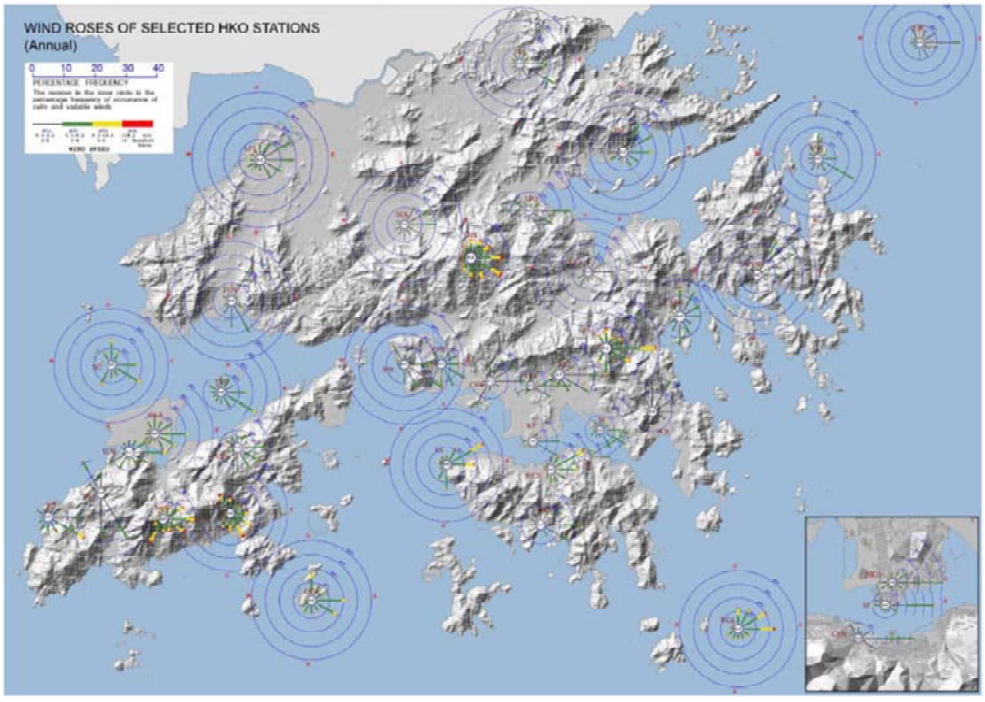

Fig. 4: Wind roses of Hong Kong Observatory wind stations (annual)

This first cut understanding demonstrates the complex wind field of Hong Kong due to the seasons, topography and the land and sea breezes. Based on the reference wind station of Walgen Island (WGL) at the bottom right corner of Figure 3 and 4, annually,

winds come from the East and north-East. In the critical summer months, winds come from the South-West. Hence, if streets have to be aligned with the winds, it is obvious that it needs to be orientated North-East South-West.

The problem with this understanding is that in many parts of Hong Kong, the wind directions are different. For example, in the Victoria Habour (inserted diagram at the bottom right hand corner), a strong channeling effect can be observed. Hence it is more important for street s to be East West orientated.

3. Land and Sea breezes

Apart from the complex topography of the land, Hong Kong is surrounded on three sides with the sea. Strong land sea breezes effects are experienced (Figure 5). It is therefore necessary to consider not only the seasonal effects of the wind availability, but also the temporal effects of daily changes.

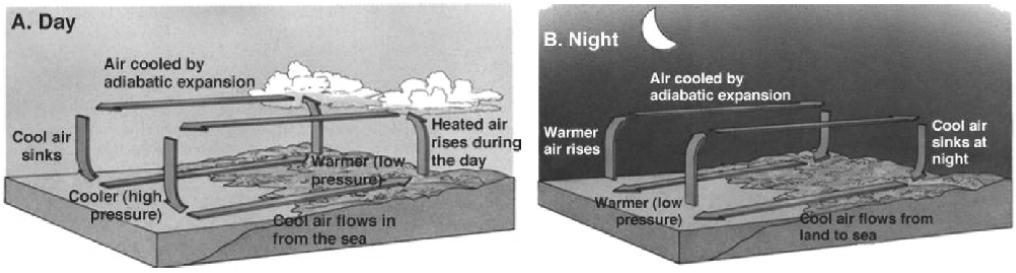

Fig. 5: A schematic understanding of the land and sea breezes effects

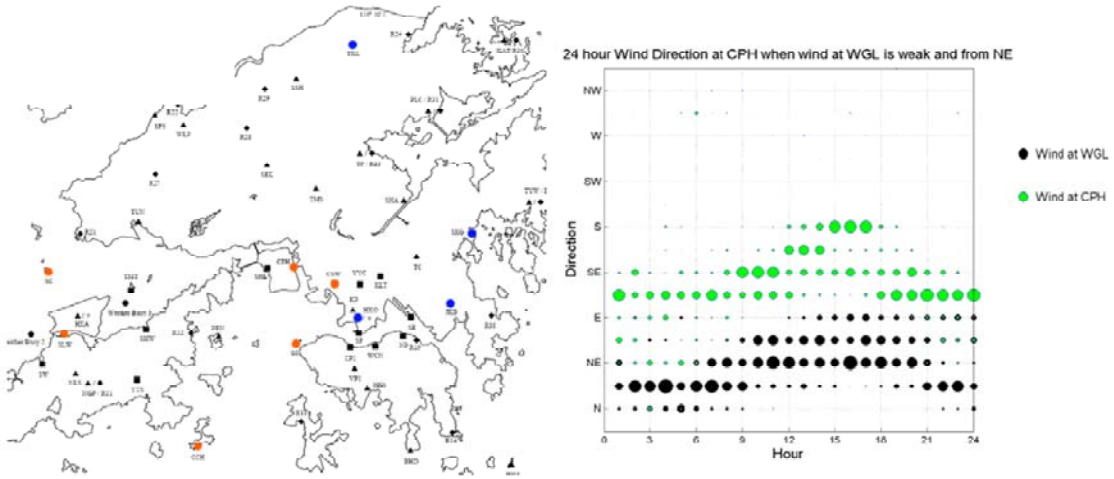

Fig. 6: (Left) Hong Kong Observatory stations on the western side of the territory shows stronger land and sea breeze effects. (Right) Hence, it is noted that when the synoptic wind of WGL, being the Hong Kong's reference wind station 9on the south-east corner of the map0 is recording North-East winds in the afternoon, a station on the western side of the territory is at the same time experiencing South winds

A 24 hour wind simulation taking into account the land and sea breeze effects has been conducted using MM5 (Figure 7).

As such it is important to note the important question: what time is wind most needed. For subtropical summer conditions of Hong Kong, it is opined that for urban human comfort, wind in the afternoon is most needed. Hence, it is more important to factor in the sea breezes than the land breezes. The prevailing directions of the sea breezes of a locality are therefore important to sort out.

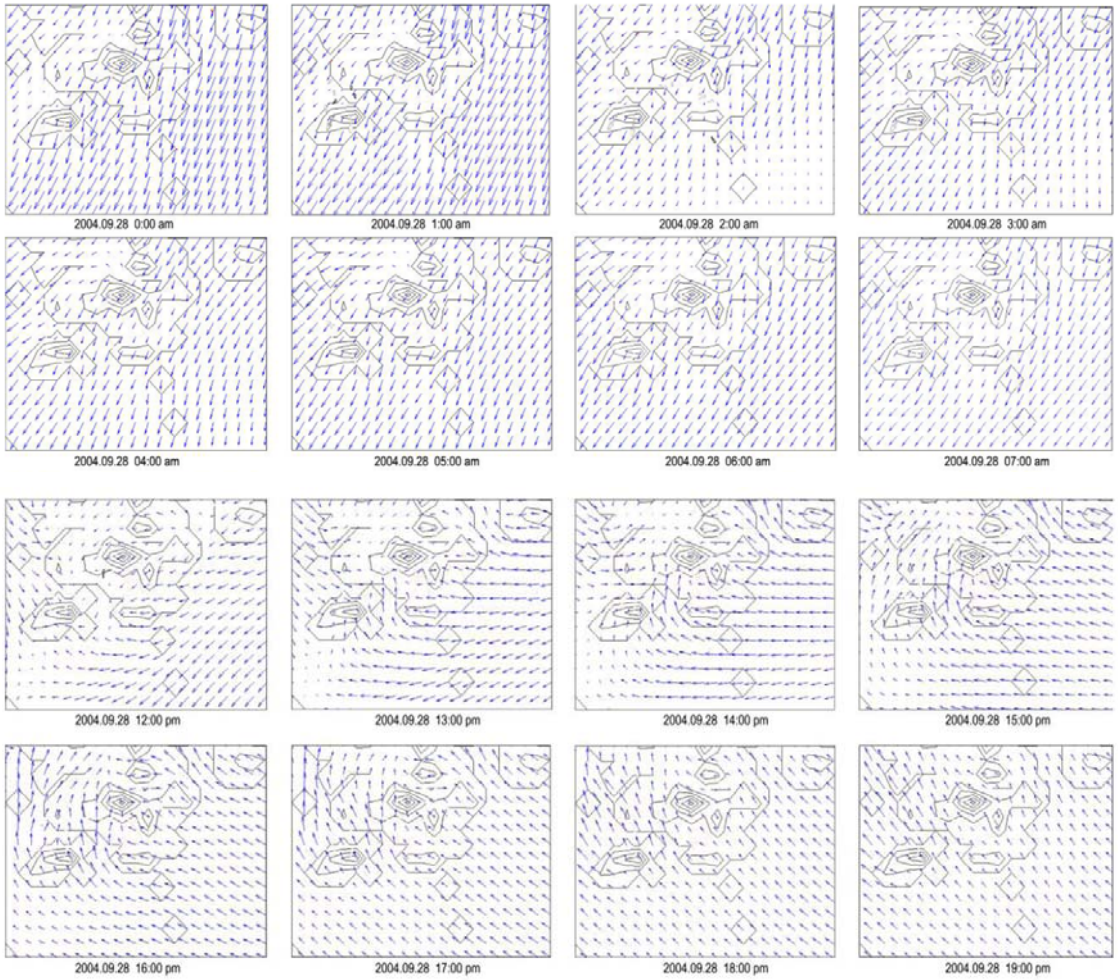

Fig. 7: A 24 hour MM5 simulation is conducted. It shows clearly the land breezes at night and the sea breezes in the afternoon hours

4. Strong vs. Weak Winds

Apart from the topographical and the temporal understanding, it is important to know the relationship between wind speeds and wind directions. Since the AVA method is a weak wind assessment method. It is important to make sure that under weak wind conditions, the streets are still well ventilated aligning with the prevailing wind directions. As demonstrated in Figure 8. In this case, at this locality, it is important to factor in a consideration of the weak summer wind coming from the South-West despite the prevailing East wind direction.

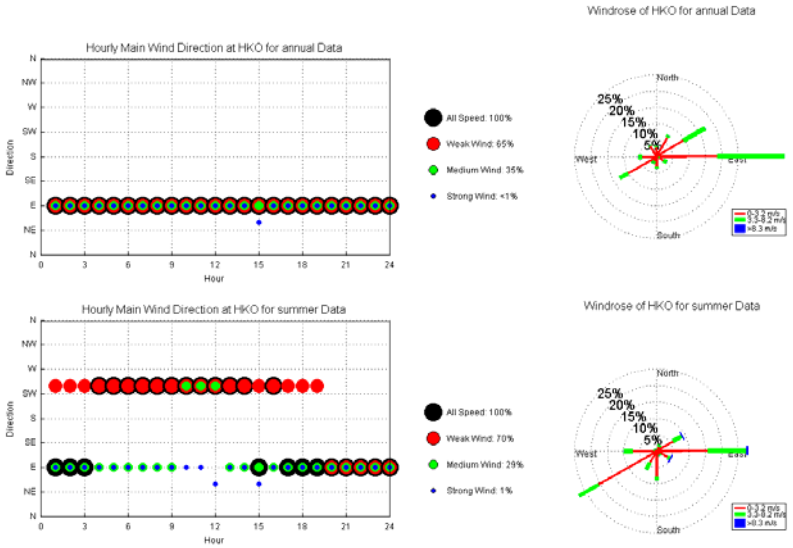

Fig. 8: A detail analysis of HKO's wind data shows that the weak wind direction is different from the strong wind direction in the summer months

5. Conclusions

This extended abstract highlights the importance of understanding the "weak wind" available for design in complex situations. It summarises various understandings that are necessary for better planning and design decision making.

Acknowledgement

Thanks are due to Professor Jimmy Fung of HKUST for providing the MM5 wind simulation data. Thanks are also due to the Hong Kong Observatory for providing the 10 year (1997 to 2006) data for analysis.

References

Team Clean, 2003: Report on Measures to Improve Environmental Hygiene in Hong Kong, HKSAR. 87.

Authors' address:

Prof. Dr. Edward Ng (edwardng@cuhk.edu.hk)
School of Architecture, Chinese University of Hong Kong
Shatin NT, Hong Kong

Mrr. Xipo An (anxipo@cuhk.edu.hk)
School of Architecture, Chinese University of Hong Kong
Shatin NT, Hong Kong

Prof. Dr. Lutz Katzschner (katzschn@uni-kassel.de)
Department of Environmental Meteorology, University Kassel
Henschelstr. 2, D-34127 Kassel, Germany

Estimation of sky view factor in complex environment as a tool for applied climatological studies

Olaf Matuschek, Andreas Matzarakis

Meteorological Institute, Albert-Ludwigs-University Freiburg,
Werthmannstr. 10, 79085 Freiburg

Abstract

Graphic processors can be implemented in computation models, e.g. in three-dimensional flow visualization. Another possibility going a step further, and propose modern graphics hardware to be used as general-purpose vector computers. These ideas and approaches use a cheap mass technology to solve specific problems. This technology and way can be applied for climate conditions or climate relevant parameters in urban scale or complex environments. Following benefits are provided from the new model: (a) short computing time and (b) low costs though the use of open source frameworks. We chose the implementation of sky view factor (SVF) for each point in a complex area, given by a digital elevation model (DEM) and urban obstacles (OBS) in order to quantify relevant climatic conditions in urban and complex areas.

1. Introduction

We show how 3D hardware can be used to improve modeling of sky view factor (SVF) in complex urban environments. Modelling of climate processes in urban areas is still challenging, some authors find it to be one of the most difficult areas in climatology (MATZARAKIS, 2001; KUTTLER, 2004a, b). The visible horizon is modified by surrounding urban structures and obstacles, radiation fluxed are altered. This results in alteration of a location's bioclimate, as radiation fluxes are one of the main factors of thermal comfort equations. The modification of urban structures can be estimated by measurement or calculation of sky view factor (MATZARAKIS *et al.*, 2007). SVF is one of the most relevant input parameters for estimating radiation fluxes in complex environments.

Powerful yet cheap graphic processors have recently been employed to implement computation intensive models, e.g. in three-dimensional flow visualization (CUNTZ *et al.* 2007). Other researchers use modern graphics hardware as a general-purpose vector computer (THOMPSON *et al.,* 2002). The idea is the same: a cheap mass technology is utilized to solve specific and specialized problems. This approach can be applied in climate or urban climate modelling as well.

We start with an overview of traditional methods of calculating SVF. A short chapter on different methods of utilizing graphics hardware follows. We then present the new efficient SVF model SkyHelios to calculate continuous SVF. In two examples, one vector, and one raster based, the chances and drawbacks of both approaches are shown. Finally the possibilities and limits of the new model are examined and discussed.

2. Methods to estimate SVF

Measurement and calculation of SVF has some history in urban climate research (STEYN 1980; JONHSON & WATSON 1984; WATSON & JOHNSON; 1987, 1988; HOLMER,

1992), though is still subject to intensive research (LITTLEFAIR, 2001; GRIMMOND *et al.*, 2001; RATTI *et al.* 2004; MATZARAKIS *et al.,* 2007; GÁL *et al.,* 2008).

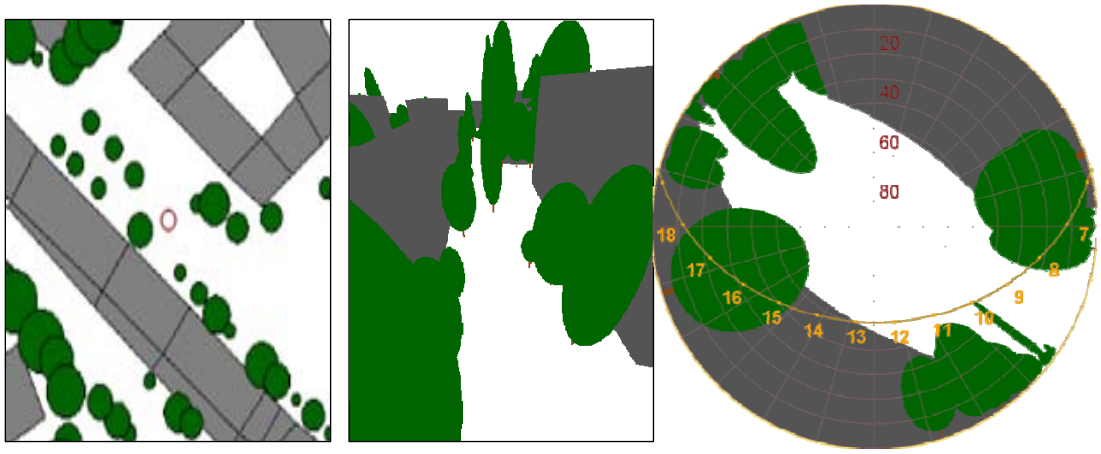

Fig. 1: Example of a modelled sky view factor image and its relation to the surrounding urban structure. a) view from top. b) birds eye view on the scene. c) sky view image. Sunpath shown for 48°N mid of April

The most traditional way to measure SVF ist to take a 180° fisheye photograph (CHEN & BLACK, 1991, LITTLEFAIR, 2001). Usually the camera sits on a tripod at 1 m height, with a fisheye lens looking into the sky. Different ways have been examined to asses sky view information from the photo, including scaled paper paper (JOHNSON & WATSON 1984; FRAZER *et al.,* 2001), computer programs helping to manual track the sourroundings (HOLMER, 1992; CHAPMAN *et al.,* 2001; HOLMER *et al.,* 2001; TELLER and AZAR, 2001; MATZARAKIS *et al.,* 2007), and fully automatic tracking of the sourroundings by software (CHAPMAN *et al.,* 2001; BRUSE and FLEER, 1998). Augmented with digital cameras, this last approach can lead to a very quick assessment of SVF at a particlar spot.

Instead of taking photographs, sky view factor can be calculated from digital models of the environment. (BRUSE and FLEER, 1998; TELLER and AZAR, 2001; MATZARAKIS *et al.,* 2007). Calculation of SVF is based on knowledge of each angle element of the hemispheric environment and associated elevation (in connection with produced shadow) angle β and azimuth angle α. Accordingly, the sky view factor Ψs can be assumed to be the sum of all this angle information over the whole hemispheric environment.

$$\Psi_s = 1 - i\sum \sin^2 \beta_i \left(\frac{a_i}{360°} \right)$$

Caclulating SVF has the benefit that is it no longer required to actually go out and take a picture, a process in which a lot of errors can occur. Instead the models, e.g. RayMan (MATZARAKIS *et al.,* 2007), allow for quickly assessing SVF at different locations. Some models even allow for calculation of continuous sky view factor, i.e. the spacial distribution of sky view factors in an area or whole city (GÁL *et al.*, 2008). Most models are based on representations of buildings (SOUZA *et al.* 2003) or digital elevation models (DEM) (GÁL *et al.*, 2008), allowing only for simple shaped building and flat roofs.

A few models are based on the idea of obstacles, allowing for modelling non-flat roofs and trees as well (MATZARAKIS *et al.,* 2007). Including non-flat roofs and trees into modelling seems to be cruical at least for modelling central european cities.

Fig. 1 shows the connection between surrounding structures and a SVF image. The sky view factor can be easily caclulated from it by dividing the area of the image that is not covered by obstacles by the total image area. Sky view factor in the example in Fig. 1 is 0.31, i.e. only 31 % of the sky is visible. The sunpath is shown for a latitude of 48° mid of April. Even though the sun is above the horizon from ca. 6:00 am to 7:00 pm, the selected location gets direct sunshine only from ca. 8:15 am to 1 pm.

3. Utilizing graphics hardware for modelling

While graphics hardware has primarily been developed to perform graphics display on a personal computer, modern 3D-graphics hardware has reached a level at which it can be seen as a general purpose vector computer (THOMPSON et al. 2002). A vector computer is one that performs the same operation on multiple data sets very efficiently. Therefore modern 3D-hardware has a lot of potential appplications in modelling, e.g. three dimensional climate flow data visualization (CUNTZ *et al.* 2007). More possibilities arise, when one does not only visualize modelling results, but reads results back from the graphics hardware. When applicable for vector processing, time intensive modelling algorithms can be transferred on the graphics hardware, with the result of a substancial reduction in processing time in the order of several magnitudes. We transferred the SVF calculation algorithm on the graphics hardware, making use both of the graphics rendering capabilities of the hardware as well of its function as a general purpose vector computer.

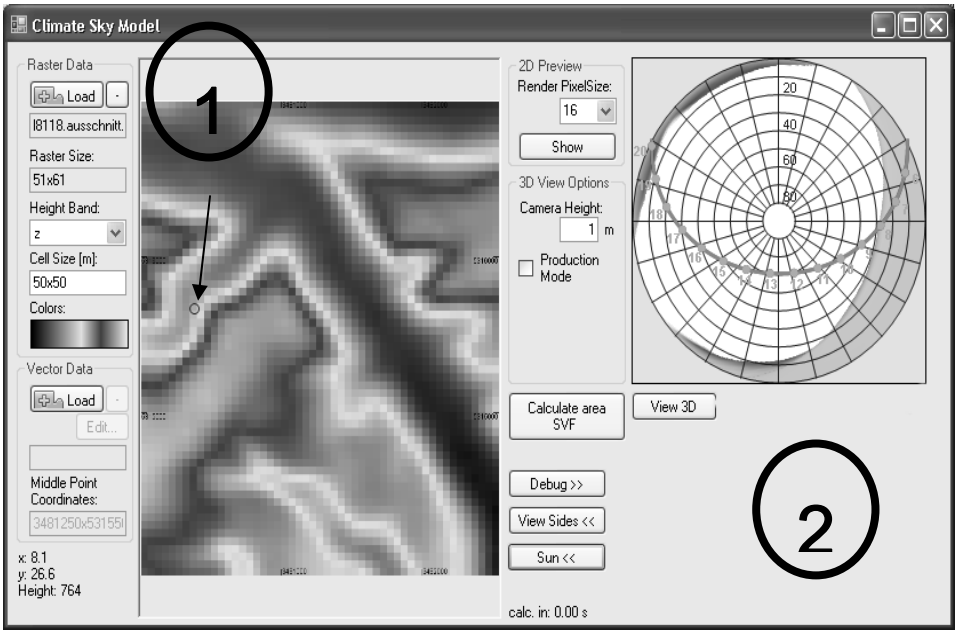

Fig. 2: Screenshot of SkyHelios and view of the sky view factor image (based on topographical data) with sun locations for Freiburg end of July. Arrow indicates selected location for the Sky View Factor

4. Raster and vector calculations with SkyHelios model

Fig. 2 shows am image of the user interface of SkyHelios. A digital elevation model (DEM) has been loaded and is shown for orientation in the left part of the sceen. A circle indicates current position for the calculation of the sky view factor image and SVF. The sky view factor image is shown on the right, overlaid with the sun positions at a latitude of 48° N for a date end of July. When "production mode" is checked, the SVF for the correspodung location is immediately calculated. Since making use of 3D graphics hardware, calculation of SVF with SkyHelios is fast. There is no delay between selecting the location and display of resulting SVF.

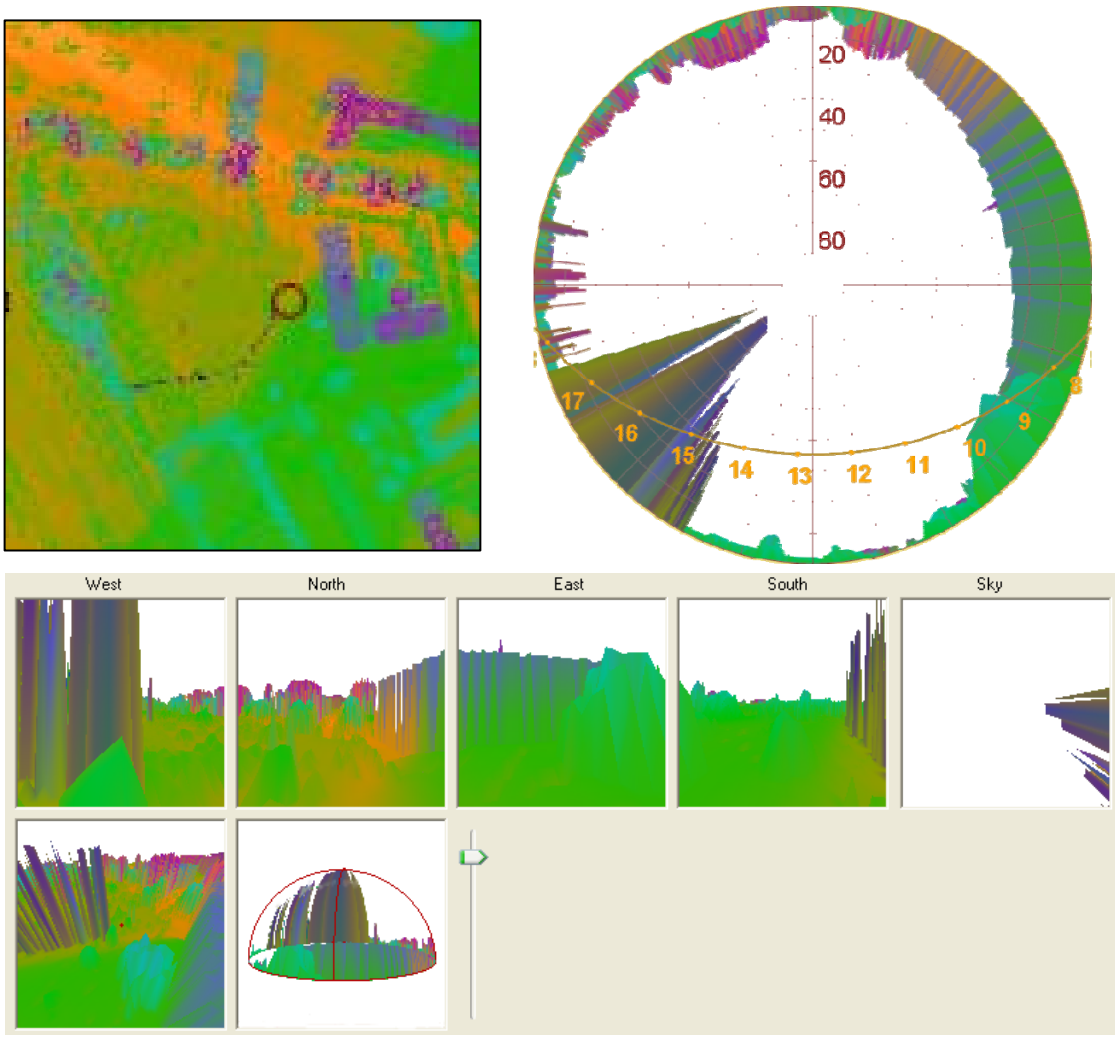

Fig. 3: A location in Freiburg, Germany, based on laser data. Top view, sky view factor image for a tripod height of 10 m and corresponding bird's eye view as well as view into all for directions and the sky

Fig. 3 shows sky view factor calculation of a location in Freiburg, Germany. The calculation is made with a DEM based on laser data with a resolution of 1 m. The top view image shows a building to the east, and a row of probably trees to the west. There are more building and trees to the north and south. The corresponding SVF image was calculated for a tripod height of 10 m, giving a SVF of 0.69. Using a laser DEM for calculation of sky view factor allows for a rapid estimation of sky view factor for a whole city (GÁL *et al.*, 2008). The sky view factor image and more so the side views and the

bird's eye view though clearly show drawbacks of using raster DEM. While the building to the east seems to be quite well modelled, what are probably trees appears to be hight but narrow "needles" looking into the sky. Their shape e.g. trunk and crown can not be modelled with a DEM based approach. The vector based approach, shown on Fig. 1, allows for modelling of trees and non-flat roof buildings as well. It has the drawback that vector models of cities are not as readily available as are DEM.

5. Discussion and conclusion

We show how computer graphics hardware can improve climate 3D modelling in applied climatology for complex environments. Several visualization techniques can help understanding of possibilities and limits when modelling SVF. SkyHelios allowes to export results for dispay in the climate mapping tools (MATUSCHEK and MATZARAKIS, 2010). Frequently-used data formats (i.e., laser or satellite data) are supported. Direct implementation of RayMan obs files (MATZARAKIS *et al.*, 2007) is an advantage, and furthermore the combination of raster and vector approaches is possible.

The visualization of morphological factors (especially in urban areas) helps to understand micrometeorological processes. The sky view factor expresses the morphological factors for a specific site in one single value, and therefore allows for an estimation of relevant climatological information. We plan to implement the spatial extension of radiation fluxes and the mean radiant temperature with very high resolution. In order to get radiation fluxes, many additional features (such as shadow generation and sunshine duration) are required from the morphological option.

SkyHelios is freely available and can be requested from the authors.

References

Chapman, L., J. E. Thornes, A.V. Bradley, 2001: Rapid determination of canyon geometry parameters for use in surface radiation budgets. Theoretical and Applied Climatology **69**, 81–89.

Chen, J. M., T. A. Black, 1991: Measuring leaf area index of plant canopies with branch architecture. Agric. Forest Meteorol. **57**, 1–12.

Cuntz, N., A. Kolb, M., Leidl, C., Rezk-Salama, M. Böttinger, 2007: GPU-based Dynamic Flow Visualization for Climate Research Applications. In: Schulze, T.; Preim, B.; Schumann, H. (Hg.): Simulation und Visualisierung 2007 (SimVis 2007), 8-9 März 2007, Magdeburg: SCS Publishing House e.V., 371–384.

Gál, T., F. Lindberg, J. Unger, 2008: Computing continuous sky view factors using 3D urban raster and vector databases: comparison and application to urban climate. Theoretical and Applied Climatology **95**, 111-123.

Grimmond, C. S. B, S. K. Potter, H. N. Zutter, C. Souch, 2001: Rapid methods to estimate sky-viw factors applied to urban areas. Int. J. Climatology **21**, 903-912.

Holmer, B., 1992: A simple operative method for determination of sky view factors in complex urban canyon from fisheye photographs. Meteorol. Z., NF **1**, 236–239.

Holmer, B., Postgärd, U., Eriksson, M., 2001: Sky view factors in forest canopies calculated with IDRISI. Theor. Appl. Climatol. **68**, 33–40.

Johnson, G. D, I. D. Watson, 1984: The determination of view-factors in urban canyons. J. Clim. Appl. Meteorol. **23**, 329–335.

Kuttler, W., 2004a: Stadtklima, Teil 1: Grundzüge und Ursachen. UWSF – Zeitschrift für Umweltchemie und Ökotoxikologie **16**, 187-199.

Kuttler, W., 2004b: Stadtklima, Teil 2: Phänomene und Wirkungen. UWSF – Zeitschrift für Umweltchemie und Ökotoxikologie **16**, 263-274.

Littlefair, P., 2001: Daylight, sunlight and solar gain in the urban environment. Solar Energy **70**, 177–185

Matzarakis, A., 2001: Die thermische Komponente des Stadtklimas. Ber. Meteorol. Inst. Univ. Freiburg Nr. 6

Matzarakis, A., F. Rutz, H. Mayer, 2007: Modelling Radiation fluxes in simple and complex environments – Application of the RayMan model. Int. J. Biometeorol. **51**, 323-334.

Matuschek, O., A. Matzarakis, 2010: Climate Mapping Tool – Creating maps for climatological and biometeorological applications. Meteorological Applications (submitted).

MOGRE, 2009: MOGRE. URL: http://www.ogre3d.org/wiki/index.php/MOGRE [Stand: 16. Januar 2009].

Ratti, C., P. Richens, 2004: Raster analysis of urban form. Environment and Planning B: Planning and Design **31**, 297–309.

Souza, L. C. L., D. S. Rodrigues, J. F. Mendes, J. F., 2003: The 3dskyview extension: an urban geometry access tool in a geographical information system. Proceedings of the Fifth International Conference on Urban Climate (ICUC-5), Lodz.

Steyn, D. M., 1980: The calculation of view factors from fisheye lens photographs. Atmosphere-Ocean **18**, 254-258.

Teller, J., S. Azar, 2001: TOWNSCOPE II - A computer system to support solar access decision-making. Solar Energy **70**, 187-200.

Thompson, C. J., S. Hahn, M. Oskin, 2002: Using modern graphics architectures for general-purpose computing: a framework and analysis. MICRO 35. Proceedings of the 35th annual ACM/IEEE international symposium on Microarchitecture. Los Alamitos, CA, USA: IEEE Computer Society Press, 306–317.

Watson, I. D., G. T. Johnson, 1987: Graphical estimation of sky viewfactors in urban environments. J. Climatology **7**, 193–197.

Watson, I. D. Johnson, G. T., 1988: Estimating person view factors from fish-eye lens photographs. Int. J. Biometeorol. **32**, 123–128.

Authors' address:

Olaf Matuschek (olaf.matuschek@uni-freiburg.de)
Prof. Dr. Andreas Matzarakis (andreas.matzarakis@meteo.uni-freiburg.de)
Meteorological Institute, Albert-Ludwigs-University of Freiburg
Werthmannstr. 10, D-79085 Freiburg, Germany

Thermal comfort issues and deficiencies in measurements and modelling

Andreas Matzarakis

Meteorological Institute, Albert-Ludwigs-University of Freiburg, Germany

Abstract

Estimations for thermal comfort contain a pronounced variability in the spatial and temporal dimension. The exact calculations of thermal comfort for humans do not only depend on the used energy balance model of the human body but also on the meteorological input variables. In addition, the spatial dimension of thermal comfort conditions in both indoors and outdoors is an important factor, which cannot be described by usually running measurements networks. Approaches concerning the temporal dimension of thermal comfort issues exist but the spatial dimension in meteorological scales is less considered.

1. Introduction

Modern human biometeorological methods use the human energy balance of the human body in order to extract thermal indices and describe the effects of the thermal environment on humans (Mayer, 1993). The approach is very suitable and if a simple result or value is described as a temperature (e.g. physiologically equivalent temperature or standard effective temperature), which is more acceptable and understandable by applied sciences (Höppe, 1999, Matzarakis, 2006, Matzarakis and Amelung, 2008). In order to determine the components of the human energy balance, meteorological data and thermo-physiological information are required. The thermo-physiological data can be summarized for clothing and activity. They are well quantified in several studies and usually can be in terms set as standard for several studies in order to have comparable conditions (e.g. VDI, 1998). The meteorological data required are air temperature, air humidity (relative humidity or vapour pressure), wind speed and the synthetically human-biometeorological quantification of the short- and long wave radiation fluxes in terms of the mean radiant temperature (VDI, 1998, Matzarakis et al., 2007).

The availability of meteorological data is the first step in order to quantify thermal comfort or stress. From the data required usually air temperature and air humidity are available at most from synoptical or climatological networks (Matzarakis, 2006). Wind is usually included in synoptical observations and measured in 10 m height a.g.l. and has to be reduced for the human weighting center of 1.1 m a.g.l. The wind information from climatological or synoptical networks has to be also transformed from wind force to wind velocity. It has to be mentioned that at most the wind has a huge variability in the spatial dimension and also modified by regional and local climatological factors, e.g. land and sea breezes. Finally the mean radiant temperature is difficult to quantify due to atmospheric influences firstly by clouds and other meteorological compounds as vapour pressure or particles. In addition, the influences of topographical or urban morphologies in terms of obstacles modify mostly not only wind but also radiation properties in the meso- and micro scale (Lin et al., 2010). The data measured is based on different instruments and are accompanied with different resolutions and accuracy. So, the high challenge is often not the used method but the required and available data in the spatial

and temporal scale. Because of the complexity of instrument systems and their prices very often because of financial reason less expensive solutions are selected.

All this parameters or factors fitted in human energy balance models delivers a specific thermal index, which describe in an appropriate manner the thermal environment and can be used for several applications from global to micro scale issues (Matzarakis, 2008, Matzarakis and Amelung, 2008, Scott et al., 2009).

As mentioned before, there are two major factors that can influence the assessment of thermal comfort: a) the input data with their accuracy and variability and b) the method used for the quantification (VDI, 1998). The methods used rely on the human energy balance in steady state and assess the thermal environment solving the human energy balance for long period with considering the change in the meteorological conditions in the temporal scale. This assumption is used for different reasons, primary because of the calculation time.

A third important factor and often not considered is the mobility of humans and the frequency of use of a specific space. Dwellers have a high mobility during the day and, depending on the time of day they spend their time, due to several reasons, in- and outdoors. This makes an assessment of their thermal comfort conditions difficult, because the periods of stay have to be known. Another issue is quantifying from another point of view, the use of different spaces (i.e., parks, indoor and outdoor). A first approach, concerning this issue, is described as affect analysis, is given in the integral climate analysis for Freiburg (Röckle et al., 2003).

2. Methods and data

For the assessment of thermal comfort issues the meteorological information needed has to be adjusted and cannot be taken directly from a meteorological station or measurement network. The needed parameters (air temperature, air humidity, and wind speed) have to be converted to the gravity center of the human body (1.1 m). More complicated is the mean radiant temperature, which has to calculated or simulated.

Table 1: Human-biometeorological parameters in their spatial and temporal dimension required for the quantification of thermal comfort

Parameter	Spatial	Temporal
Air temperature	Medium	High
Vapour pressure	Medium	High
Wind speed	Big	Medium
Mean radiant temperature (short- long-wave radiation)	Big	Big
Activity	None	High
Clothing	None	Medium

Table 1 shows the spatial and temporal variability of the input parameters. So, for a diurnal quantification of thermal comfort the input parameters have to be known and be available considering their daily variability. In complex areas wind speed and mean radiant temperature have the highest variability and are modified by surroundings and obstacles. Many measurements are performed without the required quality and appropriateness, i.e. excluding artificial ventilation or without radiation shield in air temperature leading to errors in the results.

For this study, stationary measurements of the urban climate station of the Meteorological Institute of the University of Freiburg (Matzarakis and Mayer, 2009) and mobile systems (PCE-HT100) for air temperature and relative humidity are used.

3. Exemplary results

In the following three examples are given for the spatial and temporal variability of thermal comfort and meteorological parameters from the year 2009.

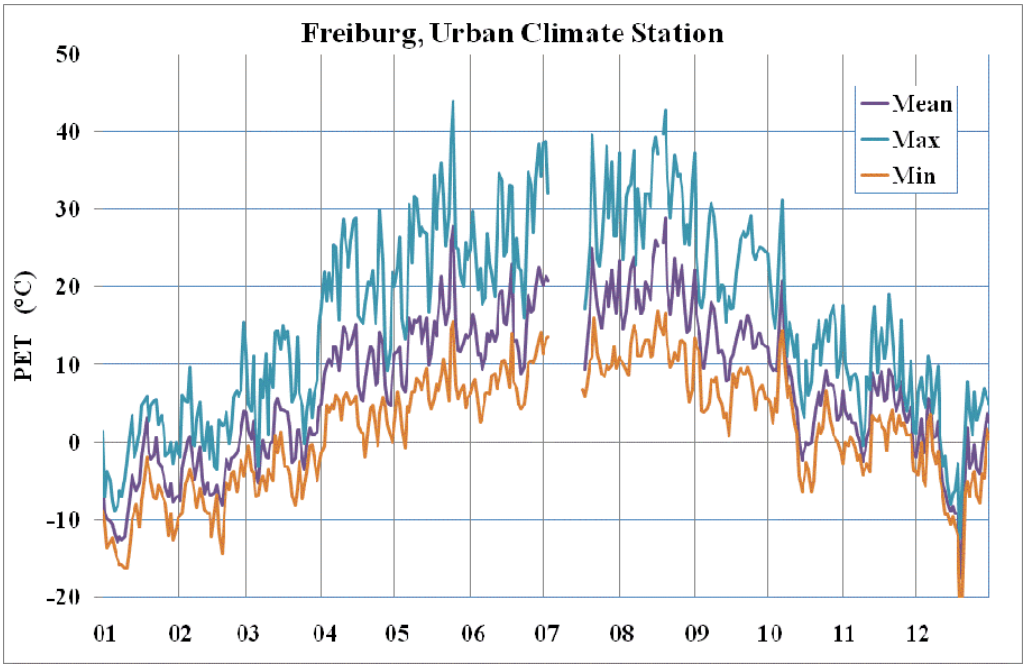

Fig. 1: Mean, maximum and minimum daily physiologically equivalent temperature PET at the urban climate station Freiburg for the period January, 1st 2009 to December 31st, 2009

Fig. 1 shows the mean, maximum and minimum daily physiologically equivalent temperature PET at the urban climate station Freiburg for the period January, 1st 2009 to December 31st, 2009. The range is from approximately -20 °C in the winter to 45 °C for summer days. In Fig. 2, the mean daily air temperature in the urban climate station Freiburg (S Mean), indoors at 1st floor (1st Mean) and 3rd floor (3rd Mean) for the period May to December 2009 are shown. Without considering the accuracy of the measurements and the different measurement systems used it can be easily seen that in the temporal pattern there is a change in the conditions indoors shifting the higher temperatures from the 3rd floor to the 1st floor from warm to cold periods. It can also be seen the decoupling of indoor and outdoor air temperature after the summer.

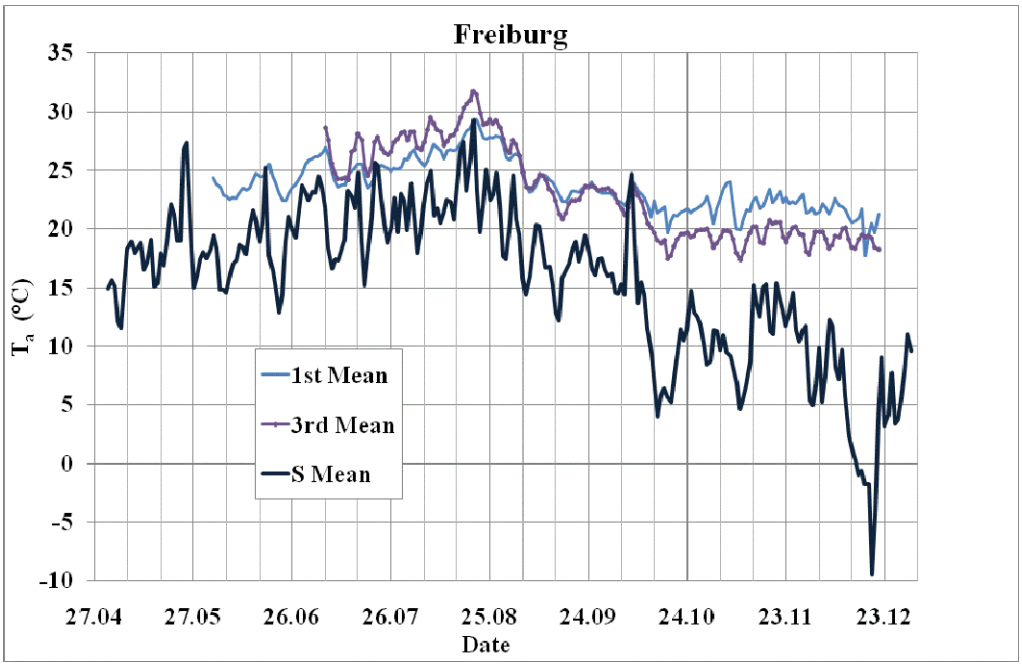

Fig. 2: Mean daily air temperature in the urban climate station Freiburg (S Mean), indoors at 1st Floor (1st Mean) and 3rd Floor (3rd Mean) for the period May to December 2009

The curve of the mean daily vapour pressure in the urban climate station Freiburg (S Mean), indoors at 1st Floor (1st Mean) and 3rd Floor (3rd Mean) is in all three sites similar depending outdoor conditions and heating conditions during the cold period of the year (not shown as figure).

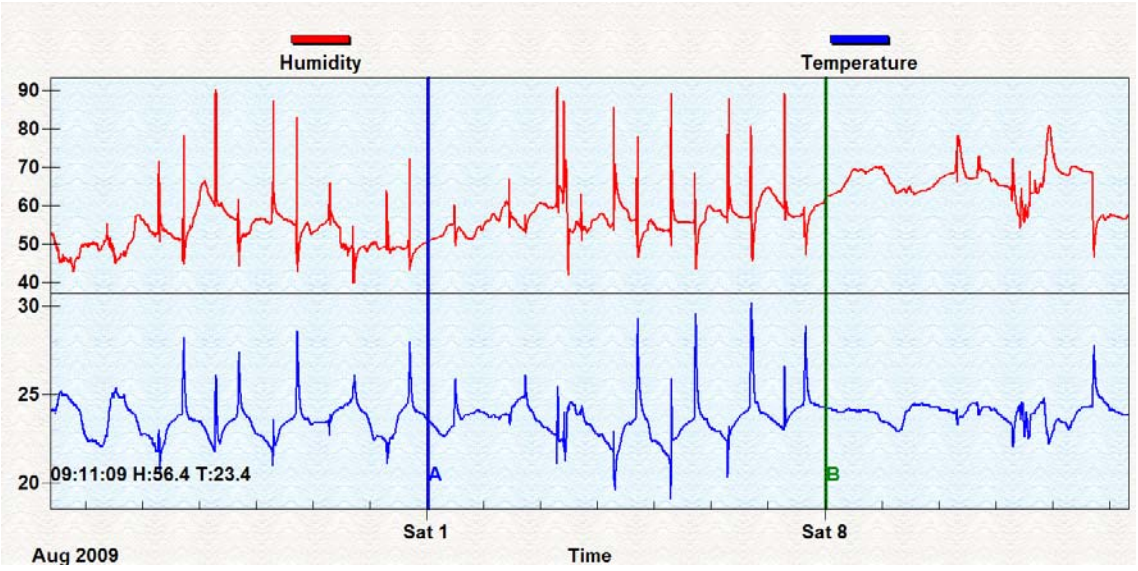

Fig. 3: Temporal development of air temperature and relative humidity in 1 minute resolution for the period July 25 to August 14, 2009

The examples shown in Fig. 1 and 2 are based on 10 minutes resolution and describe appropriately thermal and meteorological conditions in different sites. In Fig. 3 and 4

the temporal development for air temperature and relative humidity in 1 minute resolution for the periods July 25 to August 14, 2009 (Fig .3) and (Fig. 4) September 29 to October 12, 2009 are shown. There is a high variability both in both parameters (air temperature and relative humidity) not only in the diurnal pattern but also in short term indication the different exposures in indoors and outdoors conditions. Some days deviate from typical patterns and are relying in the short time mobility and stay in different spaces.

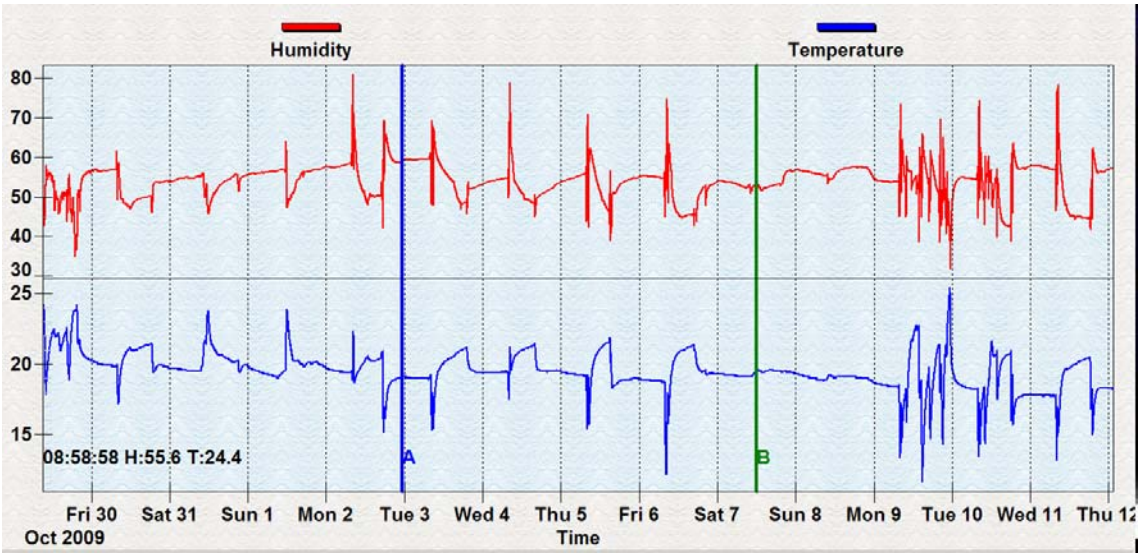

Fig. 4: Temporal development of air temperature and relative humidity in 1 minute resolution for the period September 29 to October 12, 2009

4. Discussion

The examples, based on different temporal resolutions indicate that there are difficulties and deficiencies in the quantification of thermal comfort. First of all the data used has to be accurate and in an appropriate time resolution. Mean daily data cannot accurate reproduce the thermal conditions during the day. Using specific times per day i.e. 14 LST or during the occurrence of maximum and minimum time specific parameters produce mostly appropriate typical conditions. Thermal comfort analysis based on hourly data (or 10 minutes) produce more representative condition for the diurnal quantification. As also shown in the comparison between indoor and outdoor conditions without considering the quality and accuracy of the measurements and data, it can be seen that there is modification in the air temperature in buildings from the lower to upper floors, shifting from lower to higher air temperatures from summer to winter and a decoupling between the air temperature conditions between outdoors and outdoor after the end of summer, specifically at the end of September. Air humidity shows lower differences compared to air temperature. The wind was not examined here but is known that the conditions indoors are during the night more worse that outdoors.

For the measurements of air temperature and relative humidity in 1 minute resolution can be extracted that, depending from the working hours and daily behaviours, most of the time of the day in temperate climate people spend their time indoors and only short periods they are exposed in other “climates”. Some days the diurnal variability of the meteorological conditions is very weak but in other days very high.

5. Conclusions

Thermal comfort assessment performed in the past had some deficiencies, which can be reduced with modern techniques and possibilities. This requires reliable spatial and temporal data, which are relevant as input data for thermal indexes. The periods of use of different land use areas and periods of stay indoor (also in cars and bus) and their appropriate representation of their climate is requires and of relevance in the thermal comfort quantification.

References

Höppe, P., 1999: The physiological equivalent temperature – a universal index for the biometeorological assessment of the thermal environment. Int. J. Biometeorol. 43, 71-75.

Koppe, C., Jendritzky, G., Kovats, S., Menne, B. et al., 2004: Heat-waves: risks and responses. Regional Office for Europe. Health and Global Environmental Change, Series No. 2. Kopenhagen, Denmark.

Lin, T.-P., Matzarakis, A., Hwand, R.-L., 2010: Shading effect on long-term outdoor thermal comfort. Building and Environment 45, 213-211.

Matzarakis, A., 2006: Weather and climate related information for tourism. Tourism and Hospitality Planning & Development 3, 99-115.

Matzarakis, A., Amelung, B., 2008: Physiologically Equivalent Temperature as indicator for impacts of climate change on thermal comfort of humans. In: M. C. Thomson et al. (eds.), Seasonal Forecasts, Climatic Change and Human Health. Advances in Global Change Research 30, Springer-Sciences and Business Media, 161-172.

Matzarakis A, Mayer H, 2008: Importance of urban meteorological stations - the example of Freiburg, Germany. Ber. Meteor. Inst. Univ. Freiburg 17, 119-128.

Matzarakis, A., F. Rutz, H. Mayer, 2007: Modelling Radiation fluxes in simple and complex environments – Application of the RayMan model. Int. J. Biometeorol. 51, 323-334.

Mayer, H., 1993: Urban bioclimatology, Experientia 49, 957-963.

Röckle, R.; Richter, C.-J., Höfl, H.-C.; Steinicke, W.; Streifeneder; M.; Matzarakis, A., 2003: Klimaanalyse Stadt Freiburg. Auftraggeber Stadtplanungsamt der Stadt Freiburg. November 2003.

Scott, D., de Freitas, C.R., Matzarakis, A., 2009: Adaptation in the tourism and recreation sector. In: G. R. McGregor, I. Burton, K. Ebi (Eds.), Biometeorology for Adaptation to Climate Variability and Change. Springer, 171-194.

VDI, 1998: Methods for the human-biometerological assessment of climate and air hygiene for urban and regional planning. Part I: Climate, VDI guideline 3787. Part 2. Beuth, Berlin.

Authors' address:

Prof. Dr. Andreas Matzarakis (andreas.matzarakis@meteo.uni-freiburg.de)
Meteorological Institute, Albert-Ludwigs-University of Freiburg
Werthmannstr. 10, D-79085 Freiburg, Germany

Influence of wind direction and a slanting beam angle on surface layer scintillometer estimates of sensible heat flux

Odhiambo, G. O.[1,2], Savage, M. J.[2]

[1] Department of Geography & Urban Planning, UAE University, UAE
[2] School of Environmental Sciences, University of KwaZulu-Natal, Republic of South Africa

Abstract

Understanding the partitioning of net irradiance into its component energy balance flux including sensible heat and latent energy flux measurements can provide valuable information about the local weather patterns. Such information is useful for water resource management, agriculture and environmental studies. This work was carried out with the main aim of comparing sensible heat flux estimated by the surface layer scintillometer (SLS) method with that obtained by the eddy covariance (EC) method for wind direction approximately or nearly perpendicular to the SLS beam path, with measurements obtained when the wind direction is approximately parallel to the beam path. Also investigated was the comparison of sensible heat flux measured by the SLS at slanting beam angles with that obtained by the EC method, as well as determination of the SLS footprint and comparison with the EC footprint. The investigation design as well as results obtained are presented and discussed.

1. Introduction

The comparisons of sensible heat flux measurements obtained by the EC and SLS methods can be done in terms of a number of factors, or considering several factors, such as atmospheric stability, wind direction, etc. The main objective of this paper was therefore to compare sensible heat flux estimated by the SLS method with that obtained by the EC method for wind direction approximately or nearly perpendicular to the SLS beam path, with measurements obtained when the wind direction is approximately parallel to the beam path. Also investigated was the comparison of sensible heat flux measured by the SLS at slanting beam angles with that obtained by the EC method.

2. Experimental

Field measurements were carried out from January to December 2004 over an open mixed grassland site in Ashburton ($30^{o}27'$ E, $29^{o}40'$ S) close to Pietemaritzburg in KwaZulu-Natal, South Africa, with an altitude of 671.3 m. The climate is humid and sub-tropical with summer rainfall and long dry periods in winter. Air temperature ranges between -4 and 42 ^{o}C (Savage et al., 2004). The surface within 135 m in the prevailing south east wind direction was nearly level with a slope of $1^{o}15'$ to the south east.

So as to test the scintillometry method for non-ideal (heterogeneous) surfaces, the SLS was set up in an inclined position (Fig. 1.1) from DoY 230 to 241, with the receiver set at 0.68 m above the ground level and transmitter at 1.68 m, resulting in an effective height of 1.18 m, calculated as the average height of the two heights less the vegetation height at the midpoint of the scintillometer beam path where the weighting of sensible heat flux is greatest since site where the measurements were done was relatively flat and vegetation height nearly uniform across the field.

4. Results of the study

4.1 Comparison of sensible heat flux using the SLS at a slanting beam angle with EC measurements

Corresponding sensible heat flux comparisons are presented in Figs 1.2 and 1.3, with Fig.1. showing correlation analysis results for 2-min averages of sensible heat flux for the two methods, and Fig 1.2 for the half-hourly averages. An example of the diurnal variation of sensible heat flux measured by the two methods (EC and SLS) is presented in Fig. 1.4. For the half-hourly averages comparison, higher agreement in the sensible heat measurements by the methods was obtained (e.g. r^2=0.963, with a slope of 0.940 (Fig. 1.2). Even for 2-minute averages of sensible heat measurements, the agreement between the two methods as indicated by high correlation coefficients (e.g. r^2 = 0.915; slope of 0.887- Fig. 1.2) was realised. This is further demonstrated by the diurnal variation plots (e.g. Fig. 1.4) of sensible heat flux as measured by the two methods.

4.2 Comparison of EC- and SLS-measured sensible heat flux measurements for different wind directions

Two-min wind direction and horizontal wind speed data obtained by the EC method were analysed and results for selected days when the prevailing wind direction was either approximately perpendicular, parallel to the SLS beam path, or irregular, are presented in Figs 1.6 and 1.7. The wind direction data obtained from the EC system were converted to radians and plotted using Origin software (OriginLab, 2000). Only daytime data (from 06h00 to 18h00) were plotted. Wind direction is shown by the direction of the arrows whereas horizontal wind speed is indicated by arrow length so that a longer arrow indicates greater wind speed than a shorter one. The orientation of the SLS beam path is also shown on the plots as well as the compass direction.

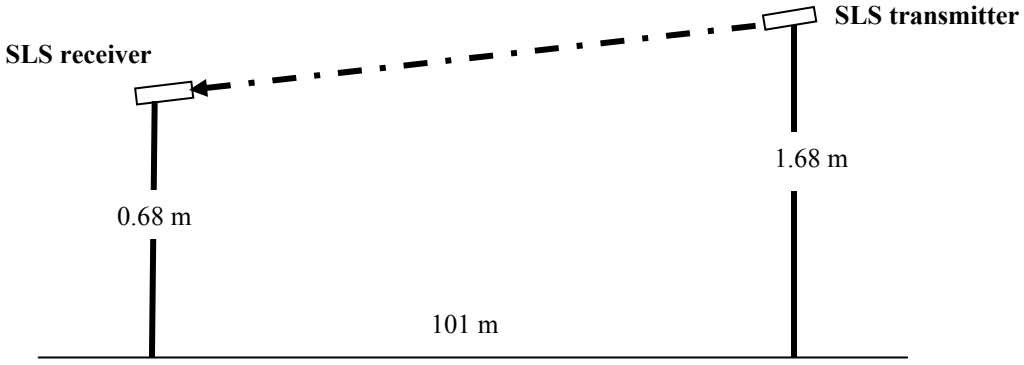

Fig. 1.1: Scintillometer set up in an inclined beam path with the receiver set at 0.68 m and transmitter at 1.68 m above the ground level. The diagram is not to scale

For most days, the prevailing wind direction was more or less perpendicular to the beam path, although there were days when the wind direction was irregular. Even for the days when the wind direction was mainly perpendicular to the SLS beam path, for some hours during the day there was irregularity in the direction (e.g. DoY 287, 2004). For those days when the wind direction was approximately perpendicular to the SLS beam

path, the sensible heat flux (F_h) values obtained by the EC and SLS methods seem to be more in agreement than for those days when the wind direction is irregular.

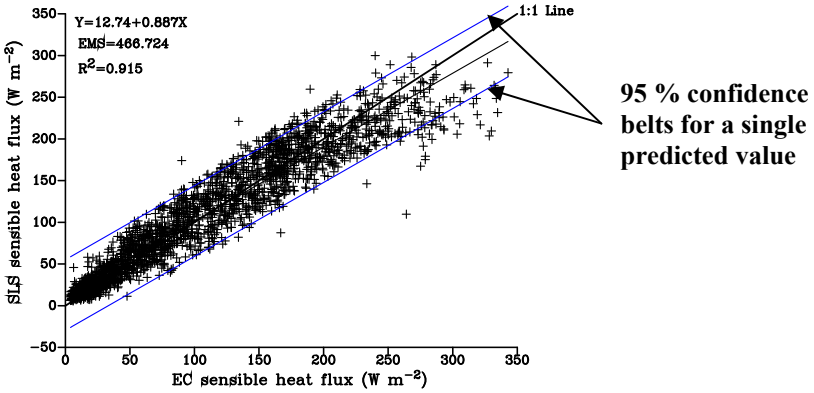

Fig. 1.2: Comparison of 2-min sensible heat flux measured by EC and SLS methods for DoY 230 to 241, with the SLS beam set at a slanting angle where the transmitter was set at a height of 1.68 m above the ground level and the receiver at a height of 0.68 m. The effective beam height was 1.18 m with the EC method at a height of 2 m.

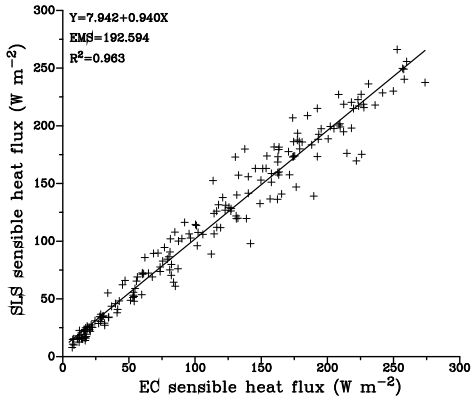

Fig. 1.3: Comparison of 30-min sensible heat flux obtained by EC and SLS methods for DoY 230 to 241, with the SLS beam set at a slanting angle

For instance, for DoY 275, r^2 = 0.945, and slope = 1.046 (Fig. 1.5). The diurnal plots (not shown) for the respective days also show good agreement in the F_h values obtained by the two methods for the days when the wind direction is mainly perpendicular to the SLS beam path. On those days when the wind direction was approximately perpendicular to the SLS beam path, the sensible heat flux (F_h) values obtained by the EC and SLS methods seem to be more in agreement than for those days when the wind direction is irregular. An example of one of the days when the wind direction was random for part of the day and perpendicular to the beam for the rest of the day is DoY 287 (Fig. 1.8) when the wind direction was irregular between 11h00 and 14h00 but perpendicular for the rest of the day. On this particular day, the diurnal plots of F_h (Figs 1.8a and b) show

the effect the wind direction has on the agreement in F_h values estimated by the EC and SLS methods.

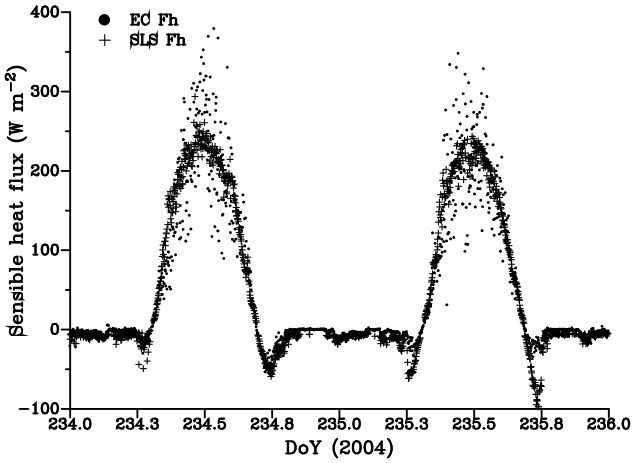

Fig. 1.4: Diurnal plot of 2-min EC- and SLS- measured sensible heat flux for DoY 234 and 235 for when the SLS beam was set at slanting angle

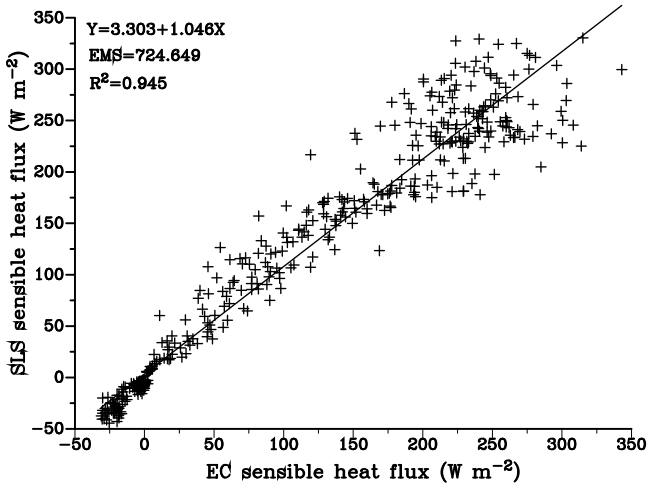

Fig. 1.5: Comparison of 2-min sensible heat flux measured by EC and SLS methods for DoY 275 for which wind direction is nearly perpendicular to the SLS beam path

It can be seen from this plot that between the hours when the wind pattern was highly irregular, there seem to be a disagreement in the F_h values. This is also reflected by the lower correlation coefficient ($r^2 = 0.88$) obtained by correlating the F_h estimates for the two methods. In Fig. 1.8b, the distinction between SLS estimates of sensible heat flux for times when the wind direction was approximately perpendicular to the beam and when the wind direction was random makes this more clearer as can be seen from the diurnal plot. In the early hours of the day (mainly before midday) the sensible heat flux measurements obtained by the two methods do not agree well - this coincides with times when the wind direction was irregular - as compared to the time after midday

when the agreement in sensible heat flux measurement by the two methods, as indicated by the coincidence in the plots, is improved.

Wind speed appears to influence the F_h measurements by the EC and SLS methods. The influence of wind speed is noticeable, for example, on DoY 107 (r^2 = 0.853) when even though the wind direction appears random, the agreement between the EC and SLS measurements of F_h is more improved compared to the agreement for DoY 131 (r^2= 0.802) when wind is more or less perpendicular to the beam path.

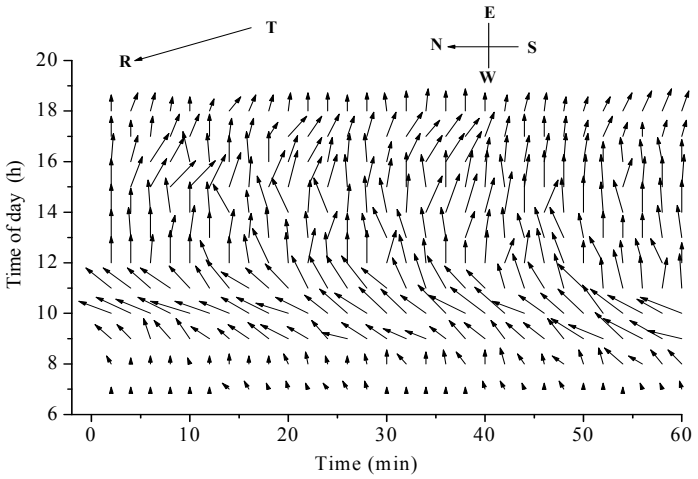

Fig. 1.6: Wind vector variation between 06h00 to 18h00 for DoY 275. The arrows point to the wind direction and wind speed is indicated by the length of the arrows. On this particular day wind direction was nearly perpendicular to the SLS beam

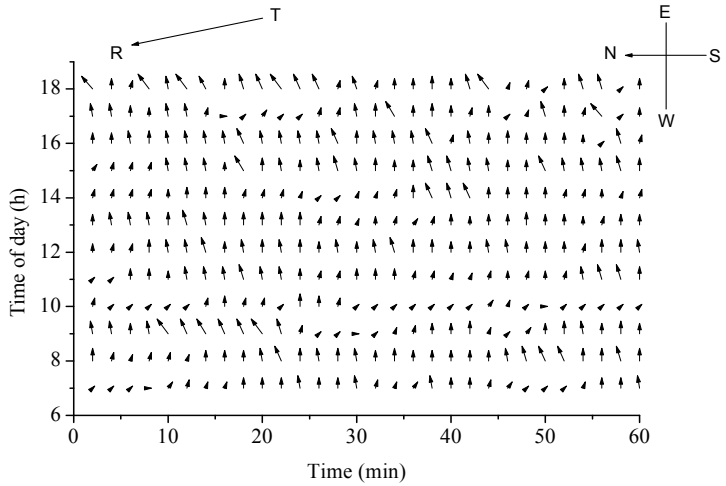

Fig. 1.7: Wind direction between 06h00 to 18h00 for DoY 131 for which wind direction was nearly perpendicular to the SLS beam path but wind speed low

On the DoY 131, the wind direction is similar to that of Fig. 1.6 - nearly perpendicular to the SLS beam path, but the wind speed is reduced for Fig. 1.7 compared to that for

DoY 107. It can be assumed that the reduced wind speed on DoY 131 resulted in the poorer agreement (r^2 = 0.888 with a slope of 0.931), since the wind direction is similar for both days.

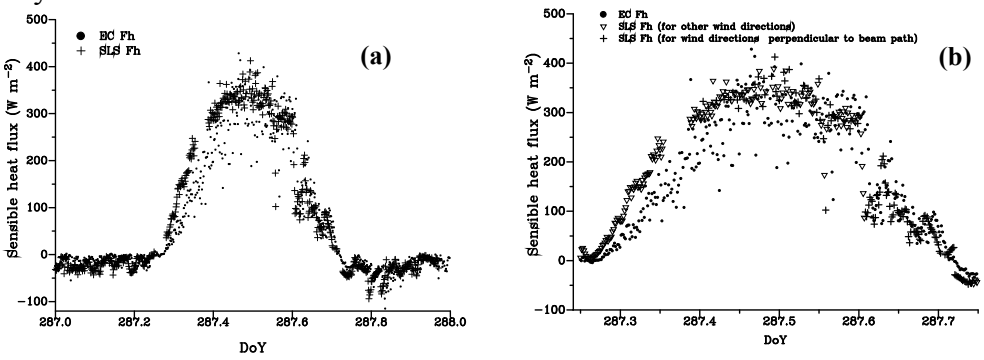

Fig. 1.8: (a) Diurnal variation of 2-min sensible heat flux measured by EC and SLS methods for DoY 287, (b) SLS sensible heat flux for the different prevailing wind directions – for wind directions nearly perpendicular to the SLS beam path or random wind directions, also for DoY 287

The influence of wind speed is also noticeable on DoY 107 when even though the wind direction appears random, the agreement between the EC and SLS measurements of F_h is more improved compared to the agreement for DoY 131 (Figs 1.6 and DoY 107) when wind is more or less perpendicular to the beam path. Wind speed plays a role in atmospheric stability and on DoY 131 the atmospheric condition was near-neutral while on DoY 107 the atmospheric condition was unstable.

5. Conclusions

There was generally good agreement in the measurements of F_h by the EC at a height of 2 m and SLS measurement methods with the SLS set up in an inclined position with the 30-min data resulting in more improved agreements. The findings confirm that the SLS set up does not impair its performance in measuring sensible heat flux. This also shows that the SLS method would also work well in heterogeneous conditions which the inclined optical beam path mimics. For those days for wind directions nearly approximately perpendicular to the beam, the F_h agreement by the EC and SLS methods improved compared to random wind directions or directions approximately parallel to the SLS beam path. Wind speed also seems to influence the F_h estimates by the two methods since the agreement in the F_h values obtained by the two methods is greater when wind speed is higher compared to times of the day when the wind speed is reduced.

Acknowledgement
The authors acknowledge the financial support from the National Research Foundation (NRF-South Africa) and the University of KwaZulu-Natal (UKZN).

References

OriginLab., 2000: Origin Software, Version 6.1. OriginLab Corporation. Northampton. Massachusetts, USA.

Savage, M. J., Everson, C. S., Odhiambo, G. O., Mengistu, M. G. and Jarmain, C., 2004: Theory and practice of evapotranspiration measurement, with special focus on surface layer scintillometer (SLS) as an operational tool for the estimation of spatially-averaged evaporation. Water Research Commission (WRC) Report No. 1335/1/04. ISBN 1-77005-247-X. WRC, Pretoria, Republic of South Africa, 204 pp.

Authors' address:

Dr. George O. Odhiambo (godhiambo@uaeu.ac.ae)
Department of Geography & Urban Planning, UAE University
P. O. Box 17771, Al Ain, UAE

Prof. Michael J. Savage (savage@ukzn.ac.za)
SPAC Research Unit, School of Environmental sciences, University of KwaZulu-Natal (UKZN)
P/Bag X01, Scottsville, 3209, Pietermaritzburg, Republic of South Africa.

Water resources of Pacific atolls: evaluating sensitivity to climatic change and variability

Manuel Helbig[1], C. R. de Freitas[2], Andreas Matzarakis[3]

[1] Institute of Geography, University of Göttingen, Germany
[2] School of Environment, University of Auckland, New Zealand
[3] Meteorological Institute, Albert-Ludwigs-University of Freiburg, Germany

Abstract

Sensitivity approaches address the problem of uncertain projections of future climates and climate variability and provide useful results for decision-makers. In light of this, a scheme is developed to quantify sensitivity of freshwater resources of atolls in the tropical Pacific to climate variability and change on a regional scale. Results refer to soil moisture availability relevant to rain-fed agriculture and to groundwater recharge rates applicable to freshwater storage amounts and extraction rates. This sensitivity approach is suitable for a variety of climate studies and represents a powerful tool to gain essential information on the influence of climate on freshwater resources of atolls.

1. Introduction

Freshwater storage capacity on most atolls is limited as these small, low-lying islands have small water catchments. Surface water resources are extremely rare on atolls and groundwater exists only as a shallow freshwater lens floating on salt water (de Freitas, 2009). They are particularly vulnerable to extended droughts or periods of below average precipitation because of their limited storage capacity. The size and surface area of the island and the aquifer geology determine the upper limit of the freshwater lens (White et al., 2007), whereas the climate determines mainly the replenishment of the lens. This means the climate defines the sustainable yield of water that can be pumped out of the freshwater lens. But only a few islands hold reliable information and data about their groundwater resources, which hinders a realisation of sustainable water management (Falkland, 1999).

Freshwater resources of atolls depend on inter-annual variability of climate and by long term climate trends. Long term changes that might be expected in the future cannot be predicted without large uncertainties on the regional scale and these uncertainties are likely to persist in the near future (Barnett, 2001). One approach to cope with these uncertainties is to identify regions of high sensitivity to change, if a change in climatic conditions were to occur (de Freitas & Fowler, 1989). In light of the above, this study critically evaluates a simple methodology to assess freshwater resources and their sensitivity to climatic change and variability on atolls in the Pacific. It focuses on the groundwater resources as well as on the soil water availability which is crucial for plant growth and thus for rain-fed agriculture on these islands.

2. Method

Atolls have little or no influence upon cloud and precipitation patterns due to their low elevation (Lavoie, 1963), thus, synoptic climatic conditions of an atoll are almost identical with that over the surrounding ocean (Giambelluca et al., 1988). Because of this,

datasets based on areal projections of satellite and surface observations and extended over large areas for latitude-longitude grid squares may be used (Uppalla et al., 2004). The ERA-40 reanalysis data that provides a consistent set of climate variables for the time period 1962 to 2000 is used here. Variables used include solar and longwave radiation, air temperature and precipitation.

The water balance for an atoll is given as

$$SD = P - EA + \Delta SM \quad (1)$$

where S_D is water surplus or deficit, P is precipitation, E_A is actual evapotranspiration and ΔS_M is change in soil moisture storage. P is given by the ERA-40 data sets. If E_P is available water balance models based on the Thornthwaite bookkeeping method (1955) can be used to estimate E_A. Priestley & Taylor (1972) estimate E_P using net allwave radiation (Q^*) and the slope of the saturation vapor pressure curve (**Δ**) as determining factors. Data on solar radiation downwards and net longwave radiation together with estimated albedo values (r) for atoll surfaces allow an estimate of Q^*. McAneney & Itier (1996) confirmed the suitability of this approach to estimate E_P in the humid tropics. The Priestley-Taylor method has been successfully used in other studies for Pacific islands as well (Giambelluca et al., 1988; Nullet, 1987). To run the simple regional water balance model assumptions have to be made on the available water capacity (*AWC)* of the predominant soil. Based on literature values (Nullet, 1987) r is assumed to be 0.25 and *AWC* to be 80 mm. Alley (1984) confirmed the accuracy of the model's estimated annual flows, but he notes problems in simulating accurate monthly flows.

Employing the above approach, one can estimate the mean monthly freshwater conditions under average climatic conditions for atolls (Figure 1). Freshwater resources can be assessed from two different points of view that require different approaches. To assess groundwater resources from a climatological viewpoint one has to examine recharge (S) rates and amounts. If impacts on agriculture are to be assessed soil moisture deficit (D) represents the crucial variable. Soil moisture availability is a key factor for agricultural planning (Giambelluca et al., 1988). D can serve as an indicator of plant water stress and agricultural drought. The sensitivity of these to climate variability or change may be used as a measure of the threat to the availability of freshwater resources. A definition of the areas of high sensitivity is given on the basis of an understanding of the interactions between freshwater resources and climate. The modified approach consists of four steps listed in Table 1.

The critical level for S varies depending on the state of development of the water management systems, population size and water using activities, which in the present circumstances is set at 100 mm. In the case of D, the critical level is assumed to be three months per year of severe deficit, which is defined in the current research as D being larger than 50% of the monthly P. This is to take into account that the negative impact on plant growth depends on the magnitude of D and varies between different plant types (Jackson, 1989). The impact of changed climatic conditions is assessed by running the water balance model under different climatic conditions. The results are mapped as shifts of isopleths on maps accounting for different freshwater resource questions. The areas of high sensitivity of freshwater resources on atolls are simulated using the water balance model and regional climate data from ERA-40.

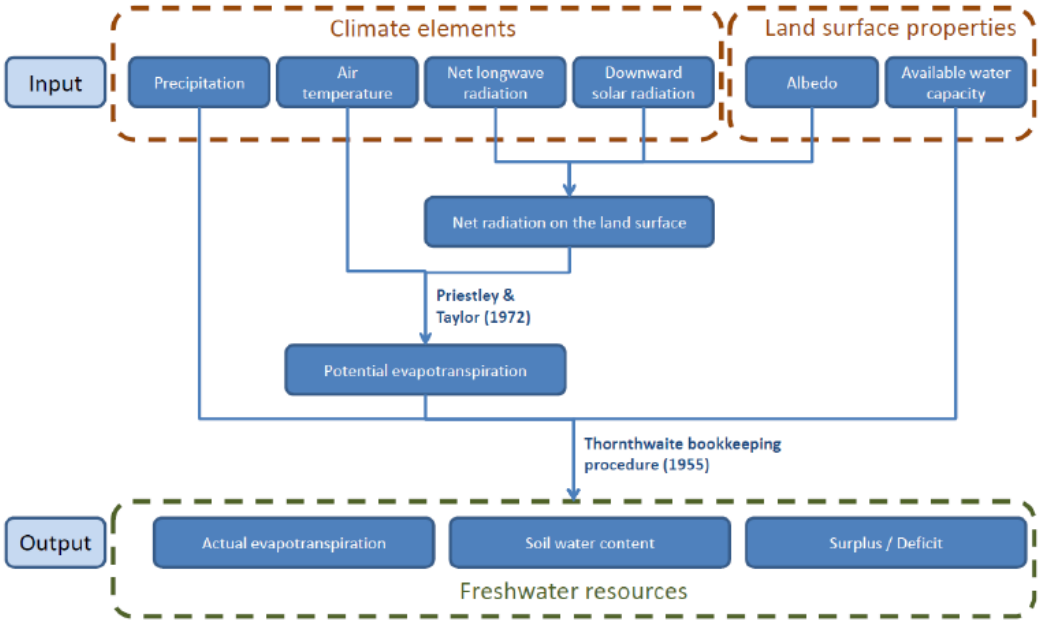

Fig. 5: Description of the water balance model with overview of the input variables, model parameters and output variables including intermediates

Tab. 1: Steps of procedure to assess areas of high sensitivity to climatic change and variability (modified after Parry 1985)

Step 1	Isolating the important climatic variables by modelling freshwater resources/climate relationships
Step 2	Establishing critical levels of freshwater resources by relating them to the use of freshwater resources on atolls
Step 3	Resolving climatic fluctuations and changes into fluctuations of the critical levels
Step 4	Mapping these as shift of isopleths to identify areas of high sensitivity

3. Results

The results focus on change and variability in P and Q^* and are divided into two sections: a) soil moisture conditions relevant for rain-fed agriculture purposes; and b) groundwater resource conditions relevant for all water extraction activities to supplement rainwater use. Some regions are not threatened by possible changed conditions, either because they exhibit a large excess of P or because the climatic conditions are too dry to benefit from variability or climatic change. Regions of interest therefore are located between very wet and very dry regions. The high sensitive areas to changing P conditions regarding the soil moisture conditions are shown in Figure 2. The results show that the islands of New Caledonia are highly sensitive to an increase in P of 20% and the Phoenix Islands to a decrease in P of 20%. Other locations, such as parts of Vanuatu and Fiji, Tonga, Niue, the Cook Islands and Kiribati, would experience deteriorated soil moisture conditions in years with 40% less P than in an average year or if average precipitation decreased by 40%.

Figure 3 illustrates the shift of the isoline representing an S of 100 mm per year assuming an increase or decrease in Q^* of 10% and 20%. Areas of high sensitivity are mainly of smaller extent than for the same change in P indicating a smaller influence of Q^* on

the *S* rates. The area of high sensitivity in the northern part of the study area has a larger extent than the narrow belts at the Phoenix Islands and New Caledonia in the southern part.

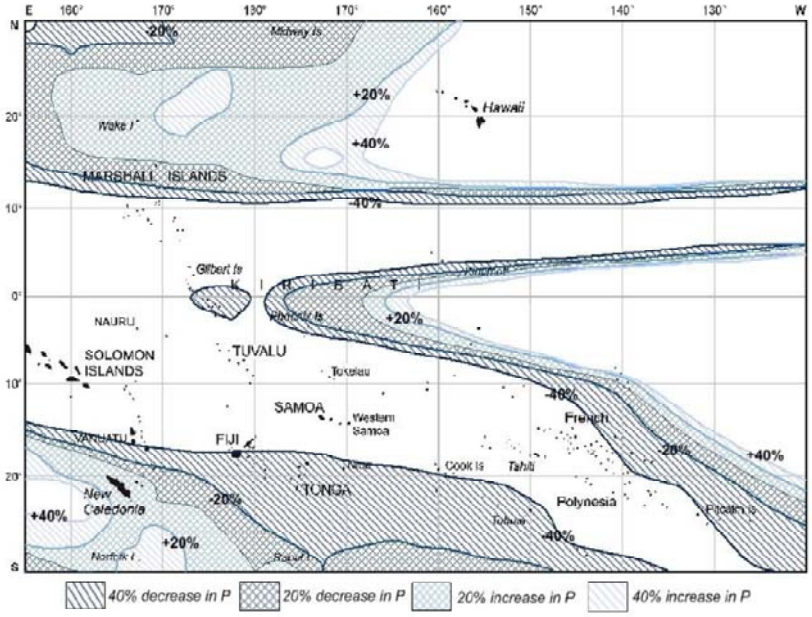

Fig. 6: Map of areas with high sensitivity to variability and change in precipitation. Shaded zones indicate the shift of the isoline of three severe deficit months assuming a specific percentage change in annual precipitation.

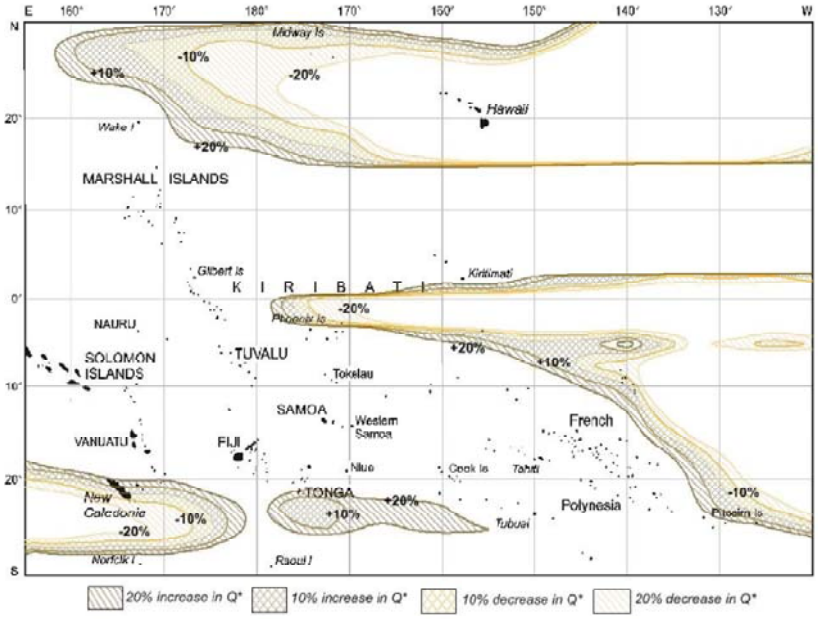

Fig. 7: Map of areas with high sensitivity to variability and change in net radiation. Shaded zones indicate the shift of the isoline of 100 mm of annual surplus assuming a specific percentage change in net radiation.

Climatic change and variability is not very likely to affect only one of both variables. Because of that a combined scenario including both variables is of greater reliability. Therefore the same procedure could be applied assuming change and variability in both variables giving more sophisticated results.

4. Discussion

The generalized nature of the method employed means that the reliability of the results needs to be carefully considered. Problems in simulating cloud properties cause an underestimation of radiation fluxes. Furthermore precipitation in tropical regions is overestimated (Uppalla et al., 2004). These biases in ERA-40 data have to be considered in the interpretation of the results of this study to avoid misleading results. Studies by Taylor (1973) and McGregor & Nieuwolt (1998) confirm the overestimation of P amounts by ERA-40 for areas near the equator, but show reasonable agreement for areas in higher latitudes of the study area. Although the various studies use data covering different time periods, it can be assumed that P is generally overestimated in equatorial areas. Only one study on E_P on atolls covering the whole tropical Pacific could be found, namely Nullet (1987), whose findings suggest E_P is largely underestimated due to an underestimation of Q^* all over the study area. In light of this, boundaries of the zones of sensitivity are very approximate. Model parameters r and AWC have to be adjusted to these to match soil and surface conditions of atolls to which the generalised result are applied. Knowledge of the patterns of change and variability of P and Q^* is also necessary to interpret the results. Change and variability of P was found to be of greater magnitude than change and variability of Q^* indicating the crucial importance of current and future patterns of P in the study area.

6. Conclusion

Possible impacts on the water budget on atolls under changed climatic conditions are examined. The approach converts changed climate conditions into impacts on freshwater resources. It provides a simple but powerful method to identify atolls that lie in areas of high sensitivity, even for regions with no data from climate stations. The results can be applied to specific atolls by adjusting model parameters to match local surface characteristics such as soil type and depth. The quality of results is not only a function of the data quality, but also of the appropriateness of the parameter setting. GPCP and ERBE data could be integrated in regional scale freshwater resource assessments based on the approach of this study. They represent more accurate datasets for the relevant climatic variables P and Q^* and thus are very likely to produce more reliable results. But for that purpose a method to adjust the different resolutions and time periods has to be developed.

References

Alley, W.M., 1984: On the treatment of evapotranspiration, soil moisture accounting and aquifer recharge in monthly water balance models. Water Resources 20, 1137-1149.

Barnett, J., 2001: Adapting to Climate Change in Pacific Island Countries: The Problem of Uncertainty. World Development 29, 977-993.

De Freitas, C.R., 2009: Adaptation and Water Resources. *In* Ebi, K.L., I. Burton, G.R. Mc Gregor (eds.): Biometeorology for Adapting to Climate Variability and Change. Springer, Netherlands, pp. 195-210.

De Freitas, C.R., A.M. Fowler, 1989: Identifying sensitivity to climatic change at the regional scale: the New Zealand example. *In* Welch, R. (ed.): Proceedings of 15th Conference New Zealand Geographical Society, New Zealand Geographical Society Conference Series No. 15, Dunedin, pp. 254-261.

Falkland, T., 1999: Impacts of Climate Change on Water Resources of Pacific Islands. PACCLIM Workshop, Modelling the effects of climate change and sea level rise in Pacific Island countries, Auckland, New Zealand, 33 pp.

Giambelluca, T.W., D. Nullet, M.A. Nullet, 1988: Agricultural drought on south-central Pacific islands. Professional Geographer 40, 404-415.

Jackson, I.J., 1989: Climate, Water and Agriculture. 2nd edition. Longman Scientific & Technical, Harlow, 377 pp.

Lavoie, R. L., 1963: Some aspects of meteorology of the tropical Pacific viewed from an atoll. Atoll Res. Bull. No. 96, Smithsonian Institute, Washington D.C., 80 pp.

McAneney, K.J., B. Itier, 1996: Operational limits to the Priestley-Taylor formula. Irrigation Sci. 17, 37-43.

McGregor, G.R., S. Nieuwolt, 1998: Tropical Climatology. 2nd edition. John Wiley & Sons Ltd, Chichester, 339 pp.

Nullet, D., 1987: Water balance of Pacific atolls. Wat. Res. Bull. 23, 1125-1132.

Parry, M.L., 1985: The impact of climatic variations on agricultural margins. *In* Kates, R. W., J.H. Ausubel, M. Berberian (eds.): Climate Impact Assessment, Studies of the Interaction of Climate and Society. John Wiley and Sons, Chichester, pp. 351-367.

Priestley, C.B., R.J. TAYLOR, 1972: On the Assessment of Surface Heat Flux and Evaporation Using Large Scale Parameters. Mon. Weather Rev. 100, 81-92.

Taylor, R.C. (1973): An atlas of Pacific Islands Rainfall. Dept. of Meteorology Publication No. 25, University of Hawaii, Honolulu, 165 pp.

Thornthwaite, C.W., J. Mather, 1955: The water balance. Publications in Climatology 8, 1-104.

White, I., T. Falkland, T. Metutera, E. Metai, M. Overmars, P. Perez, A. Dray, 2007: Climatic and human influences on groundwater in low atolls. Vadose Zone J. 6, 581–590.

Uppalla, S.M. et al (2005): The ERA-40 re-analysis. Q. J. R. Meteorol. Soc. 131, 2961–3012.

Authors' address:

Manuel Helbig BSc (manuel.helbig@stud.uni-goettingen.de)
Institute of Geography, University of Göttingen
Goldschmidtstr. 5, D-37077 Göttingen, Germany

Prof. Dr. Chris de Freitas (c.defreitas@auckland.ac.nz)
School of Environment, University of Auckland
10 Symonds Street, Auckland, New Zealand

Prof. Dr. Andreas Matzarakis (andreas.matzarakis@meteo.uni-freiburg.de)
Meteorological Institute, University of Freiburg
Werthmannstr. 10, D-79085 Freiburg, Germany

Agro-meteorology of an aromatic plant (*Valeriana officinalis*) - Borneol, Bornyl acetate and other components of essential oil in European valerian as influenced by planting time and age of harvest

K. Ramesh*, Virendra Singh, Bikram Singh and Vijayalata Pathania

Natural Plant Products Division, Institute of Himalayan Bioresource Technology

Palampur 176061 (HP)

IHBT Communication No. 0570

* Present address: Senior scientist, Indian Institute of Soil Science (ICAR), Nabibagh, Berasia Road, Bhopal 462038 (MP) India

Abstract

An experiment was conducted to study the effect of season of planting and age of harvest on yield and quality of Valerian during 2004-2006. Planting was done in autumn and spring seasons keeping 3 planting dates and 2 harvesting times. The essential oil content and the composition of subterranean parts of Valerian (*Valeriana officinalis* L.) were determined by hydrodistillation and seventy one compounds were detected by gas chromatography and GC/GC mass spectrometry analysis. Although the yield of biomass was unaffected, the oil composition did varied. The essential oil content at 12 months was slightly higher than 18 months. The major compounds were bornyl acetate, α-gurjunene, iso valeric acid, borneol, valerenal, valerenyl acetate and valerenol. Borneol, a monoterpene natural enantiomer acting on GABA (γ-amino butyric acid) receptors was found decreasing with aging whereas valerenol, valerenal and valerenyl acetate increased. Autumn planting and spring harvest recorded higher borneol content, an important constituent for use in phytomedicines.

Introduction

The root of Valerian plant (*V. officinalis*) is a medicinal herb native to Europe that is widely used for the treatment of hypertension, irritability, restlessness and insomnia. V. officinalis, popularly known as European valerian, is used in the European pharmacopoeia (European Pharmacopoeia, 1997) as a source of valerian-derived phytomedicines. Extracts of Valeriana are known to contain a large number of constituents including flavonoids and terpenoids, many of which are considered to be active at $GABA_A$ receptors (Johnston *et al.* 2006). Valerian extracts may be considered to be an "herbal valium", given that they have a benzodiazepine-like action reducing the latency of sleep onset and increasing the depth of sleep and the perception of well being. These extracts contain a large number of constituents like valerenol, maaliol, valerenal etc, many of which are thought to be active at GABA (γ-amino butyric acid) receptors. This is important for brain function since brain function is thought to be a balance between excitation mediated by glutamic acid and inhibition mediated by GABA (Johnston, 2003). Borneol showed positive modulatory properties but bornyl acetate were much less active. Borneol can be considered as a potential impulse of the new trends in food, pharmaceutical and cosmetic industries.

The growing world market for valerian and the high value for products have generated considerable interest for its cultivation in India. The overriding determinant in Valerian is the concentration of active constituents that impart health benefit. It is widely accepted that the valerenic acids are important active constituents in valerian and there is substantial industry interest in increasing the level of valerenic acids in traded products. Bornyl acetate and valerenal are considered as characteristic compounds (Granicher *et al.,* 1995) and valerenic acids are marker for valerian quality (Wills and Shohet, 2003). The maximum concentration of valerenic acid was found to occur in the roots and rhizomes in March and lowest concentration in Dec-Jan (Anon, 1994).

Borneol and other terpenoids of this plant enhance the effects of GABA, thus playing a vital role in brains chemical function. Investigating the response of valerian to environmental factors will give us a better insight into the genotype environment interactions. The objective of this investigation was, therefore, to identify optimum time of planting and optimum age of harvest that will provide maximum purported active components therein. This will provide information on optimum planting and harvesting time to commercial growth of the crop, based on industrial requirements.

Materials and methods

Plant material

Seeds of *V. officinalis* were obtained from Institute of Himalayan Bioresource Technology, Palampur, India and sown in well prepared nursery beds under protected conditions. Three months old seedlings were transferred to pots containing a pot mixture of 1:1:1 soil, sand and farmyard manure and the pH of the soil was 7. Initially two seedlings were maintained per pot and later (after a month) only one healthy seedling was maintained. 45 pots were maintained per treatment. The pots were kept in an open sunny area and periodical watering was given as and when necessary.

Experimentation

Seedlings were planted in two distinct seasons viz. autumn (Sep-Oct) and spring (Feb-Mar). Each season comprised of 3 planting dates viz., Sep15 (A_1), Sep30 (A_2), Oct 15 (A_3) and Feb 15 (A_4), Mar 2 (A_5), Mar 17 (A_6) respectively. A uniform nursery age of 3 months was followed. Total plant harvest was done at 12 (B_1) and 18 (B_2) months after planting. The roots were thoroughly washed and were used for essential oil analysis.

Essential oil analysis(Extraction and isolation procedure and GC analysis)

One kg of root and rhizomes was hydro-distilled in a Clevenger type apparatus for 3 hrs (Clevenger, 1928). All the samples were dried over anhydrous sodium sulphate and stored in sealed vials at low temperature (4-5^{0}C) in a refrigerator prior to analysis.

Qualitative analysis of the essential oils was performed on a Shimadzu QP-2010 gas chromatogram mass spectrometer equipped with BP-20 capillary column 30 m × 0.25 mm id, 0.25 μm. The initial temperature of column was 70^0 C and was raised to 220^0 C at 4^0 C/min; carrier gases He (0.8 ml/min), split ratio (50:0), injection volume 2μl. The specimen was scanned from m/z 50 to 600 amu. Retention indices (RI) relative to mix-

ture of n-alkane (C_{12}-C_{27}) were determined. Identification of the compounds was first attempted using mass spectral libraries viz., wiley, NIST etc to identify the compounds.

Results

The seasonal changes during the growing period is associated with alterations in the environmental parameters such as photoperiod, temperature, sunshine hours etc. which exert pressure on the plant not only in terms of morphology but also in their physiology and metabolism. Though there was insignificant variation on biomass for the season and age of harvest, the essential oil content at 12 MAP (0.151%) was slightly higher than 18 MAP (0.119 %, v/w fresh weight basis).

Essential oil composition

It is well known that the volatile constituents of the Valerianaceae are synthesized and stored in roots and rhizomes in the hypodermis and the contiguous parenchyma of the cortex (Granicher *et al.,* 1995). Seasonal changes in essential oil content content and composition have been shown to exist in different species, climatic factors; rates of plant metabolism and differentiation affect synthesis and secretion of essential oil (Jerkovic *et al*., 2001). Results concerning age at harvest of *V. officinalis* on the oil composition are shown in Table 1 and 2. A total of seventy one compounds have been identified in the volatile profile. In Table 2 and 3, the compounds representing the terpenic hydrocarbons profile being bornyl acetate, borneol and valerenyl acetate were the components quantified at relatively highest relative concentrations.

Effect of age of harvest

It is a well-known phenomenon over several species that the yield and composition of the volatile oil shows different behaviour both quantitatively and qualitatively at different phases of the vegetative cycle. Although many compounds tend to increase with ageing of the plants (18 months) viz., dl-limonene, β-patchoulene, α-guaiene, bornyl acetate, myrtenol, myrtenyl acetate, carvyl acetate, spathulenol and typical valerian cyclopentanoid sesquiterpenes viz., valerenol etc., but some compounds were reduced. It could be noted here that the content of borneol was found decreasing upon ageing. Ageing of the crop causes changes in essential oil composition (Runham, 1986) which was evident here.

Isovaleric acid, a compound responsible for the herb's unpleasant aroma was found decreasing upon ageing (18 months). Valerenic acid, an important component of valerian essential oil was found in only 12 months old plants. Ar-curcumene, a compound identified in Valerian oil was at lower concentration than the published reports (Granicher *et al.,* 1995), and concentration of the same was increased with ageing. The observed changes in oil composition could be explained by alterations in the level or activity of several enzymes involved in the pathway.

Table 1: Borneol and other components of Essential oil of *V. officinalis* at different ages (mean of 6 samples)

Compound	KI[a]	12 months (B_1)	18 Months (B_2)	SEm
Bornyl acetate	1575	18.89	19.23	0.17
Iso valeric acid	1676	0.73	0.44	0.14
Borneol	1694	2.02	1.70	0.16
Valerenal	2195	12.03	15.04	1.50
Valerianol	2208	0.49	0.71	0.11
Valerenyl acetate	2221	1.05	1.09	0.02
Valerenyl acetate	2273	1.85	2.45	0.30
Valerenol	2424	1.14	1.37	0.12
Valerenic acid	2642	0.16	0.00	0.08

RI[a] : retention (Kovats) indices

[b] : tentative identification

Effect of planting season

The effect of planting and harvesting season had pronounced effect on the essential oil components of *V. officinalis* possibly due to change in environmental factors such as light, temperature, and moisture status which can greatly influence the composition of essential oils (Staudt and Bertin, 1998; Gershenzon *et al.,* 2000).

Photoperiod may exert a direct influence through modulation of relevant metabolic pathways, from photosynthetic carbon production and its partitioning to the Rohmer route (non-mevalonate pyruvateglyceraldehyde- 3-phosphate driven isopentenyl pyrophosphate synthesis) leading further to generation of essential oil terpenoids (Lichtenthaler *et al.,* 1997). Spring planting and autumn harvest has recorded higher contents of borneol, Bornyl acetate, Bicyclo Germacrene, Myrtenol, β-ionone, and Longipinanol. Autumn planting favoured the higher production of dl-limonene, α-Santalene, Calarane, β-elemene, Iso valeric acid, Maaliol, valerenyl acetate etc. Under cold climatic conditions, Bernath *et al*.(1991) found a marked reduction in the contents of alpha -pinene and 1,8-cineol compared with the composition of plants grown in the field or in warmth, but the contents of β -pinene, β -selinene and ledol remained stable in the different environments Salvia sp. Among the various agronomic factors responsible for producing maximum yield in mints, planting time which primarily depends on the prevailing climatic conditions, is the most important (Singh *et al.,* 1997). α-pinene levels increased with increase in daily temperature in mints (Duriyaprapan *et al.*,1986; Ozel and Ozguven, 2002). Similar reasons may be ascribed for the change in various compounds in valerian. Growing and environmental conditions and ontogenetic developments influence the biosynthetic pathway of the oil constituents (Piccaglia *et al*., 1991). Ozguven and Tansi (1998) could not find qualitative variation in essential oil composition due to

environmental conditions, but the amount of essential oil components were changed, however, these changes did not show clear trend. The observed changes in the relative proportion of oil components could be explained by differential modifications in the levels or activities of various cyclase enzymes involved in the pathway of the plant.

Table 2: Borneol and other components of Essential oil of *V. officinalis* as influenced by planting season and harvesting season (Mean readings)

Compound	KI[a]	Planting season			Harvest season		
		Autumn (Sep-Oct)	Spring (Mar-Apr)	SEm	Autumn (Sep-Oct)	Spring (Mar-Apr)	SEm
Bornyl acetate	1575	18.63	19.49	0.43	20.14	17.99	1.08
Iso valeric acid	1676	0.69	0.48	0.11	0.43	0.74	0.15
Borneol	1694	1.36	2.36	0.50	1.98	1.74	0.12
Valerenal	2195	12.57	14.50	0.97	12.55	14.52	0.98
Valerenyl acetate	2221	1.10	1.04	0.03	1.06	1.09	0.02
Valerenyl acetate	2273	2.22	2.09	0.06	1.55	2.75	0.60
Valerenol	2424	1.17	1.34	0.08	0.78	1.73	0.48
Valerenic acid	2642	0.16	0.00	0.08	0.16	0.00	0.08

RI[a]: retention (Kovats) indices

It could be concluded that Borneol, a monoterpene natual enantiomer acting on GABA (γ-amino butyric acid) receptors was found decreasing with aging whereas valerenol, valerenal and valerenyl acetate were found to get increased. However bornyl acetate was found increasing upon ageing. Autumn planting and spring harvest recorded higher Borneol and bornyl acetate content suggesting the suitability for adoption by the growers.

References

Anonymous 1994. Report of the 41st Annual congress of medicinal plant research. Herbal Gram. 30:66

Bernath J, Danos B, Hethelyi E. 1991. Variation in essential oil spectrum on Salvia species affected by environment. Herba-Hungarica. 30(1-2): 35-46

Clevenger JF. 1928. Apparatus for the determination of volatile oil. J. Ann. Phram. Ass., 17: 346.

Duriyaprapan S, EJ Britten, KE Basford 1986. The effect of temperature on growth, oil yield and oil quality of Japanese mint. Annals of Botany, 58: 729-736.

European Pharmacopoeia. 1997. Valerianae radix (valerian root). Third Edn. European department for the quality of medicines, Council of Europe, Strasbourg, pp. 1702-1703.

Gershenzon J, McConkey ME, Croteau RB .2000. Regulation of monoterpene accumulation in leaves of peppermint. Plant Physiol. 122: 205–213

Granicher F, P. Christen, I. Kapetanidia. 1995. Essential oils from normal and hairy roots of Valeriana officinalis var. sambuctifolia. *Phytochemistry* 40(5): 1421-1424.

Jerkovic I, J. Mastelica , M. Milos.2001. The impact of both the season of collection and drying on the volatile constituents of Origanum vulgare L. ssp. hirtum grown wild in Croatia. *International Journal of Food Science and Technology* 36, 649-654

Johnston GAR. 2003. Dietary chemicals and brain function. Journal and proceedings of the Royal Society of New South Wales, 135: 57-71.

Johnston GAR, JR. Hanrahan, M Chebib, RK.Duke, KN. Mewett. 2006. Modulation of ionotropic GABA receptors by natural products of plant origin. Advances in Pharmacology, 54: 285-316

Lichtenthaler HK, Rohmer M, Schwender J. 1997. Two independent biochemical pathways for isopentenyl diphosphate and isoprenoid biosynthesis in higher plants. Physiol Plant 101: 643–652

Ozel A, Ozguven, M. 2002. Effect of different planting times on essential oil composition of different mint varieties. Turk. J. Agric. For., 26:289-294.

Ozguven M, S. Tansi. 1998. Drug Yield and Essential Oil of Thymus vulgaris L. as in Influenced by Ecological and Ontogenetical Variation. Tr. J. of Agriculture and Forestry 22 :537-542

Piccaglia R., Marotti M., Galletti .1991. J. Essential oil Res., 3: 147-152. SAC Auchincruive.

Runham R.S. 1986. An updated review of the potential uses and markets of plants grown for extracts including essential oils and factors affecting their yield and composition. MAFF Ref ST0105. RDREP03.p.33

Singh VP, Singh M., D.V. Singh. 1997. Growth, yield and quality of peppermint as influenced by planting time. J. Herbs, Spices and Med. Plants., 5(3): 33-39.

Staudt M, Bertin N.1998 Light and temperature dependence of the emission of cyclic and acyclic monoterpenes from holm oak (Quercus ilex L.) leaves. Plant Cell Environ. 21: 385–395

Wills RBH, D Shohet. 2003. Production of high quality Australian valerian products. RIRDC Pub No 03/081.

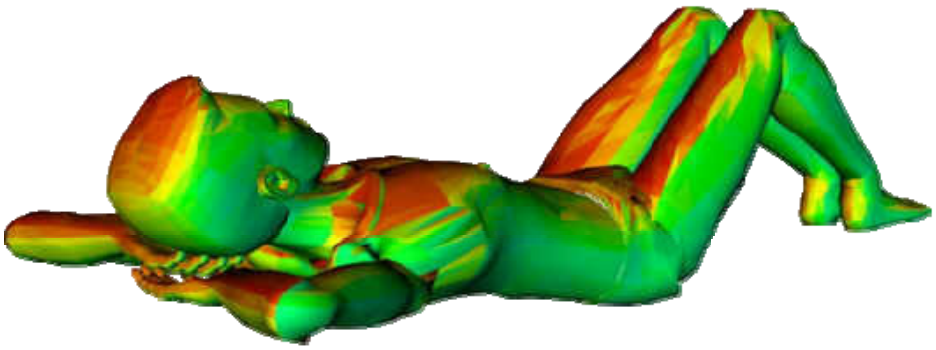

BioMet 7

April 12-14, 2010

Albert-Ludwigs-University of Freiburg, Germany

Program

7th Conference on Biometeorology of the Expert Committee "Biometeorology" of the German Meteorological Society

hosted by:

Meteorological Institute, Albert-Ludwigs-University of Freiburg, Germany

Conference website: www.mif.uni-freiburg.de/Biomet/bm7

Meteorological Institute, Albert-Ludwigs-University of Freiburg
Werthmannstrasse 10, D-79085 Freiburg, Germany
Phone: +49/761/203-3590
Fax: +49/761/203-3586
e-mail: meteo@meteo.uni-freiburg.de
http://www.meteo.uni-freiburg.de

Expert Committee “Biometeorology” of the German Meteorological Society

DMG
Deutsche Meteorologische Gesellschaft

in collaboration with:

Faculty of Agriculture and Horticulture, Professorship of Agricultural Climatology, Humboldt-University of Berlin, Germany	HUMBOLDT-UNIVERSITÄT ZU BERLIN
Society for the Promotion of Medicine-Meteorological Research in Germany	
International Society of Biometeorology	ISB
German Weather Service	DWD
Central Institute of Meteorology and Geodynamics	ZAMG

7th Conference on Biometeorology

- Program outline -

Presentations in Freiburg (Auditorium (Aula), Albert-Ludwigs-University of Freiburg)

Monday, 12 April 2010:

08:00:	Registration
09:00 - 09:30:	Welcome addresses and organisation details
09:30 - 10:15:	Phenology: 3 oral presentations
10:15 - 11:00:	*Coffee break / Poster presentations*
11:00 - 12:30:	Tourism I: 6 oral presentations
12:30 - 13:30:	*Lunch (buffet, foyer of the auditorium)*
13:30 - 14:45:	Tourism II: 5 oral presentations
14:45 - 15:15:	Animal and Forest Meteorology: 2 oral presentations
15:15 - 16:00:	*Coffee break / Poster presentations*
16:00 - 17:30:	Climate Change: 6 oral presentations
18:00 - 20:00:	*Ice-breaker (foyer of the auditorium)*

Tuesday, 13 April 2010:

09:00 - 10:15:	Human Biometeorology I: 5 oral presentations
10:15 - 11:00:	*Coffee break / Poster presentations*
11:00 - 11:45:	Human Biometeorology II: 3 oral presentations
11:45 - 12:15:	Miscellaneous: 2 oral presentations
12:15 - 13:30:	*Lunch (buffet, foyer of the auditorium)*
13:00 - 13:30:	*Assembly of the Society of the Promotion of Medical Meteorology*
13:30 - 15:30:	Urban Bioclimate I: 8 oral presentations
15:30 - 16:00:	*Coffee break / Poster presentations*
16:00 - 17:45:	Urban Bioclimate II: 7 oral presentations
18:00:	Assembly Expert Committee “Biometeorology” of the German Meteorological Society

Wednesday, 14 April 2010:

09:00 - 10:15:	Agricultural Meteorology I: 5 oral presentations
10:15 - 11:00:	*Coffee break / Poster presentations*
11:00 - 12:00:	Agricultural Meteorology II: 4 oral presentations
12:00 - 13:00:	*Lunch (buffet, foyer of the auditorium)*
13:00 - 15:00:	Human Biometeorology III: 8 oral presentations
15:00 - 15:30:	*Coffee break*
15:30:	Closing session

7th Conference on Biometeorology

Venue in Freiburg:

Auditorium (Aula), Albert-Ludwigs-University of Freiburg, Germany

Kollegiengebäude I (KG I; building No. 1 in the map below)

Platz der Universität 3, D-79098 Freiburg, Germany

7th Conference on Biometeorology

- Detailed program -

Oral presentations: 15 minutes, i.e. 12 minutes for presentation and 3 minutes for discussion

Monday, 12 April 2010:

08:00: Registration

09:00 - 09:25: Welcome addresses:

Prof. Dr. Andreas Matzarakis; Chair, Scientific and Local Organising Committee, Freiburg, Germany

Prof. Dr. Hans-Jochen Schiewer, Rector of the Albert-Ludwigs-University of Freiburg, Germany

Prof. Dr. Frank-M. Chmielewski; Chair, Expert Committee "Biometeorology" of the German Meteorological Society

09:25 - 09:30: Organisation details:

Prof. Dr. Andreas Matzarakis; Germany

Phenology (chair: Frank-M. Chmielewski, Germany)

09:30 – 09:45	Peter Braun (Forschungsanstalt Geisenheim, Germany), Markus Müller: *Limits of phenological modelling in tree species*
09:45 – 10:00	Wolfgang Janssen (Deutscher Wetterdienst, Germany): *Definition des Vegetationszeitraumes über Temperatursummen*
10:00 – 10:15	Steffi Urhausen (Meteorologisches Institut der Universität Bonn, Germany), Susanne Brienen, Alice Kapala, Clemens Simmer: *Impact of future climate conditions on viticulture in the Upper Moselle region*

10:15 - 11:00: **Coffee break**

Tourism I (chair: Chris de Freitas, New Zealand)

11:00 – 11:15	Jochen Bläsing (Deutscher Wetterdienst, Zentrum für Medizin-Meteorologische Forschung, Germany): *Auswirkungen einer durch den Klimawandel geänderten Wärmebelastung auf die Bewertung von prädikatisierten Kurorten*
11:15 – 11:30	Ksenija Zaninovic (Meteorological and Hydrological Service, Department for Climatological Research and Applied Climatology, Croatia), Lidija Srnec, Mirta Patarcic, Melita Percec Tadic, Janos Mika, Akos Nemeth: *Influence of climate change on the summer tourism potential in the Pannonian basin*
11:30 – 11:45	Hasan Yilmaz (Department of Landscape Architecture, Faculty of Agriculture, Ataturk University, Turkey), Sevgi Yilmaz, Süleyman Toy, Nalan Demircioglu Yildiz: *Evaluation of climatic characteristics for tourism and recreation in a specific area, Tortum, in Eastern Anatolia region of Turkey*
11:45 – 12:00	Raquel Machete (Centro de Estudos Geográfico, Edifício da Faculdade de Letras, Portugal), Carlos Ferreira, Eduardo Brito-Henriques, Henrique Andrade, José Couto: *Anticipating the impacts of climate change on tourism in Lisbon Metropolitan Area –*

	Assessing tourist perceptions
12:00 – 12:15	Ákos Németh (Climate Division, Hungarian Meteorological Service, Hungary), Andreas Matzarakis: *Changing thermal bioclimate and the summer tourism potential of the Lake Balaton*
12:15 – 12:30	Antonio Lopes (Centro de Estudos Geograficos, University of Lisbon, Portugal), S. Lopes, Andreas Matzarakis, Maria Joao Alcoforado: *Summer sea breeze influence on human comfort in Funchal (Madeira Island). Application to urban climate and tourism planning*

12:30 - 13:30: **Lunch (buffet, foyer of the auditorium)**

Tourism II (chair: Andreas Matzarakis, Germany)

13:30 – 13:45	Robert Steiger (Institute of Geography, Innsbruck University, Austria): *The impact of record warm winter seasons on ski touristic demand*
13:45 – 14:00	Chris de Freitas (University of Auckland, School of Environment, New Zealand), Elena A. Grigorieva: *Prediction of acclimatization thermal loading for individuals travelling between climatic extremes*
14:00 – 14:15	Sevgi Yilmaz (Department of Landscape Architecture, Faculty of Agriculture, Ataturk University, Turkey), Süleyman Toy, Hasan Yilmaz: *Determination of the winter human thermal comfort distributions in a ski-centre*
14:15 – 14:30	Chris de Freitas (University of Auckland, School of Environment, New Zealand), Andreas Matzarakis: *Gauging the sensitivity of tourism climate to change by way of an integrated thermal bioclimatic assessment scheme*
14:30 – 14:45	Christina Endler (Meteorological Institute, Albert-Ludwigs-University of Freiburg, Germany), Andreas Matzarakis: *Assessment of climate for tourism purposes in Germany*

Animal and Forest Meteorology (chair: Dirk Schindler, Germany)

14:45 – 15:00	John Gaughan (The University of Queensland, Australia), Jarrod Lees: *Development of a climate stress index for dairy cows housed outside*
15:00 – 15:15	Christian Hertel (Fachgebiet für Ökoklimatologie, Technische Universität München, Germany), Michael Leuchner: *Variability of light quality and quantity in a mixed forest stand*

15:15 - 16:00: **Coffee break / Poster presentations**

Climate Change (chair: Wilhelm Kuttler, Germany)

16:00 – 16:15	Manuel Helbig (University of Göttingen, Germany), Chris de Freitas, Andreas Matzarakis: *Water resources of Pacific atolls: evaluating sensitivity to climatic change and variability*
16:15 – 16:30	Jiri Nekovar (Czech Hydrometeorological Institute, Czech Republic), Rudolf Bagar: *Evaluation of global sunshine energy 1984-2008 over Czech climate station network*
16:30 – 16:45	Katharine Willett (Met Office Hadley Centre, UK), Steven Sherwood: *Exploring heat events in future climates for 15 regions using exceedance of WBGT thresholds*

16:45 – 17:00	Angelika Grätz (Deutscher Wetterdienst, Germany): *Stadtplanung und Klimawandel - Eine Kooperation des DWD mit der Stadtentwicklungsverwaltung von Berlin*
17:00 – 17:15	Birger Tinz (Deutscher Wetterdienst, Germany), Thomas Deutschländer, Barbara Früh: *Entwicklung der Wärmebelastung in Deutschland im 21. Jahrhundert*
17:15 – 17:30	Hans-Guido Mücke (Umweltbundesamt, Germany): *Climate change: New health risks in the air*

18:00 - 20:00: **Ice-breaker** (drinks and finger-food in the foyer of the auditorium)

Tuesday, 13 April 2010:

Human I (chair: Christina Koppe, Germany)

09:00 – 09:15	Katharina Gabriel (Leibniz-Institut für Gewässerökologie und Binnenfischerei, Germany): *Comparison of methods for heat determination*
09:15 – 09:30	Gerd Jendritzky (Meteorological Institute, Albert-Ludwigs-University of Freiburg, Germany), George Havenith, Philipp Weihs, Ekaterina Batchvarova, Richard de Dear: *Universal Thermal Climate Index UTCI*
09:30 – 09:45	Insa Thiele-Eich (Meteorologisches Institut der Universität Bonn, Germany), Susanne Brienen, Alice Kapala, Gerd Jendritzky und Clemens Simmer: *Zukünftige thermische Komfortbedingungen in Deutschland*
09:45 – 10:00	Ilian Gospodinov (National Institute of Meteorology and Hydrology, Bulgaria), Anna Tzenkova-Bratoeva: *Spatial and temporal variability of the rate of change of the winter thermal comfort conditions in Bulgaria*
10:00 – 10:15	Danuta Idzikowska (Faculty of Geography and Regional Studies, University of Warsaw, Poland): *Differences in bioclimatic conditions in four European cities: Budapest, Paris, Warsaw and Rome*

10:15 - 11:00: **Coffee break / Poster presentations**

Human II (chair: Panagiotis Nastos, Greece)

11:00 – 11:15	Makoto Nakayoshi (Tokyo Institute of Technology, Japan), Manabu Kanda: *Compact and wearable measurement system for Langrangian Human Biometeorology*
11:15 – 11:30	Henning Staiger (Freiburg, Germany), Andreas Matzarakis: *Estimating down- and up-welling thermal radiation for use in mean radiant temperature*
11:30 – 11:45	Eva R. Wanka (Klinikum der Ludwig-Maximilians-Universität München, Germany), U. Ferrari, T. Exner, C. Heumann, R. M. Huber, R. Fischer: *Longitudinale Modellierung pneumologischer Erkrankungen in Abhängigkeit von meteorologischen Einflussfaktoren - Pilotregion Bayern*

Miscellaneous (chair: Elisabeth Koch, Austria)

11:45 – 12:00	Olaf Matuschek (Meteorological Institute, Albert-Ludwigs-University of Freiburg, Germany), Andreas Matzarakis: *Estimation of sky view factor in complex environment as a tool for applied climatological studies*
12:00 – 12:15	Andreas Matzarakis (Meteorological Institute, Albert-Ludwigs-University of Freiburg, Germany): *Thermal comfort issues and deficiencies in measurements and modelling*

12:15 - 13:30: **Lunch (buffet, foyer of the auditorium)**

13:00 - 13:30: **Sitzung der Gesellschaft zur Förderung der Medizin-Meteorologischen Forschung in Deutschland e.V. (Assembly of the Society of the Promotion of Medical Meteorology in Germany) - (Room 1139) – only for members**

Urban Bioclimate I: (chair: Oded Potchter, Israel)

13:30 - 13:45	Wilhelm Kuttler (Universität Duisburg-Essen, Abt. Angewandte Klimatologie, Germany): *Einfluss des globalen Klimawandels auf die Ozon- und Feinstaubkonzentrationen in Stadt und Umland*
13:45 – 14:00	Sascha Henninger (Lehreinheit Physische Geographie, Technische Universität Kaiserslautern, Germany): *Modifikationen des lufthygienischen Wirkungskomplexes in der ruandischen Stadt Kigali*
14:00 – 14:15	Fred Meier (Fachgebiet Klimatologie, Technische Universität Berlin, Institut für Ökologie, Germany), Dieter Scherer, Jochen Richters: *Spatial and temporal variability of surface temperature of tree crowns in an urban environment*
14:15 – 14:30	B.G. Heusinkveld (Wageningen University, The Netherlands), L.W.A. van Hove, C.M.J. Jacobs, G.J. Steeneveld, J.A. Elbers, E.J. Moors, A.A.M. Holtslag: *Greening of Dutch urban canyons for heat stress reduction*
14:30 – 14:45	Sevgi Yilmaz (Department of Landscape Architecture, Faculty of Agriculture, Ataturk University, Turkey), Yahya Bulut, Süleyman Toy, Işık Sezen: *Evaluation of the relationship between air pollution and climatic elements in urban areas in the sample of Erzurum city in the respect of landscape architecture*
14:45 – 15:00	Antje Katzschner (Fachgebiet Umweltmeteorologie, Fachbereich 06, Universität Kassel, Germany): *Calibration of thermal comfort in different climates for urban planning concerns*
15:00 – 15:15	Yuk Yee Yan (Department of Geography, Hong Kong Baptist University, Kowloon Tong, Hong Kong), Ho Yan Cheng: *Summer human thermal comfort in urban open spaces in Hong Kong*
15:15 – 15:30	Chae Yeon Yi (National Institute of Meteorological Research, Meteorological Application Research Laboratory, Korea), Young-Jean Choi, Jeong-Hee Eum, Geun Hoi Kim, Kyu Rang Kim, Dieter Scherer, Ute Fehrenbach: *Development of climate analysis software for urban and environmental planning of Seoul*

15:30 - 16:00: **Coffee break / Poster presentations**

Urban Bioclimate II: (chair: Antonio Lopes, Portugal)

16:00 – 16:15	Limor Shashua-Bar (Department of Geography and Environmental Development, Ben Gurion University of the Negev, Israel), S. Cohen, O. Potchter, Y. Yaakov, J. Tanny, P. Bar-Kutiel: *The use of street trees for heat stress mitigation in hot and arid regions. Case study: Beer Sheva, Israel*
16:15 – 16:30	Oded Potchter (Laboratory for Climate and Environment, Department of Geography and Human Environment, Israel), J. Holst, L. Shashua-Bar, S. Cohen, Y. Yaakov , J. Tanny, P. Bar-Kutiel, H. Mayer: *Comparative study of trees impact on human thermal comfort in urban streets under hot-arid and temperate climates*
16:30 – 16:45	Jutta Holst (Meteorological Institute, Albert-Ludwigs-University of Freiburg, Germany), Helmut Mayer: *Impacts of street design parameters on human-biometeorological variables*
16:45 – 17:00	Ágnes Gulyás (Department of Climatology and Landscape Ecology, University of Szeged, Hungary), Andreas Matzarakis, János Unger:

	Comparison of the urban-rural thermal comfort sensation in a city with warm continental climate
17:00 – 17:15	Monika Bąkowska (Institute of Geography, Uniwersytet Kazimierza Wielkiego, Poland): *Influence of air circulation and geographical factors on daily rhythm of biothermal conditions*
17:15 – 17:30	Qun Dai (School of Architecture, The Chinese University of Hong Kong, Hong Kong): *A review on technology development in urban climatology and the application of a new enhanced urban climate model in Hong Kong*
17:30 – 17:45	Christoph Schneider (Department of Geography, Faculty of Material Sciences and Geosciences, RWTH Aachen University, Germany), Marten F. Brunk, Wolfgang Dott, Heather Hofmeister, Carmella Pfaffenbach, Christine Roll, Klaus Selle, Kunibert Wachten, Mareike Buttstädt, Katja Eßer, Julia Hahmann , Lotta Hülsmeier , Gunnar Ketzler, Marion Klemme, Antje Kröpelin, Hendrik Merbitz, Sabri: *"CITY 2020+" – assessing climate and demographic change impacts for the City of Aachen*

18:00: **Assembly Expert Committee "Biometeorology" of the German Meteorological Society**

Wednesday, 14 April 2010:

Agriculture I (chair: Ulrich Otte, Germany)

09:00 – 09:15	Franz Josef Löpmeier (Deutscher Wetterdienst Braunschweig, Germany), Cathleen Frühauf: *Die Auswirkungen des Klimawandels auf die Landwirtschaft - die Aktivitäten des Deutschen Wetterdienstes im Rahmen des Projektes ZWEK*
09:15 – 09:30	Ramona Weßnigk (Deutscher Wetterdienst Braunschweig, Germany), Jens Fildebrandt: *Agrarmeteorologische Beratung des Deutschen Wetterdienstes unter spezieller Berücksichtigung von Sonderberatungen*
09:30 – 09:45	Klaus-Peter Wittich (Deutscher Wetterdienst Braunschweig, Germany), Ralf Becker: *Klimatologische und phänologische Dürre-Indikatoren in der Agrarmeteorologie des DWD*
09:45 – 10:00	Harald Braden (Deutscher Wetterdienst Braunschweig, Germany): *Sensitivität des agrarmeteorologischen Modells AMBETI/BEKLIMA gegenüber Änderungen der meteorologischen Randbedingungen*
10:00 – 10:15	Thomas Gerersdorfer (University of Natural Resources and Applied Life Sciences, Vienna Department of Water - Atmosphere - Environment, Institute of Meteorology, Austria), Josef Eitzinger, Enno Bahrs, Christiane Brandenburg: *Der Beitrag von Landschaftsstrukturen (z.B. Windschutzhecken) zur Ertragssituation im Ackerbau in Ostösterreich*

10:15 - 11:00: **Coffee break / Poster presentations**

Agriculture II (chair: Nicola Lacetera, Italy)

11:00 – 11:15	Rakesh Kumar (Institute is Institute of Himalayan Bioresource Technology (CSIR), India), K. Ramesh, Sandeep Tehria, Bikram Singh, Rajendra Prasad: *Crop weather interaction studies in a natural sweetener plant (Stevia rebaudiana (Bert.) Bertoni) in Indian Western Himalaya*
11:15 – 11:30	Elena Grigorieva (Institute for Complex Analysis of Regional Problems, Far Eastern Branch Russian Academy of Sciences, Russian Federation), Andreas Matzarakis: *Growing degree days at the Russian Far East*
11:30 – 11:45	Kulasekaran Ramesh (Division of Soil chemistry and Fertility, Indian Institute of Soil Science (ICAR), India), Virendra Singh, Bikram Singh, Vijayalata Pathania: *Agrometeorology of an aromatic plant (Valeriana officinalis) - Borneol, Bornyl acetate and other components of essential oil in European valerian as influenced by planting time and age of harvest*
11:45 – 12:00	Frank-M. Chmielewski (Professorship of Agricultural Climatology, Humboldt-University of Berlin, Germany), Klaus Blümel, Yvonne Henniges: *Climate change and late frost damages to Apple Trees in Germany*

12:00 - 13:00: **Lunch (buffet, foyer of the auditorium)**

Human Biometeorology III (chair: Eva Regina Wanka, Germany)

13:00 – 13:15	Jereon T.M. Buters and the HIALINE working group *Ambient concentrations of the major birch, grass and olive allergen Bet v 1, Phleum*

	p 5 and Ole e 1 and pollen counts in Europe: The new EU-HIALINE project
13:15 – 13:30	Christina Koppe (Deutscher Wetterdienst, Germany), Daniel Arndt, Andreas Mügge, Jan Börgel: *The influence of meteorological parameters on hypertensive urgency*
13:30 – 13:45	Judita Liukaityte (Lithuanian Hydrometeorological Service, Latvia), Justinas Savanevicius: *Association of meteorological factors with emergency calls of ambulance in Vilnius, Lithuania*
13:45 – 14:00	Paulo Canário (Centro de Estudos Geográfico, Edifício da Faculdade de Letras, Portugal), Henrique Andrade: *Mortality spatial variations in a small scale during heat waves in Lisbon - who is at risk?*
14:00 – 14:15	Stefan Muthers (Meteorological Institute, Albert-Ludwigs-University of Freiburg, Germany), Andreas Matzarakis, Elisabeth Koch: *Relationship between climate and mortality in Vienna based on human-biometeorological data*
14:15 – 14:30	Panagiotis T. Nastos (Laboratory of Climatology and Atmospheric Environment, Department of Geography and Climatology, University of Athens, Greece), K. N. Giaouzaki, N. A. Kampanis, P. I. Agouridakis, A. Matzarakis: *Environmental impacts on human health during a saharan episode at Crete island, Greece*
14:30 – 14:45	Uwe Kaminski (Deutscher Wetterdienst, Germany), T. Glod: *Untersuchungen zum Einfluss des Klimawandels in Deutschland auf den Start der Pollensaison, die Saisonlänge und die Pollenkonzentration der wichtigsten allergenen Pollen anhand der Pollendaten der Referenzstationen des Polleninformationsdienstes PID*
14:45 – 15:00	Young-Jean Choi (National Institute of Meteorological Research, Meteorological Application Research Laboratory, Korea), Ki-Jun Park, Kyu Rang Kim, Hye-Rim Lee, Chae Yeon Yi, Jae-Won Oh: *Climate change and adaptation strategies for pollens in Korea*

15:00 - 15:30: **Coffee break**

Closing session

15:30: Closing session (Andreas Matzarakis, John Gaughan, Frank-M. Chmielewski, Helmut Mayer)

Poster presentations in Freiburg from 12-14 April 2010:

P1:	Ákos Németh: *Using digital elevation models in agroclimatology: determination of potential frost-risk territories*
P2:	Cathleen Frühauf (Deutscher Wetterdienst Braunschweig, Germany), Beate Berkelmann-Löhnertz, Bernd J. Loskill, Anja Schaldach, Harald Braden, Klaus-Uwe Gollmer, Markus Forster, Klaus-Peter Wittich: *Erweiterung und Optimierung der Geisenheimer Peronospora-Prognose und Umsetzung in die Rebschutz-Praxis im Rheingau*
P3:	Klaus-Peter Wittich (Deutscher Wetterdienst Braunschweig, Germany), Martin Kraft: *Erfassung der Vegetationsentwicklung landwirtschaftlicher Bestände mit agrarmeteorologischen Strahlungssensoren*
P4:	Elham Rahmani (Meteorologisches Institut der Universität Bonn, Germany), Andreas Hense, Jan Keller, Petra Friederichs: *The effect of climate change on agro climate zoning of wheat in Iran*
P5:	Harald Braden (Deutscher Wetterdienst Braunschweig, Germany): *"Guttation", Bedeutung, Beobachtung, Modellierung*
P6:	Frank-M. Chmielewski (Professorship of Agricultural Climatology, Humboldt-University of Berlin, Germany), Klaus Blümel, Antje Müller, Yvonne Henniges, Roland W.S. Weber: *Climate change and fruit growing in Germany*
P7:	Jürgen Junk (Département Environnement et Agro-Biotechnologies, Centre de Recherche Public - Gabriel Lippmann, Luxembourg), M. El Jarroudi, F. Pogoda, T. Dubos, K. Görgen, L. Hoffmann, M. Beyer: *Forecasting epidemic outbreaks of wheat leaf blotch based on meteorological parameters*
P8:	Fotios Xystrakis (Institute of Sylviculture, Albert-Ludwigs-University of Freiburg, Germany), Andreas Matzarakis: *The importance of meteorological variables in the bias of potential evapotranspiration estimates in Crete, southern Greece*
P9:	Andrea Vitali (Dipartimento di Produzioni Animali, Università degli Studi della Tuscia, Viterbo, Italy), Emilio Lana, Franco Guizzardi, Massimo Amadori, Umberto Bernabucci, Alessandro Nardone, Nicola Lacetera: *Seasonal pattern of mortality and relationships between mortality and temperature humidity index in heavy slaughter pigs*
P10:	Merike Fiedler (Leibniz-Institut für Agrartechnik Potsdam-Bornim e.V., Germany), Gundula Hoffmann, Kristina von Bobrutzki' Andreas Matzarakis: *Biometeorological investigations in dairy cowsheds*
P11:	Paul Neumann (Meteorological Institute, Albert-Ludwigs-University of Freiburg, Germany), Andreas Matzarakis: *Regional and local dimension of climate change: identification of the impact of climate variability and extreme events using the example of heat and drought in Baden-Württemberg*
P12:	Thomas Rötzer (Lehrstuhl für Waldwachstumskunde, Technische Universität München, Germany), Hans Pretzsch: *Water storage of Norway spruce and its possible influence on tree growth under drought stress - application of ct-scannings -*
P13:	Yan Liao (Lehrstuhl für Waldwachstumskunde, Technische Universität München, Germany),

	Thomas Rötzer, Hans Pretzsch: *Effects of climate change and adaptation strategies for Northwest European forest stands*
P14:	Steffi Röhling (Lehrstuhl für Waldwachstumskunde, Technische Universität München, Germany), Thomas Rötzer, Hans Pretzsch: *Einfluss des Klimas auf die Kohlenstoffspeicherung von Moorwäldern*
P15:	Maendy Fritz (Technologie- und Förderzentrum, Straubing, Germany), Thomas Rötzer, Uwe Hera: *Klimatische Anbaueignung von Sorghumhirsen in Deutschland unter gegebenen und veränderten Klimabedingungen*
P16:	Uwe Kaminski (Deutscher Wetterdienst, Germany), Beate Alberternst, Thomas Gabrio, Michael Böhme, Stefan Nawrath, Heidrun Behrendt: *Ambrosia Pollen-Konzentrationen in Baden-Württemberg*
P17:	Sandra Kannabei (Institut für Meteorologie, Freie Universität Berlin): *Ambrosia in Berlin: pollen emission, spread and control*
P18:	Katrin Burkart (Department of Climatology, Institute of Geography, Humboldt-Universität zu Berlin, Germany), Winfried Endlicher: *The effect of temperature and thermal atmospheric conditions on mortality in Bangladesh*
P19:	Stefan Muthers (Meteorological Institute, Albert-Ludwigs-University of Freiburg, Germany), Andreas Matzarakis, Elisabeth Koch: *Changes in heat related mortality in Vienna based on regional climate models*
P20:	Joanna Maroszek (Faculty of Geography and Regional Studies, University of Warsaw, Poland), Takeshi Morita and Krzysztof Błazejczyk: *Melatonin secretion in various climate zone*
P21:	Katarzyna Lindner (Faculty of Geography and Regional Studies, University of Warsaw, Poland): *Clothing as an indicator of human thermal comfort*
P22:	Jobst Augustin (Umweltbundesamt, Germany): *Climate change and skin cancer - relation and effects*
P23:	Panagiotis T. Nastos (Laboratory of Climatology and Atmospheric Environment, Department of Geography and Climatology, University of Athens, Greece), K. Giaouzaki, N. A. Kampanis, P. Agouridakis, A. Matzarakis: *Acute coronary syndromes and biometeorological conditions at Crete island, Greece*
P25:	Petra Gebauer (Institut für Meteorologie der FU Berlin, Germany): *The WBGT-Index – a heat index, used in international sporting events*
P25:	Anna Kunert (Institute of Geography and Spatial Organization Polish Academy of Sciences, Poland): *Modeling of UTCI index in various types of landscape*
P26:	George O. Odhiambo (Department of Geography and Urban Planning CHSS, UAE University, UAE), M. J. Savage: *Influence of wind direction and a slanting beam angle on surface layer scintillometer estimates of sensible heat flux*
P27:	Kerstin Höbart (Universität für Bodenkultur, Vienna, Austria), Christina Czachs, Christiane Brandenburg, Manfred Pintar, Erich Mursch-Radlgruber: *Bestimmung amphibischer Aktivität mittels Phänologie*

P28:	Elisabeth Koch (Central Institute of Meteorology and Geodaynamics, Vienna, Austria), Silke Adler, Wolfgang Lipa, Markus Ungersböck, Susanne Zach-Hermann *The pan European phenological database PEP725*
P29:	Elena A. Grigorieva (Institute for Complex Analysis of Regional Problems, Far Eastern Branch Russian Academy of Sciences, Russian Federation), Andreas Matzarakis: *Physiologically equivalent temperature in extreme climate regions in the Russian Far East*
P30	Gaelle Serquet (Swiss Federal Research Institute WSL), Martine Rebetez: *Relationship between tourism demand in the swiss alps and hot summer air temperatures associated with climate change*
P31:	Andreas Matzarakis (Meteorological Institute, Albert-Ludwigs-University of Freiburg, Germany), Timm Schneevoigt, Olaf Matuschek, Christina Endler: *Transfer of climate information for tourism and recreation – the CTIS software*
P32:	Christine Ketterer (Meteorological Institute, Albert-Ludwigs-University of Freiburg, Germany), Andreas Matzarakis: *The tourism climate of Engadin, Switzerland*
P33:	Philipp Schmidt (Meteorological Institute, Albert-Ludwigs-University of Freiburg, Germany), Robert Steiger, Andreas Matzarakis: *Artificial snow making in the Southern Black Forest*
P34:	Robert Steiger (Institute of Geography, Innsbruck University, Austria): *Climate change impact assessment in winter tourism*
P35:	Eleni Didaskalou (University of Pireus, Greece), Panagiotis Nastos, Paris Tsartas: *The climate as an important factor in a multicriteria decision analysis for the development planning of wellness tourism*
P36	Tzu-Ping Lin (Department of leisure planning, National Formosa University, National Formosa University, Taiwan), Andreas Matzarakis, Ruey-Lung Hwang: *Effect of pavements albedo on long-term outdoor thermal comfort*
P37:	Gudrun Schlaf (Deutscher Wetterdienst, Germany), Jochen Bläsing: *Thermal compensation systems in the outskirt areas of Rhine valley*
P38:	Noémi Kántor (Department of Climatology and Landscape Ecology, University of Szeged, Hungary), Ágnes Gulyás: *Area usage and thermal sensation vs. thermal comfort conditions- outdoor thermal comfort project in Szeged, Hungary*
P39:	Hyunjung Lee (Meteorological Institute, Albert-Ludwigs-University of Freiburg, Germany), Jutta Holst, Helmut Mayer: *Assessment of air quality indices in Seoul region by land use type*
P40:	Cornelia Kurbjuhn (Professur für Meteorologie, TU Dresden, Germany), V. Goldberg, A. Westbeld, Ch. Bernhofer: *Impact of vegetation areas on the microclimate in the city of Dresden, Germany*
P41:	Jan Herrmann (Meteorological Institute, Albert-Ludwigs-University of Freiburg, Germany), Andreas Matzarakis: *Influence of mean radiant temperature on thermal comfort of humans in idealized urban environments*
P42:	Edward Ng (School of Architecture, The Chinese University of Hong Kong), An Xipo, Lutz Katzschner: *Urban Wind and Heat Environment in Hong Kong*

P42:	Henrique Andrade (Centro de Estudos Geográfico, Edifício da Faculdade de Letras, Portugal), Maria Joao Alcoforado, Paulo Canário: *Urban thermal patterns, environmental conditions associated and synoptic factors in Lisbon*

7th Conference on Biometeorology

Freiburg, Germany, 12-14 April 2010

Scientific Committee

Paul Becker, Offenbach
Frank-M. Chmielewski, Berlin (co-chair)
Christina Koppe, Freiburg
Andreas Matzarakis, Freiburg (chair)
Helmut Mayer, Freiburg
Ulrich Otte, Offenbach

Local Organising Committee

Andrea Hug, Freiburg, Germany
Christina Koppe, Freiburg, Germany
Andreas Matzarakis, Freiburg, Germany (chair)
Helmut Mayer, Freiburg, Germany (co-chair)
Members of Meteorological Institute, Albert-Ludwigs-University of Freiburg, Germany
Student assistants, Freiburg, Germany

Berichte des Meteorologischen Institutes der Albert-Ludwigs-Universität Freiburg

Nr. 1: Fritsch, J.: Energiebilanz und Verdunstung eines bewaldeten Hanges. Juni 1998

Nr. 2: Gwehenberger, J.: Schadenpotential über den Ausbreitungspfad Atmosphäre bei Unfällen mit Tankfahrzeugen zum Transport von Benzin, Diesel, Heizöl oder Flüssiggas. August 1998

Nr. 3: Thiel, S.: Einfluß von Bewölkung auf die UV-Strahlung an der Erdoberfläche und ihre ökologische Bedeutung. August 1999

Nr. 4: Iziomon, M.G.: Characteristic variability, vertical profile and modelling of surface radiation budget in the southern Upper Rhine valley region. Juli 2000

Nr. 5: Mayer, H. (Hrsg.): Festschrift „Prof. Dr. Albrecht Kessler zum 70. Geburtstag“. Oktober 2000

Nr. 6: Matzarakis, A.: Die thermische Komponente des Stadtklimas. Juli 2001*)

Nr. 7: Kirchgäßner, A.: Phänoklimatologie von Buchenwäldern im Südwesten der Schwäbischen Alb. Dezember 2001*)

Nr. 8: Haggagy, M.E.-N.A.: A sodar-based investigation of the atmospheric boundary layer. September 2003*)

Nr. 9: Rost, J.: Vergleichende Analyse der Energiebilanz zweier Untersuchungsflächen der Landnutzungen “Grasland“ und „Wald“ in der südlichen Oberrheinebene. Januar 2004*)

Nr. 10: Peck, A.K.: Hydrometeorologische und mikroklimatische Kennzeichen von Buchenwäldern. Juni 2004*)

Nr. 11: Schindler, D.: Characteristics of the atmospheric boundary layer over a Scots pine forest. Juni 2004*)

Nr. 12: Matzarakis, A., de Freitas, C.R., Scott, D. (Eds.): Advances in Tourism Climatology. November 2004*)

Nr. 13: Dostal, P.: Klimarekonstruktion der Regio TriRhena mit Hilfe von direkten und indirekten Daten vor der Instrumentenbeobachtung. Dezember 2004*)

Nr. 14: Imbery, F.: Langjährige Variabilität der aerodynamischen Oberflächenrauhigkeit und Energieflüsse eines Kiefernwaldes in der südlichen Oberrheinebene (Hartheim). Januar 2005*)

Nr. 15: Ali Toudert, F.: Dependence of outdoor thermal comfort on street design in hot and dry climate. November 2005*)

Nr. 16: Matzarakis, A., Mayer, H. (Hrsg.): Extended Abstracts zur 6. Fachtagung BIOMET des Fachausschusses Biometeorologie der Deutschen Meteorologischen Gesellschaft e.V.. März 2007*)

Nr. 17: Mayer, H. (Ed.): Celebrating the 50 years of the Meteorological Institute, Albert-Ludwigs-University of Freiburg, Germany. May 2008*)

Nr. 18: Mayer, H., Matzarakis, A. (Eds.): 5th Japanese-German Meeting on Urban Climatology. March 2009*)

Nr. 19: Mayer, H., Schindler, D. (Eds.): Proceedings of the 2nd International Conference „Wind Effects on Trees“. October 2009*)

Nr. 20: Matzarakis, A., Mayer, H., Chmielewski, F.-M. (Eds.): Proceedings of 7th Symposium on Biometeorology. April 2010*)

*) Report online available under:
http://www.meteo.uni-freiburg.de/forschung/publikationen/berichte/index_html